DISSERTATION

EXPANDING THE MEDICINAL CHEMISTRY TOOLBOX: DEVELOPMENT OF NEW PYRIDINE AND PIPERIDINE FUNCTIONALIZATION STRATEGIES

Submitted by

Jacob W. Greenwood

Department of Chemistry

In partial fulfillment of the requirements

For the Degree of Doctor of Philosophy

Colorado State University

Fort Collins, Colorado

Summer 2022

Doctoral Committee:

Advisor: Andrew McNally

Jeffrey Bandar
Justin Sambur
Delphi Chatterjee

Copyright by Jacob W. Greenwood 2022

All Rights Reserved

ABSTRACT

EXPANDING THE MEDICINAL CHEMISTRY TOOLBOX: DEVELOPMENT OF NEW PYRIDINE AND PIPERIDINE FUNCTIONALIZATION STRATEGIES

Nitrogen-containing heterocycles, such as pyridine, are ubiquitous in pharmaceuticals, agrochemicals, ligands, and materials. Therefore, robust methods for their direct functionalization are highly desired. Chapter one focuses on the importance of pyridine-containing molecules, the reactivity of pyridine, and challenges associated with functionalization of such compounds.

In chapter two, a method for bipyridine synthesis is discussed that uses pyridylphosphonium salts as radical precursors. Other radical precursors failed to provide the desired products, highlighting the unique reactivity imparted by the phosphonium group.

In chapter three, pyridylphosphonium salts are explored as alternatives to cyanopyridines in photoredox-catalyzed radical coupling reactions. This work expands the scope of the reaction manifold to complex pyridine substrates where installation of the cyano group can be challenging.

Chapter four introduces the value of piperidines and challenges associated with their synthesis. A strategy is described to address these limitations using isolable, cyclic iminium salts as a general platform to elaborate the piperidine scaffold with several medicinally relevant functional groups.

An alternative piperidine synthesis is presented in chapter five, where the mild transformation of a range of pyridines into pyridinium salts is achieved, followed by mild hydrogenation to the desired piperidine products. This method operates under mild conditions and can tolerate substitution at the 2-position of the pyridine substrate. As a result, a large amount of pyridine starting materials can now be engaged to form piperidines that are challenging to make with other technologies.

ACKNOWLEDGEMENTS

Firstly, I want to acknowledge that I have benefitted significantly from being in the presence of incredible chemists and leaders both at Colorado State University and Merck. I would like to thank Professor Andrew McNally for taking a chance on a student who lacked a strong background in organic synthesis before graduate school and providing me with a strong foundation in chemistry. I would also like to thank all the past and present McNally group members for pushing me to be a better chemist, mentor, and person. Specifically, I'm grateful to Luke Koniarczyk for accepting the task of training me and remaining a great friend. To Ryan Dolewski, thank you for teaching me that, sometimes, the answer comes to you when enjoying life outside of the lab. To Ben Boyle and Kyle Nottingham, thank you for supporting me during my most difficult times in graduate school. I will always cherish our time as housemates. To Jeff Levy, you were the best person I could have asked to study alongside these last five years. You have an uncanny ability to ask the right questions about everything, and it will take you far. To L.-C. Campeau, thank you for taking the time to help a graduate student you didn't know well. Your advice set me on the path that led to acquiring my dream job in the pharmaceutical industry. Finally, thank you to Aaron Sather. You are an incredibly talented leader and great friend. Your advice and support were pivotal for my development over the last year, and I'm thankful to have the opportunity to continue learning from you in the coming years as I begin my career.

In addition to exposure to fantastic scientists, I value the large fan section of friends and family that have motivated and taught me to become the best version of myself. Call it stubbornness or call it persistence; whatever it is, I got it from my mother. She taught me from a very young age to fight for what I want and to never give up, and I am so fortunate to have learned

that lesson from such a strong and caring role model. My father showed me how to reflect inward, identify beliefs that are holding me back, and to transform those beliefs into characteristics that will change your life for the better. As proud as he is of his children, I think we are prouder of his achievements in the past few years. To my brother, Rob, you are my best friend, and you always know how to make me stop taking life so seriously. To my sister, Amy, you have the rare ability to sense when people need help the most, and you have been there for me in my darkest times. I would be a far lesser person without you in my life. To my future in-laws, Shannon and Jason, it is rare to be blessed with two sets of incredible parents, and you have been my second home during my studies. I can never repay you for the love and support you have given me. Thank you to my unwavering friends from Bennington, The Hernandez family, the Maldonado family, Clayton Boozer, and Austin Dudas for the laughs, memories, and support. To Paige and Bre, I would not have made it through undergraduate studies without you, and your encouragement was instrumental in pursuing my goal of a graduate degree. Finally, I must thank my fiancé, Alexsi. You are the most caring, intentional, and inspiring person I have ever met in my life. Your love and empathy can be felt everywhere you go, and if everyone in the world shared your drive and kindness, the world would be a vastly better place. I love you so much, and I thank you for helping me on my journey to become the man I want to be.

As I reflect on all the assistance I have received during my education, I find it strange that only one name will be on the diploma at the conclusion of my graduate studies. After a championship football game, the conclusion of a Broadway show, or the development of a vaccine to help end a pandemic, the entire team is acknowledged for their efforts. Analogously, it seems to me that my entire team of friends and family should be recognized for the attainment of this degree. This achievement is theirs as much as mine.

TABLE OF CONTENTS

ABSTRACT……ii

ACKNOWLEDGEMENTS ……...……...……iii

CHAPTER ONE. Introduction to Pyridines and Pyridine Functionalization Strategies……...……...…….…..….1

1.1 Prevalence of Nitrogen-Containing Heteroaromatics in Organic Molecules…...……..,…..1

1.2 Advantageous Pharmacokinetic Properties of *N*-Heterocycles...……...…..….2

1.3 Challenges in Pyridine Functionalization...……..……..….4

1.4 Classical Methods for Functionalization of the 2- and 3-Positions of Pyridine…….5

1.5 Contemporary Methods for Functionalization of the 2- and 3-Positions of Pyridine…..…7

1.6 4-Selective Pyridine Methods…...……..……...9

1.7 4-Selective Pyridine Functionalization Using Pyridylphosphonium Salts……..……..…10

1.8 Conclusion…….……...……...15

References…..……..…17

CHAPTER TWO. Pyridine-Pyridine Cross-Coupling Reaction via Dearomatized Radical Intermediates…….……..……..20

2.1 Overview……..……..…20

2.2 Introduction……..……..…20

2.3 Design Plan for Photocatalyzed Pyridine Borylation…….....…..……...22

2.4 Discovery and Importance of an Unexpected Bipyridine Coupling Reaction……...…24

2.5 Reaction Optimization.……...…….……...…28

2.6 Scope of Bipyridine Coupling Reaction…..…….……..29

2.7 Mechanistic Investigation……...……..……..…...32

2.8 Computational Insight into Mechanism of Bipyridine Formation……..…...38

2.9 Conclusion…….……..…….…..41

References……..……..……42

CHAPTER THREE. Pyridylphosphonium Salts as Alternatives to Cyanopyridines in Radical-Radical Coupling Reactions……...…….…...45

3.1 Overview……..……..……..…..45

3.2 Introduction……..……..……..…..45

3.3 Chemistry of Cyanopyridines and Synthetic Challenges for their Synthesis……...….48

3.4 Reaction Design and Optimization…….……...….49

3.5 Scope of Photoredox-Catalyzed Transformations of Pyridylphosphonium Salts…….…54

3.6 Conclusion…….…….…….…..59

References……..……..……61

CHAPTER FOUR. Iminium Ions as a Platform for *N*-(Hetero)aryl Piperidine Synthesis……64

4.1 Overview… ……...……64

4.2 Introduction ……...……64

4.3 Reaction Optimization.…….……...…69

4.4 Iminium Salt Derivatization……..….……72

4.5 Scope of Iminium Salt Formation and Subsequent Transformations…….…..…..75

4.6 Development of a Telescoped Process and Sequential Difunctionalization……..……77

4.7 Conclusion…….……..…….…..80

References…….……..…….....82

CHAPTER FIVE. Complex Piperidine Synthesis Enabled by Hydrogenation of Pyridinium Salts…….……..…….....86

5.1 Overview……..…….…….…….……..86

5.2 Introduction……..…….…….…….……..86

5.3 Improvement of Zincke Reaction via N-Triflyl Pyridinium Salts……...…….89

5.4 Pyridinium Formation from N-Triflyl Zincke Imines……...……..…..…….....92

5.5 Optimization of N-Arylpyridinium Formation……..…...……..…...94

5.6 Substrate Scope ……...……..……96

5.7 Preliminary Hydrogenation Results……...…….…….……..99

5.8 Future Directions……...……..….……101

5.9 Conclusion……...……..…….…..…103

References……..……..……...……...104

APPENDIX ONE. Pyridine-Pyridine Cross-Coupling Reaction via Dearomatized Radical Intermediates: Experimental …….…..106

APPENDIX TWO. Pyridylphosphonium Salts as Alternatives to Cyanopyridines in Radical-Radical Coupling Reactions: Experimental…….…….…….……..289

APPENDIX THREE. Iminium Ions as a Platform for *N*-(Hetero)aryl Piperidine Synthesis: Experimental……..……...……..….…....444

APPENDIX FOUR. Complex Piperidine Synthesis Enabled by Hydrogenation of Pyridinium Salts: Experimental……..613

CHAPTER ONE

INTRODUCTION TO PYRIDINES AND PYRIDINE FUNCTIONALIZATION STRATEGIES

1.1 Prevalence of Nitrogen-Containing Heteroaromatics in Organic Molecules

Pharmaceuticals have significantly impacted modern medicine, playing a crucial role in disease diagnosis, prevention, and treatment. Nearly 90% of all U.S. FDA-approved drugs are comprised of small-molecule pharmaceuticals, and 59% of these therapeutics incorporate at least one nitrogen-containing heterocycle (*N*-heterocycle).[1] An important subclass of *N*-heterocycles are electron-deficient aromatics such as pyridine, quinoline, and pyrimidine. The significance of aromatic azaarenes is highlighted by their prevalence within approved drugs, clinical lead compounds, and agrochemicals (**Figure 1.1**). Additionally, heterocycles such as pyridine are also very important in the context of organic materials and ligands designed for metal catalysis.[2–4]

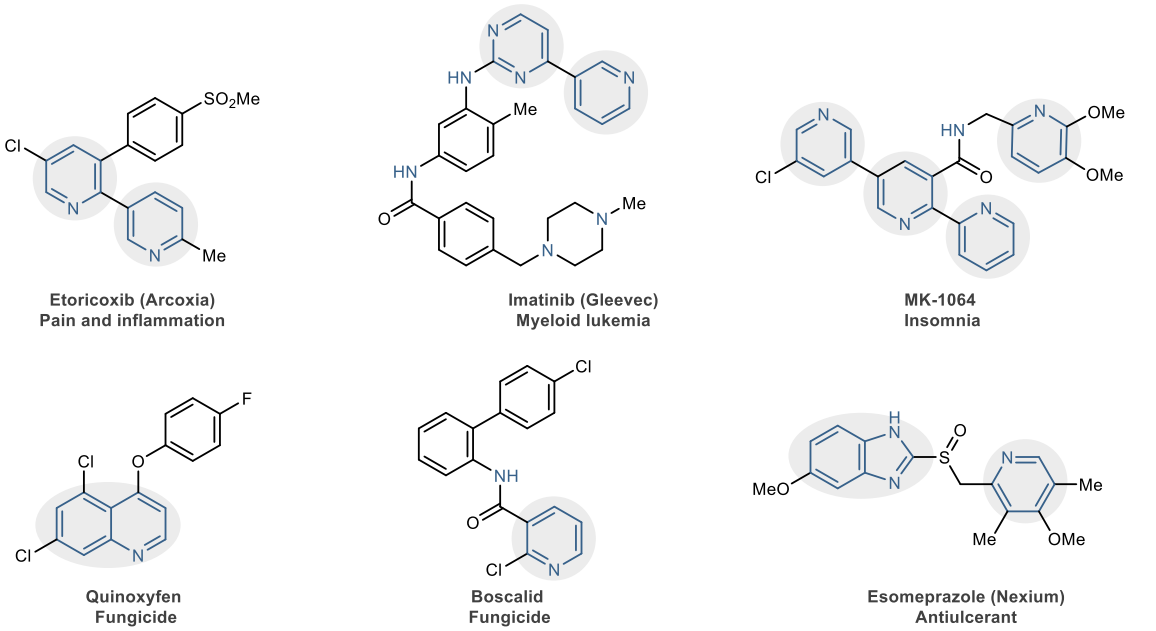

Figure 1.1: Examples of *N*-heterocycles found in drugs and agrochemicals.

1.2 Advantageous Pharmacokinetic Properties of *N*-Heterocycles

Pyridine is the second most common *N*-heterocycle and the most common nitrogen-containing aromatic within pharmaceuticals due to favorable properties it imparts for medicinal chemistry (**Figure 1.2A**).[1] Pyridine is a bioisostere of benzene where one methine group of benzene is replaced with an sp^2-hybridized nitrogen that features a lone pair positioned in the plane of the aromatic ring (**Figure 1.2B**).[5,6] Although changing from benzene to pyridine is a small change in molecular weight and structure, the substitution drastically changes the properties of the aromatic ring and confers pharmacokinetic advantages. The replacement of a carbon atom with the more electronegative nitrogen atom creates a net polarity where the electron density primarily resides on the nitrogen atom rather than delocalized equally throughout the ring, as in benzene (**Figure 1.2C**). This dipole can increase the bioavailability and aqueous solubility of a molecule, and consequently, azaarenes are commonly employed to tune the uptake of a drug into the

circulatory system.[7,8] As the amount of nitrogen atoms in the ring increases (for instance, pyrazine vs pyridine), the heterocycle continues to become more deficient thereby modifying the chemical reactivity even further. The deficiency of the ring also imparts a resistance to oxidative metabolism when compared to benzene.[5]

In addition to the dipole induced by the pyridine heteroatom, the sp^2-hybridized nitrogen atom also influences chemical reactivity exhibited by pyridines. The nitrogen-centered lone pair is positioned perpendicular to the conjugated π-system and cannot be delocalized through the aromatic structure. Instead, pyridine can act as a weak nucleophile or base, and this Lewis-basic nitrogen has been shown to play a fundamental role in binding interactions to a target molecule through important hydrogen bonding interactions.[7,8] The rigid ring shape is also exploited in drug discovery to avoid unwanted conformers that acyclic moieties can exhibit. Acyclic systems face an entropic penalty due to conformational constraints during the binding of a substrate.[9] The aromatic sp^2-hybridized structure exhibits less conformational degrees of freedom, minimizing the entropic penalty during complexation to a target molecule and leading to a more favorable binding interaction.

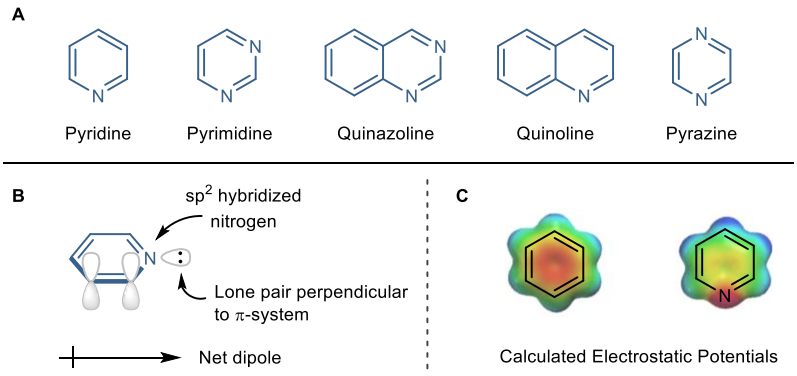

Figure 1.2: A) Top 5 most common aromatic *N*-heterocycles in U.S. FDA approved drugs.[1] B) The effects of the sp^2-hybridized nitrogen in pyridine. C) Electrostatic potential maps of benzene and pyridine.[10]

1.3 Challenges in Pyridine Functionalization

The prevalence of *N*-heterocycles within medicinal chemistry highlights the need for methods to functionalize these motifs, but development of robust and general derivatization methods is often difficult because of their inherent reactivity (**Figure 1.3**). The same properties that make pyridines attractive for medicinal chemists also make their functionalization difficult. Due to the electron-deficient nature of the pyridine ring, the heterocycle acts as a poor π-nucleophile, therefore restricting its ability to participate in classic aromatic functionalization manifolds such as electrophilic aromatic substitution (EAS).[5,6] Additionally, the Lewis-basic nitrogen can engage in unwanted reactivity, such as oxidation or ligation to metals, which can negatively impact the efficiency of *N*-heterocyles in metal-catalyzed cross couplings, one of the most widely employed strategies in synthesis.[11,12] While functionalization of pyridines is challenging with electrophiles, the electron-deficiency of the ring enables nucleophilic addition to the π-system as a viable strategy. A different set of obstacles are present when using this strategy, however, as many reactions that transform pyridine directly from the C-H bond lack regioselectivity. A mixture of 2-, 3-, and 4-position regioisomers can be formed, leading to difficult separations and diminished yields of the target product (*vide infra*). Finally, radicals can react with pyridines to provide functionalized products but also produce mixtures of regioisomers.[13]

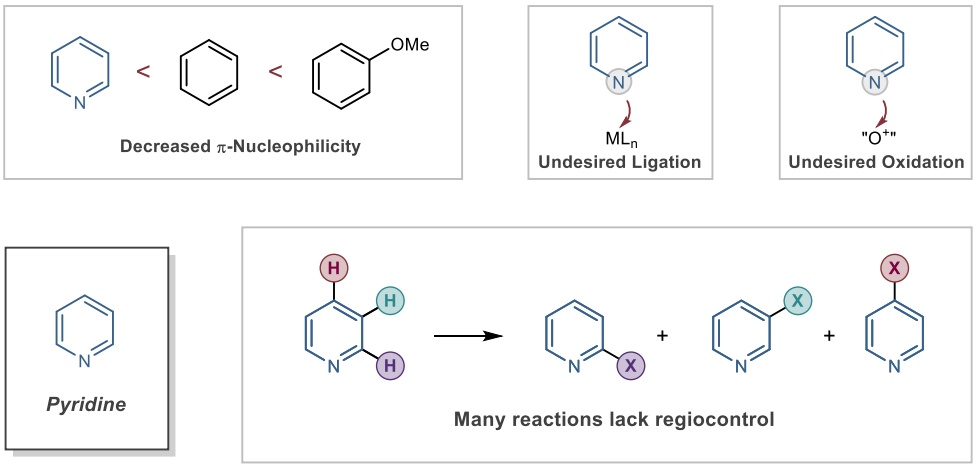

Figure 1.3: Challenges in pyridine functionalization due to inherent reactivity.

1.4 Classical Methods for Functionalization of the 2- and 3-Positions of Pyridine

The most common methods for pyridine functionalization from the C-H bonds of the aromatic ring are selective for either the 2- or 3-position of the ring, and even these established methods present challenges. A classical, 3-selective method for pyridine functionalization is halogenation using electrophilic aromatic substitution (EAS), but this requires harsh conditions to overcome the electron deficiency of the ring and often lacks regioselectivity (**Figure 1.4a**).[6] Importantly, these severe reaction conditions limit the scope of halopyridines that can be synthesized as many functional groups of interest to organic chemists will not survive the halogenation. Halogenated building blocks are irreplaceable in organic chemistry; without halogenated pyridines, a synthetic chemist's ability to access pyridyl anions, pyridyl radicals, or perform metal-catalyzed cross couplings is severely handicapped. Direct lithiation of pyridines is a classical strategy for pyridine halogenation or direct incorporation of other electrophiles[14] that employs strong bases that limit functional group tolerance. Additionally, preinstalled directing groups on the substrate are required to achieve the correct regioselectivity (**Figure 1.4B**). Finally, pyridine *N*-oxides are reagents that undergo bromination more readily than pyridines but

necessitate an oxidation-halogenation-reduction sequence that adds more steps and can limit the functional group tolerance with each operation (**Figure 1.4C**).[5] Chlorination can also occur at high temperatures with $POCl_3$, but the transformation produces a mixture of regioisomers and oxidation of the pyridine starting material is still necessary (**Figure 1.4D**).[15] Therefore, direct, selective, and mild pyridine halogenation remains a major limitation in pyridine functionalization.

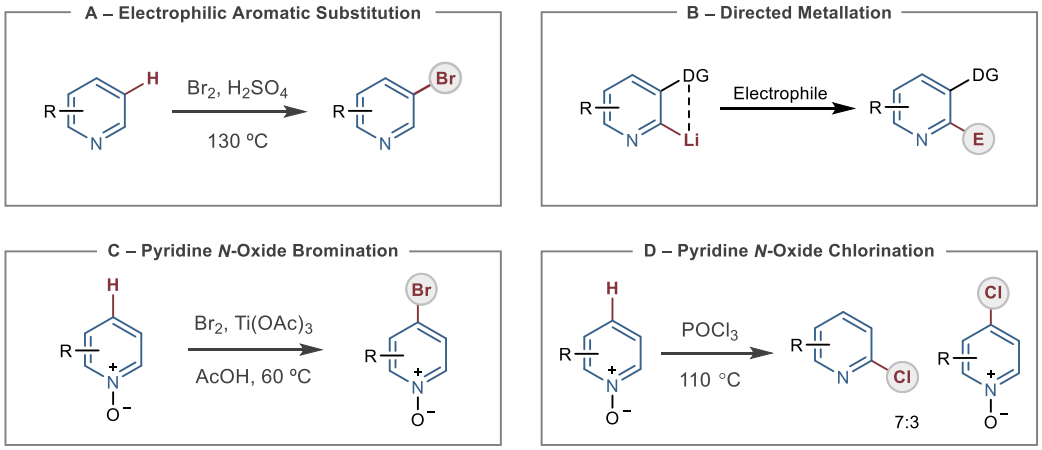

Figure 1.4: Classical strategies for pyridine halogenation.

Other classical methods for 2-selective pyridine functionalization have been reported, exploiting the electron-deficient nature of the heterocycle. For example, the Chichibabin reaction is a strategy for direct amination at the 2-position of pyridines using sodium amide as a nucleophile (**Figure 1.5A**).[16] This transformation necessitates a harsh reagent as a nucleophile that limits the functional group compatibility. A frequently employed transformation in late-stage functionalization of lead compounds is the Minisci reaction which utilizes a variety of carbon-centered radicals to add to heteroaromatic scaffolds directly from their C-H bonds (**Figure 1.5B**).[13] A prominent drawback of the Minisci reaction is the difficulty controlling the regioselectivity of the radical addition. These reactions typically furnish 2- and 4-position isomers, and even 3-position products can be formed in substantial amounts when the heterocycle is more electron

deficient.[17] By activating the pyridine via protonation or *N*-oxidation, the regioselectivity can be improved to favor the 2-position; however, regioisomers are not eliminated completely, leading to diminished yields and difficult purification of the target molecule.[18]

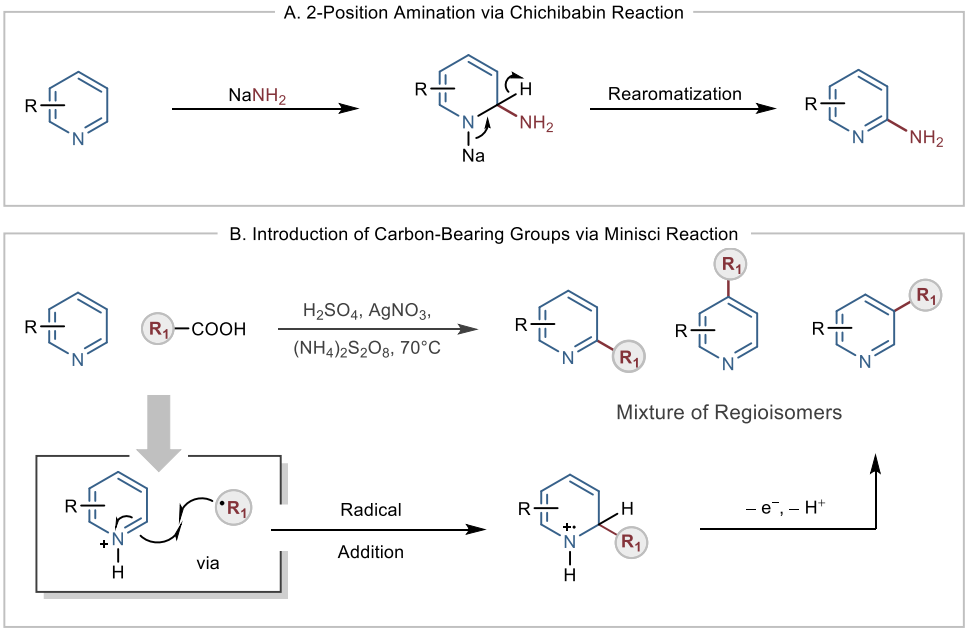

Figure 1.5: 2-Selective methods for pyridine functionalization.

1.5 Contemporary Methods for Functionalization of the 2- and 3-Positions of Pyridine

Over the last several decades, several mild methodologies have been designed to address challenges in pyridine functionalization. Examples of modern strategies that are selective for the 3-position of pyridines are illustrated in **Figure 1.6A**-**B**. While halogenation of the 3-position is challenging using EAS reactivity, pyridines readily undergo iridium-catalyzed borylation to furnish valuable cross coupling starting materials.[19,20] Alternatively, the Yu group developed a strategy for arylation of pyridines via palladium-catalyzed C-H activation.[21] The substrate scope of both strategies is generally limited to simple pyridines, and a mixture of regioisomers can be observed as the steric and electronic complexity of the substrate increases. The Chichibabin

reaction has inspired milder 2-position functionalization of pyridines, such as the silver difluoride-mediated fluorination of pyridines reported by Hartwig and Fier (**Figure 1.6C**).[22,23] Fier subsequently expanded on this strategy of nucleophilic addition to activated pyridines to eanble 2-position amination that avoids the use of harsh sodium amide nucleophile (**Figure 1.6D**).[24] Finally, advances in photoredox chemistry have enabled a renaissance in single-electron chemistry over the last several decades. Using visible light and an iridium photocatalyst DiRocco and coworkers were able to demonstrate late-stage functionalization of pyridine-containing molecules under mild conditions (**Figure 1.6E**).[25,26] The method is generally selective for the 2-position, enhanced by the addition of trifluoroacetic acid, but 4-position radical addition or bisaddition products are still formed and can be difficult to separate. Other photoredox-catalyzed Minisci reactions were developed by the MacMillan and Molander groups, among others.[27–29]

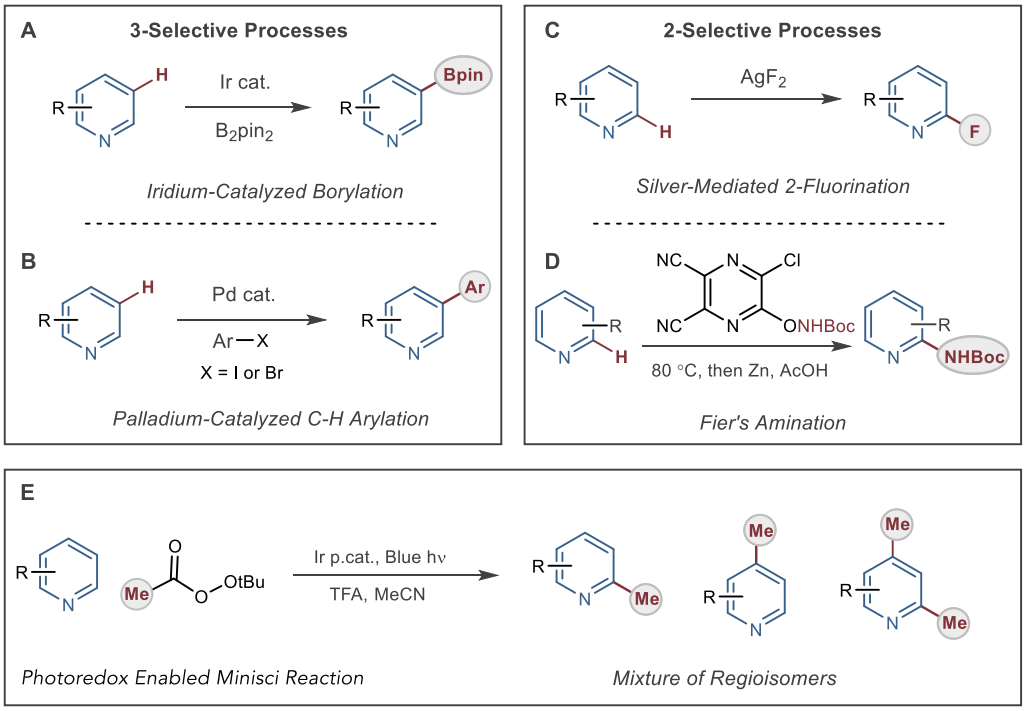

Figure 1.6: Modern methods for 2- and 3-selective pyridine functionalization.

1.6 4-Selective Pyridine Methods

Compared to functionalizing the 2- and 3-positions of pyridines, 4-selective transformations from the C-H bonds remain elusive. A handful of methods have been reported that combine Lewis acid activation and nickel catalysis to enable C-C bond formation at the 4-position of pyridines.[30–33] Both the Nakao and Ong groups reported a 4-position selective alkylation using this strategy, and the additional ability to alkenylate pyridines was demonstrated using Nakao's method (**Figure 1.7A**). This approach utilizes bulky Lewis acids that can block the 2- and 3-positions, forcing the C-H oxidative addition to preferentially occur at the 4-position. Kanai later developed methods for alkylation using an organocobalt nucleophile to add to a pyridinium salt activated by a borane Lewis acid, followed by rearomatization to provide the desired product (**Figure 1.7B**). This method was later extended to provide access to perfluoroalkylated and perfluoroarylated products, however the key pyridinium-borane adducts are typically prepared before addition of the nucleophile, and an additional oxidation step is required to provide the desired products. While the method may be 4-selective, 2-functionalized pyridines can still form in appreciable quantities (**Figure 1.7C**). Finally, Dixon and coworkers reported the direct cyanation of pyridines where N-triflyl pyridiniums are formed in-situ followed by attack by TMSCN and rearomatization with an organic base to furnish 4-cyanopyridines (**Figure 1.7D**).[34] Importantly, this process is usually only moderately selective for the 4-position, as illustrated by the 3:2 ratio of products formed when 2-phenylpyridine is used as a substrate.

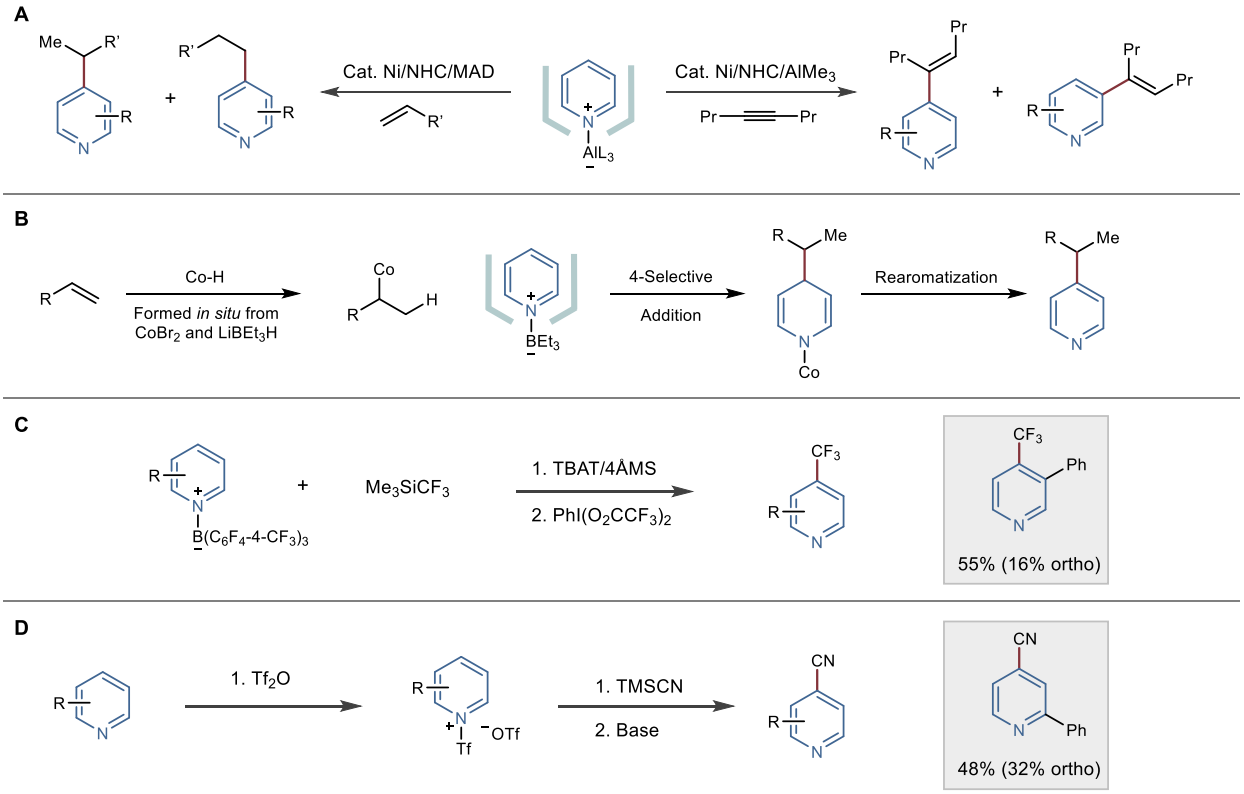

Figure 1.7: A) Nakao's synergistic aluminum- and nickel-catalyzed alkylation and alkenylation. B) Kanai's alkylation of pyridine utilizing organocobalt addition. C) Trifluoromethylation of pyridines exploiting sterically bulky borane catalyst reported by Kanai. D) Cyanation of *N*-triflyl pyridiniums developed by Dixon and coworkers.

1.7 4-Selective Pyridine Functionalization Using Pyridylphosphonium Salts

In response to the scarcity of 4-selective pyridine functionalization strategies, the McNally group has developed a platform to address this limitation using a versatile functional handle that can be installed with high regioselectivity and a broad functional group tolerance (**Figure 1.8, top**). New, regioselective methods for direct installation of a functional group to a pyridine is challenging to develop, and a distinct strategy must often be designed for each bond construction that is desired. The development of a methodology for direct, pyridine C-O bond formation versus a selective C-N bond formation, for instance, usually requires separate screening campaigns and overall different reaction design that elongates the development time. Our design would ideally

accomplish the challenging regioselective step first, providing access to a versatile reagent that can then be converted to a wide variety of different functional groups. Rapid exploration of chemical space is key to enabling successful drug development, and we wanted our strategy to work at all stages of the drug discovery process.[35] An example of such a process is illustrated in the bottom of **Figure 1.8**, showing the optimization of imatinib as a treatment of myelogenous leukemia. Synthesis of pharmaceuticals first begins with simple building blocks, which then advances to more complex lead compounds and finally to the active pharmaceutical ingredient (API). As the synthesis progresses, the challenge in compound synthesis increases due to the presence of more C-H bonds that must be distinguished to achieve selective functionalization and increase in polar functional groups that can interfere with the intended synthetic transformation. Importantly, many methods do not tolerate such structural complexity, leading medicinal chemists to repeat the entire synthetic sequence with different building blocks every time a change to the API is desired. Methods that can function at the building block stage and achieve late-stage functionalization of complex scaffolds are in high demand and can make a significant impact on drug discovery.

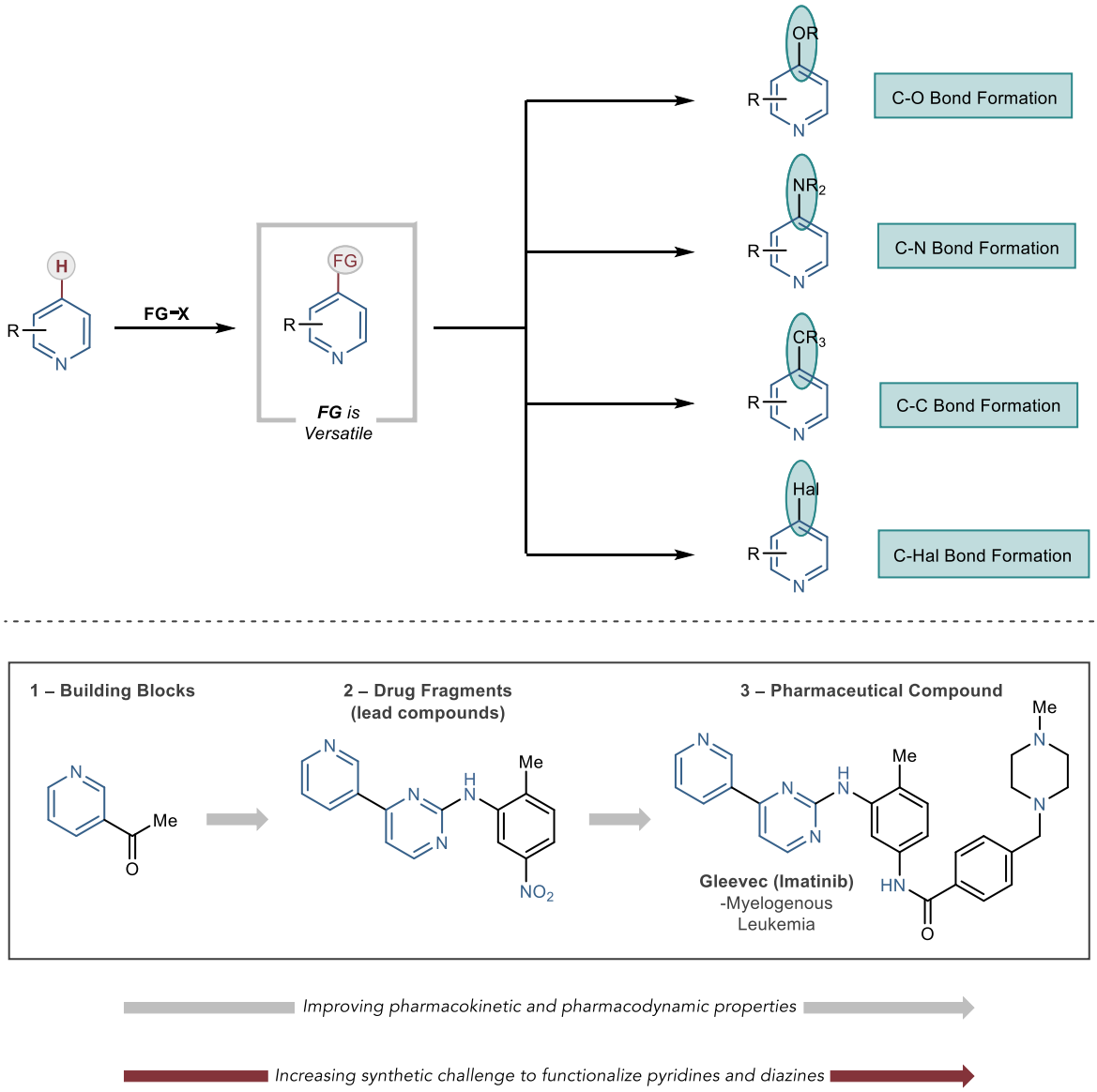

Figure 1.8: Top: Design plan for 4-selective pyridine functionalization using a versatile functional handle. Bottom: Simplified workflow of drug discovery.

An investigation commenced to identify a functional group that could be regioselectively installed to the 4-position of pyridines and diazines with a broad functional group tolerance. It was discovered that triphenylphosphine (PPh_3) could be installed selectively to the 4-position of pyridines to form pyridylphosphonium salts (**Figure 1.9**). First, pyridine is activated with triflic anhydride (Tf_2O) to make an electrophilic *N*-triflyl pyridinium (**1**). PPh_3 adds selectively to the 4-

position at low temperatures to form dearomatized intermediate **2** that is rearomatized with an organic base such as triethylamine (NEt_3) or 1,8-diazabicyclo[5.4.0]undec-7-ene (DBU) to furnish pyridylphosphonium salt **3** in 87% yield. Pyridylphosphonium salt formation was reported by Anders in the late 1980s, but only on a small selection of simple pyridine substrates.[36–38] The generality of this salt formation protocol and subsequent reactivity of the reagents remained underexplored.

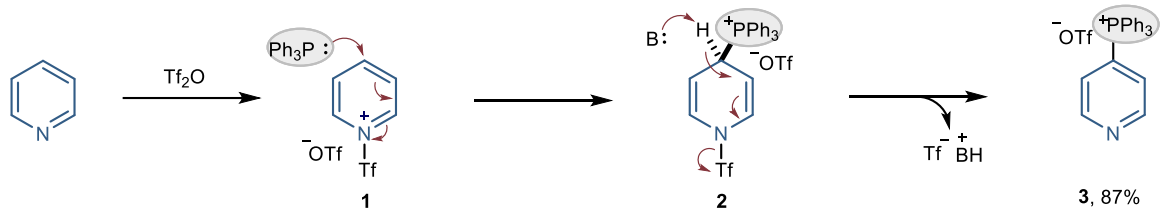

Figure 1.9: Proposed mechanism for pyridylphosphonium salt formation.

Next, the generality of the salt formation was explored (Figure 1.10). Phosphonium salts were isolated from simple pyridine building blocks (and a pyrazine) with complete regioselectivity and good yields in the cases shown below (**Figure 1.10A**, **4**-**9**), despite a wide variety of functional groups, electronics, substitution patterns, and steric environment about the bond formation site.[39–42] Pyridine-containing molecules that are more reminiscent of drug fragments in a drug discovery campaign also performed well in the reaction (**Figure 1.10 B, 10**-**13**). Importantly, the reaction is both regioselective and site-selective for one heterocycle in the presence of others, such as lead compound MK-1064 (**10**) which exhibits three different pyridine rings that could potentially be functionalized. Finally, several pharmaceuticals were converted into their corresponding phosphonium salts, highlighting the broad substrate scope of the transformation despite several polar functional groups that typically interfere with other technologies (**Figure 1.10C**, **14**-**17**).

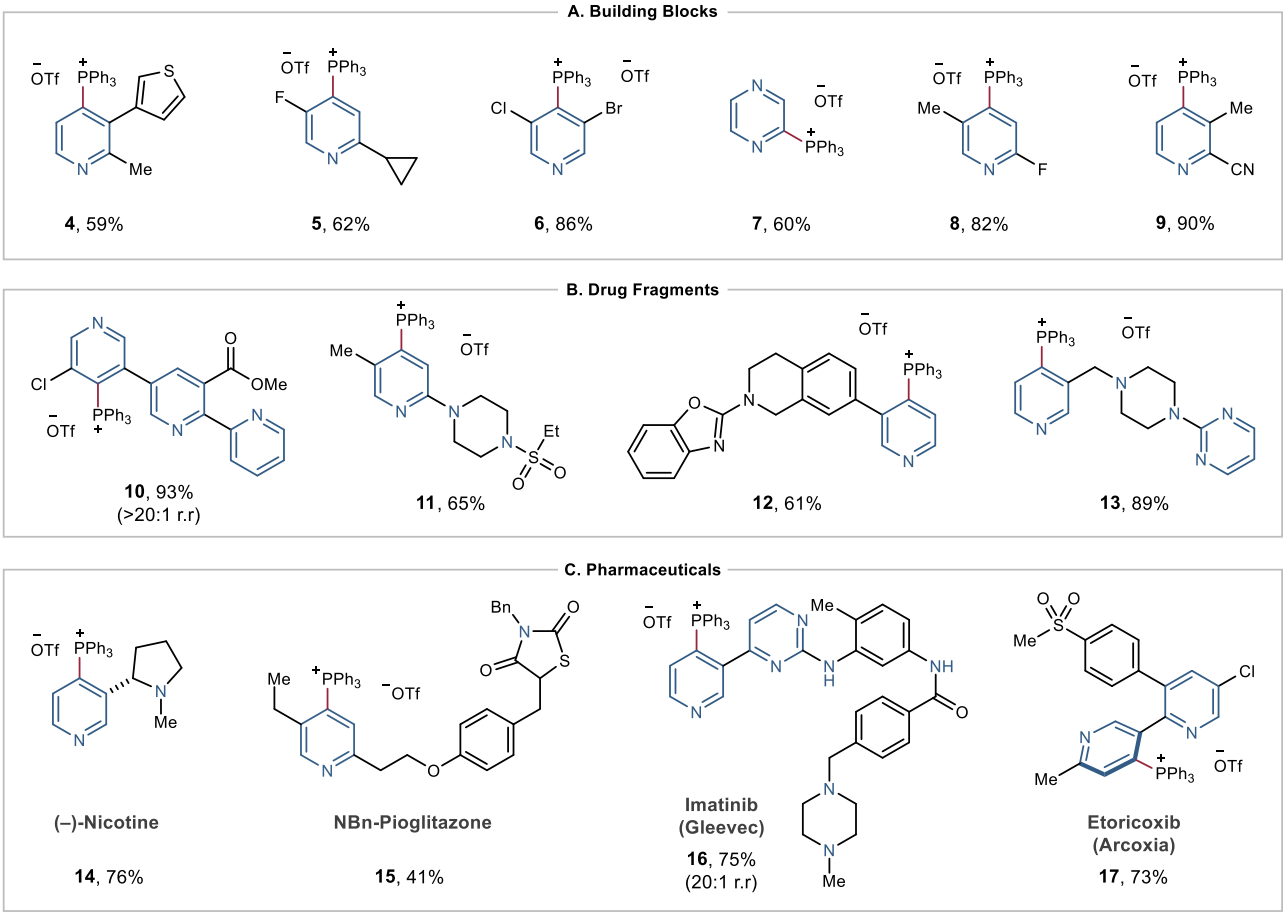

Figure 1.10: Substrate scope for phosphonium salt formation.

Finally, the McNally group developed four different reaction manifolds to enable pyridine functionalization via heteroaryl phosphonium salts (**Figure 1.11**). S_NAr-type displacement of the phosphine leaving group can be used to form products such as valuable 4-halopyridine building blocks.[43–45] Oxidative addition of a transition metal into the carbon-phosphorus bond can occur to promote carbon-carbon bond formation via metal-catalyzed cross-coupling reactions.[46,47] The reagents can undergo base-mediated decomposition driven by the formation of triphenylphosphine oxide to form a pyridyl anion that can be quenched with deuterium or tritium for radiolabeling applications.[42] Finally, the McNally group has reported several phosphorus ligand-coupling reactions from a P(V) intermediate to enable challenging bond constructions.[39,48–50] This method

has promoted challenging pyridine etherification, trifluoromethylation and difluoromethylation, and bipyridine synthesis with great 4-position selectivity. All these methods proceed through two-electron reaction manifolds, but single-electron reactivity of such reagents remained unexplored. The investigation of radical reactivity of pyridyl phosphonium salts will be the focus of the next two chapters of this dissertation.

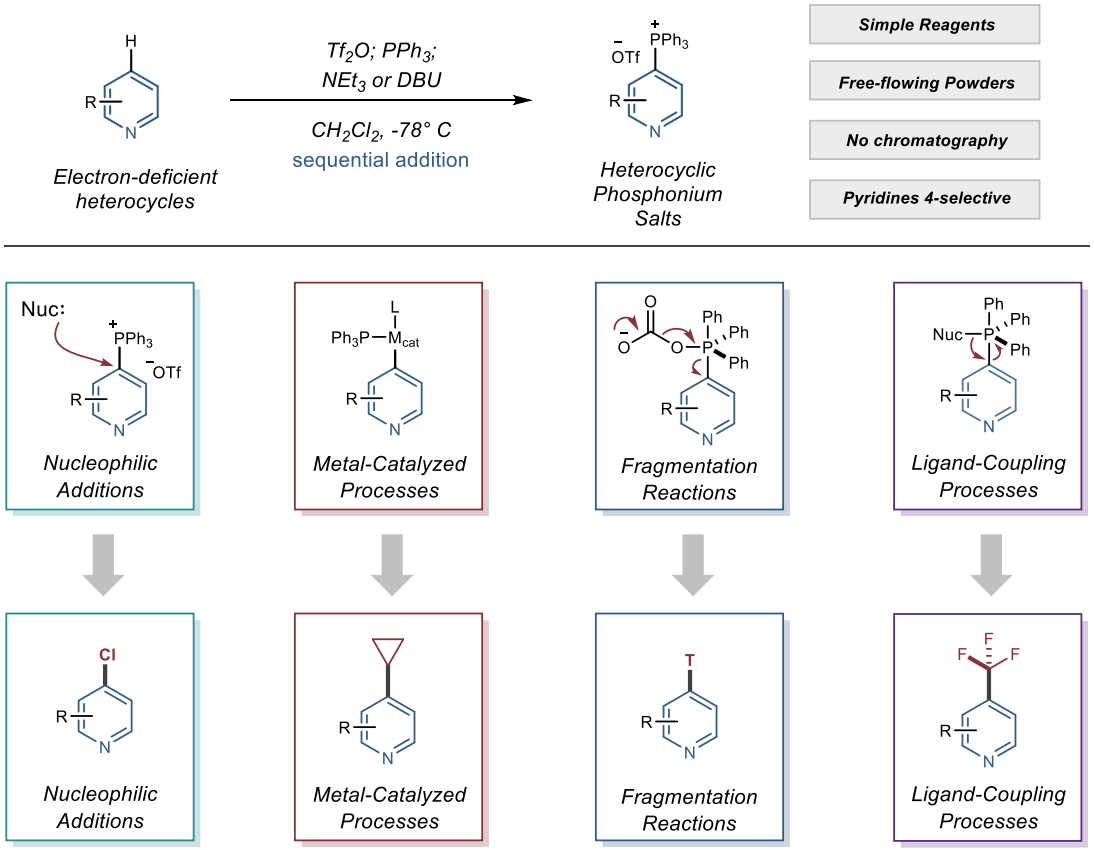

Figure 1.11: Reactivity exhibited by pyridylphosphonium salts for pyridine functionalization.

1.8 Conclusion

This section serves to introduce the importance of pyridines and diazines in materials, agrochemicals, and pharmaceuticals. The inherent challenges in pyridine functionalization are discussed, along with classical and more contemporary methods for pyridine derivatization. Most

of these methods are selective for the 2- or 3-position of pyridine, while 4-selective processes are rarer. Finally, this chapter also highlights the work of the McNally group regarding heteroaryl phosphonium salts as robust and useful reagents in organic synthesis.

References

(1) Vitaku, E.; Smith, D. T.; Njardarson, J. T. Analysis of the Structural Diversity, Substitution Patterns, and Frequency of Nitrogen Heterocycles among U.S. FDA Approved Pharmaceuticals. *J. Med. Chem.* **2014**, *57*, 10257–10274.

(2) Kaes, C.; Katz, A.; Hosseini, M. W. Bipyridine: The Most Widely Used Ligand. A Review of Molecules Comprising at Least Two 2,2'-Bipyridine Units. *Chem. Rev.* **2000**, *100*, 3553–3590.

(3) Newkome, G. R.; Patri, A. K.; Holder, E.; Schubert, U. S. Synthesis of 2,2′-Bipyridines: Versatile Building Blocks for Sexy Architectures and Functional Nanomaterials. *Eur. J. Org. Chem.* **2004**, *2004*, 235–254.

(4) Nguyen, T. P.; Easley, A. D.; Kang, N.; Khan, S.; Lim, S.-M.; Rezenom, Y. H.; Wang, S.; Tran, D. K.; Fan, J.; Letteri, R. A.; He, X.; Su, L.; Yu, C.-H.; Lutkenhaus, J. L.; Wooley, K. L. Polypeptide Organic Radical Batteries. *Nature* **2021**, *593*, 61–66.

(5) Joule, J. A.; Mills, K. *Heterocyclic Chemistry*, 5th Ed.; Wiley/Blackwell Publishing Ltd, 2010.

(6) Grimmett, M. R. *Adv. Heterocycl. Chem.* 58, 271-329.

(7) Dalvie, D.; Kang, P.; Loi, C.-M.; Goulet, L.; Nair, S. Chapter 7. Influence of Heteroaromatic Rings on ADME Properties of Drugs. In *Drug Discovery*; Smith, D. A., Royal Society of Chemistry: Cambridge, 2010; pp 328–369.

(8) Thomas, G. *Medicinal Chemistry: An Introduction*, 2nd Ed.; 2008.

(9) Silverman, R. B. *The Organic Chemistry of Drug Design and Drug Action*, 2nd Ed.; Elsevier, 2004.

(10) Lam, P. AB INITIO ELECTROSTATIC POTENTIAL SURFACES (HARTREE-FOCK 3-21G* BASIS SETS). 13.

(11) Blakemore, D. C.; Castro, L.; Churcher, I.; Rees, D. C.; Thomas, A. W.; Wilson, D. M.; Wood, A. Organic Synthesis Provides Opportunities to Transform Drug Discovery. *Nat. Chem.* **2018**, *10*, 383–394.

(12) Brown, D. G.; Boström, J. Analysis of Past and Present Synthetic Methodologies on Medicinal Chemistry: Where Have All the New Reactions Gone? *J. Med. Chem.* **2016**, *59*, 4443–4458.

(13) Duncton, M. A. J. Minisci Reactions: Versatile CH-Functionalizations for Medicinal Chemists. *Med. Chem. Comm.* **2011**, *2*, 1135.

(14) Schlosser, M.; Mongin, F. Pyridine Elaboration through Organometallic Intermediates: Regiochemical Control and Completeness. *Chem. Soc. Rev.* **2007**, *36*, 1161.

(15) Yamanaka, H.; Araki, T.; Sakamoto, T. Site-Selectivity in the Reaction of 3-Substituted Pyridine 1-Oxides with Phosphoryl Chloride. *Chem. Pharm. Bull.* **1988**, *36*, 2244–2247.

(16) Mcgill, C. K.; Rappa, A. Advances in the Chichibabin Reaction. In *Advances in Heterocyclic Chemistry*; Elsevier, **1988**; Vol. 44, pp 1–79.

(17) O'Hara, F.; Blackmond, D. G.; Baran, P. S. Radical-Based Regioselective C–H Functionalization of Electron-Deficient Heteroarenes: Scope, Tunability, and Predictability. *J. Am. Chem. Soc.* **2013**, *135*, 12122–12134.

(18) Dyall, L. K.; Pausacker, K. H. 4. Free-Radical Substitution of Pyridine 1-Oxide. *J. Chem. Soc.* **1961**, 18.

(19) Larsen, M. A.; Hartwig, J. F. Iridium-Catalyzed C–H Borylation of Heteroarenes: Scope, Regioselectivity, Application to Late-Stage Functionalization, and Mechanism. *J. Am. Chem. Soc.* **2014**, *136*, 4287–4299.

(20) Sadler, S. A.; Tajuddin, H.; Mkhalid, I. A. I.; Batsanov, A. S.; Albesa-Jove, D.; Cheung, M. S.; Maxwell, A. C.; Shukla, L.; Roberts, B.; Blakemore, D. C.; Lin, Z.; Marder, T. B.; Steel, P. G. Iridium-Catalyzed C–H Borylation of Pyridines. *Org. Biomol. Chem.* **2014**, *12*, 7318.
(21) Ye, M.; Gao, G.-L.; Yu, J.-Q. Ligand-Promoted C-3 Selective C–H Olefination of Pyridines with Pd Catalysts. *J. Am. Chem. Soc.* **2011**, *133*, 6964–6967.
(22) Fier, P. S.; Hartwig, J. F. Synthesis and Late-Stage Functionalization of Complex Molecules through C–H Fluorination and Nucleophilic Aromatic Substitution. *J. Am. Chem. Soc.* **2014**, *136*, 10139–10147.
(23) Fier, P. S.; Hartwig, J. F. Selective C-H Fluorination of Pyridines and Diazines Inspired by a Classic Amination Reaction. *Science* **2013**, *342*, 956–960.
(24) Fier, P. S.; Kim, S.; Cohen, R. D. A Multifunctional Reagent Designed for the Site-Selective Amination of Pyridines. *J. Am. Chem. Soc.* **2020**, *142*, 8614–8618.
(25) DiRocco, D. A.; Dykstra, K.; Krska, S.; Vachal, P.; Conway, D. V.; Tudge, M. Late-Stage Functionalization of Biologically Active Heterocycles Through Photoredox Catalysis. *Angew. Chem. Int. Ed.* **2014**, *53*, 4802–4806.
(26) Huff, C. A.; Cohen, R. D.; Dykstra, K. D.; Streckfuss, E.; DiRocco, D. A.; Krska, S. W. Photoredox-Catalyzed Hydroxymethylation of Heteroaromatic Bases. *J. Org. Chem.* **2016**, *81*, 6980–6987.
(27) Jin, J.; MacMillan, D. W. C. Direct α-Arylation of Ethers through the Combination of Photoredox-Mediated C□H Functionalization and the Minisci Reaction. *Angew. Chem. Int. Ed.* **2015**, *54*, 1565–1569.
(28) Jin, J.; MacMillan, D. W. C. Alcohols as Alkylating Agents in Heteroarene C–H Functionalization. *Nature* **2015**, *525*, 87–90.
(29) Presset, M.; Fleury-Brégeot, N.; Oehlrich, D.; Rombouts, F.; Molander, G. A. Synthesis and Minisci Reactions of Organotrifluoroborato Building Blocks. *J. Org. Chem.* **2013**, *78*, 4615–4619.
(30) Nakao, Y.; Yamada, Y.; Kashihara, N.; Hiyama, T. Selective C-4 Alkylation of Pyridine by Nickel/Lewis Acid Catalysis. *J. Am. Chem. Soc.* **2010**, *132*, 13666–13668.
(31) Tsai, C.-C.; Shih, W.-C.; Fang, C.-H.; Li, C.-Y.; Ong, T.-G.; Yap, G. P. A. Bimetallic Nickel Aluminun Mediated *Para* -Selective Alkenylation of Pyridine: Direct Observation of η^2 ,η^1 -Pyridine Ni(0)−Al(III) Intermediates Prior to C−H Bond Activation. *J. Am. Chem. Soc.* **2010**, *132*, 11887–11889.
(32) Nishida, T.; Ida, H.; Kuninobu, Y.; Kanai, M. Regioselective Trifluoromethylation of N-Heteroaromatic Compounds Using Trifluoromethyldifluoroborane Activator. *Nat. Commun.* **2014**, *5*, 3387.
(33) Nagase, M.; Kuninobu, Y.; Kanai, M. 4-Position-Selective C–H Perfluoroalkylation and Perfluoroarylation of Six-Membered Heteroaromatic Compounds. *J. Am. Chem. Soc.* **2016**, *138*, 6103–6106.
(34) Elbert, B. L.; Farley, A. J. M.; Gorman, T. W.; Johnson, T. C.; Genicot, C.; Lallemand, B.; Pasau, P.; Flasz, J.; Castro, J. L.; MacCoss, M.; Paton, R. S.; Schofield, C. J.; Smith, M. D.; Willis, M. C.; Dixon, D. J. C−H Cyanation of 6-Ring N-Containing Heteroaromatics. *Chem. - Eur. J.* **2017**, *23*, 14733–14737.
(35) Hughes, J.; Rees, S.; Kalindjian, S.; Philpott, K. Principles of Early Drug Discovery: Principles of Early Drug Discovery. *Br. J. Pharmacol.* **2011**, *162*, 1239–1249.

(36) Anders, E.; Markus, F. Chemie der Triphenyl-(oder Tri-n-butyl-)pyridylphosphoniumsalze, 1 Neue Methode zur regioselektiven Einführung von Phosphoniumgruppen in N-heteroaromatische Ringsysteme. *Chem. Ber.* **1989**, *122*, 113–118.
(37) Anders, E.; Markus, F. Neue methode zur regiospezifischen substitution einiger reaktionsträcer N-heteroaromatischer ringsysteme. *Tet. Lett.* **1987**, *28*, 2675–2676.
(38) Anders, E.; Korn, U.; Stankowiak, A. „Ferngesteuerte" nucleophile Eigenschaften der Anionen einiger 4-Alkylpyridine: AM 1- und MNDO-Berechnungen sowie experimentelle Untersuchungen. *Chem. Ber.* **1989**, *122*, 105–111.
(39) Hilton, M. C.; Dolewski, R. D.; McNally, A. Selective Functionalization of Pyridines via Heterocyclic Phosphonium Salts. *J. Am. Chem. Soc.* **2016**, *138*, 13806–13809.
(40) Dolewski, R. D.; Fricke, P. J.; McNally, A. Site-Selective Switching Strategies to Functionalize Polyazines. *J. Am. Chem. Soc.* **2018**, *140*, 8020–8026.
(41) Dolewski, R. D.; Fricke, P. J.; McNally, A. Site-Selective Switching Strategies to Functionalize Polyazines. *J. Am. Chem. Soc.* **2018**, *140*, 8020–8026.
(42) Koniarczyk, J. L.; Hesk, D.; Overgard, A.; Davies, I. W.; McNally, A. A General Strategy for Site-Selective Incorporation of Deuterium and Tritium into Pyridines, Diazines, and Pharmaceuticals. *J. Am. Chem. Soc.* **2018**, *140*, 1990–1993.
(43) Levy, J. N.; Alegre-Requena, J. V.; Liu, R.; Paton, R. S.; McNally, A. Selective Halogenation of Pyridines Using Designed Phosphine Reagents. *J. Am. Chem. Soc.* **2020**, *142*, 11295–11305.
(44) Anderson, R. G.; Jett, B. M.; McNally, A. Selective Formation of Heteroaryl Thioethers via a Phosphonium Ion Coupling Reaction. *Tetrahedron* **2018**, *74*, 3129–3136.
(45) Anderson, R. G.; Jett, B. M.; McNally, A. A Unified Approach to Couple Aromatic Heteronucleophiles to Azines and Pharmaceuticals. *Angew. Chem. Int. Ed.* **2018**, *57*, 12514–12518.
(46) Zhang, X.; McNally, A. Phosphonium Salts as Pseudohalides: Regioselective Nickel-Catalyzed Cross-Coupling of Complex Pyridines and Diazines. *Angew. Chem. Int. Ed.* **2017**, *56*, 9833–9836.
(47) Zhang, X.; McNally, A. Cobalt-Catalyzed Alkylation of Drug-Like Molecules and Pharmaceuticals Using Heterocyclic Phosphonium Salts. *ACS Catal.* **2019**, 4862–4866.
(48) Boyle, B. T.; Hilton, M. C.; McNally, A. Nonsymmetrical Bis-Azine Biaryls from Chloroazines: A Strategy Using Phosphorus Ligand-Coupling. *J. Am. Chem. Soc.* **2019**, *141*, 15441–15449.
(49) Hilton, M. C.; Zhang, X.; Boyle, B. T.; Alegre-Requena, J. V.; Paton, R. S.; McNally, A. Heterobiaryl Synthesis by Contractive C–C Coupling via P(V) Intermediates. *Science* **2018**, *362*, 799–804.
(50) Zhang, X.; Nottingham, K. G.; Patel, C.; Alegre-Requena, J. V.; Levy, J. N.; Paton, R. S.; McNally, A. Phosphorus-Mediated Sp2–Sp3 Couplings for C–H Fluoroalkylation of Azines. *Nature* **2021**, *594*, 217–222.

CHAPTER TWO

PYRIDINE-PYRIDINE CROSS-COUPLING REACTION VIA DEAROMATIZED RADICAL INTERMEDIATES

2.1 Overview

This chapter details the serendipitous discovery of a bipyridine synthesis that proceeds via radical-radical coupling mechanism. Pyridylphosphonium salts are reduced to a boryl-stabilized, dearomatized radical intermediate via inner sphere single-electron transfer from a cyano- and boryl-stabilized radical species. Other pyridyl radical precursors are unsuccessful as coupling partners, highlighting the unique ability of the phosphonium functional group to enable the cross-coupling reaction. Synthesis and characterization of organic compounds, design of experiments, and manuscript preparation was carried out by Luke Koniarczyk, Jacob Greenwood, and Professor Andy McNally. Computational studies were performed by Professor Rob Paton and Dr. Juan Alegre-Requena. This work led to a publication in Angewandte Chemie in 2019.

2.2 Introduction

Single-electron reaction manifolds have emerged as an important class of reactions in organic synthesis.[1] While reactions mediated by radical intermediates have been known for a long time,[2] these methodologies have experienced a renaissance over the last two decades due to the expansion of photoredox catalysis, electrochemical synthesis, and energy transfer catalysis.[3–6] These reaction platforms driven by open-shell intermediates have garnered attention due to their ability to achieve unique transformations under mild conditions using high-energy excited state intermediates. We were curious about the type of radical reactivity that could be unlocked using pyridylphosphonium salts as radical precursors. The McNally group's research program has focused on transformations

of heterocyclic phosphonium salts two electron manifolds, but we envisioned the use of these reagents in single-electron manifolds that would enable reactions challenging to accomplish through two-electron pathways (Figure 2.1). We were encouraged by our previous reports that detailed the use of the phosphonium functional group as a pseudohalide in metal-catalyzed cross-coupling reactions,[7,8] and we wondered if the pyridylphosphonium salts could act as alternatives to halopyridines pyridyl radical-forming reactions.[9–13] We hypothesized that the phosphonium salts might be amenable to facile single electron reduction, providing a valuable reaction manifold for mild pyridine diversification.

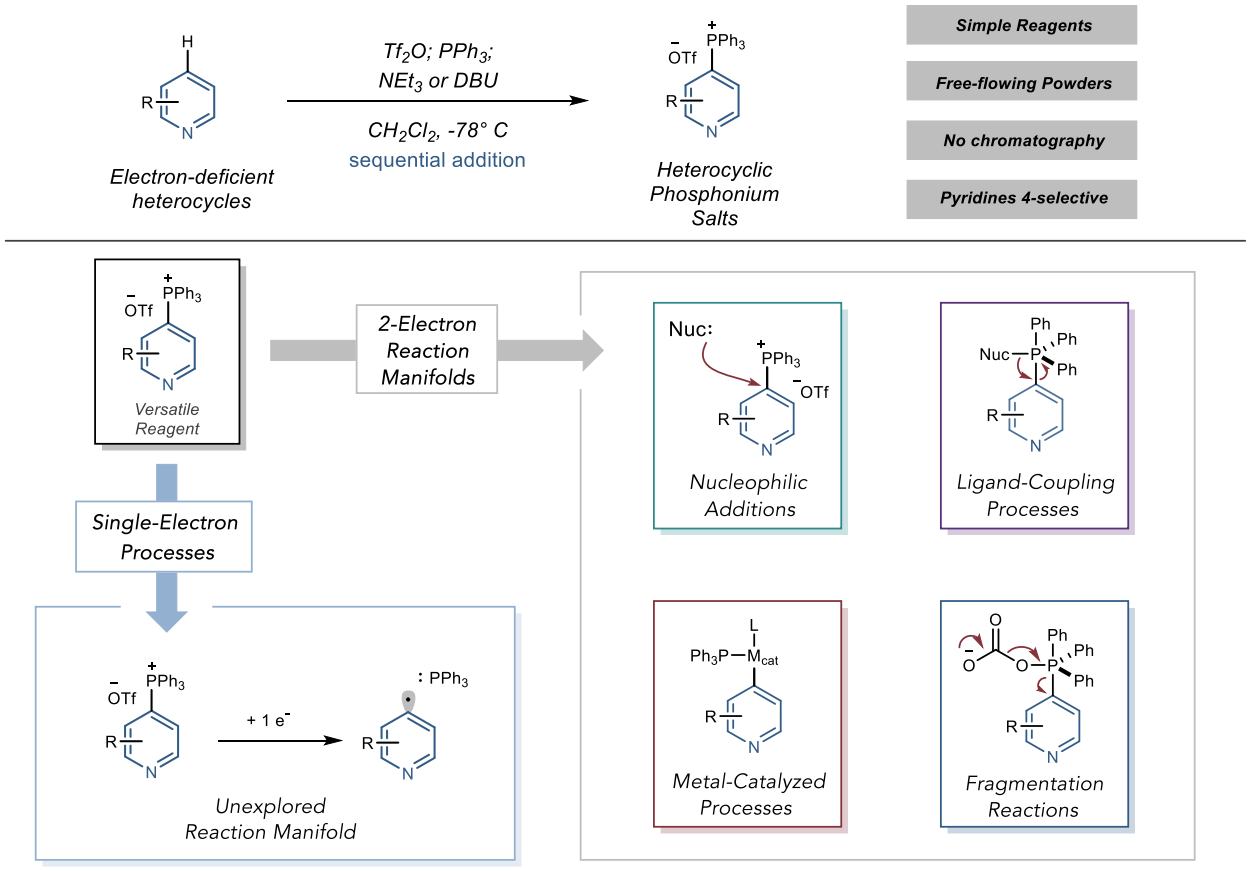

Figure 2.1: Unexplored single-electron reactivity of heterocyclic phosphonium salts.

2.3 Design Plan for Photocatalyzed Pyridine Borylation

To probe the single-electron reactivity of heterocyclic phosphonium salts, we began our investigation using photoredox chemistry to yield a pyridyl radical intermediate that could then participate in subsequent transformations. Most of the precedented reactivity of pyridyl radicals involves the addition to alkenes or metalation followed by reductive elimination. Radical-mediated borylation is a process that is well precedented using aryl halides but has not been exploited using pyridyl radicals.[14] We targeted a 4-selective, radical borylation reaction, as the 3-selective iridium-catalyzed borylation is the main strategy used to synthesize borylated pyridines and is typically constrained to simple pyridines.[15,16] Our strategy would provide a complementary method to access important borylated pyridine building blocks that could be extended to complex pyridine systems due to the mild conditions employed for both phosphonium salt formation and photoredox-catalyzed borylation.

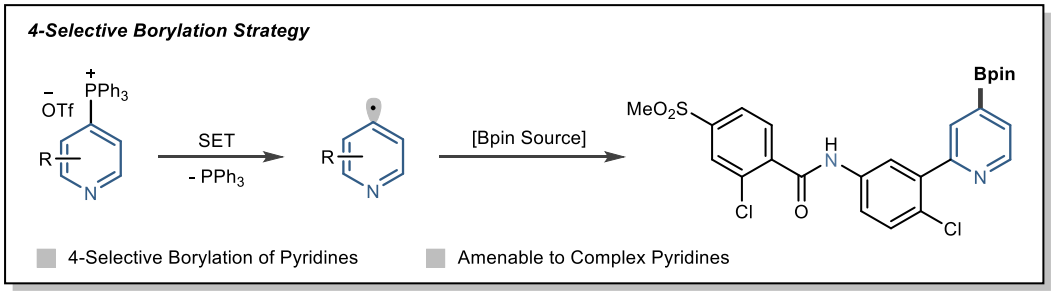

Figure 2.2: Desired 4-selective borylation of pyridines.

We were inspired by several reports in the literature detailing the borylation of aryl radicals using unusual stabilized boryl radicals. First, Li observed that two equivalents of 4-cyanopyridine (**18**) in the presence of bis(pinacolato)diboron (B_2pin_2) can form a complex capable of homolytic cleavage of the diboron bond (Figure 2.3A).[17] This process furnishes two equivalents of a boryl-stabilized radical **18a**. Li provided evidence of this proposal through the radical borylation of

benzoyl peroxide (Figure 2.3B). In 2017, Jiao documented the radical borylation of aryl halides, which occurred through reduction of the aryl halide to an aryl radical that proceeded to couple with a persistent boryl radical species, as proposed by Li (Figure 2.3C).[18]

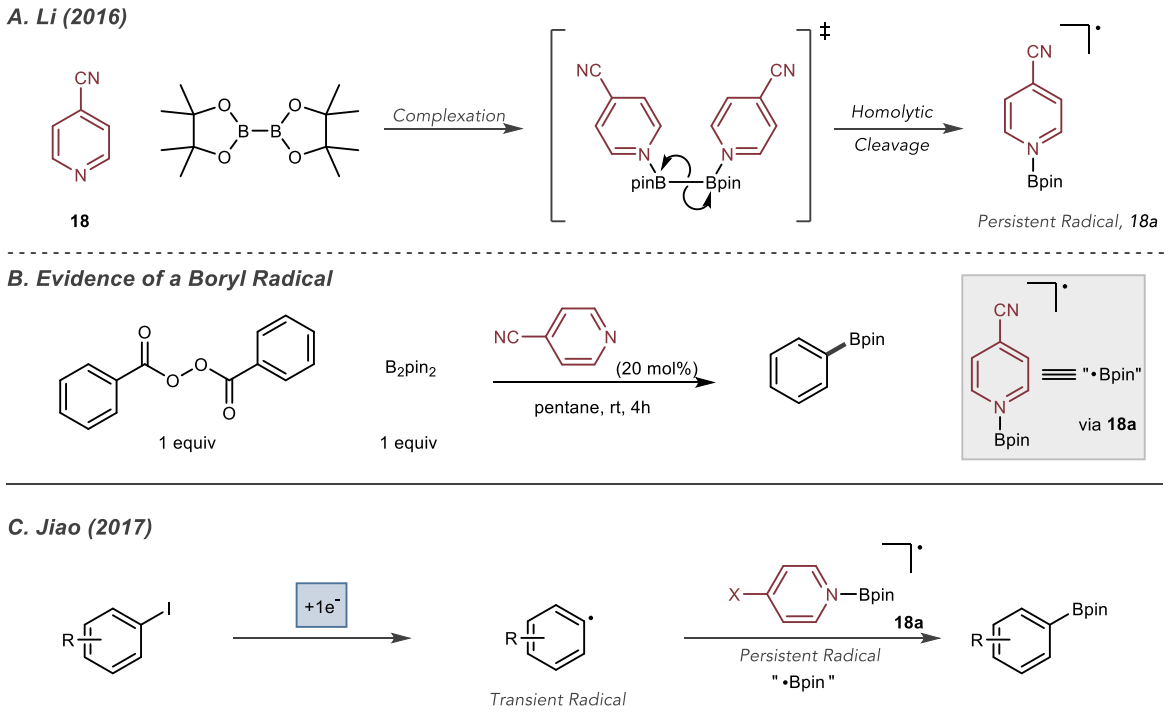

Figure 2.3: Previous reports of radical borylation using a stabilized boryl-radical intermediate.

With this precedent, we set out to design a system to promote the coupling between a persistent boryl radical intermediate and a pyridyl radical. The mechanistic proposal for this transformation is illustrated in Figure 2.4. First, excitation of an iridium photocatalyst with visible light would produce an excited state photoreductant ($E_{1/2}^{red}$ = –1.73 V vs SCE for $Ir(ppy)_3$) that can feasibly reduce pyridylphosphonium salt **19** ($E_{1/2}^{red}$ = –1.7 V vs SCE) to the corresponding pyridyl radical **19a**.[19] Next, persistent boryl radical **18a**, formed *in situ*, could couple with **19a** to deliver the desired borylated pyridine **20**. Finally, the photocatalytic cycle would be closed *via* reduction of the iridium photocatalyst with a sacrificial reductant, such as a tertiary amine.

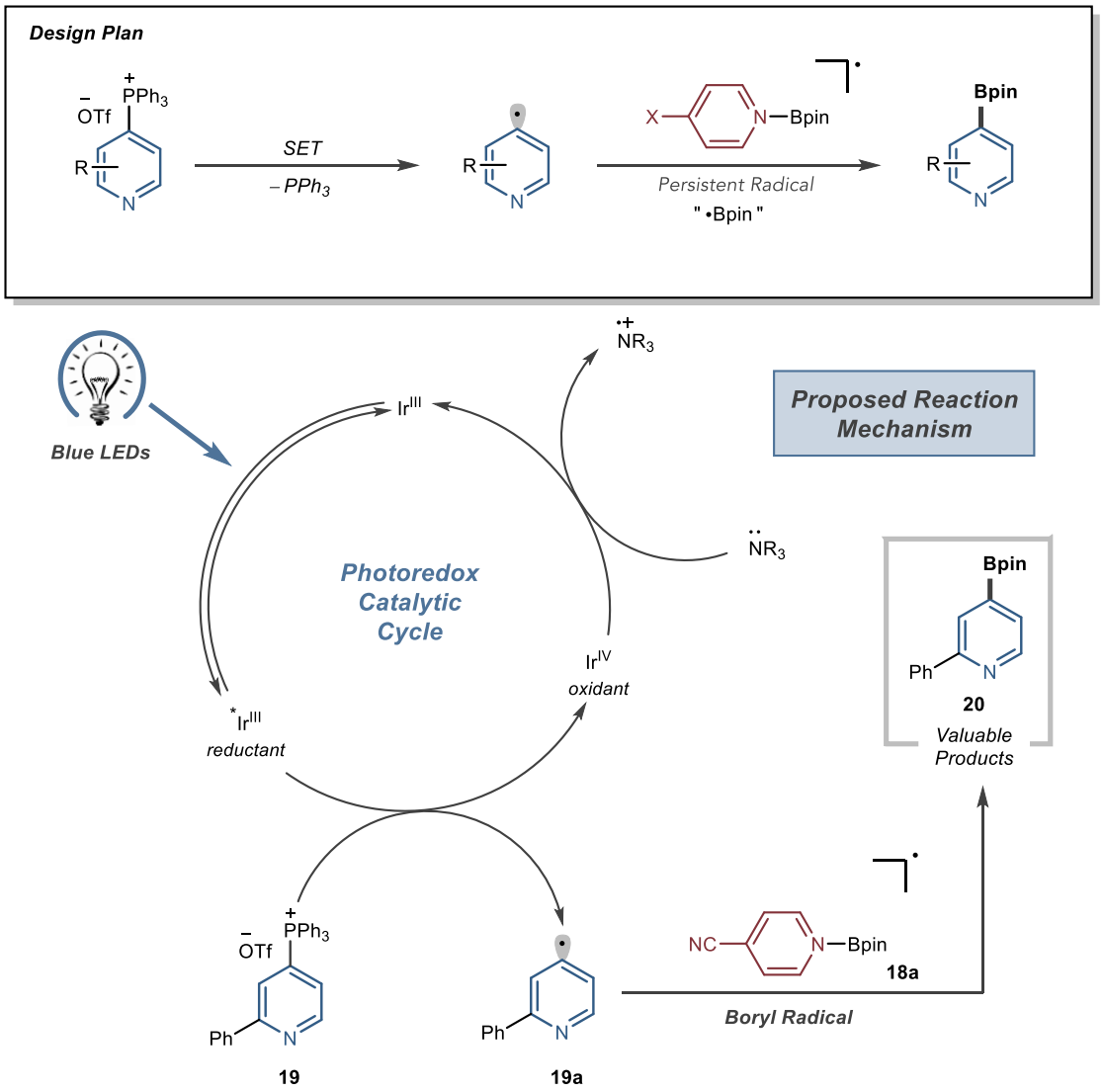

Figure 2.4: Proposed mechanism for photoredox-catalyzed borylation of pyridylphosphonium salts.

2.4 Discovery and Importance of an Unexpected Bipyridine Coupling Reaction

The results of the initial design plan are shown in Figure 2.5 using strongly reducing photocatalyst $Ir(ppy)_3$ with diisopropylethylamine (DIPEA) as a sacrificial reductant to reduce phosphonium salt **19** to pyridyl radical **19a,** which could then couple with the persistent boryl radical **18a** to furnish the borylated product **20**.[19] However, none of the desired product was observed and instead the unexpected 2,4'-bipyridine product **21** was formed in 26% yield. This

product appeared to be the result of a Minisci-type coupling between **19a** and **18** with complete regiocontrol for the 2,4' bipyridine product. Further studies revealed that neither blue light nor photocatalyst were required to promote the bipyridine coupling.

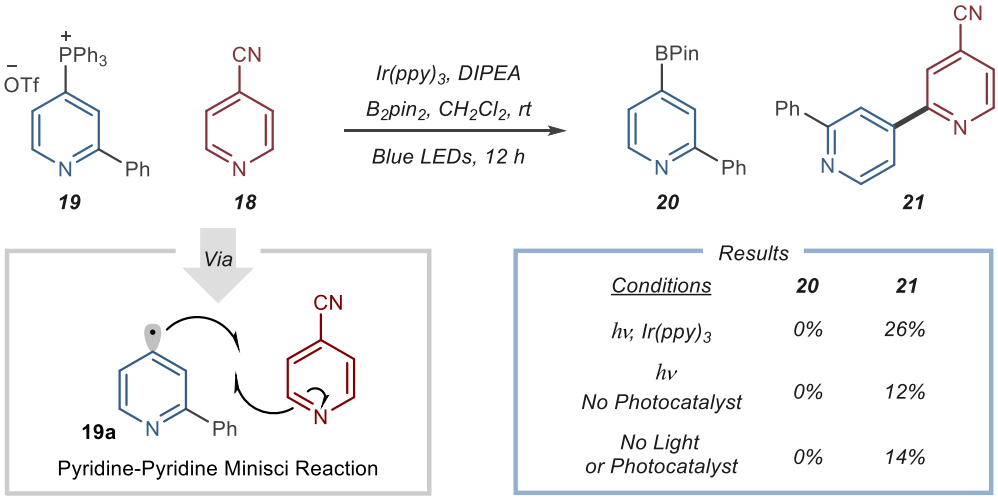

Figure 2.5: Initial attempt at radical-mediated borylation and discovery of bipyridine coupling reaction. $Ir(ppy)_3$= Tris[2-phenylpyridinato-C2,N]iridium(III).

Importantly, no pyridine-pyridine Minisci reaction has been reported in the literature despite the prevalence of the Minisci reaction in medicinal chemistry (Figure 2.6A).[20] The reaction benefits from a wide array of radical coupling partners that can be added to heteroaromatic bases directly from the C-H bond with broad functional group tolerance due to the emergence of more mild methods of radical generation. A selection of examples of modern advancements of the Minisci reaction are presented in Figure 2.6B-E. As highlighted in Chapter one, DiRocco and coworkers developed a method for late-stage methylation by leveraging photoredox catalysis (Figure 2.6B).[21] Arylation under traditional Minisci conditions was reported, but the scope of aryl coupling partners was greatly expanded by Baran with his method that used boronic acids as aryl radical precursors (Figure 2.6B).[22,23] Electrophilic radicals can also react with electron-deficient heterocycles, as reported by MacMillan, and this transformation can promote selectivity for the 3-

and 5-positions due to the nature of the radical coupling partner.[24,25] Finally, the union of aldehydes and heteroaromatics can also be achieved through a hydrogen abstraction strategy to furnish acyl radical coupling partners.[26] These advancements, among others, have allowed medicinal chemists to use the Minisci reaction for late-stage functionalization of lead compounds and pharmaceuticals, as the protocol is amenable to radical couplings between complex reaction partners. The ability to couple a pyridyl radical precursor to another pyridine directly from the corresponding C-H bond would be an invaluable tool in the synthetic toolkit since bipyridines are common throughout pharmaceuticals but can be challenging to prepare via metal-catalyzed cross-couplings.[27–30]

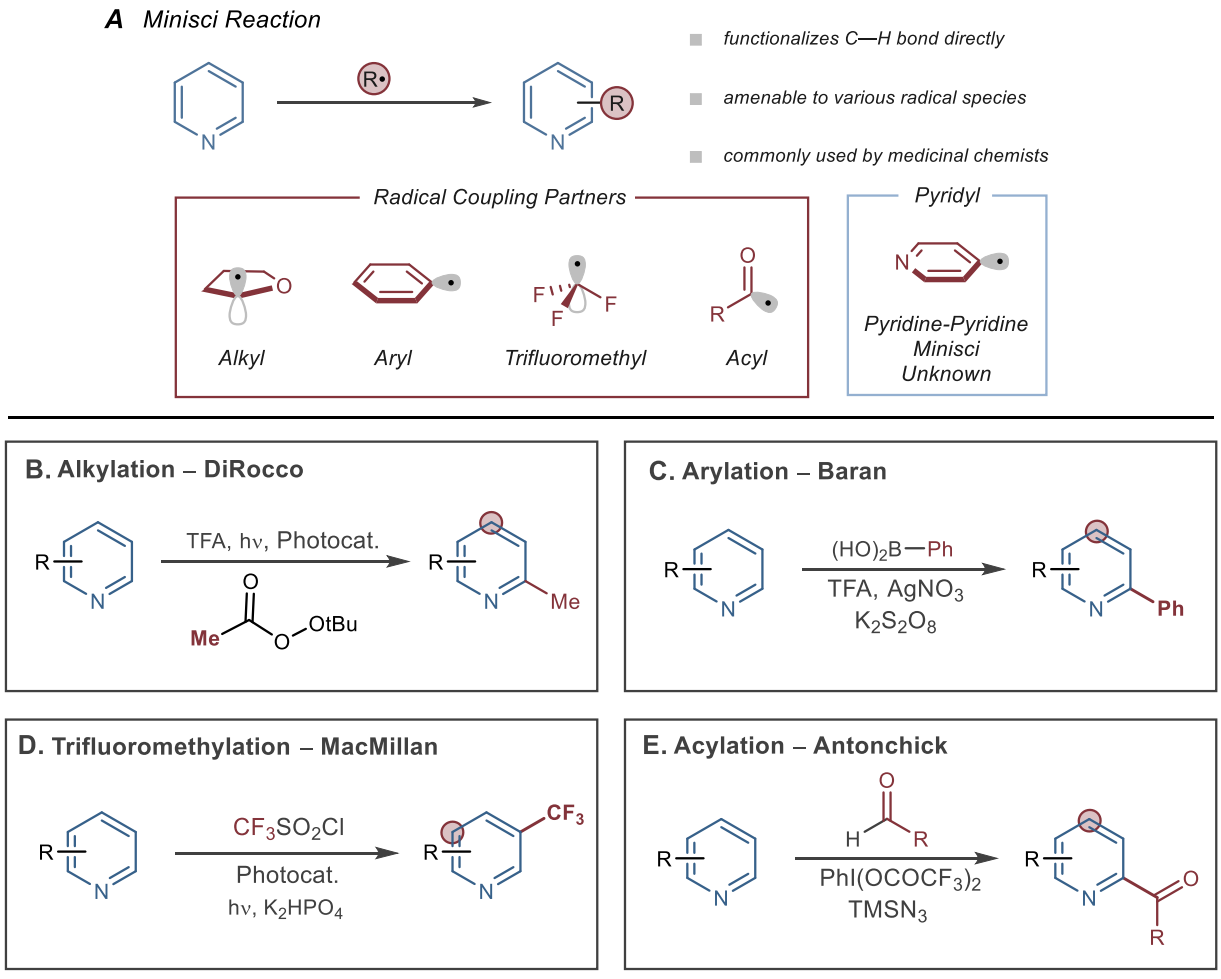

Figure 2.6: Modern advancements of the Minisci reaction to enable the introduction of a variety of carbon-bearing groups to heteroaromatic scaffolds.

We hypothesized that pyridine-pyridine Minisci couplings would be difficult because of an electronic mismatch between the pyridyl radical and the π-system of the pyridine acceptor that disfavors C-C bond formation (Figure 2.7A). A common strategy in Minisci reactions is activation of the pyridine acceptor via stoichiometric quantities of Brønsted acid to enhance the 2-position regioselectivity.[20] This strategy decreases the likelihood of a productive pyridine-pyridine Minisci coupling due to an even greater electronic incompatibility between the pyridyl radical and a pyridinium acceptor. Additionally, we suspected the pyridyl radical could react with both the desired pyridine acceptor, as well as the pyridyl radical precursor (such as 4-iodopyridine) at similar rates. This side reaction would introduce the challenge of cross-selectivity for the desired pyridine acceptor, with regioselectivity remaining an important issue. Our unexpected reaction, however, displayed precise regiocontrol and cross-selectivity with the phosphonium salt radical precursor adding exclusively to the 2-position of the cyanopyridine. For these reasons, we decided to optimize the reaction conditions and explore the scope of this transformation.

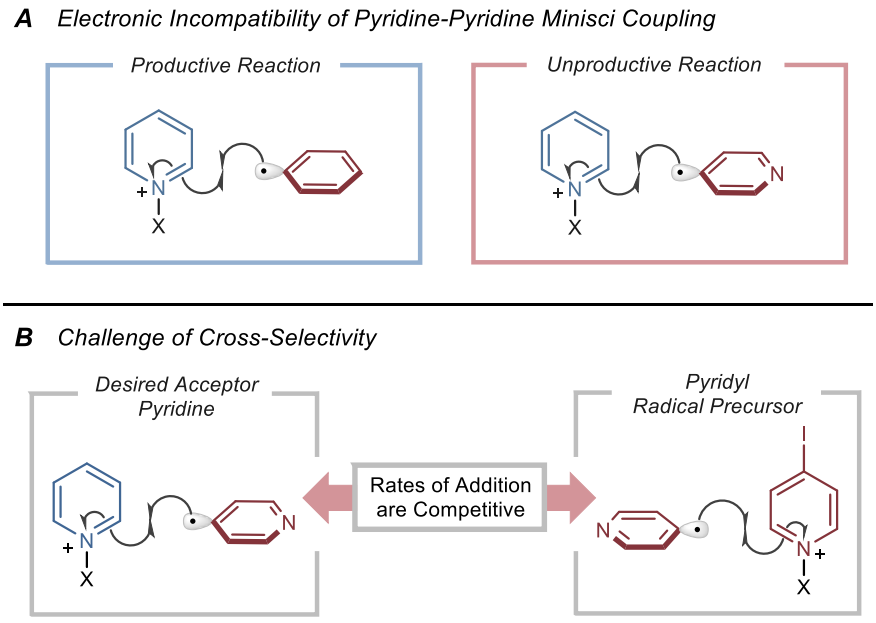

Figure 2.7: Challenges in promoting a productive pyridine-pyridine Minisci reaction.

2.5 Reaction Optimization

We began optimizing the reaction conditions to enhance the yield of the desired bipyridine product. After screening of solvents, tertiary amines, reaction concentrations, and reaction times, the optimized conditions were obtained. The key findings of the optimization are summarized in Table 2.1. By increasing the reaction concentration from 0.1 M to 0.2 M, the yield nearly doubled. Another slight increase in yield was observed when the reaction was prolonged from 8 hours to 36 hours. Notably, in the absence of B_2pin_2, the desired transformation did not occur, and 100% of the phosphonium salt remained (Entry 4). A decrease in reaction efficiency was observed when a more sterically hindered base was used (Entry 5). By switching the base to triethylamine (NEt_3), the desired product was produced in 99% NMR yield (Entry 6), and it was discovered that only 1.25 equivalents of NEt_3 were needed for bipyridine coupling in high yield (Entry 8). Importantly, even in the absence of a base additive, the reaction can proceed, albeit in significantly lower yield (Entry 7).

Table 2.1: Bipyridine Coupling Reaction Optimization

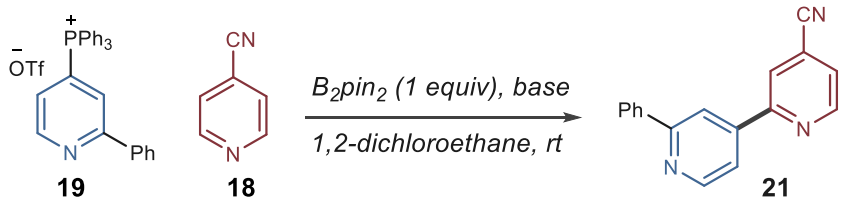

19 **18** **21**

entry	base (equiv)	time (h)	concentration (M)	% **21**[a]
1	*i*Pr$_2$NEt (2.5)	8	0.1	14
2	*i*Pr$_2$NEt (2.5)	8	0.2	26
3	*i*Pr$_2$NEt (2.5)	36	0.2	34
4[b]	*i*Pr$_2$NEt (2.5)	36	0.2	0
5	TMP (2.5)	36	0.2	16
6	NEt$_3$ (2.5)	36	0.2	99
7	none	36	0.2	26
8	NEt$_3$ (1.25)	36	0.2	97

Reaction conditions: **19** (1.0 equiv), **18** (2.0 equiv), B_2pin_2 (1.0 equiv). [a]Yields determined by ^{1}H NMR with 1,3,5-trimethoxybenzene as internal standard. [b]B_2pin_2 omitted from the reaction.

2.6 Scope of Bipyridine Coupling Reaction

With optimized reaction conditions in hand, we explored the functional group tolerance regarding the phosphonium radical precursor (Figure 2.8). A range of 2-aryl phosphonium salts and a 2-methyl salt were amenable under the reaction conditions, demonstrating tolerance of electron-rich and electron-deficient groups as well as functional groups that could undergo subsequent transformations (**22**-**26**). A chlorine atom at the 2-position provided the desired product, albeit in lower yield (**27**). Substrates containing a 3-position substituent were coupled in moderate yield (**28** and **29**), and a 2,3-disubstituted salt including a fluorine atom was accommodated (**30**). The reaction proceeded efficiently in the presence of a heteroaromatic ring and an azetidine ring (**31** and **32**), and drug-like fragments also coupled in good yield (**33** and **34**). Finally, the method was challenged with complex pharmaceuticals to show potential for late-stage

functionalization. Vismodegib, Bisacodyl, and Triprolidine (**35**-**37**), were all applicable to the reaction protocol with precise regiocontrol and cross-selectivity despite the variety of functional groups and substitution patterns displayed.

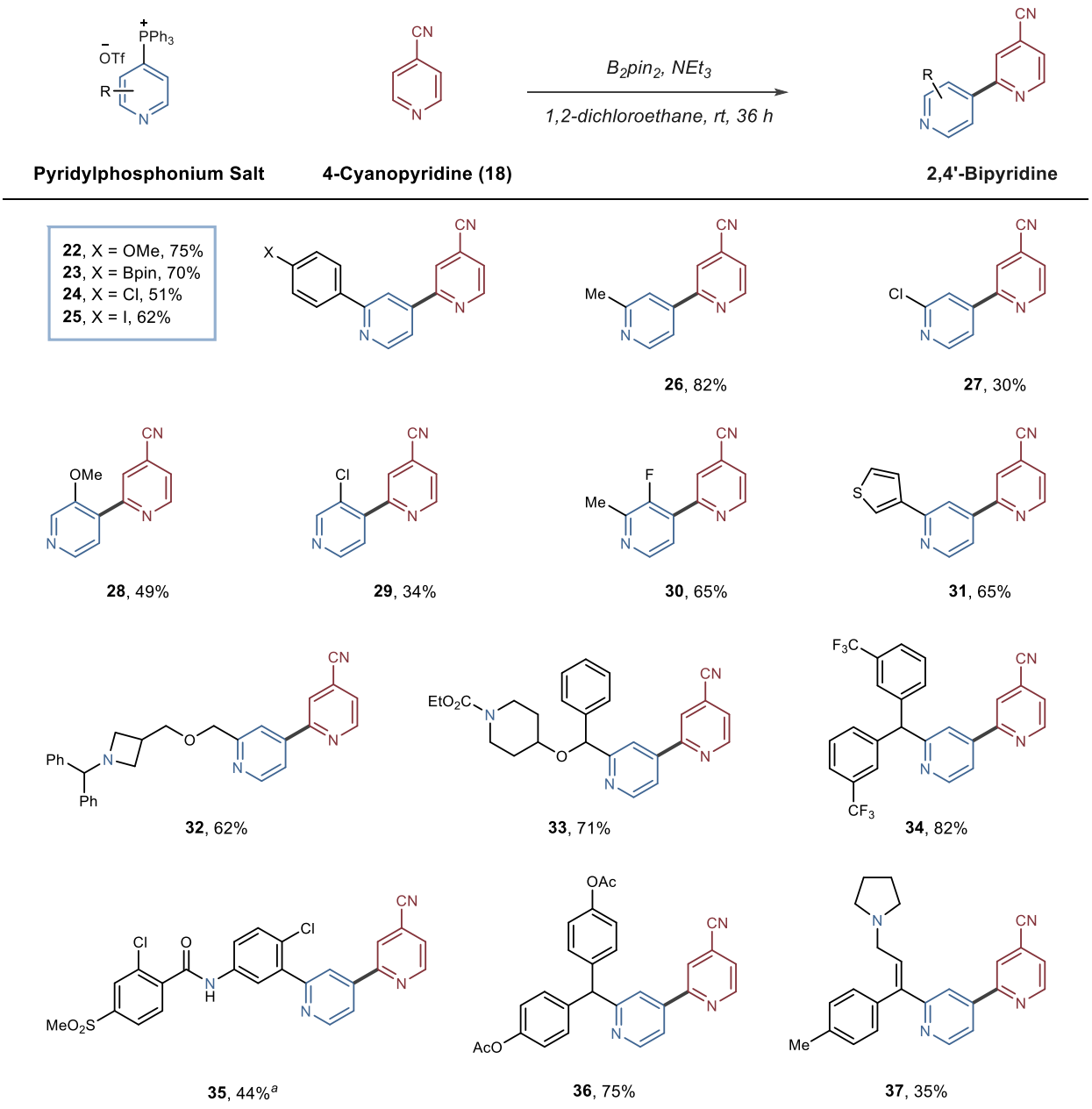

Figure 2.8: Scope of pyridylphosphonium salts in bipyridine coupling reaction. Isolated yields of single regioisomers. Conditions: phosphonium salt (1.0 equiv), 18 (2.0 equiv), B_2pin_2 (1.0 equiv), 1,2-dichloroethane (0.2 M), rt, 36 h. [a]Yield determined by ^1H NMR analysis.

Next, we explored different acceptor pyridines for this reaction (Figure 2.9). While 2-position substituents were not tolerated, a range of 3-substituted cyanopyridines did promote the transformation, producing only one regioisomer in all but one case (**43**). Alkyl substituents, as well as a silyl group were tolerated (**38**-**40**). Moderate to good yields were obtained when the acceptor pyridine contained an ester or a protected alcohol (**41** and **42**), and 3-aryl-cyanopyridines performed efficiently to produce the bipyridine products (**44** and **45**). Rapid assembly of trisheteroaryl scaffolds could be achieved, demonstrating that carbon-carbon bond formation occurs exclusively on the cyanopyridine rather than the other heteroaromatic rings (**46** and **47**). A 3,5-disubstituted cyanopyridine was tested and produced the desired product in low yield, illustrating that there is a steric impact of a substituent adjacent to the site of attack (**48**). Importantly, after screening a range of functional groups at the 4-position of the acceptor pyridine, we discovered that only a phosphonate ester could be used as an alternative to a cyano group to promote the coupling reaction, albeit in lower yield (**49**). Finally, formation of the bipyridine scaffold between complex phosphonium salts and acceptor pyridines is capable under this protocol (**50** and **51**).

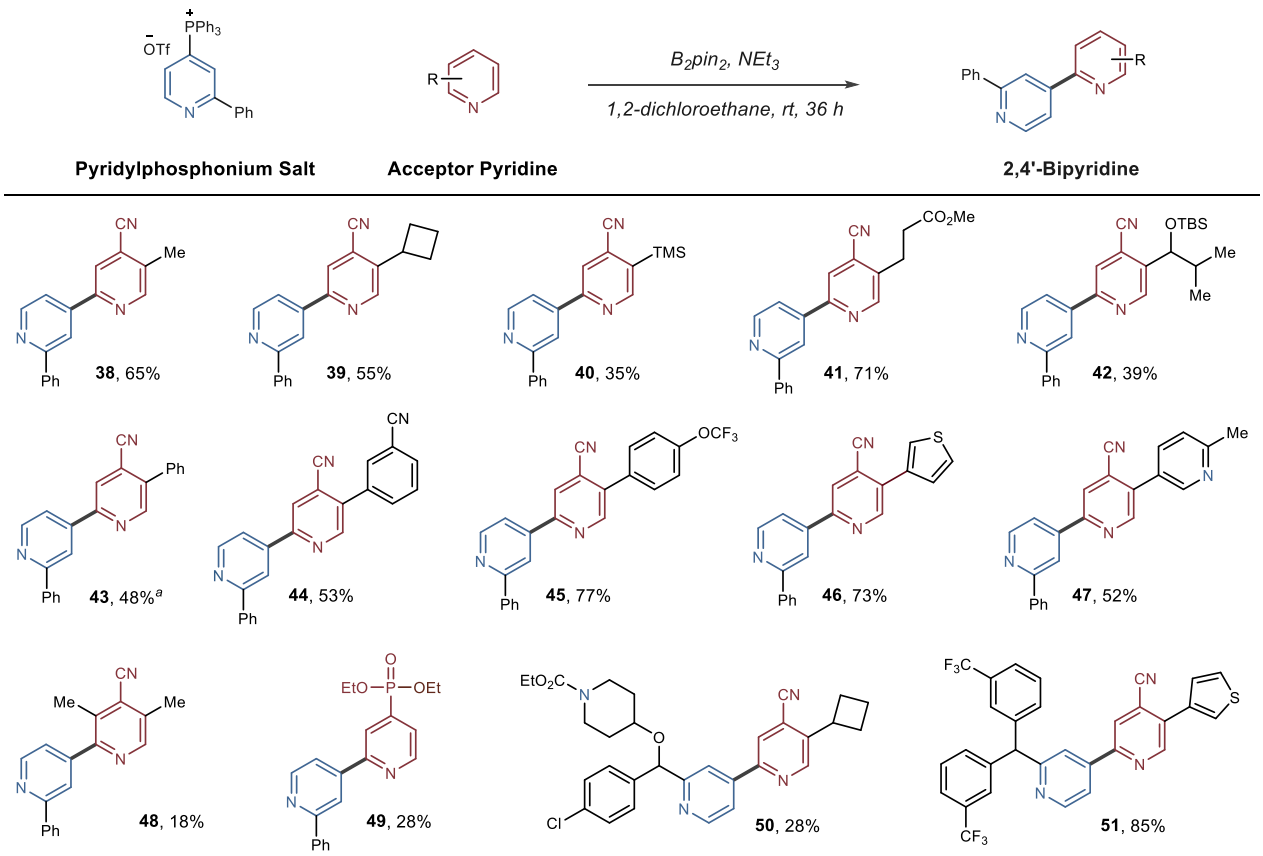

Figure 2.9: Scope of pyridine acceptors in bipyridine coupling reaction. Isolated yields of single regioisomers. Conditions: phosphonium salt 19 (1.0 equiv), pyridine acceptor (2.0 equiv), B_2pin_2 (1.0 equiv), 1,2-dichloroethane (0.2 M), rt, 36 h. [a]17:1 regioisomeric ratio.

2.7 Mechanistic Investigation

Next, we turned our attention to determining the reaction mechanism with the hypothesis that the transformation occurred through Minisci-type addition of a pyridyl radical to the cyanopyridine acceptor. In the absence of a photocatalyst capable of reducing the pyridylphosphonium salt, we focused on ascertaining a potential mechanism for the single-electron transfer. The work of Li and Jiao inspired us to pursue a borylation using the proposed stabilized boryl radical intermediate **18a** formed from cyanopyridine in the presence of B_2pin_2, but it was clear that this species was not behaving as a boryl-centered radical in our system.[17,18] As our studies

progressed, more details were published by both the Li and Jiao groups that expanded the understanding of the reactivity of boryl-stabilized radical intermediates. In Jiao's initial proposal, electron donor **52** was responsible for the SET which furnished the aryl radical that coupled with **53** to provide the product (Figure 2.10A). In 2018, Jiao published a mechanistic revision to this proposal that identified pyridine adducts **54** and **55** as the active single-electron donors in the transformation.[31] Additionally, it was determined that B_2pin_2 served as the borylation reagent rather than either SET adduct. In 2017, Li showed that persistent radical **18a** could also serve as a single-electron reductant (Figure 2.10B).[32] They demonstrated that cyclohexanone **56** could be reduced to boryl-stabilized radical **56a** that was capable of coupling with other persistent radical species.

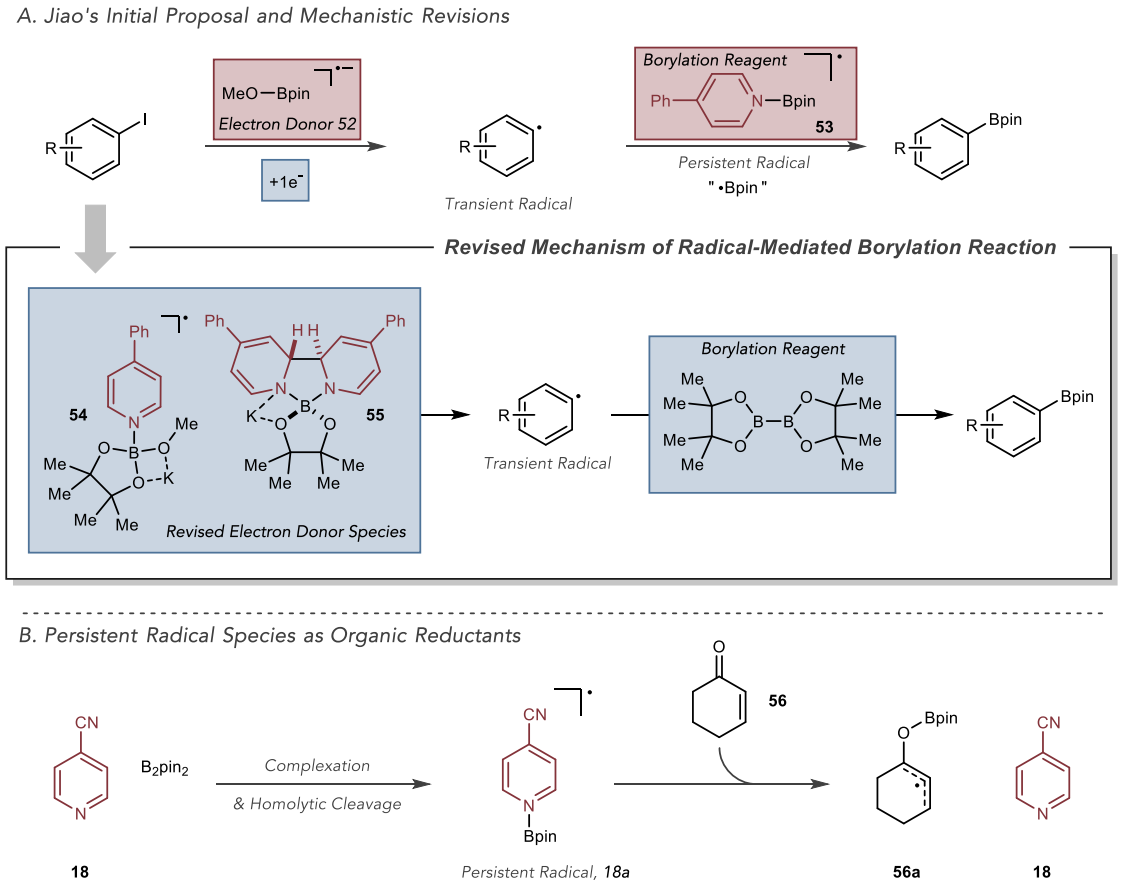

Figure 2.10: Insight into reactivity of boryl-stabilized radical intermediate.

With the understanding that boryl-stabilized radical intermediates, such as **18a**, can act as a single-electron reductant, an initial mechanistic hypothesis was proposed (Figure 2.11A). We postulated that the bipyridine coupling would begin first with the formation of organic reductant **18a**, as reported by Li. **18a** could reduce pyridylphosphonium salt **19** to pyridyl radical **19a** while simultaneously forming activated pyridinium **18b**. The intermediate pyridyl radical and activated pyridinium would then be primed for Minisci-type addition to furnish dearomatized intermediate **21a**. Finally, oxidation and rearomatization could occur to obtain the 2,4'-bipyridine product. We speculated that intermediate **21a** might exhibit a sufficient lifetime for detection by ^{1}H NMR if the reaction was kept rigorously air-free, since O_2 is known to rapidly rearomatize these intermediates.[33] Gratifyingly, visualization of the dearomatized intermediate was achieved when the reaction and NMR sample preparation was carried out in a glovebox (Figure 2.11A). In the top ^{1}H NMR spectrum, only 7% of the coupled product was detected while four doublets were observed that we attribute to **21a**. Additionally, the mass of the intermediate was also detected by low resolution mass spectrometry. After exposure to air (bottom spectrum), the dearomatized proton signals efficiently convert to coupled product **21**. While the detection of **21a** provided evidence for our hypothesis, another set of experiments stood in contradiction to this proposal. Importantly, under the optimized conditions, as well as photoredox conditions known to produce pyridyl radical intermediates from iodopyridines,[9] no other pyridyl radical precursor was successful in providing the bipyridine product (Figure 2.11B). These results imply that the phosphonium functional group is uniquely capable of promoting the desired reactivity, and further mechanistic studies were warranted.

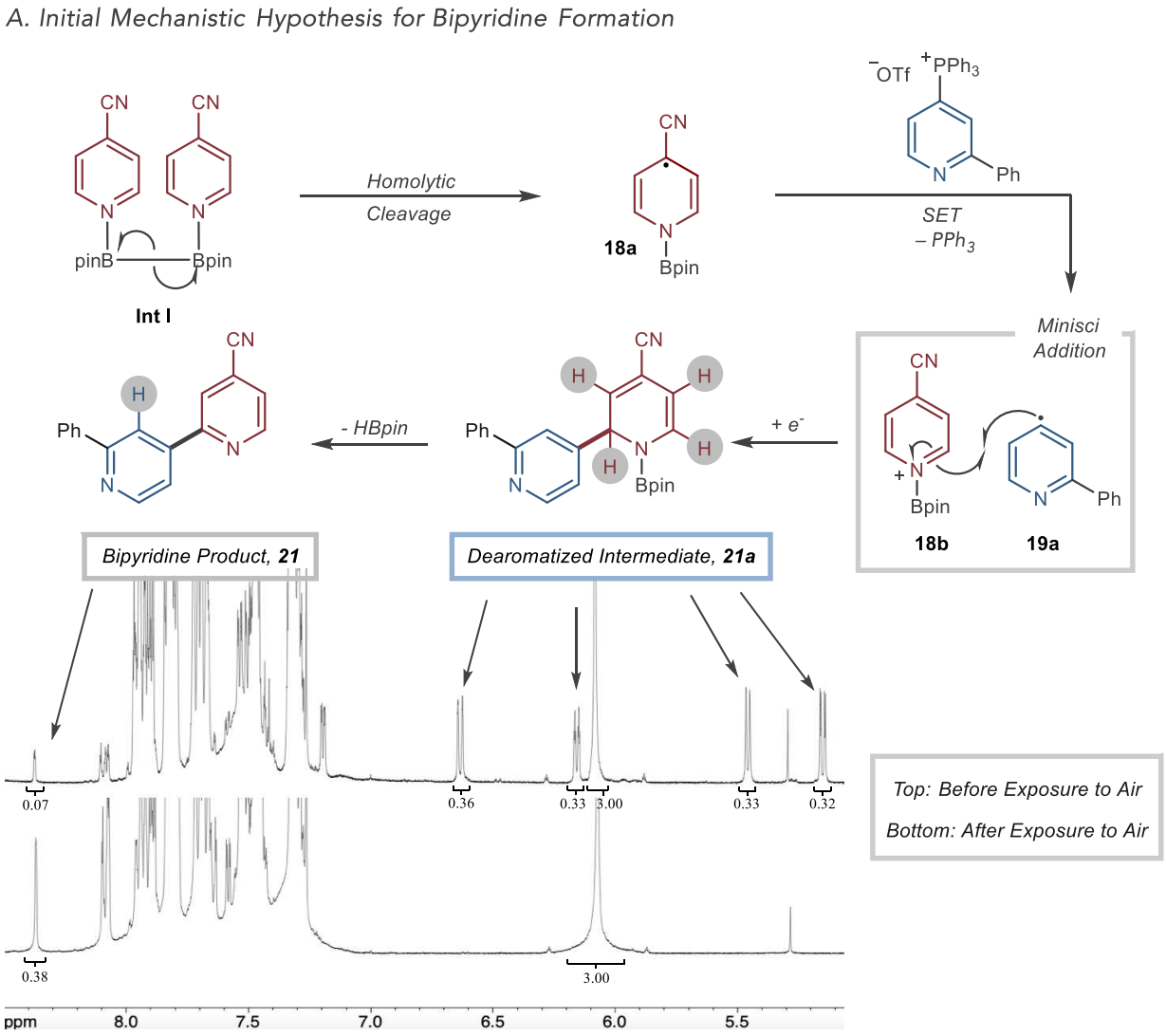

Figure 2.11: Initial mechanistic hypothesis for bipyridine formation and pyridylphosphonium salts as the only reagents that promote the transformation. 1,3,5-trimethoxybenzene used as internal standard in ^{1}H NMR assay.

A radical clock experiment was conducted to probe for the postulated radical intermediate using phosphonium salt **56** featuring a tethered alkene that could undergo a 5-exo-trig cyclization if a pyridyl radical was formed at the 4 position (Figure 2.12A).[9] These types of radical cyclizations proceed rapidly with rate constants on similar substrates ranging from 7.87 x 10^7 to 9.6 x 10^9 s^{-1}.[34–36] Under the optimized conditions, cyclized product **57** was not detected, nor any other cyclized byproducts, and the major product was bipyridine product **58**. This result suggested that a radical pathway is not operative. An alternative, two-electron mechanism could be operative where a pyridyl anion attacks the activated pyridine acceptor, especially considering that overreduction of a pyridyl radical to the anion is reported to be a facile process.[12] To probe this possibility, phosphonium salt **59**, which can undergo intramolecular cyclization with the pedant ketone upon formation of a pyridyl anion, was subjected to the reaction conditions (Figure 2.12B). The coupled bipyridine product **61** was the major product, and no cyclized products were detected. These results suggest that neither a discrete pyridyl radical nor anion were being formed in the reaction. Next, we explored intermolecular inhibition of the reaction using either an H-atom donor or a proton donor rather than intramolecular cyclization (Figure 2.12C).[37] When using Hantzsch ester, a known H-atom donor, no product arising from a pyridyl radical abstracting a hydrogen atom was detected, while the coupled product **21** was observed in 60% yield. Switching the additive to deuterium oxide (D_2O) inhibited the bipyridine formation, producing 7% of protonated 2-phenylpyridine **62** and 72% of deuterated pyridine **63**. This suggested that an anion is formed at the 4-position of the pyridine but directly contradicted the anion cyclization experiment. It is possible that the identity of intermediate **18a** or its mechanism of formation could change in the presence of deuterium oxide.

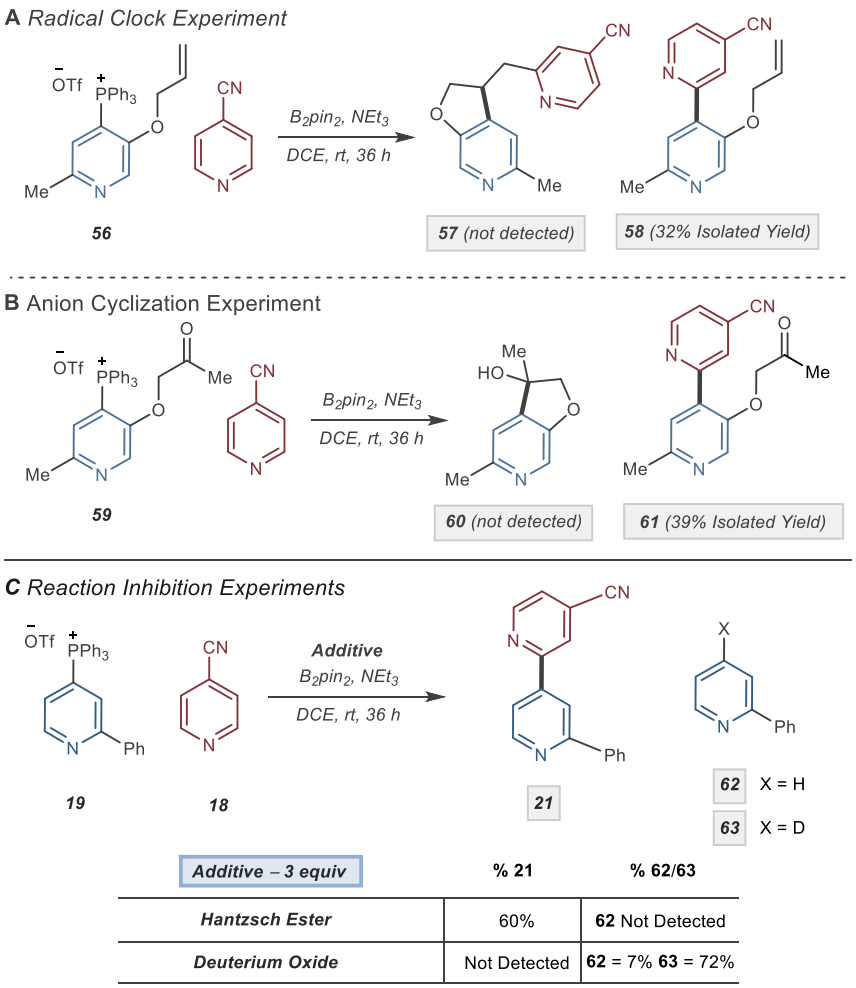

Additive – 3 equiv	% 21	% 62/63
Hantzsch Ester	60%	**62** Not Detected
Deuterium Oxide	Not Detected	**62** = 7% **63** = 72%

Figure 2.12: Experimental Probes for bipyridine Formation Mechanism.

At this junction, alternative reactive species other than a discreet pyridyl radical or anion were evaluated as the reactive intermediate during carbon-carbon bond formation. We considered the possibility that after single-electron reduction of the pyridylphosphonium salt, the resulting radical zwitterion intermediate **19b** could exhibit enhanced stability relative to radical anion intermediates of halopyridines that generally undergo rapid fragmentation to the pyridyl radical (Figure 2.13).[11,13] It is conceivable that the resonance form of **19b** that places the anion directly adjacent to the phosphonium functional group (forming an ylide) could impart unique stability of this intermediate. The unique ability of pyridylphosphonium salts to promote this transformation

compared to other pyridyl radical precursors could be explained if carbon-carbon bond formation proceeded from stabilized intermediate **19b**, rather than a discreet pyridyl radical. Additonally, productive intramolecular cyclization might be inhibited due to significant steric repulsion from the phenyl groups on the phosphonium that push the tethered electrophile away from the reactive site of the pyridine. To investigate the possibility of carbon-carbon bond formation from radical zwitterion **19b**, we initiated a collaboration to explore the reaction mechanism computationally.

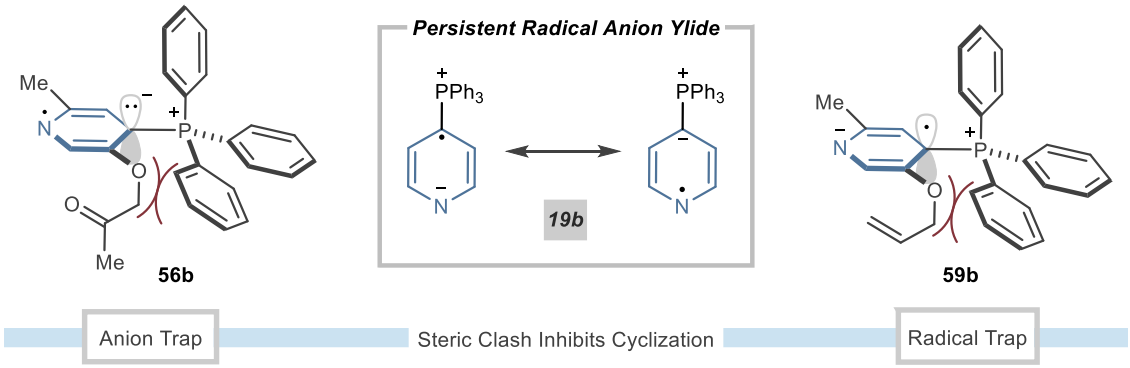

Figure 2.13: Postulated stabilized radical zwitterion intermediate that prevents intramolecular cyclization.

2.8 Computational Insight into Mechanism of Bipyridine Formation

In collaboration with the Paton group, the bipyridine cross-coupling reaction was investigated computationally. First, the feasibility of an outer sphere single electron transfer event between **18a** and **19** was explored (Figure 2.14A). The energy barrier for this SET event was calculated to be 31.9 kcal/mol, too high for a reaction proceeding at room temperature. Additionally, the radical addition of dearomatized radical intermediate **19b** to activated pyridinium **18b** was also calculated to be unfavorable, with an energy barrier of 43.1 kcal/mol. Alternatively, an inner-sphere electron transfer was determined to be feasible, where unsubstituted pyridylphosphonium salt **64** can attack the Lewis-acidic boron atom of intermediate **18a** with an

energy barrier of only 10.2 kcal/mol to form **Int I** (Figure 2.14B). The single electron transfer is spontaneous from this complex, providing a pathway to form boryl- and phosphonium-stabilized radical intermediate **64a,** where most of the spin density is located at the 2- and 4-positions, and reform **18**. Finally, to determine the pathway for C-C bond formation, we modeled several combinations of **64a** with **18** and **18a** via one- and two-electron processes, but none of these pathways were energetically feasible (see the Supporting Information for details). Instead, the most favorable pathway is a radical–radical coupling of **64a** and boryl cyanopyridine radical **18a** to form adduct **65** (Figure 2.14C). The process is rendered irreversible by losing PPh_3, and deborylation likely occurs using NEt_3 to form dearomatized intermediate **67**. Opening the reaction vessel at the end of the reaction results in a rapid color change, indicating oxidation to bipyridine **68**.

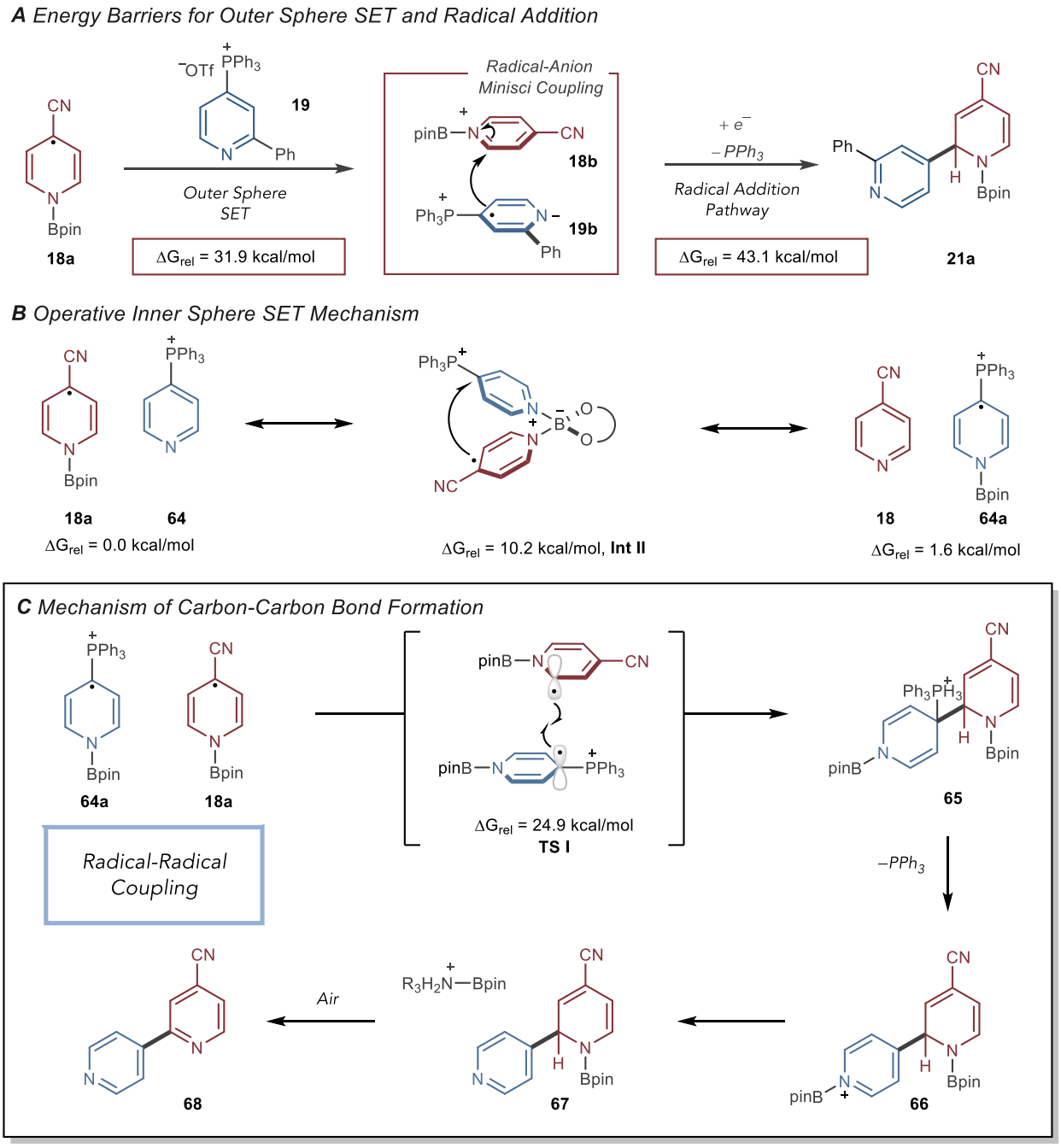

Figure 2.14: Mechanism of dearomatized radical formation and carbon-carbon bond construction.

Finally, we considered the possibility that the pyridylphosphonium salt could also serve as a Lewis base that coordinates to B_2pin_2, promoting homolytic cleave of the diboron bond (Figure 2.15). While homolytic cleavage can occur via **Int I**, **Int III**, or using a mixture of **64** and **18**, we

argue that with 2-substituted pyridylphosphonium salts, the coordination of two molecules of **18** would be more kinetically favorable. At this time, we cannot rule out the possibility that the pyridylphosphonium salt substrates are involved in the radical initiation step.

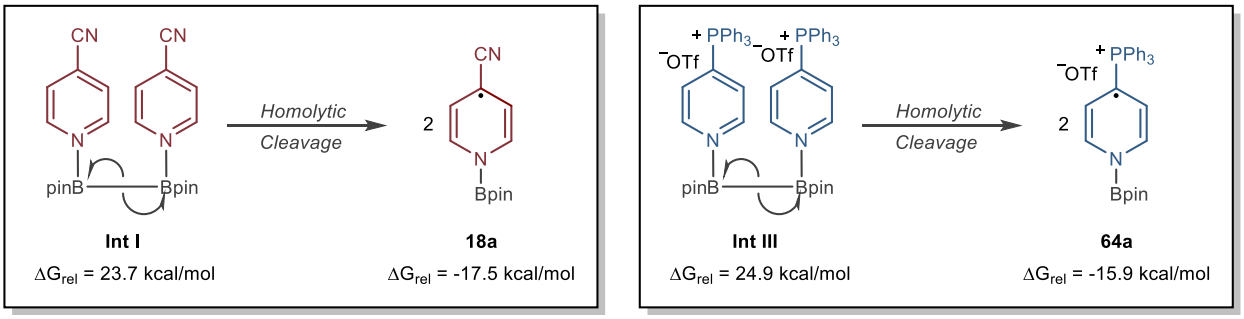

Figure 2.15: Alternative pathway for radical initiation.

2.9 Conclusion

This chapter introduces the radical reactivity of pyridylphosphonium salts. The importance of the Minisci reaction, and the challenges associated with developing a pyridine-pyridine Minisci coupling, were highlighted. Using pyridylphosphonium salts as radical precursors, we have demonstrated a useful alternative to the Minisci reaction to form 2,4'-bipyridine products through a unique mechanism, with exclusive regioselectivity. Computational and experimental studies suggest that carbon-carbon bond formation occurs via radical coupling of two dearomatized pyridyl radical intermediates, rather than a discreet pyridyl radical. This reaction only proceeds using pyridylphosphonium salt coupling partners, since other pyridyl radical precursors are unable to stabilize the dearomatized radical intermediate required for bipyridine formation. This unique reactivity will be further explored in Chapter 3.

References

(1) Yan, M.; Lo, J. C.; Edwards, J. T.; Baran, P. S. Radicals: Reactive Intermediates with Translational Potential. *J. Am. Chem. Soc.* **2016**, *138*, 12692–12714.

(2) Wille, U. Reaction Mechanisms: Radical and Radical Ion Reactions. *Annu. Rep. Sect. B Org. Chem.* **2012**, *108*, 228.

(3) Shaw, M. H.; Twilton, J.; MacMillan, D. W. C. Photoredox Catalysis in Organic Chemistry. *J. Org. Chem.* **2016**, *81*, 6898–6926.

(4) Prier, C. K.; Rankic, D. A.; MacMillan, D. W. C. Visible Light Photoredox Catalysis with Transition Metal Complexes: Applications in Organic Synthesis. *Chem Rev* **2013**, 42.

(5) Strieth-Kalthoff, F.; Glorius, F. Triplet Energy Transfer Photocatalysis: Unlocking the Next Level. *Chem* **2020**, *6*, 1888–1903.

(6) Horn, E. J.; Rosen, B. R.; Baran, P. S. Synthetic Organic Electrochemistry: An Enabling and Innately Sustainable Method. *ACS Cent. Sci.* **2016**, *2*, 302–308.

(7) Zhang, X.; McNally, A. Phosphonium Salts as Pseudohalides: Regioselective Nickel-Catalyzed Cross-Coupling of Complex Pyridines and Diazines. *Angew. Chem. Int. Ed.* **2017**, *56*, 9833–9836.

(8) Zhang, X.; McNally, A. Cobalt-Catalyzed Alkylation of Drug-Like Molecules and Pharmaceuticals Using Heterocyclic Phosphonium Salts. *ACS Catal.* **2019**, 4862–4866.

(9) Aycock, R. A.; Wang, H.; Jui, N. T. A Mild Catalytic System for Radical Conjugate Addition of Nitrogen Heterocycles. *Chem. Sci.* **2017**, *8*, 3121–3125.

(10) Boyington, A. J.; Seath, C. P.; Zearfoss, A. M.; Xu, Z.; Jui, N. T. Catalytic Strategy for Regioselective Arylethylamine Synthesis. *J. Am. Chem. Soc.* **2019**, *141*, 4147–4153.

(11) Seath, C. P.; Jui, N. T. Intermolecular Reactions of Pyridyl Radicals with Olefins via Photoredox Catalysis. *Synlett* **2019**, *30*, 1607–1614.

(12) Seath, C. P.; Vogt, D. B.; Xu, Z.; Boyington, A. J.; Jui, N. T. Radical Hydroarylation of Functionalized Olefins and Mechanistic Investigation of Photocatalytic Pyridyl Radical Reactions. *J. Am. Chem. Soc.* **2018**, *140*, 15525–15534.

(13) Senaweera, S.; Weaver, J. D. Dual C–F, C–H Functionalization via Photocatalysis: Access to Multifluorinated Biaryls. *J. Am. Chem. Soc.* **2016**, *138*, 2520–2523.

(14) Friese, F. W.; Studer, A. New Avenues for C–B Bond Formation *via* Radical Intermediates. *Chem. Sci.* **2019**, *10*, 8503–8518.

(15) Larsen, M. A.; Hartwig, J. F. Iridium-Catalyzed C–H Borylation of Heteroarenes: Scope, Regioselectivity, Application to Late-Stage Functionalization, and Mechanism. *J. Am. Chem. Soc.* **2014**, *136*, 4287–4299.

(16) Sadler, S. A.; Tajuddin, H.; Mkhalid, I. A. I.; Batsanov, A. S.; Albesa-Jove, D.; Cheung, M. S.; Maxwell, A. C.; Shukla, L.; Roberts, B.; Blakemore, D. C.; Lin, Z.; Marder, T. B.; Steel, P. G. Iridium-Catalyzed C–H Borylation of Pyridines. *Org. Biomol. Chem.* **2014**, *12*, 7318.

(17) Wang, G.; Zhang, H.; Zhao, J.; Li, W.; Cao, J.; Zhu, C.; Li, S. Homolytic Cleavage of a B−B Bond by the Cooperative Catalysis of Two Lewis Bases: Computational Design and Experimental Verification. *Angew. Chem. Int. Ed.* **2016**, *55*, 5985–5989.

(18) Zhang, L.; Jiao, L. Pyridine-Catalyzed Radical Borylation of Aryl Halides. *J. Am. Chem. Soc.* **2017**, *139*, 607–610.

(19) Koniarczyk, J. L.; Greenwood, J. W.; Alegre-Requena, J. V.; Paton, R. S.; McNally, A. A Pyridine-Pyridine Cross-Coupling Reaction via Dearomatized Radical Intermediates. *Angew. Chem. Int. Ed.* **2019**, *58*, 14882–14886.

(20) Duncton, M. A. J. Minisci Reactions: Versatile CH-Functionalizations for Medicinal Chemists. *MedChemComm* **2011**, *2*, 1135.
(21) DiRocco, D. A.; Dykstra, K.; Krska, S.; Vachal, P.; Conway, D. V.; Tudge, M. Late-Stage Functionalization of Biologically Active Heterocycles Through Photoredox Catalysis. *Angew. Chem. Int. Ed.* **2014**, *53*, 4802–4806.
(22) Seiple, I. B.; Su, S.; Rodriguez, R. A.; Gianatassio, R.; Fujiwara, Y.; Sobel, A. L.; Baran, P. S. Direct C−H Arylation of Electron-Deficient Heterocycles with Arylboronic Acids. *J. Am. Chem. Soc.* **2010**, *132*, 13194–13196.
(23) O'Hara, F.; Blackmond, D. G.; Baran, P. S. Radical-Based Regioselective C–H Functionalization of Electron-Deficient Heteroarenes: Scope, Tunability, and Predictability. *J. Am. Chem. Soc.* **2013**, *135*, 12122–12134.
(24) Nagib, D. A.; MacMillan, D. W. C. Trifluoromethylation of Arenes and Heteroarenes by Means of Photoredox Catalysis. *Nature* **2011**, *480*, 224–228.
(25) Ji, Y.; Brueckl, T.; Baxter, R. D.; Fujiwara, Y.; Seiple, I. B.; Su, S.; Blackmond, D. G.; Baran, P. S. Innate C-H Trifluoromethylation of Heterocycles. *Proc. Natl. Acad. Sci.* **2011**, *108*, 14411–14415.
(26) Matcha, K.; Antonchick, A. P. Metal-Free Cross-Dehydrogenative Coupling of Heterocycles with Aldehydes. *Angew. Chem. Int. Ed.* **2013**, *52*, 2082–2086.
(27) Basnet, A.; Thapa, P.; Karki, R.; Na, Y.; Jahng, Y.; Jeong, B.-S.; Jeong, T. C.; Lee, C.-S.; Lee, E.-S. 2,4,6-Trisubstituted Pyridines: Synthesis, Topoisomerase I and II Inhibitory Activity, Cytotoxicity, and Structure–Activity Relationship. *Bioorg. Med. Chem.* **2007**, *15*, 4351–4359.
(28) Corma, A.; García, H.; Llabrés i Xamena, F. X. Engineering Metal Organic Frameworks for Heterogeneous Catalysis. *Chem. Rev.* **2010**, *110*, 4606–4655.
(29) Campeau, L.-C.; Fagnou, K. Applications of and Alternatives to π-Electron-Deficient Azine Organometallics in Metal Catalyzed Cross-Coupling Reactions. *Chem Soc Rev* **2007**, *36*, 1058–1068.
(30) Hilton, M. C.; Zhang, X.; Boyle, B. T.; Alegre-Requena, J. V.; Paton, R. S.; McNally, A. Heterobiaryl Synthesis by Contractive C–C Coupling via P(V) Intermediates. *Science* **2018**, *362*, 799–804.
(31) Zhang, L.; Jiao, L. Super Electron Donors Derived from Diboron. *Chem. Sci.* **2018**, *9*, 2711–2722.
(32) Wang, G.; Cao, J.; Gao, L.; Chen, W.; Huang, W.; Cheng, X.; Li, S. Metal-Free Synthesis of C-4 Substituted Pyridine Derivatives Using Pyridine-Boryl Radicals via a Radical Addition/Coupling Mechanism: A Combined Computational and Experimental Study. *J. Am. Chem. Soc.* **2017**, *139*, 3904–3910.
(33) Curran, D. P.; Keller, A. I. Radical Additions of Aryl Iodides to Arenes Are Facilitated by Oxidative Rearomatization with Dioxygen. *J. Am. Chem. Soc.* **2006**, *128*, 13706–13707.
(34) Tye, J. W.; Weng, Z.; Johns, A. M.; Incarvito, C. D.; Hartwig, J. F. Copper Complexes of Anionic Nitrogen Ligands in the Amidation and Imidation of Aryl Halides. *J. Am. Chem. Soc.* **2008**, *130*, 9971–9983.
(35) Annunziata, A.; Galli, C.; Marinelli, M.; Pau, T. Determination of Rate Constants for the Reaction of Aryl Radicals with Enolate Ions. *Eur. J. Org. Chem.* **2001**, No. 7, 1323–1329.
(36) Abeywickrema, A. N.; Beckwith, A. L. J. Rate Constants for the Cyclisation of Some Aryl Radicals Bearing Unsaturated Ortho-Substituents. *J. Chem. Soc. Chem. Commun.* **1986**, No. 6, 464.

(37) Zhang, X.; Ren, J.; Tan, S. M.; Tan, D.; Lee, R.; Tan, C.-H. An Enantioconvergent Halogenophilic Nucleophilic Substitution S_N2X Reaction. *Science* **2019**, *363*, 400–404.

CHAPTER THREE

PYRIDYLPHOSPHONIUM SALTS AS ALTERNATIVES TO CYANOPYRIDINES IN RADICAL-RADICAL COUPLING REACTIONS

3.1 Overview

In this chapter, photoredox catalysis is used to form stabilized radical intermediates from heterocyclic phosphonium salts that participate in coupling reactions with other stabilized radicals. This advance serves to expand the use of phosphonium salts in reaction manifolds mediated by single electron transfer. Alkylation of heterocyclic phosphonium salts is achieved via redox neutral coupling with both trifluoroborate salts and carboxylic acids. Additionally, a mild, 4-selective amination methodology is demonstrated to form aminopyridines. Synthesis and characterization of organic compounds, design of experiments, and manuscript preparation was carried out by Jacob Greenwood and Professor Andrew McNally. Dr. Benjamin Boyle was invaluable, providing helpful conversations and completing important experiments requested during the peer review process. This work culminated in a publication in Chemical Science in 2021.

3.2 Introduction

Modern photoredox catalysis and electrochemistry have enabled new synthetic methods that proceed via transient radical intermediates.[1–7] These platforms have been advantageous to the field of pyridine functionalization as radical-based methodologies tend to be well suited to functionalization of aromatic heterocycles due to their tolerance of polar, Lewis basic functionality.[8–11] Several accounts of pyridine functionalization have been divulged that leverage pyridyl radicals generated via single-electron reduction of a halopyridine to a radical anion intermediate, that readily undergoes fragmentation, yielding the radical species and a halide anion

(**Figure 3.1 A**).[11–13] An alternative reaction manifold is accessed when 4-cyanopyridines are used as the radical precursor, as the cyano functional group is uniquely capable of stabilizing the dearomatized radical anion (**Figure 3.1 B**).[14] The stability of the radical anion intermediate enables valuable chemistry via radical-radical coupling reactions due to the persistence of the radical anion intermediate. The cyano group is essential for these methods; however, the scarcity of methods to access the required cyanopyridines limits the synthetic applicability of such reactions. This is a significant impediment in the context of applying radical anion coupling chemistry to complex pyridines, such as those found in pharmaceutical and agrochemical candidates. These structures are often devoid of preinstalled functional groups preventing regioselective nitrile installation from C-H precursors (*vide infra*). Apart from nitriles, there are no alternative functional groups that can provide the same reactivity in a general and synthetically useful manner. We envisioned pyridylphosphonium salts, regioselectively constructed from the C–H bonds of a diverse set of pyridines, could serve as alternatives to cyanopyridines (**Figure 3.1 C**).[15–26]

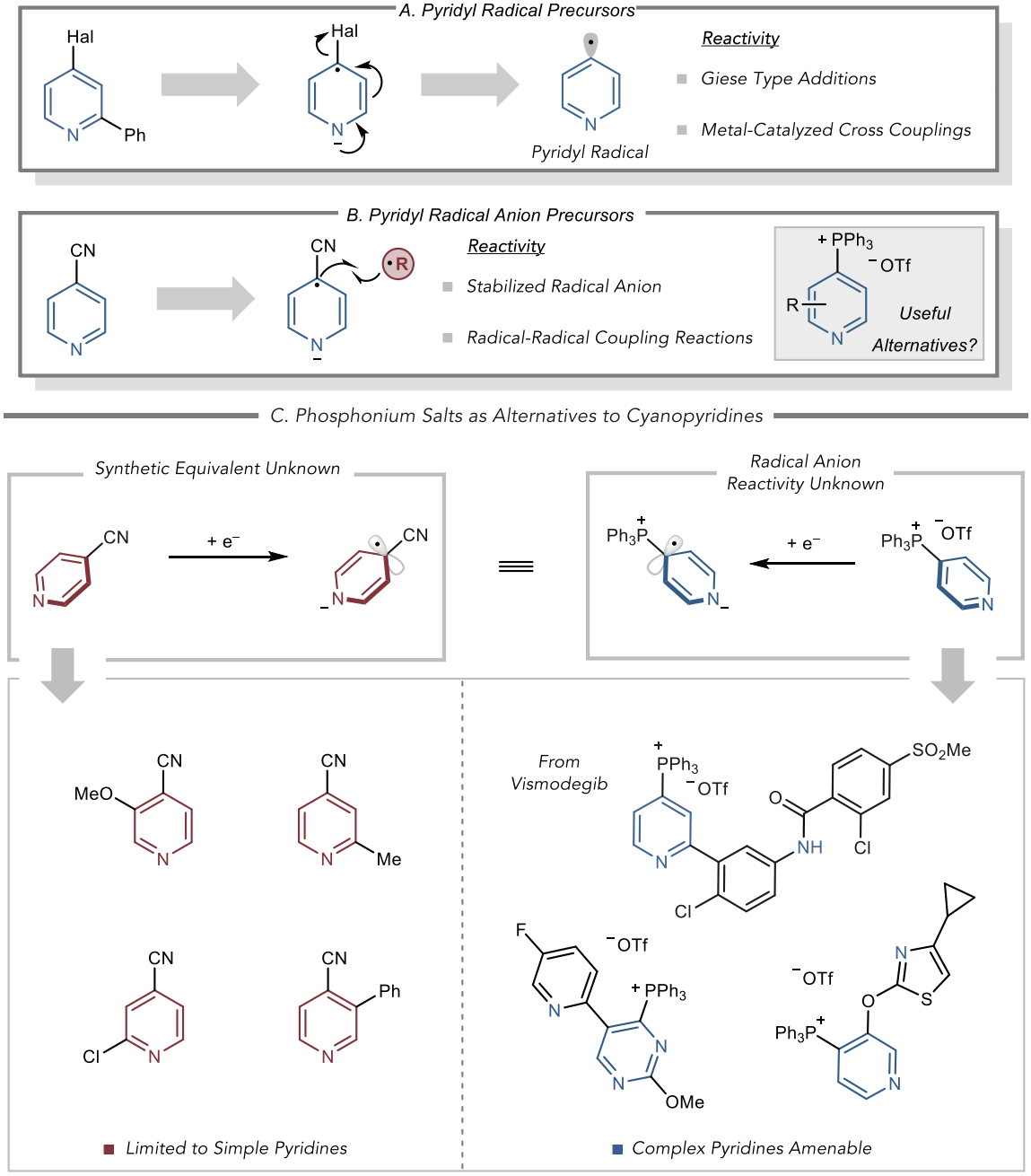

Figure 3.1: Divergent radical reactivity enabled by cyanopyridines and heteroarylphosphonium salts as alternatives to cyanopyridines.

3.3 Chemistry of Cyanopyridines and Synthetic Challenges for their Synthesis

A diverse range of transformations have been reported that proceed via dearomatized cyanopyridine radical anion intermediates (**Figure 3.2**). Redox-neutral alkylation of cyanopyridines has been demonstrated using α-amino radicals generated from tertiary amines or α-amino-acids after single-electron oxidation.[27,28] Recently, the Bandar group expanded this chemistry to include organosilane coupling partners in the absence of light or photosensitizer.[29] Allylation has been achieved using a hydrogen atom abstraction strategy to deliver the key allyl radical that can couple with the radical anion intermediate.[30] Vinylation has also been achieved by the Chu group using styrenes as coupling partners in combination with a sulfinate reagent that adds to the styrene after single-electron oxidation and undergoes base-mediated elimination after radical-radical coupling to deliver the alkenylated product.[31] Finally, sterically hindered (hetero)arylamine or alcohol synthesis has been accomplished under photoredox and electrochemical conditions where cyanopyridine radical anions couple with persistent radicals formed via reduction of ketones or imines.[32,33] Despite all the value this chemistry offers, the applications of such reactions are limited by the challenges in complex cyanopyridine synthesis. A small selection of simple building block cyanopyridines are commercially available, and even these can be prohibitively expensive for use in general methods. Complex cyanopyridine building blocks must be synthesized in most cases, typically via cross-coupling or S_NAr reaction of the corresponding halopyridine or direct addition of a cyanide nucleophile to an activated pyridinium.[34–36] Complex halopyridines also lack commercial abundance and can be expensive and/or challenging to make.[22] Direct cyanation of a complex pyridinium is an attractive alternative, but this method often provides a mixture of regioisomers that can be difficult to separate.[36]

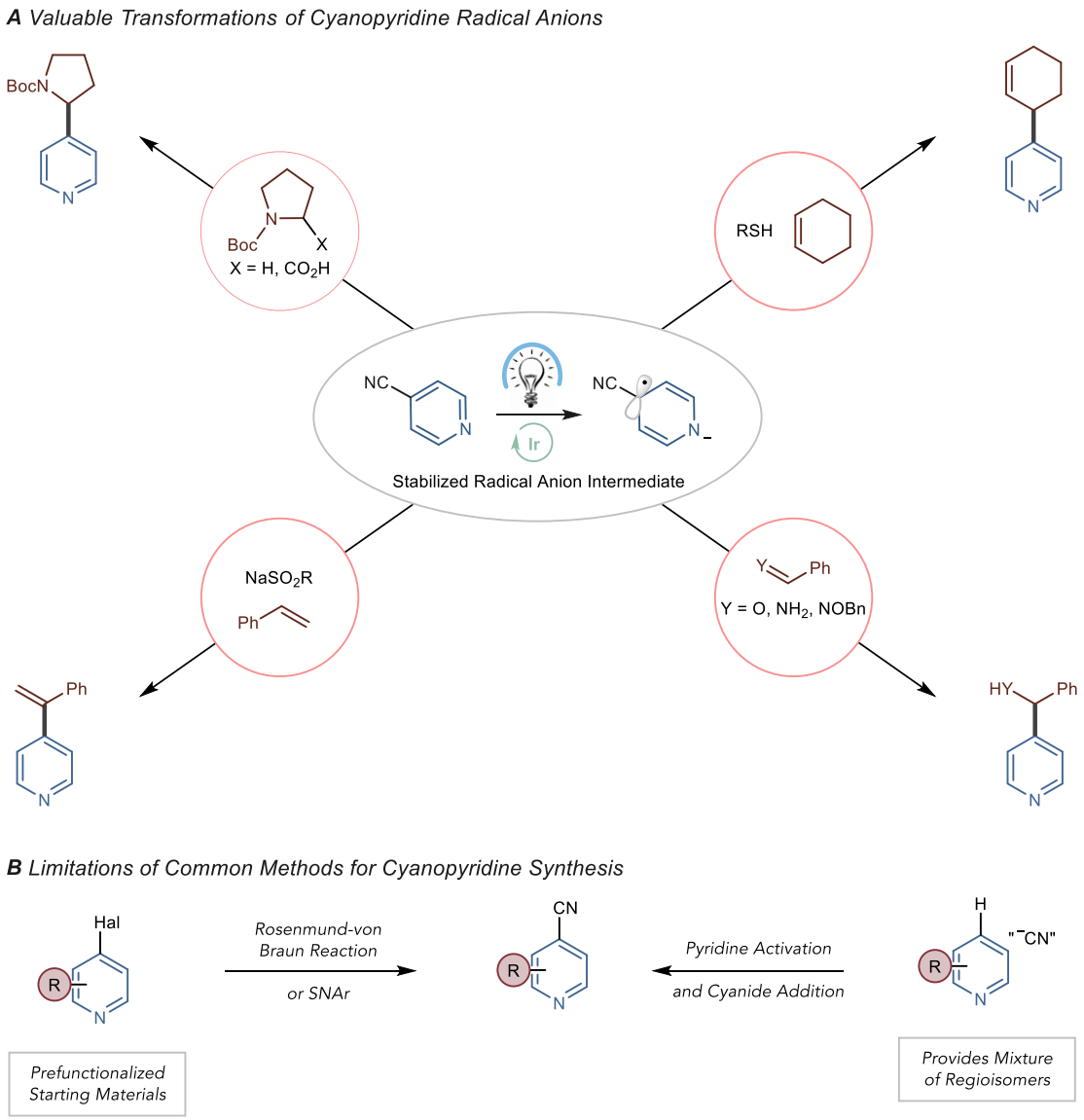

Figure 3.2: Valuable transformations of cyanopyridines and limitations in common methods used for their synthesis.

3.4 Reaction Design and Optimization

Chapter 2 detailed the discovery of an unusual radical-radical coupling reaction between a boryl-stabilized cyanopyridyl radical and a boryl-stabilized pyridylphosphonium radical.[26] While this work demonstrated the possibility that the phosphonium group could stabilize the dearomatized radical species, the intermediate radicals arose via an unusual inner-sphere process

that would be difficult to extend to other coupling reactions. The use of pyridylphosphonium salts as general radical anion precursors in photoredox and electrochemical process that can mimic the reactivity of cyanopyridines represent a significant advance. We envisioned a pyridine alkylation reaction that would begin with the single-electron reduction of a pyridylphosphonium salt ($E_{p/2}^{red}$ = –1.51 V vs. SCE) by an excited state photocatalyst to produce radical zwitterion **69** (**Figure 3.3**).[26] Next, reductive quenching of the photocatalyst could produce benzyl radical **70**, resulting from single-electron oxidation of a BF_3K salt (E_{red} = +1.10 V vs. SCE for a primary benzylic salt).[37] Finally, radical-radical coupling between persistent radicals **69** and **70** could occur, followed by loss of triphenylphosphine from dearomatized intermediate **71** to furnish the alkylated pyridine product. Notably, the redox events could invert, where single-electron oxidation of the BF_3K salt could occur first, followed by pyridylphosphonium reduction, broadening the scope of amenable photocatalysts.

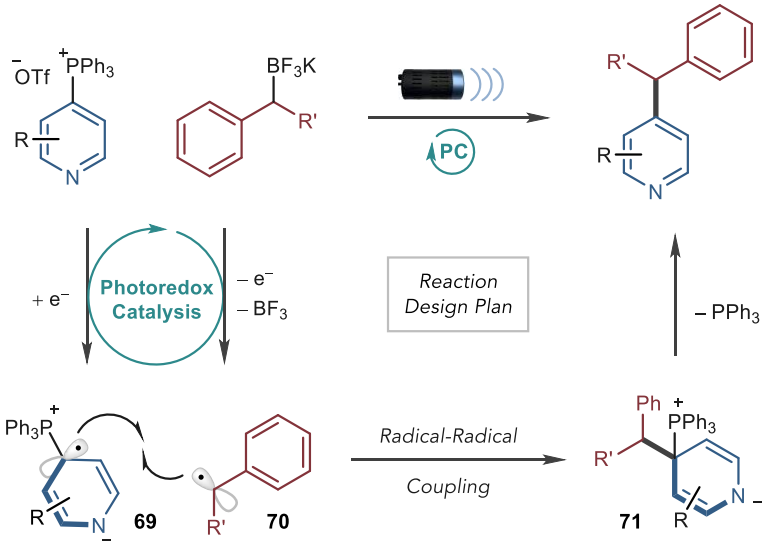

Figure 3.3: Mechanistic design for a 4-selective pyridine alkylation.

We began our investigation by examining a series of photocatalysts for the coupling reaction of phosphonium salt **72**, formed from 2-phenylpyridine with complete regioselectivity for the 4-position, and benzylic BF_3K salt **74** under irradiation from a 455 nm Kessil light (**Table 3.1A** with photocatalyst redox potentials and triplet state energies shown in **Table 3.1B**).[38] We discovered that both $Ir(ppy)_3$ and $[Ir(dF(CF_3)ppy)_2(dtbbpy)]PF_6$ catalyze the transformation despite markedly different redox properties (entries 1-2), suggesting that oxidative and reductive quenching cycles may both be operating depending on the photocatalyst employed.[2] The Adachi-type photocatalyst 3DPAFIPN improved the yield to 77% with a further increase to 82% after increasing the reaction concentration (entries 3-4).[39] Adding 2,6-lutidine, previously shown as an effective additive for photoredox cross-coupling reactions of BF_3K salts by the Molander group,[40–42] had no impact on the yield of alkylated pyridine **76** (entry 5), and $[Ir(ppy)_2(dtbbpy)]PF_6$ was a slightly less efficient photocatalyst under the same conditions (entry 6). We observed that 2,6-lutidine substantially improved the yield when the isomeric 3-Ph salt **73** was employed (entries 7-8). Without 2,6-lutidine formation of 3-phenylpyridine occurred (observable by crude ^1H NMR analysis) alongside other unidentified byproducts and the 2-benzylated pyridine product was observed (3:1 r.r., C4/C2). This outcome suggests that protodephosphination and non-selective Minisci-type pathways can occur under these conditions.[43] With 2,6-lutidine, the crude reaction profile is cleaner, and the 4- vs. 2-position ratio improved to 8:1. At this point, we have not established the role of 2,6-lutidine, although it is conceivable that it reacts with BF_3 produced as the reaction progresses. In 2-substituted systems, steric hindrance around the pyridine nitrogen atom of the salt would deter BF_3-coordination, whereas, in 3-substituted systems like salt **73**, coordination is more likely and may promote undesired background Minisci additions. Given the structural variation of pyridines that we sought to apply to this process and how those structures

could impact coordination to boron during the reaction, we elected to use 2,6-lutidine as an additive in all subsequent reactions.

Table 3.1: Pyridine Alkylation Optimization and Key Observations.

A – Reaction Optimization[a]

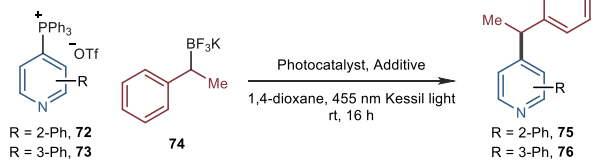

R = 2-Ph, **72**
R = 3-Ph, **73**

74

R = 2-Ph, **75**
R = 3-Ph, **76**

Entry	Salt	Photocatalyst (2 mol%)	Additive (3 equiv)	Concentration	% Prod[b]
1	**72**	$Ir(ppy)_3$	none	0.1 M	60
2	**72**	$[Ir(dF(CF_3)ppy)_2(dtbbpy)]PF_6$	none	0.1 M	66
3	**72**	3DPAFIPN	none	0.1 M	77
4	**72**	3DPAFIPN	none	0.3 M	82
5	**72**	3DPAFIPN	2,6-lutidine	0.3 M	82 (74)[c] (74)[d]
6	**72**	$[Ir(ppy)_2(dtbbpy)]PF_6$	2,6–lutidine	0.3 M	74
7	**73**	3DPAFIPN	none	0.3 M	20[e]
8	**73**	3DPAFIPN	2,6-lutidine	0.3 M	60[f] (42)[c]
9	**72**	none	2,6–lutidine	0.3 M	trace
10[g]	**72**	none	2,6–lutidine	0.3 M	66
11	**72**	$[Mes\text{-}Acr]BF_4$	2,6–lutidine	0.3 M	41

C – BF_3 Additive Enables a Previously Ineffective Photocatalyst

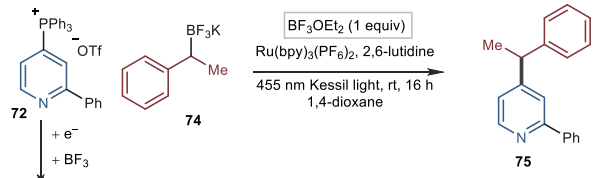

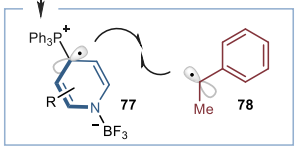

Results	% 72	% 75
Without BF_3OEt_2	98%	trace
With BF_3OEt_2	51%	47%

B – Photocatalyst Redox Properties, and Triplet State Energies[h]

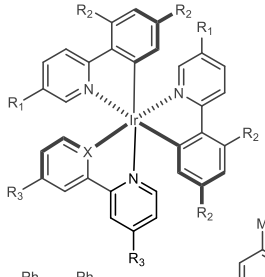

$[Ir(ppy)]_3$
X=CH, R_1=R_2=R_3=H

$[Ir(dF(CF_3)ppy)_2(dtbbpy)]PF_6$[i]
X=N, R_1=CF_3, R_2=F, R_3=tBu

$[Ir(ppy)_2(dtbbpy)]PF_6$[i]
X=N, R_1=R_2=H, R_3=tBu

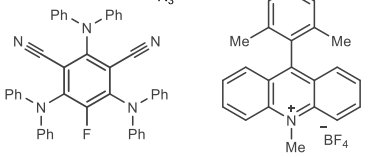

3DPAFIPN | $[Mes\text{-}Acr]BF_4$ | $[Ru(bpy)_3]PF_6$

Photocatalyst	$Ir(ppy)_3$	$[Ir(dF(CF_3)ppy)_2(dtbbpy)]PF_6$	$[Ir(ppy)_2(dtbbpy)]PF_6$
$E_{1/2}(PC^+/PC^*)$	–1.73 V	–0.89 V	–0.96 V
$E_{1/2}(PC^*/PC^-)$	+0.31 V	+1.21 V	+0.66 V
$E_{1/2}(PC^+/PC)$	+0.77 V	+1.69 V	+1.21 V
$E_{1/2}(PC/PC^-)$	–2.19 V	–1.37 V	–1.57 V
$E^{T_1}_{0,0}$(kcal/mol)	58.1	61.8	49.2

Photocatalyst	3DPAFIPN	$[Mes\text{-}Acr]BF_4$	$[Ru(bpy)_3]PF_6$
$E_{1/2}(PC^+/PC^*)$	–1.38 V		–0.81 V
$E_{1/2}(PC^*/PC^-)$	+1.09 V	+2.18 V	+0.77 V
$E_{1/2}(PC^+/PC)$	+1.30 V		+1.29 V
$E_{1/2}(PC/PC^-)$	–1.59 V	–0.49 V	–1.33 V
$E^{T_1}_{0,0}$(kcal/mol)	61.8	44.7	49.0

[a]Conditions: **72** (1.0 equiv), **74** (2.0 equiv), photocatalyst (2 mol%), additive (3.0 equiv), rt. [b]Yields determined by ^1H NMR analysis using 1,3,5-trimethoxybenzene as internal standard. [c]Isolated yield on 0.50 mmol scale. [d]Isolated yield on 2.00 mmol scale [e]3:1 4- vs. 2-regioisomeric ratio determined from the crude ^1H NMR. [f]8:1 4- vs. 2-regioisomeric ratio determined from the crude ^1H NMR. [g]Used 365 nm LEDs instead of 455 nm Kessil light for 89 h. [h]All redox potentials reported vs SCE and all values compiled from previous literature reports.[2,4,6,39] [i]Counterion omitted in structure for simplicity.

Next, we conducted a series of experiments to explore the effect of light and photocatalyst on the reaction (**Table 3.1A**, entries 9-11). Irradiating the reaction at 455 nm without photocatalyst

resulted in traces of **75**, but we did observe 66% yield of the product when we used a 365 nm light after 89 hours (entries 8-9). No evidence of an electron donor-acceptor (EDA) complex was observed by UV-Vis spectroscopy, and we propose that the reaction is initiated via direct excitation of **72** to form an excited state species capable of oxidizing **74**. We attribute the prolonged reaction time to inefficient excitation as only a small amount of overlap is observed between the LEDs emission spectrum and the absorption of **72** at 345 nm (see Supporting Information).[44] Furthermore, a photocatalyst with a redox potential incapable of promoting the reduction of **72**, [Mes-Acr]BF_4, is also competent (entry 11).[4] An energy transfer mechanism was considered, but the low triplet state energies exhibited by [Mes-Acr]BF_4 make this pathway unlikely (**Table 3.1B**).

The results in **Table 3.1C** show that activation of the pyridine nitrogen can play a significant role, in some instances. Using $Ru(bpy)_3$, a photocatalyst with insufficient redox potentials to reduce **72** or oxidize **74** from the excited state,[2] and 455 nm irradiation resulted in trace products. In the presence of one equivalent of $BF_3{\cdot}OEt_2$, however, **72** was formed in 47% yield. Here, we hypothesize that **72** reacts with BF_3 to enable single-electron reduction, and indeed, Lewis acid activation of cyanopyridines has been shown to make single-electron transfer to the radical anion intermediate more facile.[33] With this insight, we hypothesize that single-electron oxidation of **74** BF_3 extrusion occurs first when [Mes-Acr]BF_4 is used as the photocatalyst, enabling single-electron reduction of **72**. Conversely, strongly reducing catalysts, such as Ir(ppy)3 presumably initiate the catalytic cycle with reduction of **72**, followed by oxidation of **74**. Electron transfer between the oxidized state of $Ir(ppy)_3$ **74** appears to be disfavored based on redox potentials alone; however, oxidation of BF_3K salts by photocatalysts with insufficient redox potentials has been observed. Despite the similarities in photophysical properties between photocatalysts $Ru(bpy)_3(PF_6)_2$ and $Ir(ppy)_2(dtbbpy)PF_6$, the iridium photocatalyst works well in

the absence of BF_3 additive while $Ru(bpy)_3(PF_6)_2$ requires it. The reason for this is not yet understood and further studies to explain this observation are warranted.

At this stage of our investigations, we conclude that radical zwitterions **69** and **77** are likely reaction intermediates to varying extents depending on the substitution pattern of the substrate and reaction conditions employed. Using optimal catalyst 3DPAFIPN in the presence of 2,6-lutidine may favor the formation of **69** over **77**, potentially indicating that **69** is more reactive in the C–C bond-forming step. Importantly, Stern-Volmer quenching of 3DPAFIPN by pyridyl phosphonium salt **72** occurs (K_{SV} = 14.9 M^{-1} and K_q = 3.55 x 10^9 L mol^{-1} s^{-1}), indicating that zwitterions without boryl stabilization such as **69** are accessible under the reaction conditions without BF_3.[45]

3.5 Scope of Photoredox-Catalyzed Transformations of Pyridylphosphonium Salts

Next, we investigated the scope of pyridylphosphonium salts formed from building block pyridines in this coupling process (**Table 3.2**). 2-Substituted pyridines with electron-withdrawing and electron-donating groups couple effectively (**79**-**81**). Fluoropyridines such as **80** are competent coupling partners, but the presence of any other halogen on the pyridine ring (Cl, Br, or I) failed to provide the desired product with protodehalogenation being a significant decomposition pathway. Aryl and heteroaryl groups are also compatible at the 2-position (**82** and **83**), and no products resulting from the overreduction of the carbon-iodine bond was observed in **84**. An 11:1 regioisomeric mixture of compounds formed when a 3-ethyl substituent was present (**85**), but single isomers formed from 2,3- and 2,5-disubstituted pyridines (**86**-**88**). At present, pyridylphosphonium salts where the phosphonium group is situated at the pyridine 2-position are not successful coupling partners. As a representative example, when we attempted to synthesize

89, we observed significant decomposition of the starting material and only minor amounts (<5%) of the desired compound among other unidentified products.

Table 3.2: Scope of Heterocyclic Phosphonium Salt Coupling Partners

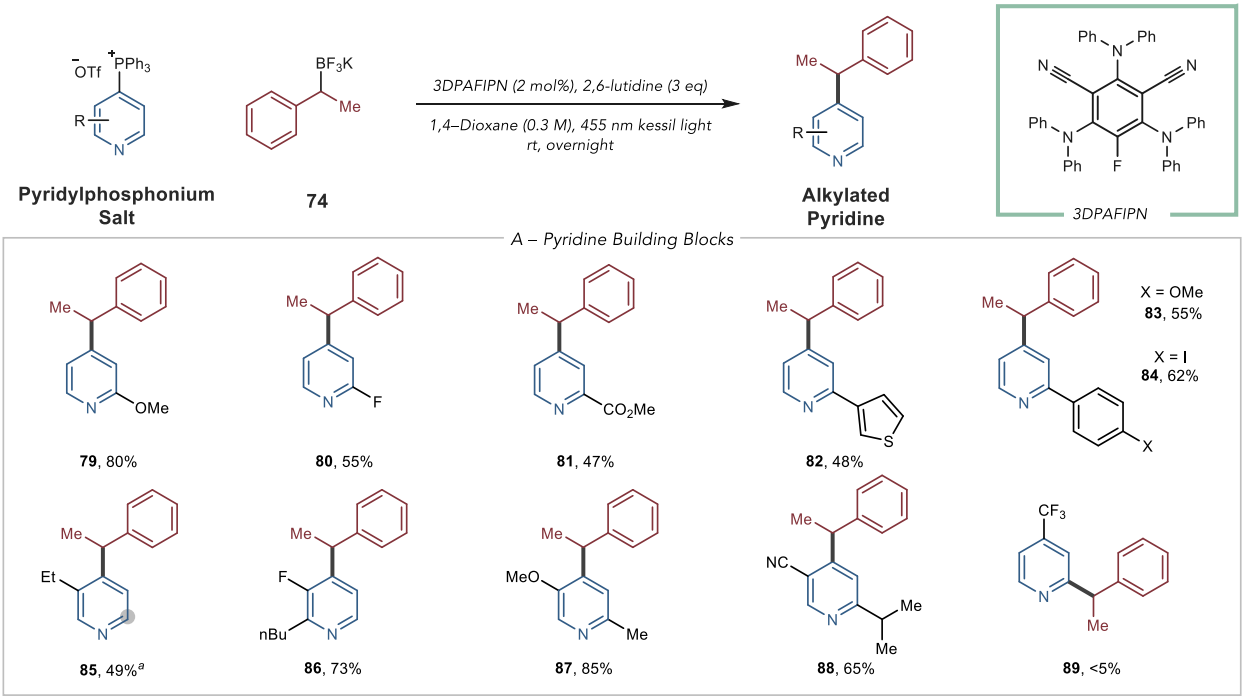

Isolated yields of single regioisomers. Conditions: pyridylphosphonium salt (1.0 equiv), **74** (2.0 equiv. [a]11:1 crude regioisomeric ratio. Grey dot denotes other regioisomer formed.

Next, we converted a series of drug-like fragments and pharmaceuticals into phosphonium salts to test as substrates in this protocol (**Table 3.3**). These examples represent the most significant advantage of this chemistry as installing a cyano group would be challenging from the C–H bond, limiting the use of radical anion chemistry for late-stage derivative synthesis. In addition, these structures contain multiple reactive sites and functional groups that could interfere with the coupling process. Nevertheless, we synthesized benzylated fragments **90**-**94** without difficulty. These substrates demonstrate the protocol's tolerance of basic nitrogen atoms, electron-rich heterocycles that could also conceivably react with free radicals, and aryl halides that can be used as functional handles for later transformations. The pyridine-pyrimidine biaryl **92** is particularly

interesting as the phosphonium salt formed site-selectively on the pyrimidine ring, and the photoredox coupling proceeded in good yield on this heterocycle. Lastly, we demonstrated coupling with four FDA-approved pharmaceuticals and an agrochemical to validate this tactic for late-stage functionalization of complex pyridines (**Figure 3.3 B**). All products were formed with exclusive regioselectivity and left functional groups such as protonated tertiary amines, amides, aryl halides, benzyl ethers, and sulfones intact (**95**-**99**).

Table 3.3: Scope of Complex Pyridine-Containing Coupling Partners

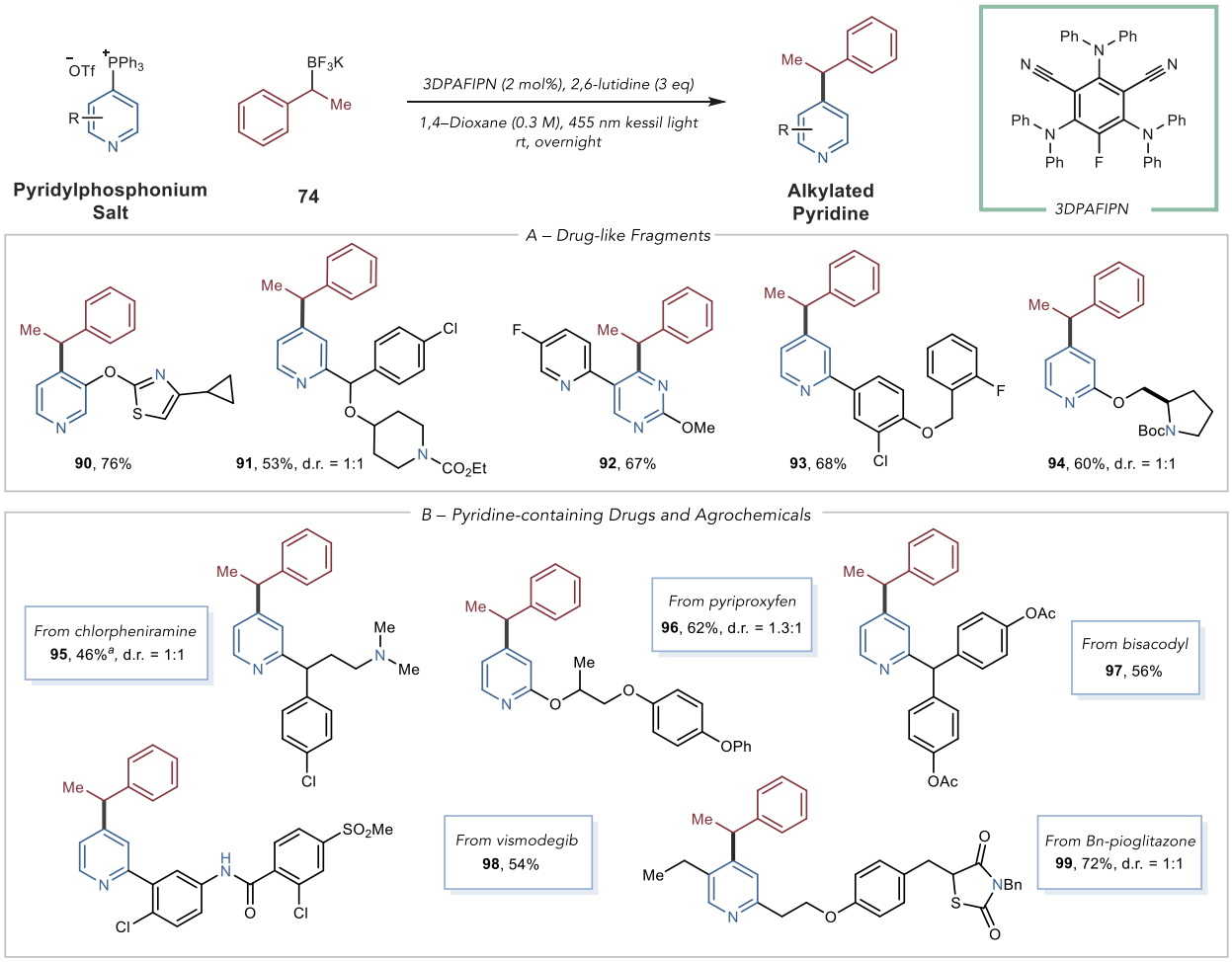

Isolated yields of single regioisomers. Conditions: pyridylphosphonium salt (1.0 equiv), **74** (2.0 equiv. [a]With 1 equiv TfOH.

Table 3.4A shows a selection of viable BF_3K salt coupling partners in the photoredox-catalyzed alkylation reaction. Secondary benzylic salts with electron-withdrawing and electron-donating groups are suitable coupling partners (**100**-**102**), and aryl halides are tolerated to provide functional handles for subsequent transformations. In the case of **101**, we added a 1.2:1 mixture of benzylic and homobenzylic BF_3K salts but only observed the benzylated product, presumably because the primary isomer is more difficult to oxidize. Secondary naphthyl and primary benzylic BF_3K salts are competent coupling partners, resulting in **103** and **104**. The reaction also tolerates α-amino BF_3K salts as evidenced by heterobenzylic amine derivative **105**. These results suggest BF_3K salts that deliver a radical intermediate that is stabilized (benzylic or adjacent to a heteroatom) are competent substrates in this protocol. Attempts to extend this reactivity to a less stabilized radical, such as tert-butyl radical, resulted in trace yield of the desired product. While trifluoroborate salts are attractive coupling partners, a wider range of diverse and commercially abundant carboxylic acid coupling partners are available. In response, we explored the use of pyridylphosphonium salts in a photoredox-catalyzed alkylation reaction using a benzylic carboxylic acid. A preliminary result (unoptimized) was obtained to yield alkylated pyridine **75** in 21% yield as a single regioisomer (**Table 3.4 B**).

Table 3.4: Scope of Alkyl Coupling Partners

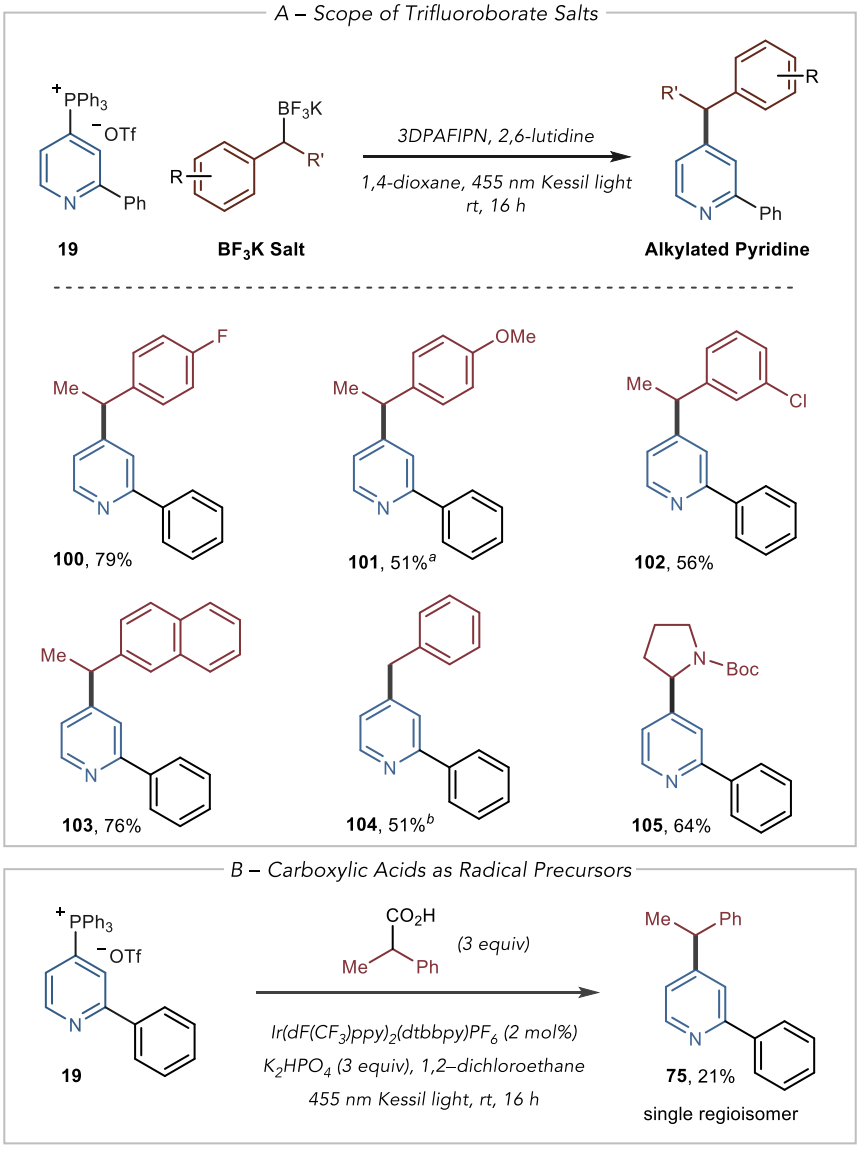

Isolated yields of single regioisomers. Conditions: **19** (1.0 equiv), BF_3K salt (2.0 equiv), 3DPAFIPN (2 mol%), 2,6-lutidine (3.0 equiv), 1,4-dioxane (0.3 M), rt. [b]BF_3K starting material is 1.2:1 mixture of regioisomers (benzylic:primary). [c]>20:1 regioisomeric ratio and 5.7:1 mono:bis alkylated product in crude ^1H NMR. Isolated as single monoalkylated regioisomer.

Finally, we evaluated pyridylphosphonium salts as alternatives to cyanopyridines in radical coupling reactions to construct carbon-heteroatom bonds rather than carbon-carbon bonds. Wu recently reported a method for photoredox-catalyzed amination using cyanopyridines as coupling

partners,[46] and we attempted to replicate this transformation using pyridylphosphonium salts (**Figure 3.4**).15 Exposure of salt **19** to the original reaction conditions and *N*-methylaniline resulted in aminopyridine **106**.16 Similarly, aminopyridine **107** was formed in good yield using N,O-dimethylhydroxylamine as a coupling partner, followed by *in situ* cleavage of the N–O bond. Consistent with the results in **Tables 3.2** and **3.3**, we expect that this reaction will be compatible with more complex pyridine phosphonium salts and further suggests that phosphonium ions can serve as surrogates for cyanopyridines in other radical anion coupling reactions.

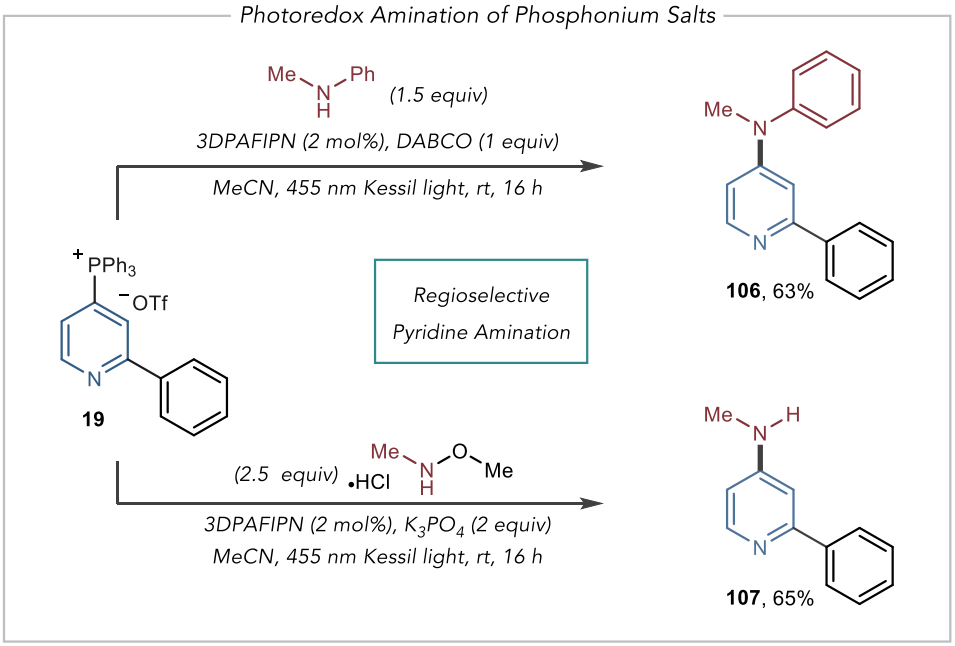

Figure 3.4: Pyridylphosphonium salts in a photoredox-catalyzed amination reaction.

3.6 Conclusion

This chapter details the investigation of pyridylphosphonium salts as alternatives to cyanopyridines in radical-radical coupling reactions under photoredox conditions. The broad scope of the phosphonium salt-forming reaction is merged with the mild reaction conditions employed for radical coupling reactions. Pyridylphosphonium salts enable the use of complex

pyridines in this regime, where installation of a cyano group would be challenging. A photoredox-catalyzed alkylation of complex pyridines was achieved using abundant trifluoroborate salts and carboxylic acids as coupling partners. The alkylation is 4-selective in almost all cases and serves as an alternative to the Minisci reaction, which is generally 2-selective. Additionally, pyridylphosphonium salts can replace cyanopyridines in a radical-mediated amination reaction to synthesize aminopyridines.

References

(1) Yan, M.; Lo, J. C.; Edwards, J. T.; Baran, P. S. Radicals: Reactive Intermediates with Translational Potential. *J. Am. Chem. Soc.* **2016**, *138*, 12692–12714.
(2) Prier, C. K.; Rankic, D. A.; MacMillan, D. W. C. Visible Light Photoredox Catalysis with Transition Metal Complexes: Applications in Organic Synthesis. *Chem Rev* **2013**, 42.
(3) Shaw, M. H.; Twilton, J.; MacMillan, D. W. C. Photoredox Catalysis in Organic Chemistry. *J. Org. Chem.* **2016**, *81*, 6898–6926.
(4) Romero, N. A.; Nicewicz, D. A. Organic Photoredox Catalysis. *Chem. Rev.* **2016**, *116*, 10075–10166.
(5) Narayanam, J. M. R.; Stephenson, C. R. J. Visible Light Photoredox Catalysis: Applications in Organic Synthesis. *Chem Soc Rev* **2011**, *40*, 102–113.
(6) Strieth-Kalthoff, F.; James, M. J.; Teders, M.; Pitzer, L.; Glorius, F. Energy Transfer Catalysis Mediated by Visible Light: Principles, Applications, Directions. *Chem. Soc. Rev.* **2018**, *47*, 7190–7202.
(7) Horn, E. J.; Rosen, B. R.; Baran, P. S. Synthetic Organic Electrochemistry: An Enabling and Innately Sustainable Method. *ACS Cent. Sci.* **2016**, *2*, 302–308.
(8) Aycock, R. A.; Wang, H.; Jui, N. T. A Mild Catalytic System for Radical Conjugate Addition of Nitrogen Heterocycles. *Chem. Sci.* **2017**, *8*, 3121–3125.
(9) Boyington, A. J.; Seath, C. P.; Zearfoss, A. M.; Xu, Z.; Jui, N. T. Catalytic Strategy for Regioselective Arylethylamine Synthesis. *J. Am. Chem. Soc.* **2019**, *141*, 4147–4153.
(10) Seath, C. P.; Jui, N. T. Intermolecular Reactions of Pyridyl Radicals with Olefins via Photoredox Catalysis. *Synlett* **2019**, *30*, 1607–1614.
(11) Seath, C. P.; Vogt, D. B.; Xu, Z.; Boyington, A. J.; Jui, N. T. Radical Hydroarylation of Functionalized Olefins and Mechanistic Investigation of Photocatalytic Pyridyl Radical Reactions. *J. Am. Chem. Soc.* **2018**, *140*, 15525–15534.
(12) Costentin, C.; Robert, M.; Savéant, J.-M. Fragmentation of Aryl Halide π Anion Radicals. Bending of the Cleaving Bond and Activation vs Driving Force Relationships. *J. Am. Chem. Soc.* **2004**, *126*, 16051–16057.
(13) Senaweera, S.; Weaver, J. D. Dual C–F, C–H Functionalization via Photocatalysis: Access to Multifluorinated Biaryls. *J. Am. Chem. Soc.* **2016**, *138*, 2520–2523.
(14) Tong, S.; Li, K.; Ouyang, X.; Song, R.; Li, J. Recent Advances in the Radical-Mediated Decyanative Alkylation of Cyano(Hetero)Arene. *Green Synth. Catal.* **2021**, *2*, 145–155.
(15) Anderson, R. G.; Jett, B. M.; McNally, A. A Unified Approach to Couple Aromatic Heteronucleophiles to Azines and Pharmaceuticals. *Angew. Chem. Int. Ed.* **2018**, *57*, 12514–12518.
(16) Dolewski, R. D.; Fricke, P. J.; McNally, A. Site-Selective Switching Strategies to Functionalize Polyazines. *J. Am. Chem. Soc.* **2018**, *140*, 8020–8026.
(17) Dolewski, R.; Hilton, M.; McNally, A. 4-Selective Pyridine Functionalization Reactions via Heterocyclic Phosphonium Salts. *Synlett* **2018**, *29*, 08–14.
(18) Hilton, M. C.; Dolewski, R. D.; McNally, A. Selective Functionalization of Pyridines via Heterocyclic Phosphonium Salts. *J. Am. Chem. Soc.* **2016**, *138*, 13806–13809.
(19) Hilton, M. C.; Zhang, X.; Boyle, B. T.; Alegre-Requena, J. V.; Paton, R. S.; McNally, A. Heterobiaryl Synthesis by Contractive C–C Coupling via P(V) Intermediates. *Science* **2018**, *362*, 799–804.

(20) Zhang, X.; McNally, A. Phosphonium Salts as Pseudohalides: Regioselective Nickel-Catalyzed Cross-Coupling of Complex Pyridines and Diazines. *Angew. Chem. Int. Ed.* **2017**, *56*, 9833–9836.
(21) Zhang, X.; Nottingham, K. G.; Patel, C.; Alegre-Requena, J. V.; Levy, J. N.; Paton, R. S.; McNally, A. Phosphorus-Mediated Sp2–Sp3 Couplings for C–H Fluoroalkylation of Azines. *Nature* **2021**, *594*, 217–222.
(22) Zhang, X.; McNally, A. Cobalt-Catalyzed Alkylation of Drug-Like Molecules and Pharmaceuticals Using Heterocyclic Phosphonium Salts. *ACS Catal.* **2019**, 4862–4866.
(23) Koniarczyk, J. L.; Hesk, D.; Overgard, A.; Davies, I. W.; McNally, A. A General Strategy for Site-Selective Incorporation of Deuterium and Tritium into Pyridines, Diazines, and Pharmaceuticals. *J. Am. Chem. Soc.* **2018**, *140*, 1990–1993.
(24) Patel, C.; Mohnike, M.; Hilton, M. C.; McNally, A. A Strategy to Aminate Pyridines, Diazines, and Pharmaceuticals via Heterocyclic Phosphonium Salts. *Org. Lett.* **2018**, *20*, 2607–2610.
(25) Levy, J. N.; Alegre-Requena, J. V.; Liu, R.; Paton, R. S.; McNally, A. Selective Halogenation of Pyridines Using Designed Phosphine Reagents. *J. Am. Chem. Soc.* **2020**, *142*, 11295–11305.
(26) Koniarczyk, J. L.; Greenwood, J. W.; Alegre-Requena, J. V.; Paton, R. S.; McNally, A. A Pyridine-Pyridine Cross-Coupling Reaction via Dearomatized Radical Intermediates. *Angew. Chem. Int. Ed.* **2019**, *58*, 14882–14886.
(27) McNally, A.; Prier, C. K.; MacMillan, D. W. C. Discovery of an A-Amino C–H Arylation Reaction Using the Strategy of Accelerated Serendipity. *Science* **2011**, *334*, 1114–1116.
(28) Zuo, Z.; MacMillan, D. W. C. Decarboxylative Arylation of α-Amino Acids via Photoredox Catalysis: A One-Step Conversion of Biomass to Drug Pharmacophore. *J. Am. Chem. Soc.* **2014**, *136*, 5257–5260.
(29) Reidl, T. W.; Bandar, J. S. Lewis Basic Salt-Promoted Organosilane Coupling Reactions with Aromatic Electrophiles. *J. Am. Chem. Soc.* **2021**, *143*, 11939–11945.
(30) Cuthbertson, J. D.; MacMillan, D. W. C. The Direct Arylation of Allylic Sp3 C–H Bonds via Organic and Photoredox Catalysis. *Nature* **2015**, *519*, 74–77.
(31) Zhu, S.; Qin, J.; Wang, F.; Li, H.; Chu, L. Photoredox-Catalyzed Branch-Selective Pyridylation of Alkenes for the Expedient Synthesis of Triprolidine. *Nat. Commun.* **2019**, *10*, 749.
(32) Lehnherr, D.; Lam, Y.; Nicastri, M. C.; Liu, J.; Newman, J. A.; Regalado, E. L.; DiRocco, D. A.; Rovis, T. Electrochemical Synthesis of Hindered Primary and Secondary Amines via Proton-Coupled Electron Transfer. *J. Am. Chem. Soc.* **2020**, *142*, 468–478.
(33) Nicastri, M. C.; Lehnherr, D.; Lam, Y.; DiRocco, D. A.; Rovis, T. Synthesis of Sterically Hindered Primary Amines by Concurrent Tandem Photoredox Catalysis. *J. Am. Chem. Soc.* **2020**, *142*, 987–998.
(34) Yu, X.; Tang, J.; Jin, X.; Yamamoto, Y.; Bao, M. Manganese-Catalyzed C−H Cyanation of Arenes with *N* -Cyano- *N-(* 4-Methoxy)Phenyl- *p* -Toluenesulfonamide. *Asian J. Org. Chem.* **2018**, *7*, 550–553.
(35) Zhao, D.; Xu, P.; Ritter, T. Palladium-Catalyzed Late-Stage Direct Arene Cyanation. *Chem* **2019**, *5*, 97–107.
(36) Elbert, B. L.; Farley, A. J. M.; Gorman, T. W.; Johnson, T. C.; Genicot, C.; Lallemand, B.; Pasau, P.; Flasz, J.; Castro, J. L.; MacCoss, M.; Paton, R. S.; Schofield, C. J.; Smith, M. D.;

Willis, M. C.; Dixon, D. J. C−H Cyanation of 6-Ring N-Containing Heteroaromatics. *Eur. J. Chem.* **2017**, *23*, 14733–14737.
(37) Matsui, J. K.; Primer, D. N.; Molander, G. A. Metal-Free C–H Alkylation of Heteroarenes with Alkyltrifluoroborates: A General Protocol for 1°, 2° and 3° Alkylation. *Chem. Sci.* **2017**, *8*, 3512–3522.
(38) Greenwood, J. W.; Boyle, B. T.; McNally, A. Pyridylphosphonium Salts as Alternatives to Cyanopyridines in Radical–Radical Coupling Reactions. *Chem. Sci.* **2021**, *12*, 10538–10543.
(39) Speckmeier, E.; Fischer, T. G.; Zeitler, K. A Toolbox Approach To Construct Broadly Applicable Metal-Free Catalysts for Photoredox Chemistry: Deliberate Tuning of Redox Potentials and Importance of Halogens in Donor–Acceptor Cyanoarenes. *J. Am. Chem. Soc.* **2018**, *140*, 15353–15365.
(40) Tellis, J. C.; Primer, D. N.; Molander, G. A. Single-Electron Transmetalation in Organoboron Cross-Coupling by Photoredox/Nickel Dual Catalysis. *Science* **2014**, *345*, 433–436.
(41) Tellis, J. C.; Amani, J.; Molander, G. A. Single-Electron Transmetalation: Photoredox/Nickel Dual Catalytic Cross-Coupling of Secondary Alkyl β-Trifluoroboratoketones and -Esters with Aryl Bromides. *Org. Lett.* **2016**, *18*, 2994–2997.
(42) Matsui, J. K.; Gutiérrez-Bonet, Á.; Rotella, M.; Alam, R.; Gutierrez, O.; Molander, G. A. Photoredox/Nickel-Catalyzed Single-Electron Tsuji-Trost Reaction: Development and Mechanistic Insights. *Angew. Chem. Int. Ed.* **2018**, *57*, 15847–15851.
(43) Duncton, M. A. J. Minisci Reactions: Versatile CH-Functionalizations for Medicinal Chemists. *MedChemComm* **2011**, *2* (12), 1135. https://doi.org/10.1039/c1md00134e.
(43) Lovett, G. H.; Chen, S.; Xue, X.-S.; Houk, K. N.; MacMillan, D. W. C. Open-Shell Fluorination of Alkyl Bromides: Unexpected Selectivity in a Silyl Radical-Mediated Chain Process. *J. Am. Chem. Soc.* **2019**, *141*, 20031–20036.
(44) Cardinale, L.; Konev, M. O.; Jacobi von Wangelin, A. Photoredox-Catalyzed Addition of Carbamoyl Radicals to Olefins: A 1,4-Dihydropyridine Approach. *Eur. J. Chem.* **2020**, *26*, 8239–8243.
(45) Zhou, C.; Lei, T.; Wei, X.-Z.; Ye, C.; Liu, Z.; Chen, B.; Tung, C.-H.; Wu, L.-Z. Metal-Free, Redox-Neutral, Site-Selective Access to Heteroarylamine via Direct Radical–Radical Cross-Coupling Powered by Visible Light Photocatalysis. *J. Am. Chem. Soc.* **2020**, *142*, 16805–16813.

CHAPTER FOUR

IMINIUM IONS AS A PLATFORM FOR *N*-(HETERO)ARYL PIPERIDINE SYNTHESIS

4.1 Overview

The importance of piperidine in pharmaceuticals, current limitations in the synthesis of piperidine scaffolds, and a new method to synthesis *N*-(hetero)arylpiperidines is presented in this chapter. Complex piperidine scaffolds that are challenging or impossible to synthesis with current technologies are built rapidly using nucleophilic and electrophilic functionalization of isolable iminium salt reagents. This research was executed during a six-month internship as a part of the Merck Future Talent program in the Discovery Process Chemistry group in Boston. Compound synthesis, experimental design, and manuscript preparation were carried out by Jacob Greenwood, Dr. Matthew Larsen, and Dr. Aaron Sather. Compound characterization was completed by Dr. Samantha Burgess and Dr. Yuan Jiang. Dr. Justin Newman provided the x-ray crystallography data. The work was published as a ChemRxiv preprint in 2022 and is currently submitted for peer review for further publication.

4.2 Introduction

Piperidine is the most common heterocycle in FDA-approved drugs and comparably prevalent in drug candidates.[1–5] Piperidine-containing therapeutics have been developed to treat a range of diseases such as cancer, arthritis, chronic pain, depression, and anxiety (**Figure 4.1**). The piperidine scaffold itself, and its substituents, are often responsible for imparting beneficial pharmacological attributes;[6] therefore, methods to synthesize complex, diverse piperidines are in high demand. Ideally, synthetic chemists must be able to introduce any functional group of interest, to any position of the scaffold, to effectively explore structure-activity relationships (SAR) in drug

discovery campaigns. In this context, methods that are amenable to late-stage functionalization are crucial to enabling rapid synthesis of drug candidate analogues.[7] Derivatization of the carbon-backbone of piperidine has been well-documented, but the identity of the group installed on the nitrogen atom also imparts different pharmacological properties to piperidine-containing molecules. Therefore, it is important a variety of groups can also be installed at this position, and this is demonstrated by the FDA-approved drugs in **Figure 4.1**, which exhibit *N*-(hetero)arylpiperidines, an alkylated piperidine, an amide, and two *N*-H piperidines. In particular, *N*-(hetero)arylpiperidines have emerged as attractive building blocks for the design of novel pharmaceuticals that continue to be highly problematic synthetic targets.[8–12] While a variety of strategies exist for the synthesis of piperidines,[13–20] challenges remain that current technology cannot adequately address.

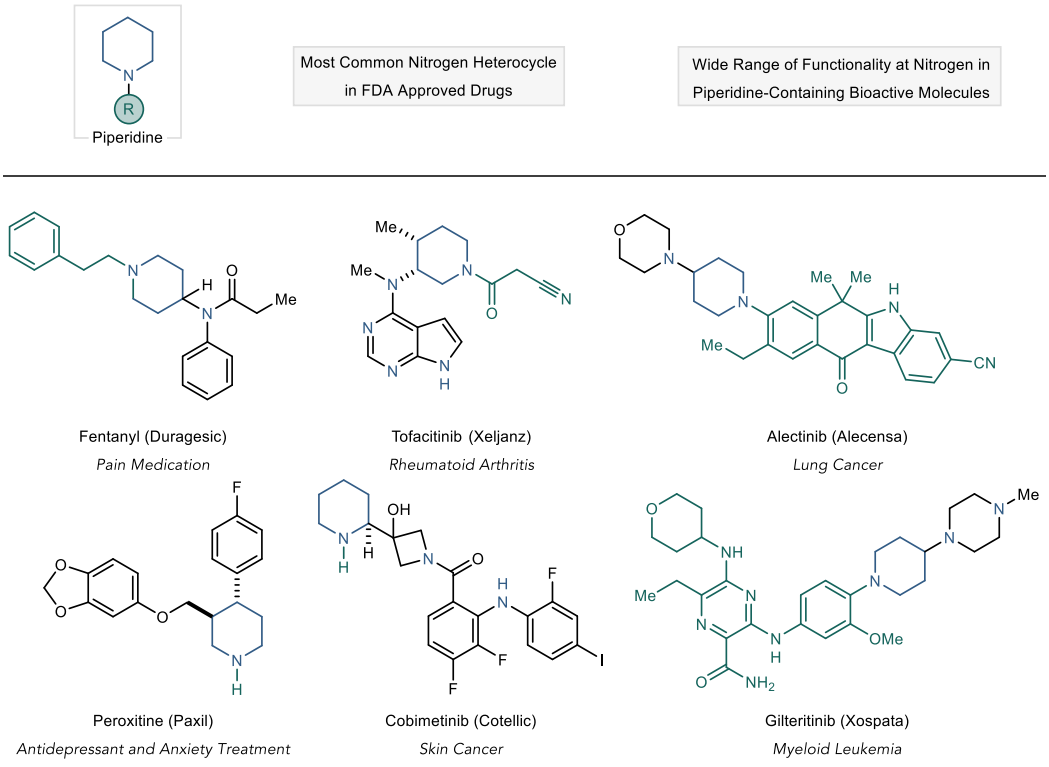

Figure 4.1: FDA-approved drugs containing the piperidine scaffold.

In general, two traditional methods are used to synthesize *N*-(hetero)arylpiperidines: nucleophilic aromatic substitution (S_NAr)[21] or the Buchwald-Hartwig cross coupling reaction between the piperidine of interest and a (hetero)aryl coupling partner.[22] While these strategies are invaluable methods in organic synthesis, deficiencies in both technologies exist depending on the identity of the two coupling partners (**Figure 4.2**). Electron-deficient aryl coupling partners are prerequisites for S_NAr type reactivity, and steric congestion around the amine nucleophile or aryl coupling partner can inhibit product formation (**Figure 4.2A**). Similarly, electron-rich aryl halides are challenging coupling partners in the Buchwald-Hartwig reaction as the increased electron density can impede C-N reductive elimination from the palladium intermediate (**Figure 4.2B**).[23,24] Heteroaryl halides often exhibit Lewis basic atoms that also can coordinate to open sites of the metal center that are required for productive catalysis. Finally, aliphatic secondary amines, such as piperidine, represents a challenging class of amine coupling partner due to their propensity to undergo β-hydride elimination. Additionally, when the amine nucleophile is sterically encumbered, coordination to the metal center to initiate transmetalation can be prevented. The inability to access C2-substituted *N*-(hetero)arylpiperidines is a serious impediment to effective optimization of piperidine-containing drugs, because C2-substitutents, and the increase in three-dimensional complexity they engender, are important means of suppressing oxidative metabolism of the piperidine ring and improving the drug's solubility, respectively.[25–28]

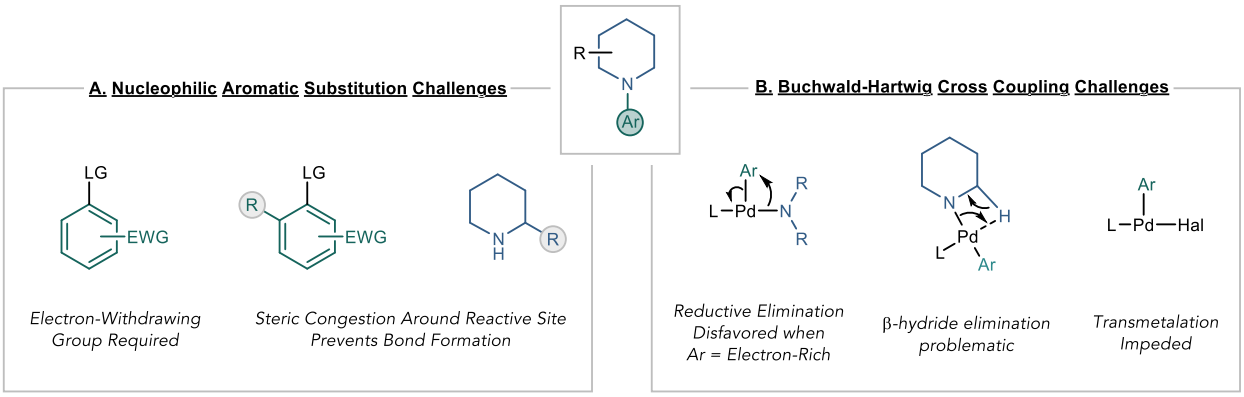

Figure 4.2: Limitations in traditional strategies for *N*-(hetero)arylpiperidine synthesis.

In recent years, important advancements have been reported to improve the scope of attainable *N*-heteroarylpiperidines. The Buchwald group developed the first palladium catalyst that enabled Buchwald-Hartwig cross coupling between α-substituted nitrogen heterocycles and arylbromides (**Figure 4.3A**).[29] A relatively modest selection of simple piperidines were coupled in good yield, and the catalyst must be synthesized in three steps, limiting the use of this method as a general platform. In 2019, Sather reported a method for cross coupling piperidines to electron-rich, five-membered (hetero)aryl halides.[30] This class of *N*-heteroarylpiperidines was of broad interest during a drug discovery campaign at Merck, but was inaccessible with the current metal-catalyzed technology. A productive palladium catalyst was discovered that catalyzed the desired transformation, but the inclusion of just a methyl group at the C2-position of the piperidine coupling partner rendered the reaction ineffective (**Figure 4.2B, 108**). In 2020, Sather presented an alternative approach to access the desired compound via a modular cyclization strategy between (hetero)arylamines and bis(electrophiles) (**Figure 4.3C**).[24] Reductive amination between ketoacrylate **109** and amine **110** occurred to form intermediate **111**, which could engage in a diastereoselective cyclization in the presence of methanol and water to furnish the desired product **112** in good yield.

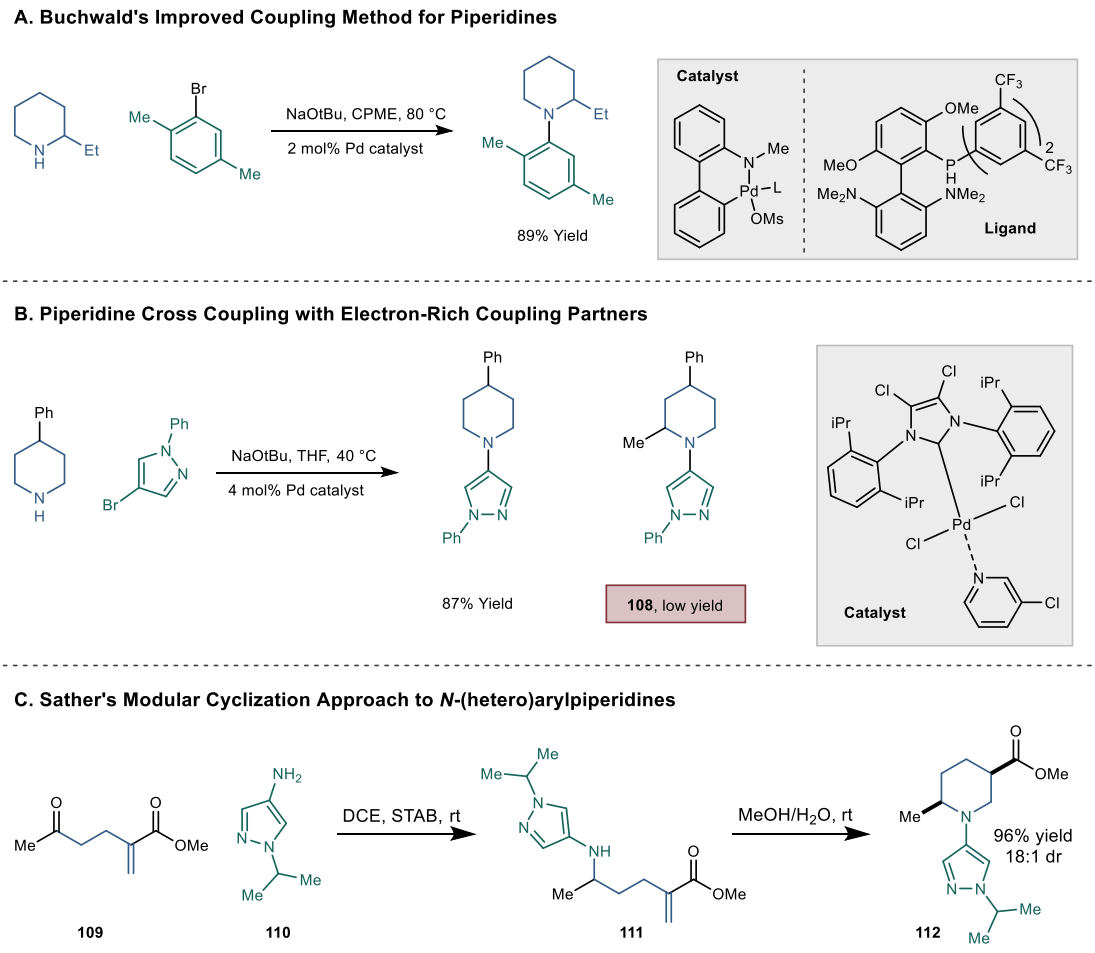

Figure 4.3: Modern advancements in *N*-(hetero)arylpiperidine synthesis.

These methods are valuable to the synthetic community but leave little opportunity for further elaboration of the key piperidine scaffold. We envisioned an alternative approach wherein heterocyclic amine nucleophiles could react with a ketoacrylate bis(electrophile) in the absence of a reducing agent via tandem condensation/aza-Michael sequence to yield either a cyclic enamine or iminium intermediate (**Figure 4.4**, **113** or **114**).[31] If the key tetrahydropiperidine intermediate could be formed, we were interested in leveraging the bimodal reactivity of this intermediate to achieve rapid diversification using either nucleophilic or electrophilic co-reactants to install substituents at C2 or C3, respectively.[32–42] The success of either derivatization strategy would greatly expand synthetic access to polyfunctionalized piperidines.

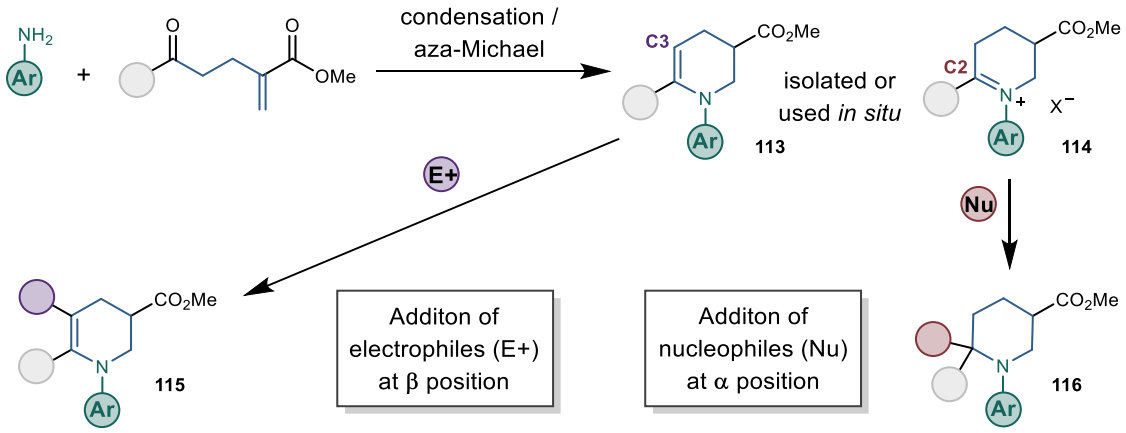

Figure 4.4: Strategy for piperidine synthesis using tetrahydropiperidine intermediates.

4.3 Reaction Optimization

We probed the feasibility of our cyclization strategy by selecting ketoacrylate **109** and amine **110** as starting materials to provide a route to a challenging class of building blocks (**Table 4.1**). We used alcoholic solvents in our starting conditions, as they are frequently effective for both condensation reactions and aza-Michael transformations. Simply heating **109** and **110** in methanol did not provide detectable amounts of product (Entry 1). Encouraged by reports that lithium salts promote some aza-Michael processes,[43] we investigated whether Lewis-acids would facilitate the proposed cyclization. Indeed, inclusion of lithium tetrafluoroborate ($LiBF_4$, 1.0 equiv) led to significant formation of iminium salt **114** (Entry 2). The iminium salt was sufficiently stable to isolate via column chromatography, and its structure was confirmed through NMR analysis and single-crystal X-ray diffraction. Interestingly, cyclic enamine **113** was not detected under the reaction conditions but could be obtained using a base to promote tautomerization (*vide infra*). Other Lewis acids (see Supporting Information) were inferior to $LiBF_4$, which is abundant and inexpensive. Strong H-bond-donor solvents, such as 2,2,2-trifluoroethanol (TFE), are also known to accelerate aza-Michael reactions,[44] and indeed, they dramatically enhanced the reactivity.

Substituting MeOH with TFE significantly improved the yield of **114** (Entries 2-3), while water suppressed the salt formation, in contrast (Entry 4). Finally, we observed the highest conversion to **114** using a modest excess (1.2 equiv) of $LiBF_4$ (Entries 5-7, Table 1). Importantly, the reaction did not go to completion at 90 °C with equimolar quantities of additive and **110** (Entry 7), and using an excess of aniline to drive conversion, though effective, hampered our efforts to develop a straightforward precipitation protocol for isolating the iminium salt. However, we isolated **114** in good yield with little difficulty on 10.0 mmol scale upon conducting the reaction at 120 °C for 48 hours to push the reaction to completion with an equimolar ratio of the two substrates (Entry 8).

Table 4.1: Effects of solvent, temperature, and additives on iminium salt (114) formation[a,b]

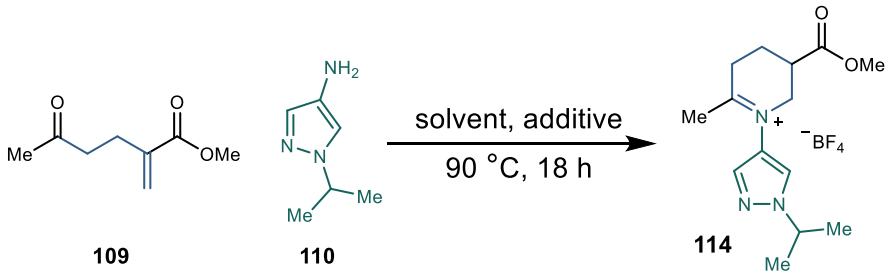

Entry	Solvent	additive	% yield
1	MeOH	-	0
2	MeOH	$LiBF_4$ (1.0 eq)	20
3	TFE	$LiBF_4$ (1.0 eq)	66
4	TFE	Water	11
5	TFE	$LiBF_4$ (0.5 eq)	44
6	TFE	$LiBF_4$ (1.2 eq)	78
7	TFE	$LiBF_4$ (1.5 eq)	45
8	TFE	$LiBF_4$ (1.0 eq)	75[c,d]

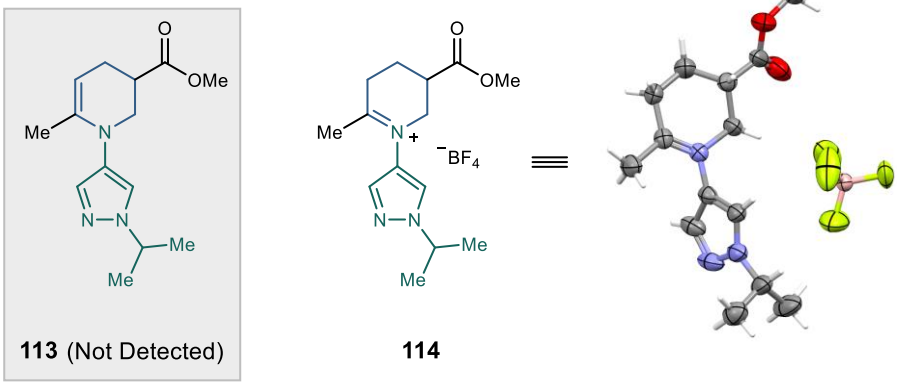

[a]Reactions were conducted on 0.1 mmol scale with 1.0 equiv **109** and 1.5 equiv **110** unless otherwise noted. Cosolvent and water mixtures were 50% v/v. Yields of **114** for individual reaction mixtures were determined using ^{1}H NMR with reference to internal 1,3,5-trimethoxybenzene. [b]Elipsoids for the single crystal x-ray structure of **114** are displayed at 50% probability. [c]The reaction was run in a microwave vial on 10 mmol scale at 120 °C for 48 h using 1.0 equiv **109**, 1.0 equiv **110**, 1.0 equiv $LiBF_4$ and 2.5 mL of TFE. [d]Isolated yield.

4.4 Iminium Salt Derivatization

Having established an optimized procedure for generating the key iminium intermediate, we focused our investigations subsequent derivatization reactions and their application to piperidine library synthesis (**Figure 4.5** and **4.6**). Facile reduction of iminium **114** with sodium triacetoxyborohydride (STAB) or sodium borohydride ($NaBH_4$) gave piperidine **115** (**Figure 4.5**) in good yield and with a very modest preference for the *trans* diastereomer in both cases. Addition of non-hydride nucleophiles smoothly delivered otherwise inaccessible 2,2-disubstituted piperidines (40-80%, **Figure 4.5**). Intermediate **114** proved to be competent for nucleophilic addition of methyl (**117**), trifluoromethyl (**118**), and cyano groups (**116**) Methyl and trifluoromethyl substituents are among the most important substituents for general SAR exploration and drug design, being broadly drug-appropriate low-MW substructures with the ability to enhance binding strength or selectivity, increase metabolic stability, induce advantageous conformational effects, and modulate numerous pharmacologically relevant properties.[45–50] On the other hand, the cyano group serves as a versatile functional handle for subsequent diversification.[51]

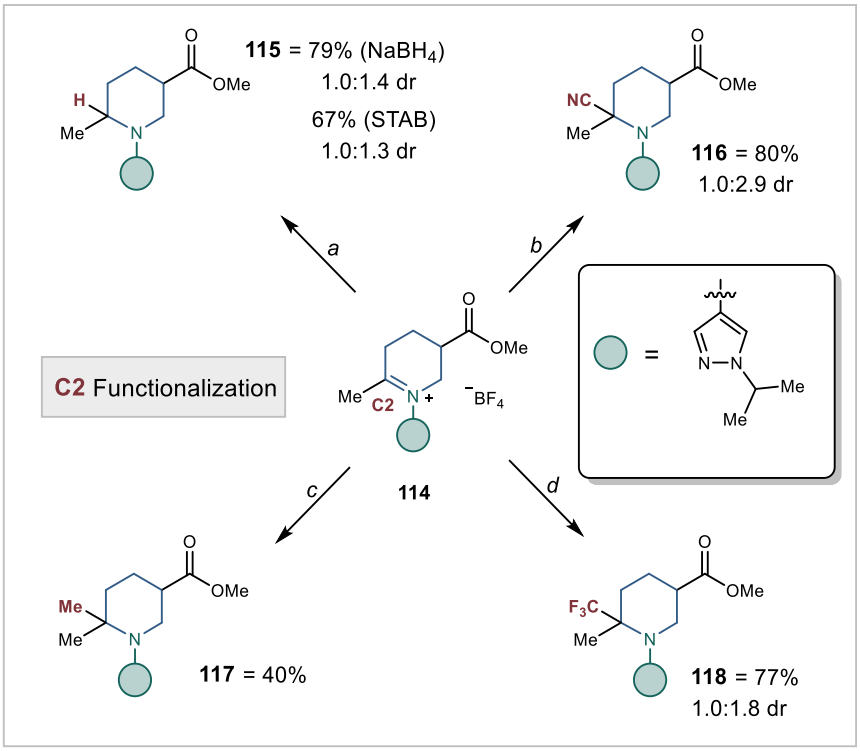

Figure 4.5: Piperidine analogue synthesis via C2-functionalization of salt 114. [a]STAB, DCE, rt. or NaBH4, MeOH, rt. [b]TMSCN, DCM, rt. [c]ZnMe2, Toluene, rt. [d]TMSCF3, KHF2, TFA, IPAc, 50°C. Isolated yields reported.

Next, we investigated base-mediated tautomerization of isolated iminium salts to the corresponding cyclic enamines to engage in C3 electrophilic functionalization. *In situ* tautomerization of iminium salt **114** mediated by Hünig's base occurred to afford the cyclic enamine compound that reacted with several common electrophiles, followed by reduction with STAB, to yield a variety of piperidines bearing synthetically useful functional handles appended to C3 (**Figure 4.6**). For example, rapid acylation with benzoyl chloride or acetyl chloride occurred to provide acylated piperidines in good yield (**119-120**). C_{sp3}-centered electrophiles were also competent reaction partners to furnish allylated and benzylated piperidines **121** and **124**, respectively. Finally, we explored the reactivity of **114** with Michael acceptors. Alkylation reactions proceeded efficiently with both methyl vinyl ketone and ethyl acrylate (**122-123**). Of

note, the transformations in Figures **4.5** and **4.6** exhibited no appreciable stereoselectivity and products are obtained as diastereomeric mixtures. However, when targeting a new drug molecule having multiple diastereomeric forms, it is important to prepare and study the biological activity of all stereoisomers. This is especially true in early drug discovery campaigns, when little information concerning the nature of the binding may be available. Heavy utilization of robust high-throughput purification capabilities for routine synthesis is standard in modern pharmaceutical discovery environments, making non-stereoselective initial preparation of a new analog generally much more efficient than executing multiple syntheses.

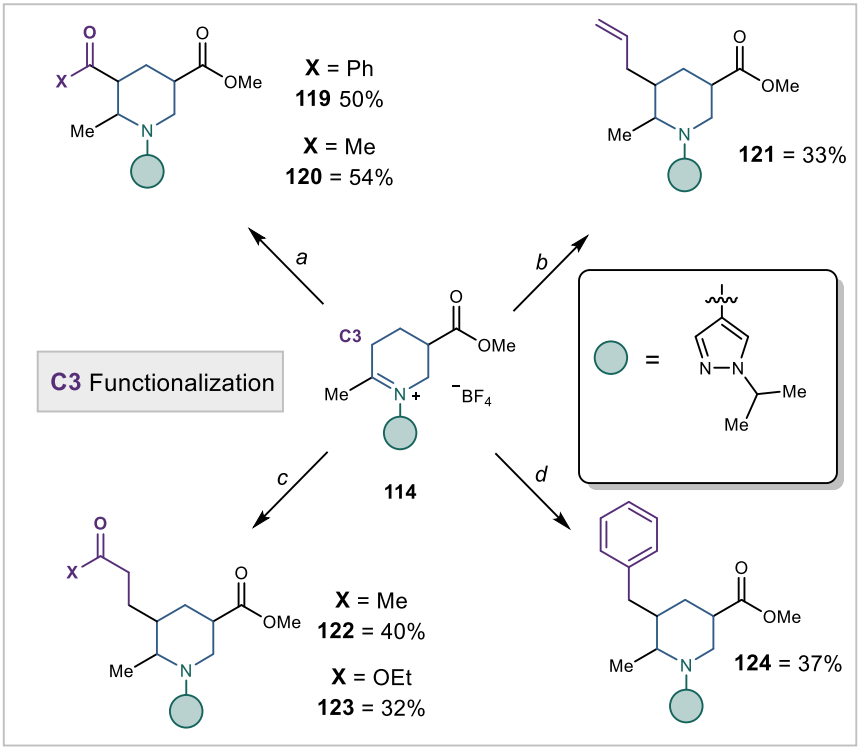

Figure 4.6: Piperidine analogue synthesis via C3-functionalization of salt 114. [a]X = Ph: benzoyl chloride, Hünig's base, DCM, rt, then STAB. X = Me: acetyl chloride, Hünig's base, DCM, rt, then STAB. [b]allyl bromide, Hünig's base, DCM, rt, then STAB. [c]X = Me: methyl vinyl ketone, Hünig's base, DCM, rt, then STAB. X = OEt: methyl acrylate, Hünig's base, DCM, rt, then STAB. dr = (cis:trans). [d]benzyl bromide, Hünig's base, DCM, rt, then STAB. Isolated yields reported.

4.5 Scope of Iminium Salt Formation and Subsequent Transformations

With a suite of transformations now in hand for introducing a variety of substituents to the piperidine scaffold, we began to explore the scope the reaction with respect to the iminium salt (**Table 4.2**). An iminium salt library was synthesized where all reactions were conducted on five mmol scale to showcase the robustness and scalability of the chemistry. Electron-rich, 5-membered heterocycles were the N1-substituents of greatest interest to us due to the challenges for their installation via alternative methods; however, we note that numerous other aryl- and heteroaryl-amine nucleophiles worked well. For example, a fused pyrazolopyridine N1-substituent was efficiently installed (**125**). In addition, aminopyridines and anilines were competent substrates regardless of the electronic bias of the ring (**126**-**128**, and **130**). The procedure tolerates bromoaryl and iodoaryl N1-substituents (**127** and **128**), making the overall diversification strategy complementary to approaches built around cross-coupling technologies. Fluoroarene C-F bonds are typically inert, but undesired displacement of fluorine could occur under the harsh conditions typically employed for challenging S_NAr reactions; however, fluoroaryl groups were well tolerated throughout formation and derivatization reactions of iminium salts **127**, **129**, and **130**. The cyclization also proved to be remarkably insensitive to the presence of steric congestion about the N1-(hetero)aryl bond, readily generating iminium ions such as **128** through **133**.

Table 4.2: Iminium Salt Scope[a]

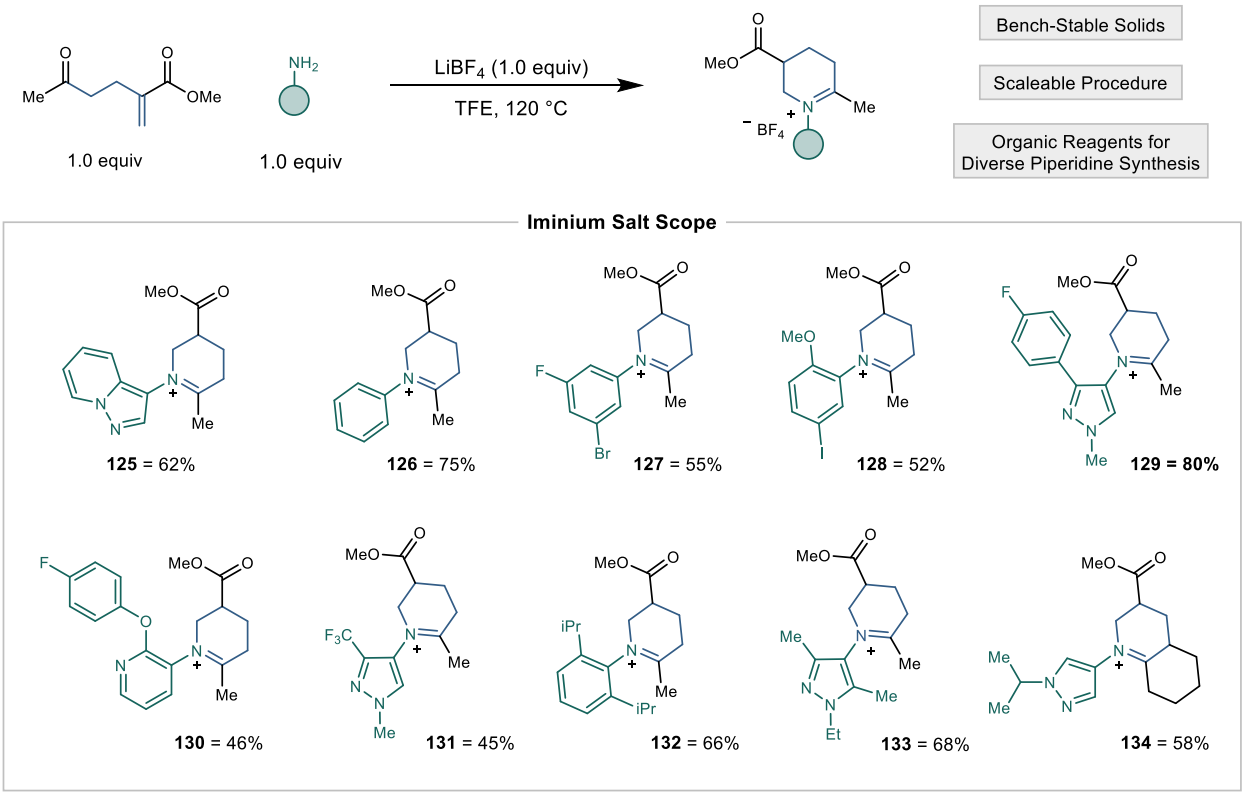

[a]BF_4 counterion omitted for clarity. Isolated yields reported.

Synthesis of C3-functionalized piperidines proceeded effectively using the platform developed in Scheme 2b despite the presence of carbon-halogen bonds, Lewis-basic nitrogen atoms, and steric hinderance around the C-N bond (**135-139**, **Table 4.3A**). Nucleophilic C2-functionalization of the iminium also performs well in sterically demanding environments, with iminium salts derived from 2,6-disubstituted anilines being the only major substrate class to exhibit a prohibitive steric barrier to this transformation (**140-144**, **Table 4.3B**). Additionally, we note that alternative choices for the ketoacrylate substrate can also be an effective strategy for engineering complexity in the piperidine ring, as exemplified in construction of a bicyclic piperidine framework in compounds **134** and **144** (**Tables 4.2** and **4.3B**).

Table 4.3: Iminium Salt Derivatization Scope.

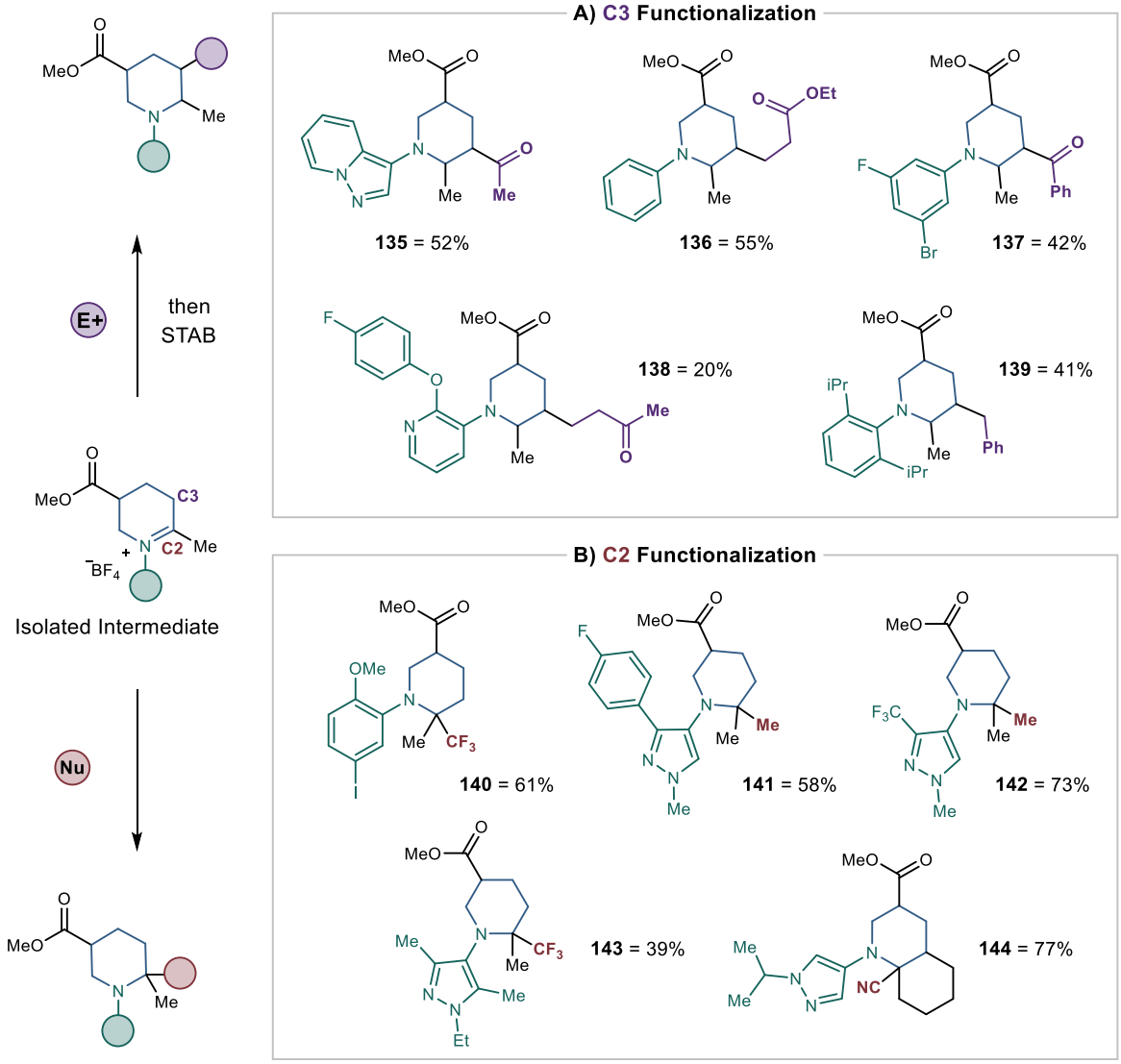

See Supporting Information for Reaction Conditions. Isolated yields reported.

4.6 Development of a Telescoped Process and Sequential Difunctionalization

For diversity-oriented synthesis, it is preferrable for the penultimate synthetic intermediate to be a stable compound that can be prepared in large quantities, stored, and used on demand for small-scale elaboration to a collection of new analogs, providing a primary motivation for developing protocols involving iminium ion isolation. However, a method that avoids an isolation

step could be useful when targeting a single product in a larger-scale preparation, or whenever isolation of the desired iminium salt is unusually challenging. Thus, we investigated the possibility of developing the iminium formation and diversification reactions into a one-pot through-process. We obtained good yields of C2-cyanated or C2-trifluoromethylated piperidines via iminium salts derivatized *in situ* (**Table 4.4**) but found C2-methylation infeasible. We first demonstrated the one-pot protocol using our model substrates (**109** and **110**, **Table 4.1**), obtaining trifluoromethylated piperidine **118** in good yield via the streamlined process. Several other iminium salts prepared from 5-membered, 6-membered, and sterically hindered anilines also reacted smoothly *in situ* to provide the series of derivatives **145**-**147**, which illustrate the readiness with which this methodology can be applied to SAR studies around an N1-(hetero)aryl substituent of interest. Notably, electron-deficient anilines (as exemplified in **145**, **146**, and **150**, **Table 4.4**) required heating at 120 °C for full conversion. Similarly, cyanation proceeded efficiently *in situ* with iminium salts derived from various aniline and aminoheterocycle nucleophiles (**116** and **148**-**150**).

Table 4.4: Scope of C2-Disubstituted Piperidines in the One-Pot Process[a]

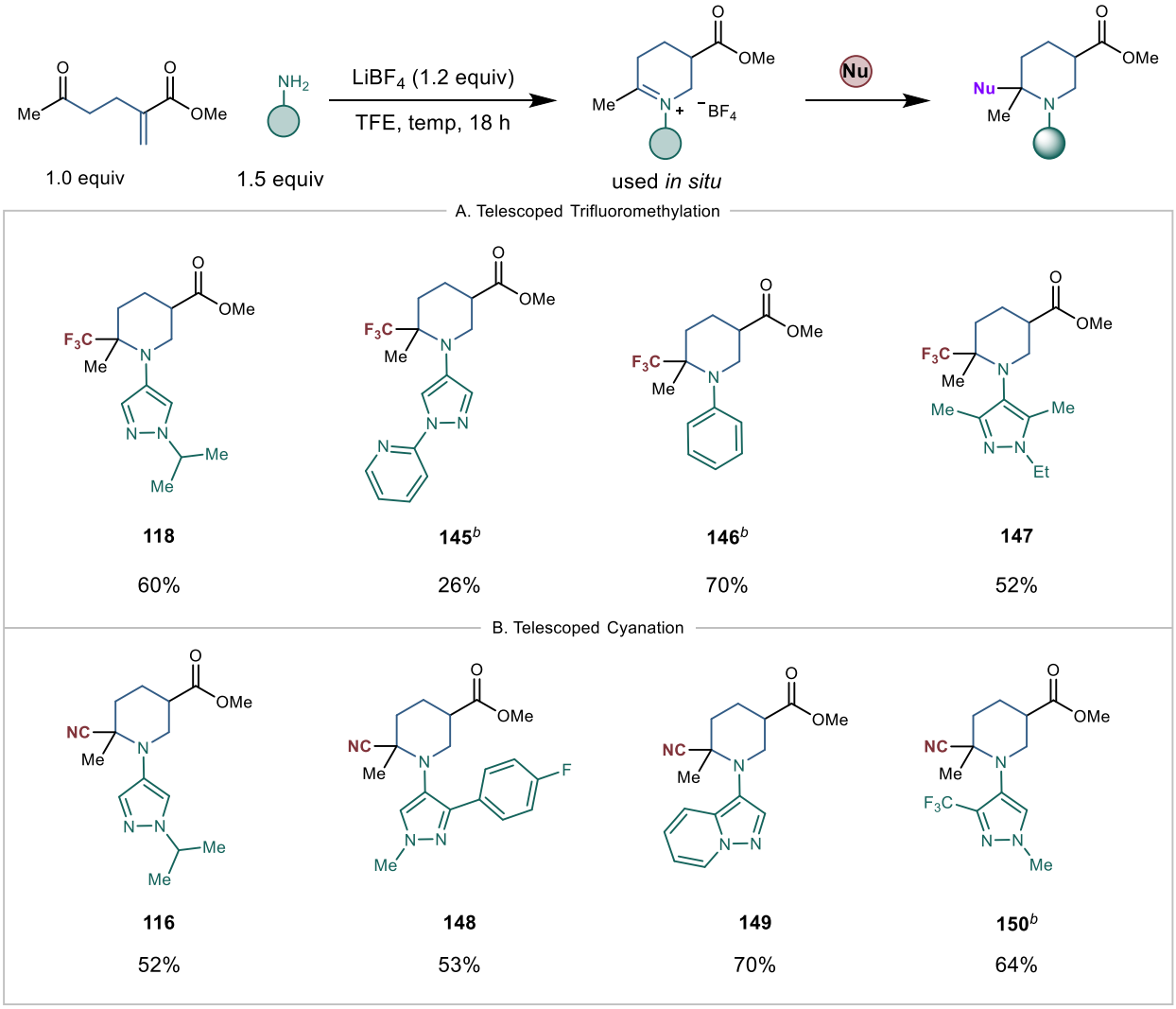

[a]Reactions were conducted on 0.5 mmol scale. Isolated yields reported. Trifluoromethylation conditions: $TSCF_3$, KHF_2, TFA, IPAc, 50°C. Cyanation conditions: TMSCN, DCM, rt. [b]Cyclization run at 120 °C.

Finally, we explored the possibility of using cyclic iminium salts in a one-pot protocol for rapid construction of heavily substituted piperidines by combining the C2 and C3 derivatization reactions (**Figure 4.7**). Thus, we allowed iminium salt **114** to undergo reaction with methyl vinyl ketone to form the β-functionalized intermediate iminium **114a**. Subsequent treatment with TMSCN *in situ* led to extensive formation of desired product **152** along with a byproduct resulting

from over-cyanation at the ketone. Deprotection of the cyanohydrin with TBAF provided **152** in 61% yield. Similarly, iminium salt **129** underwent allylation yielding **129a**, followed by *in situ* cyanation to provide **153**. Lastly, inspired by a recent report from Qiu and co-workers,[52] we acylated iminium salt **151** and subjected the resulting enamine **154** to stepwise fluorocyanation to provide hexasubstituted piperidine **154**, which bears two contiguous exhaustively functionalized carbon atoms.

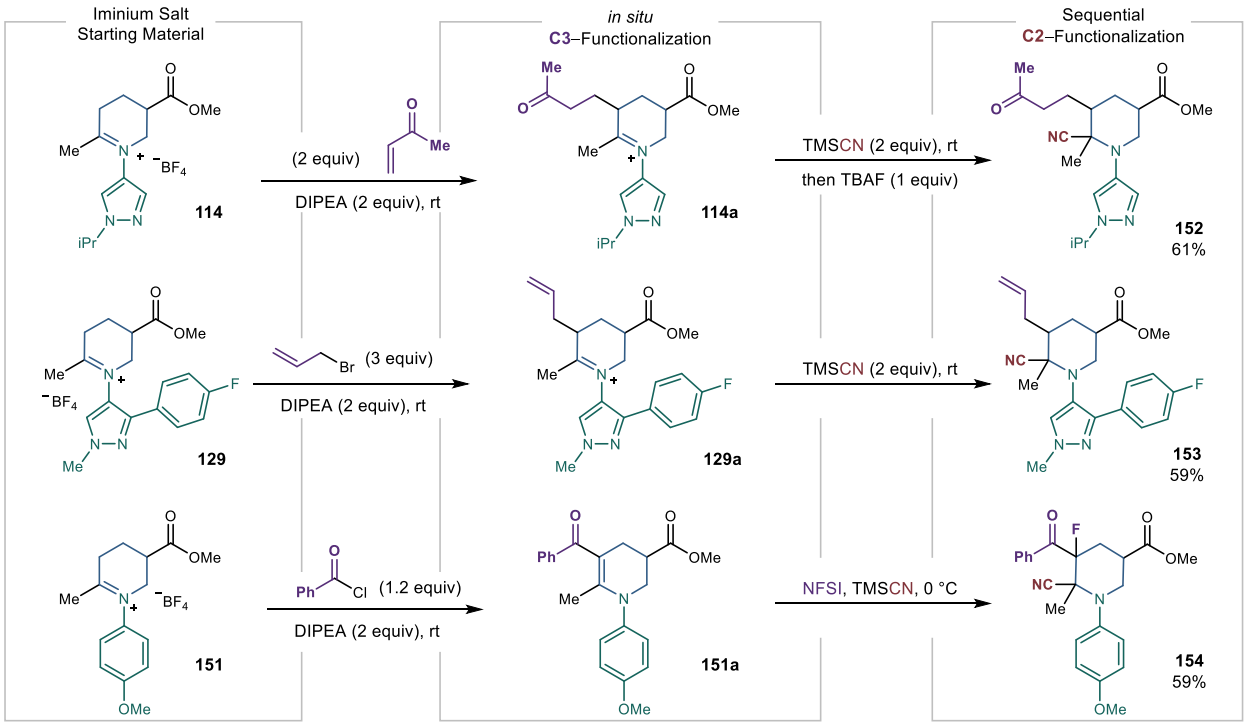

Figure 4.7: Sequential C3/C2 difunctionalization of iminium salts. Reactions were conducted on a 0.5 mmol scale. Isolated yields are reported.

4.7 Conclusion

In this chapter, a method for the synthesis of complex, medicinally relevant *N*-(hetero)arylpiperidines is described. Simple ketoacrylate electrophiles and widely available aniline nucleophiles are combined to provide access to cyclic iminium intermediates that can be harnessed

as a platform for piperidine derivatization. These intermediates can react as C3-nucleophiles after tautomerization to the corresponding enamine or as C2-electrophiles in their native iminium form, enabling synthesis of valuable *N*-(hetero)arylpiperidine derivatives using a common precursor. While the method has broad applicability, we expect that it will be especially useful for accelerating the discovery and optimization of novel piperidine-containing small-molecule drug candidates. Additionally, we report a convenient one-pot protocol that circumvents iminium ion isolation. Finally, sequential C3/C2 functionalization of the key intermediates salts was demonstrated to form densely functionalized piperidines.

References

(1) Vitaku, E.; Smith, D. T.; Njardarson, J. T. Analysis of the Structural Diversity, Substitution Patterns, and Frequency of Nitrogen Heterocycles among U.S. FDA Approved Pharmaceuticals: Miniperspective. *J. Med. Chem.* **2014**, *57*, 10257–10274.

(2) Taylor, R. D.; MacCoss, M.; Lawson, A. D. G. Rings in Drugs: Miniperspective. *J. Med. Chem.* **2014**, *57*, 5845–5859.

(3) Abdelshaheed, M. M.; Fawzy, I. M.; El-Subbagh, H. I.; Youssef, K. M. Piperidine Nucleus in the Field of Drug Discovery. *Future J. Pharm. Sci.* **2021**, *7*, 188.

(4) Källström, S.; Leino, R. Synthesis of Pharmaceutically Active Compounds Containing a Disubstituted Piperidine Framework. *Bioorg. Med. Chem.* **2008**, *16*, 601–635.

(5) Bhutani, P.; Joshi, G.; Raja, N.; Bachhav, N.; Rajanna, P. K.; Bhutani, H.; Paul, A. T.; Kumar, R. U.S. FDA Approved Drugs from 2015–June 2020: A Perspective. *J. Med. Chem.* **2021**, *64*, 2339–2381.

(6) Schnider, P.; Dolente, C.; Stalder, H.; Martin, R. E.; Reinmüller, V.; Marty, R.; Wyss Gramberg, C.; Wagner, B.; Fischer, H.; Alker, A. M.; Müller, K. Modulation of Pharmacologically Relevant Properties of Piperidine Derivatives by Functional Groups in an Equatorial or Axial B-Position to the Amino Group. *ChemBioChem* **2020**, *21*, 212–234.

(7) Cernak, T.; Dykstra, K. D.; Tyagarajan, S.; Vachal, P.; Krska, S. W. The Medicinal Chemist's Toolbox for Late Stage Functionalization of Drug-like Molecules. *Chem. Soc. Rev.* **2016**, *45*, 546–576.

(8) Goel, P.; Alam, O.; Naim, M. J.; Nawaz, F.; Iqbal, M.; Alam, M. I. Recent Advancement of Piperidine Moiety in Treatment of Cancer- A Review. *Eur. J. Med. Chem.* **2018**, *157*, 480–502.

(9) Semple, G.; Fioravanti, B.; Pereira, G.; Calderon, I.; Uy, J.; Choi, K.; Xiong, Y.; Ren, A.; Morgan, M.; Dave, V.; Thomsen, W.; Unett, D. J.; Xing, C.; Bossie, S.; Carroll, C.; Chu, Z.-L.; Grottick, A. J.; Hauser, E. K.; Leonard, J.; Jones, R. M. Discovery of the First Potent and Orally Efficacious Agonist of the Orphan G-Protein Coupled Receptor 119. *J. Med. Chem.* **2008**, *51*, 5172–5175.

(10) Paruch, K.; Dwyer, M. P.; Alvarez, C.; Brown, C.; Chan, T.-Y.; Doll, R. J.; Keertikar, K.; Knutson, C.; McKittrick, B.; Rivera, J.; Rossman, R.; Tucker, G.; Fischmann, T.; Hruza, A.; Madison, V.; Nomeir, A. A.; Wang, Y.; Kirschmeier, P.; Lees, E.; Parry, D.; Sgambellone, N.; Seghezzi, W.; Schultz, L.; Shanahan, F.; Wiswell, D.; Xu, X.; Zhou, Q.; James, R. A.; Paradkar, V. M.; Park, H.; Rokosz, L. R.; Stauffer, T. M.; Guzi, T. J. Discovery of Dinaciclib (SCH 727965): A Potent and Selective Inhibitor of Cyclin-Dependent Kinases. *ACS Med. Chem. Lett.* **2010**, *1*, 204–208.

(11) Sakairi, M.; Kogami, M.; Torii, M.; Kataoka, H.; Fujieda, H.; Makino, M.; Kataoka, D.; Okamoto, R.; Miyazawa, T.; Okabe, M.; Inoue, M.; Takahashi, N.; Harada, S.; Watanabe, N. Synthesis and SAR Studies of Bicyclic Amine Series GPR119 Agonists. *Bioorg. Med. Chem. Lett.* **2012**, *22*, 5123–5128.

(12) Watson, K. G.; Brown, R. N.; Cameron, R.; Chalmers, D. K.; Hamilton, S.; Jin, B.; Krippner, G. Y.; Luttick, A.; McConnell, D. B.; Reece, P. A.; Ryan, J.; Stanislawski, P. C.; Tucker, S. P.; Wu, W.-Y.; Barnard, D. L.; Sidwell, R. W. An Orally Bioavailable Oxime Ether Capsid Binder with Potent Activity against Human Rhinovirus. *J. Med. Chem.* **2003**, *46*, 3181–3184.

(13) Liu, G.-Q.; Opatz, T. Recent Advances in the Synthesis of Piperidines: Functionalization of Preexisting Ring Systems. In *Advances in Heterocyclic Chemistry*; Elsevier, 2018; Vol. 125, pp 107–234.
(14) Laschat, S.; Dickner, T. Stereoselective Synthesis of Piperidines. *Synthesis* **2000**, *2000*, 1781–1813.
(15) Weintraub, P. M.; Sabol, J. S.; Kane, J. M.; Borcherding, D. R. Recent Advances in the Synthesis of Piperidones and Piperidines. *Tetrahedron* **2003**, *59*, 2953–2989.
(16) Stateman, L. M.; Dare, R. M.; Paneque, A. N.; Nagib, D. A. Aza-Heterocycles via Copper-Catalyzed, Remote C–H Desaturation of Amines. *Chem* **2022**, *8*, 210-224.
(17) Zhang, Z.; Zhang, X.; Nagib, D. A. Chiral Piperidines from Acyclic Amines via Enantioselective, Radical-Mediated δ C–H Cyanation. *Chem* **2019**, *5*, 3127–3134.
(18) Buffat, M. G. P. Synthesis of Piperidines. *Tetrahedron* **2004**, *60*, 1701–1729.
(19) Chang, M.; Huang, Y.; Liu, S.; Chen, Y.; Krska, S. W.; Davies, I. W.; Zhang, X. Asymmetric Hydrogenation of Pyridinium Salts with an Iridium Phosphole Catalyst. *Angew. Chem. Int. Ed.* **2014**, *53* (47), 12761–12764. https://doi.org/10.1002/anie.201406762.
(20) Huang, Y.; Liu, S.; Liu, Y.; Chen, Y.; Weisel, M.; Williamson, R. T.; Davies, I. W.; Zhang, X. A Mechanistic Investigation of an Iridium-Catalyzed Asymmetric Hydrogenation of Pyridinium Salts. *Tetrahedron* **2018**, *74* (17), 2182–2190. https://doi.org/10.1016/j.tet.2018.03.031.
(19) Vlasov, V. M. Nucleophilic Substitution of the Nitro Group, Fluorine and Chlorine in Aromatic Compounds. *Russ. Chem. Rev.* **2003**, *72*, 681–703.
(20) Ruiz-Castillo, P.; Buchwald, S. L. Applications of Palladium-Catalyzed C–N Cross-Coupling Reactions. *Chem. Rev.* **2016**, *116*, 12564–12649.
(23) Sather, A. C.; Martinot, T. A. Data-Rich Experimentation Enables Palladium-Catalyzed Couplings of Piperidines and Five-Membered (Hetero)Aromatic Electrophiles. *Org. Process Res. Dev.* **2019**, *23* (8), 1725–1739. https://doi.org/10.1021/acs.oprd.9b00233.
(22) Larsen, M. A.; Hennessy, E. T.; Deem, M. C.; Lam, Y.; Saurí, J.; Sather, A. C. A Modular and Diastereoselective 5 + 1 Cyclization Approach to N-(Hetero)Aryl Piperidines. *J. Am. Chem. Soc.* **2020**, *142*, 726–732.
(23) Bolleddula, J.; DeMent, K.; Driscoll, J. P.; Worboys, P.; Brassil, P. J.; Bourdet, D. L. Biotransformation and Bioactivation Reactions of Alicyclic Amines in Drug Molecules. *Drug Metab. Rev.* **2014**, *46*, 379–419.
(24) Kato, K.; Jingu, S.; Ogawa, N.; Higuchi, S. Differentiation between Isomeric Oxidative Metabolites of a Piperidine-Containing Drug by Liquid Chromatography-Tandem Mass Spectrometry with Stable-Isotope Tracer Technique. *Biomed. Chromatogr.* **2002**, *16*, 25–30.
(25) Lovering, F.; Bikker, J.; Humblet, C. Escape from Flatland: Increasing Saturation as an Approach to Improving Clinical Success. *J. Med. Chem.* **2009**, *52*, 6752–6756.
(28) Hunt, J. A.; Kallashi, F.; Ruzek, R. D.; Sinclair, P. J.; Ita, I.; McCormick, S. X.; Pivnichny, J. V.; Wang, Z.; O'Keefe, S. J.; O'Neill, E. A.; Porter, G.; Thompson, J. E.; Woods, A.; Zaller, D. M.; Doherty, J. B. P38 Inhibitors: Piperidine- and 4-Aminopiperidine-Substituted Naphthyridinones, Quinolinones, and Dihydroquinazolinones. *Bioorg Med Chem Lett* **2003**, 4.

(27) Park, N. H.; Vinogradova, E. V.; Surry, D. S.; Buchwald, S. L. Design of New Ligands for the Palladium-Catalyzed Arylation of α-Branched Secondary Amines. *Angew. Chem. Int. Ed.* **2015**, *54*, 8259–8262.
(30) Sather, A. C.; Martinot, T. A. Data-Rich Experimentation Enables Palladium-Catalyzed Couplings of Piperidines and Five-Membered (Hetero)Aromatic Electrophiles. *Org Process Res Dev* **2019**, 15.
(31) Greenwood, J.; Larsen, M.; Burgess, S.; Newman, J.; Jiang, Y.; Sather, A. C. *Diversity in a Bottle: Iminium Ions as a Platform for N-(Hetero)Aryl Piperidine Synthesis*; preprint; Chemistry, 2022. https://doi.org/10.26434/chemrxiv-2022-3b427.
(32) Bláha, K.; Červinka, O. *Cyclic Enamines and Imines. In Advances in Heterocyclic Chemistry*; Elsevier, 1966; Vol. 6.
(29) Beng, T. K.; Takeuchi, H.; Weber, M.; Sarpong, R. Stereocontrolled Synthesis of Vicinally Functionalized Piperidines by Nucleophilic β-Addition of Alkyllithiums to α-Aryl Substituted Piperidine Enecarbamates. *Chem. Commun.* **2015**, *51*, 7653–7656.
(30) Chen, W.; Ma, L.; Paul, A.; Seidel, D. Direct α-C–H Bond Functionalization of Unprotected Cyclic Amines. *Nat. Chem.* **2018**, *10*, 165–169.
(31) Paul, A.; Seidel, D. α-Functionalization of Cyclic Secondary Amines: Lewis Acid Promoted Addition of Organometallics to Transient Imines. *J. Am. Chem. Soc.* **2019**, *141*, 8778–8782.
(32) Chen, W.; Paul, A.; Abboud, K. A.; Seidel, D. Rapid Functionalization of Multiple C–H Bonds in Unprotected Alicyclic Amines. *Nat. Chem.* **2020**, *12*, 545–550.
(33) Holmberg-Douglas, N.; Choi, Y.; Aquila, B.; Huynh, H.; Nicewicz, D. A. β-Functionalization of Saturated Aza-Heterocycles Enabled by Organic Photoredox Catalysis. *ACS Catal.* **2021**, 3153–3158.
(38) Rappoport, Z. *The Chemistry of Enamines*; Wiley & Sons, 1994.
(36) West, J. A. The Chemistry of Enamines. *J. Chem. Edu.* **1963**, *40*, 194.
(40) Roque, J. B.; Kuroda, Y.; Göttemann, L. T.; Sarpong, R. Deconstructive Diversification of Cyclic Amines. *Nature* **2018**, *564* (7735), 244–248. https://doi.org/10.1038/s41586-018-0700-3.
(41) Roque, J. B.; Kuroda, Y.; Göttemann, L. T.; Sarpong, R. Deconstructive Fluorination of Cyclic Amines by Carbon-Carbon Cleavage. *Science* **2018**, *361* (6398), 171–174. https://doi.org/10.1126/science.aat6365.
(42) Jurczyk, J.; Lux, M. C.; Adpressa, D.; Kim, S. F.; Lam, Y.; Yeung, C. S.; Sarpong, R. Photomediated Ring Contraction of Saturated Heterocycles. *Science* **2021**, *373* (6558), 1004–1012. https://doi.org/10.1126/science.abi7183.
(36) Lad, U. P.; Kulkarni, M. A.; Desai, U. V.; Wadgaonkar, P. P. Lithium Tetrafluoroborate Catalyzed Highly Efficient Inter- and Intramolecular Aza-Michael Addition with Aromatic Amines. *Comptes Rendus Chim.* **2011**, *14*, 1059–1064.
(37) Fedotova, A.; Kondrashov, E.; Legros, J.; Maddaluno, J.; Rulev, A. Yu. Solvent Effects in the Aza-Michael Addition of Anilines. *Comptes Rendus Chim.* **2018**, *21*, 639–643.
(38) Schönherr, H.; Cernak, T. Profound Methyl Effects in Drug Discovery and a Call for New C□H Methylation Reactions. *Angew. Chem. Int. Ed.* **2013**, *52*, 12256–12267.
(39) Aynetdinova, D.; Callens, M. C.; Hicks, H. B.; Poh, C. Y. X.; Shennan, B. D. A.; Boyd, A. M.; Lim, Z. H.; Leitch, J. A.; Dixon, D. J. Installing the "Magic Methyl" – C–H Methylation in Synthesis. *Chem. Soc. Rev.* **2021**, *50*, 5517–5563.

(40) Müller, K.; Faeh, C.; Diederich, F. Fluorine in Pharmaceuticals: Looking Beyond Intuition. *Science* **2007**, *317*, 1881–1886.
(41) Hagmann, W. K. The Many Roles for Fluorine in Medicinal Chemistry. *J. Med. Chem.* **2008**, *51*, 4359–4369.
(42) Zhou, Y.; Wang, J.; Gu, Z.; Wang, S.; Zhu, W.; Aceña, J. L.; Soloshonok, V. A.; Izawa, K.; Liu, H. Next Generation of Fluorine-Containing Pharmaceuticals, Compounds Currently in Phase II–III Clinical Trials of Major Pharmaceutical Companies: New Structural Trends and Therapeutic Areas. *Chem. Rev.* **2016**, *116*, 422–518.
(43) Gritsenko, R. T.; Levin, V. V.; Dilman, A. D.; Belyakov, P. A.; Struchkova, M. I.; Tartakovsky, V. A. Trifluoromethylation of Enamines under Acidic Conditions. *Tetrahedron Lett.* **2009**, *50*, 2994–2997.
(44) Lennox, A. J. J.; Goes, S. L.; Webster, M. P.; Koolman, H. F.; Djuric, S. W.; Stahl, S. S. Electrochemical Aminoxyl-Mediated α-Cyanation of Secondary Piperidines for Pharmaceutical Building Block Diversification. *J. Am. Chem. Soc.* **2018**, *140*, 11227–11231.
(52) Feng, T.; Wang, S.; Liu, Y.; Liu, S.; Qiu, Y. Electrochemical Desaturative β-Acylation of Cyclic N-Aryl Amines. *Angew Chem Int Ed* **2022**, *61*.

CHAPTER FIVE

COMPLEX PIPERIDINE SYNTHESIS ENABLED BY HYDROGENATION OF PYRIDINIUM SALTS

5.1 Overview

This chapter introduces a strategy for complex piperidine synthesis using a variety of commercially available and structurally diverse pyridine starting materials. Limitations in current pyridinium salt forming reactions are introduced and overcome using N-triflylpyridinium salts as an alternative to traditional Zincke salts. Pyridinium ring-opening and ring closure to the corresponding pyridinium salt is demonstrated at low temperature, exhibits a broad functional group tolerance, and 2-substituted pyridines are amenable to the process. Simple hydrogenation of the pyridinium salts with Adam's catalyst occurs rapidly under mild conditions to form piperidines that are challenging to access via other methods. This development of this method has been carried out in collaboration with Merck, as the method is of broad interest to the synthetic community. Jacob Greenwood, Dr. Chirag Patel, Barbara Pio, and Dr. Eric Phillips designed and performed the experiments. Dr. Michael Gribble performed experiments to discover and optimize the asymmetric hydrogenation of *N*-(aryl)pyridinium salts. The project has been directed by Professor Andrew McNally and Dr. Matthew Maddess. Work on this project is ongoing and will be published in due time.

5.2 Introduction

Chapter 4 introduced the prevalence of piperidines in FDA-approved drugs, common strategies used for piperidine synthesis, and current synthetic challenges for accessing *N*-(hetero)arylpiperidines.[1–5] A large percentage of methods for piperidine synthesis can be

categorized as a cyclization reaction of an amine with a 1,5-dicarbonyl electrophile (or a 1,5-dicarbonyl equivalent) (**Figure 5.1A**).[5,6] This approach benefits from a large range of amines that can be used to make various piperidine products, but generally, the key 1,5-dicarbonyl electrophile, with the desired functional group installed, must be synthesized. Complex electrophilic coupling partners may require multiple step syntheses, rendering the strategy more expensive and time-consuming than desired. Alternatively, pyridinium salt hydrogenation is an appealing and well-studied protocol to access piperidines.[7–14] The diversity of commercially available, complex pyridine starting materials makes this strategy attractive for synthetic chemists; however, the conversion of a wide range of pyridine derivatives to the corresponding pyridinium reagents can be challenging. The most common way to make pyridinium salts is via S_N2 or S_NAr activation of the pyridine substrate with a sterically accessible alkyl electrophile or electron-deficient arene (**Figure 5.1B**).[12] During pyridine alkylation, undesired byproducts can form via pyridine-mediated elimination of the leaving group rather than displacement, especially when the electrophile is sterically hindered.[15] To enable pyridine activation via S_NAr reaction, an electron-deficient and sterically accessible coupling partner is a prerequisite.[16]

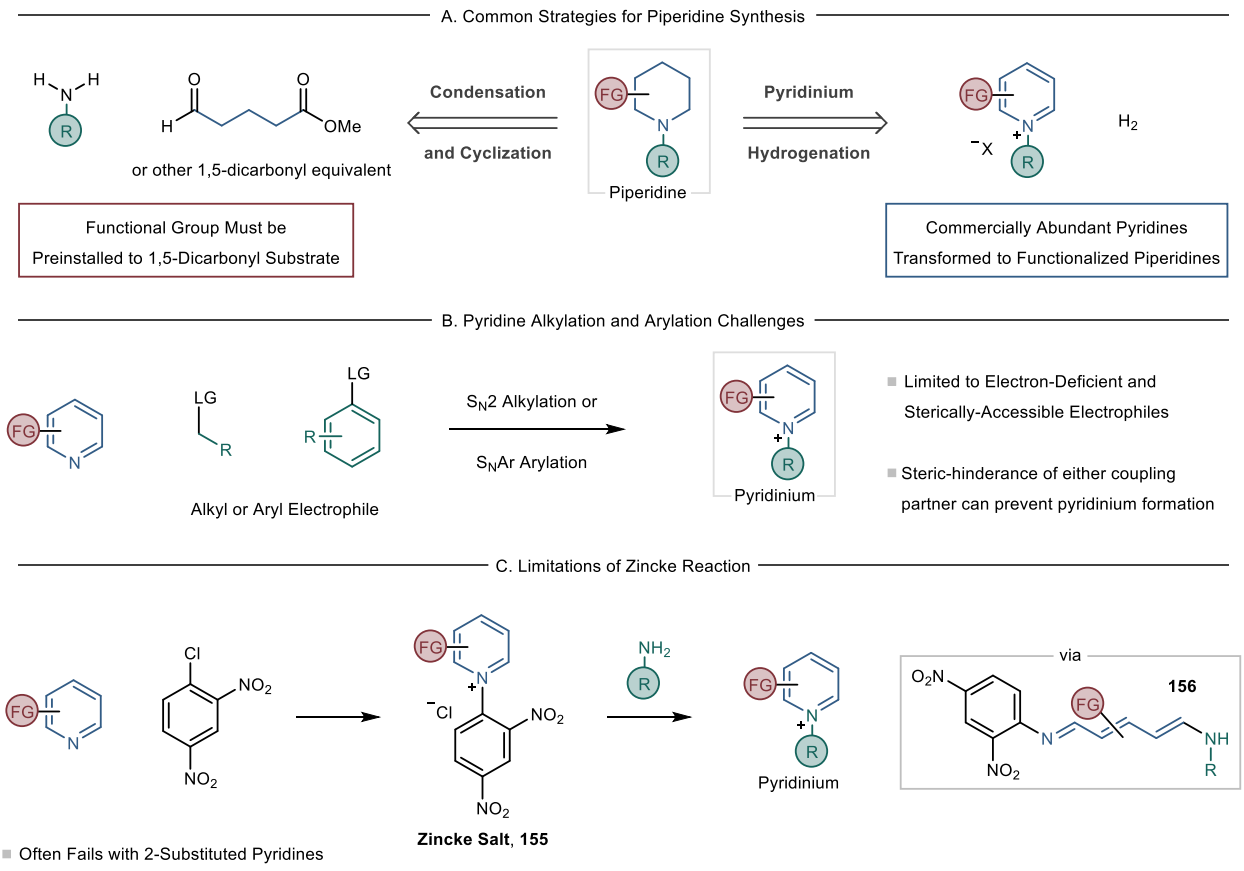

Figure 5.1: Common strategies for piperidine synthesis and limitations in pyridinium salt formation.

The Zincke reaction is a traditional method for transforming a pyridine into a pyridinium salt through a sequence of S_NAr activation, ring-opening to a triene intermediate (such as **156**) and ring-closing with the displacement of dinitroaniline to install the desired group on the pyridine nitrogen atom (**Figure 5.1C**).[17–19] While all these strategies are valuable, pyridine substrates that have a 2-position substituent often fail to undergo the activation step, severely limiting the use of pyridinium hydrogenation as a general strategy towards piperidine synthesis (**Figure 5.2**).[17]

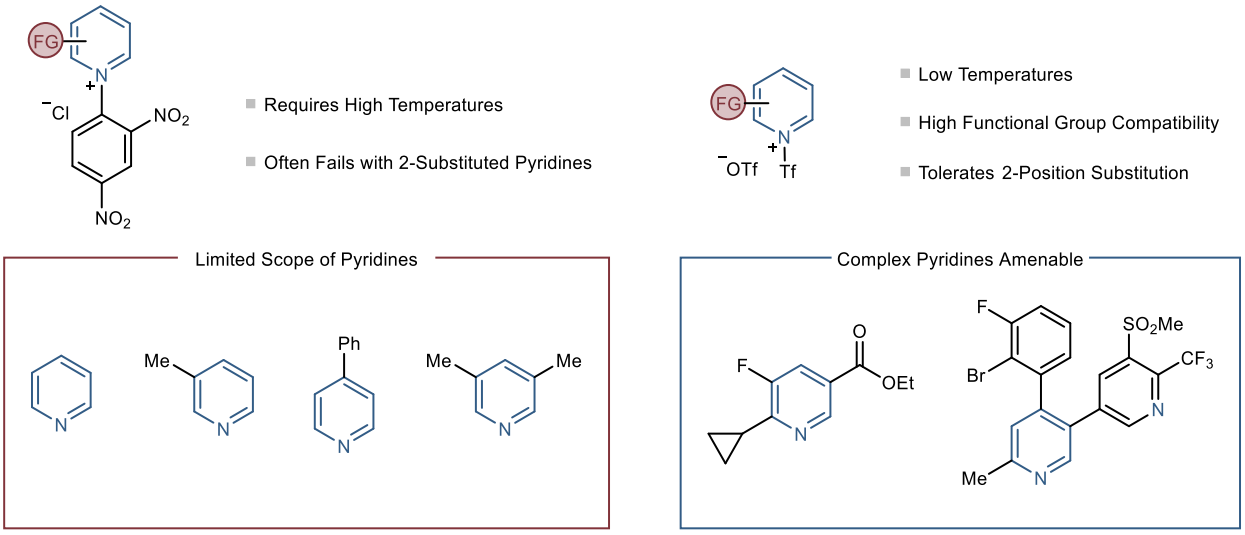

Figure 5.2: Limited scope of traditional Zincke reaction versus triflic anhydride mediated Zincke reaction.

5.3 Improvement of Zincke Reaction via *N*-Triflyl Pyridinium Salts

The McNally group has focused on developing 4-selective methods for pyridine functionalization, but protocols that enable selective derivatization of any other position are also valuable. We were interested in using the Zincke reaction as a general method for pyridine functionalization through a ring-opening, functionalization, and ring-closing strategy (**Figure 5.3**). We envisioned the appropriate combination of a pyridine activator and a nucleophile could promote the conversion of a range of electron-deficient pyridines, regardless of electronic bias or substitution pattern, to electron-rich triazine intermediates, such as **157**, via ring-opening. These intermediates would be more reactive towards electrophiles to enable functionalization of the C3- or C5-positions. Finally, cyclization with ammonia could occur to produce functionalized pyridines.

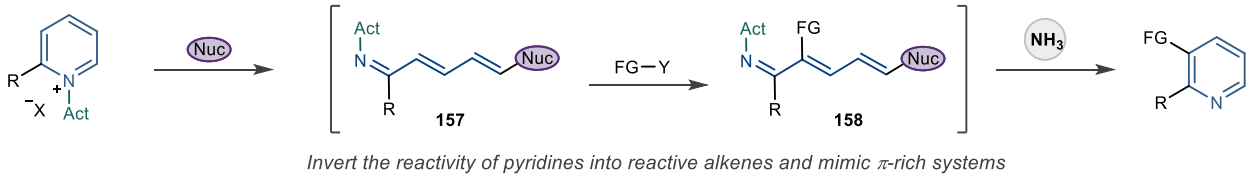

Figure 5.3: Design plan for electrophilic functionalization of pyridines.

In pursuit of this goal, it was discovered that dibenzylamine attacks the 2-position of a variety *N*-triflylpyridiniums in the presence of collidine as a base, followed by ring-opening to the corresponding Zincke imine intermediates (**Table 5.1**). Simple, monosubstituted pyridines were were transformed to the corresponding Zincke imines in good yield with electron donating and electron withdrawing groups at either position (**159**-**162**, **165**). 2,3- and 2,5-disubstituted pyridines also served as competent substrates (**163**-**164**, **166**). More complex, medicinally relevant pyridines were amenable to the protocol, providing the corresponding Zincke imines in good yields, demonstrating the method's functional group tolerance for halogens, trifluoromethyl groups, heterocycles with basic nitrogen atoms, sulfones, ethers, amides, and carbamates (**167**-**172**). Importantly, this reaction occurs at low temperature and tolerates 2-position substituents on the pyridine, addressing limitations currently experienced using traditional conditions for Zincke chemistry. Finally, two sets of conditions were identified for transforming the Zincke imine back to the pyridine starting material (**Table 5.1D** and **E**). Most pyridines will ring-close effectively in the presence of ammonium acetate as the ammonia source in ethanol at 60 °C. Zincke imines that are substituted at the C3- or C5-position were observed to ring close at room temperature in the absence of an ammonia source when exposed to 2 equivalents of trifluoroacetic acid.

Table 5.1: Selected Substrate Scope of Zincke Imine Formation.

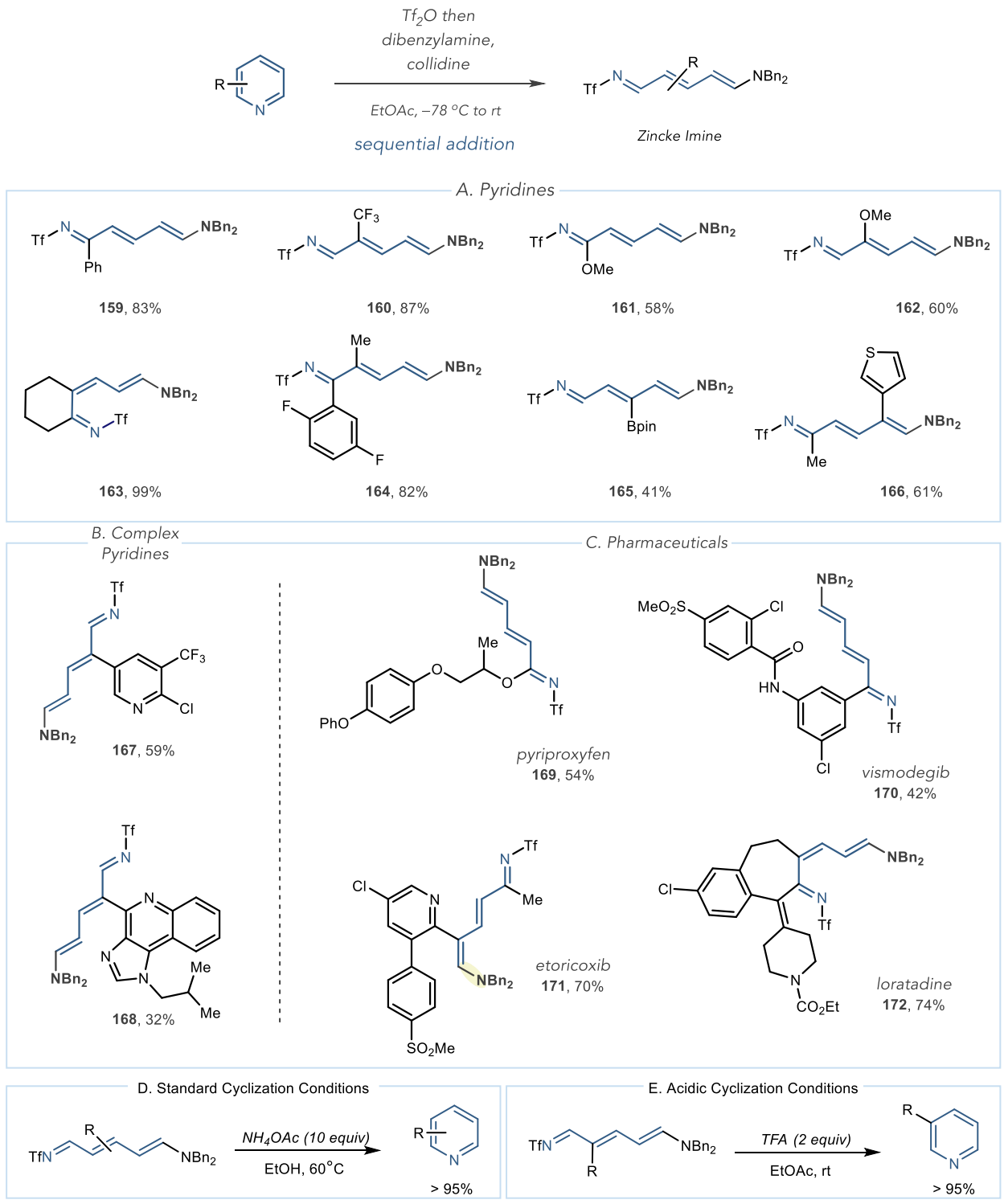

Yields determined by ^{1}H NMR using triphenylmethane as an internal standard.

5.4 Pyridinium Formation from *N*-Triflyl Zincke Imines

With tools to ring-open and ring-close a range of pyridine substrates, the group began to focus on functionalization reactions of the intermediate Zincke imines. We also suspected that the recyclization step could serve as a valuable point of diversification, however. Specifically, we were curious if the ring-closing procedure of *N*-triflyl Zincke imines could be adapted to enable pyridinium formation when using primary amines as a nucleophile, rather than ammonia. This would represent a significant advance over the traditional Zincke reaction because more complex, medicinally relevant pyridines would be amenable to pyridinium formation. Using well-understood pyridinium hydrogenation methodologies, complex piperidines could be accessed from pyridines via the improved Zincke reaction.

As a proof of concept, Zincke adduct 173, derived from 2-phenylpyridine, and 1-butylamine were combined in ethyl acetate at 50 °C for five hours to produce *N*-butylpyridinium salt 174, in high yield after isolation via precipitation (Figure 5.4A). Subsequent hydrogenation of the *N*-butylpyridinium at room temperature with Adam's catalyst under one atmosphere of hydrogen gas produced the desired piperidine 175 in 30 minutes.[13,14] We were also interested in the use of 174 as an electrophile prior to hydrogenation to introduce functionality to the resulting piperidine scaffold. Trifluoromethylation of 174 was achieved using Rupert's reagent in the presence of cesium fluoride to form dihydropyridine 176 in 69% NMR yield.[13,14] Subsequent hydrogenation of this compound also proceeded smoothly to furnish the trifluoromethylated piperidine. Finally, we were interested in extending this protocol to a one-pot reaction where isolation of the intermediate Zincke imine adduct and pyridinium was subverted (Figure 5.4B). Accordingly, 2-phenylpyridine was successfully activated, ring-opened, ring-closed with 1-

butylamine, and reduced by Adam's catalyst in 50% NMR yield in a single-telescoped process with no isolations or workups necessary.

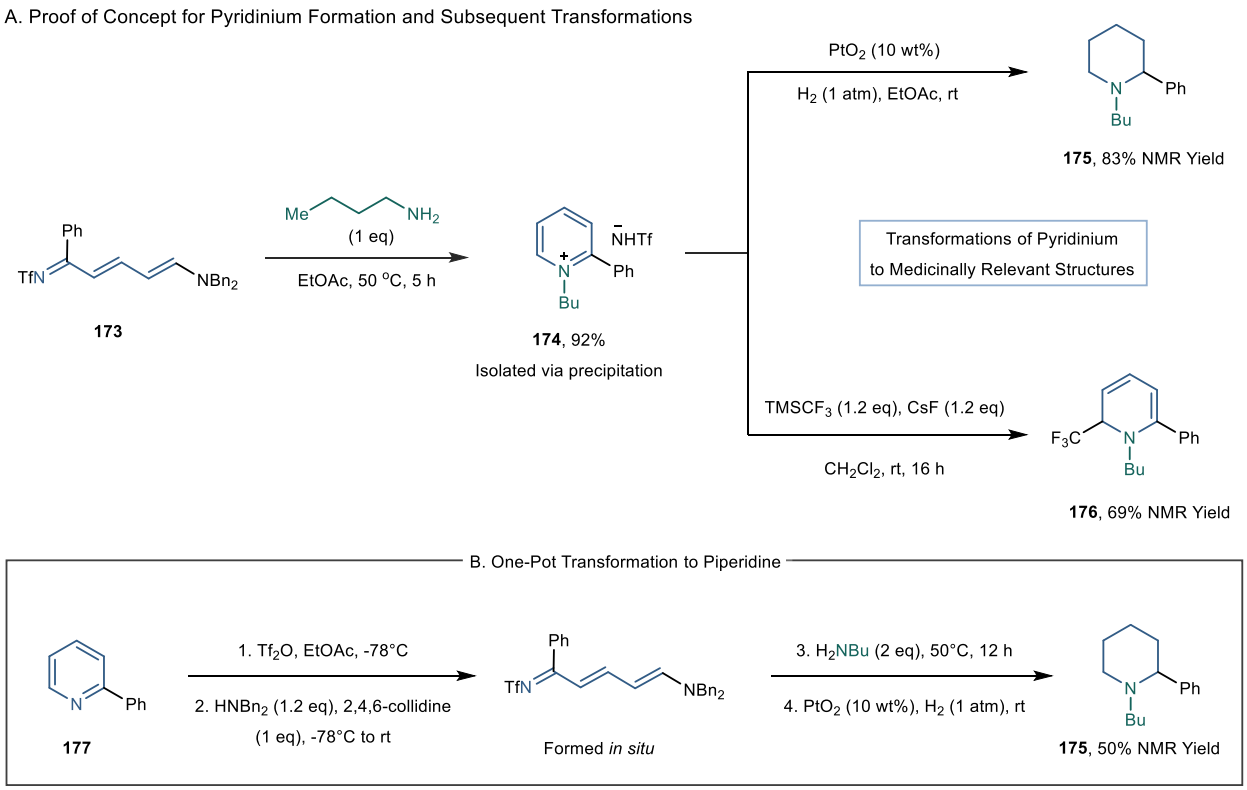

Figure 5.4: *N*-alkylpyridinium formation and subsequent transformations.

Due to the importance of *N*-heteroarylpiperidines in medicinal chemistry and the challenges that exist in current technologies for their synthesis, as discussed in Chapter 4, we attempted to extend this cyclization strategy to include aniline coupling partners (**Figure 5.5**). While cyclization with 1-butylamine was met with success, formation of *N*-phenylpyridinium salt **176** failed with complete recovery the Zincke imine. At this point, we decided to explore reaction conditions to promote pyridinium formation with less nucleophilic aniline coupling partners when compared to alkylamines.

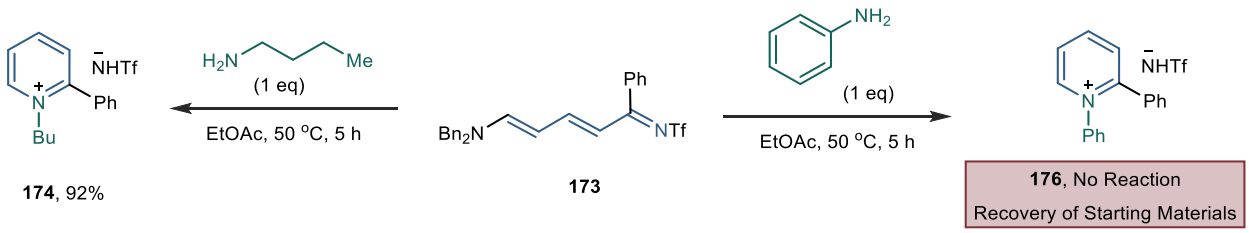

Figure 5.5: Failed attempt to form *N*-arylpyridinium substrate with aniline coupling partner.

5.5 Optimization of *N*-Arylpyridinium Formation

First, we optimized the reaction between Zincke imine adduct 173 and aniline to explore the factors that could promote the desired reactivity (Table 5.2). Isopropyl acetate (IPAc) was chosen as a reaction medium because it is regarded as an ideal solvent choice for medicinal chemists.[20] Simply heating the reagents in IPAc at 50 °C failed to provide any desired pyridinium and quantitative recovery of both coupling partners was observed (Entry 1). We hypothesized that activation of the Zincke imine electrophile with a Bronsted acid could promote nucleophilic addition of the aniline and initiate the cyclization. We discovered that acetic acid (AcOH) could enable the desired reactivity, and ten equivalents of AcOH was optimal to provide the pyridinium salt 177 in good yield (Entries 2-4). We evaluated the conditions for the formation of ***N***-aryl pyridinium, and found that 1.5 equivalents of aniline, with a reaction concentration of 0.1 M with respect to 173, resulted in a significant decrease in yield because the reaction did not go to completion (Entry 5). Increasing the concentration accelerated the reaction rate to yield 94% of 177 (Entries 6 and 7).

Next, we examined the optimized reaction conditions with less nucleophilic aniline 178 and found that the corresponding pyridinium 178 was only formed in 50% yield (Entry 8). Only a small increase in yield was observed when the reaction was heated to 70 °C (Entry 9). Alcoholic solvents are known to be effective solvents for the pyridinium formation between anilines and

Zincke aldehydes,[18] and the use of MeOH as the reaction solvent improved the cyclization with Zincke imine 173, as well (Entry 10). Finally, heating the reaction in MeOH to 70 °C resulted in the highest yield of 178 (Entry 11). We hypothesized that both sets of conditions could be beneficial based on the nucleophilicity of the aniline coupling partner, so we subjected a small set of anilines to both conditions to evaluate this theory (Table 5.2B). The brief survey supported our hypothesis that electron-neutral or electron-rich anilines perform better at 50 °C in IPAc, while pyridinium formation should be executed in MeOH at 70 °C for electron-deficient anilines.

Table 5.2: Optimization of *N*-Arylpyridinium Formation

A. Reaction Optimization

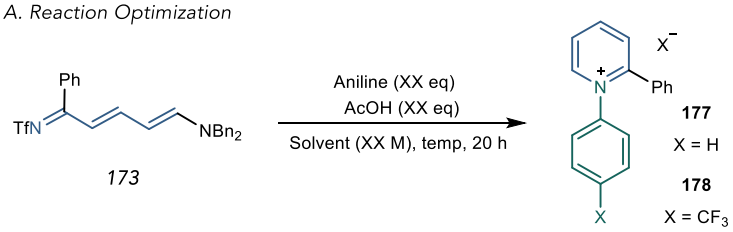

Entry	Aniline (eq)	AcOH (eq)	Solvent (M)	Temp. (°C)	% Prod.
1	177 (3.0)	0	IPAc (0.1)	50	Trace
2	177 (3.0)	1	IPAc (0.1)	50	28
3	177 (3.0)	5	IPAc (0.1)	50	47
4	177 (3.0)	10	IPAc (0.1)	50	92
5	177 (1.5)	10	IPAc (0.1)	50	44
6	177 (1.5)	10	IPAc (0.2)	50	67
7	177 (1.5)	10	IPAc (0.4)	50	94
8	178 (1.5)	10	iPAc (0.4)	50	50
9	178 (1.5)	10	IPAc (0.4)	70	54
10	178 (1.5)	10	MeOH (0.4)	50	61
11	178 (1.5)	10	MeOH (0.4)	70	74

Aniline Coupling Partners

B. Evaluation of Substrate-Dependent Conditions

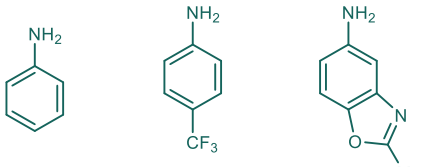

Conditions	177	178	179
iPAc, 50 °C	94	50	87
MeOH, 70 °C	84	74	64

Yields determined by ^{1}H NMR using triphenylmethane as an internal standard.

With conditions optimized to form the desired ***N***-heteroarylpyridiniums, a collaboration was initiated with Merck to further explore the scope of this reaction, with a focus on substrates that are more representative of the molecules that medicinal chemists work with every day in the pursuit of new medicines. Additionally, our teams were interested in elucidating the mechanism of cyclization, investigating the hydrogenation of the *N*-(hetero)arylpyridinium salts, and developing new methodologies that make use of these reagents. Preliminary results in pursuit of these goals are detailed below.

5.6 Substrate Scope

Using the conditions discovered in our optimization, we evaluated the effectiveness of the protocol using fifteen anilines via ^{1}H NMR assay with triphenylmethane as internal standard (**Table 5.3**). Anilines ranging from electron-neutral to electron-rich were coupled using the appropriate coupling conditions to form the corresponding pyridiniums in good yield (**182**-**184**). Anilines appending to other heteroaromatics such as a quinoline, pyrazole, and pyridine were tolerated in the protocol (**185**-**187**). 3-aminopyridine is the most electron-deficient aniline coupling partner we evaluated using the conditions that were optimized for electron-rich anilines, and three equivalents of the nucleophile were required to obtain pyridinium **187** in good yield. Sterically hindered anilines are challenging substrates that did not undergo significant product formation with Zincke imine **173**, but 2-methoxy-6-methylaniline was a competent coupling partner with a Zincke imine derived from 2-methylpyridine (**188**). Pyridiniums (and the corresponding piperidines) resembling **188** that exhibit extreme steric congestion about the carbon-nitrogen bond are an important class of compounds that cannot be accessed via any other methods currently.[6,21]

Next, the conditions suited for electron-deficient (hetero)arylamines were assessed. We discovered that electron-neutral 2-methylaniline with imine **173** to provide pyridinium **189** without the need for three equivalents of the aniline. With this observation, we hypothesize that the rate determining step in this reaction for sterically hindered or electronic-deficient anilines could be the displacement of the triflamide leaving group. Employing the conditions that use MeOH as solvent at higher temperatures may provide a hydrogen-bond donor that can accelerate the rate of this step. Further studies on the mechanism of this transformation are ongoing. While 4-aminopyrazole reacts readily with **173** to form pyridinium **186**, we found that 3-aminopyrazole did not form significant amounts of pyridinium salt **191** using the first set of conditions. The conditions developed to promote electron-deficient anilines proved to also enable less nucleophilic anilines that exhibit conjugation to another heteroatom. Conjugated anilines bearing pyrazoles, isoxazoles, quinolines, and pyridines were all tolerated under the reaction conditions (**191**-**195**). Finally, trimethylaniline failed to react with **173** but reacted effectively with 2-methyl Zincke imine to provide another sterically congested pyridinium, and only 1.5 equivalents of the aniline were required (**196**).

Table 5.3: Preliminary Scope of Aniline Coupling Partners

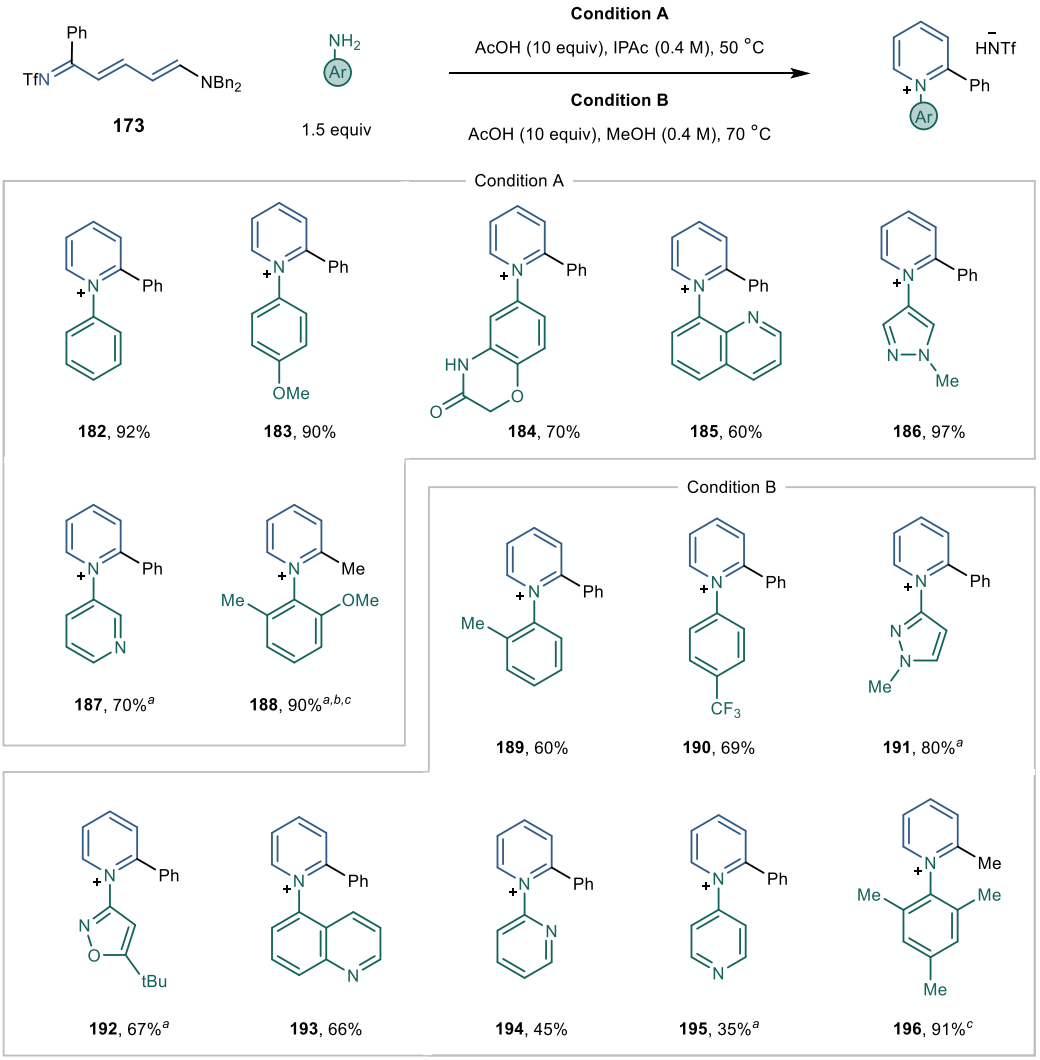

Yields determined by ^{1}H NMR using triphenylmethane as an internal standard. Triflamide counterions omitted for clarity. [a]3.0 equivalents of aniline used. [b]Reaction conducted at 70 °C. [c]Used Zincke imine derived from 2-methylpyridine.

Finally, a selection of pyridines was evaluated as coupling partners in the pyridinium formation reaction (**Table 5.4**). Notably, all the pyridiniums shown below were synthesized in a one-pot process where no isolation of the intermediate Zincke imine adduct was required. Pyridines with substituents at the 2-, 3-, and 4-positions performed well in the transformation, and the presence of functional groups such as esters, trifluoromethyl groups, and bromides were

tolerated under the reaction conditions (**197**-**200**). We found that a pyrimidine could also serve as a competent substrate to form pyrimidinium **201** in excellent yield. Lastly, three more complex pyridines were assessed in the protocol showing the methods tolerance of medicinally relevant motifs such as carbon-fluorine bonds, tertiary amines, alkenes, and electron-rich heterocycles.

Table 5.4: Preliminary Scope of Pyridine Substrates

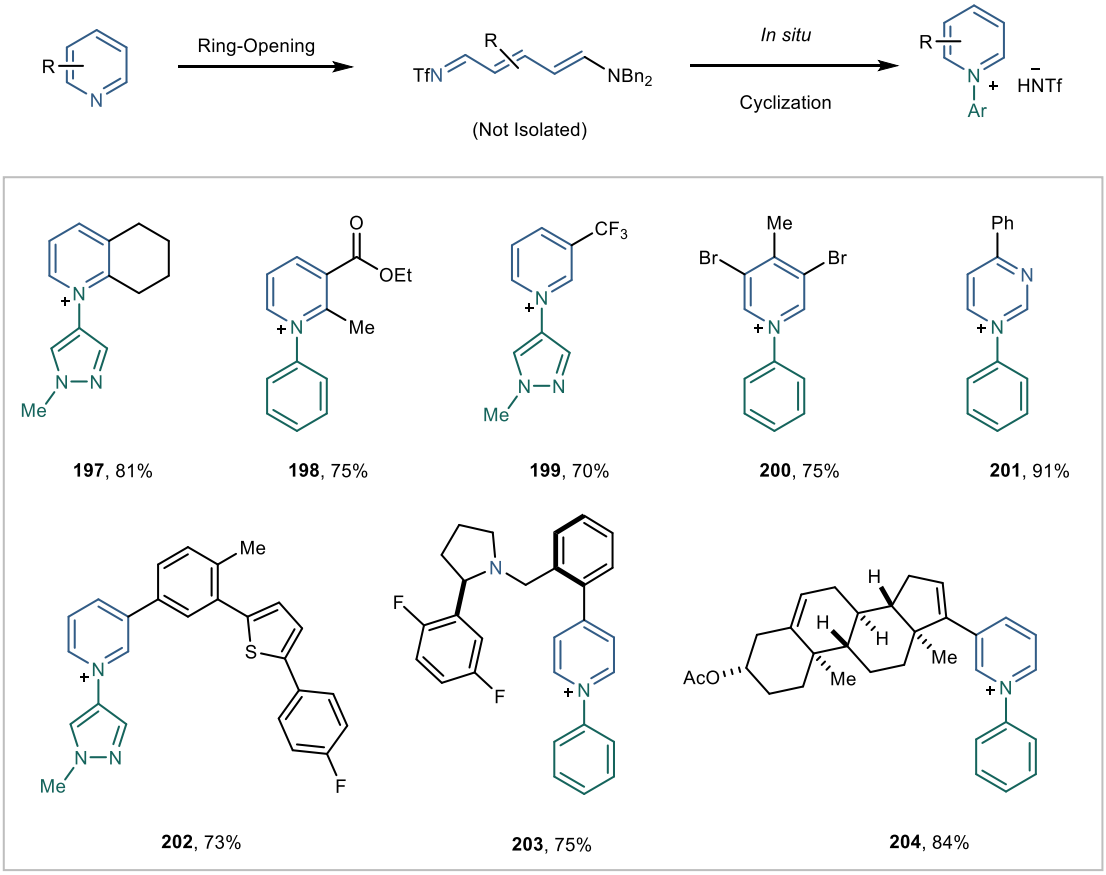

Yields determined by ^{1}H NMR using triphenylmethane as an internal standard. Triflamide counterions omitted for clarity.

5.7 Preliminary Hydrogenation Results

A variety of different pyridinium substrates are accessible through our cyclization strategy that are challenging to synthesize with other methods, and we investigated the performance of a selection of substrates under hydrogenation conditions (**Table 5.5A**). Pyridinium formation was

conducted directly from the corresponding Zincke imine, followed by *in situ* hydrogenation with no isolation required. *N*-aryl substituents spanning from electron-deficient to electron-rich were well tolerated, and carbon-halogen bonds that can be used as functional handles for subsequent functionalization remained intact (**205**-**207**). Two different 2,3-disubstituted piperidines were also synthesized diastereospecifically from the corresponding Zincke imines in good yield (**208** and **209**). Finally, an asymmetric hydrogenation was demonstrated by our Merck collaborators using an iridium-based hydrogenation in the presence of a chiral ligand to provide **210** in good yield and reasonably high enantioselectivity. Efforts to improve this protocol are ongoing. Notably, the effective ligand for *N*-alkylpyridinium salt hydrogenation is distinct from the ligand we identified for enantioselective hydrogenation of *N*-arylpyridinium salts.[7,10]

Table 5.5: Preliminary Pyridinium Salt Hydrogenation Results

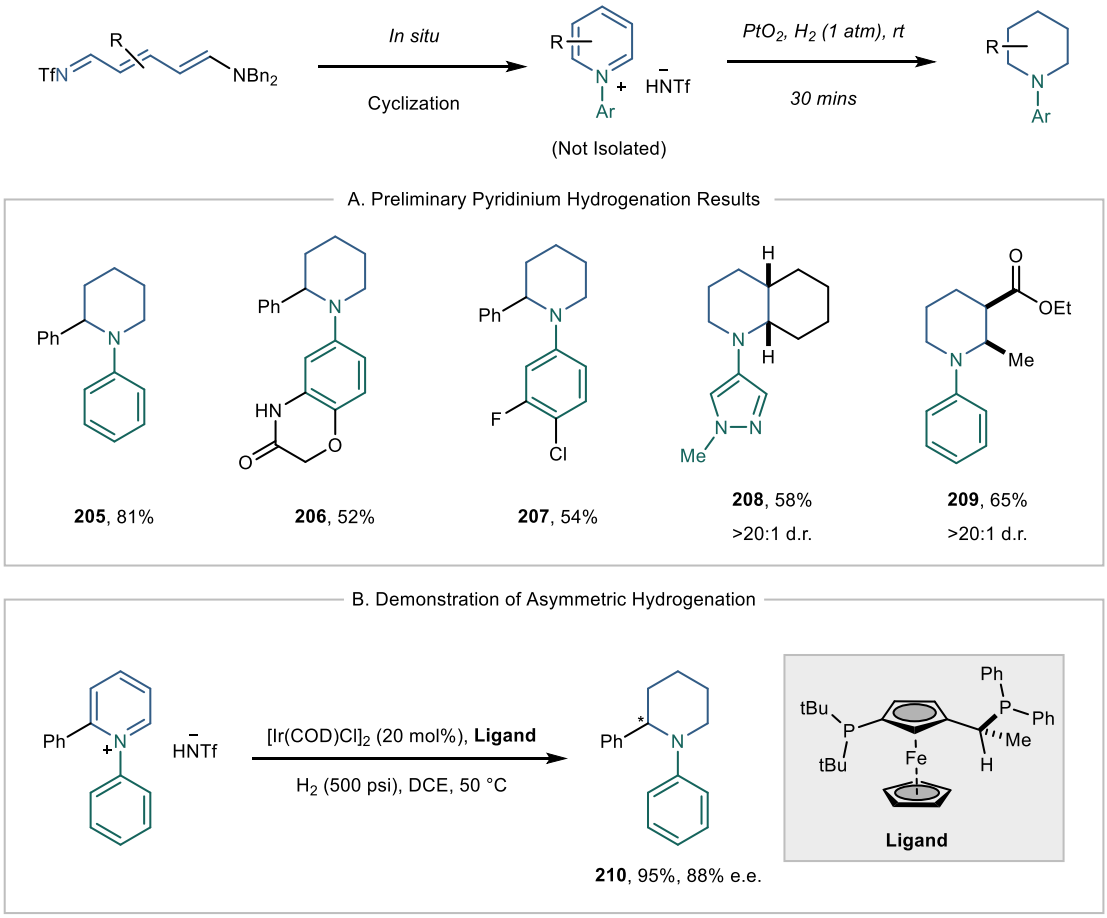

Yields determined by ^{1}H NMR using triphenylmethane as an internal standard. Results for asymmetric hydrogenation determined via HPLC.

5.8 Future Directions

Combining all the preliminary results detailed above, we are optimistic that this protocol will exhibit a broad scope of anilines and pyridines amenable to the procedure. In response, our team and Merck collaborators have decided to use high throughput experimentation (HTE) to identify pyridinium salts that can be formed from the cyclization between a library of Zincke imine adducts synthesized by the McNally group and complex, medicinally relevant (hetero)aryl amines from Merck's internal building block collection. Representative examples of each reagent and the

products that can potentially be synthesized using this protocol are shown in **Figure 5.6**. 12 Zincke imines and 24 anilines will be combined to map out the viability of 288 different reaction outcomes on microgram scale to define the effectiveness of the protocol on complex substrates.

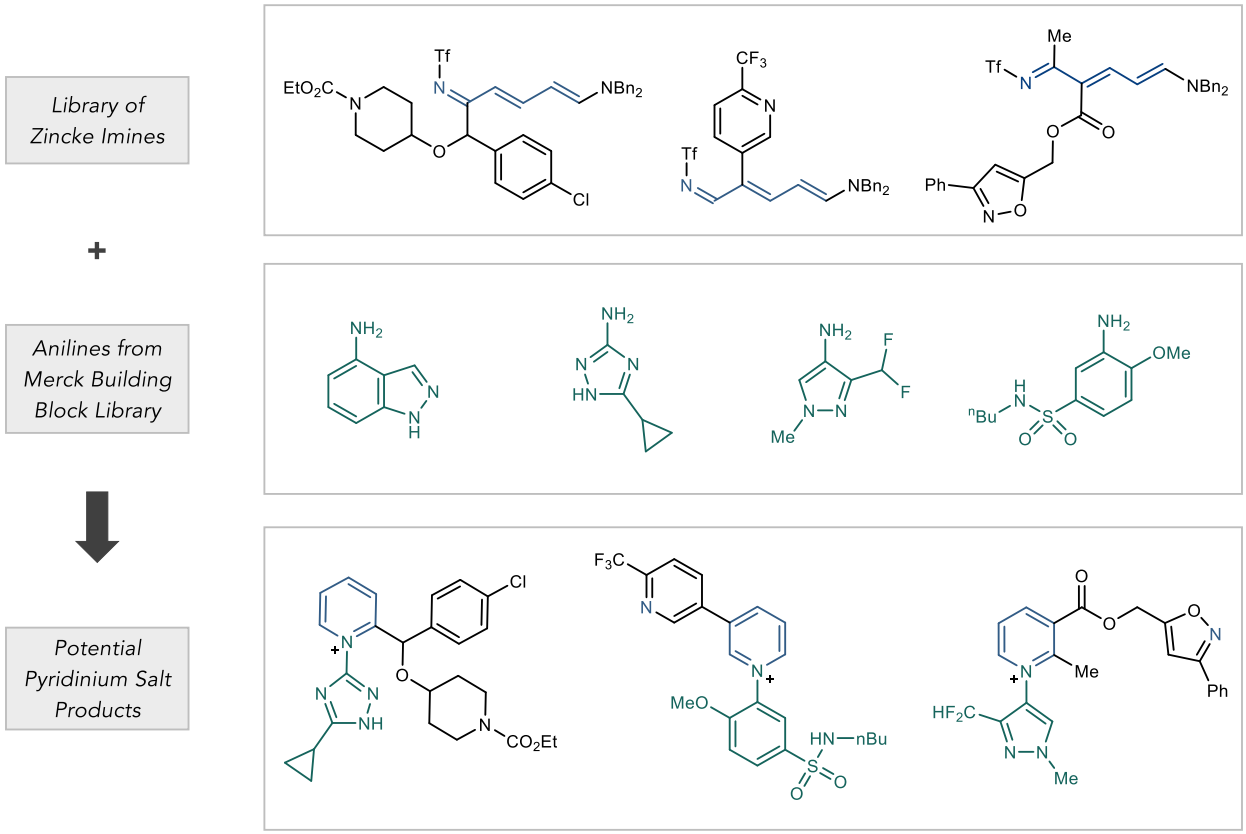

Figure 5.6: Representatives coupling partners and potential products informed via HTE. Triflamide counterion excluded for clarity.

Finally, we will explore methods to append other substituents to the eventual piperidine scaffold via nucleophilic addition to the pyridinium salt reagents and subsequent transformations of the intermediate dihydropyridine (**Figure 5.7**). Limited methods exist for the sequential functionalization of piperidine C-H bonds to form densely functionalized piperidines. Pyridinium salts functionalization with nucleophiles is well precedented, but the study of electrophilic

derivatization of the dihydropyridine intermediate is limited. We will attempt to leverage pyridinium salts as powerful reagents in the synthesis of complex piperidines.

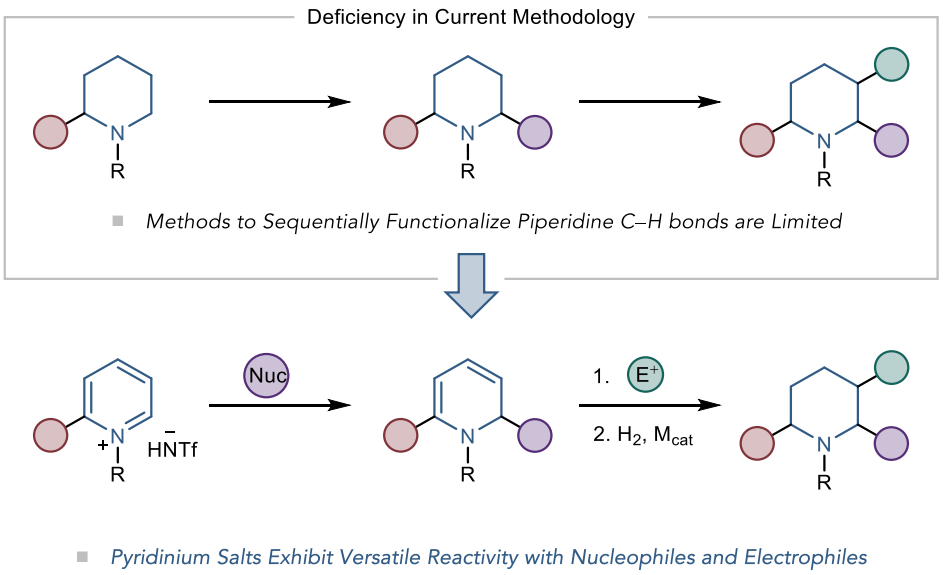

Figure 5.7: Pyridinium reactivity can address challenges in piperidine functionalization.

5.9 Conclusion

An alternative approach toward the synthesis of *N*-(hetero)arylpiperidines was presented in this chapter. A wide range of *N*-triflylpyridinium salts ring-opened under mild conditions, greatly expanding the scope of the original Zincke reaction. The intermediate Zincke imines can be ring closed with a variety of primary amine nucleophiles to form the corresponding pyridiniums that can be hydrogenated to form piperidines that are challenging to access with any other method.

References

(1) Vitaku, E.; Smith, D. T.; Njardarson, J. T. Analysis of the Structural Diversity, Substitution Patterns, and Frequency of Nitrogen Heterocycles among U.S. FDA Approved Pharmaceuticals: Miniperspective. *J. Med. Chem.* **2014**, *57*, 10257–10274.

(2) Goel, P.; Alam, O.; Naim, M. J.; Nawaz, F.; Iqbal, M.; Alam, M. I. Recent Advancement of Piperidine Moiety in Treatment of Cancer- A Review. *Eur. J. Med. Chem.* **2018**, *157*, 480–502.

(3) Semple, G.; Fioravanti, B.; Pereira, G.; Calderon, I.; Uy, J.; Choi, K.; Xiong, Y.; Ren, A.; Morgan, M.; Dave, V.; Thomsen, W.; Unett, D. J.; Xing, C.; Bossie, S.; Carroll, C.; Chu, Z.-L.; Grottick, A. J.; Hauser, E. K.; Leonard, J.; Jones, R. M. Discovery of the First Potent and Orally Efficacious Agonist of the Orphan G-Protein Coupled Receptor 119. *J. Med. Chem.* **2008**, *51*, 5172–5175.

(4) Weintraub, P. M.; Sabol, J. S.; Kane, J. M.; Borcherding, D. R. Recent Advances in the Synthesis of Piperidones and Piperidines. *Tetrahedron* **2003**, *59*, 2953–2989.

(5) Buffat, M. G. P. Synthesis of Piperidines. *Tetrahedron* **2004**, *60*, 1701–1729.

(6) Larsen, M. A.; Hennessy, E. T.; Deem, M. C.; Lam, Y.; Saurí, J.; Sather, A. C. A Modular and Diastereoselective 5 + 1 Cyclization Approach to N-(Hetero)Aryl Piperidines. *J. Am. Chem. Soc.* **2020**, *142*, 726–732.

(7) Chang, M.; Huang, Y.; Liu, S.; Chen, Y.; Krska, S. W.; Davies, I. W.; Zhang, X. Asymmetric Hydrogenation of Pyridinium Salts with an Iridium Phosphole Catalyst. *Angew. Chem. Int. Ed.* **2014**, *53*, 12761–12764.

(8) Huang, W.-X.; Wu, B.; Gao, X.; Chen, M.-W.; Wang, B.; Zhou, Y.-G. Iridium-Catalyzed Selective Hydrogenation of 3-Hydroxypyridinium Salts: A Facile Synthesis of Piperidin-3-Ones. *Org. Lett.* **2015**, *17*, 1640–1643.

(9) Huang, Y.; Liu, S.; Liu, Y.; Chen, Y.; Weisel, M.; Williamson, R. T.; Davies, I. W.; Zhang, X. A Mechanistic Investigation of an Iridium-Catalyzed Asymmetric Hydrogenation of Pyridinium Salts. *Tetrahedron* **2018**, *74*, 2182–2190.

(10) Qu, B.; Mangunuru, H. P. R.; Tcyrulnikov, S.; Rivalti, D.; Zatolochnaya, O. V.; Kurouski, D.; Radomkit, S.; Biswas, S.; Karyakarte, S.; Fandrick, K. R.; Sieber, J. D.; Rodriguez, S.; Desrosiers, J.-N.; Haddad, N.; McKellop, K.; Pennino, S.; Lee, H.; Yee, N. K.; Song, J. J.; Kozlowski, M. C.; Senanayake, C. H. Enantioselective Synthesis of α-(Hetero)Aryl Piperidines through Asymmetric Hydrogenation of Pyridinium Salts and Its Mechanistic Insights. *Org. Lett.* **2018**, *20*, 1333–1337.

(11) Legault, C. Y.; Charette, A. B. Catalytic Asymmetric Hydrogenation of *N* -Iminopyridinium Ylides: Expedient Approach to Enantioenriched Substituted Piperidine Derivatives. *J. Am. Chem. Soc.* **2005**, *127*, 8966–8967.

(12) Sowmiah, S.; Esperança, J. M. S. S.; Rebelo, L. P. N.; Afonso, C. A. M. Pyridinium Salts: From Synthesis to Reactivity and Applications. *Org. Chem. Front.* **2018**, *5*, 453–493.

(13) Carreira, E. M.; Rössler, S.; Jelier, B.; Tripet, P.; Shemet, A.; Jeschke, G.; Togni, A. Pyridyl Radical Cation for C-H Amination of Arenes. *Angew. Chem. Int. Ed.* **2018**, *58*, 526-531.

(14) Tierno, A. F.; Walters, J. C.; Vazquez-Lopez, A.; Xiao, X.; Wengryniuk, S. E. Heterocyclic Group Transfer Reactions with I(III) *N* -HVI Reagents: Access to *N* -Alkyl(Heteroaryl)Onium Salts *via* Olefin Aminolactonization. *Chem. Sci.* **2021**, *12*, 6385–6392.

(15) Sauers, R. R. The Effect of Structure on the Course of Phosphoryl Chloride-Pyridine Dehydration of Tertiary Alcohols. *J. Am. Chem. Soc.* **1959**, *81*, 4873–4876.
(16) Vlasov, V. M. Nucleophilic Substitution of the Nitro Group, Fluorine and Chlorine in Aromatic Compounds. *Russ. Chem. Rev.* **2003**, *72*, 681–703.
(17) Cheng, W.-C.; Kurth, M. J. THE ZINCKE REACTION. A REVIEW. *Org. Prep. Proced. Int.* **2002**, *34*, 585–608.
(18) Asskar, G.; Rivard, M.; Martens, T. Glutaconaldehyde as an Alternative Reagent to the Zincke Salt for the Transformation of Primary Amines into Pyridinium Salts. *J. Org. Chem.* **2020**, *85*, 1232–1239.
(19) Genisson, Y.; Marazano, C.; Mehmandoust, M.; Gnecco, D.; Das, B. C. Zincke's Reaction with Chiral Primary Amines: A Practical Entry to Pyridinium Salts of Interest in Asymmetric Synthesis. *Synlett* **2002**, *1992*, 431–434.
(20) Byrne, F. P.; Jin, S.; Paggiola, G.; Petchey, T. H. M.; Clark, J. H.; Farmer, T. J.; Hunt, A. J.; Robert McElroy, C.; Sherwood, J. Tools and Techniques for Solvent Selection: Green Solvent Selection Guides. *Sustain. Chem. Process.* **2016**, *4*, 7.
(21) Sather, A. C.; Martinot, T. A. Data-Rich Experimentation Enables Palladium-Catalyzed Couplings of Piperidines and Five-Membered (Hetero)Aromatic Electrophiles. *Org. Process Res. Dev.* **2019**, *23*, 1725–1739.

APPENDIX ONE

PYRIDINE-PYRDIINE CROSS-COUPLING REACTION VIA DEAROMATIZED RADICAL INTERMEDIATES: EXPERIMENTAL

A1.1 General Information

Proton nuclear magnetic resonance (^{1}H NMR) spectra were recorded at ambient temperature on a Varian 400 MR spectrometer (400 MHz), an Agilent Inova 400 (400 MHz) spectrometer, an Agilent Inova 500 (500 MHz) spectrometer, or a Bruker AV-111 400 (400 MHz) spectrometer. Chemical shifts (δ) are reported in ppm and quoted to the nearest 0.01 ppm relative to the residual protons in $CDCl_3$ (7.26 ppm), C_6D_6 (7.16 ppm), $(CD_3)_2SO$ (2.50 ppm), CD_3OD (3.31 ppm) or CD_3CN (1.94 ppm) and coupling constants (*J*) are quoted in Hertz (Hz). Data are reported as follows: Chemical shift (number of protons, multiplicity, coupling constants, proton assignment). Coupling constants were quoted to the nearest 0.1 Hz and multiplicity was reported according to the following convention: s = singlet, d = doublet, t = triplet, q = quartet, qn = quintet, sext = sextet, sp = septet, oct = octet, m = multiplet, br = broad. Where coincident coupling constants have been observed, the apparent (app) multiplicity of the proton resonance has been reported. Carbon nuclear magnetic resonance (^{13}C NMR) spectra were recorded at ambient temperature on a Varian 400 MR spectrometer (100 MHz) or an Agilent Inova 400 (100 MHz) spectrometer. Chemical shift (δ) was measured in ppm and quoted to the nearest 0.1 ppm relative to the residual solvent peaks in $CDCl_3$ (77.16 ppm), C_6D_6 (128.06 ppm), $(CD_3)_2SO$ (39.51 ppm), CD_3OD (49.00 ppm) or CD_3CN (1.32 ppm). 2-dimensional experiments (COSY, HMBC and HSQC) were used to support assignments where appropriate.

Absorption spectra were obtained with a Hewlett-Packard 8453 spectrometer in quartz cuvettes with a 1 cm or 0.17 cm path length. Electrochemical experiments were performed in 0.1 M

solutions of Bu_4NPF_6 in CH_2Cl_2. Cyclic voltammograms (CVs) and square-wave voltammograms (SWVs) were recorded with a CH Instruments potentiostat (Model 1230A or 660C) using a 0.25 mm glassy carbon disk working electrode, Ag^+/Ag reference electrode, and a Pt wire auxiliary electrode. Scans were collected at 100 mV/s. Reported potentials are referenced to the $[Cp2Fe]^+/[Cp2Fe]$ (Fc^+/Fc), where Cp = cyclopentadiene, redox couple, and were determined by adding ferrocene as an internal standard at the conclusion of each electrochemical experiment. The potentials in reference to SCE are estimates based on the reported of Fc^+/Fc^0 in 0.1 M solution of Bu_4NPF_6 in dichloromethane.[1]

Low-resolution mass spectra (LRMS) were measured on an Agilent 6310 Quadrupole Mass Spectrometer. Infrared (IR) spectra were recorded on a Bruker Tensor 27 FT-IR spectrometer as either solids or neat films, either through direct application or deposited in $CHCl_3$, with absorptions reported in wavenumbers (cm^{-1}).

Analytical thin layer chromatography (TLC) was performed using pre-coated Merck glass-backed silica gel plates (Silicagel 60 F254) or foil-backed basic aluminum oxide plates (Baker-flex 4467). Flash column chromatography was undertaken on Fluka or Material Harvest silica gel (230–400 mesh) or Sigma-Aldrich aluminum oxide (activated, basic) under a positive pressure of air. Preparative thin layer chromatography was performed using pre-coated Silicycle glass-backed silica gel plates (Siliaplate 60Å, 20 cm×20 cm, 2000 μm, TLG–R10011B–353). Visualization was achieved using ultraviolet light (254 nm) and chemical staining with ceric ammonium molybdate or basic potassium permanganate solutions as appropriate.

Tetrahydrofuran (THF), toluene, hexane, diethyl ether and dichloromethane were dried and distilled using standard methods.[1] 1,2-Dichloroethane (DCE), 1,4-dioxane, chloroform, chlorobenzene and acetone were purchased anhydrous from Sigma Aldrich chemical company.

All reagents were purchased at the highest commercial quality and used without further purification. Reactions were carried out under an atmosphere of nitrogen unless otherwise stated. All reactions were monitored by TLC, ^{1}H NMR spectra taken from reaction samples, gas chromatography (GC) and gas chromatography-mass spectrometry (GCMS) using an Agilent 5977A fitted with an Agilent *J*&W HP-5ms Ultra Inert Column (30 m, 0.25 mm, 0.25 μm film) for MS analysis and an Agilent *J*&W VF-5ms column (10 m, 0.15 mm, 0.15 μm film) for FID analysis or liquid chromatography mass spectrometry (LCMS) using an Agilent 6310 Quadrupole Mass Spectrometer. Melting points (mp) were recorded using a Büchi B-450 melting point apparatus and are reported uncorrected.

PPh_3 (99%) was purchased from Oakwood Chemical and is most effective when crushed to a powder before use. Tf_2O (99%) was purchased from Oakwood Chemical and used without further purification and was routinely stored in a –20 ºC fridge. NEt_3 and DBU were distilled before use. 4-cyanopyridine was recrystallized from a 50:50 mixture of CH_2Cl_2:Et_2O and stored in the glovebox before use.

A1.2 Evidence of Dearomatized Species

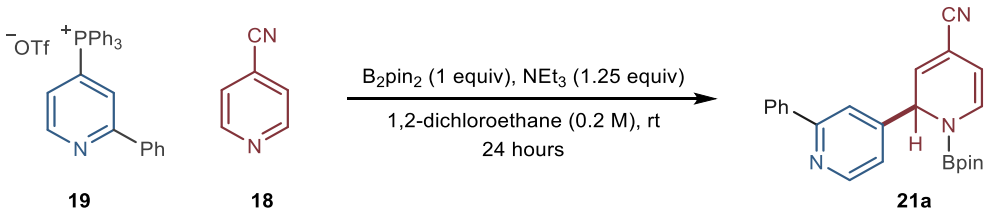

Evidence of the proposed dearomatized species was observed using **19** as the phosphonium salt to form dearomatized species **21a**. The standard reaction was set up and ran in a glovebox using degassed $CDCl_3$. After 24 hours, the ^{1}H NMR and MS samples were prepared in the glovebox to

avoid exposure to air. By ^{1}H NMR analysis, four protons appeared in the alkenyl region of the spectra (see below). The sample was transferred from the NMR tube to a vial and stirred open to air for thirty minutes and reanalyzed by ^{1}H NMR and LCMS. The alkenyl peaks seen before were no longer present and had converted almost completely to rearomatized product **21**. For integration values in ^{1}H NMR, 1,3,5-trimethoxybenzene was used as internal standard.

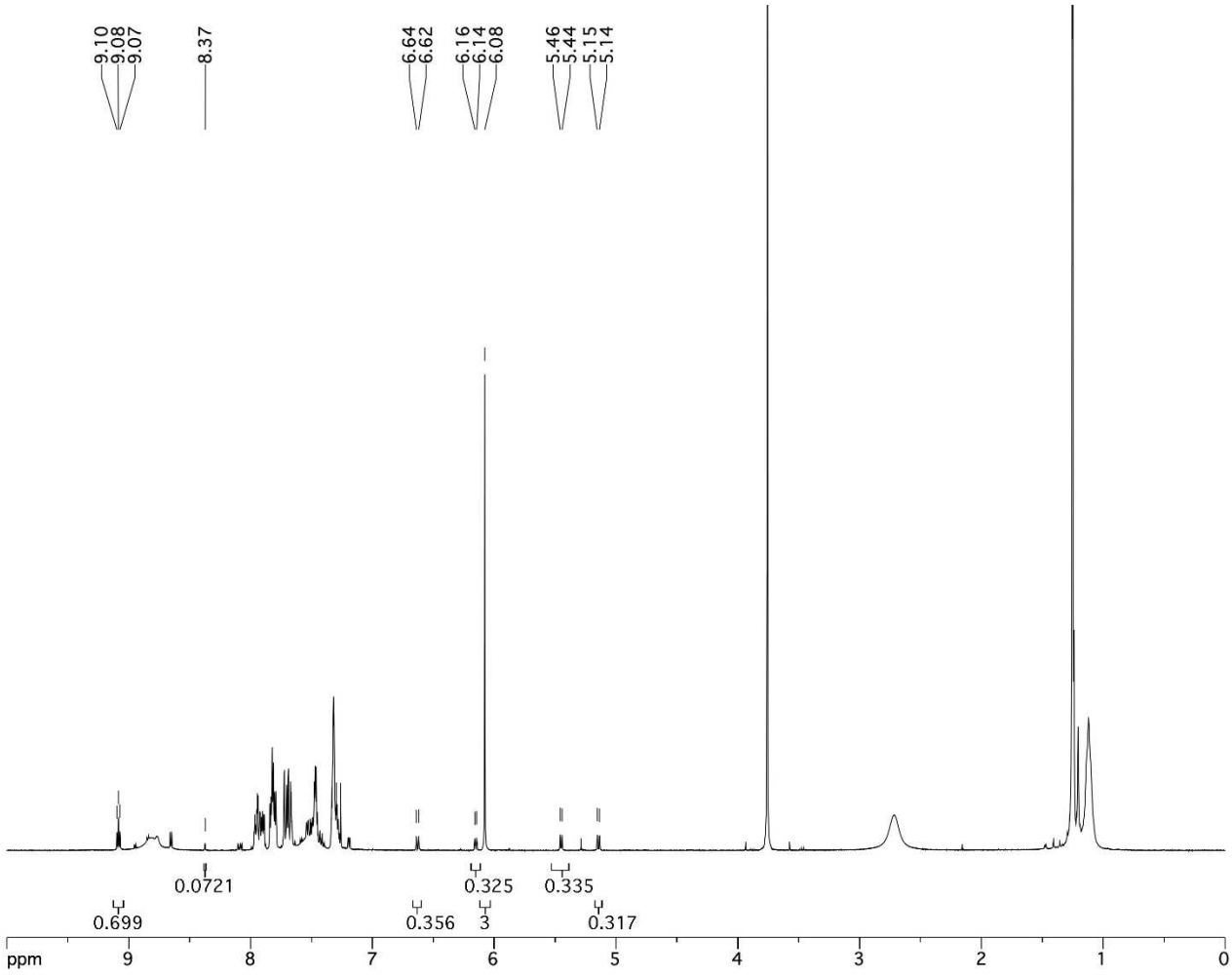

Figure A1.1. ^{1}H NMR before exposure to air.

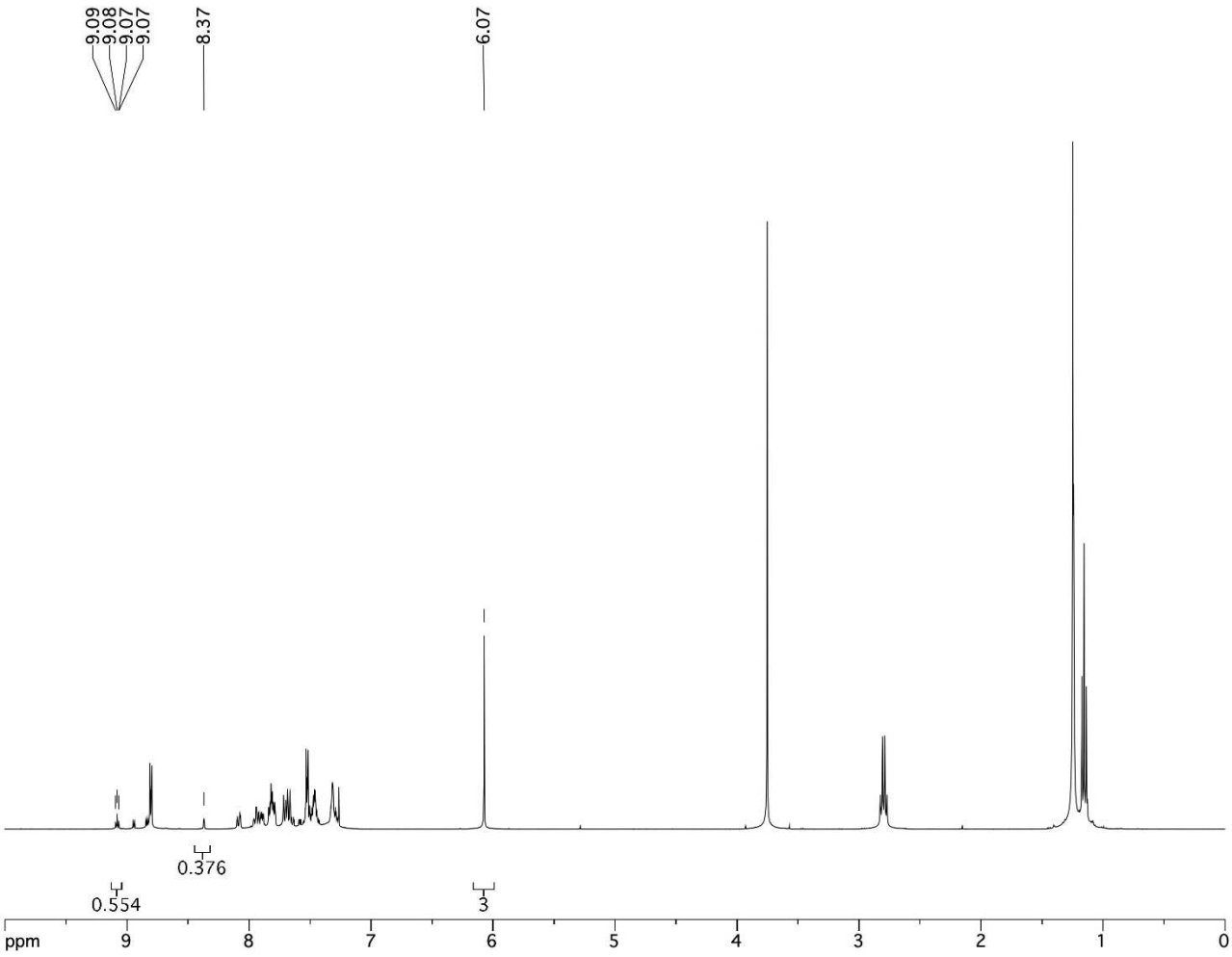

Figure A1.2. ^{1}H NMR after exposure to air for 30 minutes.

A1.3 Radical Clock Experiments

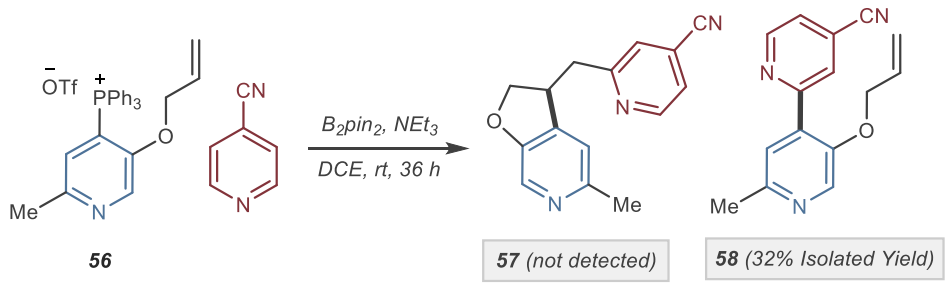

Figure A1.3. Radical clock experiments.

To probe the intermediacy of a free radical, we synthesized phosphonium **56**, which should be able to undergo a 5-exo-trig cyclization with the allyloxy substituent upon reduction and formation of a discrete pyridyl radical intermediate. The reaction was subjected to the standard reaction conditions at 0.1 mmol scale and analyzed after 36 hours. Through ^{1}H NMR analysis, no cyclized product **57**, nor any other cyclized products were detected. The major product formed in the reaction was coupled product **58** and isolated in 32% yield.

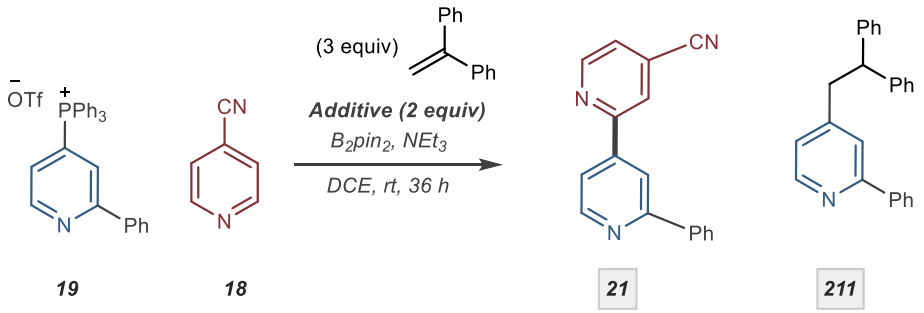

entry	additive	% **19**	% **21**	% **211**
1	none	23	78	0
2	benzyl mercaptan	75	30	0
3	Hantzsch ester	37	40	0

Figure A1.4. Radical trapping experiments.

Additionally, we attempted to trap the postulated pyridyl radical formed from **19** with 1,1-diphenylethylene and a hydrogen atom source (benzyl mercaptan or Hantzsch ester). The reaction was subjected to the standard reaction conditions at 0.1 mmol scale and analyzed after 24 hours. In all cases, bipyridine **21** was the major product, none of the trapped product **211** was observed, and unreacted starting material **19** remained.

A1.4 Anion cyclization trap experiment

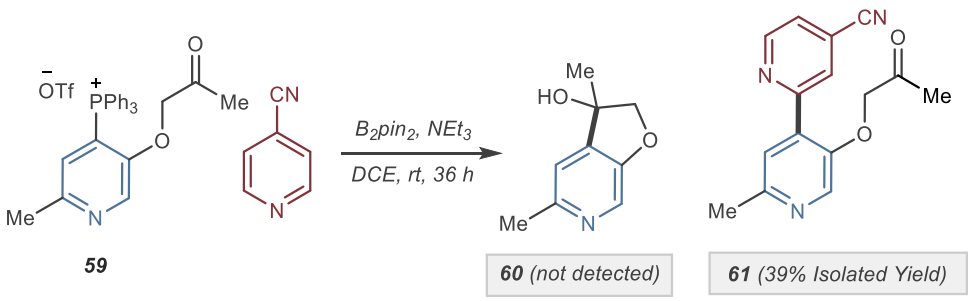

Figure A1.5. Anion trapping experiments.

To probe the intermediacy of a pyridyl anion or a pyridyl radical anion, we synthesized phosphonium **59**, which should be able to undergo a 5-exo-trig cyclization with the allyloxy substituent upon reduction and formation of a discreet pyridyl anion or a pyridyl radical anion. The reaction was subjected to the standard reaction conditions at 0.1 mmol scale and analyzed after 36 hours. Through ^{1}H NMR analysis, no cyclized product **60**, nor any other cyclized products were detected. The major product formed in the reaction was coupled product **61** and was isolated at 39% yield.

A1.5 Inhibition Experiment with Hantzsch Ester as an H-atom Donor

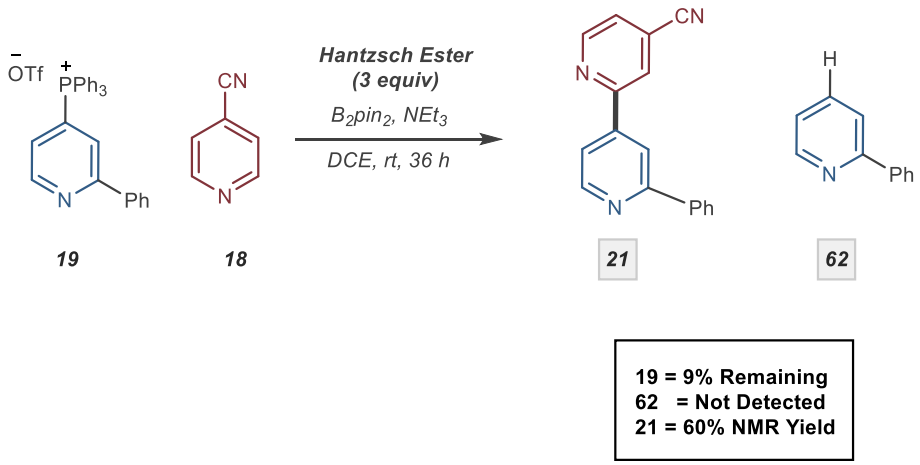

Figure A1.6. H-atom donor experiments.

We attempted to inhibit the reaction using Hantzsch Ester as an H-atom source. If a pyridyl radical was formed, we expect to see product **62** arising from H-atom abstraction. The reaction was subjected to the standard reaction conditions at 0.1 mmol scale with 3 equivalents of Hantzsch Ester and analyzed after 24 hours. The results of the reaction are shown in the figure above. 9% of phosphonium salt **19** remained, no product **62** detected, and 60% ^{1}H NMR yield of the bipyridine coupled product **21**. This suggests that the reaction is not proceeding through a discrete pyridyl-radical.

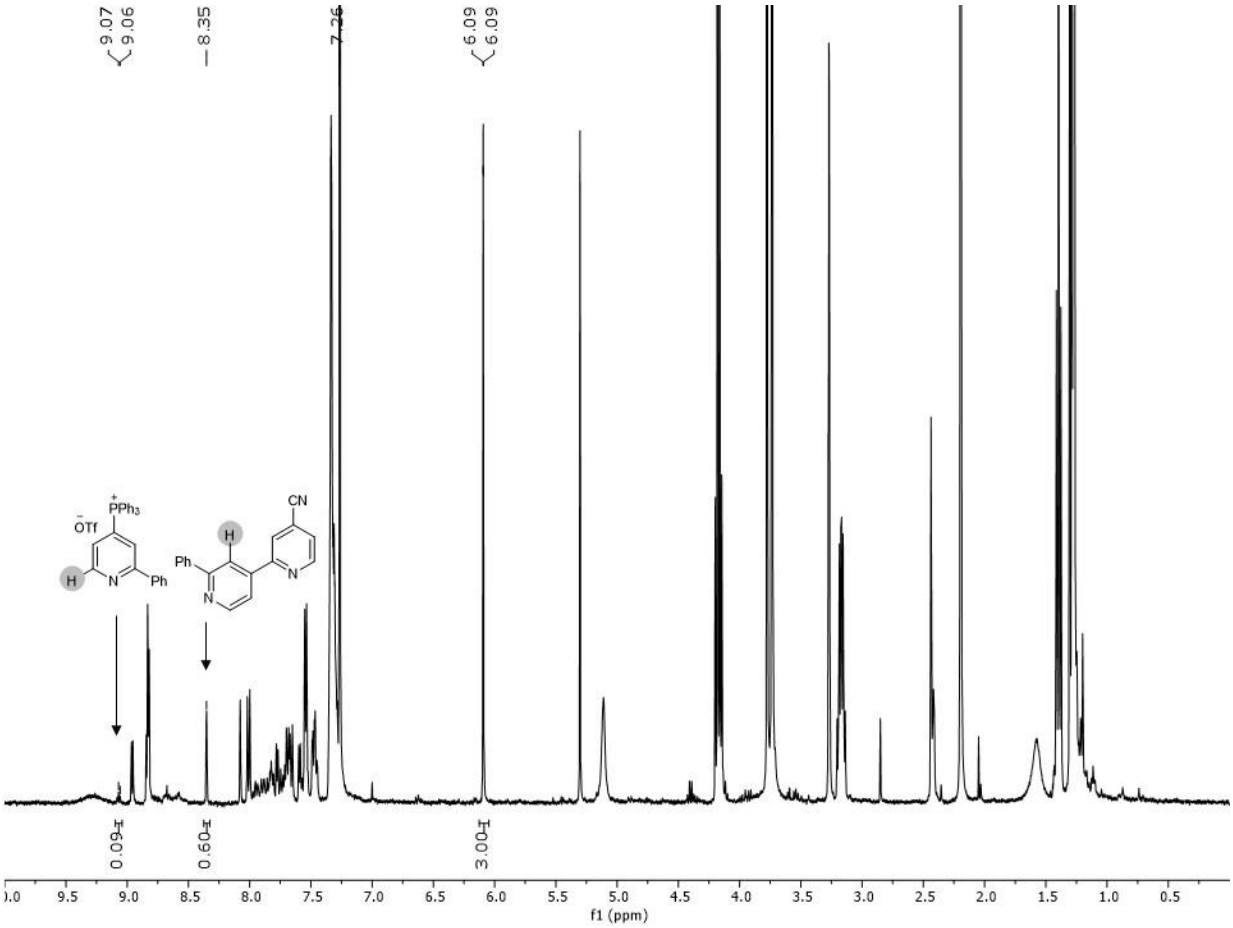

Figure A1.7. Crude ^{1}H NMR spectrum of coupling reaction using Hantzsch as H-atom donor.

A1.6 Inhibition Experiment with Deuterium Oxide (D_2O) as a Proton Donor

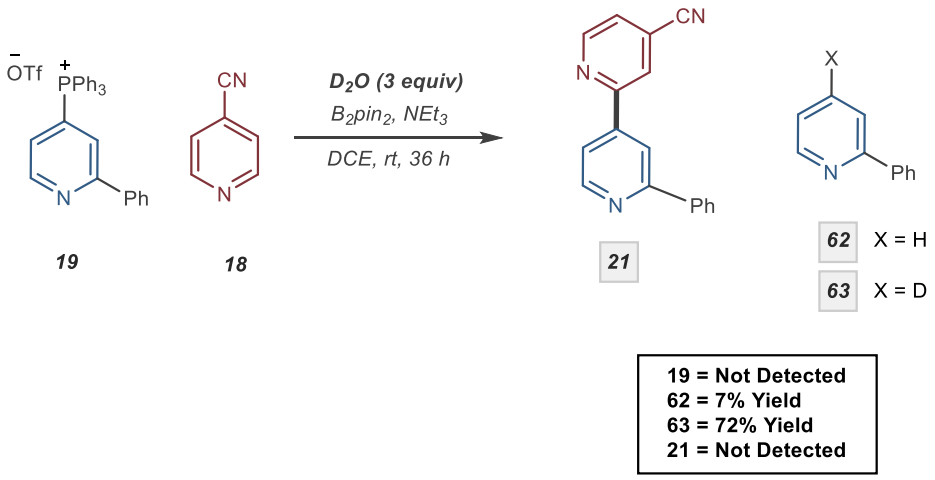

Figure A1.7. Deuterium donor experiment.

We attempted to trap the possible pyridyl anion using D_2O as an acidic deuterium source. If a pyridyl anion, or the proposed radical phosphonium ylide was formed, we should observe deuteration of the anion from D_2O to make product **63**. The reaction was subjected to the standard reaction conditions at 0.1 mmol scale with 3 equivalents of D_2O and analyzed after 24 hours. The results of the reaction are shown in the figure above. Phosphonium salt **19** and bipyridine product **21** were not detected, however a mixture of product **62** and **63** was isolated (silica gel plug, 30% EtOAc:hexane) giving 72% of deuterated product **63** and 7% of product **62** (79% yield overall with 91% deuterium incorporation by ^1H NMR using 1,3,5-trimethoxybenzene as an internal standard). This suggests that the reaction could proceed either through a pyridyl anion or the proposed radical phosphonium ylide. It also could suggest that the presence of D_2O changes the mechanism and identity of the intermediates formed after coordination to B_2pin_2.

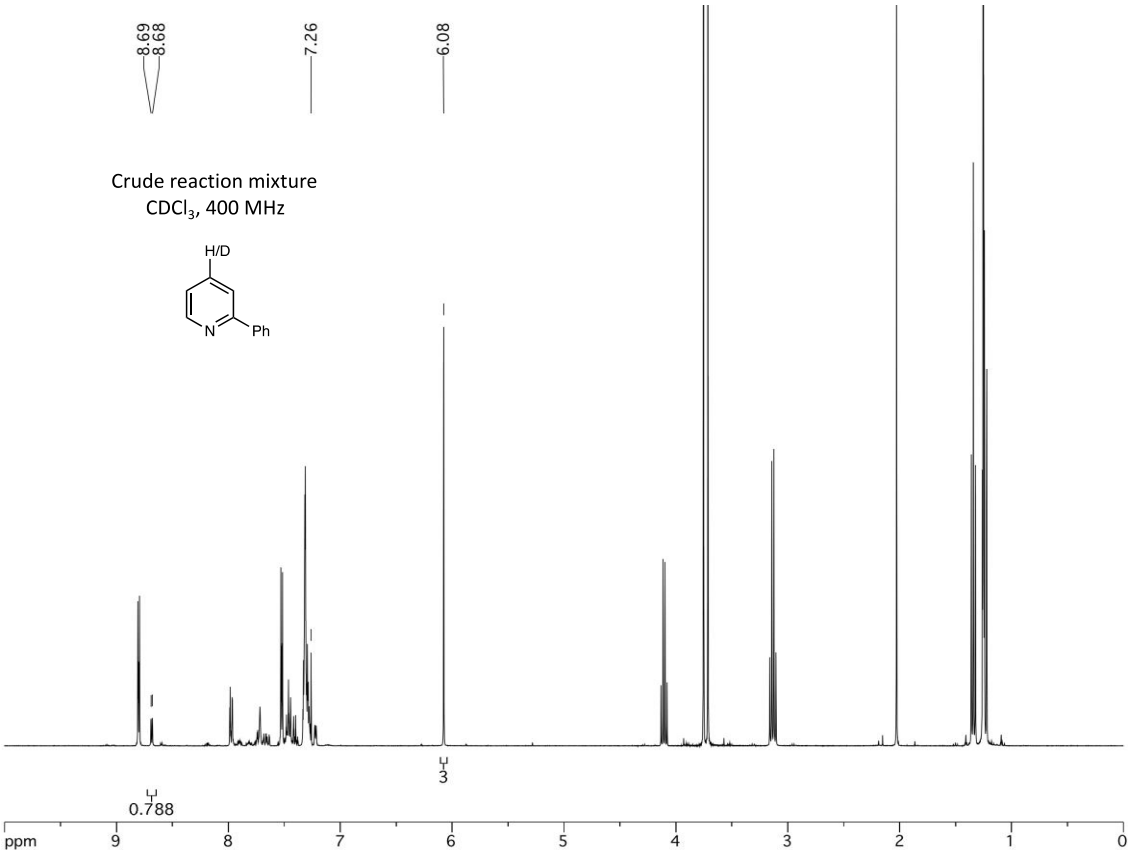

Figure A1.8. Crude ^{1}H NMR spectrum of coupling reaction using D_2O as deuterium donor.

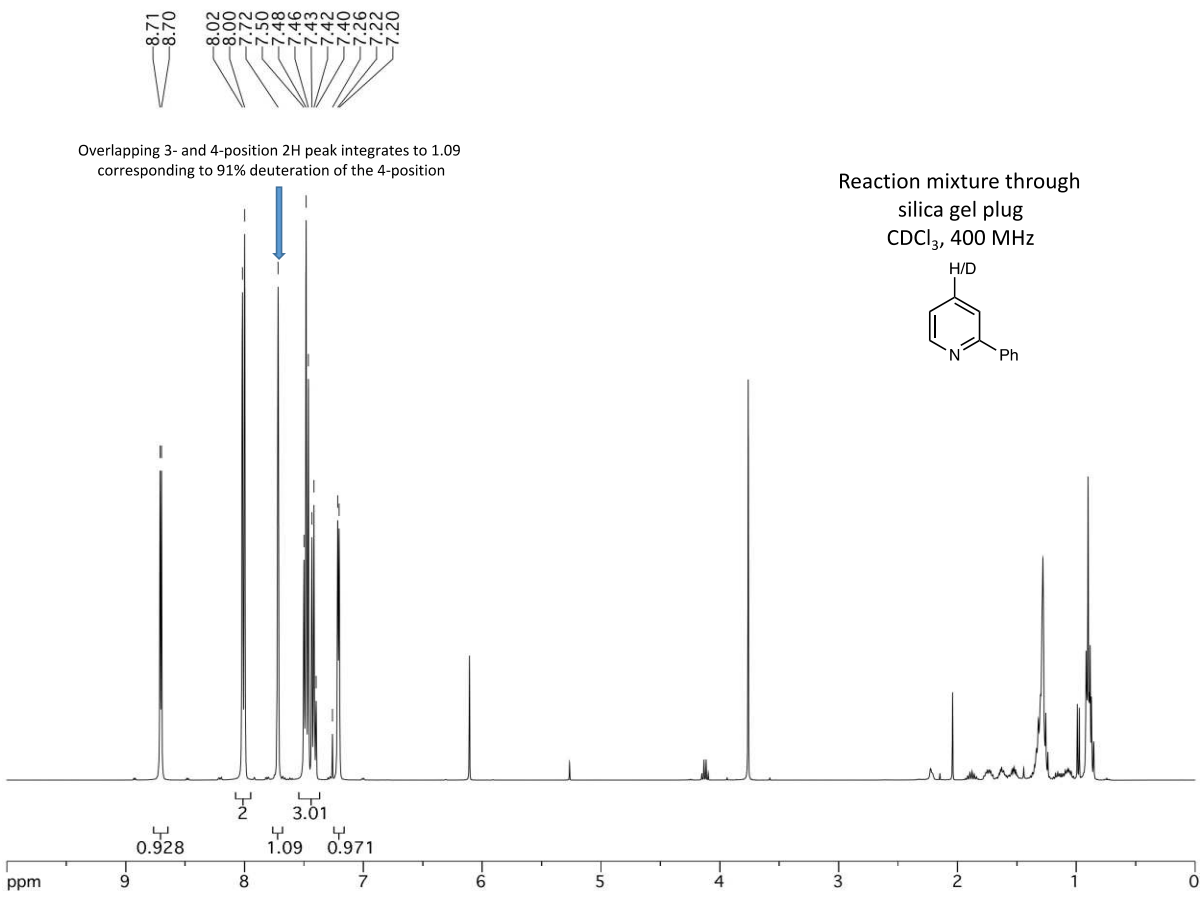

Figure A1.9. ^{1}H NMR spectrum of isolated C-H/D product reaction using D_2O as deuterium donor.

A1.7 Control reaction of phosphonium in presence of D_2O and LiOD

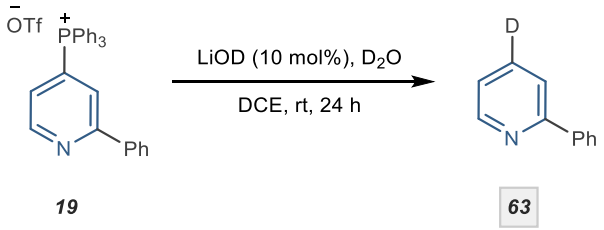

19 *63*

To assure that a catalytic amount of LiOD was not initiating the decomposition and subsequent deuteration of **19** to produce **63** in the previous mechanistic experiment, the following study was performed. A LiOD/D_2O solution (LiOD 10 mol % relative to phosphonium salt) was prepared by adding *n*BuLi (2.3 M in hexane) (0.025 mmol, 10.9 µL) to D_2O (0.75 mmol, 13.5 µL) at 0 °C and warmed to rt. This LiOD/D_2O solution was then added to a solution of phosphonium **19** (141 mg, 0.25 mmol), 1,2-dichloroethane (1.25 mL, 0.2 M), and let stir at rt for 24 h. Analysis by ^{1}H NMR and LCMS confirmed that there was no degradation of the phosphonium salt **19** to deuterated product **63**. This result suggests that LiOD in the reaction mixture does not decompose the phosphonium salt in the above reaction conditions.

A1.8. Aryl Group Substitution Study: Initial Rates

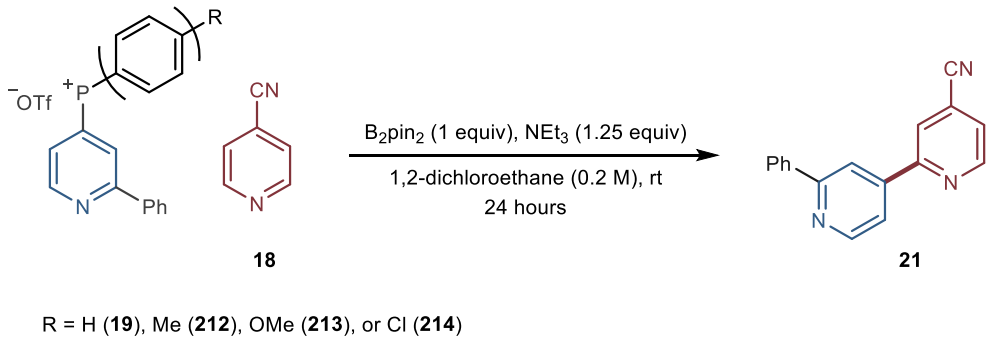

18 **21**

R = H (**19**), Me (**212**), OMe (**213**), or Cl (**214**)

Figure A1.10. Initial rate studies of electronically differentiated phosphonium salts.

The standard reaction was monitored for 1-2 hours in duplicate and the average was used for comparison of initial rates with phosphonium salt derivatives **212** to **214**. The linear range for the standard reaction was chosen for analysis of the initial rate. Yields were determined at the given time points using ^{1}H NMR in $CDCl_3$ with 1,3,5-trimethoxybenzene as the internal standard. Procedure for data collection is detailed below. Each reaction performed for the kinetic analysis was carried to completion to validate method of monitoring product formation instead of starting material consumption; each reaction regardless of phosphonium salt derivative gave 84-104% yield.

Procedure for Aryl Group Substitution Study:

An oven dried 8 mL vial with a septa cap was charged with the phosphonium salt (Characterization of phosphonium salts shown in Preparation of Heteroaryl Phosphonium Salt section (**19, 212** to **214**) (0.5 mmol), 4-cyanopyridine **18** (104 mg, 1.0 mmol), B_2pin_2 (127 mg, 0.5

mmol), NEt_3 (87 µL, 0.625 mmol), 1,3,5-trimethoxybenzene (84 mg, 0.5 mmol), 1,2-dichloroethane (2.5 mL) and sealed under a nitrogen atmosphere in a glovebox. At each time point, 100 µL of the reaction mixture was sampled via a syringe and charged to a vial open to air. EtOAc (4 mL) was then added to the vial and was allowed to stir for 30 minutes open to air. The vial was then concentrated *in vacuo* and the resulting residue was dissolved in $CDCl_3$ and ^1H NMR spectrum was obtained on the sample. The reaction was allowed to progress until the phosphonium salt was fully consumed and the final yield for the reaction was obtained via ^1H NMR in $CDCl_3$ (48 hours). Each reaction profile was performed in duplicate and the average of the two runs used for initial rate analysis.

Data:

Time (min)	Average [Product] (M)
15	0
30	0.002
45	0.002
60	0.02
75	0.022
90	0.03
105	0.034
120	0.043
135	0.052
150	0.054
165	0.059
180	0.064
195	0.072
210	0.076
225	0.081
240	0.085

Average yield after 60 h: 103%

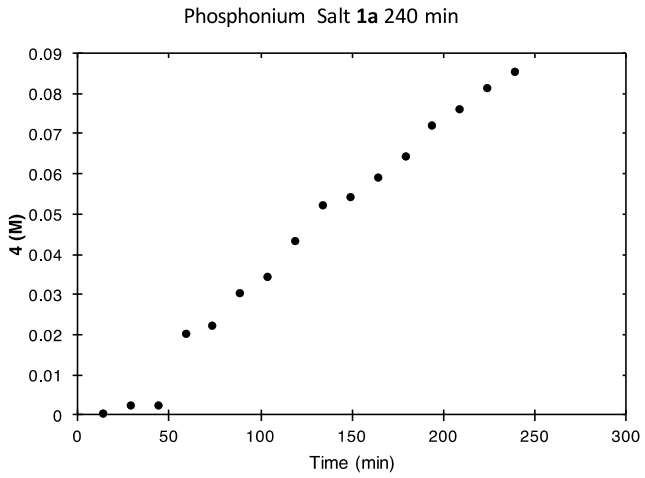

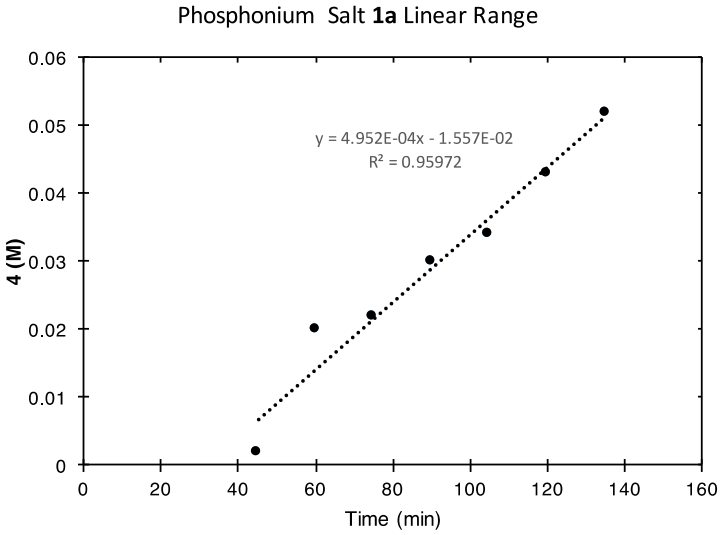

Figure A1.11. Standard reaction conditions ran with phosphonium salt **19** to obtain the initial reaction rate. Study was run in duplicate, and the average yield was used. Yields were determined at the given time points using ^{1}H NMR in $CDCl_3$ with 1,3,5-trimethoxybenzene as the internal standard.

Time (min)	Average [Product] (M)
15	0.008
30	0.009
45	0.001
60	0.005
75	0.003
90	0.009
105	0.019
120	0.03
135	0.037
150	0.042
165	0.047
180	0.053
195	0.059
210	0.063
225	0.066
240	0.071

Average yield after 60 h: 93.5%

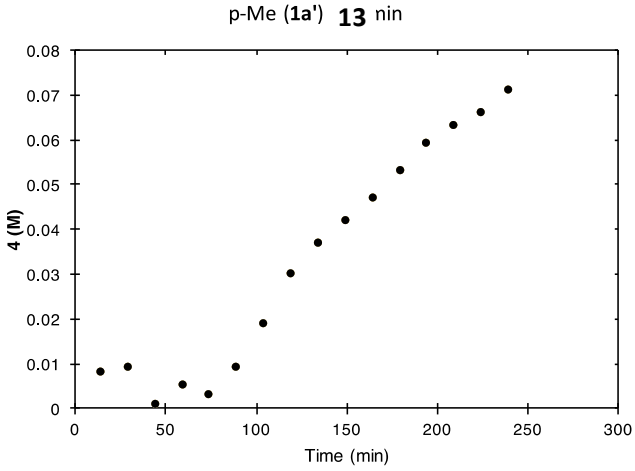

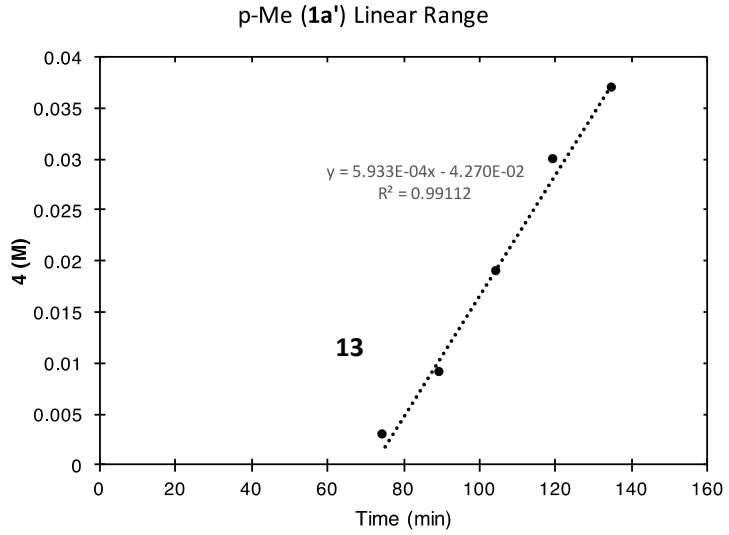

Figure A1.12. Standard reaction conditions ran with phosphonium salt **212** to obtain the initial reaction rate. Study was run in duplicate, and the average yield was used. Yields were determined at the given time points using ^{1}H NMR in $CDCl_3$ with 1,3,5-trimethoxybenzene as the internal standard.

Time (min)	Average [Product] (M)
15	0.006
30	0.001
45	0.002
60	0.004
75	0.011
90	0.014
105	0.025
120	0.033

Average yield after 60 h: 84%

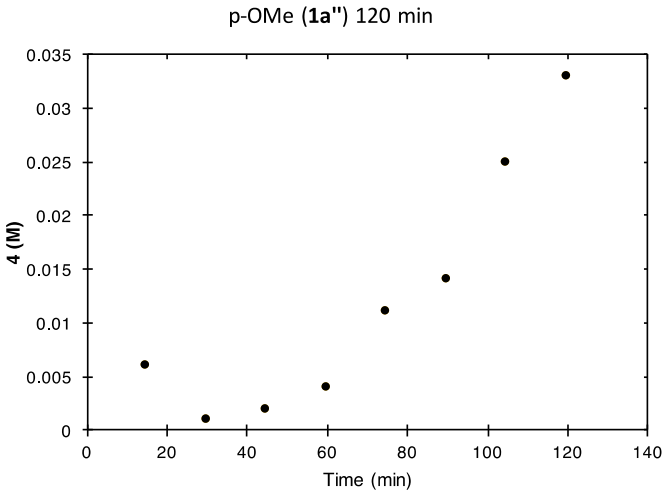

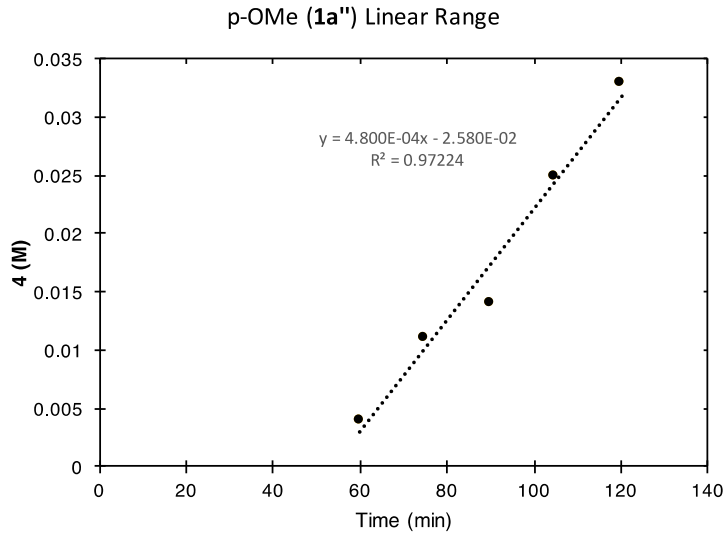

Figure A1.13. Standard reaction conditions ran with phosphonium salt **213** to obtain the initial reaction rate. Study was run in duplicate, and the average yield was used. Yields were determined at the given time points using ^{1}H NMR in $CDCl_3$ with 1,3,5-trimethoxybenzene as the internal standard.

Time (min)	Average [Product] (M)
15	0.001
30	0.013
45	0.01
60	0.011
75	0.025
90	0.024
105	0.039
120	0.047
150	0.055
165	0.067
180	0.076
195	0.084
210	0.089
225	0.095
240	0.094

Average yield after 60 h: 104%

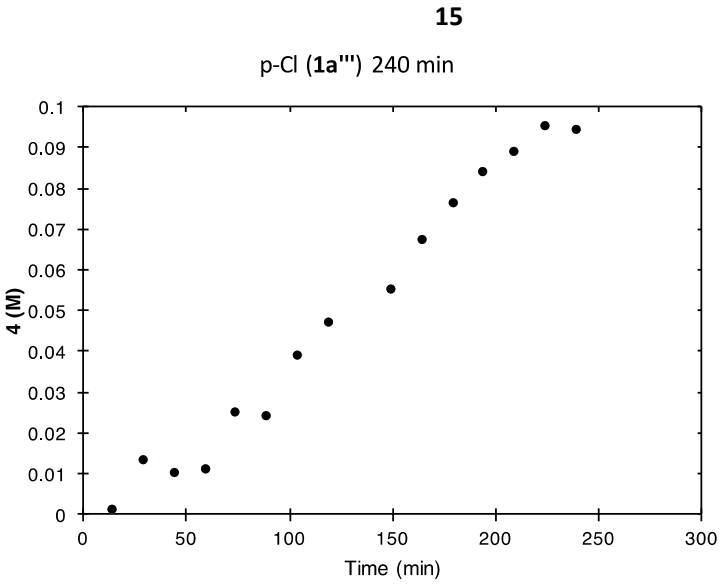

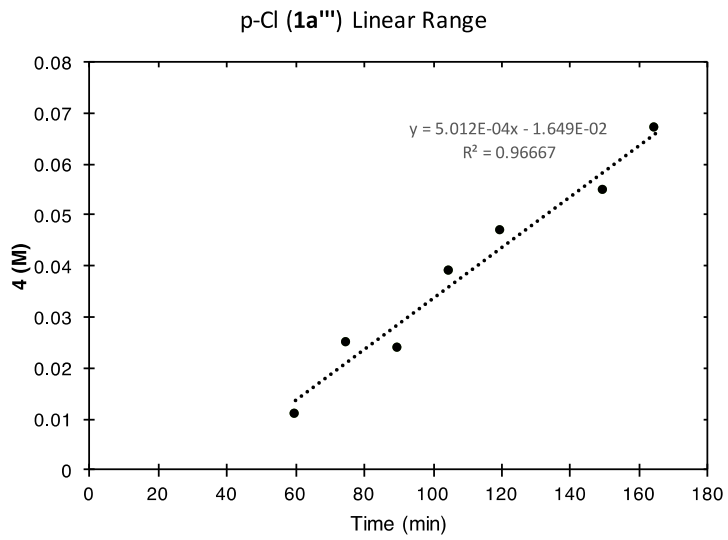

Figure A1.14. Standard reaction conditions ran with phosphonium salt **214** to obtain the initial reaction rate. Study was run in duplicate, and the average yield was used. Yields were determined at the given time points using ^{1}H NMR in $CDCl_3$ with 1,3,5-trimethoxybenzene as the internal standard.

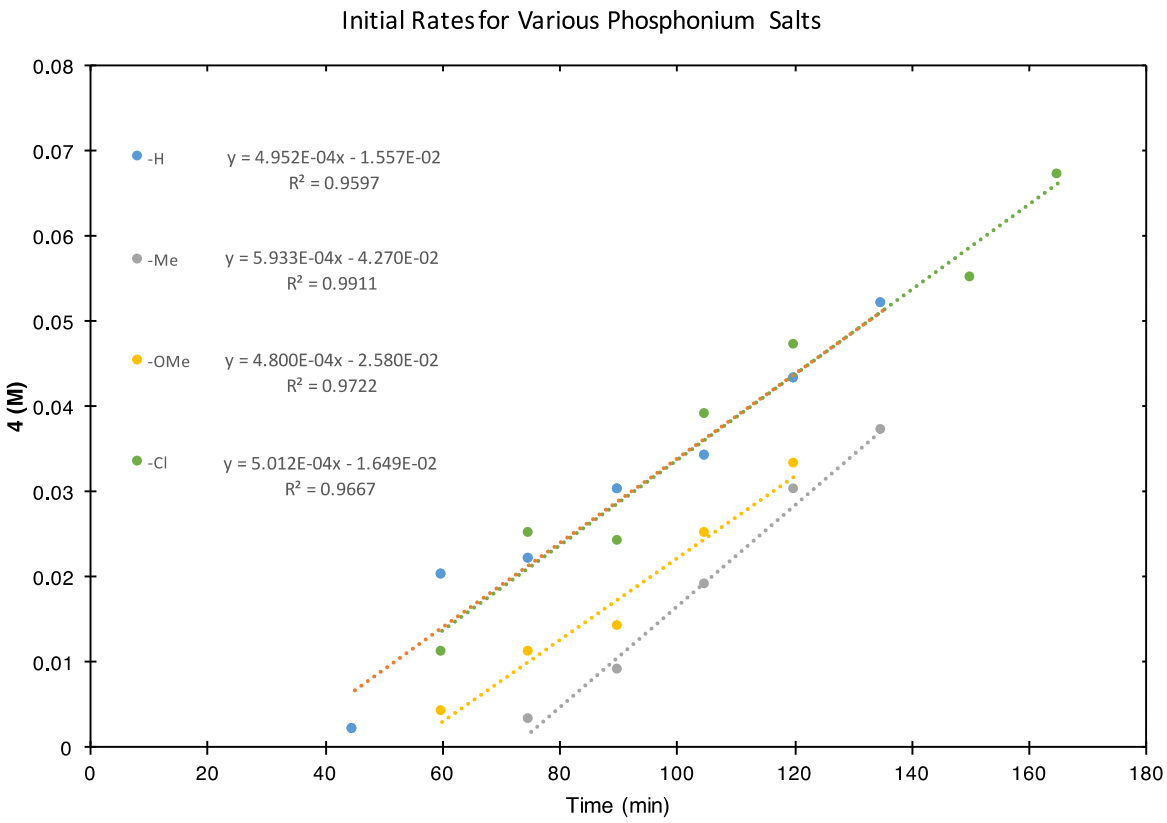

Figure A1.15. Standard reaction conditions ran with phosphonium salts **19** and **212** through **214** to obtain the initial reaction rates. Studies were run in duplicate, and the average yield was used. Yields were determined at the given time points using ^{1}H NMR in $CDCl_3$ with 1,3,5-trimethoxybenzene as the internal standard.

Table A1.1. Relative Initial Rates ($rate_X/rate_H$) of Phosphonium Salts **19, 212-214** under Standard Reaction Conditions.

Relative Rates:	
-Cl	1.01
-H	1.00
-Me	1.20
-OMe	0.97

Analysis: The investigation into the relative initial rates for the Minisci reaction shows no apparent correlation between initial reaction rate and electrophilicity (reduction potential) at the phosphorus center.

A1.9. UV-Visible Spectroscopy Study

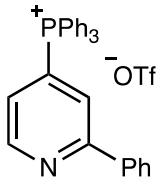

1a

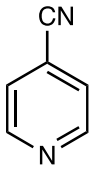

2

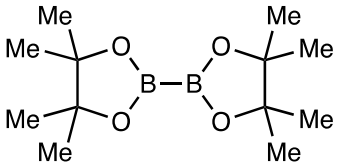

B_2pin_2

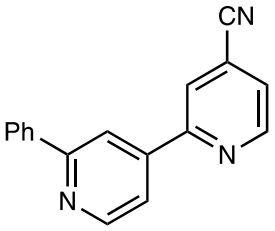

4a

a

Procedure: An oven dried 8 mL vial with a septa cap was charged with the reactants (0.05 mmol scale) (according to the standard equivalents for the optimized conditions if multiple reactants were added) under a nitrogen atmosphere in a glovebox. The vial was sealed and the mixture was stirred for 1-24 hours. Within a glovebox, a series of dilutions were made to achieve an absorbance between 0 and 1 a.u. (0.01 M – 0.0001 M) and the cuvette was then sealed under nitrogen.

UV-Vis Data:

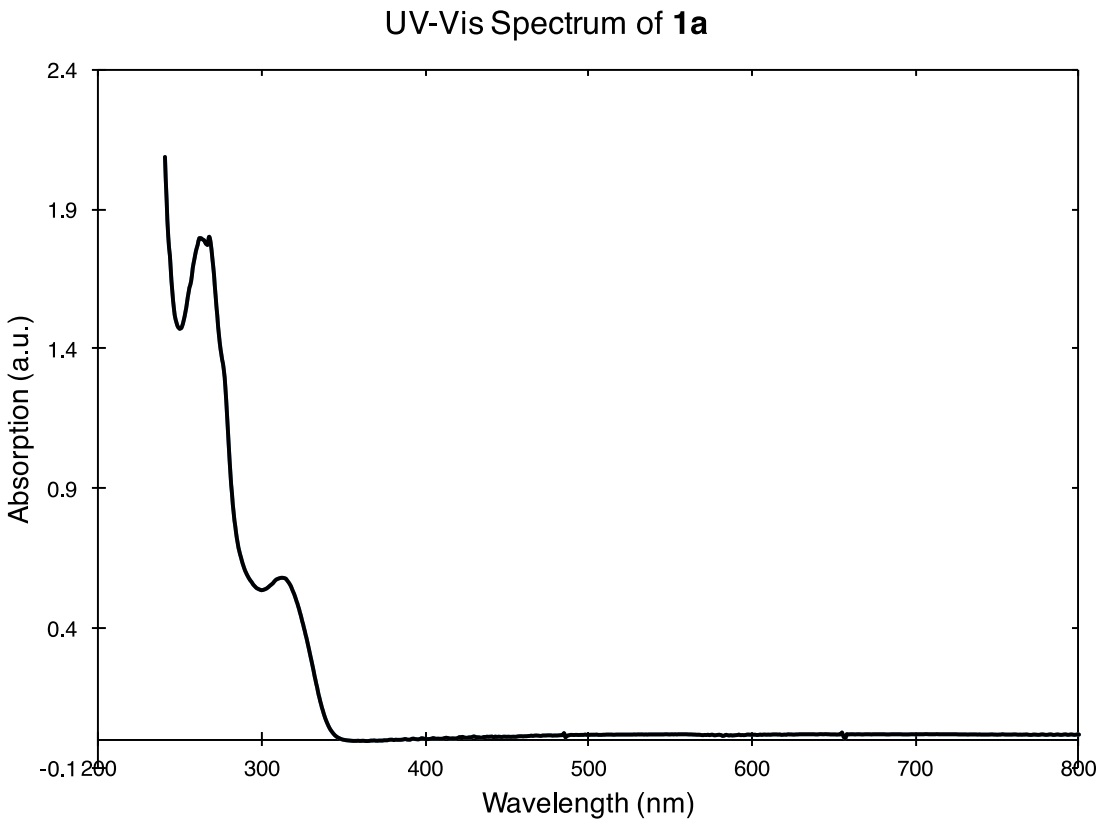

Figure A1.16. **1a** (28 mg, 0.05 mmol) in 1,2-dichloroethane (250 μL) was allowed to stir under a nitrogen atmosphere for 1 hour. The sample was then diluted with 1,2-dichloroethane to 0.0001 M and sealed in a cuvette with a 1.0 cm path length under nitrogen.

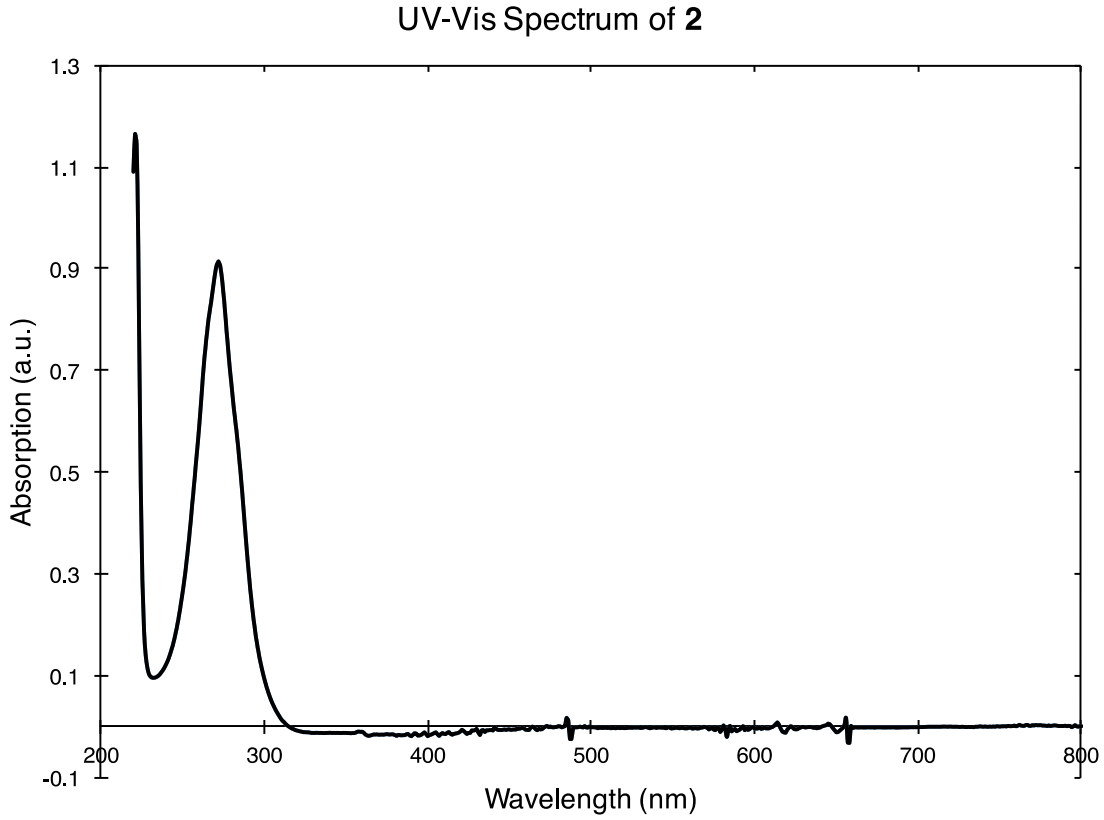

Figure A1.17. **2a** (10 mg, 0.1 mmol) in 1,2-dichloroethane (250 µL) was allowed to stir under a nitrogen atmosphere for 1 hour. The sample was then diluted with 1,2-dichloroethane to 0.001 M and sealed in a cuvette with a 0.17 cm path length under nitrogen.

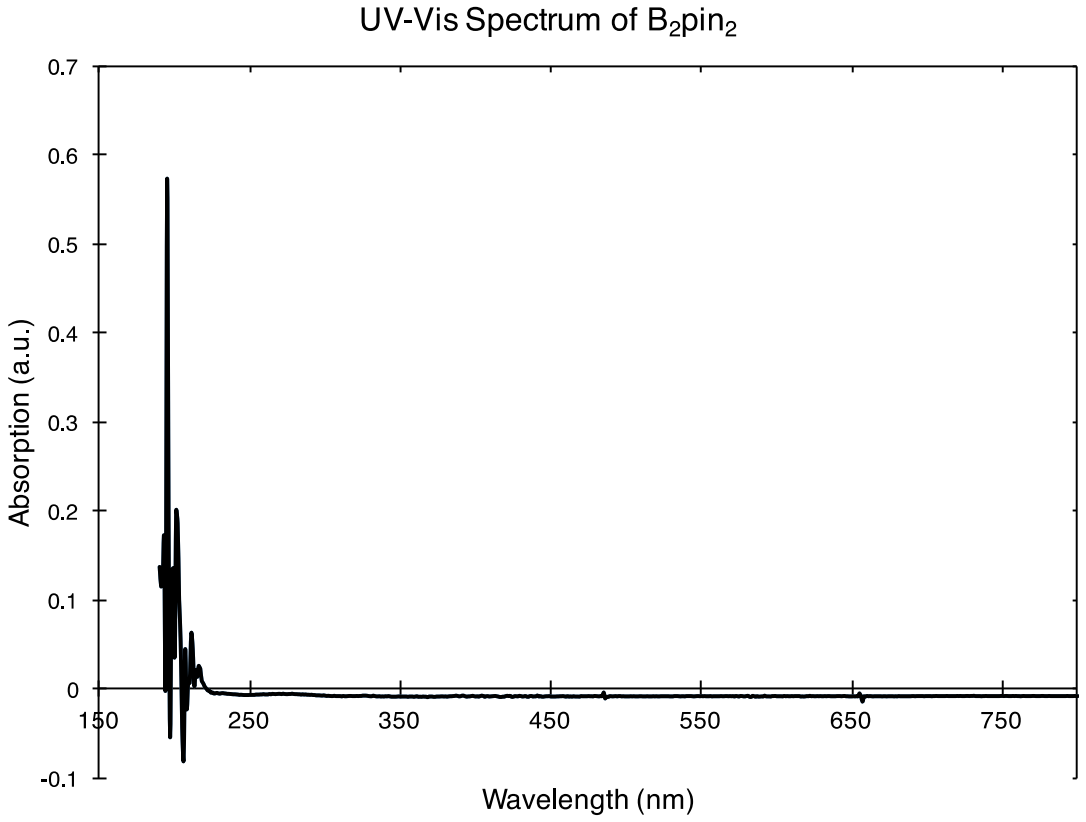

Figure A1.18. B_2pin_2 (13 mg, 0.05 mmol) in 1,2-dichloroethane (250 µL) was allowed to stir under a nitrogen atmosphere for 1 hour. The sample was then diluted with 1,2-dichloroethane to 0.01 M and sealed in a cuvette with a 0.17 cm path length under nitrogen.

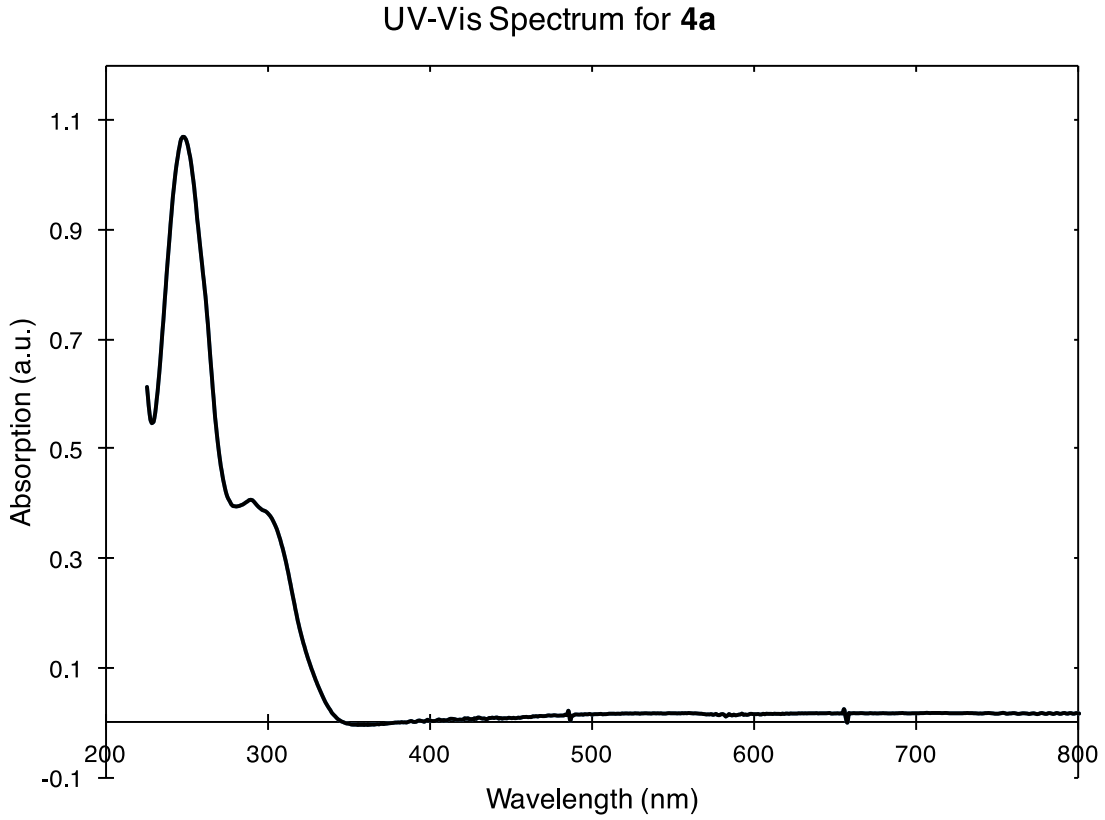

Figure A1.19. **4a** (13 mg, 0.05 mmol) in 1,2-dichloroethane (250 µL) was allowed to stir under a nitrogen atmosphere for 1 hour. The sample was then diluted with 1,2-dichloroethane to 0.0002 M and sealed in a cuvette with a 0.17 cm path length under nitrogen.

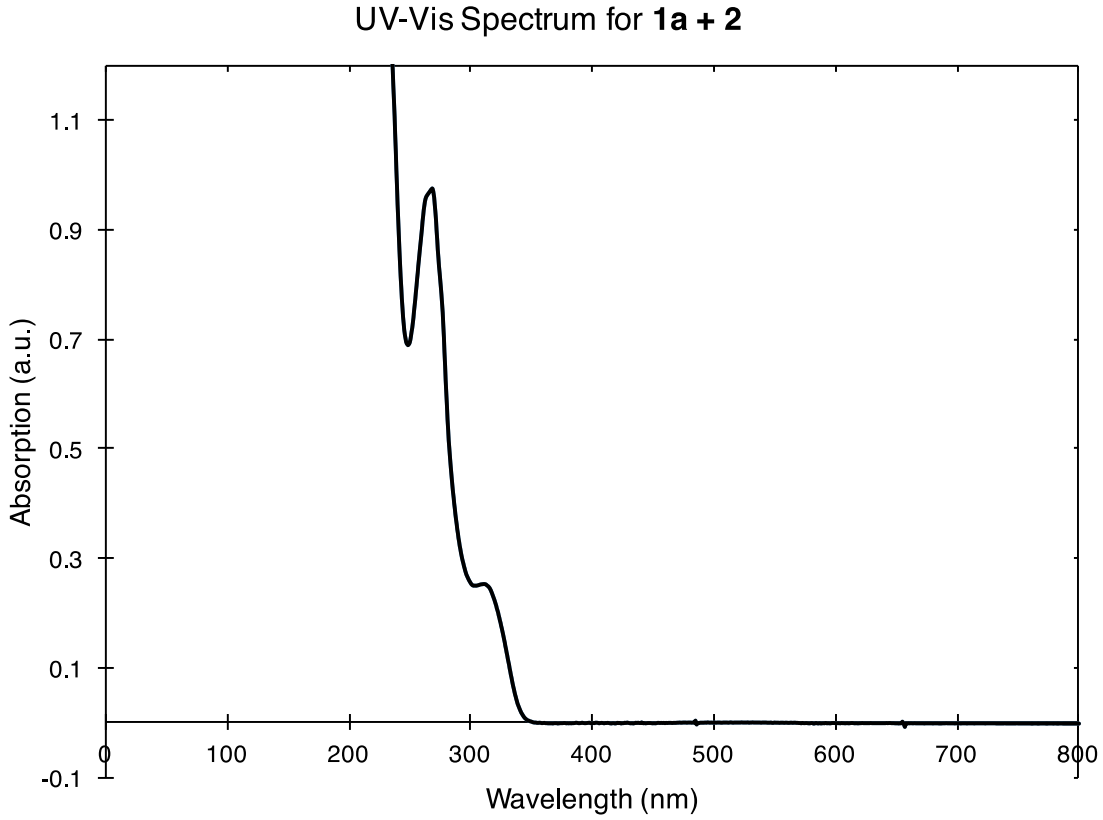

Figure A1.20. **1a** (28 mg, 0.05 mmol) and **2a** (10 mg, 0.1 mmol) in 1,2-dichloroethane (250 μL) were allowed to stir under a nitrogen atmosphere for 24 hours. The sample was then diluted with 1,2-dichloroethane to 0.001 M with respect to **1a** and sealed in a cuvette with a 0.17 cm path length under nitrogen.

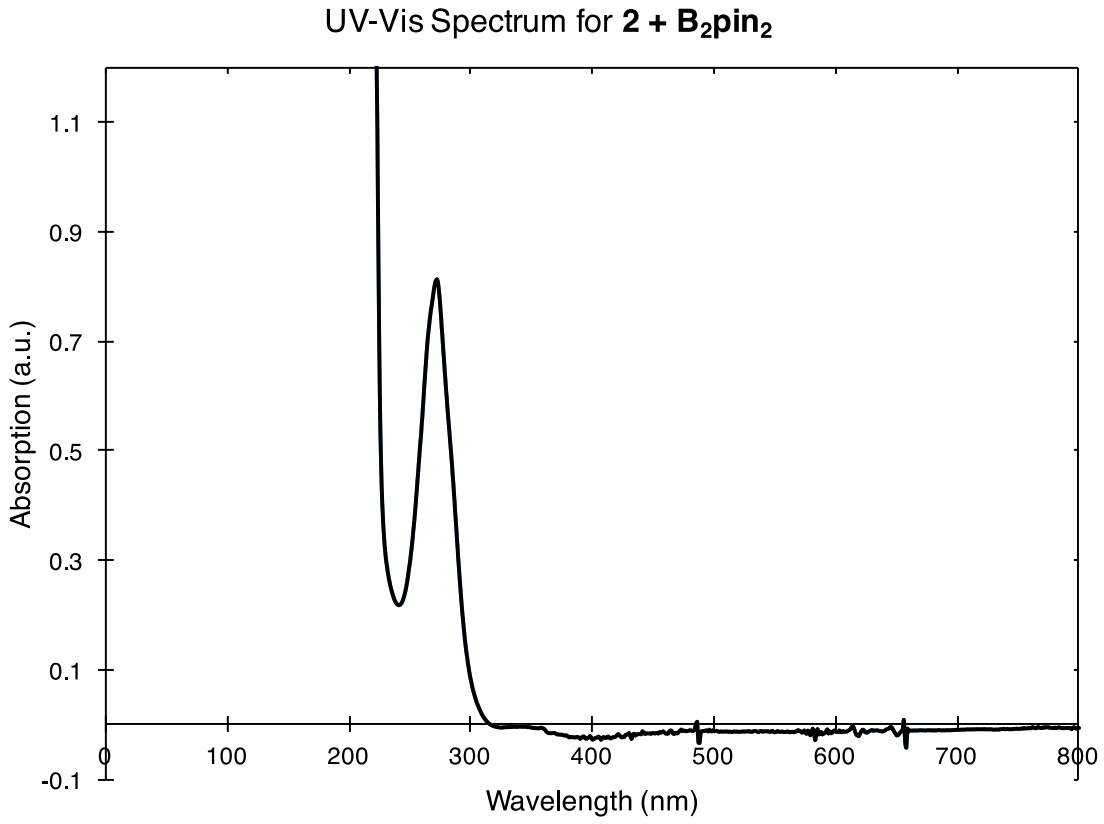

Figure A1.21. **2** (10 mg, 0.1 mmol) and B_2pin_2 (13 mg, 0.05 mmol) in 1,2-dichloroethane (250 µL) were allowed to stir under a nitrogen atmosphere for 24 hours. The sample was then diluted with 1,2-dichloroethane to 0.002 M with respect to **2a** and sealed in a cuvette with a 0.17 cm path length under nitrogen.

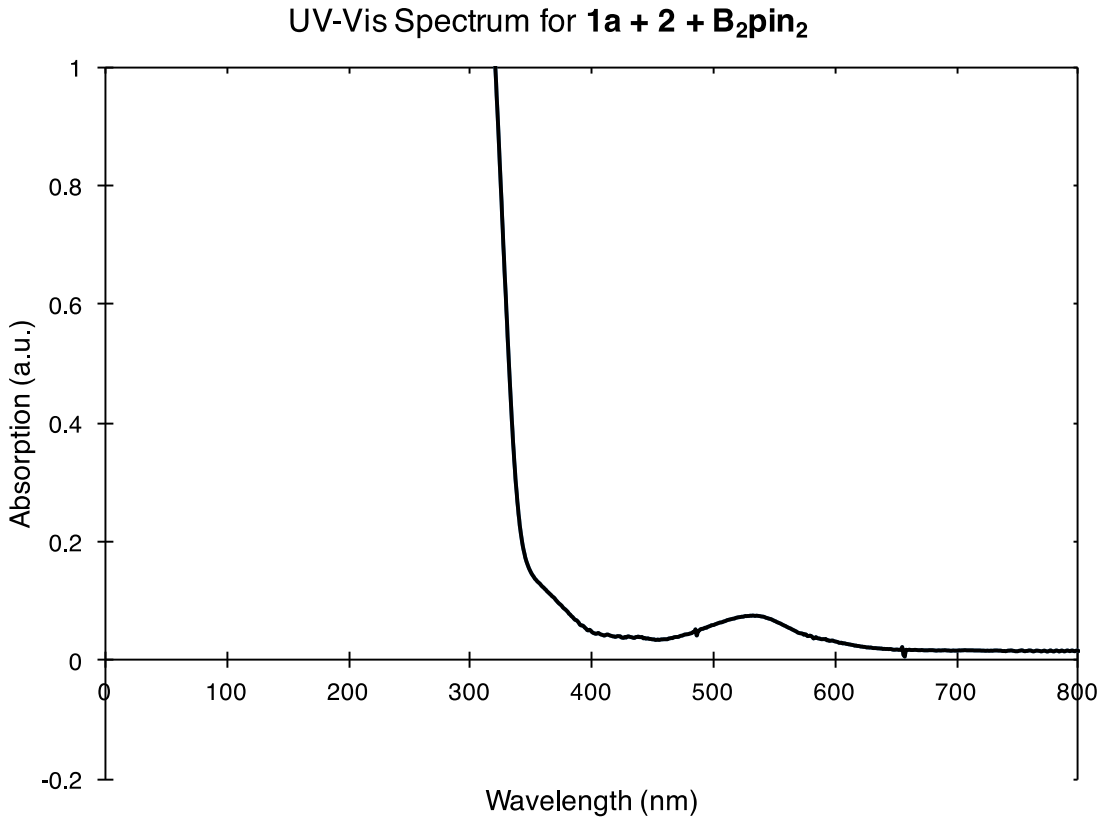

Figure A1.22. **1a** (28 mg, 0.05 mmol), **2a** (10 mg, 0.1 mmol), and B_2pin_2 (13 mg, 0.05 mmol) in 1,2-dichloroethane (250 μL) were allowed to stir under a nitrogen atmosphere for 24 hours. The sample was then diluted with 1,2-dichloroethane to 0.001 M with respect to **1a** and sealed in a cuvette with a 0.17 cm path length under nitrogen.

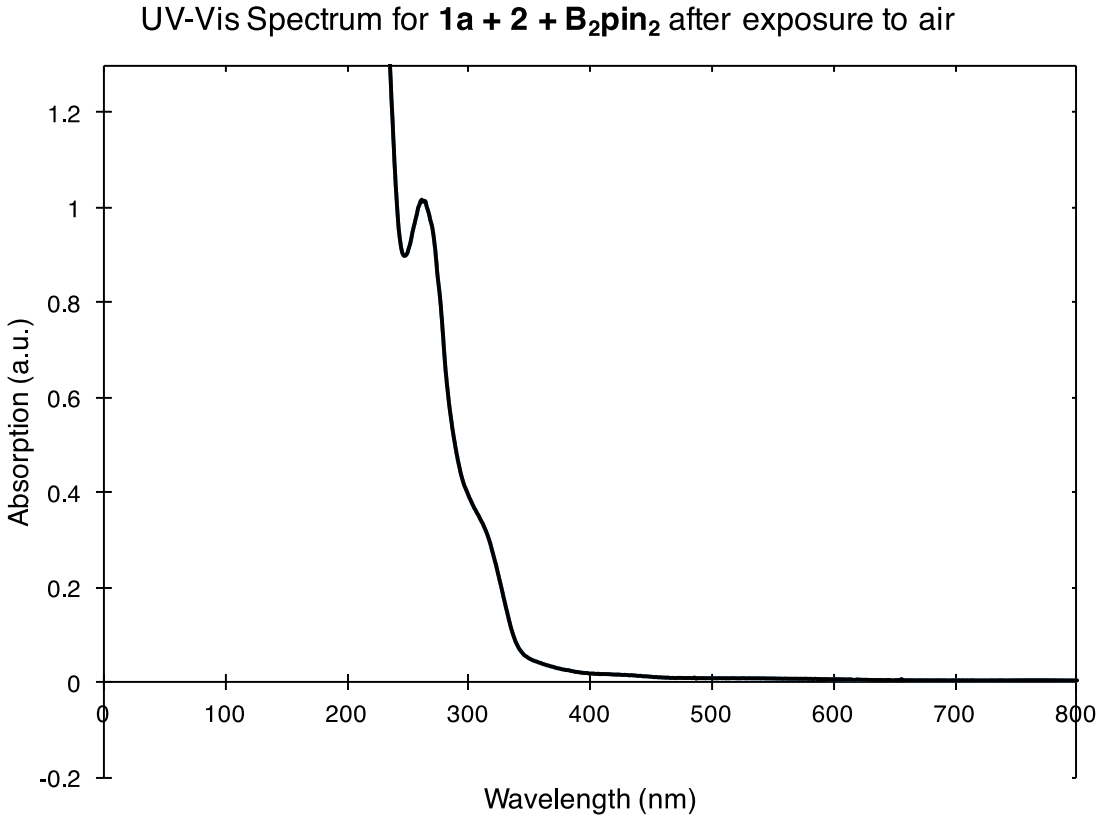

Figure A1.23. **1a** (28 mg, 0.05 mmol), **2a** (10 mg, 0.1 mmol), and B_2pin_2 (13 mg, 0.05 mmol) in 1,2-dichloroethane (250 μL) were allowed to stir under a nitrogen atmosphere for 24 hours. The sample was then diluted with 1,2-dichloroethane to 0.001 M with respect to **1a** and opened to air for 30 minutes. The sample was then placed in a cuvette with a 0.17 cm path length.

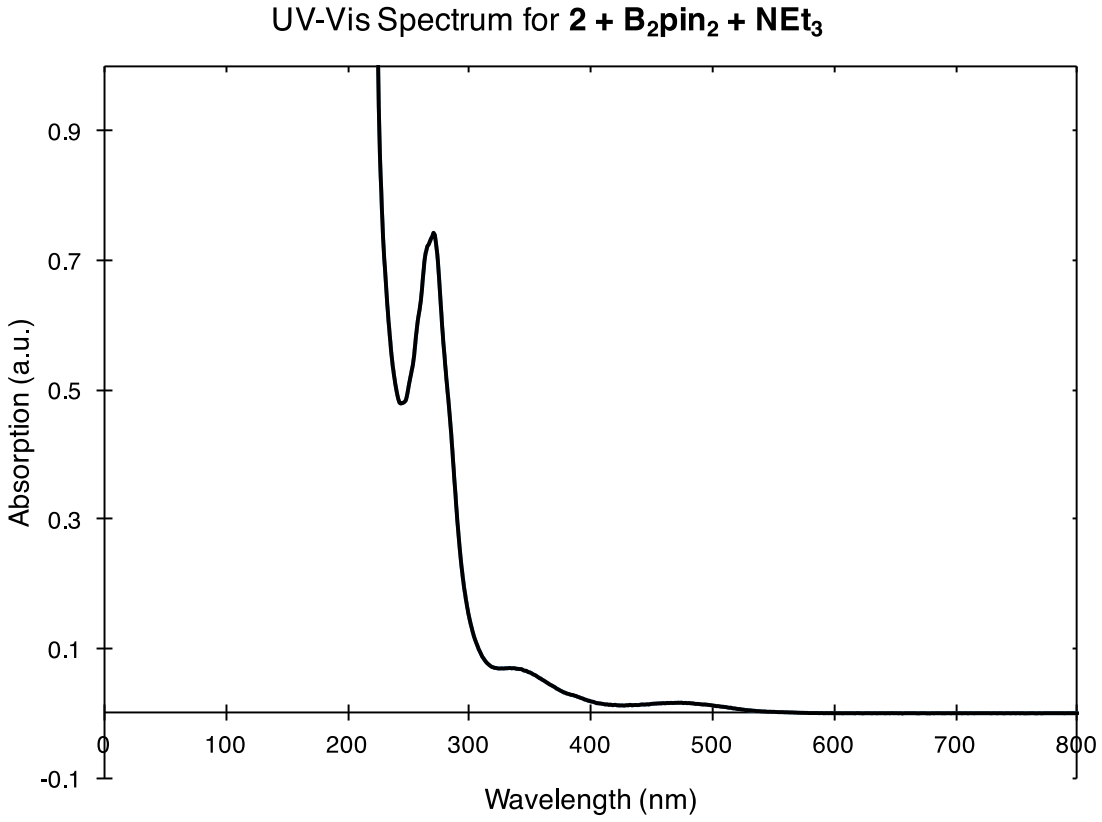

Figure A1.24. **2a** (10 mg, 0.1 mmol), B_2pin_2 (13 mg, 0.05 mmol), and NEt_3 (8.7 µL, 0.0625 mmol) in 1,2-dichloroethane (250 µL) were allowed to stir under a nitrogen atmosphere for 24 hours. The sample was then diluted with 1,2-dichloroethane to 0.002 M with respect to **2a** and sealed in a cuvette with a 0.17 cm path length under nitrogen.

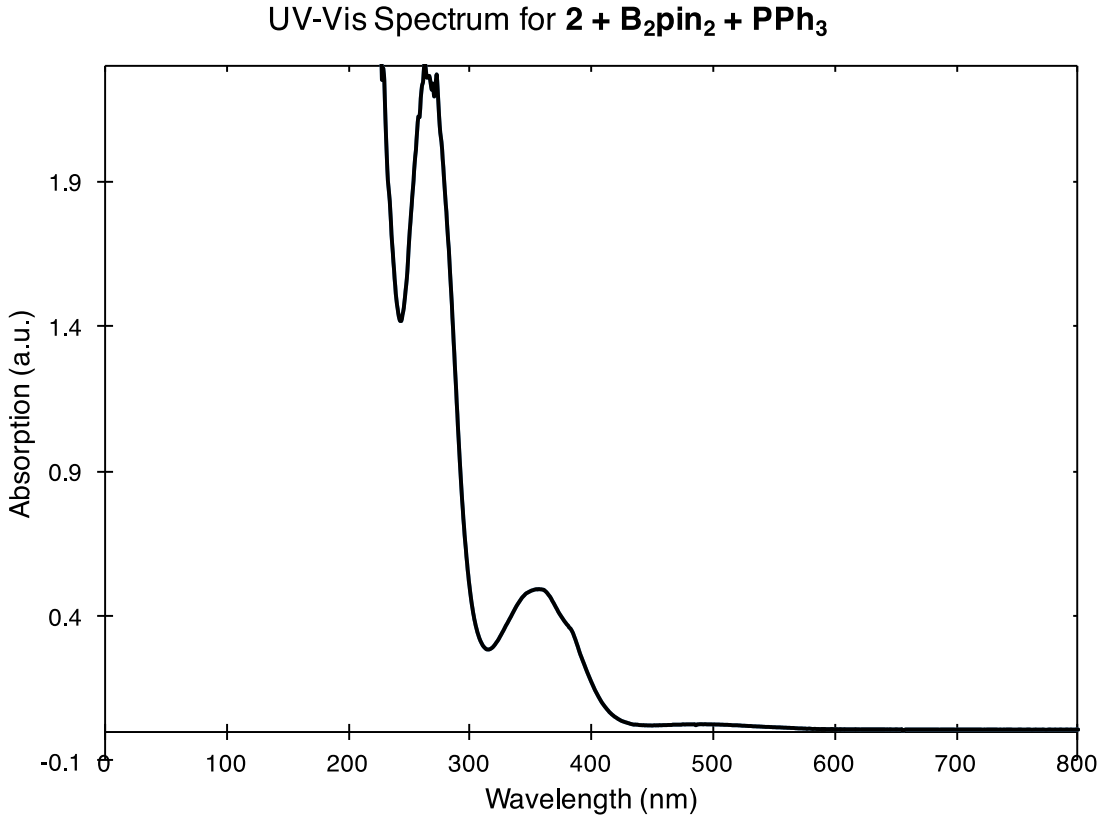

Figure A1.25. **2a** (10 mg, 0.1 mmol), B_2pin_2 (13 mg, 0.05 mmol), and PPh_3 (13 mg, 0.05 mmol) in 1,2-dichloroethane (250 μL) were allowed to stir under a nitrogen atmosphere for 24 hours. The sample was then diluted with 1,2-dichloroethane to 0.002 M with respect to **2a** and sealed in a cuvette with a 0.17 cm path length under nitrogen.

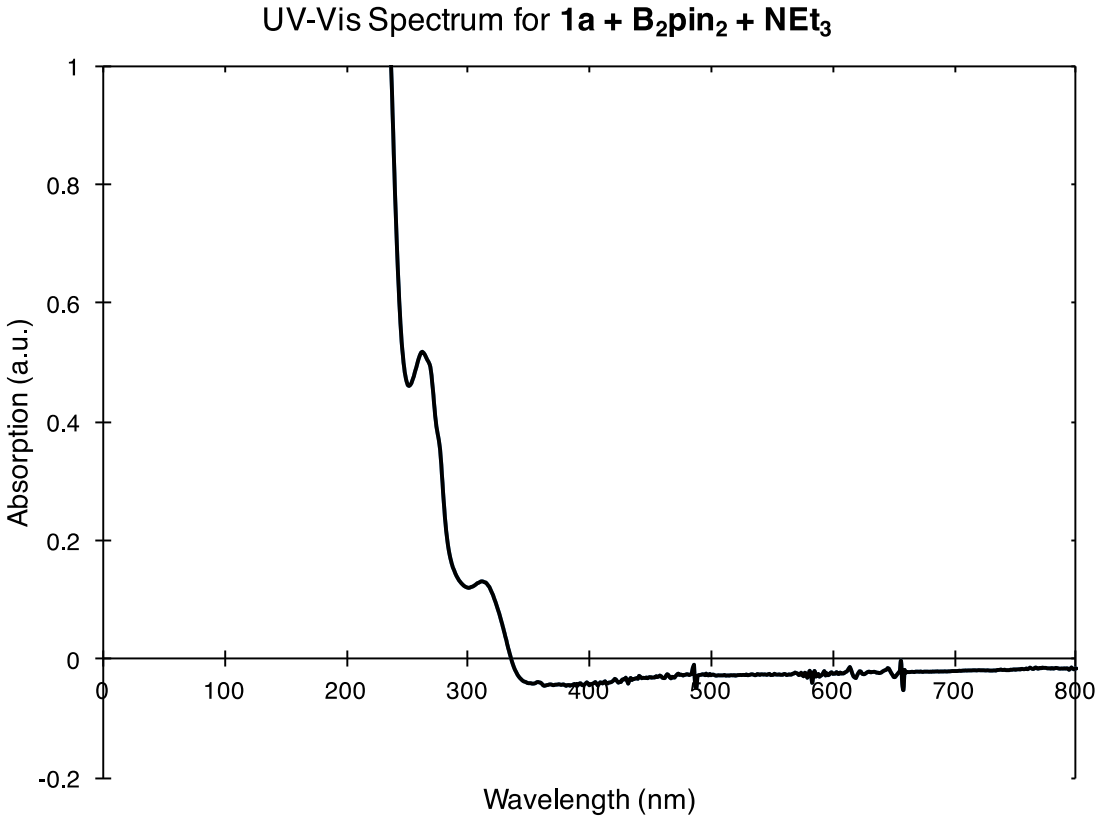

Figure A1.26. **1a** (28 mg, 0.05 mmol), B_2pin_2 (13 mg, 0.05 mmol), and NEt_3 (8.7 µL, 0.0625 mmol) in 1,2-dichloroethane (250 µL) were allowed to stir under a nitrogen atmosphere for 24 hours. The sample was then diluted with 1,2-dichloroethane to 0.0005 M with respect to **1a** and sealed in a cuvette with a 0.17 cm path length under nitrogen.

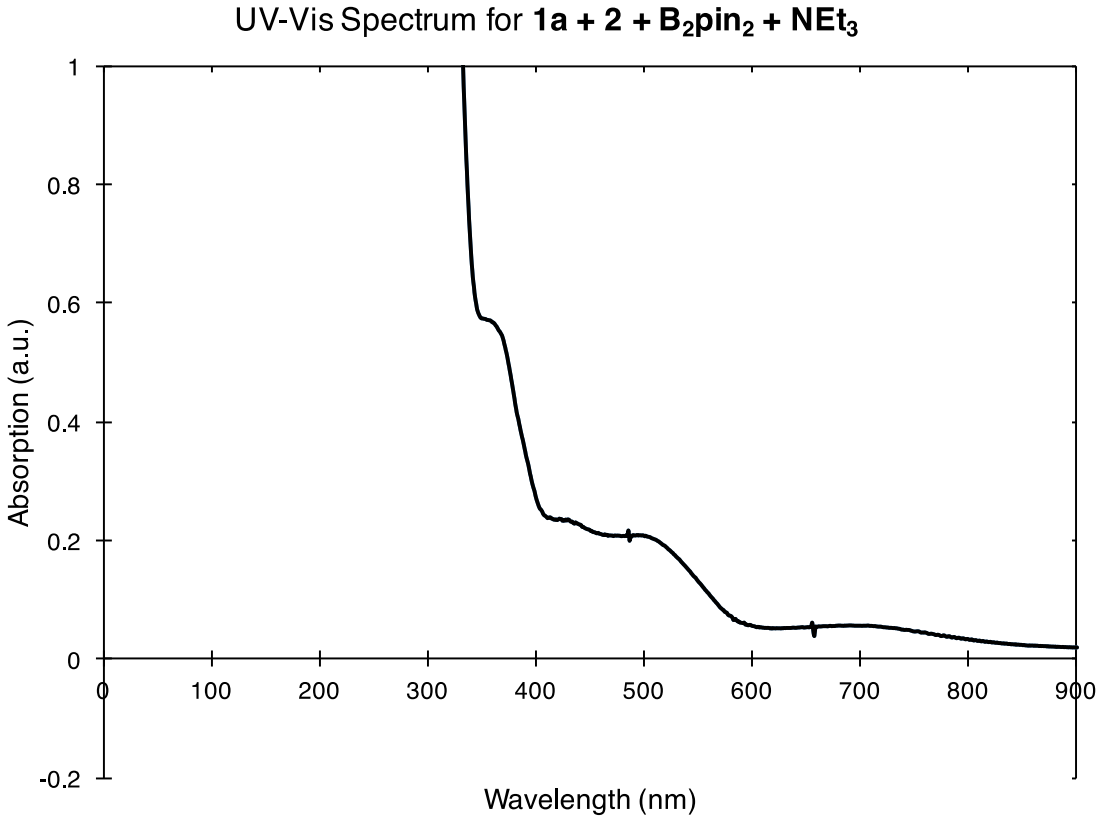

Figure A1.27. 1a (28 mg, 0.05 mmol), **2a** (13 mg, 0.1 mmol), B_2pin_2 (13 mg, 0.05 mmol), and NEt_3 (8.7 µL, 0.0625 mmol) in 1,2-dichloroethane (250 µL) were allowed to stir under a nitrogen atmosphere for 24 hours. The sample was then diluted with 1,2-dichloroethane to 0.0025 M with respect to **1a** and sealed in a cuvette with a 0.17 cm path length under nitrogen.

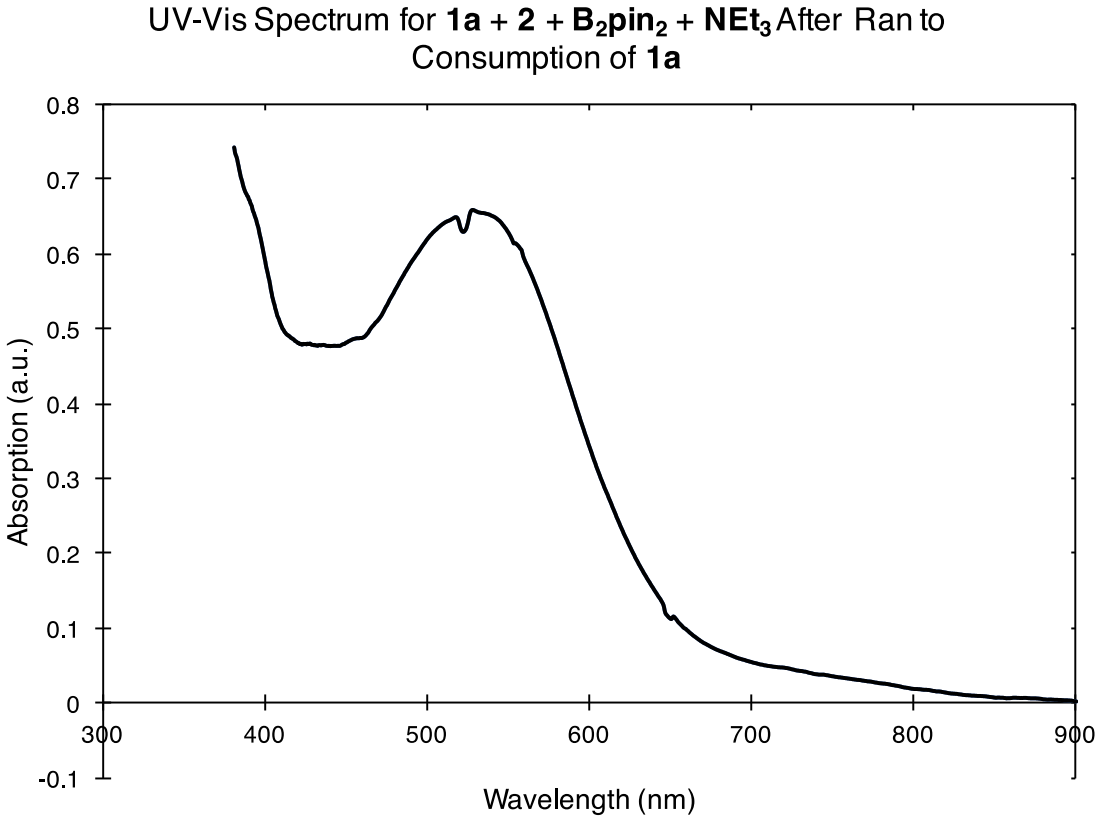

Figure A1.28. **1a** (21 mg, 0.2 mmol), **2a** (13 mg, 0.1 mmol), B_2pin_2 (13 mg, 0.05 mmol), and NEt_3 (8.7 μL, 0.0625 mmol) in 1,2-dichloroethane (250 μL) were allowed to stir under a nitrogen atmosphere for 48 hours. Consumption of **1a** was confirmed by LCMS. The sample was then diluted with 1,2-dichloroethane to 0.0025 M with respect to **1a** and sealed in a cuvette with a 0.17 cm path length under nitrogen.

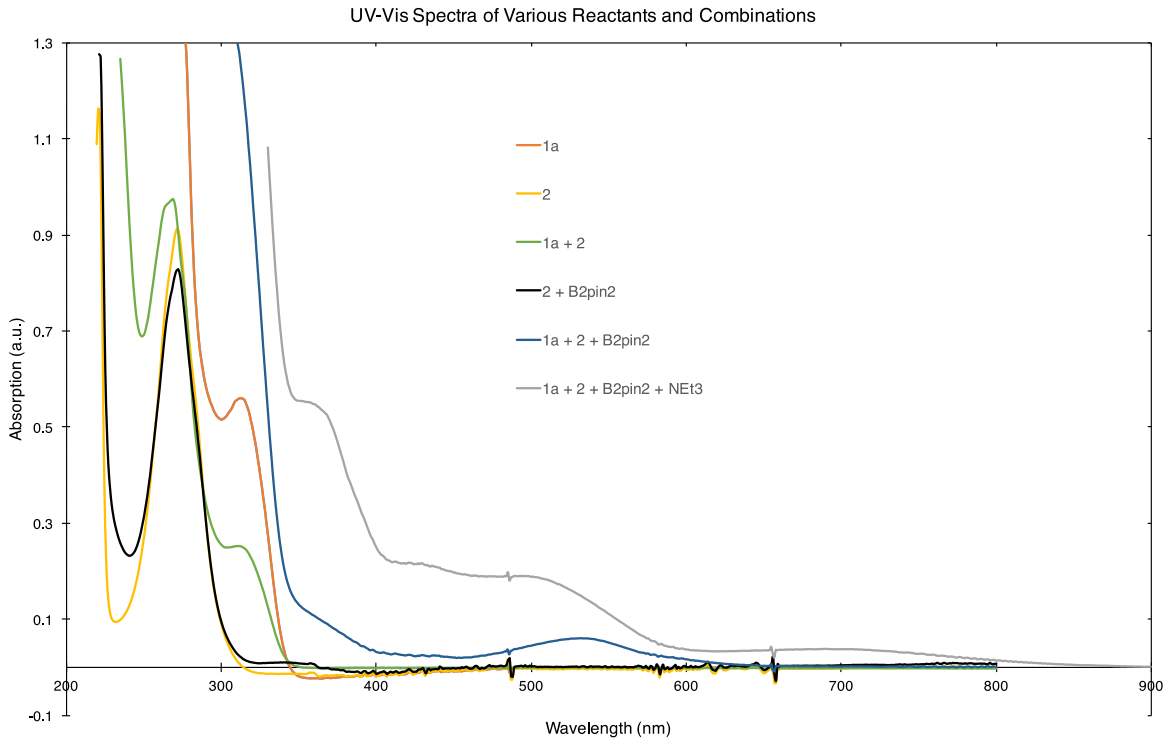

Figure A1.29. Overlaid UV-Vis spectra for various reactants and reactant combinations.

Analysis: The investigation into whether an electron donor-acceptor (EDA) complex could be observed by UV-Visible spectroscopy between the phosphonium salt **1a** and the reactants was inconclusive. A new bathochromic-shifted absorption (535 nm) was observed in Figure A1.27, however, this can most likely be attributed to dearomatized intermediate **11**. To support this hypothesis, a UV-Vis spectrum was collected from a reaction that was ran to completion (i.e. phosphonium salt **1a** was completely consumed) and the bathochromic shift was still present. At this time, an EDA complex is not supported by the UV-Vis data.

A1.10. Cyclic Voltammetry

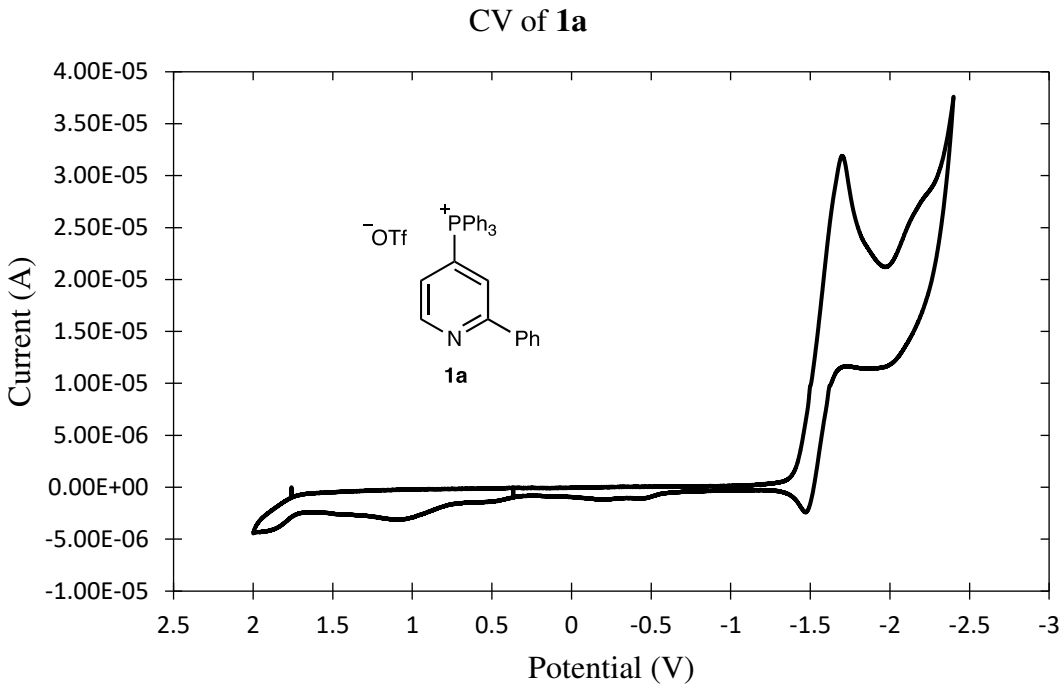

Figure A1.30. CV of **1a** in a 0.1 M CH_2Cl_2 solution of Bu_4NPF_6. Sweep rate: 100 mV/sec. Carbon working electrode, Pt auxiliary electrode, Ag pseudo-reference electrode. Referenced to Fc^+/Fc. The scan was started at the rest potential of the cell and swept cathodic. $E_p^{red} = -2.13$ V vs Fc^+/Fc (−1.67 V vs SCE), $E_{p/2} = -1.97$ V vs Fc^+/Fc (−1.51 V vs SCE).

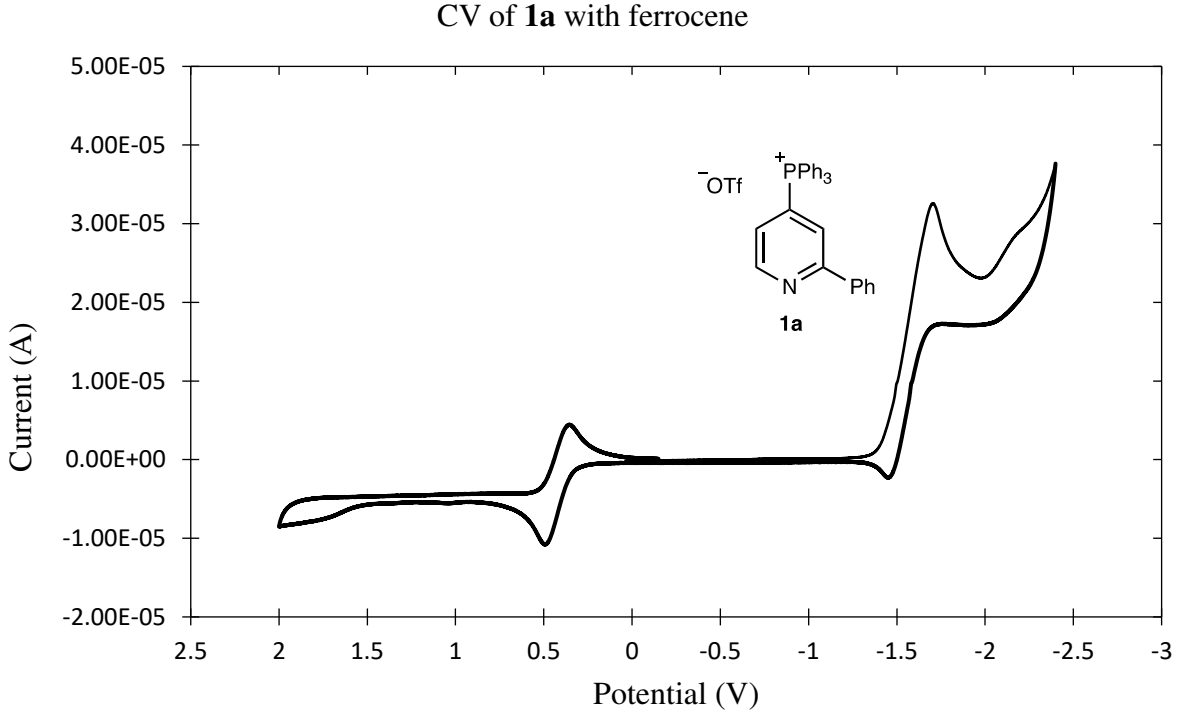

Figure A1.31. CV of **1a** and ferrocene in a 0.1 M CH_2Cl_2 solution of Bu_4NPF_6. Sweep rate: 100 mV/sec. Carbon working electrode, Pt auxiliary electrode, Ag pseudo-reference electrode. The scan was started at the rest potential of the cell and swept cathodic. Ferrocene anodic and cathodic peak difference = 127 mV, **1a** anodic and cathodic peak difference = 245 mV. Since **1a** peak difference is not 127 mV/*n* where *n* = 2 (*n* = number of electrons), this suggests that the quasi-reversible redox peak for **1a** is a single-electron event according to the Nernst equation.

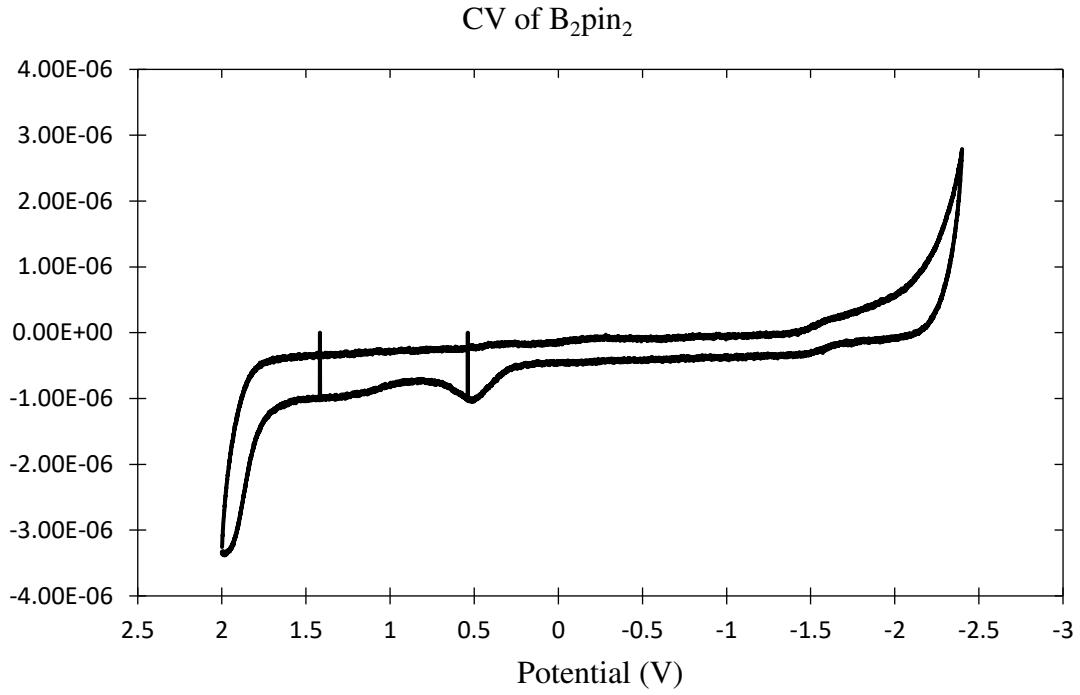

Figure A1.32. CV of B_2pin_2 in a 0.1 M CH_2Cl_2 solution of Bu_4NPF_6. Sweep rate: 100 mV/sec. Carbon working electrode, Pt auxiliary electrode, Ag pseudo-reference electrode. Referenced to Fc^+/Fc. The scan was started at the rest potential of the cell and swept cathodic. No significant redox events were observed.

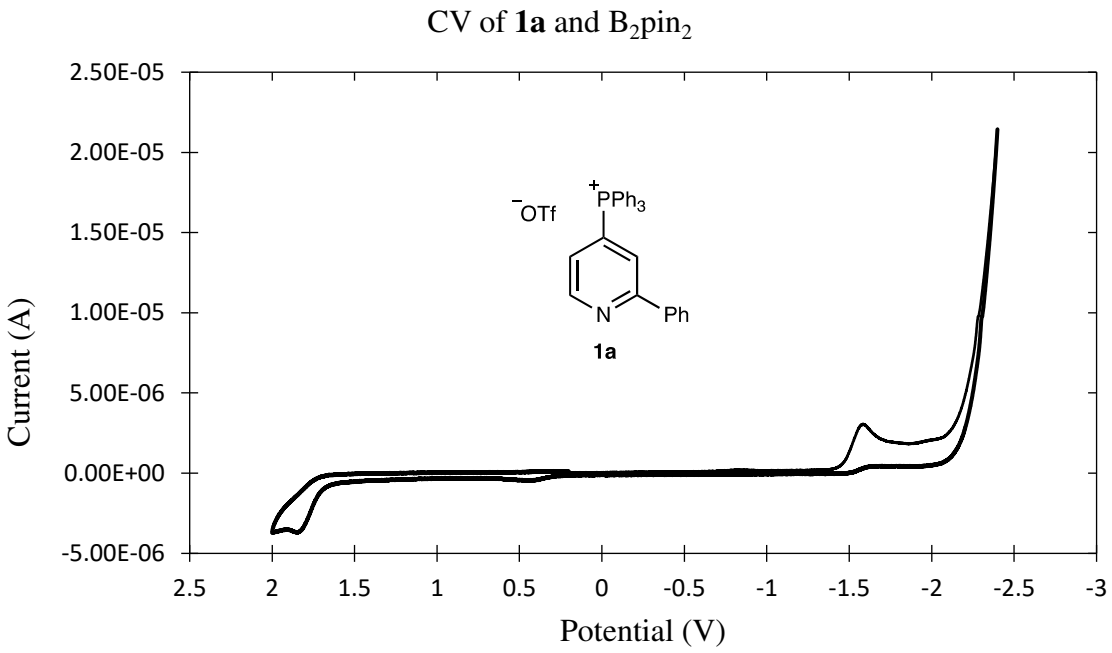

Figure A1.33. CV of **1a** and B_2pin_2 (equimolar) in a 0.1 M CH_2Cl_2 solution of Bu_4NPF_6. Sweep rate: 100 mV/sec. Carbon working electrode, Pt auxiliary electrode, Ag pseudo-reference electrode. Referenced to Fc^+/Fc. The scan was started at the rest potential of the cell and swept cathodic. $E_p^{red} = -2.13$ V vs Fc^+/Fc (−1.67 V vs SCE), $E_{p/2} = -1.96$ V vs Fc^+/Fc (−1.50 V vs SCE). This result shows that there is no change in reduction potential for **1a** when in the presence of an equimolar amount of B_2pin_2.

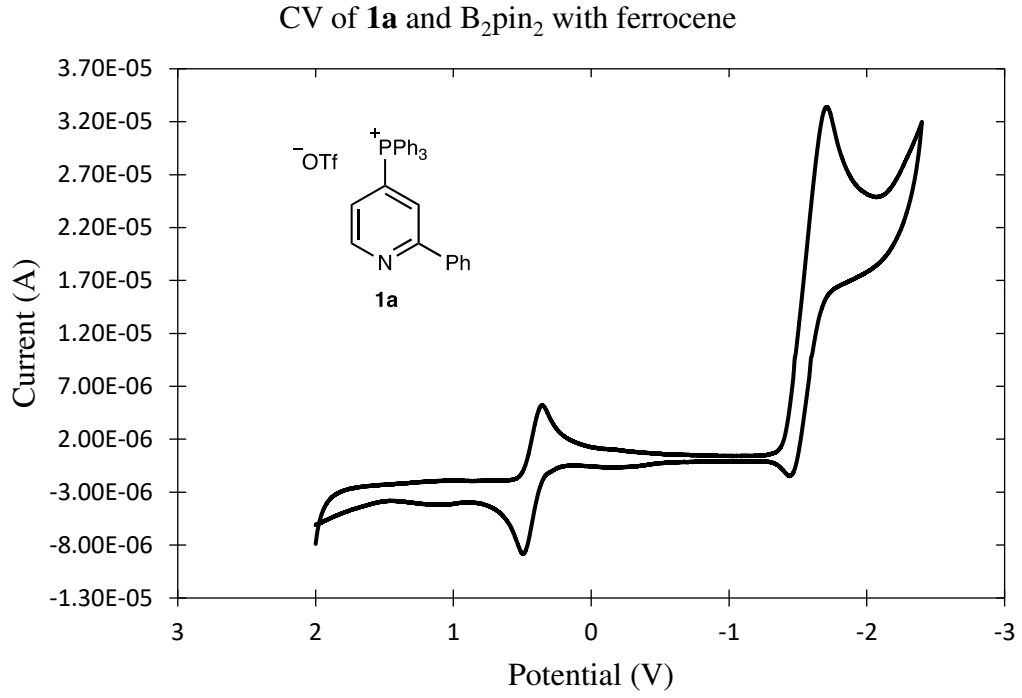

Figure A1.34. CV of **1a**, B_2pin_2, and ferrocene in a 0.1 M CH_2Cl_2 solution of Bu_4NPF_6. Sweep rate: 100 mV/sec. Carbon working electrode, Pt auxiliary electrode, Ag pseudo-reference electrode. The scan was started at the rest potential of the cell and swept cathodic. Ferrocene anodic and cathodic peak difference = 140 mV, **1a** anodic and cathodic peak difference = 263 mV. Since **1a** peak difference is not 140 mV/*n* where *n* = 2 (*n* = number of electrons), this suggests that the quasi-reversible redox peak for **1a** is a single-electron event according to the Nernst equation.

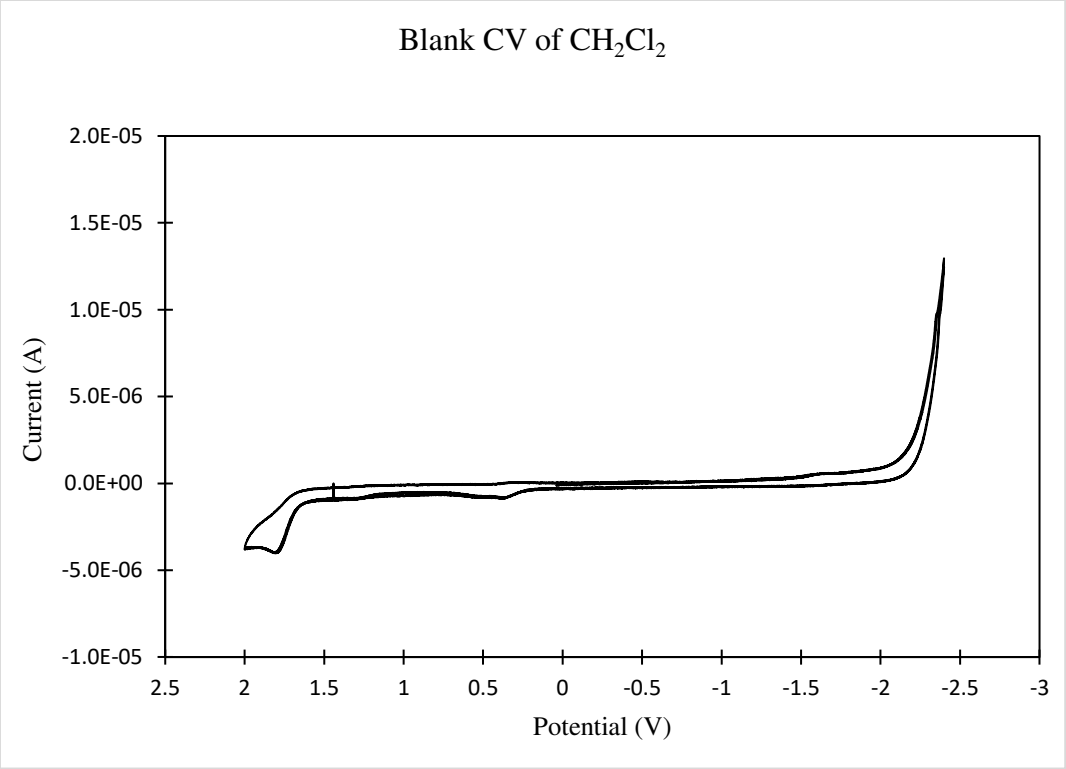

Figure A1.35. Blank CV of a 0.1 M CH_2Cl_2 solution of Bu_4NPF_6. Sweep rate: 100 mV/sec. Carbon working electrode, Pt auxiliary electrode, Ag pseudo-reference electrode. The scan was started at the rest potential of the cell and swept cathodic.

A1.11. Computational studies:

DFT calculations (ωB97X-D/def2-QZVPP with implicit solvation) were used to probe the feasibility of electron transfer. The outer sphere single electron transfer from boryl radical to a pyridyl phosphonium was found to be thermodynamically unfavorable: the reaction is endergonic by ca. 30 kcal/mol (Figure S30). **With such a barrier, the kinetics of outer-sphere electron transfer are also expected to be prohibitively slow**. The DFT result was corroborated by DLPNO-CCSD(T) calculations.

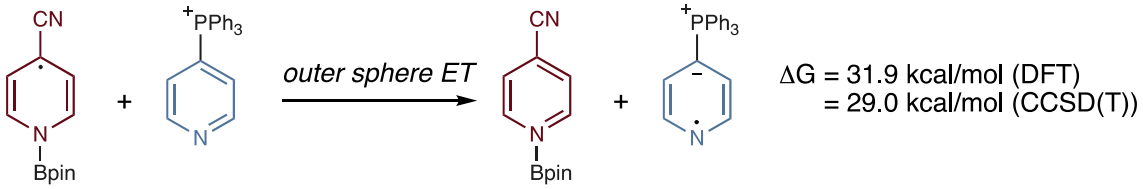

Figure A1.36. Computed thermodynamics for single-electron transfer to pyridyl phosphonium. DFT = ωB97X-D/def2-QZVPP//ωB97X-D/def2-SVP; CCSD(T) = DLPNO-CCSD(T)/cc-pV(2,3)Z//ωB97X-D/def2-SVP.

The possibility of a second single-electron reduction of putative pyridyl phosphonium radical was also examined computationally (Figure S31). Again, the thermodynamics of this process are extremely unfavorable such that this process can be dismissed from contention.

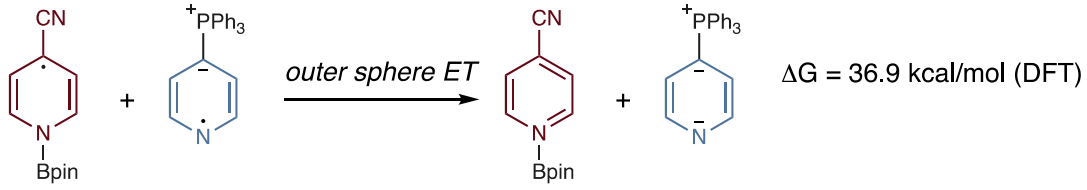

Figure A1.37. Computed thermodynamics for a second single-electron transfer to a pyridyl phosphonium radical. DFT = ωB97X-D/def2-QZVPP//ωB97X-D/def2-SVP.

In contrast, an *inner sphere* electron transfer event, mediated by the intermediacy of a boron-bridged complex was found to be much more facile (Figure S32). Formation of this intermediate is energetically favorable, with the overall endergonicity of this process resulting from the unfavorable entropic cost of bimolecular association. From this intermediate, release of a borylated pyridyl phosphonium and cyanopyridine can occur, with a very similar stability (i.e. within 2 kcal/mol) to the starting species. **The two borylated pyridine species are therefore expected to interchange readily and reversibly in solution**.

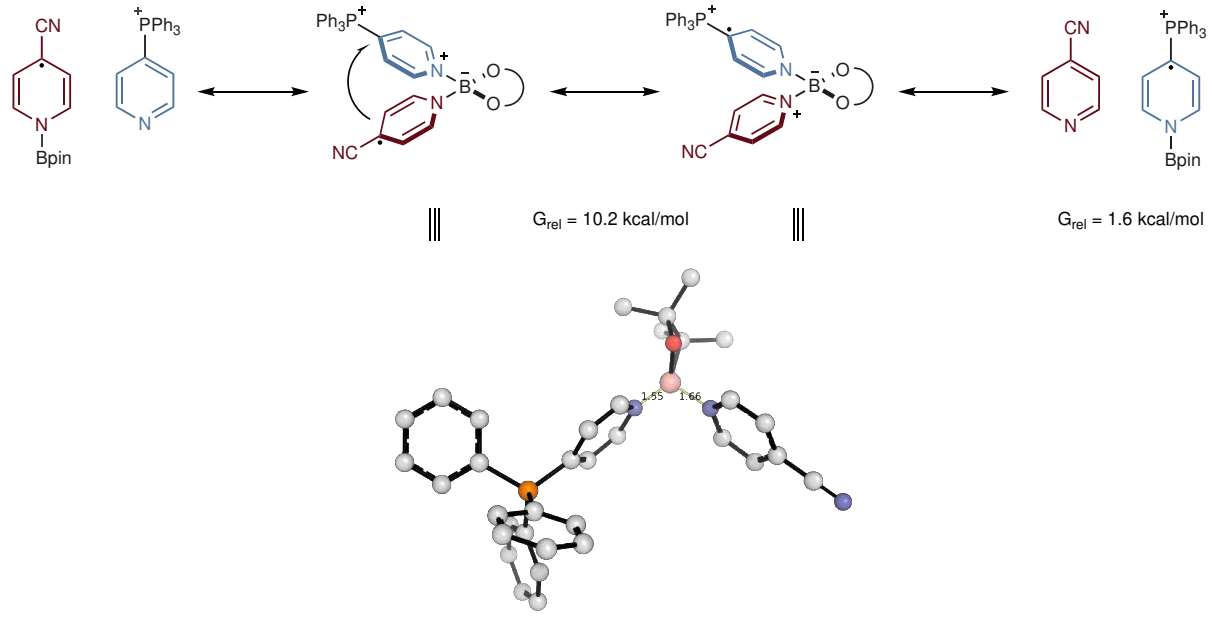

Figure A1.38. Computed thermodynamics for inner sphere single-electron transfer. DFT = ωB97X-D/def2-QZVPP//ωB97X-D/def2-SVP.

Intramolecular electron redistribution in the boron-bridged intermediate was found to occur spontaneously once the complex is formed: in the DFT optimized structure the unpaired electron resides entirely in the pyridyl phosphonium ring (spin-density plots, Figure S33), having migrated from the cyanopyridine ring. In each of the radical species shown below, the unpaired electron is delocalized around the pyridine ring, with most of the spin residing at C2 and C4-positions.

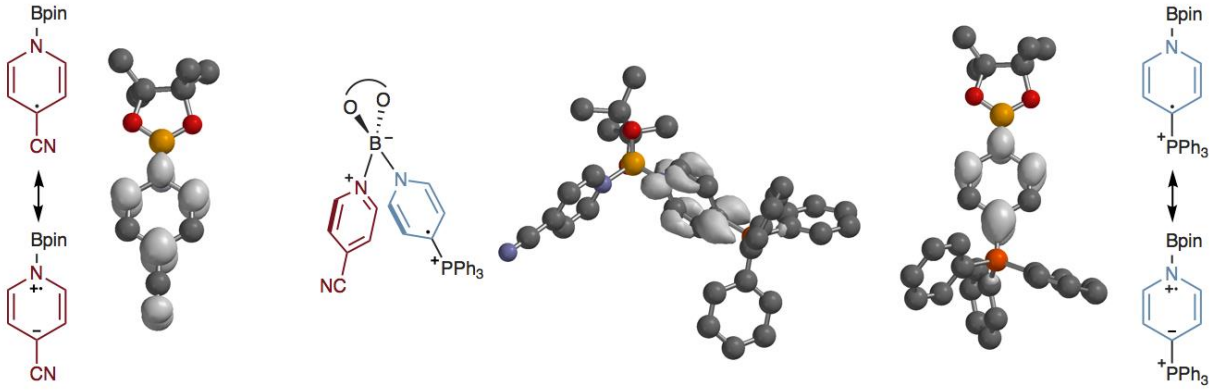

Figure A1.39. ωB97X-D Mulliken spin densities indicating localization of the unpaired electron.

Radical generation: Multiple pathways were considered to form radical pair **1b''** and **2a''** from homolytic cleavage of heterodiboron complexes (Scheme S1). The energy barriers are comparable in all the cases, indicating that all these events might occur in different degree to form the different pyridyl radicals. The importance of each pathway most likely varies depending on the electronic and steric properties of the aromatic substituents of the pyridyl phosphonium salts used.

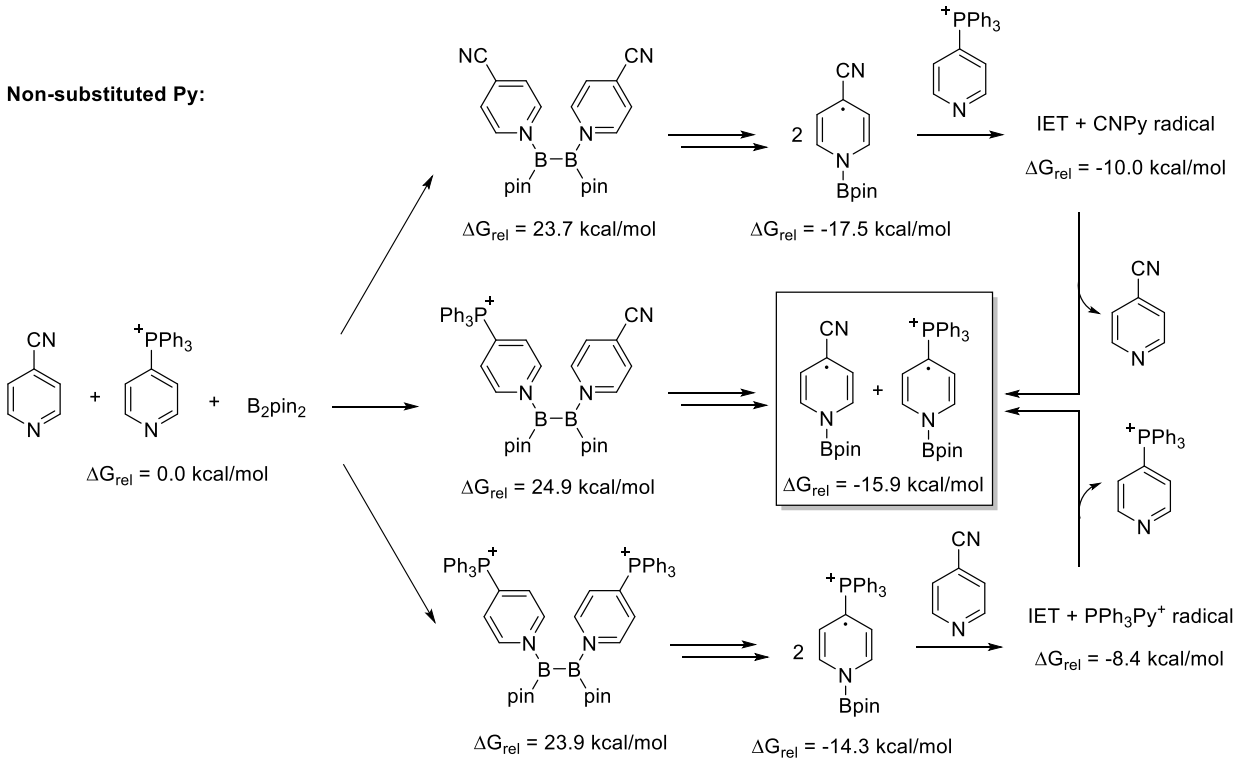

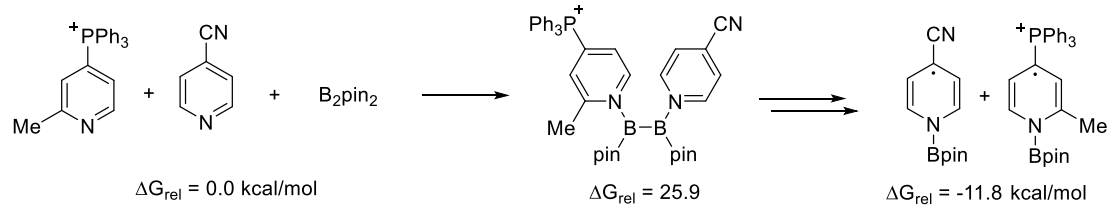

Scheme A1.1. Different pathways studied to generate radical pair **1b''** and **2a''**. IET = inner sphere electron transfer step.

Carbon-carbon bond formation: C-C bond formation can take place via radical recombination of a boryl pyridyl phosphonium radical and a boryl cyanopyridine radical. While the recombination of two boryl cyanopyridine radicals is thought to occur reversibly, this process (pyridyl phosphonium and cyanopyridine radical recombination) is irreversible due to the loss of triphenylphosphine. Subsequently, deborylation by an amine can also occur favorably, giving the adduct **11** that is observed by NMR spectroscopy (Figure S34). There is a low activation energy

barrier for this C-C bond forming TS, $\Delta E^{\ddagger}$ = 6.6 kcal/mol. The Gibbs energy of activation $\Delta G^{\ddagger}$ = 24.9 kcal/mol is higher due to the cost of bimolecular association, but nonetheless is readily attainable at ambient temperatures. Relatively little charge-transfer (< 0.2e) occurs in this TS, indicative that this is radical-radical coupling (the total spin densities on each of the two molecules, 0.47e, are equal and opposite) as opposed to a further single-electron reduction of the pyridyl phosphonium moiety. The radical-radical coupling of the borylated pyridyl phosphonium and cyanopyridyl radicals was computed to have a barrier *ca.* 20 kcal/mol lower than the alternatives considered (discussed below) and is consistent with room temperature reactivity.

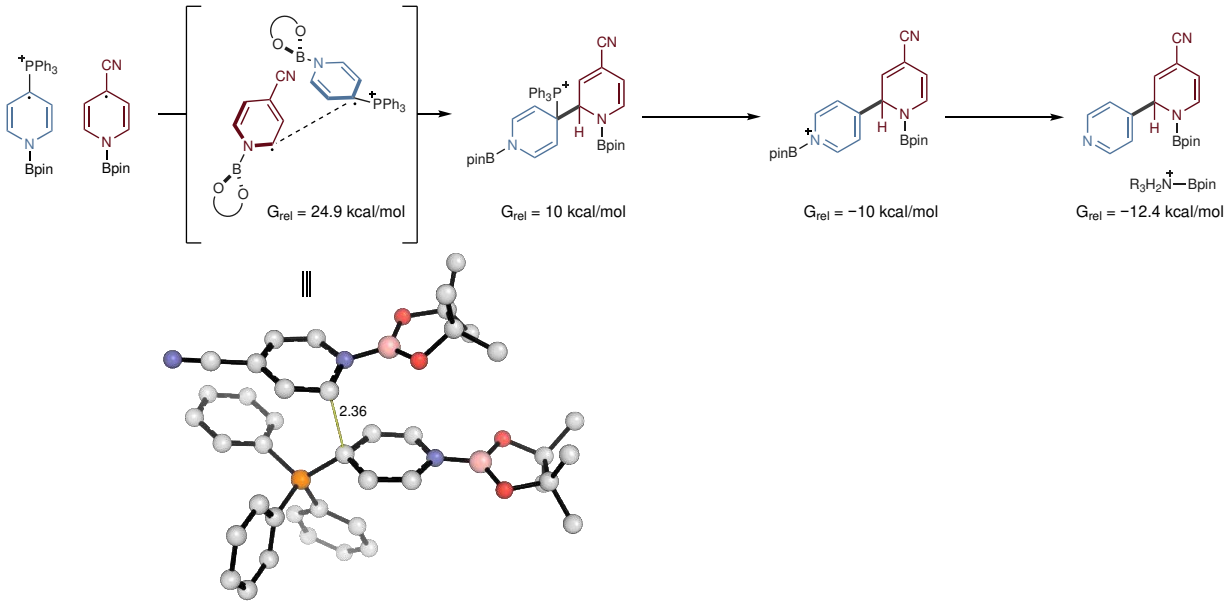

Figure A1.40. ωB97X-D computed reaction coordinate for bipyridyl formation via radical-radical coupling. Forming bond distance shown in Å, relative Gibbs energies in kcal/mol.

The alternative possibility of the pyridyl phosphonium radical reacting directly with cyanopyridine was also considered computationally (Figure S35). Gibbs energy barriers in excess of 40 kcal/mol were obtained with the boryl group still attached, indicative of an unfavorable reaction at room temperature (Figure S35b). Therefore, we considered the possibility of deborylation (for example

by amine), resulting in the formation of the free pyridyl phosphonium radical anion, that can then react with cyanopyridine. The Gibbs energy barrier for this TS, relative to these two species is a further 39.5 kcal/mol uphill, again indicative of an unfavorable coupling process at room

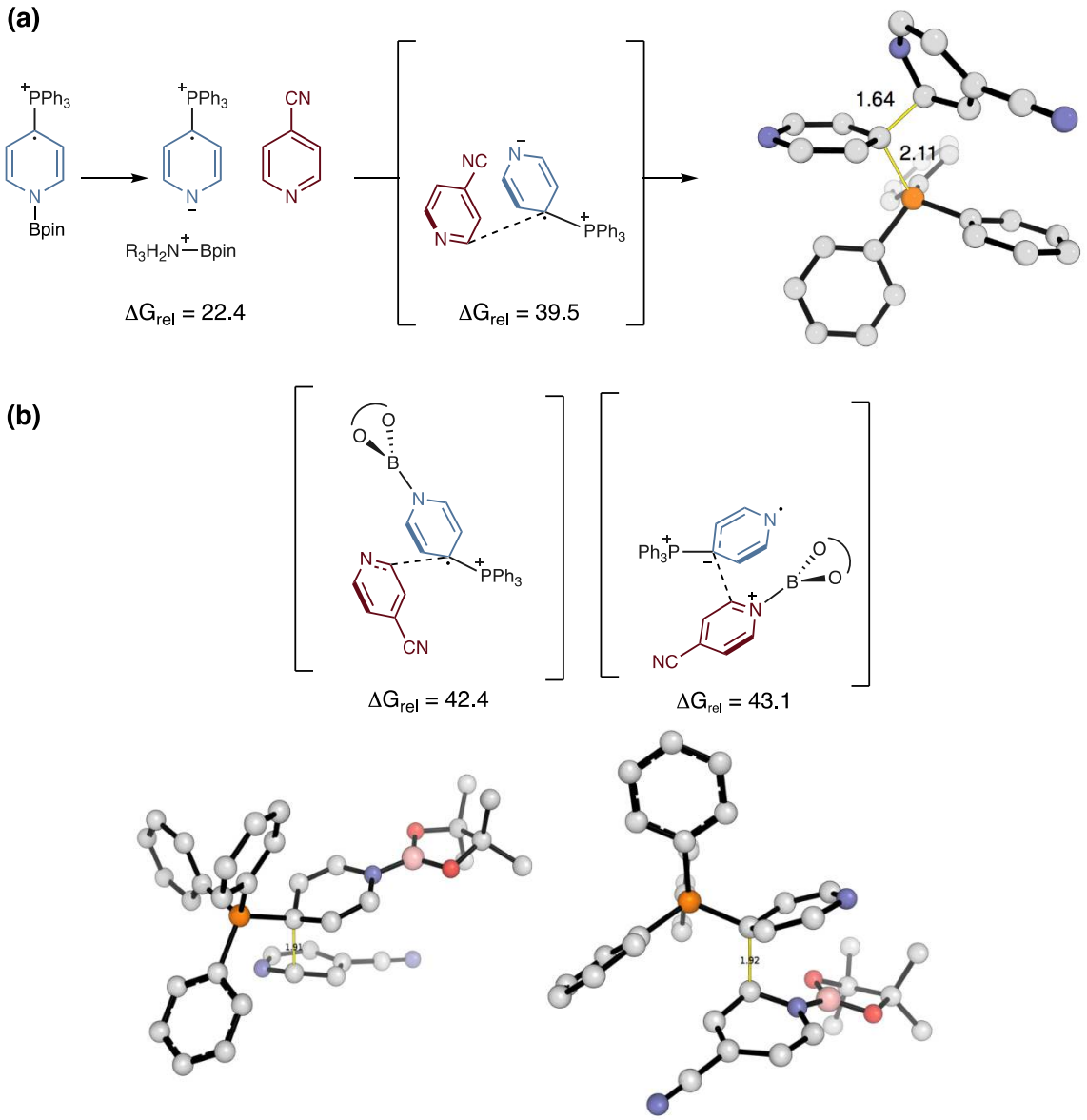

temperature. The loss of triphenylphosphine occurs in concert with C-C bond formation via this pathway.

Figure A1.41. ωB97X-D computed reaction coordinate for bipyridyl formation via radical addition to cyanopyridine. Forming bond distance shown in Å, relative Gibbs energies in kcal/mol

Computational methods: The dispersion-corrected density functional theory (DFT) functional ωB97X-D[2] was used with the def2-SVP[3] basis set for geometry optimizations. We carried out vibrational frequency calculations to obtain thermal corrections to Gibbs free energies (*G*) at 298.15 K (25 °C). Additionally, these frequency calculations were used to confirm that stationary points as minima or saddle points on the potential energy surface. An ultrafine pruned (99,950) grid was used for numerical integration and molecules were converted to their standard orientations before thermochemical analysis, which is expected to reduce the noise of rotational grid invariance. Additionally, quasi-harmonic entropy corrections were also applied.

In all the individual calculations, quasi-harmonic (QHA) vibrational corrections were applied to entropies using a frequency cut-off value of 100.0 cm^{-1}, as proposed by Grimme.[4] In a few cases, systems showed one persistent small imaginary frequency with $\nu_i < 20$ cm^{-1}. These imaginary frequencies were inverted to their respective positive values before the QHA entropic corrections were computed as seen in previous examples.[5] Additionally, a correction for the change in standard state from gas phase at 1 atm to a 1 M solution was applied when calculating G values. All of these thermodynamic corrections were calculated and automatically applied to the computed results by the *GoodVibes* program.[6]

All the optimization, frequency and single-point energy calculations included solvent effects obtained with the integral equation formalism variant of the polarizable continuum model (IEF-PCM) with the SMD solvation model (solvent = acetonitrile).[7]

Single-point energy calculations were used to refine electronic energies of optimized geometries. For this, DFT (ωB97X-D/Def2-QZVPP) was used. QHA G corrections calculated at the ωB97X-D/Def2-SVP level of theory were applied to these single point energies to obtain the final G values.

A manual conformational search was carried out in all the systems, positioning the different units in multiple interaction sites. Furthermore, for each possible interaction site, the different functional groups were rotated (see section *Thermochemical data and absolute energy values* for more information about the number of conformers used).

Gaussian 16[8] was used to perform all the DFT calculations with an "ultrafine" pruned (99,590) grid for numerical integration. Molecular graphics were generated using *PyMol*;[9] Our display settings have been made openly accessible.[10] Additionally, we used the "stable" option from Gaussian to test the stability of the wavefunctions created and detect any kind of partial or complete singlet biradical character in all the reaction steps involving singlet states.

Thermochemical data and absolute energy values: Boltzmann weighted G (G_{av}) were calculated with the *GoodVibes* program (option --pes) as:

$$G_{av} = \sum_i G_i \times p_i \quad (1)$$

where G_i is the relative Gibbs free energy of the corresponding conformers of a certain system and p_i is the probability of each conformer calculated as:

$$p_i = \frac{e^{\frac{-G_i}{RT}}}{\sum_i \left(e^{\frac{-G_i}{RT}}\right)} \quad (2)$$

G values, including the energies of all the conformers of each system, are detailed in a separate file included in the ESI. Also, the commands and options used by *GoodVibes* are represented in the same file.

Molecular coordinates: A separated XYZ file containing all the geometries considered in this study is provided along with this ESI.

A1.12. Preparation of Heterocyclic Phosphonium Salt Precursors and Pyridines

2-(((1-Benzhydrylazetidin-3-yl)methoxy)methyl)pyridine

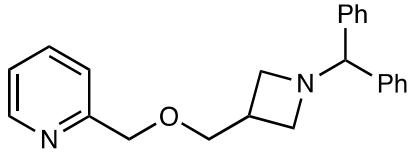

An oven dried 100 mL round bottom flask was charged with sodium hydride (60% dispersion in mineral oil, 8 equiv). The flask was subjected to three cycles of vacuum/nitrogen backfill before addition of DMF (5 mL). The mixture was cooled to 0 °C, and a mixture of (1-benzhydrylazetidin-3-yl)methanol (506 mg, 2.00 mmol) in DMF (5 mL) was added dropwise over five minutes. The mixture was warmed to room temperature and stirred for 1 hour before being cooled back down to 0 °C. A mixture of 2-(chloromethyl)pyridine hydrochloride (492 mg, 3.00 mmol) in DMF (5 mL) was added mixture, and the reaction was warmed to room temperature and stirred until the reaction was completed by TLC. The mixture was quenched with water (20 mL) and diluted with CH_2Cl_2. The organic layer was separated, and the aqueous layer was extracted with CH_2Cl_2 (3 x 20 mL). The combined organic layers were washed with brine (3 x 20 mL), dried ($MgSO_4$), filtered, and concentrated *in vacuo.* The crude material was purified by flash chromatography (silica gel: 50% EtOAc in hexanes) to provide the title compound as a white solid (601 mg, 1.74 mmol, 87% yield). mp 89-91 ºC. IR ν_{max}/cm^{-1} (film): 3061, 2934, 2858, 2843, 1584, 1489, 1448, 1348, 1127, 937, 758, 705; ^1H NMR (400 MHz, $CDCl_3$) δ: 8.63 (1H, dq, J = 4.9, 0.9 Hz), 7.78-7.72 (1H, m), 7.50 (5H, J = 7.5 Hz), 7.38-7.32 (4H, m), 7.29-7.23 (3H, m), 4.73 (2H, s), 4.44 (1H,

s), 3.81 (2H, d, J = 6.7 Hz), 3.41 (2H, t, J = 7.4 Hz), 3.03 (2H, t, J = 6.6 Hz), 2.87 (1H, sept, J = 6.8 Hz), ^{13}C NMR (100 MHz, $CDCl_3$) δ: 158.8, 149.1, 142.4, 136.6, 128.4, 127.6, 127.1, 122.4, 121.3, 78.1, 74.04, 73.7, 56.6, 29.9; m/z LRMS (ESI + APCI) found $[M+H]^+$ 345.3, $C_{23}H_{25}N_2O^+$ requires 345.2.

2-(4-Methoxyphenyl)pyridine

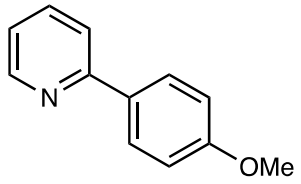

Prepared according to the method of Bao on a 5.00 mmol scale.[11] Flash chromatography by dissolving in CH_2Cl_2 and dry loading (silica gel: 20% EtOAc in hexanes) afforded the title compound as a white solid (802 mg, 4.35 mmol, 87% yield). ^{1}H NMR (400 MHz, $CDCl_3$) δ: 8.63 (1H, d, J = 4.8 Hz), 7.94 (2H, d, J = 8.8 Hz), 7.68–7.62 (2H, m), 7.15–7.11 (1H, m), 7.02 (2H, d, J = 8.8 Hz), 3.82 (3H, s); ^{13}C NMR (100 MHz, $CDCl_3$) δ: 160.6, 157.2, 149.6, 136.7, 132.1, 128.2, 121.5, 119.9, 114.2, 55.4. The spectroscopic data is in agreement with a reported synthesis.[12]

2-(4-Chlorophenyl)pyridine

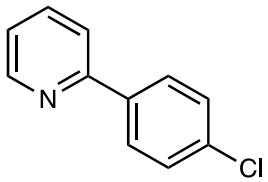

An oven-dried 100 mL round bottom flask was charged with 2-bromopyridine (0.47 mL, 5.00 mmol), (4-chlorophenyl)boronic acid (1.17 g, 7.50 mmol), $Pd(OAc)_2$ (22 mg, 0.10 mmol), and

K_3PO_4 (2.12 g, 10.0 mmol). The flask was subjected to three cycles of vacuum/nitrogen backfill before the addition of *i*PrOH (20 mL) and H_2O (20 mL). The reaction was heated to 80 °C using a condenser open to air, and monitored by TLC. After the reaction ran to completion, the reaction mixture was diluted with H_2O and extracted with CH_2Cl_2 (3 x 30 mL). The organic layer was washed with brine (3 x 20 mL), dried ($MgSO_4$), filtered, and concentrated *in vacuo*. The crude material was purified by flash chromatography (silica gel: 10% EtOAc in hexanes, and the product was dry-loaded onto the column) to provide the title compound as a pale yellow solid (695 mg, 3.65 mmol, 73% yield). ^{1}H NMR (400 MHz, $CDCl_3$) δ: 8.69 (1H, d, *J* = 4.0 Hz), 7.94 (2H, d, *J* = 8.6 Hz), 7.75 (1H, t, *J* = 7.6 Hz), 7.69 (1H, d, *J* = 7.6 Hz), 7.45 (2H, d, *J* = 8.6 Hz), 7.02 (1H, dd, *J* = 7.6 Hz, 4.0 Hz); ^{13}C NMR (100 MHz, $CDCl_3$) δ: 156.9, 150.4, 138.5, 137.5, 135.8, 129.6, 128.8, 123.0, 121.0. The spectroscopic data is in agreement with a reported synthesis.[13]

2-(4-Iodophenyl)pyridine

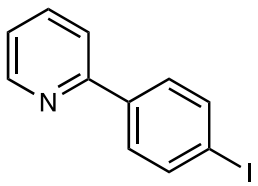

Prepared according to a method adapted from Doyle[14]. An oven-dried 100 mL round bottom flask was charged with (4-(pyridin-2-yl)phenyl)boronic acid (633 mg, 3.18 mmol), K_2CO_3 (1.097 g, 7.95 mmol), and I_2 (1.454 g, 5.23 mmol). The flask was subjected to three cycles of vacuum/nitrogen backfill before the addition of MeCN (12.7 mL), then heated to 90°C. The

reaction was monitored by TLC and diluted with H_2O after completion. The reaction mixture was extracted with EtOAc (3 x 20 mL), dried ($MgSO_4$), filtered, and concentrated *in vacuo*. The crude material was purified by flash chromatography (silica gel, gradient elution: hexanes to 10% EtOAc in hexanes) to provide the title compound as a pale orange solid (741 mg, 2.64 mmol, 83% yield). ^{1}H NMR (400 MHz, $CDCl_3$) δ: 8.68 (1H, m), 7.82-7.66 (6H, m), 7.27-7.21 (1H, m); ^{13}C NMR (100 MHz, $CDCl_3$) δ: 156.1, 149.7, 138.7, 137.8, 136.8, 128.6, 122.4, 120.1, 95.4. The spectroscopic data is in agreement with a reported synthesis.[15]

3-Phenylisonicotinonitrile

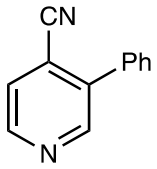

Prepared according to the method reported by Baxter on a 10.0 mmol scale.[7] The crude material was purified by flash chromatography (basic alumina, gradient elution: 15% EtOAc in hexanes to 20% EtOAc in hexanes) to provide the title compound as a pale yellow solid (406 mg, 2.30 mmol, 23%). ^{1}H NMR (400 MHz, $CDCl_{3}$) δ: 8.86 (1H, s), 8.75 (1H, d, J = 5.0 Hz), 7.63 (1H, d, J = 5.0 Hz), 7.60-7.52 (5H, m); ^{13}C NMR (100 MHz, $CDCl_3$) δ: 151.1, 148.8, 138.8, 134.5, 129.6, 129.2, 128.9, 126.1, 118.9, 116.4. The spectroscopic data is in agreement with a reported synthesis.[16]

Diethyl pyridin-4-ylphosphonate

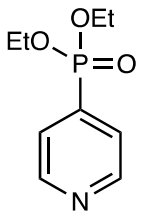

Prepared according to the procedure of Lin.[8] An oven dried 100 mL round bottom flask was charged with 4-bromopyridine hydrochloride (1.95 g, 10.0 mmol) and Tetrakis(triphenylphosphine)palladium(0) (232 mg, 0.20 mmol). The flask was subjected to three cycles of vacuum/nitrogen backfill before addition of toluene (40 mL), diethyl phosphonate (1.90 mL, 15.0 mmol), and NEt_3 (3.90 mL, 28.0 mmol). The mixture was refluxed at 120°C for 36 hours, cooled to room temperature and diluted with CH_2Cl_2 and H_2O. The organic layer was separated and washed with H_2O (2 x 20 mL). The organic layers were then dried ($MgSO_4$), filtered, and concentrated *in vacuo*. The crude material was purified by flash chromatography (silica gel: 3% MeOH in CH_2Cl_2) to provide the title compound as a colorless oil (667 mg, 3.10 mmol, 31% yield). ^{1}H NMR (400 MHz, $CDCl_3$) δ: 8.79-8.72 (2H, m), 7.69-7.60 (2H, m), 4.24-4.04 (4H, m), 1.36-1.29 (6H, m); ^{13}C NMR (100 MHz, $CDCl_3$) δ: 150.2 (d, J = 12.3 Hz), 137.6 (d, J = 189.5 Hz), 125.3 (d, J = 8.3 Hz), 62.8 (d, J = 5.55 Hz), 16.4 (d, J = 6.2 Hz); ^{31}P NMR (162 MHz, $CDCl_3$) δ: 14.59. The spectroscopic data is in agreement with a reported synthesis.[17]

3-(3-Cyanophenyl)isonicotinonitrile

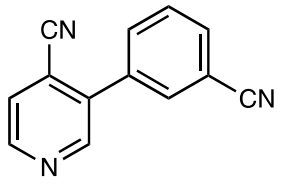

Prepared according to a method adapted from Schmidt.[9] An oven-dried 50 mL round bottom flask was charged with 3-bromoisonicotinonitrile (366 mg, 2.00 mmol), (3-cyanophenyl)boronic acid (441 mg, 3.00 mmol), $Pd(PPh_3)_4$ (69 mg, 0.06 mmol), and Na_2CO_3 (848 mg, 8.00 mmol). The flask was subjected to three cycles of vacuum/nitrogen backfill before the addition of toluene (2.86 mL), EtOH (2.86 mL), and H_2O (2.86 mL) were added, and the reaction was heated to 80 °C. The reaction was monitored by TLC and diluted with H_2O after completion. The reaction mixture was extracted with CH_2Cl_2 (3 x 20 mL), dried ($MgSO_4$), filtered, and concentrated *in vacuo*. Flash chromatography by dissolving in CH_2Cl_2 and dry loading (silica gel: 50% EtOAc in hexanes, followed by recrystallization from CH_2Cl_2 and hexanes) afforded the title compound as a white solid (175 mg, 0.86 mmol, 43% yield). mp 168-170 ºC. IR ν_{max}/cm^{-1} (film): 3095, 3019, 2220, 1582, 1490, 1416, 1399, 1205, 1174, 858, 793, 691; ^1H NMR (400 MHz, $CDCl_3$) δ: 8.82-8.86 (2H, m), 7.79-7.87 (3H, m), 7.66-7.73 (2H, m); ^{13}C NMR (100 MHz, $CDCl_3$) δ: 150.7, 150.1, 136.4, 135.9, 133.3, 133.1, 132.3, 130.2, 126.2, 119.2, 118.0, 115.7, 113.8; m/z LRMS (ESI + APCI) found $[M+H]^+$ 206.1, $C_{13}H_8N_3^+$ requires 206.1.

6'-Methyl-[3,3'-bipyridine]-4-carbonitrile

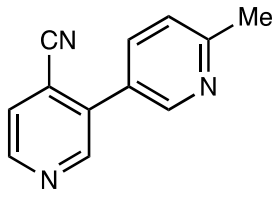

An oven-dried 50 mL round bottom flask was charged with 3-bromoisonicotinonitrile (366 mg, 2.00 mmol), pyridin-3-ylboronic acid (274 mg, 2.00 mmol), $Pd(PPh_3)_4$ (69 mg, 0.06 mmol), and K_2CO_3 (690 mg, 5.00 mmol). The flask was subjected to three cycles of vacuum/nitrogen backfill before the addition 1,4-dioxane (3.33 mL), and the reaction was heated to 95 °C. The reaction was monitored by TLC and diluted with H_2O after completion. The reaction mixture was extracted with EtOAC (3 x 20 mL), and the combined organic extracts were washed with brine (3 x 20 mL). The organic layer was dried ($MgSO_4$), filtered, and concentrated *in vacuo*. The crude material was purified by flash chromatography (silica gel, gradient elution: 80% EtOAc in hexanes to EtOAc) to provide the title compound as a white solid (135 mg, 0.68 mmol, 34% yield). mp 179-180 °C; IR ν_{max}/cm^{-1} (film): 3096, 3050, 3018, 2924, 2852, 2231, 1923, 1599, 1582, 1480, 1412, 1386, 1367, 1333, 1198, 1035, 828, 789, 584; ^1H NMR (400 MHz, $CDCl_3$) δ: 8.85 (1H, s), 8.79 (1H, d, J = 5.0 Hz), 8.69 (1H, d, J = 2.1 Hz), 7.84 (1H, dd, J = 8.1, 2.4 Hz), 7.65 (1H, d, J = 5.0 Hz), 7.30 (1H, d, J = 8.1 Hz), 2.66 (3H, m); ^{13}C NMR (100 MHz, $CDCl_3$) δ: 160.1, 150.8, 149.5, 148.6, 136.5, 135.6, 127.6, 126.2, 123.5, 119.2, 116.0, 24.5; m/z LRMS (ESI + APCI) found $[M+H]^+$ 196.1, $C_{12}H_{10}N_3^+$ requires 196.1.

3-(Thiophen-3-yl)isonicotinonitrile

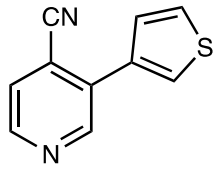

An oven-dried 50 mL round bottom flask was charged with 3-bromoisonicotinonitrile (275 mg, 1.50 mmol), thiophen-3-ylboronic acid (192 mg, 1.50 mmol), $Pd(PPh_3)_4$ (52 mg, 0.045 mmol), and K_2CO_3 (518 mg, 3.50 mmol). The flask was subjected to three cycles of vacuum/nitrogen backfill before the addition of THF (3.80 mL) and H_2O (1.90 mL), and then the reaction was heated to 95°C. The reaction was monitored by TLC and diluted with H_2O after completion. The reaction mixture was extracted with CH_2Cl_2 (3 x 20 mL), and the combined organic extracts were washed with a saturated solution of brine (3 x 20 mL). The organic layer was dried ($MgSO_4$), filtered, and concentrated *in vacuo*. The crude material was purified by flash chromatography (silica gel: 15% EtOAc in hexanes) to provide the title compound as a white solid (270 mg, 1.45 mmol, 97% yield). mp 88-89 °C; IR ν_{max}/cm^{-1} (film): 3159, 3085, 3044, 3021, 2232, 1951, 1521, 1477, 1423, 1297, 1190, 866, 802, 647, 584; ^1H NMR (400 MHz, $CDCl_3$) δ: 8.90 (1H, s), 8.65 (1H, d, *J* = 5.0 Hz), 7.75 (1H, dd, *J* = 2.9, 1.4 Hz), 7.55 (1H, dd, *J* = 5.0, 0.7 Hz), 7.49-7.42 (2H, m); ^{13}C NMR (100 MHz, $CDCl_3$) δ: 150.4, 148.3, 134.8, 133.1, 127.3, 127.0, 126.2, 125.8, 117.6, 116.6; m/z LRMS (ESI + APCI) found $[M+H]^+$ 187.1, $C_{10}H_7N_2S^+$ requires 187.0.

3-(1-((Tert-butyldimethylsilyl)oxy)-2-methylpropyl)-4-chloropyridine

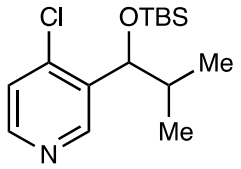

A 50 mL round bottom flask was charged with 1-(4-chloropyridin-3-yl)-2-methylpropan-1-ol (222 mg, 1.20 mmol), and the flask was subjected to three cycles of vacuum/nitrogen backfill before the addition of DMF (2 mL). A solution of tert-butyldimethylsilyl chloride (634 mg, 4.20 mmol) in DMF (2 mL) was added at 0 °C followed by addition of a solution of imidazole (408 mg, 6.00 mmol) in DMF (2 mL) at 0 °C. The flask was warmed up to room temperature and stirred for 18 hours. After completion, the reaction was quenched with a saturated solution of sodium bicarbonate (6 mL). The reaction mixture was extracted with CH_2Cl_2 (3 x 10 mL), the combined organic layers were washed with a saturated brine solution (3 x 20 mL), dried ($MgSO_4$), and concentrated *in vacuo.* The crude material was purified by flash chromatography (silica gel: 10% EtOAc in hexanes) to provide the title compound as a yellow oil (278 mg, 1.20 mmol, 77% yield). IR νmax/cm-1 (film): 2957, 2929, 2895, 2858, 1556, 1462, 1403, 1252, 1084, 1046, 837, 812, 710; ^{1}H NMR (400 MHz, $CDCl_3$) δ: 8.68 (1H, s), 8.35 (1H, d, *J* = 5.3 Hz), 7.23 (1H, d, *J* = 5.3 Hz), 4.85 (1H, d, *J* = 5.3 Hz), 1.94 (1H, oct, *J* = 6.7 Hz), 0.91 (3H, d, *J* = 1.3 Hz), 0.90 (3H, d, *J* = 1.6 Hz), 0.89 (9H, s), 0.06 (3H, s), -0.22 (3H, s); ^{13}C NMR (100 MHz, CDCl3) δ: 151.0, 148.7, 141.6, 137.9, 124.0, 74.4, 35.3, 25.9, 19.4, 18.2, 17.0, -4.6, -5.0; m/z LRMS (ESI + APCI) found $[M+H]^+$ 300.2, $C_{15}H_{27}ClNOSi^+$ requires 300.2.

3-(1-((Tert-butyldimethylsilyl)oxy)-2-methylpropyl)isonicotinonitrile

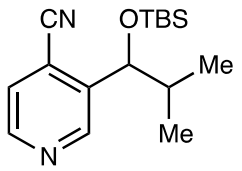

An oven dried 50 mL round bottom flask was charged with 3-(1-((tert-butyldimethylsilyl)oxy)-2-methylpropyl)-4-chloropyridine (276 mg, 0.92 mmol), dicyanozinc (64 mg, 0.55 mmol), $Pd_2(dba)_3$ (165 mg, 0.18 mmol), 1,1'-Bis(diphenylphosphino)ferrocene (205 mg, 0.37 mmol), and zinc dust (6 mg, 0.09 mmol). The flask was subjected to three cycles of vacuum/nitrogen backfill before the addition of DMA (2.0 mL). The reaction was heated to 120 °C for 12 hours before diluting with water, and extracting the mixture with CH_2Cl_2 (3 x 10 mL). After extraction, the combined organic layers were washed with a saturated solution of NH_4Cl (10 mL), dried ($MgSO_4$), filtered, and concentrated *in vacuo*. The crude material was purified by flash chromatography (silica gel: 5% EtOAc in hexanes) to provide the title compound as a yellow oil (149 mg, 0.52 mmol, 56 %). IR ν_{max}/cm^{-1} (film): 2958, 2930, 2858, 1585, 1471, 1409, 1253, 1077, 1054, 836, 775; ^1H NMR (400 MHz, $CDCl_3$) δ: 8.87 (1H, s), 8.65 (1H, d, *J* = 5.0 Hz), 7.45 (1H, d, *J* = 5.0 Hz), 4.71 (1H, d, *J* = 6.2 Hz), 2.01 (1H, oct, *J* = 6.7 Hz), 0.97 (3H, d, *J* = 6.7 Hz), 0.89 (9H, s), 0.88 (3H, d, *J* = 6.8 Hz), 0.09 (3H, s), -0.20 (3H, s); ^{13}C NMR (100 MHz, $CDCl_3$) δ: 150.6, 148.8, 141.6, 125.0, 118.5, 115.6, 76.7, 36.5, 25.9, 19.1, 18.2, 17.7, -4.6, -5.0; m/z LRMS (ESI + APCI) found $[M+H]^+$ 291.2, $C_{16}H_{27}N_2OSi^+$ requires 291.2.

Methyl (E)-3-(4-cyanopyridin-3-yl)acrylate

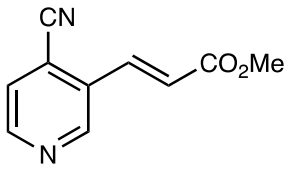

An oven-dried 50 mL round bottom flask was charged with 3-bromoisonicotinonitrile (368 mg, 2.00 mmol), $Pd(OAc)_2$ (45 mg, 0.20 mmol), triphenylphosphine (105 mg, 0.40 mmol), and K_2CO_3 (552 mg, 4.00 mmol). The flask was subjected to 3 cycles of vacuum/nitrogen backfill before being addition of DMF (20 mL), followed by addition of methyl acrylate (1.81 mL, 20.0 mmol). The reaction was heated to 110 °C and monitored by TLC until completion. The reaction mixture was diluted with water and extracted with EtOAc (3 x 20 mL). The combined organic extracts were washed with water (3 x 20 mL), dried ($MgSO_4$), filtered, and concentrated *in vacuo.* Flash chromatography by dissolving in CH_2Cl_2 and dry loading (silica gel: 30% EtOAc in hexanes) afforded the title compound as a white solid (149 mg, 0.80 mmol, 30% yield). mp 117-119 °C; IR ν_{max}/cm^{-1} (film): 3095, 3061, 3021, 2956, 2230, 1720, 1639, 1581, 1435, 1325, 1207, 980, 847; ^1H NMR (400 MHz, $CDCl_3$) δ: 9.02 (1H, s), 8.75 (1H, d, *J* = 5.0 Hz), 7.88 (1H, d, *J* = 16.2 Hz), 7.57 (1H, dd, *J* = 5.0, 0.5 Hz), 6.76 (1H, d, *J* = 16.1 Hz), 3.85 (3H, s); ^{13}C NMR (100 MHz, $CDCl_3$) δ: 165.5, 150.6, 148.9, 136.5, 131.0, 125.8, 124.3, 119.4, 114.9, 52.1; *m/z* LRMS (ESI + APCI) found $[M+H]^+$ 189.1, $C_{10}H_9N_2O_2^+$ requires 189.1.

Methyl 3-(4-cyanopyridin-3-yl)propanoate

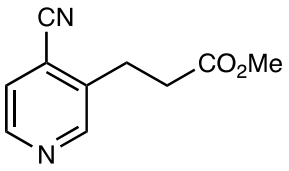

An oven-dried 50 mL round bottom flask was charged with methyl (E)-3-(4-cyanopyridin-3-yl)acrylate (123 mg, 0.65 mmol) and Pd/C(10 w%) (12 mg, 10 w%). The flask was subjected to 3 cycles of vacuum/nitrogen backfill before being addition of MeOH (6.5 mL). The reaction mixture atmosphere was exchanged with a balloon of H_2 gas, then capped with a second balloon of H_2 gas (1 atm) and stirred for 48 hours. The reaction mixture was filtered through celite, extracted with EtOAc (3 x 20 mL), dried ($MgSO_4$), filtered, and concentrated *in vacuo.* Flash chromatography by dissolving in CH_2Cl_2 and dry loading (silica gel: 30% EtOAc in hexanes) afforded the title compound as a colorless oil (73 mg, 0.39 mmol, 60% yield). IR ν_{max}/cm^{-1} (film): 3097, 2955, 2928, 2855, 2233, 1728, 1587, 1486, 1442, 1410, 1370, 1203, 1167, 847; ^1H NMR (400 MHz, $CDCl_3$) δ: 8.68 (1H, s), 8.60 (1H, d, *J* = 5.0 Hz), 7.45 (1H, d, *J* = 5.0 Hz), 3.63 (3H, s), 3.13 (2H, t, *J* = 7.4 Hz), 2.71 (2H, t, *J* = 7.4 Hz); ^{13}C NMR (100 MHz, $CDCl_3$) δ: 171.8, 151.3, 148.5, 137.6, 125.4, 120.4, 115.4, 51.9, 34.0, 26.8; *m/z* LRMS (ESI + APCI) found $[M+H]^+$ 191.1, $C_{10}H_{11}N_2O_2^+$ requires 191.1.

A1.13. Preparation of Heterocyclic Phosphonium Salts

General Procedure A

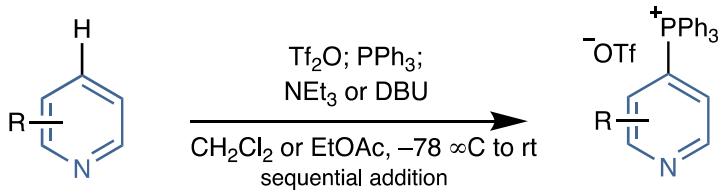

An oven dried 8 mL vial (≤ 0.5 mmol scale) or a round bottom flask (> 0.5 mmol scale) equipped with a stir bar was charged with the heterocycle (1.0 equiv) and placed under a nitrogen atmosphere. CH_2Cl_2 (0.1 M) was added, the reaction vessel cooled to –78 ºC, and Tf_2O (1.0 equiv) was added dropwise over 5 minutes. The reaction was stirred for 30 minutes then warmed to –50 °C before PPh_3 (1.1 equiv) was added in one portion. The reaction was subjected to three rapid cycles of vacuum/nitrogen backfill and was stirred for a further 30 minutes at –78 ºC. The stated organic base (NEt_3 or DBU, 1.0 equiv) was added dropwise via syringe, the cooling bath was removed, and the reaction was allowed to warm to room temperature while stirring (approximately 15-30 minutes). When the reaction mixture reached room temperature, it was then quenched with H_2O (approximately the same volume as CH_2Cl_2) and the mixture was transferred to a separatory funnel. The mixture was diluted with CH_2Cl_2 and the resulting organic layer was washed three times with H_2O. The organic layer was dried ($MgSO_4$), filtered and concentrated *in vacuo*. Approximately 2-10 mL (depending on the scale of the reaction) of CH_2Cl_2 was added to reaction mixture and was then added dropwise to an excess of chilled Et_2O (0 ºC). The flask was then placed in a –20 ºC refrigerator for approximately 1 hour. The resulting suspension was filtered on

a frit, the solid washed with chilled Et_2O (0 ºC), and dried *in vacuo* to provide the pure phosphonium salt.

Notes.

1) PPh_3 was crushed into a powder prior to use.
2) Certain substrates require longer periods for the precipitation step and specific cases are indicated below.
3) In a small number of cases, residual CH_2Cl_2 can become trapped in the phosphonium salt products. In these cases, heating the salts under vacuum (50-100 ºC) removed the solvent.
4) In order to evaluate regioselectivity from the crude reaction mixtures, a duplicate reaction was performed and aliquots taken after addition of the organic base and warming to room temperature. These aliquots were concentrated *in vacuo* and analyzed by ^1H and ^{31}P NMR.

Triphenyl(2-phenylpyridin-4-yl)phosphonium trifluoromethanesulfonate

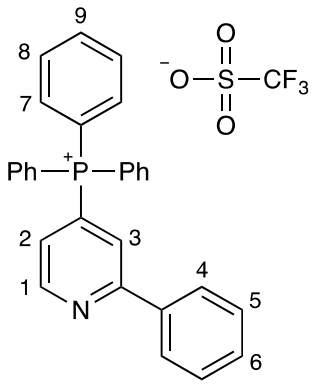

Prepared according to our previous report.[19] ^1H NMR (400 MHz, $CDCl_3$) δ: 9.01 (1H, app t, J = 5.1 Hz, H_1), 7.93-7.54 (18H, m, H_3, H_7, H_8, H_9, and H_4), 7.50 (1H, ddd, J = 17.8, 5.1, 1.1 Hz, H_2),

7.42-7.36 (3H, m, H_5 and H_6); ^{13}C NMR (100 MHz, $CDCl_3$) δ: 159.1 (d, *J* = 9.9 Hz), 151.6 (d, *J* = 10.7 Hz), 136.7 (d, *J* = 1.5 Hz), 136.1 (d, *J* = 3.2 Hz), 134.3 (d, *J* = 9.8 Hz), 130.9 (d, *J* = 13.0 Hz), 130.3, 129.2 (d, *J* = 84.1 Hz), 129.0, 127.0, 125.2 (d, *J* = 7.8 Hz), 123.1, (d, *J* = 8.4 Hz), 120.7 (q, *J* = 321.1 Hz), 115.5 (d, *J* = 89.1 Hz).

(2-(Bis(3-(trifluoromethyl)phenyl)methyl)pyridin-4-yl)triphenylphosphonium trifluoromethanesulfonate

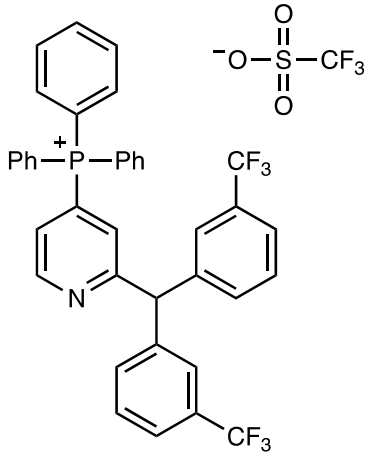

Prepared according to our previous report.[20] ^{1}H NMR (400 MHz, $CDCl_3$) δ: 8.99 (1H, app t, *J* = 5.1 Hz), 7.91-7.80 (3H, m), 7.78-7.66 (6H, m), 7.63-7.37 (15H, m), 7.29 (1H, d, *J* = 13.8 Hz), 5.97 (1H, s); ^{13}C NMR (100 MHz, $CDCl_3$) δ: 164.0 (d, *J* = 9.8), 151.6 (d, *J* = 10.4 Hz), 141.7, 136.1 (d, *J* = 3.1 Hz), 134.3 (d, *J* = 10.5 Hz), 132.9 (d, *J* = 1.1 Hz), 130.9 (d, *J* = 13.1 Hz), 130.7 (q, *J* = 32.2 Hz), 130.0, 129.6 (d, *J* = 83.7 Hz), 127.0 (d, *J* = 8.7 Hz), 125.6-125.4 (2C, m), 124.0 (q, *J* = 3.8 Hz), 123.8 (q, *J* = 272.5 Hz), 120.78 (q, *J* = 321.2 Hz), 115.4 (d, *J* = 89.5 Hz), 57.7; ^{19}F NMR (365 MHz, $CDCl_3$) δ: –62.46, –78.13; ^{31}P NMR (162 MHz, $CDCl_3$) δ: 22.38.

(2-((4-Chlorophenyl)((1-(ethoxycarbonyl)piperidin-4-yl)oxy)methyl)pyridin-4-yl) triphenylphosphonium trifluoromethanesulfonate

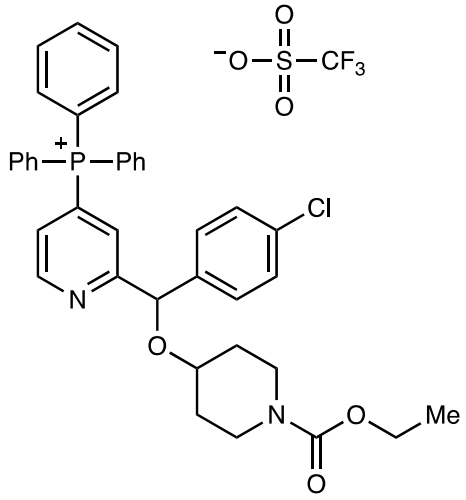

Prepared according to our previous report.[20] ^{1}H NMR (400 MHz, $CDCl_3$) δ: 8.90 (1H, t, *J* = 5.1 Hz), 7.94-7.86 (3H, m), 7.82-7.73 (6H, m), 7.71-7.59 (7H, m), 7.49 (1H, ddd, *J* = 12.6, 5.0, 1.1 Hz), 7.34-7.25 (4H, m), 5.71 (1H, s), 4.11 (2H, q, *J* = 7.1 Hz), 3.70-3.60 (1H, m), 3.55-3.42 (2H, m), 3.25-3.12 (2H, m), 1.79-1.56 (2H, m), 1.54-1.37 (2H, m), 1.25 (3H, t, *J* = 7.1 Hz); ^{13}C NMR (100 MHz, $CDCl_3$) δ: 164.4 (d, *J* = 9.6 Hz), 155.4, 151.1 (d, *J* =10.5 Hz), 138.7, 136.2 (d, *J* = 3.1 Hz), 134.5 (d, *J* = 10.5 Hz), 134.0, 130.9 (d, *J* = 13.1 Hz), 129.3 (d, *J* = 84.1 Hz), 128.8, 128.5, 125.9 (d, *J* = 8.4 Hz), 123.9 (d, *J* = 9.1 Hz), 120.8 (q, *J* = 321.2 Hz), 115.8 (d, *J* = 89.4 Hz), 79.9, 72.8, 61.3, 40.7 (rot), 40.7, 31.3, 30.3 (rot), 14.7; ^{19}F NMR (365 MHz, $CDCl_3$) δ: –78.15; ^{31}P NMR (162 MHz, $CDCl_3$) δ: 22.67.

(E)-Triphenyl(2-(3-(pyrrolidin-1-yl)-1-(p-tolyl)prop-1-en-1-yl)pyridin-4-yl)phosphonium trifluoromethanesulfonate

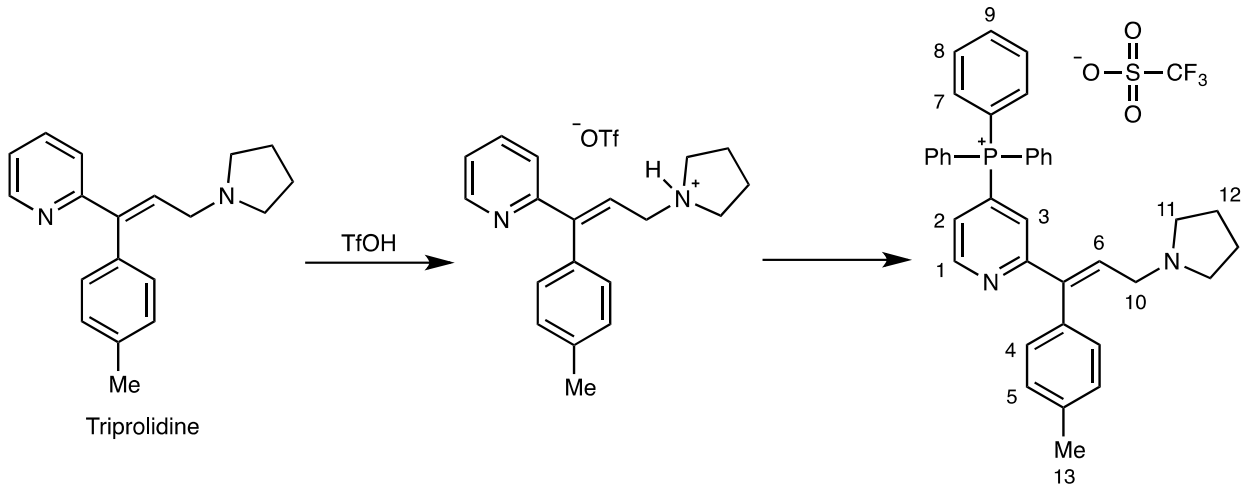

Prepared according to our previous report.[21] ^{1}H NMR (400 MHz, $CDCl_3$) δ: 8.93 (1H, app t, J = 5.3 Hz, H_1), 7.92-7.56 (15H, m, H_7, H_8, and H_9), 7.38 (1H, dd, J = 12.3, 4.8 Hz, H_2), 7.26 (1H, d, J = 14.3 Hz, H_3), 7.18-6.98 (5H, m, H_4, H_5, and H_6), 3.71 (2H, d, J = 6.9 Hz, H_{10}), 3.13 (4H, br s, H_{11}), 2.37 (3H, s, H_{13}), 1.99 (4H, br s, H_{12}); ^{13}C NMR (100 MHz, $CDCl_3$) δ: 159.3 (d, J = 10.1 Hz), 150.9 (d, J = 10.5 Hz), 144.2, 138.2, 136.0 (d, J = 3.0 Hz), 134.3 (d, J = 10.6 Hz), 132.3, 130.9 (d, J = 13.1 Hz), 129.7, 129.1, 128.8 (d, J = 84.7 Hz), 126.3, 125.6 (d, J = 9.2 Hz), 125.3 (d, J = 8.0 Hz), 120.6 (q, J = 320.4 Hz), 115.6 (d, J = 89.6 Hz), 54.0, 53.7, 23.0, 21.2; ^{19}F NMR (365 MHz, $CDCl_3$) δ: –78.05; ^{31}P NMR (162 MHz, $CDCl_3$) δ: 22.34.

(2-(2-Chloro-5-(2-chloro-4-(methylsulfonyl)benzamido)phenyl)pyridin-4-yl)triphenylphosphonium trifluoromethanesulfonate and (6-(2-chloro-5-(2-chloro-4-(methylsulfonyl)benzamido)phenyl)pyridin-2-yl)triphenylphosphonium trifluoromethanesulfonate

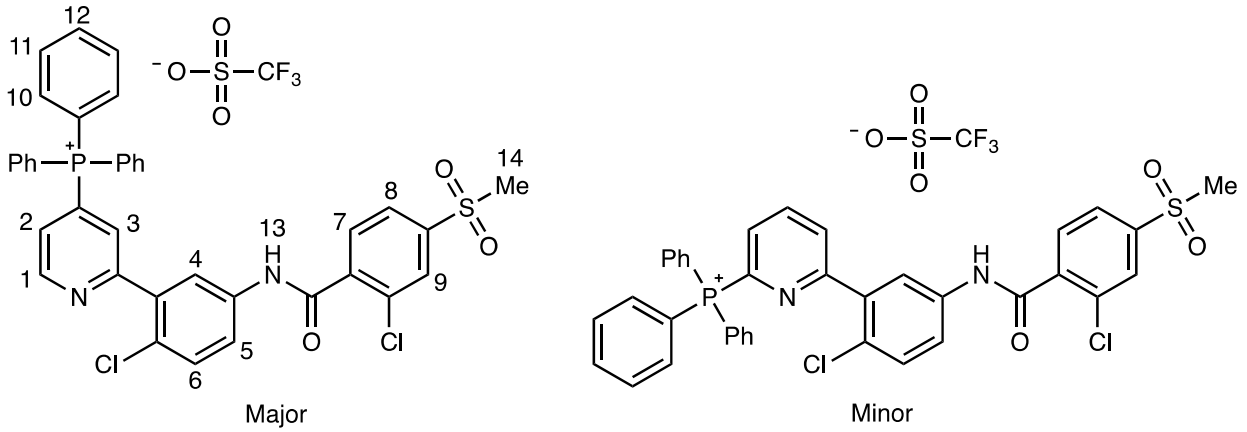

7:1 Mixture of Regioisomers

Prepared according to our previous report.[21] Major isomer, ^{1}H NMR (400 MHz, $CDCl_3$) δ: 9.98 (1H, s, H_{13}), 8.98 (1H, app t, J = 4.9 Hz, H_1), 8.15-7.33 (23H, m, H_2, H_3, H_4, H_5, H_6, H_7, H_8, H_9, H_{10}, H_{11}, and H_{12}), 3.01 (3H, s, H_{14}); Major isomer, ^{13}C NMR (100 MHz, $CDCl_3$) δ: 164.5, 158.5 (d, J = 10.8 Hz), 151.2 (d, J = 10.9 Hz), 142.3, 140.4, 137.9, 136.8, 136.2 (d, J = 2.9 Hz), 134.4 (d, J = 10.5 Hz), 132.5, 130.9 (d, J = 13.1 Hz), 130.5, 130.0, 128.7, 128.5 (d, J = 84.4 Hz), 128.1 (d, J = 8.8 Hz), 126.4, 125.8, 125.4 (d, J = 8.4 Hz), 123.2, 122.6, 120.4 (q, J = 320.6 Hz), 115.6 (d, J = 89.6 Hz), 44.3; Both isomers, ^{19}F NMR (365 MHz, $CDCl_3$) δ: –78.34; Both isomers, ^{31}P NMR (162 MHz, $CDCl_3$) δ: 22.60 (major), 17.95 (minor).

(3-Methoxypyridin-4-yl)triphenylphosphonium trifluoromethanesulfonate

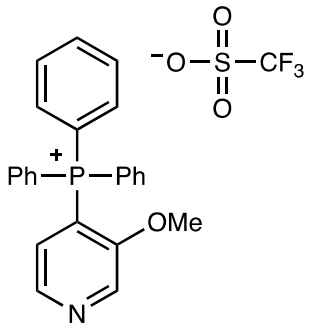

Prepared according to our previous report.[22] ^{1}H NMR (400 MHz, $CDCl_3$) δ: 8.72 (1H, d, *J* = 6.8 Hz), 8.58 (1H, app t, *J* = 3.9 Hz), 7.90–7.86 (3H, m), 7.79–7.74 (6H, m), 7.66–7.60 (6H, m), 7.09 (1H, dd, *J* = 4.9, 15.0 Hz), 3.74 (3H, s); ^{13}C NMR (100 MHz, $CDCl_3$) δ: 155.8 (d, *J* = 0.6 Hz), 143.9 (d, *J* = 10.9 Hz), 136.6 (d, *J* = 4.6 Hz), 135.6 (d, *J* = 3.0 Hz), 133.8 (d, *J* = 10.6 Hz), 130.6 (d, *J* =13.2 Hz), 127.9 (d, *J* = 7.0 Hz), 120.7 (q, *J* = 319.4 Hz), 116.4 (d, *J* = 90.9 Hz), 115.2 (d, *J* = 86.4 Hz), 57.2; ^{19}F NMR (365 MHz, $CDCl_3$) δ: –78.14; ^{31}P NMR (162 MHz, $CDCl_3$) δ: 21.45.

(**2-Chloropyridin-4-yl)triphenylphosphonium trifluoromethanesulfonate**

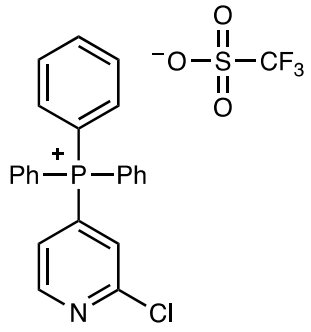

Prepared according to our previous report.[19] ^{1}H NMR (400 MHz, $CDCl_3$) δ: 8.82 (1H, app t, *J* = 5.1 Hz), 7.98-7.89 (3H, m), 7.86-7.77 (6H, m), 7.75-7.62 (7H, m), 7.40 (1H, d, *J* = 13.2 Hz); ^{13}C NMR (100 MHz, $CDCl_3$) δ: 153.4 (d, *J* = 15.1 Hz), 152.3 (d, *J* = 11.3 Hz), 136.4 (d, *J* = 3.0 Hz),

134.5 (d, J = 10.4 Hz), 132.0 (d, J = 83.2 Hz), 131.1 (d, J = 13.0 Hz), 127.4 (d, J = 9.5 Hz), 126.3 (d, J = 8.4 Hz), 120.7 (q, J = 320.4 Hz), 115.0 (d, J = 90.0 Hz); ^{19}F NMR (365 MHz, $CDCl_3$) δ: –78.19; ^{31}P NMR (162 MHz, $CDCl_3$) δ: 22.27.

(2-(Bis(4-acetoxyphenyl)methyl)pyridin-4-yl)triphenylphosphonium trifluoromethanesulfonate

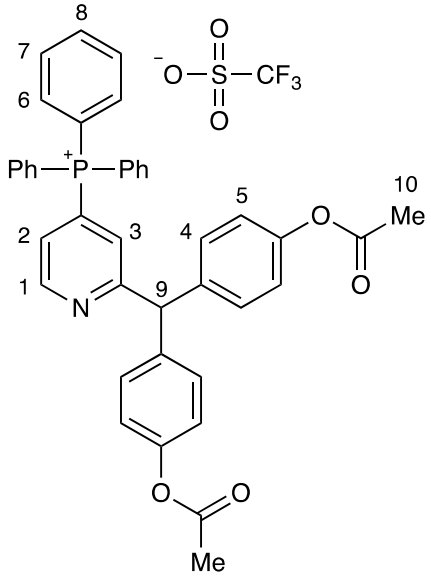

Prepared according to our previous report.[21] ^{1}H NMR (400 MHz, $CDCl_3$) δ: 8.90 (1H, app t, J = 5.1 Hz, H_1), 7.86-7.80 (3H, m, H_8), 7.73-7.66 (6H, m, H_7), 7.56-7.39 (7H, m, H_2 and H_6), 7.18 (1H, d, J = 13.7 Hz, H_3), 7.13-7.08 (4H, m, H_4), 6.97–6.91 (4H, m, H_5), 5.72 (1H, s, H_9), 2.21 (6H, s, H_{10}); ^{13}C NMR (100 MHz, $CDCl_3$) δ: 169.1, 165.0 (d, J = 9.4 Hz), 151.2 (d, J = 10.4 Hz), 149.3, 138.4, 135.9 (d, J = 3.0 Hz), 134.1 (d, J = 10.6 Hz), 130.7 (d, J = 13.0 Hz), 129.9, 129.0 (d, J = 83.8 Hz), 126.6 (d, J = 8.7 Hz), 124.9 (d, J = 7.9 Hz), 121.5, 120.6 (q, J = 321.2 Hz), 115.3 (d, J = 89.4 Hz), 57.4, 20.8; ^{19}F NMR (365 MHz, $CDCl_3$) δ: –78.05; ^{31}P NMR (162 MHz, $CDCl_3$) δ: 22.34.

Triphenyl(2-(thiophen-3-yl)pyridin-4-yl)phosphonium trifluoromethanesulfonate

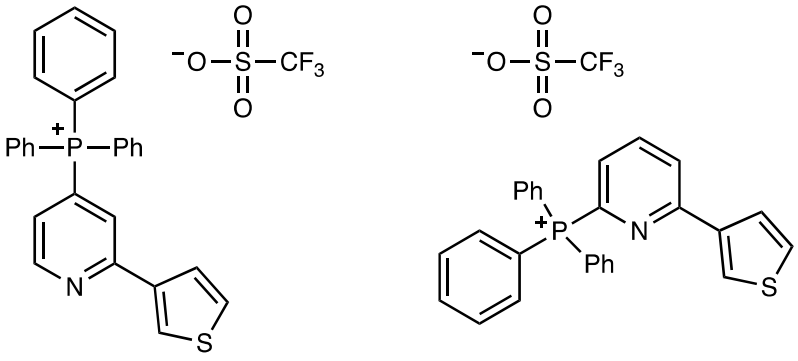

Major Minor

10:1 mixture of regioisomers

Prepared according to general procedure A (except immediately after addition of Tf_2O, the reaction was warmed up to -50 °C) using 2-(thiophen-3-yl)pyridine (460 mg, 2.86 mmol), Tf_2O (280 μL, 2.86 mmol), PPh_3 (823 mg, 3.14 mmol), DBU (427 μL, 2.86 mmol) and CH_2Cl_2 (30 mL). After the purification procedure, the title compound was isolated as a white, amorphous solid (611 mg, 1.06 mmol, 37% yield). IR ν_{max}/cm^{-1} (film): 3090, 3064, 1577, 1438, 1260, 1223, 1108, 1029, 725, 650; ^1H NMR (400 MHz, $CDCl_3$) δ: 8.99 (1H, td, *J* = 5.1, 0.9 Hz), 8.00 (1H, dd, *J* = 3.0, 1.3 Hz), 7.90-7.96 (3H, m), 7.66-7.86 (13H, m), 7.55 (1H, dd, *J* = 5.1, 1.3 Hz), 7.44 (1H, dd, *J* = 5.0, 1.6 Hz), 7.38-7.42 (1H, m); ^{13}C NMR (100 MHz, $CDCl_3$) δ: 155.1 (d, *J* = 10.9 Hz), 151.7 (d, *J* = 10.6 Hz), 139.8 (d, *J* = 1.6 Hz), 136.3 (d, *J* = 3.1 Hz), 134.4 (d, *J* = 10.3 Hz), 131.0 (d, *J* = 12.8 Hz), 129.3 (d, *J* = 84.2 Hz), 127.3, 126.4, 125.9, 124.8 (d, *J* = 8.2 Hz), 123.0 (d, *J* = 8.7 Hz), 120.8 (q, *J* = 321.1 Hz), 115.6 (d, *J* = 89.4 Hz); ^{19}F NMR (365 MHz, $CDCl_3$) δ: –78.15; ^{31}P NMR (162 MHz, $CDCl_3$) δ: 22.69; m/z LRMS (ESI + APCI) found $[M–OTf]^+$ 422.2, $C_{27}H_{21}NPS^+$ requires 422.1.

Triphenyl(2-(4-(4,4,5,5-tetramethyl-1,3,2-dioxaborolan-2-yl)phenyl)pyridin-4-yl)phosphonium trifluoromethanesulfonate

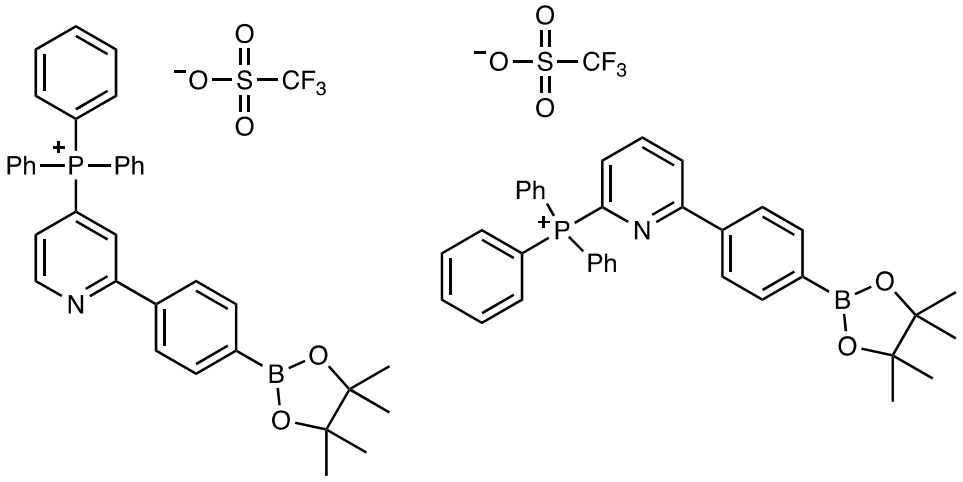

Major Minor

>20:1 mixture of regioisomers

Prepared according to general procedure A (except PPh_3 was added and stirred at –30 °C) using 2-(4-(4,4,5,5-tetramethyl-1,3,2-dioxaborolan-2-yl)phenyl)pyridine (1.615 g, 5.75 mmol), Tf_2O (0.97 mL, 5.75 mmol), PPh_3 (1.656 g, 6.32 mmol), DBU (0.86 mL, 5.75 mmol) and CH_2Cl_2 (58 mL). After the purification procedure, the title compound was isolated as a white, amorphous solid (2.84 g, 5.00 mmol, 87% yield). IR ν_{max}/cm^{-1} (film): 3062, 2978, 2929, 1578, 1439, 1357, 1260, 1142, 1030; ^1H NMR (400 MHz, $CDCl_3$) δ: 9.10 (1H, td, *J* = 5.1, 0.7 Hz), 7.67-7.97 (20H, m), 7.57 (1H, ddd, *J* = 7.7, 5.0, 1.6 Hz), 1.34 (12H, s); ^{13}C NMR (100 MHz, $CDCl_3$) δ: 159.2 (d, *J* = 10.2 Hz), 152.0 (d, *J* = 10.5 Hz), 139.3 (d, *J* = 1.5 Hz), 136.4 (d, *J* = 3.1 Hz), 135.5, 134.5 (d, *J* = 10.4 Hz), 131.1 (d, *J* = 13.2 Hz), 130.6 (d, *J* = 12.7 Hz), 129.5 (d, *J* = 83.9 Hz), 126.3, 125.8 (d, *J* = 8.0 Hz), 123.6 (d, *J* = 8.7 Hz), 120.9 (q, *J* = 324.7 Hz), 115.7 (d, *J* = 89.4 Hz), 84.1, 24.9; ^{19}F NMR (365 MHz, $CDCl_3$) δ: –78.11; ^{31}P NMR (162 MHz, CD_3CN) δ: 22.71, 16.07; m/z LRMS

(ESI + APCI) found $[M–OTf]^+$ 542.3, $C_{35}H_{34}BNO_2P^+$ requires 542.2.

(2-Methylpyridin-4-yl)triphenylphosphonium trifluoromethanesulfonate

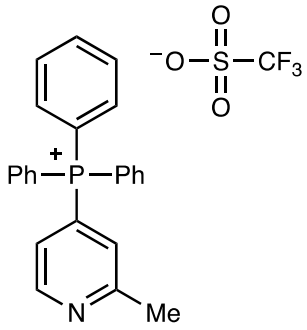

Prepared according to general procedure A using 2-methylpyridine (1.97 mL, 20.0 mmol), Tf_2O (3.36 mL, 20.0 mmol), PPh_3 (5.76 g, 22.0 mmol), NEt_3 (2.78 mL, 20.0 mmol) and CH_2Cl_2 (200 mL). After the purification procedure, the title compound was isolated as a white solid (7.47 g, 14.8 mmol, 74% yield). mp 187-189 ºC; IR ν_{max}/cm^{-1} (film): 3067, 3042, 2974, 2925, 2854, 2239, 1591, 1546, 1514, 1355, 1328, 1286, 1141, 1092, 961, 829, 774, 663; ^1H NMR (400 MHz, $CDCl_3$) δ: 8.88 (1H, app t, *J* = 5.2 Hz), 7.97-7.60 (15H, m), 7.42-7.30 (2H, m), 2.69 (3H, s); ^{13}C NMR (100 MHz, $CDCl_3$) δ: 160.9 (d, *J* = 10.0 Hz), 150.6 (d, *J* = 10.7 Hz), 135.7 (d, *J* = 2.9 Hz), 134.1 (d, *J* = 10.4 Hz), 130.6 (d, *J* = 13.0 Hz), 128.2 (d, *J* = 83.5 Hz), 126.2 (d, *J* = 7.9 Hz), 123.8 (d, *J* = 11.1 Hz), 120.4 (q, *J* = 321.3 Hz), 115.4 (d, *J* = 89.4 Hz), 24.4; ^{19}F NMR (365 MHz, $CDCl_3$) δ: –78.14; ^{31}P NMR (162 MHz, $CDCl_3$) δ: 22.39; m/z LRMS (ESI + APCI) found $[M–OTf]^+$ 354.2, $C_{24}H_{21}NP^+$ requires 354.1.

(3-Fluoro-2-methylpyridin-4-yl)triphenylphosphonium trifluoromethanesulfonate

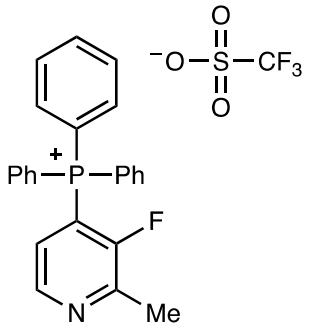

Prepared according to general procedure using 3-fluoro-2-methylpyridine (618 μL, 6.00 mmol), Tf_2O (1.00 mL, 6.00 mmol), PPh_3 (1.73 g, 6.60 mmol), DBU (896 μL, 6.00 mmol) and CH_2Cl_2 (60 mL). After the purification procedure, the title compound was isolated as a tan solid (1.41 g, 2.70 mmol, 45% yield). mp 205-209 ºC; IR ν_{max}/cm^{-1} (film): 3088, 3063, 1586, 1482, 1437, 1408, 1260, 1225, 1143, 1106, 1030, 724, 635; ^{1}H NMR (400 MHz, $CDCl_3$) δ: 8.66 (1H, app t, *J* = 4.1 Hz), 7.94-7.86 (3H, m), 7.83-7.75 (6H, m), 7.70-7.61 (6H, m), 7.09 (1H, dt, *J* = 14.0, 4.6 Hz), 2.64 (3H, d, *J* = 3.0 Hz); ^{13}C NMR (100 MHz, $CDCl_3$) δ: 157.1 (d, *J* = 264.9 Hz), 150.0 (dd, *J* = 17.0, 4.4 Hz), 147.0 (dd, *J* = 11.0, 6.8 Hz), 136.2 (d, *J* = 3.1 Hz), 134.0 (d, *J* = 11.2 Hz), 131.0 (d, *J* = 13.6 Hz), 125.9 (dd, *J* = 6.0, 2.3 Hz), 120.8 (q, *J* = 321.6 Hz), 115.6 (dd, *J* = 84.1, 14.6 Hz), 115.3 (d, *J* = 91.0 Hz), 18.2 (d, *J* = 2.4 Hz); ^{19}F NMR (365 MHz, $CDCl_3$) δ: –78.18, –107.41; ^{31}P NMR (162 MHz, $CDCl_3$) δ: 20.66 (d, *J* = 3.7 Hz); m/z LRMS (ESI + APCI) found $[M–OTf]^+$ 372.2, $C_{24}H_{20}FNP^+$ requires 372.1.

(2-(((1-Benzhydrylazetidin-3-yl)methoxy)methyl)pyridin-4-yl)triphenylphosphonium trifluoromethanesulfonate

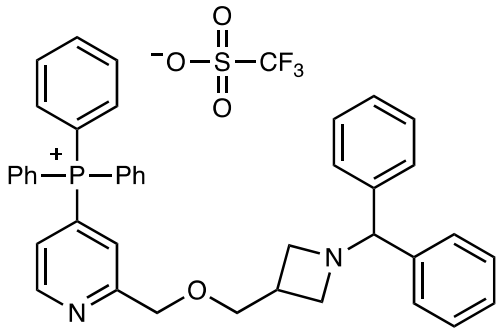

Prepared according to general procedure A using 2-(((1-benzhydrylazetidin-3-yl)methoxy)methyl)pyridine (962 mg, 2.79 mmol), Tf_2O (468 μL, 2.79 mmol), PPh_3 (812 mg, 3.10 mmol), DBU (416 μL, 2.79 mmol) and CH_2Cl_2 (28 mL). After the purification procedure, the title compound was isolated as a white solid (1.77 g, 2.34 mmol, 84% yield). mp 201-203 ºC; IR ν_{max}/cm^{-1} (film): 3060, 2949, 2851, 1582, 1485, 1439, 1264, 1223, 1147, 1108, 1029, 689, 636, 558; ^1H NMR (400 MHz, $CDCl_3$) δ: 8.93 (1H, app t, *J* = 5.0 Hz), 7.82-7.11 (27H, m), 4.71 (2H, s), 4.29 (1H, br), 3.68 (2H, d, *J* = 6.9 Hz), 3.15 (2H, br), 2.93-2.49 (3H, m); ^{13}C NMR (100 MHz, $CDCl_3$) δ: 161.5 (d, *J* = 9.9 Hz), 150.7 (d, *J* = 10.4 Hz), 141.3-140.8 (br), 135.9 (d, *J* = 2.79 Hz), 134.1 (d, *J* = 10.6 Hz), 130.6 (d, *J* = 13.0 Hz), 128.8 (d, *J* = 84.0 Hz), 128.3, 127.2, 127.1, 125.5 (d, *J* = 8.1 Hz), 123.8 (d, *J* = 9.1 Hz), 120.6 (q, *J* = 324.3 Hz), 115.8, 115.4 (d, *J* = 89.4 Hz), 78.0, 72.3, 56.0, 29.0; ^{19}F NMR (365 MHz, $CDCl_3$) δ: –78.08; ^{31}P NMR (162 MHz, $CDCl_3$) δ: 22.64; m/z LRMS (ESI + APCI) found $[M–OTf]^+$ 605.3, $C_{41}H_{38}N_2OP^+$ requires 605.3.

(2-(4-Methoxyphenyl)pyridin-4-yl)triphenylphosphonium trifluoromethanesulfonate

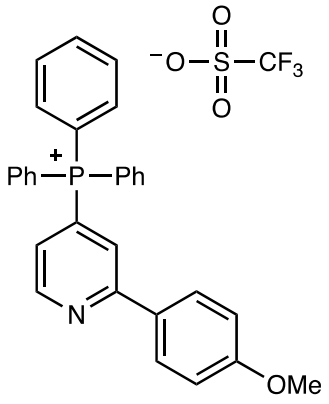

Major

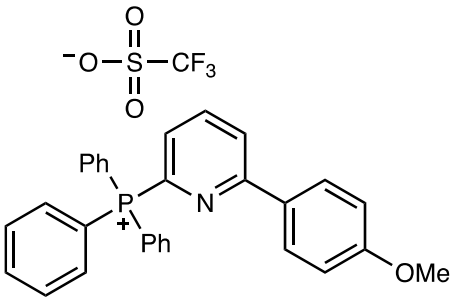

Minor

>20:1 mixture of regioisomers

Prepared according to general procedure A using 2-(4-methoxyphenyl)pyridine (92 mg, 0.50 mmol), Tf_2O (84 μL, 0.50 mmol), PPh_3 (144 mg, 0.55 mmol), NEt_3 (70 μL, 0.50 mmol) and CH_2Cl_2 (5 mL). After the purification procedure, the title compound was isolated as a white solid (298 mg, 0.38 mmol, 75% yield). mp 123-125 ºC; IR ν_{max}/cm^{-1} (film): 3062, 2963, 2937, 2839, 2231, 1606, 1582, 1515, 1463, 1438, 1377, 1260, 1222, 1148, 1108, 1029, 830, 725, 689, 635; Major isomer, ^1H NMR (400 MHz, $CDCl_3$) δ: 9.00 (1H, app t, *J* = 5.1 Hz), 7.99-7.62 (18H, m), 7.41 (1H, dd, *J* = 12.7, 4.9 Hz), 6.97 (2H, d, *J* = 8.8 Hz), 3.83 (3H, s); Major isomer, ^{13}C NMR (100 MHz, $CDCl_3$) δ: 161.5, 158.8 (d, *J* = 10.5 Hz), 151.5 (d, *J* = 10.8 Hz), 136.2 (d, *J* = 2.9 Hz), 134.3 (d, *J* = 10.5 Hz), 130.9 (d, *J* = 13.0 Hz), 129.2 (d, *J* = 1.3 Hz), 129.0 (d, *J* = 84.0 Hz), 128.5, 124.6 (d, *J* = 8.1 Hz), 122.4 (m), 120.7 (q, *J* = 323.7 Hz), 115.6 (d, *J* = 89.5 Hz), 114.4, 55.4; ^{19}F NMR (365 MHz, $CDCl_3$) δ: –78.12; ^{31}P NMR (162 MHz, $CDCl_3$) δ: 22.77, 15.16; m/z LRMS (ESI + APCI) found $[M–OTf]^+$ 446.2, $C_{30}H_{25}NOP^+$ requires 446.2.

(2-(4-Iodophenyl) pyridin-4-yl)triphenylphosphonium trifluoromethanesulfonate

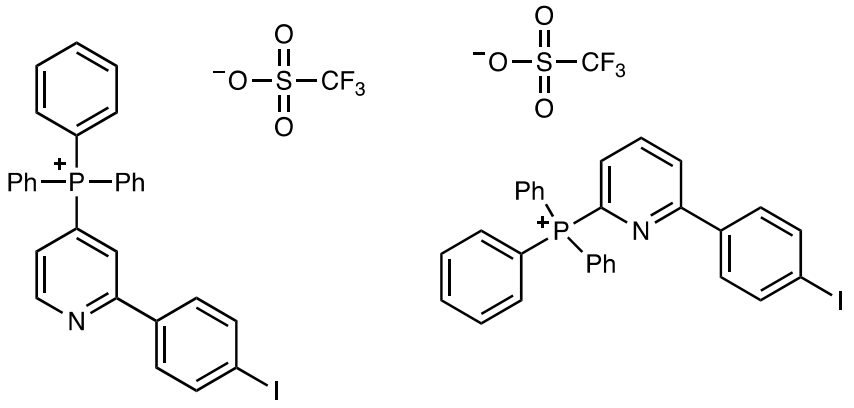

Major Minor

19:1 Mixture of Regioisomers

Prepared according to general procedure A (except that PPh_3 was stirred at -30 °C) 2-(4-iodophenyl)pyridine (843 mg, 3.00 mmol), Tf_2O (504 μL, 3.00 mmol), PPh_3 (865 mg, 3.30 mmol), DBU (448 μL, 3.00 mmol) and CH_2Cl_2 (30 mL). After the purification procedure, the title compound was isolated as a yellow solid (2.00 g, 2.91 mmol, 97% yield). mp 204-207 ºC; IR ν_{max}/cm^{-1} (film): 3061, 1585, 1438, 1285, 1147, 1108, 1029, 635; Major isomer, ^1H NMR (400 MHz, $CDCl_3$) δ: 9.05 (1H, td, *J* = 5.1, 0.7 Hz), 7.96-7.63 (20H, m), 7.54 (1H, ddd, *J* = 12.7, 5.0, 1.6 Hz); Major isomer, ^{13}C NMR (100 MHz, $CDCl_3$) δ: 158.4 (d, *J* = 10.6 Hz), 151.8 (d, *J* = 10.7 Hz), 138.3, 136.5 (d, *J* = 1.5 Hz), 136.3 (d, *J* = 3.0 Hz), 135.6 (d, *J* = 10.6 Hz), 131.1 (d, *J* = 13.1 Hz), 129.7 (d, *J* = 83.9 Hz), 129.0, 125.8 (d, *J* = 8.0 Hz), 123.2 (d, *J* = 8.6 Hz), 121.1 (q, *J* = 321.2 Hz), 115.7 (d, *J* = 89.4 Hz), 97.4; ^{19}F NMR (365 MHz, $CDCl_3$) δ: –78.14; ^{31}P NMR (162 MHz, $CDCl_3$) δ: 22.78, 15.72; m/z LRMS (ESI + APCI) found $[M–OTf]^+$ 542.1, $C_{29}H_{22}INP^+$ requires 542.1.

(2-(4-Chlorophenyl)pyridin-4-yl)triphenylphosphonium trifluoromethanesulfonate

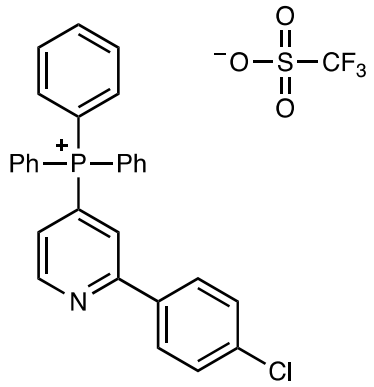

Prepared according to general procedure A using 2-(4-chlorophenyl)pyridine (95 mg, 0.50 mmol), Tf_2O (84 μL, 0.50 mmol), PPh_3 (144 mg, 0.55 mmol), NEt_3 (70 μL, 0.50 mmol) and CH_2Cl_2 (5 mL). After the purification procedure, the title compound was isolated as a white solid (300 mg, 0.35 mmol, 69% yield). mp 211-213 ºC; IR ν_{max}/cm^{-1} (film): 3060, 1582, 1439, 1373, 1260, 1223, 1148, 1108, 1029, 725, 636, 545; ^1H NMR (400 MHz, $CDCl_3$) δ: 9.05 (1H, app t, *J* = 5.1 Hz), 7.97-7.63 (18H, m), 7.52 (1H, ddd, *J* = 12.7, 5.0, 1.6 Hz), 7.40 (2H, d, *J* = 8.6 Hz); ^{13}C NMR (100 MHz, $CDCl_3$) δ: 158.0 (d, *J* = 10.5 Hz), 151.7 (d, *J* = 10.7 Hz), 136.5, 136.2 (d, *J* = 3.0 Hz), 135.5 (d, *J* = 1.5 Hz), 134.5 (d, *J* = 10.5 Hz), 131.0 (d, *J* = 13.0 Hz), 129.7 (d, *J* = 84.1 Hz), 129.2, 128.6, 125.7 (d, *J* = 8.2 Hz), 123.2 (d, *J* = 8.6 Hz), 122.8 (q, *J* = 327.4 Hz), 115.6 (d, *J* = 89.5 Hz); ^{19}F NMR (365 MHz, $CDCl_3$) δ: –78.15; ^{31}P NMR (162 MHz, $CDCl_3$) δ: 22.75; m/z LRMS (ESI + APCI) found $[M–OTf]^+$ 450.2, $C_{29}H_{22}ClNP^+$ requires 450.1.

(3-Chloropyridin-4-yl)triphenylphosphonium trifluoromethanesulfonate

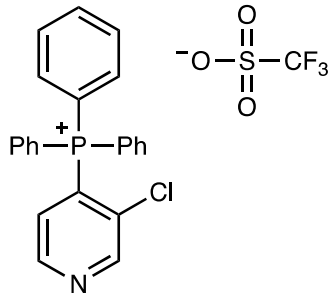

Prepared according to general procedure A using 3-chloroisonicotinonitrile (48 μL, 0.50 mmol), Tf_2O (84 μL, 0.50 mmol), PPh_3 (144 mg, 0.55 mmol), DBU (75 μL, 0.50 mmol) and CH_2Cl_2 (5 mL). After the purification procedure, the title compound was isolated as a white solid (262 mg, 0.38 mmol, 76% yield). mp 197-200 ºC; IR ν_{max}/cm^{-1} (film): 3064, 1587, 1483, 1437, 1391, 1260, 1224, 1182, 1147, 1107, 1029, 749, 701, 634, 528; ^{1}H NMR (400 MHz, $CDCl_3$) δ: 8.93-8.84 (2H, m), 7.95-7.65 (15H, m), 7.31 (1H, dd, *J* = 14.6, 4.9 Hz; ^{13}C NMR (100 MHz, $CDCl_3$) δ: 151.6 (d, *J* = 5.0 Hz), 149.8 (d, *J* = 9.9 Hz), 135.8 (d, *J* = 3.0 Hz), 134.5 (d, *J* = 1.5 Hz), 134.0 (d, *J* = 10.7 Hz), 130.8 (d, *J* = 13.4 Hz), 130.2 (d, *J* = 8.3 Hz), 127.1 (d, *J* = 88.4 Hz), 120.6 (q, *J* = 321.4 Hz), 115.0 (d, *J* = 90.5 Hz); ^{19}F NMR (365 MHz, $CDCl_3$) δ: –78.15; ^{31}P NMR (162 MHz, $CDCl_3$) δ: 22.68; *m/z* LRMS (ESI + APCI) found $[M–OTf]^+$ 374.1, $C_{23}H_{18}ClNP^+$ requires 374.1.

(5-(allyloxy)-2-methylpyridin-4-yl)triphenylphosphonium trifluoromethanesulfonate

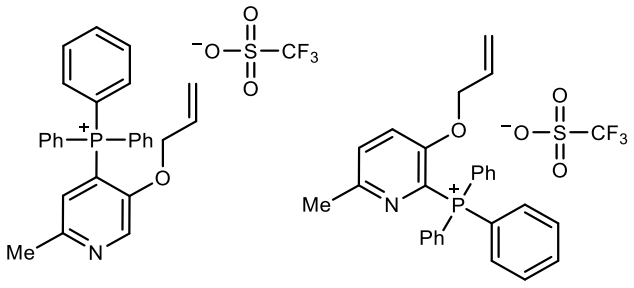

Major **Minor**

16:1 mixture of regioisomers

Prepared according to general procedure A (except PPh_3 was added and stirred at -78°C) using 5-(allyloxy)-2-methylpyridine (885 mg, 5.90 mmol), Tf_2O (0.99 mL, 5.90 mmol), PPh_3 (1.700 g, 6.49 mmol), DBU (0.88 mL, 5.90 mmol) and CH_2Cl_2 (59 mL). After the purification procedure, the title compound was isolated as a white amorphous solid (2.467 g, 4.43 mmol, 75% yield); IR ν_{max}/cm^{-1} (film): 3061, 3026, 2995, 2926, 1586, 1484, 1438, 1350, 1260, 1222, 1146, 1107, 1029, 983, 722, 689, 635; ^1H NMR (400 MHz, $CDCl_3$) δ: 8.54 (1H, d, J = 6.9 Hz), 7.91-7.86 (3H, m), 7.79-7.72 (6H, m), 7.68-7.60 (6H, m), 6.88 (1H, d, J = 15.1 Hz), 5.32-5.21 (1H, m), 5.01 (1H, dq, J = 10.5, 1.1 Hz), 4.91 (1H, dq, J =17.1, 1.2 Hz), 4.46 (2H, dt, J = 5.6, 1.3 Hz), 2.54 (3H, s); ^{13}C NMR (100 MHz, $CDCl_3$) d: 152.6, 136.0 (d, *J* = 4.7 Hz), 135.2, 133.6 (d, *J* = 10.6 Hz), 130.3 (d, *J* = 13.1 Hz), 129.6, 127.0 (d, *J* = 6.8 Hz), 120.5 (q, *J* = 321.2 Hz), 119.1, 117.7 (d, *J* = 90.9 Hz), 116.2 (d, *J* = 91.3 Hz), 115.0, 70.3, 23.3; ^{19}F NMR (365 MHz, $CDCl_3$) d: –78.18; ^{31}P NMR (162 MHz, $CDCl_3$) d: 22.46 (major), 17.78 (minor); *m/z* LRMS (ESI + APCI) found $[M–OTf]^+$ 410.2, $C_{23}H_{18}ClNP^+$ requires 410.2.

(2-methyl-5-(2-oxopropoxy)pyridin-4-yl)triphenylphosphonium trifluoromethanesulfonate

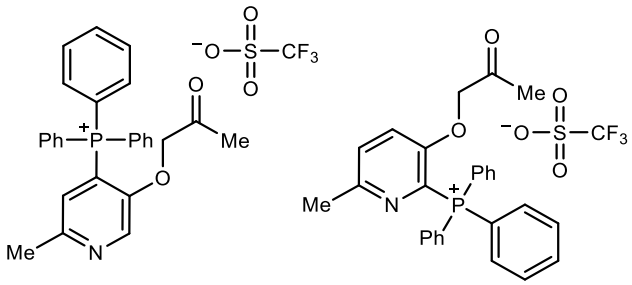

Major **Minor**

6:1 mixture of regioisomers

Prepared according to general procedure A using 1-((6-methylpyridin-3-yl)oxy)propan-2-one (885 mg, 5.0 mmol), Tf_2O (0.84 mL, 5.0 mmol), PPh_3 (1.441 g, 5.5 mmol), DBU (0.75 mL, 5.0 mmol) and CH_2Cl_2 (50 mL). After the purification procedure, the title compound was isolated as a brown amorphous solid (1.526 g, 2.65 mmol, 53% yield); IR ν_{max}/cm^{-1} (film): 3071, 3023, 2923, 1726, 1493, 1437, 1353, 1259, 1153, 1106, 1027, 722, 689, 635, 569; ^1H NMR (400 MHz, $CDCl_3$) δ: 8.42 (1H, d, *J* = 6.8 Hz), 7.95 – 7.60 (16H, m), 6.84 (1H, d, *J* = 15.2 Hz), 4.80 (2H, s), 2.51 (3H, s), 2.01 (3H, s); ^{13}C NMR (100 MHz, $CDCl_3$) δ: 201.1, 153.3 (d, *J* = 2.0 Hz), 136.0 (d, *J* = 3.1 Hz), 134.7 (d, *J* = 10.8 Hz), 131.1 (d, *J* = 13.3 Hz), 130.3 (d, *J* = 13.1 Hz), 128.2 (d, *J* = 7.1 Hz), 121.2 (q, *J* = 320.8 Hz), 118.7 (d, *J* = 90.4 Hz), 117.0 (d, *J* = 91.3 Hz), 116.5 (d, *J* = 85.9 Hz), 73.77, 26.3, 23.8; ^{19}F NMR (365 MHz, $CDCl_3$) δ -78.22; ^{31}P NMR (162 MHz, $CDCl_3$) δ: 21.72 (Major), 17.88 (Minor). *m/z* LRMS (ESI + APCI) found $[M–OTf]^+$ 426.2, $C_{27}H_{25}NO_2P^+$ requires 426.2.

A1.14. Synthesis of Bipyridines

General Procedure B

An oven-dried 8 mL vial (≤ 0.5 mmol scale) or a round bottom flask (> 0.5 mmol scale) equipped with a stir bar was charged with the phosphonium salt (1 equiv), the pyridyl coupling partner (2 equiv), B_2Pin_2 (1.0 equiv), and placed under a nitrogen atmosphere. 1,2-Dichloroethane (0.2 M) was added, followed by addition of NEt_3 (1.25 equiv) at room temperature, and the reaction was stirred for 36 hours. The reaction mixture was then opened, diluted with EtOAc (2 mL), and allowed to stir under air for 30 minutes. The crude mixture was directly concentrated *in vacuo*, and the residue was purified by flash chromatography under the stated conditions to provide the bisheterobiaryl product.

2'-(4-Methoxyphenyl)-[2,4'-bipyridine]-4-carbonitrile

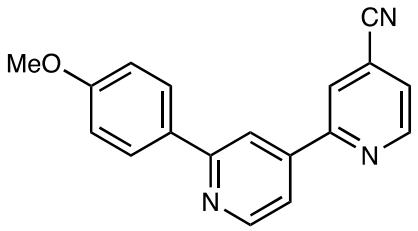

Prepared according to general procedure B using (2-(4-methoxyphenyl)pyridin-4-yl)triphenylphosphonium trifluoromethanesulfonate (238 mg, 0.40 mmol), isonicotinonitrile (83 mg, 0.80 mmol), B_2Pin_2 (102 mg, 0.40 mmol), NEt_3 (70 μL, 0.50 mmol), and 1,2-dichloroethane (2.0 mL). Flash column chromatography (silica gel: 30% EtOAc in hexanes) afforded the title compound as a white solid (86 mg, 0.30 mmol, 75% yield). mp 156-158 ºC; IR ν_{max}/cm^{-1} (film): 3020, 2956, 2927, 2237, 1607, 1546, 1516, 1426, 1259, 1177, 833; ^1H NMR (400 MHz, $CDCl_3$)

δ: 8.91 (1H, d, *J* = 4.8 Hz), 8.77 (1H, d, *J* = 5.0 Hz), 8.27 (1H, s), 7.98-8.10 (3H, m), 7.69 (1H, d, 5.0 Hz) 7.55 (1H, s, *J* = 4.7 Hz), 7.01 (2H, d, *J* = 8.7 Hz), 3.86 (3H, s); ^{13}C NMR (100 MHz, $CDCl_3$) δ: 160.8, 158.2, 156.4, 151.0, 150.5, 145.0, 131.5, 128.4, 124.9, 122.4, 121.6, 118.6, 117.0, 116.4, 114.2, 55.4; m/z LRMS (ESI + APCI) found $[M+H]^+$ 288.1, $C_{18}H_{14}N_3O^+$ requires 288.1.

2'-(4-(4,4,5,5-Tetramethyl-1,3,2-dioxaborolan-2-yl)phenyl)-[2,4'-bipyridine]-4-carbonitrile

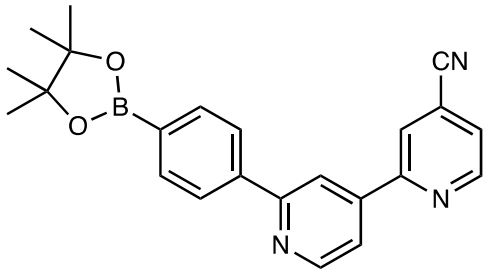

Prepared according to general procedure B using triphenyl(2-(4-(4,4,5,5-tetramethyl-1,3,2-dioxaborolan-2-yl)phenyl)pyridin-4-yl)phosphonium trifluoromethanesulfonate (346 mg, 0.50 mmol), isonicotinonitrile (104 mg, 1.00 mmol), B_2Pin_2 (127 mg, 0.50 mmol), NEt_3 (87 μL, 1.25 mmol), and 1,2-dichloroethane (2.5 mL). Flash column chromatography by dissolving in CH_2Cl_2 and dry loading (silica gel, gradient elution: 15% EtOAc in hexanes) afforded the title compound as a white solid (135 mg, 0.35 mmol, 70% yield). mp 189-191 ºC; IR ν_{max}/cm^{-1} (film): 3067, 3042, 2974, 2925, 2854, 2239, 1608, 1546, 1355, 1328, 1286, 1141, 1093, 961, 829, 663; ^{1}H NMR (400 MHz, $CDCl_3$) δ: 8.93 (1H, d, *J* = 4.9 Hz), 8.84 (1H, d, *J* = 5.1 Hz), 8.38 (1H, s), 8.10 (2H, d, *J* = 8.2 Hz), 8.06 (1H, s), 7.94 (2H, d, *J* = 8.1 Hz), 7.78 (1H, dd, *J* = 5.1, 1.5 Hz), 7.56 (1H, dd, *J* = 4.9, 1.2 Hz), 1.37 (12H, s); ^{13}C NMR (100 MHz, $CDCl_3$) δ: 158.3, 156.2, 151.0, 150.6, 145.1, 141.2, 135.3, 130.0, 126.2, 125.0, 122.5, 121.6, 119.5, 118.0, 116.3, 84.0, 25.0; m/z LRMS (ESI + APCI) found $[M+H]^+$ 384.3, $C_{23}H_{23}BN_3O_2^+$ requires 384.2.

2'-(4-Chlorophenyl)-[2,4'-bipyridine]-4-carbonitrile

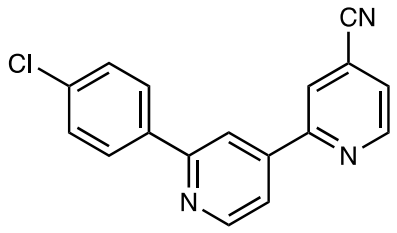

Prepared according to general procedure B using (2-(4-chlorophenyl)pyridin-4-yl)triphenylphosphonium trifluoromethanesulfonate (300 mg, 0.50 mmol), isonicotinonitrile (104 mg, 1.00 mmol), B_2Pin_2 (127 mg, 0.50 mmol), NEt_3 (87 μL, 0.63 mmol), and 1,2-dichloroethane (2.5 mL). Flash column chromatography (silica gel, gradient elution: EtOAc to 1% MeOH in CH_2Cl_2, followed by 6% EtOAc in toluene) afforded the title compound as a white solid (75 mg, 0.26 mmol, 51% yield). mp 164-166 ºC; IR νmax/cm-1 (film): 3089, 3040, 3021, 2235, 1590, 1545, 1473, 1425, 1372, 1097, 843, 829; ^{1}H NMR (400 MHz, $CDCl_3$) δ: 8.96 (1H, d, *J* = 4.9 Hz), 8.84 (1H, d, *J* = 5.1 Hz), 8.36 (1H, s), 8.07 (3H, m), 7.80 (1H, dd, *J* = 5.1, 1.6 Hz), 7.60 (1H, dd, *J* = 4.9, 1.3 Hz), 7.48 (2H, m); ^{13}C NMR (100 MHz, $CDCl_3$) δ: 157.6, 156.3, 151.2, 150.8, 145.4, 137.5, 135.7, 129.2, 128.5, 125.2, 122.6, 121.9, 119.6, 117.8, 116.4; m/z LRMS (ESI + APCI) found $[M+H]^+$ 292.1, $C_{17}H_{11}ClN_3^+$ requires 292.1.

2'-(4-Iodophenyl)-[2,4'-bipyridine]-4-carbonitrile

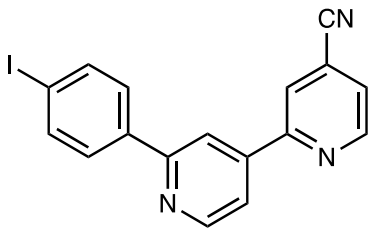

Prepared according to general procedure B using (2-(4-iodophenyl)pyridin-4-yl)triphenylphosphonium trifluoromethanesulfonate (276 mg, 0.40 mmol), isonicotinonitrile (83 mg, 0.80 mmol), B_2Pin_2 (102 mg, 0.40 mmol), NEt_3 (70 μL, 0.50 mmol), and 1,2-dichloroethane (2.0 mL). Flash column chromatography (silica gel: 17% EtOAc in hexanes) afforded the title compound as a white solid (95 mg, 0.25 mmol, 62% yield). mp 209-211 ºC. IR ν_{max}/cm^{-1} (film): 3138, 3091, 3020, 2958, 2923, 2852, 2236, 1592, 1544, 1462, 1423, 1368, 818, 646; ^1H NMR (400 MHz, $CDCl_3$) δ: 8.95 (1H, dd, *J* = 4.9, 0.9 Hz), 8.84 (1H, d, *J* = 5.1 Hz), 8.36 (1H, m), 8.07 (1H, m), 7.85 (4H, s), 7.80 (1H, dd, *J* = 5.1, 1.6 Hz), 7.59 (1H, dd, *J* = 4.9, 1.4 Hz); ^{13}C NMR (100 MHz, $CDCl_3$) δ: 157.7, 156.3, 151.2, 150.8, 145.4, 138.5, 138.1, 128.9, 125.2, 122.6, 121.9, 119.7, 117.7, 116.4, 96.0; m/z LRMS (ESI + APCI) found $[M+H]^+$ 384.1, $C_{17}H_{11}IN_3^+$ requires 384.0.

2'-Methyl-[2,4'-bipyridine]-4-carbonitrile

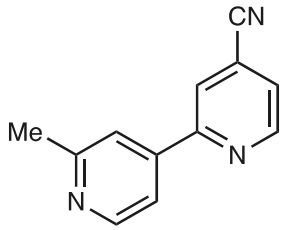

Prepared according to general procedure B using (2-methylpyridin-4-yl)triphenylphosphonium trifluoromethanesulfonate (252 mg, 0.50 mmol), isonicotinonitrile (104 mg, 1.00 mmol), B_2Pin_2 (127 mg, 0.50 mmol), NEt_3 (87 μL, 0.63 mmol), and 1,2-dichloroethane (2.5 mL). Flash column chromatography (silica gel: 40% EtOAc in hexanes) afforded the title compound as a white solid (80 mg, 0.41 mmol, 82% yield). mp 123-125 ºC; IR ν_{max}/cm^{-1} (film): 3099, 3009, 2957, 2922, 2239, 1593, 1547, 1463, 833, 644; ^1H NMR (400 MHz, $CDCl_3$) δ: 8.89 (1H, d, *J* = 4.8 Hz), 8.63

(1H, d, *J* = 5.1 Hz), 7.98 (1H, s), 7.75 (1H, s), 7.65 (1H, d, *J* = 4.8 Hz), 7.54 (1H, d, *J* = 4.7 Hz), 2.64 (3H, s); ^{13}C NMR (100 MHz, $CDCl_3$) δ: 159.7, 156.4, 151.0, 150.2, 144.6, 124.9, 122.5, 121.6, 120.5, 118.1, 116.3, 24.7; m/z LRMS (ESI + APCI) found $[M+H]^+$ 196.1, $C_{12}H_{10}N_3^+$ requires 196.1.

2'-Chloro-[2,4'-bipyridine]-4-carbonitrile

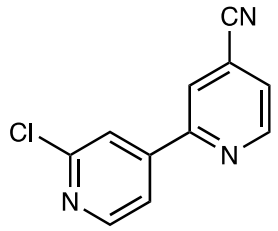

Prepared according to general procedure B using (2-chloropyridin-4-yl)triphenylphosphonium trifluoromethanesulfonate (262 mg, 0.50 mmol), isonicotinonitrile (104 mg, 1.00 mmol), B_2Pin_2 (127 mg, 0.50 mmol), $^{44}NEt_3$ (87 μL, 0.63 mmol), and 1,2-dichloroethane (2.5 mL). Flash column chromatography (basic alumina: 15% EtOAc in hexanes) afforded the title compound as a white solid (33 mg, 0.15 mmol, 30% yield). mp 199-200 ºC; IR ν_{max}/cm^{-1} (film): 3097, 3064, 2240, 1590, 1540, 1403, 1364, 1098, 836, 769, 644; ^{1}H NMR (400 MHz, $CDCl_3$) δ: 8.94 (1H, d, *J* = 4.8 Hz), 8.55 (1H, d, *J* = 5.1 Hz), 8.00 (2H, m), 7.82 (1H, d, *J* = 5.1 Hz), 7.61 (1H, d, *J* = 4.8 Hz); ^{13}C NMR (100 MHz, $CDCl_3$) δ: 154.9, 153.0, 151.4, 150.8, 147.4, 125.7, 122.6, 122.1, 121.9, 119.7, 116.1; m/z LRMS (ESI + APCI) found $[M+H]^+$ 216.1, $C_{11}H_7ClN_3^+$ requires 216.0.

3'-Methoxy-[2,4'-bipyridine]-4-carbonitrile

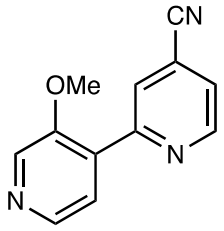

Prepared according to general procedure B using (3-methoxypyridin-4-yl)triphenylphosphonium trifluoromethanesulfonate (519 mg, 1.00 mmol), isonicotinonitrile (208 mg, 2.00 mmol), B_2Pin_2 (254 mg, 1.00 mmol), NEt_3 (254 μL, 1.25 mmol), and 1,2-dichloroethane (5.0 mL). Flash column chromatography (silica gel: 50% EtOAc in hexanes, followed by recrystallization from CH_2Cl_2 and hexanes) afforded the title compound as a white solid (103 mg, 0.49 mmol, 49% yield). mp 122-124 ºC; IR ν_{max}/cm^{-1} (film): 3054, 2948, 2943, 2236, 1752, 1592, 1556, 1494, 1424, 1230, 1055, 840, 636; ^{1}H NMR (400 MHz, $CDCl_3$) δ: 8.89 (1H, dd, *J* = 5.0, 0.9 Hz), 8.47 (1H, s), 8.40 (1H, d, *J* = 4.9 Hz), 8.27 (1H, m), 7.85 (1H, d, *J* = 4.9 Hz), 7.50 (1H, dd, *J* = 5.0, 1.5 Hz), 4.03 (3H, s); ^{13}C NMR (100 MHz, $CDCl_3$) δ: 154.4, 152.6, 150.5, 143.3, 134.9, 132.8, 127.1, 124.2, 123.8, 120.6, 116.7, 56.4; m/z LRMS (ESI + APCI) found $[M+H]^+$ 212.1, $C_{12}H_{10}N_3O^+$ requires 212.1.

3'-Chloro-[2,4'-bipyridine]-4-carbonitrile

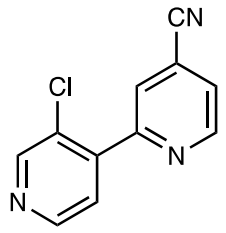

Prepared according to general procedure B (except ran for 115 hours) using (3-chloropyridin-4-yl)triphenylphosphonium trifluoromethanesulfonate (262 mg, 0.50 mmol), isonicotinonitrile (104 mg, 1.00 mmol), B_2Pin_2 (127 mg, 0.50 mmol), NEt_3 (87 μL, 0.63 mmol), and 1,2-dichloroethane (2.5 mL). Flash column chromatography (silica gel: 30% EtOAc in hexanes) afforded the title compound as a white solid (37 mg, 0.17 mmol, 34% yield). mp 136-138 ºC. IR ν_{max}/cm^{-1} (film): 3092, 3060, 3025, 2240, 1595, 1461, 1388, 851, 640; ^{1}H NMR (400 MHz, $CDCl_3$) δ: 8.96 (1H, d, J = 4.9 Hz), 8.75 (1H, s), 8.65 (1H, d, J = 4.6 Hz), 8.02 (1H, s), 7.60 (2H, m); ^{13}C NMR (100 MHz, $CDCl_3$) δ: 155.5, 151.2, 150.8, 148.5, 143.8, 129.5, 126.3, 125.2, 125.0, 121.1, 116.2; m/z LRMS (ESI + APCI) found $[M+H]^+$ 216.1, $C_{11}H_7ClN_3^+$ requires 216.0.

3'-Fluoro-2'-methyl-[2,4'-bipyridine]-4-carbonitrile

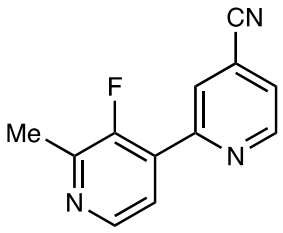

Prepared according to general procedure B using triphenyl(2-(prop-1-en-2-yl)pyridin-4-yl)phosphonium trifluoromethanesulfonate (261 mg, 0.50 mmol), isonicotinonitrile (104 mg, 1.00

mmol), B_2Pin_2 (127 mg, 0.50 mmol), NEt_3 (87 μL, 1.25 mmol), and 1,2-dichloroethane (2.5 mL). Flash column chromatography by dissolving in CH_2Cl_2 and dry loading (silica gel, gradient elution: 15% EtOAc in toluene) afforded the title compound as a white solid (70 mg, 0.33 mmol, 65% yield). mp 102-104 ºC; IR ν_{max}/cm^{-1} (film): 3068, 2957, 2923, 2852, 2241, 1596, 1564, 1474, 1395, 1298, 1200, 1123, 850, 532; ^1H NMR (400 MHz, $CDCl_3$) δ: 8.92 (1H, d, *J* = 4.9 Hz), 8.42 (1H, d, *J* = 5.0 Hz), 8.12 (1H, s), 7.78 (1H, t, *J* = 3.8 Hz), 7.56 (1H, d, *J* = 4.9 Hz), 2.61 (3H, d, *J* = 3.3 Hz); ^{13}C NMR (100 MHz, $CDCl_3$) δ: 155.1 (d, *J* = 260.3 Hz), 152.5, 150.8, 148.3 (d, *J* = 18.6 Hz), 145.1 (d, *J* = 7.0 Hz), 131.3 (d, *J* = 9.5 Hz), 126.3 (d, *J* = 11.5 Hz), 124.9, 121.8, 121.3, 116.1, 18.1; ^{19}F NMR (365 MHz, $CDCl_3$) δ: –129.52; *m/z* LRMS (ESI + APCI) found $[M+H]^+$ 214.1, $C_{12}H_9FN_3^+$ requires 214.1.

2'-(((1-Benzhydrylazetidin-3-yl)methoxy)methyl)-[2,4'-bipyridine]-4-carbonitrile

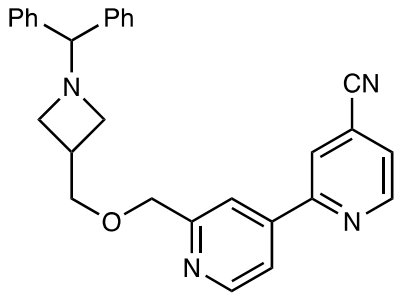

Prepared according to general procedure B using (2-(((1-benzhydrylazetidin-3-yl)methoxy)methyl)pyridin-4-yl)triphenylphosphonium trifluoromethanesulfonate (226 mg, 0.30 mmol), isonicotinonitrile (62 mg, 0.60 mmol), B_2Pin_2 (76 mg, 0.30 mmol), NEt_3 (52 μL, 0.38 mmol), and 1,2-dichloroethane (1.5 mL). Flash column chromatography (basic alumina: 25% EtOAc in hexanes) followed by a second flash column (silica gel: 40% EtOAc in hexanes) afforded

the title compound as a light yellow, amorphous solid (83 mg, 0.19 mmol, 62% yield). IR ν_{max}/cm^{-1} (film): 3098, 3062, 3024, 2962, 2845, 2831, 2242, 1593, 1453, 1123, 840, 783, 706, 699, 544; ^{1}H NMR (400 MHz, $CDCl_3$) δ: 8.87 (1H, d, *J* = 4.8 Hz), 8.71 (1H, d, *J* = 5.1 Hz), 8.04 (1H, s), 8.00 (1H, s), 7.79 (1H, d, *J* = 3.9 Hz), 7.54 (1H, d, *J* = 4.9 Hz), 7.40 (4H, d, *J* = 7.4 Hz), 7.13-7.29 (6H, m), 4.73 (2H, s), 4.37 (1H, s), 3.78 (2H, d, *J* = 6.6 Hz), 3.34 (2H, t, *J* = 7.5 Hz), 2.98 (2H, t, *J* = 6.6 Hz), 2.83 (1H, qn, *J* = 6.6 Hz); ^{13}C NMR (100 MHz, $CDCl_3$) δ: 160.2, 156.4, 151.1, 150.1, 145.1, 142.4, 128.5, 127.6, 127.1, 125.0, 122.5, 121.7, 119.7, 118.6, 116.4, 78.2, 73.9, 73.9, 56.7, 29.9; m/z LRMS (ESI + APCI) found $[M+H]^+$ 447.3, $C_{29}H_{27}N_4O^+$ requires 447.2.

2'-(Thiophen-3-yl)-[2,4'-bipyridine]-4-carbonitrile

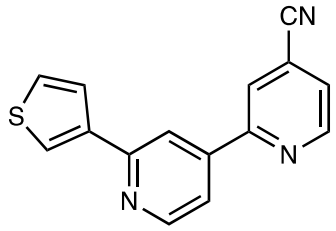

Prepared according to general procedure B using triphenyl(2-(thiophen-3-yl)pyridin-4-yl)phosphonium trifluoromethanesulfonate (172 mg, 0.30 mmol), isonicotinonitrile (62 mg, 0.60 mmol), B_2Pin_2 (76 mg, 0.30 mmol), NEt_3 (52 μL, 0.38 mmol), and 1,2-dichloroethane (1.5 mL). Flash column chromatography (silica gel: 20% EtOAc in hexanes) afforded the title compound as a white solid (57 mg, 0.20 mmol, 65% yield). mp 165-166 ºC; IR ν_{max}/cm^{-1} (film): 3130, 3090, 3058, 3024, 2238, 1590, 1559, 1543, 1463, 1433, 1382, 789, 670, 526; ^{1}H NMR (400 MHz, $CDCl_3$) δ: 8.94 (1H, d, *J* = 4.9 Hz), 8.77 (1H, d, *J* = 5.2 Hz), 8.25 (1H, s), 8.05 (1H, s), 8.02 (1H, d, *J* = 2.8 Hz), 7.76 (1H, d, *J* = 5.6 Hz), 7.72 (1H, dd, *J* = 5.0, 1.5 Hz), 7.58 (1H, d, *J* = 5.0 Hz),

7.44 (1H, dd, J = 4.9, 3.0 Hz); ^{13}C NMR (100 MHz, $CDCl_3$) δ: 156.4, 154.8, 151.2, 150.7, 145.2, 141.9, 126.7, 126.4, 125.1, 124.3, 122.5, 121.8, 119.0, 117.7, 116.4; m/z LRMS (ESI + APCI) found $[M+H]^+$ 264.1, $C_{15}H_{10}N_3S^+$ requires 264.1.

Ethyl 4-((4-cyano-[2,4'-bipyridin]-2'-yl)(phenyl)methoxy)piperidine-1-carboxylate

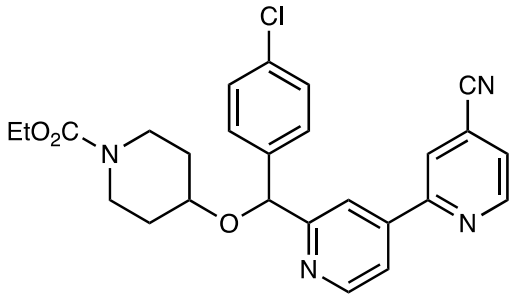

Prepared according to general procedure B using (2-((4-chlorophenyl)((1-(ethoxycarbonyl)piperidin-4-yl)oxy)methyl)pyridin-4-yl)triphenylphosphonium trifluoromethanesulfonate (393 mg, 0.30 mmol), isonicotinonitrile (62 mg, 0.60 mmol), B_2Pin_2 (76 mg, 0.30 mmol), NEt_3 (52 μL, 0.38 mmol), and 1,2-dichloroethane (1.5 mL). Flash column chromatography (silica gel: 15% EtOAc in hexanes) afforded the title compound as a tan solid (102 mg, 0.21 mmol, 71% yield). mp 46-48 ºC; IR ν_{max}/cm^{-1} (film): 3059, 2979, 2928, 2866, 2239, 1690, 1592, 1428, 1273, 1227, 1085, 833, 806, 526; ^{1}H NMR (400 MHz, $CDCl_3$) δ: 8.92 (1H, d, J = 4.9 Hz), 8.66 (1H, d, J = 5.1 Hz), 8.11 (1H, s), 7.99 (1H, s), 7.77 (1H, dd, J = 5.1, 1.7 Hz), 7.57 (1H, dd, J = 4.9, 1.3 Hz), 7.42 (2H, d, J = 8.6 Hz), 7.30 (2H, d, J = 8.5 Hz), 5.71 (1H, s), 4.11 (2H, q, J = 7.1 Hz), 3.81 (2H, m), 3.68 (1H, sp, J = 3.8 Hz), 3.18 (2H, m), 1.87 (2H, m), 1.69 (2H, m), 1.25 (3H, t, J = 7.1 Hz); ^{13}C NMR (100 MHz, $CDCl_3$) δ: 163.4, 156.3, 155.6, 151.2, 150.1, 145.6, 139.9, 133.7, 128.8, 128.3, 125.1, 122.6, 121.8, 120.0, 117.9, 116.4, 81.0, 73.1, 61.4, 41.3 (rot),

41.2, 31.4 (rot), 31.2, 14.8; m/z LRMS (ESI + APCI) found $[M+H]^+$ 477.2, $C_{26}H_{26}ClN_4O_3^+$ requires 477.2.

2'-(Bis(3-(trifluoromethyl)phenyl)methyl)-[2,4'-bipyridine]-4-carbonitrile

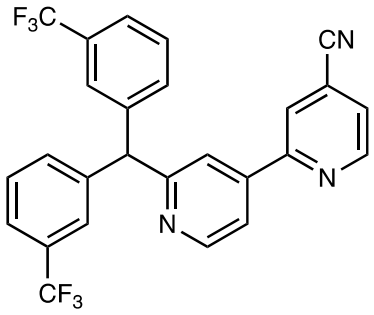

Prepared according to general procedure B using (2-(bis(3-(trifluoromethyl)phenyl)methyl)pyridin-4-yl)triphenylphosphonium trifluoromethanesulfonate (158 mg, 0.20 mmol), isonicotinonitrile (42 mg, 0.40 mmol), B_2Pin_2 (51 mg, 0.20 mmol), NEt_3 (35 μL, 0.25 mmol), and 1,2-dichloroethane (1.0 mL). Flash column chromatography (silica gel: 30% EtOAc in hexanes) afforded the title compound as a light yellow solid (79 mg, 0.16 mmol, 82% yield). mp 86-89 ºC; IR ν_{max}/cm^{-1} (film): 3058, 2925, 2853, 2239, 1593, 1543, 1310, 1161, 1118, 1075, 701; ^1H NMR (400 MHz, $CDCl_3$) δ: 8.90 (1H, dd, *J* = 5.0, 0.8 Hz), 8.80 (1H, d, *J* = 5.1 Hz), 7.96 (1H, app t, *J* = 1.0 Hz), 7.84 (1H, s), 7.78 (1H, dd, *J* = 5.1, 1.7 Hz), 7.41-7.55 (9H, m), 5.83 (1H, s); ^{13}C NMR (100 MHz, $CDCl_3$) δ: 162.5, 156.0, 151.2, 151.0, 145.5, 142.8, 132.7, 131.0 (q, *J* = 32.3 Hz), 129.3, 126.0 (q, *J* = 3.9 Hz), 124.1 (q, *J* = 272.5 Hz), 124.1 (q, *J* = 3.7 Hz), 122.6, 121.8, 121.2, 120.1, 119.5, 116.3, 58.8; ^{19}F NMR (365 MHz, $CDCl_3$) δ: –62.54; m/z LRMS (ESI + APCI) found $[M+H]^+$ 484.2, $C_{23}H_{17}N_4^+$ requires 484.1.

2-Chloro-N-(4-chloro-3-(4-cyano-[2,4'-bipyridin]-2'-yl)phenyl)-4-(methylsulfonyl)benzamide

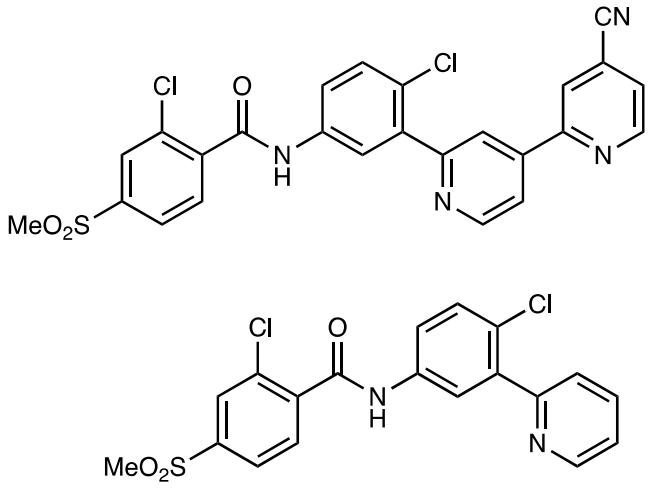

Major Minor

Isolated as 3.8:1 mixture of products

Prepared according to general procedure B (except bubbled 1 atm of O_2 through the reaction instead of opening to air and used 2 equivalents of B_2pin_2) using (2-(2-Chloro-5-(2-chloro-4-(methylsulfonyl)benzamido)phenyl)pyridin-4-yl)triphenylphosphonium trifluoromethanesulfonate (208 mg, 0.25 mmol), 3,5-dimethylisonicotinonitrile (52 mg, 0.50 mmol), B_2Pin_2 (127 mg, 0.50 mmol), NEt_3 (43 μL, 0.31 mmol), and 1,2-dichloroethane (1.25 mL). Flash column chromatography (silica gel: 40% EtOAc and 1% Acetic Acid in hexanes followed by recrystallization from CH_2Cl_2 and hexanes) afforded the title compound as a 3.8:1 mixture of products as a white solid with a crude ^1H NMR yield = 44% using 1,3,5-trimethoxybenzene as an internal standard. *m/z* LRMS (ESI + APCI) found $[M+H]^+$ 523.1, $C_{25}H_{17}Cl_2N_4O_3S^+$ requires 523.0.

((4-Cyano-[2,4'-bipyridin]-2'-yl)methylene)bis(4,1-phenylene) diacetate

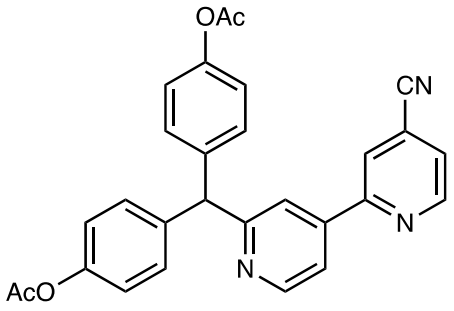

Prepared according to general procedure B using ((4-cyano-[2,4'-bipyridin]-2'-yl)methylene)bis(4,1 phenylene) diacetate (232 mg, 0.30 mmol), isonicotinonitrile (162 mg, 0.60 mmol), B_2Pin_2 (76 mg, 0.30 mmol), NEt_3 (52 μL, 0.38 mmol), and 1,2-dichloroethane (1.5 mL). Flash column chromatography (silica gel: 35% EtOAc in hexanes) afforded the title compound as a light brown oil (104 mg, 0.23 mmol, 75% yield). IR ν_{max}/cm^{-1} (film): 2920, 2850, 2260, 1756, 1592, 1503, 1369, 1190, 1165, 1017, 912, 834, 644; ^1H NMR (400 MHz, $CDCl_3$) δ: 8.84 (1H, dd, *J* = 4.9, 0.6 Hz), 8.73 (1H, d, *J* = 5.1 Hz), 7.91 (1H, s), 7.78 (1H, s), 7.71 (1H, dd, *J* = 5.2, 1.6 Hz), 7.50 (1H, dd, *J* = 4.9 Hz, 1.3 Hz), 7.27-7.22 (4H, m), 7.06-7.01 (4H, m), 5.74 (1H, m), 2.26 (6H, m); ^{13}C NMR (100 MHz, CD_3CN) δ: 170.5, 164.5, 156.4, 151.9, 151.3, 150.6, 146.3, 141.4, 131.2, 126.5, 124.2, 122.7, 122.3, 121.9, 120.0, 117.5, 58.4, 21.2; m/z LRMS (ESI + APCI) found $[M+H]^+$ 464.2, $C_{28}H_{22}N_3O_4^+$ requires 464.2

(E)-2'-(3-(Pyrrolidin-1-yl)-1-(p-tolyl)prop-1-en-1-yl)-[2,4'-bipyridine]-4-carbonitrile

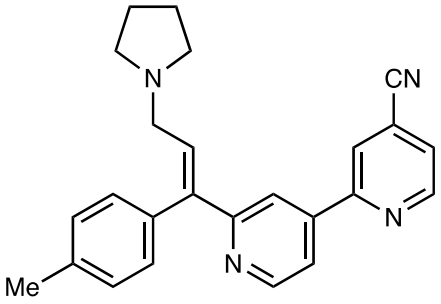

Prepared according to general procedure B using (E)-triphenyl(2-(3-(pyrrolidin-1-yl)-1-(p-tolyl)prop-1-en-1-yl)pyridin-4-yl)phosphonium trifluoromethanesulfonate (207 mg, 0.30 mmol), isonicotinonitrile (62 mg, 0.60 mmol), B_2Pin_2 (76 mg, 0.30 mmol), NEt_3 (52 μL, 0.38 mmol), and 1,2-dichloroethane (1.5 mL). Flash column chromatography (silica gel, gradient elution: 50% Et_2O and 1% NEt_3 in CH_2Cl_2 to 10% MeOH in CH_2Cl_2) followed by a second flash column (silica gel: 3% MeOH in CH_2Cl_2), then the product was recrystallized from CH_2Cl_2 and hexanes, collected on a frit, and washed with brine (2 x 20 mL) and a saturated solution of $NaHCO_3$ (20 mL) afforded the title compound as a white solid (40 mg, 0.11 mmol, 35% yield). mp 112-114 ºC; IR ν_{max}/cm^{-1} (film): 3045, 3000, 2960, 2926, 2909, 2874, 2787, 2238, 1586, 1419, 840, 526; ^1H NMR (400 MHz, $CDCl_3$) δ: 8.85 (1H, d, *J* = 4.9 Hz), 8.72 (1H, d, *J* = 5.1 Hz), 7.83 (1H, s), 7.71 (1H, dd, *J* = 5.1, 1.6 Hz), 7.62 (1H, s), 7.50 (1H, dd, *J* = 4.9, 1.3 Hz), 7.23 (2H, d, *J* = 7.9 Hz), 7.13 (2H, d, *J* = 8.0 Hz), 6.99 (1H, t, *J* = 6.8 Hz), 3.25 (2H, d, *J* = 6.8 Hz), 2.58-2.51 (4H, m), 2.41 (3H, s), 1.80-1.74 (4H, m); ^{13}C NMR (100 MHz, $CDCl_3$) δ: 160.3, 156.7, 151.0, 150.3, 144.8, 141.9, 137.3, 135.2, 131.7, 129.8, 129.4, 124.8, 122.5, 121.6, 119.3, 119.2, 116.4, 54.9, 54.3, 23.6, 21.5; m/z LRMS (ESI + APCI) found $[M+H]^+$ 381.3, $C_{25}H_{25}N_4^+$ requires 381.2.

5-Methyl-2'-phenyl-[2,4'-bipyridine]-4-carbonitrile

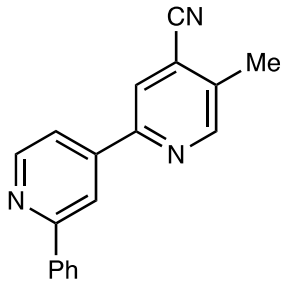

Prepared according to general procedure B using triphenyl(2-phenylpyridin-4-yl)phosphonium trifluoromethanesulfonate (283 mg, 0.50 mmol), 3-methylisonicotinonitrile (118 mg, 1.00 mmol), B_2Pin_2 (127 mg, 0.50 mmol), NEt_3 (87 μL, 0.63 mmol), and 1,2-dichloroethane (2.50 mL). Flash column chromatography (silica gel: 15% EtOAc in hexanes) afforded the title compound as white solid (95 mg, 0.36 mmol, 71% yield). mp 181-182 ºC; IR ν_{max}/cm^{-1} (film): 3057, 2923, 2237, 1581, 1542, 1467, 1367, 1211, 855, 780, 690; ^1H NMR (400 MHz, $CDCl_3$) δ: 8.82 (1H, d, *J* = 5.1 Hz), 8.79 (1H, s), 8.34 (1H, s), 8.06-8.12 (2H, m), 8.00 (1H, s), 7.76 (1H, dd, *J* = 5.1, 1.6 Hz), 7.42-7.54 (3H, m), 2.62 (3H, s); ^{13}C NMR (100 MHz, $CDCl_3$) δ: 158.6, 153.5, 151.9, 150.6, 145.3, 139.1, 135.6, 129.4, 128.9, 127.1, 122.2, 121.9, 119.1, 117.7, 115.7, 17.4; m/z LRMS (ESI + APCI) found $[M+H]^+$ 272.1, $C_{18}H_{14}N_3^+$ requires 272.1.

5-Cyclobutyl-2'-phenyl-[2,4'-bipyridine]-4-carbonitrile

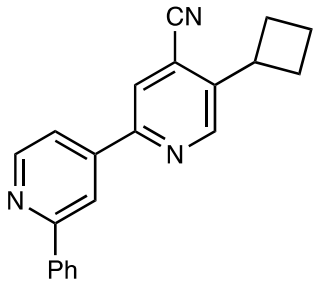

Prepared according to general procedure B using triphenyl(2-phenylpyridin-4-yl)phosphonium trifluoromethanesulfonate (283 mg, 0.50 mmol), 3-cyclobutylisonicotinonitrile (158 mg, 1.00 mmol), B_2Pin_2 (127 mg, 0.50 mmol), NEt_3 (87 μL, 0.63 mmol), and 1,2-dichloroethane (2.5 mL). Flash column chromatography (silica gel: 15% EtOAc in hexanes, followed by recrystallization from CH_2Cl_2 and hexanes) afforded the title compound as a white solid (85 mg, 0.28 mmol, 55% yield). mp 160-161 ºC; IR ν_{max}/cm^{-1} (film): 2995, 2975, 2943, 2862, 2229, 1597, 1531, 1481, 1390, 1364, 1207, 864, 779, 692; ^1H NMR (400 MHz, $CDCl_3$) δ: 8.85 (1H, s), 8.79 (1H, dd, *J* = 5.1, 0.7 Hz), 8.32 (1H, dd, *J* = 1.6, 0.7 Hz), 8.08 (2H, m), 7.95 (1H, d, *J* = 0.7 Hz), 7.74 (1H, dd, *J* = 5.1, 1.7 Hz), 7.39-7.53 (3H, m), 3.90 (1H, qn, *J* = 8.8 Hz), 2.58 (2H, m), 2.35 (2H, m), 2.18 (1H, m), 1.98 (1H, m); ^{13}C NMR (100 MHz, $CDCl_3$) δ: 158.5, 153.3, 150.6, 149.5, 145.2, 142.5, 139.1, 129.3, 128.9, 127.1, 122.5, 120.1, 119.1, 117.7, 115.9, 36.8, 28.9, 18.7; m/z LRMS (ESI + APCI) found $[M+H]^+$ 312.2, $C_{21}H_{18}N_3^+$ requires 312.2.

2'-Phenyl-5-(trimethylsilyl)-[2,4'-bipyridine]-4-carbonitrile

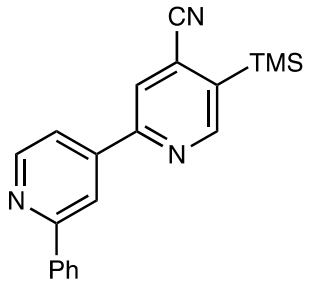

Prepared according to general procedure B using triphenyl(2-phenylpyridin-4-yl)phosphonium trifluoromethanesulfonate (283 mg, 0.50 mmol), 3-(3-cyanophenyl)isonicotinonitrile (176 mg, 1.00 mmol), B_2Pin_2 (127 mg, 0.50 mmol), NEt_3 (87 μL, 0.63 mmol), and 1,2-dichloroethane (2.5 mL). Flash column chromatography (silica gel: 10% EtOAc in hexanes, followed by recrystallization from CH_2Cl_2 and hexanes) afforded the title compound as a white solid (57 mg, 0.18 mmol, 35% yield). mp 128-130 ºC; IR ν_{max}/cm^{-1} (film): 3053, 2956, 2925, 2895, 2228, 1579, 1512, 1500, 1346, 1252, 1208, 820, 766, 691; ^1H NMR (400 MHz, $CDCl_3$) δ: 8.97 (1H, s), 8.83 (1H, d, *J* = 5.1 Hz), 8.37 (1H, s), 8.10 (2H, m), 8.05 (1H, s), 7.79 (1H, dd, *J* = 5.1, 1.4 Hz), 7.42-7.54 (3H, m), 0.52 (9H, s); ^{13}C NMR (100 MHz, $CDCl_3$) δ: 158.7, 156.0, 155.5, 150.6, 145.3, 139.0, 137.5, 129.4, 128.9, 127.1, 126.8, 123.3, 119.3, 117.8, 117.7, 1.4; m/z LRMS (ESI + APCI) found $[M+H]^+$ 330.2, $C_{20}H_{20}N_3Si^+$ requires 330.1.

Methyl 3-(4-cyano-2'-phenyl-[2,4'-bipyridin]-5-yl)propanoate

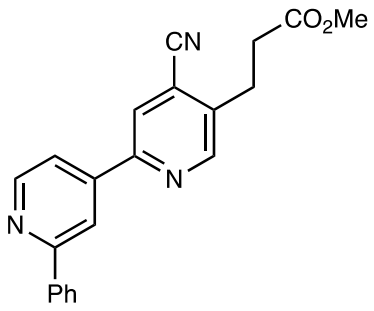

Prepared according to general procedure B using triphenyl(2-phenylpyridin-4-yl)phosphonium trifluoromethanesulfonate (96 mg, 0.17 mmol), methyl 3-(4-cyanopyridin-3-yl)propanoate (67 mg, 0.35 mmol), B_2Pin_2 (43 mg, 0.17 mmol), NEt_3 (30 μL, 0.21 mmol), and 1,2-dichloroethane (0.85 mL). Flash column chromatography (silica gel: 30% EtOAc in hexanes) afforded the title compound as a colorless oil (41 mg, 0.12 mmol, 71% yield). IR ν_{max}/cm^{-1} (film): 3060, 2952, 2920, 2852, 2237, 1730, 1622, 1488, 1442, 1371, 1196, 1182, 1161, 854, 691; ^{1}H NMR (400 MHz, $CDCl_3$) δ: 8.83 (1H, s), 8.81 (1H, d, *J* = 5.1 Hz), 8.33 (1H, s), 8.09 (2H, m), 8.01 (1H, s), 7.75 (1H, dd, *J* = 5.1, 1.6 Hz), 7.41-7.54 (3H, m), 3.70 (3H, s), 3.24 (2H, t, *J* = 7.4 Hz), 2.80 (2H, t, *J* = 7.3 Hz); ^{13}C NMR (100 MHz, $CDCl_3$) δ: 171.9, 158.7, 154.2, 151.8, 150.6, 145.1, 139.1, 137.8, 129.4, 128.9, 127.1, 122.6, 121.7, 119.2, 117.8, 115.5, 52.1, 34.0, 26.8; *m/z* LRMS (ESI + APCI) found $[M+H]^+$ 344.2, $C_{21}H_{18}N_3O_2^+$ requires 344.1.

5-(1-((Tert-butyldimethylsilyl)oxy)-2-methylpropyl)-2'-phenyl-[2,4'-bipyridine]-4-carbonitrile

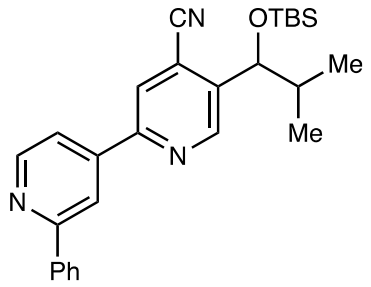

Prepared according to general procedure B using triphenyl(2-phenylpyridin-4-yl)phosphonium trifluoromethanesulfonate (147 mg, 0.26 mmol), 3-(1-((tert-butyldimethylsilyl)oxy)-2-methylpropyl)isonicotinonitrile (149 mg, 0.51 mmol), B_2Pin_2 (66 mg, 0.26 mmol), NEt_3 (45 μL, 0.33 mmol), and 1,2-dichloroethane (1.3 mL). Flash column chromatography (silica gel: 5% EtOAc in hexanes) afforded the title compound as a colorless oil (45 mg, 0.10 mmol, 39% yield). IR ν_{max}/cm^{-1} (film): 2957, 2929, 2857, 1590, 1540, 1465, 1253, 1074, 884, 774, 693; ^1H NMR (400 MHz, $CDCl_3$) δ: 9.01 (1H, s), 8.84 (1H, d, *J* = 5.1 Hz), 8.39 (1H, s) 8.11 (2H, d, *J* = 7.2 Hz), 8.01 (1H s), 7.80 (1H, dd, *J* = 5.1, 1.5 Hz), 7.42-7.54 (3H, m), 4.80 (1H, d, *J* = 6.0 Hz), 2.06 (1H, sext, *J* = 6.6 Hz), 1.00 (3H, d, *J* = 6.6 Hz), 0.93 (12H, m), 0.13 (3H, s), -0.14 (3H, s); ^{13}C NMR (100 MHz, $CDCl_3$) δ: 158.8, 154.4, 150.9, 150.7, 145.2, 141.7, 139.1, 129.4, 129.0, 127.2, 122.2, 119.6, 119.2, 117.9, 115.6, 76.5, 36.6, 25.9, 19.1, 18.3, 17.6 (rot), -4.4, -4.9 (rot); m/z LRMS (ESI + APCI) found $[M+H]^+$ 444.3, $C_{27}H_{34}N_3OSi^+$ requires 444.3.

2',5-Diphenyl-[2,4'-bipyridine]-4-carbonitrile

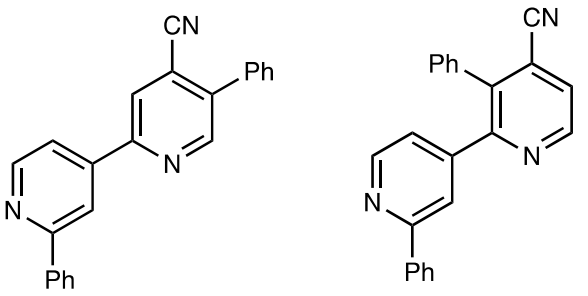

Major Minor

17:1 mixture of regioisomers

Prepared according to general procedure B using triphenyl(2-phenylpyridin-4-yl)phosphonium trifluoromethanesulfonate (283 mg, 0.50 mmol), 3-phenylisonicotinonitrile (180 mg, 1.00 mmol), B_2Pin_2 (127 mg, 0.50 mmol), NEt_3 (87 μL, 0.63 mmol), and 1,2-dichloroethane (2.5 mL). Flash column chromatography (silica gel: 10% EtOAc in hexanes, followed by recrystallization from CH_2Cl_2 and hexanes) afforded the title compound as a white solid (80 mg, 0.24 mmol, 48% yield). mp 184-186 ºC; IR ν_{max}/cm^{-1} (film): 3057, 3037, 3026, 2238, 1959, 1624, 1537, 1470, 1443, 1365, 1212, 904, 768, 693, 532; ^{1}H NMR (400 MHz, $CDCl_3$) δ: 8.99 (1H, m), 8.86 (1H, d, J = 5.1 Hz), 8.42 (1H, m), 8.09-8.17 (3H, m), 7.84 (1H, dd, J = 5.1, 1.6 Hz), 7.42-7.71 (8H, m); ^{13}C NMR (100 MHz, $CDCl_3$) δ: 158.8, 154.3, 151.4, 150.7, 145.0, 139.1, 138.6, 134.1, 130.0, 129.5, 129.4, 129.0, 128.9, 127.2, 123.4, 120.0, 119.3, 117.9, 116.5; m/z LRMS (ESI + APCI) found $[M+H]^+$ 334.2, $C_{23}H_{16}N_3^+$ requires 334.1.

5-(3-Cyanophenyl)-2'-phenyl-[2,4'-bipyridine]-4-carbonitrile

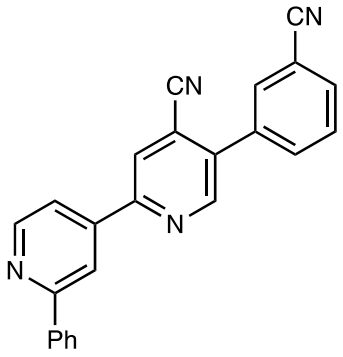

Prepared according to general procedure B except the reaction was diluted to 0.1 M. Triphenyl(2-phenylpyridin-4-yl)phosphonium trifluoromethanesulfonate (188 mg, 0.33 mmol), 3-(3-cyanophenyl)isonicotinonitrile (135 mg, 0.66 mmol), B_2Pin_2 (84 mg, 0.33 mmol), NEt_3 (58 μL, 0.41 mmol), and 1,2-dichloroethane (3.3 mL, 0.1 M) were combined in the reaction vessel. Flash column chromatography (silica gel: 40% EtOAc in hexanes) afforded the title compound as a white solid (63 mg, 0.18 mmol, 53% yield). mp 223-225 ºC; IR ν_{max}/cm^{-1} (film): 3063, 3013, 2235, 1601, 1588, 1535, 1469, 1448, 1366, 1215, 1182, 891, 816, 779, 692, 544; ^{1}H NMR (400 MHz, $CDCl_3$) δ: 8.97 (1H, s), 8.89 (1H, d, J = 5.1 Hz), 8.43 (1H, m), 8.21 (1H, m), 8.12 (2H, m), 7.80-7.98 (4H, m), 7.69-7.77 (1H, m), 7.42-7.59 (3H, m); ^{13}C NMR (100 MHz, $CDCl_3$) δ: 159.0, 155.7, 151.0, 150.9, 144.6, 139.0, 136.1, 135.5, 133.4, 133.2, 132.3, 130.4, 129.6, 129.0, 127.2, 123.4, 120.4, 119.3, 118.0, 117.9, 115.8, 114.0; m/z LRMS (ESI + APCI) found $[M+H]^+$ 359.2, $C_{24}H_{15}N_4^+$ requires 359.1.

2'-Phenyl-5-(4-(trifluoromethoxy)phenyl)-[2,4'-bipyridine]-4-carbonitrile

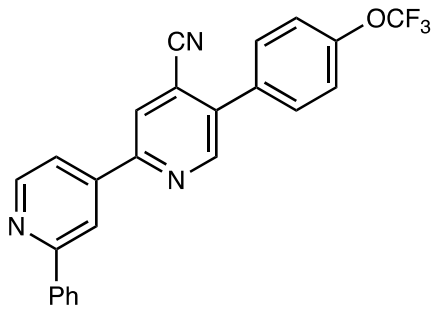

Prepared according to general procedure B using triphenyl(2-phenylpyridin-4-yl)phosphonium trifluoromethanesulfonate (283 mg, 0.50 mmol), 3-(4-(trifluoromethoxy)phenyl)isonicotinonitrile (264 mg, 1.00 mmol), B_2Pin_2 (127 mg, 0.50 mmol), NEt_3 (87 μL, 0.63 mmol), and 1,2-dichloroethane (2.5 mL). Flash column chromatography (silica gel: 20% EtOAc in hexanes) afforded the title compound as a tan solid (161 mg, 0.39 mmol, 77% yield). mp 194-196 ºC; IR ν_{max}/cm^{-1} (film): 3051, 3012, 2924, 2852, 2236, 1601, 1582, 1467, 1254, 1203, 852; ^1H NMR (400 MHz, $CDCl_3$) δ: 8.96 (1H, s), 8.85 (1H, d, *J* = 4.9 Hz), 8.40 (1H, s), 8.15 (1H, s), 8.11 (2H, d, *J* = 7.3 Hz), 7.82 (1H, d, *J* = 4.4 Hz), 7.69 (2H, d, *J* = 8.6 Hz), 7.39-7.55 (5H, m); ^{13}C NMR (100 MHz, $CDCl_3$) δ: 158.7, 154.8, 151.1, 150.7, 150.5 (m), 144.7, 139.0, 137.0, 132.6, 130.5, 129.5, 128.9, 127.1, 123.3, 121.6, 120.4 (q, *J* = 258.5 Hz), 120.0, 119.2, 117.8, 116.1; ^{19}F NMR (365 MHz, $CDCl_3$) δ: –57.68; m/z LRMS (ESI + APCI) found $[M+H]^+$ 418.2, $C_{24}H_{15}F_3N_3O^+$ requires 418.1.

2'-Phenyl-5-(thiophen-3-yl)-[2,4'-bipyridine]-4-carbonitrile

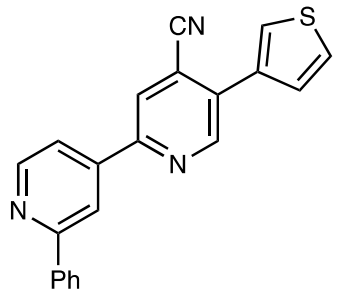

Prepared according to general procedure B using triphenyl(2-phenylpyridin-4-yl)phosphonium trifluoromethanesulfonate (283 mg, 0.50 mmol), 3-(thiophen-3-yl)isonicotinonitrile (186 mg, 1.00 mmol), B_2Pin_2 (127 mg, 0.50 mmol), NEt_3 (87 μL, 0.63 mmol), and 1,2-dichloroethane (2.5 mL). Flash column chromatography (silica gel: 20% EtOAc in hexanes, followed by silica gel, gradient elution: CH_2Cl_2 to 1% MeOH in CH_2Cl_2) afforded the title compound as a white solid (123 mg, 0.37 mmol, 73% yield). mp 195-197 ºC; IR ν_{max}/cm^{-1} (film): 3114, 3092, 3074, 2228, 1567, 1583, 1469, 1423, 1375, 1201, 782, 693, 526; ^1H NMR (400 MHz, $CDCl_3$) δ: 9.06 (1H, d, *J* = 0.7 Hz), 8.85 (1H, dd, *J* = 5.1, 0.6 Hz), 8.39 (1H, m), 8.12 (3H, m), 7.88 (1H, m), 7.81 (1H, dd, *J* = 5.1, 1.7 Hz), 7.43-7.57 (5H, m); ^{13}C NMR (100 MHz, $CDCl_3$) δ: 158.8, 153.8, 150.8, 150.8, 145.0, 139.1, 134.5, 133.0, 129.5, 129.0, 127.7, 127.2, 127.1, 126.3, 123.5, 119.2, 118.8, 117.8, 116.8; m/z LRMS (ESI + APCI) found $[M+H]^+$ 340.2, $C_{21}H_{14}N_3S^+$ requires 340.1.

6-Methyl-2''-phenyl-[3,3':6',4''-terpyridine]-4'-carbonitrile

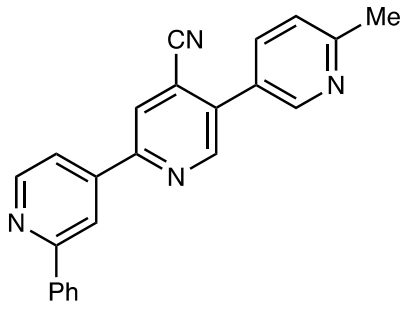

Prepared according to general procedure B using triphenyl(2-phenylpyridin-4-yl)phosphonium trifluoromethanesulfonate (170 mg, 0.30 mmol), 6'-methyl-[3,3'-bipyridine]-4-carbonitrile (118 mg, 0.60 mmol), B_2Pin_2 (76 mg, 0.30 mmol), NEt_3 (52 μL, 0.38 mmol), and 1,2-dichlorethane (1.5 mL). Flash column chromatography (silica gel: 60% EtOAc in hexanes, followed by recrystallization from CH_2Cl_2 and hexanes) afforded the title compound as a white solid (55 mg, 0.16 mmol, 52% yield). mp 209-211 ºC; IR ν_{max}/cm^{-1} (film): 3061, 3027, 2920, 2851, 2230, 1596, 1468, 1383, 1037, 840, 730, 687; ^{1}H NMR (400 MHz, $CDCl_3$) δ: 8.99 (1H, s), 8.87 (1H, d, *J* = 5.1 Hz), 8.77 (1H, d, *J* = 2.0 Hz), 8.42 (1H, s), 8.19 (1H, s) 8.11 (2H, d, *J* = 7.2 Hz), 7.92 (1H, dd, *J* = 8.0, 2.3 Hz) 7.84 (1H, dd, *J* = 5.1, 1.2 Hz), 7.44-7.56 (3H, m), 7.38 (1H, d, *J* = 8.0 Hz), 2.69 (3H, s); ^{13}C NMR (100 MHz, $CDCl_3$) δ: 160.4, 158.9, 155.1, 151.0, 150.8, 148.6, 144.8, 139.1, 136.5, 135.4, 129.6, 129.0, 127.3, 127.2, 123.6, 123.4, 120.3, 119.3, 117.9, 116.1, 24.6; m/z LRMS (ESI + APCI) found $[M+H]^+$ 349.2, $C_{23}H_{17}N_4^+$ requires 349.1.

3,5-Dimethyl-2'-phenyl-[2,4'-bipyridine]-4-carbonitrile

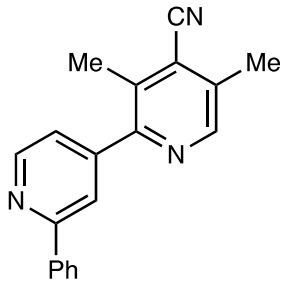

Prepared according to general procedure B (except used 4 equivalents of the cyanopyridine instead of 2 equivalents, 2 equivalents of B_2pin_2 instead of 1 equivalent, and ran the reaction for 48 hours instead of 36) using triphenyl(2-phenylpyridin-4-yl)phosphonium trifluoromethanesulfonate (170 mg, 0.30 mmol), 3,5-dimethylisonicotinonitrile (158 mg, 1.20 mmol), B_2Pin_2 (76 mg, 0.30 mmol), NEt_3 (52 μL, 0.38 mmol), and 1,2-dichloroethane (1.5 mL). Flash column chromatography by dissolving in CH_2Cl_2 and dry loading (silica gel, gradient elution: 20% EtOAc in hexanes to 25% EtOAc in hexanes, followed by recrystallization from CH_2Cl_2) afforded the title compound as a white solid (26 mg, 0.05 mmol, 18% yield). mp 156-158 ºC; IR ν_{max}/cm^{-1} (film): 3058, 2919, 2852, 2224, 1596, 1540, 1388, 1219, 765, 694, 530; ^1H NMR (400 MHz, $CDCl_3$) δ: 8.80 (1H, d, J = 4.9 Hz), 8.59 (1H, s), 8.05-8.00 (2H, m), 7.84 (1H, s), 7.51-7.40 (3H, m), 7.34 (1H, dd, J = 5.0, 1.6 Hz), 2.59 (6H, s); ^{13}C NMR (100 MHz, $CDCl_3$) δ: 158.0, 155.1, 149.9, 148.6, 147.5, 139.1, 135.4, 132.9, 129.3, 128.9, 127.1, 132.2, 122.0, 120.7, 115.0, 18.6, 17.8; m/z LRMS (ESI + APCI) found $[M+H]^+$ 286.2, $C_{19}H_{16}N_3^+$ requires 286.1.

Diethyl (2'-phenyl-[2,4'-bipyridin]-4-yl)phosphonate

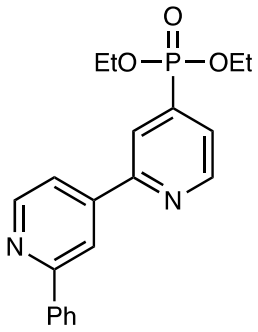

Prepared according to general procedure B (except 2 equivalents of B_2pin_2 and 4 equivalents of diethyl pyridin-4-ylphosphonate). Triphenyl(2-phenylpyridin-4-yl)phosphonium trifluoromethanesulfonate (141 mg, 0.25 mmol), diethyl pyridin-4-ylphosphonate (216 mg, 1.00 mmol), B_2Pin_2 (127 mg, 0.50 mmol), NEt_3 (44 μL, 0.31 mmol), and 1,2-dichloroethane (1.25 mL). Flash column chromatography (basic alumina: 60% EtOAc in hexanes) followed by a second flash column (silica gel: 75% EtOAc in hexanes) afforded the title compound as colorless oil (26 mg, 0.07 mmol, 28% yield; IR ν_{max}/cm^{-1} (film): 3052, 2981, 2926, 2852, 1589, 1256, 1047, 1010, 967, 776, 694, 558; ^1H NMR (400 MHz, $CDCl_3$) δ: 8.90 (1H, app t, *J* = 5.1 Hz), 8.82 (1H, d, *J* = 5.1), 8.41 (1H, s), 8.22 (1H, d, *J* = 14.1 Hz), 8.10 (2H, d, *J* = 7.3 Hz), 7.86 (1H, dd, *J* = 5.1, 1.3 Hz), 7.69 (1H, dd, *J* = 13.0, 4.7 Hz), 7.48 (3H, m), 4.22 (4H, m), 1.38 (6H, t, *J* = 7.1 Hz); ^{13}C NMR (100 MHz, $CDCl_3$) δ: 158.6, 155.6 (d, *J* = 15.8 Hz), 150.5, 150.5 (d, *J* = 13.1 Hz), 146.4 (d, *J* = 2.2 Hz), 139.3, 139.1 (d, *J* = 185.9), 129.3, 128.9, 127.2, 125.3 (d, *J* = 7.9 Hz), 122.7 (d, *J* = 9.3 Hz), 119.6, 118.2, 63.1 (d, *J* = 5.8 Hz), 16.5 (d, *J* = 6.3 Hz); ^{31}P NMR (162 MHz, $CDCl_3$) δ: 14.38; m/z LRMS (ESI + APCI) found $[M+H]^+$ 369.2, $C_{20}H_{22}N_2O_3P^+$ requires 369.1.

Ethyl 2'-phenyl-[2,4'-bipyridine]-4-carboxylate

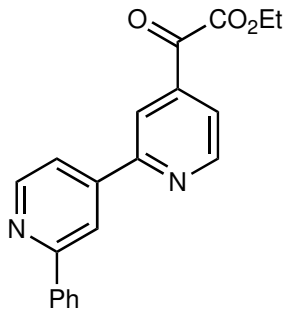

Prepared according to general procedure B using triphenyl(2-phenylpyridin-4-yl)phosphonium trifluoromethanesulfonate (226 mg, 0.40 mmol), ethyl isonicotinate (120 μL, 0.80 mmol), B_2pin_2 (102 mg, 0.40 mmol), NEt_3 (70 μL, 0.50 mmol), and 1,2-dichloroethane (2.0 mL). Crude ^1H NMR spectrum of reaction suggests that the product was made in ca. 12% yield (8.81 ppm, 1H, d, J = 5.2 Hz).

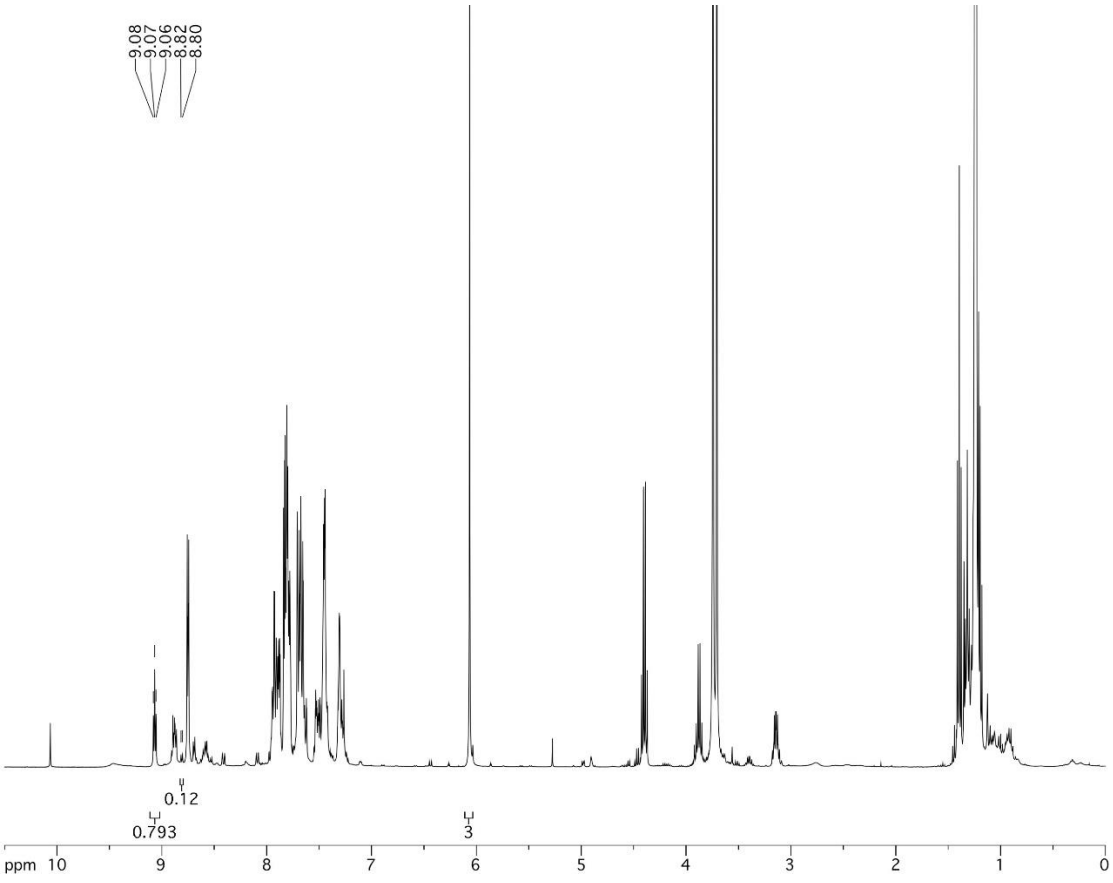

Ethyl 4-(2-(4-chlorophenyl)-2-(4-cyano-5-cyclobutyl-[2,4'-bipyridin]-2'-yl)ethyl)piperidine-1-carboxylate

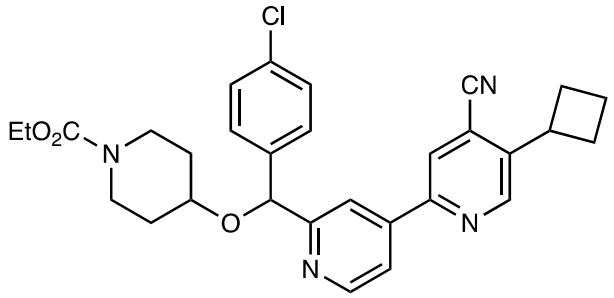

Prepared according to general procedure B using (2-((4-chlorophenyl)((1-(ethoxycarbonyl)piperidin-4-yl)oxy)methyl)pyridin-4-yl)triphenylphosphonium trifluoromethanesulfonate (196 mg, 0.25 mmol), 3-cyclobutylisonicotinonitrile (79 mg, 0.50 mmol), B_2Pin_2 (64 mg, 0.25 mmol), NEt_3 (44 μL, 0.31 mmol), and 1,2-dichloroethane (1.25 mL). Flash column chromatography (silica gel: 80% Et_2O in hexanes, then silica gel: 65% EtOAc in hexanes, then recrystallized from CH_2Cl_2 and hexanes) afforded the title compound as a colorless oil (37 mg, 0.07 mmol, 28% yield). IR ν_{max}/cm^{-1} (film): 2979, 2944, 2866, 2233, 1689, 1600, 1590, 1488, 1433, 1227, 1085, 728; ^1H NMR (400 MHz, $CDCl_3$) δ: 8.87 (1H, s), 8.63, (1H, d, *J* = 5.0 Hz), 8.08 (1H, s), 7.89 (1H, s), 7.74 (1H, m), 7.42 (2H, *J* = 7.4 Hz), 7.29 (2H, d, *J* = 7.6 Hz), 5.70 (1H, s), 4.11 (2H, q, *J* = 7.0 Hz), 3.62-3.96 (4H, m), 3.10-3.24 (2H, m), 2.53-2.64 (2H, m), 2.34 (2H, qn, *J* = 9.6 Hz), 2.18 (1H, sext, *J* = 9.5 Hz), 1.93-2.04 (1H, m), 1.78-193 (2H, m), 1.59-1.78 (2H, m), 1.24 (3H, t, *J* = 6.9 Hz); ^{13}C NMR (100 MHz, $CDCl_3$) δ: 163.2, 155.6, 153.2, 150.0, 149.6, 145.7, 142.7, 140.0, 133.7, 128.8, 128.3, 122.6, 120.2, 119.8, 117.7, 115.9, 81.1, 73.0, 61.4, 41.3 (rot), 41.2, 36.8, 31.3 (rot), 31.2, 29.0, 18.7, 14.8; m/z LRMS (ESI + APCI) found $[M+H]^+$ 531.3, $C_{30}H_{32}ClN_4O_3^+$ requires 531.2.

2'-(Bis(3-(trifluoromethyl)phenyl)methyl)-5-(thiophen-3-yl)-[2,4'-bipyridine]-4-carbonitrile

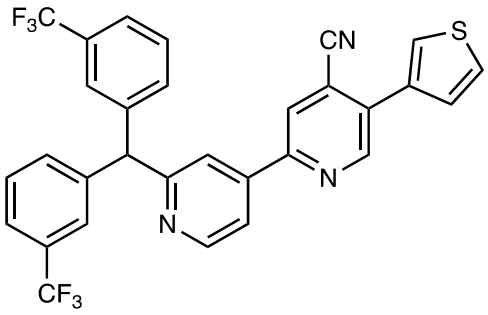

Prepared according to general procedure B using 2-(bis(3-(trifluoromethyl)phenyl)methyl)-4-(triphenyl-l4-phosphaneyl)pyridine trifluoromethanesulfonate (119 mg, 0.15 mmol), 3-(thiophen-3-yl)isonicotinonitrile (56 mg, 0.30 mmol), B_2Pin_2 (38 mg, 0.15 mmol), NEt_3 (26 μL, 0.19 mmol), and 1,2-dichloroethane (0.75 mL). Flash column chromatography (silica gel: 2% Et_2O in toluene) afforded the title compound as a white solid (72 mg, 0.13 mmol, 85% yield). mp 131-133 ºC; IR ν_{max}/cm^{-1} (film): 3059, 2924, 2852, 2232, 1596, 1528, 1469, 1449, 1320, 1159, 1118, 1074, 790, 700, 532; ^1H NMR (400 MHz, $CDCl_3$) δ: 9.02 (1H, s), 8.80 (1H, d, *J* = 5.1 Hz), 8.01 (1H, s), 7.86 (2H, m), 7.80 (1H, dd, *J* = 5.1, 1.6 Hz), 7.40-7.58 (10H, m), 5.84 (1H, s); ^{13}C NMR (100 MHz, $CDCl_3$) δ: 162.5, 153.3, 151.1, 150.8, 145.2, 142.8, 134.4, 133.1, 132.8, 131.1 (q, *J* = 32.3 Hz), 129.3, 127.7, 127.1, 126.4, 126.1 (q, *J* = 3.9 Hz), 124.2 (q, *J* = 272.7 Hz), 124.1 (q, *J* = 3.9 Hz), 123.6, 121.0, 119.3, 118.8, 116.7, 58.9; ^{19}F NMR (365 MHz, $CDCl_3$) δ: –62.54; *m/z* LRMS (ESI + APCI) found $[M+H]^+$ 566.2, $C_{30}H_{18}F_6N_3S^+$ requires 566.1.

5'-(allyloxy)-2'-methyl-[2,4'-bipyridine]-4-carbonitrile

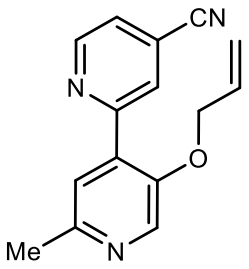

Prepared according to general procedure B using (5-(allyloxy)-2-methylpyridin-4-yl)triphenylphosphonium trifluoromethanesulfonate (280 mg, 0.50 mmol), isonicotinonitrile (104 mg, 1.00 mmol), B_2Pin_2 (127 mg, 0.50 mmol), NEt_3 (87 μL, 1.25 mmol), and 1,2-dichloroethane (2.5 mL). Flash column chromatography (silica gel: 25% EtOAc in hexanes) afforded the title compound as a yellow solid (40.1 mg, 0.16 mmol, 32% yield). mp 157-160 ºC; IR ν_{max}/cm^{-1} (film): 3071, 3032, 2922, 2851, 2238, 1599, 1540, 1423, 1400, 1354, 1282, 1195, 894, 856, 786; ^{1}H NMR (400 MHz, $CDCl_3$) δ: 12.98 (1H, s), 8.77 (1H, dd, *J* = 5.2, 1.0 Hz), 8.22 (1H, t, *J* = 1.2 Hz), 7.58 (1H, dd, *J* = 5.2, 1.4 Hz), 7.26 (1H, s), 6.15 (1H, ddt, *J* = 16.8, 10.1, 6.6 Hz), 5.19 (1H, dq, *J* = 17.2, 1.7 Hz), 5.10 (1H, dq, *J* = 10.1, 1.6 Hz), 3.72 (2H, dt, *J* = 6.6, 1.6 Hz), 2.56 (3H, s). ^{13}C NMR (100 MHz, $CDCl_3$) δ: 157.60, 151.14, 149.98, 147.56, 147.22, 134.94, 123.77, 122.61, 122.19, 121.96, 116.15, 115.91, 115.65, 37.28, 23.46; *m/z* LRMS (ESI + APCI) found $[M+H]^+$ 252.2, $C_{15}H_{14}N_3O^+$ requires 252.1.

2'-methyl-5'-(2-oxopropoxy)-[2,4'-bipyridine]-4-carbonitrile

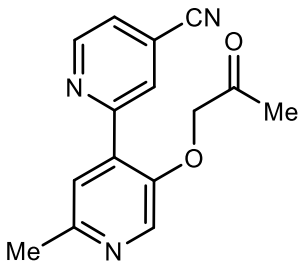

Prepared according to general procedure B using 1-((6-methyl-4-(triphenyl-l4-phosphaneyl)pyridin-3-yl)oxy)propan-2-one trifluoromethanesulfonate (287 mg, 0.50 mmol), isonicotinonitrile (105 mg, 1.00 mmol), B_2Pin_2 (127 mg, 0.50 mmol), NEt_3 (87 μL, 1.25 mmol), and 1,2-dichloroethane (2.5 mL). Flash column chromatography (silica gel: 85% EtOAc in hexanes) afforded the title compound as a tan solid (52 mg, 0.19 mmol, 39% yield). mp 142-148 ºC; IR ν_{max}/cm^{-1} (film): 3448, 3043, 2922, 2900, 2234, 1732, 1591, 1492, 1255, 1178, 1080, 1043, 865, 644; ^{1}H NMR (400 MHz, $CDCl_3$) δ: 8.90 (1H, d, *J* = 4.9 Hz), 8.45 (1H, s), 8.17 (1H, s), 7.73 (1H, s), 7.53 (1H, d, *J* = 4.9H z), 4.80 (2H, s), 2.58 (3H, s), 2.26 (3H, s); ^{13}C NMR (100 MHz, $CDCl_3$) δ: 202.4, 154.5, 152.9, 150.7, 149.5, 134.8, 134.3, 127.5, 124.5, 124.0, 120.9, 116.6, 73.7, 26.5, 23.7; *m/z* LRMS (ESI + APCI) found $[M+H]^+$ 268.1, $C_{15}H_{14}N_3O_2^+$ requires 268.1.

A1.15. References

S1. Connelly, N. G.; Geiger, W. E. Chemical Redox Agents for Organometallic Chemistry. *Chem. Rev.* **1996**, 96, 877-910.

S2. (a) Becke, A. D. Density-functional thermochemistry. V. Systematic Optimization of Exchange-Correlation Functionals. *J. Chem. Phys*. **1997**, *107*, 8554–8560. (b) Chai, J.-D.; Head-Gordon, M. Long-Range Corrected Hybrid Density Functionals with Damped Atom–Atom Dispersion Corrections. *Phys. Chem. Chem. Phys*. **2008**, *10*, 6615–6620.

S3. (a) Weigend, F.; Ahlrichs, R. Balanced Basis Sets of Split Valence, Triple Zeta Valence and Quadruple Zeta Valence Quality for H to Rn: Design and Assessment of Accuracy. *Phys. Chem. Chem. Phys.* **2005**, *7*, 3297−3305. (b) Weigend, F. Accurate Coulomb-Fitting Basis Sets for H to Rn. *Phys. Chem. Chem. Phys.* **2006**, *8*, 1057−1065.

S4. Grimme, S. Supramolecular Binding Thermodynamics by Dispersion-corrected Density Functional Theory. *Chem. Eur. J*. **2012**, *18*, 9955–9964.

S5. R. Sure, R.; S. Grimme, S. Comprehensive Benchmark of Association (Free) Energies of Realistic Host–Guest Complexes. *J. Chem. Theory Comput.* **2015**, *11*, 3785–3801.

S6. GoodVibes, version 3.0.0, Luchini, G.; Alegre-Requena J. V.; Guan, Y.; Funes-Ardoiz, I.; Paton, R. S. 2019, http://doi.org/10.5281/zenodo.595246

S7. (a) Cancès, E.; Mennucci, B.; Tomasi, J. A New Integral Equation Formalism for the Polarizable Continuum Model: Theoretical Background and Applications to Isotropic and Anisotropic Dielectrics. *J. Chem. Phys.* **1997**, *107*, 3032–3041. (b) Mennucci, B.; Cancès, E.; Tomasi, J. Evaluation of Solvent Effects in Isotropic and Anisotropic Dielectrics and in Ionic Solutions with a Unified Integral Equation Method: Theoretical Bases, Computational Implementation, and Numerical Applications. *J. Phys. Chem. B.* **1997**, *101*, 10506–10517. (c) Mennucci, B.; Tomasi, J. Continuum Solvation Models: A New Approach to the Problem of Solute's Charge Distribution and Cavity Boundaries. *J. Chem. Phys.* **1997**, *106*, 5151–5158. (d) Tomasi, J.; Mennucci, T. B.; Cancès, E. The IEF Version of the PCM Solvation Method: An Overview of a New Method Addressed to Study Molecular Solutes at the QM Ab Initio Level. *J. Mol. Struct. THEOCHEM* **1999**, *464*, 211–226. (e) Scalmani, G.; Frisch, M. J. Continuous Surface Charge Polarizable Continuum Models of Solvation. I. General formalism. *J. Chem. Phys.* **2010**, *132*, 114110. (f) Marenich, A. V.; Cramer, C. J.; Truhlar, D. G. Universal Solvation Model Based on Solute Electron Density and on a Continuum Model of the Solvent Defined by the Bulk Dielectric Constant and Atomic Surface Tensions. *J. Phys. Chem. B.* **2009**, *113*, 6378–6396.

S8. Gaussian 16, Revision B.01, Frisch, M. J.; Trucks, G. W.; Schlegel, H. B.; Scuseria, G. E.; Robb, M. A.; Cheeseman, J. R.; Scalmani, G.; Barone, V.; Petersson, G. A.; Nakatsuji, H.; Li, X.; Caricato, M.; Marenich, A. V.; Bloino, J.; Janesko, B. G.; Gomperts, R.; Mennucci, B.; Hratchian, H. P.; Ortiz, J. V.; Izmaylov, A. F.; Sonnenberg, J. L.; Williams-Young, D.; Ding, F.; Lipparini, F.; Egidi, F.; Goings, J.; Peng, B.; Petrone, A.; Henderson, T.; Ranasinghe, D.; Zakrzewski, V. G.; Gao, J.; Rega, N.; Zheng, G.; Liang, W.; Hada, M.; Ehara, M.; Toyota, K.; Fukuda, R.; Hasegawa, J.; Ishida, M.; Nakajima, T.; Honda, Y.; Kitao, O.; Nakai, H.; Vreven, T.; Throssell, K.; Montgomery, Jr., J. A.; Peralta, J. E.; Ogliaro, F.; Bearpark, M. J.; Heyd, J. J.;

Brothers, E. N.; Kudin, K. N.; Staroverov, V. N.; Keith, T. A.; Kobayashi, R.; Normand, J.; Raghavachari, K.; Rendell, A. P.; Burant, J. C.; Iyengar, S. S.; Tomasi, J.; Cossi, M.; Millam, J. M.; Klene, M.; Adamo, C.; Cammi, R.; Ochterski, J. W.; Martin, R. L.; Morokuma, K.; Farkas, O.; Foresman, J. B.; Fox, D. J. Gaussian, Inc., Wallingford CT, 2016.

S9. The PyMOL Molecular Graphics System, version 2.0.7, Schrödinger, LLC.

S10. https://gist.github.com/bobbypaton (accessed 13 April 2018).

S11. Yu, X.; Tang, *J*.; *J*in, X.; Yamamoto, Y.; Bao, M. Manganese-Catalyzed C−H Cyanation of Arenes with N -Cyano- N-(4-Methoxy)Phenyl- p -Toluenesulfonamide. *Asian J. Org. Chem.* **2018**, 7, 550-553.

S12. Kim, K. D.; Lee, *J*. H. Visible-Light Photocatalyzed Deoxygenation of N-Heterocyclic N -Oxides. *Org. Lett.* **2018**, 20, 7712-7716.

S13. Kitamura, Y.; Sako, S.; Tsutsui, A.; Monguchi, Y.; Maegawa, T.; Kitade, Y.; Sa*J*iki, H. Ligand-Free and Heterogeneous Palladium on Carbon-Catalyzed Hetero-Suzuki-Miyaura Cross-Coupling. *Adv. Synth. Catal.* **2010**, 352, 718-730.

S14. Shields, B. *J*.; Doyle, A. G. Direct C(sp3)–H Cross Coupling Enabled by Catalytic Generation of Chlorine Radicals. *J. Am. Chem. Soc.* **2016**, 138, 12719-12722.

S15. Cumpstey, N.; Bera, R. N.; Burn, P. L.; Samuel, I. D. W. Investigating the Effect of Steric Crowding in Phosphorescent Dendrimers. *Macromolecules* **2005**, 38, 9564-9570.

S16. Galloway, *J*. D.; Mai, D. N.; Baxter, R. D. Silver-Catalyzed Minisci Reactions Using Selectfluor as a Mild Oxidant. *Org. Lett.* **2017**, 19, 5772-5775.

S17. Ayyappan, P.; Evans, O. R.; Foxman, B. M.; Wheeler, K. A.; Warren, T. H.; Lin, W. New Open Frameworks Based on Metal Pyridylphosphonates. *Inorg. Chem.* **2001**, 40, 5954-5961.

S18. Neumann, T.; Bena*J*iba, L.; Göring, S.; Stegmaier, K.; Schmidt, B. Evaluation of Improved Glycogen Synthase Kinase-3α Inhibitors in Models of Acute Myeloid Leukemia. *J. Med. Chem.* **2015**, *58*, 8907-8919.

S19. Hilton, M.; Dolewski, R.; McNally, A. Selective Functionalization of Pyridines via Heterocyclic Phosphonium Salts. *J. Am. Chem. Soc.* **2016**, 138, pp 13806-13809.

S20. Patel, C.; Mohnike, M.; Hilton, M. C.; McNally, A. A Strategy to Aminate Pyridines, Diazines, and Pharmaceuticals via Heterocyclic Phosphonium Salts. *Org. Lett.* **2018**, *20*, 2607-2610.

S21. Koniarczyk, *J*. L.; Hesk, D.; Overgard, A.; Davies, I. W.; McNally, A. A General Strategy for Site-Selective Incorporation of Deuterium and Tritium into Pyridines, Diazines, and Pharmaceuticals. *J. Am. Chem. Soc.* **2018**, *140*, 1990–1993.

S22. Zhang, X.; McNally, A. Phosphonium Salts as Pseudohalides: Regioselective Nickel-Catalyzed Cross-Coupling of Complex Pyridines and Diazines. *Angew. Chem. Int. Ed.* **2017**, *56*, 9833-9836.

A1.15. Spectra

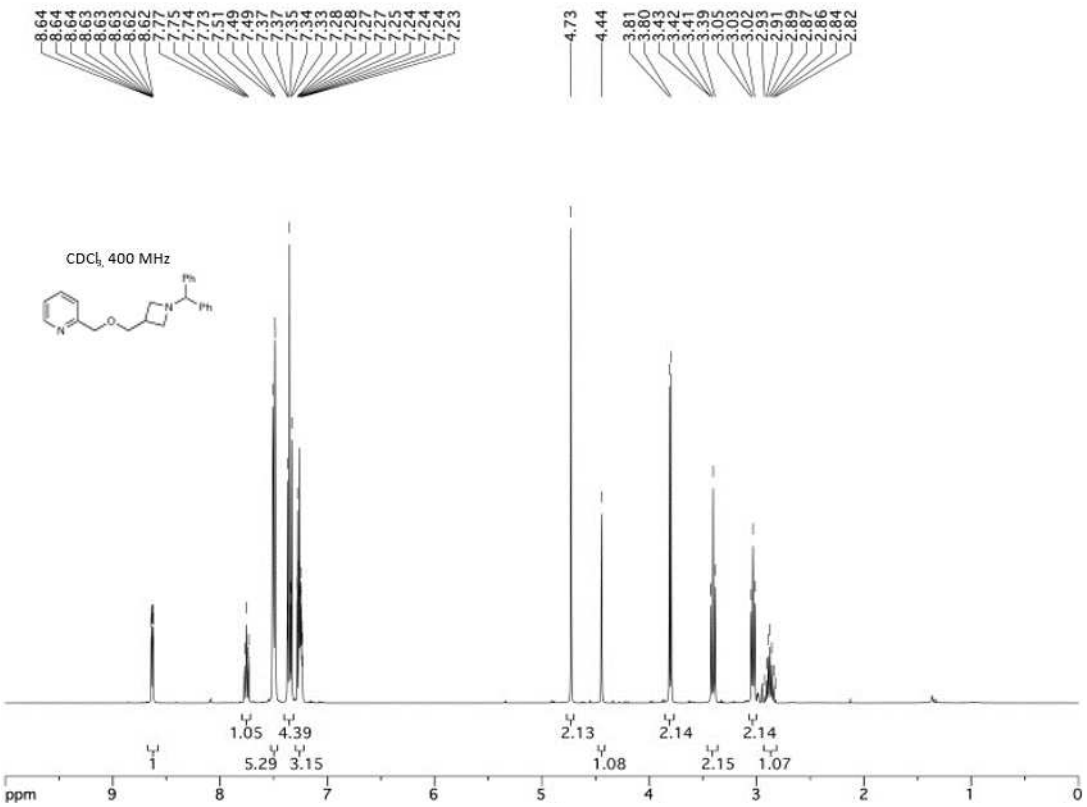

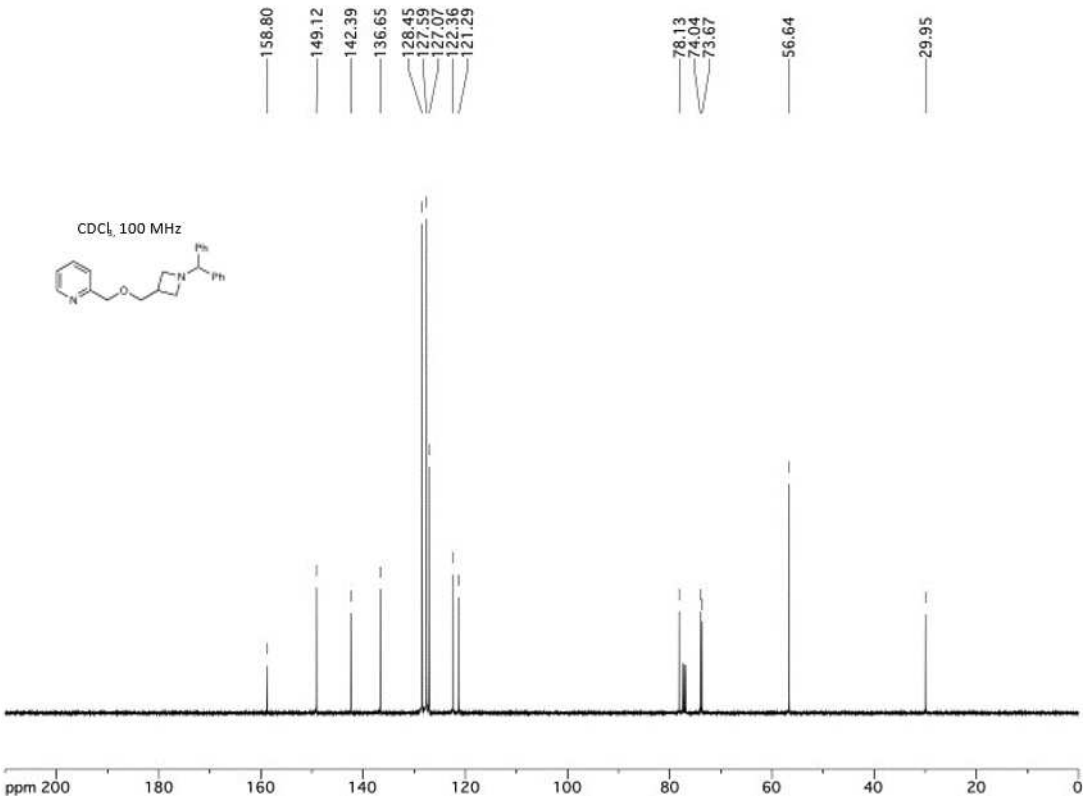

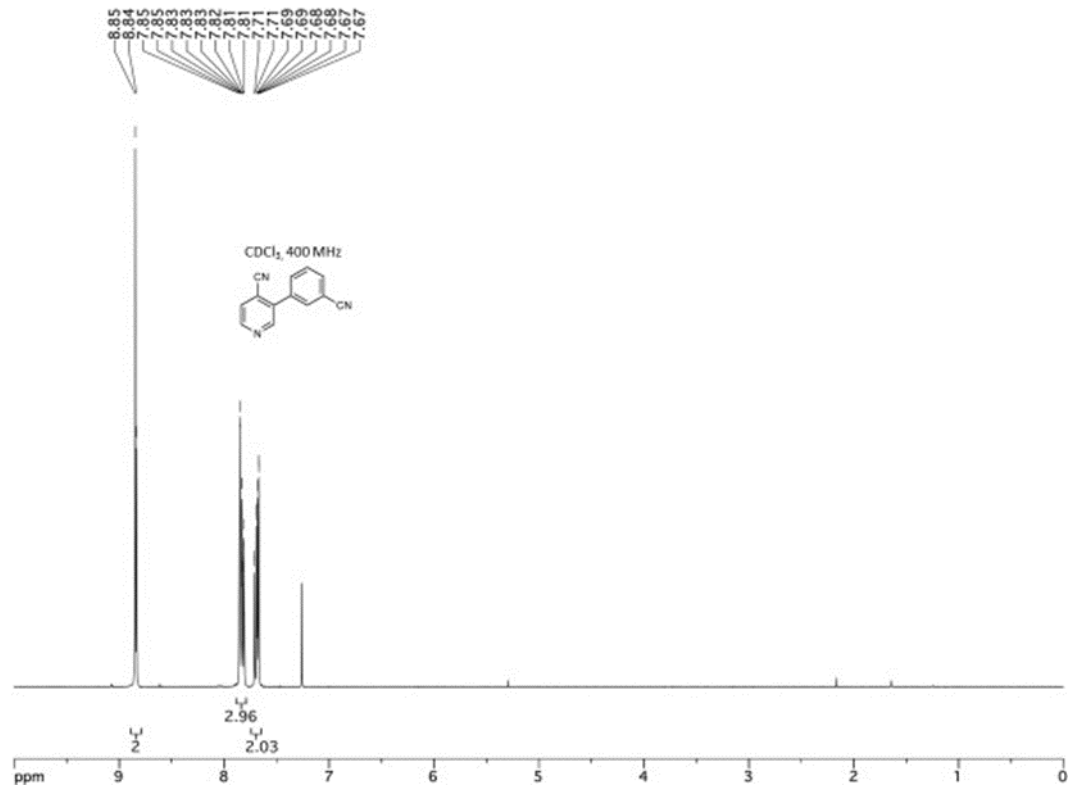
8.85
8.84
7.85
7.85
7.83
7.83
7.82
7.81
7.81
7.71
7.71
7.69
7.69
7.68
7.68
7.67
7.67
CDCl3, 400 MHz
CN
CN
N
2.96
2.03
2
ppm
9
8
7
6
5
4
3
2
1
0

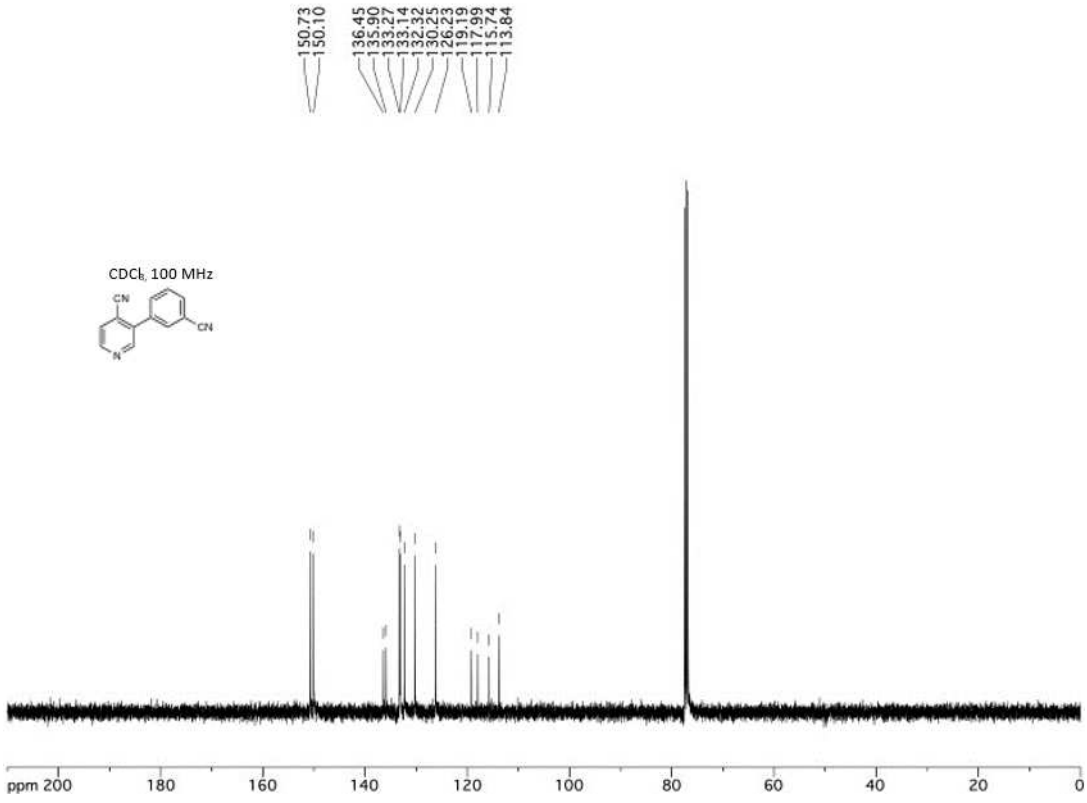
150.73
150.10
136.45
135.90
133.27
133.14
132.32
130.25
126.23
119.19
117.99
115.74
113.84
CDCl3, 100 MHz
CN
CN
N
ppm 200
180
160
140
120
100
80
60
40
20
0

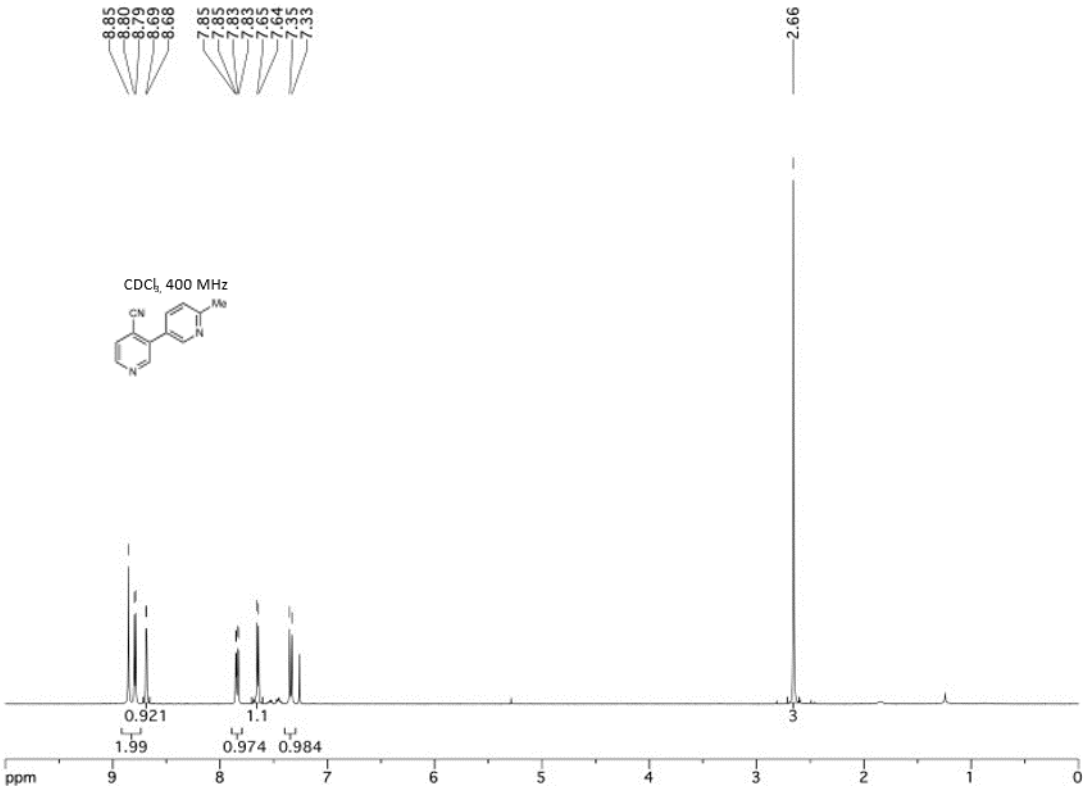
8.85
8.80
8.79
8.69
8.68
7.85
7.85
7.83
7.83
7.65
7.64
7.35
7.33
2.66
CDCl3 400 MHz
CN
Me
N
N
0.921
1.99
1.1
0.974
0.984
3
ppm
9
8
7
6
5
4
3
2
1
0

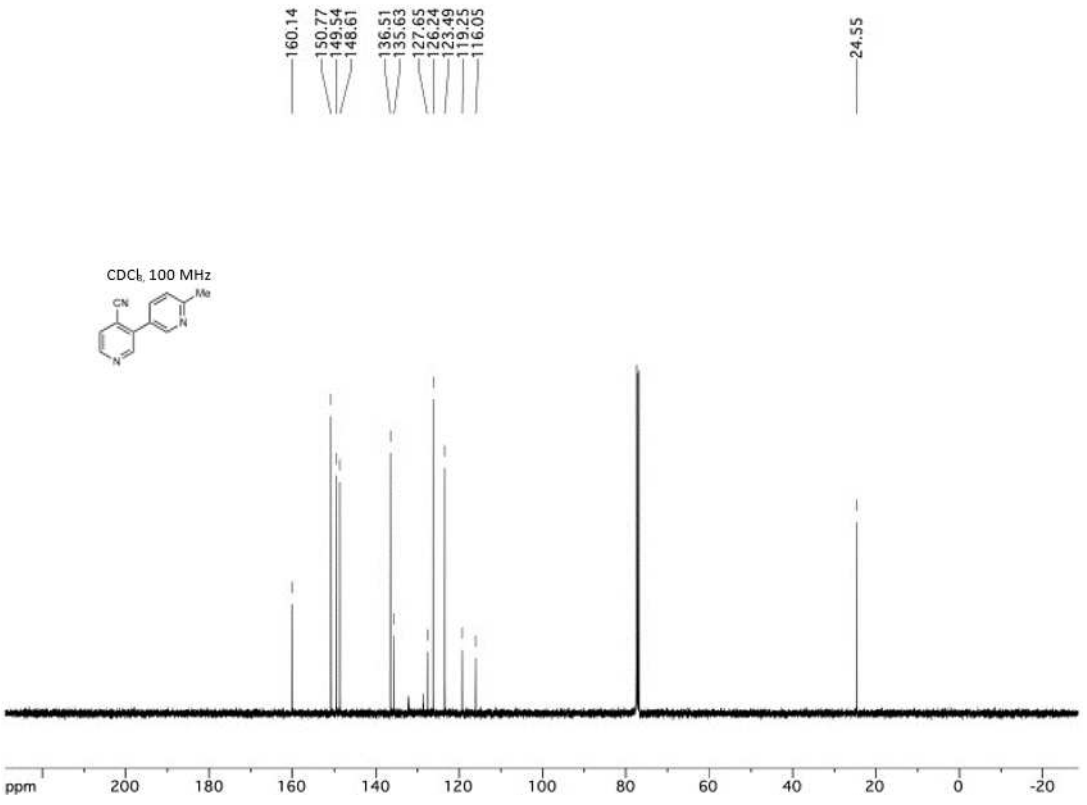
160.14
150.77
149.54
148.61
136.51
135.63
127.65
126.24
123.49
119.25
116.05
24.55
CDCl3 100 MHz
CN
Me
N
N
ppm
200
180
160
140
120
100
80
60
40
20
0
-20

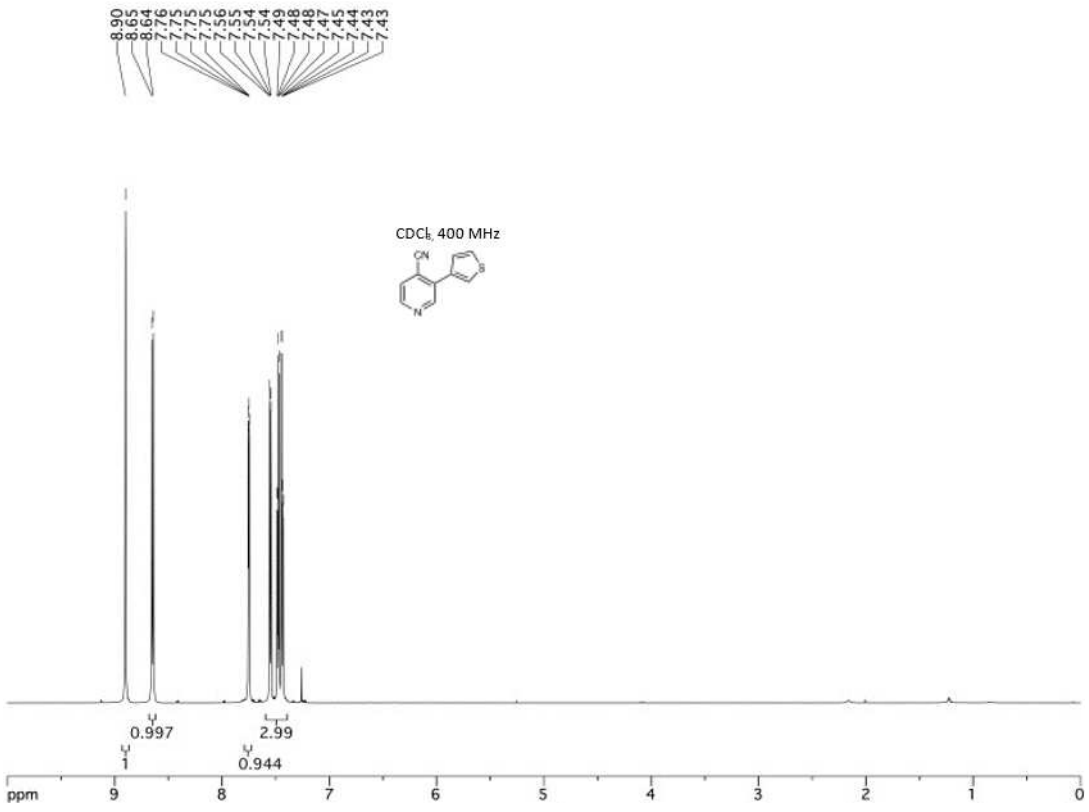
8.90
8.65
8.64
7.76
7.75
7.75
7.75
7.56
7.55
7.54
7.54
7.49
7.48
7.48
7.47
7.45
7.44
7.43
7.43
CDCl3, 400 MHz
CN
S
N
0.997
2.99
1
0.944
ppm
9
8
7
6
5
4
3
2
1
0

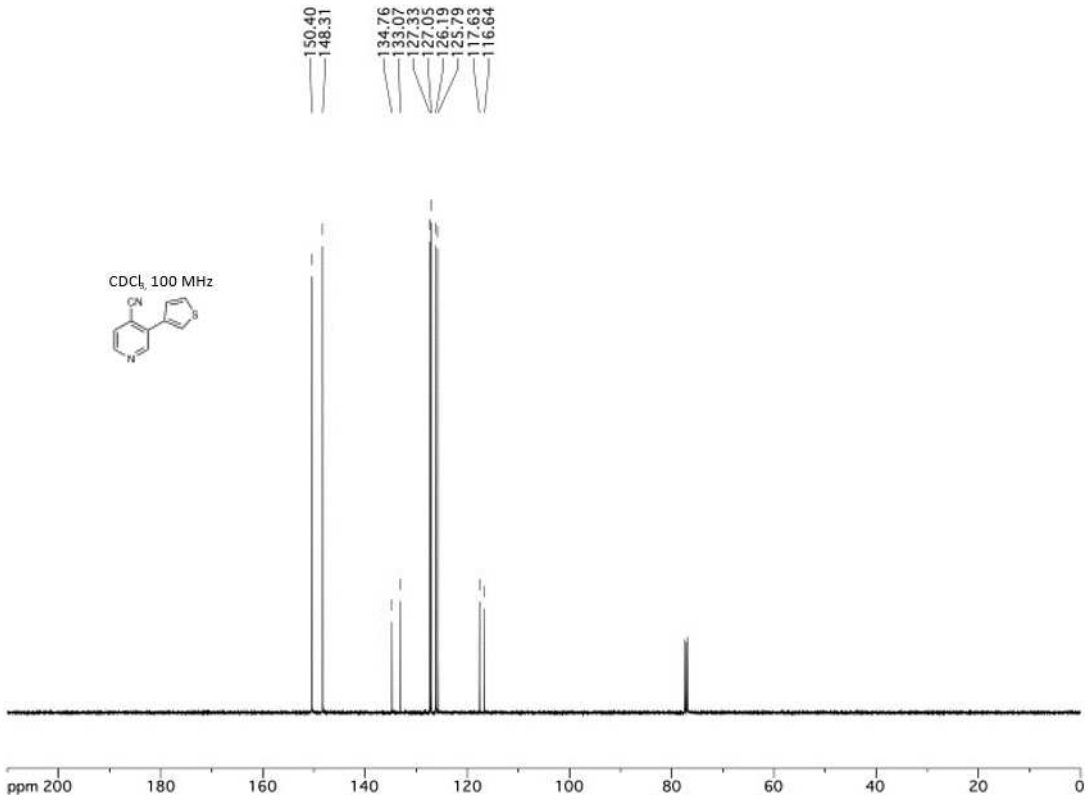
150.40
148.31
134.76
133.07
127.33
127.05
126.19
125.79
117.63
116.64
CDCl3, 100 MHz
CN
S
N
ppm 200
180
160
140
120
100
80
60
40
20
0

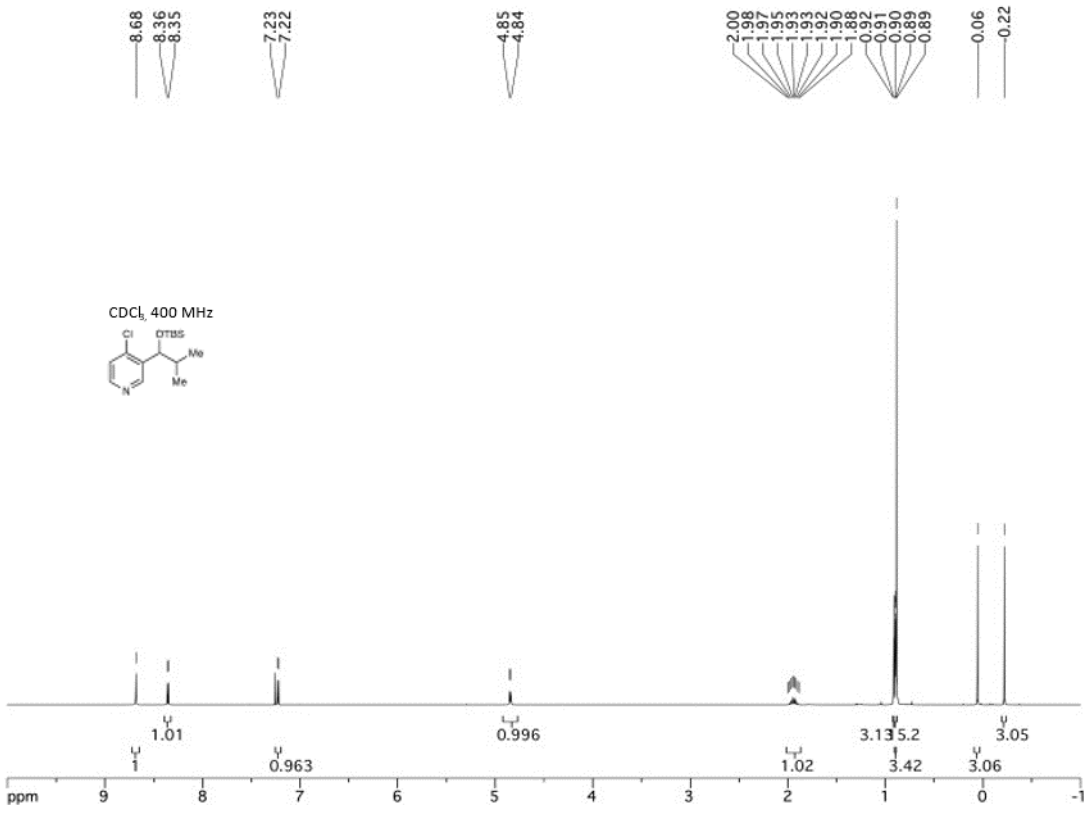
8.68
8.36
8.35
7.23
7.22
4.85
4.84
2.00
1.98
1.97
1.95
1.93
1.93
1.92
1.90
1.88
0.92
0.91
0.90
0.89
0.89
0.06
0.22
CDCl3 400 MHz
Cl
OTBS
Me
Me
N
1.01
0.996
3.13
5.2
3.05
1
0.963
1.02
3.42
3.06
ppm
9
8
7
6
5
4
3
2
1
0
-1

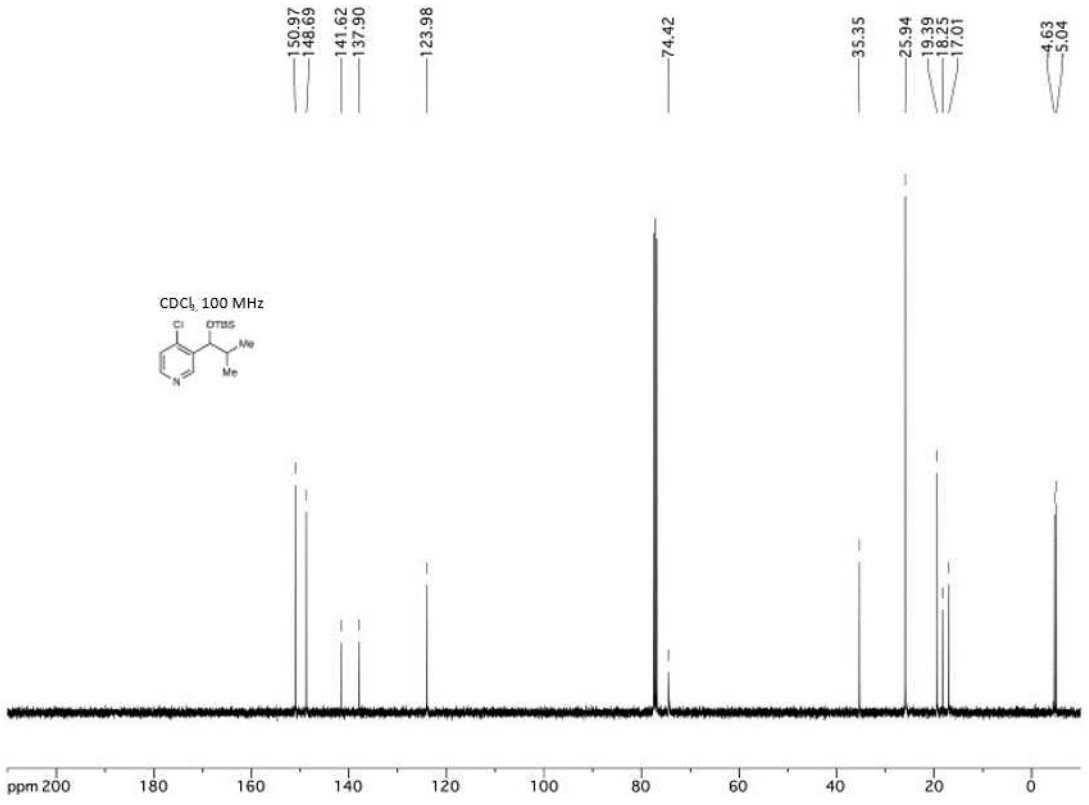
150.97
148.69
141.62
137.90
123.98
74.42
35.35
25.94
19.39
18.25
17.01
4.63
5.04
CDCl3 100 MHz
Cl
OTBS
Me
Me
N
ppm 200
180
160
140
120
100
80
60
40
20
0

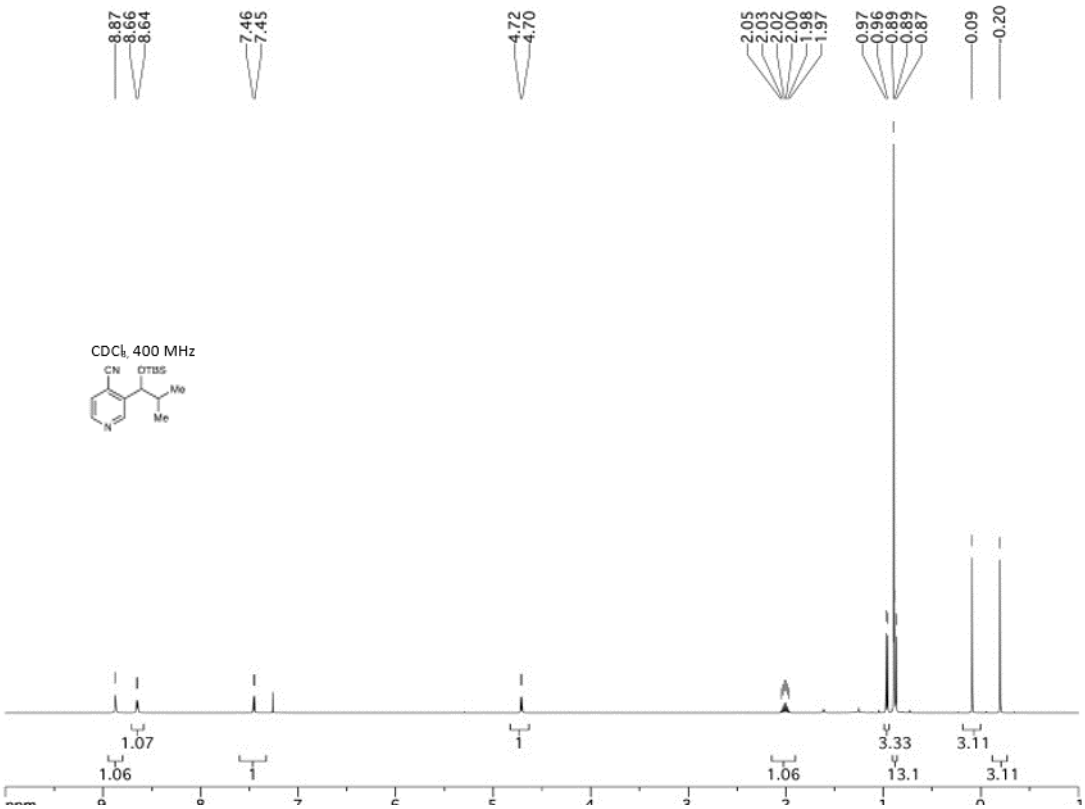
8.87
8.66
8.64
7.46
7.45
4.72
4.70
2.05
2.03
2.02
2.00
1.98
1.97
0.97
0.96
0.89
0.89
0.87
0.09
0.20
CDCl3, 400 MHz
CN
OTBS
Me
Me
1.07
1
3.33
3.11
1.06
1
1.06
13.1
3.11

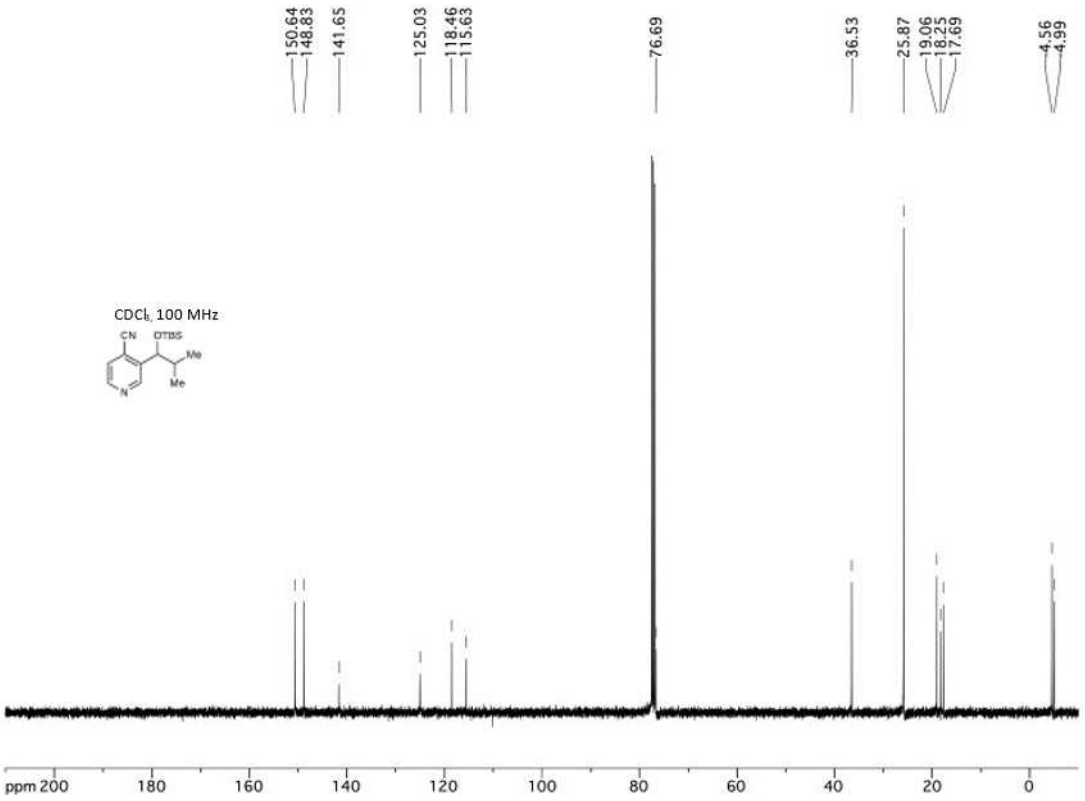
150.64
148.83
141.65
125.03
118.46
115.63
76.69
36.53
25.87
19.06
18.25
17.69
4.56
4.99
CDCl3, 100 MHz
CN
OTBS
Me
Me
ppm 200
180
160
140
120
100
80
60
40
20
0

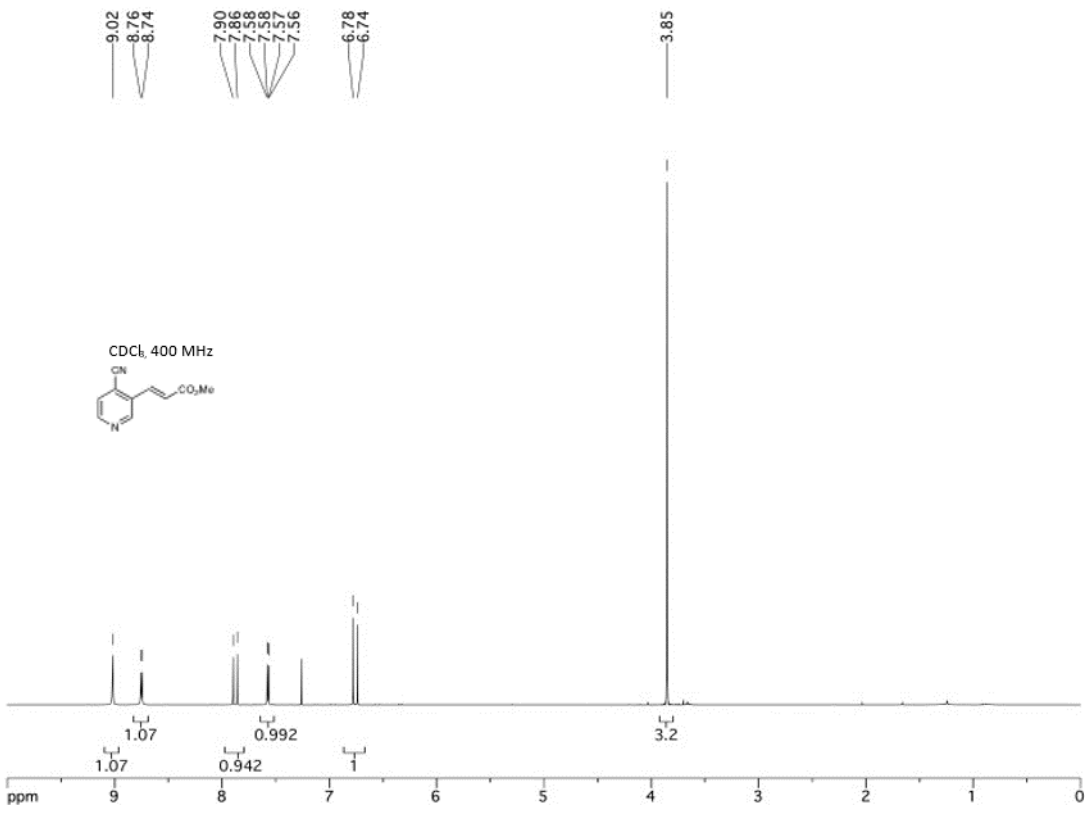
9.02
8.76
8.74
7.90
7.86
7.58
7.58
7.57
7.56
6.78
6.74
3.85
CDCl3 400 MHz
CN
CO2Me
N
1.07
0.992
3.2
1.07
0.942
1
ppm
9
8
7
6
5
4
3
2
1
0

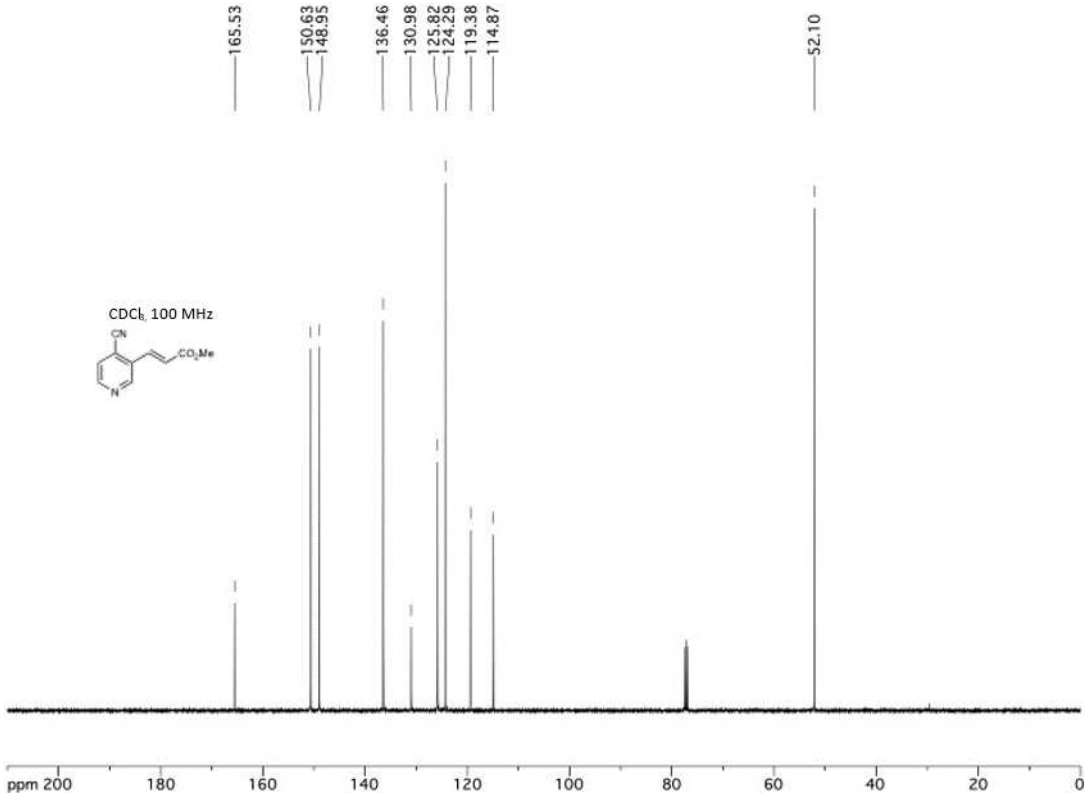
165.53
150.63
148.95
136.46
130.98
125.82
124.29
119.38
114.87
52.10
CDCl3 100 MHz
CN
CO2Me
N
ppm 200
180
160
140
120
100
80
60
40
20
0

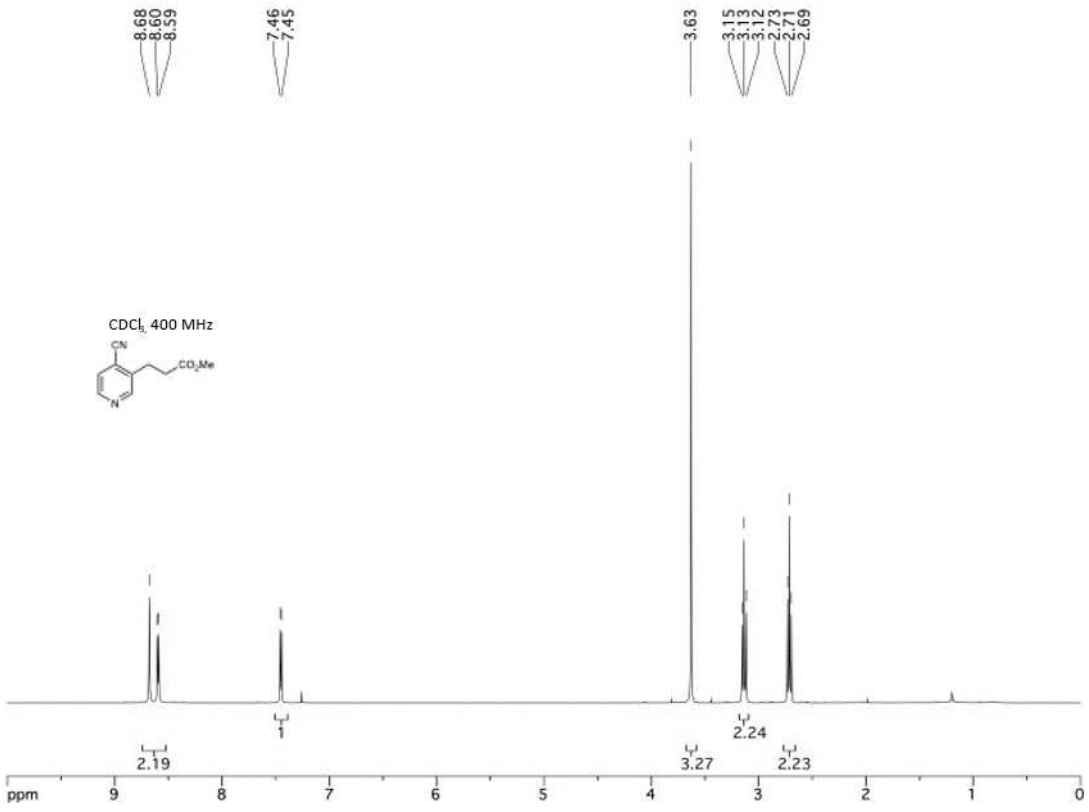
8.68
8.60
8.59
7.46
7.45
3.63
3.15
3.13
3.12
2.73
2.71
2.69
CDCl3 400 MHz
CN
CO2Me
N
2.19
1
2.24
3.27
2.23
ppm
9
8
7
6
5
4
3
2
1
0

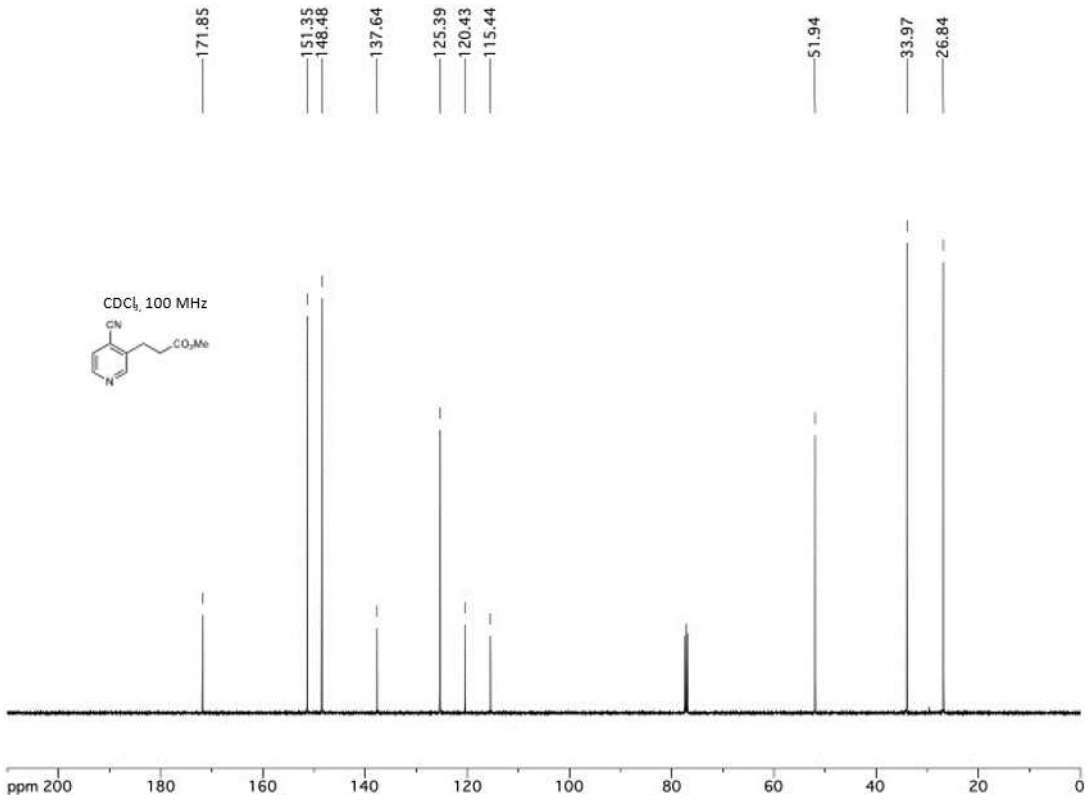
171.85
151.35
148.48
137.64
125.39
120.43
115.44
51.94
33.97
26.84
CDCl3 100 MHz
CN
CO2Me
N
ppm 200
180
160
140
120
100
80
60
40
20
0

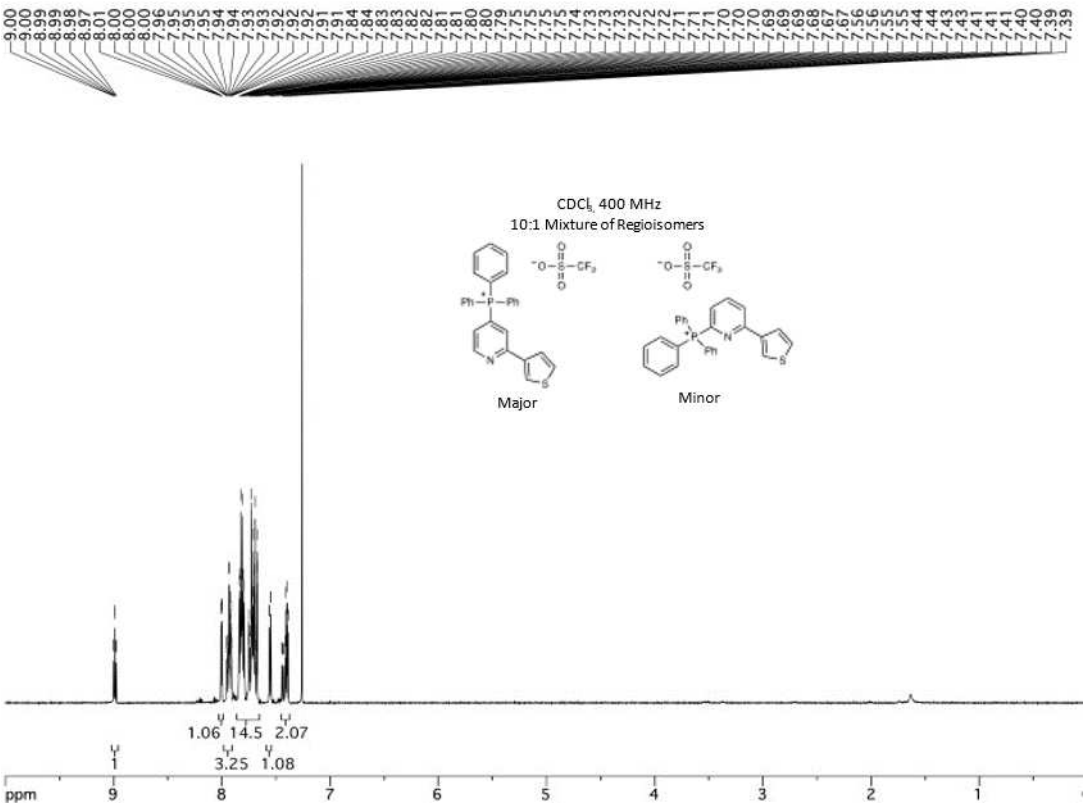
CDCl3 400 MHz
10:1 Mixture of Regioisomers
Major
Minor
1.06 14.5 2.07
1 3.25 1.08
ppm

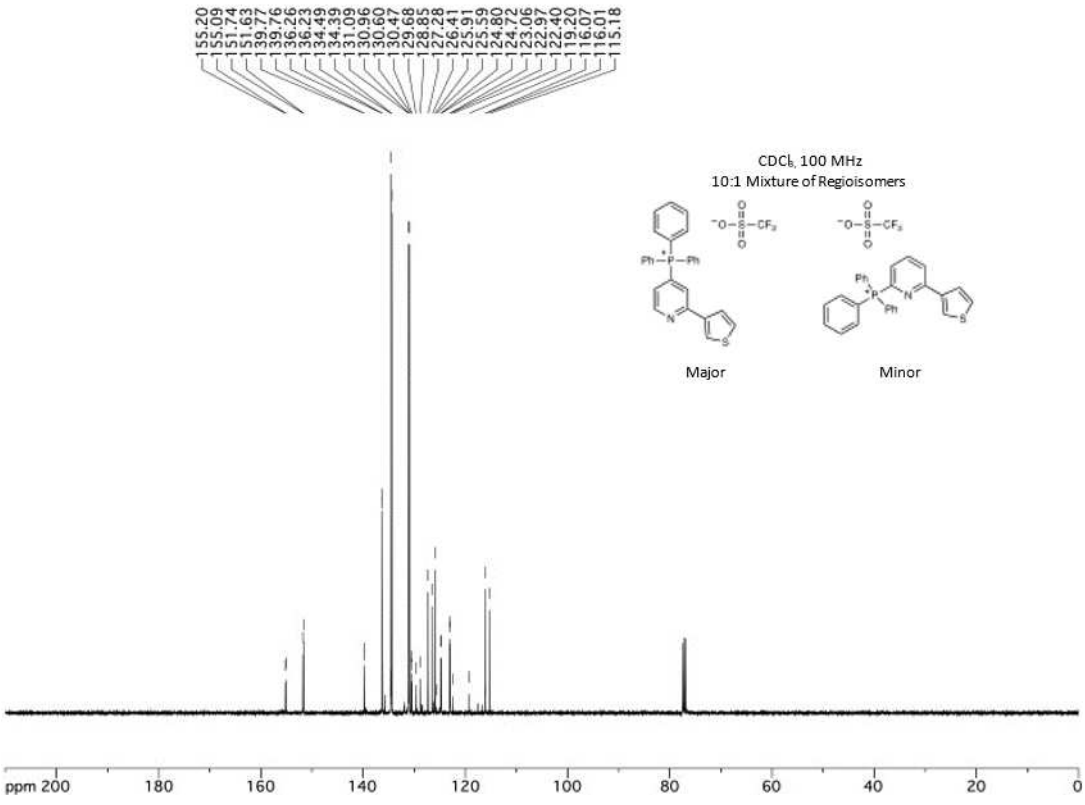
CDCl3 100 MHz
10:1 Mixture of Regioisomers
Major
Minor
ppm

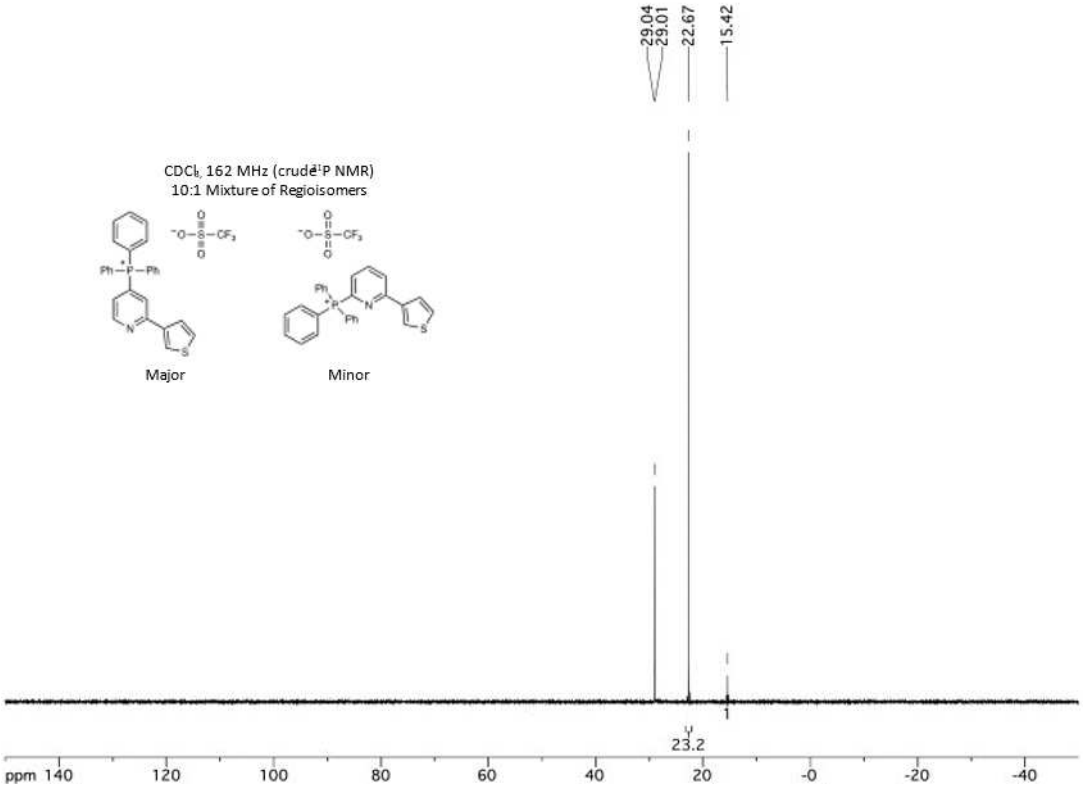
29.04
29.01
22.67
15.42
CDCl3 162 MHz (crude 31P NMR)
10:1 Mixture of Regioisomers
Major
Minor
1
23.2
ppm 140
120
100
80
60
40
20
-0
-20
-40

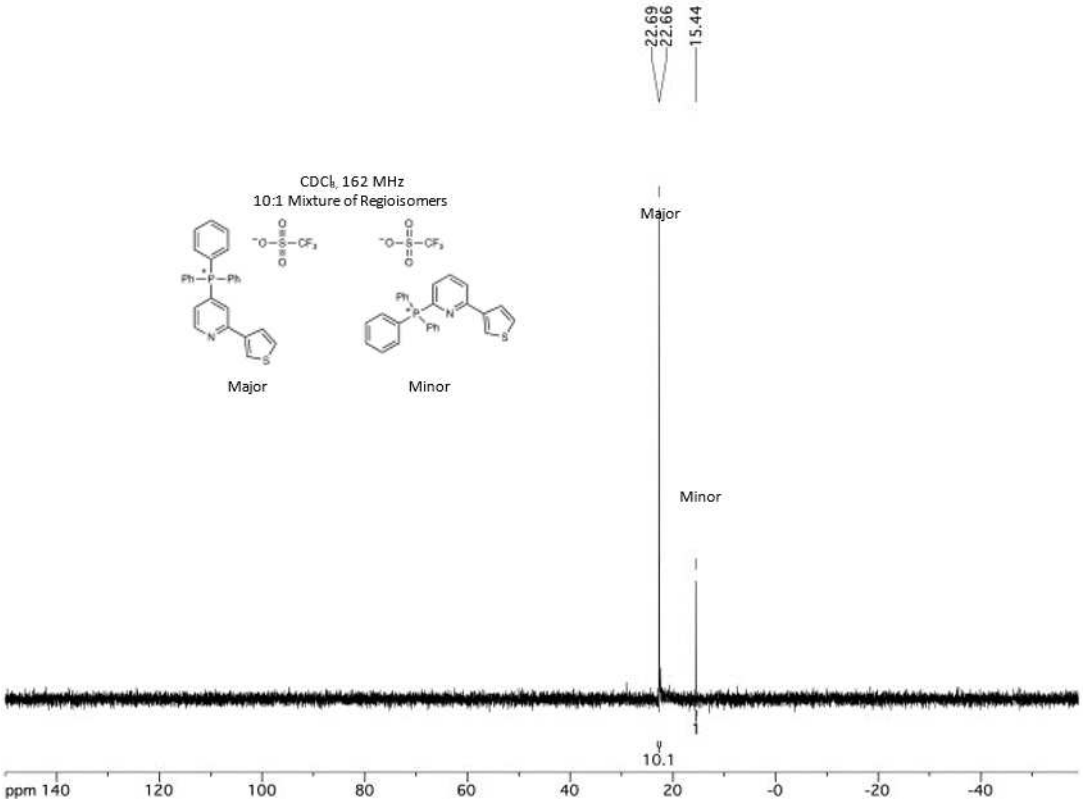
22.69
22.66
15.44
CDCl3 162 MHz
10:1 Mixture of Regioisomers
Major
Minor
Major
Minor
1
10.1
ppm 140
120
100
80
60
40
20
-0
-20
-40

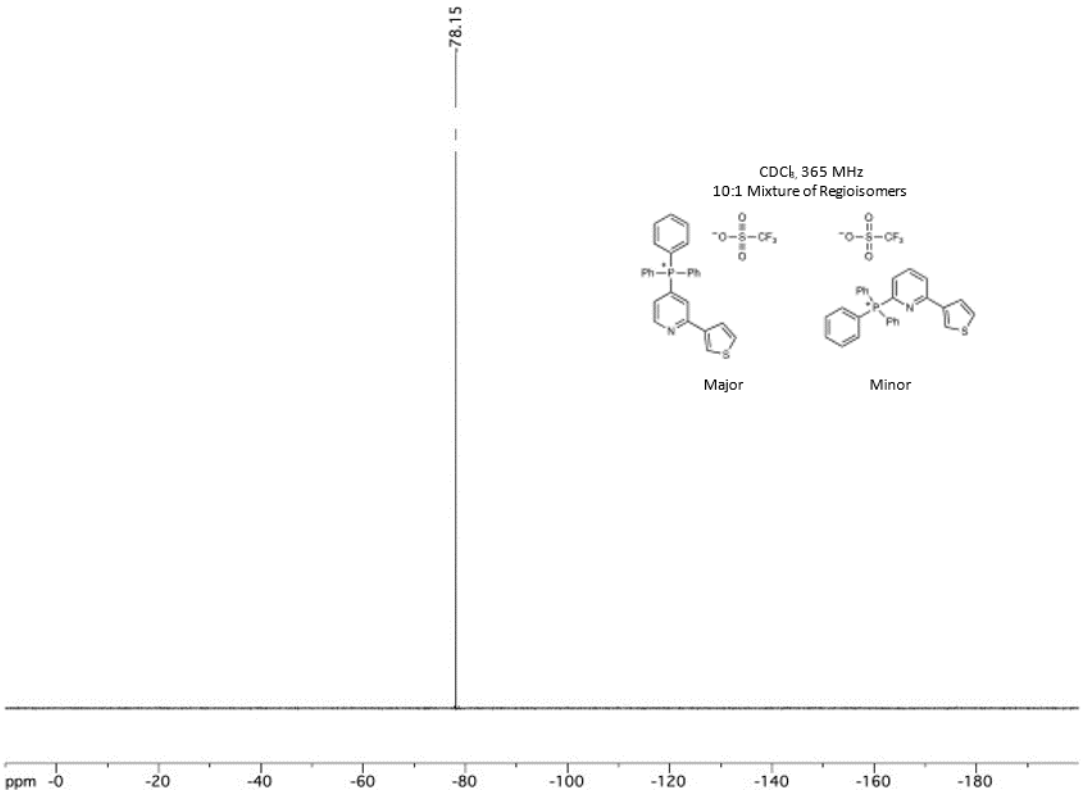
78.15
CDCl3 365 MHz
10:1 Mixture of Regioisomers
Major
Minor
ppm -0 -20 -40 -60 -80 -100 -120 -140 -160 -180

9.12 9.11 9.10 9.10 9.09 9.09 7.96 7.96 7.95 7.95 7.94 7.94 7.93 7.93 7.92 7.92 7.91 7.91 7.91 7.90 7.90 7.89 7.89 7.87 7.87 7.85 7.84 7.84 7.83 7.83 7.82 7.81 7.81 7.80 7.80 7.79 7.76 7.76 7.76 7.75 7.75 7.74 7.73 7.73 7.73 7.71 7.71 7.71 7.70 7.70 7.69 7.68 7.68 7.67 7.60 7.59 7.59 7.58 7.57 7.56 7.55 7.55 1.34

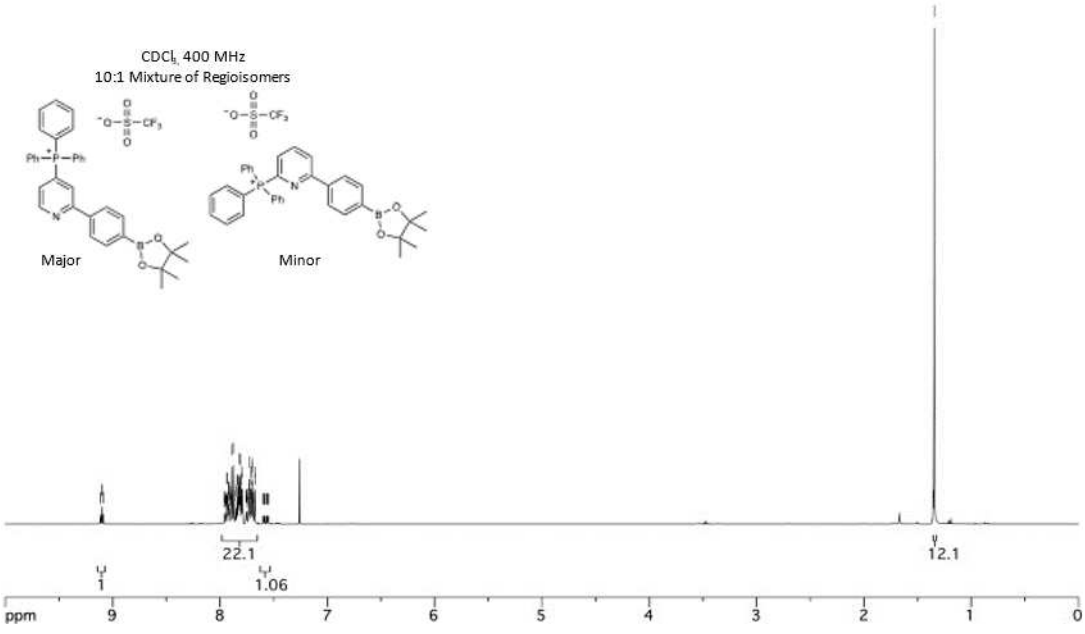
CDCl3 400 MHz
10:1 Mixture of Regioisomers
Major
Minor
22.1
1.06
12.1
1
ppm 9 8 7 6 5 4 3 2 1 0

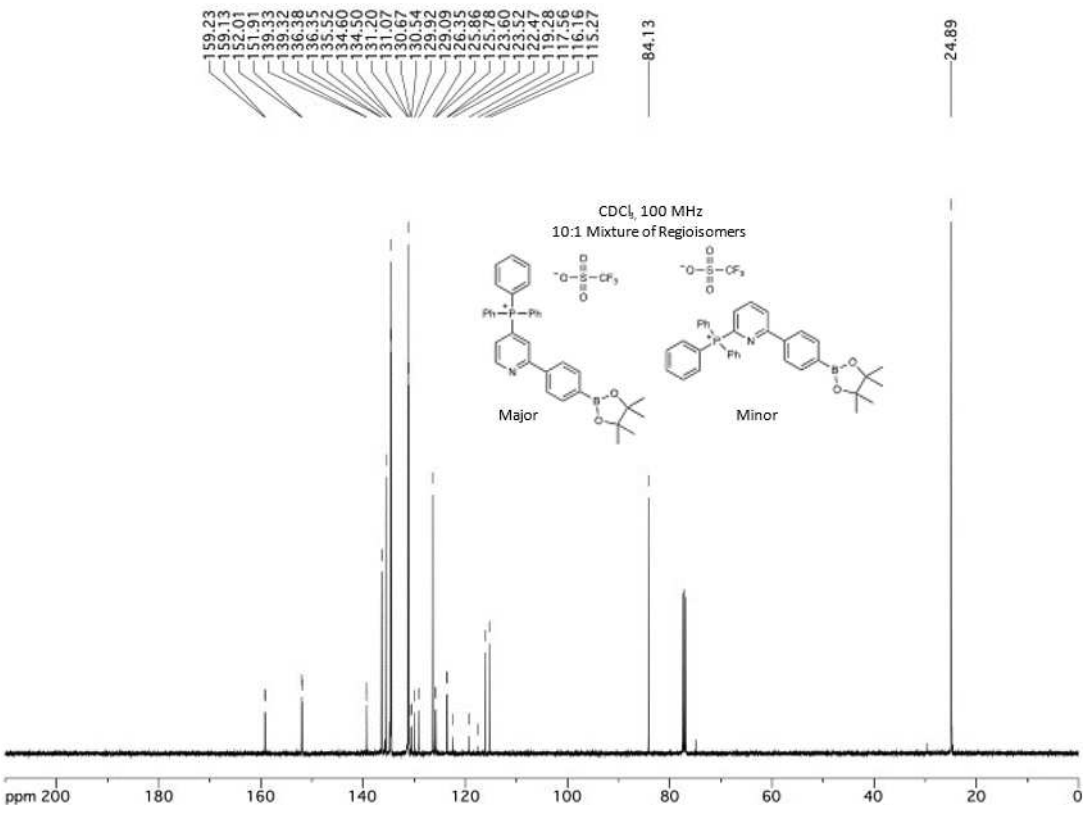
159.23
159.13
152.01
151.91
139.33
139.32
136.38
136.35
135.52
134.60
134.50
131.20
131.07
130.67
130.54
129.92
129.09
126.35
125.86
125.78
123.60
123.52
122.47
119.28
117.56
116.16
115.27
84.13
24.89
CDCl3 100 MHz
10:1 Mixture of Regioisomers
Major
Minor
ppm 200
180
160
140
120
100
80
60
40
20
0

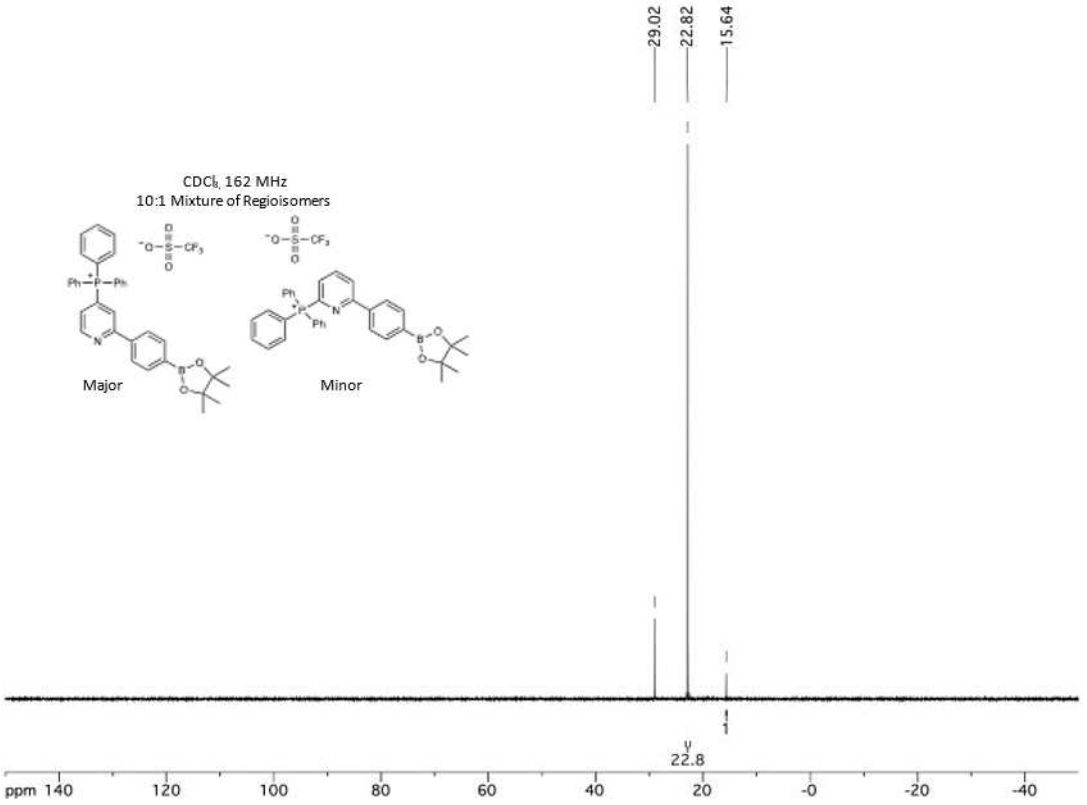
29.02
22.82
15.64
CDCl3 162 MHz
10:1 Mixture of Regioisomers
Major
Minor
22.8
ppm 140
120
100
80
60
40
20
-0
-20
-40

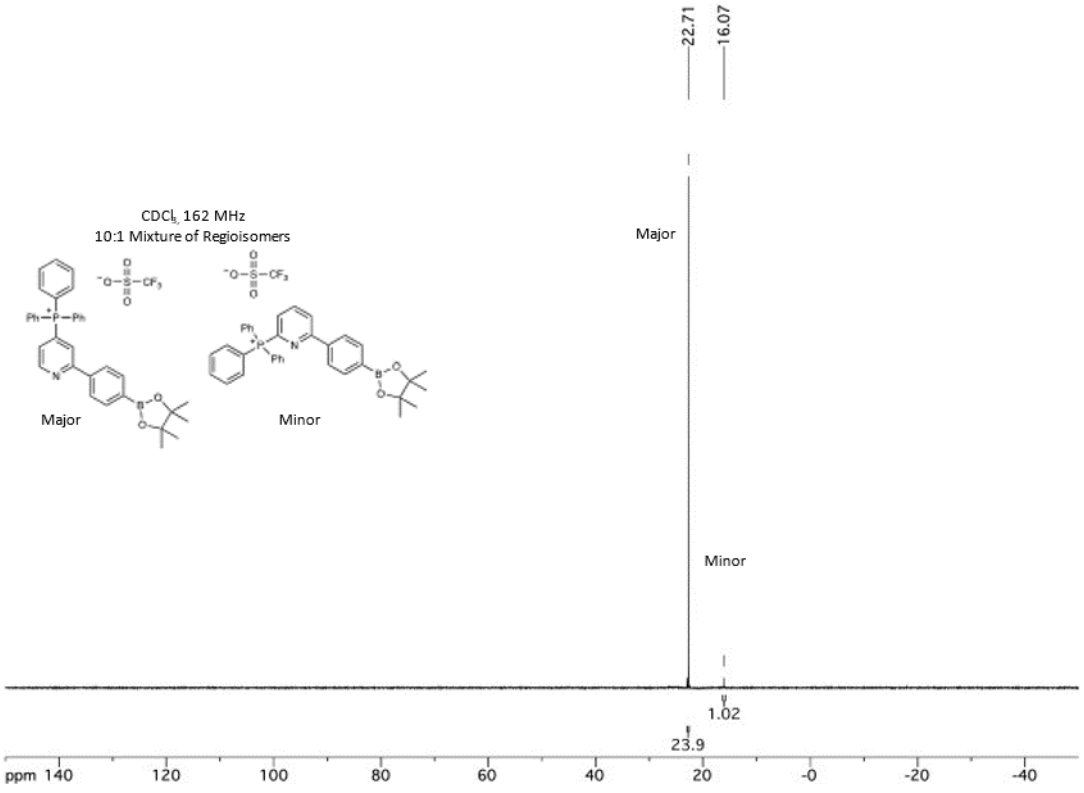
22.71
16.07
CDCl3, 162 MHz
10:1 Mixture of Regioisomers
Major
Minor
Major
Minor
1.02
23.9
ppm 140
120
100
80
60
40
20
-0
-20
-40

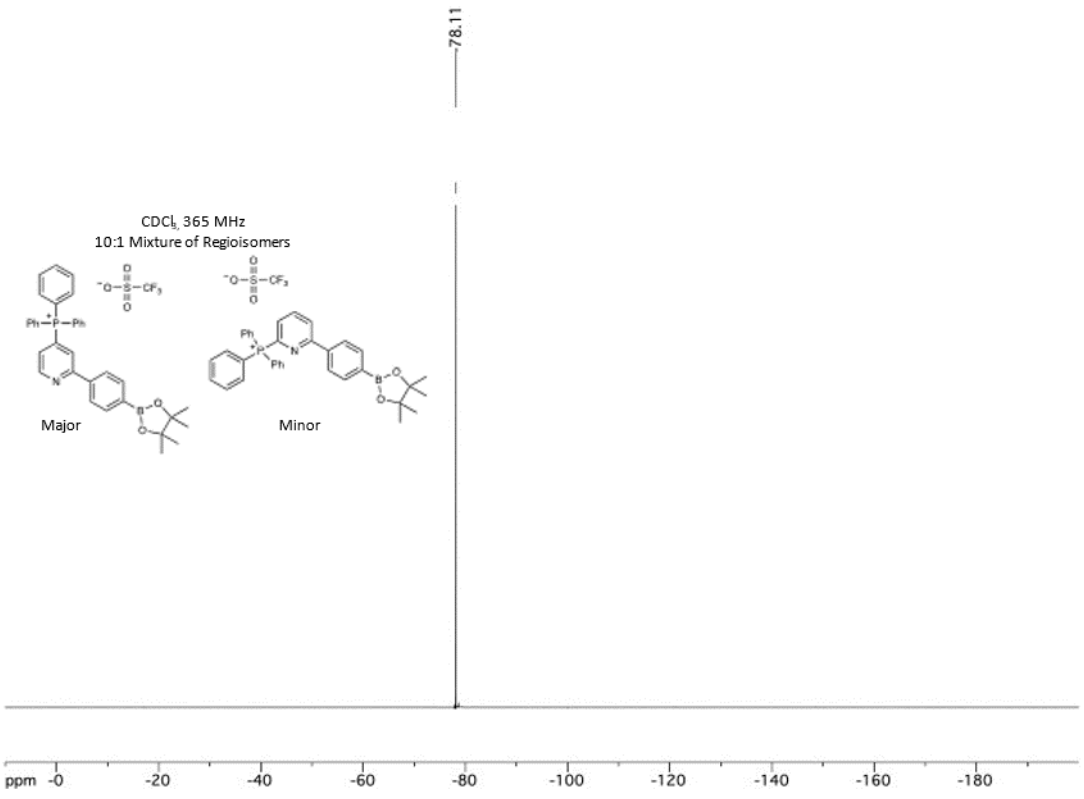
78.11
CDCl3, 365 MHz
10:1 Mixture of Regioisomers
Major
Minor
ppm -0
-20
-40
-60
-80
-100
-120
-140
-160
-180

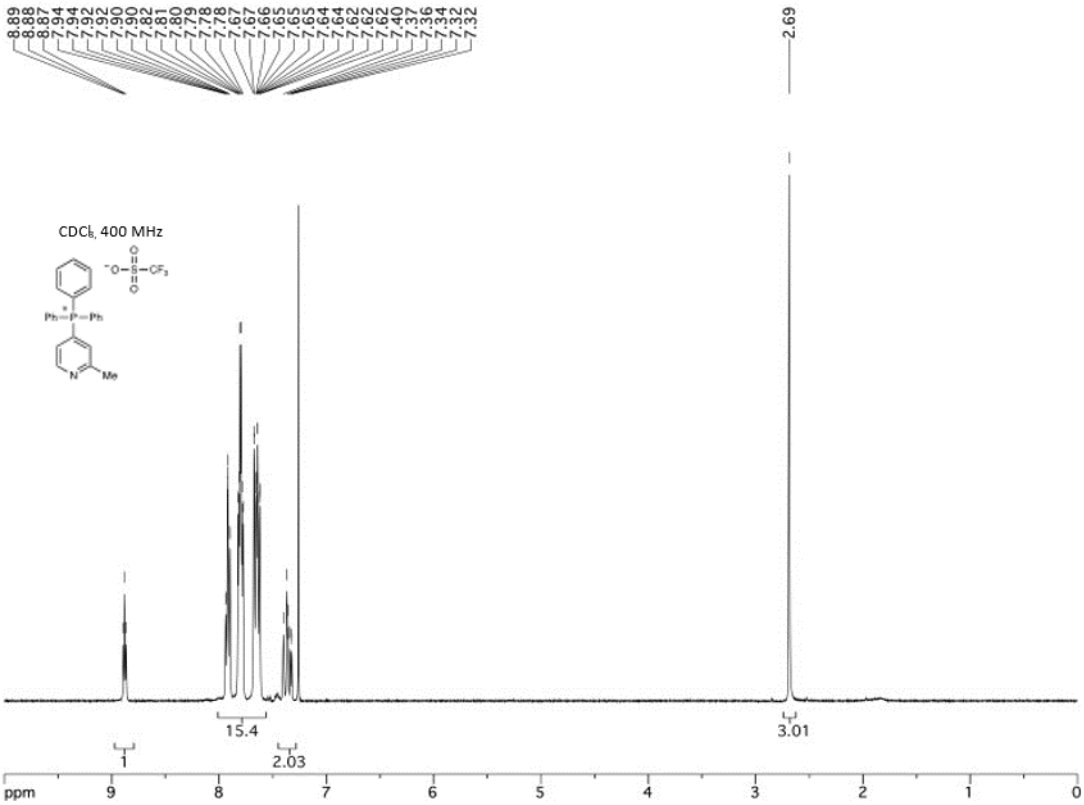
8.89
8.88
8.87
7.94
7.94
7.92
7.92
7.90
7.90
7.82
7.81
7.80
7.79
7.78
7.78
7.67
7.67
7.66
7.65
7.65
7.65
7.64
7.64
7.62
7.62
7.42
7.40
7.37
7.36
7.34
7.32
7.32
2.69
CDCl3, 400 MHz
15.4
3.01
1
2.03
ppm
9
8
7
6
5
4
3
2
1
0

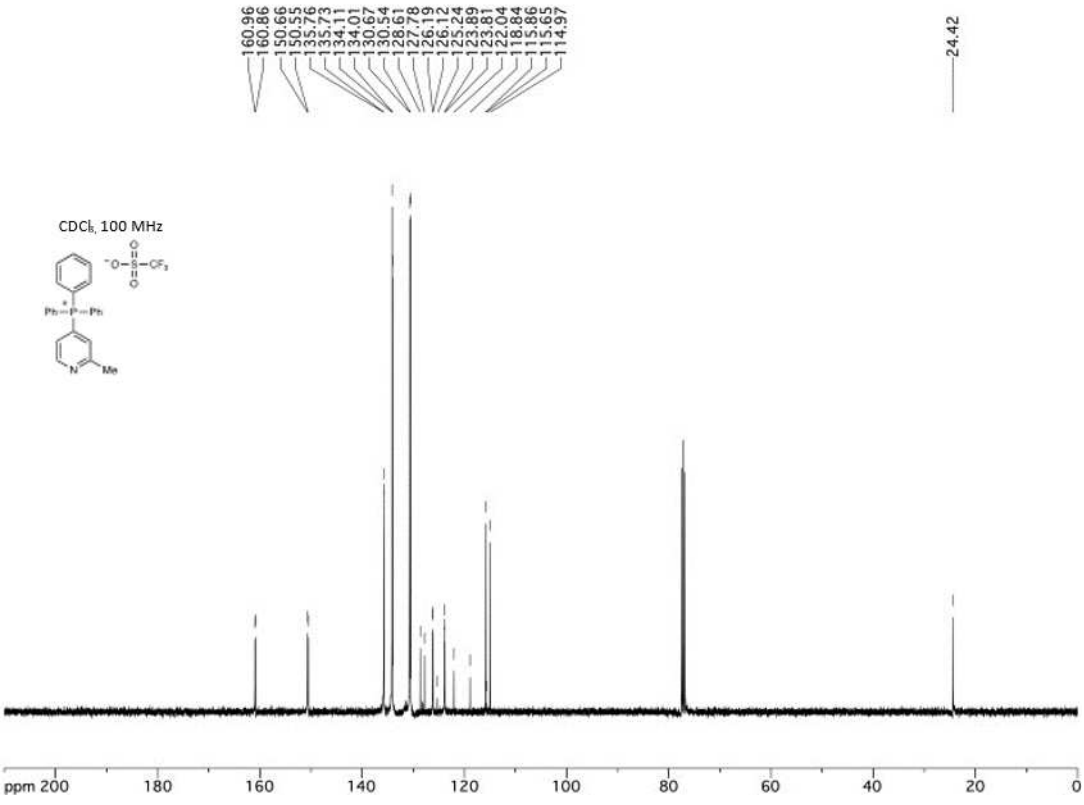
160.96
160.86
150.66
150.55
135.76
135.73
134.11
134.01
130.67
130.54
128.61
127.78
126.19
126.12
125.24
123.89
123.81
122.04
118.84
115.86
115.65
114.97
24.42
CDCl3, 100 MHz
ppm 200
180
160
140
120
100
80
60
40
20
0

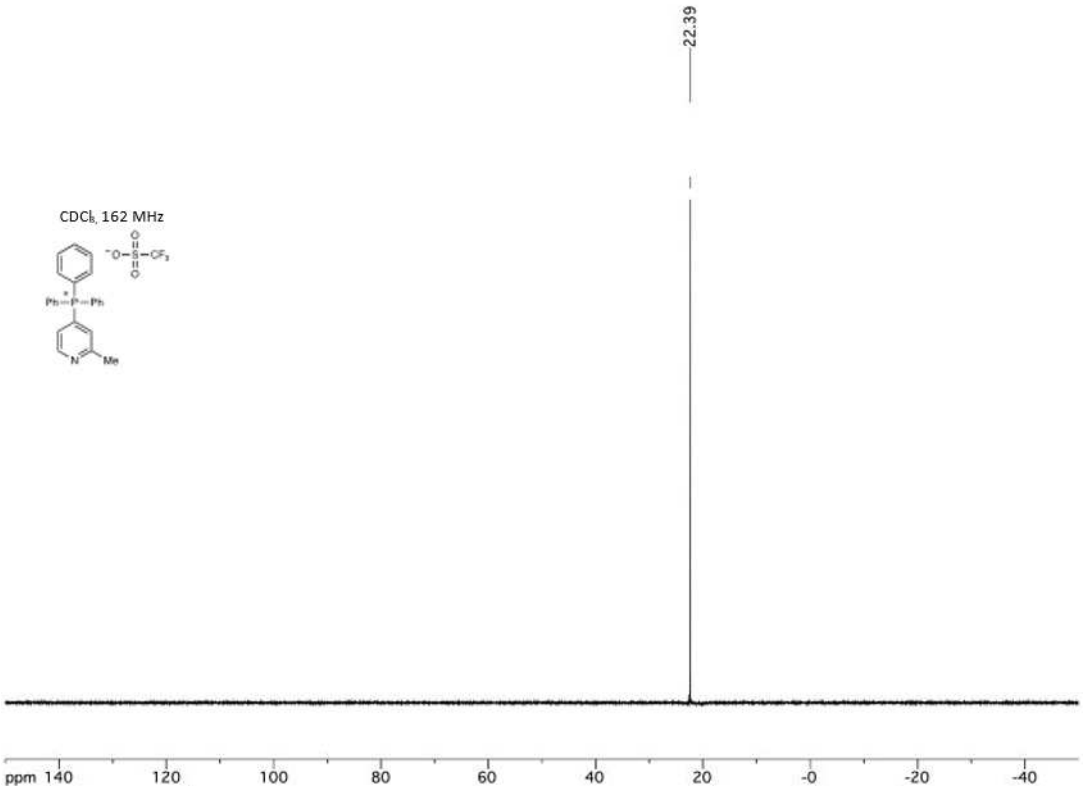
22.39
CDCl3, 162 MHz
ppm 140
120
100
80
60
40
20
-0
-20
-40

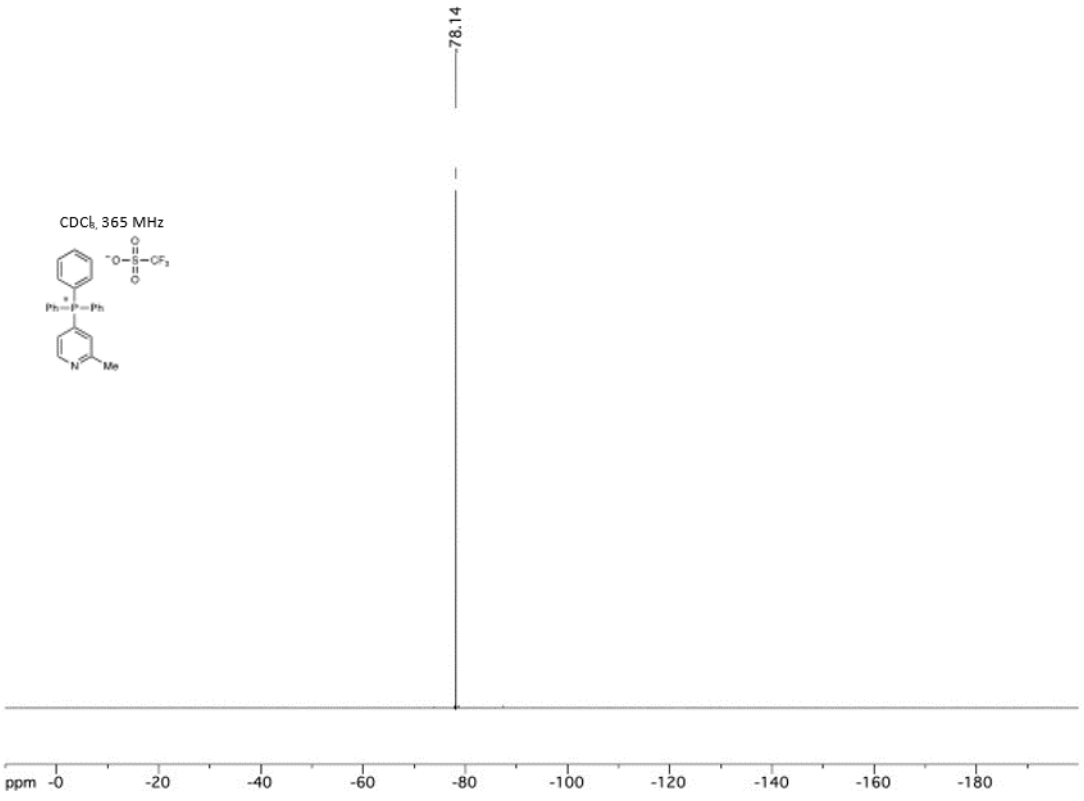
78.14
CDCl3, 365 MHz
ppm -0
-20
-40
-60
-80
-100
-120
-140
-160
-180

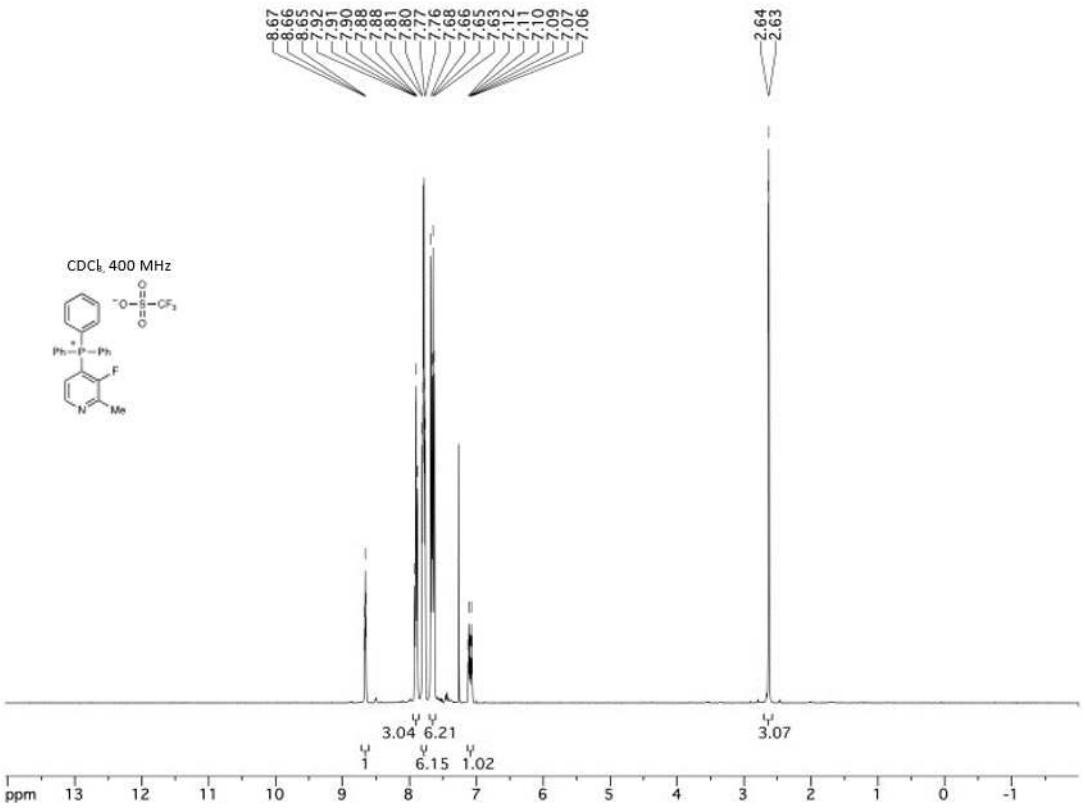
8.67
8.66
8.65
7.92
7.91
7.90
7.88
7.88
7.81
7.80
7.77
7.76
7.68
7.66
7.65
7.63
7.12
7.11
7.10
7.09
7.07
7.06
2.64
2.63
CDCl3 400 MHz
3.04
6.21
3.07
1
6.15
1.02
ppm

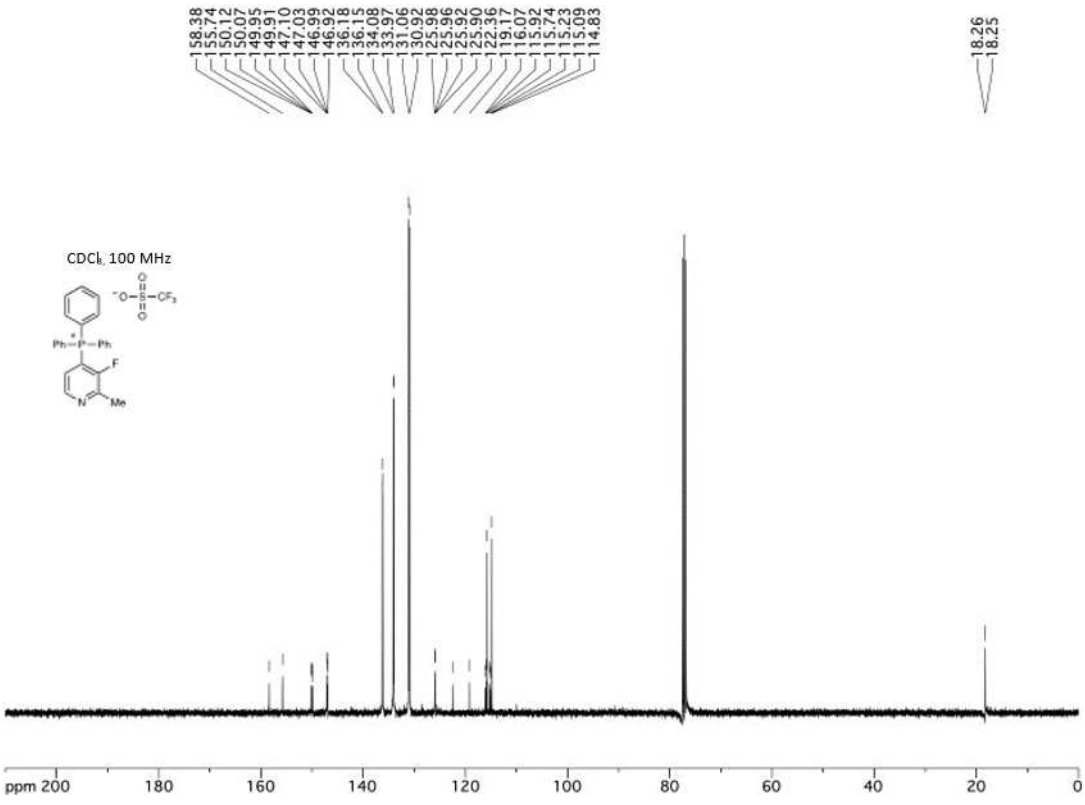
158.38
155.74
150.12
150.07
149.95
149.91
147.10
147.03
146.99
146.92
136.18
136.15
134.08
133.97
131.06
130.92
125.98
125.96
125.92
125.90
122.36
119.17
116.07
115.92
115.74
115.23
115.09
114.83
18.26
18.25
CDCl3 100 MHz
ppm

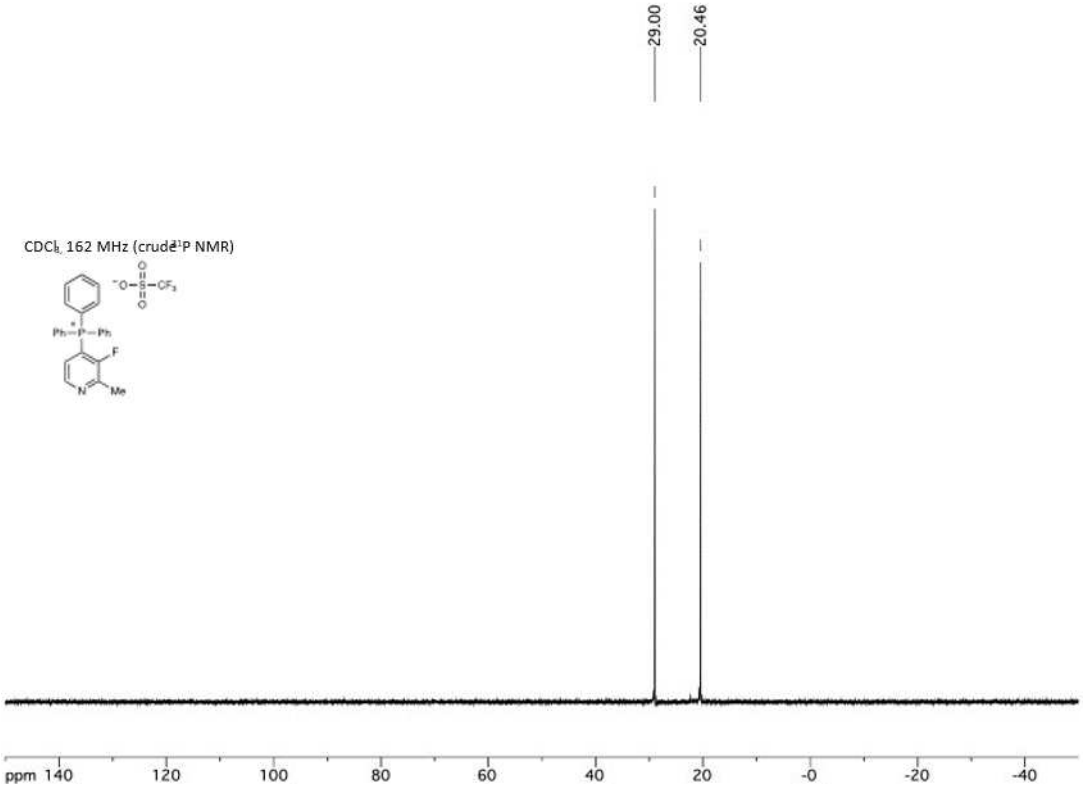
29.00
20.46
CDCl3 162 MHz (crude 31P NMR)
ppm 140
120
100
80
60
40
20
-0
-20
-40

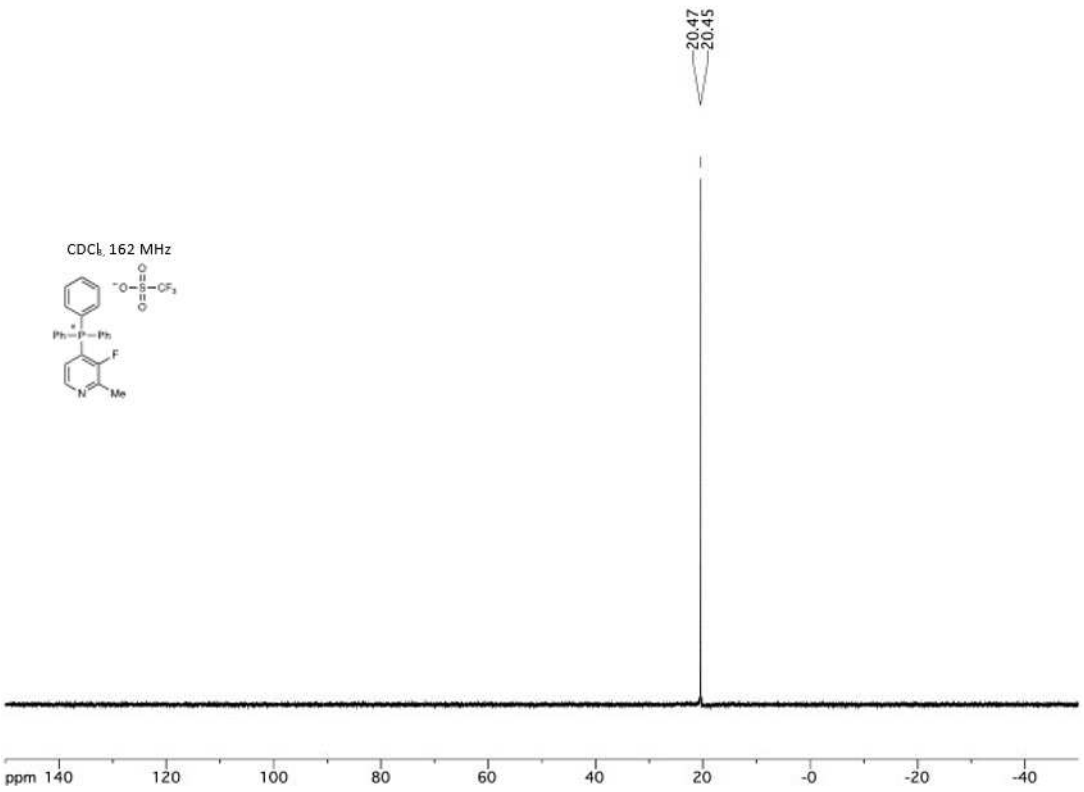
20.47
20.45
CDCl3 162 MHz
ppm 140
120
100
80
60
40
20
-0
-20
-40

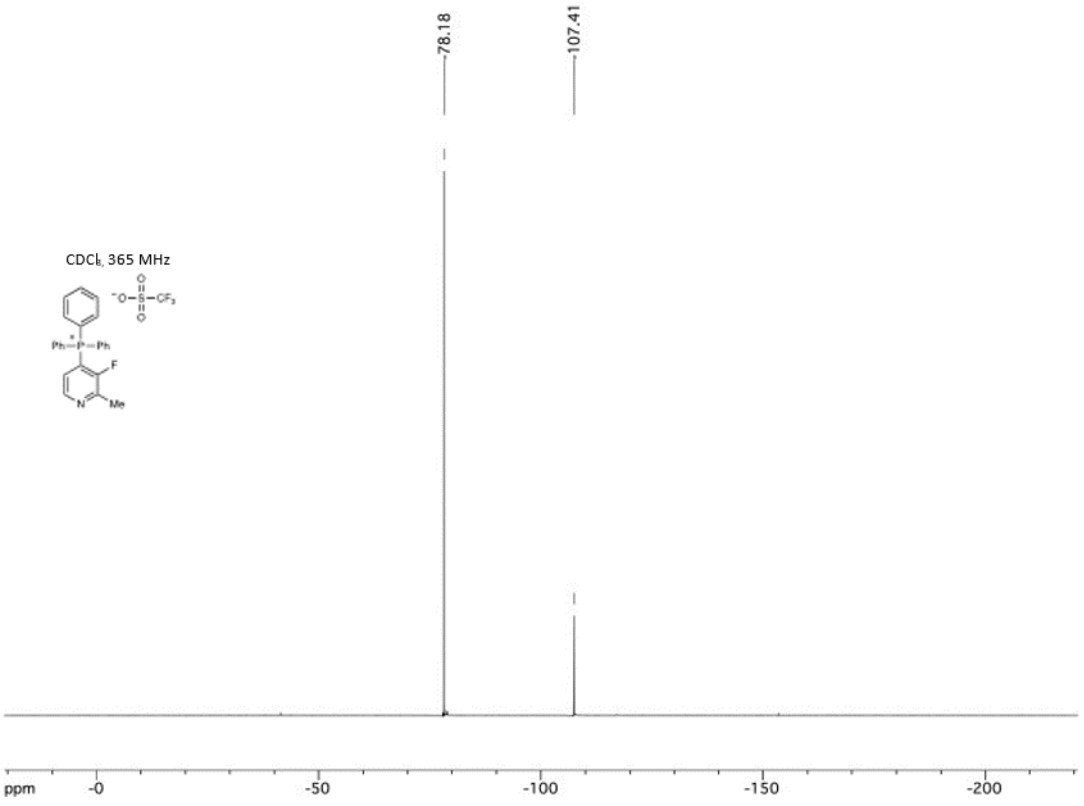
78.18
107.41
CDCl3 365 MHz
ppm
-0
-50
-100
-150
-200

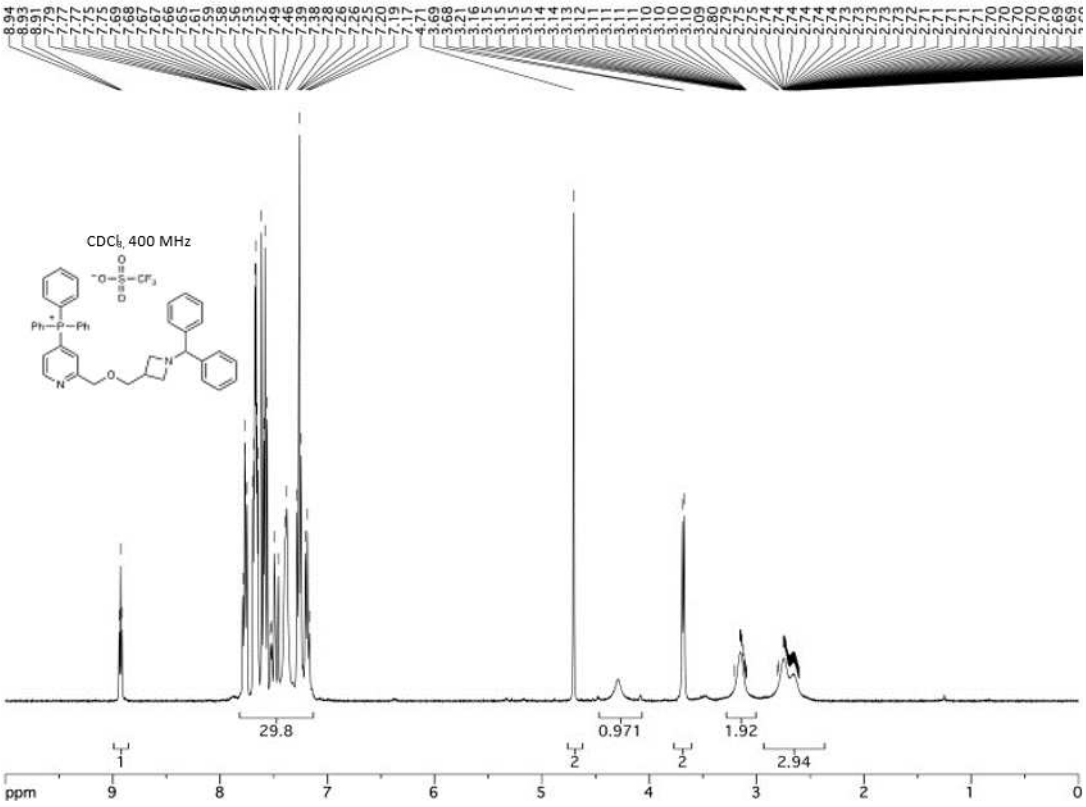
CDCl3 400 MHz
29.8
0.971
1.92
2.94
1
2
2
ppm
9
8
7
6
5
4
3
2
1
0

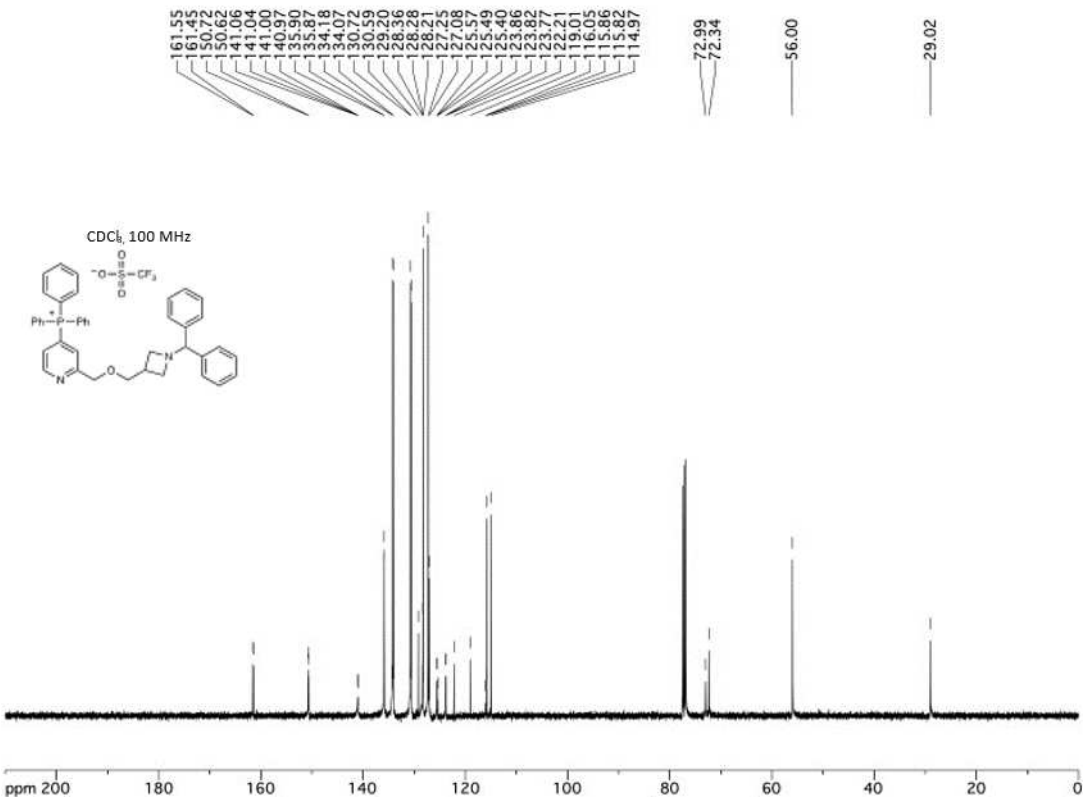
161.55
161.45
150.72
150.62
141.06
141.04
141.00
140.97
135.90
135.87
134.18
134.07
130.72
130.59
129.20
128.36
128.28
128.21
127.25
127.08
125.57
125.49
125.40
123.86
123.82
123.77
122.21
119.01
116.05
115.86
115.82
114.97
72.99
72.34
56.00
29.02
CDCl3, 100 MHz
ppm 200
180
160
140
120
100
80
60
40
20
0

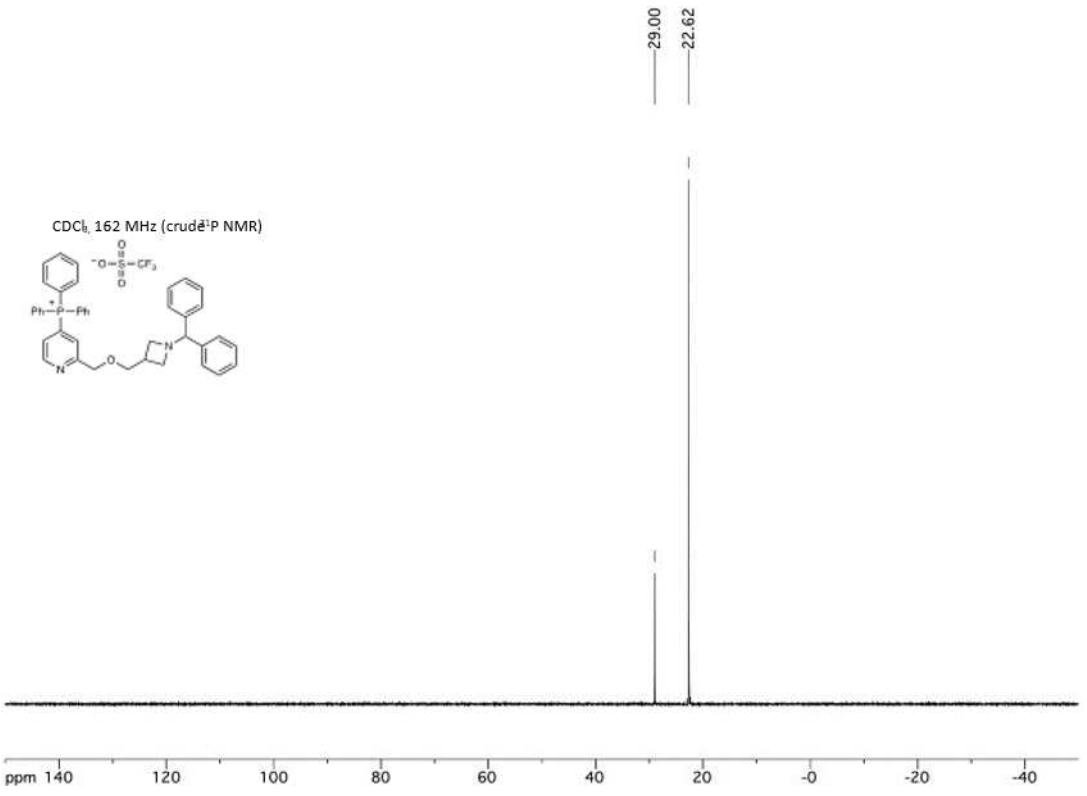
29.00
22.62
CDCl3, 162 MHz (crude 31P NMR)
ppm 140
120
100
80
60
40
20
-0
-20
-40

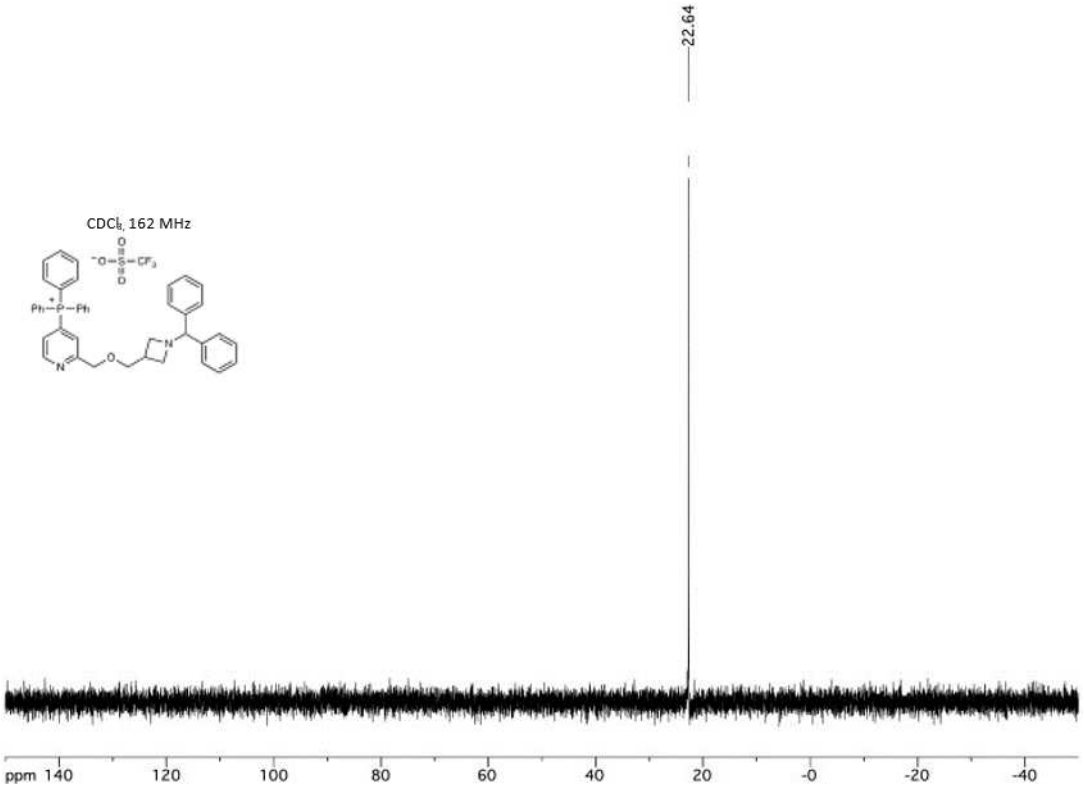
22.64
CDCl3, 162 MHz
ppm 140
120
100
80
60
40
20
-0
-20
-40

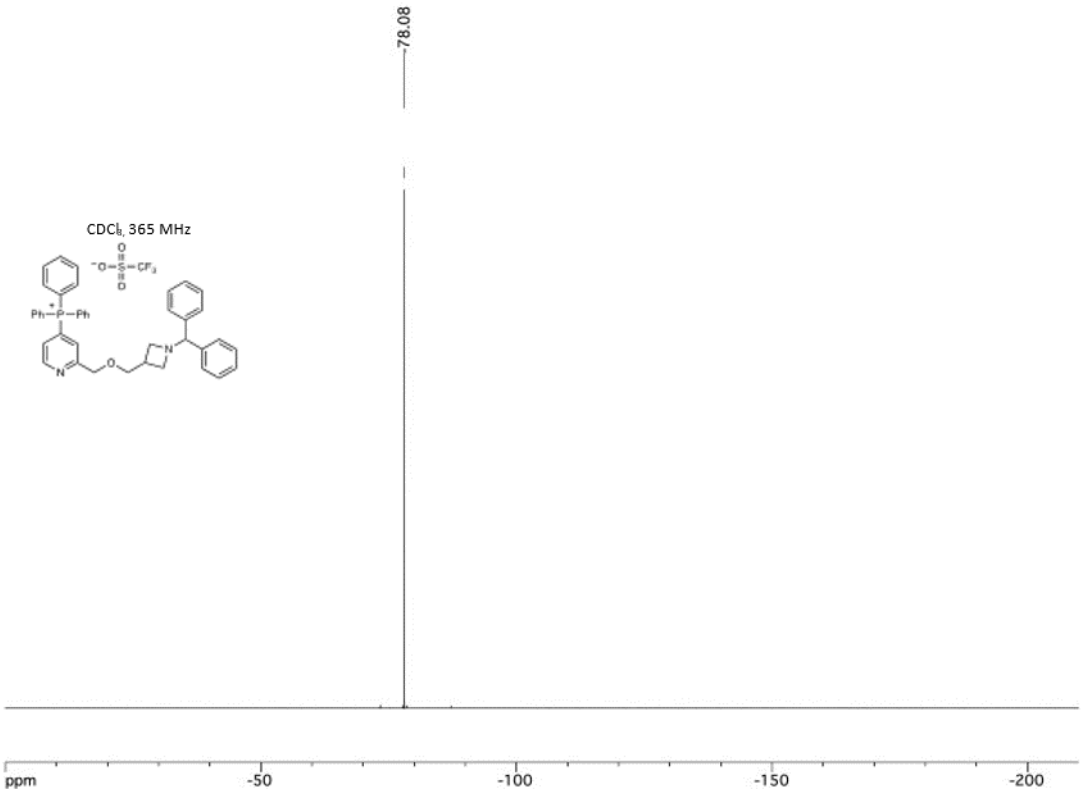
-78.08
CDCl3, 365 MHz
ppm
-50
-100
-150
-200

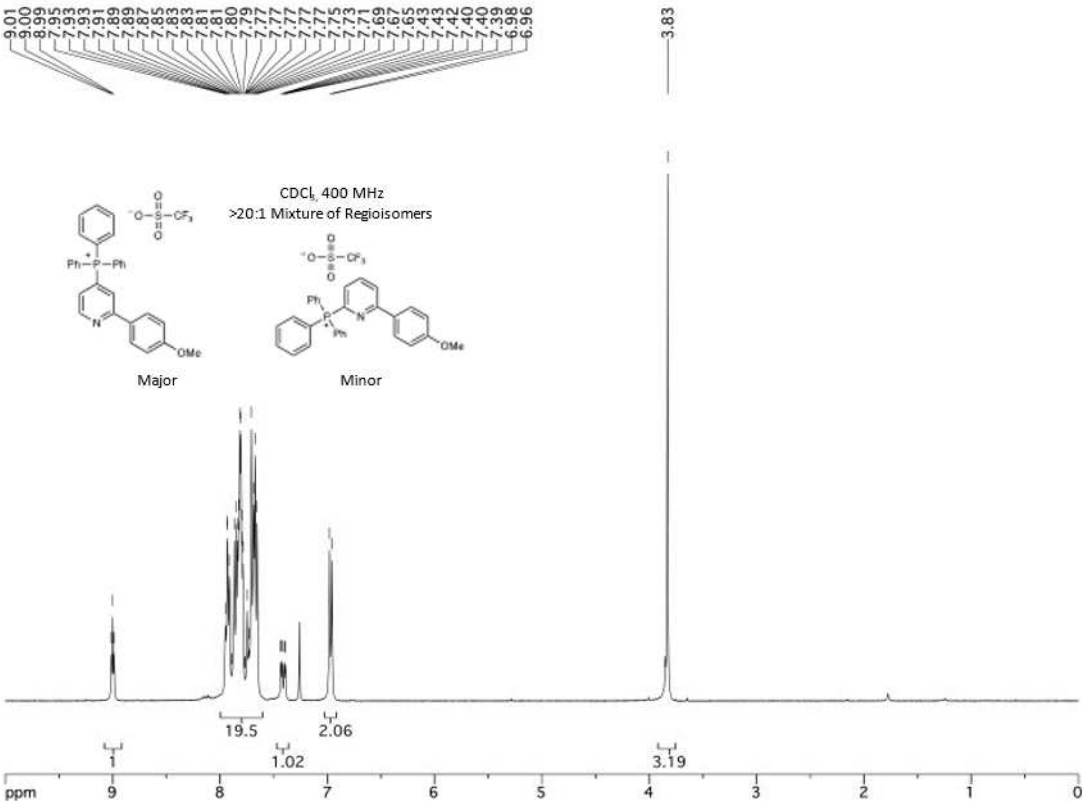
9.01
9.00
8.99
7.95
7.93
7.93
7.91
7.89
7.89
7.87
7.85
7.83
7.83
7.81
7.81
7.80
7.79
7.77
7.77
7.77
7.77
7.77
7.75
7.73
7.71
7.69
7.67
7.65
7.43
7.42
7.40
7.40
7.39
6.98
6.96
3.83
CDCl3 400 MHz
>20:1 Mixture of Regioisomers
Major
Minor
19.5
2.06
1
1.02
3.19
ppm

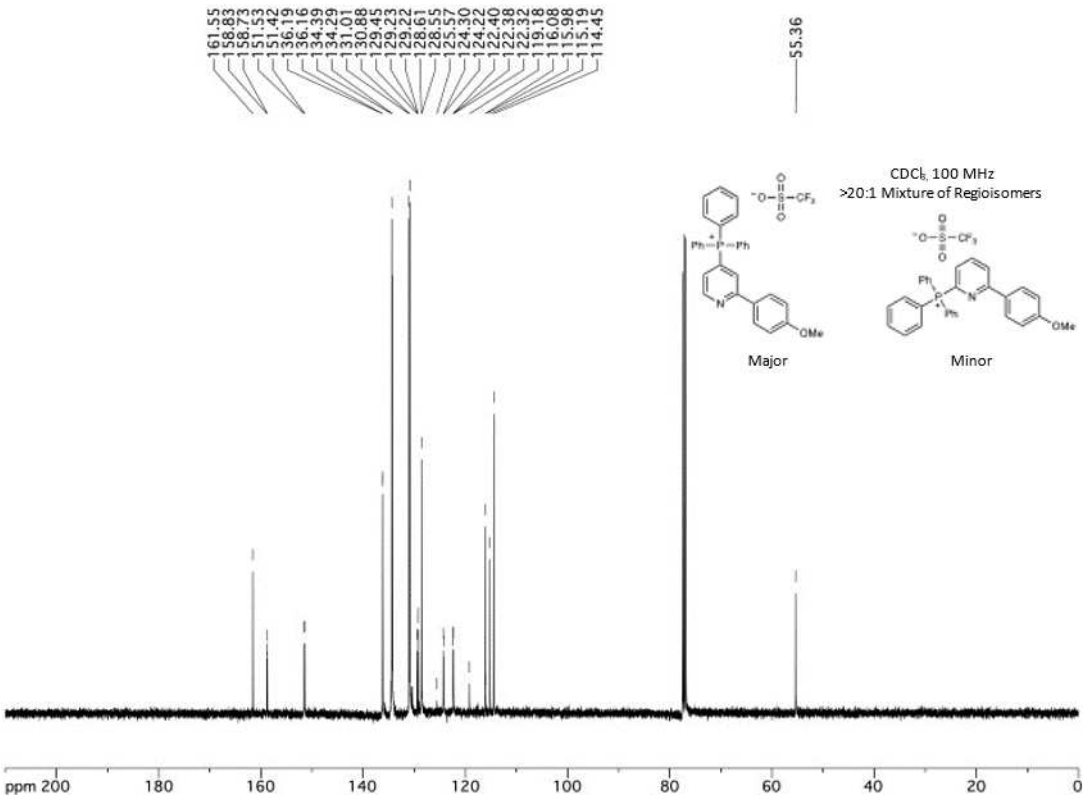
161.55
158.83
158.73
151.53
151.42
136.19
136.16
134.39
134.29
131.01
130.88
129.45
129.23
129.22
128.61
128.55
125.57
124.30
124.22
122.40
122.38
122.32
119.18
116.08
115.98
115.19
114.45
55.36
CDCl3 100 MHz
>20:1 Mixture of Regioisomers
Major
Minor
ppm

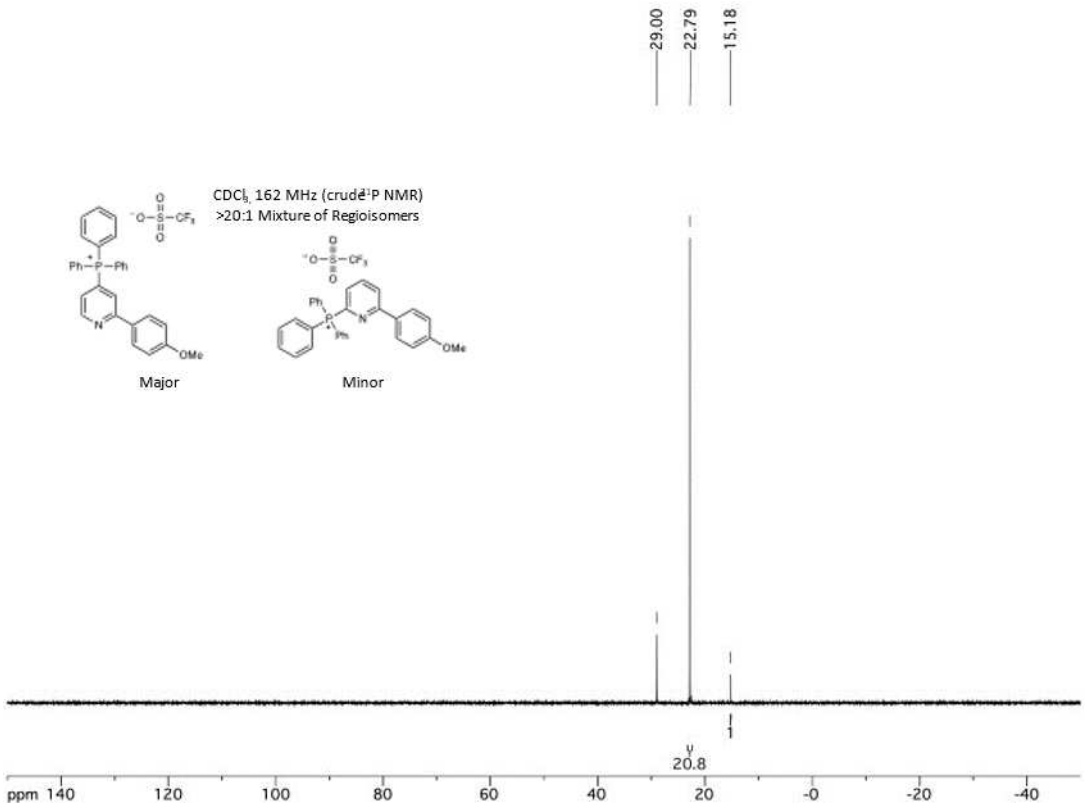
29.00
22.79
15.18
CDCl3, 162 MHz (crude 31P NMR)
>20:1 Mixture of Regioisomers
Major
Minor
20.8
ppm 140
120
100
80
60
40
20
-0
-20
-40

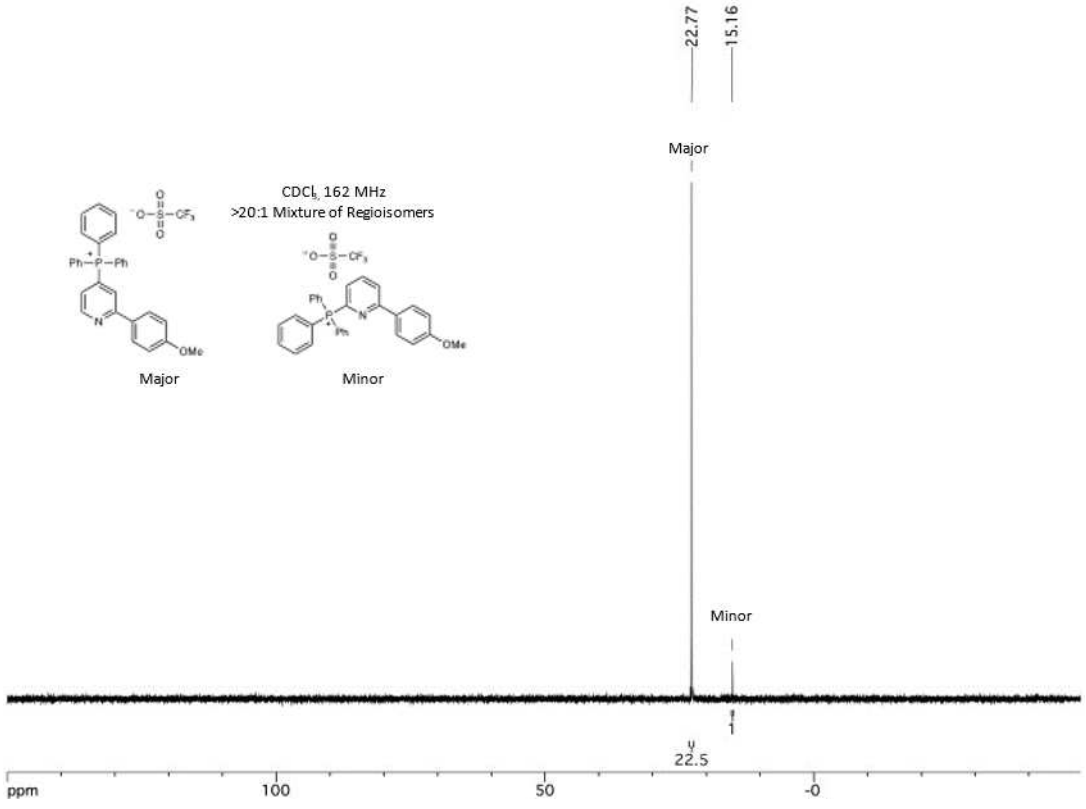
22.77
15.16
Major
CDCl3, 162 MHz
>20:1 Mixture of Regioisomers
Major
Minor
Minor
22.5
ppm
100
50
-0

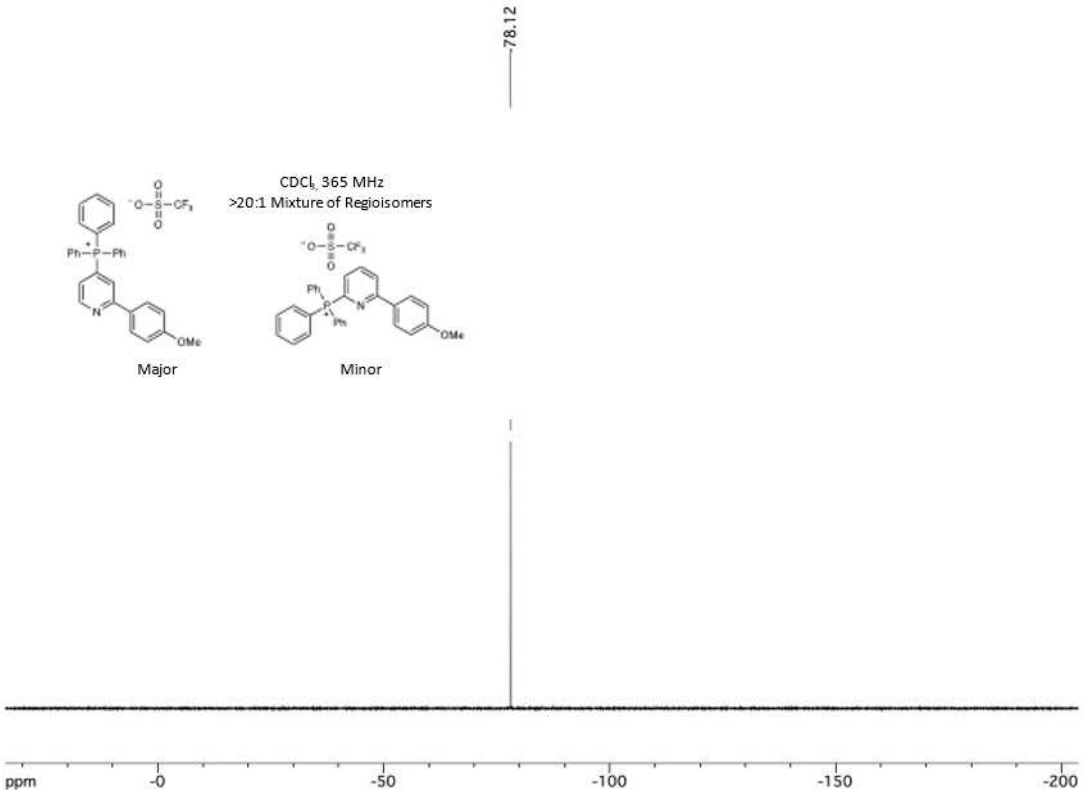
-78.12
CDCl3, 365 MHz
>20:1 Mixture of Regioisomers
Major
Minor
ppm
0
-50
-100
-150
-200

9.07
9.06
9.05
9.05
9.04
9.04
7.94
7.94
7.94
7.94
7.93
7.93
7.92
7.92
7.91
7.91
7.90
7.90
7.90
7.83
7.83
7.82
7.82
7.81
7.80
7.80
7.79
7.79
7.78
7.78
7.77
7.73
7.73
7.72
7.72
7.70
7.70
7.70
7.69
7.69
7.68
7.68
7.67
7.67
7.66
7.65
7.65
7.57
7.56
7.56
7.55
7.54
7.53
7.52
7.52

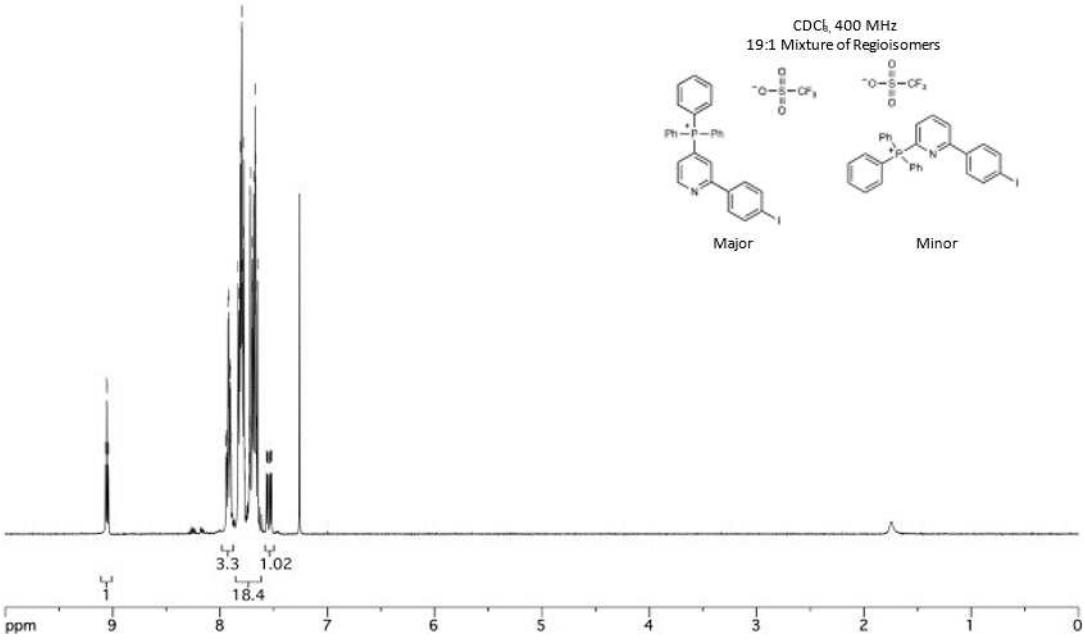
CDCl3, 400 MHz
19:1 Mixture of Regioisomers
Major
Minor
3.3
1.02
1
18.4
ppm
9
8
7
6
5
4
3
2
1
0

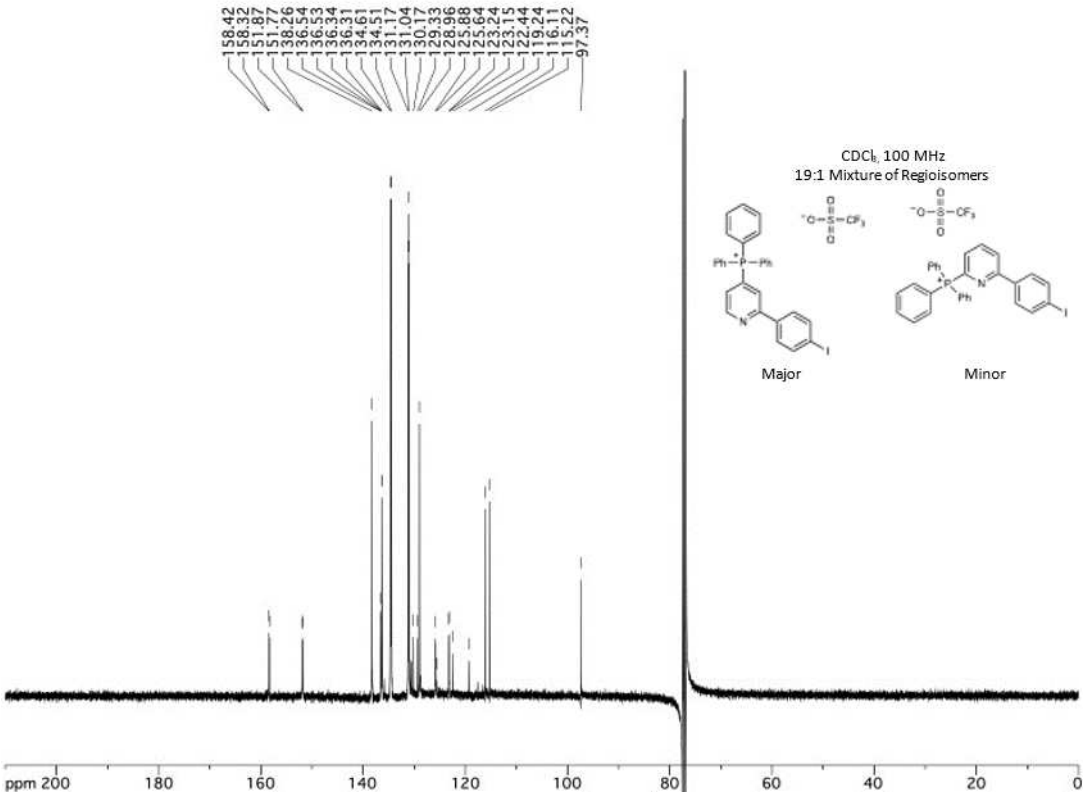
158.42
158.32
151.87
151.77
138.26
136.54
136.53
136.34
136.31
134.61
134.51
131.17
131.04
130.17
129.33
128.96
125.88
125.64
123.24
123.15
122.44
119.24
116.11
115.22
97.37
CDCl3, 100 MHz
19:1 Mixture of Regioisomers
Major
Minor
ppm 200
180
160
140
120
100
80
60
40
20
0

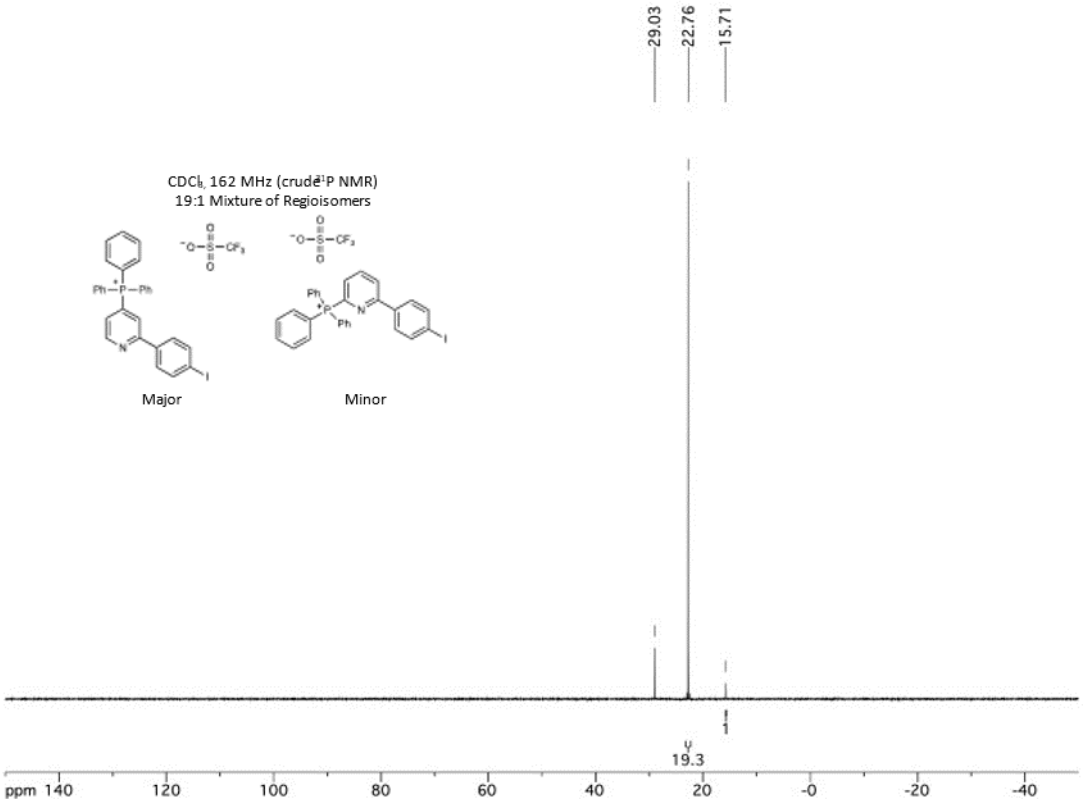
29.03
22.76
15.71
CDCl3, 162 MHz (crude 31P NMR)
19:1 Mixture of Regioisomers
Major
Minor
19.3
ppm 140
120
100
80
60
40
20
-0
-20
-40

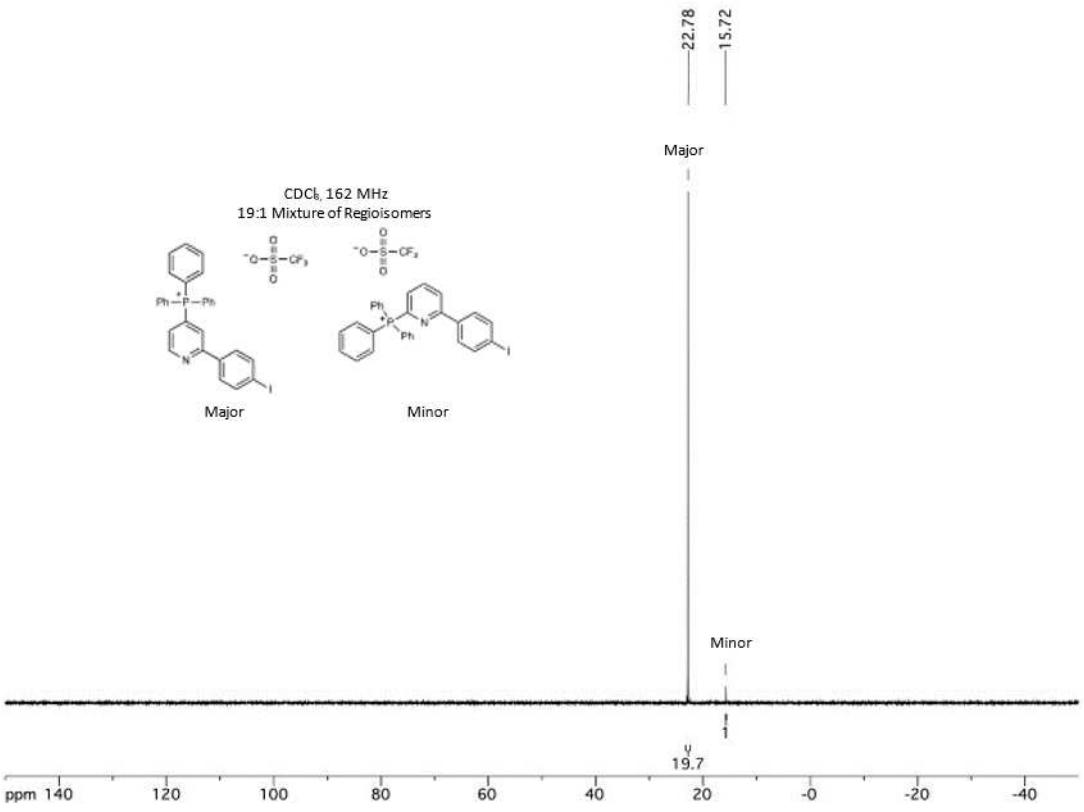
22.78
15.72
Major
CDCl3, 162 MHz
19:1 Mixture of Regioisomers
Major
Minor
Minor
1
19.7
ppm 140 120 100 80 60 40 20 0 -20 -40

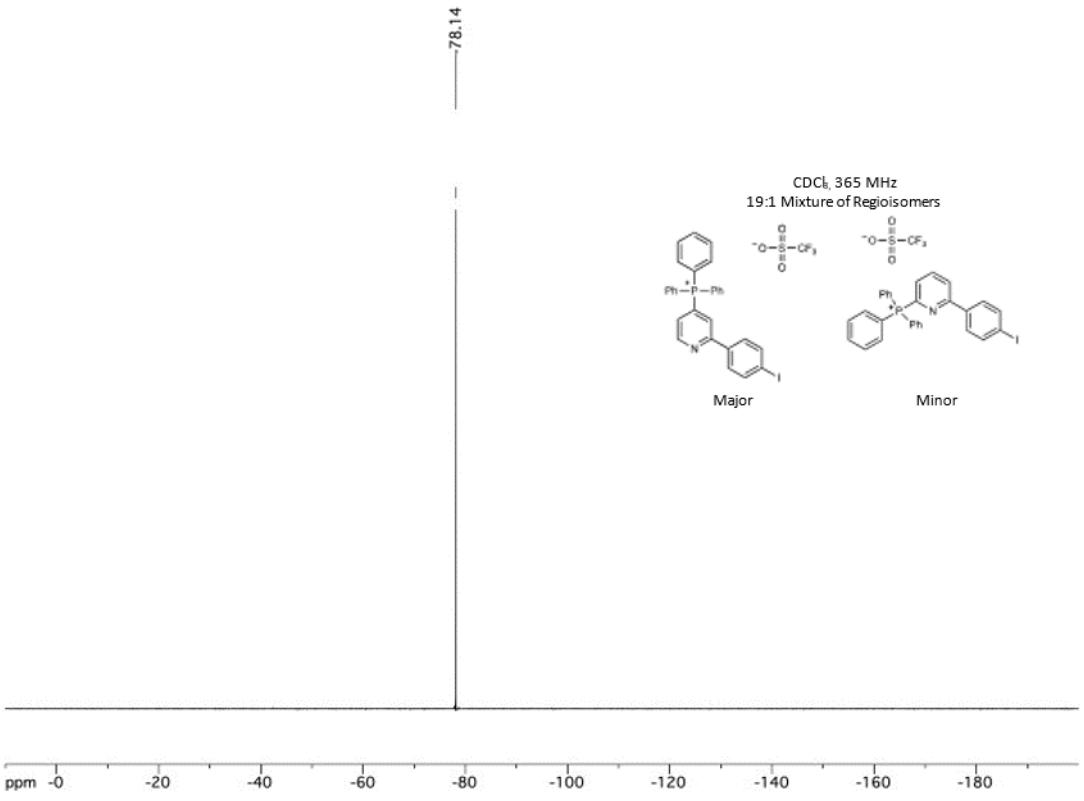
78.14
CDCl3, 365 MHz
19:1 Mixture of Regioisomers
Major
Minor
ppm 0 -20 -40 -60 -80 -100 -120 -140 -160 -180

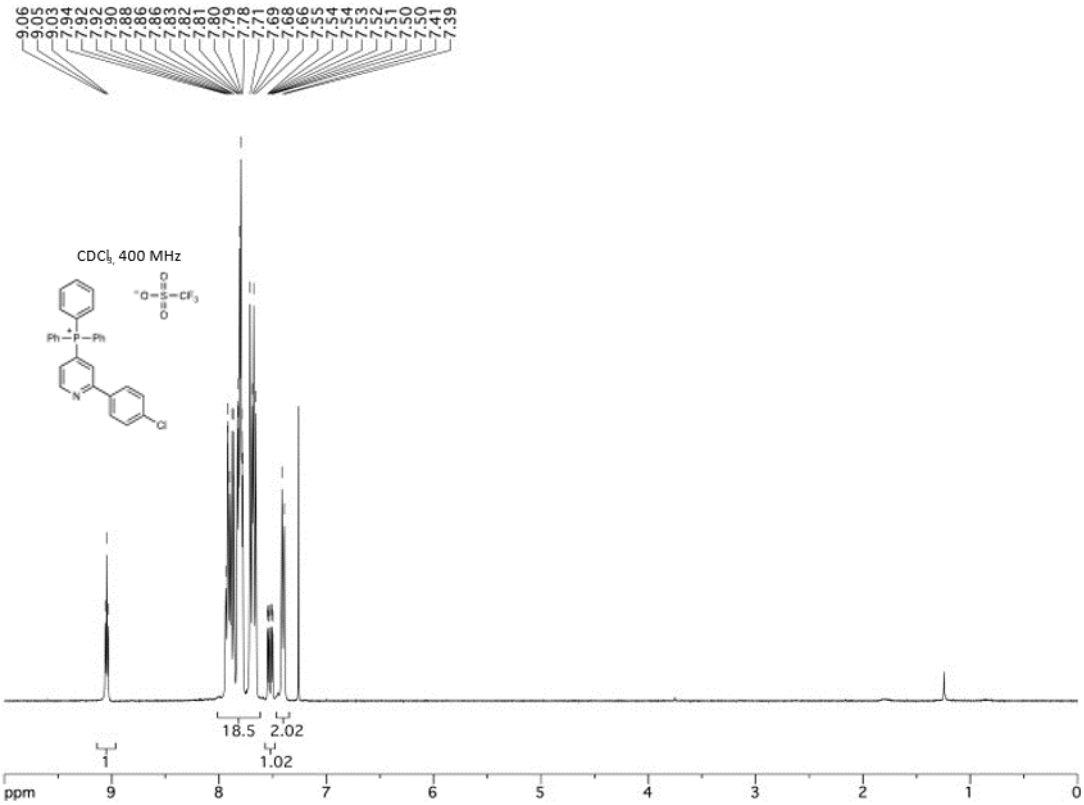
9.06
9.05
9.03
7.94
7.92
7.90
7.88
7.86
7.86
7.83
7.82
7.81
7.80
7.79
7.78
7.71
7.69
7.68
7.66
7.55
7.54
7.54
7.53
7.52
7.51
7.50
7.50
7.41
7.39
CDCl3, 400 MHz
18.5
2.02
1
1.02
ppm
9
8
7
6
5
4
3
2
1
0

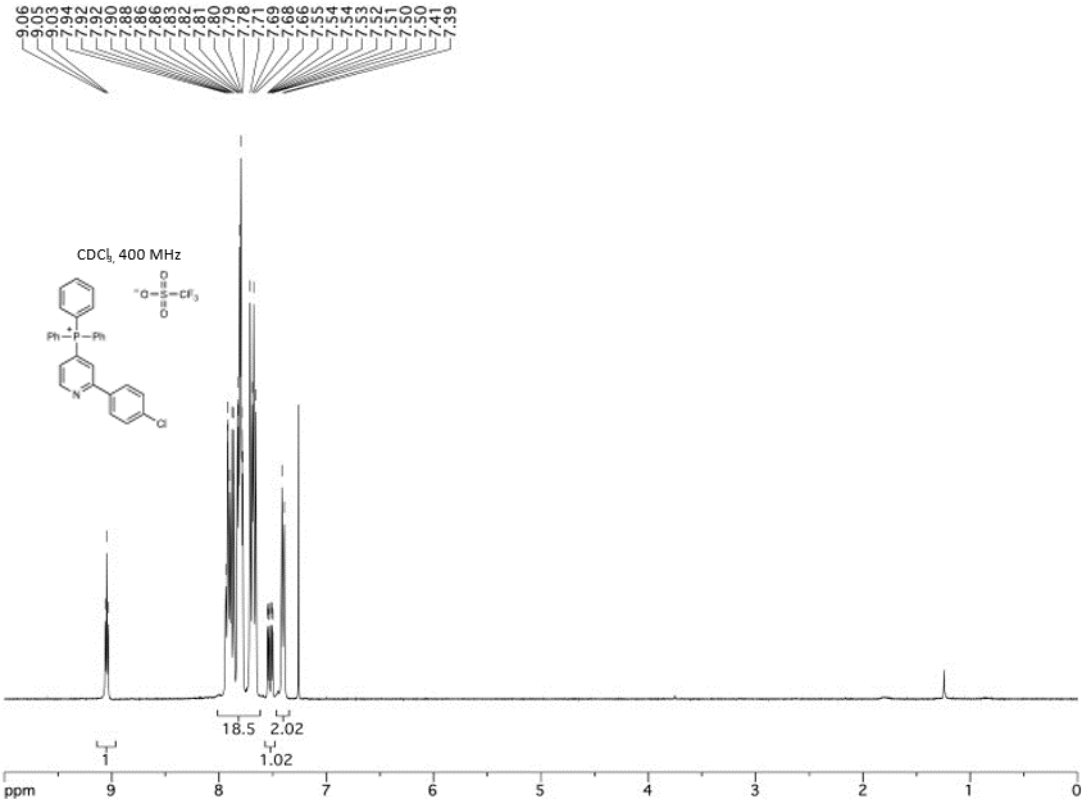
9.06
9.05
9.03
7.94
7.92
7.90
7.88
7.86
7.86
7.83
7.82
7.81
7.80
7.79
7.78
7.71
7.69
7.68
7.66
7.55
7.54
7.54
7.53
7.52
7.51
7.50
7.50
7.41
7.39
CDCl3, 400 MHz
18.5
2.02
1
1.02
ppm
9
8
7
6
5
4
3
2
1
0

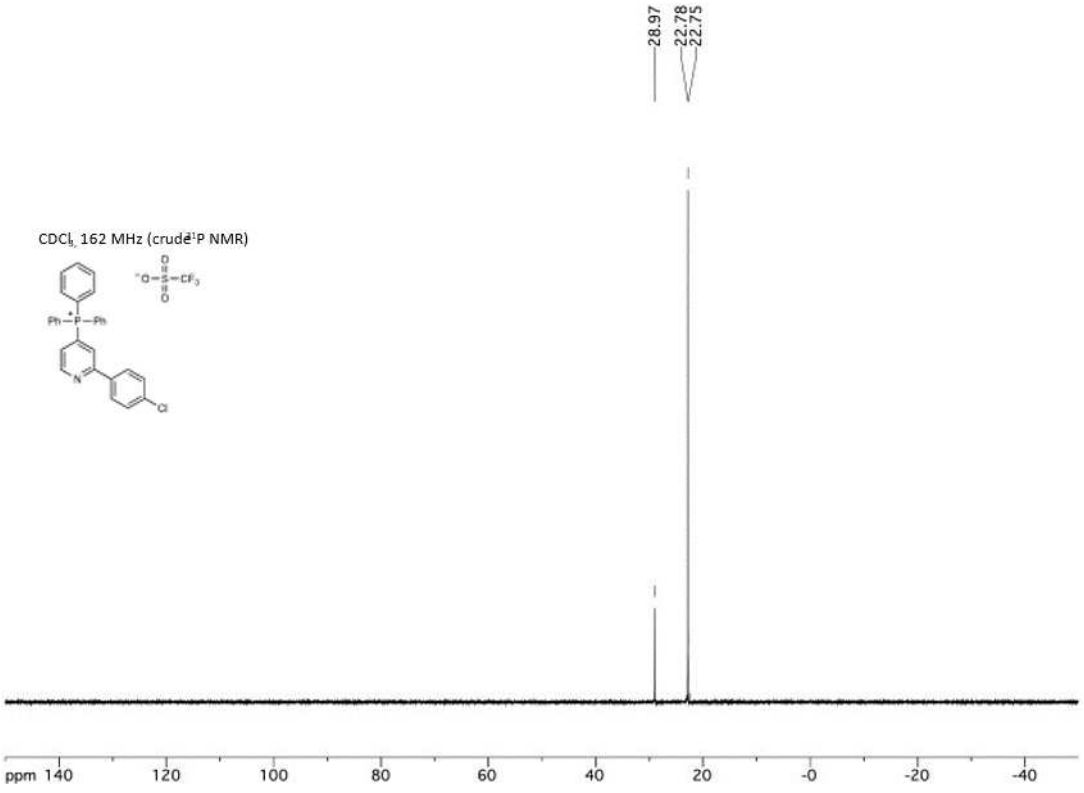
28.97
22.78
22.75
CDCl3, 162 MHz (crude) 31P NMR)
ppm 140
120
100
80
60
40
20
-0
-20
-40

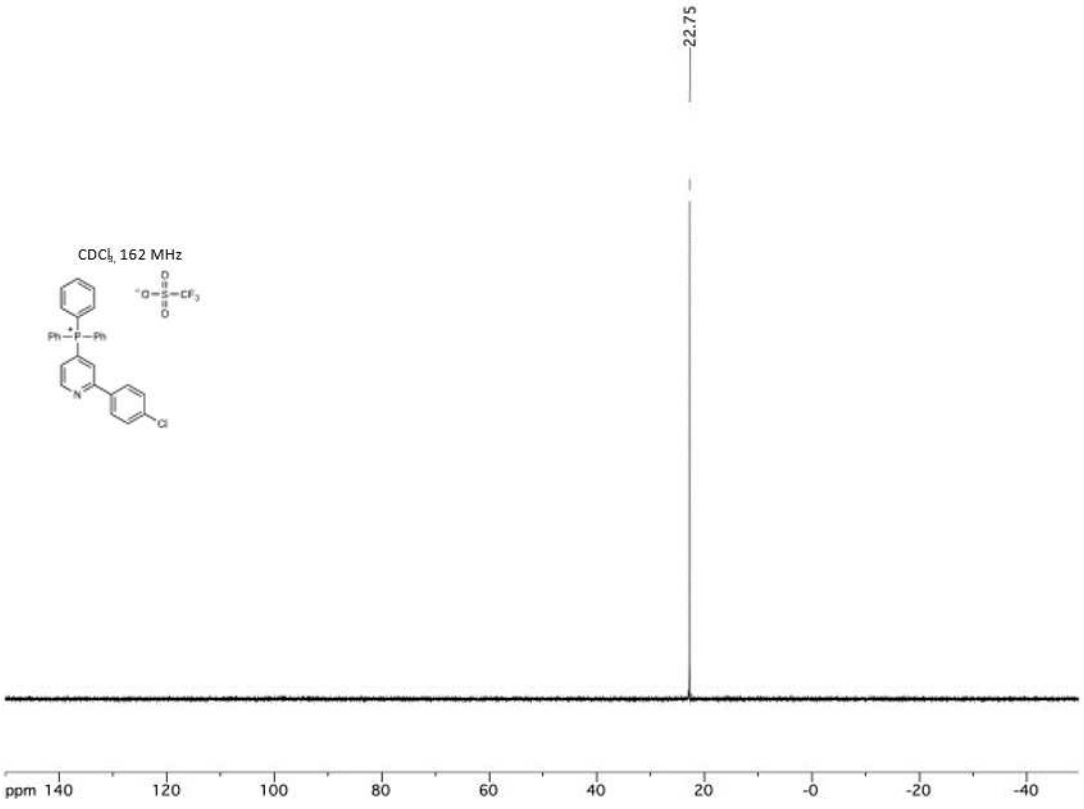
22.75
CDCl3, 162 MHz
ppm 140
120
100
80
60
40
20
-0
-20
-40

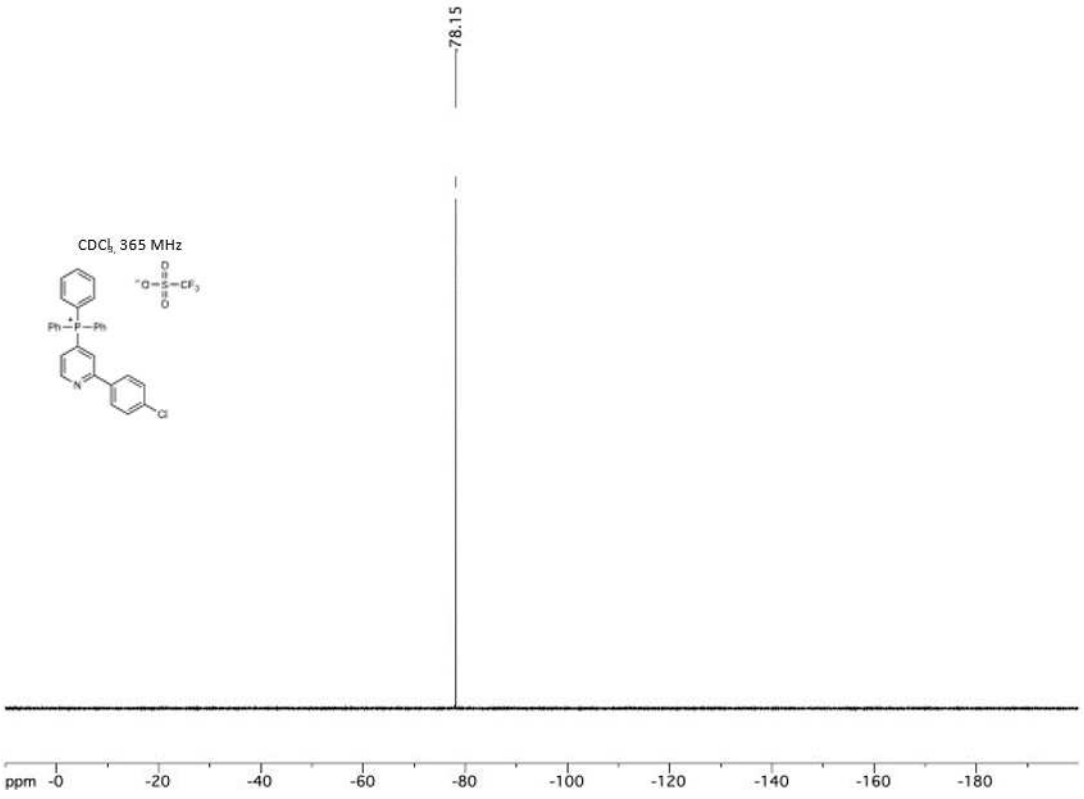
78.15
CDCl3, 365 MHz
ppm -0 -20 -40 -60 -80 -100 -120 -140 -160 -180

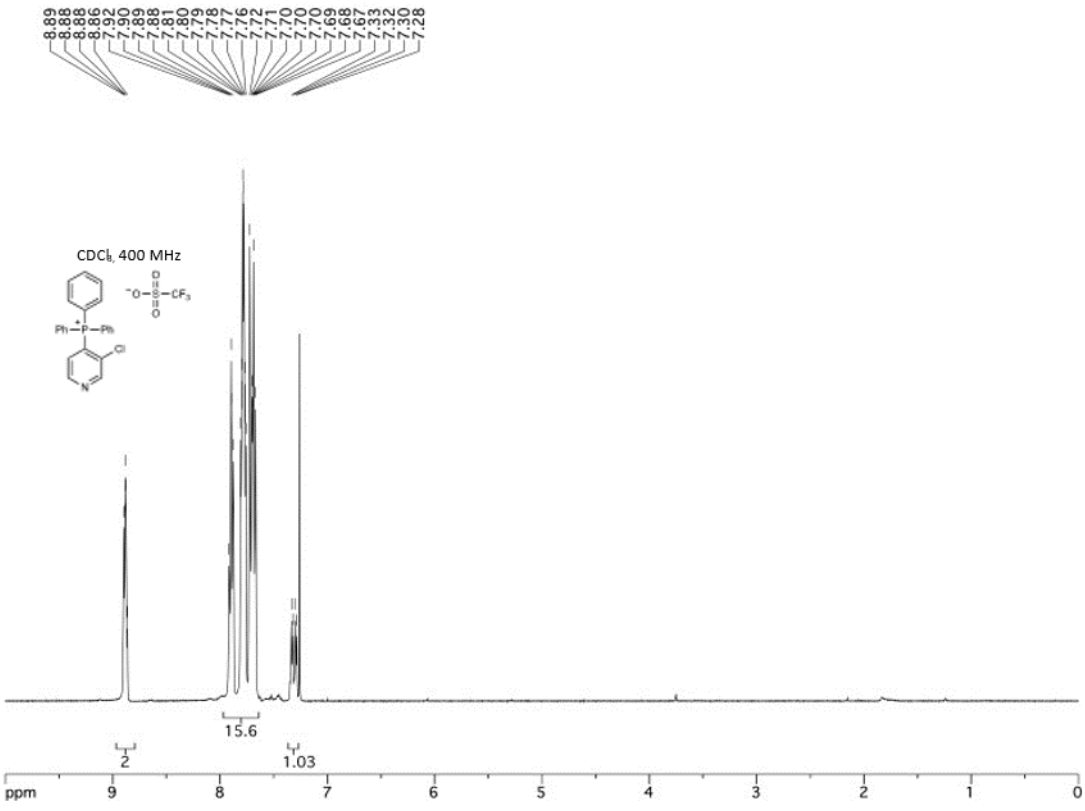
8.89 8.88 8.88 8.86 7.92 7.90 7.89 7.88 7.81 7.80 7.79 7.78 7.77 7.76 7.72 7.71 7.70 7.70 7.70 7.69 7.68 7.67 7.33 7.32 7.30 7.28
CDCl3, 400 MHz
15.6
2
1.03
ppm 9 8 7 6 5 4 3 2 1 0

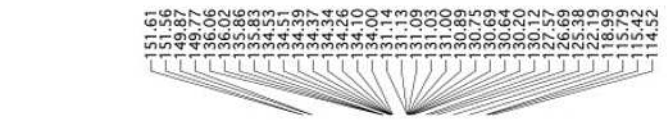
151.61
151.56
149.87
149.77
136.06
136.02
135.86
135.83
134.53
134.51
134.39
134.37
134.34
134.26
134.10
134.00
131.14
131.13
131.09
131.03
131.00
130.89
130.75
130.69
130.64
130.20
130.12
127.57
126.69
125.38
122.19
118.99
115.79
115.42
114.52

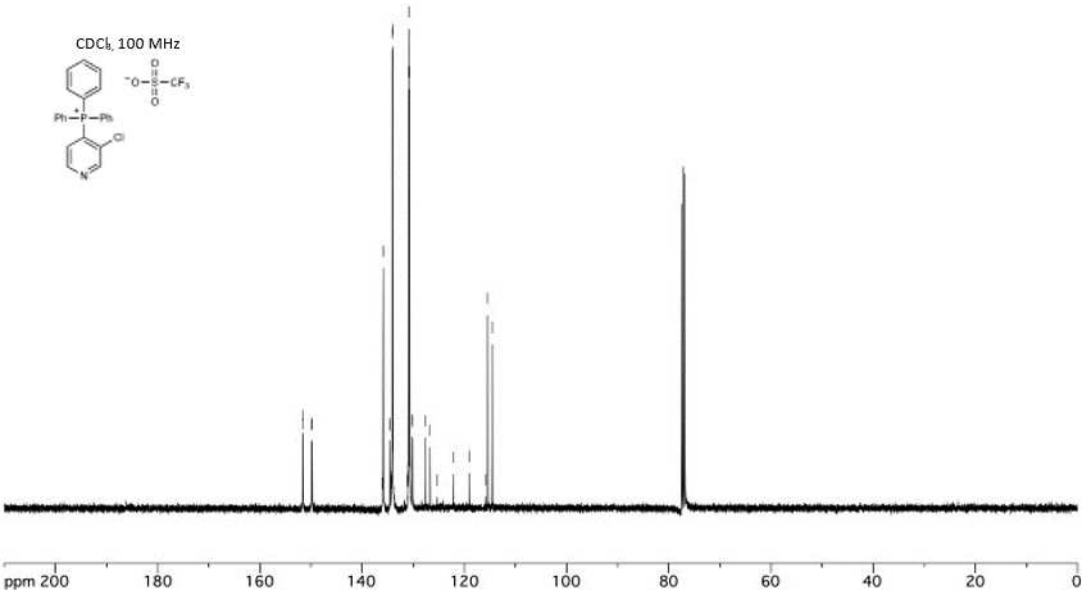
CDCl3, 100 MHz
ppm 200
180
160
140
120
100
80
60
40
20
0

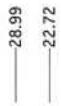
28.99
22.72

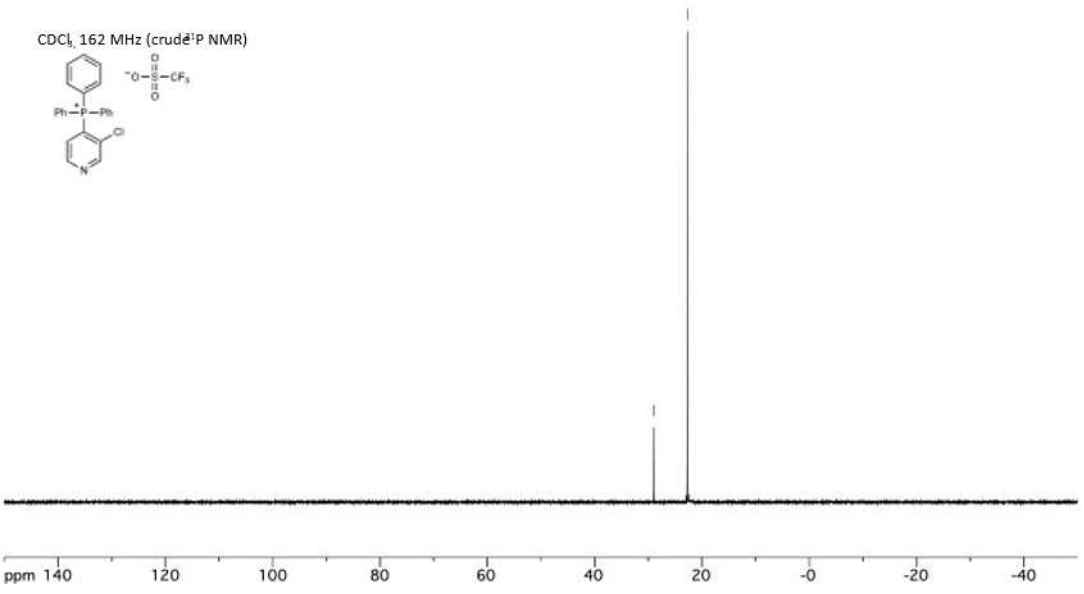
CDCl3, 162 MHz (crude 31P NMR)
ppm 140
120
100
80
60
40
20
-0
-20
-40

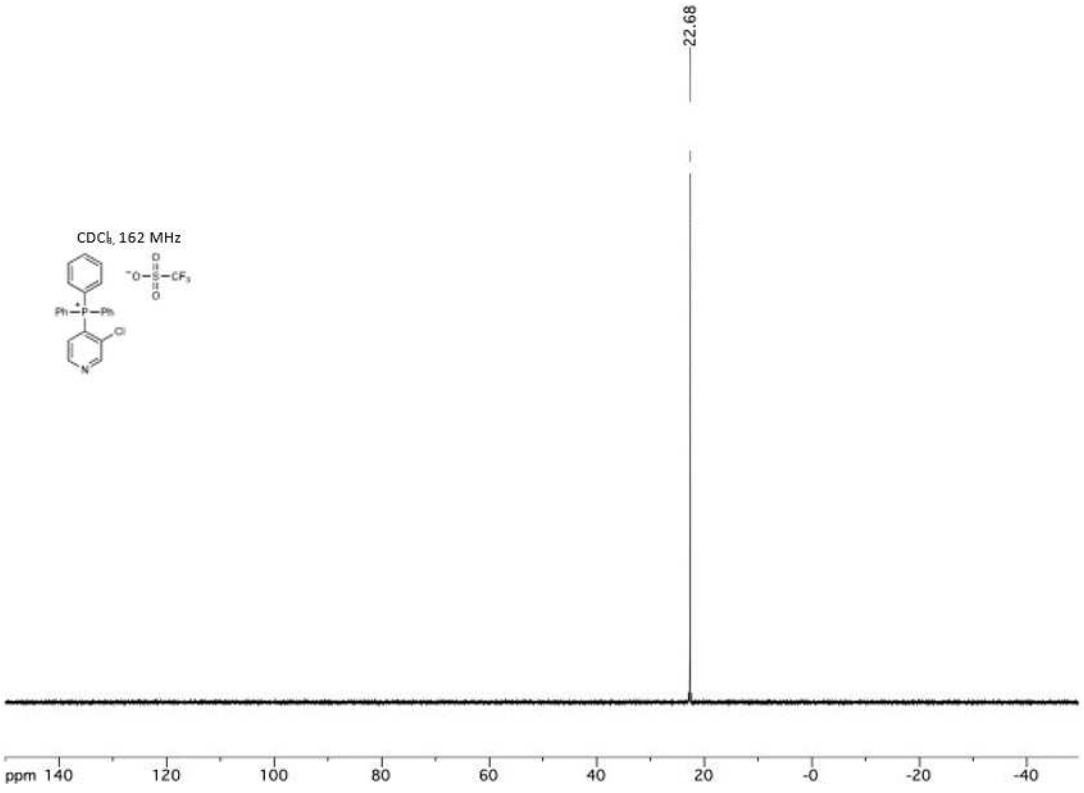
22.68
CDCl3, 162 MHz
ppm 140
120
100
80
60
40
20
-0
-20
-40

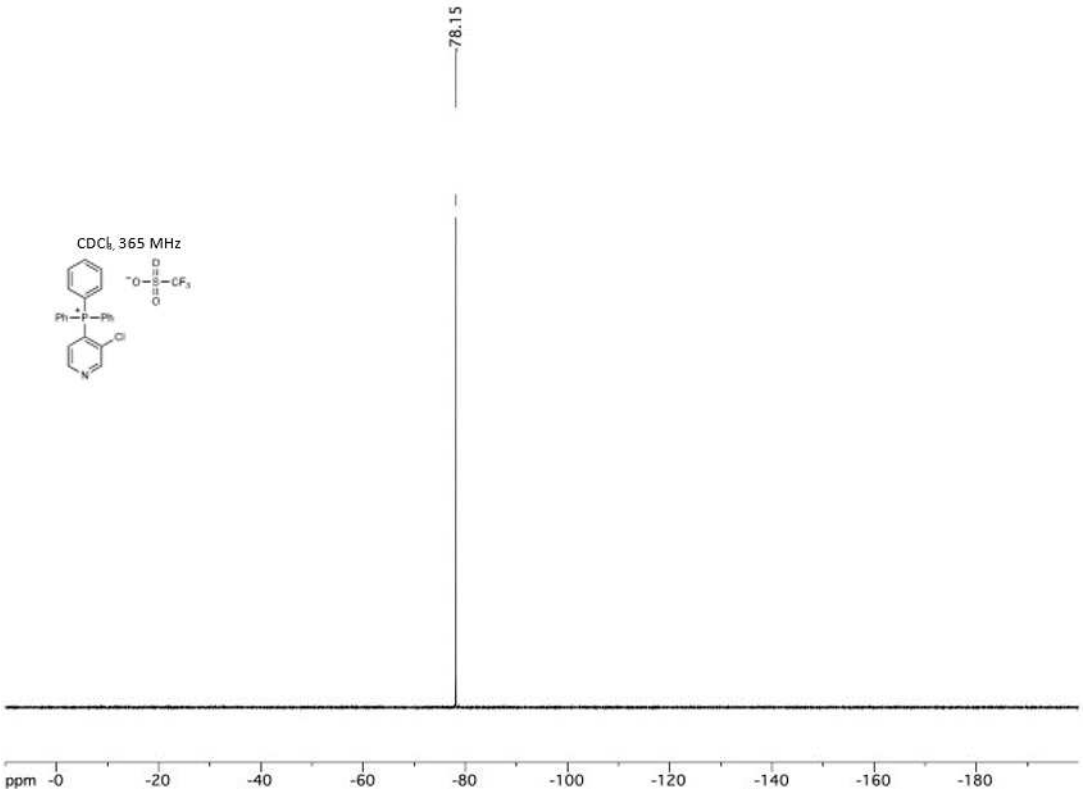
78.15
CDCl3, 365 MHz
ppm -0
-20
-40
-60
-80
-100
-120
-140
-160
-180

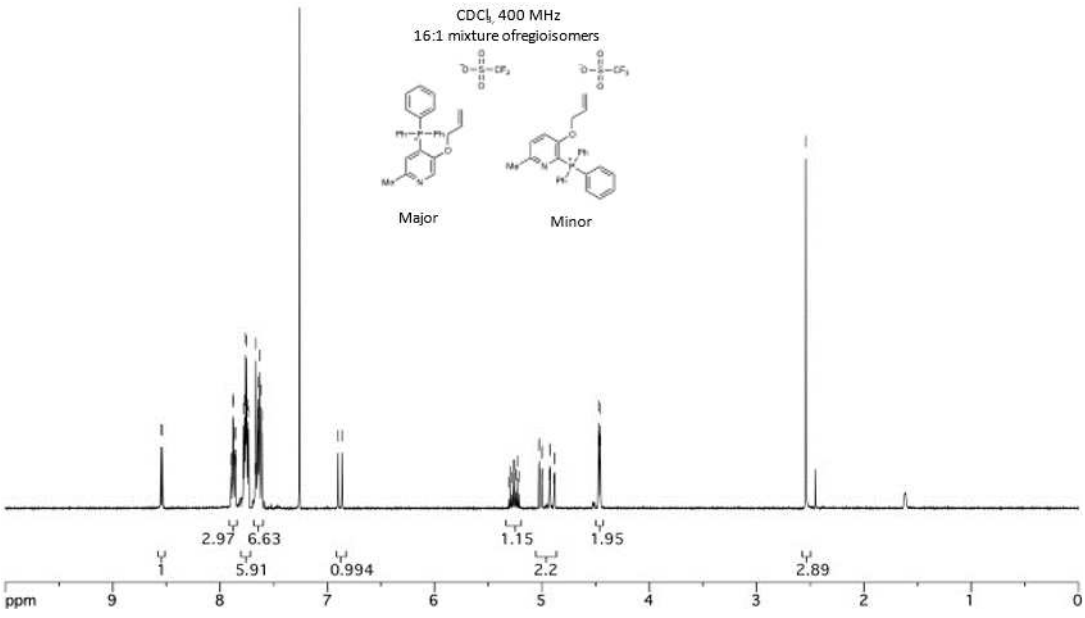
CDCl3 400 MHz
16:1 mixture ofregioisomers
Major
Minor
2.97
6.63
1.15
1.95
1
5.91
0.994
2.2
2.89
ppm

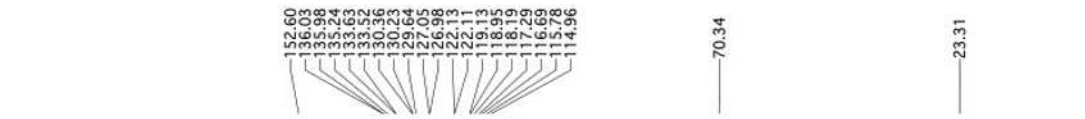

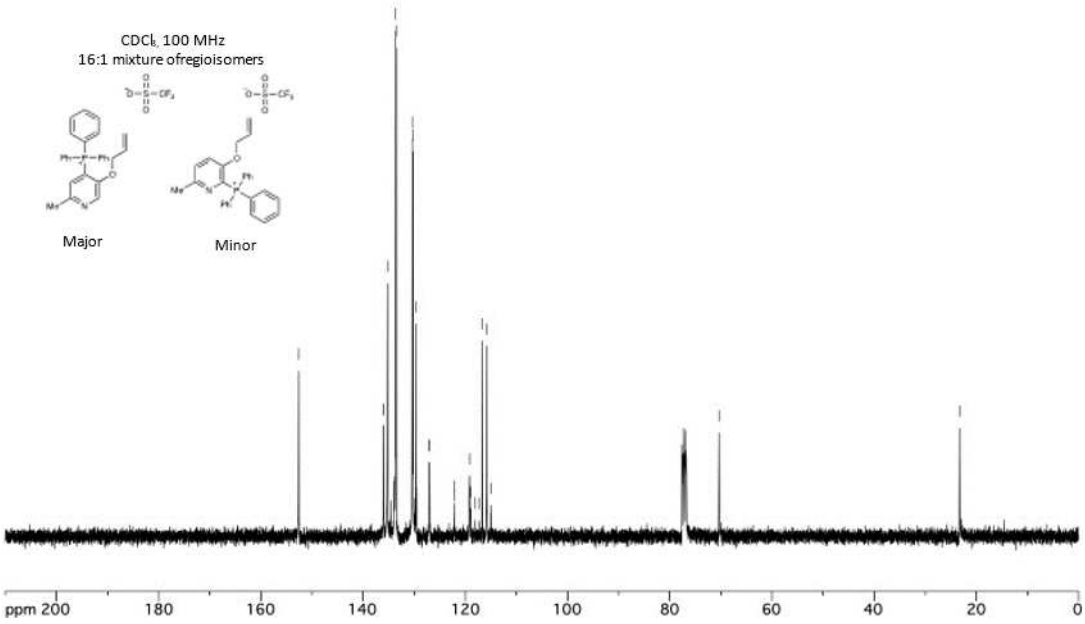
CDCl3 100 MHz
16:1 mixture ofregioisomers
Major
Minor
ppm

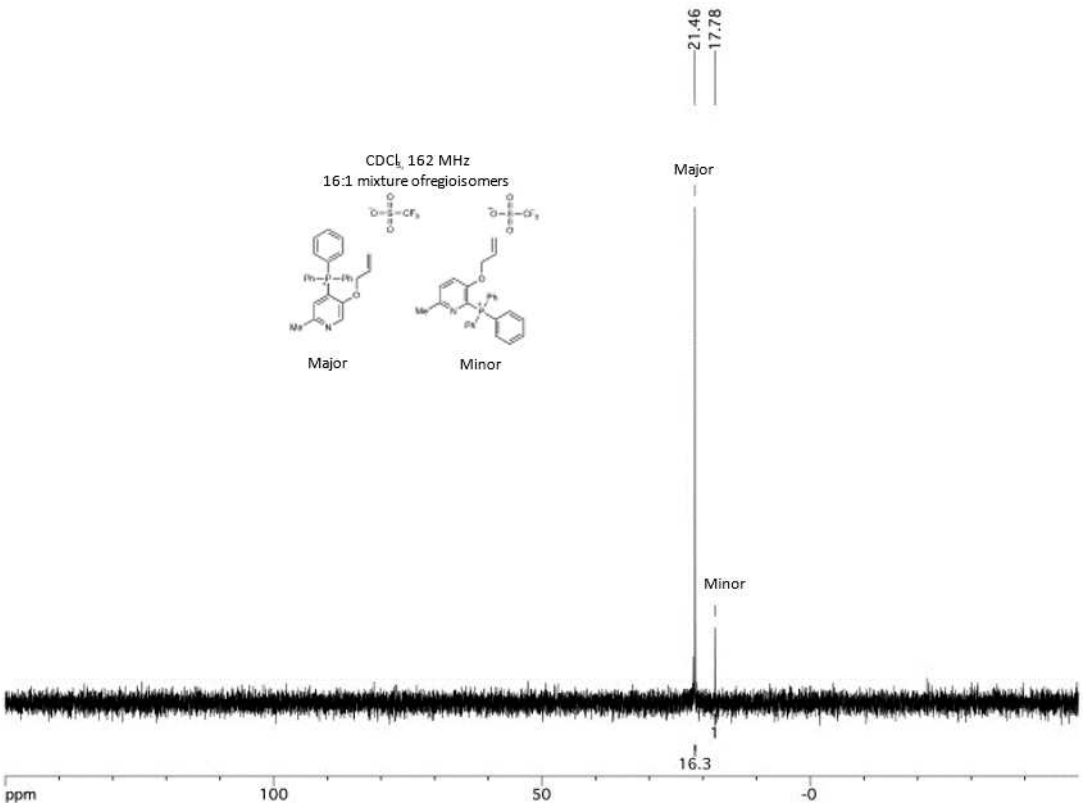
21.46
17.78
CDCl3, 162 MHz
16:1 mixture ofregioisomers
Major
Minor
Major
Minor
1
16.3
ppm
100
50
-0

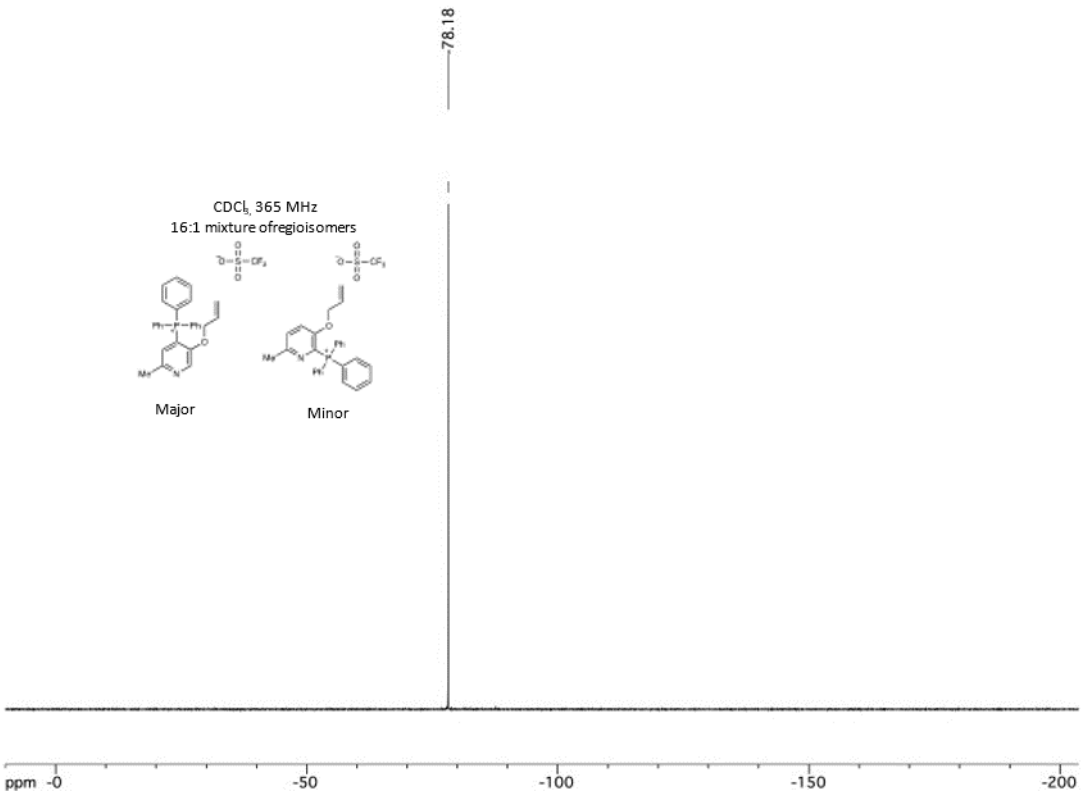
78.18
CDCl3, 365 MHz
16:1 mixture ofregioisomers
Major
Minor
ppm -0
-50
-100
-150
-200

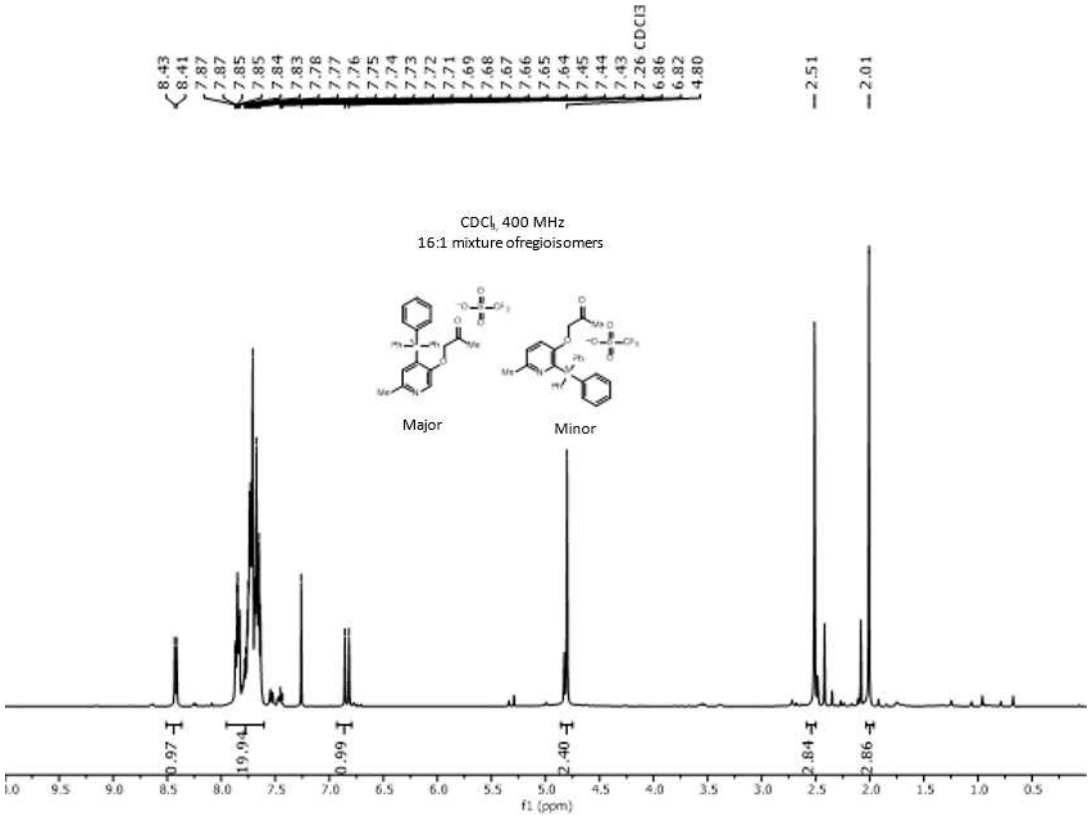
8.43
8.41
7.87
7.87
7.85
7.85
7.84
7.83
7.78
7.77
7.76
7.75
7.74
7.73
7.72
7.71
7.69
7.68
7.67
7.66
7.65
7.64
7.45
7.44
7.43
7.26 CDCl3
6.86
6.82
4.80
2.51
2.01
CDCl3 400 MHz
16:1 mixture ofregioisomers
Major
Minor
0.97
19.94
0.99
2.40
2.84
2.86
f1 (ppm)

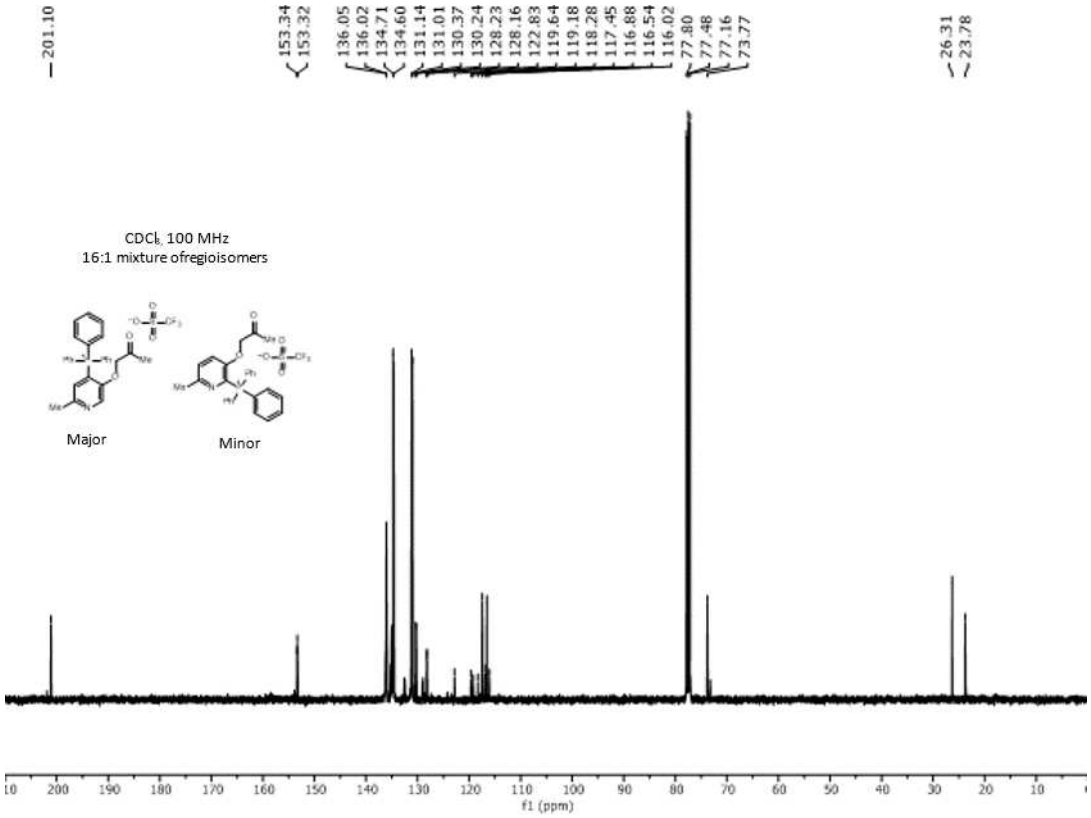
201.10
153.34
153.32
136.05
136.02
134.71
134.60
131.14
131.01
130.37
130.24
128.23
128.16
122.83
119.64
119.18
118.28
117.45
116.88
116.54
116.02
77.80
77.48
77.16
73.77
26.31
23.78
CDCl3 100 MHz
16:1 mixture ofregioisomers
Major
Minor
f1 (ppm)

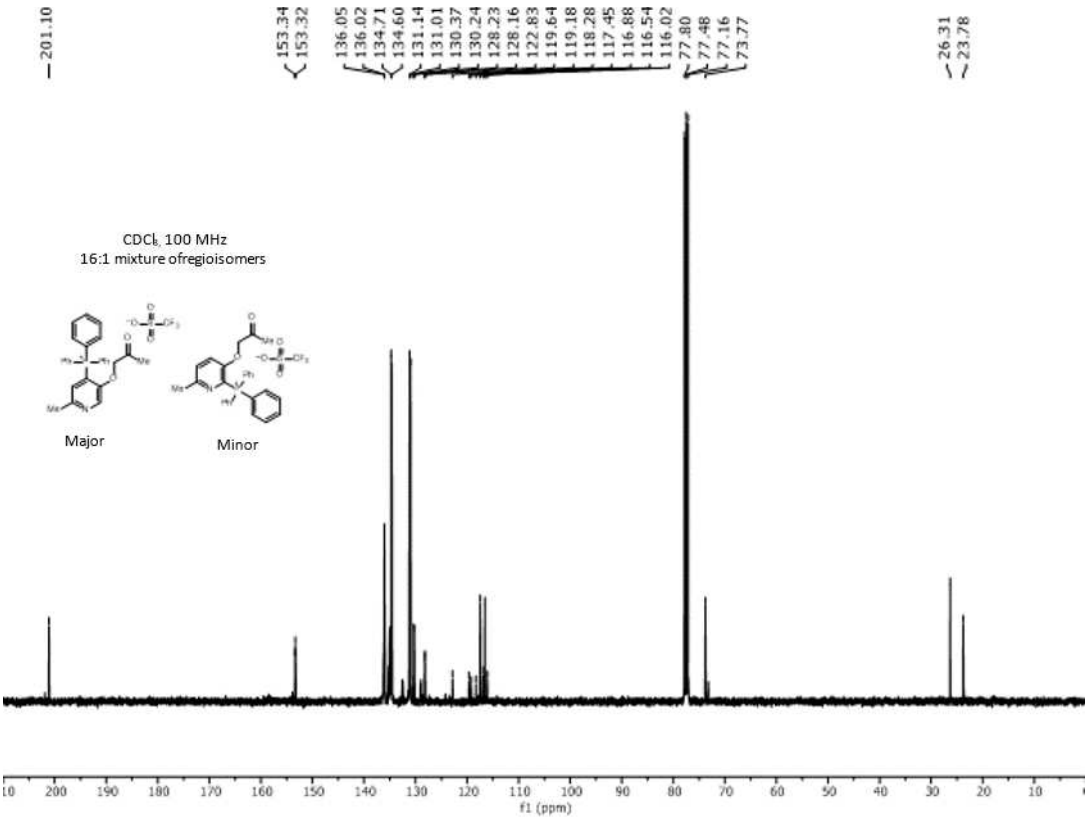
201.10
153.34
153.32
136.05
136.02
134.71
134.60
131.14
131.01
130.37
130.24
128.23
128.16
122.83
119.64
119.18
118.28
117.45
116.88
116.54
116.02
77.80
77.48
77.16
73.77
26.31
23.78
CDCl3 100 MHz
16:1 mixture ofregioisomers
Major
Minor
f1 (ppm)

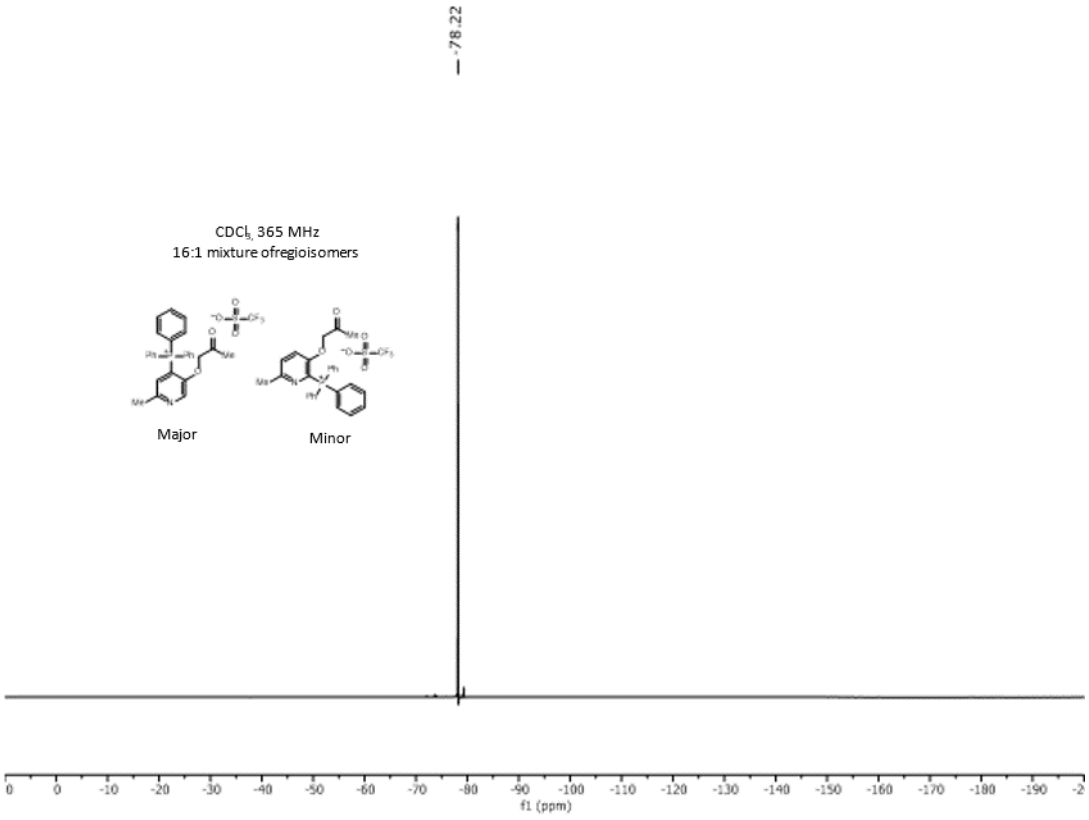
-78.22
CDCl3 365 MHz
16:1 mixture ofregioisomers
Major
Minor
f1 (ppm)

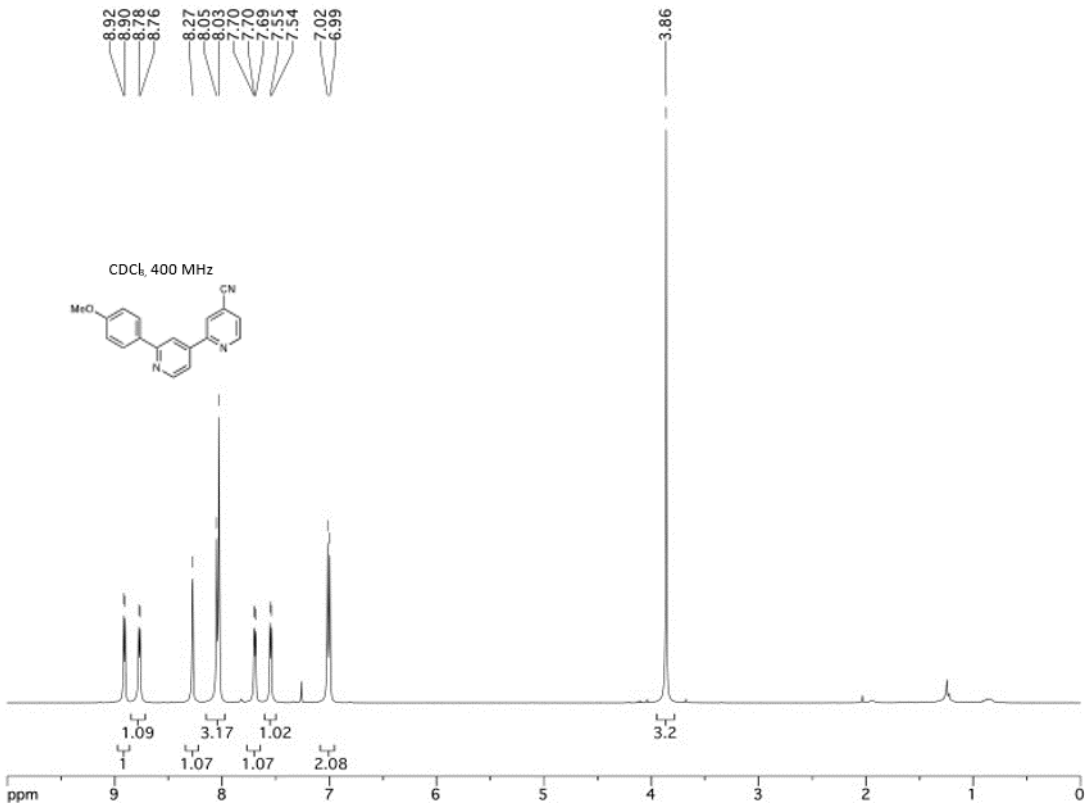
8.92
8.90
8.78
8.76
8.27
8.05
8.03
7.70
7.70
7.69
7.55
7.54
7.02
6.99
3.86
CDCl3 400 MHz
MeO
CN
N
N
1.09
3.17
1.02
3.2
1
1.07
1.07
2.08
ppm
9
8
7
6
5
4
3
2
1
0

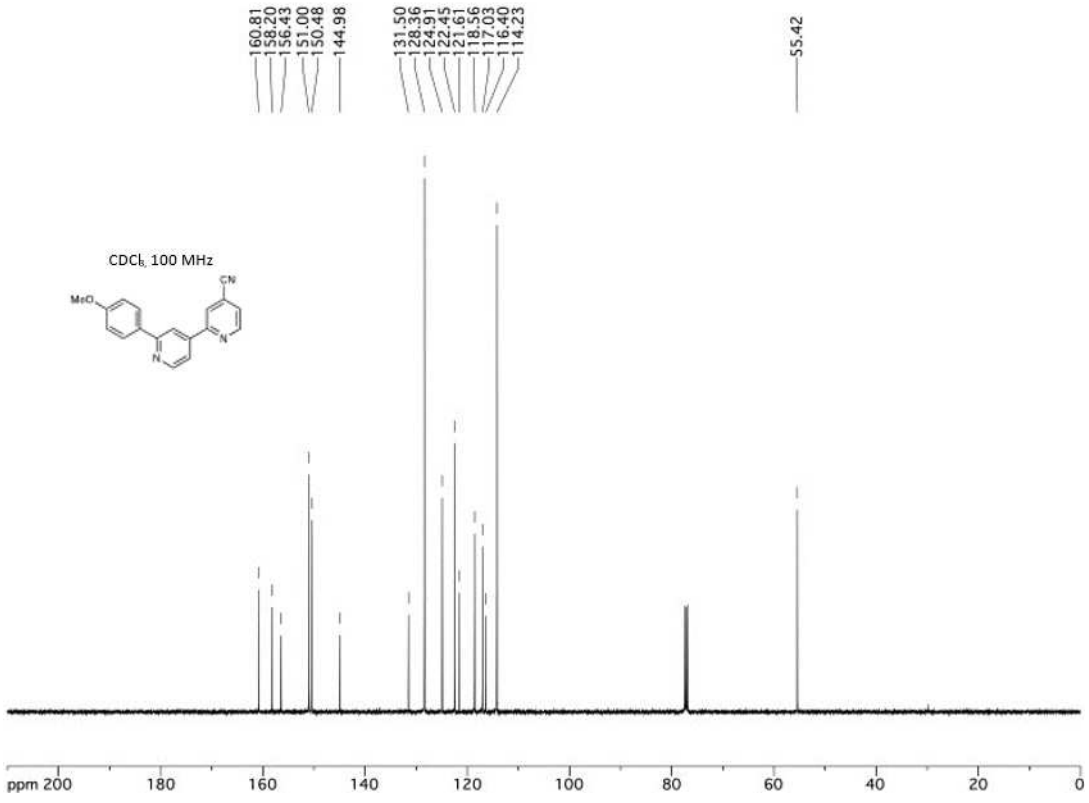
160.81
158.20
156.43
151.00
150.48
144.98
131.50
128.36
124.91
122.45
121.61
118.56
117.03
116.40
114.23
55.42
CDCl3 100 MHz
MeO
CN
N
N
ppm 200
180
160
140
120
100
80
60
40
20
0

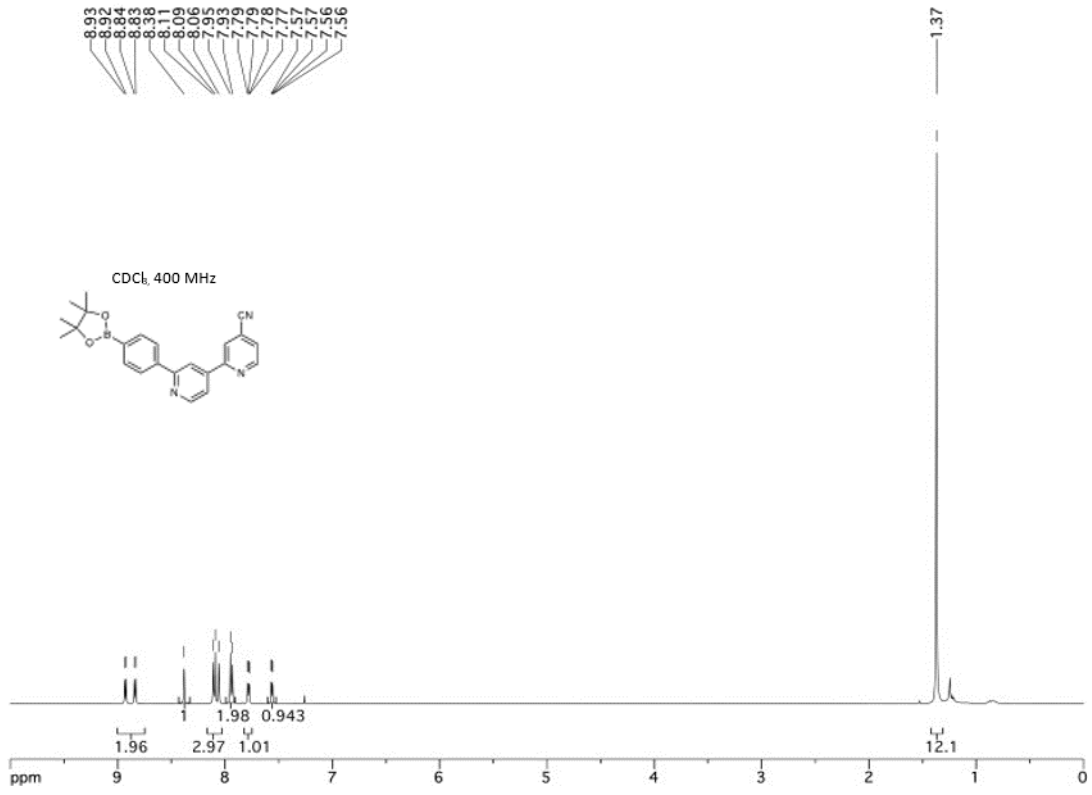
8.93
8.92
8.84
8.83
8.38
8.11
8.09
8.06
7.95
7.93
7.79
7.79
7.78
7.77
7.57
7.57
7.56
7.56
1.37
CDCl3 400 MHz
CN
N
N
1
1.98
0.943
1.96
2.97
1.01
12.1
ppm
9
8
7
6
5
4
3
2
1
0

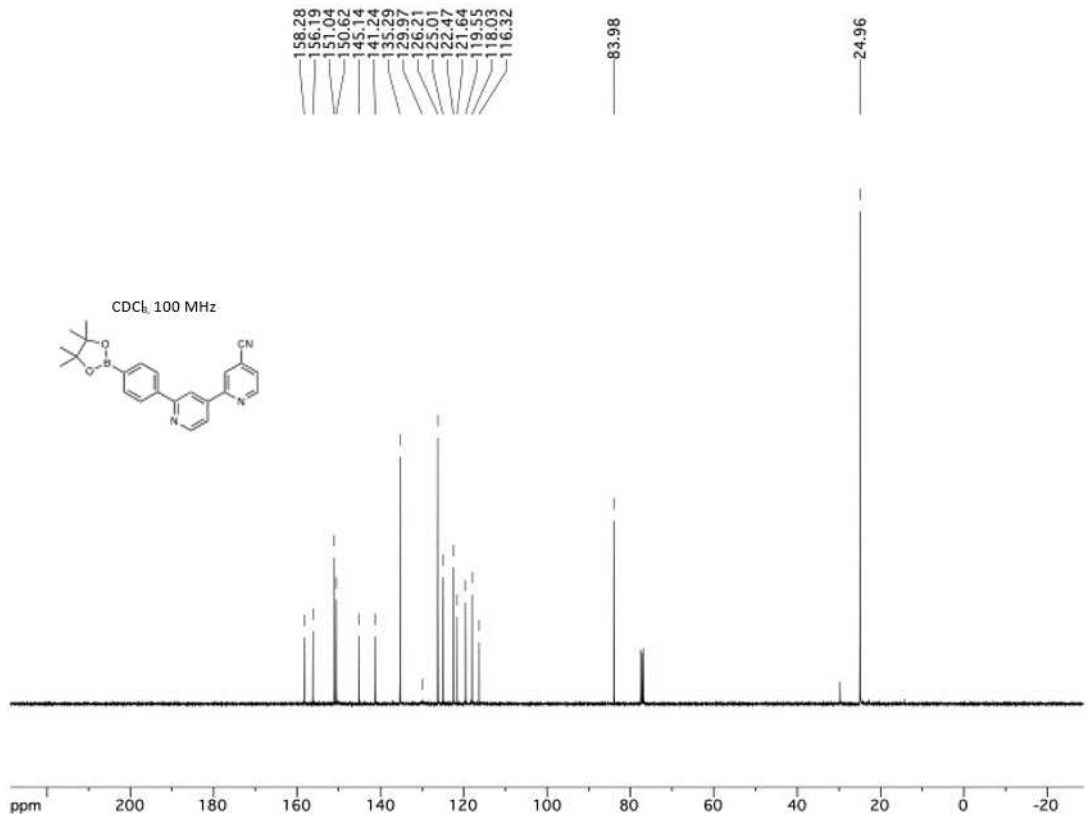
158.28
156.19
151.04
150.62
145.14
141.24
135.29
129.97
126.21
125.01
122.47
121.64
119.55
118.03
116.32
83.98
24.96
CDCl3 100 MHz
CN
N
N
ppm
200
180
160
140
120
100
80
60
40
20
0
-20

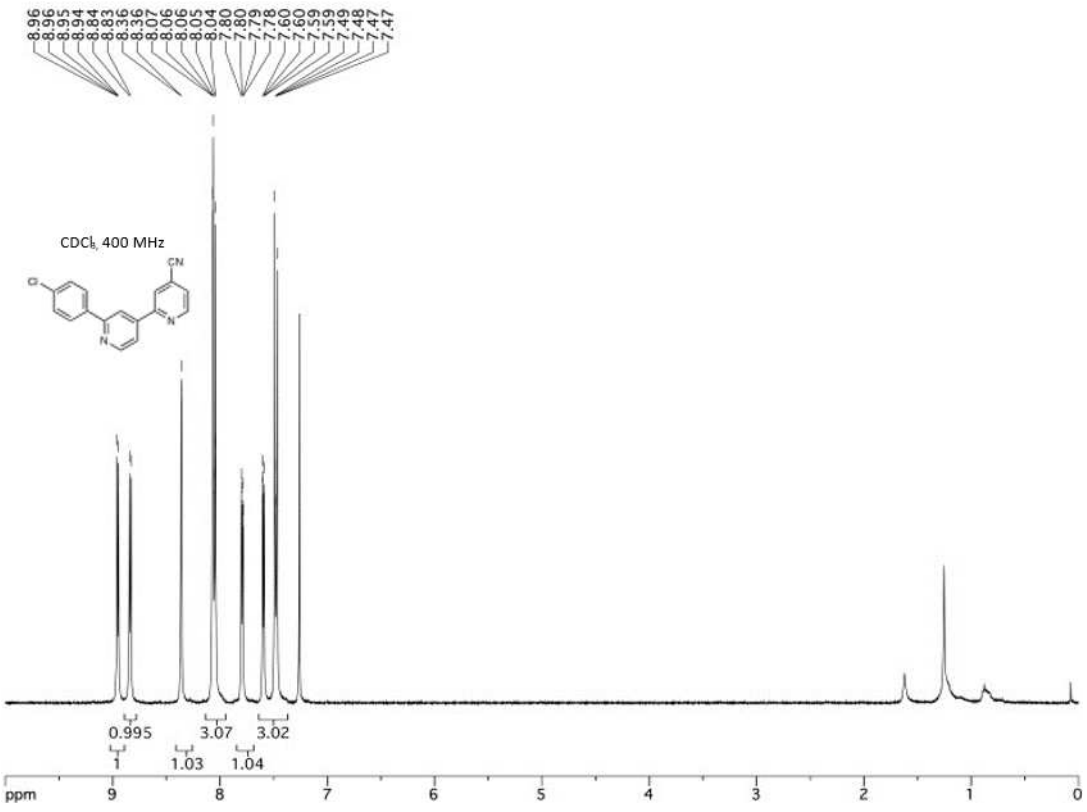
8.96
8.96
8.95
8.94
8.84
8.83
8.36
8.36
8.07
8.06
8.06
8.05
8.04
7.80
7.80
7.79
7.78
7.60
7.60
7.59
7.59
7.49
7.48
7.47
7.47
CDCl3, 400 MHz
CN
Cl
N
N
0.995
3.07
3.02
1
1.03
1.04
ppm
9
8
7
6
5
4
3
2
1
0

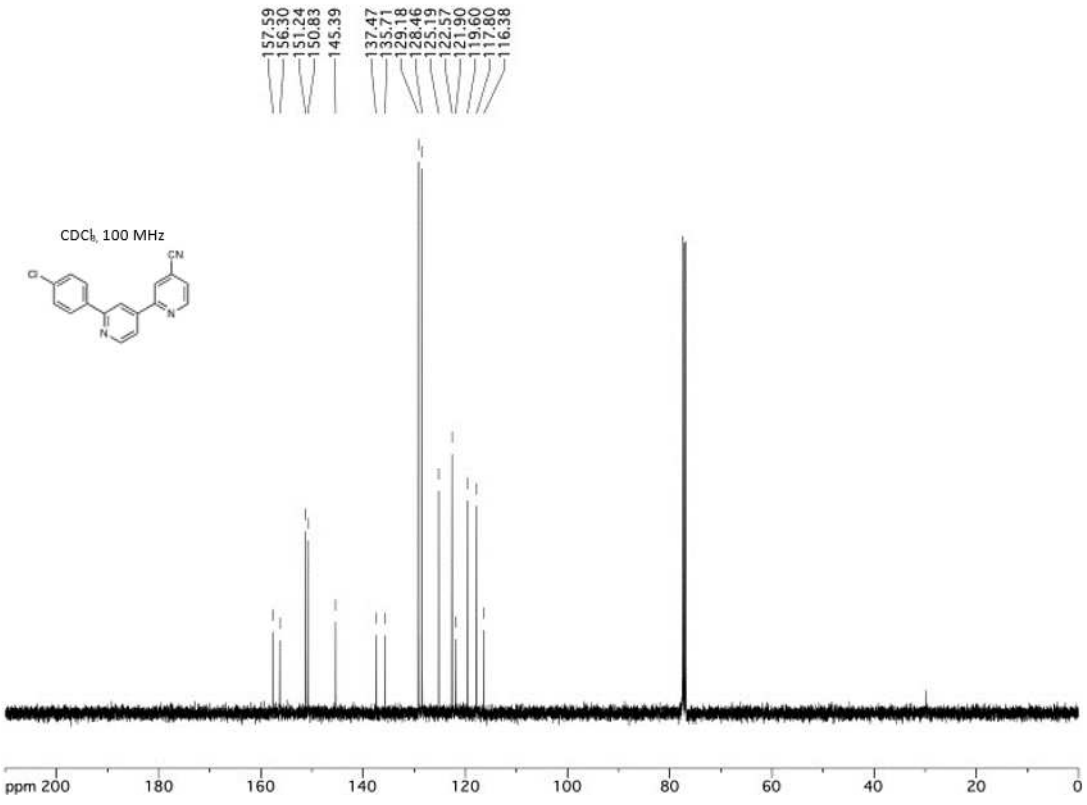
157.59
156.30
151.24
150.83
145.39
137.47
135.71
129.18
128.46
125.19
122.57
121.90
119.60
117.80
116.38
CDCl3, 100 MHz
CN
Cl
N
N
ppm 200
180
160
140
120
100
80
60
40
20
0

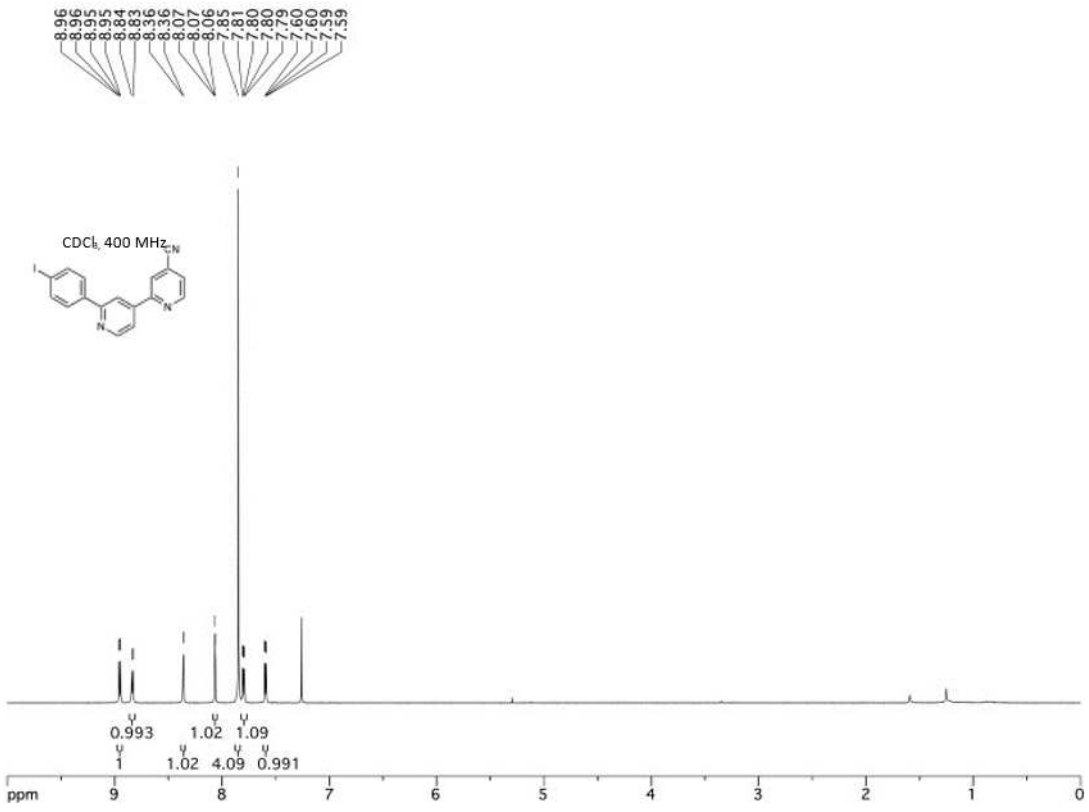
8.96
8.96
8.95
8.95
8.84
8.83
8.36
8.36
8.07
8.07
8.06
7.85
7.81
7.80
7.80
7.79
7.60
7.60
7.59
7.59
CDCl3, 400 MHz
0.993
1.02
1.09
1
1.02
4.09
0.991
ppm
9
8
7
6
5
4
3
2
1
0

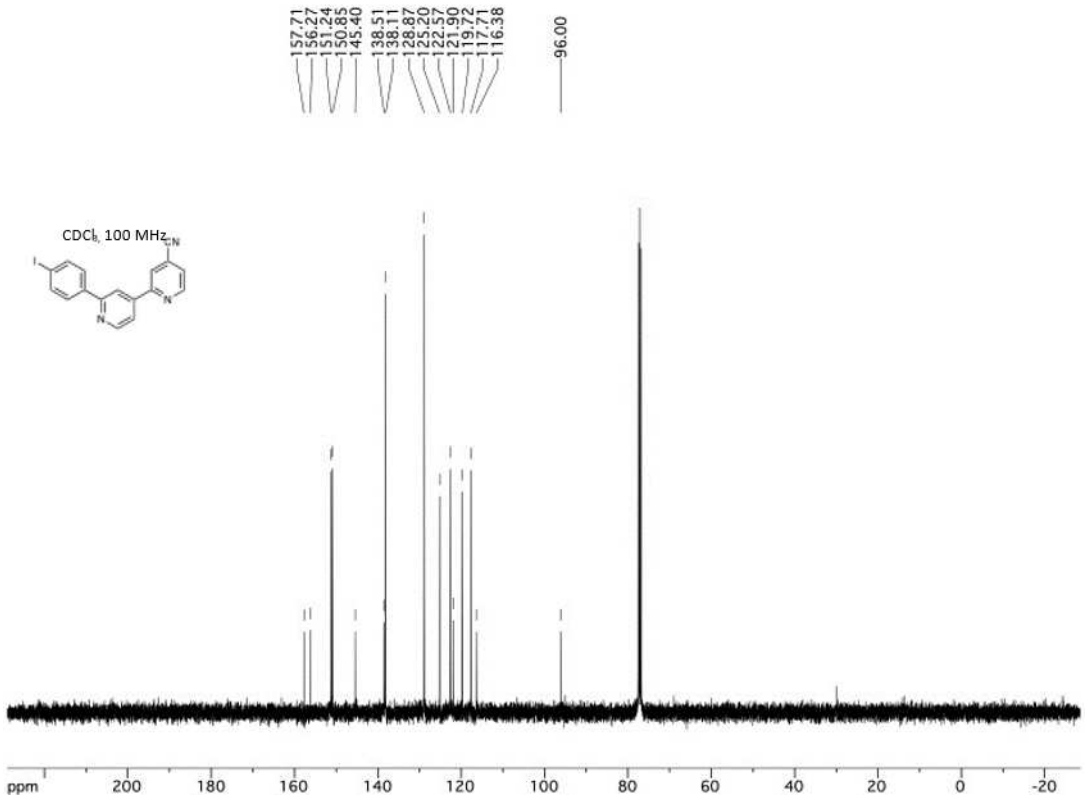
157.71
156.27
151.24
150.85
145.40
138.51
138.11
128.87
125.20
122.57
121.90
119.72
117.71
116.38
96.00
CDCl3, 100 MHz
ppm
200
180
160
140
120
100
80
60
40
20
0
-20

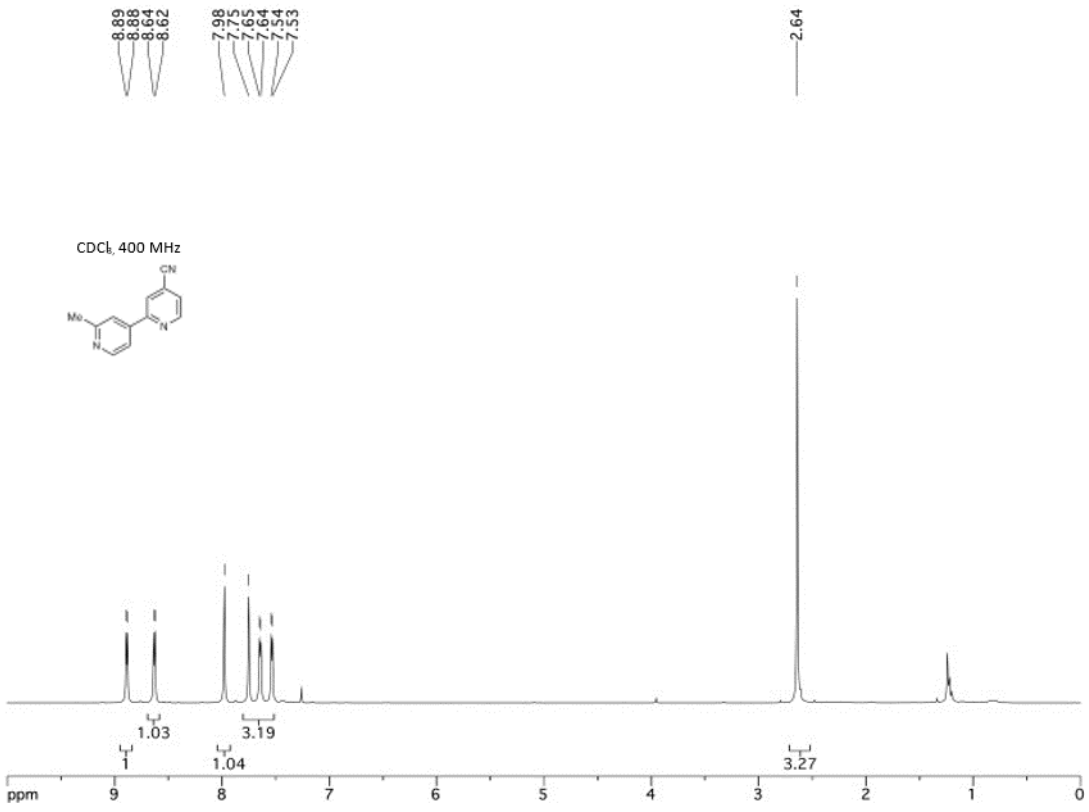
8.89
8.88
8.64
8.62
7.98
7.75
7.65
7.64
7.54
7.53
2.64
CDCl3, 400 MHz
Me
CN
N
1.03
3.19
1
1.04
3.27
ppm
9
8
7
6
5
4
3
2
1
0

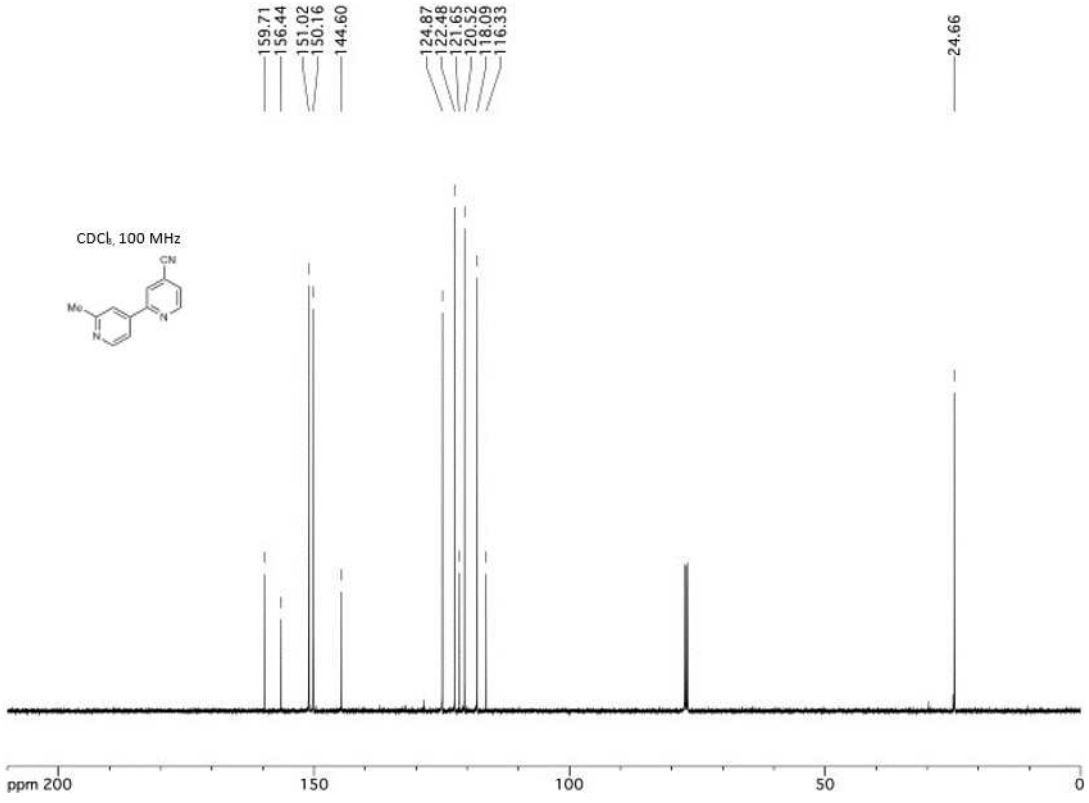
159.71
156.44
151.02
150.16
144.60
124.87
122.48
121.65
120.52
118.09
116.33
24.66
CDCl3, 100 MHz
Me
CN
N
ppm 200
150
100
50
0

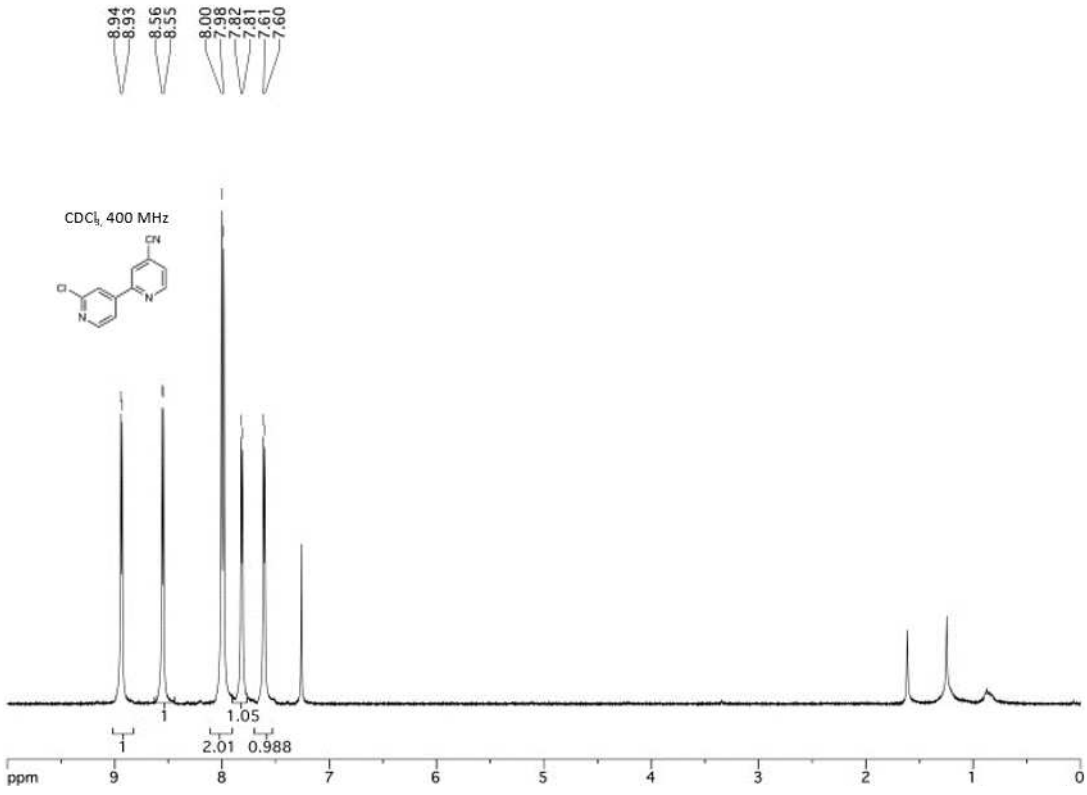
8.94
8.93
8.56
8.55
8.00
7.98
7.82
7.81
7.61
7.60
CDCl3, 400 MHz
CN
Cl
N
N
1
1.05
1
2.01
0.988
ppm
9
8
7
6
5
4
3
2
1
0

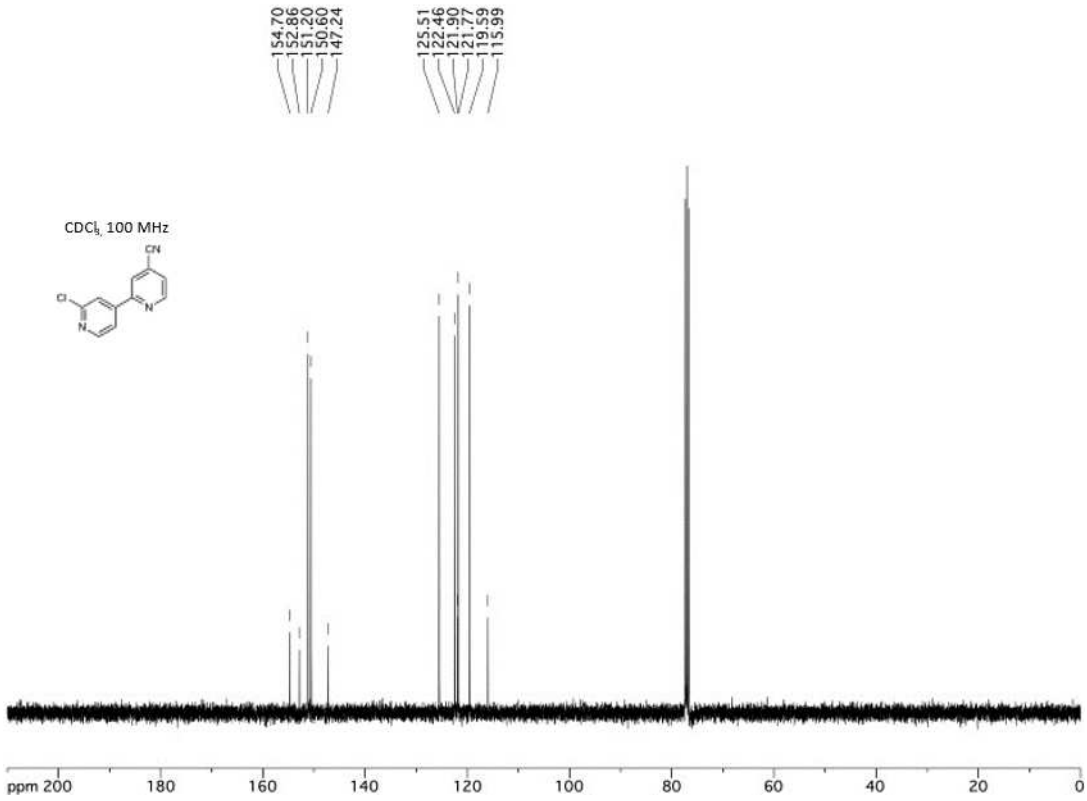
154.70
152.86
151.20
150.60
147.24
125.51
122.46
121.90
121.77
119.59
115.99
CDCl3, 100 MHz
CN
Cl
N
N
ppm 200
180
160
140
120
100
80
60
40
20
0

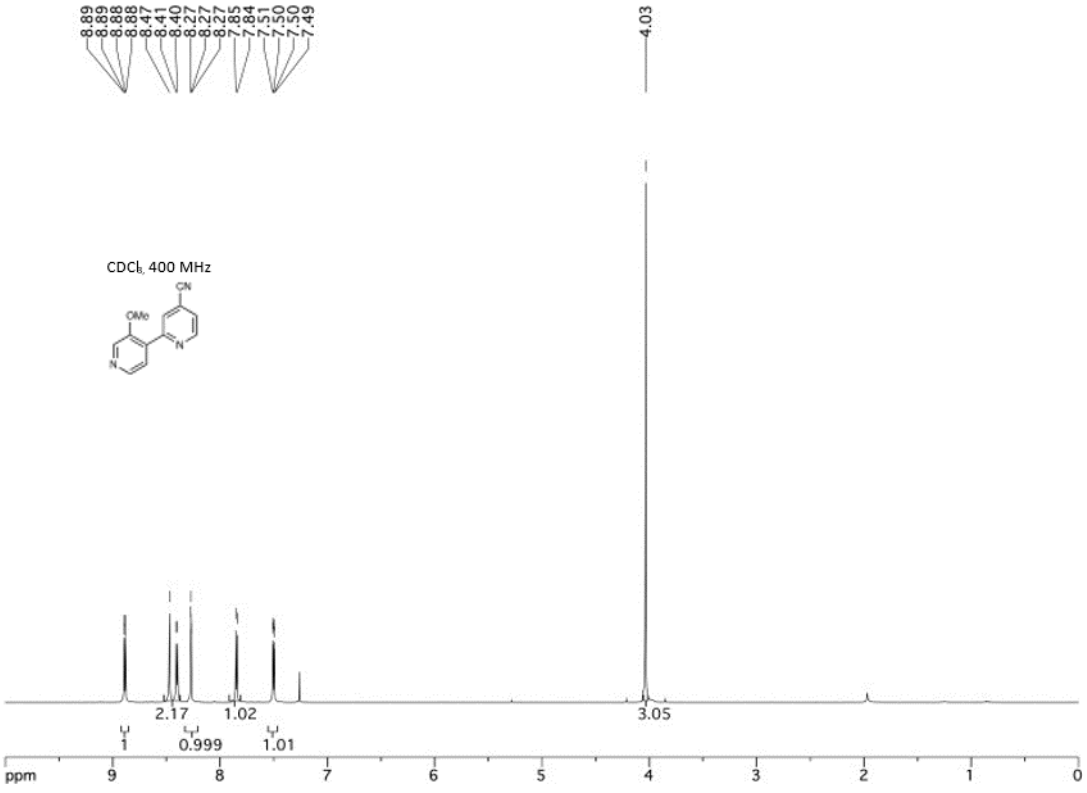
8.89
8.89
8.88
8.88
8.47
8.41
8.40
8.27
8.27
8.27
7.85
7.84
7.51
7.50
7.50
7.49
4.03
CDCl3, 400 MHz
OMe
CN
N
N
2.17
1.02
3.05
1
0.999
1.01
ppm
9
8
7
6
5
4
3
2
1
0

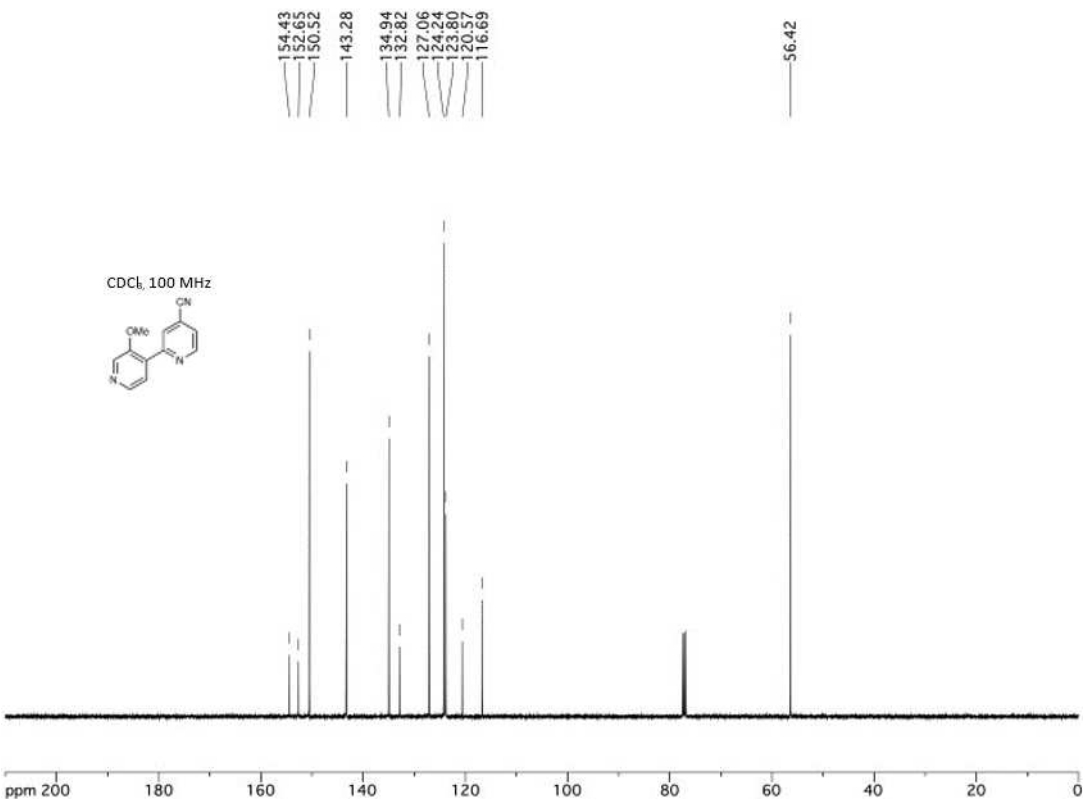
154.43
152.65
150.52
143.28
134.94
132.82
127.06
124.24
123.80
120.57
116.69
56.42
CDCl3, 100 MHz
OMe
CN
N
N
ppm 200
180
160
140
120
100
80
60
40
20
0

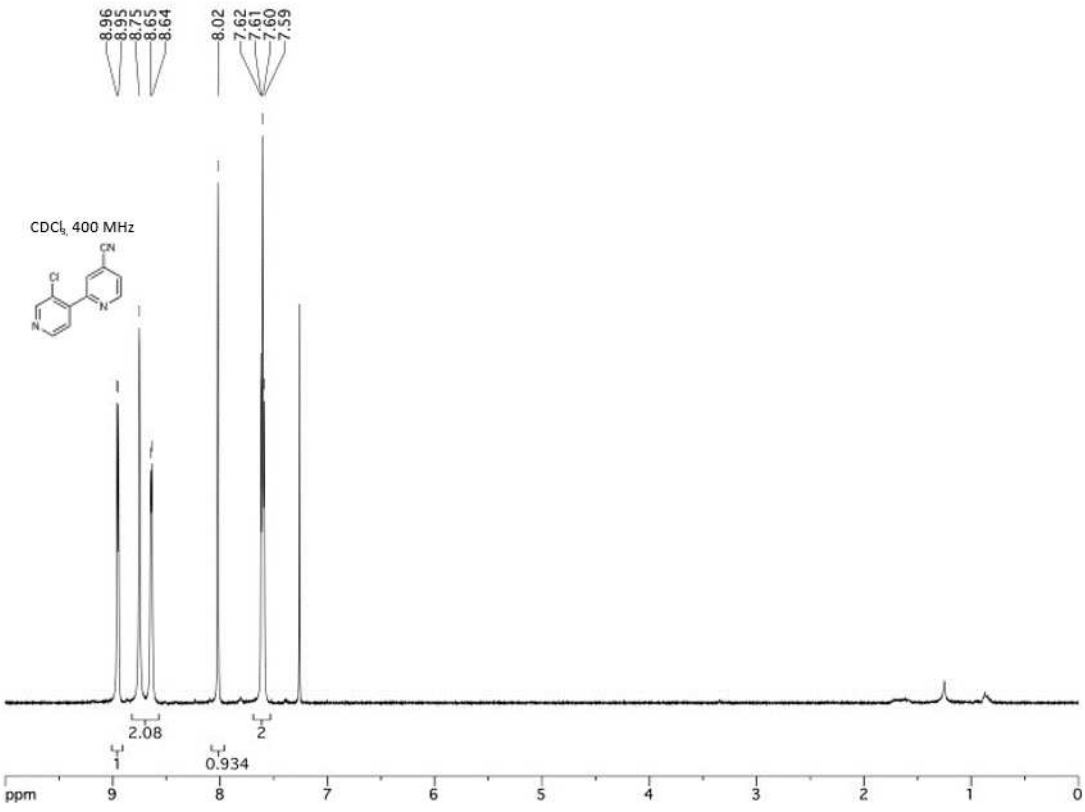
8.96
8.95
8.75
8.65
8.64
8.02
7.62
7.61
7.60
7.59
CDCl3, 400 MHz
2.08
2
1
0.934
ppm
9
8
7
6
5
4
3
2
1
0

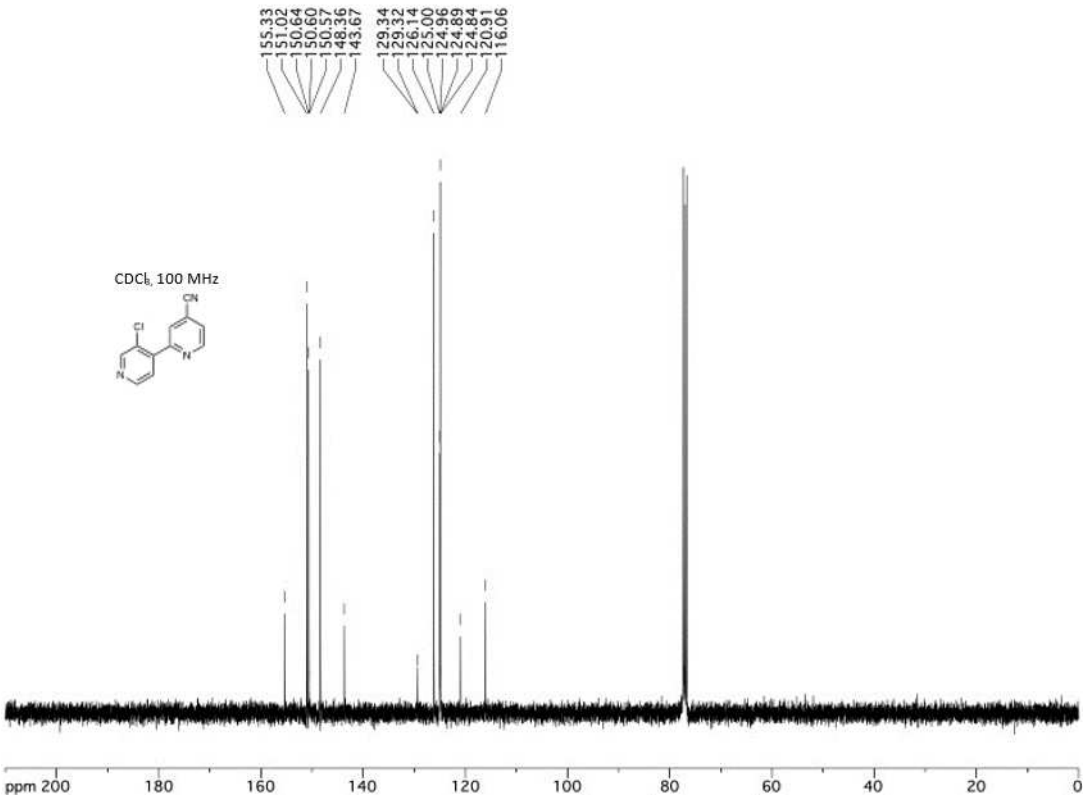
155.33
151.02
150.64
150.60
150.57
148.36
143.67
129.34
129.32
126.14
125.00
124.96
124.89
124.84
120.91
116.06
CDCl3, 100 MHz
ppm 200
180
160
140
120
100
80
60
40
20
0

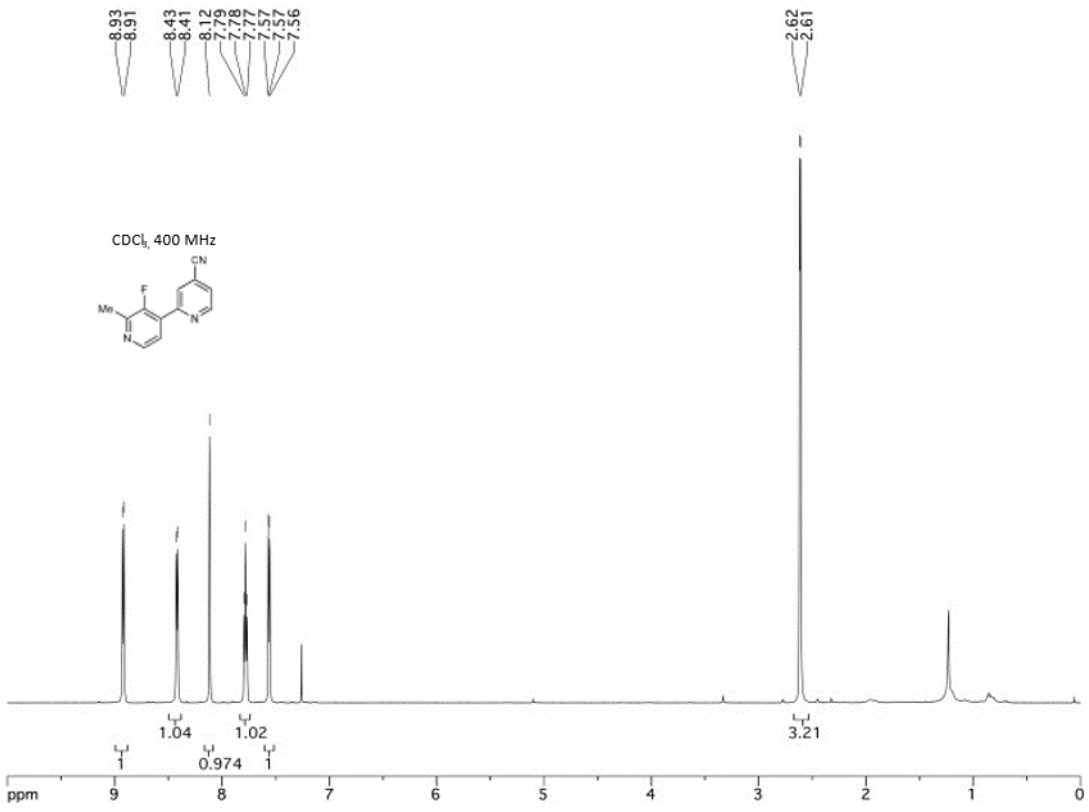
8.93
8.91
8.43
8.41
8.12
7.79
7.78
7.77
7.57
7.57
7.56
2.62
2.61
CDCl3 400 MHz
CN
F
Me
N
N
1.04
1.02
3.21
1
0.974
1
ppm
9
8
7
6
5
4
3
2
1
0

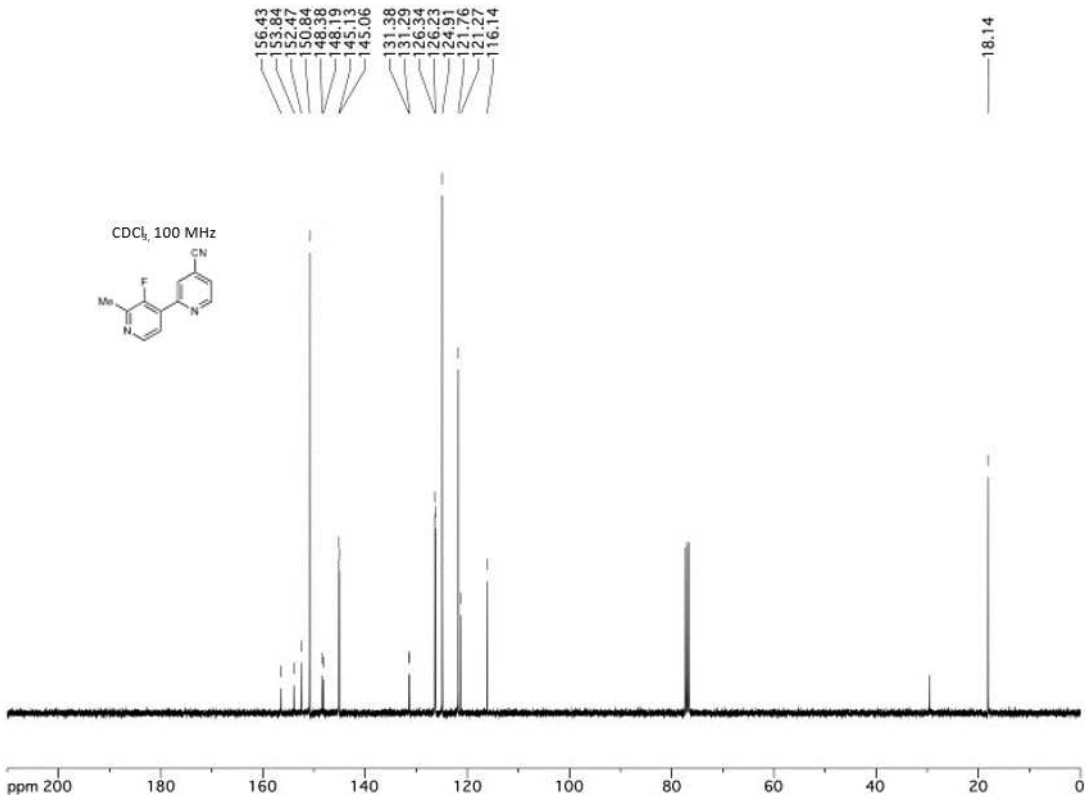
156.43
153.84
152.47
150.84
148.38
148.19
145.13
145.06
131.38
131.29
126.34
126.23
124.91
121.76
121.27
116.14
18.14
CDCl3 100 MHz
CN
F
Me
N
N
ppm 200
180
160
140
120
100
80
60
40
20
0

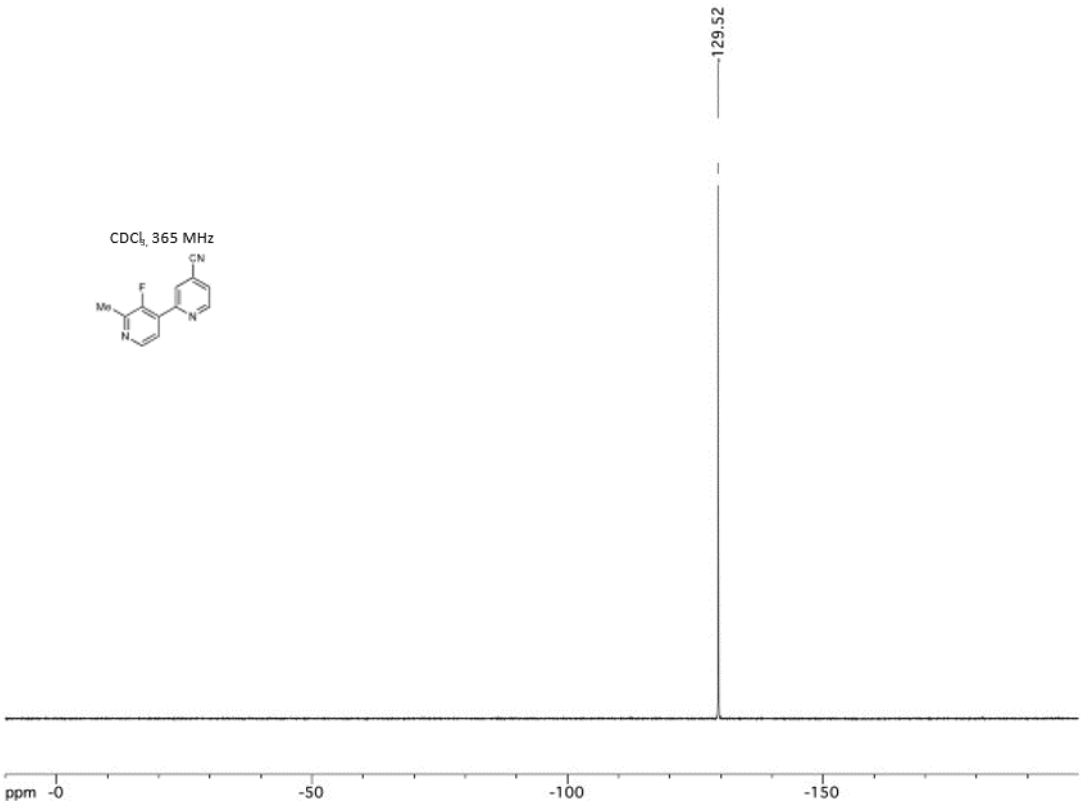
CDCl3, 365 MHz
129.52
ppm -0
-50
-100
-150

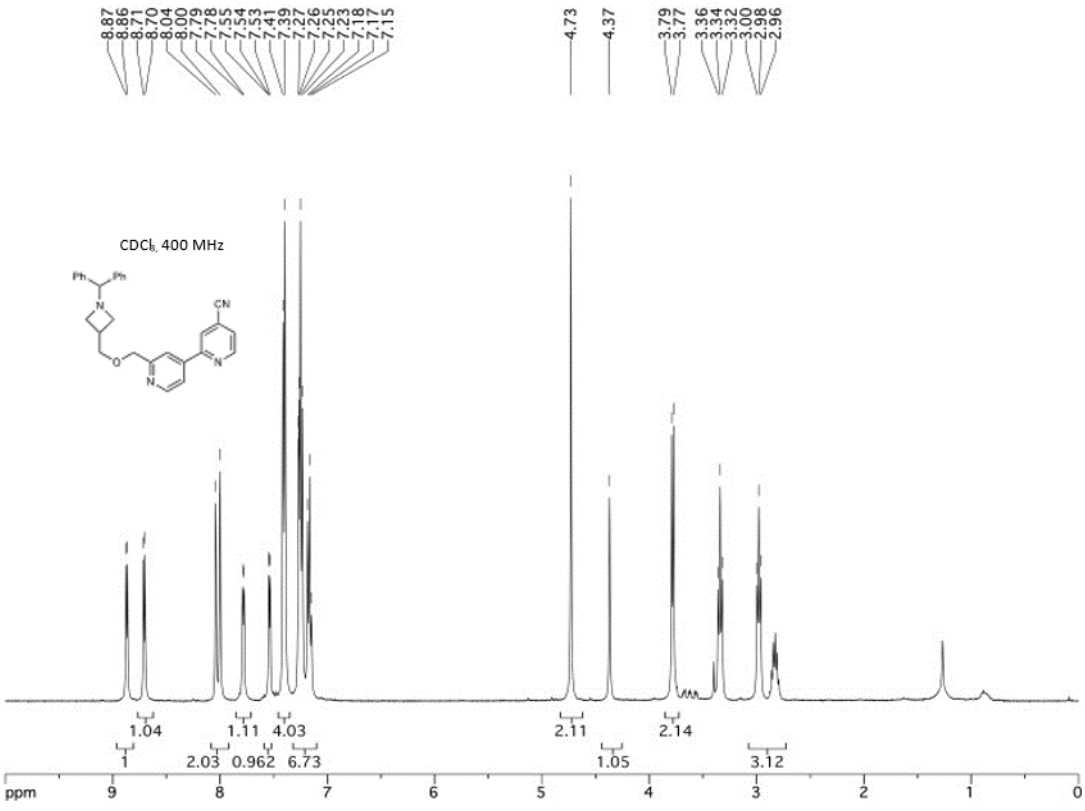
8.87
8.86
8.71
8.70
8.04
8.00
7.79
7.78
7.55
7.54
7.53
7.41
7.39
7.27
7.26
7.25
7.23
7.18
7.17
7.15
4.73
4.37
3.79
3.77
3.36
3.34
3.32
3.00
2.98
2.96
CDCl3, 400 MHz
1.04
1.11
4.03
2.11
2.14
1
2.03
0.962
6.73
1.05
3.12
ppm 9
8
7
6
5
4
3
2
1
0

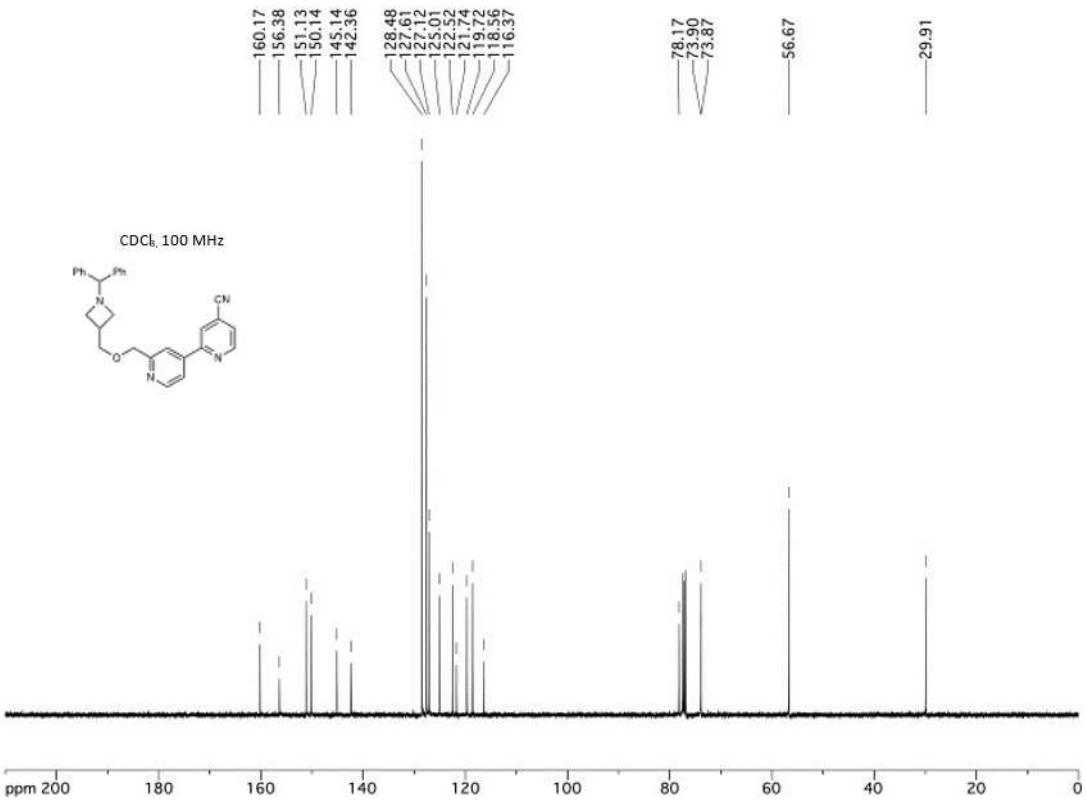
160.17
156.38
151.13
150.14
145.14
142.36
128.48
127.61
127.12
125.01
122.52
121.74
119.72
118.56
116.37
78.17
77.90
73.87
56.67
29.91
CDCl3, 100 MHz
ppm 200
180
160
140
120
100
80
60
40
20
0

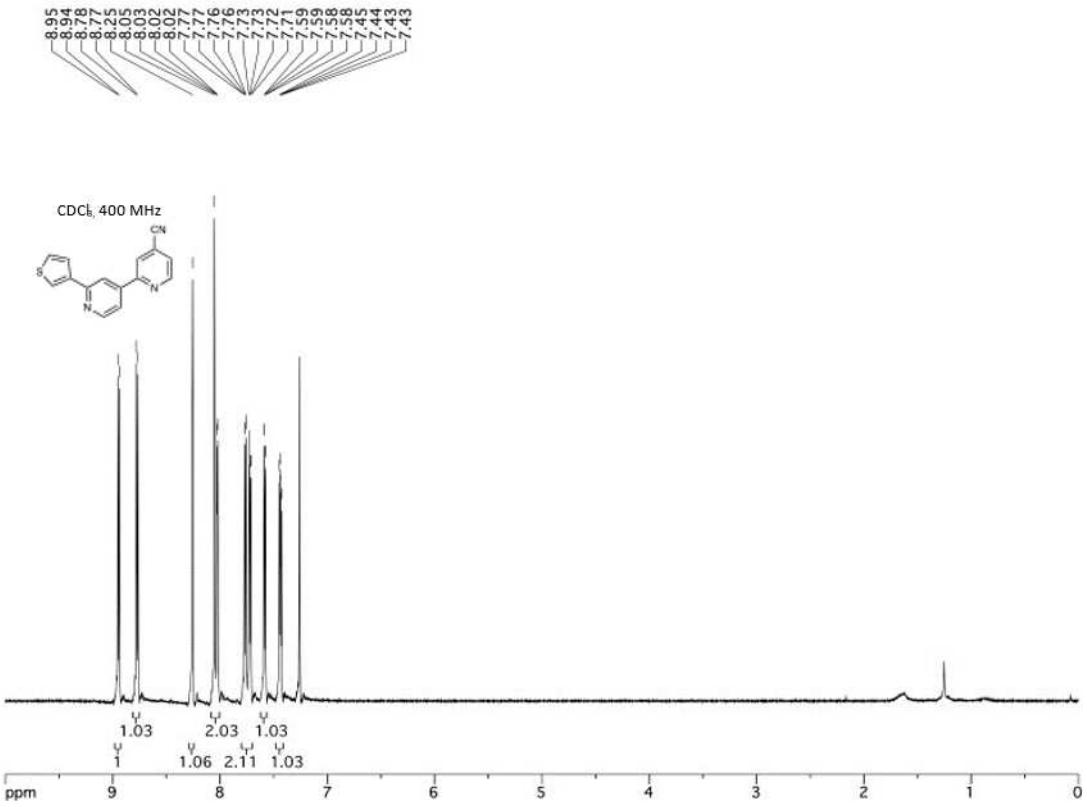
8.95
8.94
8.78
8.77
8.25
8.05
8.03
8.02
8.02
7.77
7.77
7.76
7.76
7.73
7.73
7.72
7.71
7.59
7.59
7.58
7.58
7.45
7.44
7.43
7.43
CDCl3, 400 MHz
1.03
2.03
1.03
1
1.06
2.11
1.03
ppm
9
8
7
6
5
4
3
2
1
0

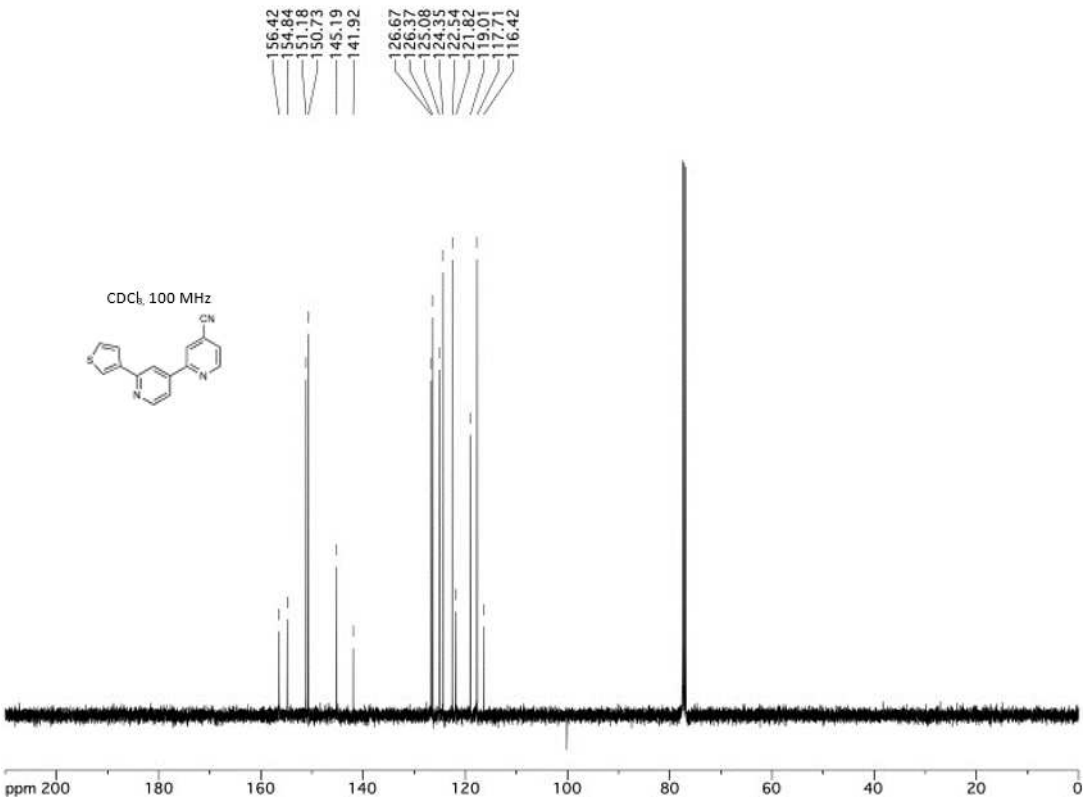
156.42
154.84
151.18
150.73
145.19
141.92
126.67
126.37
125.08
124.35
122.54
121.82
119.01
117.71
116.42
CDCl3, 100 MHz
ppm 200
180
160
140
120
100
80
60
40
20
0

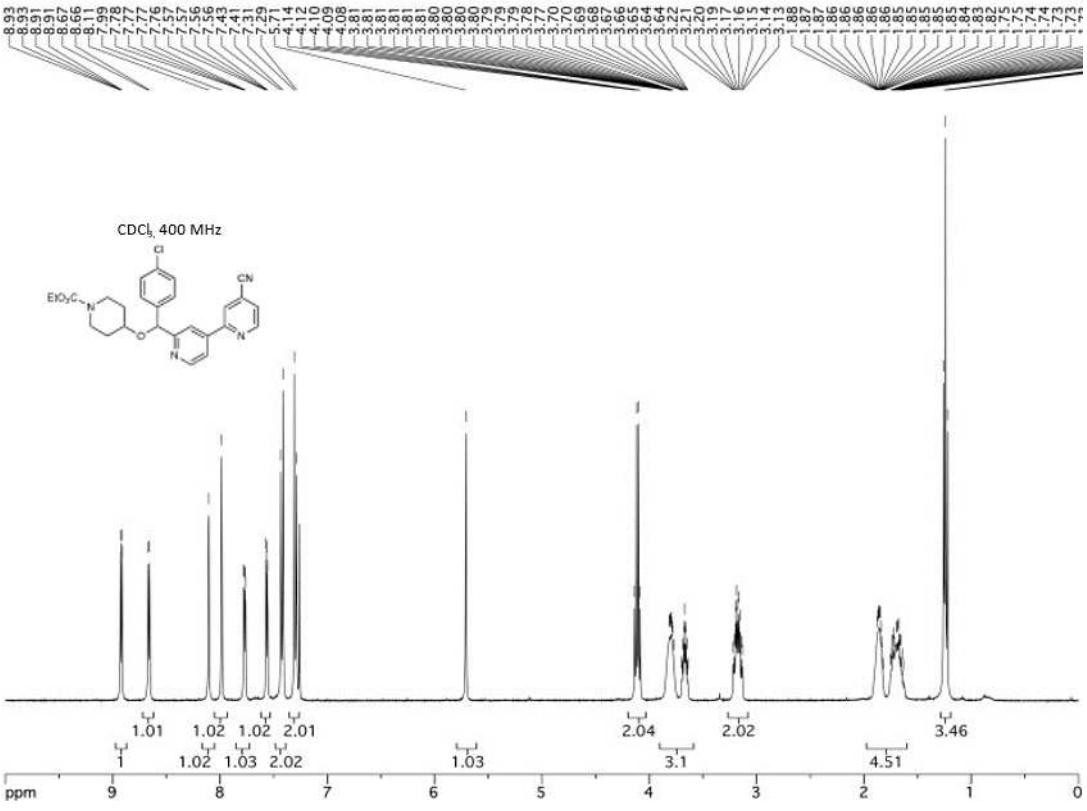
CDCl3, 400 MHz
1.01
1.02
1.02
1.02
2.01
2.04
2.02
3.46
1
1.02
1.03
2.02
1.03
3.1
4.51
ppm
9
8
7
6
5
4
3
2
1
0

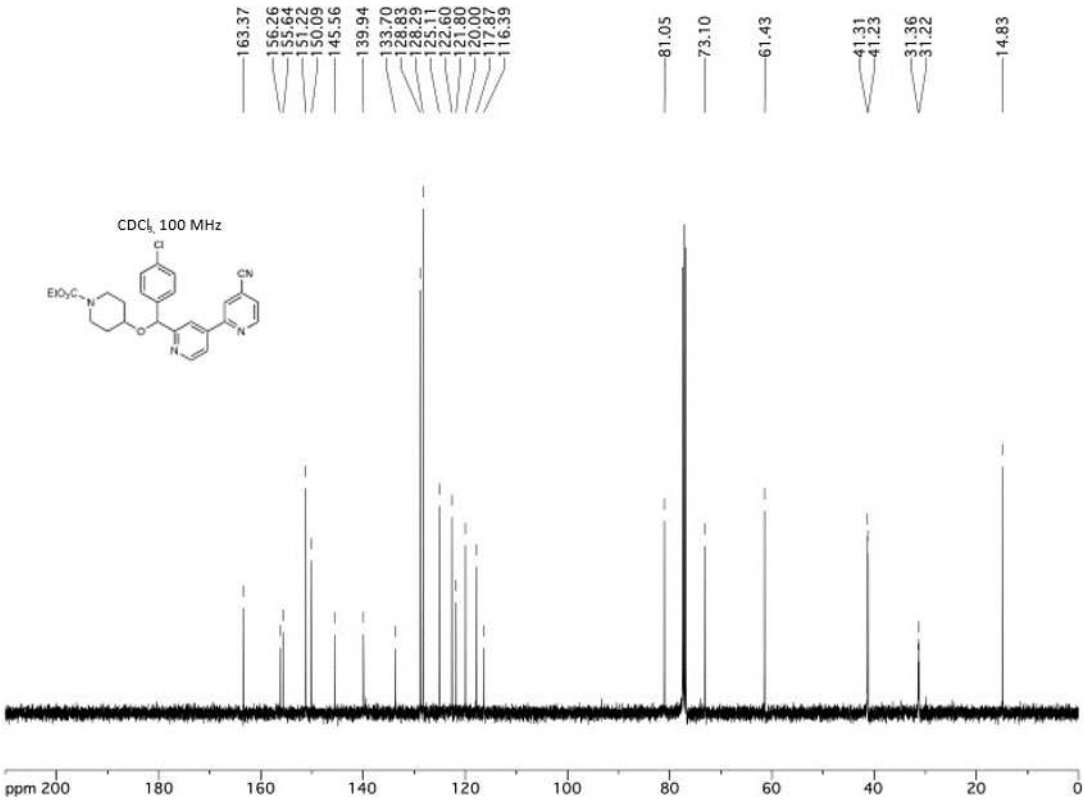
163.37
156.26
155.64
151.22
150.09
145.56
139.94
133.70
128.83
128.29
125.11
122.60
121.80
120.00
117.87
116.39
81.05
73.10
61.43
41.31
41.23
31.36
31.22
14.83
CDCl3 100 MHz
ppm 200
180
160
140
120
100
80
60
40
20
0

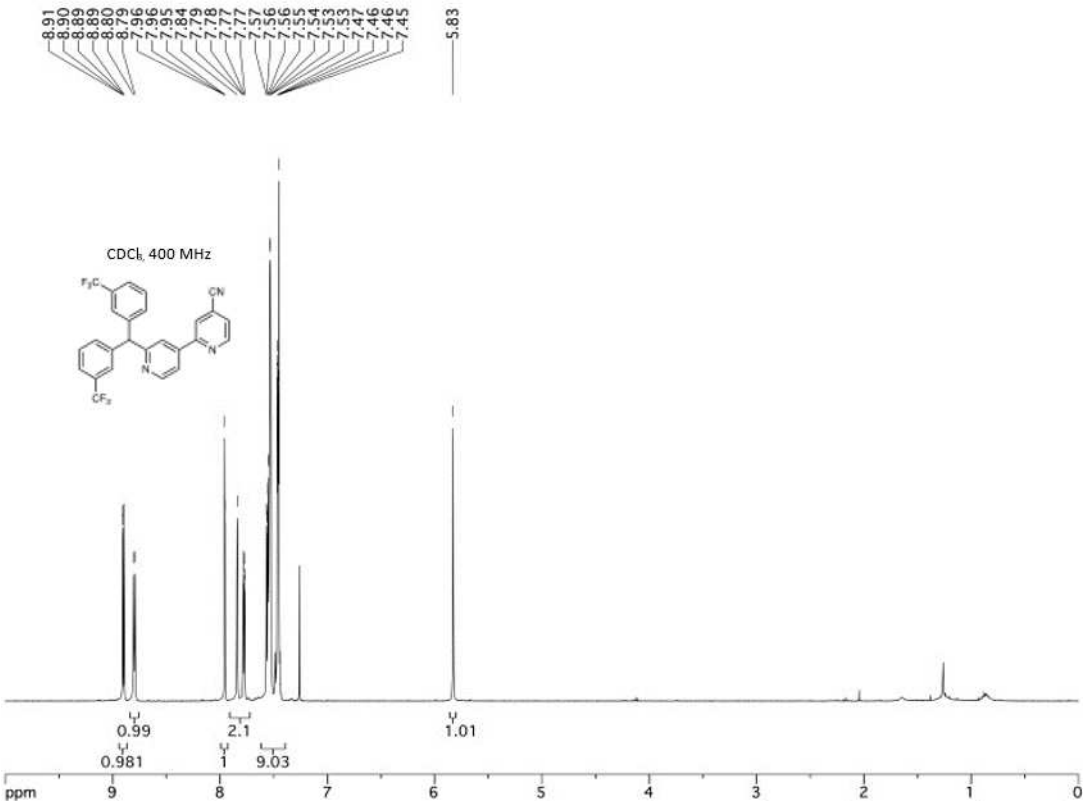
8.91
8.90
8.89
8.89
8.80
8.79
7.96
7.96
7.95
7.84
7.79
7.78
7.77
7.77
7.57
7.56
7.56
7.55
7.54
7.53
7.53
7.47
7.46
7.46
7.45
5.83
CDCl3 400 MHz
0.99
2.1
1.01
0.981
1
9.03
ppm
9
8
7
6
5
4
3
2
1
0

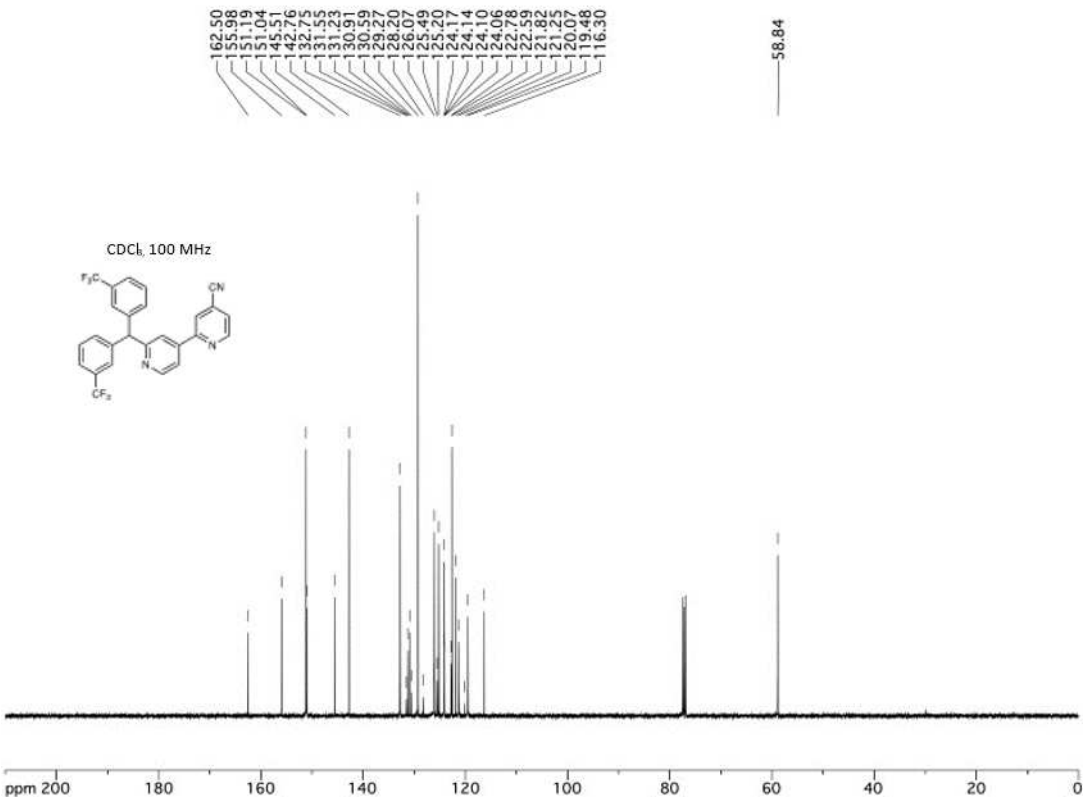
162.50
155.98
151.19
151.04
145.51
142.76
132.75
131.55
131.23
130.91
130.59
129.27
128.20
126.07
125.49
125.20
124.17
124.14
124.10
124.06
122.78
122.59
121.82
121.25
120.07
119.48
116.30
58.84
CDCl3, 100 MHz
ppm 200
180
160
140
120
100
80
60
40
20
0

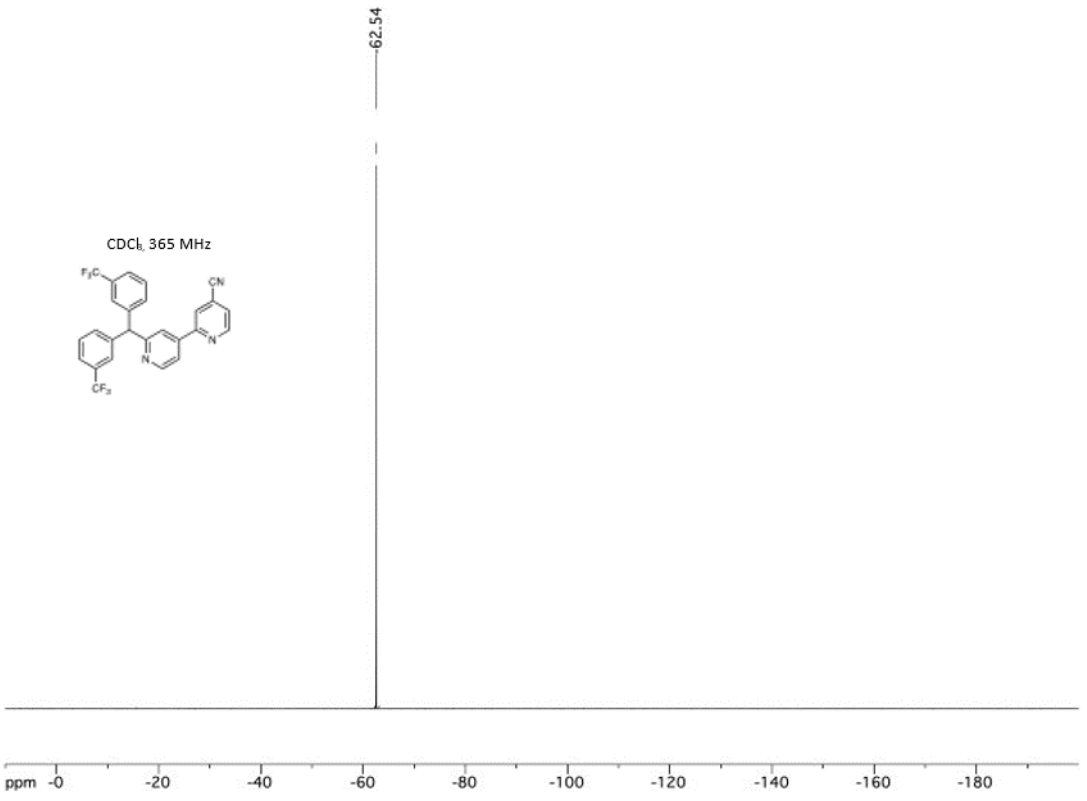
62.54
CDCl3, 365 MHz
ppm -0
-20
-40
-60
-80
-100
-120
-140
-160
-180

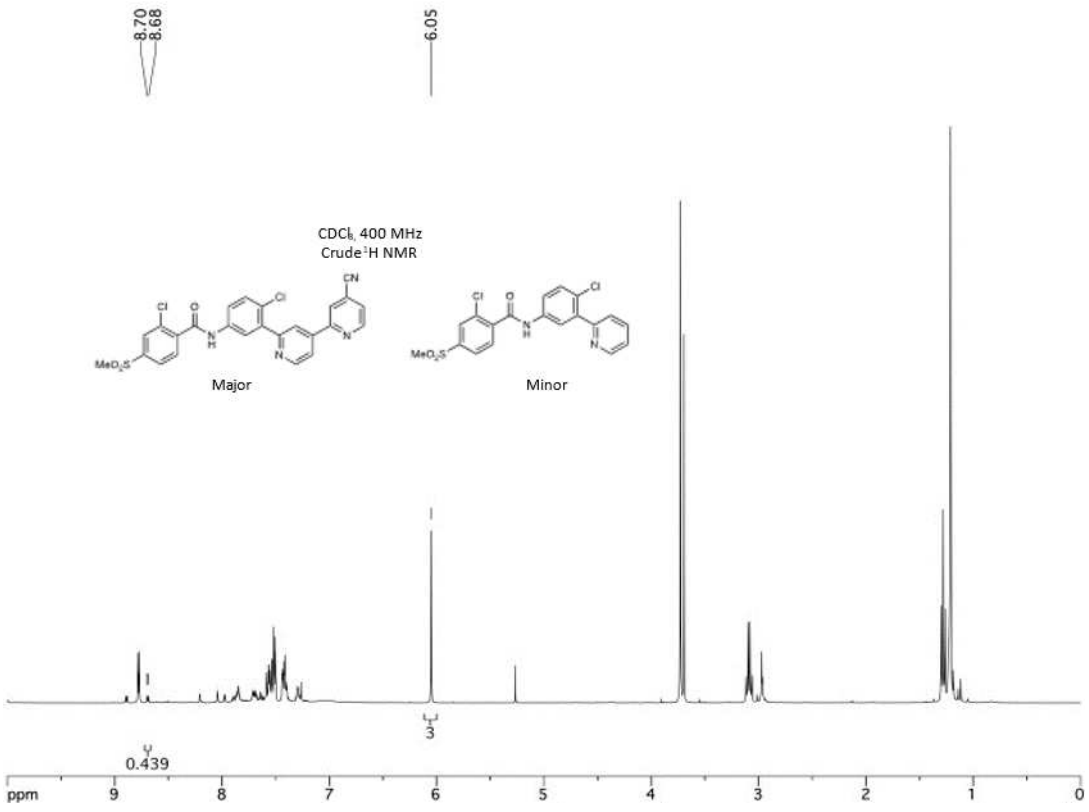
8.70
8.68
6.05
CDCl3, 400 MHz
Crude 1H NMR
Major
Minor
0.439
3
ppm

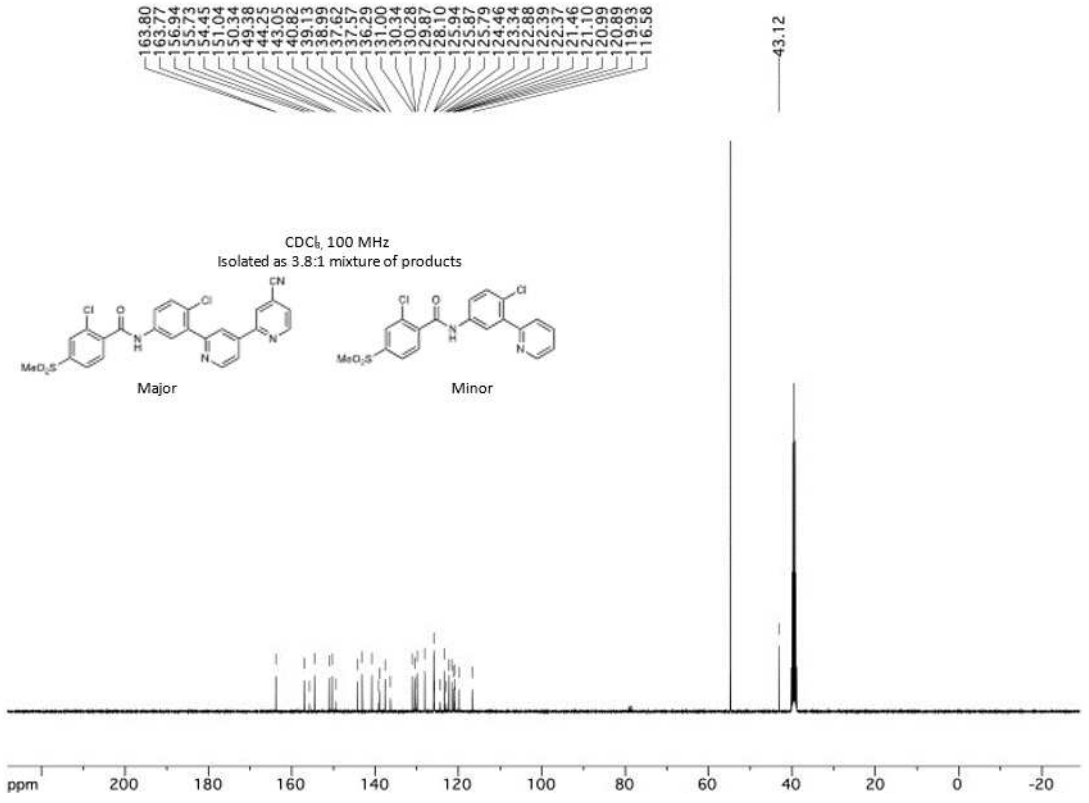
163.80
163.77
156.94
155.73
154.45
151.04
150.34
149.38
144.25
143.05
140.82
139.13
138.99
137.62
137.57
136.29
131.00
130.34
130.28
129.87
128.10
125.94
125.87
125.79
124.46
123.34
122.88
122.39
122.37
121.46
121.10
120.99
120.89
119.93
116.58
43.12
CDCl3, 100 MHz
Isolated as 3.8:1 mixture of products
Major
Minor
ppm

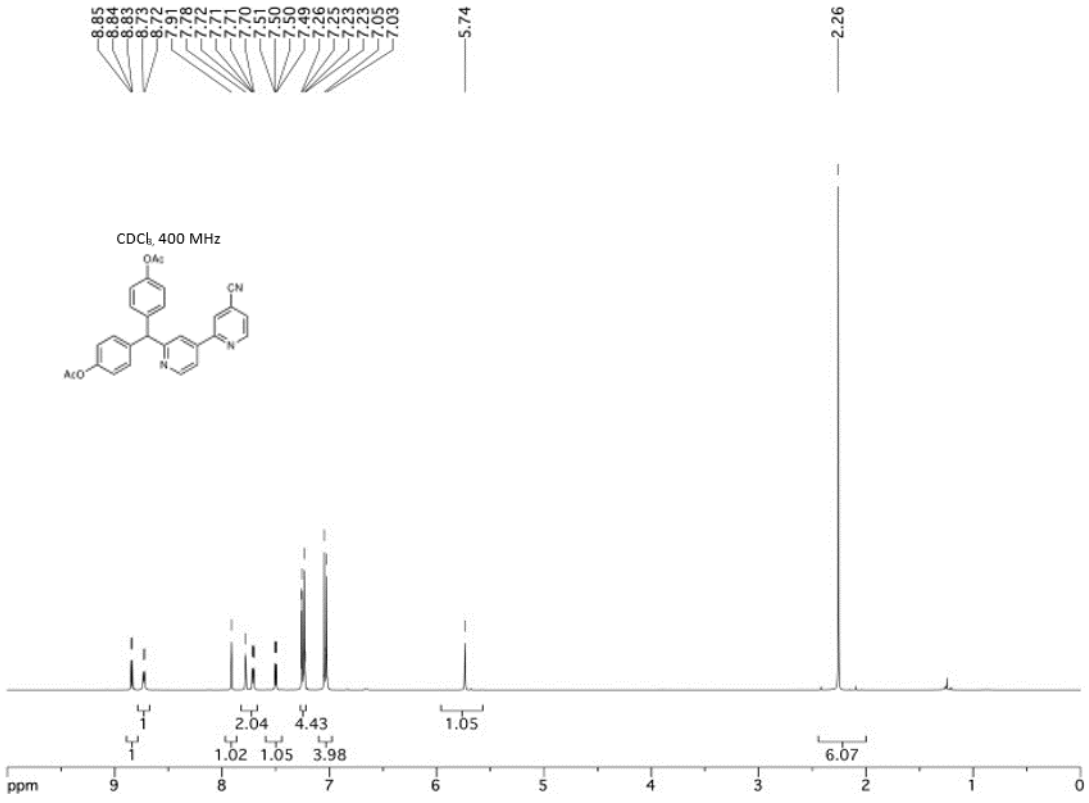
8.85
8.84
8.83
8.73
8.72
7.91
7.78
7.72
7.71
7.71
7.70
7.51
7.50
7.50
7.49
7.26
7.25
7.23
7.23
7.05
7.03
5.74
2.26
CDCl3, 400 MHz
OAc
CN
AcO
N
N
1
2.04
4.43
1.05
1
1.02
1.05
3.98
6.07
ppm
9
8
7
6
5
4
3
2
1
0

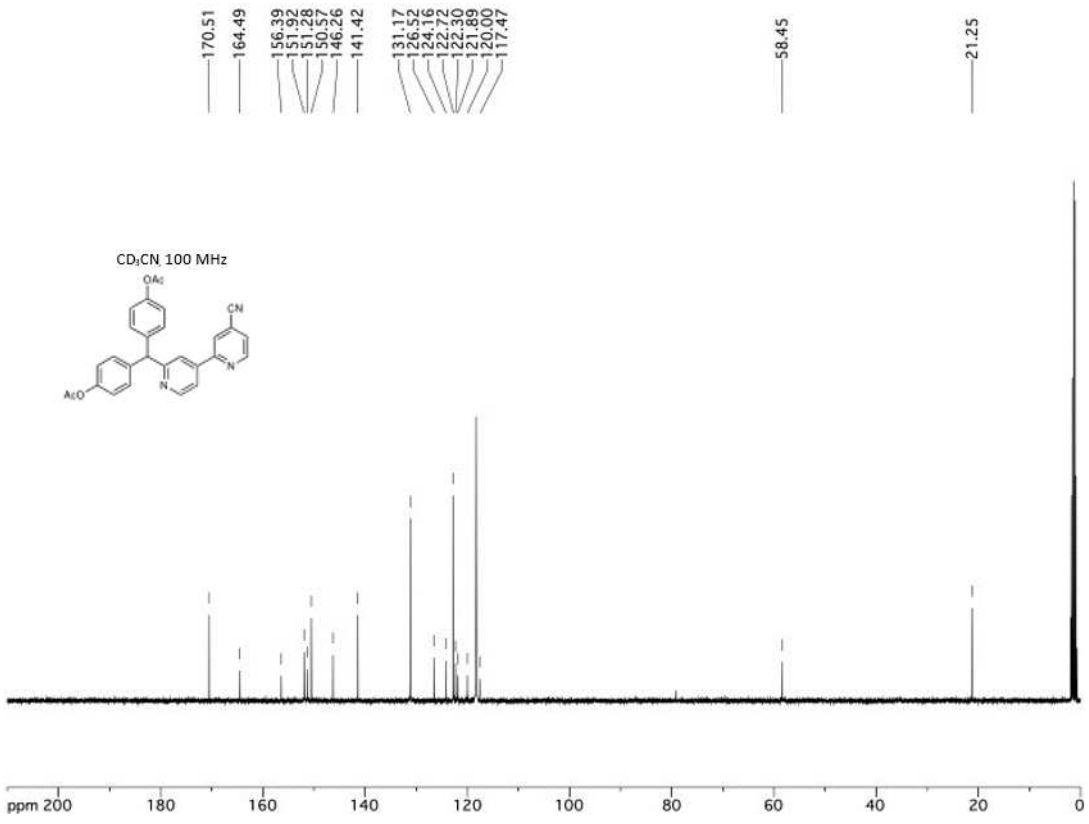
170.51
164.49
156.39
151.92
151.28
150.57
146.26
141.42
131.17
126.52
124.16
122.72
122.30
121.89
120.00
117.47
58.45
21.25
CD3CN, 100 MHz
OAc
CN
AcO
N
N
ppm
200
180
160
140
120
100
80
60
40
20
0

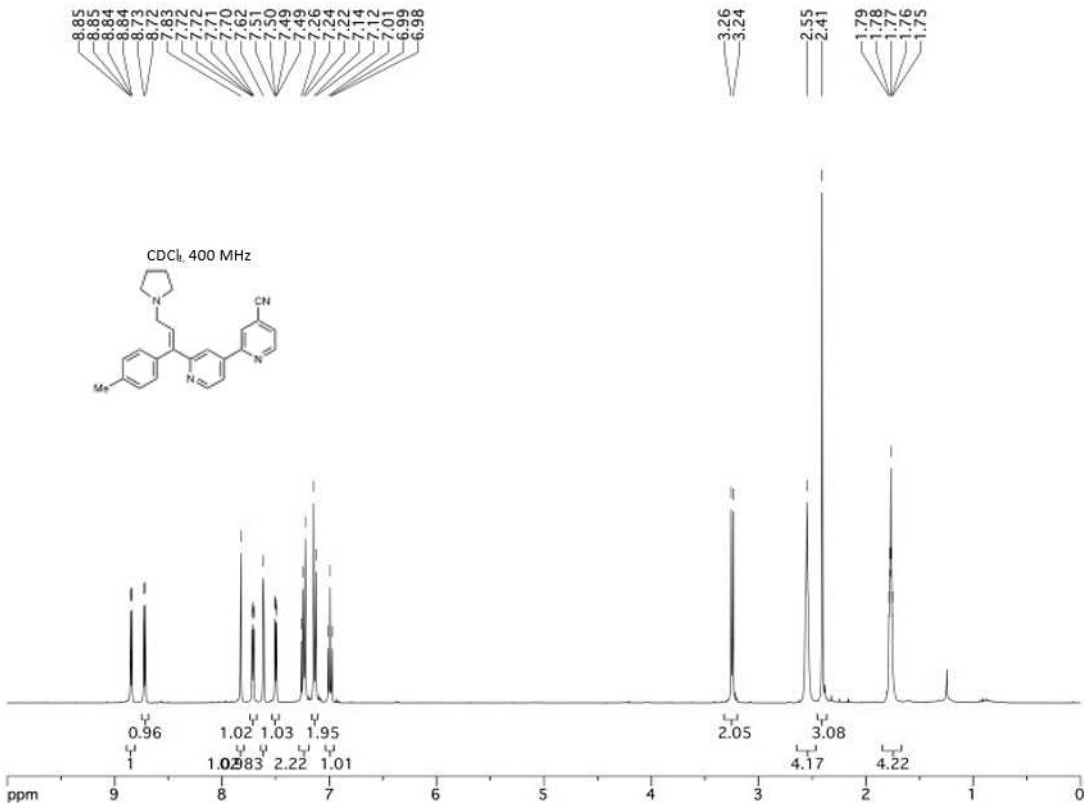
8.85
8.85
8.84
8.84
8.73
8.72
7.83
7.72
7.72
7.71
7.70
7.62
7.51
7.50
7.49
7.49
7.26
7.24
7.22
7.14
7.12
7.01
6.99
6.98
3.26
3.24
2.55
2.41
1.79
1.78
1.77
1.76
1.75
CDCl3, 400 MHz
CN
N
N
Me
0.96
1.02
1.03
1.95
2.05
3.08
1
1.07
1.83
2.22
1.01
4.17
4.22
ppm
9
8
7
6
5
4
3
2
1
0

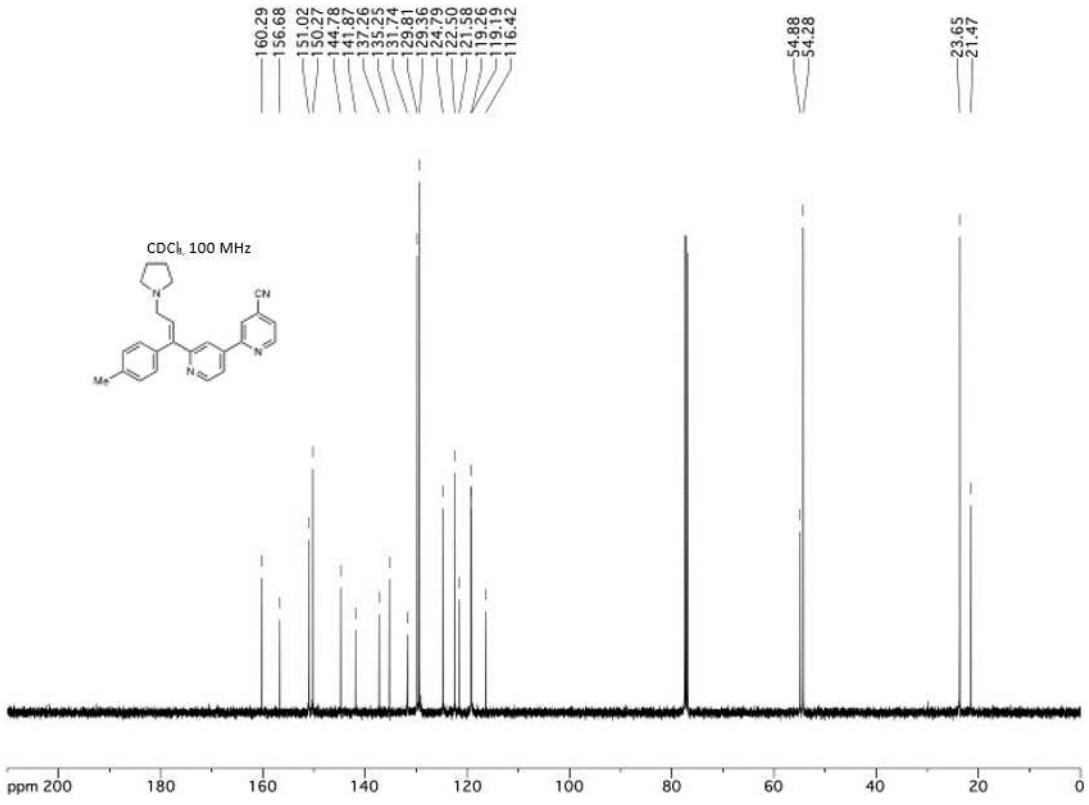
160.29
156.68
151.02
150.27
144.78
141.87
137.26
135.25
131.74
129.81
129.36
124.79
122.50
121.58
119.26
119.19
116.42
54.88
54.28
23.65
21.47
CDCl3, 100 MHz
CN
N
N
Me
ppm 200
180
160
140
120
100
80
60
40
20
0

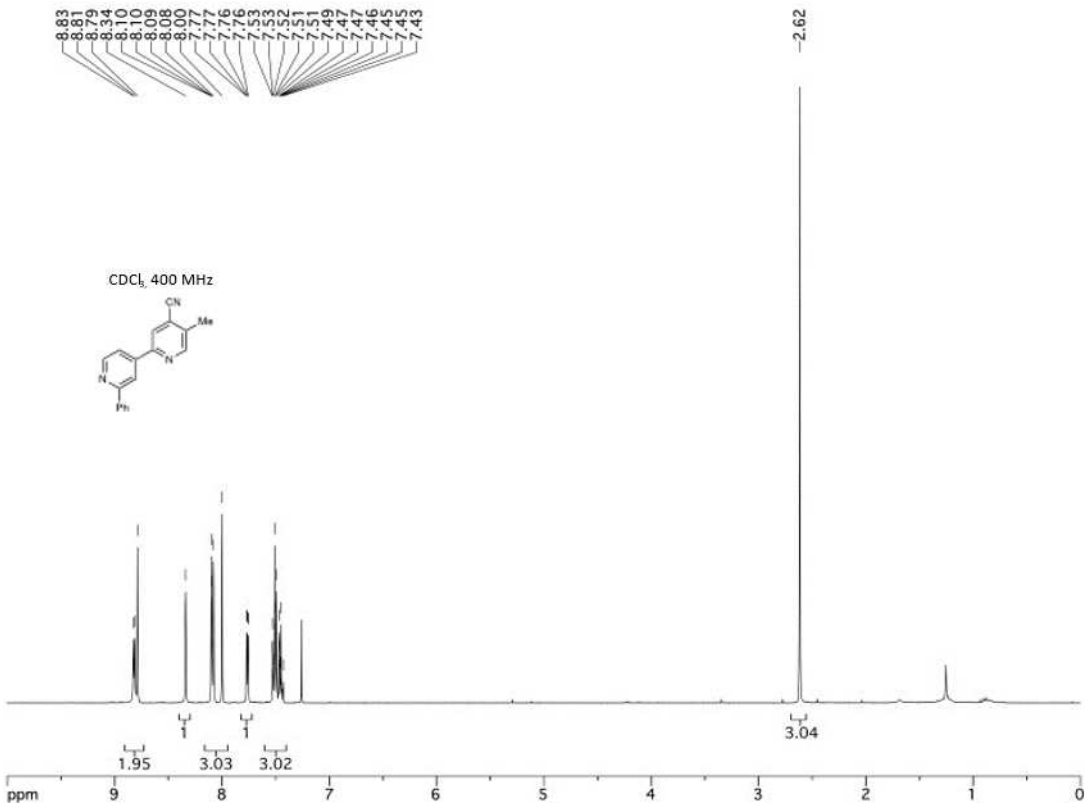
8.83
8.81
8.79
8.34
8.10
8.10
8.09
8.08
8.00
7.77
7.77
7.76
7.76
7.53
7.52
7.51
7.51
7.49
7.47
7.47
7.46
7.45
7.45
7.43
2.62
CDCl3 400 MHz
CN
Me
N
N
Ph
1.95
3.03
1
3.02
1
3.04
ppm
9
8
7
6
5
4
3
2
1
0

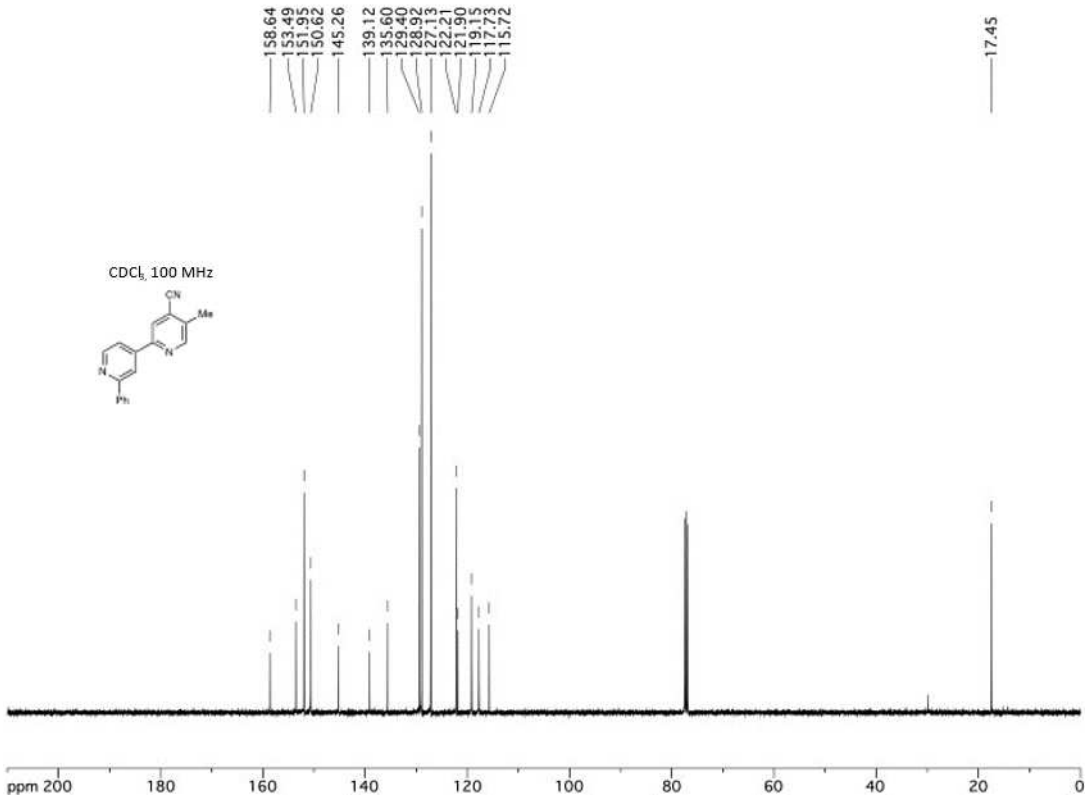
158.64
153.49
151.95
150.62
145.26
139.12
135.60
129.40
128.92
127.13
122.21
121.90
119.15
117.73
115.72
17.45
CDCl3 100 MHz
CN
Me
N
N
Ph
ppm 200
180
160
140
120
100
80
60
40
20
0

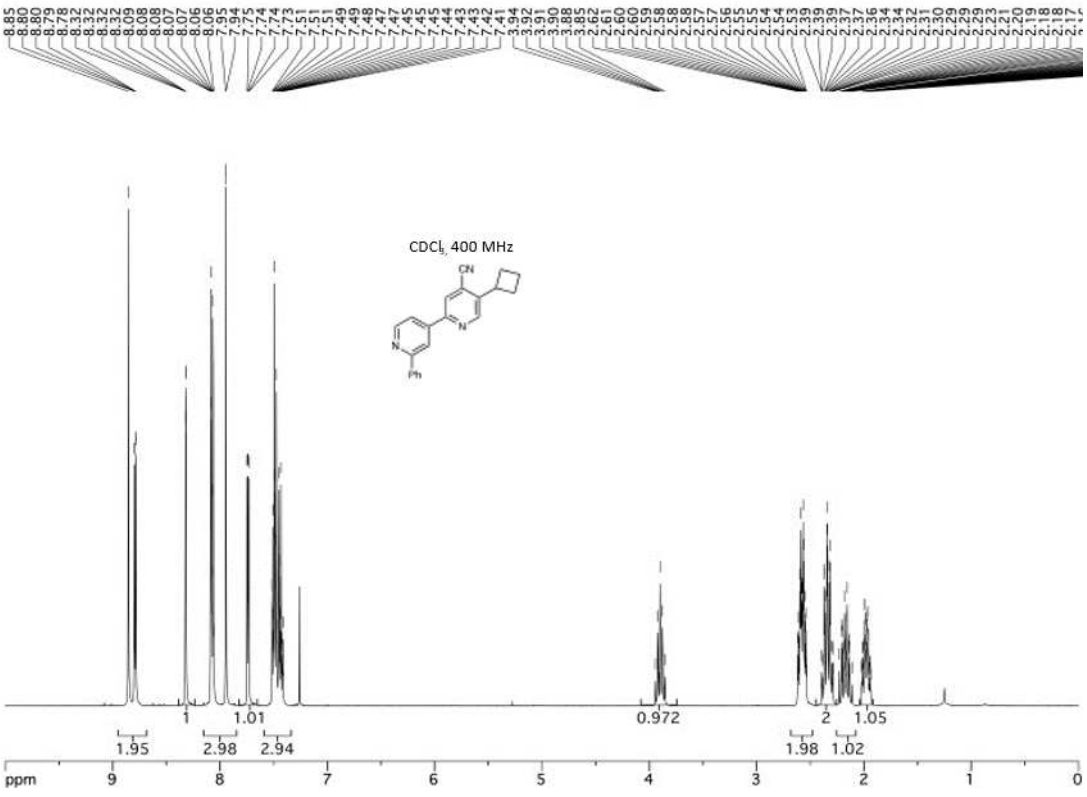
CDCl3 400 MHz
1
1.01
0.972
2
1.05
1.95
2.98
2.94
1.98
1.02
ppm

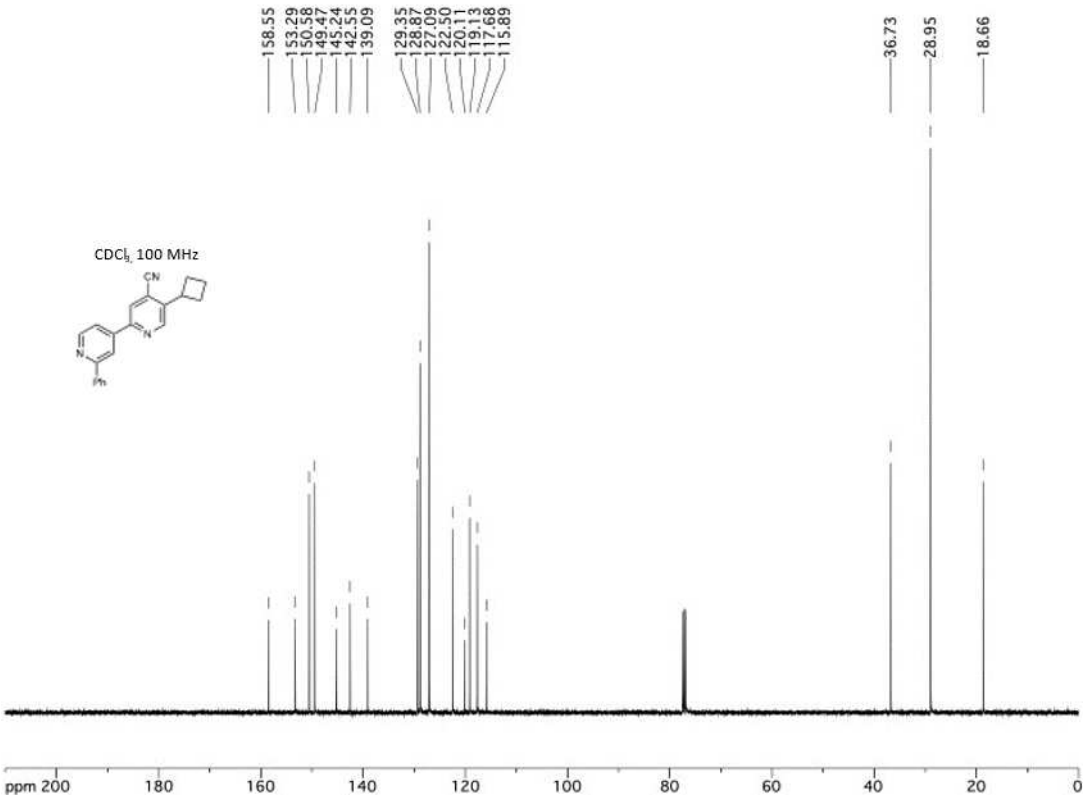
158.55
153.29
150.58
149.47
145.24
142.55
139.09
129.35
128.87
127.09
122.50
120.11
119.13
117.68
115.89
36.73
28.95
18.66
CDCl3 100 MHz
ppm

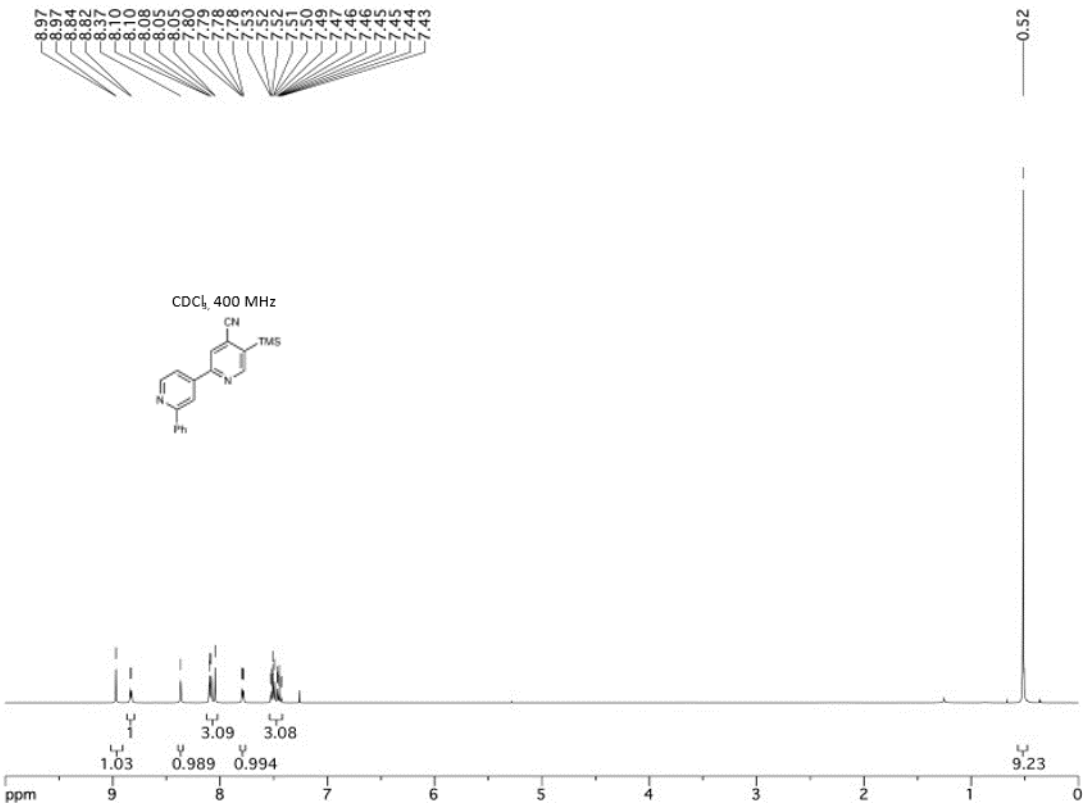
8.97
8.97
8.84
8.82
8.37
8.10
8.08
8.05
8.05
7.80
7.79
7.78
7.78
7.53
7.52
7.52
7.51
7.50
7.49
7.47
7.46
7.46
7.45
7.45
7.44
7.43
0.52
CDCl3, 400 MHz
CN
TMS
N
N
Ph
1
3.09
3.08
1.03
0.989
0.994
9.23
ppm
9
8
7
6
5
4
3
2
1
0

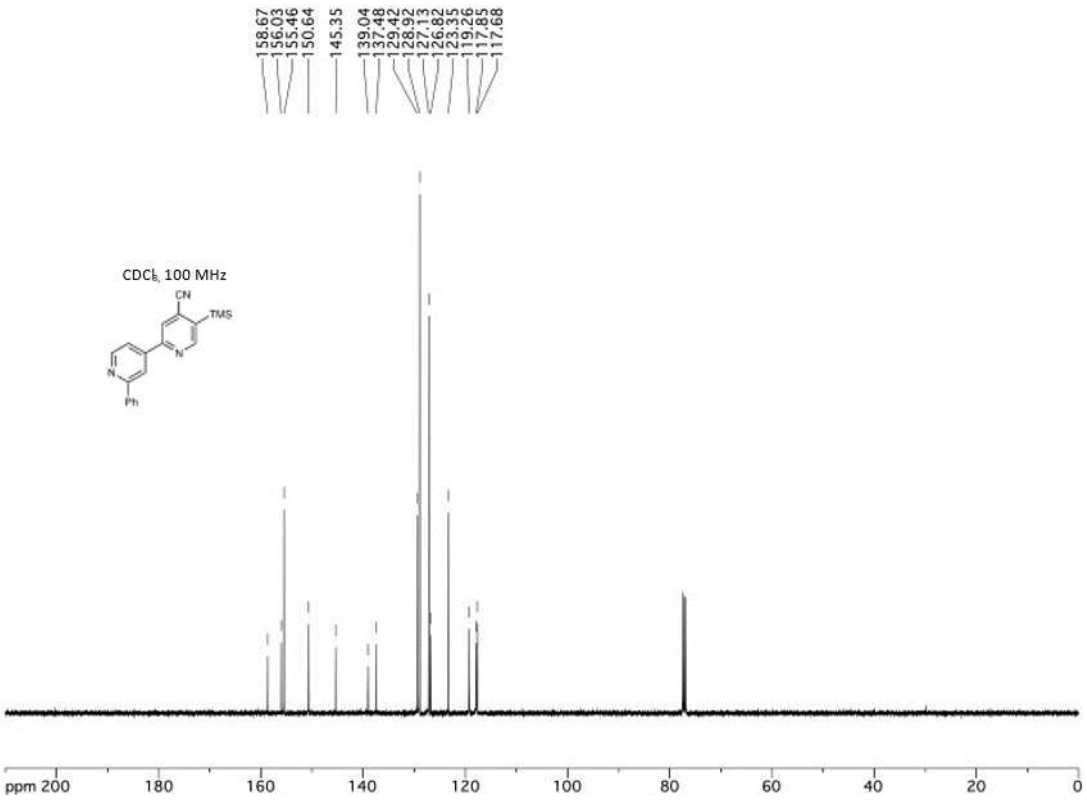
158.67
156.03
155.46
150.64
145.35
139.04
137.48
129.42
128.92
127.13
126.82
123.35
119.26
117.85
117.68
CDCl3, 100 MHz
CN
TMS
N
N
Ph
ppm 200
180
160
140
120
100
80
60
40
20
0

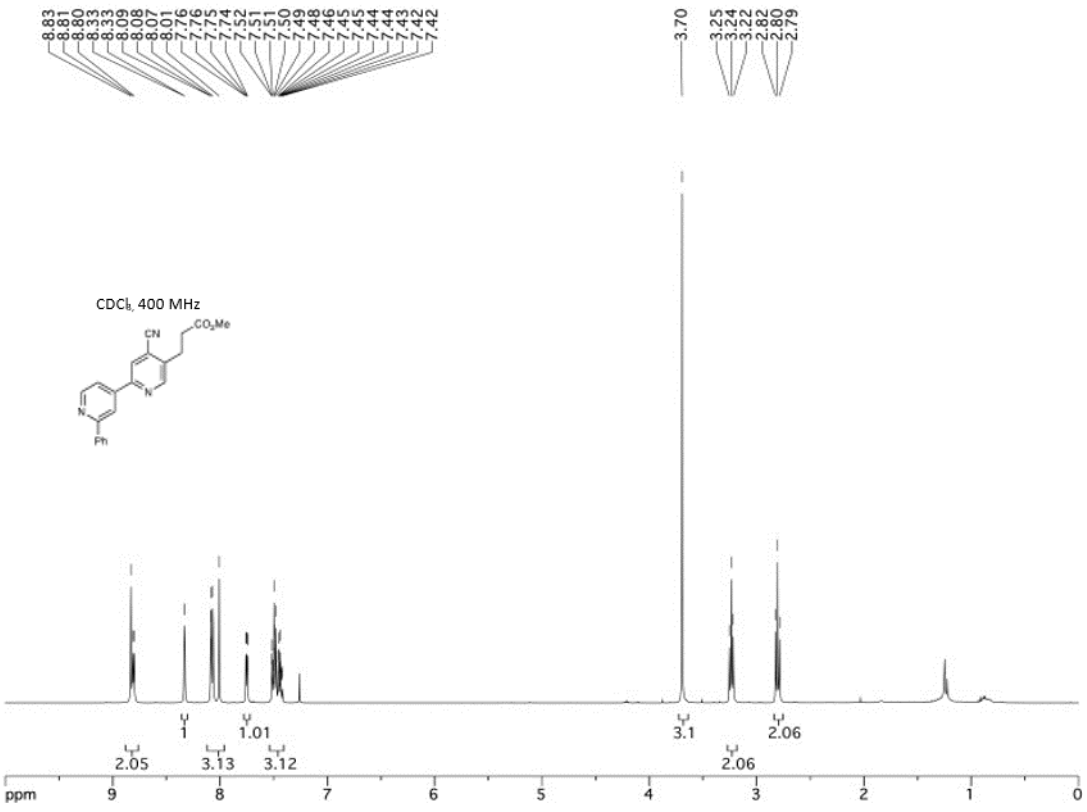
8.83
8.81
8.80
8.33
8.33
8.09
8.08
8.07
8.01
7.76
7.76
7.75
7.74
7.52
7.51
7.51
7.50
7.49
7.48
7.46
7.45
7.45
7.44
7.44
7.43
7.42
7.42
3.70
3.25
3.24
3.22
2.82
2.80
2.79
CDCl3, 400 MHz
CN
CO2Me
N
N
Ph
1
1.01
3.1
2.06
2.05
3.13
3.12
2.06
ppm
9
8
7
6
5
4
3
2
1
0

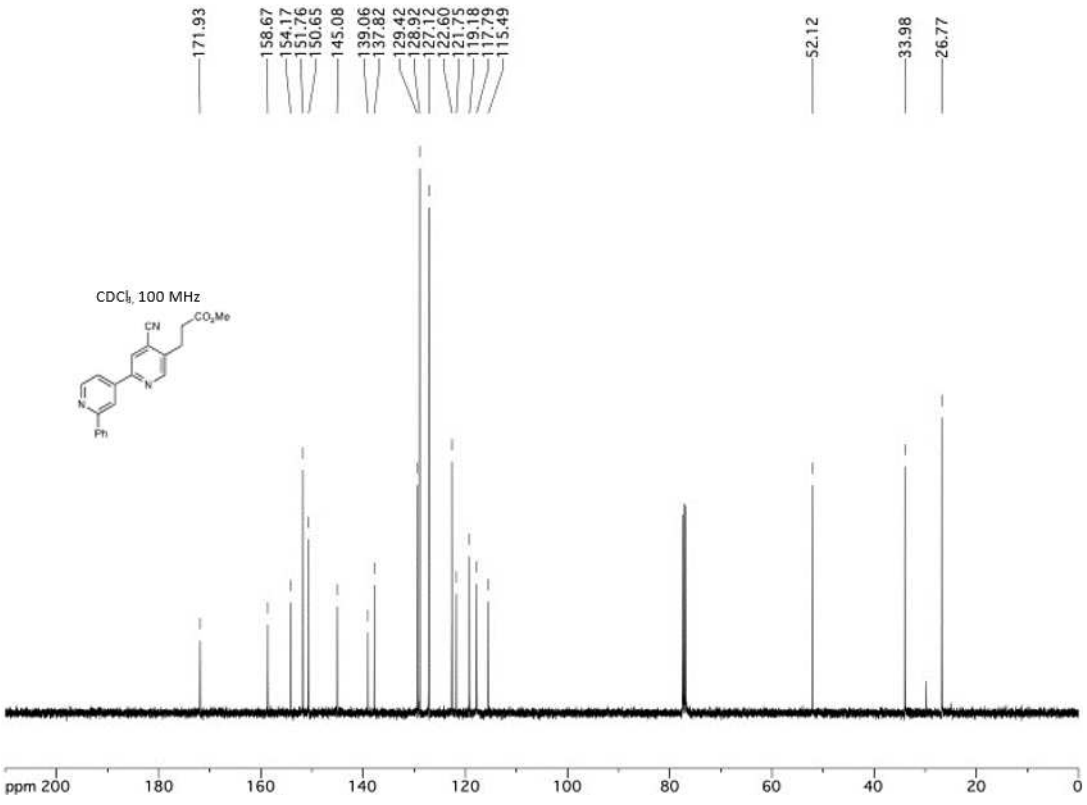
171.93
158.67
154.17
151.76
150.65
145.08
139.06
137.82
129.42
128.92
127.12
122.60
121.75
119.18
117.79
115.49
52.12
33.98
26.77
CDCl3, 100 MHz
CN
CO2Me
N
N
Ph
ppm 200
180
160
140
120
100
80
60
40
20
0

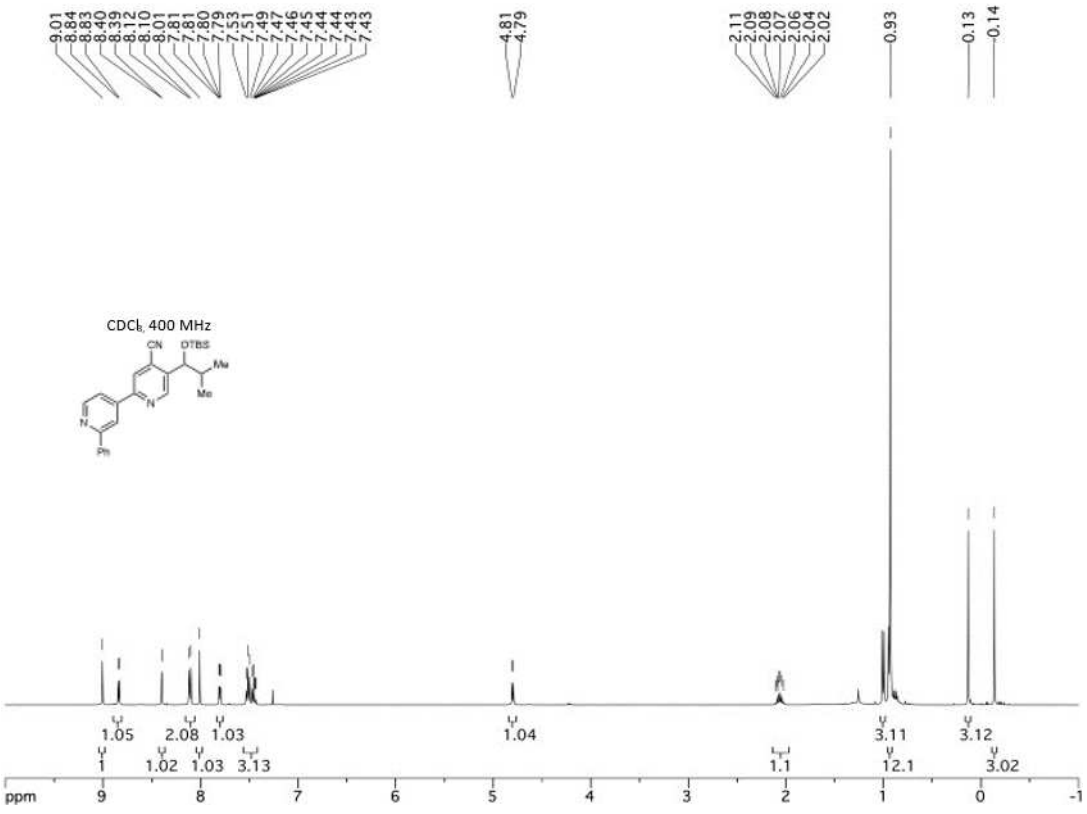
9.01
8.84
8.83
8.40
8.39
8.12
8.10
8.01
8.01
7.81
7.81
7.80
7.79
7.53
7.51
7.49
7.47
7.46
7.45
7.44
7.44
7.43
7.43
4.81
4.79
2.11
2.09
2.08
2.07
2.06
2.04
2.02
0.93
0.13
0.14
CDCl3 400 MHz
CN
OTBS
Me
Me
Ph
1.05
2.08
1.03
1.04
3.11
3.12
1
1.02
1.03
3.13
1.1
12.1
3.02
ppm
9
8
7
6
5
4
3
2
1
0
-1

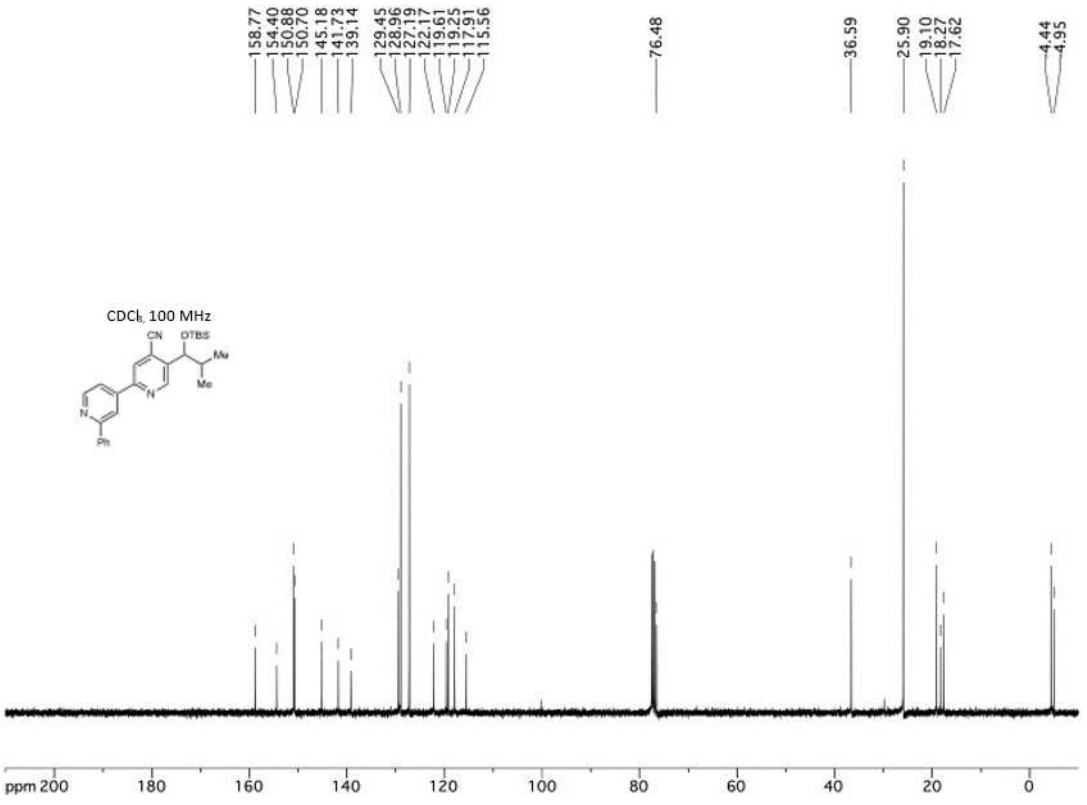
158.77
154.40
150.88
150.70
145.18
141.73
139.14
129.45
128.96
127.19
122.17
119.61
119.25
117.91
115.56
76.48
36.59
25.90
19.10
18.27
17.62
4.44
4.95
CDCl3 100 MHz
CN
OTBS
Me
Me
Ph
ppm 200
180
160
140
120
100
80
60
40
20
0

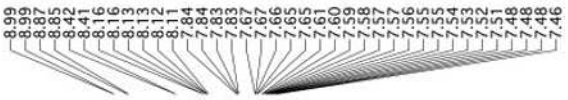
8.99
8.99
8.87
8.85
8.42
8.41
8.16
8.16
8.13
8.13
8.12
8.11
7.84
7.84
7.83
7.83
7.67
7.67
7.66
7.65
7.65
7.61
7.60
7.59
7.58
7.57
7.57
7.56
7.55
7.55
7.54
7.53
7.52
7.51
7.48
7.48
7.48
7.46

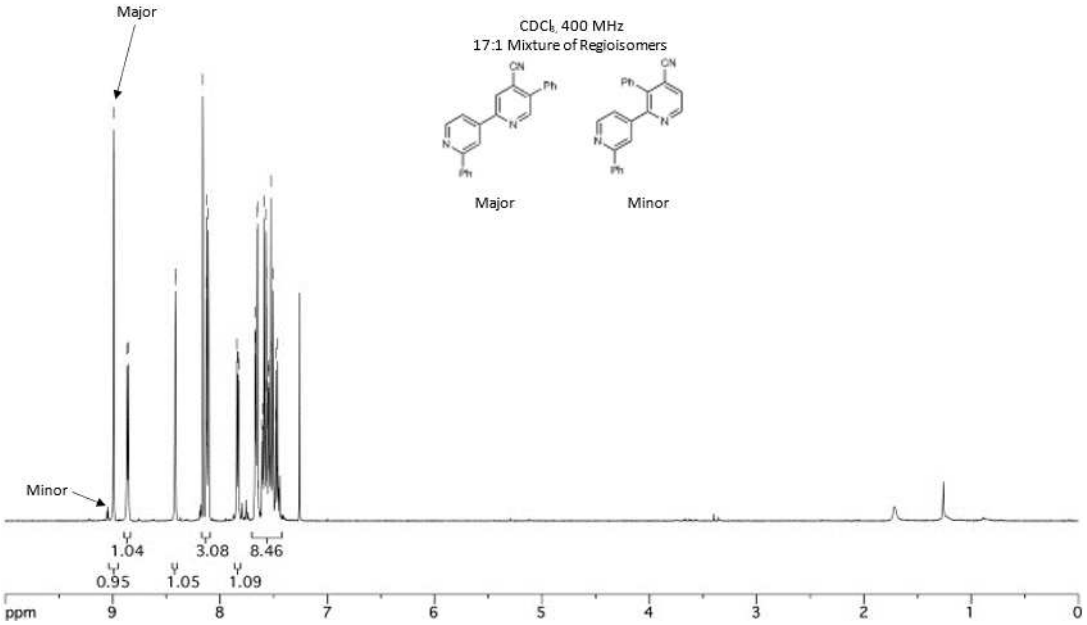
Major
CDCl3, 400 MHz
17:1 Mixture of Regioisomers
Major
Minor
Minor
1.04
3.08
8.46
0.95
1.05
1.09
ppm
9
8
7
6
5
4
3
2
1
0

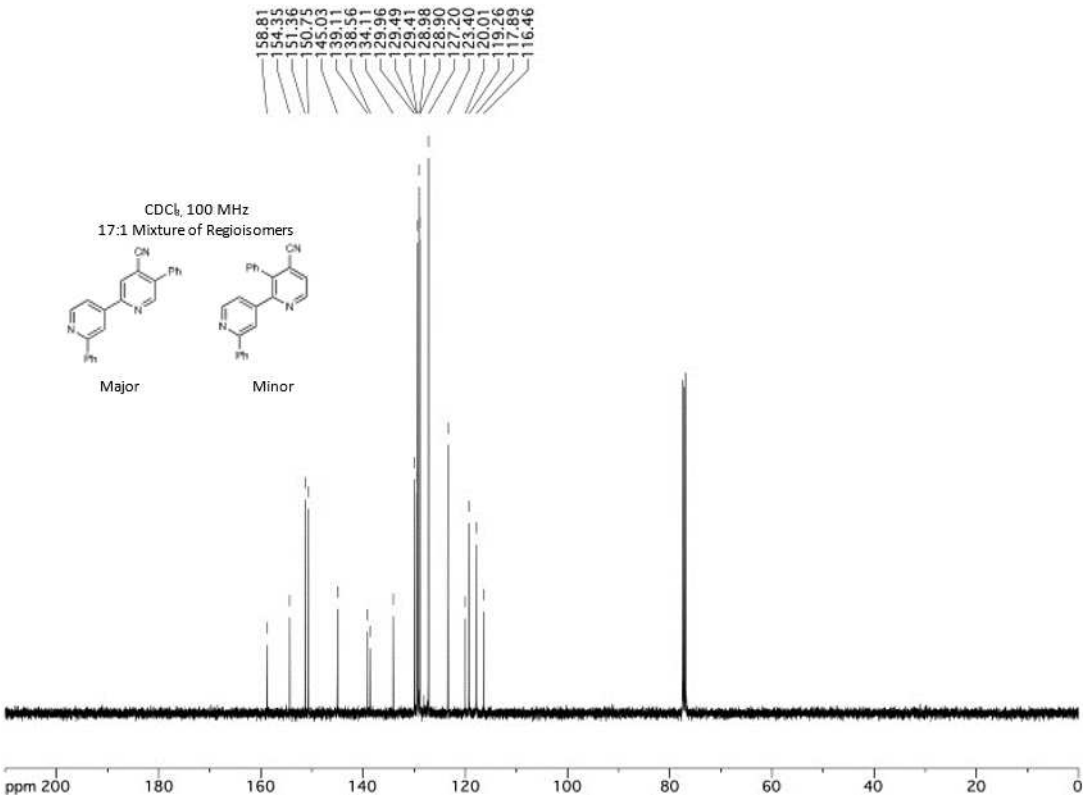
158.81
154.35
151.36
150.75
145.03
139.11
138.56
134.11
129.96
129.49
129.41
128.98
128.90
127.20
123.40
120.01
119.26
117.89
116.46
CDCl3, 100 MHz
17:1 Mixture of Regioisomers
Major
Minor
ppm 200
180
160
140
120
100
80
60
40
20
0

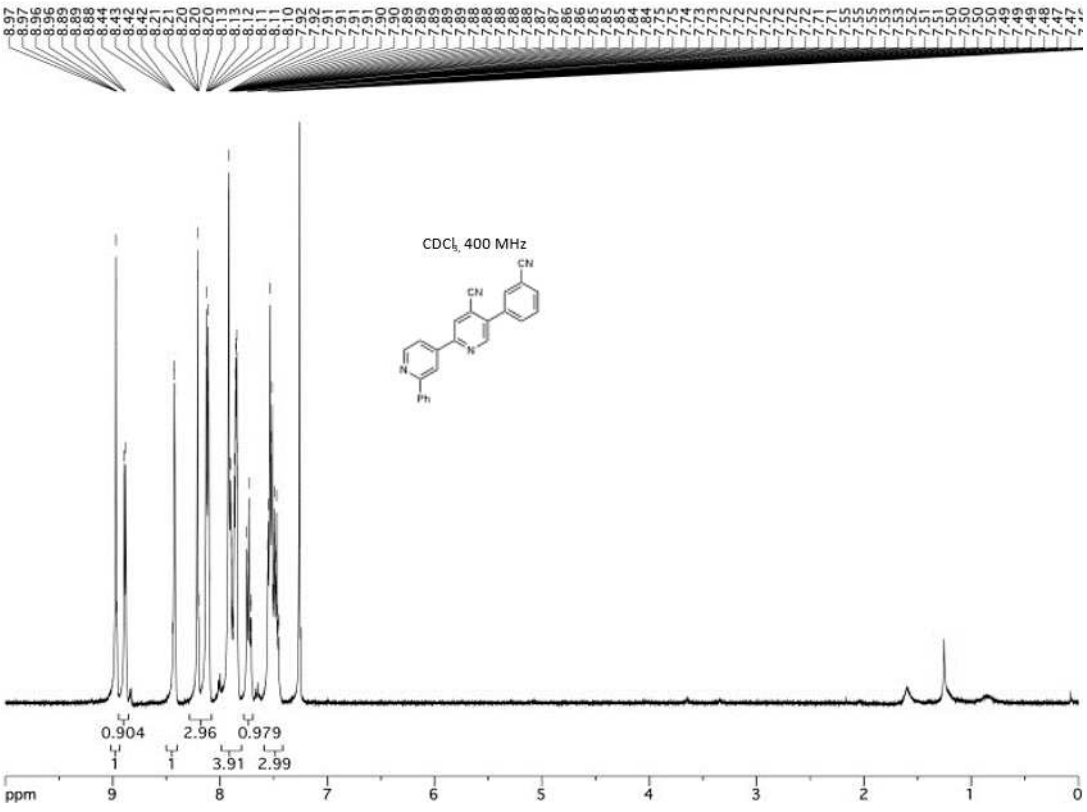
CDCl3, 400 MHz
0.904
2.96
0.979
1
1
3.91
2.99
ppm

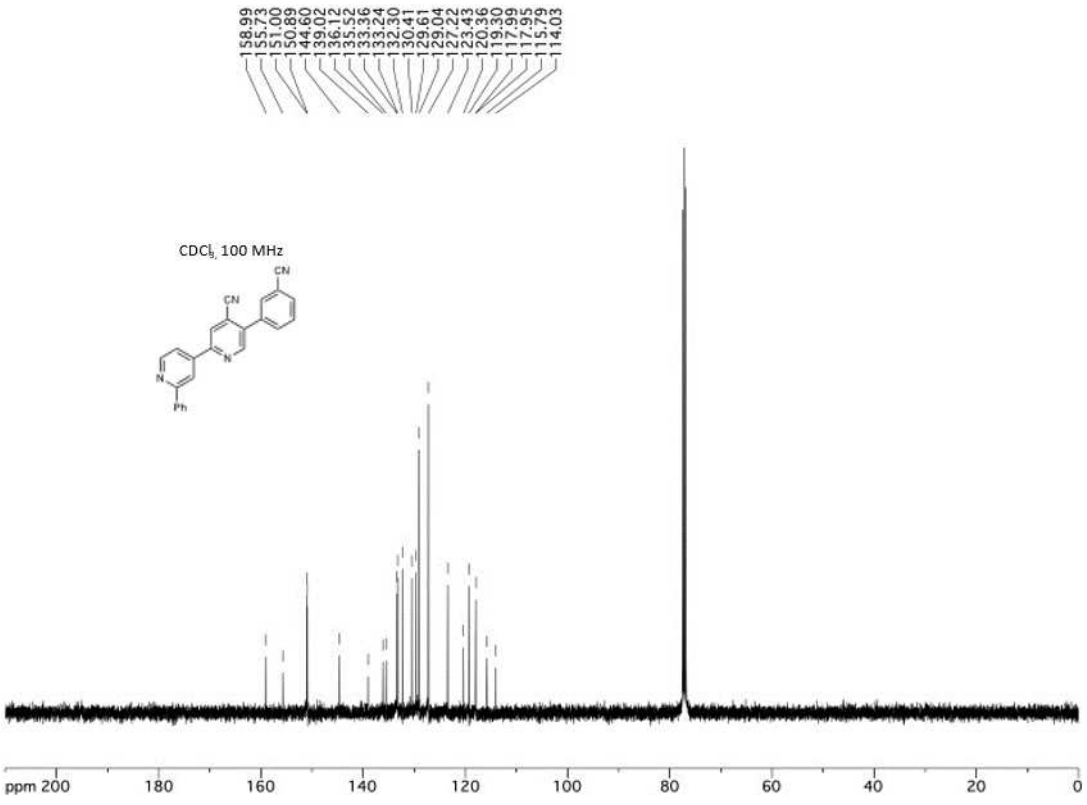
CDCl3, 100 MHz
ppm

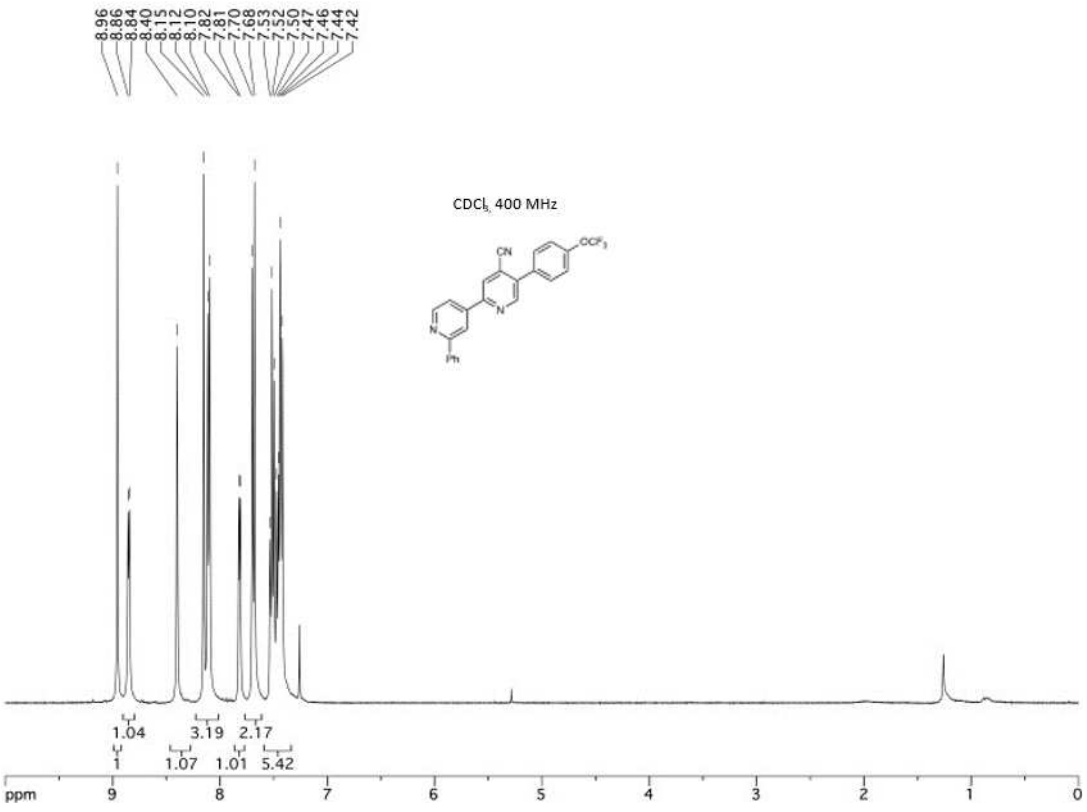
8.96
8.86
8.84
8.40
8.15
8.12
8.10
7.82
7.81
7.70
7.68
7.53
7.52
7.50
7.47
7.46
7.44
7.42
CDCl3 400 MHz
CN
CF3
N
N
Ph
1.04
3.19
2.17
1
1.07
1.01
5.42
ppm
9
8
7
6
5
4
3
2
1
0

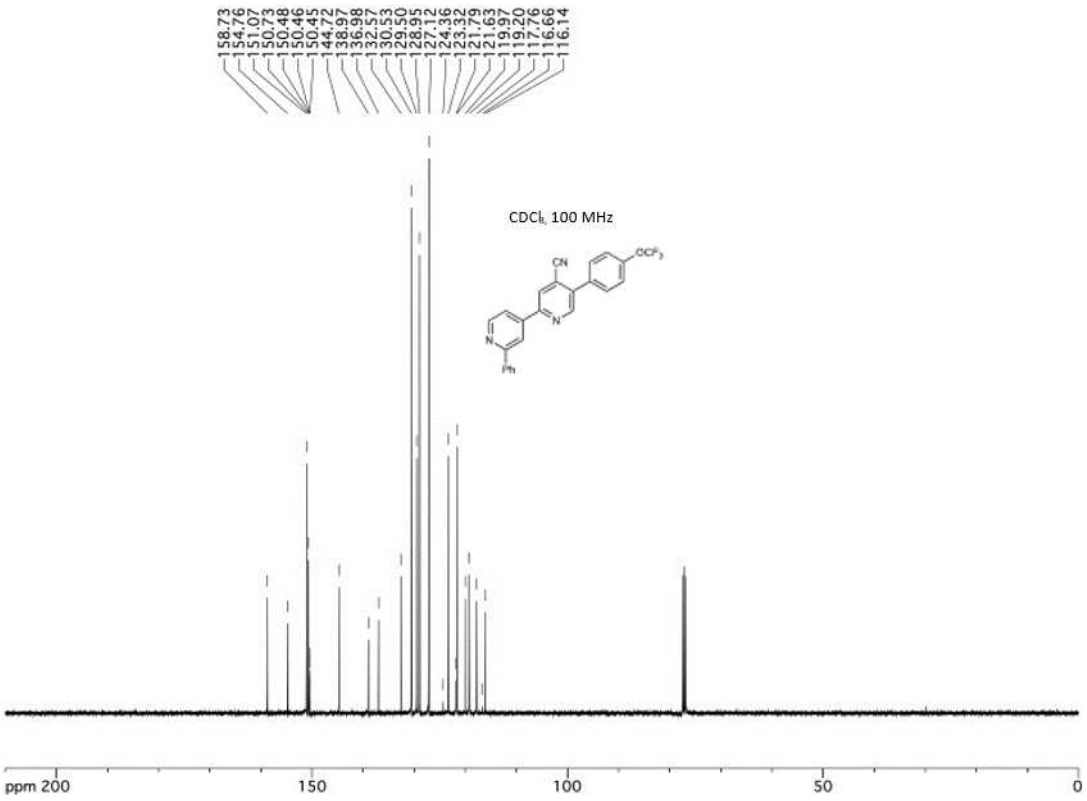
158.73
154.76
151.07
150.73
150.48
150.46
150.45
144.72
138.97
136.98
132.57
130.53
129.50
128.95
127.12
124.36
123.32
121.79
121.63
119.97
119.20
117.76
116.66
116.14
CDCl3 100 MHz
CN
CF3
N
N
Ph
ppm
200
150
100
50
0

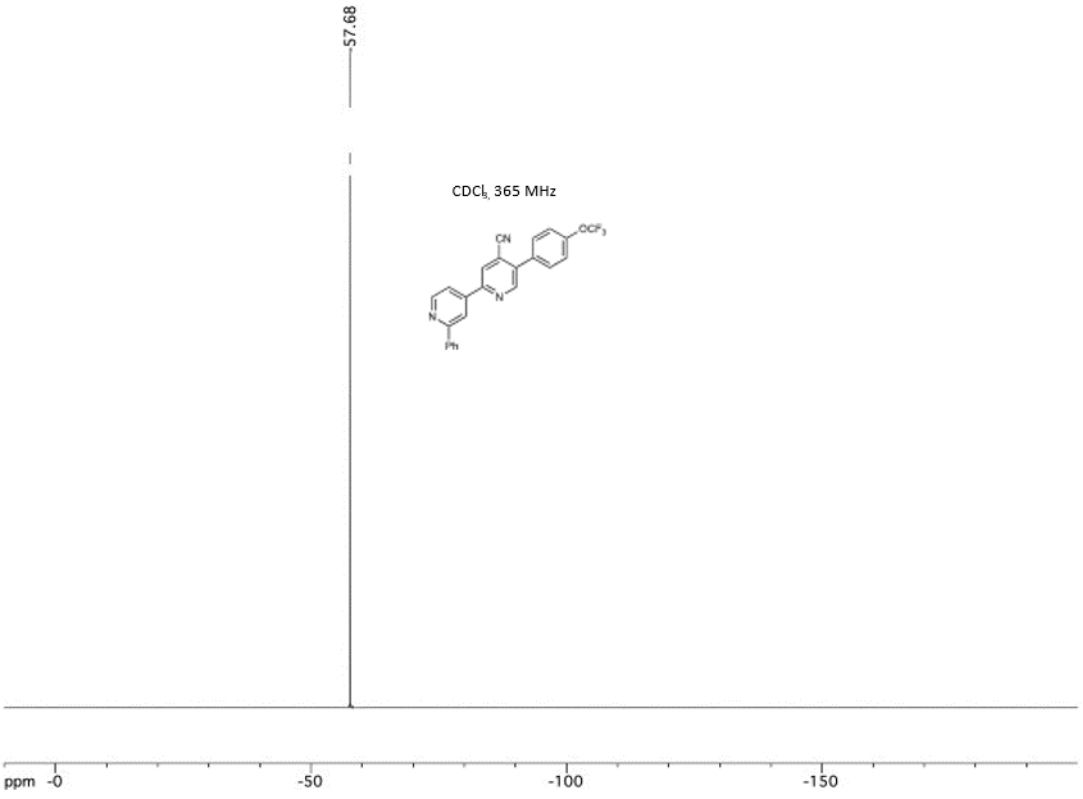
57.68
CDCl3, 365 MHz
CN
OCF3
N
N
Ph
ppm -0
-50
-100
-150

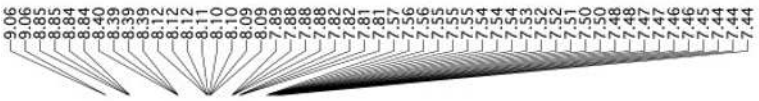
9.06
9.06
8.85
8.85
8.84
8.84
8.40
8.39
8.39
8.39
8.12
8.12
8.11
8.11
8.10
8.10
8.09
8.09
7.89
7.88
7.88
7.88
7.82
7.82
7.81
7.81
7.57
7.56
7.56
7.55
7.55
7.55
7.54
7.54
7.54
7.53
7.52
7.52
7.51
7.50
7.50
7.48
7.48
7.47
7.47
7.46
7.46
7.45
7.44
7.44
7.44

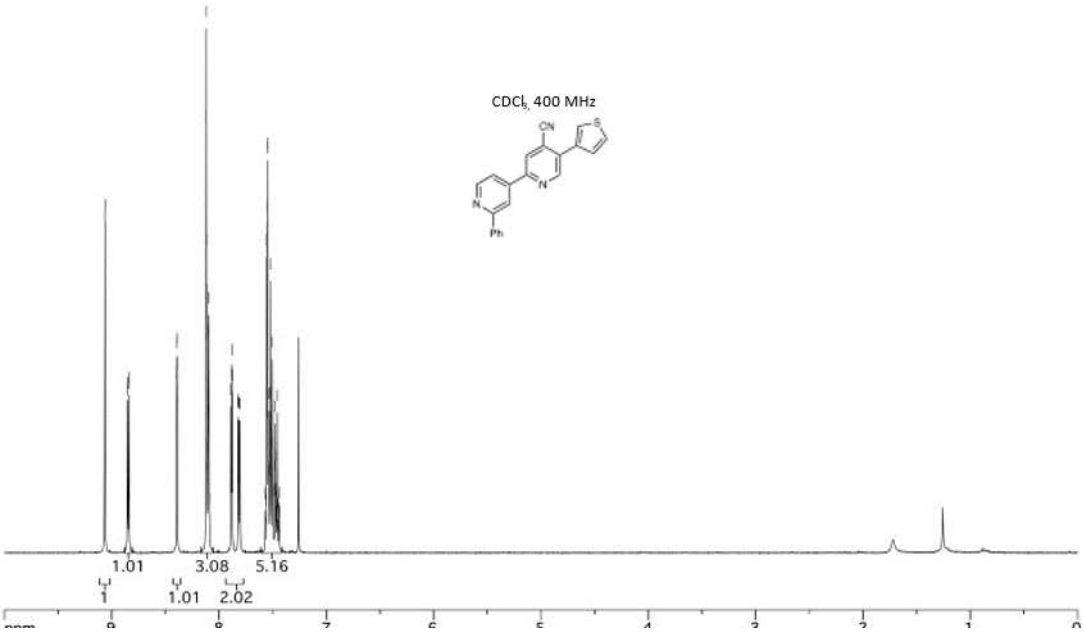
CDCl3, 400 MHz
CN
S
N
N
Ph
1.01
3.08
5.16
1
1.01
2.02

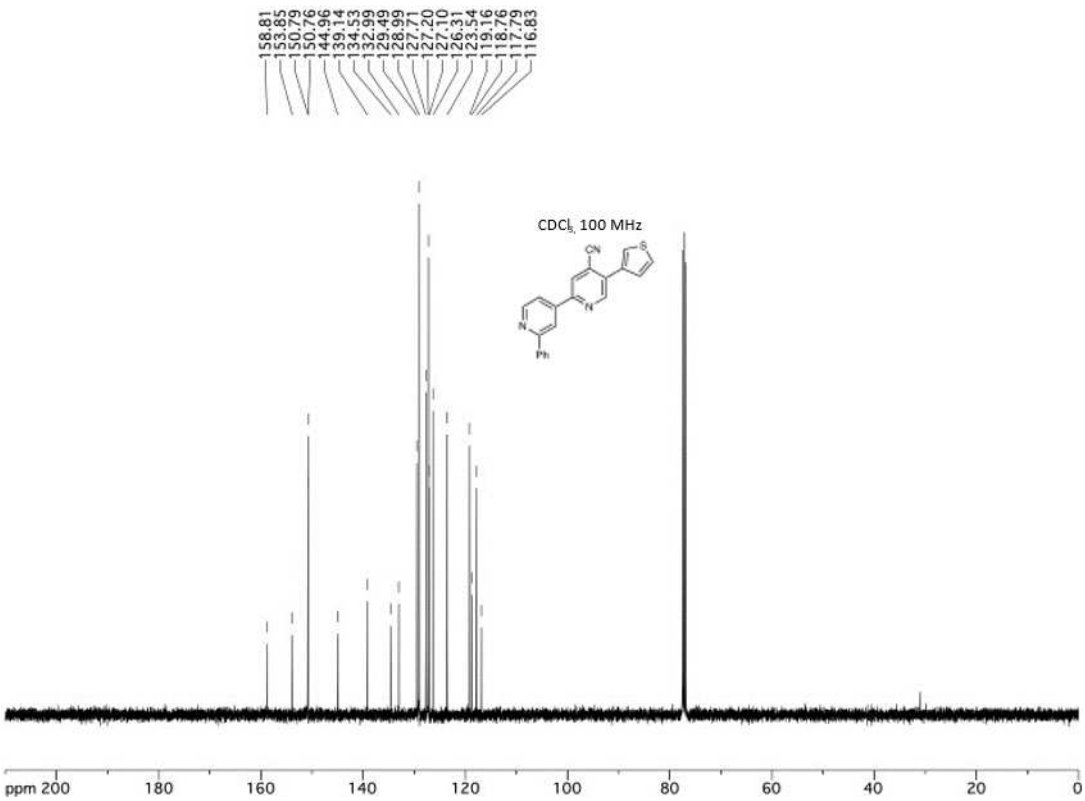
158.81
153.85
150.79
150.76
144.96
139.14
134.53
132.99
128.49
128.09
127.71
127.20
127.10
126.31
123.54
119.16
118.76
117.79
116.83
CDCl3, 100 MHz
CN
S
N
N
Ph
ppm 200
180
160
140
120
100
80
60
40
20
0

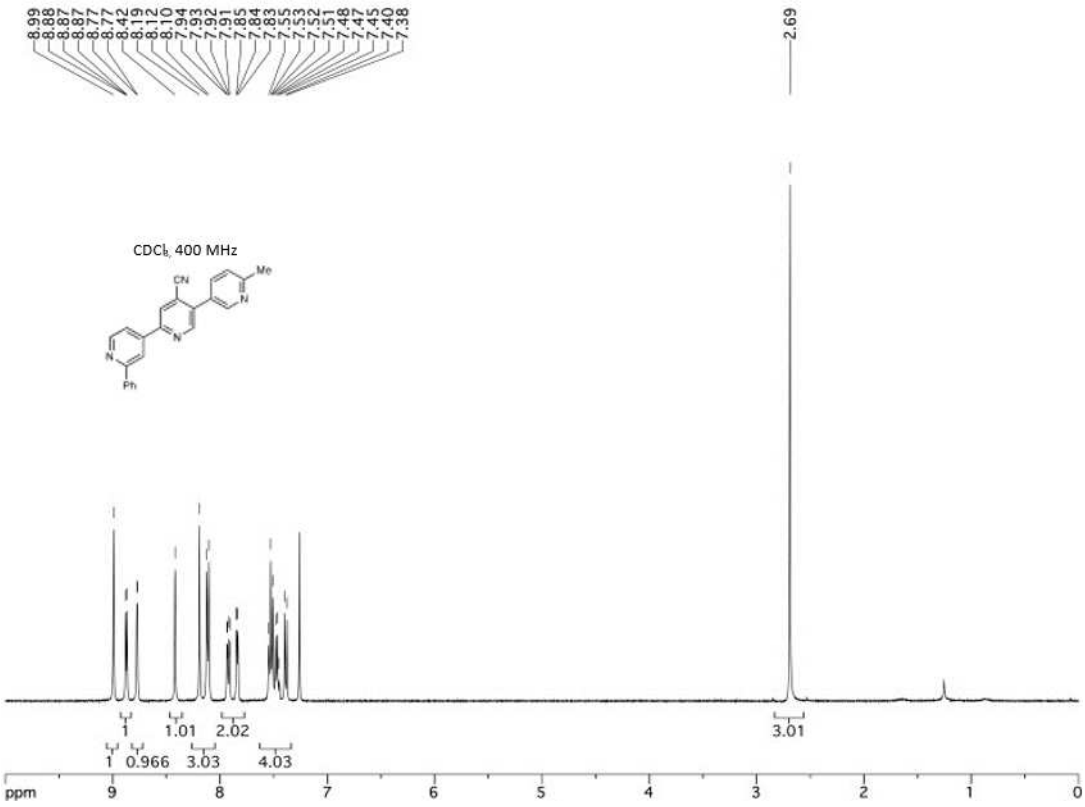
8.99
8.88
8.87
8.87
8.77
8.77
8.42
8.19
8.12
8.10
7.94
7.93
7.92
7.91
7.85
7.84
7.83
7.55
7.53
7.52
7.51
7.48
7.47
7.45
7.40
7.38
2.69
CDCl3, 400 MHz
CN
Me
N
N
N
Ph
1
1.01
2.02
3.01
1
0.966
3.03
4.03
ppm
9
8
7
6
5
4
3
2
1
0

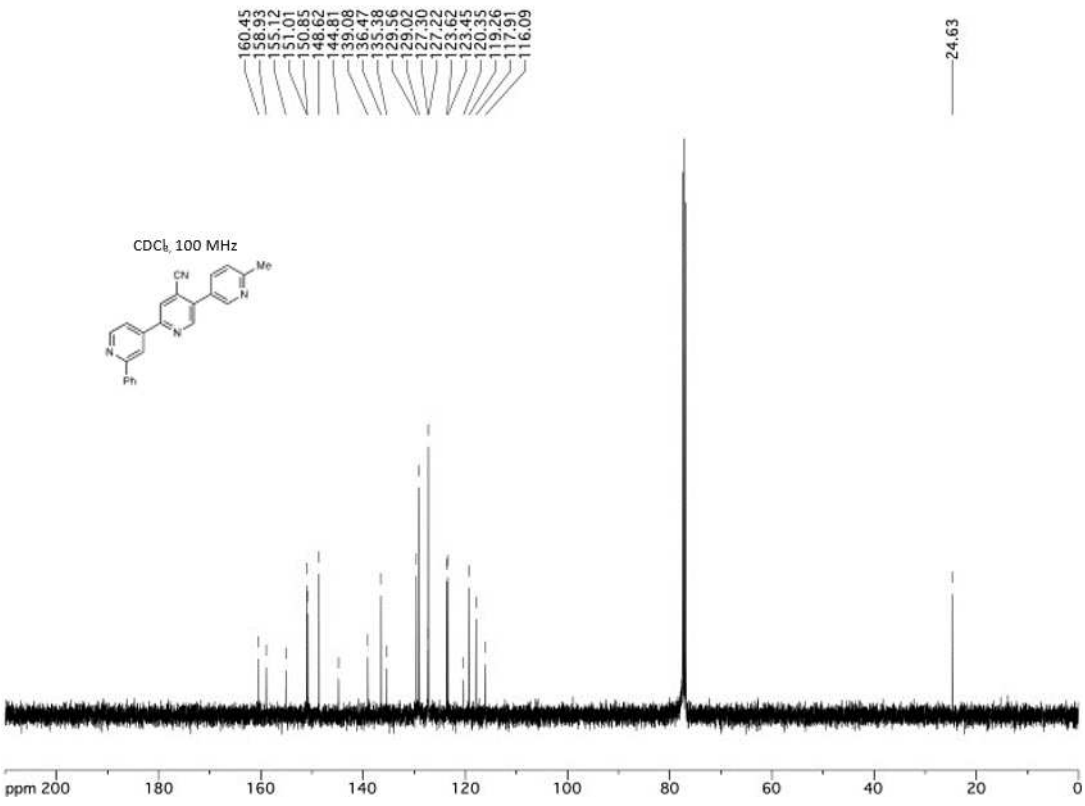
160.45
158.93
155.12
151.01
150.85
148.62
144.81
139.08
136.47
135.38
129.56
129.02
127.30
127.22
123.62
123.45
120.35
119.26
117.91
116.09
24.63
CDCl3, 100 MHz
CN
Me
N
N
N
Ph
ppm 200
180
160
140
120
100
80
60
40
20
0

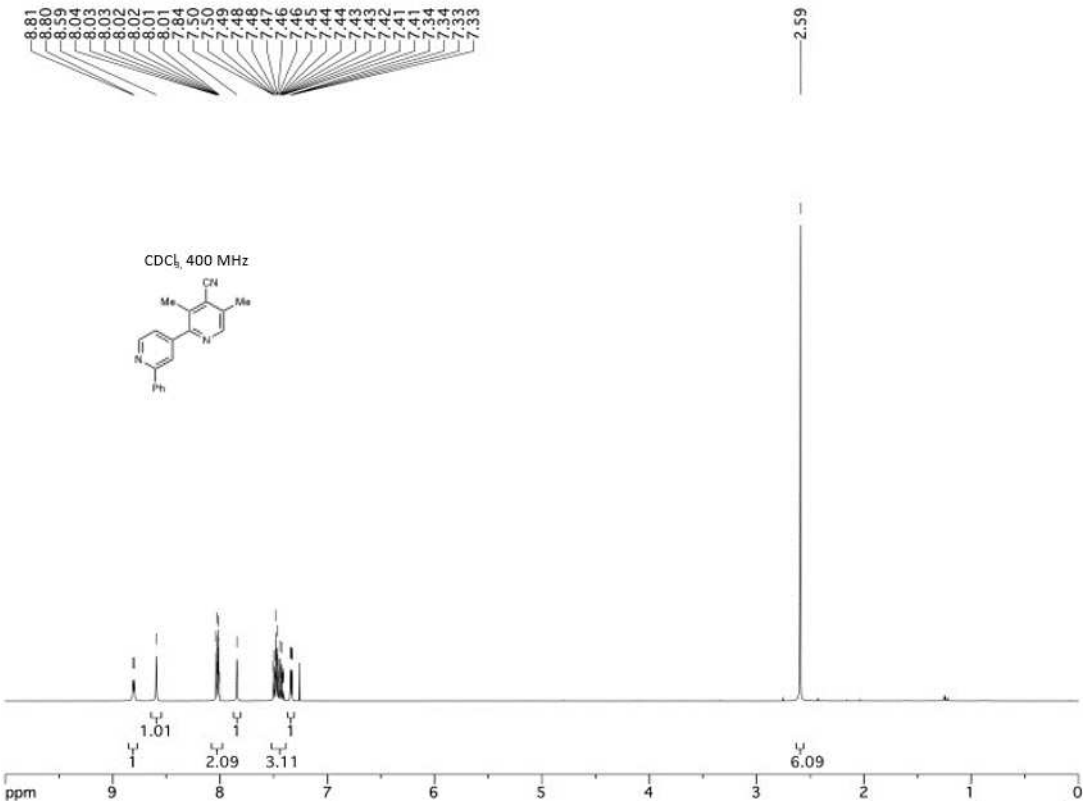
8.81
8.80
8.59
8.04
8.03
8.03
8.02
8.02
8.01
8.01
7.84
7.50
7.50
7.49
7.48
7.48
7.47
7.46
7.46
7.45
7.44
7.44
7.43
7.43
7.42
7.41
7.41
7.34
7.34
7.33
7.33
2.59
CDCl3, 400 MHz
CN
Me
Me
N
N
Ph
1
1.01
1
1
1
2.09
3.11
6.09
ppm
9
8
7
6
5
4
3
2
1
0

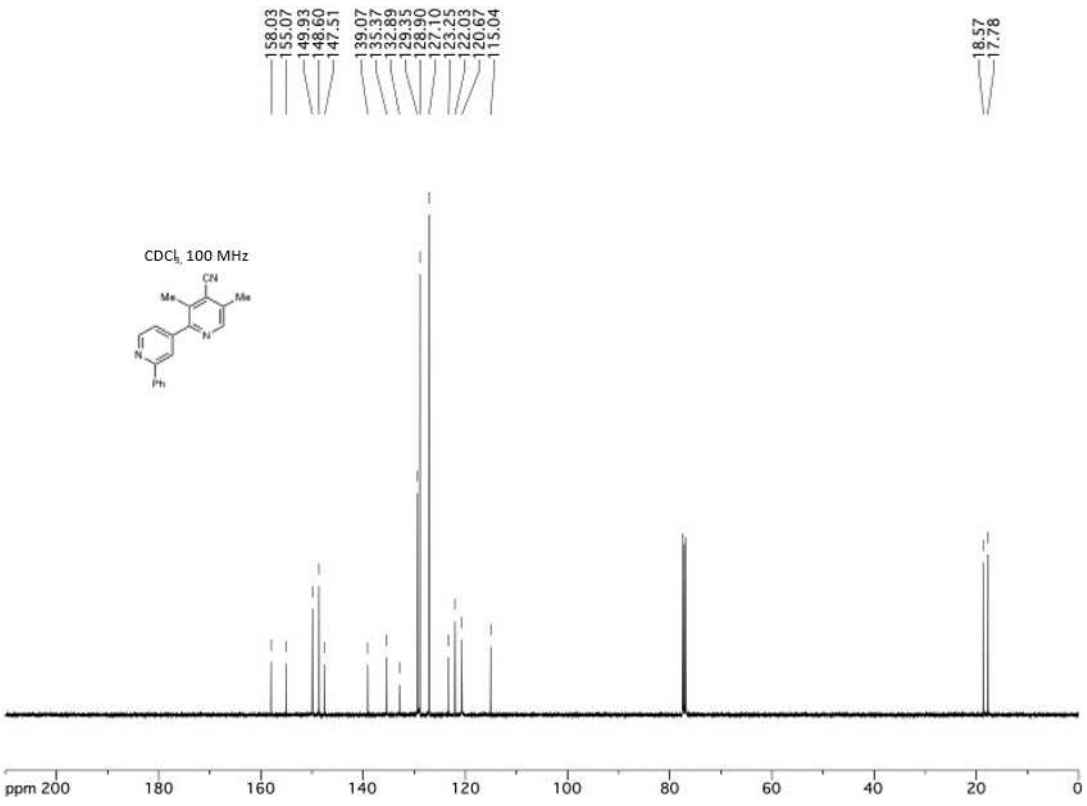
158.03
155.07
149.93
148.60
147.51
139.07
135.37
132.89
129.35
128.90
127.10
123.25
122.03
120.67
115.04
18.57
17.78
CDCl3, 100 MHz
CN
Me
Me
N
N
Ph
ppm 200
180
160
140
120
100
80
60
40
20
0

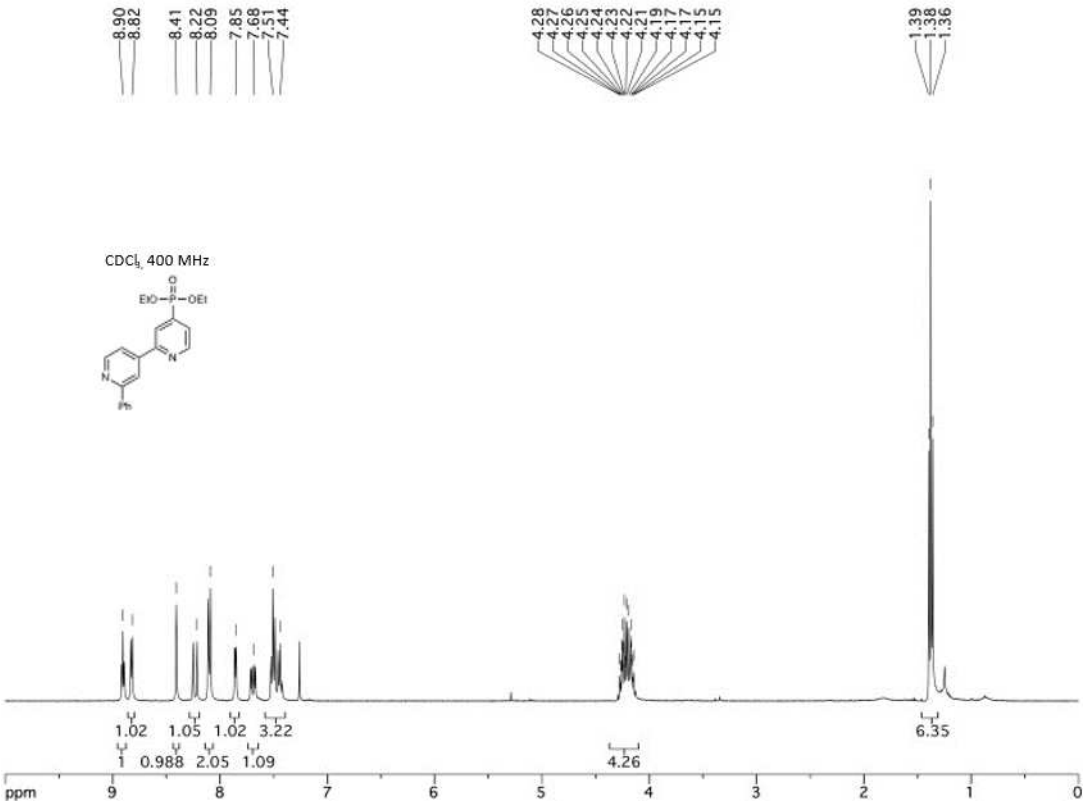
8.90
8.82
8.41
8.22
8.09
7.85
7.68
7.51
7.44
4.28
4.27
4.26
4.25
4.24
4.23
4.22
4.21
4.19
4.17
4.17
4.15
4.15
1.39
1.38
1.36
CDCl3, 400 MHz
EtO
P
O
OEt
N
N
Ph
1.02
1.05
1.02
3.22
1
0.988
2.05
1.09
4.26
6.35
ppm
9
8
7
6
5
4
3
2
1
0

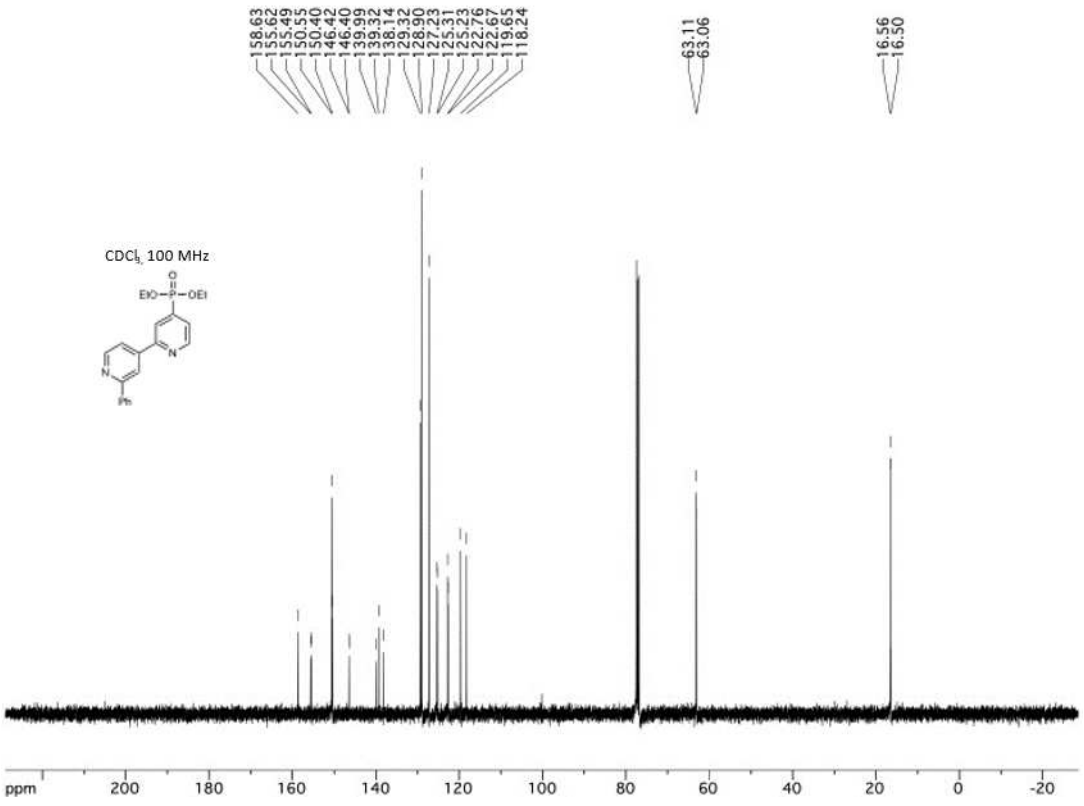
158.63
155.62
155.49
150.55
150.40
146.42
146.40
139.99
139.32
138.14
129.32
128.90
127.23
125.31
125.23
122.76
122.67
119.65
118.24
63.11
63.06
16.56
16.50
CDCl3, 100 MHz
EtO
P
OEt
N
Ph
ppm
200
180
160
140
120
100
80
60
40
20
0
-20

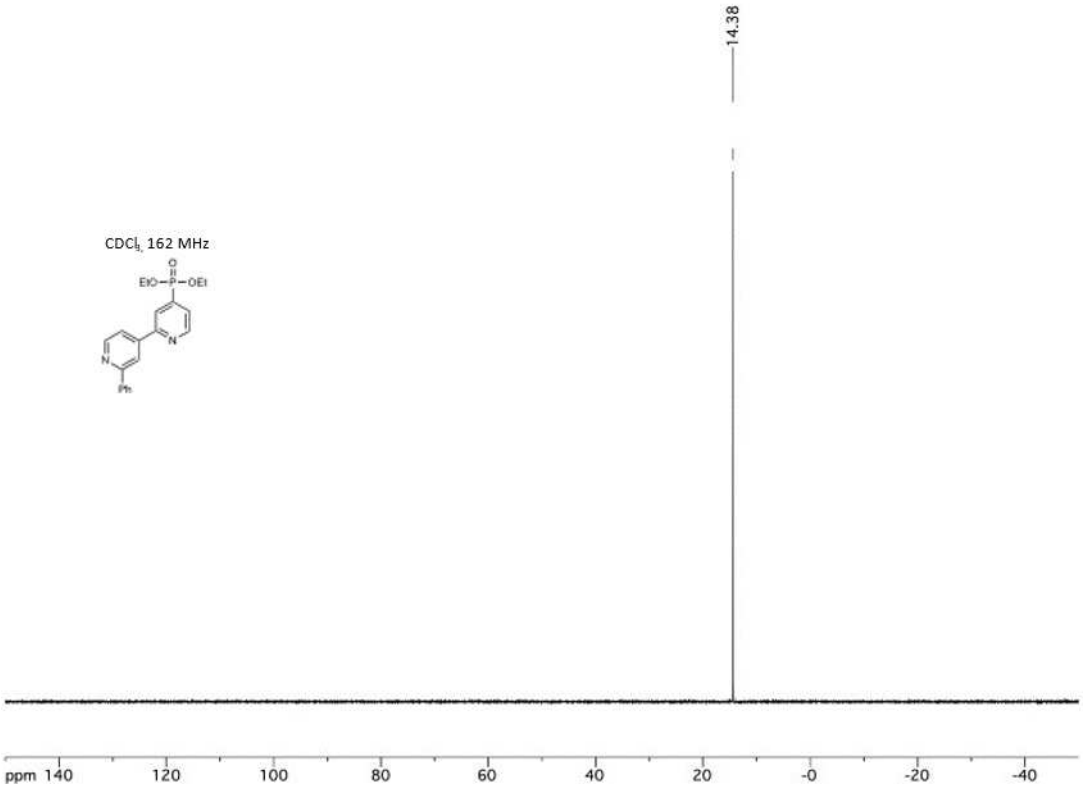
14.38
CDCl3, 162 MHz
EtO
P
OEt
N
Ph
ppm
140
120
100
80
60
40
20
-0
-20
-40

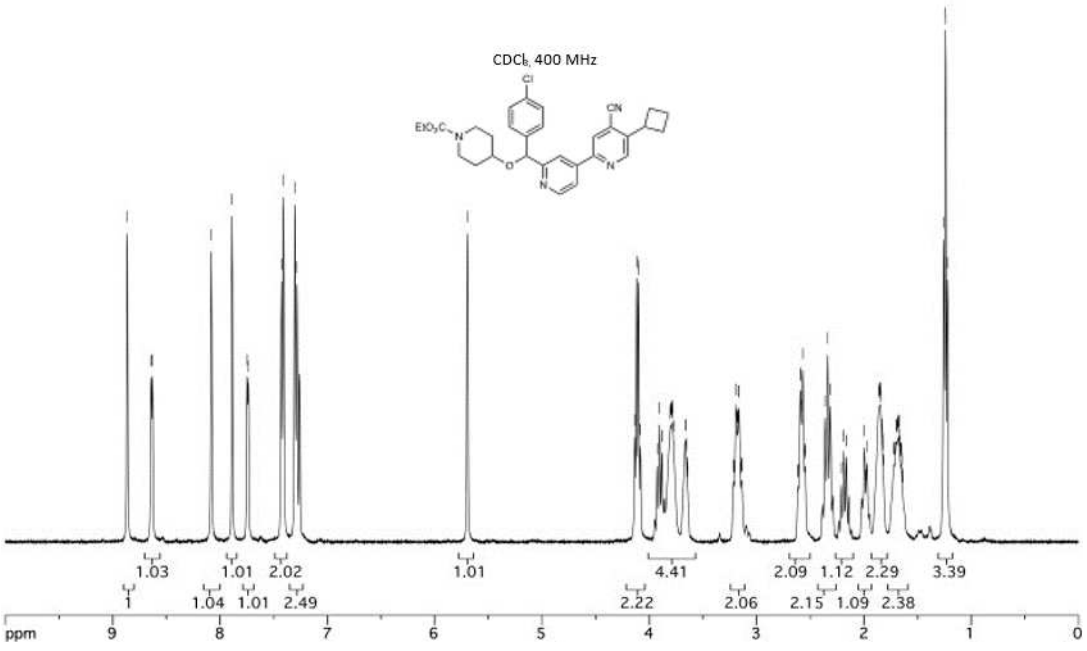
CDCl3, 400 MHz
1.03
1.01
2.02
1.01
4.41
2.09
1.12
2.29
3.39
1
1.04
1.01
2.49
2.22
2.06
2.15
1.09
2.38
ppm
9
8
7
6
5
4
3
2
1
0

163.21
155.65
153.19
149.99
149.64
145.70
142.73
140.01
133.67
128.81
128.29
122.62
120.18
119.80
117.70
115.93
81.09
73.05
61.43
41.30
41.23
36.79
31.32
31.24
29.02
18.70
14.83

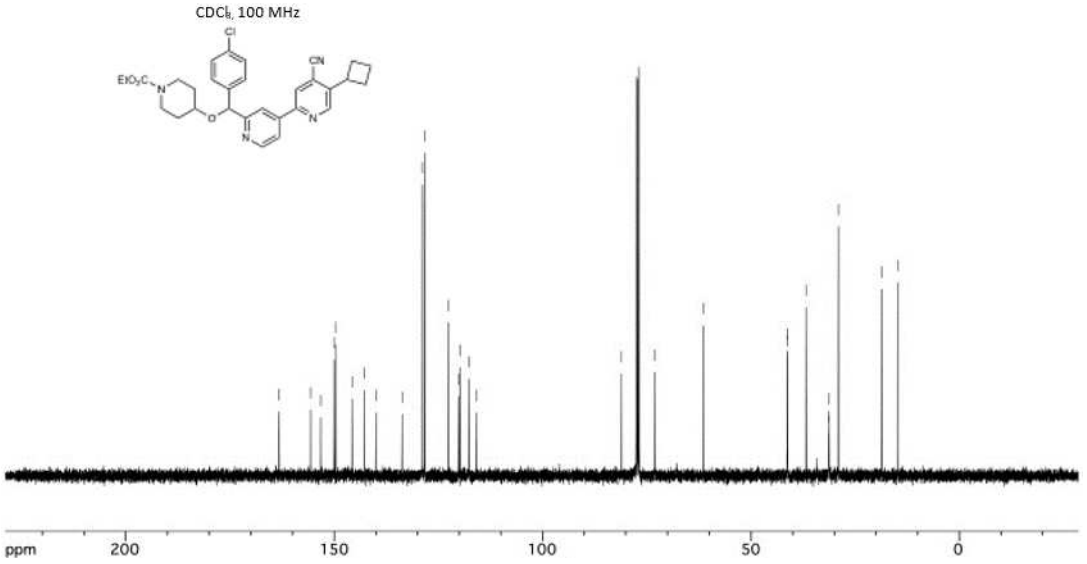
CDCl3, 100 MHz
ppm
200
150
100
50
0

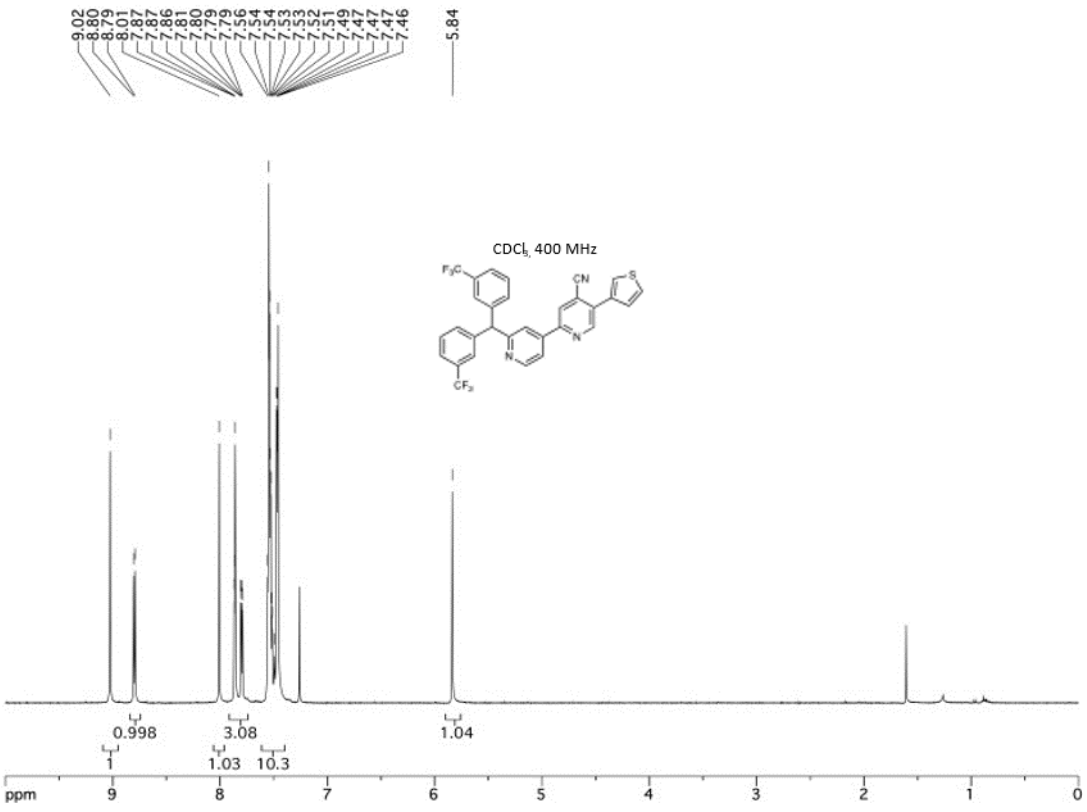
9.02
8.80
8.79
8.01
7.87
7.87
7.86
7.81
7.80
7.79
7.79
7.56
7.54
7.54
7.53
7.53
7.52
7.31
7.49
7.47
7.47
7.47
7.46
5.84
CDCl3, 400 MHz
0.998
3.08
1.04
1
1.03
10.3
ppm

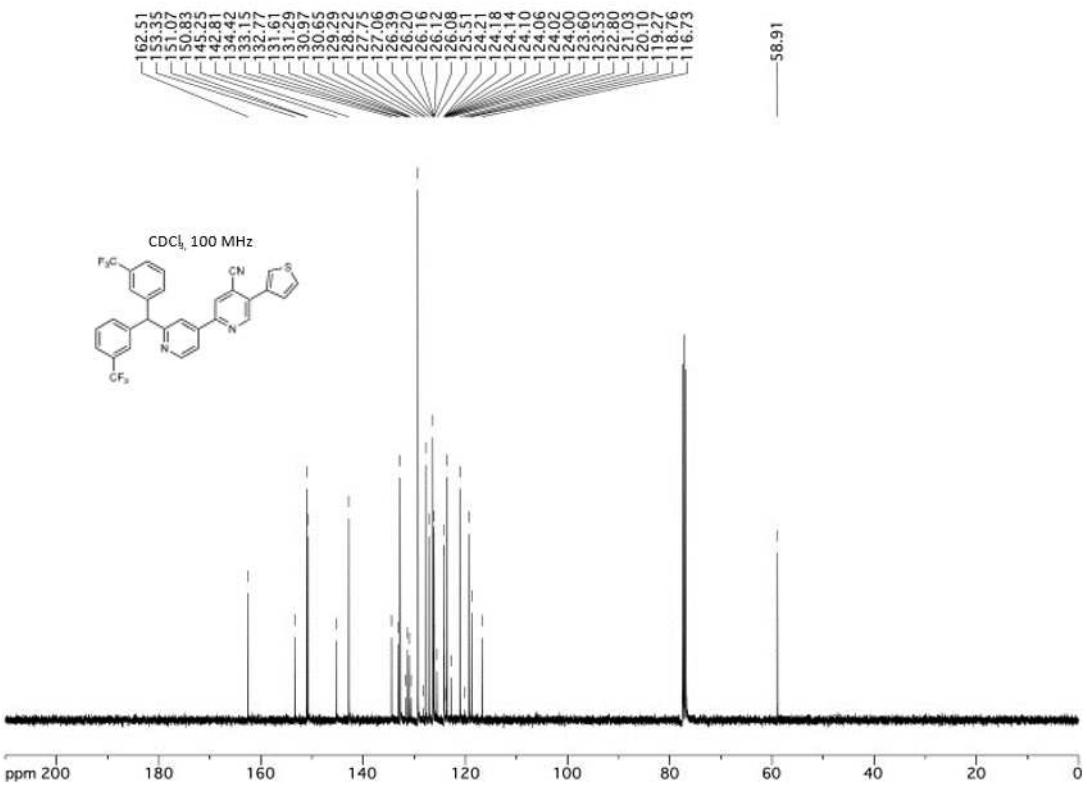
162.51
153.35
151.07
150.83
145.25
142.81
134.42
133.15
132.77
131.61
131.29
130.97
130.65
129.29
128.22
127.75
127.06
126.39
126.20
126.16
126.12
126.08
125.51
124.21
124.18
124.14
124.10
124.06
124.02
124.00
123.60
123.53
122.80
121.03
120.10
119.27
118.76
116.73
58.91
CDCl3, 100 MHz
ppm

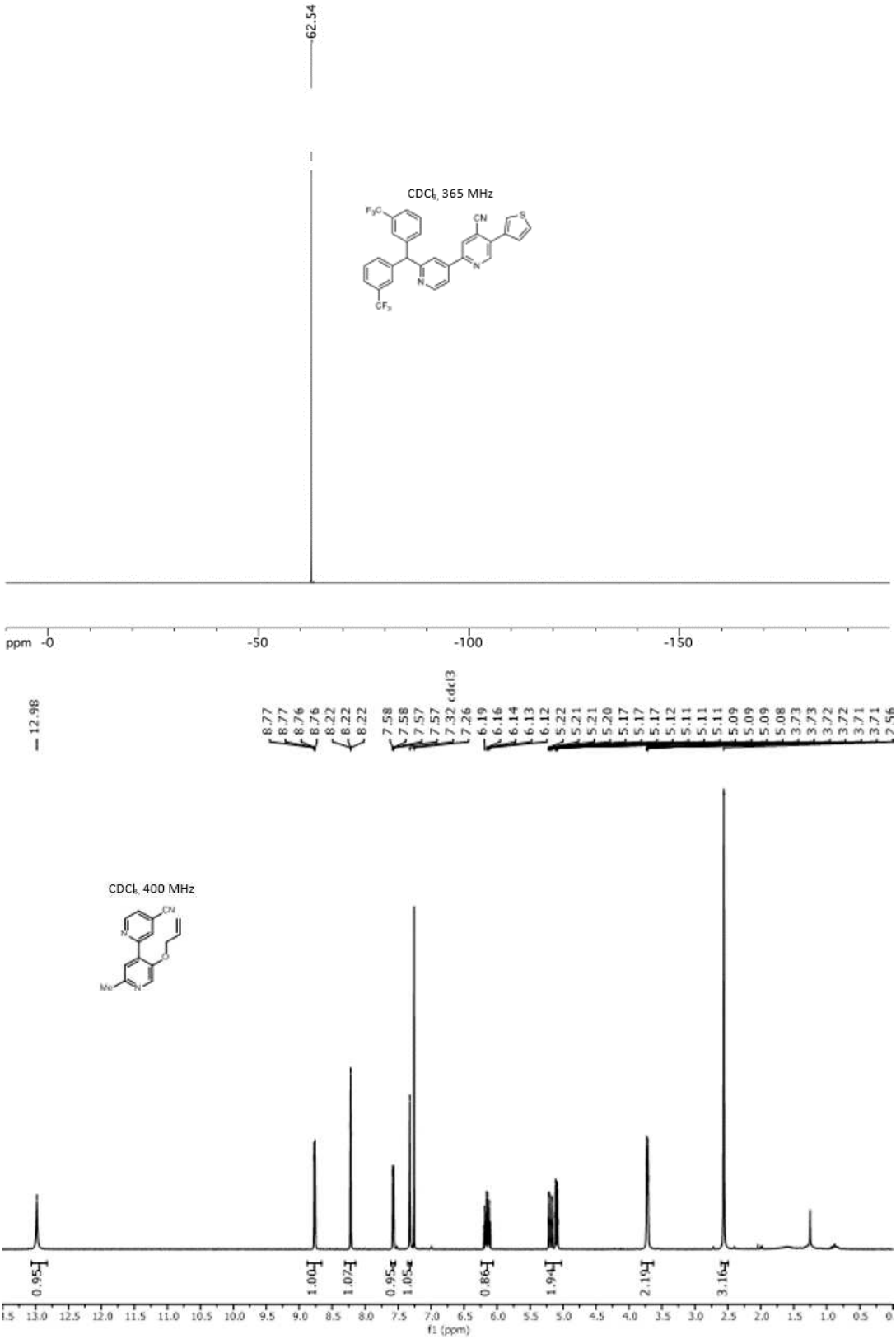
62.54
CDCl3, 365 MHz
ppm -0
-50
-100
-150
12.98
8.77
8.77
8.76
8.76
8.22
8.22
8.22
7.58
7.58
7.57
7.57
7.32 cdcl3
7.26
6.19
6.16
6.14
6.13
6.12
5.22
5.21
5.21
5.20
5.17
5.17
5.17
5.12
5.11
5.11
5.11
5.09
5.09
5.09
5.08
3.73
3.73
3.72
3.72
3.71
3.71
CDCl3, 400 MHz
0.95
1.00
1.07
0.95
1.05
0.86
1.94
2.19
3.16
f1 (ppm)

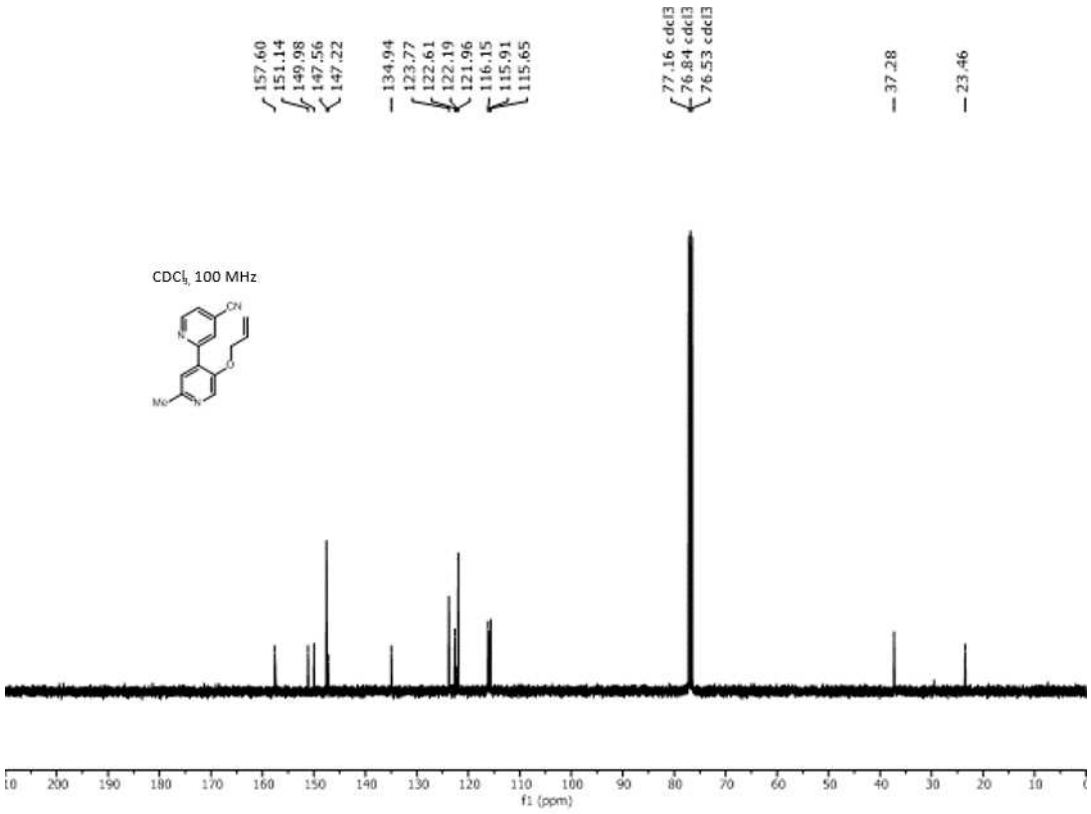
157.60
151.14
149.98
147.56
147.22
134.94
123.77
122.61
122.19
121.96
116.15
115.91
115.65
77.16 cdcl3
76.84 cdcl3
76.53 cdcl3
37.28
23.46
CDCl3, 100 MHz
f1 (ppm)

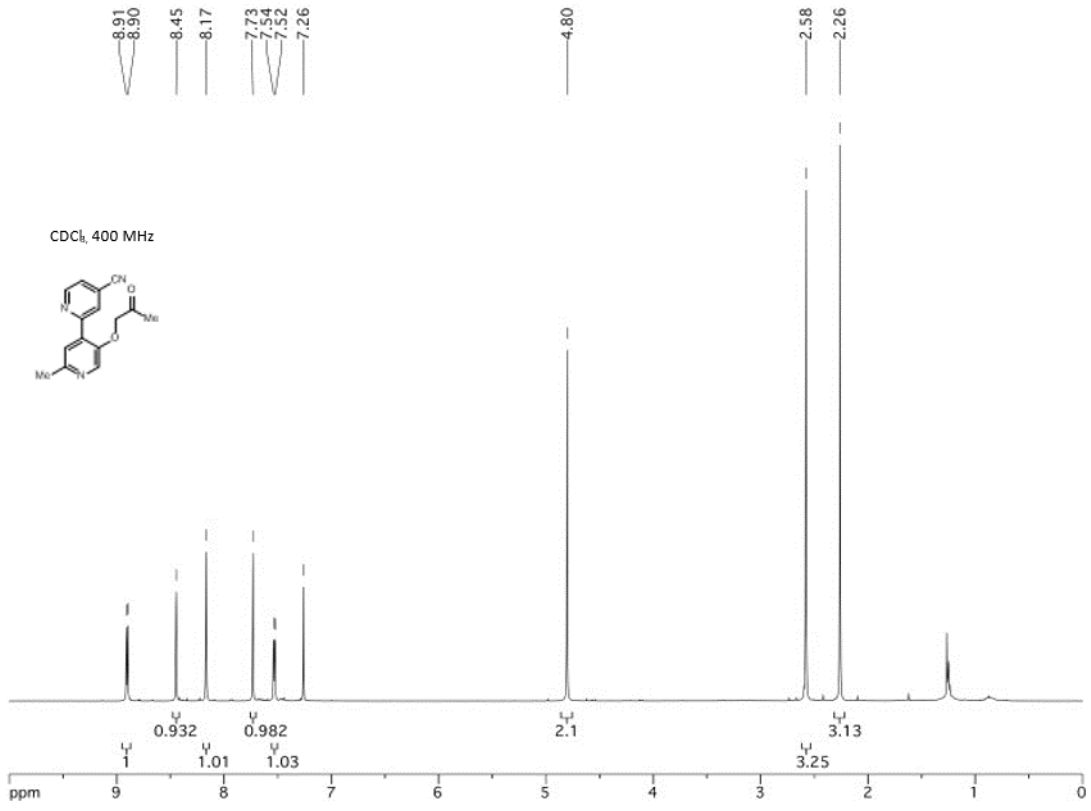
8.91
8.90
8.45
8.17
7.73
7.54
7.52
7.26
4.80
2.58
2.26
CDCl3, 400 MHz
0.932
0.982
2.1
3.13
1
1.01
1.03
3.25
ppm

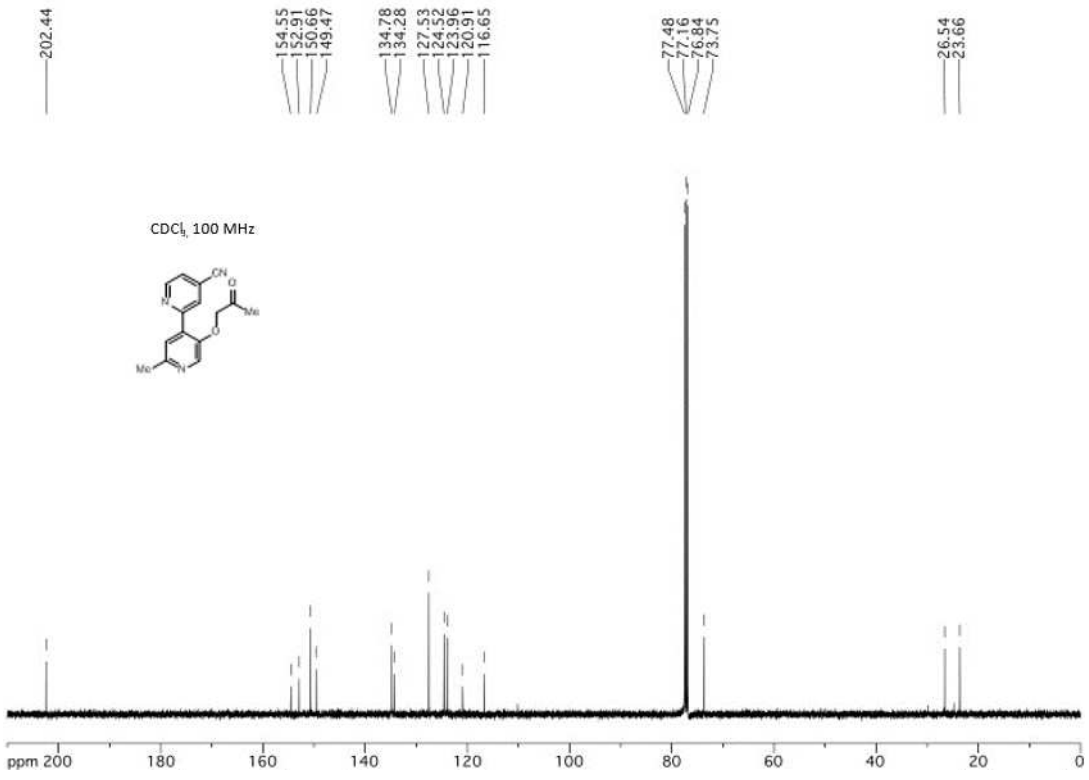
202.44
154.55
152.91
150.66
149.47
134.78
134.28
127.53
124.52
123.96
120.91
116.65
77.48
77.16
76.84
73.75
26.54
23.66
CDCl3, 100 MHz
ppm 200
180
160
140
120
100
80
60
40
20
0

APPENDIX TWO

PYRIDYLPHOSPHONIUM SALTS AS ALTERNATIVES TO CYANOPYRIDINES IN RADICAL-RADICAL COUPLING REACTIONS: EXPERIMENTAL

A2.1. General Information

Proton nuclear magnetic resonance (^{1}H NMR) spectra were recorded at ambient temperature on either a Bruker Ultrashield–400 (400 MHz) spectrometer, a Varian 400 MR (400 MHz) spectrometer or an Agilent Inova 400 (400 MHz) spectrometer. Chemical shifts (δ) are reported in ppm and quoted to the nearest 0.01 ppm relative to the residual protons in $CDCl_3$ (7.26 ppm), C_6D_6 (7.16 ppm), $(CD_3)_2SO$ (2.50 ppm), CD_3OD (3.31 ppm) or CD_3CN (1.94 ppm) and coupling constants (*J*) are quoted in Hertz (Hz). Data are reported as follows: Chemical shift (number of protons, multiplicity, coupling constants). Coupling constants were quoted to the nearest 0.1 Hz and multiplicity reported according to the following convention: s = singlet, d = doublet, t = triplet, q = quartet, qn = quintet, sext = sextet, sp = septet, m = multiplet, br = broad. Where coincident coupling constants have been observed, the apparent (app) multiplicity of the proton resonance has been reported. Carbon nuclear magnetic resonance (^{13}C NMR) spectra were recorded at ambient temperature on either a Bruker Ultrashield–400 (100 MHz) spectrometer, a Varian 400 MR spectrometer (100 MHz) or an Agilent Inova 400 (100 MHz) spectrometer. Chemical shift (δ) was measured in ppm and quoted to the nearest 0.1 ppm relative to the residual solvent peaks in $CDCl_3$ (77.16 ppm), C_6D_6 (128.06 ppm), $(CD_3)_2SO$ (39.51 ppm), CD_3OD (49.00 ppm) or CD_3CN (1.32 ppm). DEPT135, NOE experiments and 2–dimensional experiments (COSY, HMBC, and HSQC) were used to support assignments where appropriate.

Absorption spectra were obtained with a Hewlett-Packard 8453 spectrometer in quartz cuvettes with a 1 cm path length. Emission spectroscopy was performed on an Edinburgh Instruments FS5 spectrometer using a sealed quartz cuvette.

Low–resolution mass spectra (LRMS) were measured on an Agilent 6310 Quadrupole Mass Spectrometer. Infrared (IR) spectra were recorded on a Bruker Tensor 27 FT–IR spectrometer as either

solids or neat films, either through direct application or deposited in $CHCl_3$, with absorptions reported in wavenumbers (cm^{-1}).

Analytical thin layer chromatography (TLC) was performed using pre–coated glass backed silica gel plates (Silicagel 60 F254). Flash column chromatography was undertaken on Silicycle silica gel (230–400 mesh) under a positive pressure of air. Visualization was achieved using ultraviolet light (254 nm) and chemical staining with ceric ammonium molybdate or basic potassium permanganate solutions as appropriate.

Tetrahydrofuran (THF), toluene, hexane, diethyl ether and dichloromethane were dried and distilled using standard methods.[1] Ethyl acetate (EtOAc), 1,2–Dichloroethane (DCE), 1,4–dioxane, chloroform, chlorobenzene and acetone were purchased anhydrous from Sigma Aldrich chemical company. All reagents were purchased at the highest commercial quality and used without further purification unless stated otherwise. Reactions were carried out under an atmosphere of nitrogen unless otherwise stated. All reactions were monitored by TLC, ^1H NMR spectra taken from reaction samples, and/or liquid chromatography mass spectrometry (LCMS) using an Agilent 6310 Quadrupole Mass Spectrometer. Melting points (mp) were recorded using a Büchi B–450 melting point apparatus and are reported uncorrected.

PPh_3 (99%) was purchased from Oakwood Chemical and is most effective when crushed to a powder before use. Tf_2O (99%) was purchased from Oakwood Chemical and used without further purification and was routinely stored in a –20 ºC fridge. NEt_3 and DBU were distilled before use. 2,6-lutidine was distilled then sparged with a stream of N_2 for 20 mins before use. Sparged, distilled 2,6-lutidine was stored in the glovebox to prevent exposure to oxygen or moisture.

All photoredox reactions were conducted under a nitrogen atmosphere while subject to irradiation from a 455 nm kessil lamp (Kessil PR160 set at 100% intensity or Kessil H150-Blue) at room temperature (see photoredox setup below). Irradiation of the reaction mixture with UV light was done with realUV™

LED Lights (365 nm) which can be purchased from waveformlighting.com. These LEDs were wrapped around the inside of a Pyrex crystallization dish and reaction vials were placed inside the dish as close to the lights as possible. 3DPAFIPN (2,4,6-Tris(diphenylamino)-5-fluoroisophthalonitrile), 5CzBn (2,3,4,5,6-Penta(9H-carbazol-9-yl)benzonitrile), and 3DPA2FBN (2,4,6-Tris(diphenylamino)-3,5-difluorobenzonitrile) photocatalysts were prepared according to a previously reported procedure.[2]

A2.2. Photoredox Setup

All reactions were conducted under nitrogen at room temperature. Ambient temperature was maintained by using a compressed air line. Shown below is a photograph of the reaction setup, where the LED array was positioned approximately 6 inches away from the vials containing reaction mixture. If using the Kessil PR160 lamps, the intensity dial was set at 100%. **Be sure to wear proper protective eyewear that blocks harmful wavelengths of light when lights are in use until the light has been properly covered or blocked.** An example of appropriate protective goggles from HepatoChem is provided: Skyper eyewear protective goggles, product number HCK1015-01-001. Note: the reactions shown below were covered fully with cardboard after the lights were turned on.

Figure A2.1. Photoredox setup with lights off

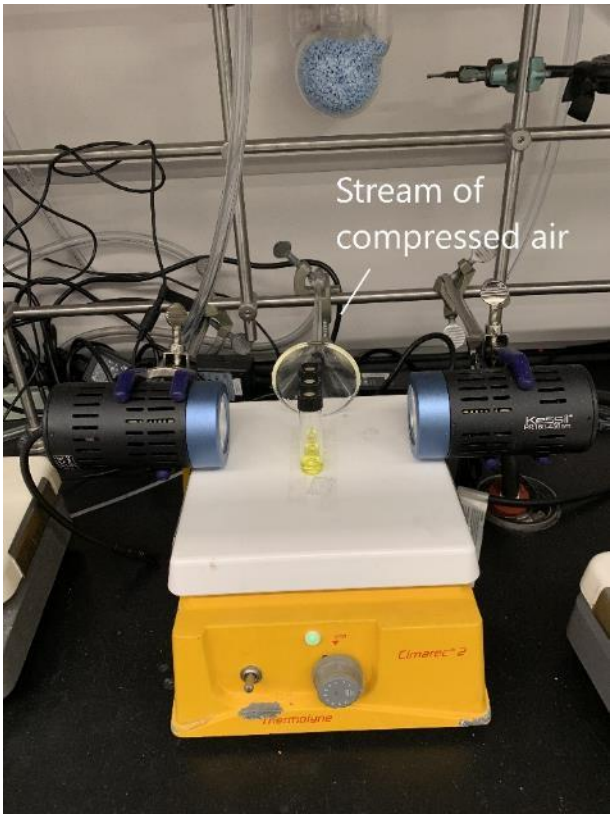

Figure A2.2. Photoredox setup with lights on

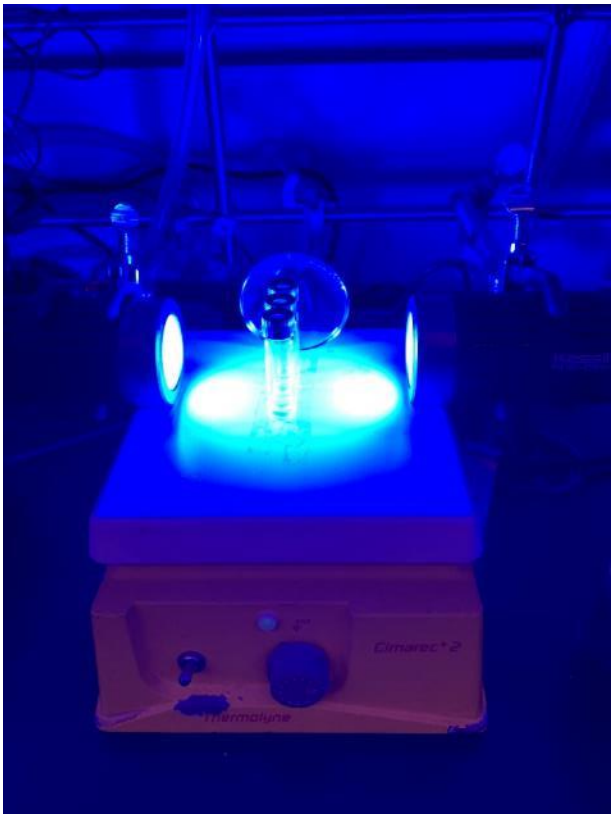

A2.3. Optimization Studies

For optimization studies, an oven dried 8 mL vial equipped with a magnetic stir bar was charged with the triphenyl(2-phenylpyridin-4-yl)phosphonium trifluoromethane sulfonate (56.6 mg, 0.10 mmol, 1.0 equiv), potassium trifluoro(1-phenylethyl)borate (42.4 mg, 0.20 mmol, 2.0 equiv) and photocatalyst (2 mol%). The vial was pumped into a glovebox and then dioxane (333 μL, 0.3 M) and 2,6-lutidine (35 μL, 3.0 equiv) were added via a microliter syringe. The vial was sealed and removed from the glovebox and pre-stirred for ten minutes before irradiation with a 455 nm kessil lamp (5 cm away, with stream of air blowing over vials to keep reaction at 25 °C) for 16 hours. The reaction was quenched with water and the aqueous layer was extracted with CH_2Cl_2 (4x). The combined organic extracts were dried ($MgSO_4$), filtered, and concentrated *in vacuo*. $CDCl_3$ and trimethoxybenzene (16.8 mg, 0.10 mmols) was added, and the sample was analyzed by ^1H NMR. The integral values were used to calculate the data given in **Table S1**. Examples of substrates that worked better with the inclusion of the 2,6-lutidine additive are summarized in **Tables S2 and S3**. Redox potentials and triplet energies of pertinent photocatalysts are included below in **Table 4** that were compiled from previous literature reports.[2-5]

Table A2.1. Optimization of Pyridine Alkylation[a]

A – Reaction Optimization

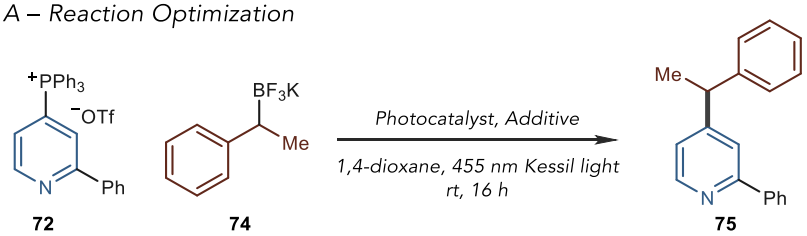

Entry	Photocatalyst (2 mol%)	Additive (3 equiv)	Concentration	% **75**[b]
1	$Ir(ppy)_3$	none	0.1 M	60
2	$[Ir(dF(CF_3)ppy)_2(dtbbpy)]PF_6$	none	0.1 M	66
3	3DPAFIPN	none	0.1 M	77
4	3DPAFIPN	none	0.3 M	82
5	3DPAFIPN	2,6–lutidine	0.3 M	82 (74)[c]
6	4CzIPN	2,6–lutidine	0.3 M	40
7	5CzBn	2,6–lutidine	0.3 M	71
8	3DPA2FBN	2,6–lutidine	0.3 M	73
9	$[Ir(ppy)_2(dtbbpy)]PF_6$	2,6–lutidine	0.3 M	74
10	$[Mes\text{-}Acr]BF_4$	2,6–lutidine	0.3 M	41
11	none	2,6–lutidine	0.3 M	trace
12[d]	none	2,6–lutidine	0.3 M	66

B – BF_3 Additive Enables Previously Ineffective Photocatalyst

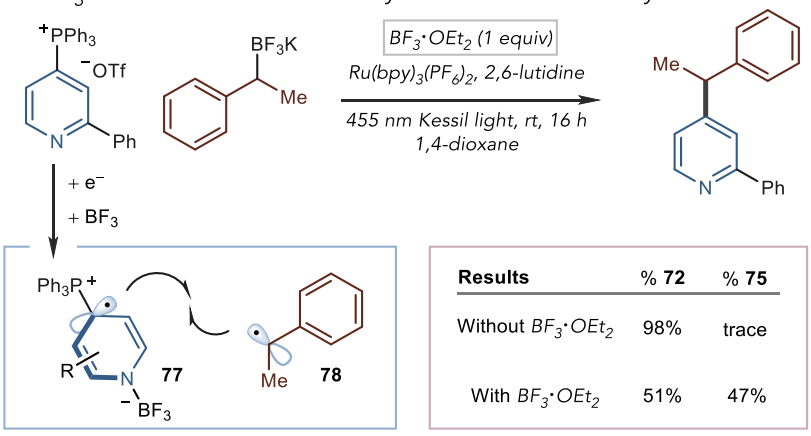

Results	% 72	% 75
Without $BF_3{\cdot}OEt_2$	98%	trace
With $BF_3{\cdot}OEt_2$	51%	47%

[a]Conditions: **72** (1.0 equiv), **74** (2.0 equiv), photocatalyst (2 mol%), additive (3.0 equiv), rt. [b]Yields determined by ^{1}H NMR analysis using 1,3,5-trimethoxybenzene as internal standard. [c]Isolated yield on 0.50 mmol scale. [d]Used 365 nm LEDs instead of 455 nm Kessil light for 89 h.

Table A2.2. Example of BF_3K Salt that Requires 2,6-lutidine Additive[a,b]

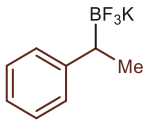

vs.

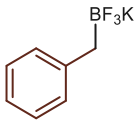

	Yield of Product **75**	Yield of Product **3aa**
With 2,6-lutidine	82%	50%[c]
Without 2,6-lutidine	82%	29%[d]

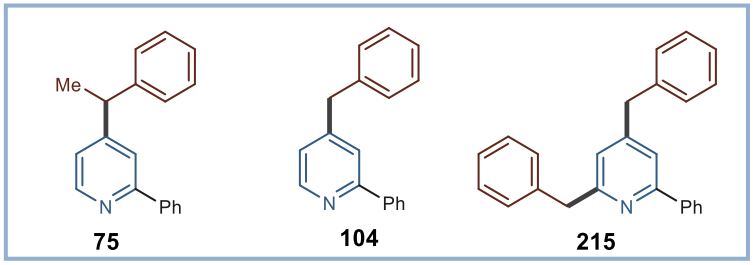

[a]Conditions: **72** (1.0 equiv), **BF_3K Salt** (2.0 equiv) photocatalyst (2 mol%), additive (3.0 equiv), rt. [b]Yields detemined by ^{1}H NMR analysis using 1,3,5-trimethoxybenzene as internal standard. [c]Ratio of desired product **104** to bis-addition **215** = 5.7:1. [d]Ratio of desired product **104** to bis-addition **215** = 1.6:1.

Table A2.3. Example of Phosphonium Salt that Requires 2,6-lutidine Additive[a,b]

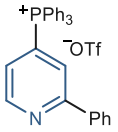

72

vs.

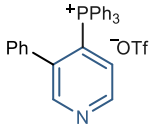

73

	Yield of Product **75**	Yield of Product **76**
With 2,6-lutidine	82%	60%
Without 2,6-lutidine	82%	20%[c]

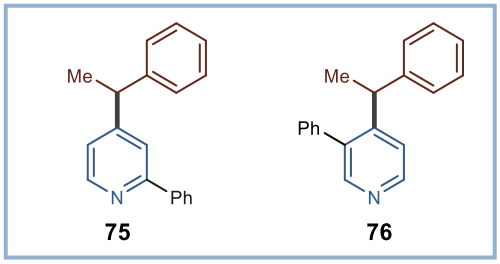

[a]Conditions: **Phosphonium Salt** (1.0 equiv), **74** (2.0 equiv) photocatalyst (2 mol%), additive (3.0 equiv), rt. [b]Yields detemined by ^{1}H NMR analysis using 1,3,5-trimethoxybenzene as internal standard. [c]Reaction provided complex mixture of byproducts

Table A2.4. Pertinent Photocatalyst Redox Properties and Triplet Energies

Photocatalyst	$E_{1/2}(M^+/M^*)$	$E_{1/2}(M^*/M^-)$	$E_{1/2}(M^+/M)$	$E_{1/2}(M/M^-)$	$E_{0,0}^{T_1}$(kcal/mol)
Ir(ppy)$_3$	*−1.73 V*	*+0.31 V*	*+0.77 V*	*−2.19 V*	58.1
[Ir(dF(CF$_3$)ppy)$_2$(dtbbpy)]PF$_6$	*−0.89 V*	*+1.21 V*	*+1.69 V*	*−1.37 V*	61.8
3DPAFIPN	*−1.38 V*	*+1.09 V*	*+1.30 V*	*−1.59 V*	61.8
[Ir(ppy)$_2$(dtbbpy)]PF$_6$	*−0.96 V*	*+0.66 V*	*+1.21 V*	*−1.57 V*	49.2
[Mes-Acr]BF$_4$		*+2.18 V*		*−0.49 V*	44.7
[Ru(bpy)$_3$]PF$_6$	*−0.81 V*	*+0.77 V*	*+1.29 V*	*−1.33 V*	49.0

All redox potentials are reported vs SCE. All values are compiled from previous literature reports.

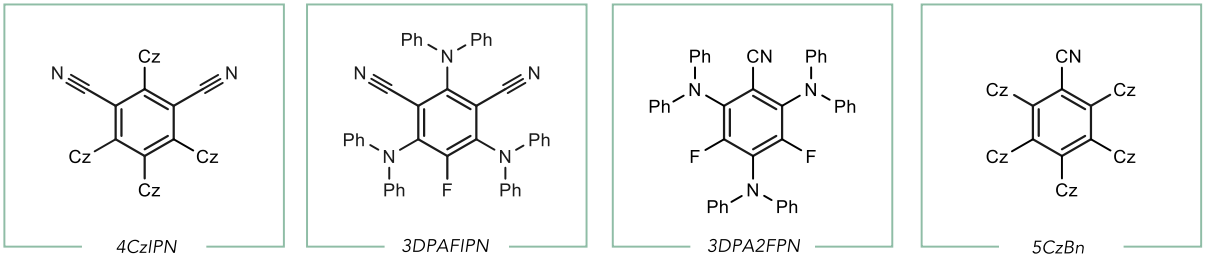

A2.4. UV-Vis Spectroscopy Studies

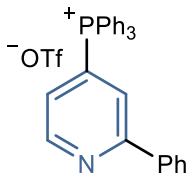

72

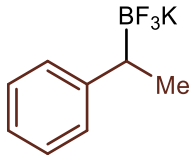

74

Procedure: An oven dried 8 mL vial was charged with either triphenyl(2-phenylpyridin-4-yl)phosphonium trifluoromethanesulfonate, (5.7 mg, 0.01 mmol), potassium trifluoro(1-phenylethyl)borate (2.1 mg, 0.01 mmol), or both (1:1 mixture, 0.01 mmol each). 1,4-dioxane (1.0 mL, 0.01 M) was added to each of the three vials, and a series of dilutions were made to achieve an absorbance between 0 and 1 a.u. (0.001 M – 0.0001 M). The solutions were transferred to a quartz cuvette with 1 cm pathlength and analyzed via UV-Vis spectroscopy. Results are shown below.

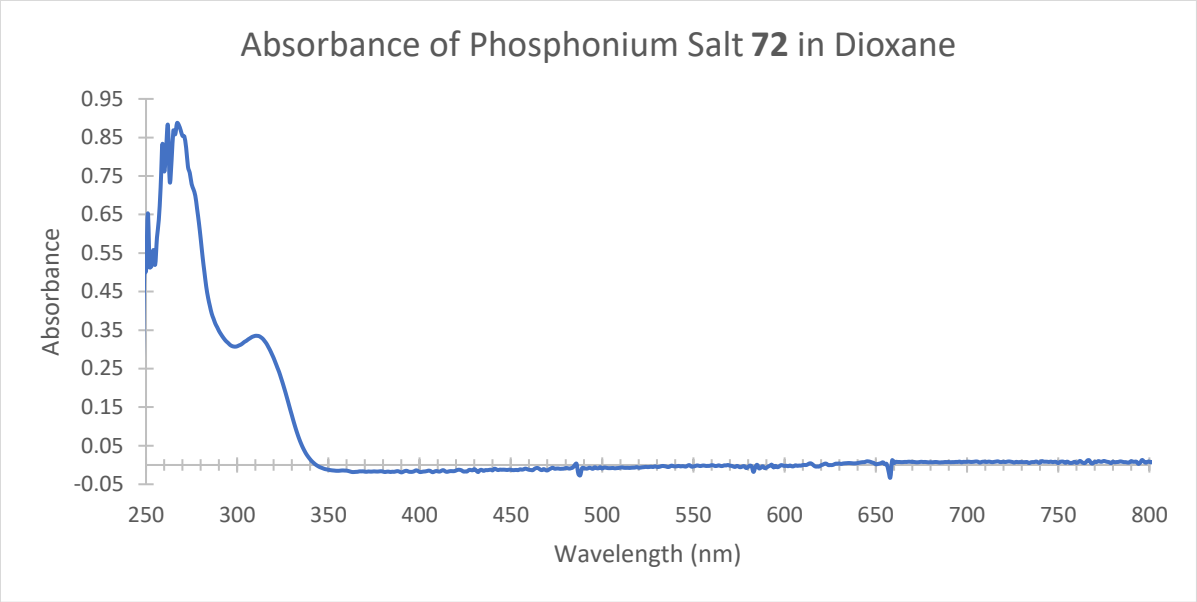

Figure A2.3: **72** (5.7 mg, 0.01 mmol) in 1,4-dioxane (1 mL) were added to an 8 mL vial. The sample was then diluted with 1,4-dioxane to 0.0001 M with respect to **72** and transferred to a cuvette with a 1 cm path length.

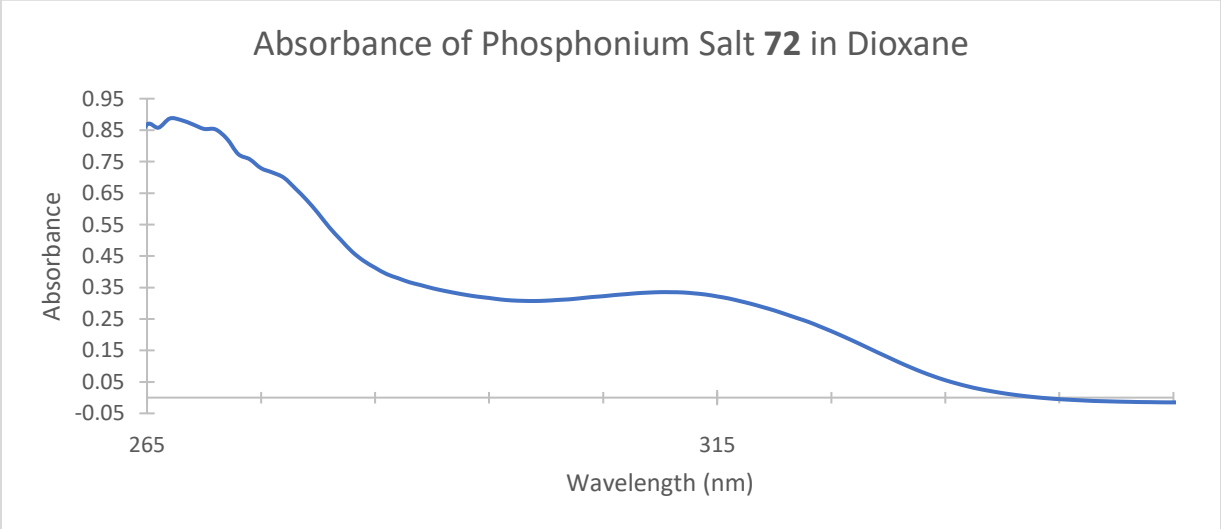

Figure A2.4: Zoomed in spectra from **Figure A2.3.**

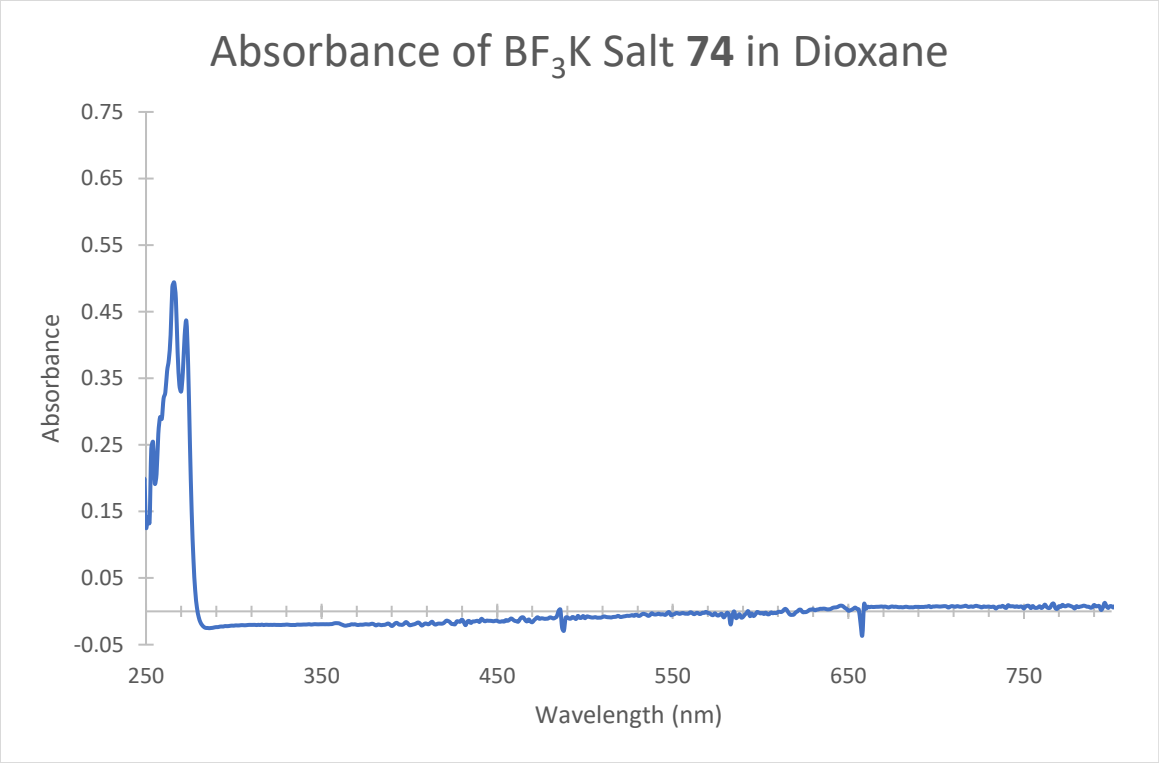

Figure A2.5: **74** (2.1 mg, 0.01 mmol) in 1,4-dioxane (1 mL) were added to an 8 mL vial. The sample was then diluted with 1,4-dioxane to 0.001 M with respect to **74** and transferred to a cuvette with a 1 cm path length.

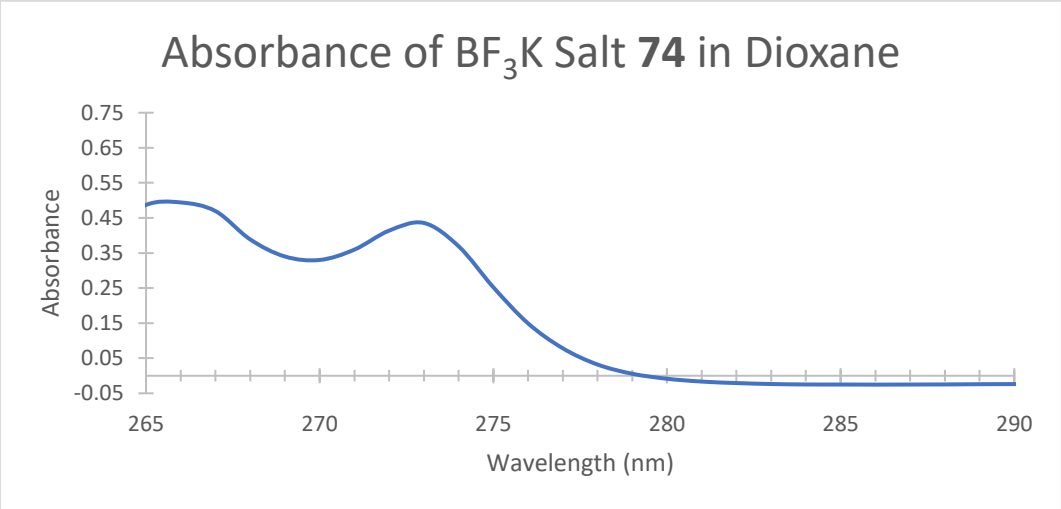

Figure A2.6: Zoomed in spectra from **Figure A2.5**.

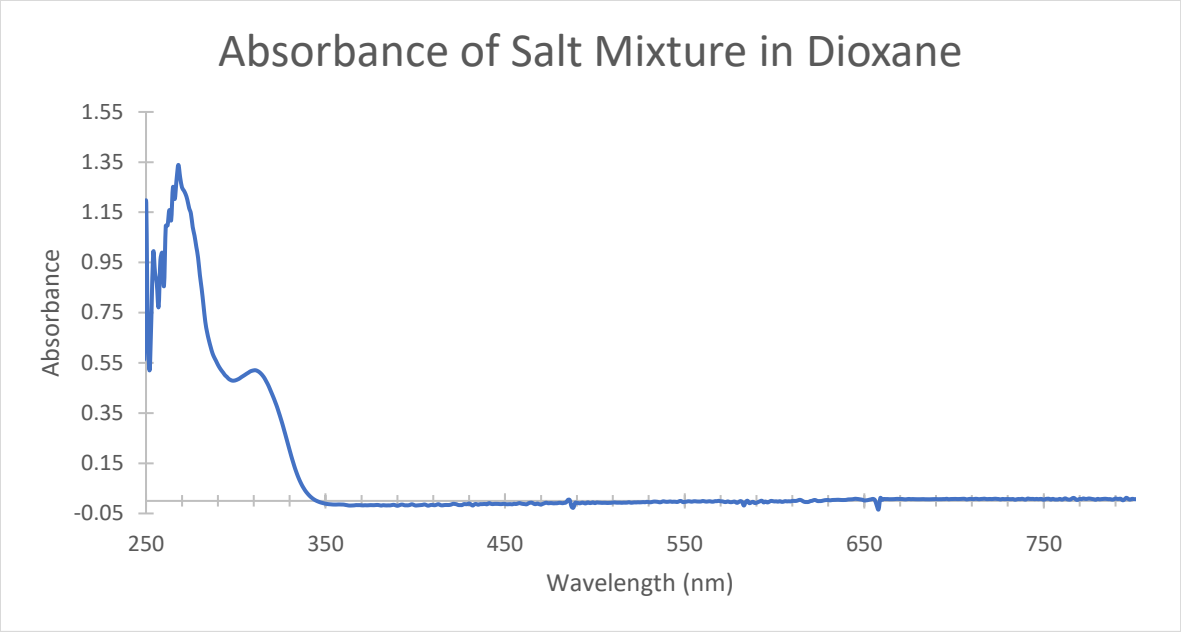

Figure S7: **72** (5.7 mg, 0.01 mmol) and **74** (2.1 mg, 0.01 mmol) in 1,4-dioxane (1 mL) were added to an 8 mL vial. The sample was then diluted with 1,4-dioxane to 0.0001 M with respect to both **72** and **74** (1:1 mixture) and transferred to a cuvette with a 1 cm path length.

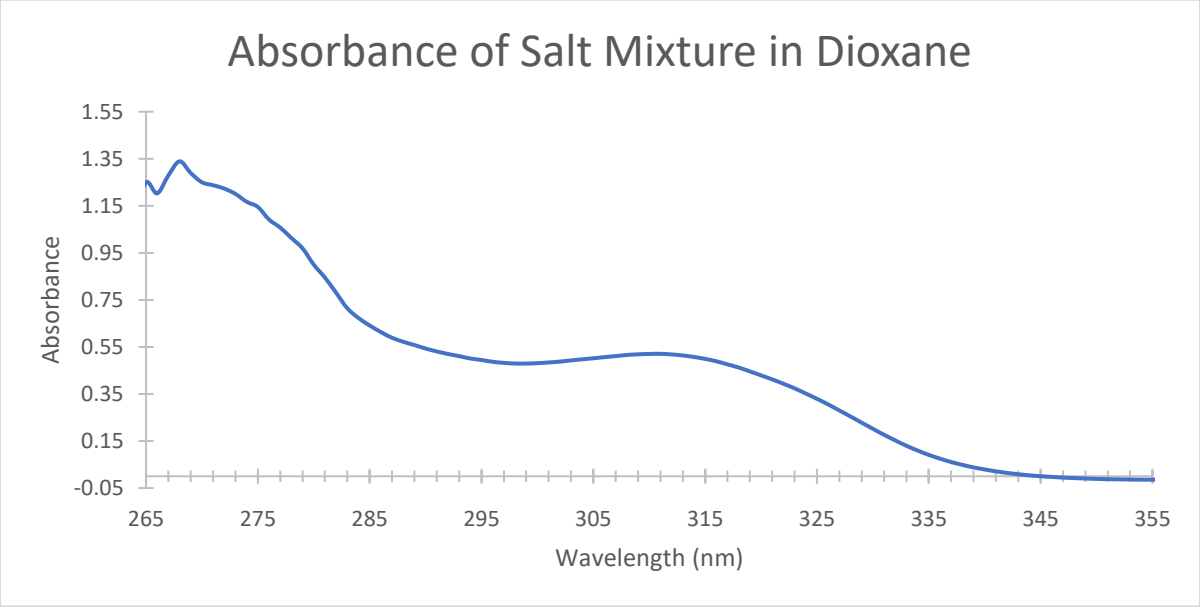

Figure A2.8: Zoomed in spectra from **Figure A2.7**.

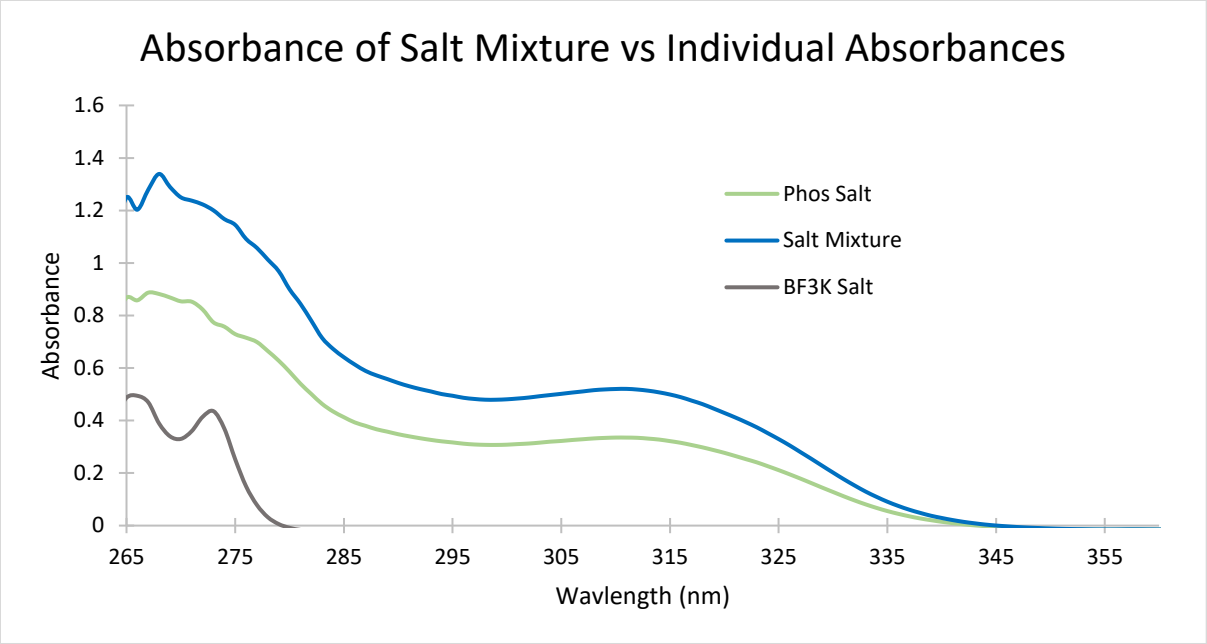

Figure A2.9. Overlaid UV-Vis spectra for each salt and a 1:1 mixture of both salts.

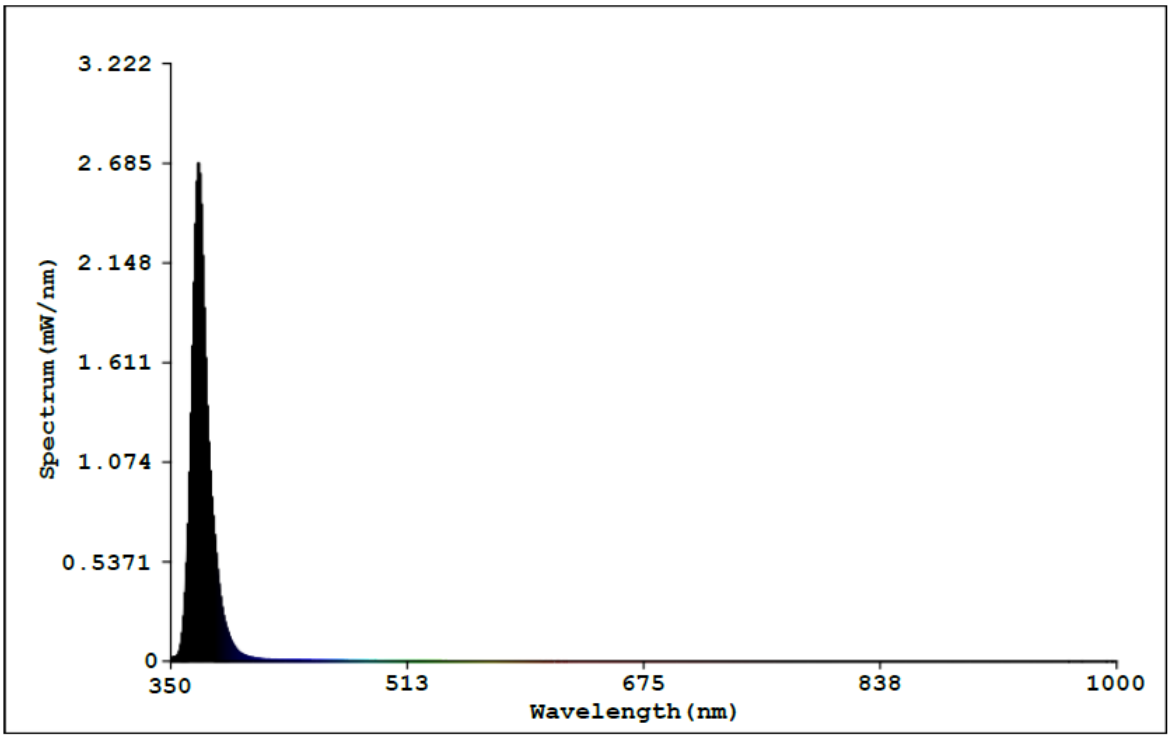

Figure A2.10. 365 nm LEDs emission spectrum provided by manufacturer.

Analysis: The investigation into whether an electron donor-acceptor (EDA) complex could be observed by UV-Visible spectroscopy between the phosphonium salt **72** and BF_3K salt **74** demonstrated that the two salts do not form an EDA complex. No bathochromic-shifted absorption was observed in comparison to the UV-Vis spectra for the two salts on their own. Phosphonium salt **72** displays a minor absorbance of light approaching 345 nm at low concentration while the emission spectrum of the 365 nm LEDs shows minor emission tailing off past 350 nms. We attribute the success of the reaction irradiated with 365 nm LEDs in the absence of photocatalyst to the overlap of this absorbance and emission, and this minor overlap is consistent with the prolonged reaction time needed.

A2.5. Stern-Volmer Quenching Studies

Fluorescence measurements were acquired at room temperature using an Edinburgh Instruments FS5 spectrometer. Emission quenching of the different samples were done using a screw-top 1.0 cm quartz cuvette with the corresponding solvent (1,4-dioxane or 1,2-dichloroethane) with a photocatalyst concentration of 9 mM. All the prepared solutions were transferred to the cuvette and degassed for 5 minutes with a stream of argon. The solution was excited at a wavelength of 400 nm and the emission spectra was recorded from 420 to 700 nm. Raw fluorescence intensity was measured at the emission λ_{max} (525 nm in 1,2-dichloroethane and 510 nm in 1,4-dioxane). Quenching of the excited state of 3DPAFIPN with phosphonium salt **72** was carried out in 1,2-dichloroethane the solution of salt **72** in 1,4-dioxane was heterogeneous without the BF_3K salt. Quenching of the excited state of 3DPAFIPN with BF_3K salt **74** was carried out in 1,4-dioxane.

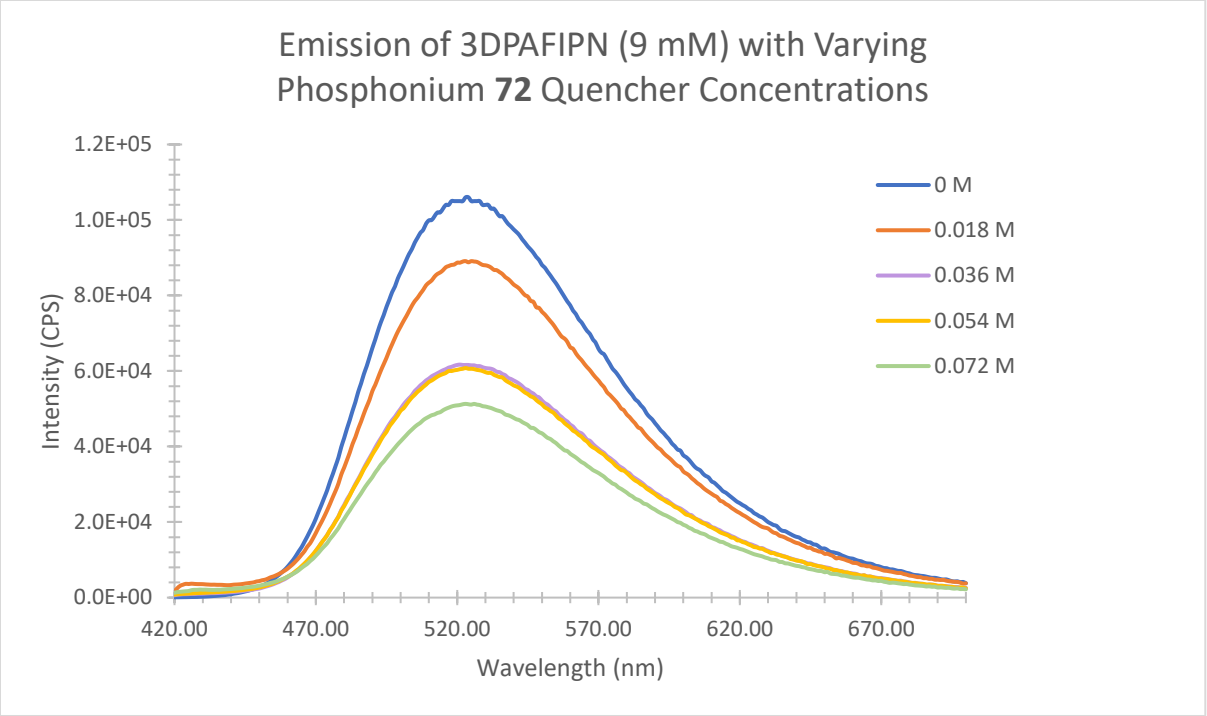

Figure A2.11. Emission spectra of 9 mM 3DPAFIPN with varying concentrations of phosphonium salt **72** in 1,2-dichloroethane with excitation slit open at 4 nm and emission slit open at 0.5 nm.

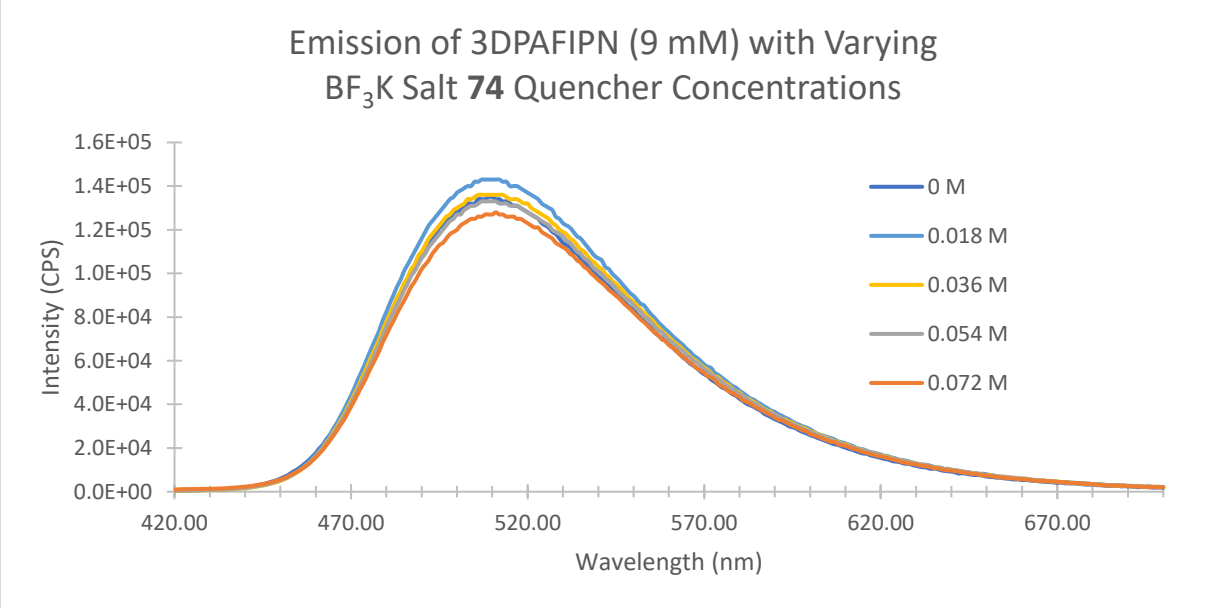

Figure A2.12. Emission spectra of 9 mM 3DPAFIPN with varying concentrations of BF_3K salt **74** in 1,4-dioxane with excitation slit open at 2.5 nm and emission slit open at 0.5 nm.

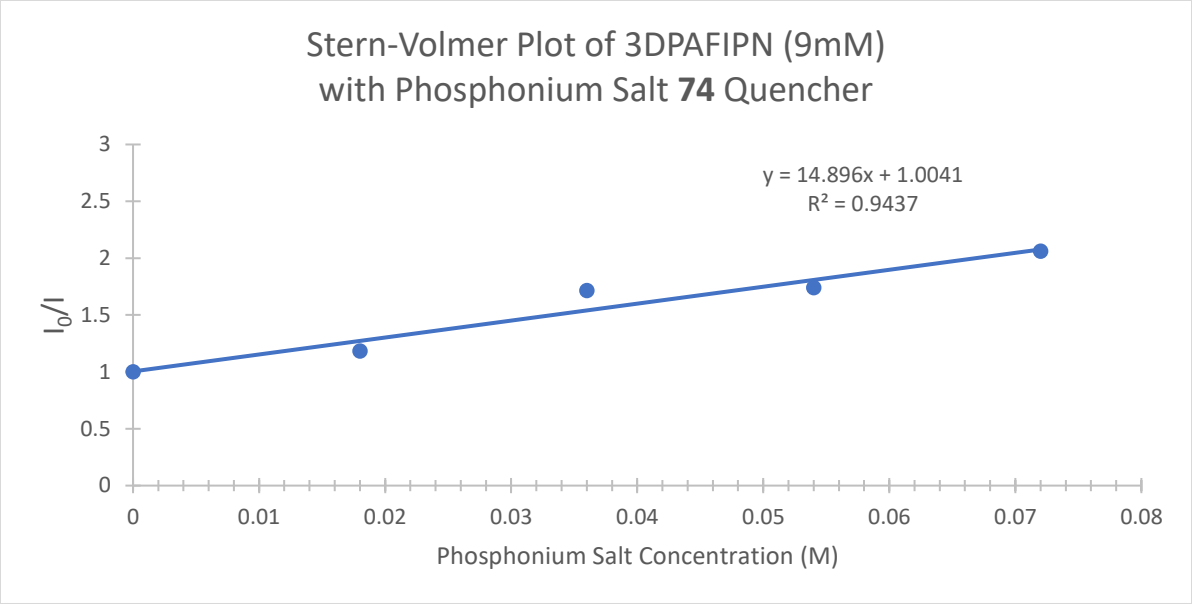

Figure A2.13. Stern-Volmer plot analysis derived from the data extracted from Figure **A2.11**. The Kq was determined from Stern-Volmer equation [Ksv = Kq τ] using a lifetime of τ = 4.2 ns for 3DPAFIPN[2]. K_{SV} = 14.9 M^{-1} and the resulting Kq for phosphonium salt **72** is 3.55 x 10^9 L mol^{-1} s^{-1}.

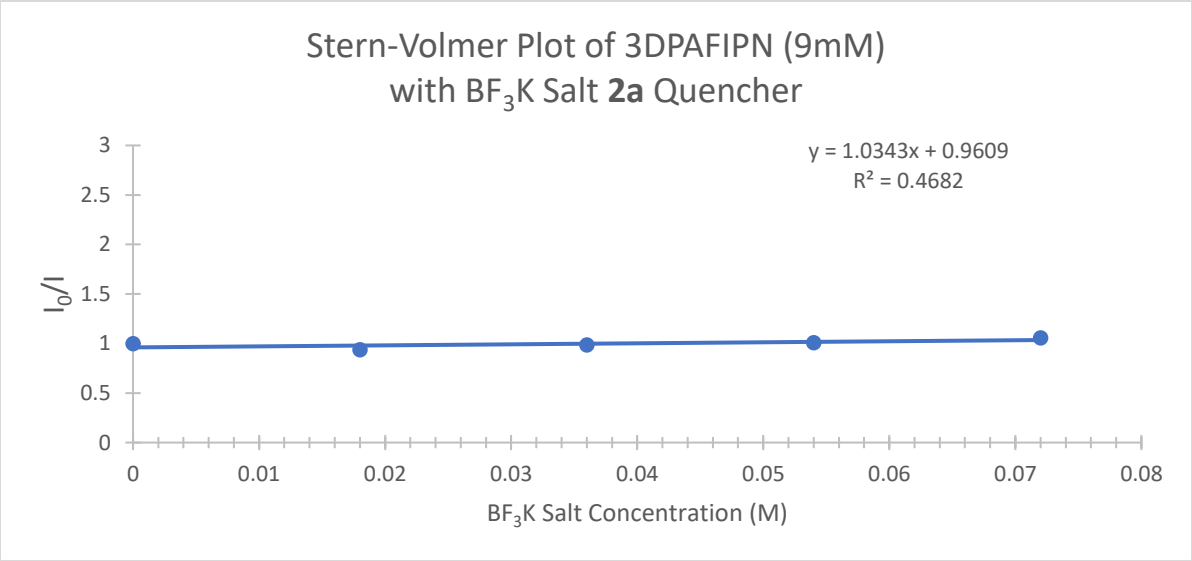

Figure A2.14. Stern-Volmer plot analysis derived from the data extracted from Figure **A2.12**. The Kq was determined from Stern-Volmer equation [Ksv = Kq τ] using a lifetime of τ = 4.2 ns for 3DPAFIPN[2]. K_{SV} = 1.0 M^{-1} and the resulting Kq for BF_3K salt **2a** is 2.4 x 10^8 L mol^{-1} s^{-1}. No significant quenching of 3DPAFIPN excited state was observed.

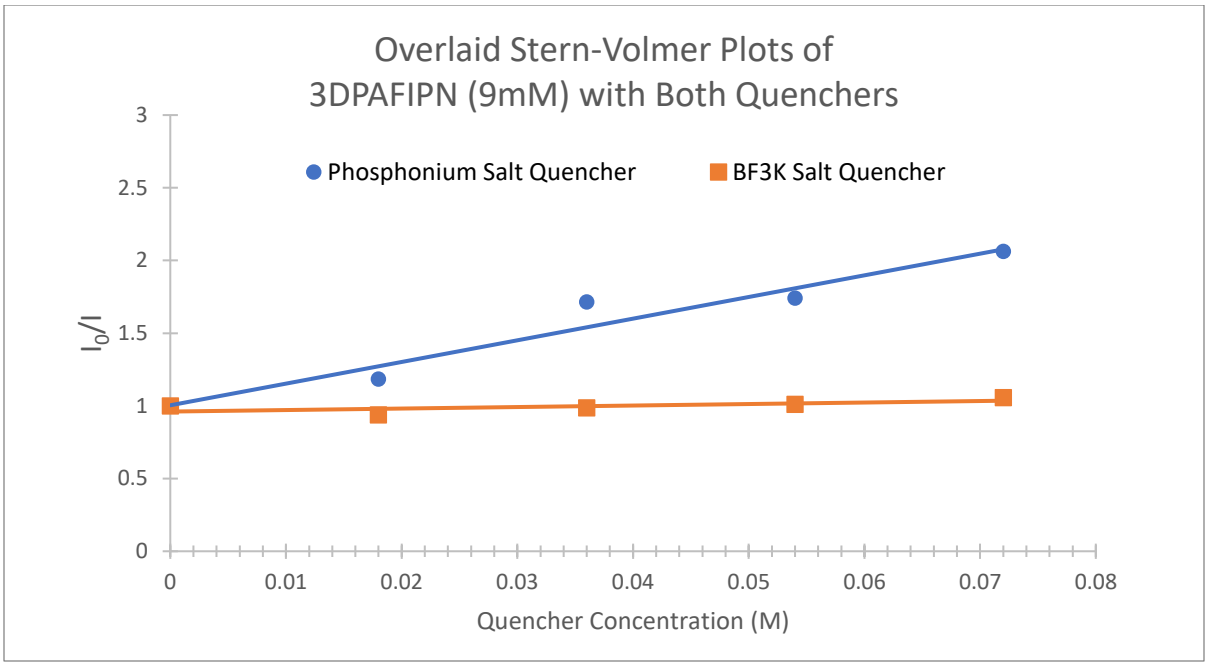

Figure A2.15. Stern-Volmer plots of both phosphonium salt **72** and BF3K salt **74**.

A2.6. Preparation of Heteroaryl Precursors

2-(3-Chloro-4-((2-fluorobenzyl)oxy)phenyl)pyridine

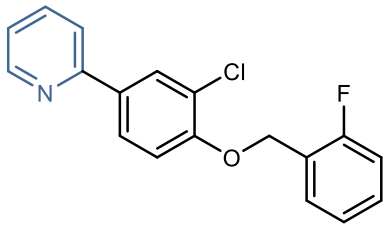

An oven dried 50 mL pressure tube was charged with (3-chloro-4-((2-fluorobenzyl)oxy)phenyl)boronic acid (843.0 mg, 3.00 mmol), K_2CO_3 (828.0 mg, 6 mmol), $Pd(OAc)_2$ (33.8 mg, 0.15 mmol), triphenylphosphine (157.2 mg, 0.60 mmol) and subjected to three cycles of vacuum/nitrogen backfill. Degassed H_2O (9.4 mL), degassed dimethoxyethane (9.4 mL), and 2-bromopyridine (0.29 mL, 3.00 mmol) was charged to the tube and the mixture was heated at 90℃ for 16 hours, then cooled to room temperature and diluted with EtOAc. The organic layer was separated, and the aqueous layer was extracted 2x with EtOAc. The combined organic layers were dried ($MgSO_4$), filtered over a frit, and concentrated *in vacuo*. Flash column chromatography (silica gel: 10% EtOAc in hexanes) afforded the title compound as a white crystalline solid (835.6 mg, 2.67 mmol, 89% yield). m.p. 74-76 □C; IR □$_{max}$/cm^{-1} (film): 3072, 3053, 2955, 2886, 1623, 1601, 1588, 1494, 1455, 1434, 1306, 1253, 1230, 1011, 772, 749, 693; ^{1}H NMR (400 MHz, $CDCl_3$) δ: 8.42 (d, *J* = 4.8 Hz, 1H), 7.91 (d, *J* = 2.3 Hz, 1H), 7.60 (dd, *J* = 8.5, 2.2 Hz, 1H), 7.48 – 7.29 (m, 3H), 7.15 – 6.73 (m, 5H), 4.98 (s, 2H); ^{13}C NMR (100 MHz, $CDCl_3$) δ: 160.0 (d, *J* = 246.7 Hz), 155.3, 154.4, 149.4, 136.6, 133.1, 129.6 (d, *J* = 8.0 Hz), 129.2 (d, *J* = 3.8 Hz), 128.7, 126.0, 124.3 (d, *J* = 3.5 Hz), 123.5 (d, *J* = 1.9 Hz), 123.3, 121.8, 119.6, 115.1 (d, *J* = 20.9 Hz), 113.4, 64.4 (d, *J* = 4.7 Hz); ^{19}F NMR (365 MHz, CDCl3) δ: -118.46; *m/z* LRMS (ESI + APCI) found $[M+H]^+$ 314.1, $C_{18}H_{14}ClFNO^+$ requires 314.1.

2-(4-Methoxyphenyl)pyridine

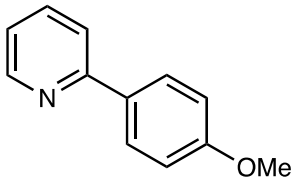

Prepared according to our previous report.[6] ^{1}H NMR (400 MHz, $CDCl_3$) δ: 8.63 (d, *J* = 4.8 Hz, 1H), 7.94 (d, *J* = 8.8 Hz, 2H), 7.68–7.62 (m, 2H), 7.15–7.11 (m, 1H), 7.02 (d, *J* = 8.8 Hz, 2H), 3.82 (s, 3H); ^{13}C NMR (100 MHz, $CDCl_3$) δ: 160.6, 157.2, 149.6, 136.7, 132.1, 128.2, 121.5, 119.9, 114.2, 55.4.

2-(4-Iodophenyl)pyridine

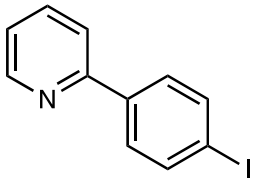

Prepared according to our previous report.[6] ^{1}H NMR (400 MHz, $CDCl_3$) δ: 8.68 (m, 1H), 7.82-7.66 (m. 6H), 7.27-7.21 (m, 1H); ^{13}C NMR (100 MHz, $CDCl_3$) δ: 156.1, 149.7, 138.7, 137.8, 136.8, 128.6, 122.4, 120.1, 95.4.

4-Cyclopropyl-2-(pyridin-3-yloxy)thiazole

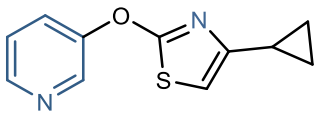

An oven dried mL round-bottom flask was charged with pyridin-3-ol (414.3 mg, 4.36 mmol), 2-bromo-4-cyclopropylthiazole (807.5 mg, 3.96 mmol), K_2CO_3 (658.7 mg, 4.25 mmol), and

subjected to three cycles of vacuum/nitrogen backfill. The flask was charged with DMF (10 mL) and heated to 135℃ for four hours. The brown suspension was cooled to room temperature and poured into H_2O (100 mL). The aqueous phase was extracted with EtOAc (3x) and the combined organic layer was washed with brine, dried (Na_2SO_4), filtered through a frit, and concentrated *in vacuo*. Flash column chromatography (silica gel, gradient elution: 33% EtOAc in hexanes) afforded the title compound as a yellow oil (337.1 mg, 1.64 mmol, 41% yield); IR ν_{max}/cm^{-1} (film): 3025, 2955, 2923, 2852, 1604, 1559, 1478, 1422, 1231, 837, 799, 734; ^1H NMR (400 MHz, $CDCl_3$) δ: 8.66 (s, 1H), 8.51 (s, 1H), 7.80 – 7.62 (m, 1H), 7.35 (s, 1H), 6.40 (s, 1H), 1.95 – 1.81 (m, 1H), 1.30 – 1.20 (m, 2H), 0.88 – 0.83 (m, 2H); ^{13}C NMR (100 MHz, $CDCl_3$) δ: 171.2, 153.7, 146.4, 142.1, 127.2, 124.3, 104.9, 12.8, 7.8 *m/z* LRMS (ESI + APCI) found $[M+H]^+$ 219.1, $C_{11}H_{11}N_2OS^+$ requires 219.1.

5-(5-Fluoropyridin-2-yl)-2-methoxypyrimidine

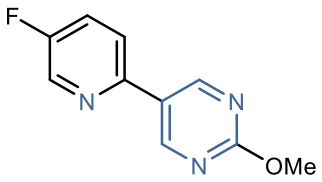

An oven dried 50 mL pressure tube was charged with 2-bromo-5-fluoropyridine (415.4 mg, 2.36 mmol), (2-methoxypyrimidin-5-yl)boronic acid (436.2 mg, 2.8 mmol), K_2CO_3 (651.4 mg, 4.72 mmol), $Pd(OAc)_2$ (79.7 mg, 0.35 mmol), triphenylphosphine (123.7 mg, 0.47 mmol) and subjected to three cycles of vacuum/nitrogen backfill. Degassed H_2O (9.4 mL) and degassed dimethoxyethane (9.4 mL) was charged to the tube and the mixture was heated at 90℃ for 16 hours, then cooled to room temperature and diluted with EtOAc. The organic layer was separated, and the aqueous layer was extracted 2x with EtOAc. The combined organic layers were dried

($MgSO_4$), filtered over a frit, and concentrated *in vacuo*. Flash column chromatography (silica gel: 35% EtOAc in hexanes) afforded the title compound as a white crystalline solid (201.1 mg, 0.99 mmol, 42% yield). m.p. 132-134 °C; IR ν_{max}/cm^{-1} (film): 3088, 3064, 3008, 2924, 2852, 1576, 1538, 1504, 1474, 1425, 1322, 1227, 1022, 908, 730, 703; ^{1}H NMR (400 MHz, $CDCl_3$) δ: 9.00 (s, 2H), 8.48 (d, *J* = 2.9 Hz, 1H), 7.60 (dd, *J* = 8.7, 4.2 Hz, 1H), 7.44 (td, *J* = 8.3, 2.9 Hz, 1H), 4.01 (s, 3H); ^{13}C NMR (100 MHz, $CDCl_3$) δ: 165.9, 159.2 (d, *J* = 257.5 Hz), 157.7, 148.8 (d, *J* = 4.0 Hz), 138.7 (d, *J* = 23.8 Hz), 126.0, 124.1 (d, *J* = 18.9 Hz), 120.6 (d, *J* = 4.4 Hz), 55.4; ^{19}F NMR (365 MHz, CDCl3) δ: -78.17; *m/z* LRMS (ESI + APCI) found $[M+H]^+$ 206.1, $C_{10}H_9FN_3O^+$ requires 206.1.

(R)-Tert-butyl 2-((pyridin-2-yloxy)methyl)pyrrolidine-1-carboxylate

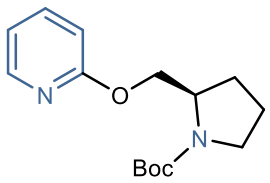

Prepared according to our previous report.[7] ^{1}H NMR (400 MHz, $CDCl_3$) δ: 8.11 (dd, J = 5.0, 1.5 Hz, 1H), 7.52 (dt, *J* = 7.6, 1.4 Hz, 1H), 6.82 (t, *J* = 5.7 Hz, 1H), 6.70 (d, *J* = 8.4 Hz, 1H), 4.37-4.35 (m, 1H), 4.21-4.11 (m, 2H), 3.37 (br s, 2H), 1.98-1.90 (m, 3H), 1.83-1.77 (m, 1H), 1.43 (s, 9H); ^{13}C NMR (100 MHz, $CDCl_3$) δ: 163.70, 154.48, 146.81, 138.44, 116.67, 110.89, 79.32, 66.05, 56.00, 46.36, 28.74, 28.45, 22.91; m/z LRMS (ESI + APCI) found $[M + H]^+$ 279.2, $C_{15}H_{23}N_2O_3^+$ requires 279.2.

3-Benzyl-5-(4-(2-(5-ethylpyridin-2-yl)ethoxy)benzyl)thiazolidine-2,4-dione

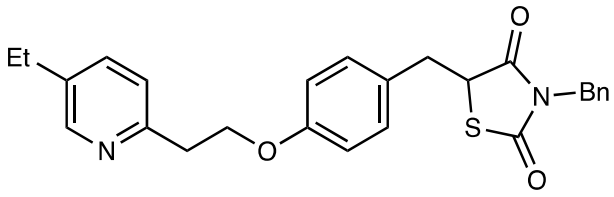

To a mixture of 5-(4-(2-(5-ethylpyridin-2-yl)ethoxy)benzyl)thiazolidine-2,4-dione (535 mg, 1.5 mmol) in DMF (15 mL) was added NaH (60% dispersion in oil) (66 mg, 1.65 mmol) at 0 °C. The reaction was warmed to rt over 15 minutes, then benzyl bromide (196 μL, 1.65 mmol) was added. The reaction was stirred at rt for 25 hours and then concentrated in vacuo. The crude material was purified by flash chromatography (silica gel: 100 % hexanes to 25 % EtOAc in hexanes) to provide the title compound as a light yellow solid (625 mg, 1.40 mmol, 93 % yield). m.p. 94-97 °C; ^{1}H NMR (400 MHz, $CDCl_3$) δ: 8.42 (d, *J* = 2.2 Hz, 1H), 7.48 (dd, *J* = 7.9, 2.3 Hz, 1H), 7.32 – 7.23 (m, 5H), 7.21 (d, *J* = 7.9 Hz, 1H), 7.05 (d, *J* = 8.6 Hz, 2H), 6.77 (d, *J* = 8.5 Hz, 2H), 4.79 – 4.59 (m, 2H), 4.43 (dd, *J* = 8.7, 4.0 Hz, 1H), 4.31 (t, *J* = 6.6 Hz, 2H), 3.38 (dd, *J* = 14.1, 4.0 Hz, 1H), 3.24 (t, *J* = 6.6 Hz, 2H), 3.09 (dd, *J* = 14.1, 8.7 Hz, 1H), 2.64 (q, *J* = 7.6 Hz, 2H), 1.25 (t, *J* = 7.6 Hz, 3H); ^{13}C NMR (101 MHz, $CDCl_3$) δ: 173.78, 171.03, 158.32, 155.73, 149.02, 137.24, 136.01, 135.09, 130.49, 128.72, 128.16, 127.45, 123.47, 115.98, 114.83, 67.32, 51.73, 45.22, 37.64, 37.62, 25.82, 15.44. IR υ_{max}/cm^{-1} (film): 3033, 2966, 2931, 2874, 2360, 2342, 1749, 1680, 1611, 1512, 1490, 1430, 1382, 1330, 1247, 1179, 1146, 1029, 908, 730, 700. *m/z* HRMS (DART): $[M+H]^+$ calculated for $C_{26}H_{27}N_2O_3S^+$ = 447.1737, found 447.1748.

A2.7. Preparation of Heterocyclic Phosphonium Salts

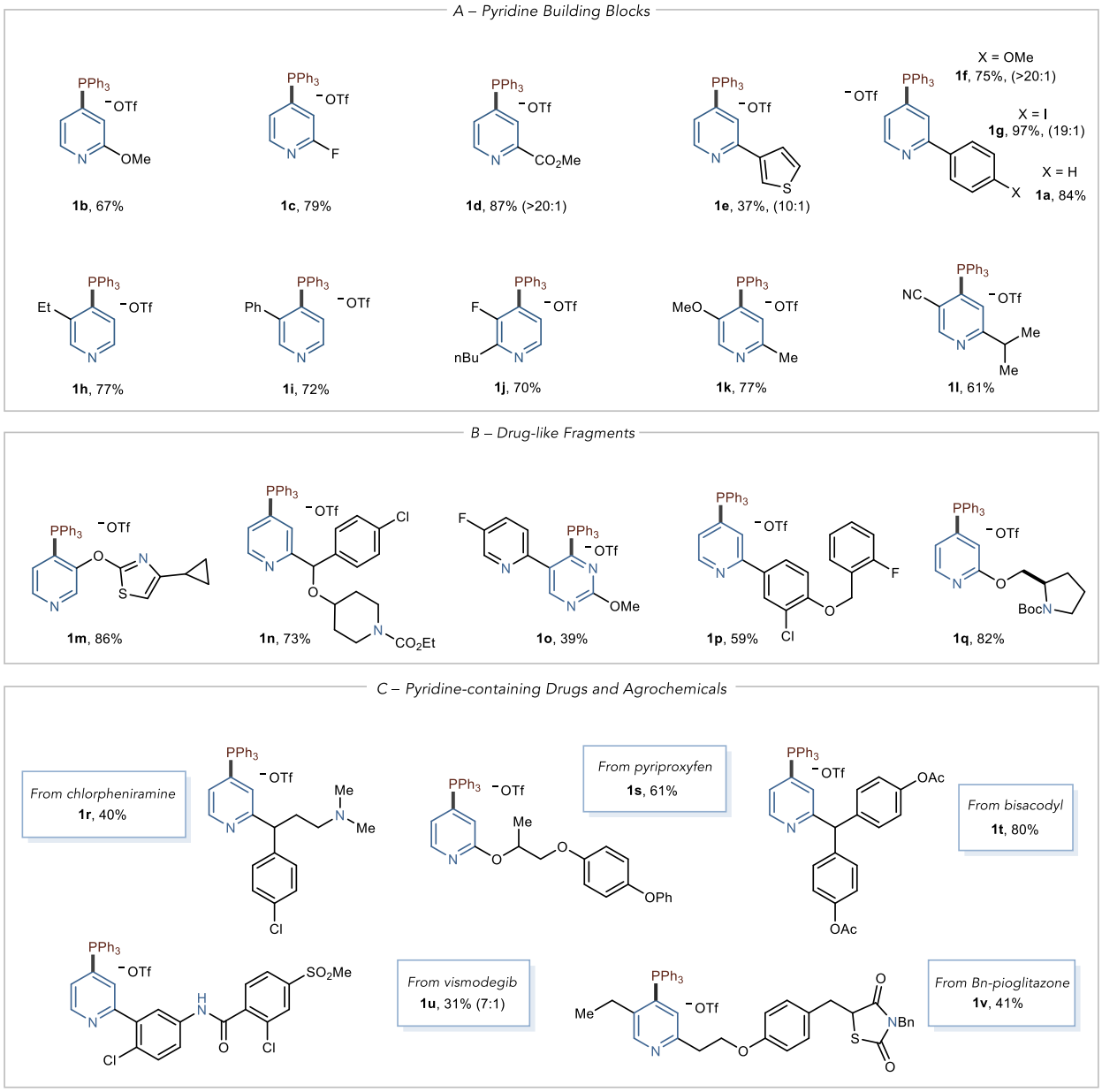

All yields are isolated yields of phosphonium salt as single regioisomers unless stated otherwise. Ratio in parenthesis denotes the ratio of 4-position regioisomer to 2-position regioisomer if any minor regioisomer was detected

Table A2.5. Yields and Regioselectivities for Phosphonium Salt Formation Reaction of Salts Used in this Study

General Procedure A

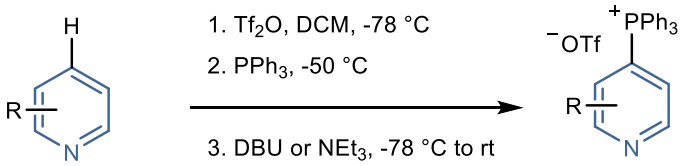

An oven dried 8 mL vial (≤ 0.5 mmol scale) or a round bottom flask (> 0.5 mmol scale) equipped with a stir bar was charged with the heterocycle (1.0 equiv) and placed under a nitrogen atmosphere. CH_2Cl_2 (0.1 M) was added, the reaction vessel cooled to –78 °C, and Tf_2O (1.0 equiv) was added dropwise over 5 minutes. The reaction was stirred for 30 minutes then warmed to –50 °C before PPh_3 (1.1 equiv) was added in one portion. The reaction was subjected to three rapid cycles of vacuum/nitrogen backfill and was stirred for a further 30 minutes at –78 °C. The stated organic base (NEt_3 or DBU, 1.0 equiv) was added dropwise via syringe, the cooling bath was removed, and the reaction was allowed to warm to room temperature while stirring (approximately 15-30 minutes). When the reaction mixture reached room temperature, it was then quenched with H_2O (approximately the same volume as CH_2Cl_2) and the mixture was transferred to a separatory funnel. The mixture was diluted with CH_2Cl_2 and the resulting organic layer was washed three times with H_2O. The organic layer was dried ($MgSO_4$), filtered and concentrated *in vacuo*. Approximately 2-10 mL (depending on the scale of the reaction) of CH_2Cl_2 was added to reaction mixture and was then added dropwise to an excess of Et_2O at room temperature. The flask was then placed in a –20 °C refrigerator for until the solid has settled to the bottom of the flask. The resulting suspension was filtered on a frit, washed with Et_2O, and dried *in vacuo* to provide the pure phosphonium salt.

General Procedure B

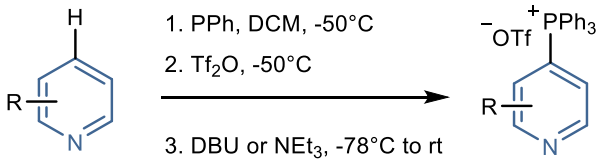

An oven dried round bottom flask equipped with a stir bar was charged with the heterocycle (1.0 equiv), PPh_3 (1.0 equiv), and placed under a nitrogen atmosphere. CH_2Cl_2 (0.1 M) was added, the reaction vessel cooled to –50 °C and Tf_2O (1.0 equiv) was added dropwise. After stirring for 1 hour, the reaction was cooled to –78 °C and DBU or NEt_3 (1.0 equiv) was added dropwise via syringe. The cooling bath was removed, and the reaction was allowed to warm to room temperature while stirring (approximately 20-30 minutes). The reaction mixture was diluted with CH_2Cl_2 and washed with H_2O (3x). The organic layer was dried ($MgSO_4$), filtered and concentrated in vacuo to approximately 2-5 mL (depending on the scale of the reaction). Approximately 2-10 mL (depending on the scale of the reaction) of CH_2Cl_2 was added to reaction mixture and was then added dropwise to an excess of Et_2O at room temperature which was then placed in a –20 °C refrigerator until the solid has settled to the bottom of the flask. The suspension was filtered on a frit, washed with Et_2O, and dried in vacuo to provide the pure product.

Notes.

5) PPh_3 was crushed into a powder prior to use.
6) If the product forms an oil rather than a solid during the crash-out purification, allow the oil to settle to the bottom of the flask overnight at -20 °C. Decant the Et_2O away from the oil, and dissolve the oil in CH_2Cl_2. Transfer the solution to an appropriately sized round bottom flask (typically 250 mL round bottom flask for a 1-3 mmol scale salt reaction), concentrate *in vacuo*, and place the flask on high vac to solidify the residue.

Triphenyl(2-phenylpyridin-4-yl)phosphonium trifluoromethanesulfonate

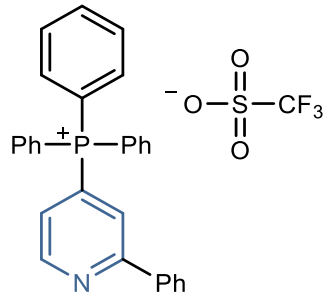

Prepared according to our previous report.[8] ^{1}H NMR (400 MHz, $CDCl_3$) δ: 9.01 (app t, *J* = 5.1 Hz, 1H), 7.93-7.54 (m, 18H), 7.50 (ddd, *J* = 17.8, 5.1, 1.1 Hz, 1H), 7.42-7.36 (m, 3H); ^{13}C NMR (100 MHz, $CDCl_3$) δ: 159.1 (d, *J* = 9.9 Hz), 151.6 (d, *J* = 10.7 Hz), 136.7 (d, *J* = 1.5 Hz), 136.1 (d, *J* = 3.2 Hz), 134.3 (d, *J* = 9.8 Hz), 130.9 (d, *J* = 13.0 Hz), 130.3, 129.2 (d, *J* = 84.1 Hz), 129.0, 127.0, 125.2 (d, *J* = 7.8 Hz), 123.1, (d, *J* = 8.4 Hz), 120.7 (q, *J* = 321.1 Hz), 115.5 (d, *J* = 89.1 Hz).

Triphenyl(2-methoxypyridin-4-yl)phosphonium trifluoromethanesulfonate

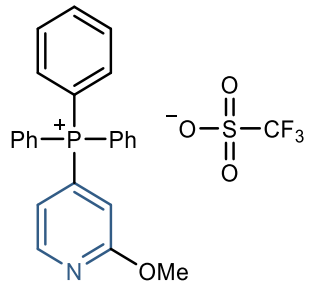

Prepared according to our previous report.[9] ^{1}H NMR (400 MHz, CDCl3) δ: 8.57 (t, *J* = 5.3 Hz, 1H), 7.97-7.87 (m, 3H), 7.85-7.74 (m, 6H), 7.71-7.59 (m, 6H), 7.12 (dd, *J* = 11.5 Hz, 5.0 Hz, 1H), 6.84 (d, *J* = 15.0 Hz, 1H), 4.01 (s, 3H); ^{13}C NMR (100 MHz, CDCl3) δ: 164.5 (d, *J* = 15.7 Hz), 149.8 (d, *J* = 10.5 Hz), 136.1 (d, *J* = 2.9 Hz), 134.2 (d, *J* = 10.5 Hz), 130.9 (d, *J* = 13.5 Hz), 130.5 (d, *J* = 85.2 Hz), 120.7 (q, *J* = 321.2 Hz), 118.8 (d, *J* = 8.3 Hz), 116.2 (d, *J* = 10.0 Hz), 115.6 (d, *J* = 89.6 Hz), 54.3; ^{19}F NMR (365 MHz, CDCl3) δ: -78.17; ^{31}P NMR (162 MHz, CDCl3) δ: 22.37.

(2-Fluoropyridin-4-yl)triphenylphosphonium trifluoromethanesulfonate

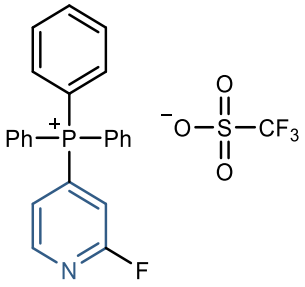

Prepared according to our previous report.[8] ^{1}H NMR (400 MHz, CDCl3) δ: 8.67 (app t, *J* = 5.3 Hz, 1H), 7.99-7.88 (m, 3H), 7.87-7.75 (m, 6H), 7.74-7.60 (m, 7H), 7.10 (d, *J* = 13.4 Hz, 1H); ^{13}C NMR (100 MHz, CDCl3) δ: 163.28 (dd, *J* = 245.4, 16.9 Hz), 150.63 (dd, *J* = 13.7, 12.7 Hz), 136.09 (d, *J* = 3.2 Hz), 134. 21 (d, *J* = 10.7 Hz), 133.95 (dd, *J* = 84.4, 6.6 Hz), 130.81 (d, *J* = 13.8 Hz), 125.18 (dd, *J* = 8.2, 5.1 Hz), 122.44 (q, *J* = 321.6 Hz), 114.81 (d, *J* = 90.1 Hz), 114.19 (dd, *J* = 40.3, 10.2 Hz).

(2-(Ethoxycarbonyl)pyridin-4-yl)triphenylphosphonium trifluoromethanesulfonate

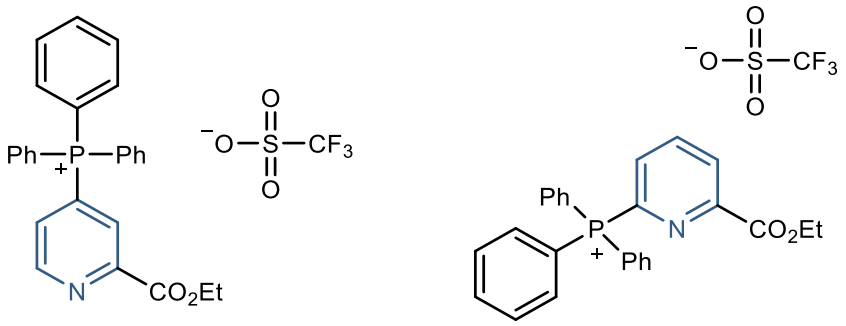

>20:1 Mixture of Regioisomers

Prepared according to general procedure A using ethyl picolinate (130 µL, 1.00 mmol), Tf_2O (170 µL, 1.00 mmol), PPh_3 (288.2 mg, 1.10 mmol), NEt_3 (140 µL, 1.00 mmol) and CH_2Cl_2 (10 mL). After the purification procedure, the title compound was isolated as a white solid (359.9 mg, 0.87 mmol, 87% yield). m.p. 52–56 °C; IR ν_{max}/cm^{-1} (film): 3062, 1720, 1578, 1485, 1439, 1304, 1260, 1223, 1145, 1107, 1029, 997, 753, 726,

689; major isomer: ^{1}H NMR (400 MHz, $CDCl_3$) δ: 9.18 (t, *J* = 4.8 Hz, 1H), 8.21 (dd, *J* = 13.1, 1.7 Hz, 1H), 8.06 – 7.88 (m, 4H), 7.81 (td, *J* = 7.8, 3.7 Hz, 6H), 7.71 – 7.63 (m, 6H), 4.47 (q, *J* = 7.2 Hz, 2H), 1.41 (t, *J* = 7.1 Hz, 3H); ^{13}C NMR (100 MHz, $CDCl_3$) δ: 163.9 (d, *J* = 2.7 Hz) 152.5 (d, *J* = 10.0 Hz), 149.9 (d, *J* = 10.2 Hz), 136.6 (d, *J* = 3.2 Hz), 134.8 (d, *J* = 10.6 Hz), 131.3 (d, *J* = 13.1 Hz), 130.2, 127.7 (d, *J* = 9.1 Hz), 120.9 (q, *J* = 321.0 Hz), 115.4 (d, *J* = 89.7 Hz), 63.1, 14.3; ^{19}F NMR (365 MHz, $CDCl_3$) δ: –78.21; ^{31}P NMR (162 MHz, $CDCl_3$) δ: 22.55. *m/z* LRMS (ESI + APCI) found $[M\text{-}OTf]^+$ 412.2, $C_{26}H_{23}NO_2P^+$ requires 412.1.

Triphenyl(2-(thiophen-3-yl)pyridin-4-yl)phosphonium trifluoromethanesulfonate

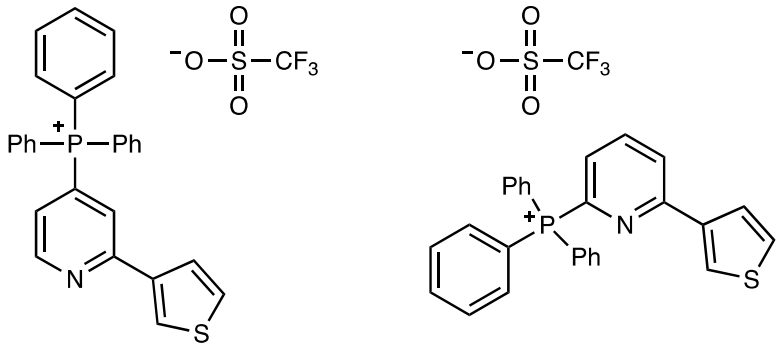

Major Minor

13:1 mixture of regioisomers

Prepared according to our previous report.[6] Major isomer, ^{1}H NMR (400 MHz, $CDCl_3$) δ: 8.99 (td, *J* = 5.1, 0.9 Hz, 1H), 8.00 (dd, *J* = 3.0, 1.3 Hz, 1H), 7.90-7.96 (m, 3H), 7.66-7.86 (m, 13H), 7.55 (dd, *J* = 5.1, 1.3 Hz, 1H), 7.44 (dd, *J* = 5.0, 1.6 Hz, 1H), 7.38-7.42 (m, 1H); ^{13}C NMR (100 MHz, $CDCl_3$) δ: 155.1 (d, *J* = 10.9 Hz), 151.7 (d, *J* = 10.6 Hz), 139.8 (d, *J* = 1.6 Hz), 136.3 (d, *J* = 3.1 Hz), 134.4 (d, *J* = 10.3 Hz), 131.0 (d, *J* = 12.8 Hz), 129.3 (d, *J* = 84.2 Hz), 127.3, 126.4, 125.9, 124.8 (d, *J* = 8.2 Hz), 123.0 (d, *J* = 8.7 Hz), 120.8 (q, *J* = 321.1 Hz), 115.6 (d, *J* = 89.4 Hz); ^{19}F NMR (365 MHz, $CDCl_3$) δ: –78.15; ^{31}P NMR (162 MHz, $CDCl_3$) δ: 22.69; m/z LRMS (ESI + APCI) found $[M–OTf]^+$ 422.2, $C_{27}H_{21}NPS^+$ requires 422.1.

(2-(4-Methoxyphenyl)pyridin-4-yl)triphenylphosphonium trifluoromethanesulfonate

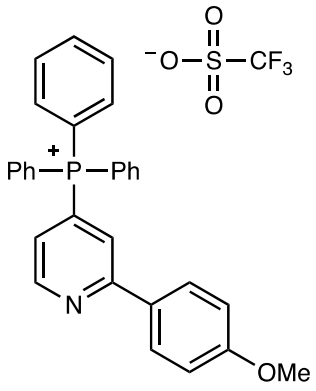

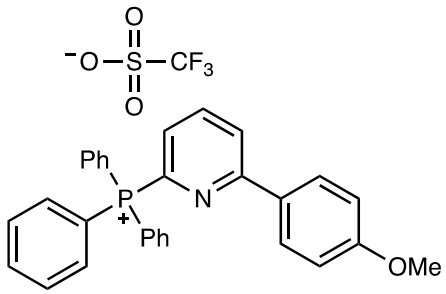

Major Minor

>20:1 mixture of regioisomers

Prepared according to our previous report.[6] Major Isomer, ^{1}H NMR (400 MHz, $CDCl_3$) δ: 9.00 (app t, *J* = 5.1 Hz, 1H), 7.99-7.62 (m, 18H), 7.41 (dd, *J* = 12.7, 4.9 Hz, 1H), 6.97 (d, *J* = 8.8 Hz, 2H), 3.83 (s, 3H); Major isomer, ^{13}C NMR (100 MHz, $CDCl_3$) δ: 161.5, 158.8 (d, *J* = 10.5 Hz), 151.5 (d, *J* = 10.8 Hz), 136.2 (d, *J* = 2.9 Hz), 134.3 (d, *J* = 10.5 Hz), 130.9 (d, *J* = 13.0 Hz), 129.2 (d, *J* = 1.3 Hz), 129.0 (d, *J* = 84.0 Hz), 128.5, 124.6 (d, *J* = 8.1 Hz), 122.4 (m), 120.7 (q, *J* = 323.7 Hz), 115.6 (d, *J* = 89.5 Hz), 114.4, 55.4; ^{19}F NMR (365 MHz, $CDCl_3$) δ: –78.12; ^{31}P NMR (162 MHz, $CDCl_3$) δ: 22.77 (major), 15.16 (minor); m/z LRMS (ESI + APCI) found $[M–OTf]^+$ 446.2, $C_{30}H_{25}NOP^+$ requires 446.2.

(2-(4-Iodophenyl) pyridin-4-yl)triphenylphosphonium trifluoromethanesulfonate

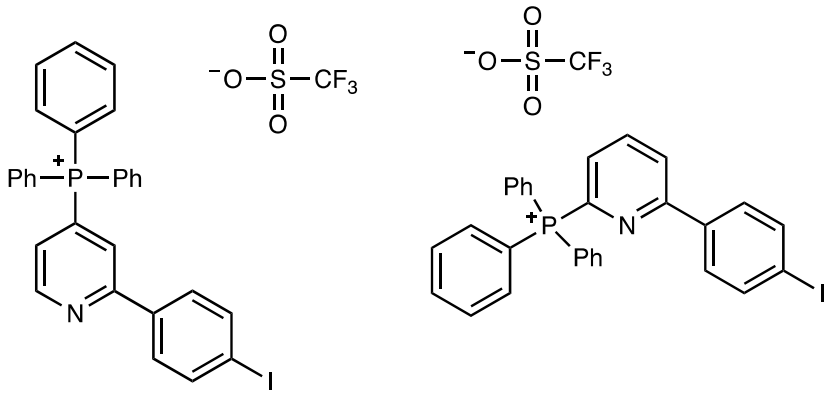

Major Minor

19:1 Mixture of Regioisomers

Prepared according to our previous report.[6] Major isomer, ^{1}H NMR (400 MHz, $CDCl_3$) δ: 9.05 (td, *J* = 5.1, 0.7 Hz, 1H), 7.96-7.63 (m, 20H), 7.54 (ddd, *J* = 12.7, 5.0, 1.6 Hz, 1H); Major isomer, ^{13}C NMR (100 MHz, $CDCl_3$) δ: 158.4 (d, *J* = 10.6 Hz), 151.8 (d, *J* = 10.7 Hz), 138.3, 136.5 (d, *J* = 1.5 Hz), 136.3 (d, *J* = 3.0 Hz), 135.6 (d, *J* = 10.6 Hz), 131.1 (d, *J* = 13.1 Hz), 129.7 (d, *J* = 83.9 Hz), 129.0, 125.8 (d, *J* = 8.0 Hz), 123.2 (d, *J* = 8.6 Hz), 121.1 (q, *J* = 321.2 Hz), 115.7 (d, *J* = 89.4 Hz), 97.4; ^{19}F NMR (365 MHz, $CDCl_3$) δ: –78.14; ^{31}P NMR (162 MHz, $CDCl_3$) δ: 22.78, 15.72; m/z LRMS (ESI + APCI) found $[M–OTf]^+$ 542.1, $C_{29}H_{22}INP^+$ requires 542.1.

(3-Ethylpyridin-4-yl)triphenylphosphonium trifluoromethanesulfonate

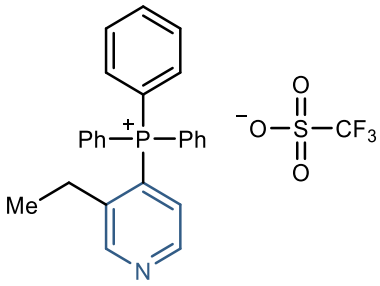

Prepared according to general procedure A using 3-ethylpyridine (110 μL, 1.00 mmol), Tf_2O (170 μL, 1.00 mmol), PPh_3 (288.2 mg, 1.10 mmol), DBU (150 μL, 1.00 mmol) and CH_2Cl_2 (10 mL). After the purification procedure, the title compound was isolated as a tan solid (282.0 mg, 0.77 mmol, 77% yield). m.p. 155–157 °C; IR ν_{max}/cm^{-1} (film): 2976, 1586, 1569, 1437, 1399, 1266, 1257, 1223, 1166, 1106, 1027, 752, 724, 708, 691; major isomer: ^{1}H NMR (400 MHz, $CDCl_3$) δ: 8.92 (d, *J* = 6.8 Hz, 1H), 8.76 (t, *J* = 4.7 Hz, 1H), 7.94 – 7.86 (m, 3H), 7.85 – 7.77 (m, 6H), 7.72 – 7.63 (m, 6H), 7.09 (dd, *J* = 15.2, 5.1 Hz, 1H), 2.44 (q, *J* = 7.4 Hz, 2H), 0.78 (t, *J* = 7.4 Hz, 3H); ^{13}C NMR (100 MHz, $CDCl_3$) δ: 153.2 (d, *J* = 8.1 Hz), 149.4 (d, *J* = 10.5 Hz), 142.4 (d, *J* = 7.0 Hz), 136.2 (d, *J* = 3.1 Hz), 134.4 (d, *J* = 10.5 Hz), 131.3 (d, *J* = 13.1 Hz), 128.1 (d, *J* = 10.1 Hz), 126.4 (d, *J* = 83.4 Hz), 121.0 (q, *J* = 321.3 Hz), 116.7 (d, *J* = 88.7 Hz), 27.3 (d, *J* = 5.2 Hz), 13.7; ^{19}F NMR (365 MHz, $CDCl_3$) δ: –78.13; ^{31}P NMR (162 MHz, $CDCl_3$) δ: 21.33. *m/z* LRMS (ESI + APCI) found $[M\text{-}OTf]^+$ 368.2, $C_{25}H_{23}NP^+$ requires 368.2.

Triphenyl(3-phenylpyridin-4-yl)phosphonium trifluoromethanesulfonate

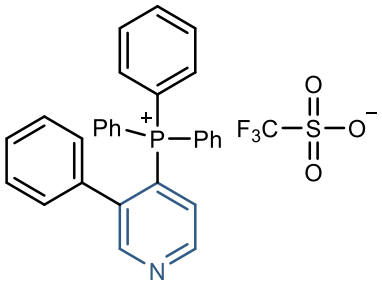

Prepared according to our previous report.[8] ^{1}H NMR (400 MHz, CDCl3) δ: 8.95 (app t, *J* = 4.7 Hz, 1H), 8.74 (d, *J* = 6.8 Hz, 1H), 7.85-7.73 (m, 3H), 7.73-7.40 (m, 13H), 7.11 (t, *J* = 7.6 Hz, 1H), 6.91 (app t, *J* = 7.6 Hz, 2H), 6.71 (d, *J* = 7.5 Hz, 2H); ^{13}C NMR (100 MHz, CDCl3) δ: 153.6 (d, *J* = 8.0 Hz), 150.0 (d, *J* = 10.4 Hz), 141.7 (d, *J* = 7.3 Hz), 135.4 (d, *J* = 3.0 Hz), 134.4 (d, *J* = 4.5 Hz), 134.2 (d, *J* = 10.3 Hz), 130.6 (d, *J* = 13.0 Hz), 129.2, 128.9, 128.3, 128.2, 126.4 (d, *J* = 83.4 Hz), 120.8 (q, *J* = 321.2 Hz), 116.9 (d, *J* = 89.2 Hz).

(2-Butyl-3-fluoropyridin-4-yl)triphenylphosphonium trifluoromethanesulfonate

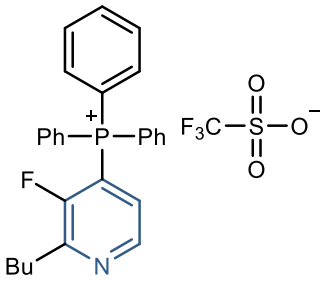

Prepared according to our previous report.[5] ^{1}H NMR (400 MHz, $CDCl_3$) δ: 8.73 (t, *J* = 4.0 Hz, 1H), 7.94–7.90 (m, 3H), 7.82–7.78 (m, 6H), 7.69–7.64 (m, 6H), 7.12 (dt, *J* = 14.0, 4.7 Hz, 1H), 2.95 (td, *J* = 7.6, 2.5 Hz, 2H), 1.73 (qn, *J* = 7.5 Hz, 2H), 1.37 (sext, *J* = 7.5 Hz, 2H), 0.92 (t, *J* = 7.2 Hz, 3H); ^{13}C NMR (100 MHz, $CDCl_3$) δ: 156.80 (d, *J* = 263.2 Hz), 153.64 (dd, *J* = 16.0, 4.0 Hz), 147.23 (dd, *J* = 10.7, 6.6 Hz),

136.16 (d, *J* = 3.1 Hz), 133.98 (d, *J* = 10.7 Hz), 130.96 (d, *J* = 13.4 Hz), 125.87 (dd, *J* = 6.0, 2.3 Hz), 120.75 (q, *J* = 319.5 Hz), 115.64 (dd, *J* = 83.5, 15.0 Hz), 115.30 (d, *J* = 90.6 Hz), 31.07, 30.01, 22.18, 13.61.

(5-Methoxy-2-methylpyridin-4-yl)triphenylphosphonium trifluoromethanesulfonate

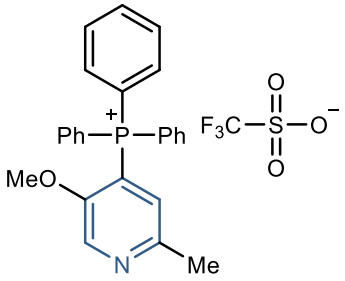

Prepared according to our previous report.[10] ^{1}H NMR (400 MHz, $CDCl_3$) δ: 8.52 (d, *J* = 6.9 Hz, 1H), 7.95–7.40 (m, 15H), 6.79 (d, *J* = 15.0 Hz, 1H), 3.62 (s, 3H), 2.46 (s, 3H); ^{13}C NMR (100 MHz, $CDCl_3$) δ: 153.72, 153.05 (d, *J* = 10.7 Hz), 135.62 (d, *J* = 4.6 Hz), 135.46 (d, *J* = 3.1 Hz), 133.71 (d, *J* = 10.7 Hz), 130.51 (d, *J* = 13.0 Hz), 127.12 (d, *J* = 6.9 Hz), 120.72 (q, *J* = 321.2 Hz), 116.46 (d, *J* = 91.6 Hz), 115.62 (d, *J* = 87.0 Hz), 57.01, 23.55.

(5-Cyano-2-isopropylpyridin-4-yl)triphenylphosphonium trifluoromethanesulfonate

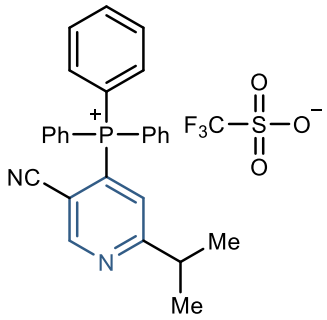

Prepared according to our previous report.[9] ^{1}H NMR (400 MHz, $CDCl_3$) δ: 9.10 (d, *J* = 5.8 Hz, 1H), 7.96-7.90 (m, 3H), 7.86-7.73 (m, 12H), 7.34 (d, *J* = 15.3 Hz, 1H), 3.20 (sp, *J* = 6.9 Hz, 1H), 1.27 (d, *J* = 6.8 Hz,

6H); ^{13}C NMR (100 MHz, $CDCl_3$) δ: 174.5 (d, *J* = 8.9 Hz), 154.8 (d, *J* = 6.1 Hz), 136.3 (d, *J* = 3.0 Hz), 134.6 (d, *J* = 10.8 Hz), 131.0 (d, *J* = 82.5 Hz), 131.0 (d, *J* = 13.4 Hz), 127.6 (d, *J* = 7.5 Hz), 120.6 (q, *J* = 321.2 Hz), 114.4 (d, *J* = 89.8 Hz), 113.9 (d, *J* = 5.2 Hz), 108.9 (d, *J* = 3.7 Hz), 36.9, 21.5.

(3-((4-Cyclopropylthiazol-2-yl)oxy)pyridin-4-yl)triphenylphosphonium trifluoromethanesulfonate

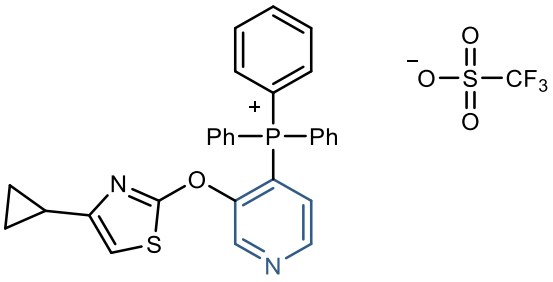

Prepared according to general procedure A using 4-cyclopropyl-2-(pyridin-3-yloxy)thiazole (382 mg, 1.75 mmol), Tf_2O (295 μL, 1.75 mmol), PPh_3 (506.1 mg, 1.83 mmol), DBU (263 μL, 1.75 mmol) and CH_2Cl_2 (17.5 mL). After the purification procedure, the title compound was isolated as a white solid (947 mg, 1.51 mmol, 86% yield). mp 160–164 °C; IR ν_{max}/cm^{-1} (film): 3112, 3063, 3002, 1533, 1438, 1406, 1287, 1266, 1219, 1107, 1029, 736, 710; ^{1}H NMR (400 MHz, $CDCl_3$) δ: 9.12 (d, *J* = 6.2 Hz, 1H), 8.81 (t, *J* = 4.4 Hz, 1H), 7.87 (td, *J* = 7.2, 1.9 Hz, 3H), 7.80 – 7.60 (m, 12H), 7.35 (dd, *J* = 14.4, 4.9 Hz, 1H), 6.33 (s, 1H), 1.79 (tt, *J* = 8.5, 4.9 Hz, 1H), 0.93 – 0.80 (m, 2H), 0.72 – 0.61 (m, 2H); ^{13}C NMR (100 MHz, $CDCl_3$) δ: 167.3, 153.3, 152.0, 148.0 (d, *J* = 10.5 Hz), 144.4 (d, *J* = 4.3 Hz), 136.1 (d, *J* = 3.2 Hz), 134.2 (d, *J* = 10.9 Hz), 131.1 (d, *J* = 13.4 Hz), 128.5 (d, *J* = 6.6 Hz), 120.9 (q, *J* = 321.2 Hz), 119.2 (d, *J* = 85.5 Hz), 115.8 (d, *J* = 91.1 Hz), 106.7, 12.6, 8.0. ^{19}F NMR (365 MHz, $CDCl_3$) δ: –78.11; ^{31}P NMR (162 MHz, $CDCl_3$) δ: 21.12. *m/z* LRMS (ESI + APCI) found $[M\text{-}OTf]^+$ 479.2, $C_{29}H_{24}N_2OPS^+$ requires 479.1.

(2-((4-Chlorophenyl)((1-(ethoxycarbonyl)piperidin-4-yl)oxy)methyl)pyridin-4-yl) triphenylphosphonium trifluoromethanesulfonate

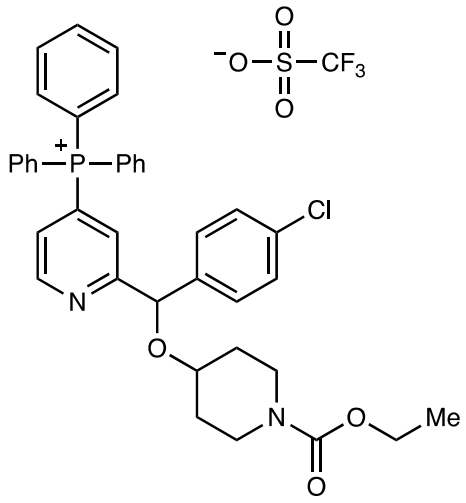

Prepared according to our previous report.[11] ^{1}H NMR (400 MHz, $CDCl_3$) δ: 8.90 (t, *J* = 5.1 Hz, 1H), 7.94-7.86 (m, 3H), 7.82-7.73 (m, 6H), 7.71-7.59 (m, 7H), 7.49 (ddd, *J* = 12.6, 5.0, 1.1 Hz, 1H), 7.34-7.25 (m, 4H), 5.71 (s, 1H), 4.11 (q, *J* = 7.1 Hz, 2H), 3.70-3.60 (m, 1H), 3.55-3.42 (m, 2H), 3.25-3.12 (m, 2H), 1.79-1.56 (m, 2H), 1.54-1.37 (m, 2H), 1.25 (t, *J* = 7.1 Hz, 3H); ^{13}C NMR (100 MHz, $CDCl_3$) δ: 164.4 (d, *J* = 9.6 Hz), 155.4, 151.1 (d, *J* =10.5 Hz), 138.7, 136.2 (d, *J* = 3.1 Hz), 134.5 (d, *J* = 10.5 Hz), 134.0, 130.9 (d, *J* = 13.1 Hz), 129.3 (d, *J* = 84.1 Hz), 128.8, 128.5, 125.9 (d, *J* = 8.4 Hz), 123.9 (d, *J* = 9.1 Hz), 120.8 (q, *J* = 321.2 Hz), 115.8 (d, *J* = 89.4 Hz), 79.9, 72.8, 61.3, 40.7 (rot), 40.7, 31.3, 30.3 (rot), 14.7.

((Trifluoromethyl)sulfonyl)-l1-oxidane, (5-(5-fluoropyridin-2-yl)-2-methoxypyrimidin-4-yl)triphenylphosphonium trifluoromethanesulfonate

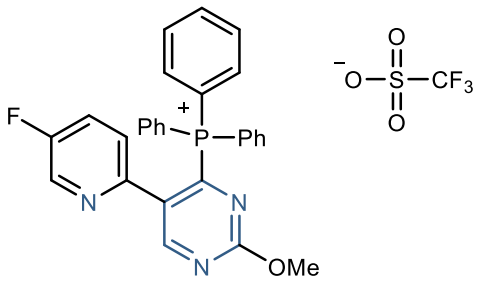

Prepared according to general procedure B using 5-(5-fluoropyridin-2-yl)-2-methoxypyrimidine (201.1 mg, 0.98 mmol), Tf_2O (170 μL, 0.98 mmol), PPh_3 (256.8 mg, 0.98 mmol), DBU (150 μL, 0.98 mmol) and CH_2Cl_2 (9.8 mL). After the purification procedure, the title compound was isolated as a white solid (237.1 mg, 0.38 mmol, 39% yield). mp 238–240 °C; IR ν_{max}/cm^{-1} (film): 3098, 3060, 1585, 1566, 1474, 1412, 1381, 1276, 1257, 1226, 1160, 1136, 1112, 1028, 709; ^1H NMR (400 MHz, $CDCl_3$) δ: 9.32 (d, *J* = 9.3 Hz, 1H), 8.17 – 8.08 (m, 1H), 7.87 – 7.38 (m, 17H), 3.80 (s, 3H); ^{13}C NMR (100 MHz, $CDCl_3$) δ: 165.0 (d, *J* = 20.9 Hz), 162.7 (d, *J* = 5.4 Hz), 159.4 (d, *J* = 261.0 Hz), 151.5 (d, *J* = 118.5 Hz), 145.5 (d, *J* = 4.1 Hz), 136.2 (d, *J* = 25.3 Hz), 134.8 (d, *J* = 3.1 Hz), 134.5 (d, *J* = 9.9 Hz), 132.0 (d, *J* = 15.4 Hz), 130.0 (d, *J* = 13.2 Hz), 125.3 (d, *J* = 18.9 Hz), 124.7 (d, *J* = 5.3 Hz), 121.0 (q, *J* = 320.2 Hz), 119.4 (d, *J* = 92.2 Hz), 56.2; ^{19}F NMR (365 MHz, $CDCl_3$) δ: –78.20, -124.03; ^{31}P NMR (162 MHz, $CDCl_3$) δ: 25.76. *m/z* LRMS (ESI + APCI) found $[M\text{-}OTf]^+$ 466.2, $C_{28}H_{22}FN_3OP^+$ requires 466.1.

(2-(3-Chloro-4-((2-fluorobenzyl)oxy)phenyl)pyridin-4-yl)triphenylphosphonium trifluoromethanesulfonate

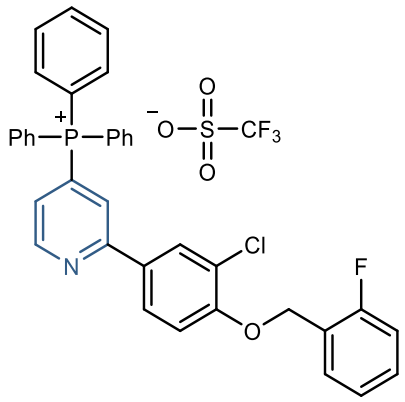

Prepared according to general procedure A using 2-(3-chloro-4-((2-fluorobenzyl)oxy)phenyl)pyridine (800.0 mg, 2.55 mmol), Tf_2O (430 μL, 2.55 mmol), PPh_3 (734 mg, 2.80 mmol), NEt_3 (360 μL, 2.55 mmol) and CH_2Cl_2 (25.5 mL). After the purification procedure, the title compound was isolated as a white solid (1.085 g, 1.50 mmol, 59% yield). mp 76–82 °C; IR ν_{max}/cm^{-1} (film): 3493, 3063, 2963, 2872, 2288, 1599, 1586, 1503, 1459, 1438, 1259, 1223, 1147, 1108, 1029, 997, 753, 725, 689; ^{1}H NMR (400 MHz, $(CD_3)_2SO$) δ: 9.03 (t, *J* = 5.1 Hz, 1H), 8.29 (d, *J* = 13.8 Hz, 1H), 8.20 (d, *J* = 2.3 Hz, 1H), 8.09 – 7.95 (m, 4H), 7.90 – 7.79 (m, 12H), 7.64 – 7.54 (m, 2H), 7.48 – 7.41(m, 2H), 7.31 – 7.23 (m, 2H), 5.33 (s, 2H); ^{13}C NMR (100 MHz, $(CD_3)_2SO$) δ: 160.4 (d, *J* = 246.5 Hz), 155.8 (d, *J* = 10.7 Hz), 155.1, 151.2 (d, *J* = 10.9 Hz), 135.7 (d, *J* = 3.1 Hz), 134.9 (d, *J* = 10.7 Hz), 130.9 (d, *J* = 1.8 Hz), 130.8 (d, *J* = 8.4 Hz), 130.6, 130.6 (d, *J* = 4.3 Hz), 130.5, 129.7 (d, *J* = 84.6 Hz), 128.0 (d, *J* = 127.2 Hz), 126.1 (d, *J* = 8.6 Hz), 124.7 (d, *J* = 3.4 Hz), 123.7 (d, *J* = 9.1 Hz), 123.1 (d, *J* = 14.4 Hz), 122.3, 120.7 (q, *J* = 324.2 Hz), 116.5 (d, *J* = 89.3 Hz), 115.6 (d, *J* = 20.8 Hz), 114.5, 64.8 (d, *J* = 3.8 Hz); ^{19}F NMR (365 MHz, $(CD_3)_2SO$) δ: –77.74, -117.95; ^{31}P NMR (162 MHz, $(CD_3)_2SO$) δ: 22.08. *m/z* LRMS (ESI + APCI) found $[M\text{-}OTf]^+$ 574.2, $C_{36}H_{27}ClFNOP^+$ requires 574.2.

(R)-(2-((1-(Tert-butoxycarbonyl)pyrrolidin-2-yl)methoxy)pyridin-4-yl)triphenylphosphonium trifluoromethanesulfonate

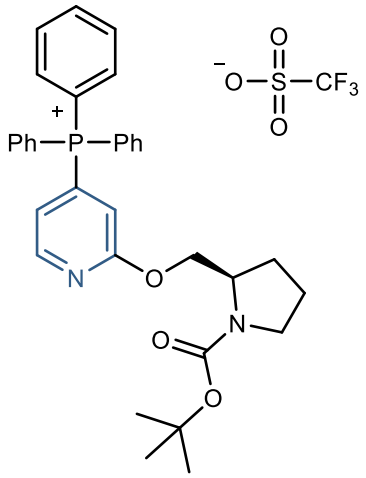

Prepared according to our previous report.[7] ^{1}H NMR (400 MHz, $CDCl_3$) δ: 8.52 (t, *J* = 5.0 Hz, 1H), 7.94-7.90 (m, 3H), 7.82-7.79 (m, 6H), 7.67-7.62 (m, 6H), 7.10 (br s, 1H), 6.81 (*J* = 14.5 Hz, 1H), 4.48 (dd, *J* = 10.4, 4.1 Hz, 1H), 4.30 (t, *J* = 7.8 Hz, 1H), 4.18-4.12 (m, 1H), 3.48-3.33 (m, 2H), 1.94-1.87 (m, 4H), 1.42 (s, 9H); ^{13}C NMR (100 MHz, $CDCl_3$) δ: 164.19, 164.03, 154.29, 149.71 (d, *J* = 12.3 Hz), 136.07 (d, *J* = 1.0 Hz), 134.22 (d, *J* = 10.3 Hz), 130.85 (d, *J* = 13.0 Hz), 120.69 (q, *J* = 319.5 Hz), 119.00, 116.02 (d, *J* = 11.0 Hz), 115.52 (d, *J* = 89.2 Hz), 79.36, 67.17, 55.38, 46.24, 28.25, 27.78, 23.43-22.74 (rot); ^{19}F NMR (365 MHz, CDCl3) δ: –78.14; ^{31}P NMR (162 MHz, CDCl3) δ: 22.32.

(2-(1-(4-Chlorophenyl)-3-(dimethylamino)propyl)pyridin-4-yl)triphenylphosphonium trifluoromethanesulfonate

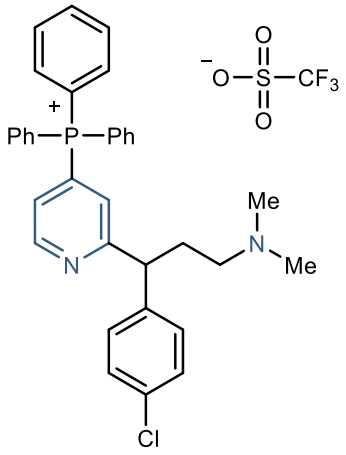

Prepared according to our previous report.[8] ^{1}H NMR (400 MHz, $CDCl_3$) d: 8.97 (app t, *J* = 5.1 Hz, 1H), 7.93-7.86 (m, 3H), 7.80-7.70 (m, 6H), 7.61-7.50 (m, 6H), 7.39 (ddd, *J* = 12.8, 5.1, 1.5 Hz, 1H), 7.25-7.16 (m, 5H), 4.28 (app t, *J* = 6.8 Hz, 1H), 2.56-2.43 (m, 1H), 2.32-2.11 (m, 9H); ^{13}C NMR (100 MHz, $CDCl_3$) d: 165.55 (d, *J* = 9.9 Hz), 150.97 (d, *J* = 9.9 Hz), 140.26, 135.82 (d, *J* = 3.1 Hz), 134.02 (d, *J* = 10.7 Hz), 132.25, 130.61 (d, *J* = 13.0 Hz), 128.92 (d, *J* = 85.5 Hz), 128.75, 127.92, 126.26 (d, *J* = 8.4 Hz), 124.42 (d, *J* = 7.6 Hz), 120.46 (q, *J* = 321.2 Hz), 115.31 (d, *J* = 89.3 Hz), 56.73, 49.77, 44.88, 31.99.

(2-((1-(4-Phenoxyphenoxy)propan-2-yl)oxy)pyridin-4-yl)triphenylphosphonium trifluoromethanesulfonate

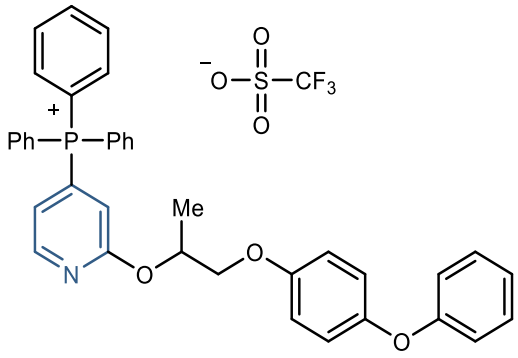

Prepared according to our previous report.[12] ^{1}H NMR (400 MHz, $CDCl_3$) d: 8.55 (app t, *J* = 5.3 Hz, 1H), 7.93-7.87 (m, 3H), 7.82-7.74 (m, 6H), 7.67-7.59 (m, 6H), 7.30-7.23 (m, 2H), 7.13 (ddd, *J* = 11.7, 5.3, 1.2 Hz, 1H), 7.02 (t, *J* = 7.4 Hz, 1H), 6.94-6.77 (m, 7H), 5.66 (sext, *J* = 5.3 Hz, 1H), 4.18-4.07 (m, 2H), 1.48 (d, *J* = 6.4 Hz, 3H); ^{13}C NMR (100 MHz, $CDCl_3$) d: 163.72 (d, *J* = 15.9 Hz), 158.13, 154.71, 150.29, 149.77 (d, *J* = 12.1 Hz), 136.11 (d, *J* = 3.0 Hz), 134.32 (d, *J* = 10.6 Hz), 130.91 (d, *J* = 13.0 Hz), 130.78 (d, *J* = 84.2 Hz), 129.50, 122.43, 120.78 (q, *J* = 321.2 Hz), 120.56, 119.08 (d, *J* = 8.1 Hz), 117.47, 116.55 (d, *J* = 10.0 Hz), 115.62 (d, *J* = 89.4 Hz), 115.61, 71.50, 70.49, 16.41.

(2-(Bis(4-Acetoxyphenyl)methyl)pyridin-4-yl)triphenylphosphonium trifluoromethanesulfonate

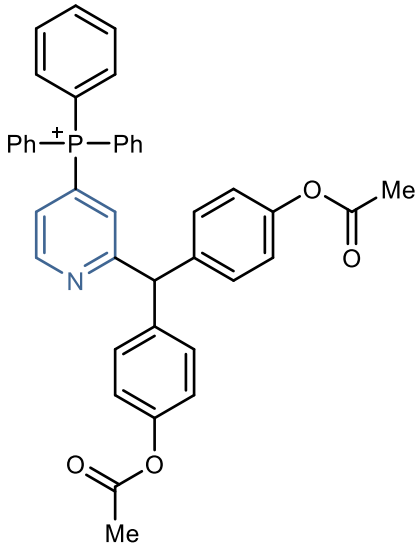

Prepared according to our previous report.[12] ^{1}H NMR (400 MHz, $CDCl_3$) δ: 8.90 (app t, *J* = 5.1 Hz, 1H), 7.86-7.80 (m, 3H), 7.73-7.66 (m, 6H), 7.56-7.39 (m, 7H), 7.18 (d, *J* = 13.7 Hz, 1H), 7.13-7.08 (m, 4H), 6.97–6.91 (m, 4H), 5.72 (s, 1H), 2.21 (s, 6H); ^{13}C NMR (100 MHz, $CDCl_3$) δ: 169.1, 165.0 (d, *J* = 9.4 Hz), 151.2 (d, *J* = 10.4 Hz), 149.3, 138.4, 135.9 (d, *J* = 3.0 Hz), 134.1 (d, *J* = 10.6 Hz), 130.7 (d, *J* = 13.0 Hz), 129.9, 129.0 (d, *J* = 83.8 Hz), 126.6 (d, *J* = 8.7 Hz), 124.9 (d, *J* = 7.9 Hz), 121.5, 120.6 (q, *J* = 321.2 Hz), 115.3 (d, *J* = 89.4 Hz), 57.4, 20.8; ^{19}F NMR (365 MHz, $CDCl_3$) δ: –78.05; ^{31}P NMR (162 MHz, $CDCl_3$) δ: 22.34.

(2-(2-Chloro-5-(2-chloro-4-(methylsulfonyl)benzamido)phenyl)pyridin-4-yl)triphenylphosphonium trifluoromethanesulfonate and (6-(2-chloro-5-(2-chloro-4-(methylsulfonyl)benzamido)phenyl)pyridin-2-yl)triphenylphosphonium trifluoromethanesulfonate

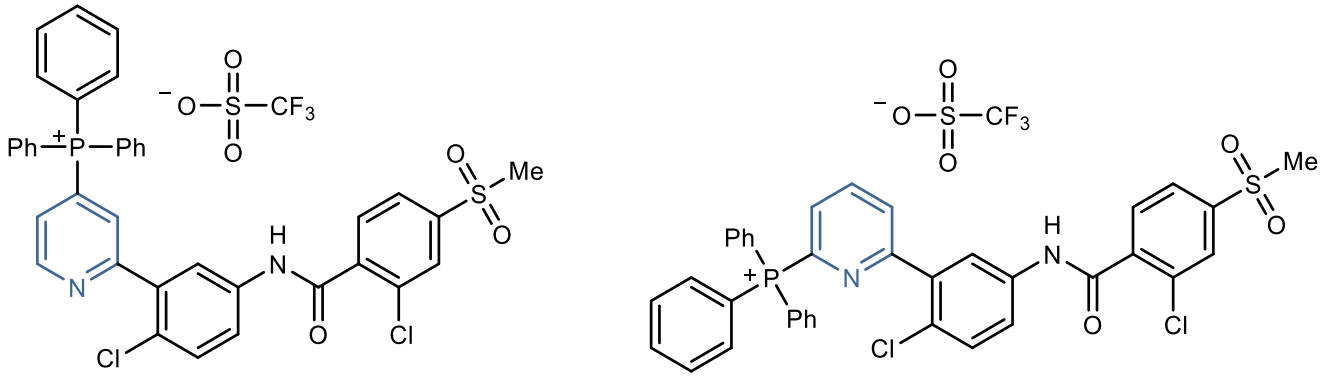

7:1 Mixture of Regioisomers

Prepared according to our previous report.[12] Major isomer, ^{1}H NMR (400 MHz, $CDCl_3$) δ: 9.98 (s, 1H), 8.98 (app t, *J* = 4.9 Hz, 1H), 8.15-7.33 (m, 23H), 3.01 (s, 3H); Major isomer, ^{13}C NMR (100 MHz, $CDCl_3$) δ: 164.5, 158.5 (d, *J* = 10.8 Hz), 151.2 (d, *J* = 10.9 Hz), 142.3, 140.4, 137.9, 136.8, 136.2 (d, *J* = 2.9 Hz), 134.4 (d, *J* = 10.5 Hz), 132.5, 130.9 (d, *J* = 13.1 Hz), 130.5, 130.0, 128.7, 128.5 (d, *J* = 84.4 Hz), 128.1 (d, *J* = 8.8 Hz), 126.4, 125.8, 125.4 (d, *J* = 8.4 Hz), 123.2, 122.6, 120.4 (q, *J* = 320.6 Hz), 115.6 (d, *J* = 89.6 Hz), 44.3; Both isomers, ^{19}F NMR (365 MHz, $CDCl_3$) δ: –78.34; Both isomers, ^{31}P NMR (162 MHz, $CDCl_3$) δ: 22.60 (major), 17.95 (minor).

(2-(2-(4-((3-Benzyl-2,4-dioxothiazolidin-5-yl)methyl)phenoxy)ethyl)-5-ethylpyridin-4-yl)triphenylphosphonium trifluoromethanesulfonate

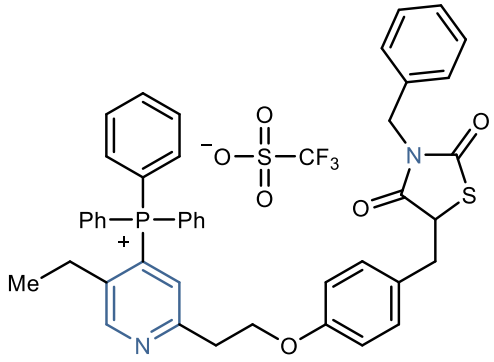

Prepared according to general procedure B using 3-benzyl-5-(4-(2-(5-ethylpyridin-2-yl)ethoxy)benzyl)thiazolidine-2,4-dione (450.1 mg, 1.01 mmol), Tf_2O (170 μL, 1.01 mmol), PPh_3 (264.6 g, 1.01 mmol), DBU (150 μL, 1.01 mmol) and CH_2Cl_2 (10.1 mL). After the purification procedure, the title compound was isolated as a white solid (355.1 mg, 0.41 mmol, 41% yield). mp 80–85 °C; IR ν_{max}/cm^{-1} (film): 3234, 3135, 3085, 3031, 2959, 2932, 1748, 1676, 1608, 1438, 1264, 1239, 1152, 1052, 1029, 723, 690; ^{1}H NMR (400 MHz, CD_3CN) δ: 8.88 (d, *J* = 7.0 Hz, 1H), 7.97 – 7.81 (m, 3H), 7.78 – 7.60 (m, 12H), 7.26 – 7.18 (m, 3H), 7.07 (ddd, *J* = 12.6, 6.5, 3.2 Hz, 5H), 6.67 – 6.52 (m, 2H), 4.76 – 4.53 (m, 3H), 4.23 (t, *J* = 6.0 Hz, 2H), 3.40 – 3.08 (m, 4H), 2.39 (qd, *J* = 7.4, 1.1 Hz, 2H), 0.70 (t, *J* = 7.4 Hz, 3H); ^{13}C NMR (100 MHz, CD_3CN) δ: 174.9, 172.2, 159.5 (d, *J* = 10.8 Hz), 158.7, 153.6 (d, *J* = 8.9 Hz), 141.2 (d, *J* = 7.4 Hz), 136.6 (d, *J* = 3.2 Hz), 136.6, 135.5 (d, *J* = 10.5 Hz), 131.8, 131.6 (d, *J* = 13.0 Hz), 129.5, 129.1, 128.7, 128.7, 127.6, 126.7, 122.2 (q, *J* = 322.2 Hz), 118.0 (d, *J* = 88.9 Hz), 115.3, 66.9, 52.2, 45.7, 38.0, 37.1, 27.4 (d, *J* = 5.2 Hz), 13.9; ^{19}F NMR (365 MHz, CD_3CN) δ: –79.16; ^{31}P NMR (162 MHz, CD_3CN) δ: 21.48; *m/z* LRMS (ESI + APCI) found $[M\text{-}OTf]^+$ 707.3, $C_{28}H_{22}FN_3OP^+$ requires 707.2.

A2.8. Preparation of Pinacol Boronic Esters

General Procedure C

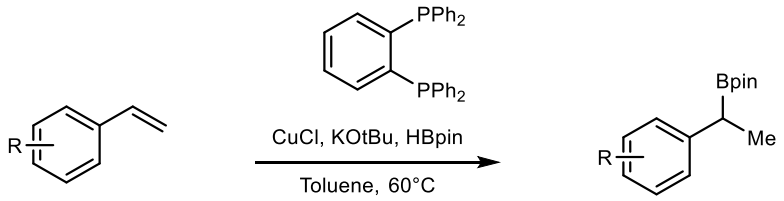

Boronic esters were prepared according to the report of Noh et al.[13] An oven dried pressure tube of appropriate size was equipped with a magnetic stir bar was charged with CuCl (3 mol%), KOtBu (6 mol%), and 1,2-bis(diphenylphosphaneyl)benzene (5 mol%), and the pressure tube was subjected to three rapid cycles of vacuum/nitrogen backfill followed by addition of toluene (2.5 M). The reaction was stirred at room temperature for ten minutes before addition of pinacolborane (1.2 equiv). After stirring for another ten minutes, the reaction mixture was diluted with toluene (1M) and charged with the corresponding styrene (1 equiv). The reaction was sealed with the pressure tube cap and heated to 60 °C overnight. The reaction was filtered through a pad of celite, concentrated *in vacuo*, and purified by flash column chromatography under the stated conditions to provide the benzyl boronic ester.

4,4,5,5-Tetramethyl-2-(1-phenylethyl)-1,3,2-dioxaborolane

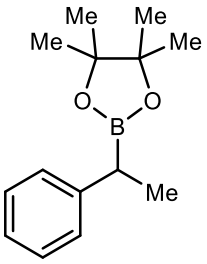

Prepared according to General Procedure C with CuCl (89.1 mg, 0.9 mmol, 3 mol%), KOtBu (201.6 mg, 1.8 mmol, 6 mol%), 1,2-bis(diphenylphosphaneyl)benzene (669.0 mg, 1.5, 5 mol%), and toluene (12 mL, 2.5 M). Then, pinacolborane was added (5.2 mL, 36 mmols, 1.2 equiv) followed by dilution with toluene (18 mL, 1 M) and addition of styrene (3.4 mL, 30 mmol, 1 equiv) to provide the title compound (5.7135 g, 24.6 mmols, 82% yield). The compound was purified via flash column chromatography (silica gel: 5% Et_2O in hexanes) as a colorless oil. ^1H NMR (400 MHz, $CDCl_3$) δ: 7.3 – 7.2 (m, 4H), 7.2 (t, J = 7.1 Hz, 1H), 2.5 (q, J = 7.6 Hz, 1H), 1.4 (d, J = 7.6 Hz, 3H), 1.2 (d, J = 5.7 Hz, 12H); ^{13}C NMR (100 MHz, $CDCl_3$) δ: 145.0, 128.3, 127.8, 125.1, 83.3, 24.6, 24.6, 17.1. All characterization data are consistent with previous reports.[10]

2-(1-(4-Fluorophenyl)ethyl)-4,4,5,5-tetramethyl-1,3,2-dioxaborolane

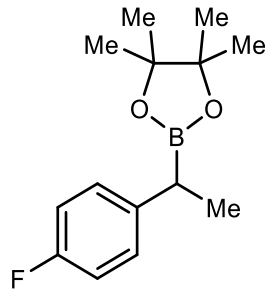

Prepared according to General Procedure C with CuCl (14.9 mg, 0.15 mmol, 3 mol%), KOtBu (33.6 mg, 1.30 mmol, 6 mol%), 1,2-bis(diphenylphosphaneyl)benzene (111.5 mg, 0.25, 5 mol%), and toluene (2 mL, 2.5 M). Then, pinacolborane was added (0.87 mL, 6 mmols, 1.2 equiv) followed by dilution with toluene (3 mL, 1 M) and addition of 1-fluoro-4-vinylbenzene (0.60 mL, 5 mmol, 1 equiv). The compound was purified via flash column chromatography (silica gel: 5% Et_2O in hexanes) to provide the title compound (1.0505 g, 4.2 mmols, 84% yield) as a colorless oil. ^{1}H NMR (400 MHz, $CDCl_3$) δ: 7.21 – 7.11 (m, 2H), 7.07 – 6.87 (m, 2H), 2.41 (q, *J* = 7.5 Hz, 1H), 1.31 (d, *J* = 7.6 Hz, 3H), 1.21 (s, 6H), 1.20 (s, 6H); ^{13}C NMR (100 MHz, $CDCl_3$) δ: 161.0 (d, *J* = 242.3 Hz), 140.7 (d, *J* = 3.1 Hz), 129.1 (d, *J* = 7.8 Hz), 115.1 (d, *J* = 21.0 Hz), 83.5, 24.8, 24.7, 17.4; ^{19}F NMR (365 MHz, $CDCl_3$) δ: -119.03. All characterization data are consistent with previous reports.[13]

2-(1-(3-Chlorophenyl)ethyl)-4,4,5,5-tetramethyl-1,3,2-dioxaborolane

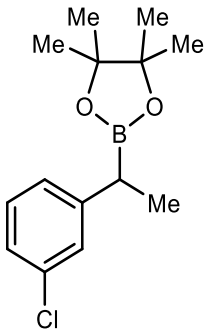

Prepared according to General Procedure C with CuCl (14.9 mg, 0.15 mmol, 3 mol%), KOtBu (33.6 mg, 1.30 mmol, 6 mol%), 1,2-bis(diphenylphosphaneyl)benzene (111.5 mg, 0.25, 5 mol%), and toluene (2 mL, 2.5 M). Then, pinacolborane was added (0.87 mL, 6 mmols, 1.2 equiv) followed by dilution with toluene (3 mL, 1 M) and addition of 1-chloro-3-vinylbenzene (0.64 mL, 5 mmol, 1 equiv). The compound was purified via flash column chromatography (silica gel: 3% Et_2O in hexanes) to provide the title compound (1.1366 g, 4.25 mmols, 85% yield) as a colorless oil. ^{1}H NMR (400 MHz, $CDCl_3$) δ: 7.23 – 7.14 (m, 2H), 7.14 – 7.06 (m, 2H), 2.42 (q, *J* = 7.5 Hz, 1H), 1.32 (d, *J* = 7.5 Hz, 3H), 1.22 (s, 6H), 1.21 (s, 6H); ^{13}C NMR (100 MHz, $CDCl_3$) δ: 147.2, 134.1, 129.6, 128.0, 126.2, 125.4, 83.6, 24.7, 24.7, 16.9. All characterization data are consistent with previous reports.[13]

4,4,5,5-Tetramethyl-2-(1-(naphthalen-2-yl)ethyl)-1,3,2-dioxaborolane

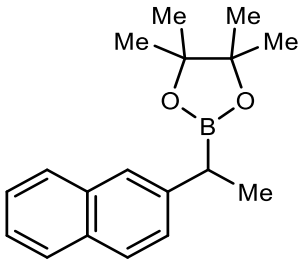

Prepared according to General Procedure C with CuCl (14.9 mg, 0.15 mmol, 3 mol%), KOtBu (33.6 mg, 1.30 mmol, 6 mol%), 1,2-bis(diphenylphosphaneyl)benzene (111.5 mg, 0.25, 5 mol%), and toluene (2 mL, 2.5 M). Then, pinacolborane was added (0.87 mL, 6 mmols, 1.2 equiv) followed by dilution with toluene (3 mL, 1 M) and addition of 2-vinylnaphthalene (770 mg, 5 mmol, 1 equiv). The compound was purified via flash column chromatography (silica gel: 5% Et_2O in hexanes) to provide the title compound (1.0142 g, 3.6 mmols, 84% yield) as a colorless oil. ^1H NMR (400 MHz, $CDCl_3$) δ: 7.86 – 7.73 (m, 3H), 7.67 (d, *J* = 1.7 Hz, 1H), 7.42 (pd, *J* = 7.0, 1.5 Hz, 3H), 2.64 (q, *J* = 7.5 Hz, 1H), 1.45 (d, *J* = 7.5 Hz, 3H), 1.23 (s, 6H), 1.22 (s, 6H); ^{13}C NMR (100 MHz, $CDCl_3$) δ: 142.71, 134.00, 131.86, 127.79, 127.65, 127.60, 127.37, 125.76, 125.39, 124.89, 83.50, 24.77, 24.74, 16.95. All characterization data are consistent with previous reports.[13]

2-(1-(4-Methoxyphenyl)ethyl)-4,4,5,5-tetramethyl-1,3,2-dioxaborolane

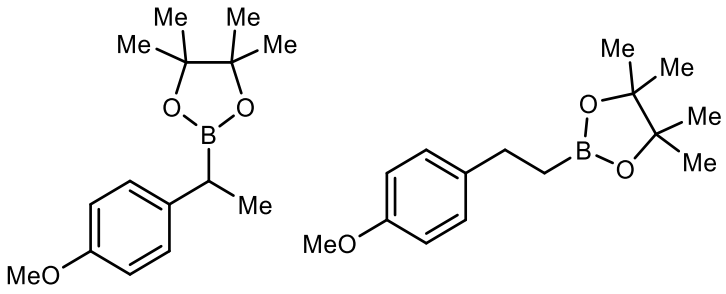

A **B**

3.7 **1**

Prepared according to procedure of Endo et al.[14] To a mixture of [RhCl(cod)]2 (98.6 mg, 0.20 mmol, 5 mol% Rh), DPPB (102.3 mg, 0.24 mmol, 6.0 mol%), and DMAP (29.3 mg, 0.24 mmol, 6.0 mol%) in DCE (4 mL) were added 1-methoxy-4-vinylbenzene (.52 mL, 4.0 mmol) and pinacolborane (0.70 mL, 4.8 mmol, 1.2 equiv) at r.t. The reaction mixture was stirred at r.t. for 10 min and filtered through a pad of silica gel with Et_2O (50 mL) and concentrated *in vacuo*. The crude ^1H NMR analysis shows a mixture of A:B with a ratio of 3.6:1. The compound was purified via flash column chromatography (silica gel: 5% Et_2O in hexanes) to provide the title compound (0.814 g, 3.1 mmols, 78% yield) as a colorless oil. Purified product is a 3.7:1 mixture of regioisomers A:B. ^1H NMR (400 MHz, CD_3CN) δ: 7.16 – 7.05 (m, 2H), 6.82 (d, J = 8.3 Hz, 2H), 3.75 (s, 3H), 2.63 (t, J = 8.0 Hz, regio), 2.32 (q, J = 7.6 Hz, 1H), 1.24 (d, J = 7.5 Hz, 3H), 1.20 (s, 6H), 1.18 (s, 6H), 1.02 (t, J = 7.9 Hz, regio); ^{13}C NMR (100 MHz, CD_3CN) δ: 158.4, 138.3, 129.6, 114.7, 84.1, 55.8, 25.0 (d, J = 2.2 Hz), 17.9. All characterization data are consistent with previous reports.[13]

A2.9. Preparation of Trifluoroborate Salts

General Procedure D

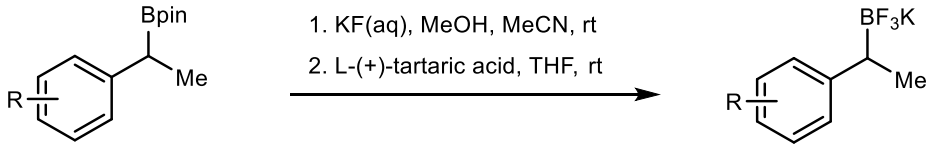

Potassium trifluoroborate salts were prepared according to the report of Lennox and Lloyd-Jones.[15] To the organoboronic acid pinacol ester (1.0 mmol, 1 equiv) was added methanol (2 mL, 0.5M) then acetonitrile (2 mL, 0.5 M), followed by potassium fluoride (4 equiv, 4.0 mmol) in H_2O (0.4 mL, 10 M with respect to KF) at room temperature. The mixture was stirred until complete dissolution of the boronic ester (0.5 - 1 min). L-(+)-tartaric acid (5) (2.05 equiv., 2.05 mmol) was dissolved into THF (1.5 mL, 1.4 M with respect to tartaric acid, gentle heat and agitation is required for rapid dissolution) and added drop-wise to the rapidly (≈ 1000 rpm) stirring biphasic mixture over a period of 5 minutes, as a white precipitate formed. The reaction was stirred for 2 min, diluted with acetonitrile (3 mL) and stirred for a further 2 min before being diluted again with acetonitrile (1 mL) and filtered. The flask and filter cake were rinsed with further portions of acetonitrile (3 x 5 mL) and then the combined filtrates were concentrated *in vacuo* to give a mixture of the corresponding potassium organotrifluoroborate and pinacol. Pinacol was removed by evaporation at 6 mmHg with gentle heating using a heat gun, until there were no visible signs of the condensed pinacol around the flask (5- 10 min). The solid was scrapped off the sides of the flask and subjected to further heating (10 – 15 min) at this low pressure. In most cases this amount was sufficient however in some cases more heating was required.

Notes:

1. It is crucial to remove any excess potassium fluoride for the subsequent photoredox catalyzed alkylation, as the fluoride anion can decompose the heterocyclic phosphonium salts, decreasing the yield of alkylated product.
2. To prevent isolation with small amounts of potassium fluoride when the reaction is scaled up, Et_2O was used as an antisolvent to effect precipitation of the pure product after pinacol was removed under vacuum.
3. As well as the method developed by Lennox and Lloyd-Jones, the procedure reported by Molander that uses KHF_2 is also a viable option for synthesis of the trifluoroborate salts.[16-17]

Potassium trifluoro(1-phenylethyl)borate

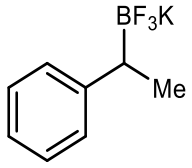

Prepared according to general procedure D using 4,4,5,5-tetramethyl-2-(1-phenylethyl)-1,3,2-dioxaborolane (4.1643 g, 18.0 mmol), potassium fluoride (4.164 g, 71.8 mmol), H_2O (7.2 mL, 10 M with respect to KF), MeOH (36.0 mL, 0.5 M with respect to 4,4,5,5-tetramethyl-2-(1-phenylethyl)-1,3,2-dioxaborolane), MeCN (36.0 mL, 0.5 M with respect to 4,4,5,5-tetramethyl-2-(1-phenylethyl)-1,3,2-dioxaborolane), L-(+)-tartaric acid (5.535 g, 36.9 mmol), and THF (26.4 mL, 1.4 M with respect to tartaric acid). Filtration, concentration, and trituration of the crude reaction mixture with Et_2O afforded the title compound as a white crystalline solid (3.0665 g, 14.4 mmol, 80% yield). ^{1}H NMR (400 MHz, $CDCl_3$) δ: 7.20 – 7.11 (m, 4H), 6.96 (tt, *J* = 5.7, 2.8 Hz, 1H), 1.72 (s, 1H), 1.12 (d, *J* = 7.4 Hz, 3H); ^{13}C NMR (100 MHz, $CDCl_3$) δ: 153.23, 128.64, 128.15, 123.70, 17.28; The carbon attached to boron could not be observed

due to quadrupolar relaxation. ^{19}F NMR (365 MHz, CD_3CN) δ: -144.90--147.40 (m). The data is consistent with those previously reported.[18]

Potassium trifluoro(1-(4-fluorophenyl)ethyl)borate

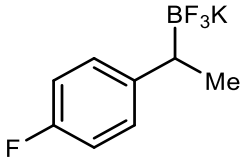

Prepared according to general procedure D using 2-(1-(4-Fluorophenyl)ethyl)-4,4,5,5-tetramethyl-1,3,2-dioxaborolane (1.0505 g, 4.2 mmol), potassium fluoride (763.8 mg, 71.8 mmol), H_2O (1.3 mL, 10 M with respect to KF), MeOH (6.6 mL, 0.5 M with respect to 2-(1-(4-Fluorophenyl)ethyl)-4,4,5,5-tetramethyl-1,3,2-dioxaborolane), MeCN (6.6 mL, 0.5 M with respect to 2-(1-(4-Fluorophenyl)ethyl)-4,4,5,5-tetramethyl-1,3,2-dioxaborolane), L-(+)-tartaric acid (1.013 g, 36.9 mmol), and THF (26.4 mL, 1.4 M with respect to tartaric acid). Filtration and concentration of the crude reaction mixture afforded the title compound as a white crystalline solid (468.8 g, 1.61 mmol, 49% yield). m.p. 142-145 °C; IR ν_{max}/cm^{-1} (film): 2957, 2931, 2872, 1601, 1505, 1459, 1373, 1241, 1221, 1142, 1087, 1022, 1012, 905, 835, 753; ^1H NMR (400 MHz, CD_3CN) δ: 7.17 (dd, *J* = 8.5, 5.8 Hz, 2H), 6.92 (t, *J* = 9.0 Hz, 2H), 1.81 (qn, *J* = 6.3 Hz, 1H), 1.15 (d, *J* = 7.4 Hz, 3H); ^{13}C NMR (100 MHz, CD_3CN) δ: 160.8 (d, *J* = 237.5 Hz), 148.1, 129.7 (d, *J* = 7.3 Hz), 114.8 (d, *J* = 20.5 Hz), 31.4, 17.4; ^{19}F NMR (365 MHz, CD_3CN) δ: -123.05, -146.14.

Potassium trifluoro(1-(4-methoxyphenyl)ethyl)borate (2c)

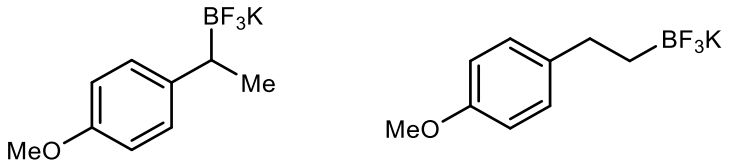

2c **2c'**

1.2 **1**

Prepared according to general procedure D using 2-(1-(4-methoxyphenyl)ethyl)-4,4,5,5-tetramethyl-1,3,2-dioxaborolane (3.8:1 mixture of regioisomers) (749.8 mg, 2.9 mmol), potassium fluoride (667 mg, 11.5 mmol), H_2O (1.2 mL, 10 M with respect to KF mg), MeOH (5.7 mL, 0.5 M with respect to 2-(1-(4-methoxyphenyl)ethyl)-4,4,5,5-tetramethyl-1,3,2-dioxaborolane), MeCN (5.7 mL, 0.5 M with respect to 2-(1-(4-methoxyphenyl)ethyl)-4,4,5,5-tetramethyl-1,3,2-dioxaborolane), L-(+)-tartaric acid (879 mg, 5.9 mmol), and THF (4.2 mL, 1.4 M with respect to tartaric acid). Filtration, concentration, and trituration of the crude reaction mixture with Et_2O afforded the title compound as a white crystalline solid as a mixture of regioisomers 2c and 2c' (1.2:1) (203 g, 0.83 mmol, 29% yield). m.p. 162-164 °C; IR ν_{max}/cm^{-1} (film): 3008, 2953, 2906, 2837, 1612, 1512, 1247, 1089, 1030, 1018, 934, 860, 838, 812, 757; ^{1}H NMR (400 MHz, CD_3CN) δ: 7.08 (dd, *J* = 21.0, 8.3 Hz, 2H), 6.88 – 6.66 (m, 2H), 3.73 (s, regio), 3.72 (s, 3H), 2.55 – 2.40 (m, regio), 1.64 (s, 1H), 1.08 (d, *J* = 7.5 Hz, 3H), 0.57 – 0.22 (m, regio); ^{13}C NMR (100 MHz, CD_3CN) δ: 156.94, 141.23, 129.27, 113.73, 55.69, 31.91, 17.67; ^{19}F NMR (365 MHz, $CDCl_3$) δ: -141.26 (regio), -146.06.

Potassium (1-(3-chlorophenyl)ethyl)trifluoroborate

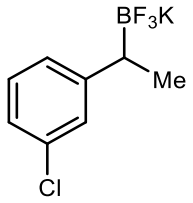

Prepared according to general procedure D using 2-(1-(3-Chlorophenyl)ethyl)-4,4,5,5-tetramethyl-1,3,2-dioxaborolane (1.0718 g, 4.0 mmol), potassium fluoride (933.8 mg, 16.1 mmol), H_2O (1.6 mL, 10 M with respect to KF), MeOH (8.1 mL, 0.5 M with respect to 2-(1-(3-Chlorophenyl)ethyl)-4,4,5,5-tetramethyl-1,3,2-dioxaborolane), MeCN (8.1 mL, 0.5 M with respect to 2-(1-(3-Chlorophenyl)ethyl)-4,4,5,5-tetramethyl-1,3,2-dioxaborolane), L-(+)-tartaric acid (1.239 g, 8.3 mmol), and THF (5.9 mL, 1.4 M with respect to tartaric acid). Filtration, and concentration of the crude reaction mixture afforded the title compound as a tan crystalline solid (673.3 mg, 2.7 mmol, 68% yield). m.p. 99-105 °C; IR ν_{max}/cm^{-1} (film): 3061, 2960, 2932, 2872, 1591, 1565, 1468, 1426, 1270, 1225, 1111, 1078, 1020, 999, 958, 901, 844, 790, 698; ^{1}H NMR (400 MHz, $CDCl_3$) δ: 7.23 – 7.08 (m, 3H), 7.01 (d, J = 7.5, 1H), 1.90 – 1.75 (m, 1H), 1.16 (d, J = 7.4 Hz, 3H); ^{13}C NMR (100 MHz, $CDCl_3$) δ: 155.19, 133.64, 129.82, 128.29, 127.08, 123.90, 32.46, 16.85; ^{19}F NMR (365 MHz, $CDCl_3$) δ: -146.17.

Potassium trifluoro(1-(naphthalen-2-yl)ethyl)borate (2e)

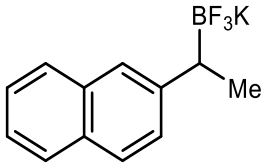

Prepared according to general procedure D using 4,4,5,5-Tetramethyl-2-(1-(naphthalen-2-yl)ethyl)-1,3,2-dioxaborolane (977.5 mg, 3.5 mmol), potassium fluoride (804.5 mg, 13.9 mmol), H_2O (1.4 mL, 10 M with respect to KF mg), MeOH (6.9 mL, 0.5 M with respect to 4,4,5,5-Tetramethyl-2-(1-(naphthalen-2-yl)ethyl)-1,3,2-dioxaborolane), MeCN (6.9 mL, 0.5 M with respect to 4,4,5,5-Tetramethyl-2-(1-(naphthalen-2-yl)ethyl)-1,3,2-dioxaborolane), L-(+)-tartaric acid (1.067 g, 7.1 mmol), and THF (5.1 mL, 1.4 M with respect to tartaric acid). Filtration, concentration, and trituration of the crude reaction mixture with Et_2O afforded the title compound as a tan amorphous solid (720.1 mg, 2.7, 79% yield). IR ν_{max}/cm^{-1} (film): 3414, 3054, 2973, 2930, 2870, 1709, 1678, 1629, 1365, 1226, 1093, 1016, 982, 912, 748; ^{1}H NMR (400 MHz, $CDCl_3$) δ: 7.74 (t, *J* = 7.4 Hz, 2H), 7.64 (d, *J* = 8.5 Hz, 1H), 7.52 (s, 1H), 7.44 (d, *J* = 8.4 Hz, 1H), 7.40 – 7.34 (m, 1H), 7.34 – 7.27 (m, 1H), 1.93 (s, 1H), 1.14 (d, *J* = 1.0 Hz, 3H); ^{13}C NMR (100 MHz, $CDCl_3$) δ: 151.6, 134.9, 131.8, 129.8, 128.2, 127.8, 126.8, 126.0, 124.7, 124.4, 25.2, 17.2; ^{19}F NMR (365 MHz, $CDCl_3$) δ: -145.66.

A2.10. Preparation of Alkylated Pyridines and Diazines

General Procedure E

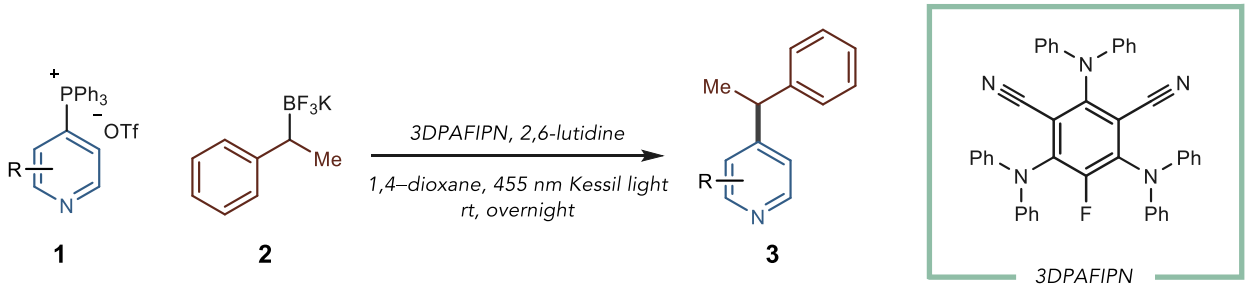

An oven dried 8 mL vial equipped with a magnetic stir bar was charged with the heterocyclic phosphonium salt (1.0 equiv), potassium trifluoroborate salt (2.0 equiv) and photocatalyst 3DPAFIPN (2 mol%). The vial was pumped into a glovebox and then dioxane (0.3 M) and 2,6-lutidine (3.0 equiv) were added via a syringe. The vial was sealed and removed from the glovebox and pre-stirred for ten minutes before irradiation with a 455 nm kessil lamp (5 cm away, with stream of air blowing over vials to keep reaction at 25 °C) for 16 hours. The reaction was quenched with water and the aqueous layer was extracted with CH_2Cl_2 (4x). The combined organic extracts were dried ($MgSO_4$), filtered, and concentrated *in vacuo*. The crude residue was put under vacuum for an hour to remove 2,6-lutidine from the crude mixture, then purified by flash column chromatography under the stated conditions to provide the alkylated heteroaryl product.

NOTES:

1. The presence of potassium fluoride leftover from the trifluoroborate salt synthesis has a detrimental effect on the heteroaromatic alkylation reaction, as the fluoride anion can decompose the heterocyclic phosphonium salt back to the heterocycle precursor. To remove excess potassium fluoride (especially when making trifluoroborate salt on large scale) recrystallize the product as described in the notes for Section 7.
2. The pre-stirring step is important to bring the heterocyclic phosphonium salt into solution before any redox events occur, leading to undesired byproducts. The authors note the observation that heterocyclic phosphonium salts that are difficult to dissolve by themselves, dissolve easier upon stirring with the trifluoroborate salt.
3. Putting the crude residue under vacuum for an hour to remove the 2,6-lutidine before flash column chromatography is not necessary but was done to provide consistent and reproducible column conditions for purification.
4. Protonation of tertiary amines within the substrate with an equivalent of TfOH resulted in slightly higher yields of coupled product.

Heterocyclic Phosphonium Salt Scope for Heteroaromatic Alkylation

2-Phenyl-4-(1-phenylethyl)pyridine

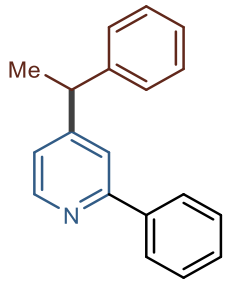

Prepared according to general procedure E using triphenyl(2-phenylpyridin-4-yl)phosphonium trifluoromethane sulfonate (283.0 mg, 0.50 mmol), potassium trifluoro(1-phenylethyl)borate (212.0 mg, 1.00 mmol), 3DPAFIPN (6.5 mg, 0.01 mmol), 2,6-lutidine (175 mL, 1.5 mmol), and 1,4-dioxane (1.67 mL, 0.3M). Flash column chromatography (silica gel: 7% Et_2O in hexanes) afforded the title compound as a pale yellow oil (85.5 mg, 0.40 mmol, 74% yield).; IR $\tilde{\nu}_{max}/cm^{-1}$ (film): 3084, 3028, 2969, 2930, 2874, 1596, 1554, 1474, 1446, 1403, 1265, 1029, 991, 800, 741, 697; ^1H NMR (400 MHz, $CDCl_3$) δ: 8.47 (d, *J* = 5.1 Hz, 1H), 7.88 – 7.78 (m, 2H), 7.46 (d, *J* = 1.6 Hz, 1H), 7.38 – 7.24 (m, 3H), 7.24 – 7.06 (m, 5H), 6.96 (dd, *J* = 5.1, 1.7 Hz, 1H), 4.05 (q, *J* = 7.2 Hz, 1H), 1.56 (d, *J* = 7.2 Hz, 3H); ^{13}C NMR (100 MHz, $CDCl_3$) δ: 157.7, 155.9, 149.8, 144.5, 139.7, 128.9, 128.7, 128.7, 127.7, 127.1, 126.7, 121.5, 120.0, 44.5, 21.2; *m/z* LRMS (ESI + APCI) found $[M+H]^+$ 260.2, $C_{19}H_{18}N^+$ requires 260.1.

Large scale: Prepared according to general procedure E except a 16 mL vial was used rather than an 8 mL vial using triphenyl(2-phenylpyridin-4-yl)phosphonium trifluoromethane sulfonate (1.132 g, 2.00 mmol), potassium trifluoro(1-phenylethyl)borate (848.0 mg, 4.00 mmol), 3DPAFIPN (26.0 mg, 0.04 mmol), 2,6-lutidine (692 mL, 6.00 mmol), and 1,4-dioxane (6.67 mL, 0.3M). Flash column chromatography (silica gel: 7% Et_2O in hexanes) afforded the title compound

as a pale yellow oil (383 mg, 1.48 mmol, 74% yield). Spectra consistent with that obtained upon isolation of small scale reaction.

3-Phenyl-4-(1-phenylethyl)pyridine

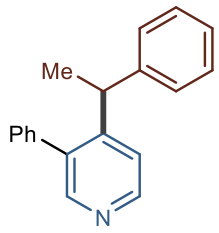

Prepared according to general procedure E using triphenyl(3-phenylpyridin-4-yl)phosphonium trifluoromethanesulfonate (283.0 mg, 0.50 mmol), potassium trifluoro(1-phenylethyl)borate (212.0 mg, 1.00 mmol), 3DPAFIPN (6.5 mg, 0.01 mmol), 2,6-lutidine (175 □L, 1.5 mmol), and 1,4-dioxane (1.67 mL, 0.3M). ^{1}H NMR analysis of the crude reaction mixture gave a mixture of regioisomers with a ratio of 8:1 (4 position:2 position alkylation). Flash column chromatography (silica gel: 5% Et_2O in hexanes) afforded the title compound as a single regioisomer as a yellow oil (54.5 mg, 0.21 mmol, 42% yield). IR □$_{max}$/cm^{-1} (film): 3058, 3025, 2968, 1585, 1494, 1444, 1007, 838, 761, 697; ^{1}H NMR (400 MHz, $CDCl_3$) δ: 8.70 – 8.43 (m, 2H), 7.59 – 7.46 (m, 3H), 7.42 – 7.26 (m, 6H), 7.14 (dd, *J* = 7.32, 1.78 Hz, 2H), 4.41 (q, *J* = 7.16 Hz, 1H), 1.65 (d, *J* = 7.19 Hz, 3H); ^{13}C NMR (100 MHz, $CDCl_3$) δ: 152.8, 150.4, 149.0, 144.7, 137.9, 137.5, 129.6, 128.5, 128.5, 127.8, 127.6, 126.4, 122.3, 40.0, 21.7□ *m/z* LRMS (ESI + APCI) found $[M+H]^+$ 260.2, $C_{19}H_{18}N^+$ requires 260.1.

2-Methoxy-4-(1-phenylethyl)pyridine

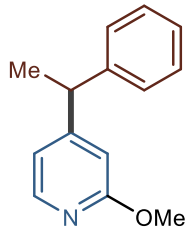

Prepared according to general procedure E using triphenyl(2-methoxypyridin-4-yl)phosphonium trifluoromethanesulfonate (260.0 mg, 0.50 mmol), potassium trifluoro(1-phenylethyl)borate (212.0 mg, 1.00 mmol), 3DPAFIPN (6.5 mg, 0.01 mmol), 2,6-lutidine (175 mL, 1.5 mmol), and 1,4-dioxane (1.67 mL, 0.3M). Flash column chromatography (silica gel: 5% Et_2O in hexanes) afforded the title compound as a pale yellow oil (85.5 mg, 0.40 mmol, 80% yield). IR ν_{max}/cm^{-1} (film): 3061, 3025, 2945, 2875, 1607, 1557, 1394, 1317, 1027, 698; ^1H NMR (400 MHz, $CDCl_3$) δ: 8.05 (d, *J* = 8.0 Hz 1H), 7.36 – 7.27 (m, 2H), 7.22 (td, *J* = 7.1, 1.2 Hz, 3H), 6.72 (dd, *J* = 5.4, 1.6 Hz, 1H), 6.63 (m, 1H), 4.07 (q, *J* = 7.2 Hz, 1H), 3.93 (s, 3H), 1.62 (d, *J* = 7.3 Hz, 3H). ^{13}C NMR (100 MHz, $CDCl_3$) δ: 164.7, 158.1, 146.7, 144.6, 128.7, 127.7, 126.7, 116.9, 109.6, 53.4, 44.3, 21.0. *m/z* LRMS (ESI + APCI) found $[M+H]^+$ 214.2, $C_{14}H_{16}NO^+$ requires 214.1.

2-Fluoro-4-(1-phenylethyl)pyridine

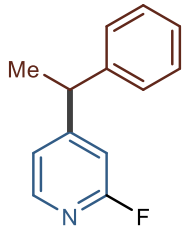

Prepared according to general procedure E using (2-fluoropyridin-4-yl)triphenylphosphonium trifluoromethanesulfonate (253.5 mg, 0.50 mmol), potassium trifluoro(1-phenylethyl)borate (212.0 mg, 1.00 mmol), 3DPAFIPN (6.5 mg, 0.01 mmol), 2,6-lutidine (175 mL, 1.5 mmol), and 1,4-dioxane (1.67 mL, 0.3M). Flash column chromatography (silica gel: 5% Et_2O in hexanes) afforded the title compound as a yellow oil (55.2 mg, 0.275 mmol, 55% yield). IR ν_{max}/cm^{-1} (film): 3062, 2972, 2933, 1609, 1563, 1480, 1407, 1271, 1148, 919, 699; ^1H NMR (400 MHz, $CDCl_3$) δ: 8.00 (d, *J* = 5.3 Hz, 1H), 7.31 – 7.20 (m, 2H), 7.20 – 7.08 (m, 3H), 6.93 (dt, *J* = 5.3, 1.8 Hz, 1H), 6.73 – 6.65 (m, 1H), 4.06 (q, *J* = 7.2 Hz, 1H), 1.56 (d, *J* = 7.2 Hz, 3H). ^{13}C NMR (100 MHz, $CDCl_3$) δ: 164.3 (d, *J* = 238.2 Hz), 161.4 (d, *J* = 7.5 Hz), 147.5 (d, *J* = 15.3 Hz), 143.8, 128.9, 127.7, 127.0, 121.0 (d, *J* = 3.9 Hz), 108.4 (d, *J* = 37.2 Hz), 44.3 (d, *J* = 2.8 Hz), 21.1; ^{19}F (365 MHz, $CDCl_3$) δ: -68.47; *m/z* LRMS (ESI + APCI) found $[M+H]^+$ 202.1, $C_{13}H_{13}FN^+$ requires 202.1.

Ethyl 4-(1-phenylethyl)picolinate

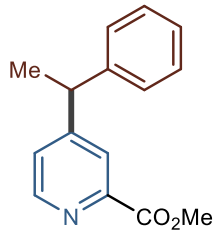

Prepared according to general procedure E using (2-(ethoxycarbonyl)pyridin-4-yl)triphenylphosphonium trifluoromethanesulfonate (281.0 mg, 0.50 mmol), potassium trifluoro(1-phenylethyl)borate (212.0 mg, 1.00 mmol), 3DPAFIPN (6.5 mg, 0.01 mmol), 2,6-lutidine (175 mL, 1.5 mmol), and 1,4-dioxane (1.67 mL, 0.3M). Flash column chromatography (silica gel: 50% Et_2O in hexanes) afforded the title compound as a yellow oil (60.8 mg, 0.24 mmol, 47% yield). IR ν_{max}/cm^{-1} (film): 3059, 2973, 2931, 1738, 1714, 1595, 1451, 1296, 1191, 1097, 1021, 859, 788, 699; ^1H NMR (400 MHz, $CDCl_3$) δ: 8.54 (dd, J = 4.9, 0.7 Hz, 1H), 7.94 (d, J = 1.8 Hz, 1H), 7.29 – 7.02 (m, 6H), 4.38 (q, J = 7.1 Hz, 2H), 4.11 (q, J = 7.2 Hz, 1H), 1.58 (d, J = 7.3 Hz, 3H), 1.34 (t, J = 7.2 Hz, 3H).^{13}C NMR (100 MHz, $CDCl_3$) δ: 165.5, 156.5, 149.9, 148.4, 143.8, 128.8, 127.6, 126.9, 126.1, 124.4, 62.0, 44.3, 21.0, 14.4. *m/z* LRMS (ESI + APCI) found $[M+H]^+$ 256.2, $C_{16}H_{18}NO_2^+$ requires 256.1.

4-(1-Phenylethyl)-2-(thiophen-3-yl)pyridine

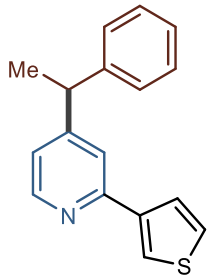

Prepared according to general procedure E using triphenyl(2-(thiophen-3-yl)pyridin-4-yl)phosphonium trifluoromethanesulfonate (286.0 mg, 0.50 mmol), potassium trifluoro(1-phenylethyl)borate (212.0 mg, 1.00 mmol), 3DPAFIPN (6.5 mg, 0.01 mmol), 2,6-lutidine (175 mL, 1.5 mmol), and 1,4-dioxane (1.67 mL, 0.3M). Flash column chromatography (silica gel: 20% Et_2O in hexanes), followed by a second column (silica gel, gradient elution: CH_2Cl_2 to 10% Et_2O in CH_2Cl_2) afforded the title compound as a pale yellow oil (64 mg, 0.24 mmol, 48% yield). IR ν_{max}/cm^{-1} (film): 3084, 3060, 2967, 2929, 2873, 1595, 1552, 1451, 1424, 840, 792, 744, 698, 672; ^1H NMR (400 MHz, $CDCl_3$) δ 8.4 (d, *J* = 5.13 Hz, 1H), 7.8 (dd, *J* = 3.09, 1.25 Hz, 1H), 7.5 (dd, *J* = 5.03, 1.29 Hz, 1H), 7.4 (d, *J* = 1.70 Hz, 1H), 7.3 (dd, *J* = 5.04, 3.00 Hz, 1H), 7.3 – 7.2 (m, 2H), 7.2 – 7.1 (m, 3H), 6.9 (dd, *J* = 5.31, 1.73 Hz, 1H), 4.1 (q, *J* = 7.20 Hz, 1H), 1.6 (d, *J* = 7.24 Hz, 3H).; ^{13}C NMR (100 MHz, $CDCl_3$) δ 155.9, 153.7, 149.8, 144.5, 142.4, 128.8, 127.7, 126.8, 126.4, 126.3, 123.6, 121.4, 119.8, 44.5, 21.2. *m/z* LRMS (ESI + APCI) found $[M+H]^+$ 266.1, $C_{17}H_{16}NS^+$ requires 266.1.

2-(4-Methoxyphenyl)-4-(1-phenylethyl)pyridine

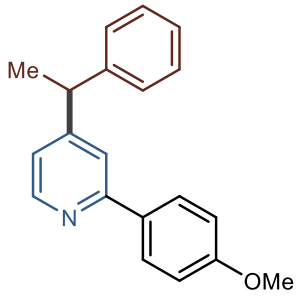

Prepared according to general procedure E using (2-(4-methoxyphenyl)pyridin-4-yl)triphenylphosphonium trifluoromethanesulfonate (178.8 mg, 0.30 mmol), potassium trifluoro(1-phenylethyl)borate (127.2 mg, 0.60 mmol), 3DPAFIPN (3.9 mg, 0.006 mmol), 2,6-lutidine (105 □L, 0.9 mmol), and 1,4-dioxane (1.00 mL, 0.3M). Flash column chromatography (silica gel: 10% EtOAc in hexanes) followed by a second column (silica gel: 30% Et_2O in hexanes) afforded the title compound as a yellow amorphous solid (48.1 mg, 0.17 mmol, 55% yield). m.p. 57-60 °C; IR $\square_{max}/cm^{-1}$ (film): 3001, 2966, 2933, 2839, 1597, 1550, 1514, 1245, 1172, 1026, 831, 703; ^1H NMR (400 MHz, $CDCl_3$) δ 8.55 (d, *J* = 5.10 Hz, 1H), 8.14 – 7.78 (m, 2H), 7.52 (s, 1H), 7.39 – 7.20 (m, 5H), 7.04 (dd, *J* = 5.15, 1.64 Hz, 1H), 6.99 (dd, *J* = 8.70, 1.53 Hz, 2H), 4.18 (q, *J* = 7.22 Hz, 1H), 3.86 (s, 3H), 1.69 (d, *J* = 7.26 Hz, 3H). ^{13}C NMR (100 MHz, $CDCl_3$) δ 160.39, 157.24, 155.75, 149.55, 144.53, 132.18, 128.63, 128.24, 127.63, 126.61, 120.84, 119.20, 114.05, 55.34, 44.48, 21.15. *m/z* LRMS (ESI + APCI) found $[M+H]^+$ 290.2, $C_{20}H_{20}NO^+$ requires 290.2.

2-(4-Iodophenyl)-4-(1-phenylethyl)pyridine

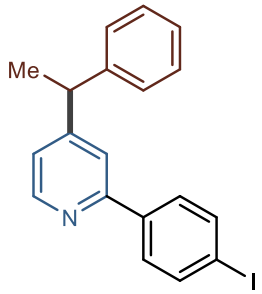

Prepared according to general procedure E using (2-(4-iodophenyl)pyridin-4-yl)triphenylphosphonium trifluoromethanesulfonate (207.6 mg, 0.30 mmol), potassium trifluoro(1-phenylethyl)borate (127.2 mg, 0.60 mmol), 3DPAFIPN (3.9 mg, 0.006 mmol), 2,6-lutidine (105 □L, 0.9 mmol), and 1,4-dioxane (1.00 mL, 0.3M). Flash column chromatography (silica gel, gradient elution: 5% Et_2O in hexanes to 10% EtOAc in hexanes) afforded the title compound as a yellow oil (71.3 mg, 0.19 mmol, 62% yield). IR $\square_{max}/cm^{-1}$ (film): 3058, 2966, 2927, 1596, 1468, 1411, 1003, 821, 698; ^1H NMR (400 MHz, $CDCl_3$) δ: 8.47 (d, J = 5.10 Hz, 1H), 7.72 – 7.66 (m, 2H), 7.64 – 7.57 (m, 2H), 7.47 – 7.41 (m, 1H), 7.27 – 7.20 (m, 2H), 7.18 – 7.11 (m, 3H), 7.01 (dd, J = 5.15, 1.66 Hz, 1H), 4.09 (q, J = 7.20 Hz, 1H), 1.59 (d, J = 7.20 Hz, 3H); ^{13}C NMR (100 MHz, $CDCl_3$) δ: 156.52, 156.11, 149.84, 144.33, 139.05, 137.81, 128.77, 128.73, 127.65, 126.75, 121.89, 119.70, 95.24, 44.48, 21.20; *m/z* LRMS (ESI + APCI) found $[M+H]^+$ 386.1, $C_{19}H_{17}IN^+$ requires 386.0.

3-Ethyl-4-(1-phenylethyl)pyridine

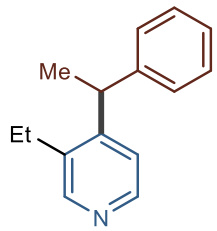

Prepared according to general procedure E using (3-ethylpyridin-4-yl)triphenylphosphonium trifluoromethanesulfonate (259.0 mg, 0.50 mmol), potassium trifluoro(1-phenylethyl)borate (212.0 mg, 1.00 mmol), 3DPAFIPN (6.5 mg, 0.01 mmol), 2,6-lutidine (175 □L, 1.5 mmol), and 1,4-dioxane (1.67 mL, 0.3M). Flash column chromatography (silica gel: 60% EtOAc in hexanes) followed by a second column (silica gel: 30% EtOAc in hexanes) afforded the title compound as a yellow solid (51.4 mg, 0.25 mmol, 49% yield). m.p. 46-48 °C; IR $\square_{max}$/cm^{-1} (film): 3062, 2966, 2928, 2871, 1589, 1490, 1449, 843, 764, 725; ^{1}H NMR (400 MHz, $CDCl_3$) δ: 8.31 (m, 2H), 7.48 – 6.80 (m, 6H), 4.28 (q, *J* = 7.13 Hz, 1H), 2.56 (ddt, *J* = 27.03, 14.63, 7.33 Hz, 2H), 1.52 (d, *J* = 7.20 Hz, 3H), 1.08 (t, *J* = 7.57 Hz, 3H); ^{13}C NMR (100 MHz, $CDCl_3$) δ: 152.27, 150.29, 147.75, 144.77, 137.10, 128.64, 127.64, 126.49, 121.94, 39.83, 23.23, 21.86, 15.29. *m/z* LRMS (ESI + APCI) found $[M+H]^+$ 212.1, $C_{15}H_{18}N^+$ requires 212.1.

2-Butyl-3-fluoro-4-(1-phenylethyl)pyridine

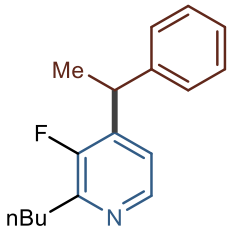

Prepared according to general procedure E using (2-butyl-3-fluoropyridin-4-yl)triphenylphosphonium trifluoromethanesulfonate (225.6 mg, 0.40 mmol), potassium trifluoro(1-phenylethyl)borate (169.6 mg, 0.80 mmol), 3DPAFIPN (2.6 mg, 0.004 mmol), 2,6-lutidine (140 □L, 1.20 mmol), and 1,4-dioxane (1.33 mL, 0.3M). Flash column chromatography (silica gel: 10% EtOAc in hexanes) afforded the title compound as a pale yellow oil (75.2 mg, 0.29 mmol, 73% yield). IR $\square_{max}$/cm^{-1} (film): 3063, 2958, 2930, 1601, 1496, 1426, 1176, 837, 757, 698; ^{1}H NMR (400 MHz, $CDCl_3$) δ: 8.21 (d, *J* = 5.0 Hz, 1H), 7.36 – 7.27 (m, 2H), 7.25 – 7.17 (m, 3H), 6.95 (t, *J* = 5.3 Hz, 1H), 4.45 (q, *J* = 7.2 Hz, 1H), 2.86 – 2.75 (m, 2H), 1.68 (qn, *J* = 8.0 Hz, 2H), 1.61 (d, *J* = 7.2 Hz, 3H), 1.38 (h, *J* = 7.4 Hz, 2H), 0.92 (t, *J* = 8.0 Hz, 3H). ^{13}C NMR (100 MHz, $CDCl_3$) δ: 155.9 (d, *J* = 254.4 Hz), 150.5 (d, *J* = 17.2 Hz), 144.8 (d, *J* = 6.6 Hz), 143.6, 141.2 (d, *J* = 13.4 Hz), 128.7, 127.6, 126.8, 121.0 (d, *J* = 1.4 Hz), 38.0 – 36.6 (m), 31.5 (d, *J* = 1.8 Hz), 30.8 (d, *J* = 1.3 Hz), 22.7, 20.3, 14.0. ^{19}F NMR (365 MHz, $CDCl_3$) □□□□132□4□ *m/z* LRMS (ESI + APCI) found $[M+H]^+$ 258.2, $C_{17}H_{21}FN^+$ requires 258.2.

5-Methoxy-2-methyl-4-(1-phenylethyl)pyridine

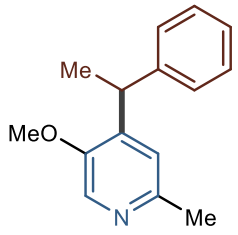

Prepared according to general procedure E using (5-methoxy-2-methylpyridin-4-yl)triphenylphosphonium trifluoromethanesulfonate (267.0 mg, 0.50 mmol), potassium trifluoro(1-phenylethyl)borate (212.0 mg, 1.00 mmol), 3DPAFIPN (6.5 mg, 0.01 mmol), 2,6-lutidine (175 □L, 1.5 mmol), and 1,4-dioxane (1.67 mL, 0.3M). Flash column chromatography (silica gel: 35% EtOAc in hexanes) afforded the title compound as a pale yellow amorphous solid (96.4 mg, 0.43 mmol, 85% yield). IR $\square_{max}$/cm^{-1} (film): 3025, 2968, 2930, 2874, 2839, 1597, 1590, 1492, 1450, 1272, 1028, 699; ^{1}H NMR (400 MHz, $CDCl_3$) δ: 7.96 (s, 1H), 7.23 – 7.02 (m, 5H), 6.80 (s, 1H), 4.40 (q, *J* = 7.25 Hz, 1H), 3.71 (s, 3H), 2.35 (s, 3H), 1.46 (d, *J* = 7.25 Hz, 3H); ^{13}C NMR (100 MHz, $CDCl_3$) δ: 151.4, 150.9, 144.5, 143.7, 132.3, 128.3, 127.7, 126.2, 121.7, 56.1, 37.1, 23.7, 20.2.□ *m/z* LRMS (ESI + APCI) found $[M+H]^+$ 228.2, $C_{15}H_{18}NO^+$ requires 228.1.

6-Isopropyl-4-(1-phenylethyl)nicotinonitrile

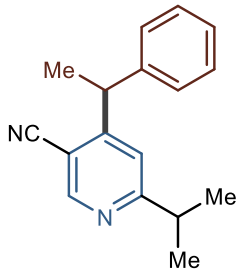

Prepared according to general procedure E using (3-cyano-2-isopropylpyridin-4-yl)triphenylphosphonium trifluoromethanesulfonate (224.0 mg, 0.40 mmol), potassium trifluoro(1-phenylethyl)borate (169.6 mg, 0.80 mmol), 3DPAFIPN (2.6 mg, 0.004 mmol), 2,6-lutidine (140 □L, 1.20 mmol), and 1,4-dioxane (1.33 mL, 0.3M). Flash column chromatography (silica gel: 5% EtOAc in hexanes) afforded the title compound as a pale yellow oil (64.8 mg, 0.26 mmol, 65% yield). IR $\square_{max}$/cm^{-1} (film): 3062, 2968, 2933, 2225, 1591, 1452, 1064, 916, 762, 699; ^{1}H NMR (400 MHz, $CDCl_3$) δ: 8.69 (s, 1H), 7.38 – 7.27 (m, 2H), 7.27 – 7.18 (m, 3H), 7.10 (s, 1H), 4.50 (q, *J* = 7.2 Hz, 1H), 3.03 (hept, *J* = 6.9 Hz, 1H), 1.68 (d, *J* = 7.2 Hz, 3H), 1.25 (d, *J* = 7.0 Hz, 6H); ^{13}C NMR (100 MHz, $CDCl_3$) δ: 171.8, 158.6, 152.8 (d, *J* = 1.9 Hz), 142.2, 128.8, 127.6, 127.1, 119.2 (d, *J* = 1.8 Hz), 116.5, 107.4, 42.8 (d, *J* = 2.4 Hz), 36.7, 22.2 (d, *J* = 6.5 Hz), 20.6.□ *m/z* LRMS (ESI + APCI) found $[M+H]^+$ 251.2, $C_{17}H_{19}N_2^+$ requires 251.2.

4-Cyclopropyl-2-((4-(1-phenylethyl)pyridin-3-yl)oxy)thiazole

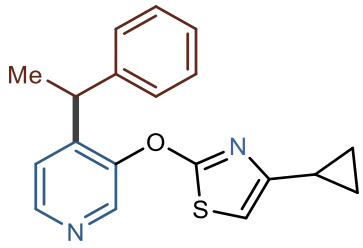

Prepared according to general procedure E using (3-((4-cyclopropylthiazol-2-yl)oxy)pyridin-4-yl)triphenylphosphonium trifluoromethanesulfonate (188.7 mg, 0.30 mmol), potassium trifluoro(1-phenylethyl)borate (127.2 mg, 0.60 mmol), 3DPAFIPN (3.9 mg, 0.006 mmol), 2,6-lutidine (105 □L, 0.90 mmol), and 1,4-dioxane (1.00 mL, 0.3 M). Flash column chromatography (silica gel: 20% EtOAc in hexanes) afforded the title compound as a yellow oil (73.8 mg, 0.23 mmol, 76% yield). IR $\square_{max}$/cm^{-1} (film): 3061, 3007, 2969, 2923, 2859, 1676, 1595, 1538, 1503, 1485, 1409, 1233, 1213, 1194, 967, 698; ^{1}H NMR (400 MHz, $CDCl_3$) □: 8.44 (s, 1H), 8.33 (d, *J* = 5.1 Hz, 1H), 7.23 – 7.06 (m, 6H), 6.24 (s, 1H), 4.40 (q, *J* = 7.2 Hz, 1H), 1.88 – 1.67 (m, 1H), 1.53 (d, *J* = 7.2 Hz, 3H), 0.87 – 0.64 (m, 4H); ^{13}C NMR (100 MHz, $CDCl_3$) □□□172.2, 153.6, 150.0, 147.4, 147.1, 143.2, 128.6, 127.7, 126.7, 123.1, 104.5, 37.8, 20.4, 12.7, 7.7; *m/z* LRMS (ESI + APCI) found $[M+H]^+$ 323.2, $C_{19}H_{19}N_2OS^+$ requires 323.1.

Ethyl 4-((4-chlorophenyl)(4-(1-phenylethyl)pyridin-2-yl)methoxy)piperidine-1-carboxylate

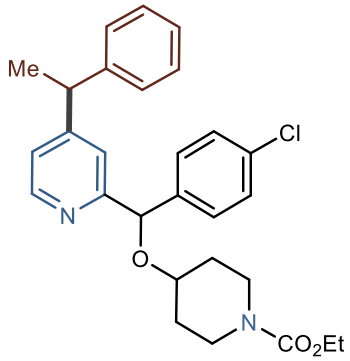

Prepared according to general procedure E using (2-((4-chlorophenyl)((1-(ethoxycarbonyl)piperidin-4-yl)oxy)methyl)pyridin-4-yl)triphenylphosphonium trifluoromethanesulfonate (196.0 mg, 0.25 mmol), potassium trifluoro(1-phenylethyl)borate (106.0 mg, 0.50 mmol), 3DPAFIPN (3.2 mg, 0.005 mmol), 2,6-lutidine (87.2 □L, 0.75 mmol), and 1,4-dioxane (833 □L, 0.3M). Flash column chromatography (silica gel: 15% acetone in hexanes) afforded the title compound as a yellow oil as a 1:1 mixture of diastereomers (63.9 mg, 0.13 mmol, 53% yield). IR $\square_{max}$/cm^{-1} (film): 3059, 2923, 2851, 1693, 1597, 1489, 1471, 1451, 1432, 1273, 1085, 1014, 767, 699; ^{1}H NMR (400 MHz, $CDCl_3$) δ: 8.31 (dd, *J* = 7.3, 5.1 Hz, 1H), 7.32 – 7.03 (m, 10H), 6.94 (ddd, *J* = 13.9, 5.1, 1.8 Hz, 1H), 5.48 (s, 1H), 4.10 – 3.98 (m, 3H), 3.71 – 3.53 (m, 2H), 3.50 – 3.40 (m, 1H), 3.14 – 2.96 (m, 2H), 1.80 – 1.68 (m, 1H), 1.64 – 1.37 (m, 6H), 1.17 (t, *J* = 8.0 Hz, 3H); ^{13}C NMR (100 MHz, $CDCl_3$) δ: 161.9, 156.2, 155.6, 149.2, 144.7, 140.2, 133.4, 128.7, 128.6, 128.3, 127.7, 126.8, 122.1, 120.1, 81.1, 72.8, 61.4, 44.5, 41.1, 31.2, 21.3, 14.8.□ *m/z* LRMS (ESI + APCI) found $[M+H]^+$ 479.3, $C_{28}H_{32}ClN_2O_3^+$ requires 479.2

5-(5-Fluoropyridin-2-yl)-2-methoxy-4-(1-phenylethyl)pyrimidine

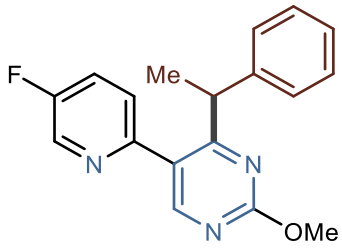

Prepared according to general procedure E using (5-(5-fluoropyridin-2-yl)-2-methoxypyrimidin-4-yl)triphenylphosphonium trifluoromethanesulfonate (154.0 mg, 0.25 mmol), potassium trifluoro(1-phenylethyl)borate (106.0 mg, 0.50 mmol), 3DPAFIPN (3.2 mg, 0.005 mmol), 2,6-lutidine (87.2 □L, 0.75 mmol), and 1,4-dioxane (833 □L, 0.3 M). Flash column chromatography (silica gel: 20% EtOAc in hexanes) afforded the title compound as a pale yellow oil (52.1 mg, 0.17 mmol, 67% yield). IR $\tilde{\nu}_{max}$/cm^{-1} (film): 3070, 2956, 2918, 2849, 1685, 1586, 1461, 1379, 1226, 1013, 845, 772, 748, 696; ^{1}H NMR (400 MHz, $CDCl_3$) □: 8.5 (d, *J* = 3.0 Hz, 1H), 8.3 (s, 1H), 7.3 (td, *J* = 8.3, 3.0 Hz, 1H), 7.1 – 6.9 (m, 6H), 4.5 (q, *J* = 7.0 Hz, 1H), 4.0 (s, 3H), 1.6 (d, *J* = 7.0 Hz, 3H); ^{13}C NMR (100 MHz, $CDCl_3$) □□□172.9, 165.1, 159.4, 158.8 (d, *J* = 256.0 Hz), 151.4 (d, *J* = 4.2 Hz), 143.8, 138.0 (d, *J* = 23.6 Hz), 128.4, 127.8, 126.6, 126.5, 125.4 (d, *J* = 4.4 Hz), 123.5 (d, *J* = 18.4 Hz), 55.0, 42.8, 20.8; ^{19}F NMR (365 MHz, $CDCl_3$) □□□□128□14□ *m/z* LRMS (ESI + APCI) found $[M+H]^+$ 310.2, $C_{18}H_{17}FN_3O^+$ requires 310.1.

2-(3-Chloro-4-((2-fluorobenzyl)oxy)phenyl)-4-(1-phenylethyl)pyridine

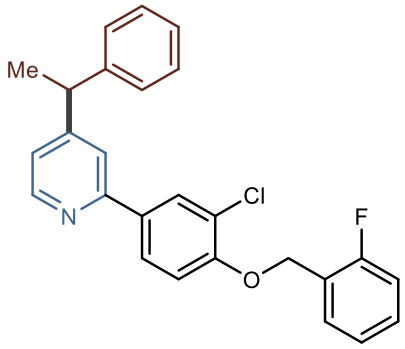

Prepared according to general procedure E using (2-(3-chloro-4-(2-fluorophenoxy)phenyl)pyridin-4-yl)triphenylphosphonium trifluoromethanesulfonate (217.2 mg, 0.30 mmol), potassium trifluoro(1-phenylethyl)borate (127.2 mg, 0.60 mmol), 3DPAFIPN (3.9 mg, 0.006 mmol), 2,6-lutidine (105 □L, 0.9 mmol), and 1,4-dioxane (1.00 mL, 0.3M). Flash column chromatography (silica gel: 10% Et_2O in hexanes) followed by a second column (silica gel: 100% CH_2Cl_2 to 20% Et_2O in hexanes) afforded the title compound as a yellow oil (84.7 mg, 0.20 mmol, 68% yield). IR □$_{max}$/cm^{-1} (film): 2961, 2919, 2850, 1596, 1551, 1451, 1260, 1060, 855, 756, 699; ^{1}H NMR (400 MHz, $CDCl_3$) □: 8.42 (d, *J* = 5.1 Hz, 1H), 7.94 (d, *J* = 2.2 Hz, 1H), 7.69 (dd, *J* = 8.6, 2.3 Hz, 1H), 7.49 (td, *J* = 7.5, 1.8 Hz, 1H), 7.38 (d, *J* = 1.7 Hz, 1H), 7.29 – 6.90 (m, 10H), 5.14 (s, 2H), 4.05 (q, *J* = 7.2 Hz, 1H), 1.56 (d, *J* = 7.2 Hz, 3H); ^{13}C NMR (100 MHz, $CDCl_3$) □□□ 160.2 (d, *J* = 246.5 Hz), 156.0, 155.9, 154.5, 149.7, 144.4, 133.6, 129.7 (d, *J* = 8.2 Hz), 129.3 (d, *J* = 3.9 Hz), 129.0, 128.7, 127.6, 126.7, 126.3, 124.4 (d, *J* = 3.6 Hz), 123.7, 123.5, 121.4, 119.3, 115.2 (d, *J* = 21.0 Hz), 113.8, 64.5 (d, *J* = 4.7 Hz), 44.5, 21.1; ^{19}F NMR (365 MHz, $CDCl_3$) □□□□118.69□ *m/z* LRMS (ESI + APCI) found $[M+H]^+$ 418.2, $C_{26}H_{22}ClFNO^+$ requires 418.1.

Tert-butyl (2R)-2-(((4-(1-phenylethyl)pyridin-2-yl)oxy)methyl)pyrrolidine-1-carboxylate

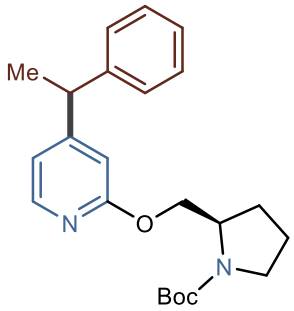

Prepared according to general procedure E using (R)-(2-((1-(tert-butoxycarbonyl)pyrrolidin-2-yl)methoxy)pyridin-4-yl)triphenylphosphonium trifluoromethanesulfonate (344.5 mg, 0.50 mmol), potassium trifluoro(1-phenylethyl)borate (212.0 mg, 1.00 mmol), 3DPAFIPN (6.5 mg, 0.01 mmol), 2,6-lutidine (175 □L, 1.5 mmol), and 1,4-dioxane (1.67 mL, 0.3M). Flash column chromatography (silica gel: 30% Et_2O in hexanes) followed by a second column (silica gel: 20% Et_2O in hexanes) afforded the title compound as a clear oil as a 1:1 mixture of diastereomers (114.5 mg, 0.30 mmol, 60% yield). IR □$_{max}$/cm^{-1} (film): 2970, 2917, 2849, 1690, 1608, 1557, 1415, 1390, 1365, 1162, 1105, 1026, 700; ^{1}H NMR (400 MHz, $CDCl_3$) δ: 7.99 (d, *J* = 5.4 Hz, 1H), 7.35 – 7.27 (m, 2H), 7.25 – 7.16 (m, 3H), 6.70 (d, *J* = 4.9 Hz, 1H), 6.59 (s, 1H), 4.49 – 4.27 (m, 1H), 4.22 – 3.98 (m, 3H), 3.38 (s, 2H), 2.13 – 1.76 (m, 4H), 1.61 (d, *J* = 7.2 Hz, 3H), 1.44 (s, 9H); ^{13}C NMR (100 MHz, $CDCl_3$) δ: 164.3, 158.1, 154.7, 146.7, 144.6, 128.7, 127.7, 126.7, 117.0, 109.6, 79.5, 66.3, 56.2, 46.5, 44.3, 28.9, 28.6, 23.1, 21.1□ *m/z* LRMS (ESI + APCI) found $[M+H]^+$ 383.3, $C_{23}H_{31}N_2O_3^+$ requires 383.2.

3-(4-Chlorophenyl)-N,N-dimethyl-3-(4-(1-phenylethyl)pyridin-2-yl)propan-1-amine

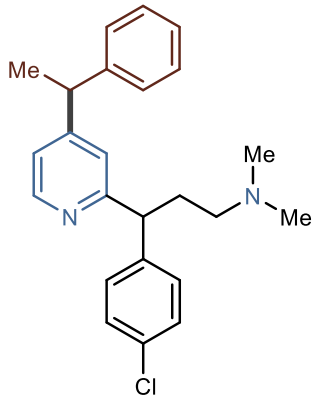

Prepared according to general procedure E using (2-(1-(4-chlorophenyl)-3-(dimethylamino)propyl)pyridin-4-yl)triphenylphosphonium trifluoromethanesulfonate (205.5 mg, 0.30 mmol), potassium trifluoro(1-phenylethyl)borate (127.2 mg, 0.60 mmol), 3DPAFIPN (3.9 mg, 0.01 mmol), 2,6-lutidine (105 □L, 0.90 mmol), 1,4-dioxane (1.00 mL, 0.3M), and trifluoromethanesulfonic acid (26.5 □L, 0.30) mmol. Flash column chromatography (silica gel: 90% EtOAc in hexanes with 1% NEt_3) afforded the title compound as a brown oil as a 1:1 mixture of diastereomers (52.8 mg, 0.14 mmol, 46% yield). IR $\square_{max}/cm^{-1}$ (film): 3061, 3027, 2923, 2851, 1596, 1456, 1284, 756, 699; ^{1}H NMR (400 MHz, $CDCl_3$) δ: 8.42 (app t, *J* = 4.0, 1H), 7.31 – 7.18 (m, 7H), 7.16 – 7.09 (m, 2H), 6.99 (s, 1H), 6.95 – 6.89 (m, 1H), 4.14 – 3.96 (m, 2H), 2.42 – 2.25 (m, 1H), 2.20 – 2.05 (m, 9H), 1.57 (d, *J* = 7.2 Hz, 3H).^{13}C NMR (100 MHz, $CDCl_3$) δ: 163.1, 155.7, 149.5, 144.7, 142.4, 132.2, 129.5, 128.7, 128.6, 127.7, 126.7, 122.4, 121.0, 57.7, 50.6, 45.5, 44.4, 33.1, 21.2□ *m/z* LRMS (ESI + APCI) found $[M+H]^+$ 379.3, $C_{24}H_{28}ClN_2^+$ requires 379.2.

2-((1-(4-Phenoxyphenoxy)propan-2-yl)oxy)-4-(1-phenylethyl)pyridine

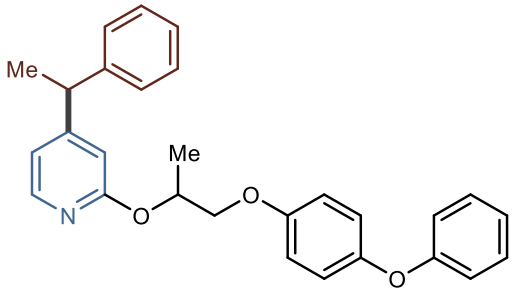

Prepared according to general procedure E using (2-((1-(4-phenoxyphenoxy)propan-2-yl)oxy)pyridin-4-yl)triphenylphosphonium trifluoromethanesulfonate (219.0 mg, 0.30 mmol), potassium trifluoro(1-phenylethyl)borate (127.2 mg,0.60 mmol), 3DPAFIPN (3.9 mg, 0.006 mmol), 2,6-lutidine (105 □L, 0.9 mmol), and 1,4-dioxane (1.00 mL, 0.3 M). Flash column chromatography (silica gel: 5% Et_2O in hexanes) afforded the title compound as a brown oil as a 1.3:1 mixture of diastereomers (79.1 mg, 0.19 mmol, 62% yield). IR $\square_{max}/cm^{-1}$ (film): 3027, 2927, 2873, 1607, 1556, 1503, 1488, 1412, 1216, 1157, 829, 699, 691; ^1H NMR (400 MHz, $CDCl_3$) δ: 7.92 (d, *J* = 5.3 Hz, 1H), 7.24 – 7.15 (m, 4H), 7.15 – 7.08 (m, 3H), 6.93 (t, *J* = 7.4 Hz, 1H), 6.88 – 6.78 (m, 6H), 6.61 (dd, *J* = 5.4, 1.5 Hz, 1H), 6.53 (s, 1H), 5.47 (q, *J* = 5.7 Hz, 1H), 4.07 (dd, *J* = 9.9, 5.2 Hz, 1H), 4.01 – 3.88 (m, 2H), 1.51 (d, *J* = 7.2 Hz, 3H), 1.37 (d, *J* = 6.4 Hz, 3H); ^{13}C NMR (100 MHz, $CDCl_3$) δ: 163.7, 158.6, 158.3, 155.3, 150.4, 146.6, 144.6, 129.7, 128.7, 127.7, 126.7, 122.5, 120.9, 117.7, 117.0, 115.9, 110.2, 71.2, 69.4, 44.3, 21.1, 17.1; *m/z* LRMS (ESI + APCI) found $[M+H]^+$ 426.3, $C_{28}H_{28}NO_3^+$ requires 426.2.

((4-(1-Phenylethyl)pyridin-2-yl)methylene)bis(4,1-phenylene) diacetate

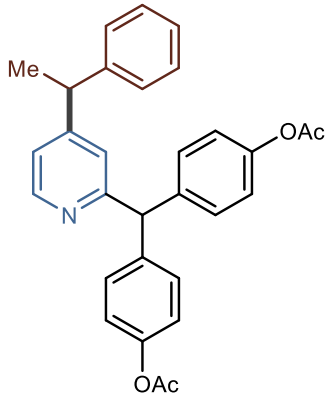

Prepared according to general procedure E using (2-(bis(4-acetoxyphenyl)methyl)pyridin-4-yl)triphenylphosphonium trifluoromethanesulfonate (231.6 mg, 0.30 mmol), potassium trifluoro(1-phenylethyl)borate (127.2 mg, 0.60 mmol), 3DPAFIPN (3.9 mg, 0.006 mmol), 2,6-lutidine (105 □L, 0.90 mmol), and 1,4-dioxane (1.00 mL, 0.3 M). Flash column chromatography (silica gel: 30% EtOAc in hexanes) afforded the title compound as a yellow oil (86.7 mg, 0.17 mmol, 56% yield). IR $\square_{max}$/cm^{-1} (film): 3107, 3030, 2933, 1753, 1595, 1503, 1368, 1195, 1164, 1018, 910, 701; ^{1}H NMR (400 MHz, $CDCl_3$) □: 8.38 (d, *J* = 5.2, 1H), 7.29 – 7.02 (m, 10H), 6.95 – 6.87 (m, 6H), 3.98 (q, *J* = 7.2 Hz, 1H), 2.19 (s, 6H), 1.50 (d, *J* = 7.2 Hz, 3H); ^{13}C NMR (100 MHz, $CDCl_3$) □□□169.6, 162.5, 156.0, 149.7, 149.4, 144.5, 140.3, 130.3, 128.7, 127.7, 126.7, 123.3, 121.5, 121.0, 58.1, 44.4, 21.3, 21.2; *m/z* LRMS (ESI + APCI) found $[M+H]^+$ 466.3 $C_{30}H_{28}NO_4^+$ requires 466.2.

2-Chloro-N-(4-chloro-3-(4-(1-phenylethyl)pyridin-2-yl)phenyl)-4-(methylsulfonyl)benzamide

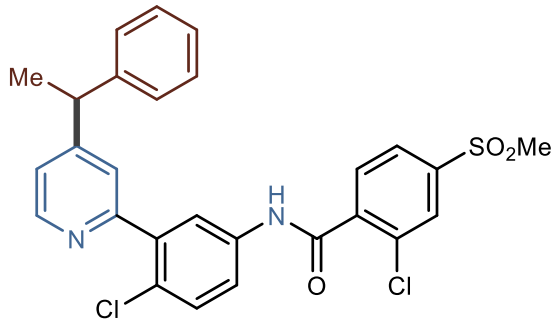

Prepared according to general procedure E using (2-(3-(2-chloro-4-(methylsulfonyl)benzamido)phenyl)pyridin-4-yl)triphenylphosphonium trifluoromethanesulfonate (166.4 mg, 0.20 mmol), potassium trifluoro(1-phenylethyl)borate (84.8 mg, 0.40 mmol), 3DPAFIPN (2.6 mg, 0.004 mmol), 2,6-lutidine (69.8 □L, 0.60 mmol), and 1,4-dioxane (666 □L, 0.3 M). Flash column chromatography (silica gel: 60% EtOAc in hexanes) afforded the title compound as a tan crystalline solid (57.1 mg, 0.11 mmol, 54% yield). m.p. 81-83 °C; IR $\square_{max}$/cm^{-1} (film): 3252, 3106, 3059, 3028, 1680, 1540, 1316, 1153, 700; ^{1}H NMR (400 MHz, $CDCl_3$) □□ 10.37 – 10.17 (m, 1H), 8.13 (dd, *J* = 5.5, 2.7 Hz, 1H), 8.08 (dd, *J* = 8.8, 2.5 Hz, 1H), 7.81 (q, *J* = 1.6 Hz, 1H), 7.67 – 7.60 (m, 2H), 7.51 – 7.41 (m, 3H), 7.34 – 7.28 (m, 2H), 7.25 – 7.14 (m, 3H), 7.02 – 6.97 (m, 1H), 4.13 (q, *J* = 7.2 Hz, 1H), 2.92 (d, *J* = 1.7 Hz, 3H), 1.64 (d, *J* = 7.2 Hz, 3H); ^{13}C NMR (100 MHz, $CDCl_3$) □□□164.1, 156.2, 155.7, 148.5, 144.0, 142.6, 140.9, 138.6, 137.4, 132.4, 131.0, 129.9, 128.9, 128.8, 127.7, 127.2, 126.9, 125.8, 124.9, 122.8, 122.3, 121.8, 44.4, 44.4, 21.0□ *m/z* LRMS (ESI + APCI) found $[M+H]^+$ 525.2, $C_{27}H_{23}Cl_2N_2O_3S^+$ requires 525.1.

3-Benzyl-5-(4-(2-(5-ethyl-4-((S)-1-phenylethyl)pyridin-2-yl)ethoxy)benzyl)thiazolidine-2,4-dione

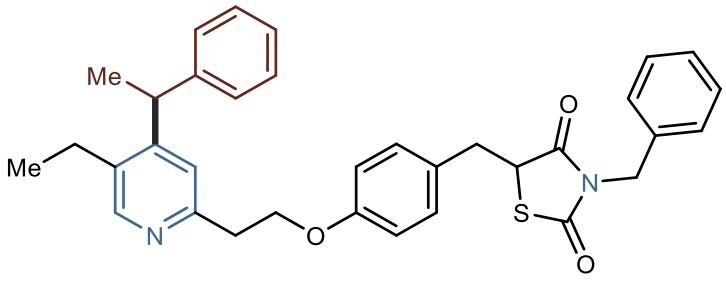

Prepared according to general procedure E using (2-(2-(4-((3-benzyl-2,4-dioxothiazolidin-5-yl)methyl)phenoxy)ethyl)-5-ethylpyridin-4-yl)triphenylphosphonium trifluoromethanesulfonate (169.5 mg, 0.20 mmol), potassium trifluoro(1-phenylethyl)borate (84.0 mg, .40 mmol), 3DPAFIPN (2.6 mg, 0.004 mmol), 2,6-lutidine (69 mL, .59 mmol), and 1,4-dioxane (659 □L, 0.3M). Flash column chromatography (silica gel: 75% Et_2O in hexanes) afforded the title compound as a yellow amorphous solid as a 1:1 mixture of diastereomers (76.2 mg, 0.14 mmol, 72% yield). IR $\square_{max}/cm^{-1}$ (film): 3033, 2968, 2931, 2874, 1749, 1680, 1512, 1381, 1329, 1244, 759, 699; ^1H NMR (400 MHz, CD_3CN) δ: 8.30 (s, 1H), 7.33 – 7.14 (m, 9H), 7.12 – 7.03 (m, 4H), 6.75 – 6.67 (m, 2H), 4.72 – 4.54 (m, 3H), 4.40 (q, *J* = 7.1 Hz, 1H), 4.35 – 4.21 (m, 2H), 3.30 (ddd, *J* = 14.3, 4.4, 2.5 Hz, 1H), 3.23 – 3.06 (m, 3H), 2.76 – 2.52 (m, 2H), 1.57 (dd, *J* = 7.2, 1.9 Hz, 3H), 1.10 (td, *J* = 7.6, 1.7 Hz, 3H). ^{13}C NMR (100 MHz, CD_3CN) δ: 174.9, 172.3, 159.1, 157.3, 153.4, 150.6, 146.2, 136.6, 135.9, 131.8, 129.5, 128.8, 128.7, 128.7, 128.6, 128.5, 127.3, 122.8, 115.3, 68.0, 52.3, 45.7, 40.5, 38.2, 37.2, 23.5, 22.2, 15.7; *m/z* LRMS (ESI + APCI) found $[M+H]^+$ 551.3, $C_{34}H_{35}N_2O_3S^+$ requires 551.2.

Potassium Trifluoroborate Scope for Heteroaromatic Alkylation

4-(1-(4-Fluorophenyl)ethyl)-2-phenylpyridine

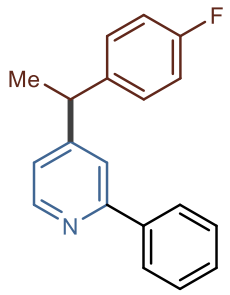

Prepared according to general procedure E using triphenyl(2-phenylpyridin-4-yl)phosphonium trifluoromethane sulfonate (169.8 mg, 0.30 mmol), potassium trifluoro(1-(4-fluorophenyl)ethyl)borate (138.0 mg, 0.60 mmol), 3DPAFIPN (3.9 mg, 0.006 mmol), 2,6-lutidine (105 □L, 0.90 mmol), and 1,4-dioxane (1.00 mL, 0.3 M). Flash column chromatography (silica gel: 10% Et_2O in hexanes) afforded the title compound as a yellow oil (65.9 mg, 0.24 mmol, 79% yield). IR $\tilde{\nu}_{max}/cm^{-1}$ (film): 2969, 2930, 1888, 1596, 1553, 1507, 1403, 1221, 1159, 832, 820, 775, 693; ^1H NMR (400 MHz, $CDCl_3$) □: 8.48 (d, *J* = 5.1 Hz, 1H), 7.89 – 7.82 (m, 2H), 7.43 (d, *J* = 1.7 Hz, 1H), 7.40 – 7.25 (m, 3H), 7.07 (dd, *J* = 8.5, 5.4 Hz, 2H), 6.98 – 6.85 (m, 3H), 4.04 (q, *J* = 7.2 Hz, 1H), 1.55 (d, *J* = 7.2 Hz, 3H); ^{13}C NMR (100 MHz, $CDCl_3$) 161.6 (d, *J* = 245.1 Hz), 157.8, 155.7, 149.9, 140.2 (d, *J* = 3.2 Hz), 139.6, 129.2 (d, *J* = 7.9 Hz), 129.0, 128.8, 127.1, 121.4, 119.9, 115.5 (d, *J* = 21.3 Hz), 43.8, 21.4□ ^{19}F NMR (365 MHz, $CDCl_3$) □□□□116□24□ *m/z* LRMS (ESI + APCI) found $[M+H]^+$ 278.2, $C_{19}H_{17}FN^+$ requires 278.1.

4-(1-(4-Methoxyphenyl)ethyl)-2-phenylpyridine

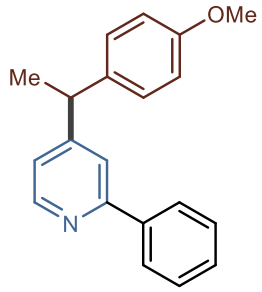

Prepared according to general procedure E using triphenyl(2-phenylpyridin-4-yl)phosphonium trifluoromethane sulfonate (226.4 mg, 0.30 mmol), potassium trifluoro(1-(4-methoxyphenyl)ethyl)borate (1.2:1 regiomeric mixture of 2c:2c') (145.2 mg, 0.60 mmol), 3DPAFIPN (3.9 mg, 0.006 mmol), 2,6-lutidine (105 □L, 0.90 mmol), and 1,4-dioxane (1.00 mL, 0.3 M). Flash column chromatography (silica gel: 100% CH_2Cl_2 to 15% Et_2O in hexanes) afforded the title compound as a clear oil (51.1 mg, 0.15 mmol, 51% yield). IR $\tilde{\nu}_{max}/cm^{-1}$ (film): 3030, 3002, 2966, 2931, 2834, 1595, 1580, 1510, 1445, 1402, 1244, 1178, 1033, 829, 776, 694; ^{1}H NMR (400 MHz, $CDCl_3$) □: 8.59 (dd, *J* = 5.2, 0.8 Hz, 1H), 8.07 – 7.87 (m, 2H), 7.60 – 7.54 (m, 1H), 7.51 – 7.37 (m, 3H), 7.20 – 7.14 (m, 2H), 7.08 (dd, *J* = 5.1, 1.7 Hz, 1H), 6.87 (d, *J* = 8.7 Hz, 2H), 4.15 (q, *J* = 7.2 Hz, 1H), 3.79 (s, 3H), 1.67 (d, *J* = 7.2 Hz, 3H).^{13}C NMR (100 MHz, $CDCl_3$) □□□158.4, 157.7, 156.4, 149.8, 139.7, 136.7, 128.9, 128.8, 128.7, 127.1, 121.5, 120.0, 114.1, 55.4, 43.7, 21.4□ *m/z* LRMS (ESI + APCI) found $[M+H]^+$ 290.2, $C_{20}H_{20}NO^+$ requires 290.2.

4-(1-(3-Chlorophenyl)ethyl)-2-phenylpyridine

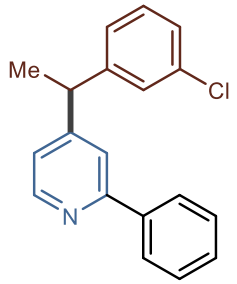

Prepared according to general procedure E using triphenyl(2-phenylpyridin-4-yl)phosphonium trifluoromethane sulfonate (169.8 mg, 0.30 mmol), potassium (1-(3-chlorophenyl)ethyl)trifluoroborate (148.2 mg, 0.60 mmol), 3DPAFIPN (3.9 mg, 0.006 mmol), 2,6-lutidine (105 □L, 0.90 mmol), and 1,4-dioxane (1.00 mL, 0.3 M). Flash column chromatography (silica gel: 100% CH_2Cl_2 to 10% Et_2O in hexanes) afforded the title compound as a yellow oil (87.9 mg, 0.17 mmol, 56% yield). IR $\square_{max}$/cm^{-1} (film): 3056, 2970, 2932, 2875, 1593, 1579, 1553, 1473, 1403, 1082, 883, 866, 775, 694; ^{1}H NMR (400 MHz, $CDCl_3$) □: 8.63 (d, *J* = 5.1 Hz, 1H), 8.05 – 7.93 (m, 2H), 7.58 (d, *J* = 1.7 Hz, 1H), 7.53 – 7.41 (m, 3H), 7.32 – 7.22 (m, 3H), 7.19 – 7.11 (m, 1H), 7.09 (dd, *J* = 5.1, 1.7 Hz, 1H), 4.18 (q, *J* = 7.2 Hz, 1H), 1.70 (d, *J* = 7.2 Hz, 3H); ^{13}C NMR (100 MHz, $CDCl_3$) □□□ 157.9, 155.1, 150.0, 146.6, 139.5, 134.6, 130.0, 129.1, 128.8, 127.9, 127.1, 127.0, 126.0, 121.4, 119.9, 44.3, 21.1□ *m/z* LRMS (ESI + APCI) found $[M+H]^+$ 294.2, $C_{19}H_{17}ClN^+$ requires 294.1.

4-(1-(Naphthalen-2-yl)ethyl)-2-phenylpyridine

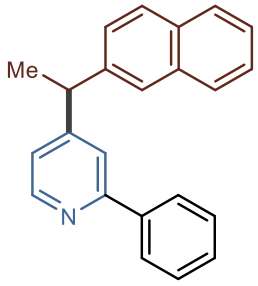

Prepared according to general procedure E using triphenyl(2-phenylpyridin-4-yl)phosphonium trifluoromethane sulfonate (169.8 mg, 0.30 mmol), potassium trifluoro(1-(naphthalen-2-yl)ethyl)borate (157.2 mg, 0.60 mmol), 3DPAFIPN (3.9 mg, 0.006 mmol), 2,6-lutidine (105 mL, 0.90 mmol), and 1,4-dioxane (1.00 mL, 0.3 M). Flash column chromatography (silica gel: 10% Et_2O in hexanes) afforded the title compound as a yellow oil (70.1 mg, 0.23 mmol, 76% yield). IR ν_{max}/cm^{-1} (film): 3052, 2966, 2917, 2849, 1595, 1580, 1473, 1445, 1403, 907, 891, 818, 751, 693; ^{1}H NMR (400 MHz, $CDCl_3$) δ: 8.63 (d, *J* = 5.1 Hz, 1H), 7.99 (d, *J* = 7.0 Hz, 2H), 7.88 – 7.79 (m, 2H), 7.75 (d, *J* = 1.9 Hz, 1H), 7.65 (s, 1H), 7.57 – 7.39 (m, 6H), 7.33 (dd, *J* = 8.6, 1.8 Hz, 1H), 7.14 (dd, *J* = 5.1, 1.6 Hz, 1H), 4.37 (q, *J* = 7.2 Hz, 1H), 1.81 (d, *J* = 7.2 Hz, 3H); ^{13}C NMR (100 MHz, $CDCl_3$) δ: 157.7, 155.7, 149.8, 141.9, 139.6, 133.5, 132.3, 128.9, 128.7, 128.4, 127.8, 127.7, 127.0, 126.4, 126.3, 125.8, 125.8, 121.6, 120.1, 44.6, 21.1; *m/z* LRMS (ESI + APCI) found $[M+H]^+$ 310.2, $C_{23}H_{20}N^+$ requires 310.2.

4-Benzyl-2-phenylpyridine

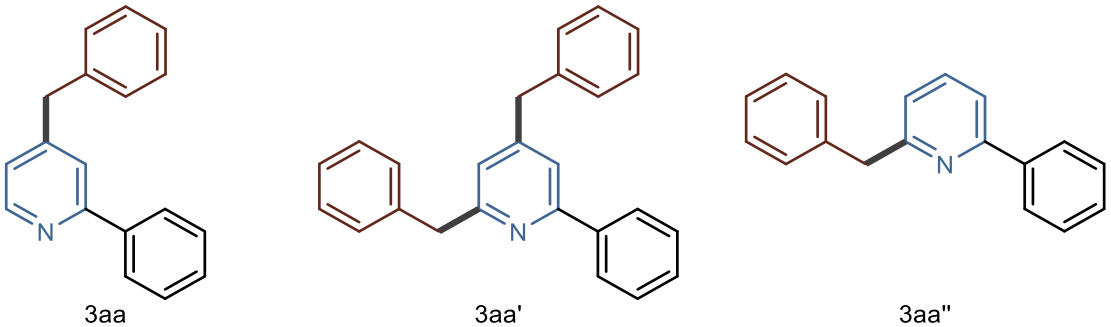

3aa		3aa'		3aa''
5.7	**:**	**1**	**:**	**<1**

Prepared according to general procedure E using triphenyl(2-phenylpyridin-4-yl)phosphonium trifluoromethane sulfonate (226.4 mg, 0.40 mmol), potassium benzyltrifluoroborate (158.4 mg, 0.80 mmol), 3DPAFIPN (5.2 mg, 0.01 mmol), 2,6-lutidine (140 □L, 1.20 mmol), and 1,4-dioxane (1.33 mL, 0.3 M). The product as well as the bis addition product (3aa') and regioisomer (3aa'') were formed in the crude reaction mixture in a ratio of 5.7:1:<1(3aa:3aa':3aa''). Flash column chromatography (silica gel: 5% Et_2O in hexanes) afforded the title compound (**3aa**) as a yellow oil as a single regioisomer (49.6 mg, 0.20 mmol, 51% yield).; IR $\square_{max}/cm^{-1}$ (film): 3060, 3028, 2922, 2852, 1595, 1555, 1474, 1445, 1402, 774, 762, 731, 693; ^1H NMR (400 MHz, $CDCl_3$) □: 8.48 (d, *J* = 5.0 Hz, 1H), 7.86 (dd, *J* = 7.2, 2.8 Hz, 2H), 7.45 (s, 1H), 7.40 – 7.08 (m, 8H), 6.94 (d, *J* = 5.1 Hz, 1H), 3.92 (s, 2H); ^{13}C NMR (100 MHz, $CDCl_3$) □□ 157.8, 150.8, 149.8, 139.6, 139.1, 129.1, 129.0, 128.9, 128.8, 127.1, 126.8, 122.8, 121.2, 41.6.□ *m/z* LRMS (ESI + APCI) found $[M+H]^+$ 246.2, $C_{18}H_{16}N^+$ requires 246.1.

Tert-butyl 2-(2-phenyl-1l4-pyridin-4-yl)pyrrolidine-1-carboxylate

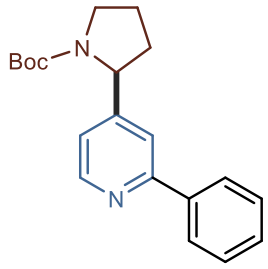

Prepared according to general procedure E using triphenyl(2-phenylpyridin-4-yl)phosphonium trifluoromethane sulfonate (141.5 mg, 0.25 mmol), potassium (1-(tert-butoxycarbonyl)pyrrolidin-2-yl)trifluoroborate (138.5 mg, 0.50 mmol), 3DPAFIPN (3.2 mg, 0.005 mmol), 2,6-lutidine (87.2 □L, 0.75 mmol), and 1,4-dioxane (833 □L, 0.3 M). Flash column chromatography (silica gel: 40% Et_2O in hexanes) afforded the title compound as a yellow oil (59.7 mg, 0.16 mmol, 64% yield). The product gives two sets of NMR signals, owing to the presence of rotamers around the tertiary amide.[19] IR □$_{max}$/cm^{-1} (film): 3059, 2974, 2930, 2876, 1690, 1598, 1446, 1388 1365, 1156, 1115, 775, 733, 694; ^{1}H NMR (400 MHz, $CDCl_3$) □: 8.61 (d, *J* = 5.1 Hz, 1H), 8.01 – 7.91 (m, 2H), 7.66 – 7.36 (m, 4H), 7.05 (dd, *J* = 5.1, 1.6 Hz, 1H), 5.09 – 4.73 (m, 1H), 3.74 – 3.45 (m, 2H), 2.48 – 2.28 (m, 1H), 1.98 – 1.79 (m, 3H), 1.48 (s, 3H), 1.21 (s, 6H); ^{13}C NMR (100 MHz, $CDCl_3$) □□□157.7, 155.1, 154.5, 149.8, 139.5, 129.1, 128.9, 127.0, 119.4, 117.5, 79.9, 60.9, 47.3, 35.7, 28.3, 23.4; *m/z* LRMS (ESI + APCI) found $[M+H]^+$ 325.3, $C_{20}H_{25}N_2O_2^+$ requires 325.2.

A2.11. Pyridine Alkylation Using Carboxylic Acid as Alkyl Radical Precursor

2-Phenyl-4-(1-phenylethyl)pyridine

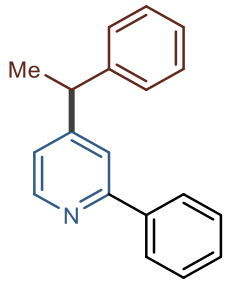

An oven dried 8 mL vial equipped with a magnetic stir bar was charged with triphenyl(2-phenylpyridin-4-yl)phosphonium trifluoromethane sulfonate (169.8 mg, 0.30 mmol), $Ir(dF(CF_3)ppy)_2(dtbbpy)PF_6$ (6.7 mg, 0.006 mmol), and potassium phosphate dibasic (157.0 mg, 0.90 mmol). The reaction vessel was pumped into a glovebox and then 2-phenylpropanoic acid (124.0 □L, 0.90 mmol) and 1,2-dichloroethane (960.0 mL) were added via a syringe. The vial was sealed and removed from the glovebox followed by irradiation with a 455 nm kessil lamp (5 cm away, with stream of air blowing over vials to keep reaction at 25 °C) for 16 hours. Flash column chromatography (silica gel: 7% Et_2O in hexanes) afforded the title compound as a pale yellow oil (16.4 mg, 0.06 mmol, 21% yield).; Spectra match that obtained from **3a** obtained from coupling with BF_3K salt.

A2.12. Pyridine Amination

N-Methyl-N,2-diphenylpyridin-4-amine

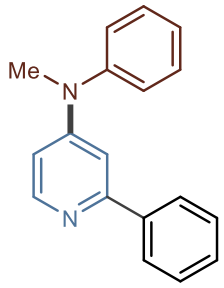

Prepared according to procedure reported by Zhou et al.[20] An oven dried 8 mL vial equipped with a magnetic stir bar was charged with triphenyl(2-phenylpyridin-4-yl)phosphonium trifluoromethane sulfonate (169.8 mg, 0.30 mmol), 3DPAFIPN (3.9 mg, 0.006 mmol), and 1,4-Diazabicyclo[2.2.2]octane (33.6 mg, 0.30 mmol). The reaction vessel was pumped into a glovebox and then *N*-methylaniline (49 □L, 0.45 mmol) and MeCN (3.00 mL) were added via a syringe. The vial was sealed and removed from the glovebox followed by irradiation with a 455 nm kessil lamp (5 cm away, with stream of air blowing over vials to keep reaction at 25 °C) for 16 hours. The reaction was quenched with water and the aqueous layer was extracted with CH_2Cl_2 (3x). The combined organic extracts were dried ($MgSO_4$), filtered, and concentrated *in vacuo*. Flash column chromatography (neutralized silica gel: 25% EtOAc in hexanes) afforded the title compound as a yellow oil (48.7 mg, 0.19 mmol, 62% yield). IR $\square_{max}/cm^{-1}$ (film): 3056, 3033, 2922, 2852, 2816, 1604, 1586, 1575, 1493, 1480, 1360, 1001, 772, 693; ^1H NMR (400 MHz, $CDCl_3$) □: 8.22 (d, *J* = 5.9 Hz, 1H), 7.83 – 7.74 (m, 2H), 7.41 – 7.08 (m, 8H), 6.89 (d, *J* = 2.4 Hz, 1H), 6.43 (dd, *J* = 5.9, 2.5 Hz, 1H), 3.26 (s, 3H); ^{13}C NMR (100 MHz, $CDCl_3$) □□□ 158.0, 154.6, 149.9, 146.4, 140.4, 130.0, 128.6, 128.6, 127.0, 126.7, 126.4, 107.3, 105.4, 39.6; *m/z* LRMS (ESI + APCI) found $[M+H]^+$ 261.2, $C_{18}H_{17}N_2^+$ requires 261.1.

N-Methyl-2-phenylpyridin-4-amine

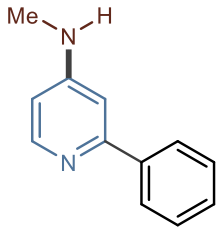

Prepared according to procedure reported by Zhou et al.[20] An oven dried 8 mL vial equipped with a magnetic stir bar was charged with triphenyl(2-phenylpyridin-4-yl)phosphonium trifluoromethanesulfonate (169.8 mg, 0.30 mmol), N,O-dimethylhydroxylammonium chloride (75.6 mg, 0.75 mmol), 3DPAFIPN (3.9 mg, 0.006 mmol), and K_3PO_4 (190.8 mg, 0.90 mmol). The reaction vessel was pumped into a glovebox and MeCN (3.00 mL) was added via a syringe. The vial was sealed and removed from the glovebox followed by irradiation with a 455 nm kessil lamp (5 cm away, with stream of air blowing over vials to keep reaction at 25 °C) for 16 hours. The reaction was quenched with water and the aqueous layer was extracted with CH_2Cl_2 (3x). The combined organic extracts were dried ($MgSO_4$), filtered, and concentrated *in vacuo*. Flash column chromatography (neutralized silica gel: 55% EtOAc in hexanes) afforded the title compound as a yellow solid (35.8 mg, 0.20 mmol, 65% yield). m.p. 89-92 □C; IR □$_{max}$/cm^{-1} (film): 3231, 3136, 3085, 3032, 2959, 1605, 1598, 1535, 1476, 1355, 1238, 983, 858, 772, 690; ^{1}H NMR (400 MHz, $CDCl_3$) □: 8.28 (d, *J* = 5.7 Hz, 1H), 7.96 – 7.87 (m, 2H), 7.53 – 7.33 (m, 3H), 6.81 (d, *J* = 2.3 Hz, 1H), 6.37 (dd, *J* = 5.7, 2.3 Hz, 1H), 4.55 (d, *J* = 5.8 Hz, 1H), 2.84 (d, *J* = 4.9 Hz, 3H); ^{13}C NMR (100 MHz, $CDCl_3$) □□□158.0, 155.2, 149.8, 140.3, 128.6, 128.6, 127.0, 106.1, 104.2, 29.5; *m/z* LRMS (ESI + APCI) found $[M+H]^+$ 185.2, $C_{12}H_{13}N_2^+$ requires 185.1.

A2.12. References

1. D. D. Perrin, W. L. F. Amerego, Purification of Laboratory Chemicals (Pergamon, ed. 3, 1988).

2. E. Speckmeier, T. Fischer, K. J. Zeitler, *Am. Chem. Soc.* 2018, **140**, 15353–15365.

3. F. Strieth-Kalthoff, M. J. James, M. Teders, L. Pitzer, F. Glorius, *Chem. Soc. Rev.* 2018, **47**, 7190–7202.

4. N. A. Romero, D. A. Nicewicz, *Chemical Reviews* 2016, **116**, 10075–10166.

5. C. K. Prier, D. A. Rankic, D. W. C. MacMillan, *Chem. Rev.* 2013, **42**.

6. J. L. Koniarczyk, J. W. Greenwood, J. V. Alegre-Requena, R. S. Paton, A. McNally, *Angew. Chem. Int. Ed.* 2019, **58**, 14882–14886.

7. X. Zhang, A. McNally, *ACS Catal.* 2019, **9**, 4862–4866.

8. M. C. Hilton, R. D. Dolewski, A. McNally, *J. Am. Chem. Soc.* 2016, **138**, 13806–13809.

9. R. G. Anderson, B. M. Jett, A. McNally, *Angew. Chem. Int. Ed.* 2018, **57**, 12514–12518.

10. X. Zhang, A. McNally, *Angew. Chem. Int. Ed.* 2017, **56**, 9833–9836.

11. C. Patel, M. Mohnike, M. C. Hilton, A. McNally, *Org. Lett.* 2018, **20**, 2607–2610.

12. J. L. Koniarczyk, D. Hesk, A. Overgard, I. W. Davies, A. McNally, *J. Am. Chem. Soc.* 2018, **140**, 1990–1993.

13. D. Noh, H. Chea, J. Ju, J. Yun, *Angew. Chem. Int. Ed.* 2009, **48**, 6062–6064.

14. K. Endo, M. Hirokami, K. Takeuchi, T. Shibata, *Synlett* 2008, **20**, 3231–3233.

15. A. J. J. Lennox, G. C. Lloyd-Jones, *Angew. Chem. Int. Ed.* 2012, **51**, 9385–9388.

16. J. C. Tellis, D. N. Primer, G. A. Molander, *Science* 2014, **345**, 433–436.

17. D. N. Primer, I. Karakaya, J. C. Tellis, G. A. Molander, *J. Am. Chem. Soc.* 2015, **137**, 2195–2198.

18. V. Bagutski, A. Ros, V. K. Aggarwal, *Tetrahedron* 2009, **65**, 9956–9960.

19. Z. Zuo, D. W. C. MacMillan, *J. Am. Chem. Soc.* 2014, **136**, 5257–5260.

20. C. Zhou, T. Lei, X.-Z. Wei, C. Ye, Z. Liu, B. Chen, C.-H. Tung, L.-Z. Wu, *J. Am. Chem. Soc.* 2020, **142**, 16805–16813.

A2.13. Spectra

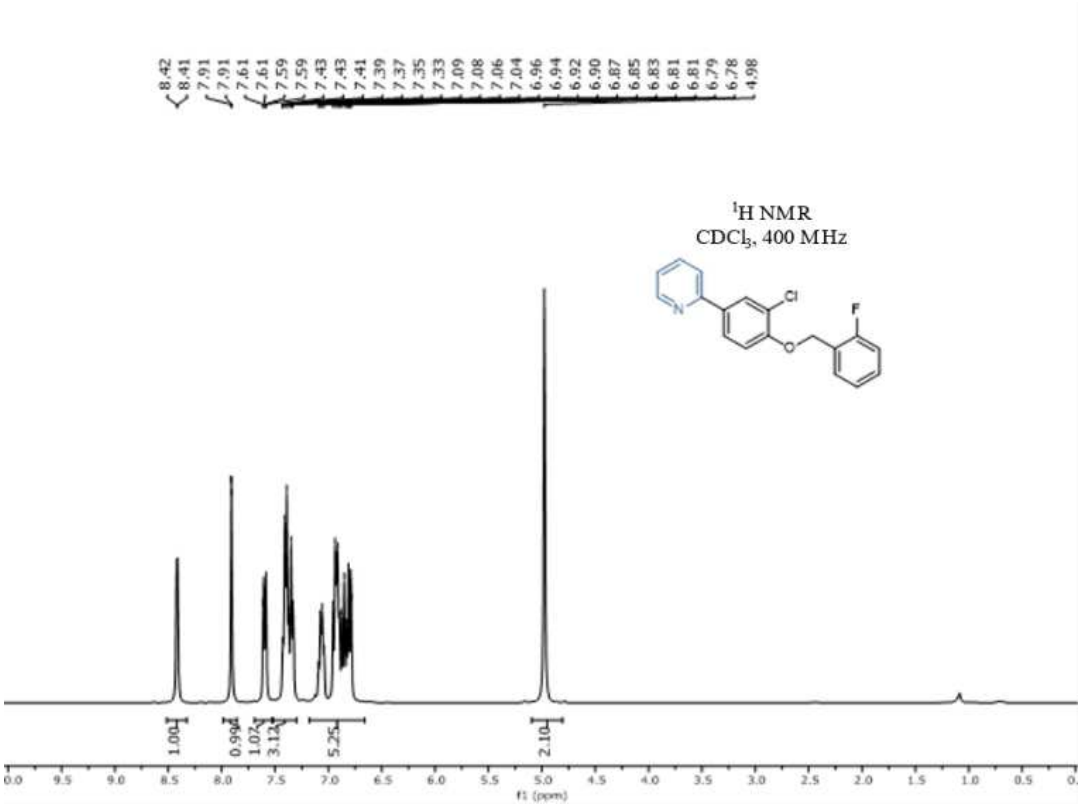

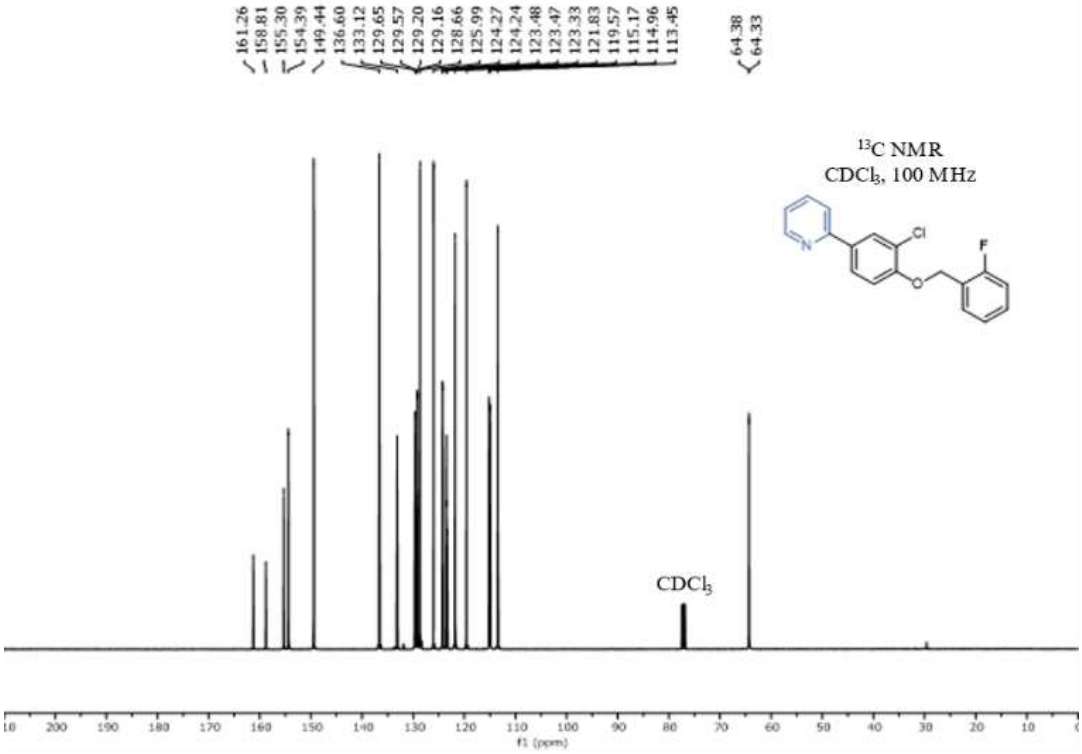

^{19}F NMR
$CDCl_3$, 365 MHz

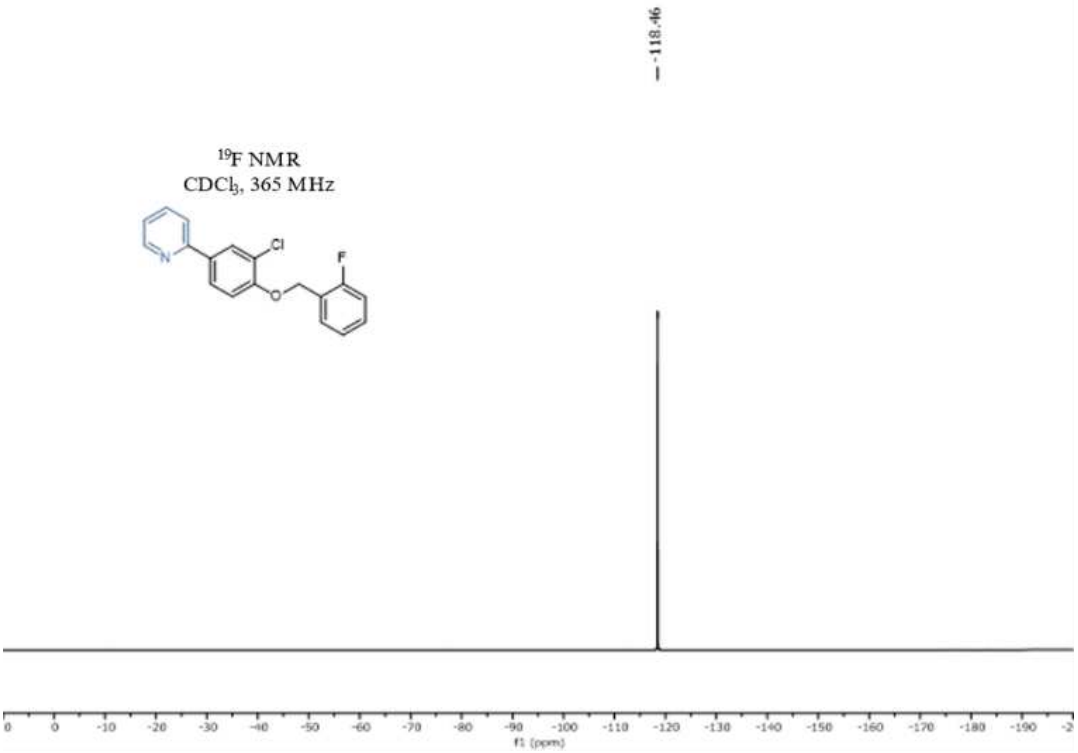

^{1}H NMR
$CDCl_3$, 400 MHz

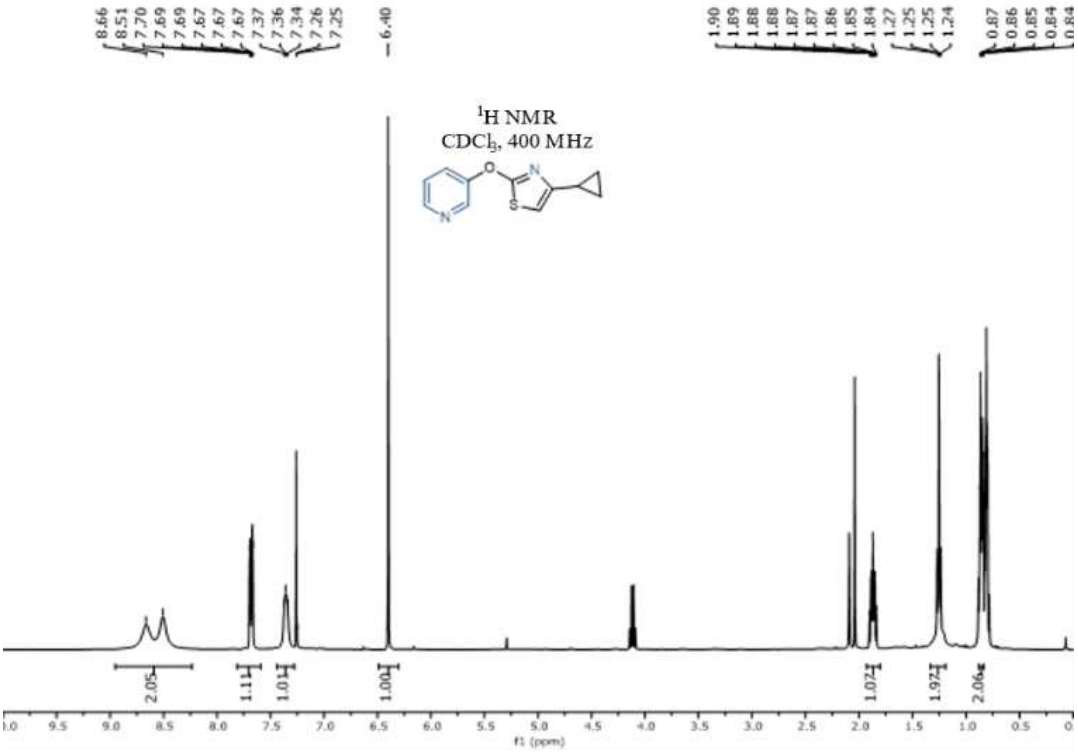

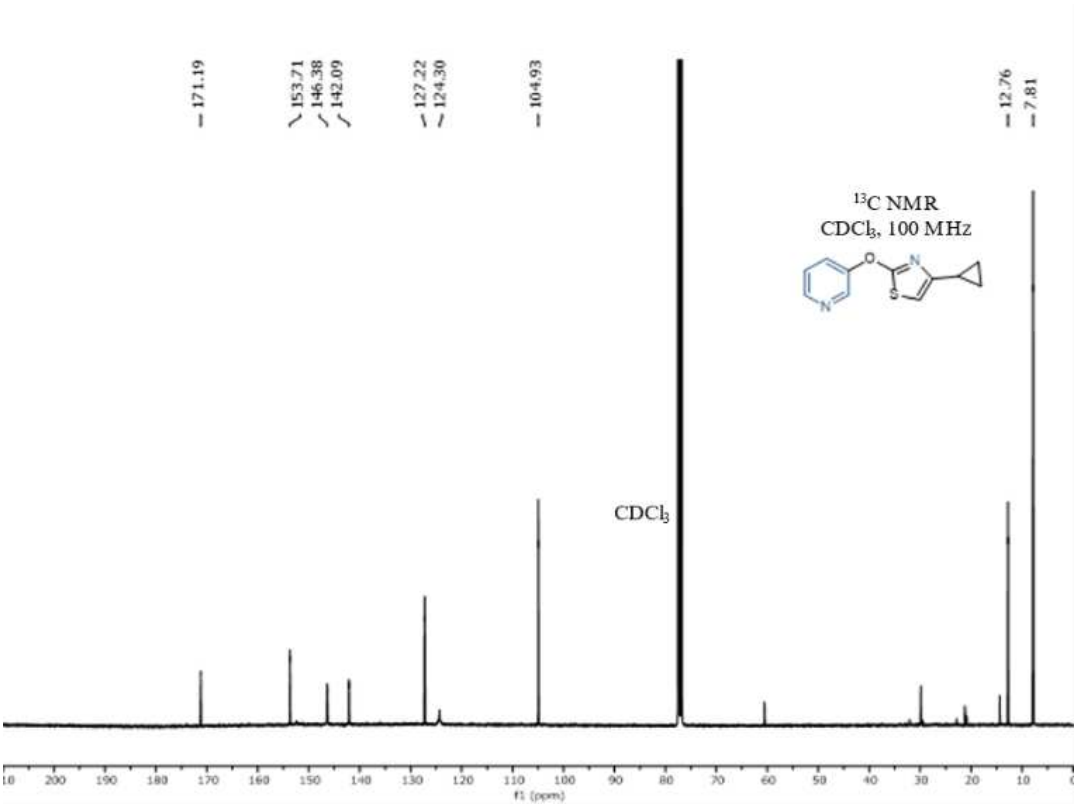
171.19
153.71
146.38
142.09
127.22
124.30
104.93
12.76
7.81
^{13}C NMR
$CDCl_3$, 100 MHz
$CDCl_3$
f1 (ppm)

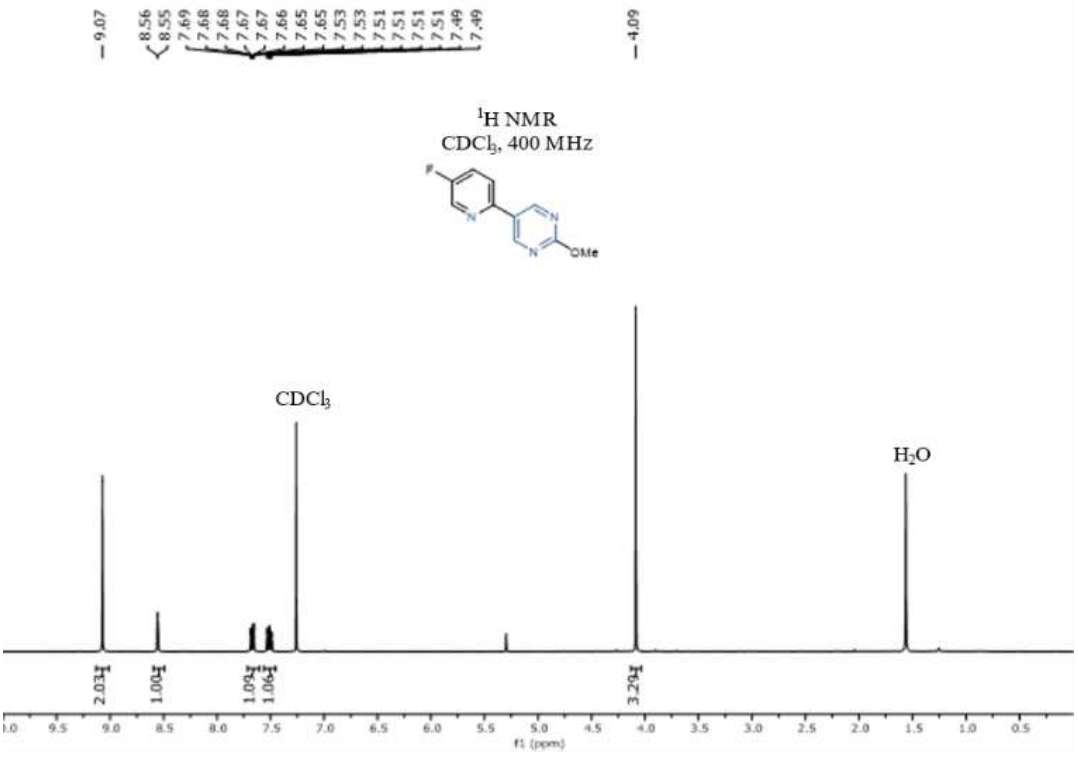
9.07
8.56
8.55
7.69
7.68
7.68
7.67
7.67
7.66
7.65
7.65
7.53
7.53
7.51
7.51
7.51
7.51
7.49
7.49
4.09
^{1}H NMR
$CDCl_3$, 400 MHz
OMe
$CDCl_3$
H_2O
2.03
1.00
1.09
1.06
3.29
f1 (ppm)

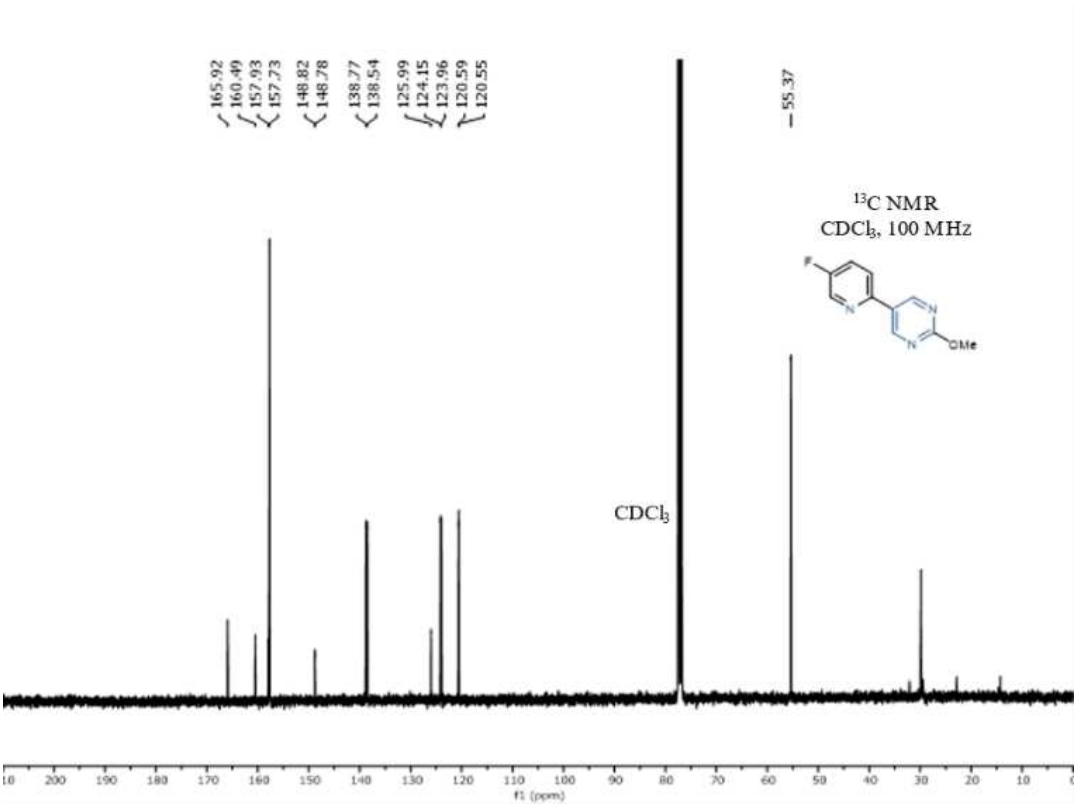
165.92
160.49
157.93
157.73
148.82
148.78
138.77
138.54
125.99
124.15
123.96
120.59
120.55
55.37
^{13}C NMR
$CDCl_3$, 100 MHz
$CDCl_3$
f1 (ppm)

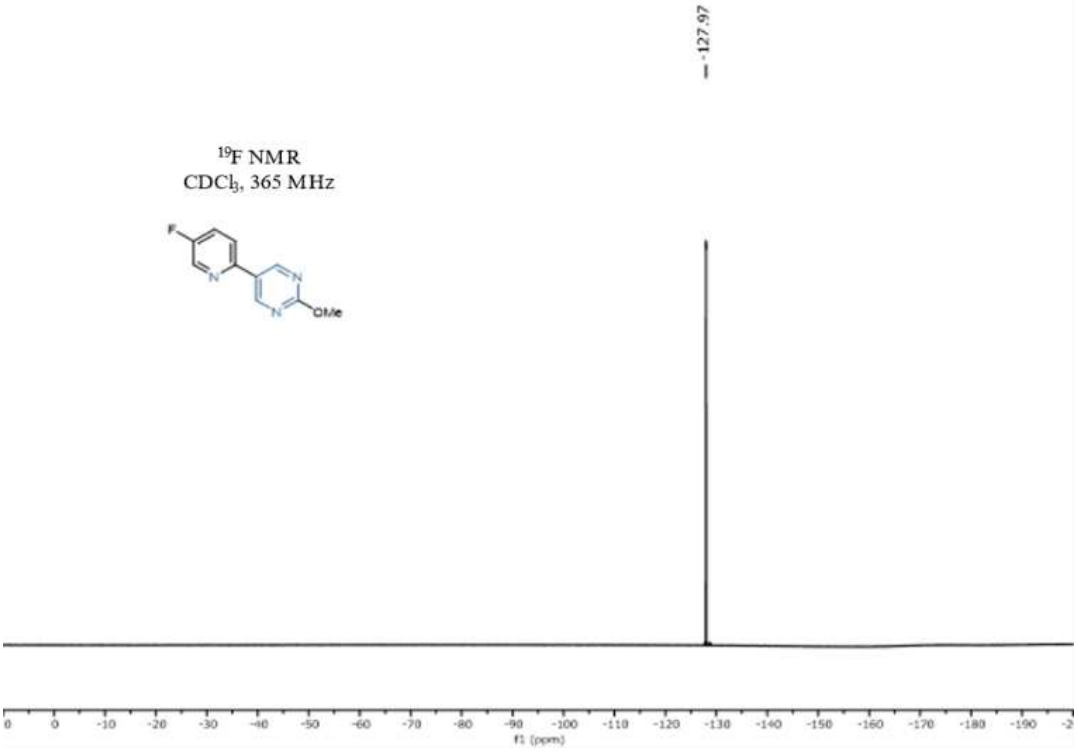
-127.97
^{19}F NMR
$CDCl_3$, 365 MHz
f1 (ppm)

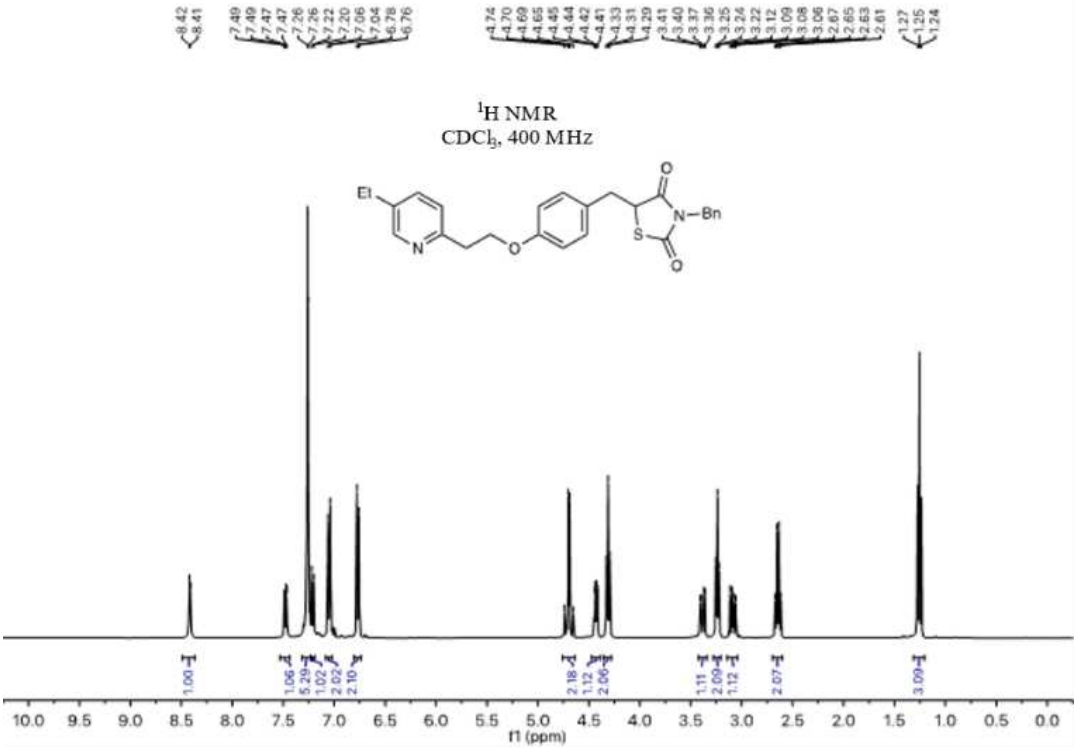
^{1}H NMR
$CDCl_3$, 400 MHz
Et
N
O
S
N–Bn
f1 (ppm)

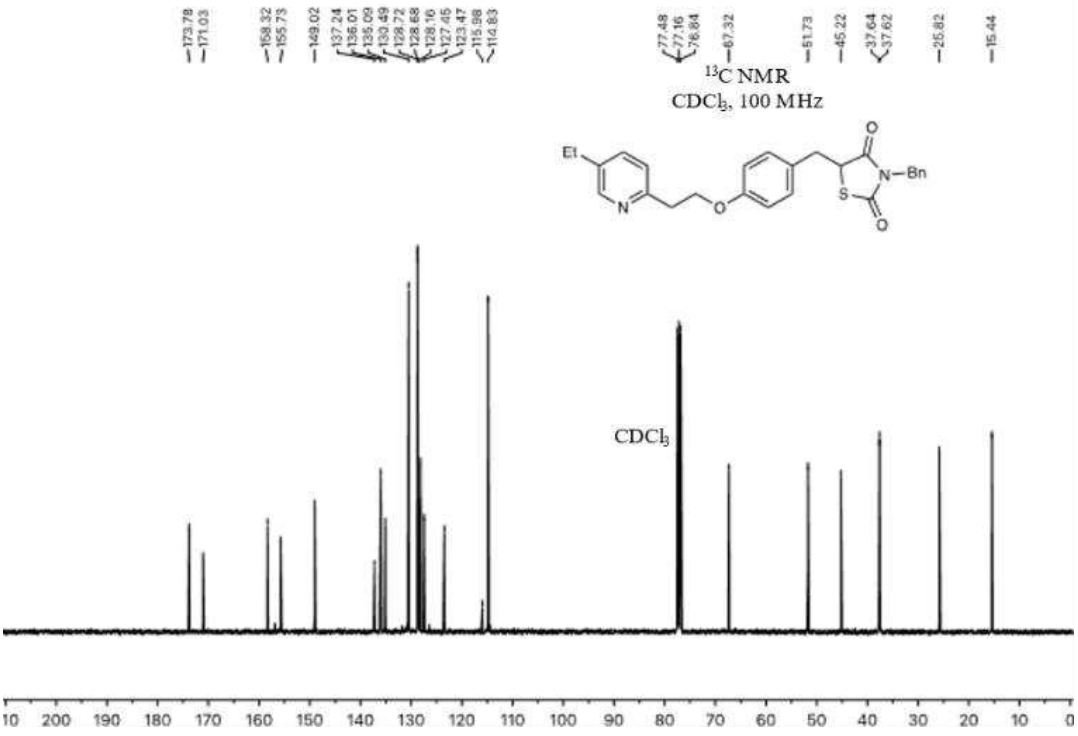
^{13}C NMR
$CDCl_3$, 100 MHz
Et
N
O
S
N–Bn
$CDCl_3$

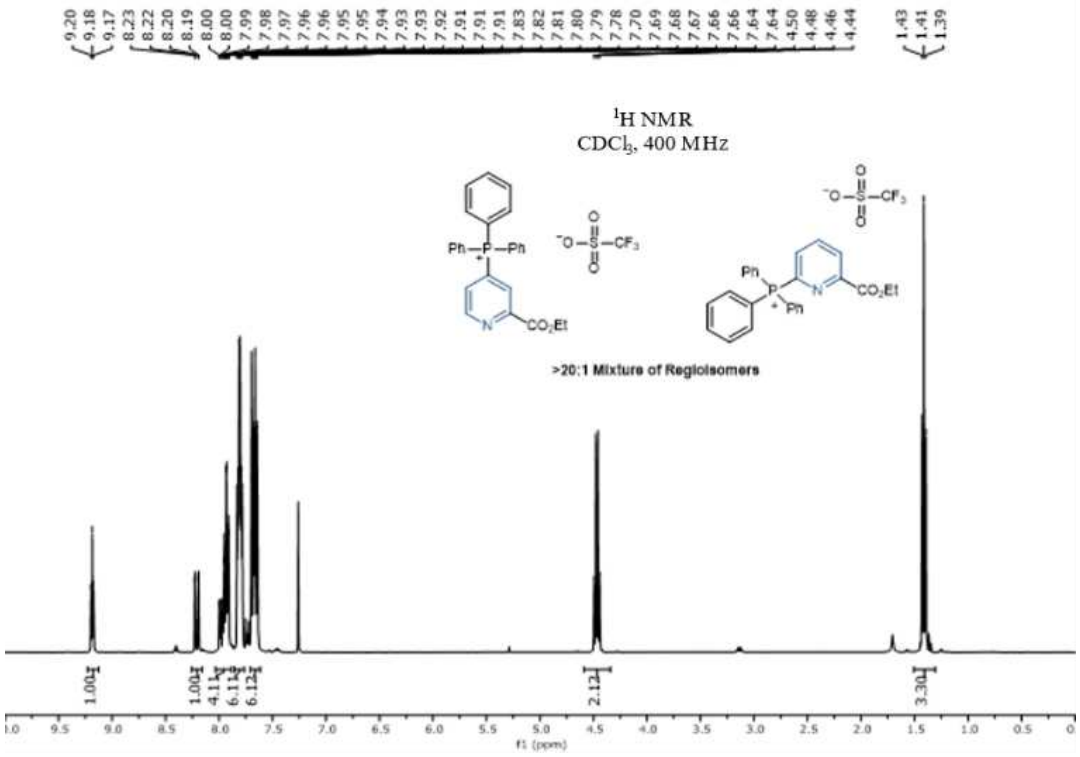
9.20
9.18
9.17
8.23
8.22
8.20
8.19
8.00
8.00
7.99
7.98
7.97
7.96
7.96
7.95
7.95
7.94
7.93
7.93
7.92
7.91
7.91
7.91
7.83
7.82
7.81
7.80
7.79
7.78
7.70
7.69
7.68
7.67
7.66
7.66
7.64
7.64
4.50
4.48
4.46
4.44
1.43
1.41
1.39
1H NMR
CDCl3, 400 MHz
>20:1 Mixture of Regioisomers
1.00
1.00
4.11
6.11
6.12
2.12
3.30
f1 (ppm)

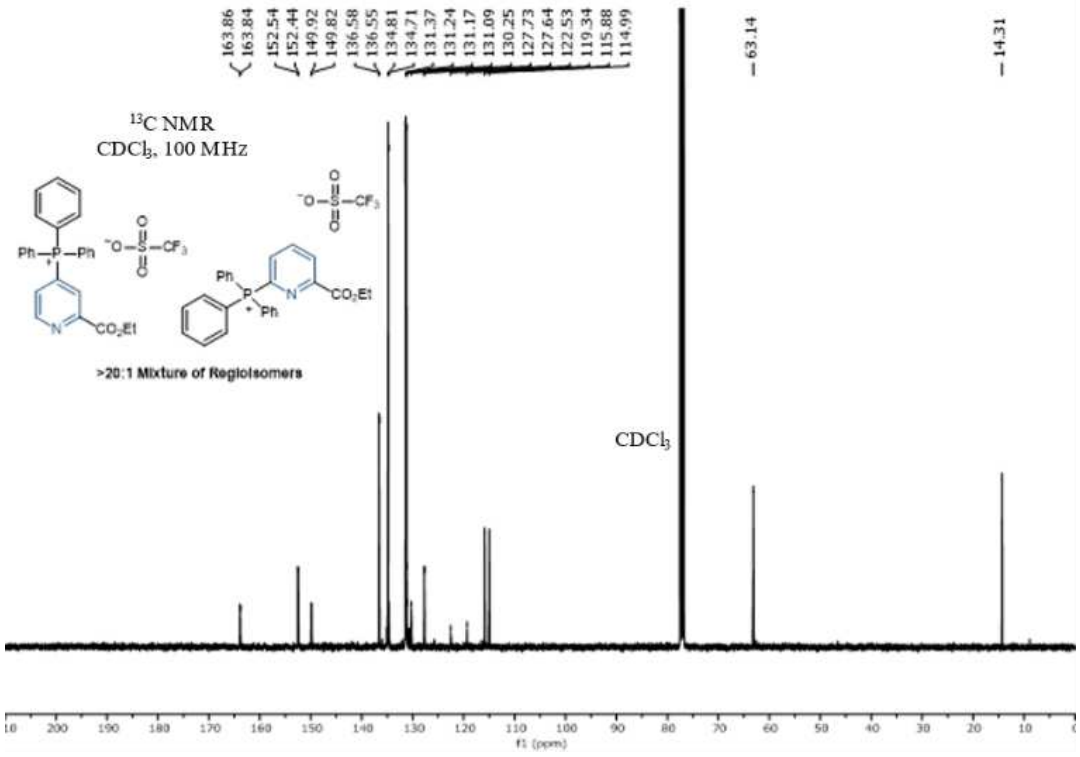
163.86
163.84
152.54
152.44
149.92
149.82
136.58
136.55
134.81
134.71
131.37
131.24
131.17
131.09
130.25
127.73
127.64
122.53
119.34
115.88
114.99
63.14
14.31
13C NMR
CDCl3, 100 MHz
>20:1 Mixture of Regioisomers
CDCl3
f1 (ppm)

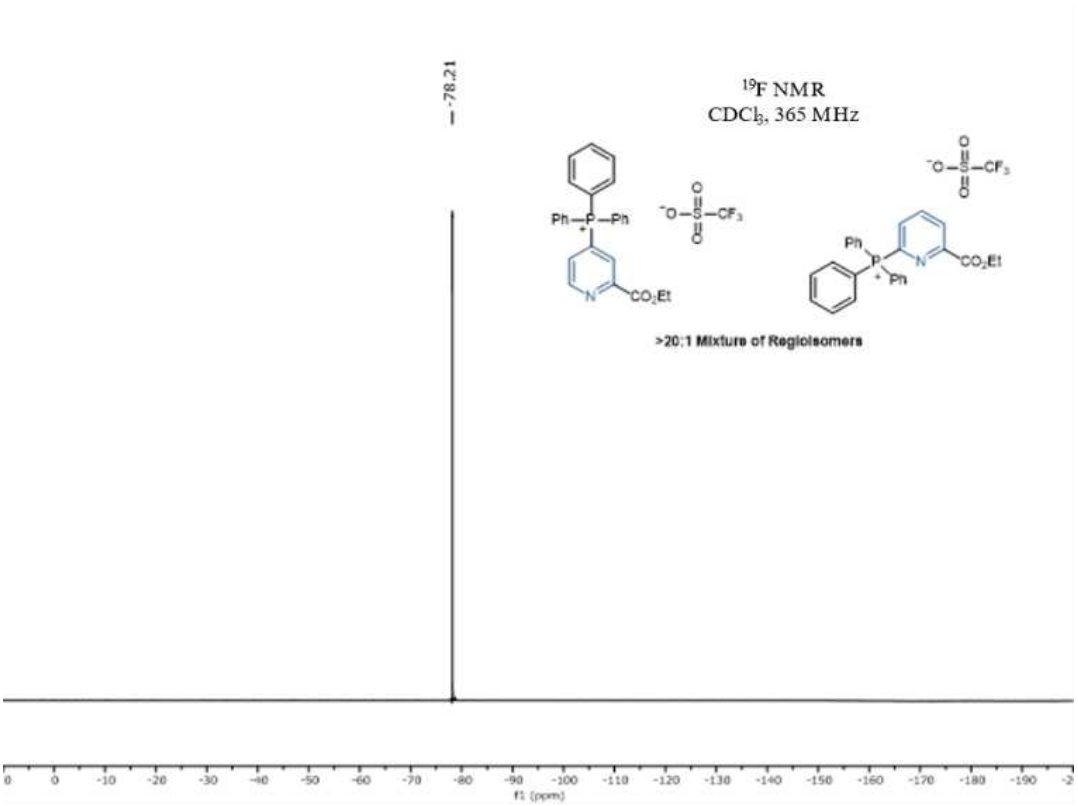
-78.21
^{19}F NMR
$CDCl_3$, 365 MHz
>20:1 Mixture of Regioisomers
f1 (ppm)

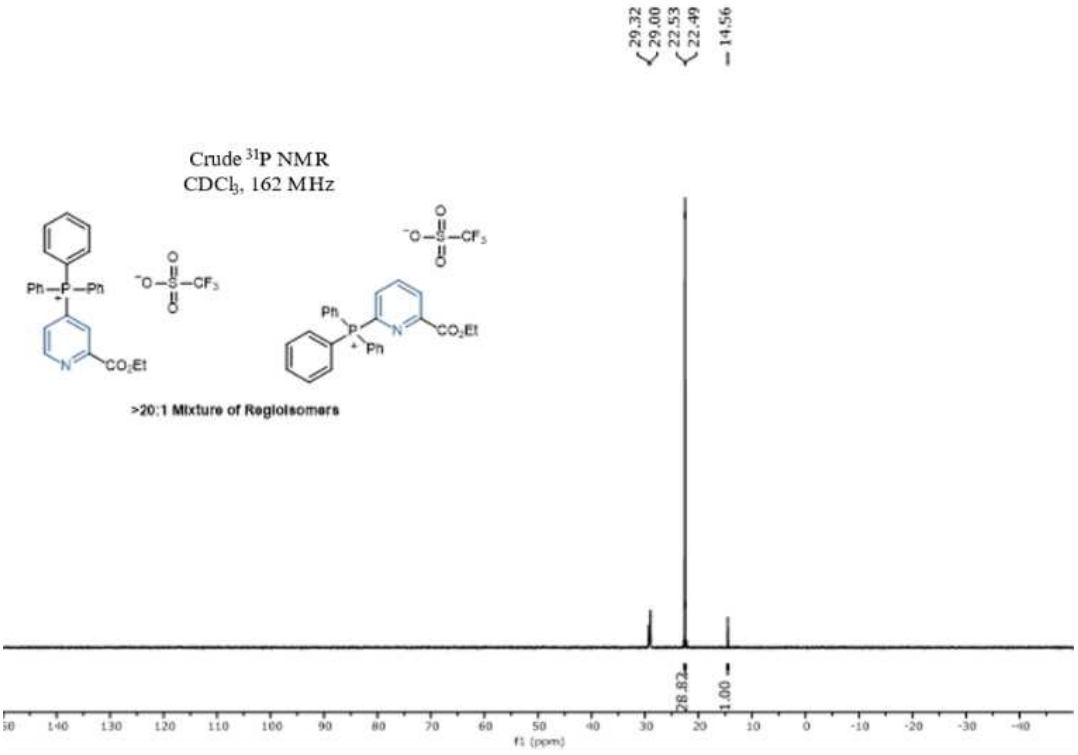
29.32
29.00
22.53
22.49
14.56
Crude ^{31}P NMR
$CDCl_3$, 162 MHz
>20:1 Mixture of Regioisomers
26.82
1.00
f1 (ppm)

^{31}P NMR
$CDCl_3$, 162 MHz

>20:1 Mixture of Regioisomers

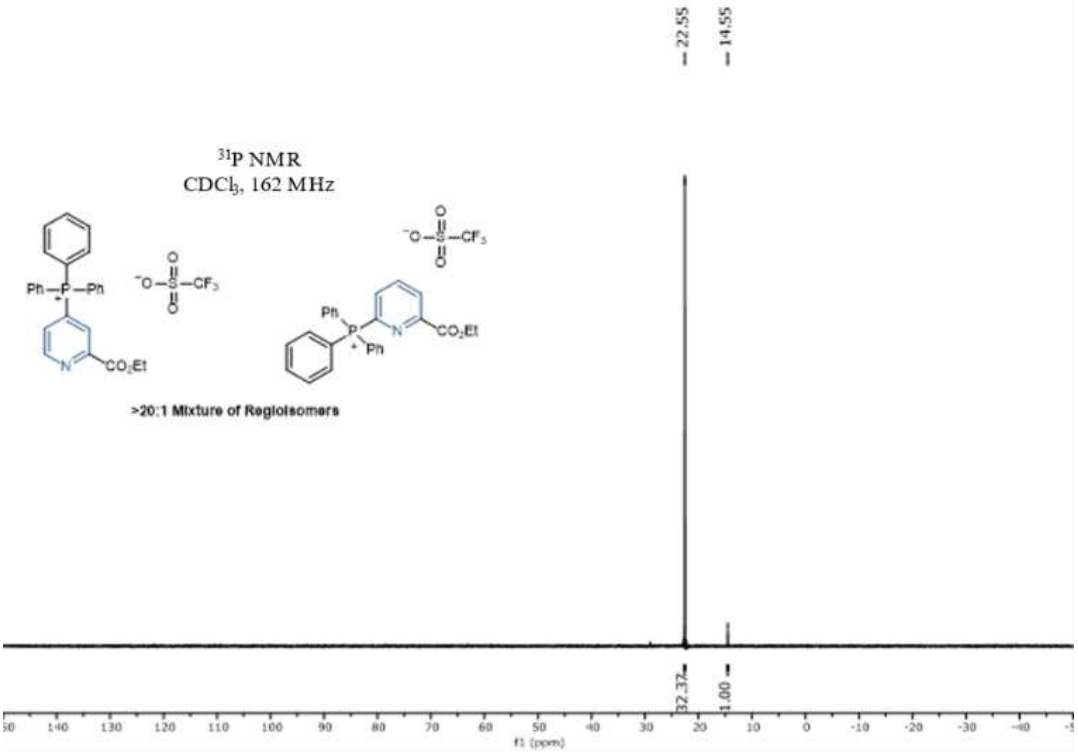

^{1}H NMR
$CDCl_3$, 400 MHz

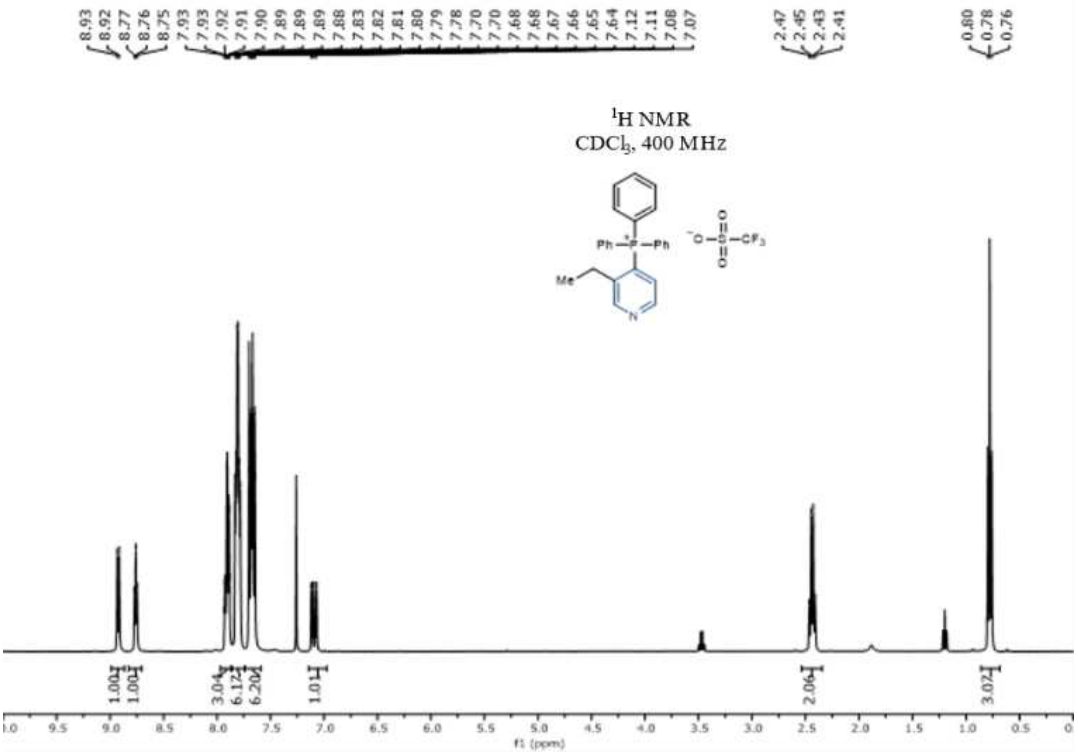

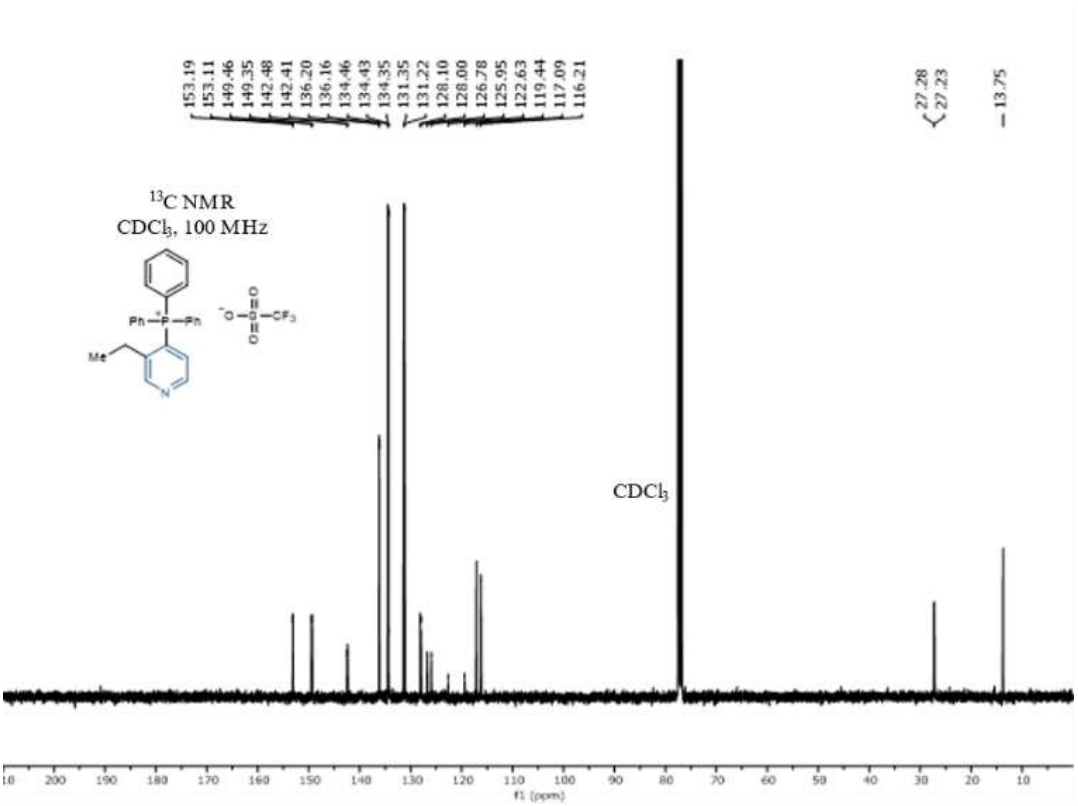
153.19
153.11
149.46
149.35
142.48
142.41
136.20
136.16
134.46
134.43
134.35
131.35
131.22
128.10
128.00
126.78
125.95
122.63
119.44
117.09
116.21
27.28
27.23
13.75
^{13}C NMR
$CDCl_3$, 100 MHz
Ph
P
Ph
Me
N
O
O
O
CF_3
$CDCl_3$
f1 (ppm)

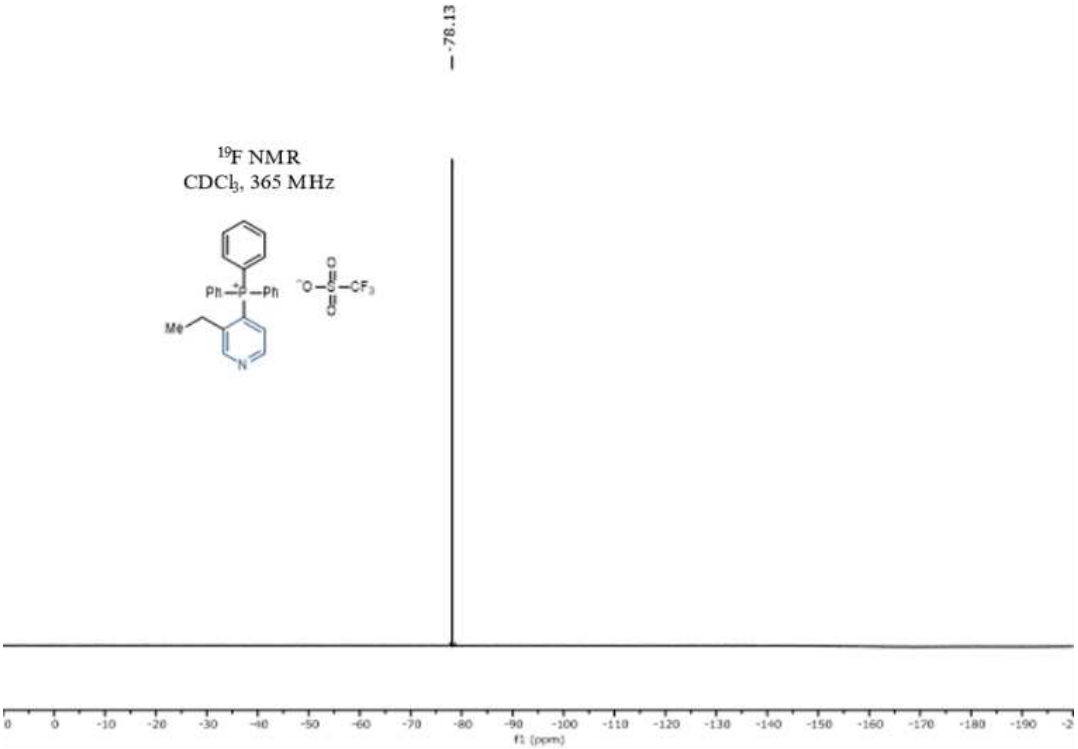
-78.13
^{19}F NMR
$CDCl_3$, 365 MHz
Ph
P
Ph
Me
N
O
O
O
CF_3
f1 (ppm)

Crude ^{31}P NMR
$CDCl_3$, 162 MHz

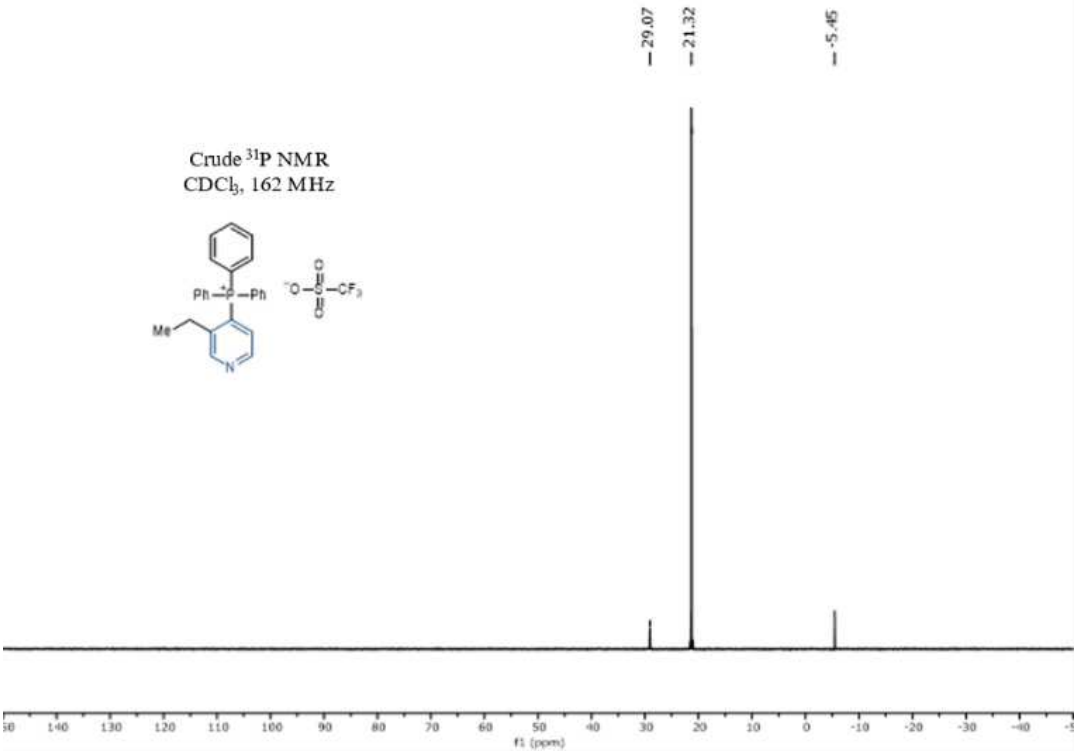

^{31}P NMR
$CDCl_3$, 162 MHz

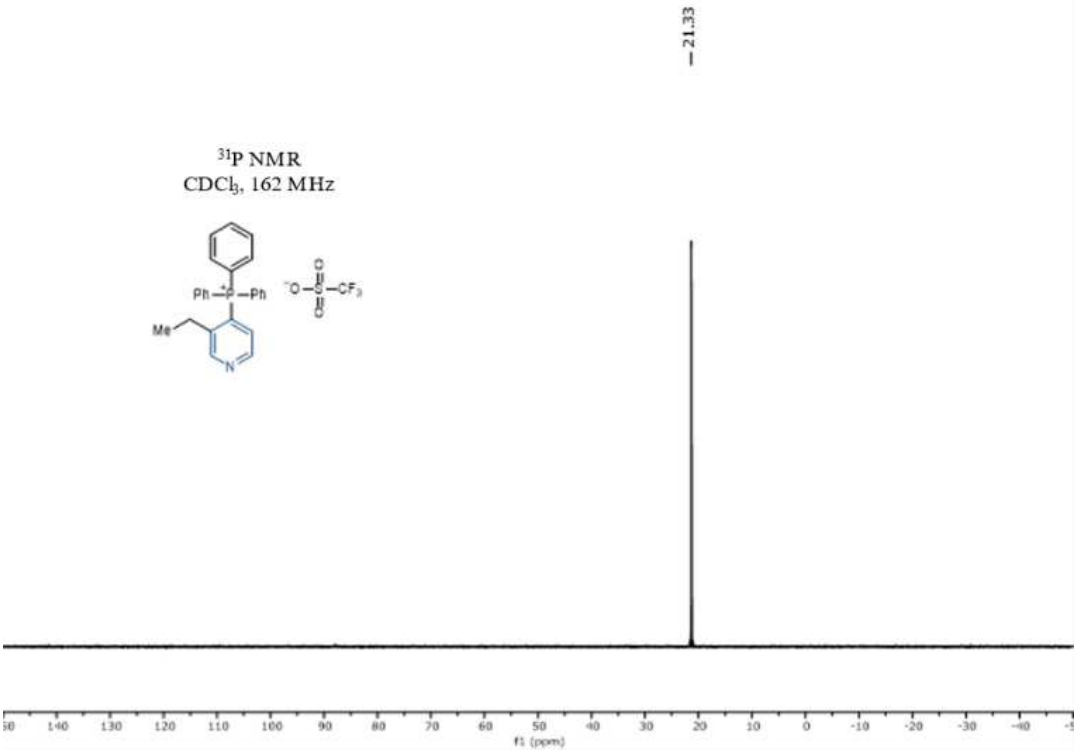

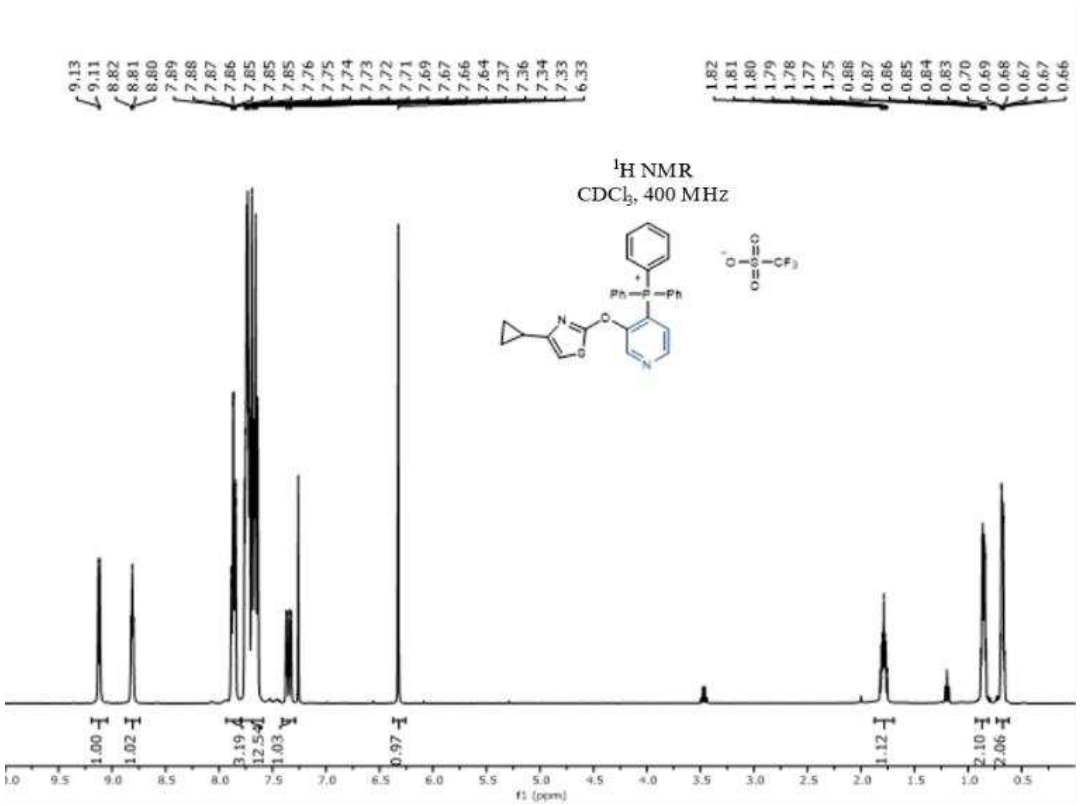
9.13
9.11
8.82
8.81
8.80
7.89
7.88
7.87
7.86
7.85
7.85
7.85
7.76
7.75
7.74
7.73
7.72
7.71
7.69
7.67
7.66
7.64
7.37
7.36
7.34
7.33
6.33
1.82
1.81
1.80
1.79
1.78
1.77
1.75
0.88
0.87
0.86
0.85
0.84
0.83
0.70
0.69
0.68
0.67
0.67
0.66
1H NMR
CDCl3, 400 MHz
1.00
1.02
3.19
12.54
1.03
0.97
1.12
2.10
2.06
f1 (ppm)

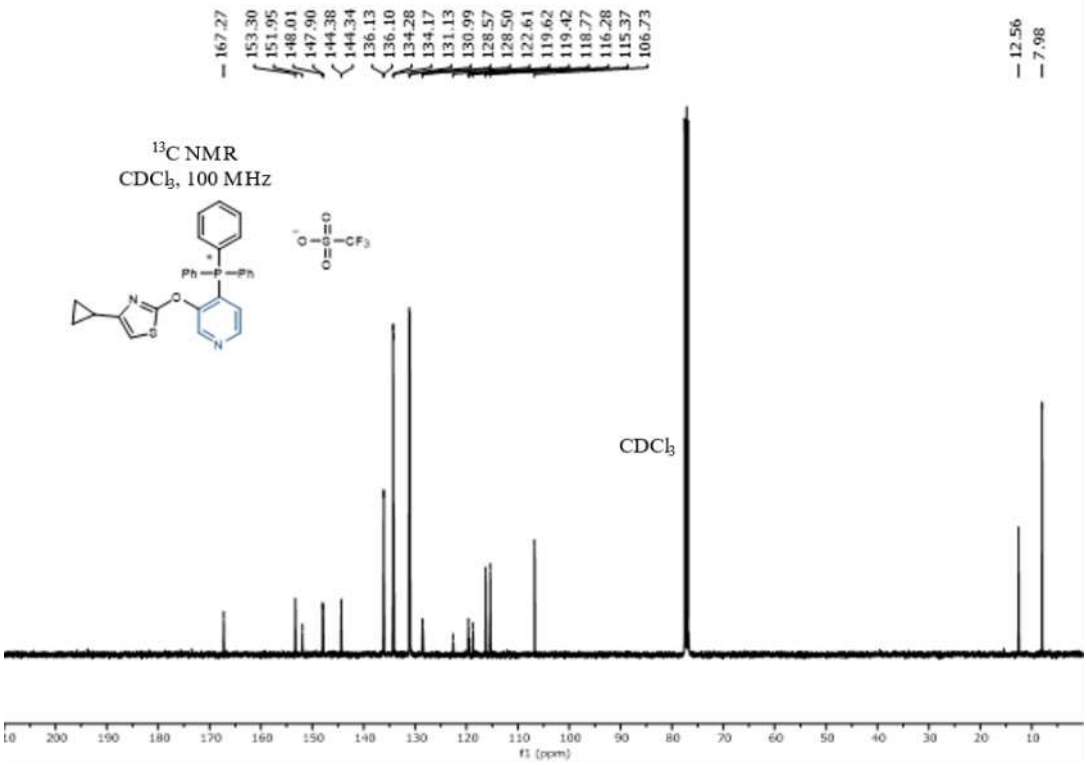
167.27
153.30
151.95
148.01
147.90
144.38
144.34
136.13
136.10
134.28
134.17
131.13
130.99
128.57
128.50
122.61
119.62
119.42
118.77
116.28
115.37
106.73
12.56
7.98
13C NMR
CDCl3, 100 MHz
CDCl3
f1 (ppm)

^{19}F NMR
$CDCl_3$, 365 MHz

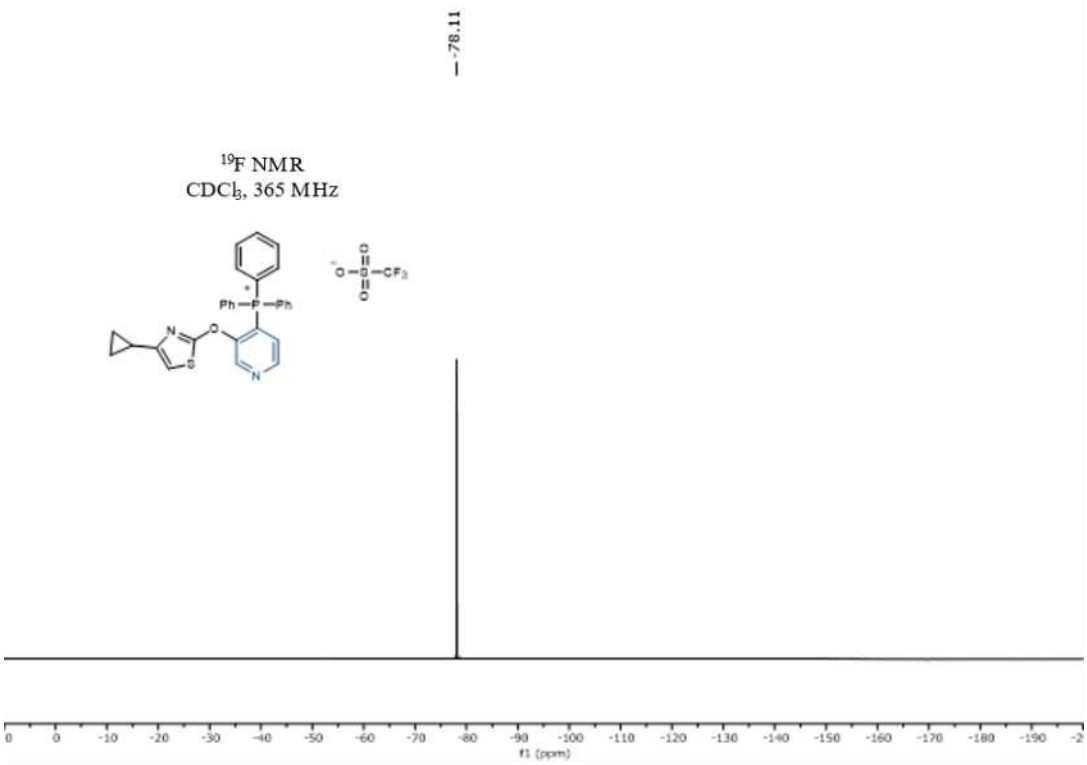

^{31}P NMR
$CDCl_3$, 162 MHz

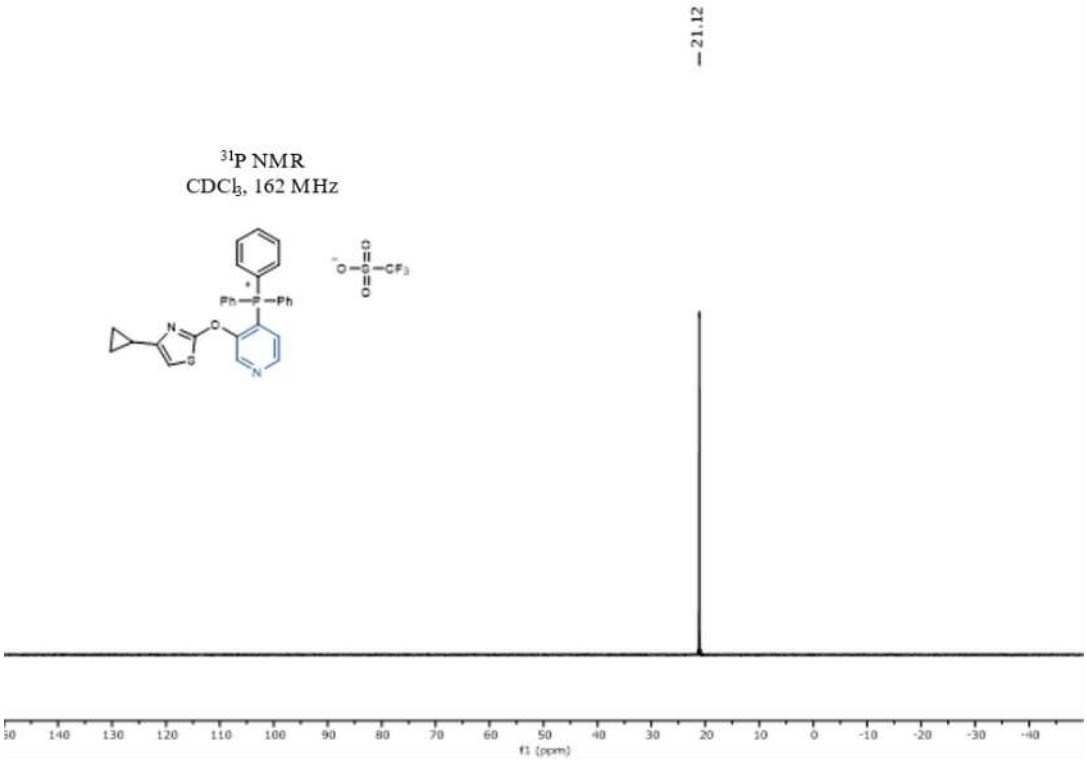

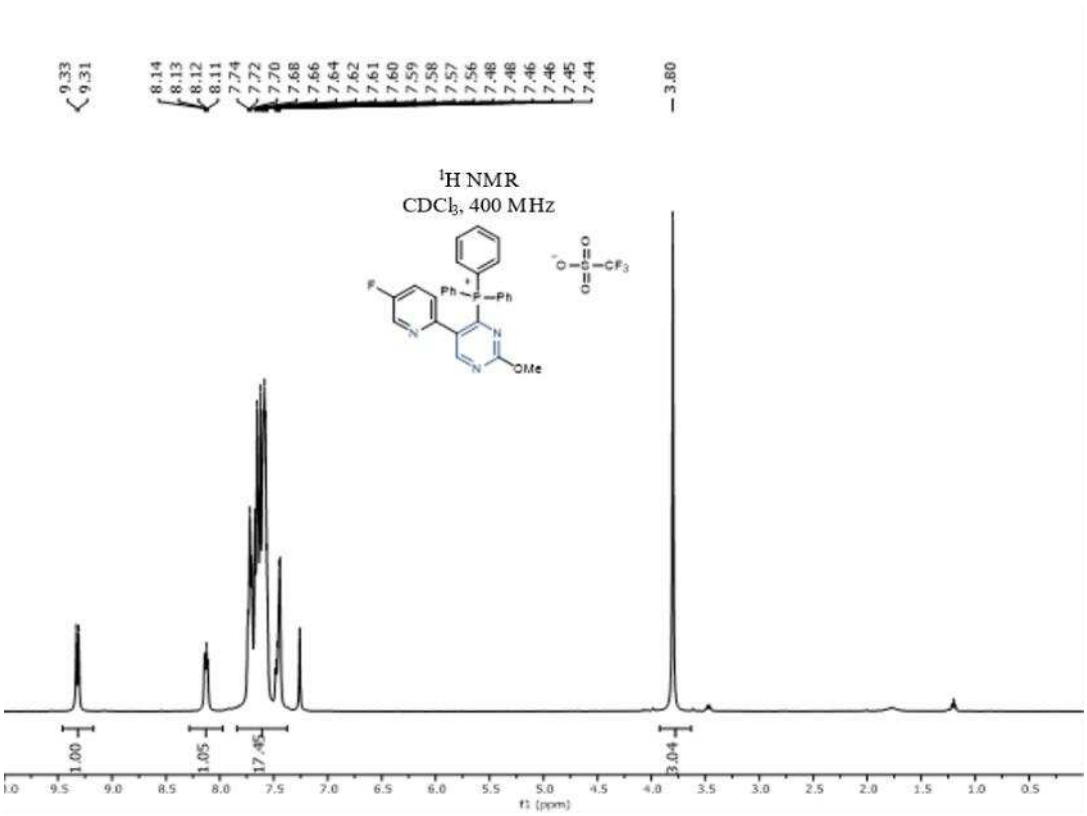
9.33
9.31
8.14
8.13
8.12
8.11
7.74
7.72
7.70
7.68
7.66
7.64
7.62
7.61
7.60
7.59
7.58
7.57
7.56
7.48
7.48
7.46
7.46
7.45
7.44
3.80
1H NMR
CDCl3, 400 MHz
F
Ph
P
Ph
N
N
OMe
O
O
O
CF3
1.00
1.05
17.45
3.04
f1 (ppm)

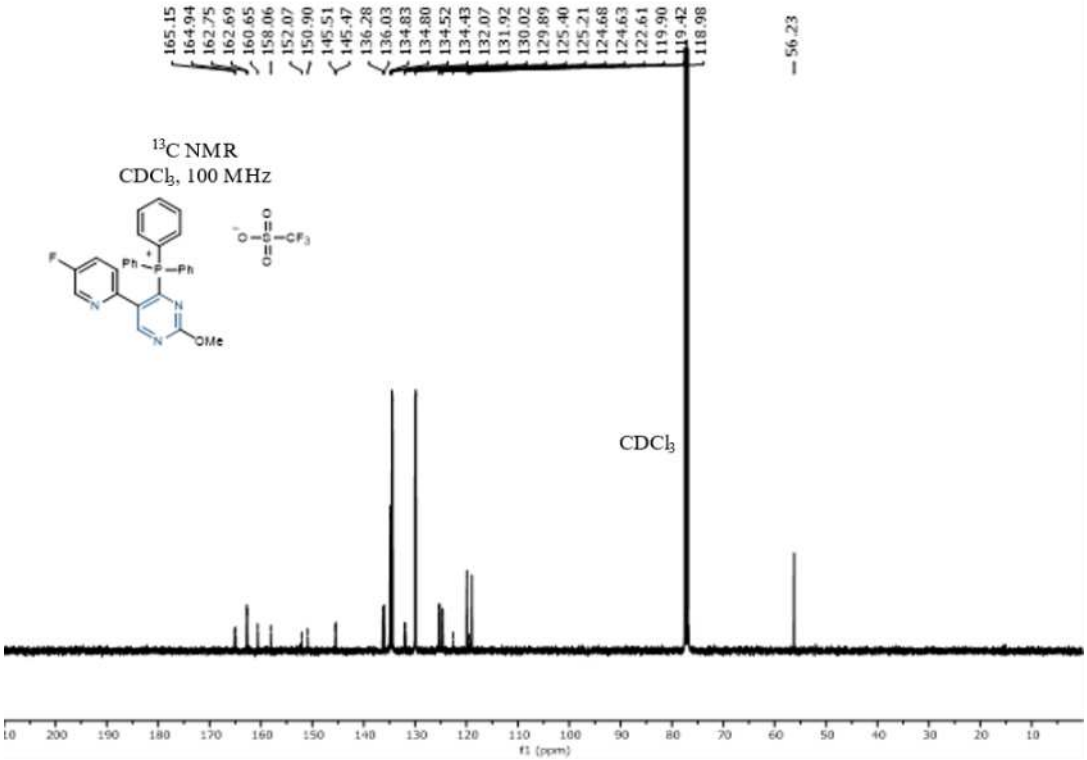
165.15
164.94
162.75
162.69
160.65
158.06
152.07
150.90
145.51
145.47
136.28
136.03
134.83
134.80
134.52
134.43
132.07
131.92
130.02
129.89
125.40
125.21
124.68
124.63
122.61
119.90
119.42
118.98
56.23
13C NMR
CDCl3, 100 MHz
F
Ph
P
Ph
N
N
OMe
O
O
O
CF3
CDCl3
f1 (ppm)

^{19}F NMR
$CDCl_3$, 365 MHz

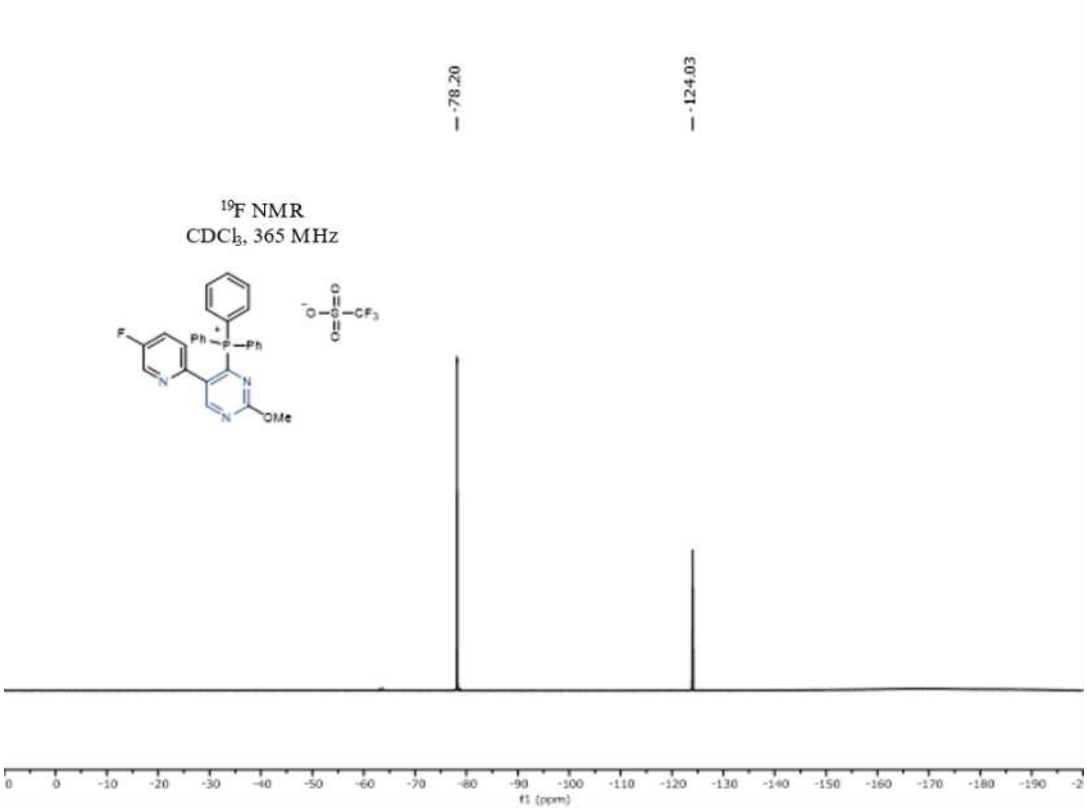

Crude ^{31}P NMR
$CDCl_3$, 162 MHz

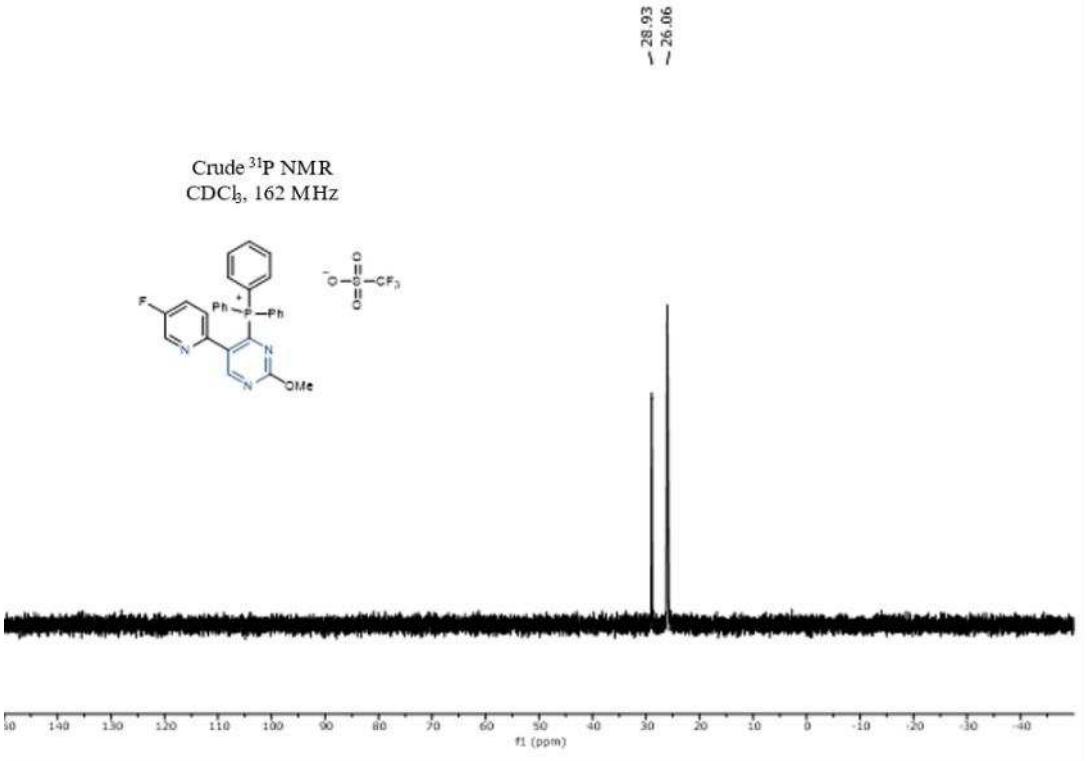

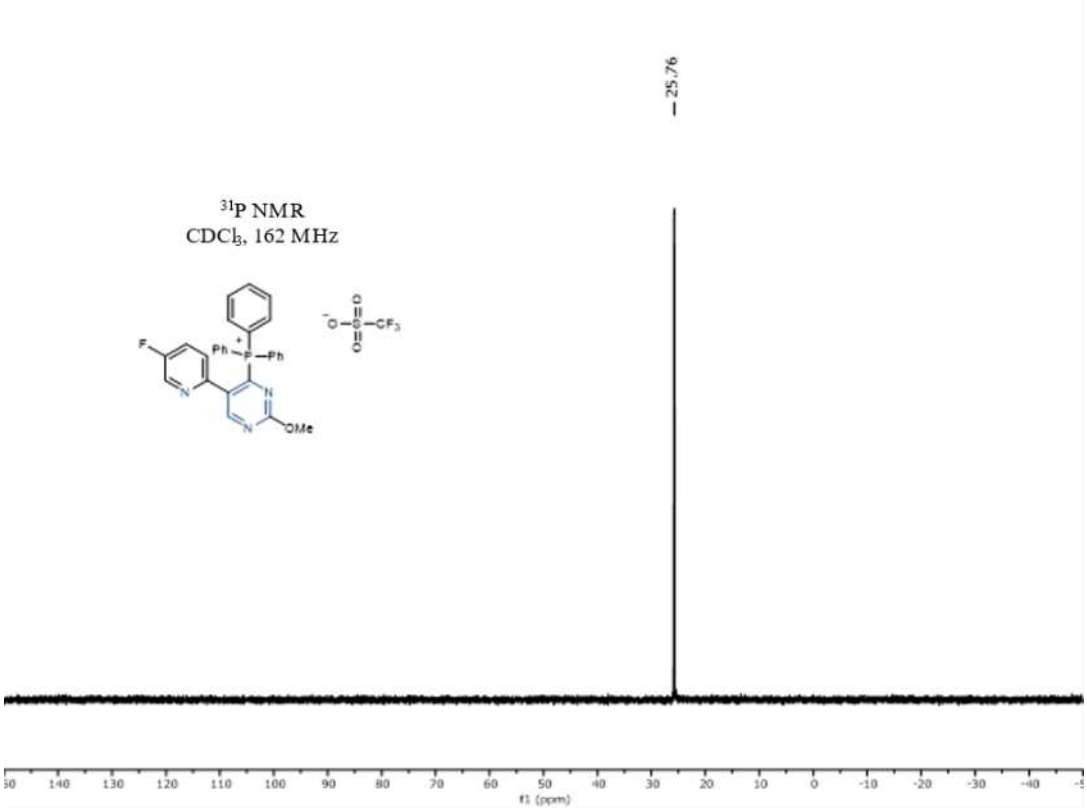
25.76
31P NMR
CDCl3, 162 MHz
f1 (ppm)

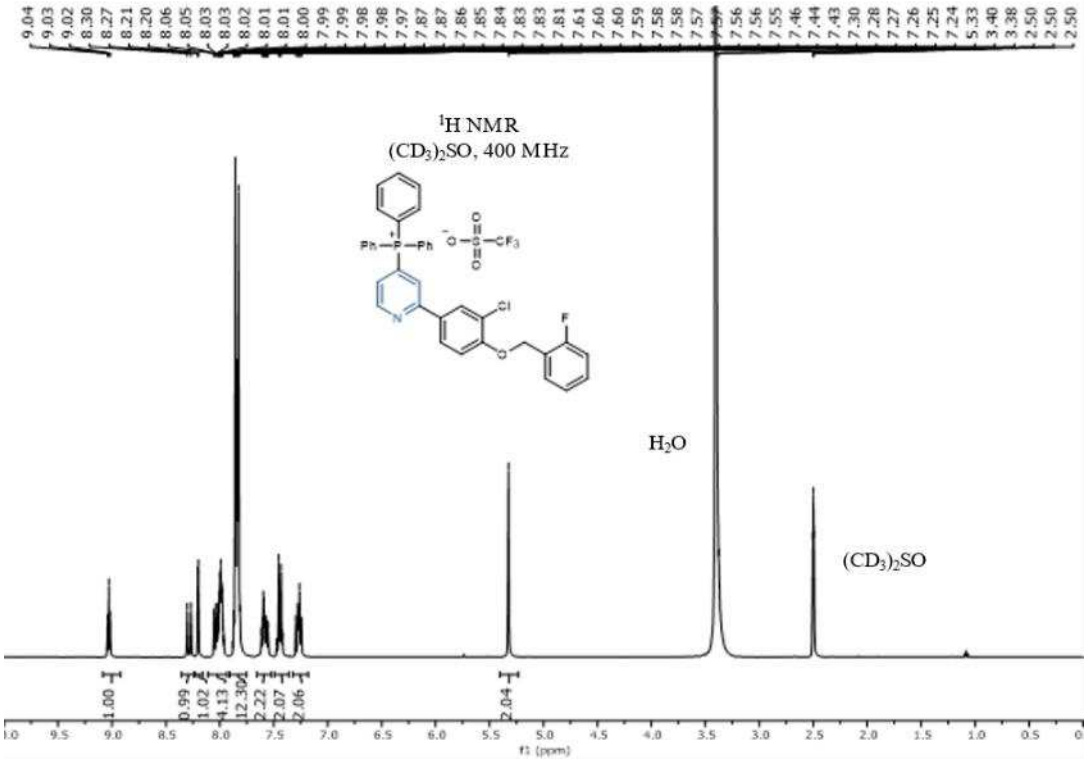
1H NMR
(CD3)2SO, 400 MHz
H2O
(CD3)2SO
f1 (ppm)

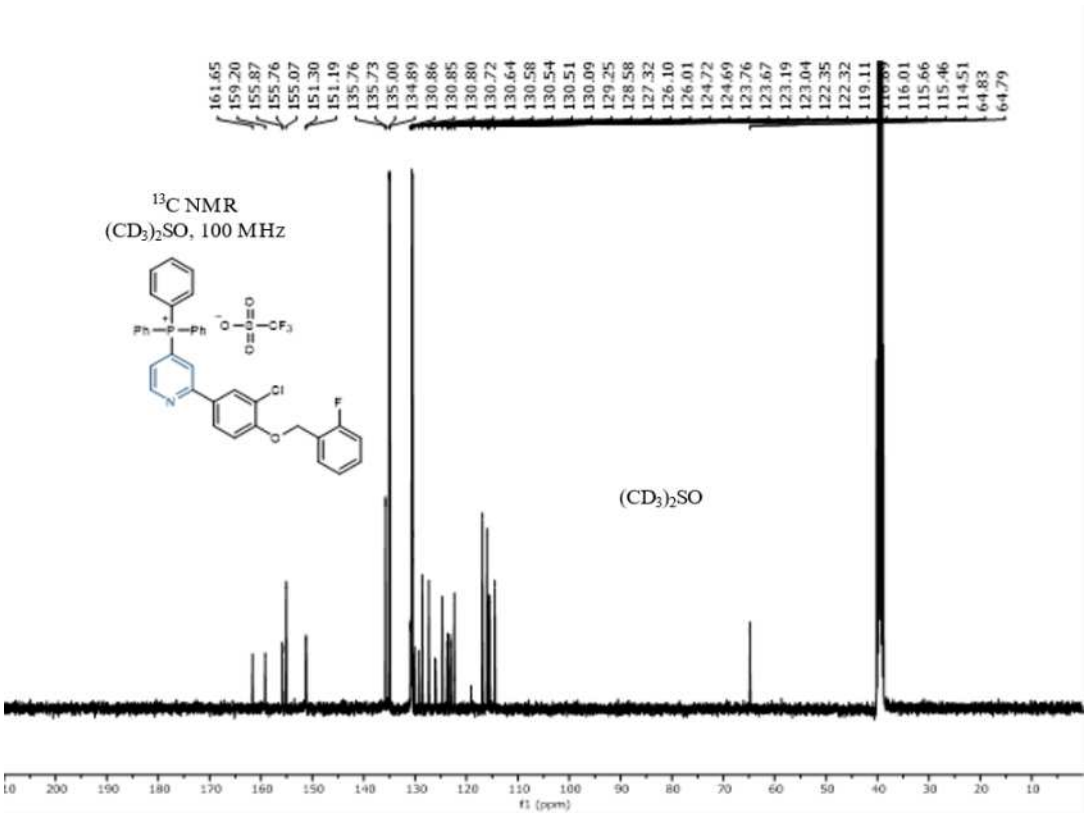
161.65
159.20
155.87
155.76
155.07
151.30
151.19
135.76
135.73
135.00
134.89
130.86
130.85
130.80
130.72
130.64
130.58
130.54
130.51
130.09
129.25
128.58
127.32
126.10
126.01
124.72
124.69
123.76
123.67
123.19
123.04
122.35
122.32
119.11
116.01
115.66
115.46
114.51
64.83
64.79
^{13}C NMR
$(CD_3)_2SO$, 100 MHz
$(CD_3)_2SO$
f1 (ppm)

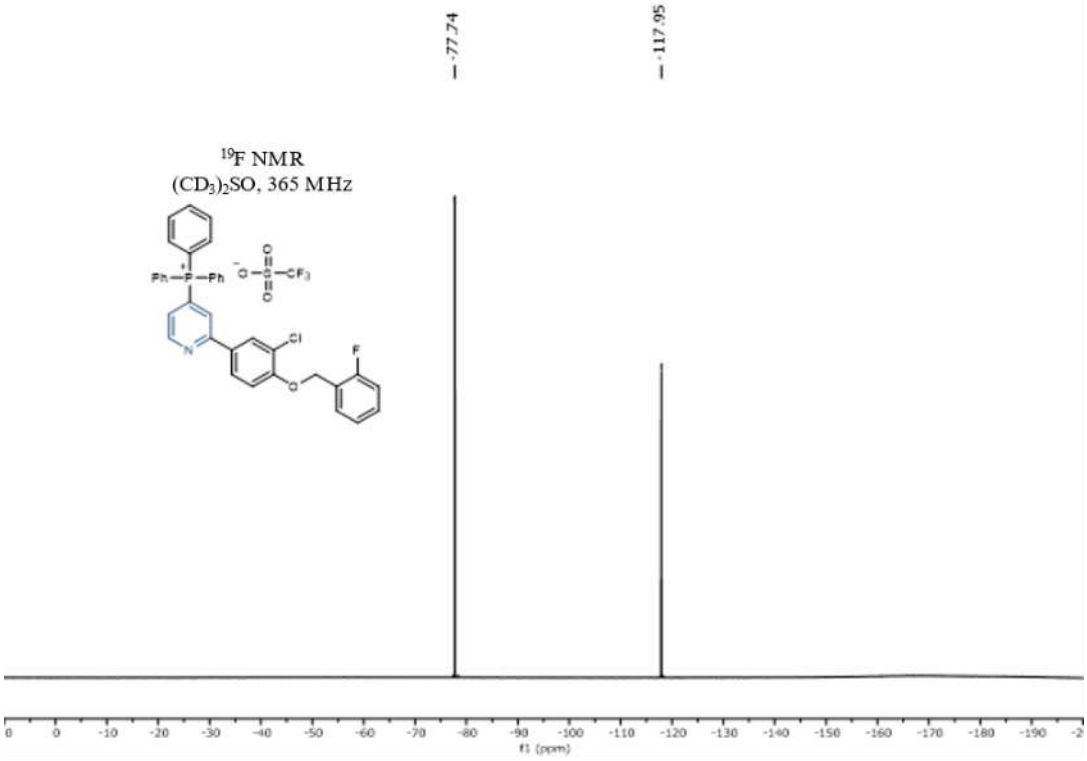
-77.74
-117.95
^{19}F NMR
$(CD_3)_2SO$, 365 MHz
f1 (ppm)

Crude ^{31}P NMR
$CDCl_3$, 162 MHz

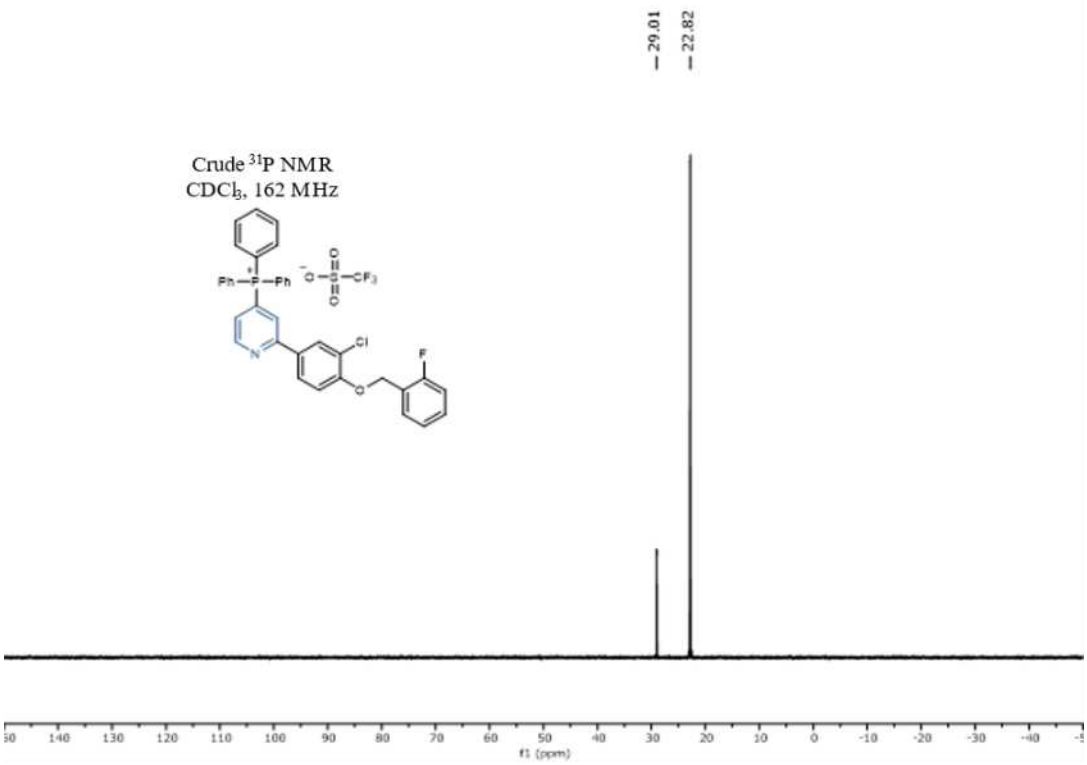

^{31}P NMR
$(CD_3)_2SO$, 162 MHz

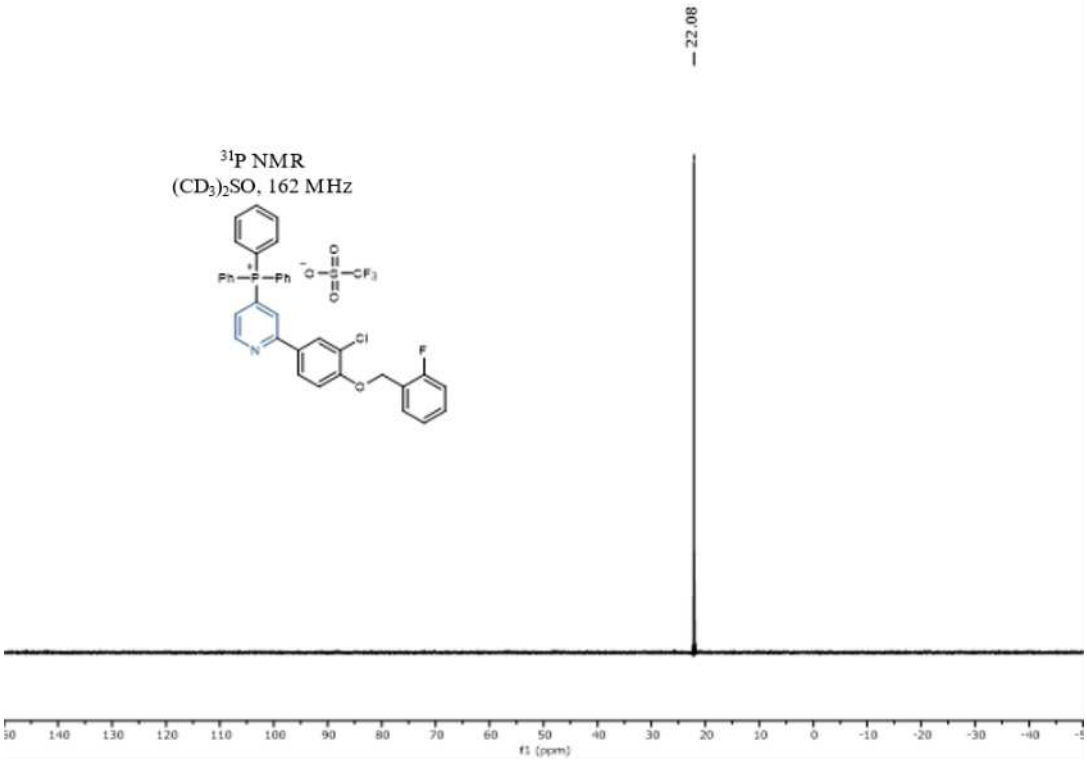

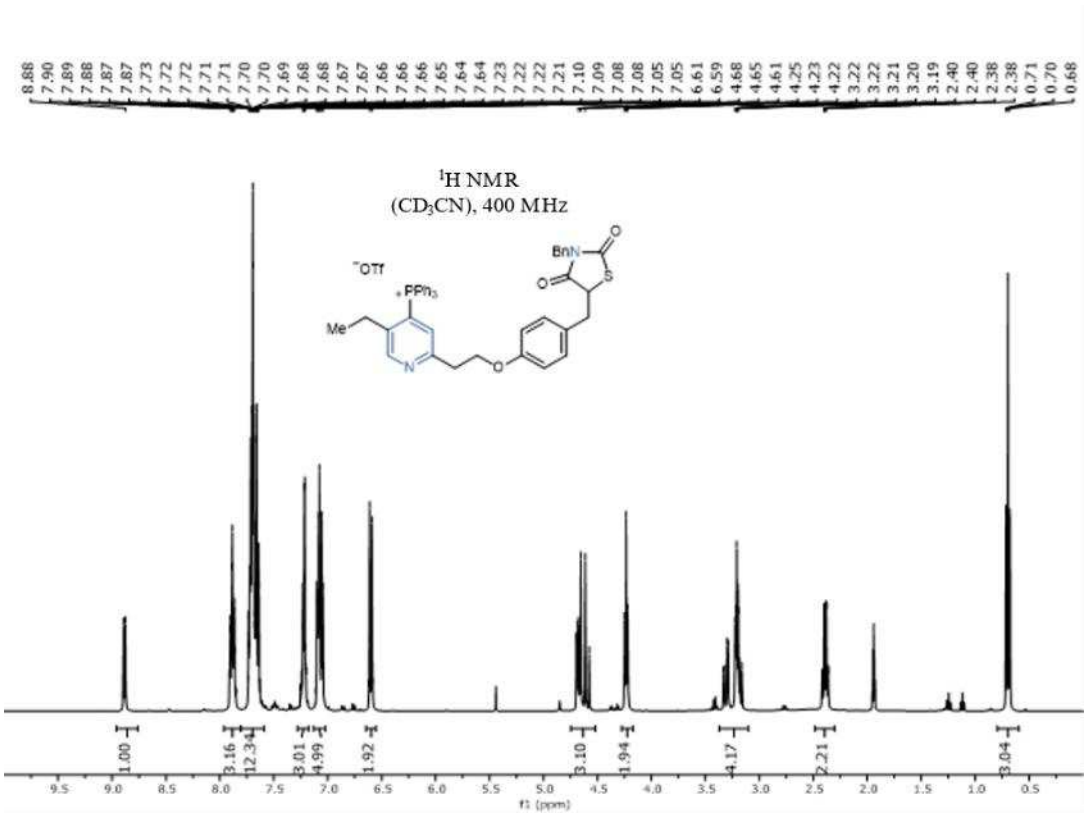
8.88 7.90 7.89 7.88 7.87 7.73 7.72 7.72 7.71 7.71 7.70 7.70 7.69 7.68 7.68 7.67 7.67 7.66 7.66 7.66 7.65 7.64 7.64 7.23 7.22 7.22 7.21 7.10 7.09 7.08 7.08 7.05 7.05 6.61 6.59 4.68 4.65 4.61 4.25 4.23 4.22 3.22 3.22 3.21 3.20 3.19 2.40 2.40 2.38 2.38 0.71 0.70 0.68
1H NMR
(CD3CN), 400 MHz
OTf
PPh3
Me
BnN
O
S
1.00 3.16 12.34 3.01 4.99 1.92 3.10 1.94 4.17 2.21 3.04
f1 (ppm)

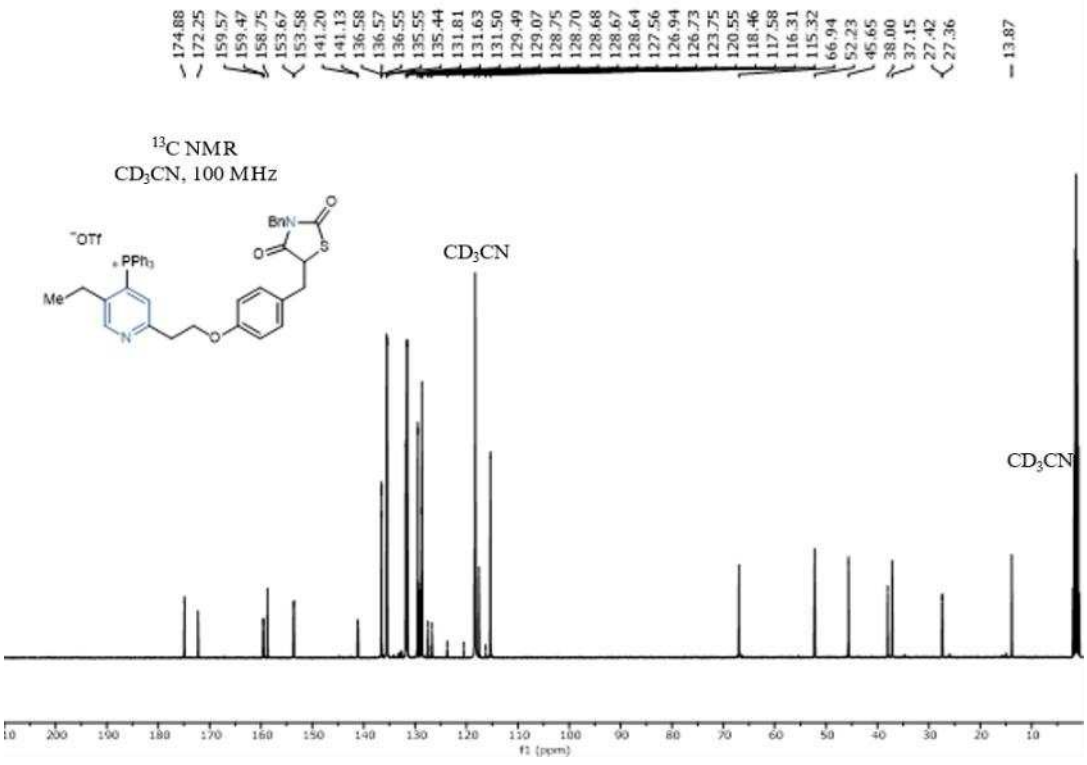
174.88 172.25 159.57 159.47 158.75 153.67 153.58 141.20 141.13 136.58 136.57 136.55 135.55 135.44 131.81 131.63 131.50 129.49 129.07 128.75 128.70 128.68 128.67 128.64 127.56 126.94 126.73 123.75 120.55 118.46 117.58 116.31 115.32 66.94 52.23 45.65 38.00 37.15 27.42 27.36 13.87
13C NMR
CD3CN, 100 MHz
OTf
PPh3
Me
BnN
CD3CN
CD3CN
f1 (ppm)

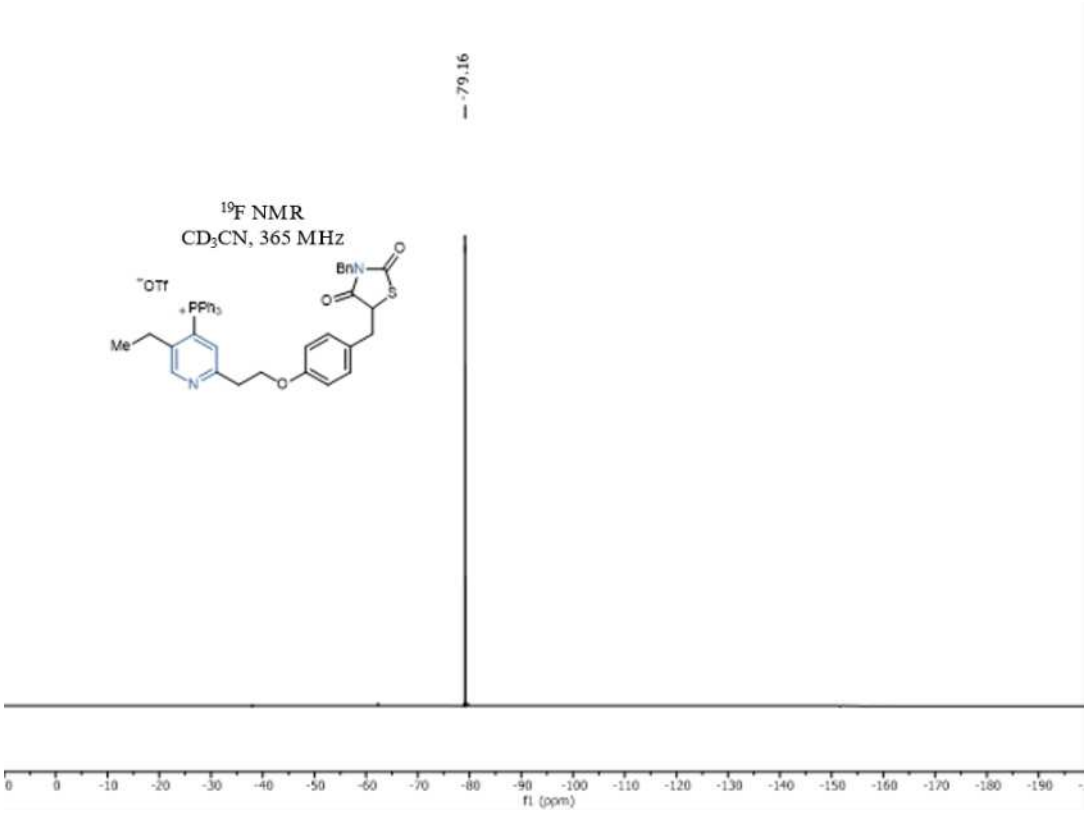
-79.16
19F NMR
CD3CN, 365 MHz
BnN
OTf
PPh3
Me
f1 (ppm)

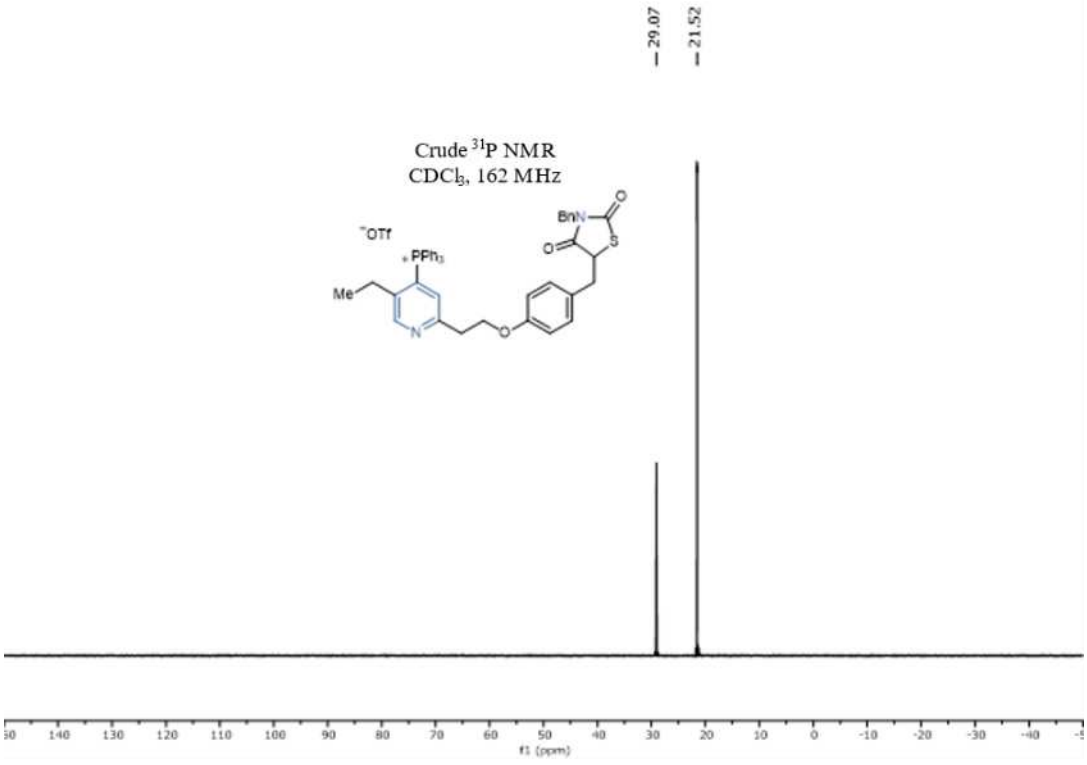
-29.07
-21.52
Crude 31P NMR
CDCl3, 162 MHz
BnN
OTf
PPh3
Me
f1 (ppm)

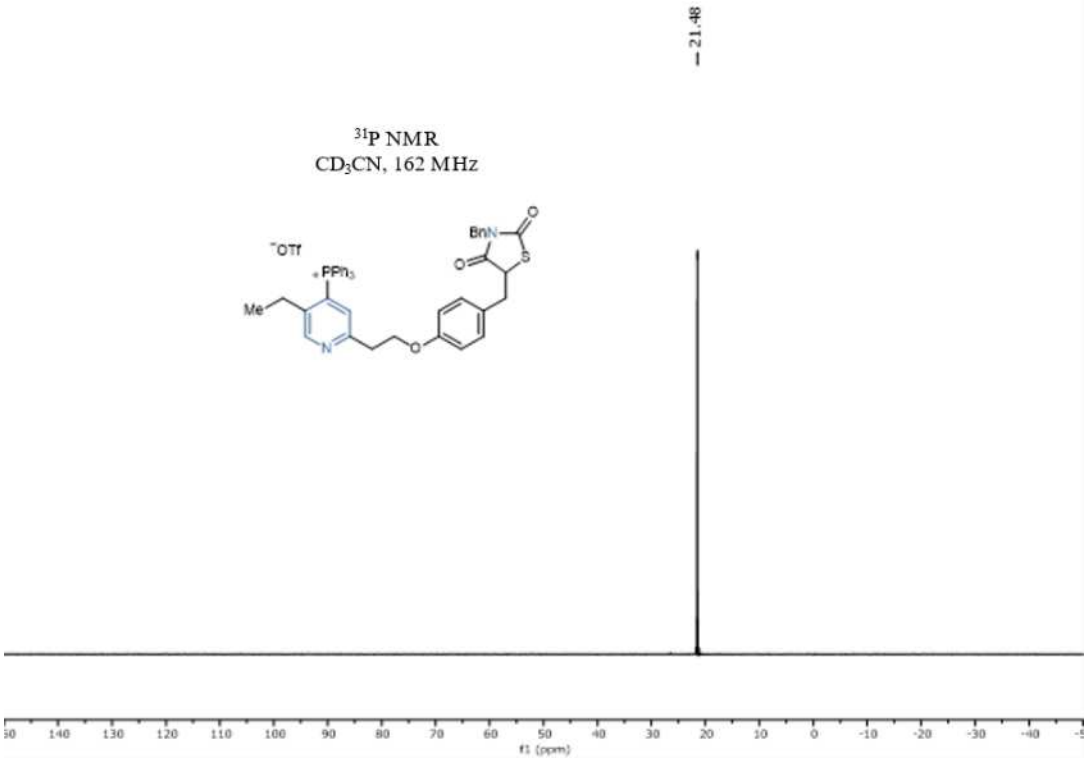
21.48
31P NMR
CD3CN, 162 MHz
−OTf
+PPh3
Me
BnN
O
O
S
O
N
f1 (ppm)

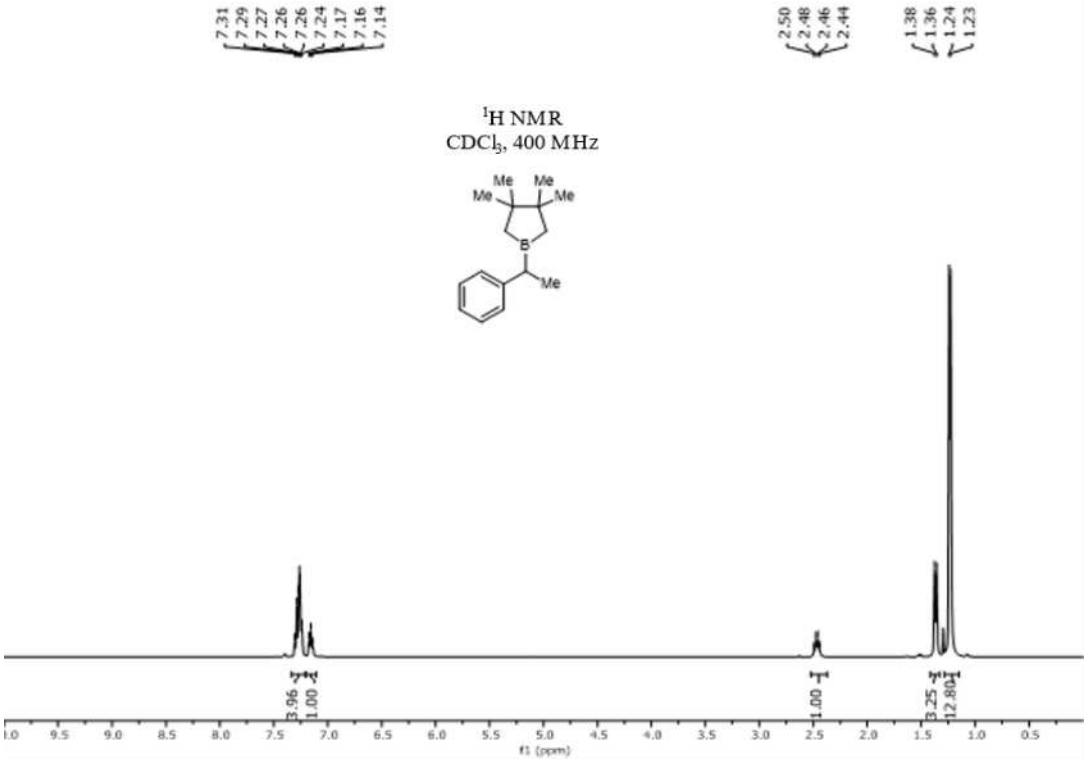
7.31
7.29
7.27
7.26
7.26
7.24
7.17
7.16
7.14
2.50
2.48
2.46
2.44
1.38
1.36
1.24
1.23
1H NMR
CDCl3, 400 MHz
Me
Me
Me
Me
B
Me
3.96
1.00
1.00
3.25
12.80
f1 (ppm)

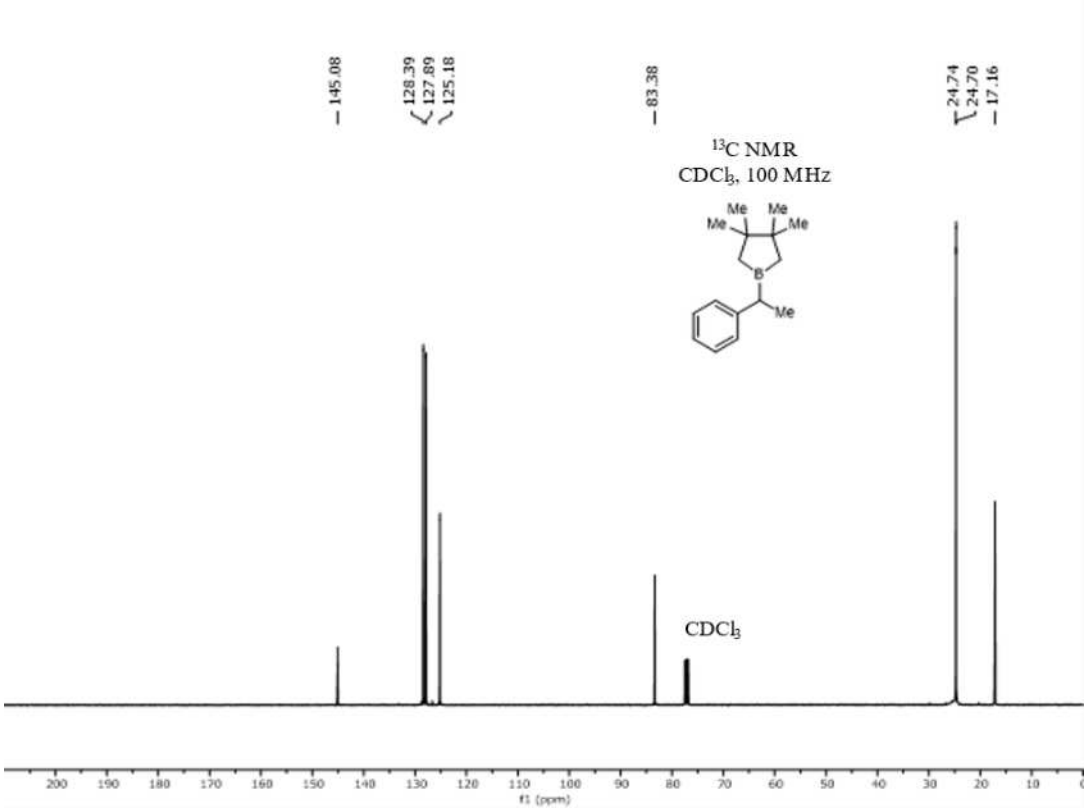
145.08
128.39
127.89
125.18
83.38
24.74
24.70
17.16
^{13}C NMR
$CDCl_3$, 100 MHz
Me
Me
Me
Me
B
Me
$CDCl_3$
200 190 180 170 160 150 140 130 120 110 100 90 80 70 60 50 40 30 20 10
f1 (ppm)

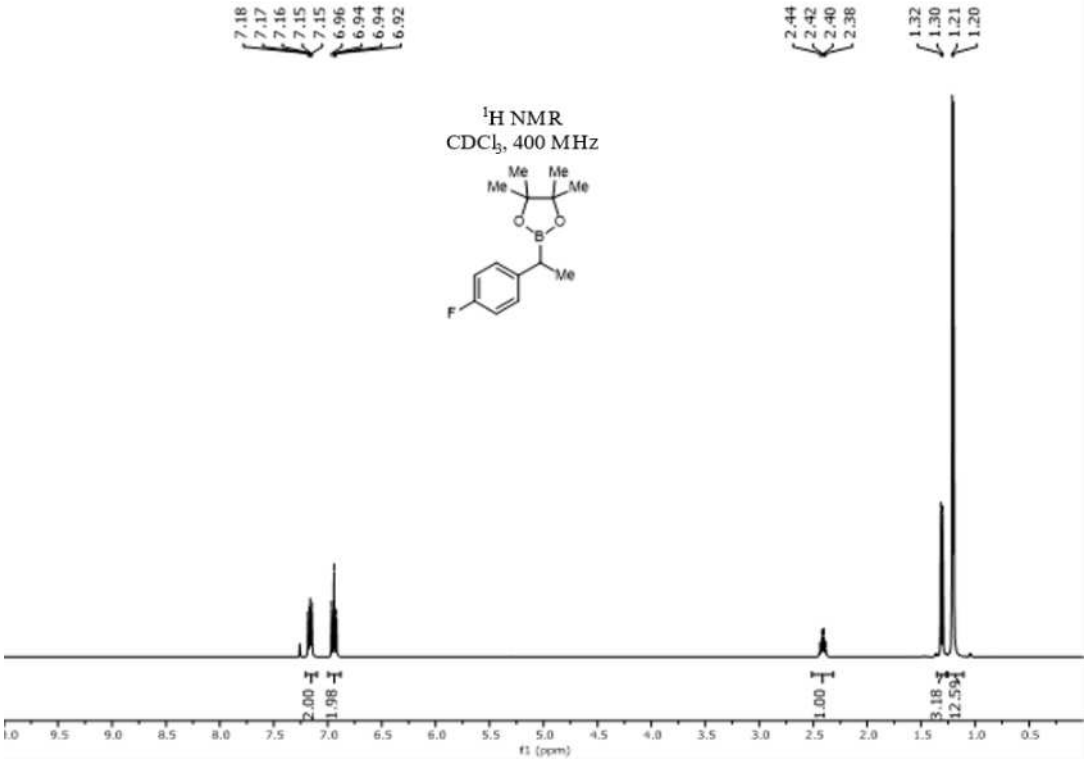
7.18
7.17
7.16
7.15
7.15
6.96
6.94
6.94
6.92
2.44
2.42
2.40
2.38
1.32
1.30
1.21
1.20
^{1}H NMR
$CDCl_3$, 400 MHz
Me
Me
Me
Me
B
Me
F
2.00
1.98
1.00
3.18
12.59
9.5 9.0 8.5 8.0 7.5 7.0 6.5 6.0 5.5 5.0 4.5 4.0 3.5 3.0 2.5 2.0 1.5 1.0 0.5
f1 (ppm)

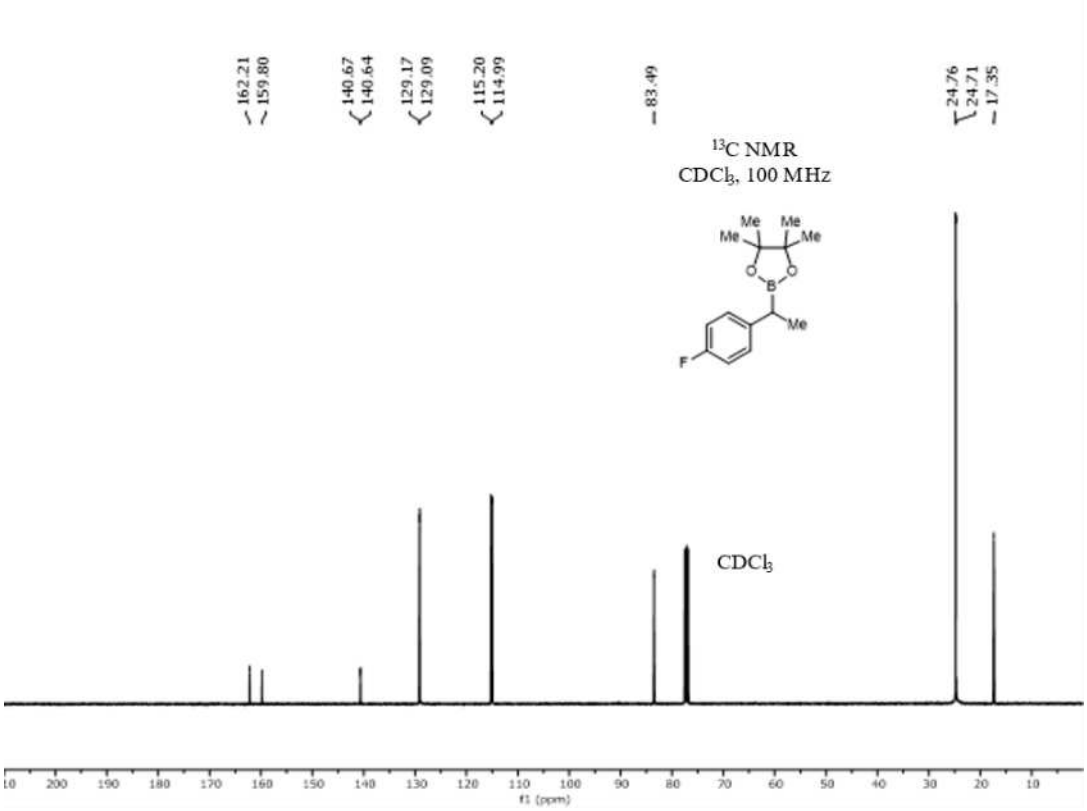
162.21
159.80
140.67
140.64
129.17
129.09
115.20
114.99
83.49
24.76
24.71
17.35
13C NMR
CDCl3, 100 MHz
Me
Me
Me
Me
B
O
O
Me
F
CDCl3
f1 (ppm)

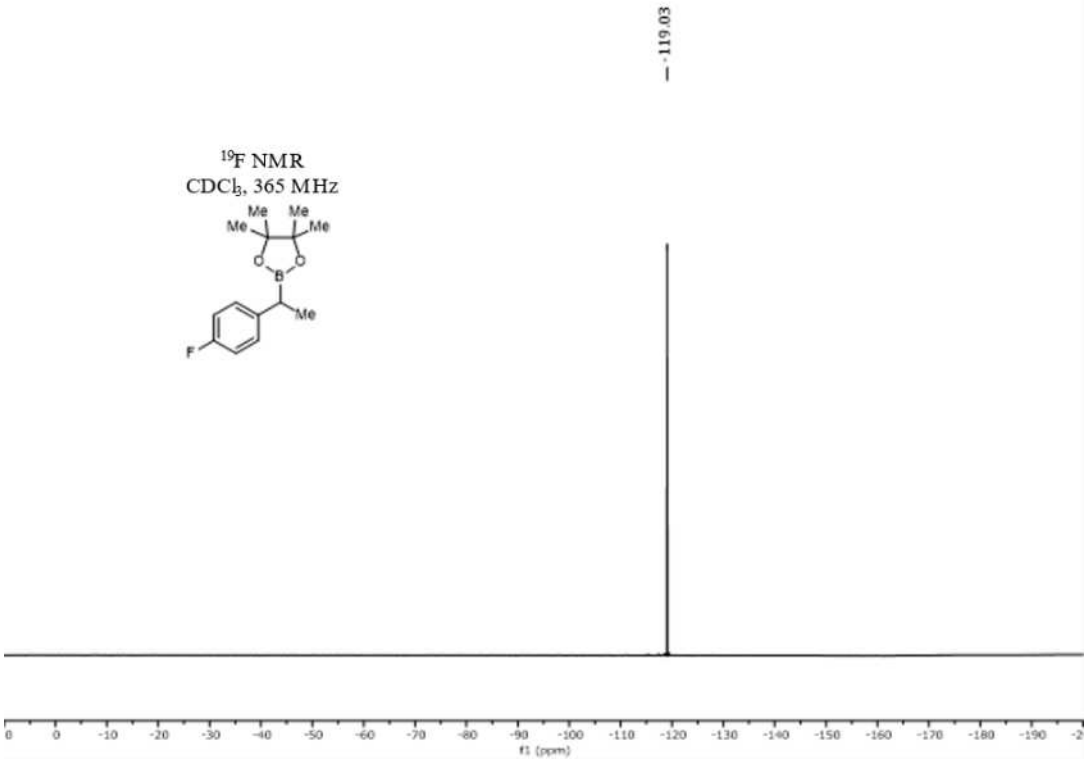
-119.03
19F NMR
CDCl3, 365 MHz
Me
Me
Me
Me
B
O
O
Me
F
f1 (ppm)

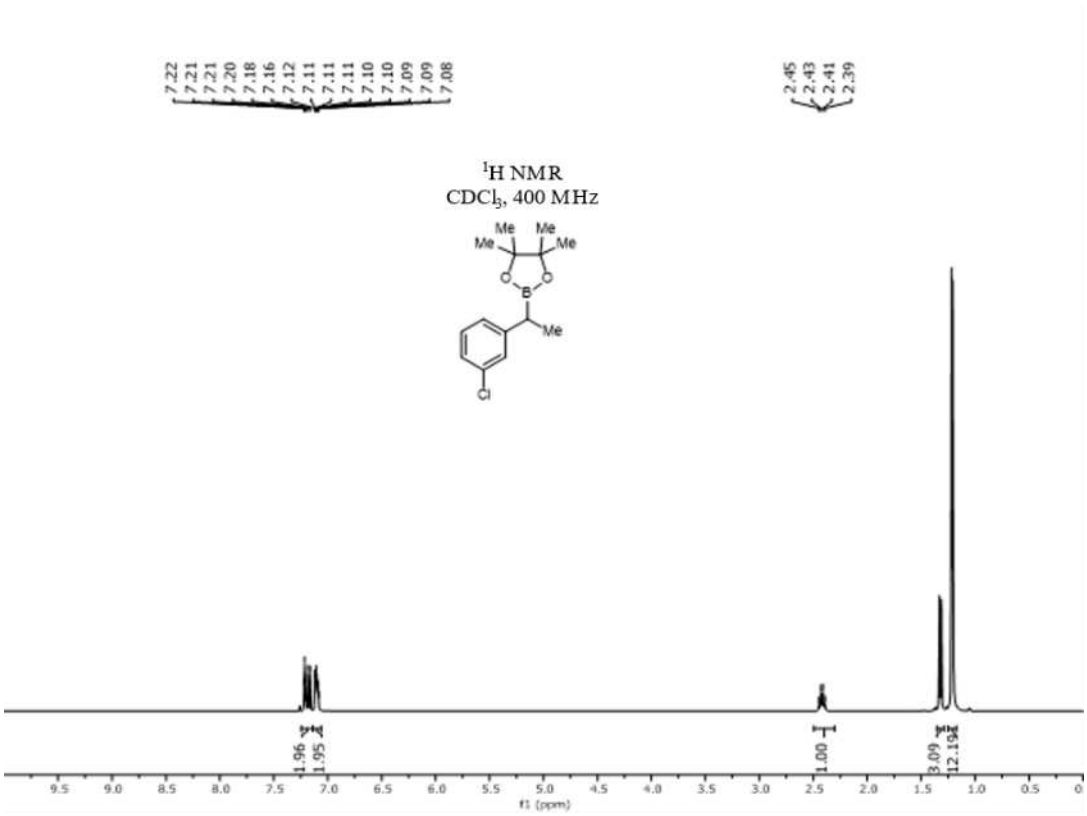
7.22
7.21
7.21
7.20
7.18
7.16
7.12
7.11
7.11
7.11
7.10
7.10
7.09
7.09
7.08
2.45
2.43
2.41
2.39
^{1}H NMR
$CDCl_3$, 400 MHz
Me
Me
Me
Me
B
O
O
Me
Cl
1.96
1.95
1.00
3.09
12.19
9.5
9.0
8.5
8.0
7.5
7.0
6.5
6.0
5.5
5.0
4.5
4.0
3.5
3.0
2.5
2.0
1.5
1.0
0.5
f1 (ppm)

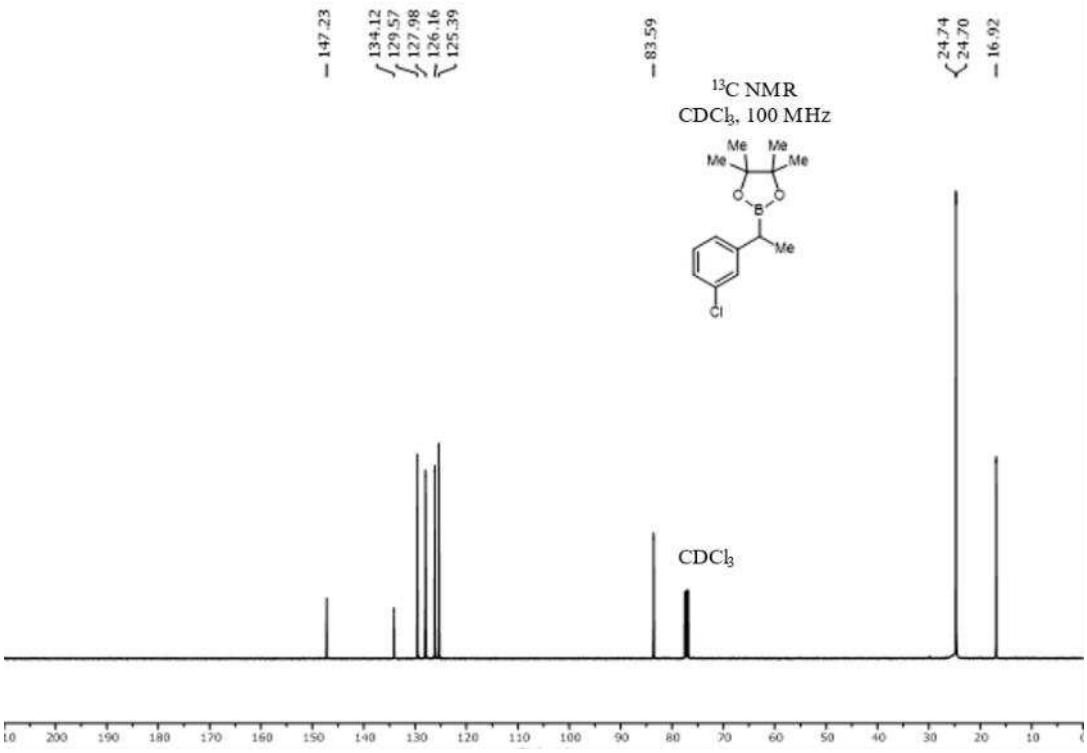
147.23
134.12
129.57
127.98
126.16
125.39
83.59
24.74
24.70
16.92
^{13}C NMR
$CDCl_3$, 100 MHz
Me
Me
Me
Me
B
O
O
Me
Cl
$CDCl_3$
200
190
180
170
160
150
140
130
120
110
100
90
80
70
60
50
40
30
20
10

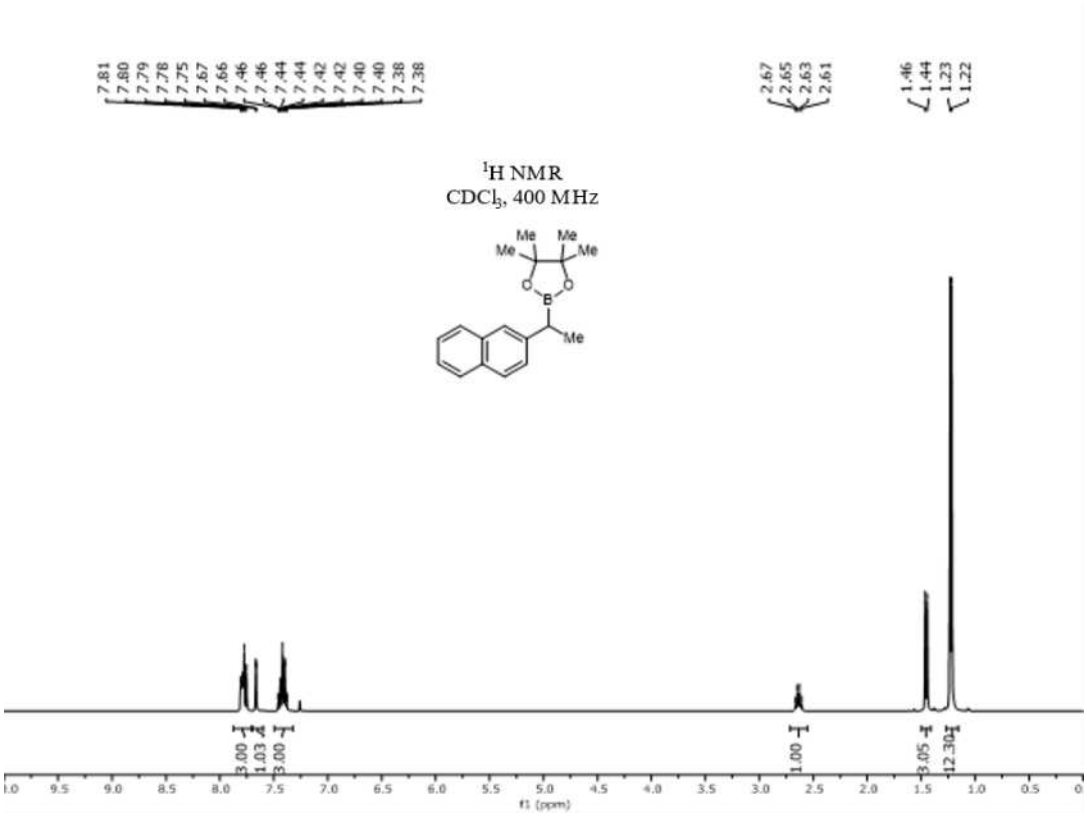
7.81
7.80
7.79
7.78
7.75
7.67
7.66
7.46
7.46
7.44
7.44
7.42
7.42
7.40
7.40
7.38
7.38
2.67
2.65
2.63
2.61
1.46
1.44
1.23
1.22
^{1}H NMR
$CDCl_3$, 400 MHz
Me
Me
Me
Me
B
Me
3.00
1.03
3.00
1.00
3.05
12.30
f1 (ppm)

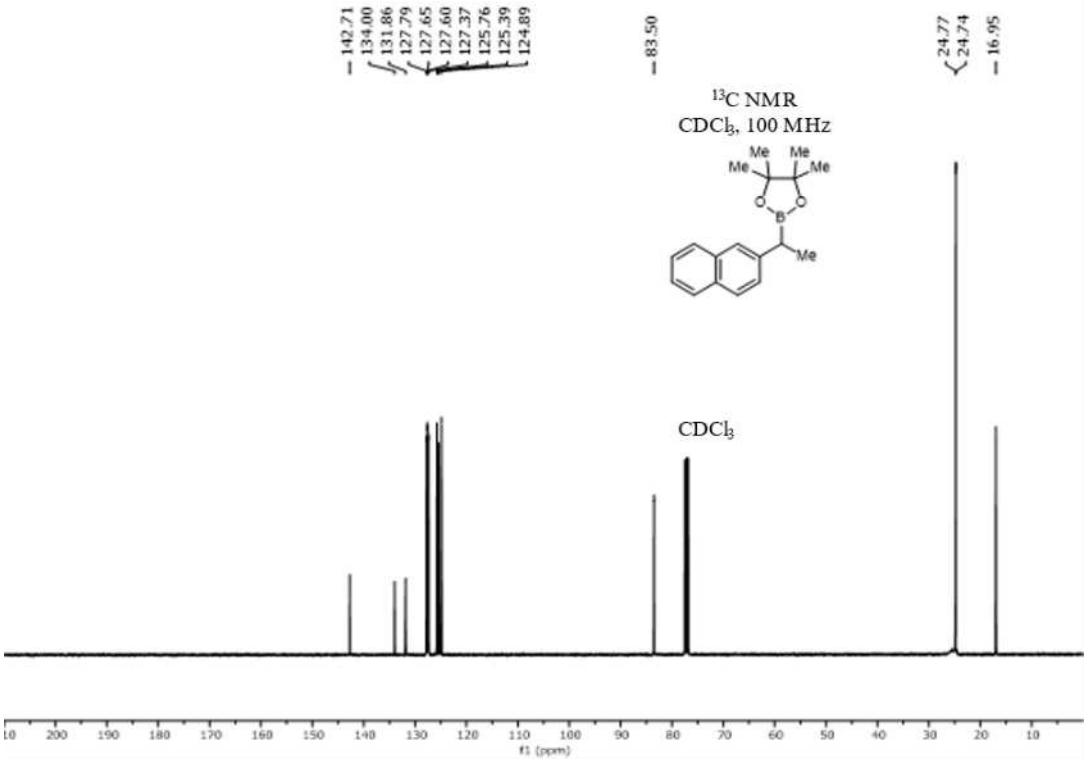
142.71
134.00
131.86
127.79
127.65
127.60
127.37
125.76
125.39
124.89
83.50
24.77
24.74
16.95
^{13}C NMR
$CDCl_3$, 100 MHz
Me
Me
Me
Me
B
Me
$CDCl_3$
f1 (ppm)

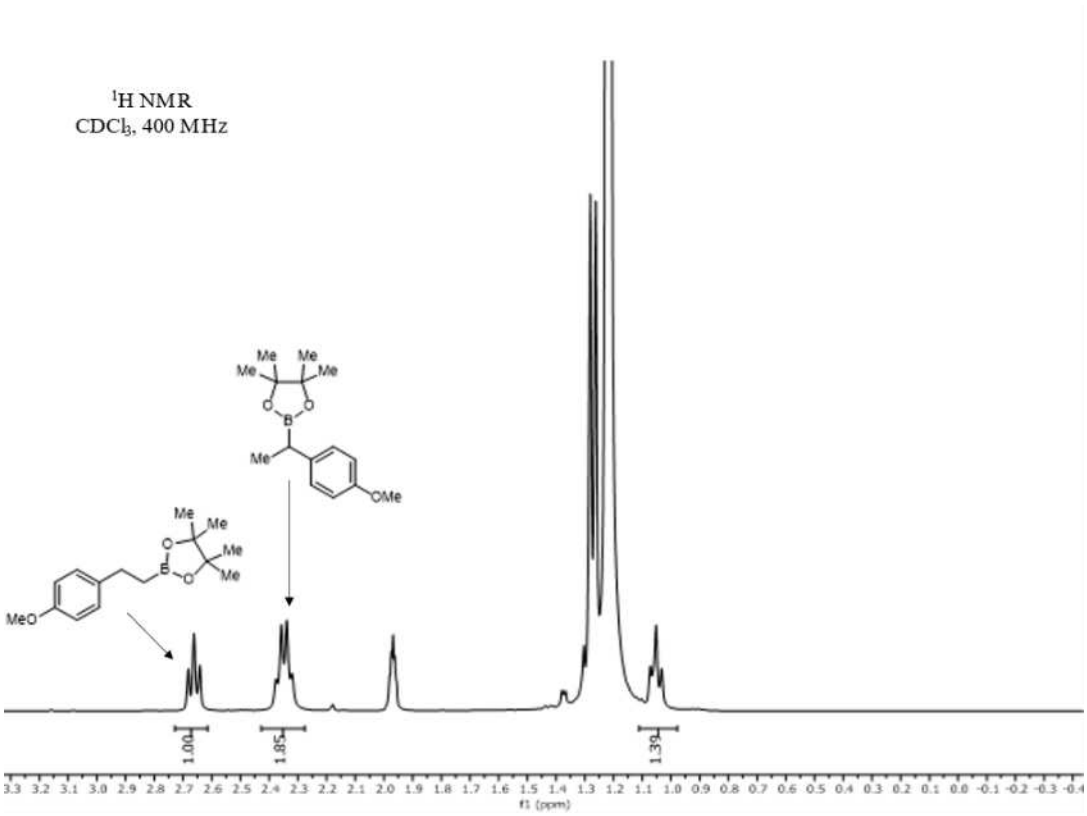
^{1}H NMR
$CDCl_3$, 400 MHz
Me
Me
Me
Me
Me
Me
Me
Me
Me
Me
B
O
O
OMe
MeO
1.00
1.85
1.39
f1 (ppm)

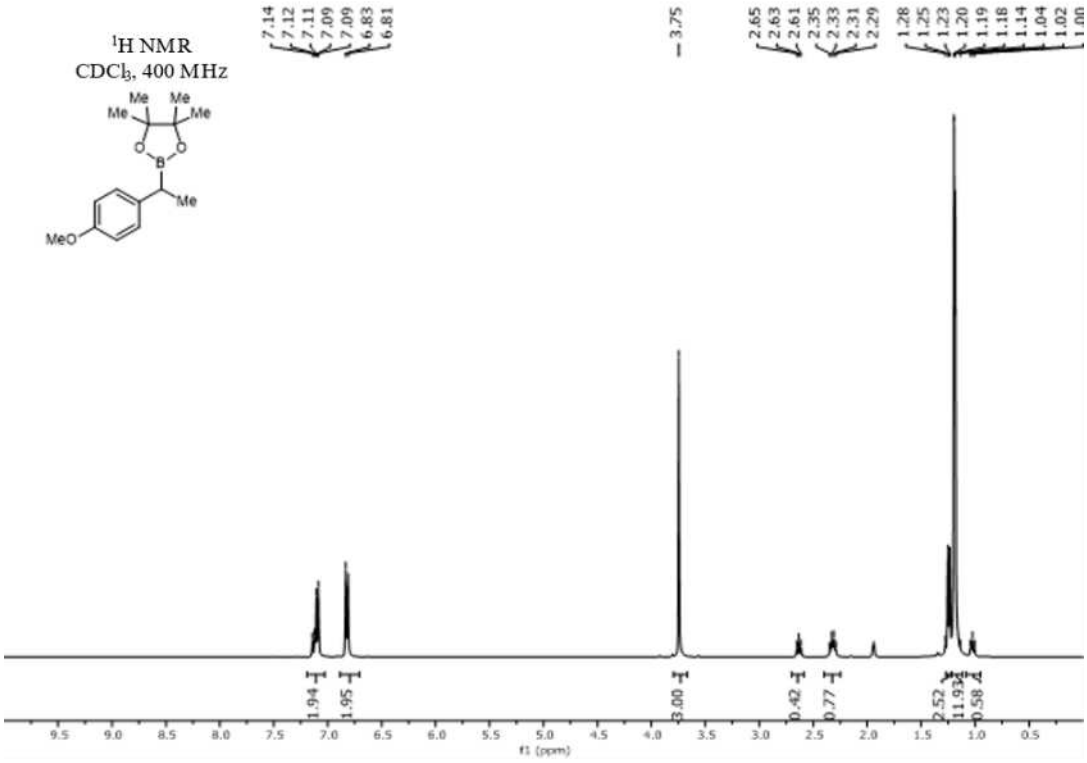
^{1}H NMR
$CDCl_3$, 400 MHz
7.14
7.12
7.11
7.09
7.09
6.83
6.81
3.75
2.65
2.63
2.61
2.35
2.33
2.31
2.29
1.28
1.25
1.23
1.20
1.19
1.18
1.14
1.04
1.02
1.00
Me
Me
Me
Me
Me
Me
B
O
O
MeO
1.94
1.95
3.00
0.42
0.77
2.52
11.93
0.58
f1 (ppm)

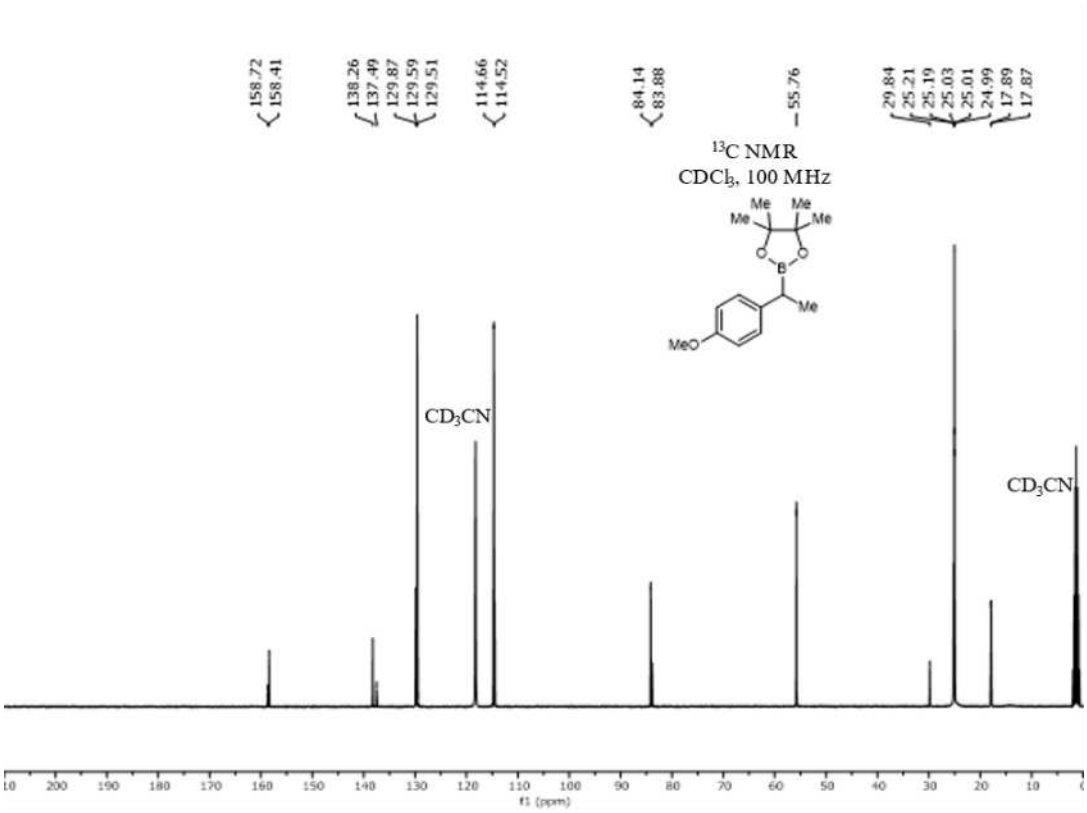
158.72
158.41
138.26
137.49
129.87
129.59
129.51
114.66
114.52
84.14
83.88
55.76
29.84
25.21
25.19
25.03
25.01
24.99
17.89
17.87
13C NMR
CDCl3, 100 MHz
Me
Me
Me
Me
B
Me
MeO
CD3CN
CD3CN
f1 (ppm)

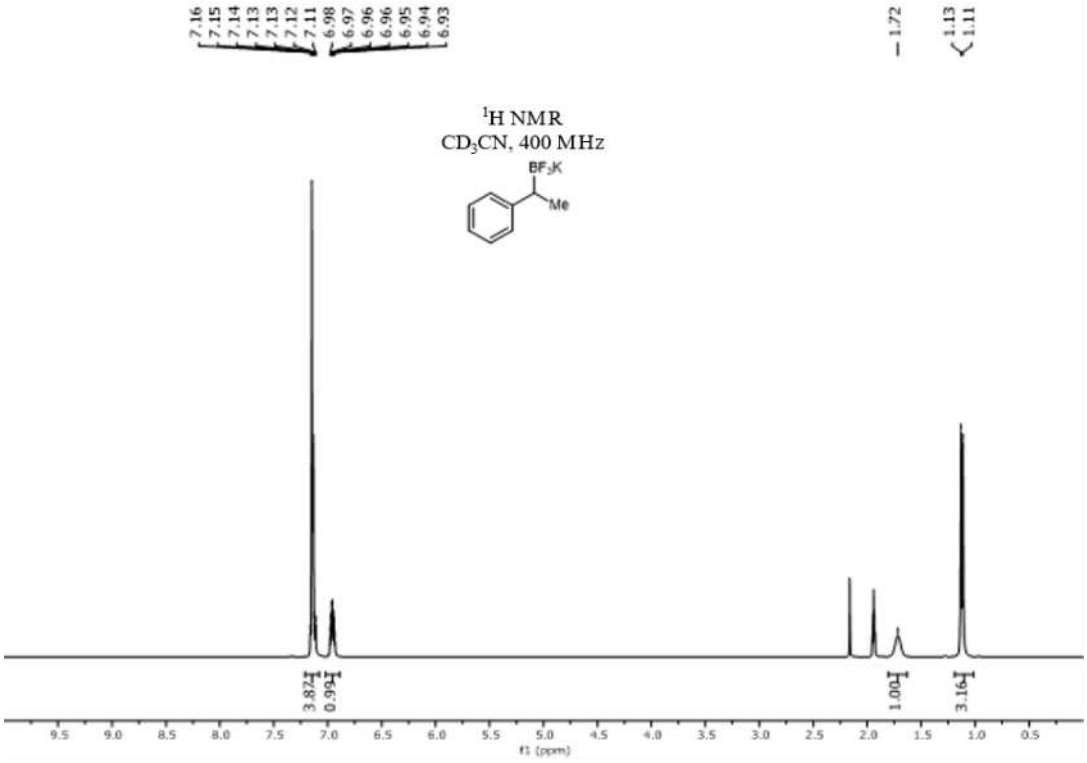
7.16
7.15
7.14
7.13
7.13
7.12
7.11
6.98
6.97
6.96
6.96
6.95
6.94
6.93
1.72
1.13
1.11
1H NMR
CD3CN, 400 MHz
BF3K
Me
3.82
0.99
1.00
3.16
f1 (ppm)

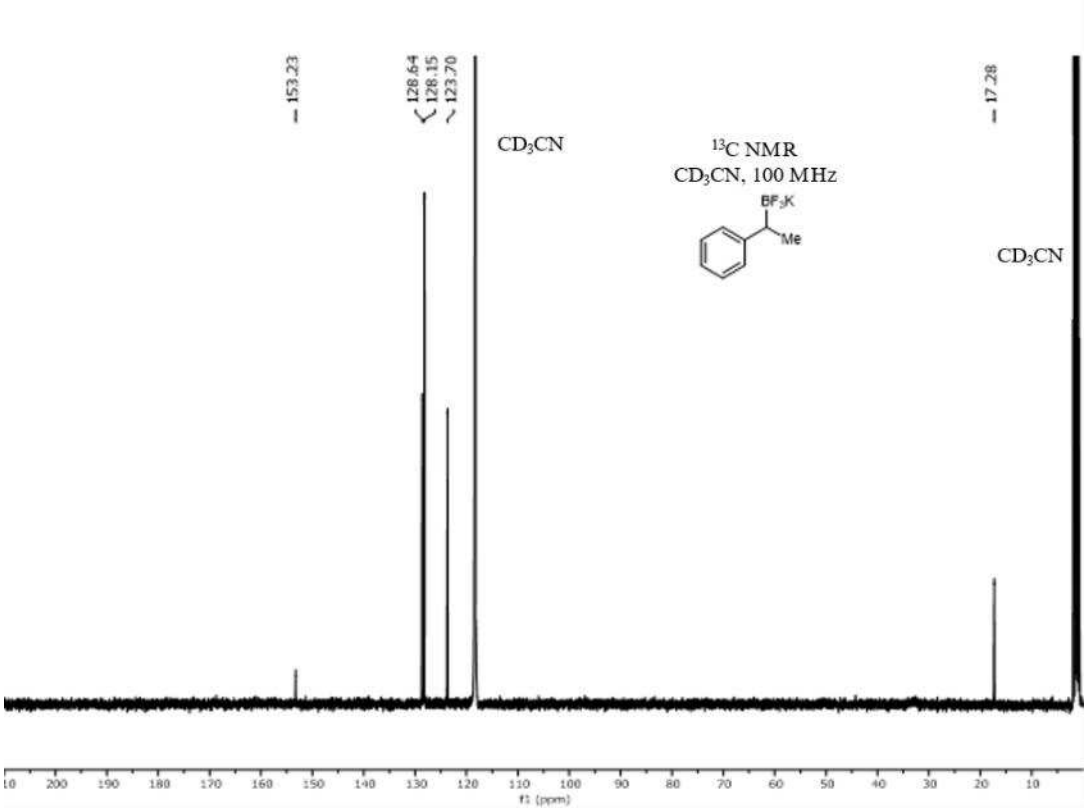
153.23
128.64
128.15
123.70
CD3CN
17.28
13C NMR
CD3CN, 100 MHz
BF3K
Me
CD3CN
f1 (ppm)

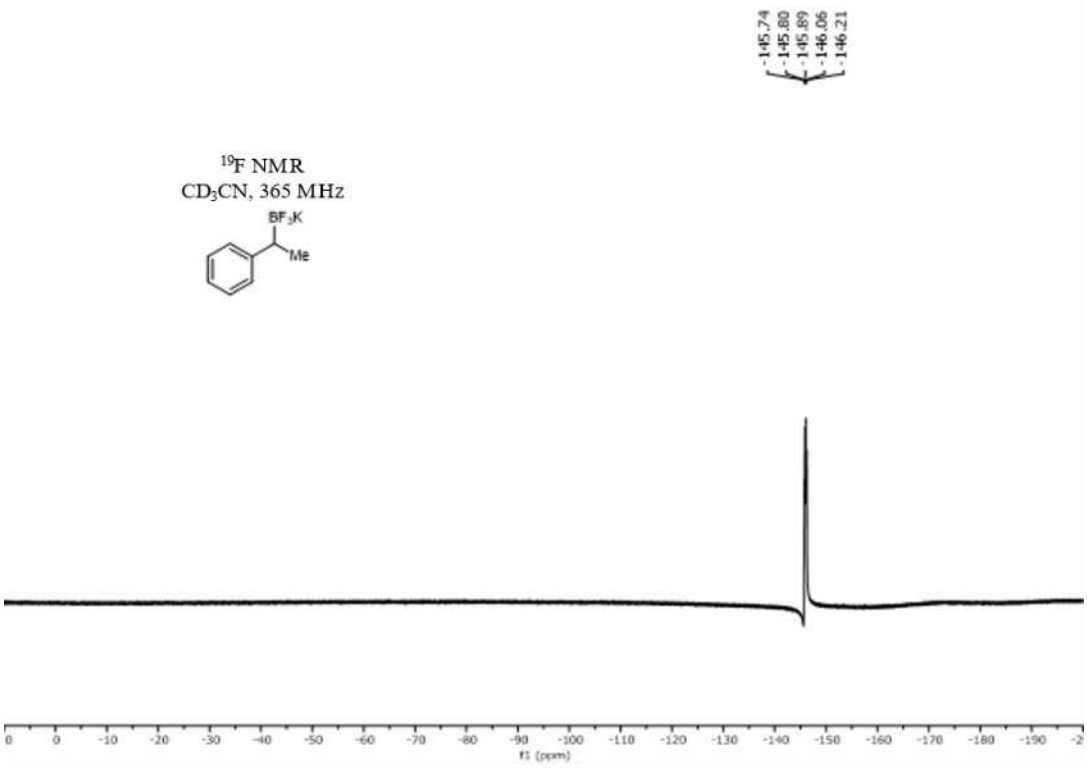
-145.74
-145.80
-145.89
-146.06
-146.21
19F NMR
CD3CN, 365 MHz
BF3K
Me
f1 (ppm)

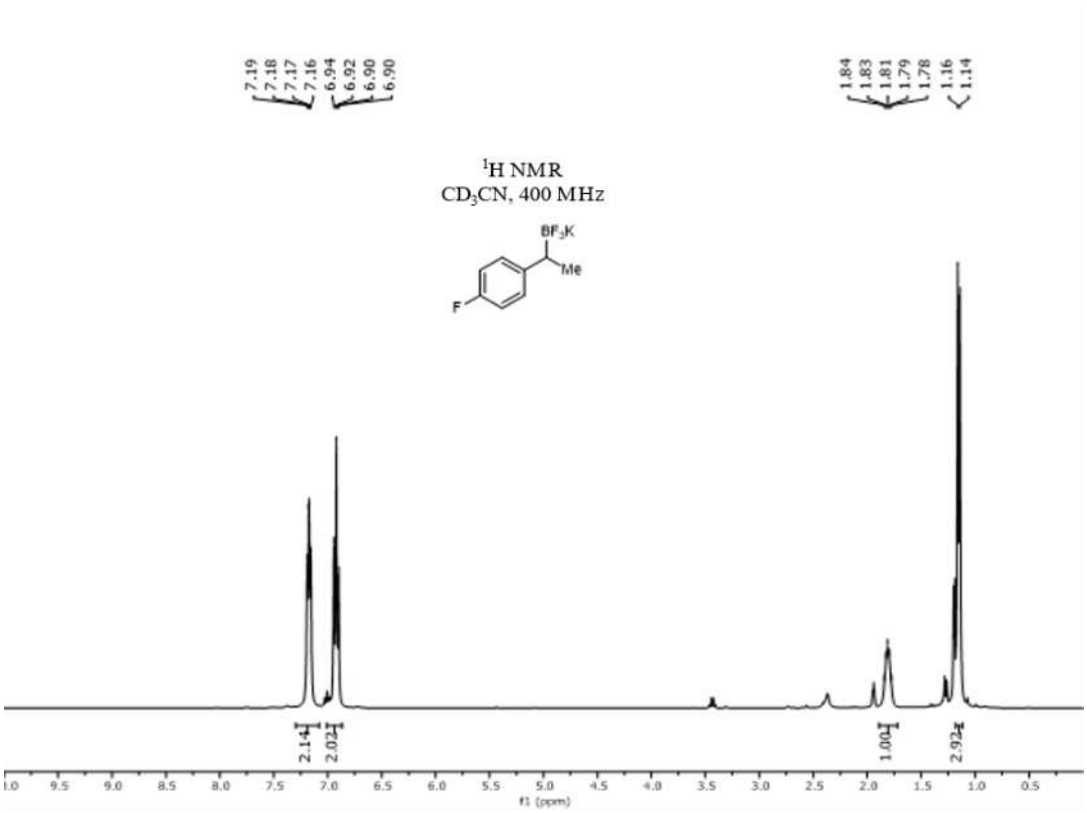
7.19
7.18
7.17
7.16
6.94
6.92
6.90
6.90
1.84
1.83
1.81
1.79
1.78
1.16
1.14
^{1}H NMR
CD_3CN, 400 MHz
BF_3K
Me
F
2.14
2.02
1.00
2.92
f1 (ppm)

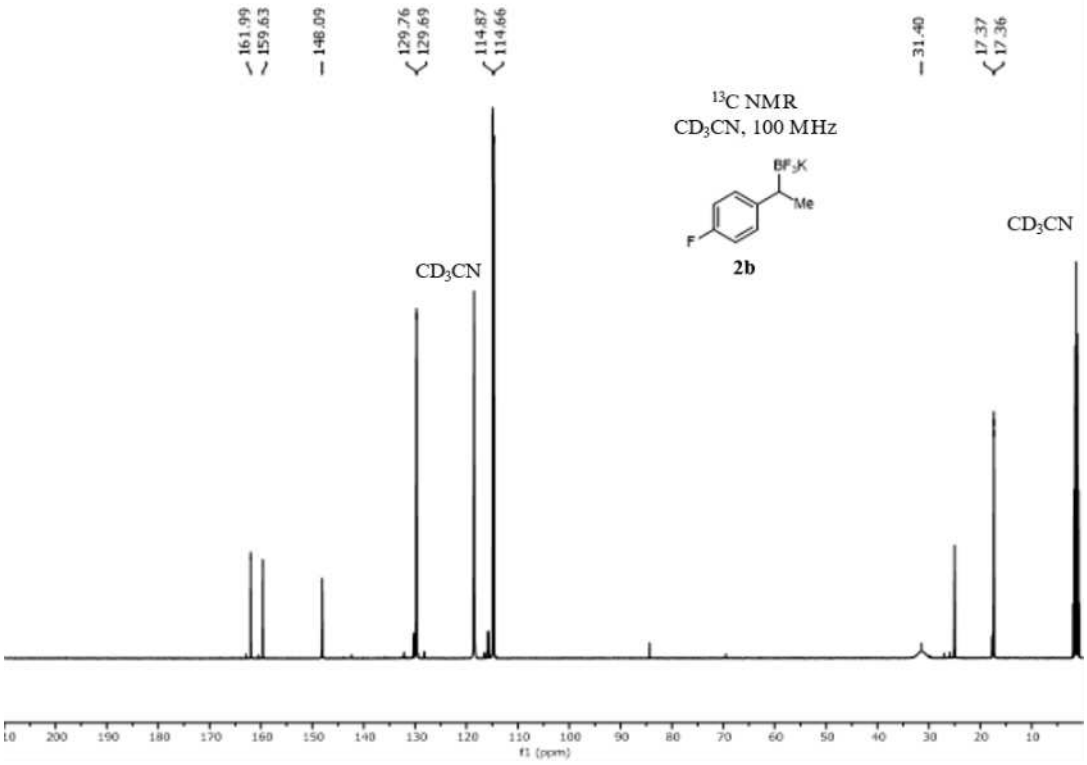
161.99
159.63
148.09
129.76
129.69
114.87
114.66
31.40
17.37
17.36
^{13}C NMR
CD_3CN, 100 MHz
BF_3K
Me
F
2b
CD_3CN
CD_3CN
f1 (ppm)

^{19}F NMR
CD_3CN, 365 MHz

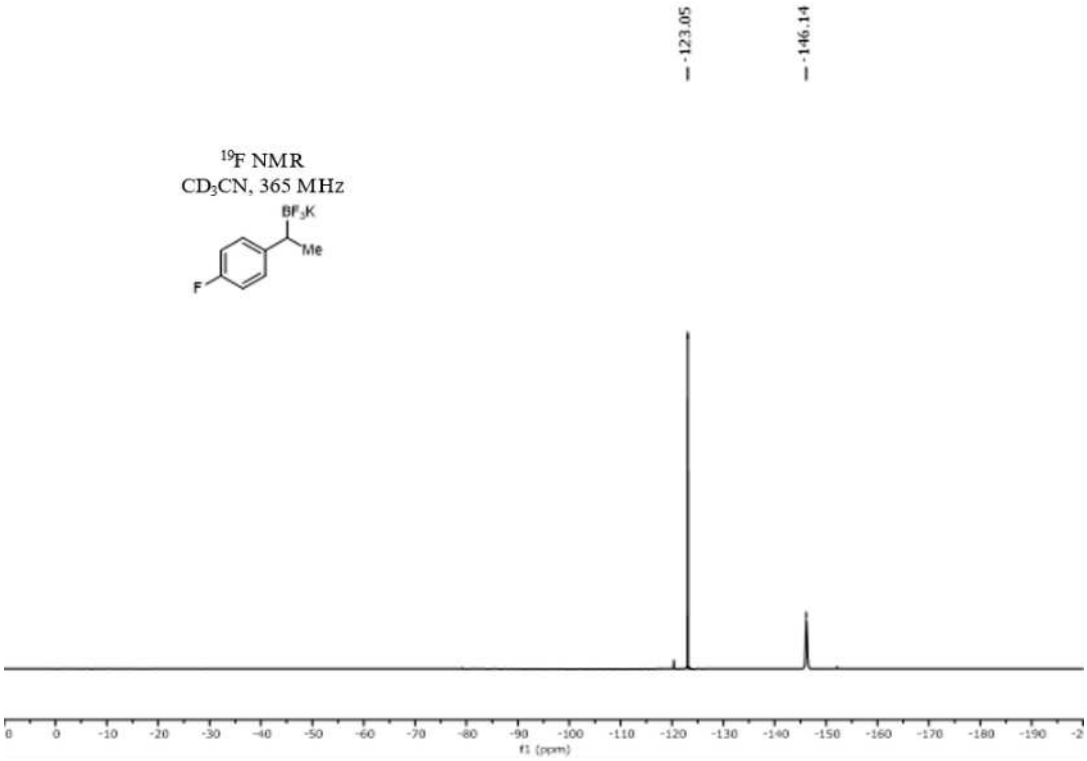

^{1}H NMR
CD_3CN, 400 MHz

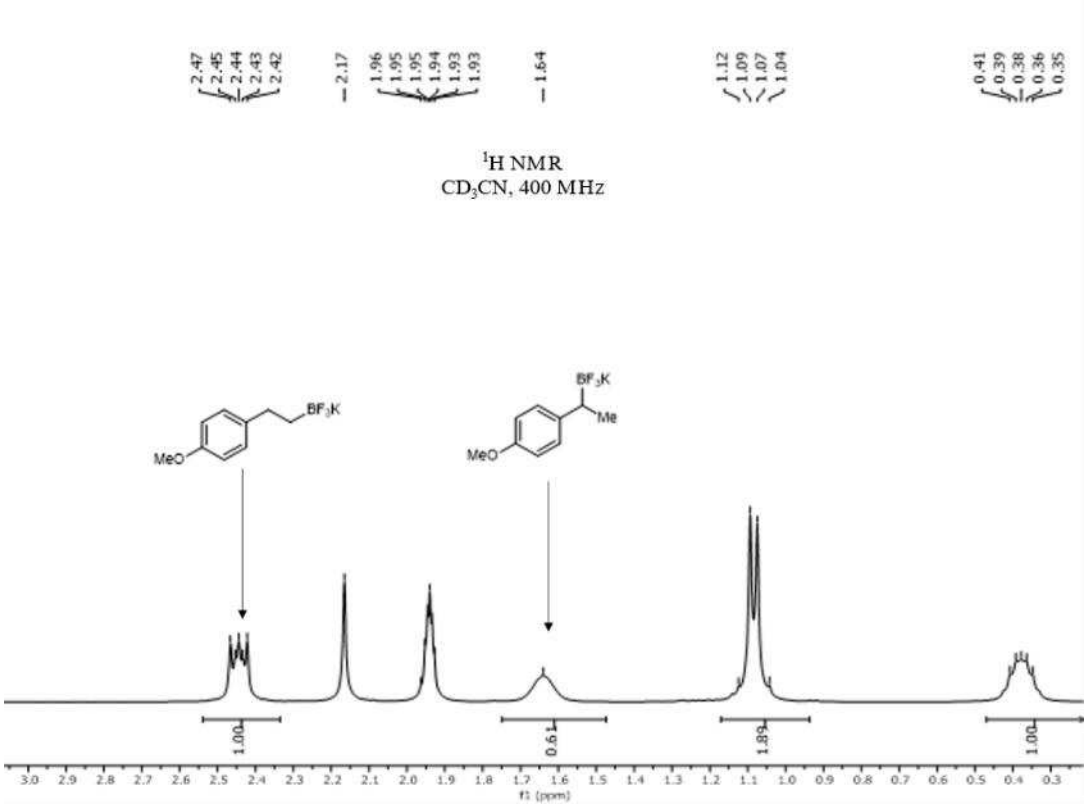

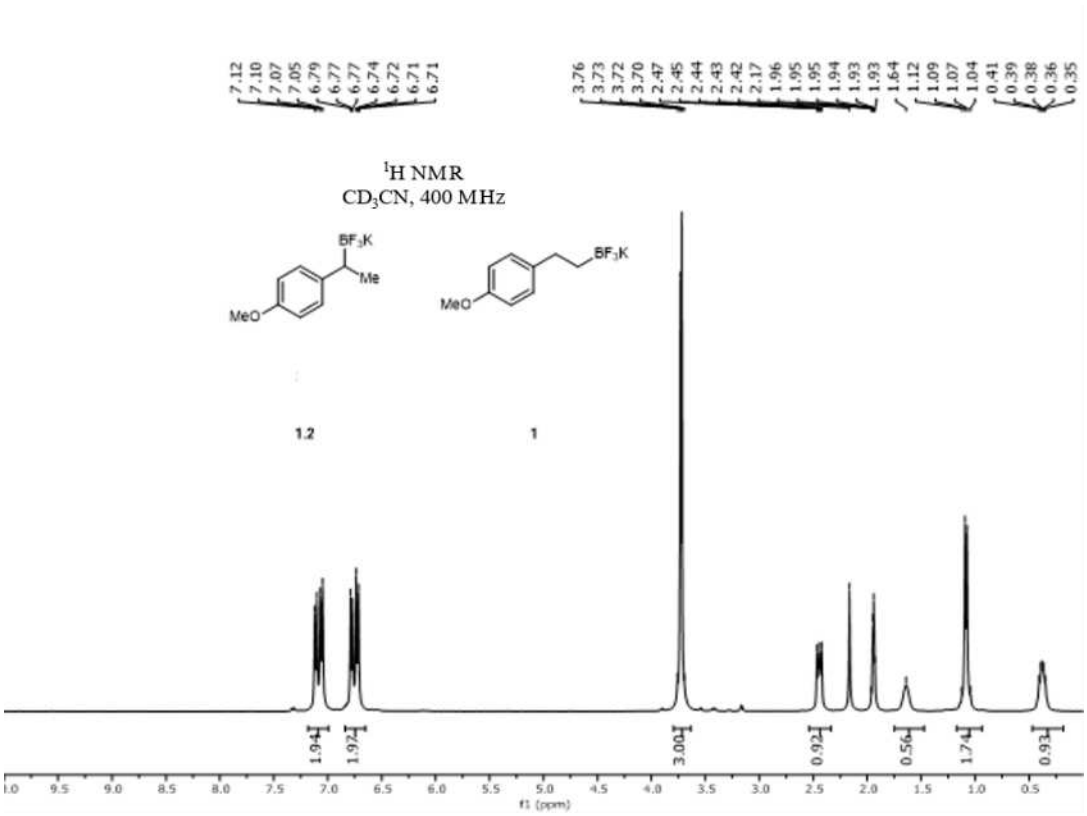
7.12
7.10
7.07
7.05
6.79
6.77
6.77
6.74
6.72
6.71
6.71
3.76
3.73
3.72
3.70
2.47
2.45
2.44
2.43
2.42
2.17
1.96
1.95
1.95
1.94
1.93
1.93
1.64
1.12
1.09
1.07
1.04
0.41
0.39
0.38
0.36
0.35
1H NMR
CD3CN, 400 MHz
BF3K
Me
MeO
BF3K
MeO
1.2
1
1.94
1.92
3.00
0.92
0.56
1.74
0.93
f1 (ppm)

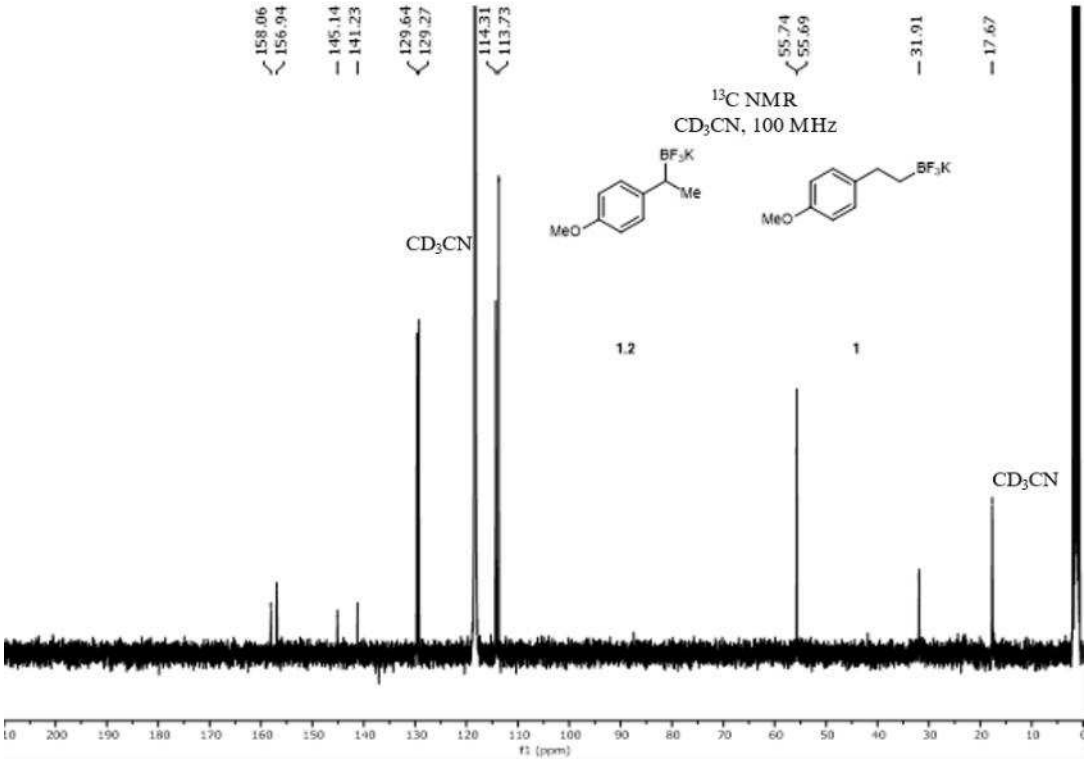
158.06
156.94
145.14
141.23
129.64
129.27
114.31
113.73
55.74
55.69
31.91
17.67
13C NMR
CD3CN, 100 MHz
BF3K
Me
MeO
BF3K
MeO
CD3CN
1.2
1
CD3CN
f1 (ppm)

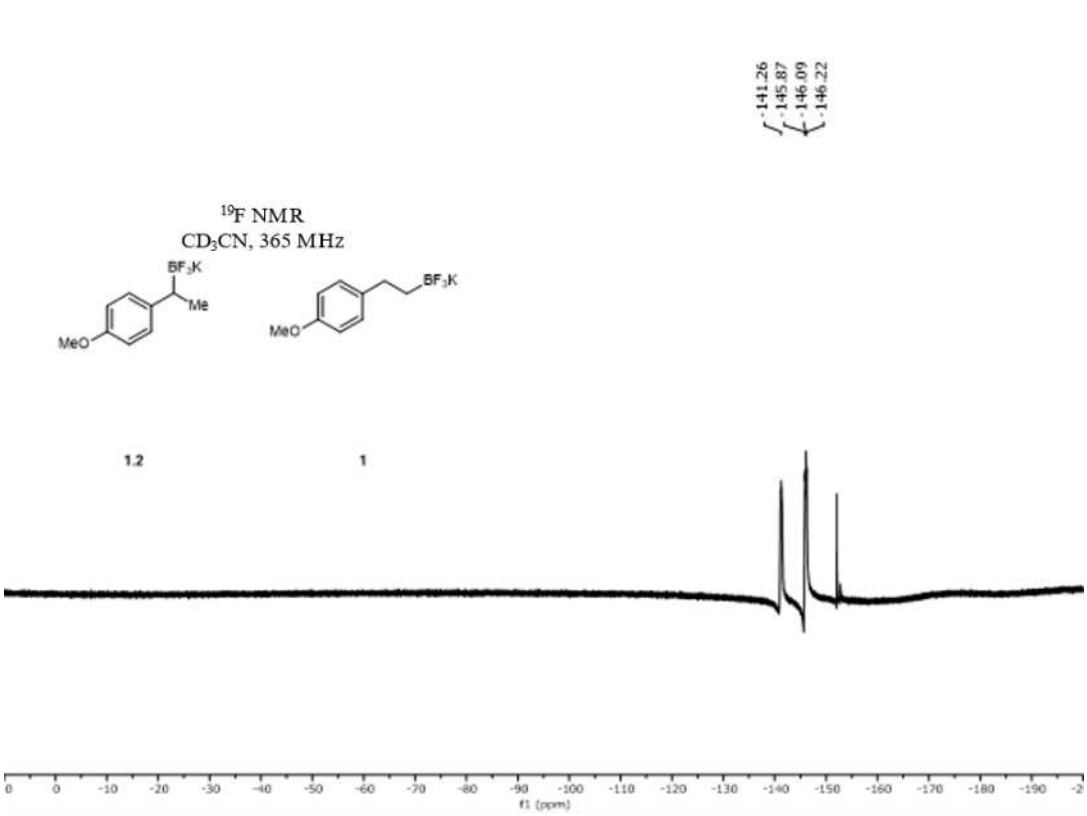
-141.26
-145.87
-146.09
-146.22
19F NMR
CD3CN, 365 MHz
BF3K
Me
MeO
BF3K
MeO
1.2
1
f1 (ppm)

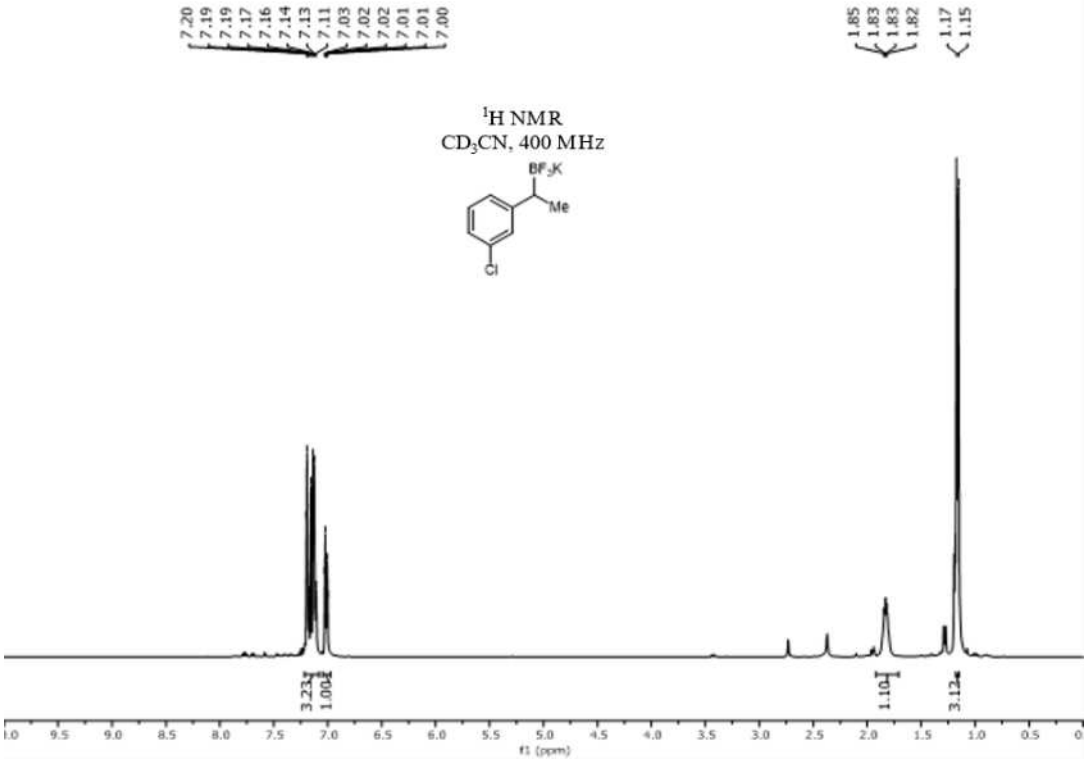
7.20
7.19
7.19
7.17
7.16
7.14
7.13
7.11
7.03
7.02
7.02
7.01
7.01
7.00
1.85
1.83
1.83
1.82
1.17
1.15
1H NMR
CD3CN, 400 MHz
BF3K
Me
Cl
3.23
1.00
1.10
3.12
f1 (ppm)

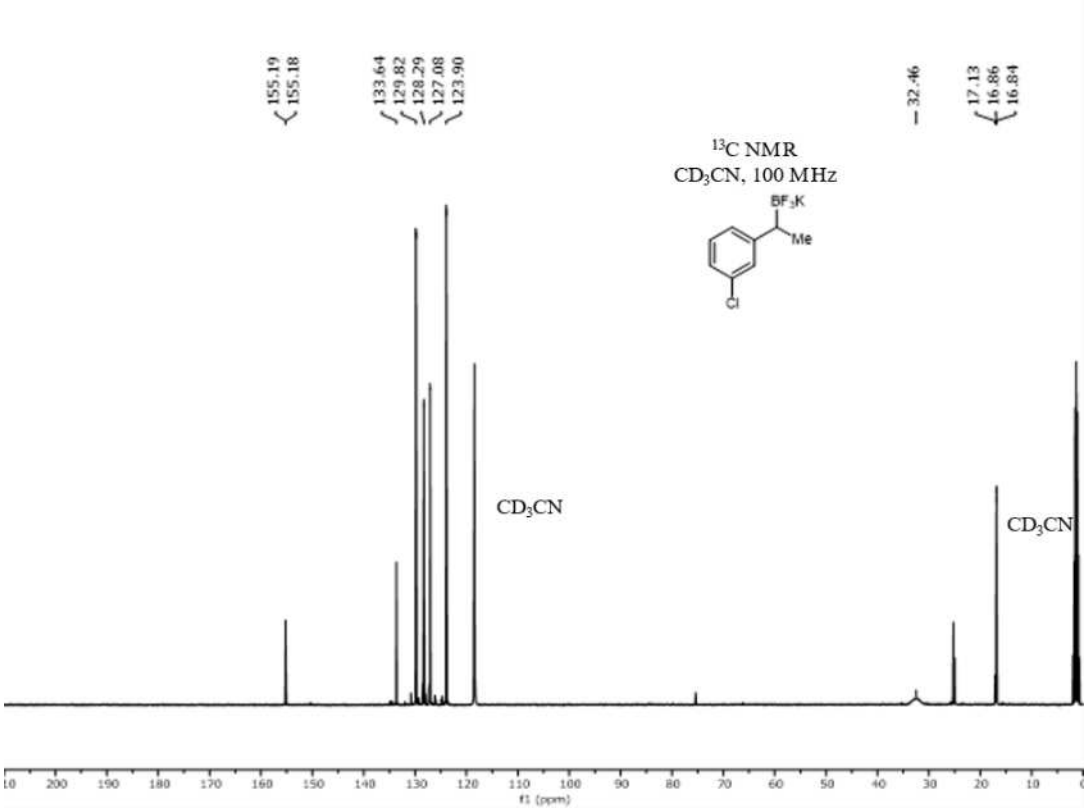
155.19
155.18
133.64
129.82
128.29
127.08
123.90
32.46
17.13
16.86
16.84
^{13}C NMR
CD_3CN, 100 MHz
BF_3K
Me
Cl
CD_3CN
CD_3CN
f1 (ppm)

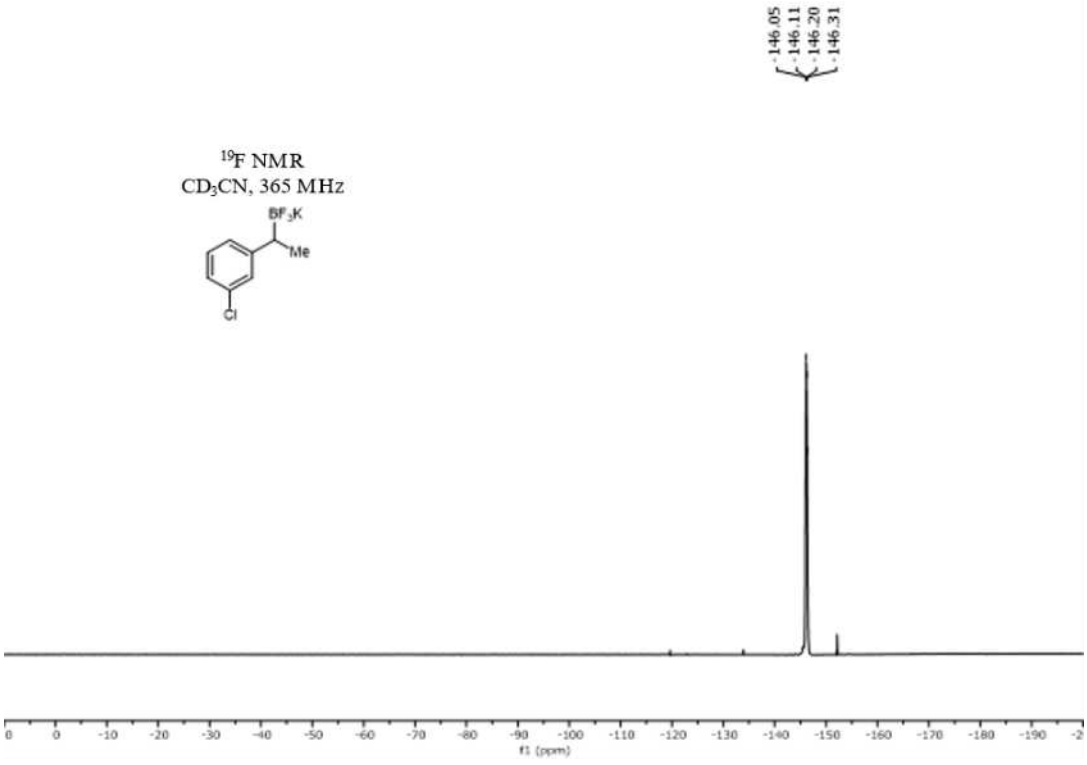
-146.05
-146.11
-146.20
-146.31
^{19}F NMR
CD_3CN, 365 MHz
BF_3K
Me
Cl
f1 (ppm)

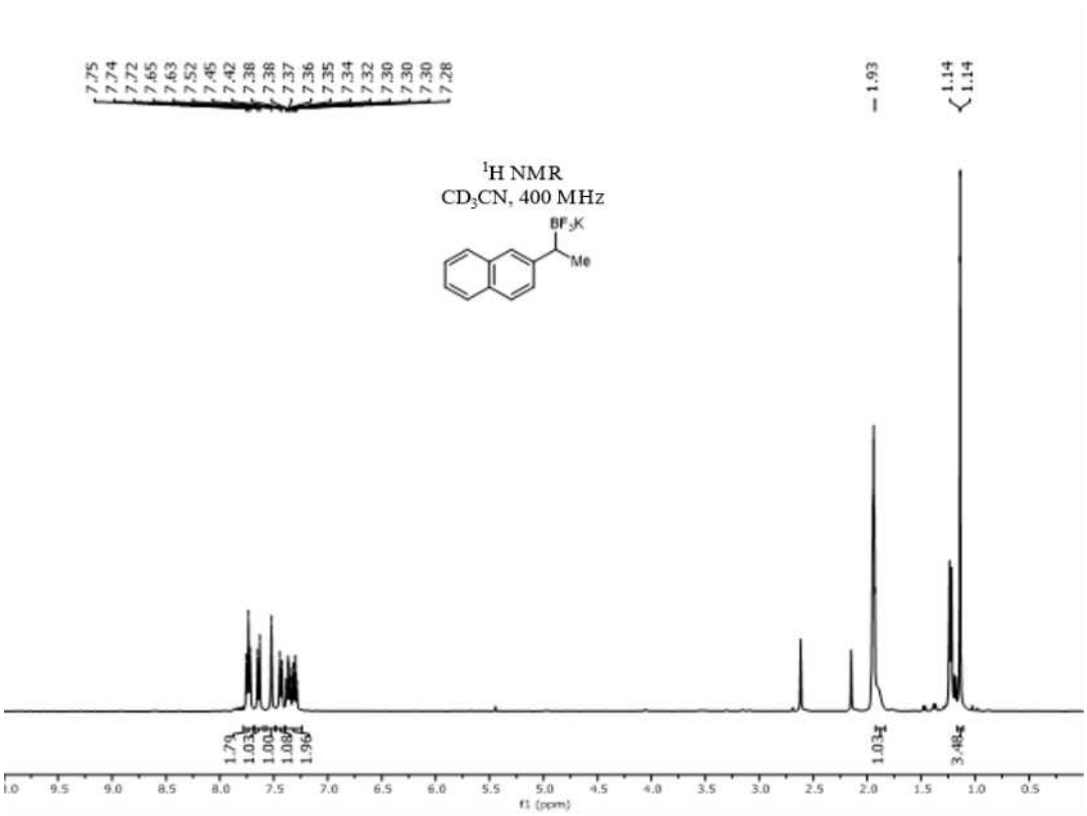
7.75
7.74
7.72
7.65
7.63
7.52
7.45
7.42
7.38
7.38
7.37
7.36
7.35
7.34
7.32
7.30
7.30
7.30
7.28
1.93
1.14
1.14
^{1}H NMR
CD_3CN, 400 MHz
BF_3K
Me
1.79
1.03
1.00
1.09
1.96
1.03
3.48
f1 (ppm)

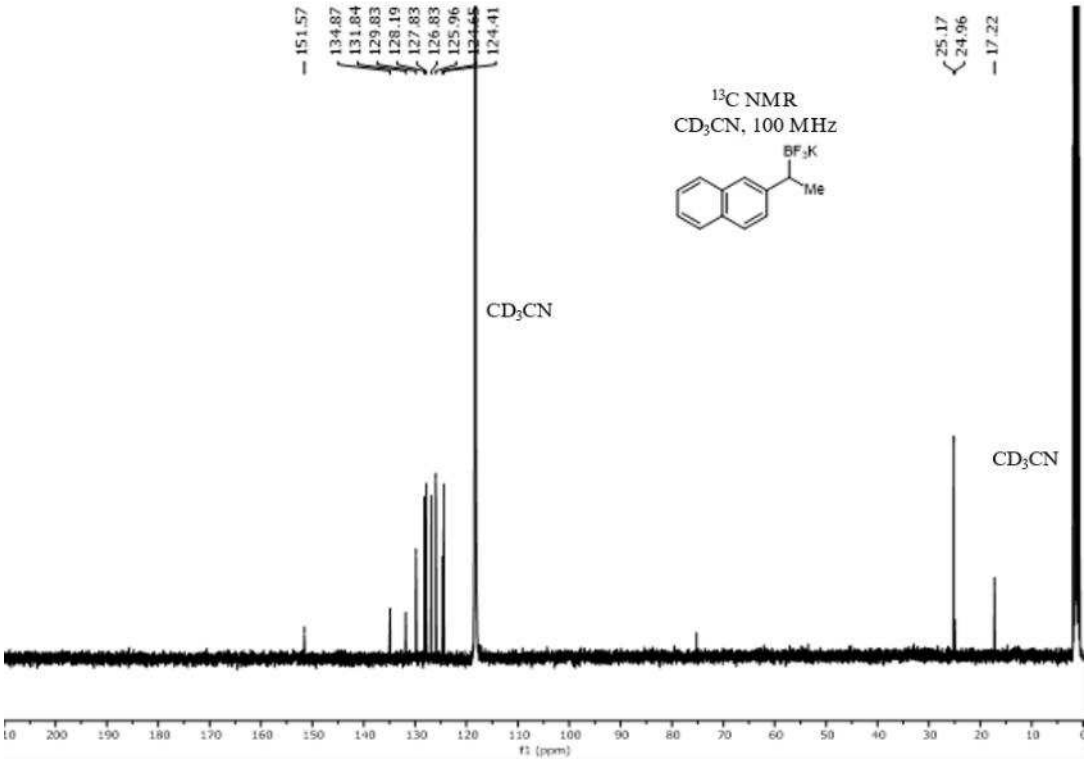
151.57
134.87
131.84
129.83
128.19
127.83
126.83
125.96
124.65
124.41
25.17
24.96
17.22
^{13}C NMR
CD_3CN, 100 MHz
BF_3K
Me
CD_3CN
CD_3CN
f1 (ppm)

^{19}F NMR
CD_3CN, 365 MHz

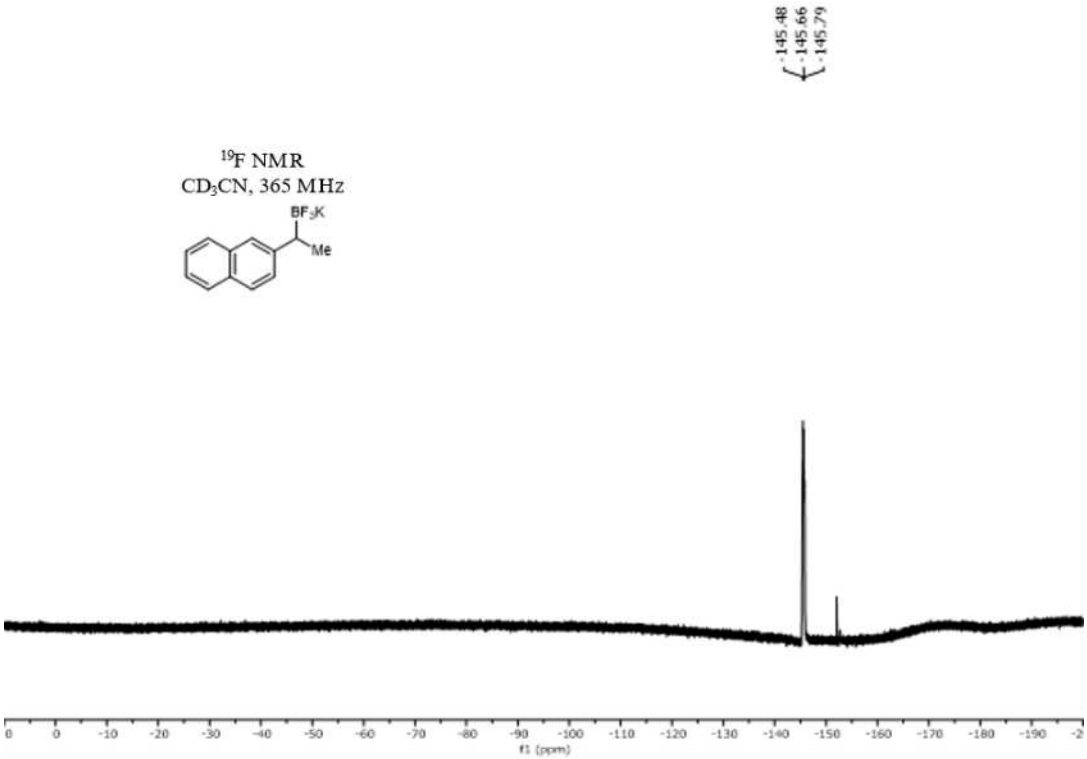

^{1}H NMR
$CDCl_3$, 400 MHz

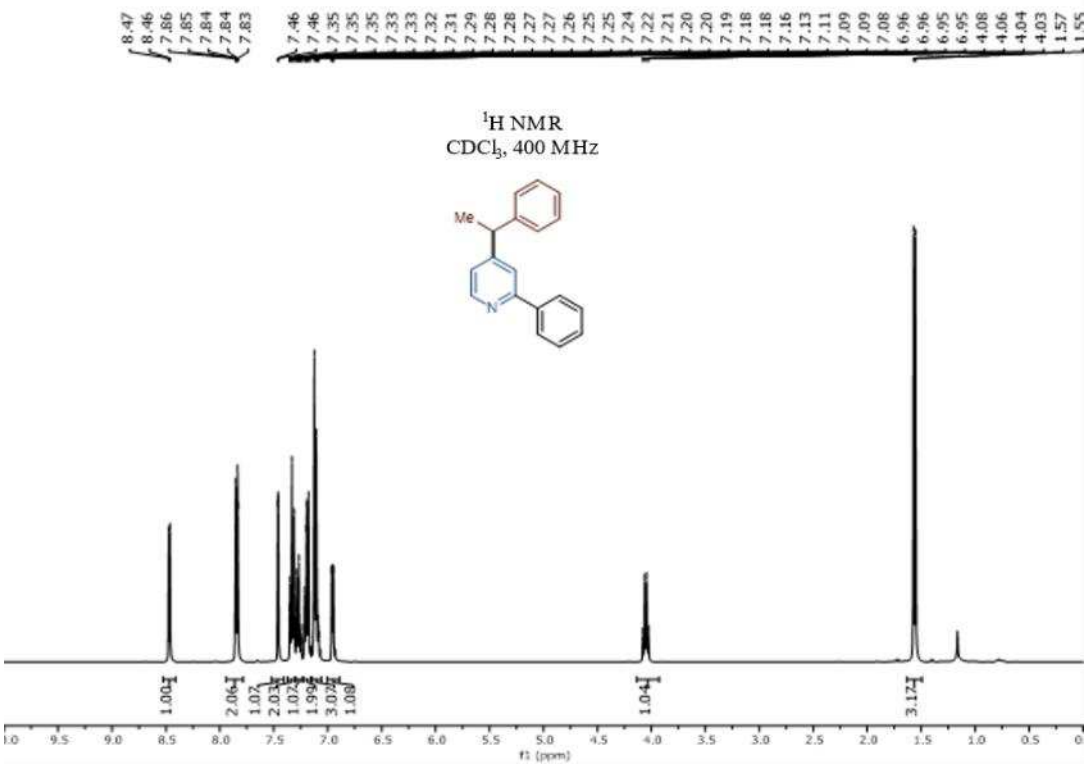

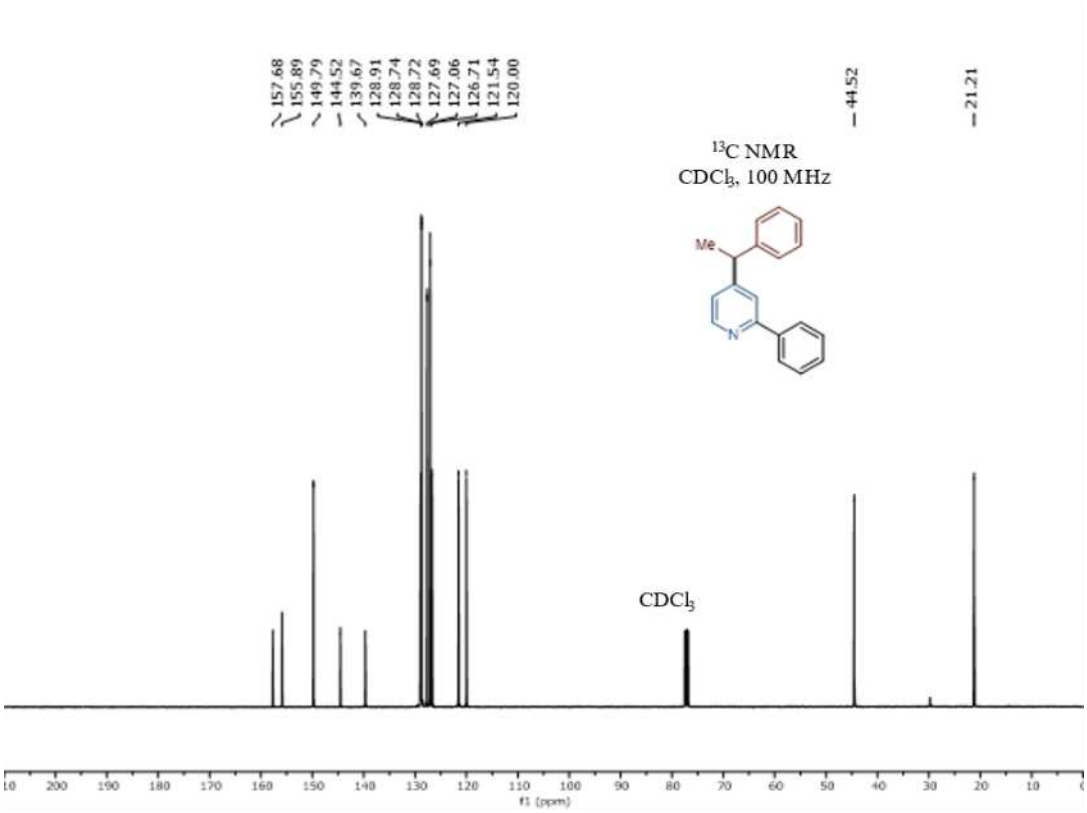
157.68
155.89
149.79
144.52
139.67
128.91
128.74
128.72
127.69
127.06
126.71
121.54
120.00
44.52
21.21
^{13}C NMR
$CDCl_3$, 100 MHz
Me
N
$CDCl_3$
f1 (ppm)

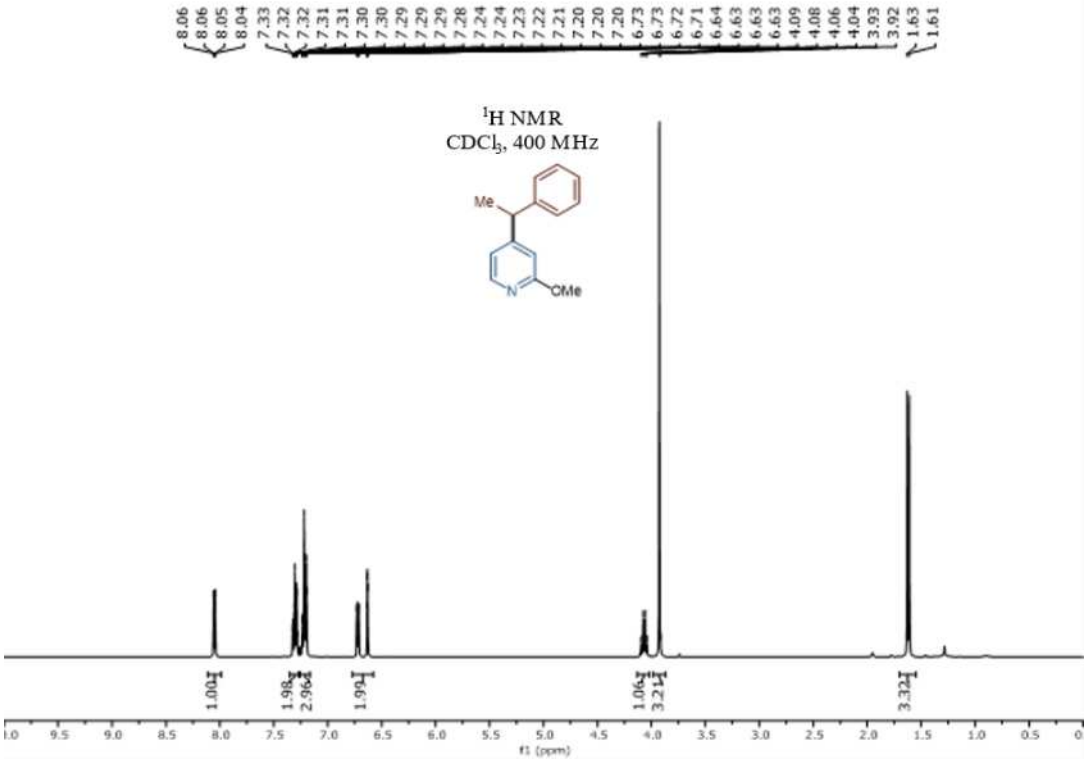
8.06
8.06
8.05
8.04
7.33
7.32
7.32
7.31
7.31
7.30
7.30
7.29
7.29
7.29
7.28
7.24
7.24
7.23
7.22
7.21
7.20
7.20
7.20
6.73
6.73
6.72
6.71
6.64
6.63
6.63
6.63
4.09
4.08
4.06
4.04
3.93
3.92
1.63
1.61
^{1}H NMR
$CDCl_3$, 400 MHz
Me
N
OMe
1.00
1.98
2.96
1.99
1.06
3.21
3.32
f1 (ppm)

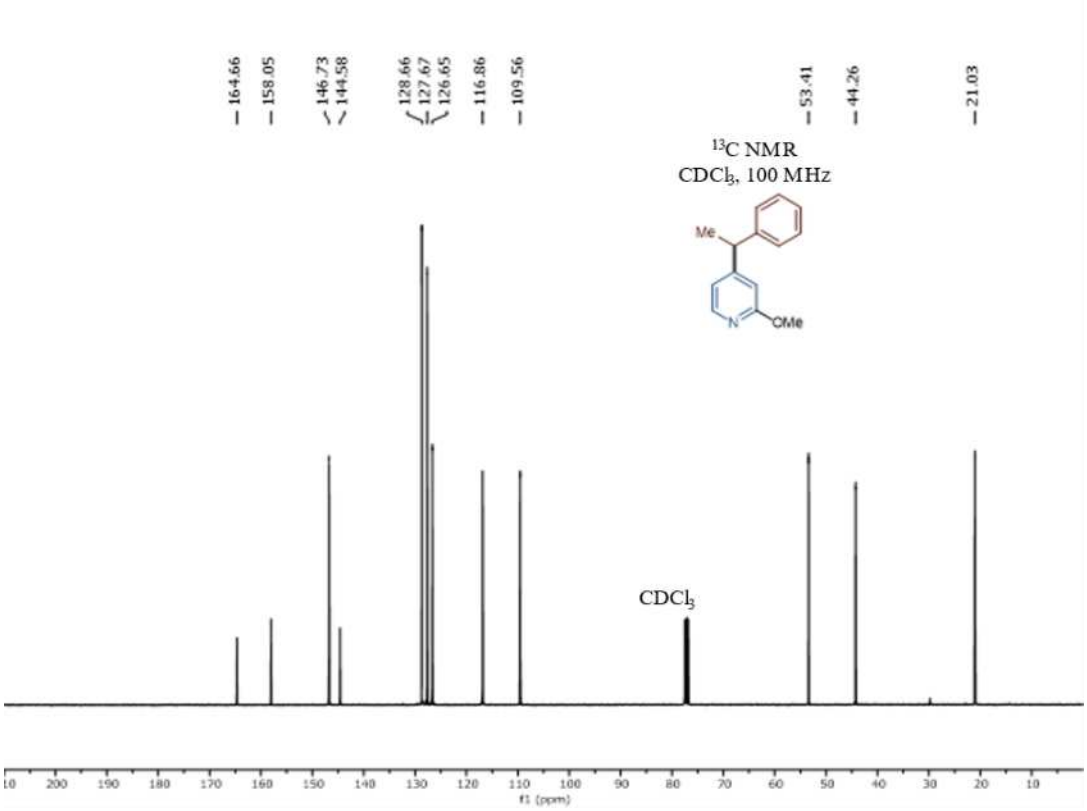
164.66
158.05
146.73
144.58
128.66
127.67
126.65
116.86
109.56
53.41
44.26
21.03
^{13}C NMR
$CDCl_3$, 100 MHz
Me
N
OMe
$CDCl_3$
f1 (ppm)

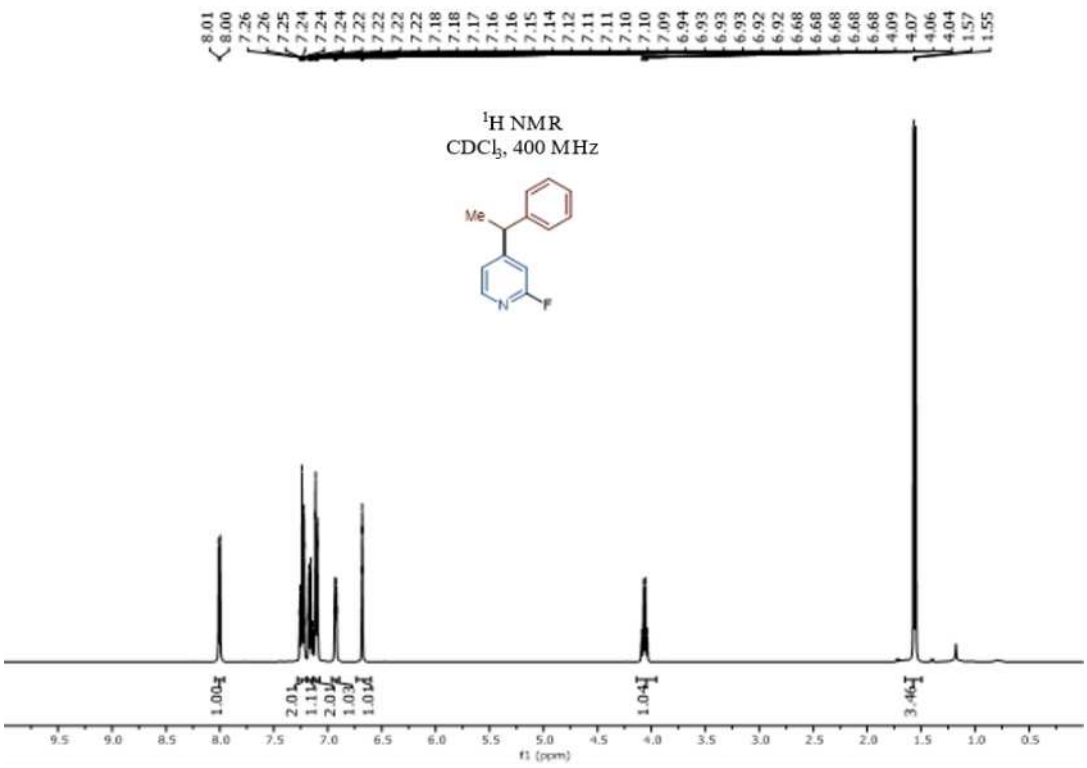
8.01
8.00
7.26
7.26
7.25
7.24
7.24
7.24
7.22
7.22
7.22
7.22
7.18
7.18
7.17
7.16
7.16
7.15
7.14
7.12
7.11
7.11
7.10
7.10
7.09
6.94
6.93
6.93
6.93
6.92
6.92
6.68
6.68
6.68
6.68
6.68
4.09
4.07
4.06
4.04
1.57
1.55
^{1}H NMR
$CDCl_3$, 400 MHz
Me
N
F
1.00
2.01
1.11
2.03
1.03
1.01
1.04
3.46
f1 (ppm)

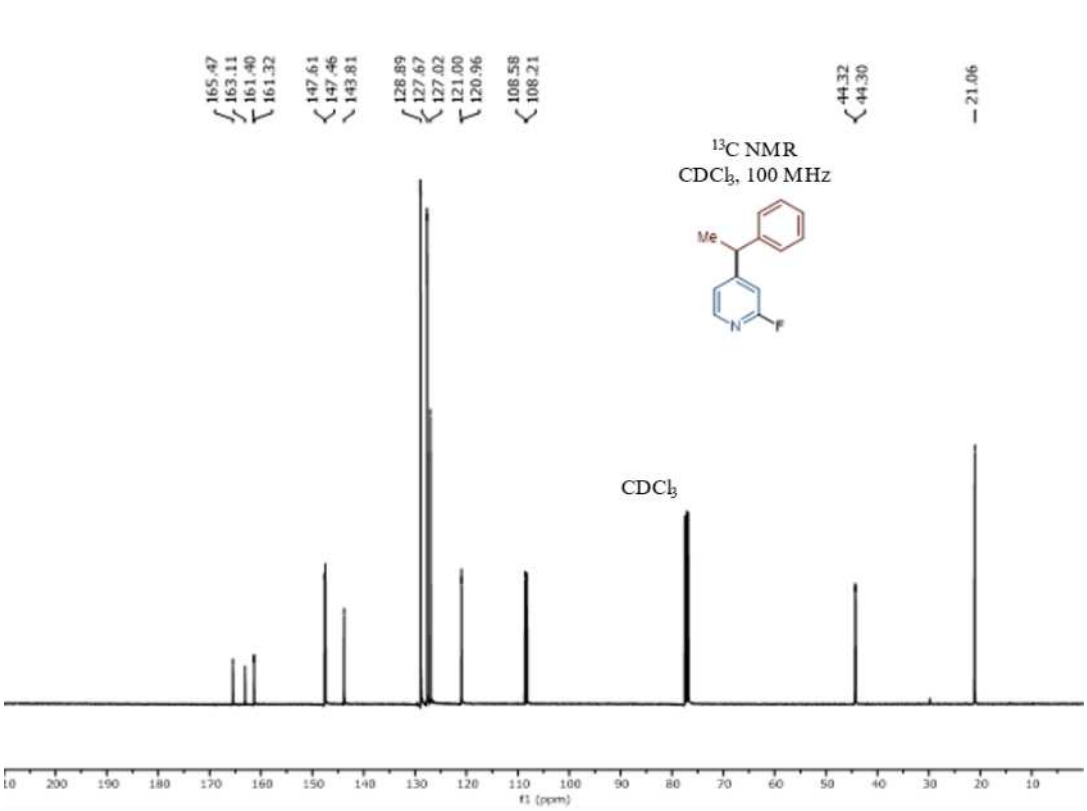
165.47
163.11
161.40
161.32
147.61
147.46
143.81
128.89
127.67
127.02
121.00
120.96
108.58
108.21
44.32
44.30
21.06
^{13}C NMR
$CDCl_3$, 100 MHz
Me
N
F
$CDCl_3$
f1 (ppm)

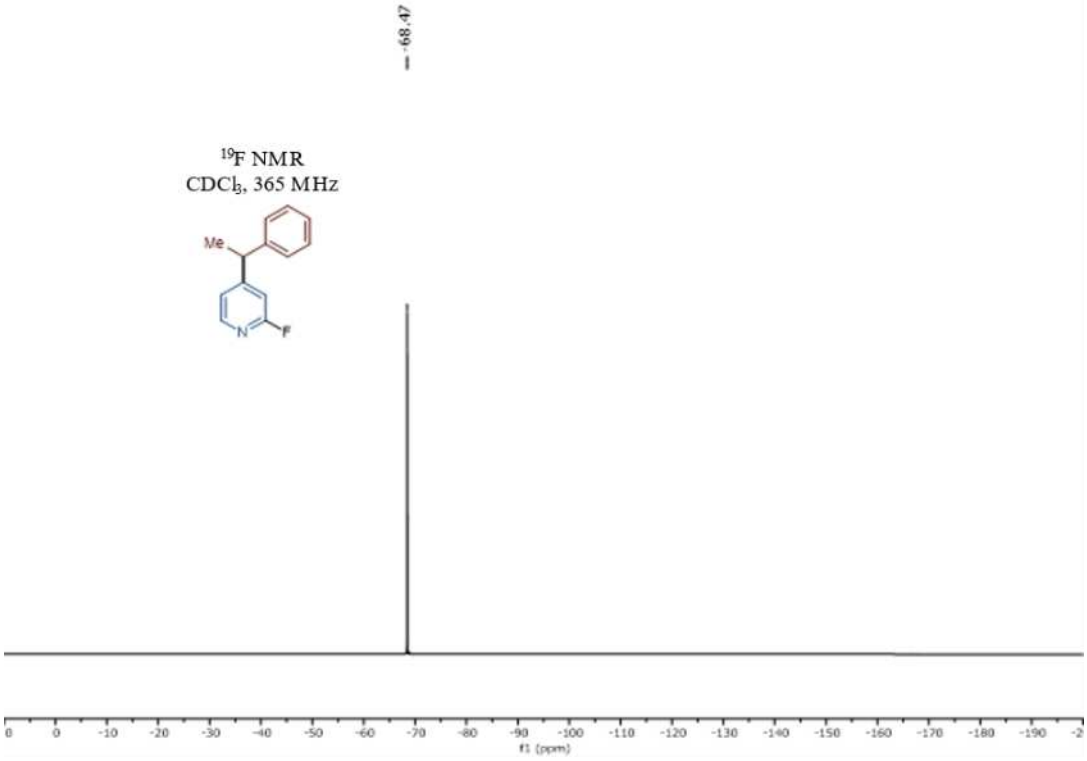
-68.47
^{19}F NMR
$CDCl_3$, 365 MHz
Me
N
F
f1 (ppm)

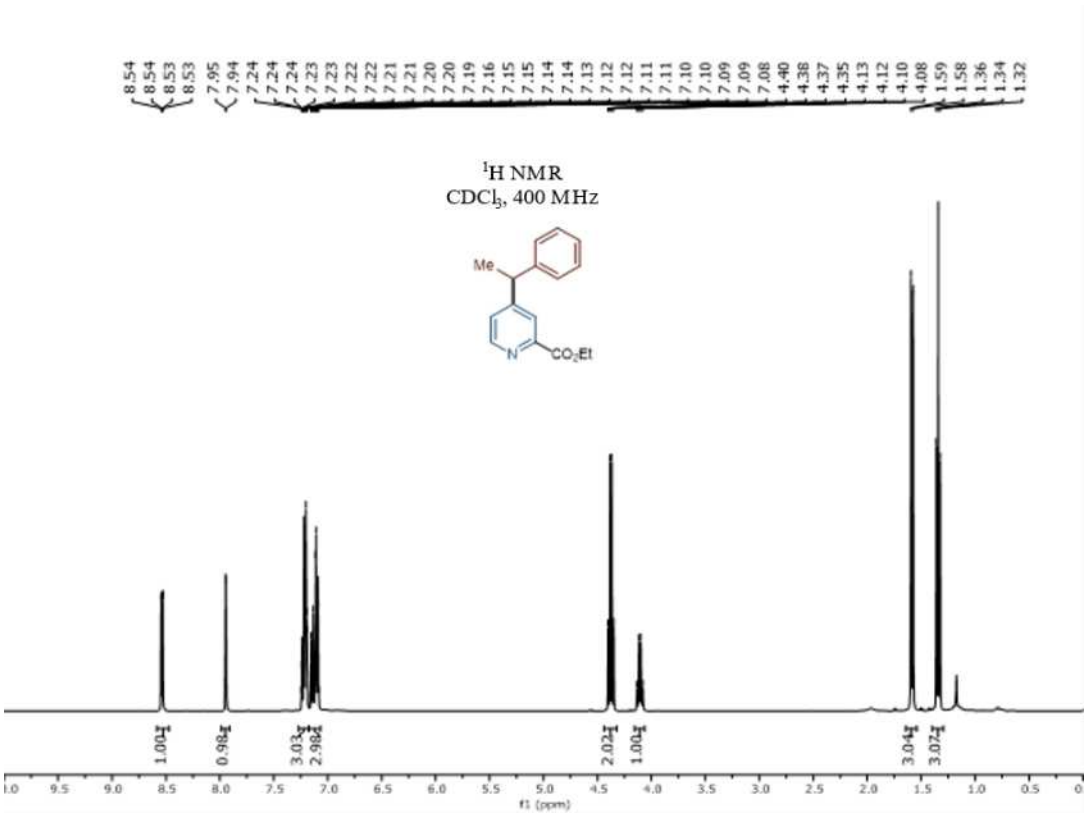
8.54
8.54
8.53
8.53
7.95
7.94
7.24
7.24
7.24
7.23
7.23
7.22
7.22
7.21
7.21
7.20
7.20
7.19
7.16
7.15
7.15
7.14
7.14
7.13
7.12
7.12
7.11
7.11
7.10
7.10
7.09
7.09
7.08
4.40
4.38
4.37
4.35
4.13
4.12
4.10
4.08
1.59
1.58
1.36
1.34
1.32
1H NMR
CDCl3, 400 MHz
Me
N
CO2Et
1.00
0.98
3.03
2.98
2.02
1.00
3.04
3.07
f1 (ppm)

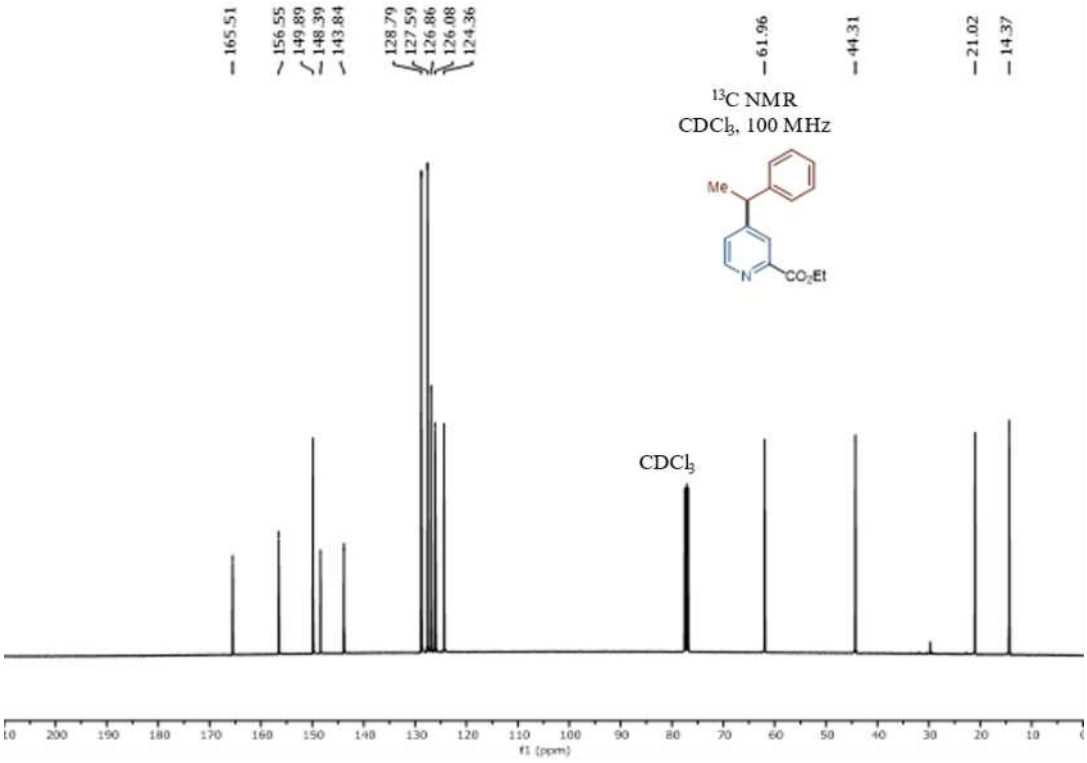
165.51
156.55
149.89
148.39
143.84
128.79
127.59
126.86
126.08
124.36
61.96
44.31
21.02
14.37
13C NMR
CDCl3, 100 MHz
Me
N
CO2Et
CDCl3
f1 (ppm)

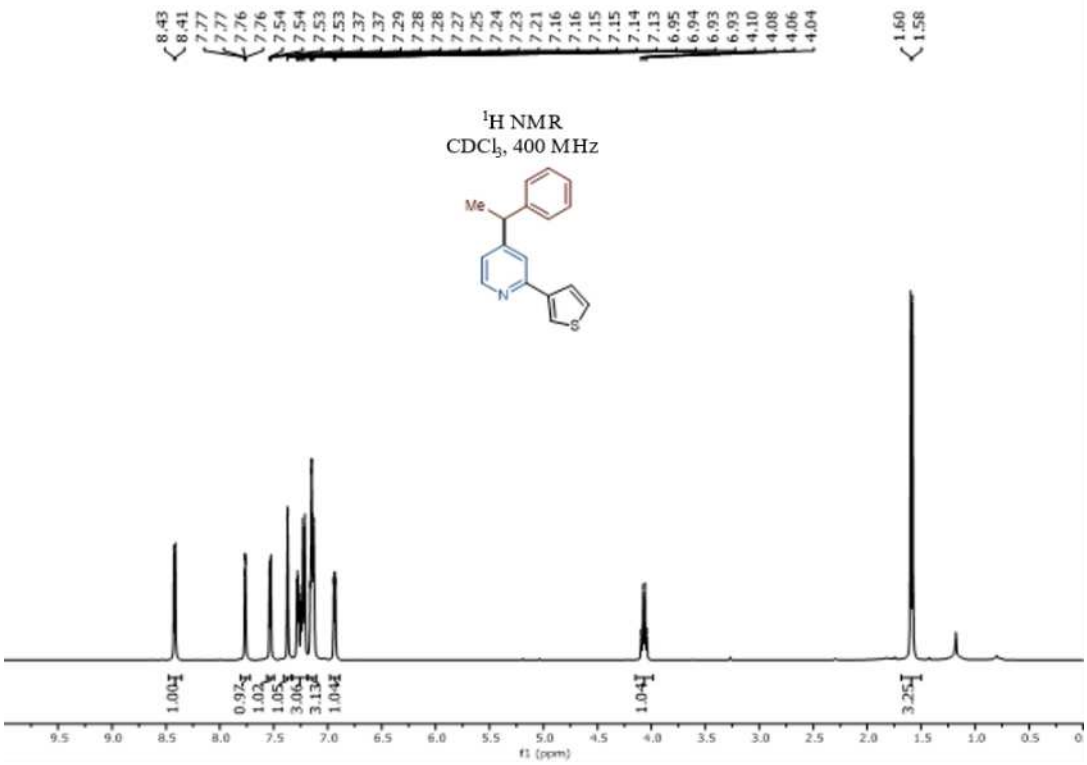
8.43
8.41
7.77
7.77
7.76
7.76
7.54
7.54
7.53
7.53
7.37
7.37
7.29
7.28
7.28
7.27
7.25
7.24
7.23
7.21
7.16
7.16
7.15
7.15
7.14
7.13
6.95
6.94
6.93
6.93
4.10
4.08
4.06
4.04
1.60
1.58
1H NMR
CDCl3, 400 MHz
Me
N
S
1.00
0.92
1.02
1.05
3.06
3.13
1.04
1.04
3.25
f1 (ppm)

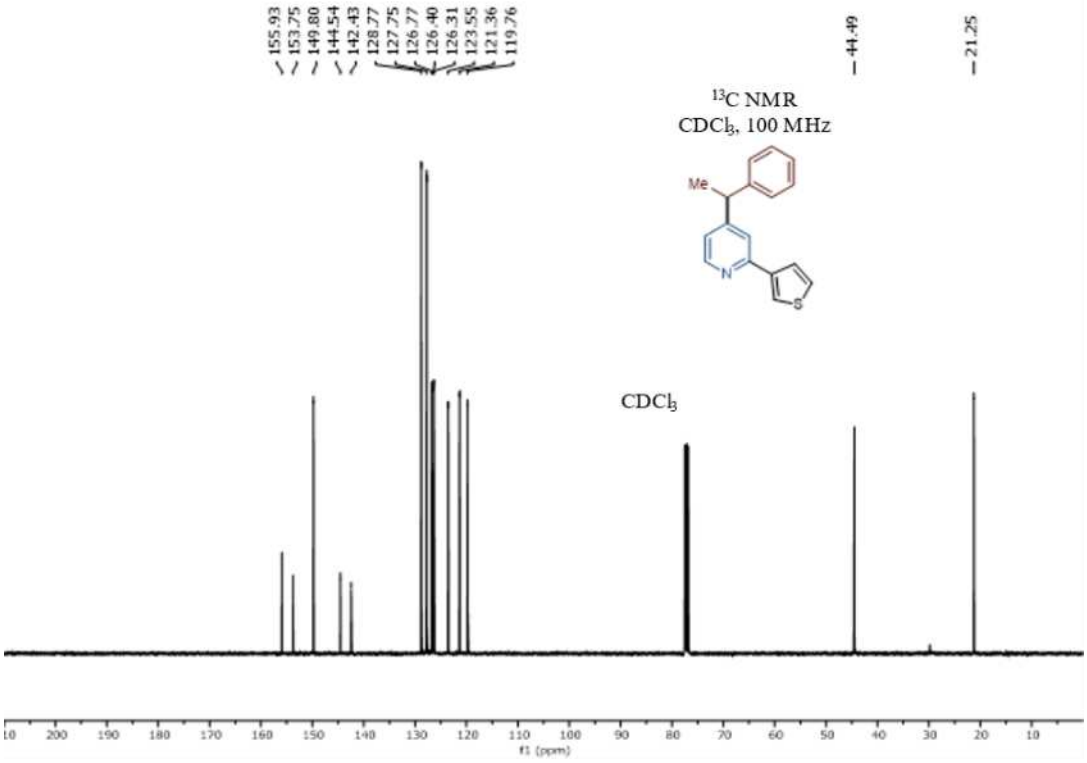
155.93
153.75
149.80
144.54
142.43
128.77
127.75
126.77
126.40
126.31
123.55
121.36
119.76
44.49
21.25
13C NMR
CDCl3, 100 MHz
Me
N
S
CDCl3
f1 (ppm)

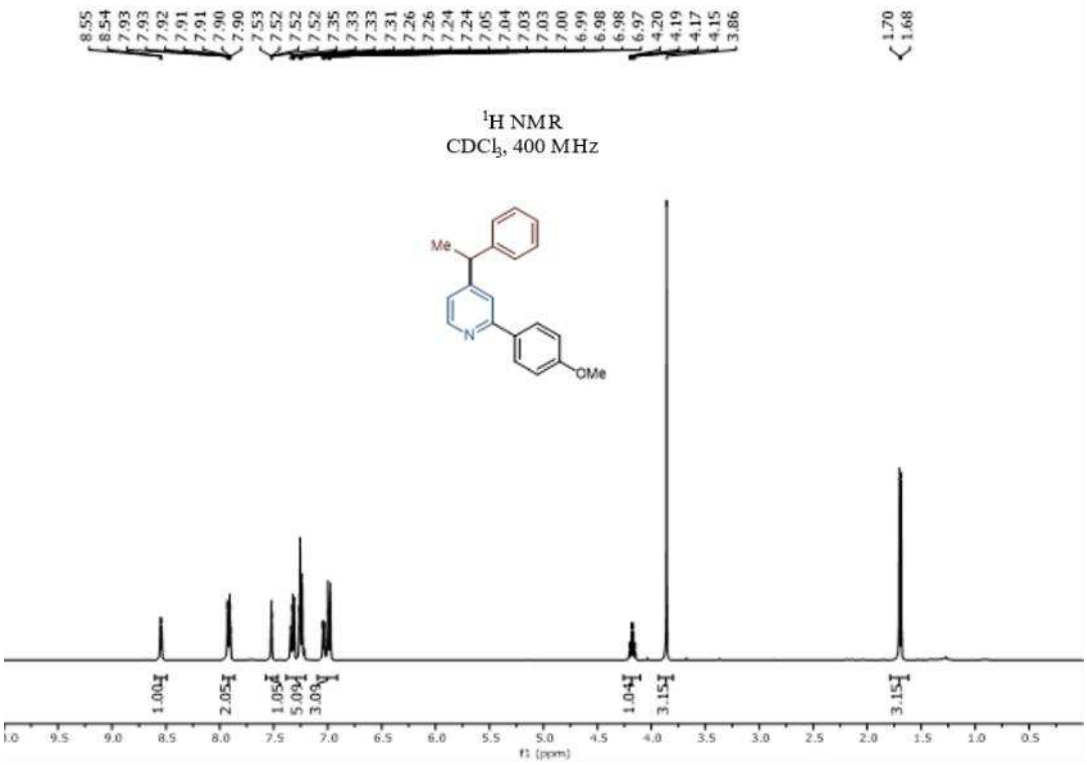

^{1}H NMR
$CDCl_3$, 400 MHz

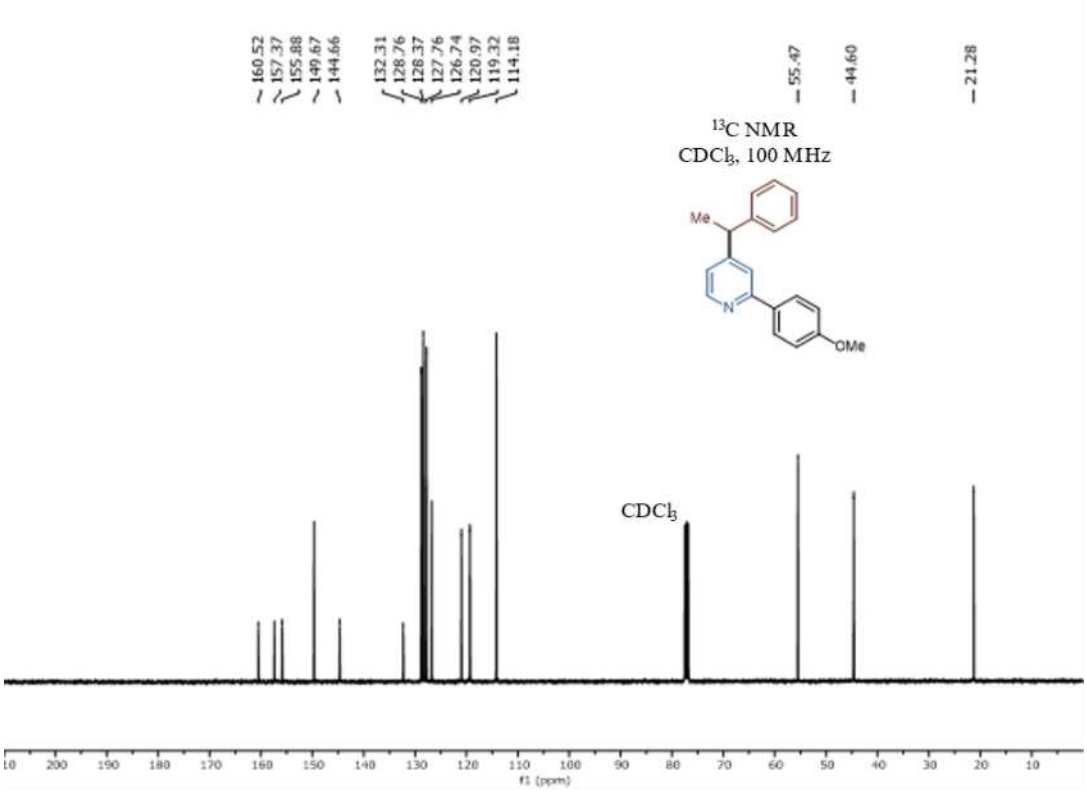

^{13}C NMR
$CDCl_3$, 100 MHz

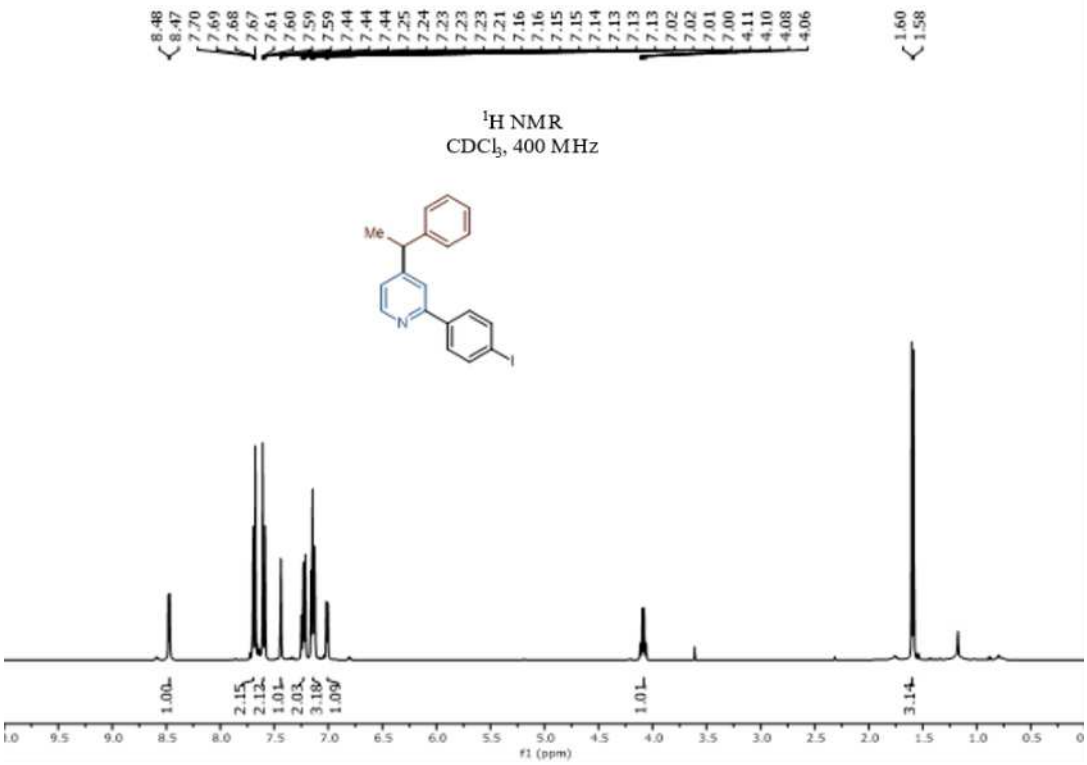

^{1}H NMR
$CDCl_3$, 400 MHz

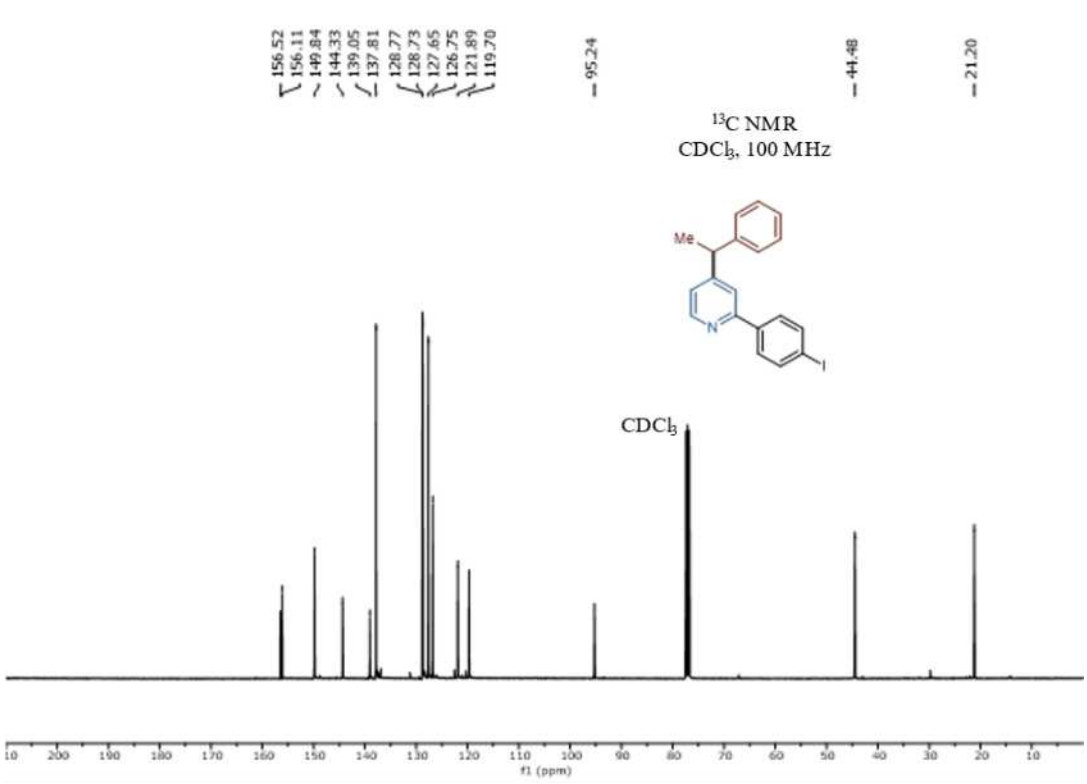

^{13}C NMR
$CDCl_3$, 100 MHz

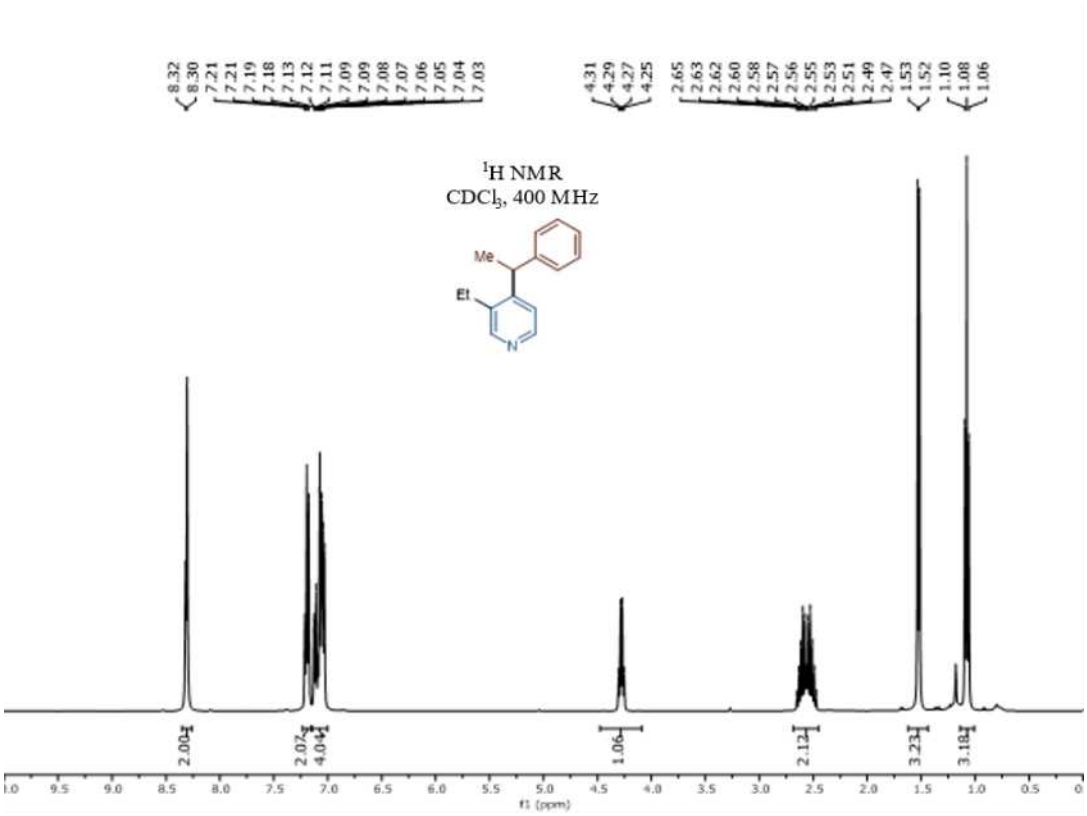
8.32
8.30
7.21
7.21
7.19
7.18
7.13
7.12
7.11
7.09
7.09
7.08
7.07
7.06
7.05
7.04
7.03
4.31
4.29
4.27
4.25
2.65
2.63
2.62
2.60
2.58
2.57
2.56
2.55
2.53
2.51
2.49
2.47
1.53
1.52
1.10
1.08
1.06
^{1}H NMR
$CDCl_3$, 400 MHz
Me
Et
N
2.00
2.07
4.04
1.06
2.12
3.23
3.18
f1 (ppm)

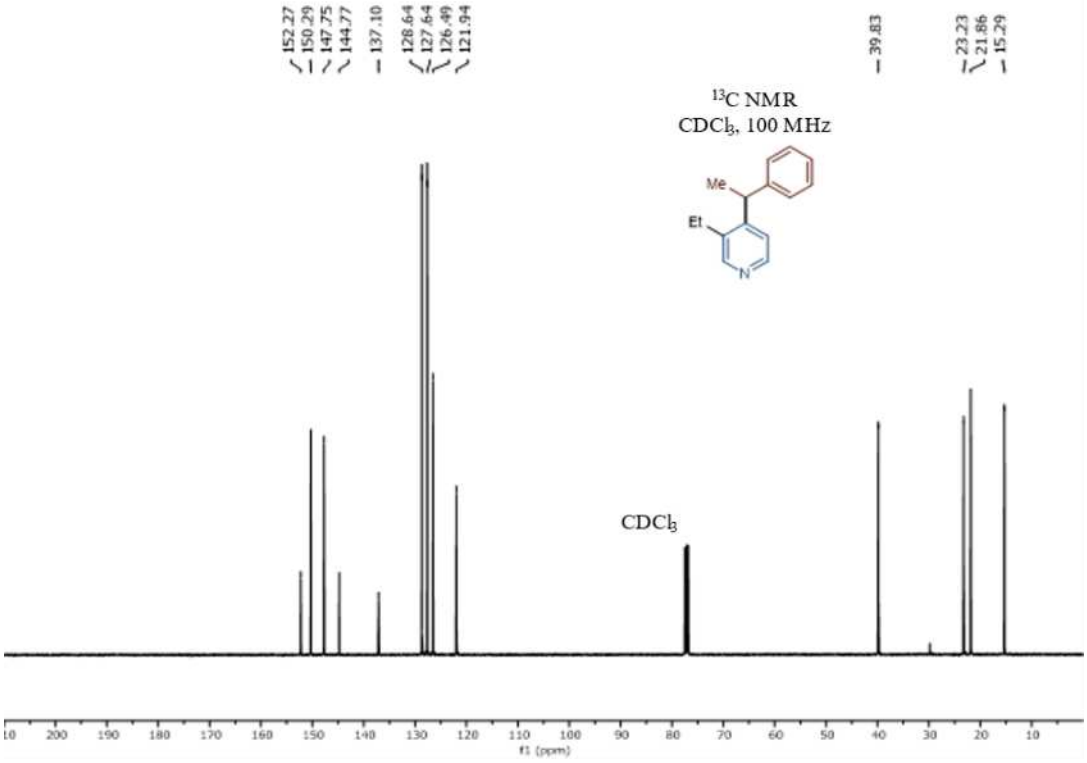
152.27
150.29
147.75
144.77
137.10
128.64
127.64
126.49
121.94
39.83
23.23
21.86
15.29
^{13}C NMR
$CDCl_3$, 100 MHz
Me
Et
N
$CDCl_3$
f1 (ppm)

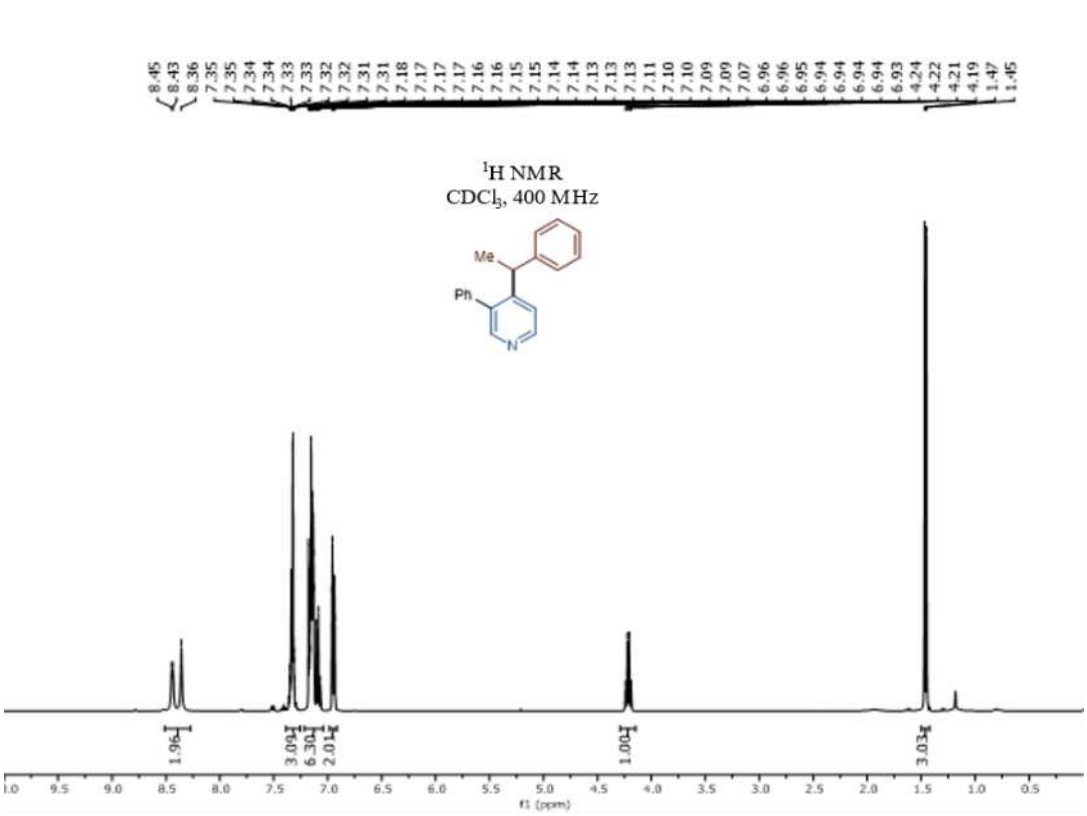
8.45
8.43
8.36
7.35
7.35
7.34
7.34
7.33
7.33
7.32
7.32
7.31
7.31
7.18
7.17
7.17
7.17
7.16
7.16
7.15
7.15
7.14
7.14
7.13
7.13
7.13
7.11
7.10
7.10
7.09
7.09
7.07
6.96
6.96
6.95
6.94
6.94
6.94
6.94
6.93
4.24
4.22
4.21
4.19
1.47
1.45
1H NMR
CDCl3, 400 MHz
Me
Ph
N
1.96
3.09
6.30
2.01
1.00
3.03
f1 (ppm)

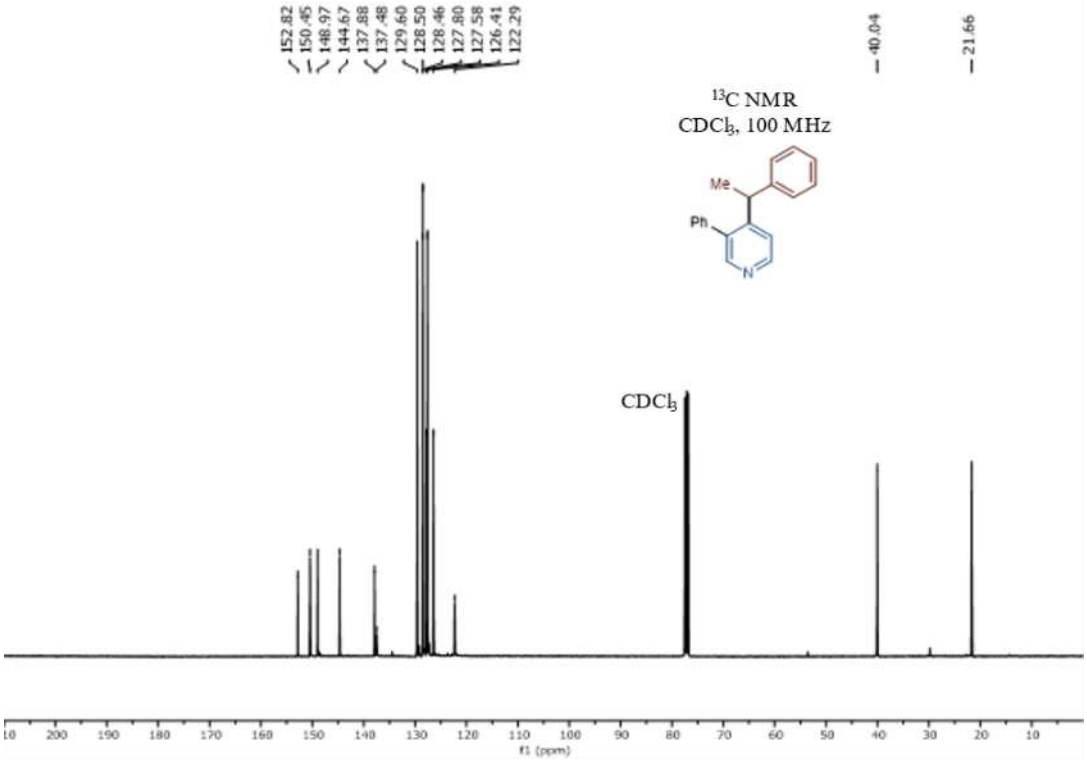
152.82
150.45
148.97
144.67
137.88
137.48
129.60
128.50
128.46
127.80
127.58
126.41
122.29
40.04
21.66
13C NMR
CDCl3, 100 MHz
Me
Ph
N
CDCl3
f1 (ppm)

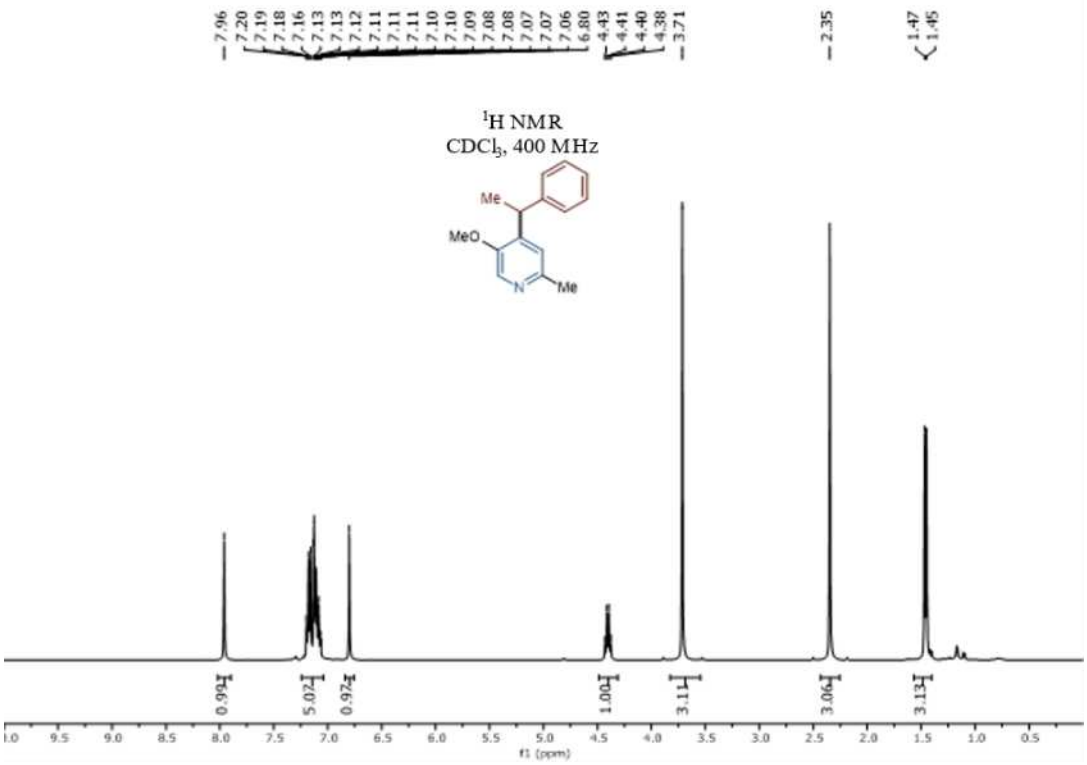

^{1}H NMR
$CDCl_3$, 400 MHz

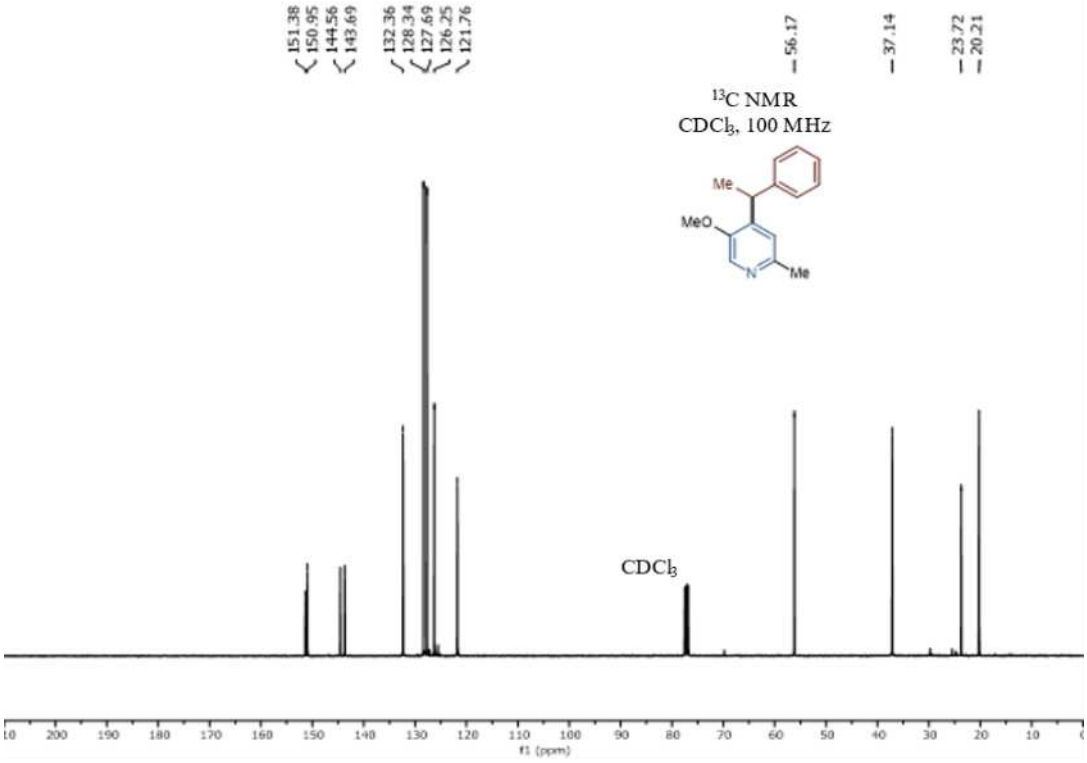

^{13}C NMR
$CDCl_3$, 100 MHz

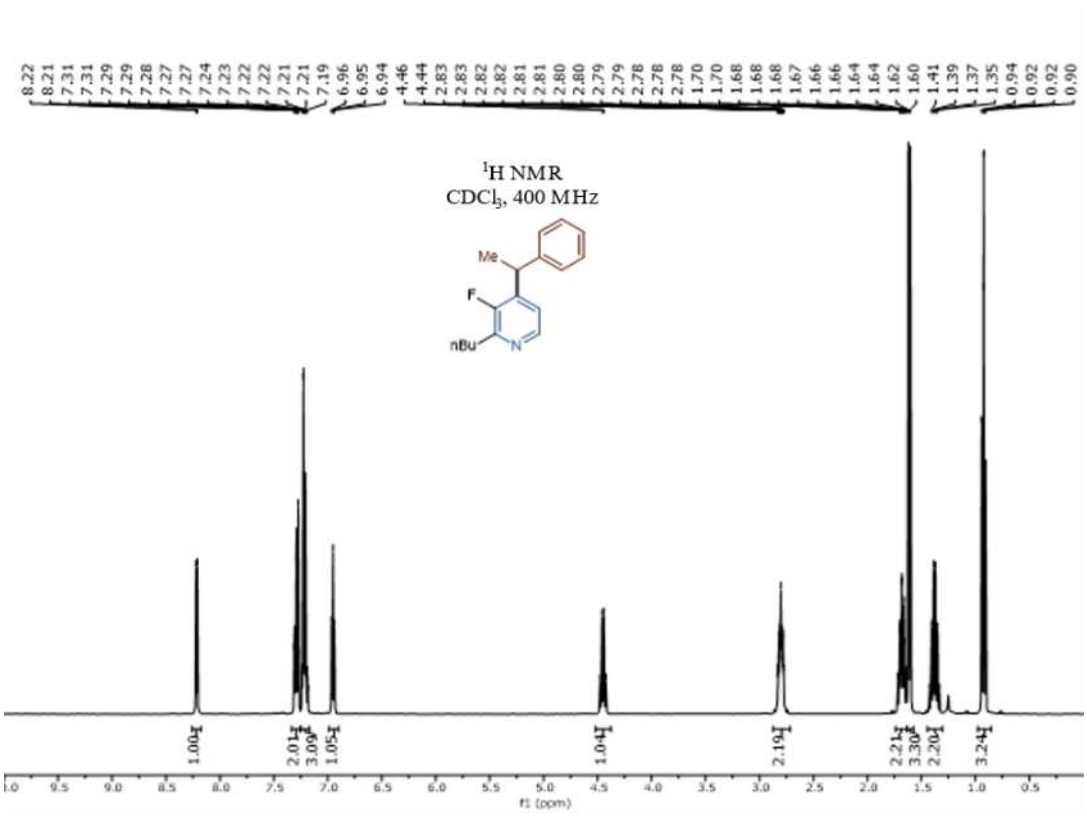
8.22
8.21
7.31
7.31
7.29
7.29
7.28
7.27
7.27
7.24
7.23
7.22
7.22
7.21
7.21
7.19
6.96
6.95
6.94
4.46
4.44
2.83
2.82
2.82
2.81
2.81
2.80
2.80
2.79
2.79
2.78
2.78
2.78
1.70
1.70
1.68
1.68
1.68
1.67
1.66
1.66
1.64
1.64
1.62
1.60
1.41
1.39
1.37
1.35
0.94
0.92
0.92
0.90
^{1}H NMR
$CDCl_3$, 400 MHz
Me
F
nBu
N
1.00
2.01
3.09
1.05
1.04
2.19
2.21
3.30
2.20
3.24
f1 (ppm)

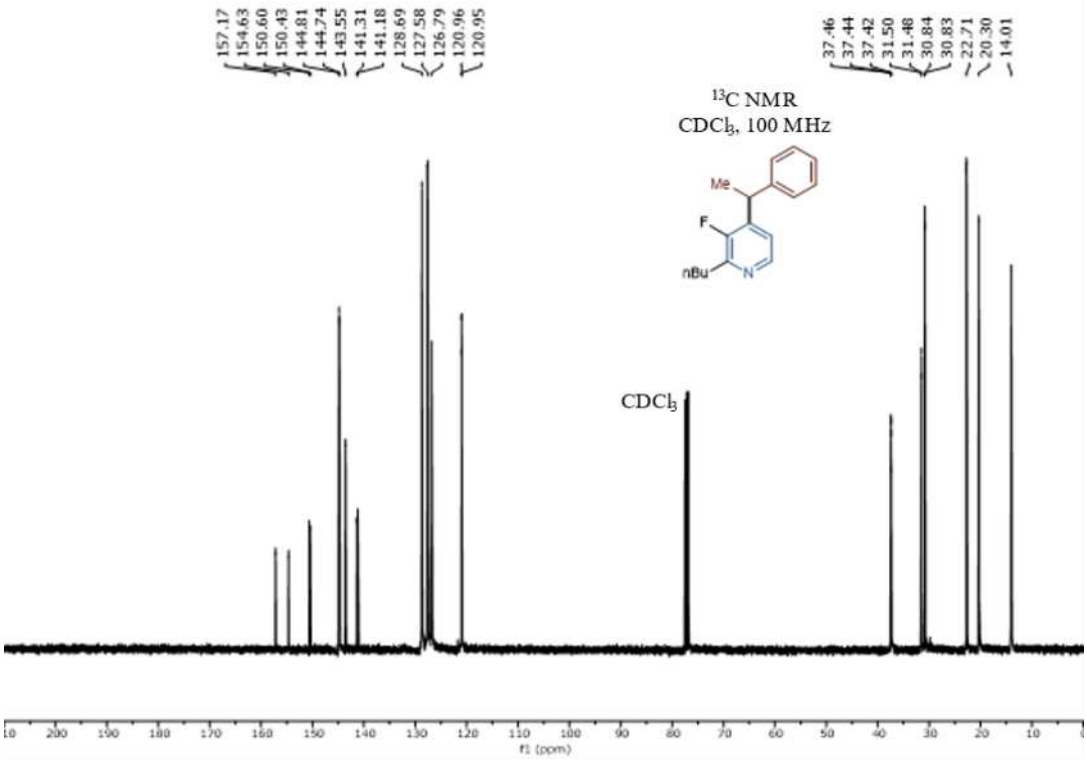
157.17
154.63
150.60
150.43
144.81
144.74
143.55
141.31
141.18
128.69
127.58
126.79
120.96
120.95
37.46
37.44
37.42
31.50
31.48
30.84
30.83
22.71
20.30
14.01
^{13}C NMR
$CDCl_3$, 100 MHz
Me
F
nBu
N
$CDCl_3$
f1 (ppm)

^{19F} NMR
$CDCl_3$, 365 MHz

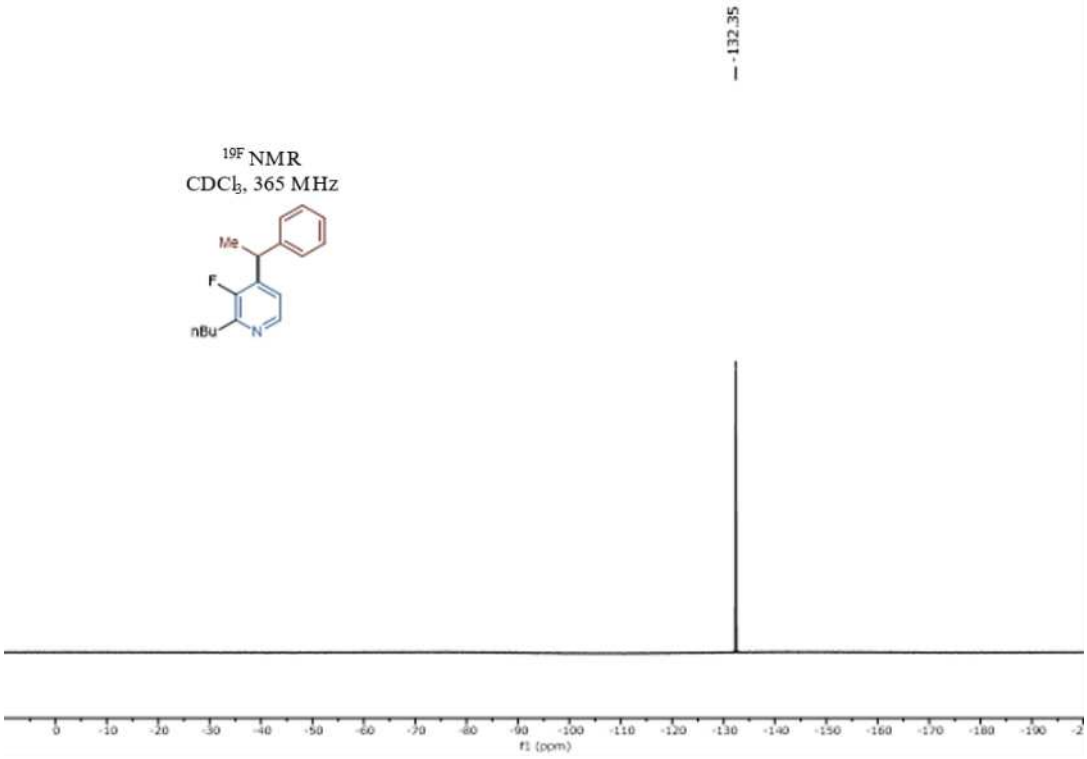

^{1}H NMR
$CDCl_3$, 400 MHz

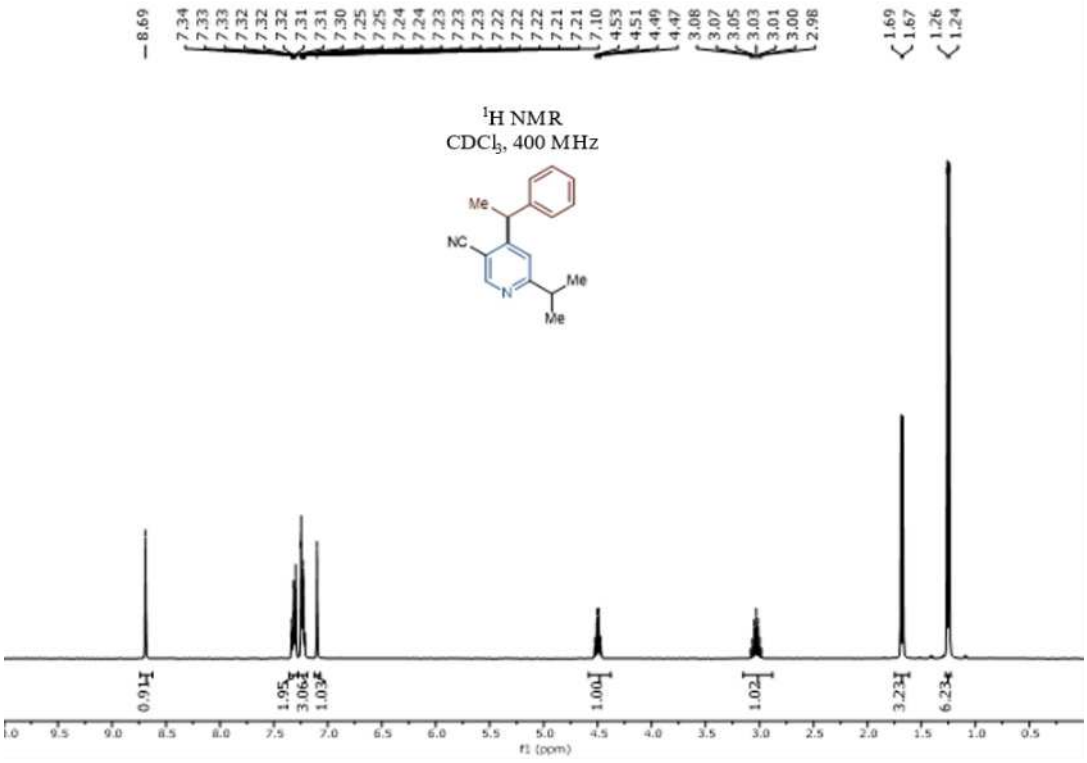

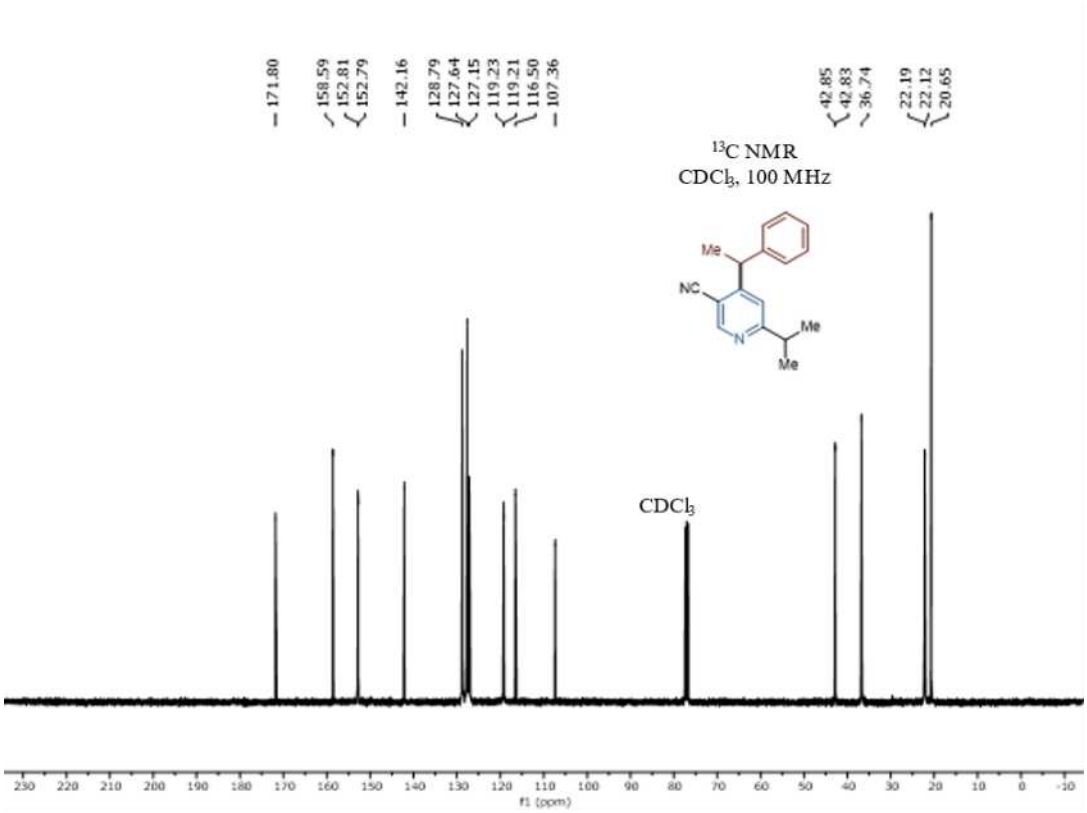
171.80
158.59
152.81
152.79
142.16
128.79
127.64
127.15
119.23
119.21
116.50
107.36
42.85
42.83
36.74
22.19
22.12
20.65
13C NMR
CDCl3, 100 MHz
Me
NC
N
Me
Me
CDCl3
f1 (ppm)

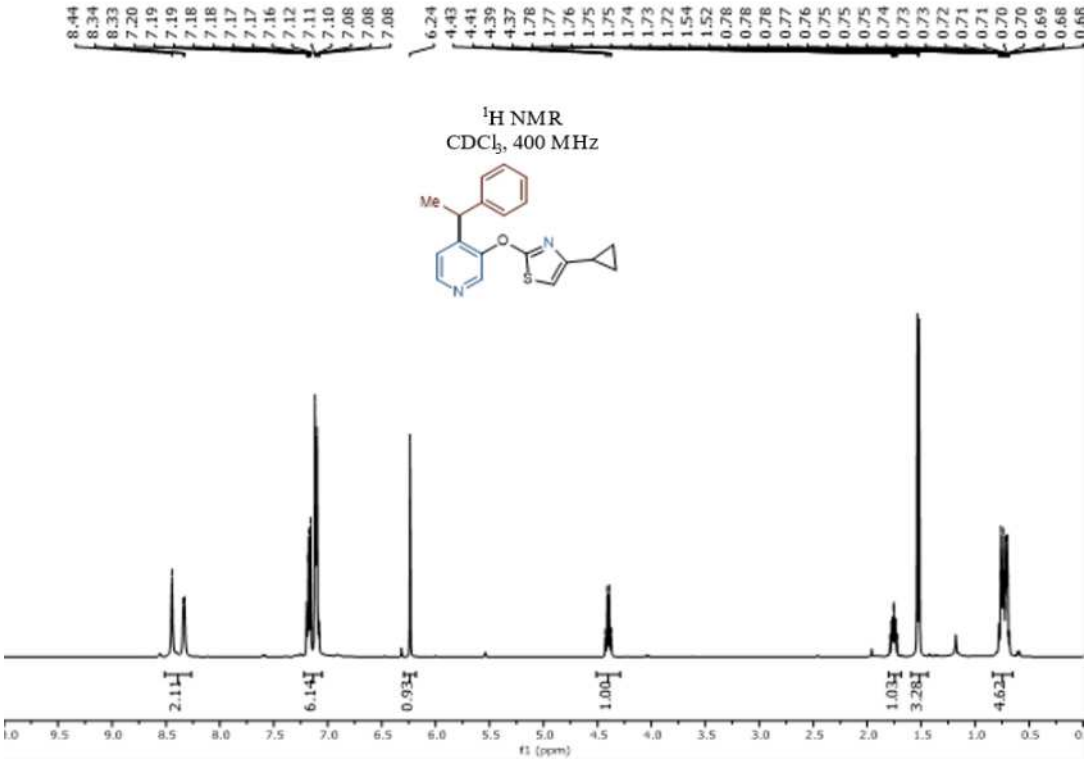
8.44
8.34
8.33
7.20
7.19
7.19
7.18
7.18
7.17
7.17
7.16
7.12
7.11
7.10
7.08
7.08
7.08
6.24
4.43
4.41
4.39
4.37
1.78
1.77
1.76
1.75
1.75
1.74
1.73
1.72
1.54
1.52
0.78
0.78
0.78
0.77
0.76
0.75
0.75
0.75
0.74
0.73
0.73
0.72
0.71
0.71
0.70
0.70
0.69
0.68
1H NMR
CDCl3, 400 MHz
Me
O
N
S
N
2.11
6.14
0.93
1.00
1.03
3.28
4.62
f1 (ppm)

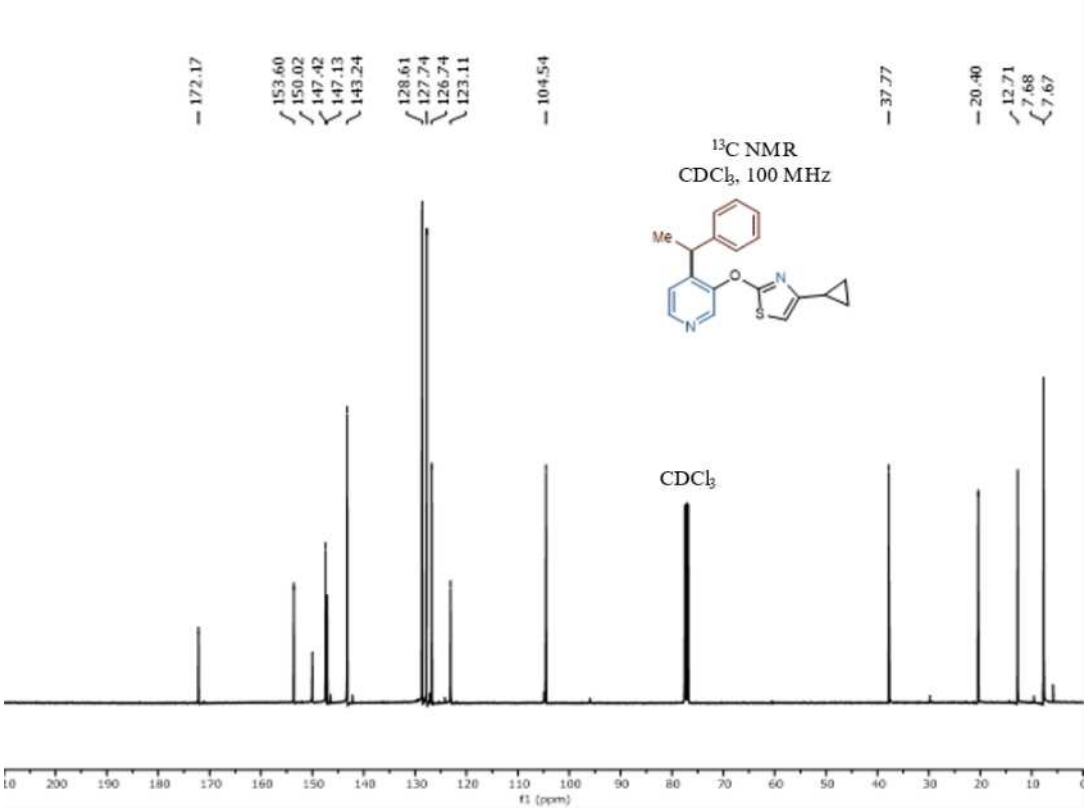
172.17
153.60
150.02
147.42
147.13
143.24
128.61
127.74
126.74
123.11
104.54
37.77
20.40
12.71
7.68
7.67
13C NMR
CDCl3, 100 MHz
Me
N
O
S
N
CDCl3
f1 (ppm)

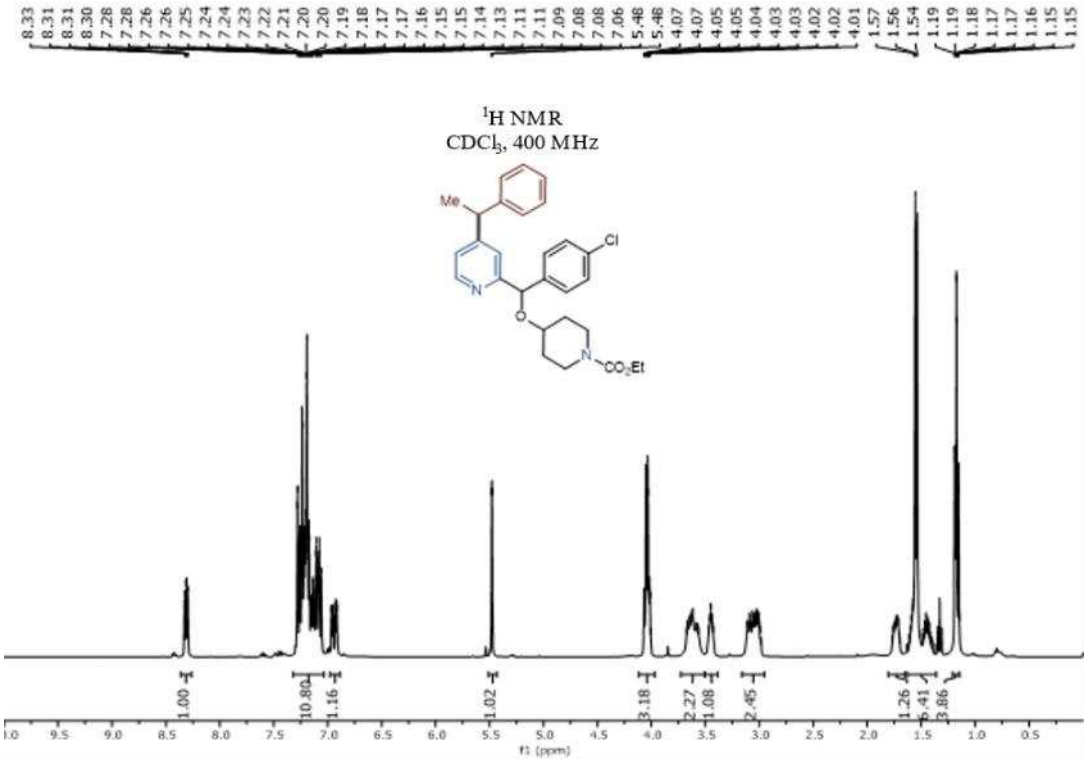
8.33
8.31
8.31
8.30
7.28
7.26
7.26
7.25
7.24
7.24
7.23
7.22
7.21
7.20
7.20
7.19
7.18
7.17
7.17
7.16
7.15
7.15
7.14
7.13
7.11
7.11
7.09
7.08
7.08
7.06
5.48
5.48
4.07
4.07
4.05
4.05
4.04
4.03
4.03
4.02
4.02
4.01
1.57
1.56
1.54
1.19
1.19
1.18
1.17
1.17
1.16
1.15
1.15
1H NMR
CDCl3, 400 MHz
Me
Cl
N
O
N
CO2Et
1.00
10.80
1.16
1.02
3.18
2.27
1.08
2.45
1.26
6.41
3.86
f1 (ppm)

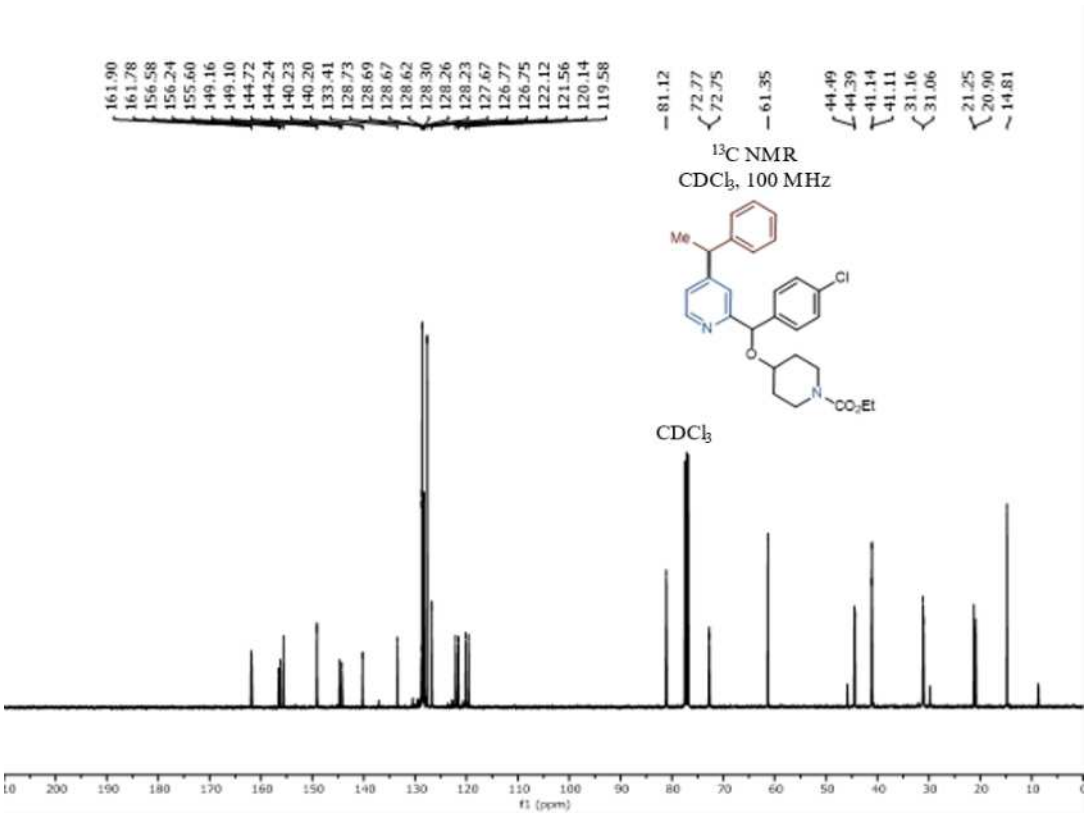
161.90
161.78
156.58
156.24
155.60
149.16
149.10
144.72
144.24
140.23
140.20
133.41
128.73
128.69
128.67
128.62
128.30
128.26
128.23
127.67
126.77
126.75
122.12
121.56
120.14
119.58
81.12
72.77
72.75
61.35
44.49
44.39
41.14
41.11
31.16
31.06
21.25
20.90
14.81
13C NMR
CDCl3, 100 MHz
Me
Cl
N
O
N
CO2Et
CDCl3
f1 (ppm)

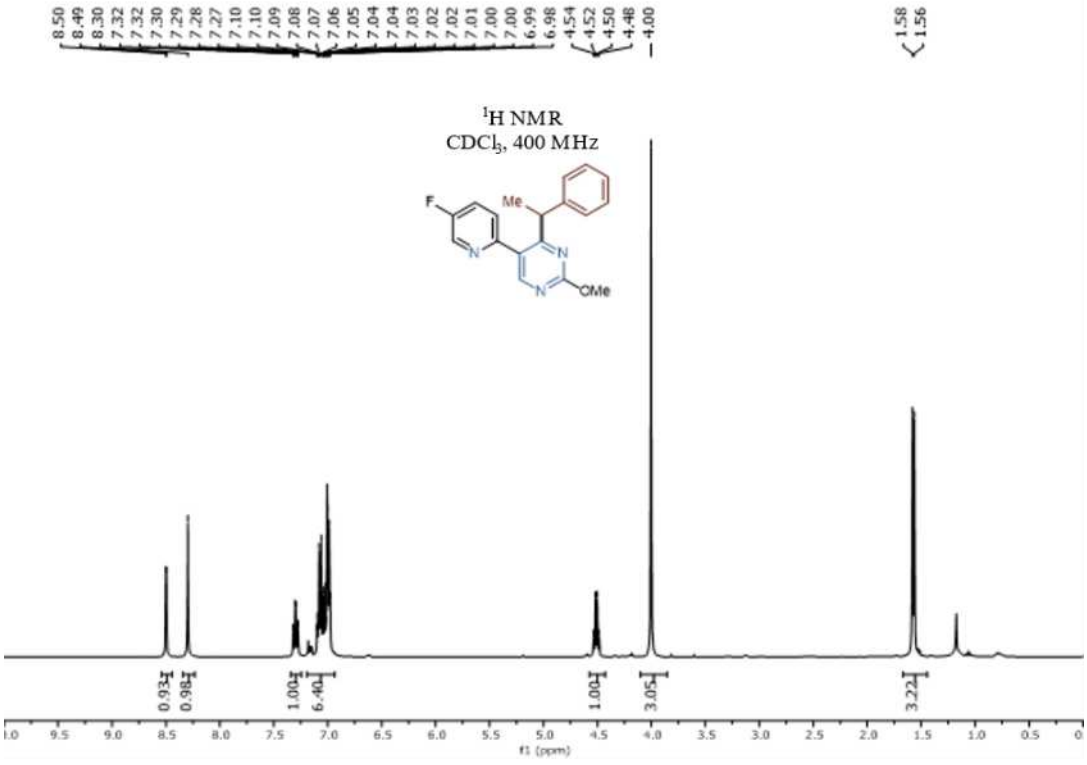
8.50
8.49
8.30
7.32
7.32
7.30
7.29
7.28
7.27
7.10
7.10
7.09
7.08
7.07
7.06
7.05
7.04
7.04
7.03
7.02
7.02
7.01
7.00
7.00
6.99
6.98
4.54
4.52
4.50
4.48
4.00
1.58
1.56
1H NMR
CDCl3, 400 MHz
F
Me
N
N
N
OMe
0.93
0.98
1.00
6.40
1.00
3.05
3.22
f1 (ppm)

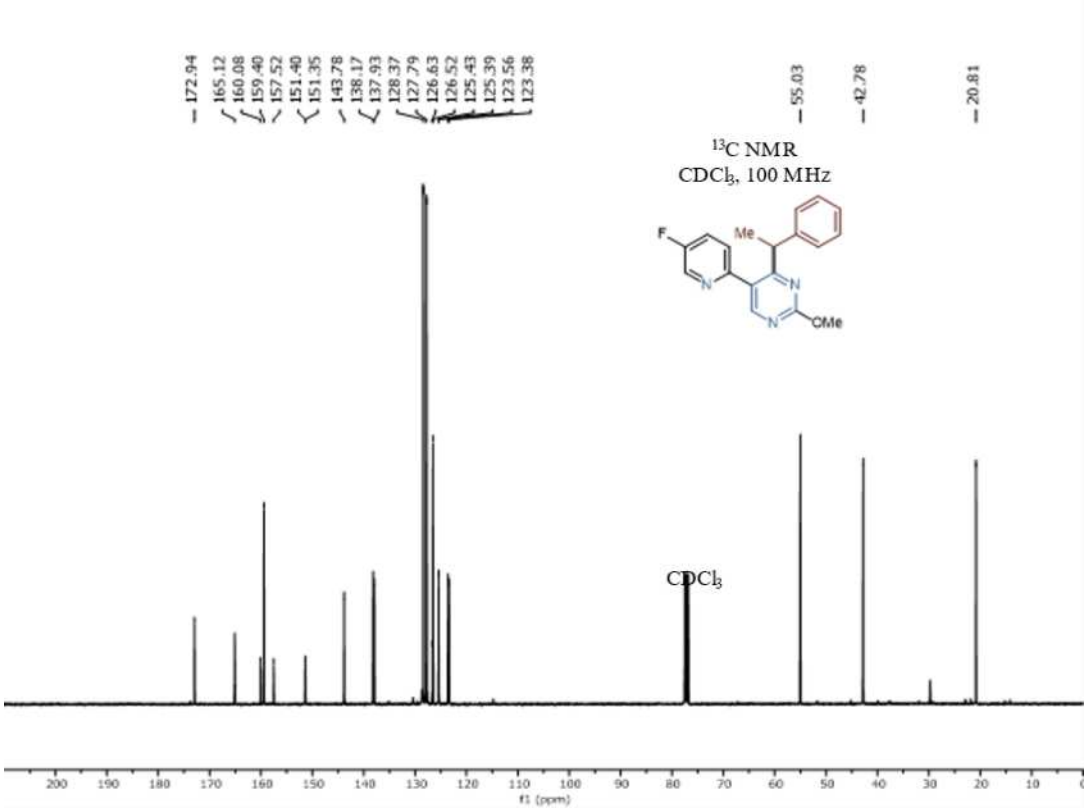
172.94
165.12
160.08
159.40
157.52
151.40
151.35
143.78
138.17
137.93
128.37
127.79
126.63
126.52
125.43
125.39
123.56
123.38
55.03
42.78
20.81
13C NMR
CDCl3, 100 MHz
F
Me
N
N
OMe
CDCl3
200 190 180 170 160 150 140 130 120 110 100 90 80 70 60 50 40 30 20 10
f1 (ppm)

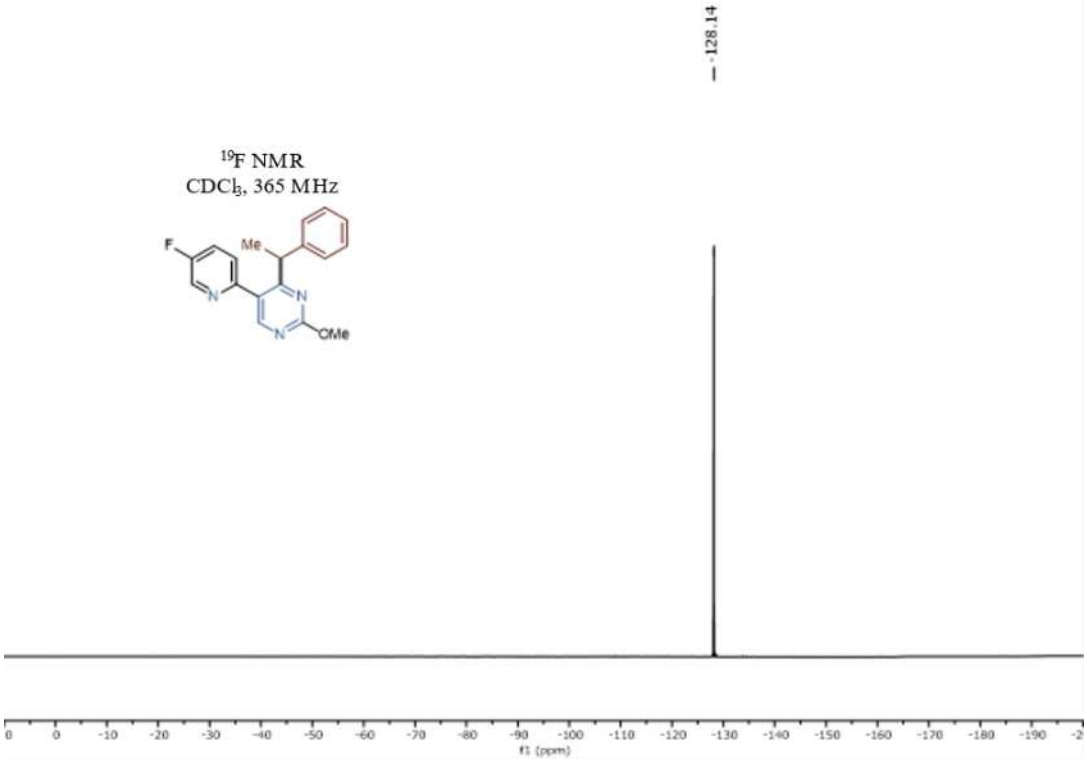
-128.14
19F NMR
CDCl3, 365 MHz
F
Me
N
N
OMe
0 0 -10 -20 -30 -40 -50 -60 -70 -80 -90 -100 -110 -120 -130 -140 -150 -160 -170 -180 -190
f1 (ppm)

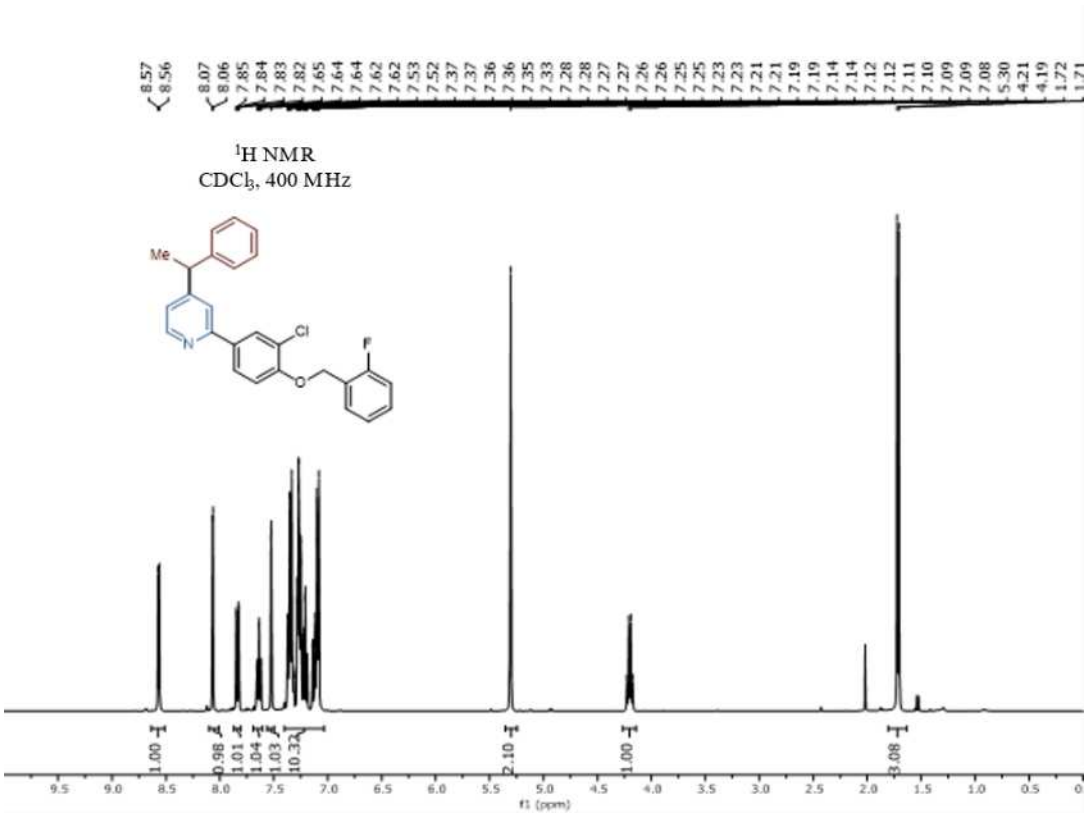

^{1}H NMR
$CDCl_3$, 400 MHz

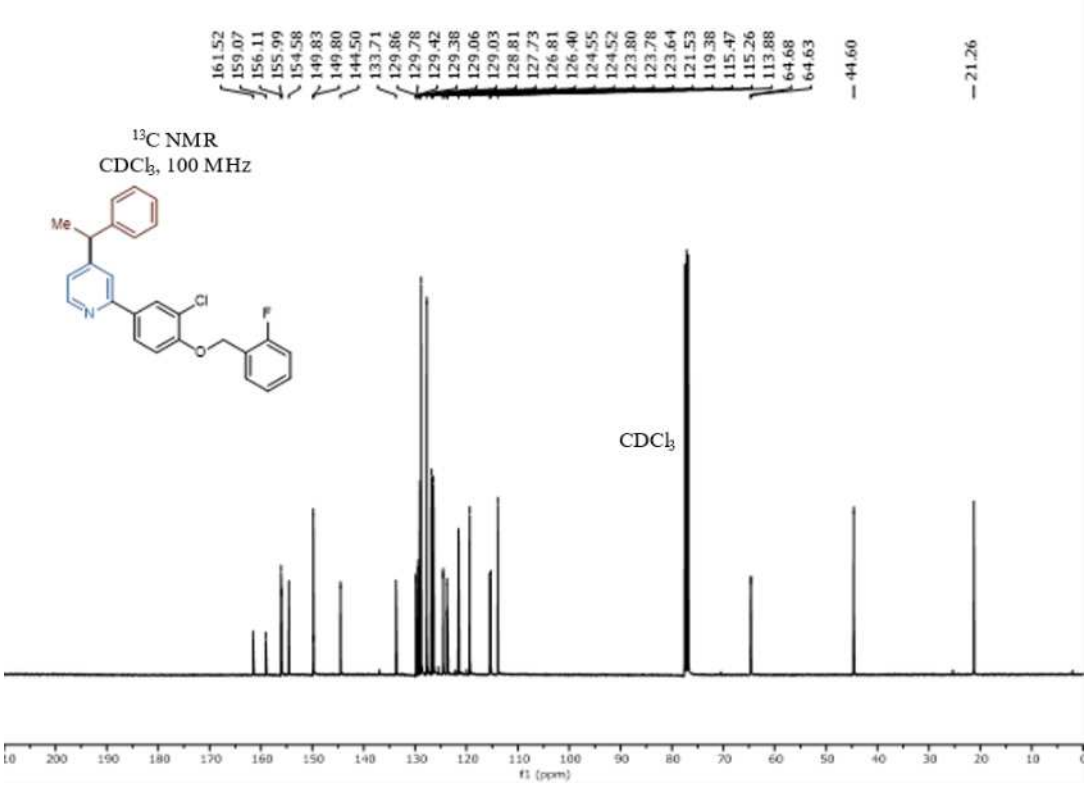

^{13}C NMR
$CDCl_3$, 100 MHz

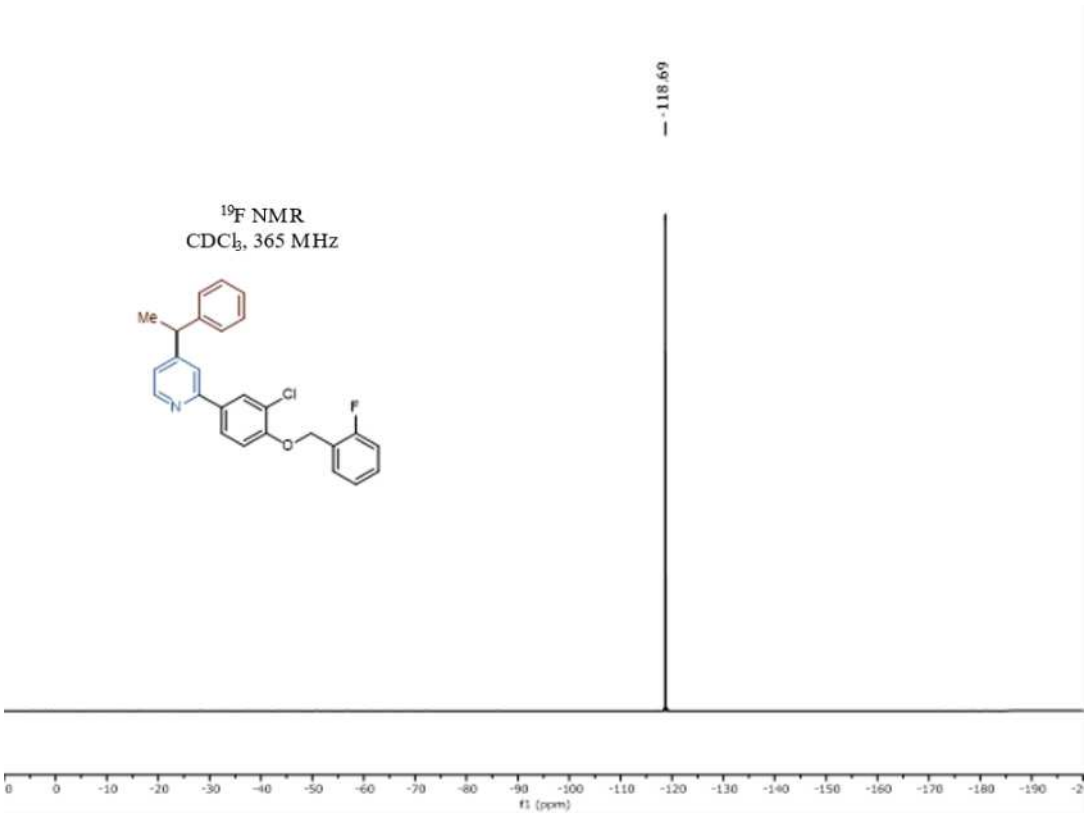
-118.69
19F NMR
CDCl3, 365 MHz
Me
Cl
F
O
N
f1 (ppm)

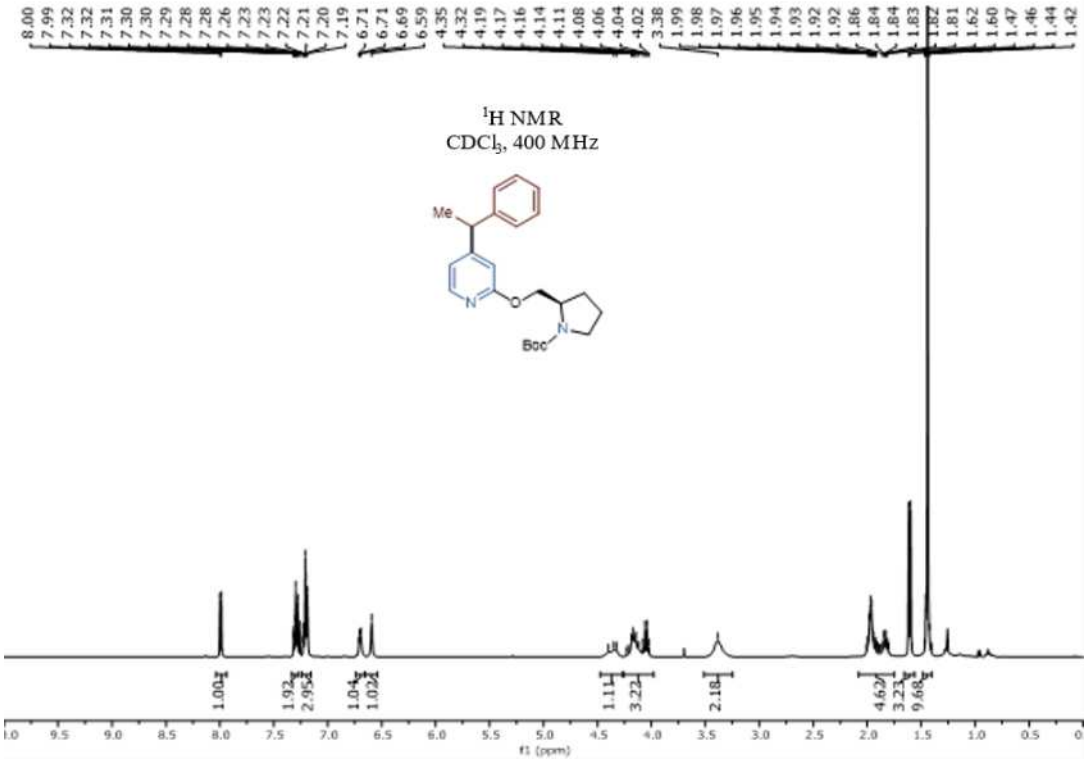
8.00
7.99
7.32
7.32
7.31
7.30
7.30
7.29
7.28
7.28
7.26
7.23
7.22
7.21
7.20
7.19
6.71
6.71
6.69
6.59
4.35
4.32
4.19
4.17
4.16
4.14
4.11
4.08
4.06
4.04
4.02
3.38
1.99
1.98
1.97
1.96
1.95
1.94
1.93
1.92
1.92
1.86
1.84
1.84
1.83
1.82
1.81
1.62
1.60
1.47
1.46
1.44
1.42
1H NMR
CDCl3, 400 MHz
Me
O
N
Boc
1.00
1.92
2.95
1.04
1.02
1.11
3.22
2.18
4.62
3.23
9.68
f1 (ppm)

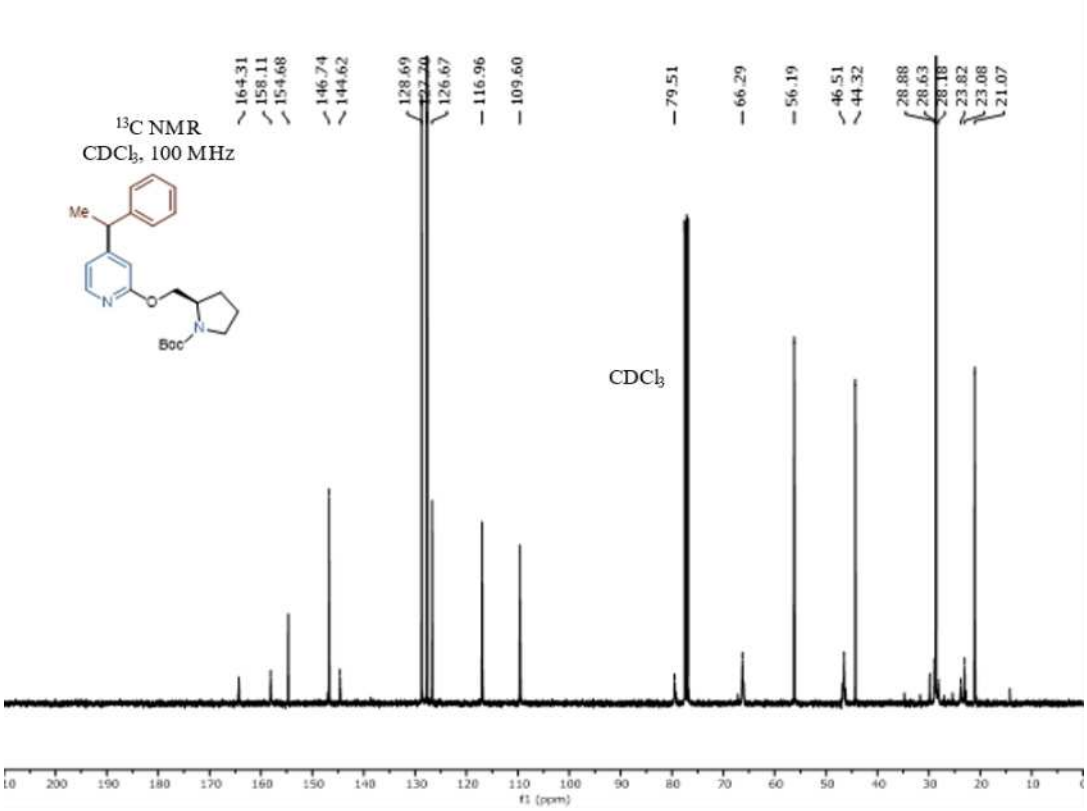
164.31
158.11
154.68
146.74
144.62
128.69
122.70
126.67
116.96
109.60
79.51
66.29
56.19
46.51
44.32
28.88
28.63
28.18
23.82
23.08
21.07
13C NMR
CDCl3, 100 MHz
Me
O
N
Boc
CDCl3
f1 (ppm)

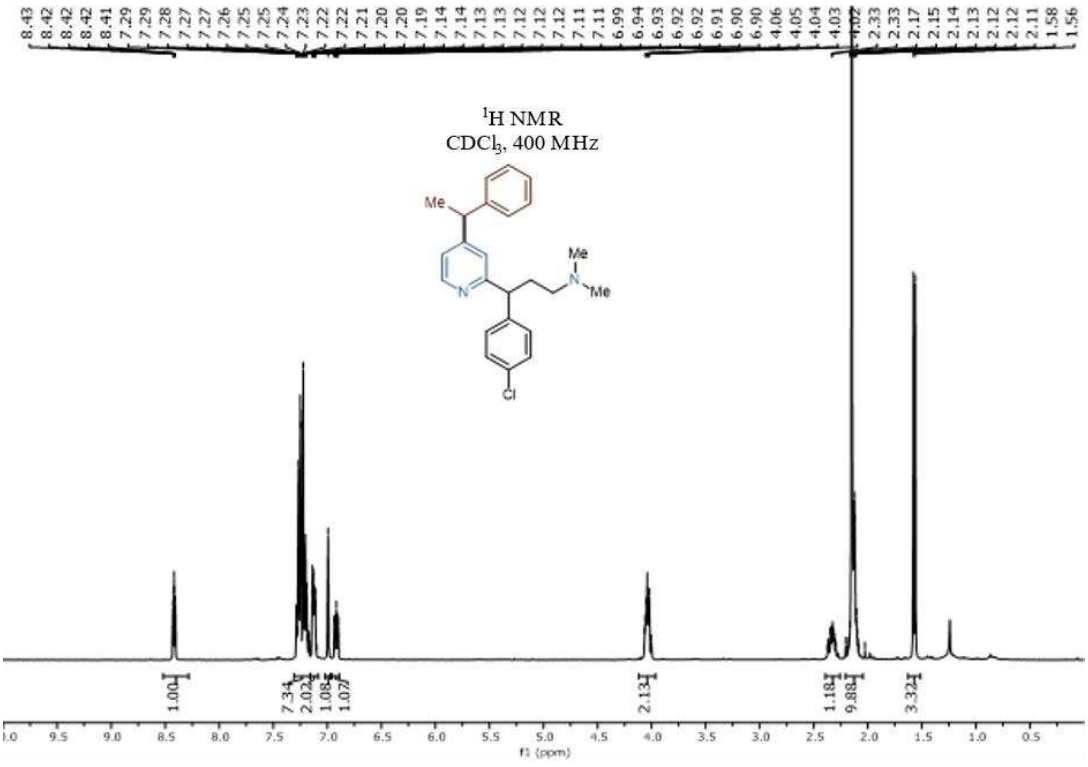
8.43
8.42
8.42
8.42
8.41
7.29
7.29
7.28
7.27
7.27
7.26
7.25
7.25
7.24
7.23
7.22
7.22
7.21
7.20
7.20
7.19
7.14
7.14
7.13
7.13
7.12
7.12
7.12
7.11
7.11
6.99
6.94
6.93
6.92
6.92
6.91
6.90
6.90
4.06
4.05
4.04
4.03
4.02
2.33
2.33
2.17
2.15
2.14
2.13
2.12
2.12
2.11
1.58
1.56
1H NMR
CDCl3, 400 MHz
Me
N
Me
Me
Cl
1.00
7.34
2.02
1.08
1.07
2.13
1.18
9.88
3.32
f1 (ppm)

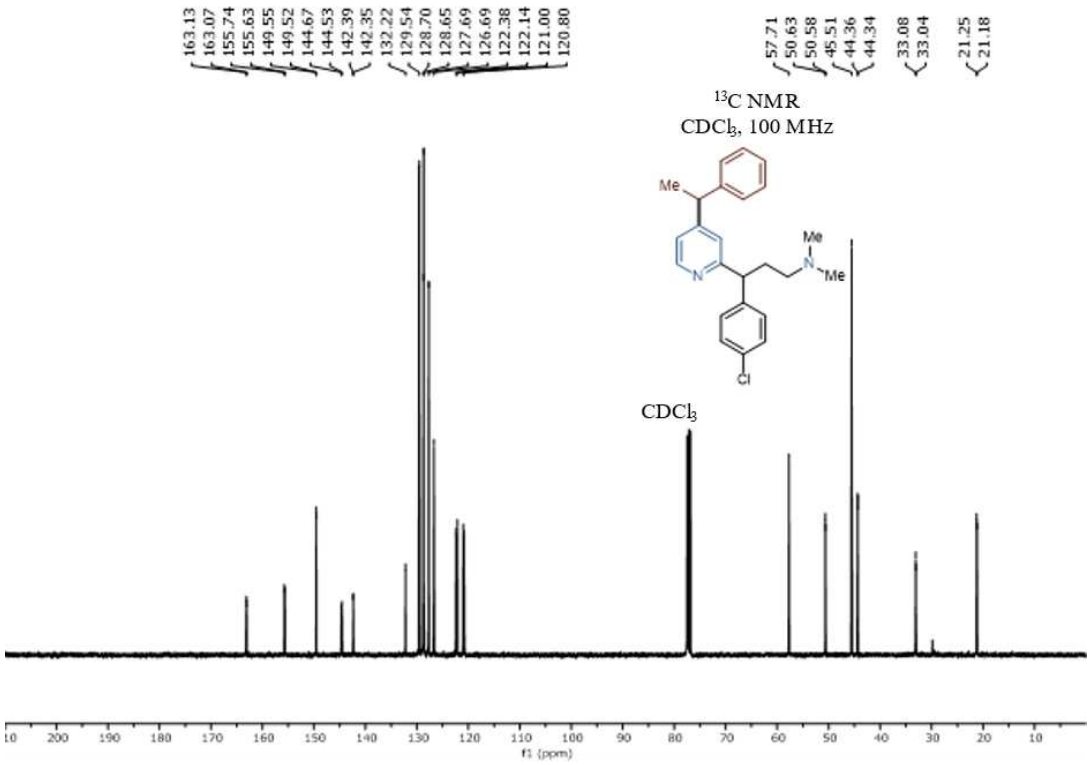
163.13
163.07
155.74
155.63
149.55
149.52
144.67
144.53
142.39
142.35
132.22
129.54
128.70
128.65
127.69
126.69
122.38
122.14
121.00
120.80
57.71
50.63
50.58
45.51
44.36
44.34
33.08
33.04
21.25
21.18
13C NMR
CDCl3, 100 MHz
Me
N
Me
Me
Cl
CDCl3
f1 (ppm)

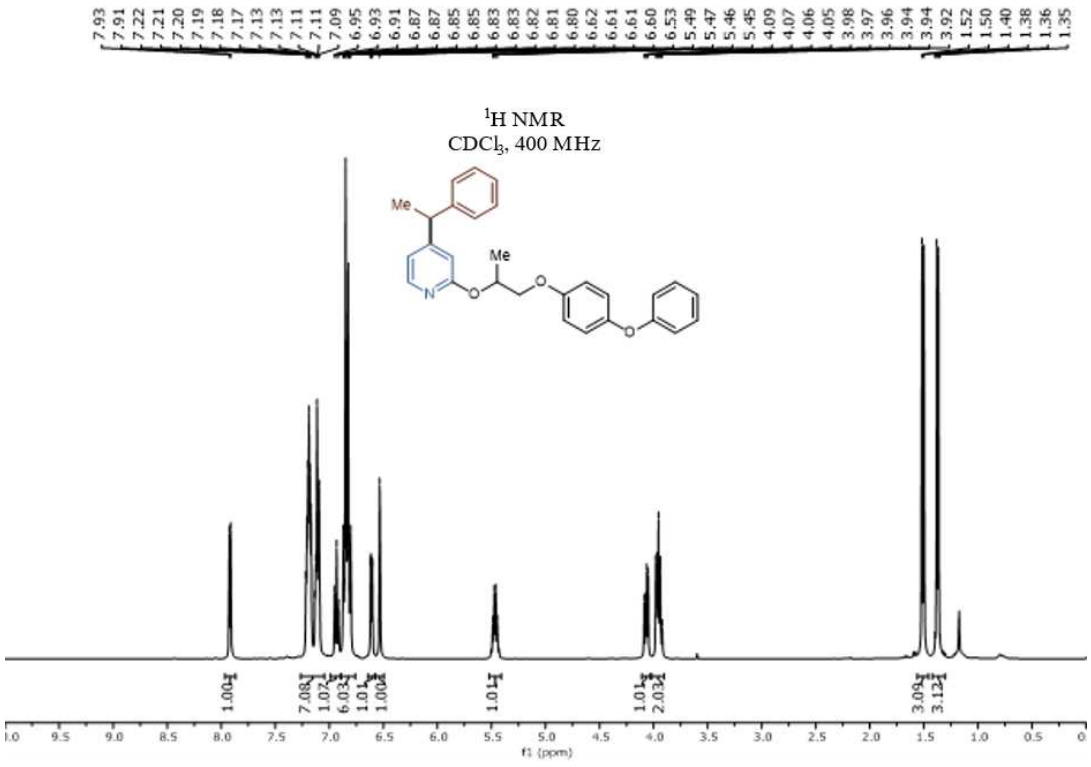
7.93
7.91
7.22
7.21
7.20
7.19
7.18
7.17
7.13
7.13
7.11
7.11
7.09
6.95
6.93
6.91
6.87
6.87
6.85
6.85
6.83
6.83
6.82
6.81
6.80
6.62
6.61
6.61
6.60
6.53
5.49
5.47
5.46
5.45
4.09
4.07
4.06
4.05
3.98
3.97
3.96
3.94
3.94
3.92
1.52
1.50
1.40
1.38
1.36
1.35
1H NMR
CDCl3, 400 MHz
Me
N
Me
O
O
O
1.00
7.08
1.07
6.03
1.01
1.00
1.01
1.01
2.03
3.09
3.12
f1 (ppm)

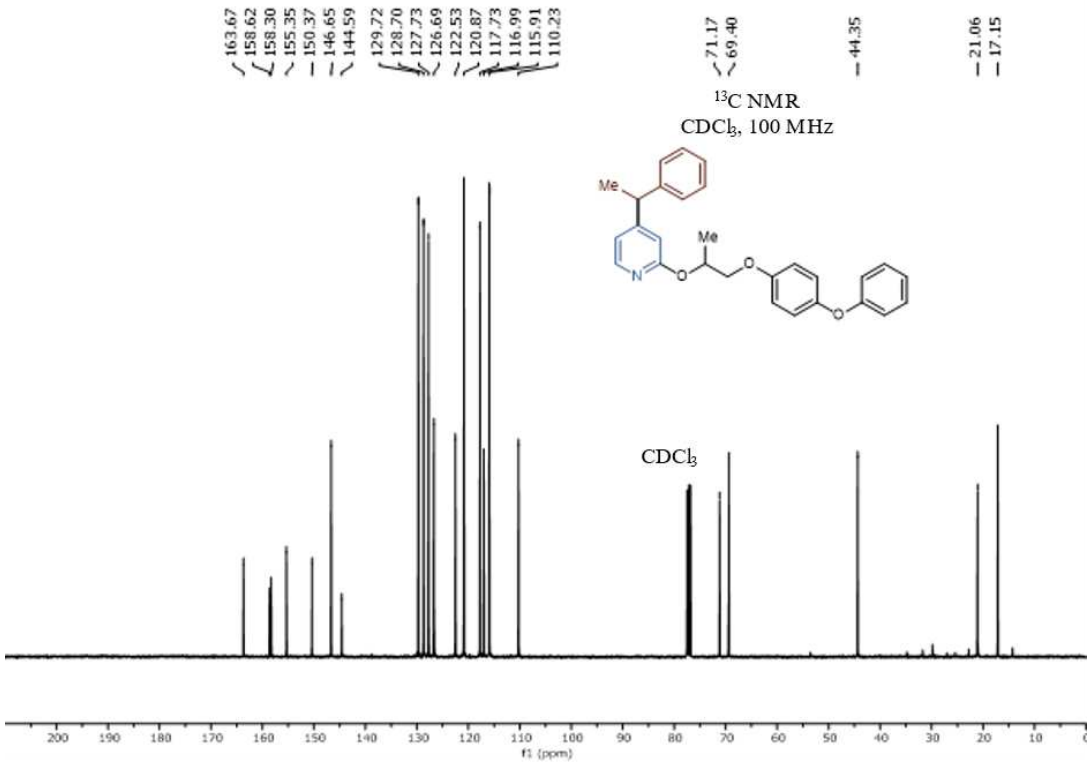
163.67
158.62
158.30
155.35
150.37
146.65
144.59
129.72
128.70
127.73
126.69
122.53
120.87
117.73
116.99
115.91
110.23
71.17
69.40
44.35
21.06
17.15
13C NMR
CDCl3, 100 MHz
Me
Me
O
O
O
N
CDCl3
200 190 180 170 160 150 140 130 120 110 100 90 80 70 60 50 40 30 20 10
f1 (ppm)

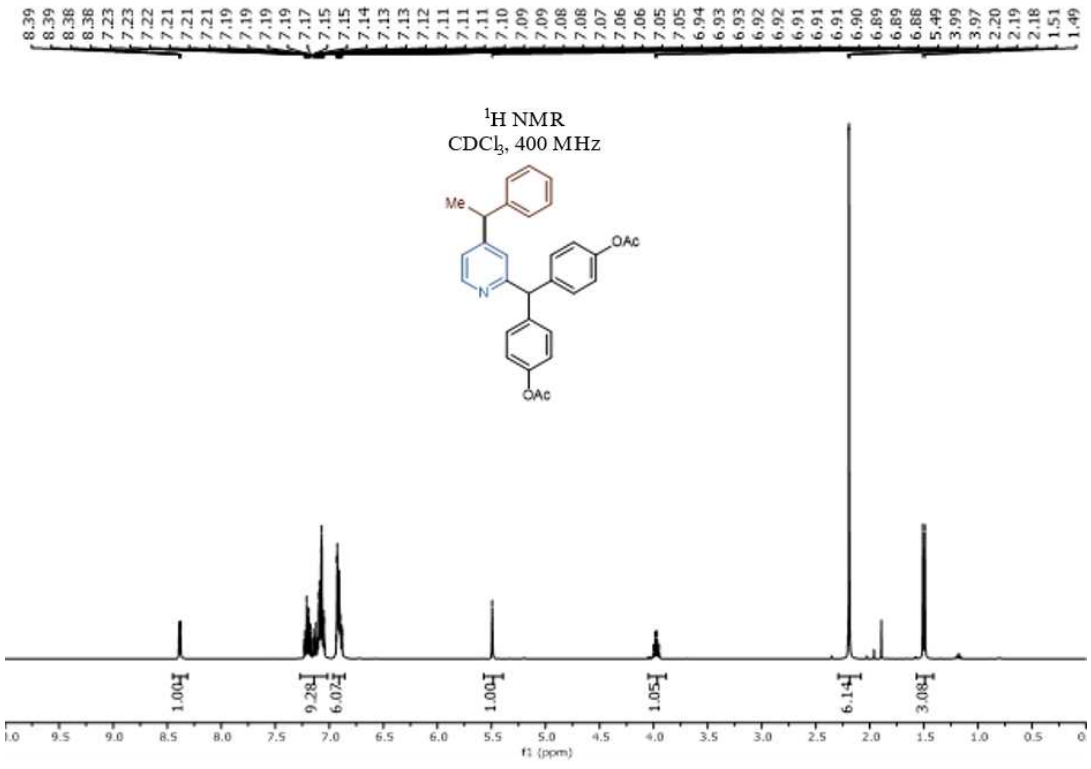
8.39
8.39
8.38
8.38
7.23
7.22
7.21
7.21
7.21
7.19
7.19
7.19
7.19
7.17
7.15
7.15
7.14
7.13
7.13
7.12
7.11
7.11
7.11
7.10
7.09
7.09
7.08
7.08
7.07
7.06
7.06
7.05
7.05
6.94
6.93
6.93
6.92
6.92
6.91
6.91
6.91
6.90
6.89
6.89
6.88
5.49
3.99
3.97
2.20
2.19
2.18
1.51
1.49
1H NMR
CDCl3, 400 MHz
Me
OAc
OAc
N
1.00
9.28
6.07
1.00
1.05
6.14
3.08
f1 (ppm)

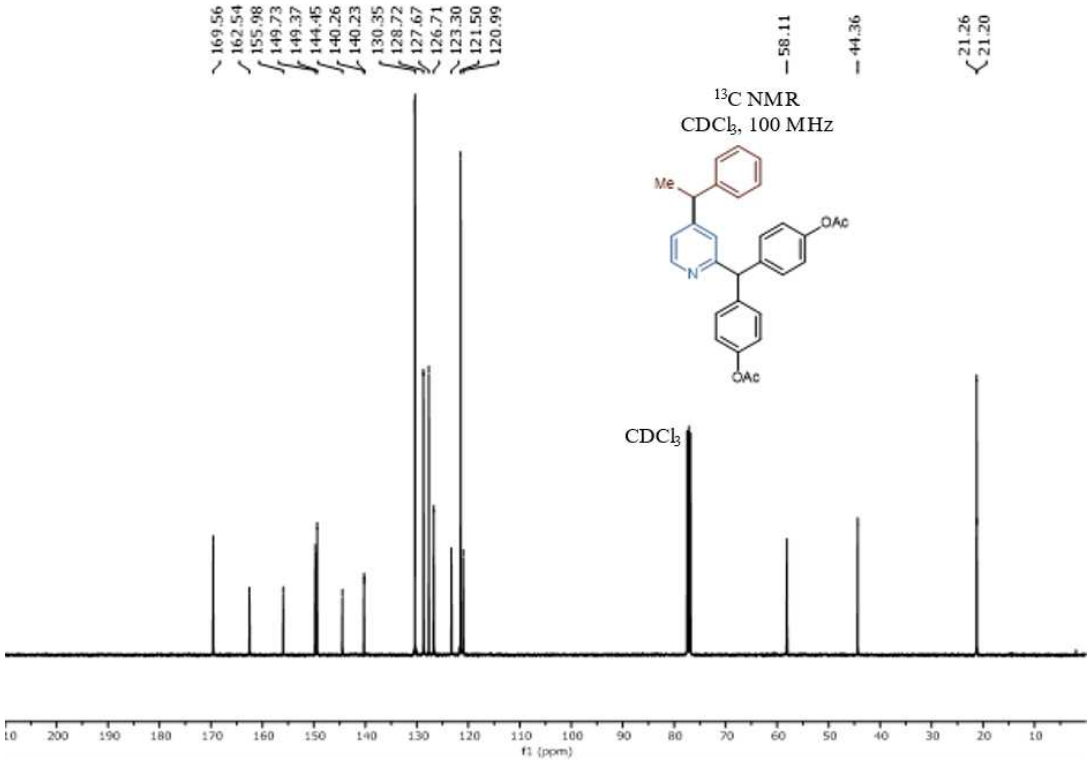
169.56
162.54
155.98
149.73
149.37
144.45
140.26
140.23
130.35
128.72
127.67
126.71
123.30
121.50
120.99
58.11
44.36
21.26
21.20
^{13}C NMR
$CDCl_3$, 100 MHz
Me
OAc
OAc
N
$CDCl_3$
f1 (ppm)

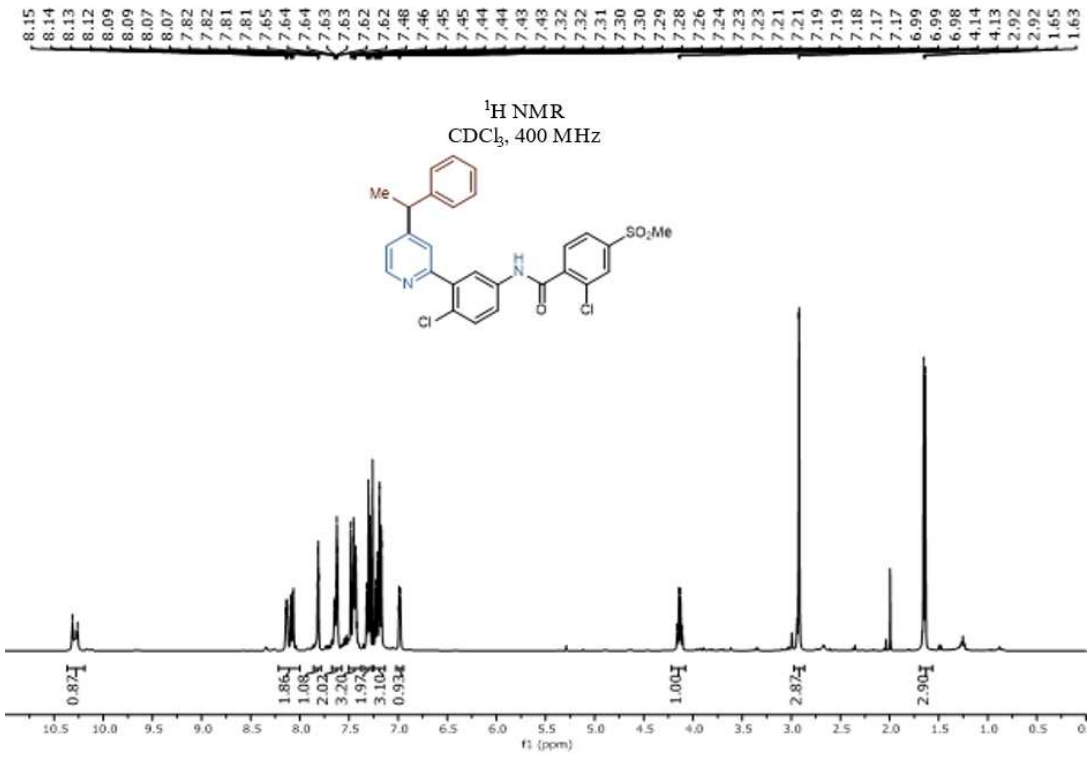
8.15
8.14
8.13
8.12
8.09
8.09
8.07
8.07
7.82
7.82
7.81
7.81
7.65
7.64
7.64
7.63
7.63
7.62
7.62
7.48
7.46
7.45
7.45
7.44
7.44
7.43
7.43
7.32
7.32
7.31
7.30
7.30
7.29
7.28
7.26
7.24
7.23
7.23
7.21
7.21
7.19
7.19
7.18
7.17
7.17
6.99
6.99
6.98
4.14
4.13
2.92
2.92
1.65
1.63
^{1}H NMR
$CDCl_3$, 400 MHz
Me
SO_2Me
N
H
O
Cl
Cl
0.87
1.86
1.08
2.02
3.20
1.97
3.10
0.93
1.00
2.87
2.90
f1 (ppm)

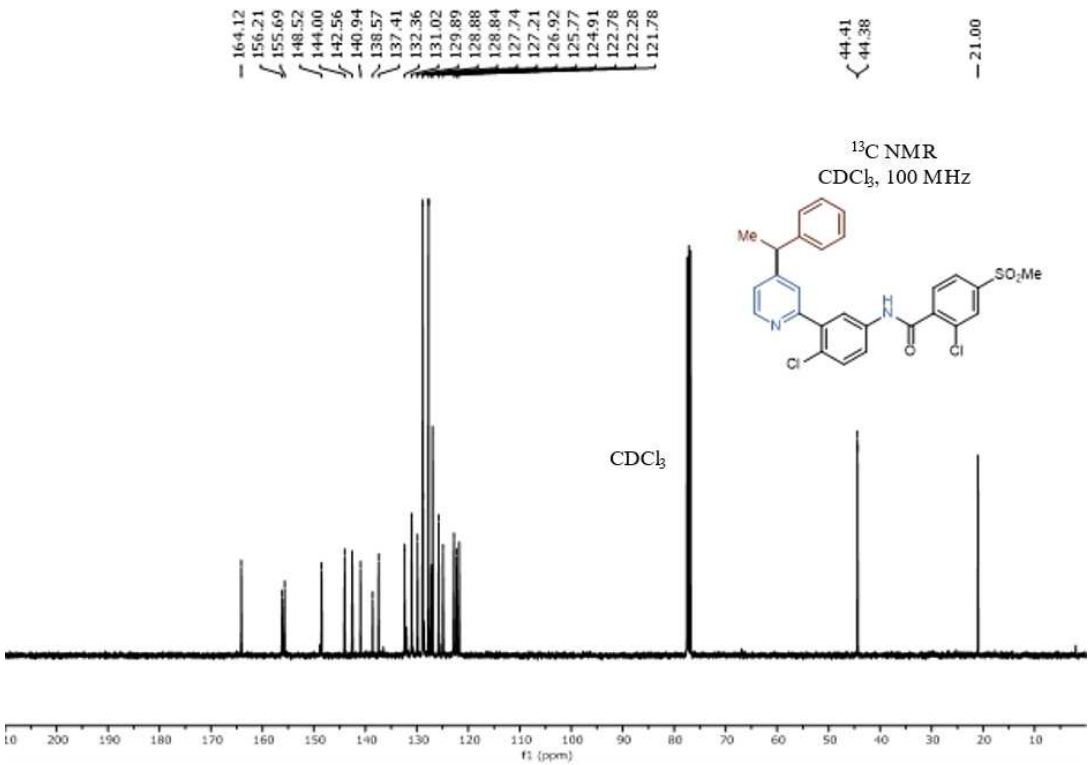
164.12
156.21
155.69
148.52
144.00
142.56
140.94
138.57
137.41
132.36
131.02
129.89
128.88
128.84
127.74
127.21
126.92
125.77
124.91
122.78
122.28
121.78
44.41
44.38
21.00
13C NMR
CDCl3, 100 MHz
Me
SO2Me
N
H
O
Cl
Cl
CDCl3
f1 (ppm)

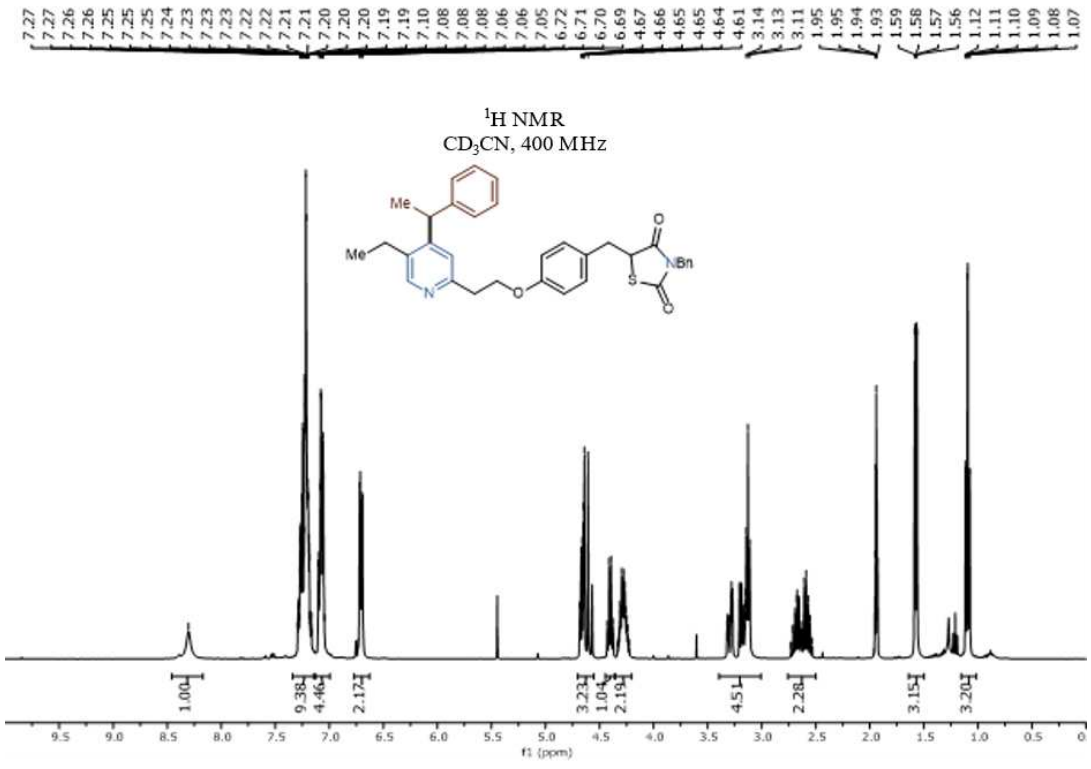
7.27
7.27
7.26
7.26
7.25
7.25
7.25
7.24
7.23
7.23
7.22
7.22
7.21
7.21
7.20
7.20
7.20
7.19
7.19
7.10
7.08
7.08
7.08
7.06
7.06
7.05
6.72
6.71
6.70
6.69
4.67
4.66
4.65
4.65
4.64
4.61
3.14
3.13
3.11
1.95
1.95
1.94
1.93
1.59
1.58
1.57
1.56
1.12
1.11
1.10
1.09
1.08
1.07
1H NMR
CD3CN, 400 MHz
Me
Me
N
O
O
NBn
S
O
1.00
9.38
4.46
2.17
3.23
1.04
2.19
4.51
2.28
3.15
3.20
f1 (ppm)

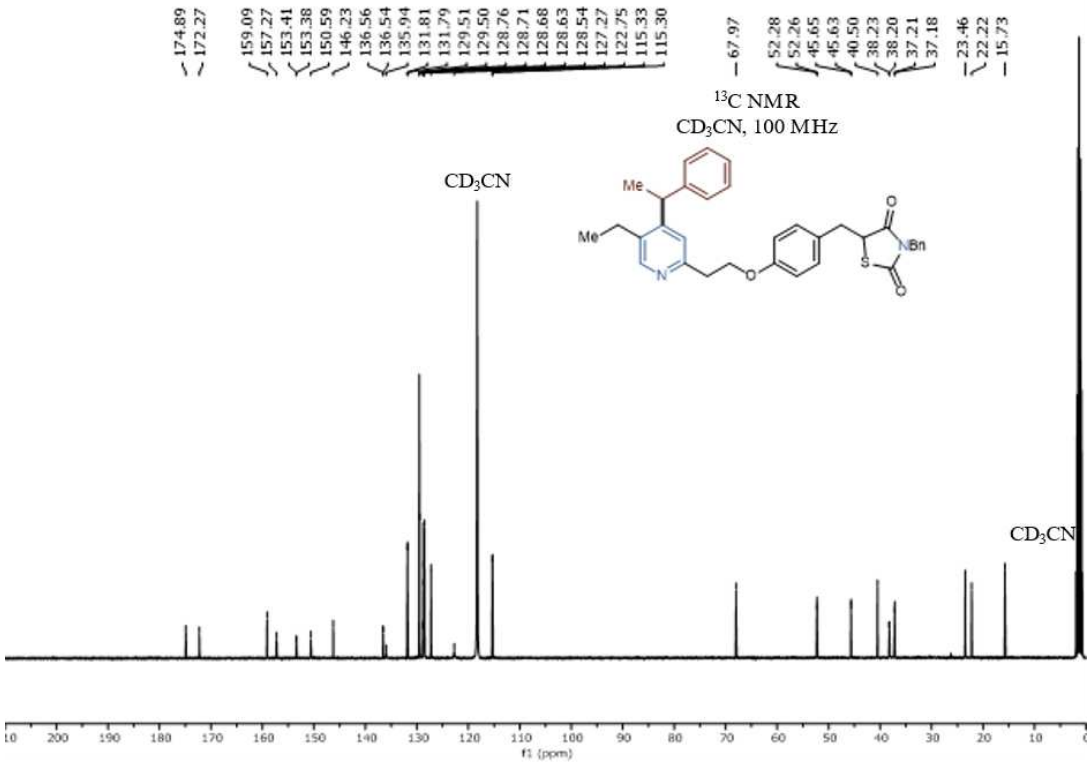
174.89
172.27
159.09
157.27
153.41
153.38
150.59
146.23
136.56
136.54
135.94
131.81
131.79
129.51
129.50
128.76
128.71
128.68
128.63
128.54
127.27
122.75
115.33
115.30
67.97
52.28
52.26
45.65
45.63
40.50
38.23
38.20
37.21
37.18
23.46
22.22
15.73
13C NMR
CD3CN, 100 MHz
CD3CN
CD3CN
Me
Me
N
O
O
S
NBn
O
f1 (ppm)

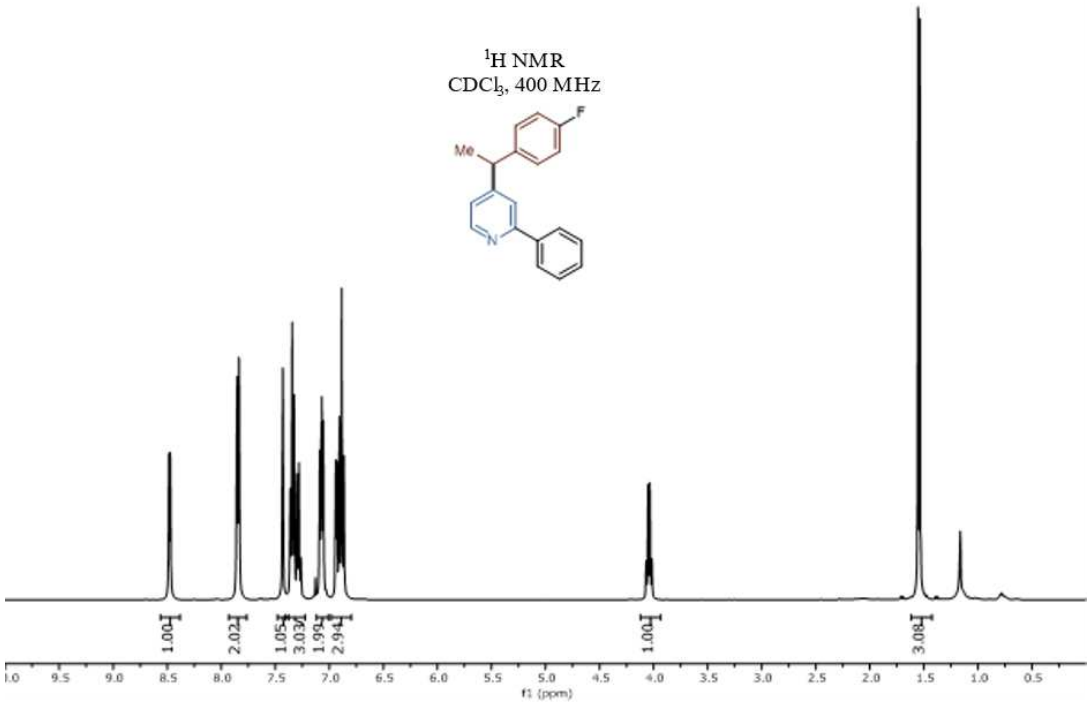
1H NMR
CDCl3, 400 MHz
F
Me
N
1.00
2.02
1.05
3.03
1.99
2.94
1.00
3.08
f1 (ppm)

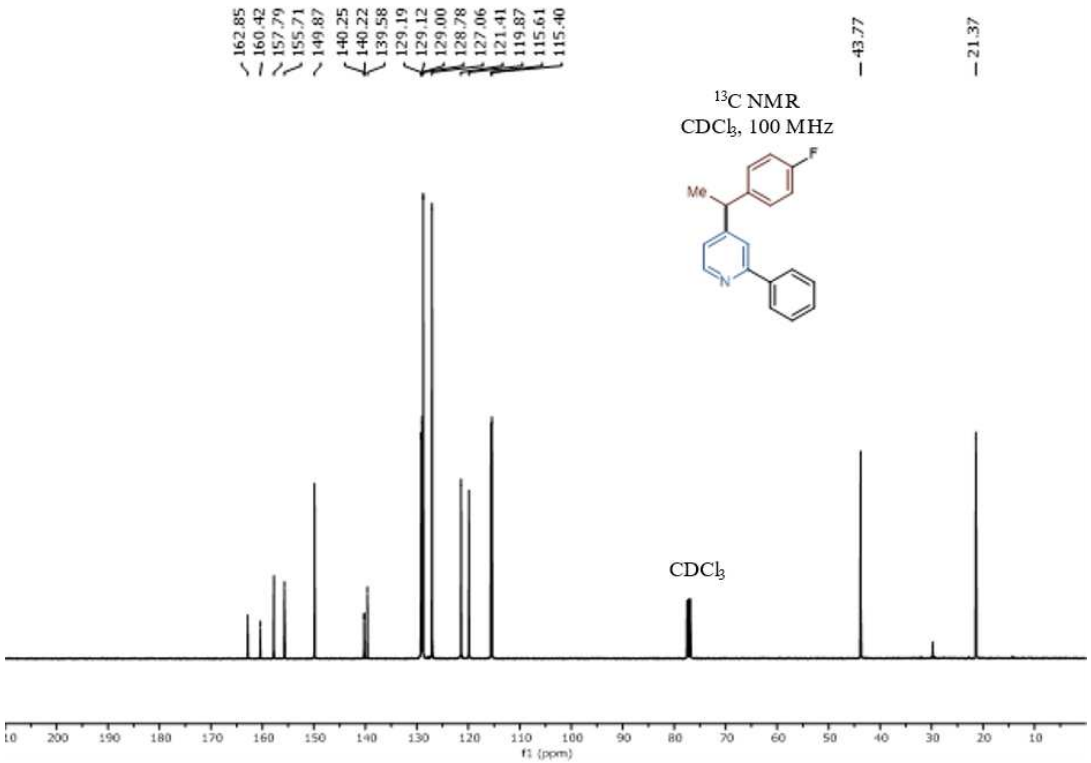
162.85
160.42
157.79
155.71
149.87
140.25
140.22
139.58
129.19
129.12
129.00
128.78
127.06
121.41
119.87
115.61
115.40
43.77
21.37
13C NMR
CDCl3, 100 MHz
Me
F
N
CDCl3
f1 (ppm)

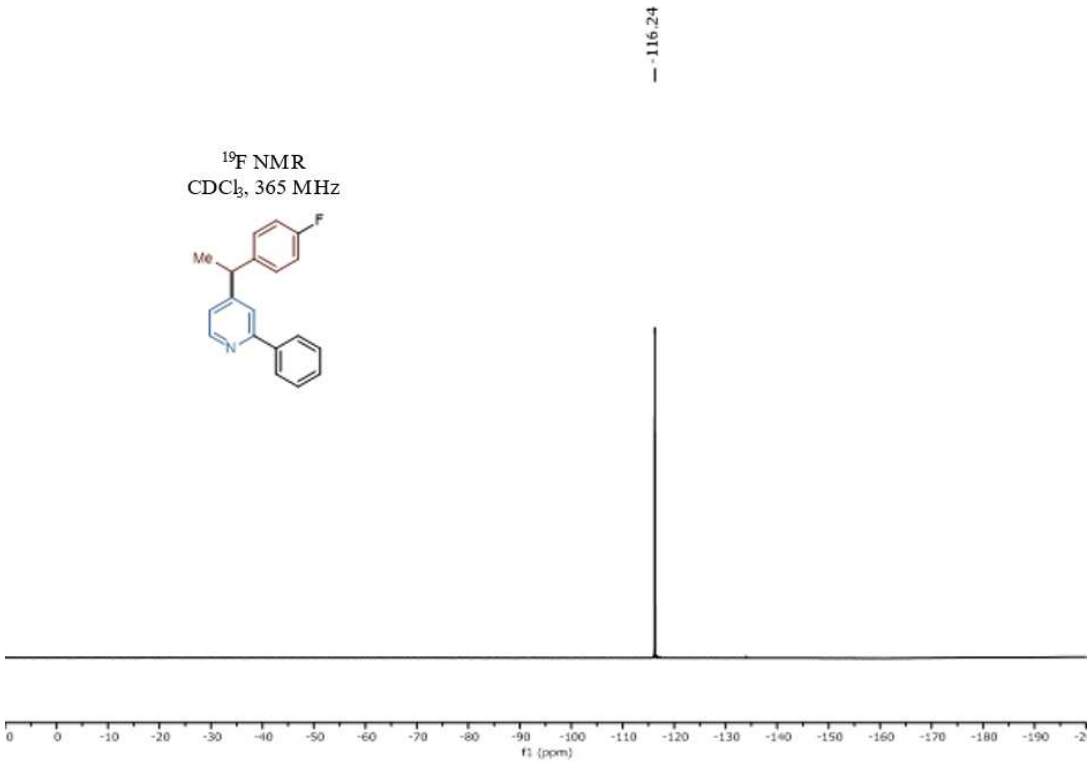
-116.24
19F NMR
CDCl3, 365 MHz
Me
F
N
f1 (ppm)

^{1}H NMR
$CDCl_3$, 400 MHz

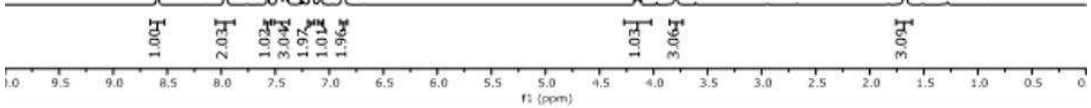

^{13}C NMR
$CDCl_3$, 100 MHz

$CDCl_3$

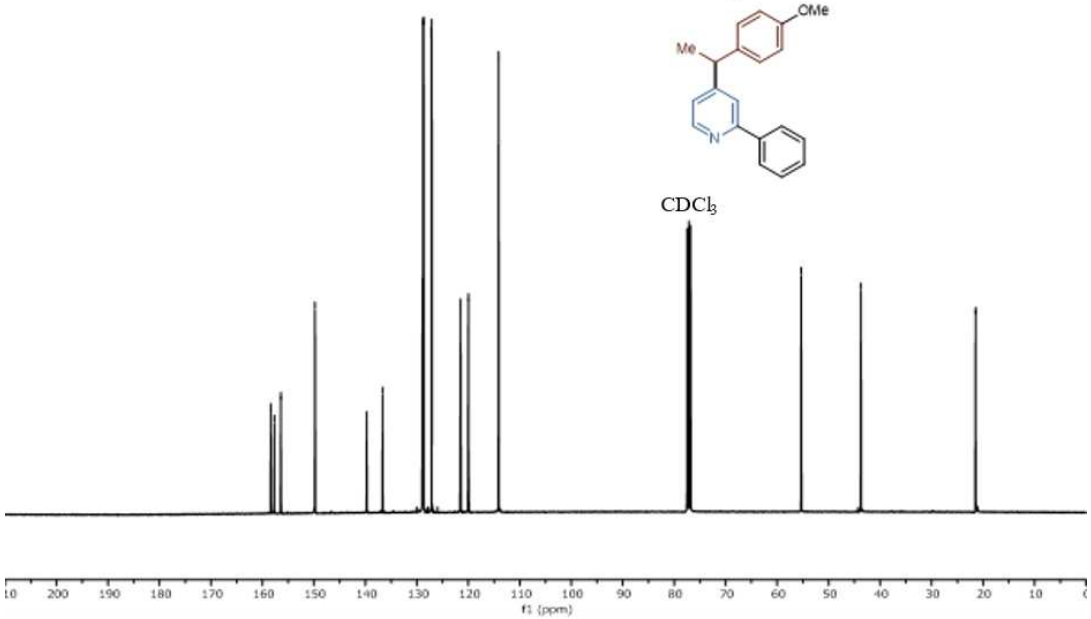

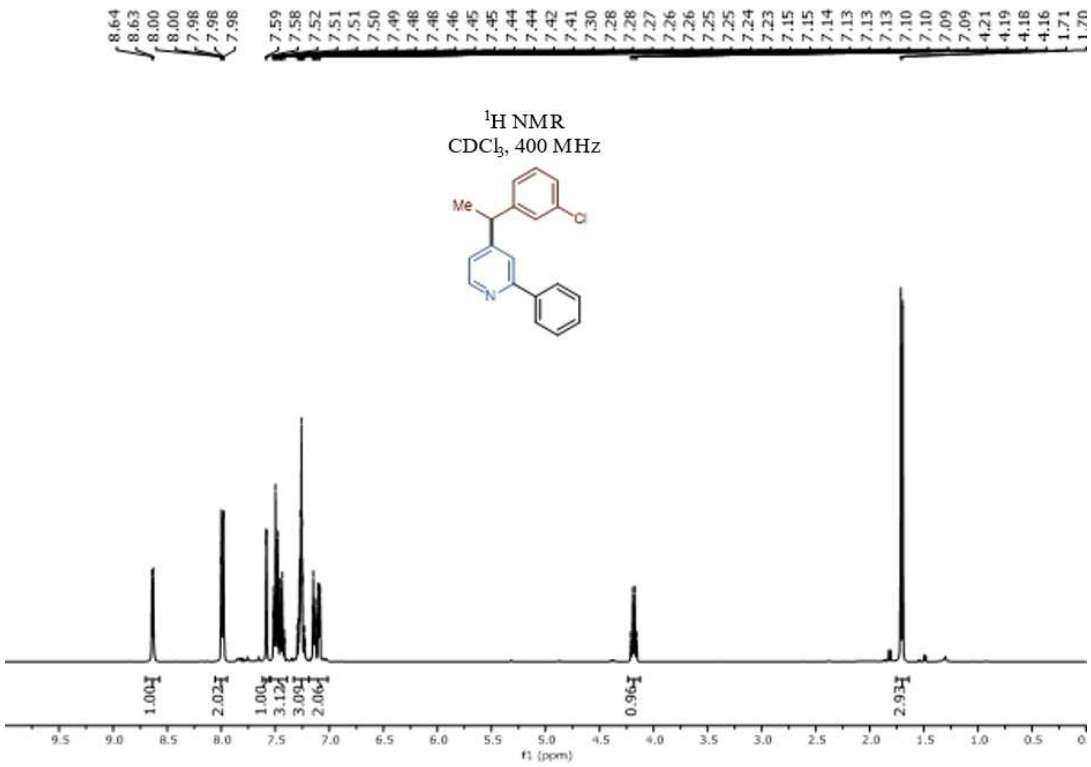
8.64
8.63
8.00
8.00
7.98
7.98
7.98
7.59
7.58
7.52
7.51
7.51
7.50
7.49
7.48
7.48
7.46
7.45
7.45
7.44
7.44
7.42
7.41
7.30
7.28
7.28
7.27
7.26
7.26
7.25
7.25
7.24
7.23
7.15
7.15
7.14
7.13
7.13
7.13
7.10
7.10
7.09
7.09
4.21
4.19
4.18
4.16
1.71
1.70
1H NMR
CDCl3, 400 MHz
Me
Cl
N
1.00
2.02
1.00
3.12
3.09
2.06
0.96
2.93
f1 (ppm)

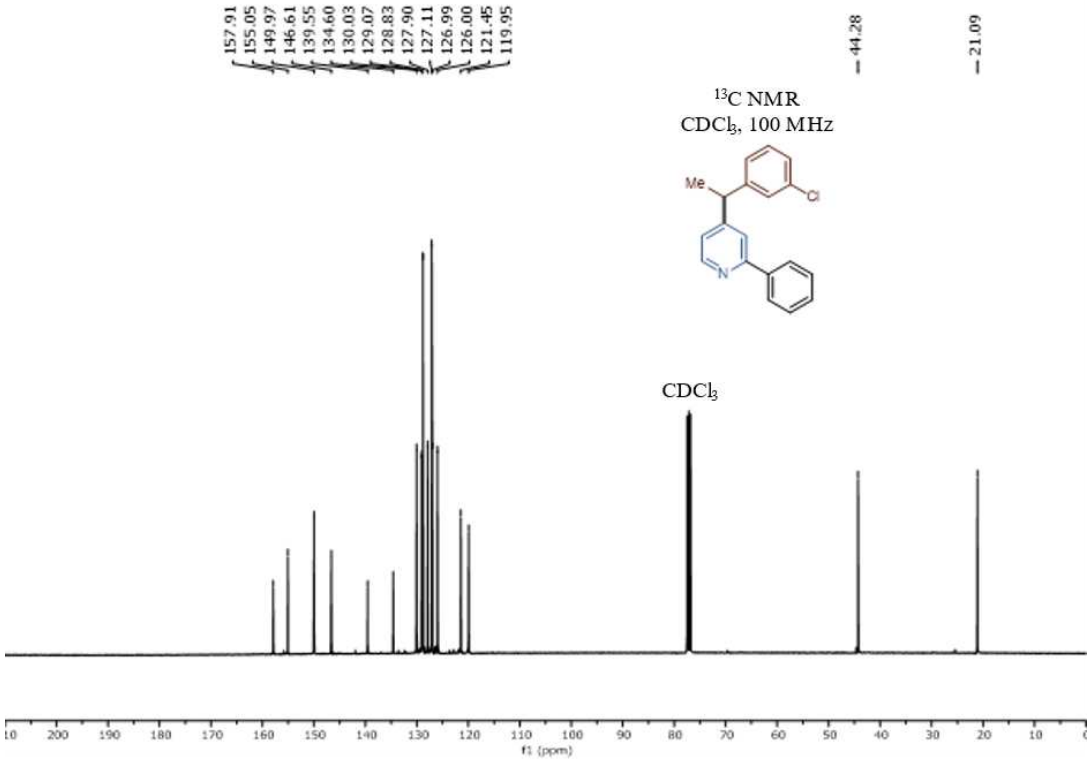
157.91
155.05
149.97
146.61
139.55
134.60
130.03
129.07
128.83
127.90
127.11
126.99
126.00
121.45
119.95
44.28
21.09
13C NMR
CDCl3, 100 MHz
Me
Cl
N
CDCl3
f1 (ppm)

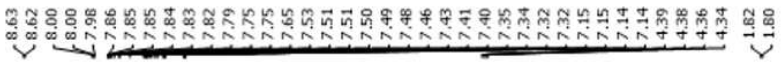

^{1}H NMR
$CDCl_3$, 400 MHz

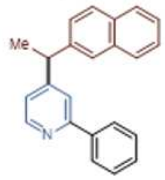

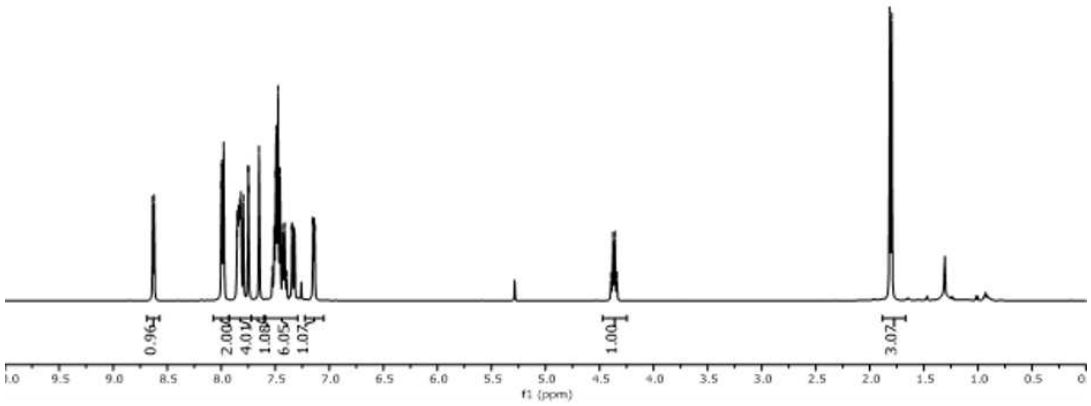

^{13}C NMR
$CDCl_3$, 100 MHz

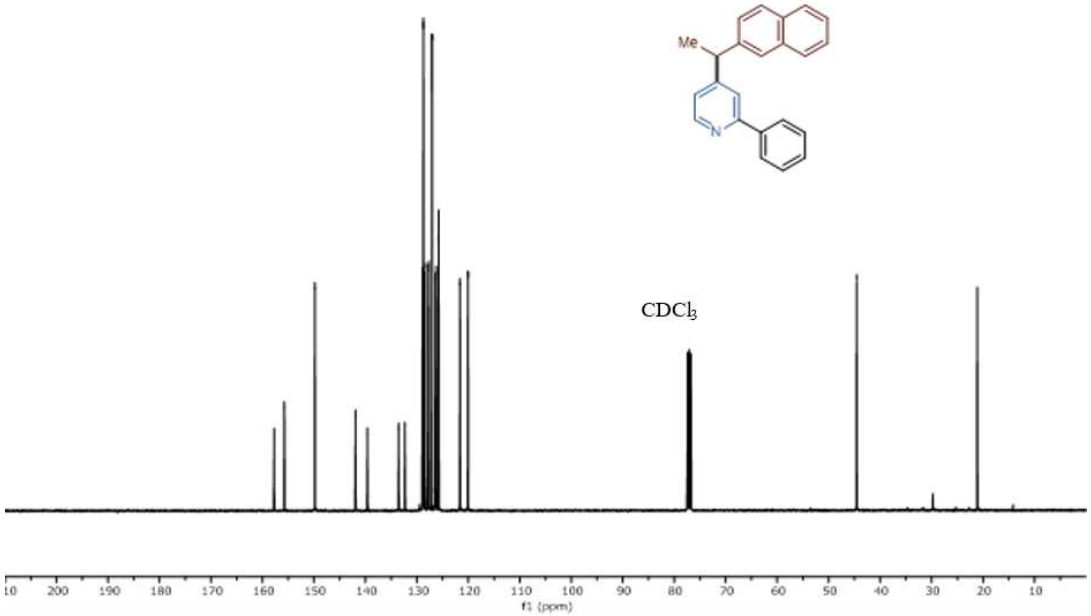

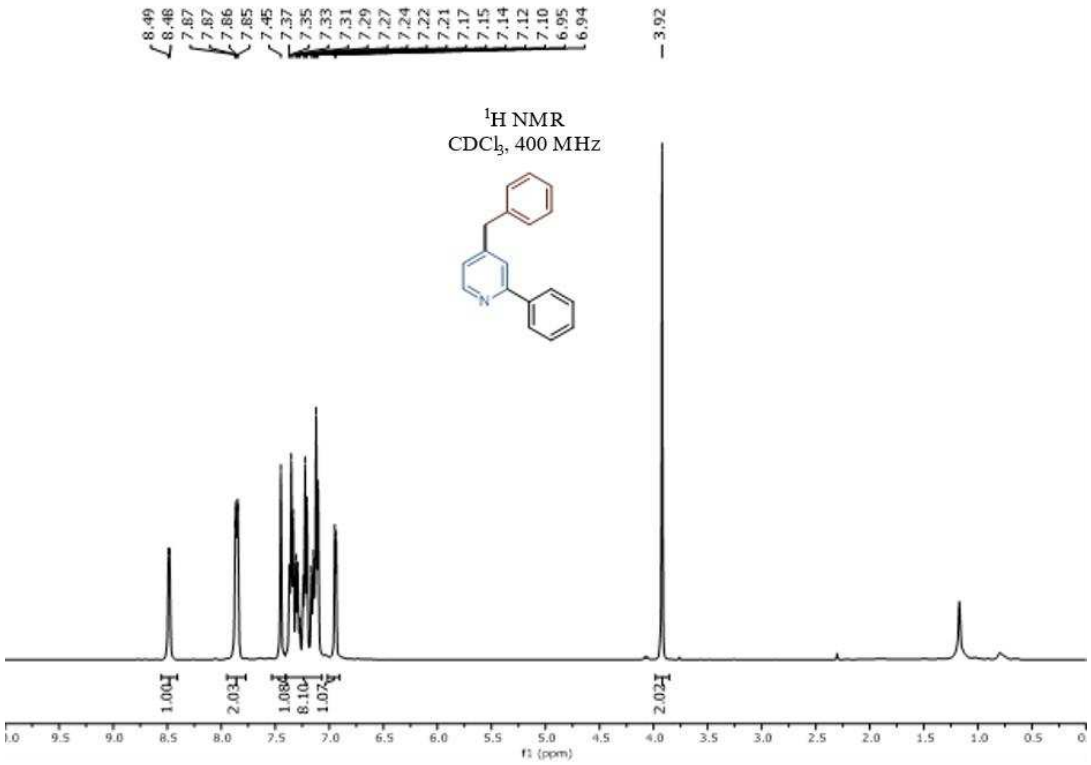
8.49
8.48
7.87
7.87
7.86
7.85
7.45
7.37
7.35
7.33
7.31
7.29
7.27
7.24
7.22
7.21
7.17
7.15
7.14
7.12
7.10
6.95
6.94
3.92
1H NMR
CDCl3, 400 MHz
1.00
2.03
1.08
8.10
1.07
2.02
f1 (ppm)

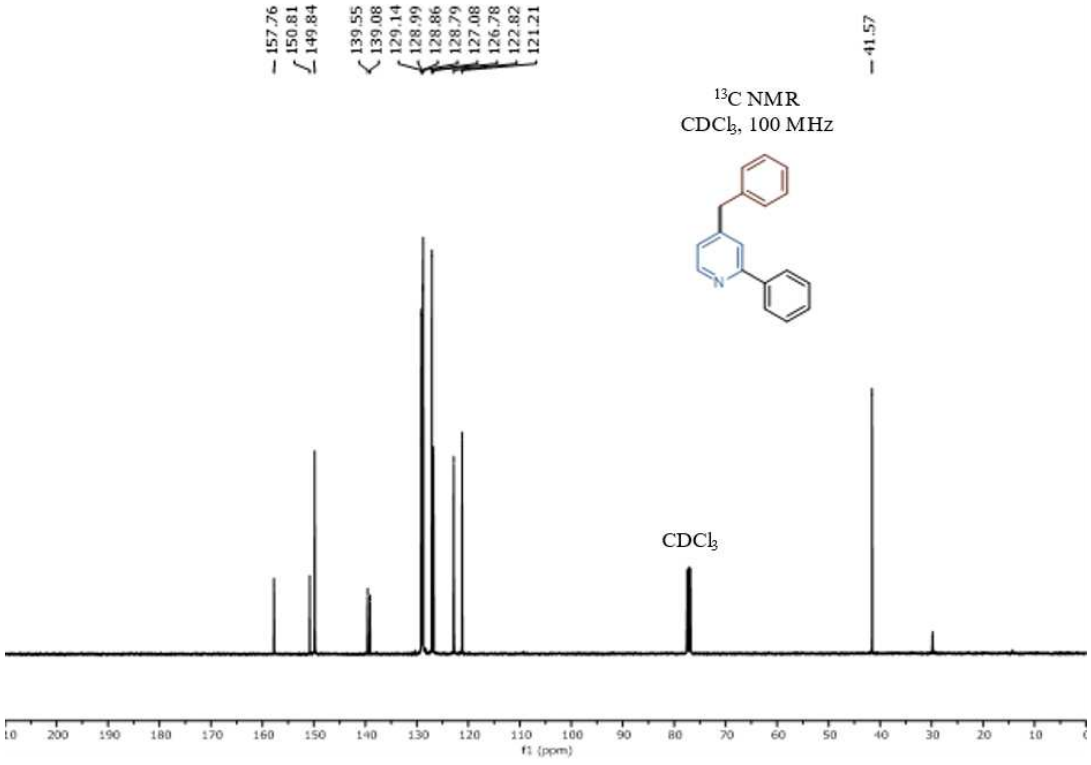
157.76
150.81
149.84
139.55
139.08
129.14
128.99
128.86
128.79
127.08
126.78
122.82
121.21
41.57
13C NMR
CDCl3, 100 MHz
CDCl3
f1 (ppm)

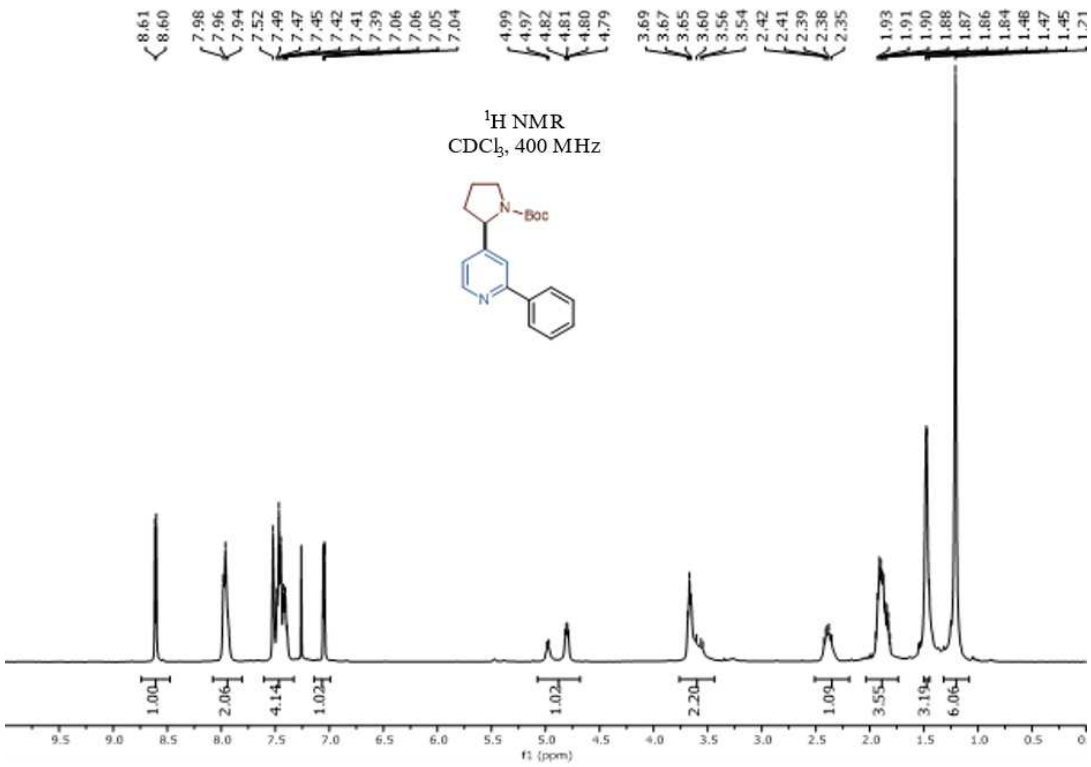
8.61
8.60
7.98
7.96
7.94
7.52
7.49
7.47
7.45
7.42
7.41
7.39
7.06
7.06
7.05
7.04
4.99
4.97
4.82
4.81
4.80
4.79
3.69
3.67
3.65
3.60
3.56
3.54
2.42
2.41
2.39
2.38
2.35
1.93
1.91
1.90
1.88
1.87
1.86
1.84
1.48
1.47
1.45
1.21
1H NMR
CDCl3, 400 MHz
Boc
1.00
2.06
4.14
1.02
1.02
2.20
1.09
3.55
3.19
6.06
f1 (ppm)

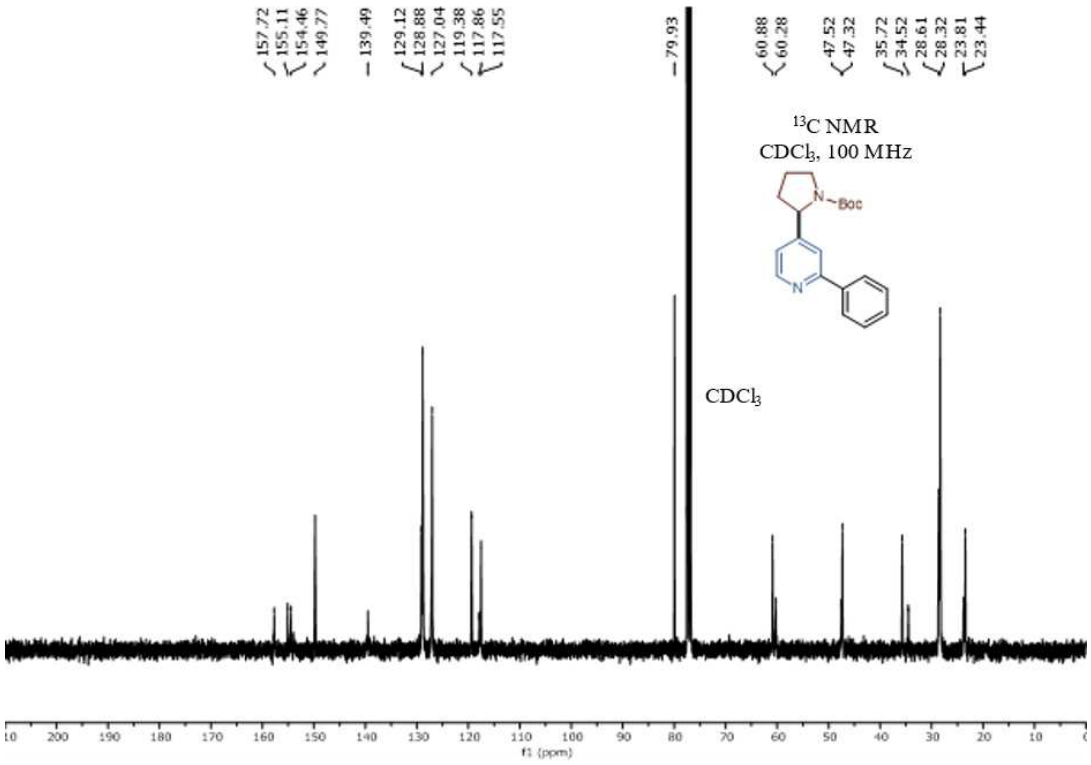
157.72
155.11
154.46
149.77
139.49
129.12
128.88
127.04
119.38
117.86
117.55
79.93
60.88
60.28
47.52
47.32
35.72
34.52
28.61
28.32
23.81
23.44
13C NMR
CDCl3, 100 MHz
Boc
CDCl3
f1 (ppm)

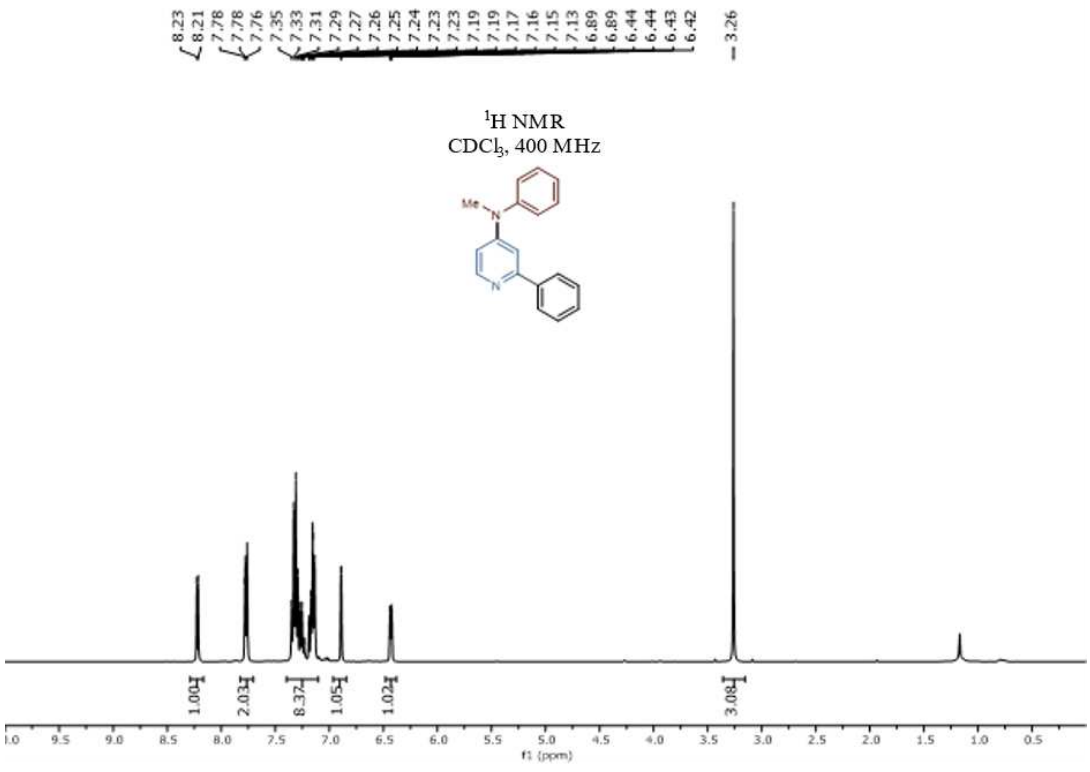
8.23
8.21
7.78
7.78
7.76
7.35
7.33
7.31
7.29
7.27
7.26
7.25
7.24
7.23
7.23
7.19
7.19
7.17
7.16
7.15
7.13
6.89
6.89
6.44
6.44
6.43
6.42
3.26
1H NMR
CDCl3, 400 MHz
Me
N
1.00
2.03
8.37
1.05
1.02
3.08
f1 (ppm)

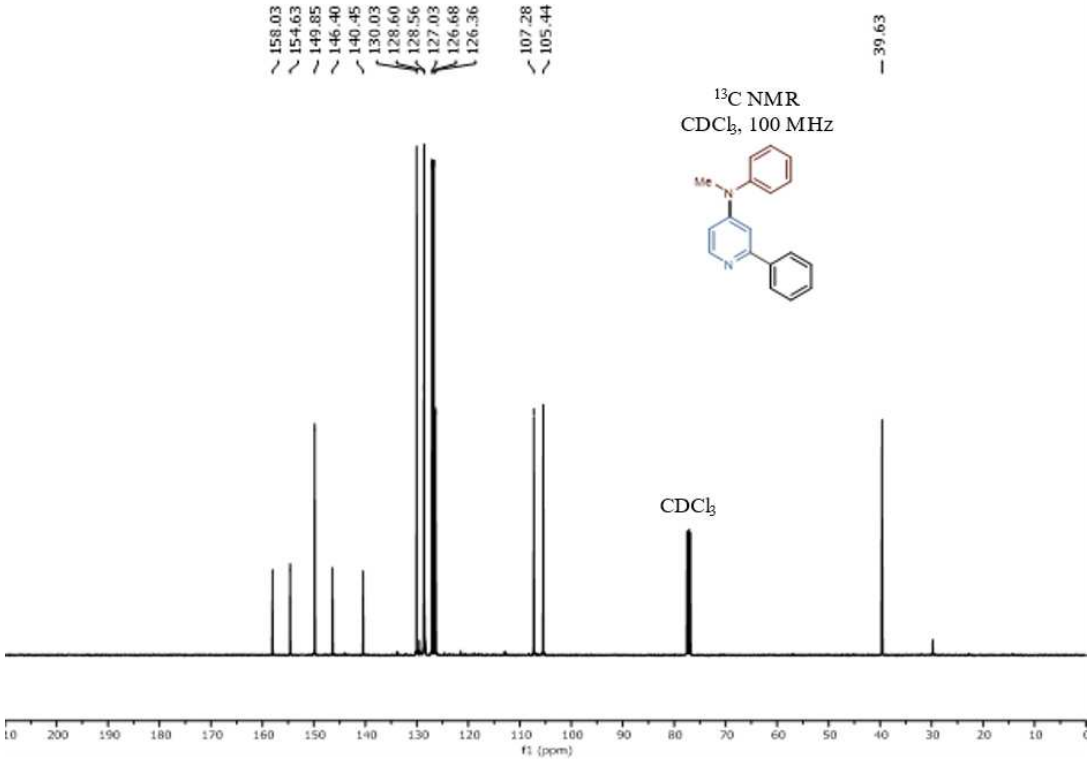
158.03
154.63
149.85
146.40
140.45
130.03
128.60
128.56
127.03
126.68
126.36
107.28
105.44
39.63
13C NMR
CDCl3, 100 MHz
Me
N
CDCl3
f1 (ppm)

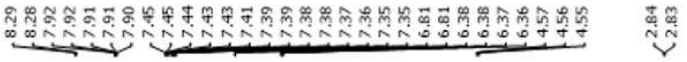

^{1}H NMR
$CDCl_3$, 400 MHz

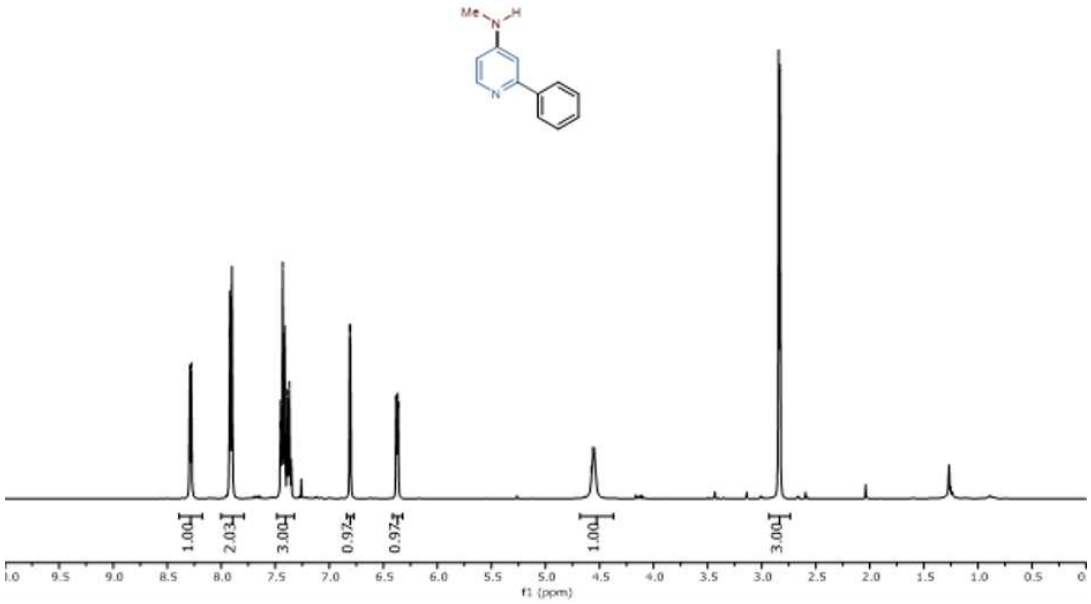

^{13}C NMR
$CDCl_3$, 100 MHz

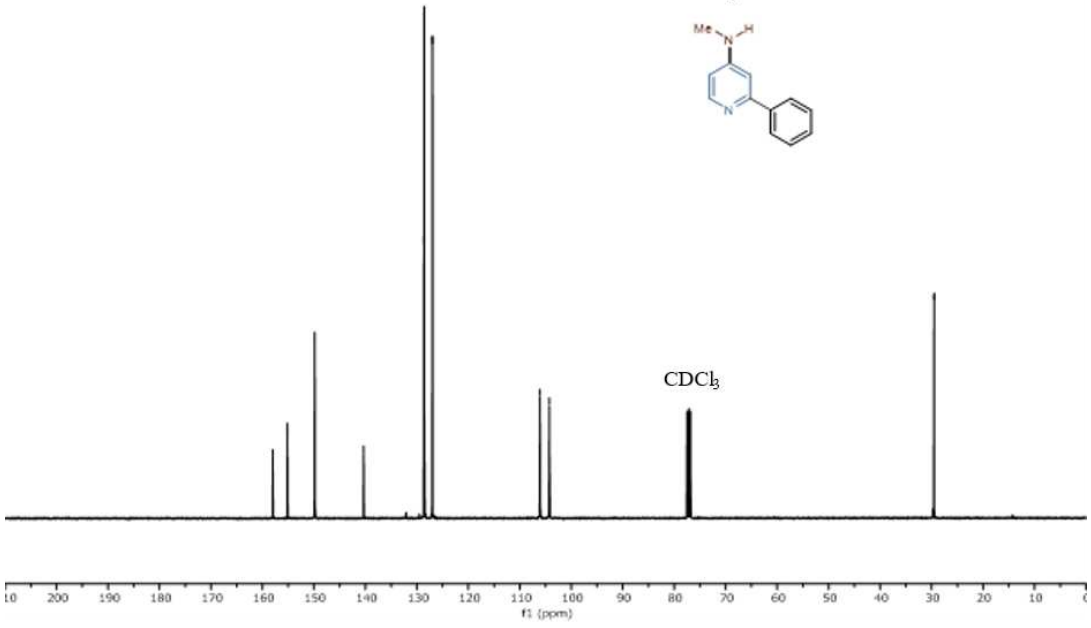

APPENDIX THREE

IMINIUM IONS AS A PLATFORM FOR *N*-(HETERO)ARYL PIPERIDINE SYNTHESIS: EXPERIMENTAL

A3.1. General Experimental:

Reactions were performed in scintillation vials with Teflon septa unless otherwise specified. Reactions were monitored by liquid chromatography/mass spectrometry (LCMS) or by thin-layer chromatography (TLC) on silica gel60 F254 plates (EMD) and visualized with UV light (254 nm). Flash chromatography was performed using prepacked RediSep gold Rf silica gel columns on a Teledyne Isco CombiFlash Rf automated chromatography system. Organic solutions were concentrated under reduced pressure on a Buchi rotary evaporator. Tetrahydrofuran (THF), toluene (PhMe or Tol), 1,4-dioxane, and acetonitrile (MeCN), were purchased from Sigma-Aldrich in Sure-Seal™ bottles and used as received. $CDCl_3$, CD_3OD, DMSO-d_6, acetone-d_6 and MeCN-d_3 were purchased from Cambridge Isotope Laboratories, Inc. and used as received. Acetonitrile (LC-MS grade), water (LC-MS grade), and 0.1% formic acid in water (LC-MS grade) were obtained from Fisher Scientific (Pittsburgh, PA, USA). Anilines were obtained from Merck's internal building block collection or purchased from commercial sources. If obtained as the corresponding salt, the salt was freebased using a saturated solution of sodium carbonate, followed by extraction with DCM x 3. Ketoacrylate coupling partners were synthesized as reported previously.[1] All other reagents were purchased from commercial sources and used as received.

NMR experiments were acquired at 298 K on a Bruker Avance III HD 600 MHz NMR with a prodigy cryoprobe TCI H&F-C/N-D (PP TCI 600S3 H&F-C/N-D-05 Z; probe ID Z129773-0040) "bos600b" or a Bruker Avance Neo 600 MHz NMR spectrometer with a room temperature probe (PA BBO 600 SE BBF-H-D-05-ZSP; probe ID Z114607-0276). ^{1}H, ^{13}C, HSQC and HMBC NMR experiments were acquired for all compounds. For reported compounds that contain

fluorine, a ^{19}F NMR experiment was also acquired. For several samples COSY experiments were also acquired to aid in structure assignment. All NMR data was processed and analyzed in MestReNova. For each compound only one major isomer was assigned. In instance where there were peak overlap integrations were normalized to the expected number of protons in the ^{1}H NMR report and the raw values are shown on the ^{1}H NMR spectrum. Chemical shifts are reported in parts per million (ppm, δ), downfield from tetramethylsilane (TMS, δ = 0.00 ppm) and are referenced to residual solvent (DMSO-d_6, δ = 2.50 ppm (^{1}H) and 39.52 ppm (^{13}C); CD_3CN 1.94 ppm (^{1}H) and 118.26 (^{13}C); $CDCl_3$ 7.26 ppm (^{1}H) and 77.16 (^{13}C)). Coupling constants were reported in Hertz (Hz). Data for ^{1}H NMR spectra were reported as follows: chemical shift in ppm (s = singlet, d = doublet, t = triplet, q = quartet, p = pentet, h (or hept) = heptet, dd = doublet of doublets, dt = doublet of triplets, td = triplet of doublets, tt = triplet of triplets, dq = doublet of quartets, ddd = doublet of doublet of doublets or m = multiplet, coupling constant (Hz), integration). For carbon resonances coupled to fluorine, ^{13}C NMR data were reported as follows: chemical shift in ppm (d = doublet, q = quartet or m = multiplet, coupling constant (Hz)).

LC/HRMS experiments were performed with a Waters Acquity H-Class UPLC system equipped with a Waters Xevo G2-XS mass spectrometer (Waters Corporation, Milford, MA, USA) with Waters MassLynx V4.2 software for instrument control and data processing. Samples were prepared in acetonitrile : water 90:10 (v/v) with a concentration of 0.2 mg/mL, then injected at 1 µL onto an Acquity UPLC® BEH C18 2.1 × 100 mm, 1.7 µm column with a flow rate of 0.4 mL/min at 40 °C. The aqueous mobile phase A was 0.1% formic acid in water, and organic mobile phase B was acetonitrile, with a gradient of 5% B over 0.0-0.5 min, 5%-95% B over 0.5-4.0 min, hold 95% B for 2 min, followed by re-equilibration to 5% B for 2 min. The eluents were monitored using a photodiode array detector with a scanning range from 210 nm to 400 nm, followed by

Xevo G2-XS HRMS detection in electrospray ionization positive mode. The tuned conditions were: capillary voltage 1.5 kV, cone gas flow 10 L/h, desolvation gas 400 L/h, source temperature 120 °C, desolvation temperature 350 °C, m/z range 50-600 Da. HRMS results were found to agree with the proposed structures within 5 ppm error.

A3.2. Crystal Data and Structure Refinement for Compound 1a (CCDC 2170178)

A single crystal grown from antisolvent addition of diethyl ether into a saturated dichloromethane solution was selected for single crystal X-ray data analysis. The crystal was a cut block with dimensions of 0.18 mm x 0.14 mm x 0.12mm. Data collection was performed on a Bruker Apex II system at 100K. The unit cell was determined to be monoclinic in space group $P2_1/n$. The structure contained one molecule in the crystallographic asymmetric unit. Molecular disorder was observed where the entire molecule was replaced with the enantiomer at approximately 22% occupancy. Significant disorder was also observed in the BF_4^-. SIMU restraints were necessary for the nitrogen atoms in the pyrazole. All modeled disorder was removed from Figure S1 for clarity.

Crystallographic data is summarized in Table A3.1. Figure A3.1 shows a thermal ellipsoid representation of Compound **1a** with thermal ellipsoids set at the 50% probability level. Coordinates, refinement details and structure factors have been deposited with the Cambridge Crystallographic Data Centre (CCDC 2170178).

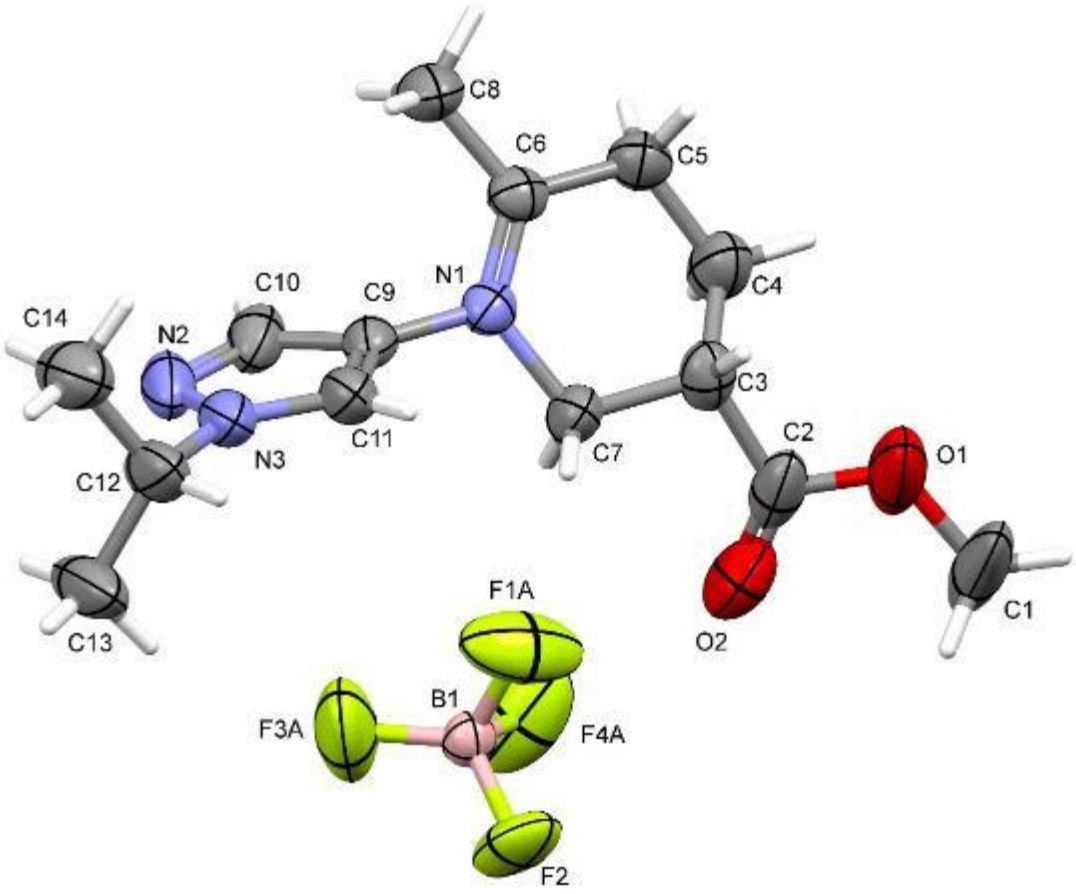

Figure A3.1: Thermal ellipsoid representation of Compound 1a with thermal ellipsoids set at the 50% probability level.

Table A3.1. Crystal data and structure refinement for mdq040.

Identification code	mdq040
Empirical formula	$C_{14}H_{22}BF_4N_3O_2$
Formula weight	351.15
Temperature	100(2) K
Radiation	CuKα (λ = 1.54178)
Crystal system	monoclinic
Space group	$P2_1/n$
Unit Cell Dimensions	a = 6.27420(10) Å α = 90°
	b = 21.3507(5) Å β = 93.7340(10)°
	c = 12.6275(3) Å γ = 90°
Volume	1687.97(6) ($Å^3$)
Z	4
Density	1.382 (g/cm^3)
Absorption coefficient	1.051 mm^{-1}
F(000)	736.0
Crystal size	0.18 × 0.14 × 0.12 mm^3
2Θ range for data collection	8.148° to 133.388°
Index ranges	$-7 \leq h \leq 7$, $-25 \leq k \leq 25$, $-15 \leq l \leq 13$
Reflections collected	19743
Independent reflections	2989 [R_{int} = 0.0363, R_{sigma} = 0.0234]
Completeness to Θ=66.694°	0.996

Absorption correction	multi-scan
Max. and min. transmission	0.7528 and 0.6780
Refinement Method	Full-matrix least-squares on F^2
Data/restraints/parameters	2989/6/268
Goodness-of-fit on F^2	1.035
Final R indexes [I>=2σ (I)]	$R_1 = 0.0924$, $wR_2 = 0.2295$
Final R indexes [all data]	$R_1 = 0.0939$, $wR_2 = 0.2306$
Largest diff. peak/hole	0.88/-0.35 $eÅ^{-3}$

A3.3. Optimization of Iminium Salt 114 Formation:

Table A2.2. Iminium salt **114** formation optimization.

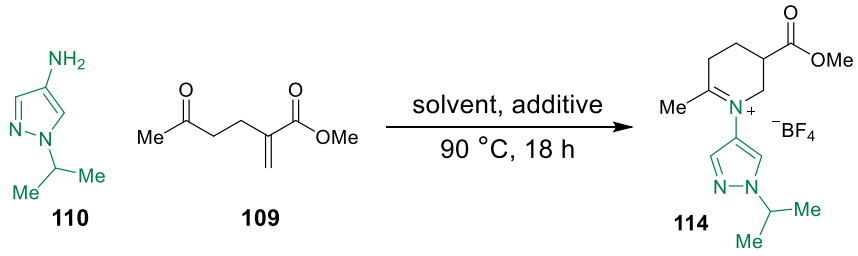

Entry	Solvent	additive	% yield
1	MeOH	-	0
2	MeOH	$LiBF_4$ (1.0 eq)	20
3	TFE	$LiBF_4$ (1.0 eq)	66
4	TFE	Water	11
5	TFE	$LiBF_4$ (0.5 eq)	44
6	TFE	$LiBF_4$ (1.2 eq)	78
7	TFE	$LiBF_4$ (1.5 eq)	45
8[c]	TFE	$LiBF_4$ (1.0 eq)	75[d]

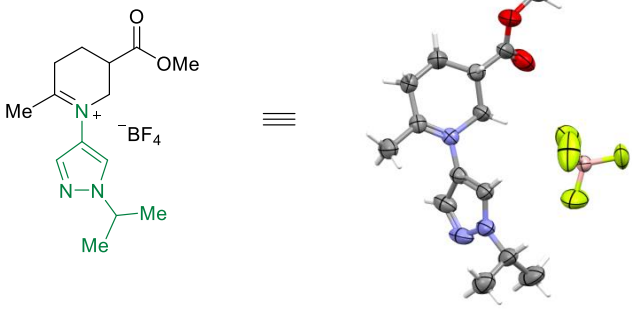

[a]Reactions were conducted on 0.1 mmol scale with 1.5 equiv **A,** 1.0 equiv **B**, and TFE (0.5 M) unless otherwise noted. Cosolvent and water mixtures were 50% v/v. Yields of **114** for individual reaction mixtures were determined using ^{1}H NMR with reference to internal 1,3,5-trimethoxybenzene. [b]Elipsoids for the single crystal x-ray structure of **114** are displayed at 50% probability. [c]The reaction was run in a microwave vial on 10 mmol scale at 120 °C for 48 h using 1.0 equiv **110**, 1.0 equiv **109**, 1.0 equiv $LiBF_4$ and 2.5 mL of TFE (4.0 M). The isolated yield for this example is given in parenthesis.

Procedure for cyclization optimization studies

A 4 mL vial with a stirbar was charged with electrophile, amine, additive, followed by TFE. The reaction vessel was sealed and heated to 90 °C unless otherwise noted. The reaction progress was followed by LCMS analysis to completion (usually 20-48 hours). The mixture was cooled to room temperature, 1,3,5-trimethoxybenzene was added, and the crude reaction was analyzed by ^{1}H NMR. The integral values were used to calculate the data given in **Table A3.2**.

Exploration of Other Lewis Acid Additives

A stock solution was made of aniline **110** (14.1 μL, 112.5 μmol, 1.50 equiv) and ketoacrylate **109** (11.7 μL, 75 μmols, 1.00 equiv) in TFE (750 μL, 0.1 M with respect to **109**) so that when plated with the corresponding Lewis Acids, there would be 20 mol% of the additive. 25 μL of the stock solution was dosed to each well with the preweighed additive (0.50 μmols, 0.20 equiv). The plate was stirred overnight at 90 °C. The reactions were cooled to room temperature, and 130 μL of a 0.10 M biphenyl solution in DMSO were added to each well. The plate was resealed and stirred for 30 seconds. 50 μL of each solution was removed and added to 1 mL of a 9:1 mixture of MeCN:H_2O in an HPLC vial. The samples were analyzed via UPLC. The numbers reported below correspond to the ratio of product:biphenyl internal standard.

Table A3.3. Results of 20 mol% additive screen.

20 mol% Catalyst Screening					
A	**B**	**C**	**D**	**E**	**F**
1	**Mg(OTf)$_2$**	**Al(OTf)$_3$**	**Ca(OTf)$_2$**	**Sc(OTf)$_3$**	**Cp$_2$Ti(OTf)$_2$**	**Fe(OTf)$_2$**
	0.50	0.72	0.32	0.76	0.51	0.39
2	**Fe(OTf)$_3$**	**Cu(OTf)$_2$**	**Ni(OTf)$_2$**	**Zn(OTf)$_2$**	**Ga(OTf)$_3$**	**Y(OTf)$_3$**
	0.38	0.00	0.48	0.53	0.71	0.88
3	**AgOTf**	**In(OTf)$_3$**	**Sn(OTf)$_2$**	**Ba(OTf)$_2$**	**La(OTf)$_3$**	**Pr(OTf)$_3$**
	0.27	0.65	0.42	0.25	0.78	0.67
4	**Nd(OTf)$_3$**	**Sm(OTf)$_3$**	**Eu(OTf)$_3$**	**Er(OTf)$_3$**	**Yb(OTf)$_3$**	**Bi(OTf)$_3$**
	0.25	0.61	0.45	0.00	0.52	0.57

Scaled up the best result to determine % yield of product via 1H NMR assay with 1,3,5-trimethoxybenzene as internal standard.

-Y(OTf)$_3$ on 0.10 mmol scale corresponded to a 38% yield of **114**.

A stock solution was made of aniline **110** (5.6 µL, 45 µmol, 1.50 equiv) and ketoacrylate **109** (4.7 µL, 30 µmols, 1.00 equiv) in TFE (300 µL, 0.1 M with respect to **109**) so that when plated with the corresponding Lewis Acids, there would be 50 mol% of the additive. 10 µL of the stock solution was dosed to each well with the preweighed additive (0.50 µmols, 0.50 equiv). The plate was stirred overnight at 90 °C. The reactions were cooled to room temperature, and 65 µL of a 0.10 M biphenyl solution in DMSO were added to each well. The plate was resealed and stirred for 30 seconds. The entire sample in each well was removed and added to 1 mL of a 9:1 mixture

of MeCN:H_2O in an HPLC vial. The samples were analyzed via UPLC. The numbers reported below orrespond to the ratio of product:biphenyl internal standard.

Table S4. Results of 50 mol% additive screen.

50 mol% Catalyst Screening					
A	**B**	**C**	**D**	**E**	**F**
1					
$Mg(OTf)_2$	**$Al(OTf)_3$**	**$Ca(OTf)_2$**	**$Sc(OTf)_3$**	**$Cp_2Ti(OTf)_2$**	**$Fe(OTf)_2$**
0.35	0.39	0.12	0.49	0.61	0.15
2					
$Fe(OTf)_3$	**$Cu(OTf)_2$**	**$Ni(OTf)_2$**	**$Zn(OTf)_2$**	**$Ga(OTf)_3$**	**$Y(OTf)_3$**
0.14	0.00	0.22	0.36	0.36	0.55
3					
AgOTf	**$In(OTf)_3$**	**$Sn(OTf)_2$**	**$Ba(OTf)_2$**	**$La(OTf)_3$**	**$Pr(OTf)_3$**
0.38	0.61	0.52	0.08	0.04	0.18
4					
$Nd(OTf)_3$	**$Sm(OTf)_3$**	**$Eu(OTf)_3$**	**$Er(OTf)_3$**	**$Yb(OTf)_3$**	**$Bi(OTf)_3$**
0.08	0.65	0.56	0.13	0.06	0.22

-$Y(OTf)_3$ on 0.10 mmol scale corresponded to a 66% yield of **114**.

-$Sm(OTf)_3$ on 0.10 mmol scale corresponded to a 72% yield of **114**.

-Attempts to increase the yield by increasing the equivalents of the additive were unsuccessful as the % conversion of the reaction was negatively impacted.

Conclusion: These optimal yields with these additives were lower than the best yield with $LiBF_4$ as additive. Additionally, 0.50 equivalents of the trifluoromethanesulfonate salt additives are more expensive than 1.2 equivalents of $LiBF_4$. For these reasons, we decided $LiBF_4$ was the best additive to use.

A3.4. Preparation of Iminium Salts:

General Procedure A: Iminium Salt Synthesis and Isolation

A microwave vial with a stirbar was charged with electrophile (1.00 equiv), amine (1.00 equiv), $LiBF_4$ (1.00 equiv), and TFE (4.0 M). The reaction vessel was sealed and heated to 120 °C unless otherwise noted. The reaction progress was followed by LCMS analysis to completion (usually 20-48 hours). The mixture was cooled to room temperature, diluted with DCM to 0.05 M, and stirred at room temperature with activated charcoal for 1 hour (DARKO® KB-WJ, 300 mg/mmol amine starting material). The suspension was filtered, the activated charcoal was washed with DCM x 3, and the filtrate was concentrated via rotary evaporation. The crude residue was dissolved in 25 mL DCM and added dropwise to a stirred, 400 mL mixture of diethyl ether and hexanes (50:50). The resulting suspension was placed in a -20 °C refrigerator for 30 minutes. The suspension was removed from the refrigerator, the mother liquor was decanted, and the remaining residue was washed with 20 mL of a mixture of diethyl ether and hexanes (50:50) x 3. The residue was then dissolved with DCM, transferred to a round bottom flask, and concentrated to dryness to provide the desired iminium salt as an amorphous solid.

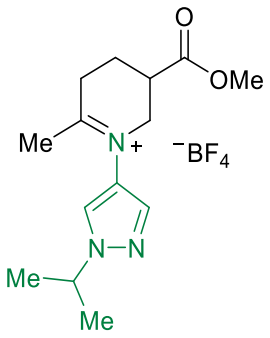

114

The synthesis and purification of **114** was conducted on 5.0 mmol scale according to General Procedure A with methyl 2-methylene-5-oxohexanoate as the electrophile and 1-isopropyl-1H-pyrazol-4-amine as the nucleophile. The cyclization was conducted for 48 h, and precipitation yielded **114** (1.32 g, 75% yield) an orange amorphous solid. ^{1}H NMR (600 MHz, $CDCl_3$) δ 8.16 (s, 1H), 7.63 (s, 1H), 4.52 (p, *J* = 6.7 Hz, 1H), 4.31 – 4.22 (m, 1H), 4.13 (dd, *J* = 15.3, 5.7 Hz, 1H), 3.76 (s, 3H), 3.30 (m, 2H), 2.94 (dt, *J* = 21.3, 6.5 Hz, 1H), 2.50 – 2.42 (m, 1H), 2.39 (s, 1H), 2.23 – 2.13 (m, 1H), 1.53 (d, *J* = 6.6 Hz, 6H). ^{13}C NMR (151 MHz, $CDCl_3$) δ 193.76, 171.83, 132.87, 124.72, 123.66, 58.98, 55.40, 52.87, 36.87, 33.11, 25.55, 22.76, 19.43. ^{19}F NMR (470 MHz, CD_3CN) δ -151.79. ESIHR $(M\text{-}BF_4)^+$ calc'd 264.1707, found 264.1713.

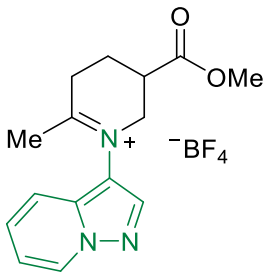

125

The synthesis of **125** was conducted on 5.0 mmol scale according to the general procedure with methyl 2-methylene-5-oxohexanoate as the electrophile and pyrazolo[1,5-a]pyridin-3-amine as the nucleophile. The cyclization was conducted for 16 h, and precipitation yielded **125** (1.11 g, 62% yield) as a brown amorphous solid. ^{1}H NMR (600 MHz, DMSO) δ 8.85 (dt, *J* = 7.0, 1.1 Hz, 1H), 8.32 (s, 1H), 7.90 (dt, *J* = 9.0, 1.2 Hz, 1H), 7.56 (ddd, *J* = 9.0, 6.8, 1.0 Hz, 1H), 7.15 (td, *J* = 6.9, 1.4 Hz, 1H), 4.34 – 4.17 (m, 2H), 3.72 (s, 3H), 3.42 – 3.38 (m, 1H), 3.21 (q, *J* = 6.0 Hz, 2H), 2.30 (d, *J* = 1.6 Hz, 3H), 2.24 – 2.19 (m, 1H), 2.09 – 2.03 (m, 1H). ^{13}C NMR (151 MHz, DMSO) δ 194.64, 171.54, 137.18, 133.31, 129.72, 126.87, 115.73, 114.08, 113.23, 57.55, 52.35, 36.60, 33.16, 24.90, 19.40. ^{19}F NMR (564 MHz, DMSO) δ -148.89. ESIHR ESIHR $(M\text{-}BF_4)^+$ calc'd 272.1399, found 272.1396.

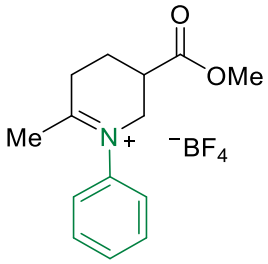

126

The synthesis of **126** was conducted on 5.0 mmol scale according to the general procedure with methyl 2-methylene-5-oxohexanoate as the electrophile and aniline as the nucleophile. The cyclization was conducted for 43 h, and precipitation yielded **126** (1.19 g, 75% yield) as a red oil. ^{1}H NMR (600 MHz, DMSO) δ 7.71 – 7.66 (m, 2H), 7.65 – 7.60 (m, 1H), 7.55 (d, *J* = 7.6 Hz, 2H), 4.21 – 4.05 (m, 2H), 3.70 (s, 3H), 3.36 – 3.32 (m, 1H), 3.14 – 3.12 (m, 2H), 2.25 – 2.18 (m, 1H), 2.16 (s, 3H), 2.05 – 1.98 (m, 1H). ^{13}C NMR (151 MHz, DMSO) δ 191.61, 171.43, 141.78, 130.66, 130.55, 123.92, 56.89, 52.31, 36.39, 32.76, 24.76, 19.42. ^{19}F NMR (564 MHz, DMSO) δ -148.91. ESIHR $(M\text{-}BF_4)^+$ calc'd 232.1338, found 232.1340.

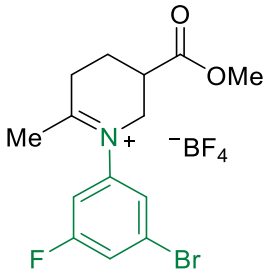

127

The synthesis of **127** was conducted on 5.0 mmol scale according to the general procedure with methyl 2-methylene-5-oxohexanoate as the electrophile and 3-bromo-5-fluoroaniline as the nucleophile. The cyclization was conducted for 42 h, and precipitation yielded **127** (1.05 g, 51% yield) as an orange amorphous solid. ^{1}H NMR (600 MHz, CD_3CN) δ 7.68 – 7.61 (m, 1H), 7.53 (s, 1H), 7.38 – 7.28 (m, 1H), 4.12 (d, *J* = 6.1 Hz, 2H), 3.73 (d, *J* = 1.9 Hz, 3H), 3.32

– 3.23 (m, 1H), 3.15 – 3.10 (m, 2H), 2.26 (d, J = 13.6 Hz, 4H), 2.14 – 2.03 (m, 1H). ^{13}C NMR (151 MHz, CD_3CN) δ 193.77, 170.17, 161.80 (d, J = 253.4 Hz), 141.89 (d, J = 10.9 Hz), 122.87 (d, J = 10.7 Hz), 122.64 (d, J = 3.9 Hz), 120.70 (d, J = 24.5 Hz), 110.54 (d, J = 26.0 Hz), 56.29, 51.18, 35.34, 31.97, 23.73, 18.16. ^{19}F NMR (564 MHz, CD_3CN) δ -108.46, -152.14. ESIHR (M-BF_4)$^+$ calc'd 328.0348, found 328.0343.

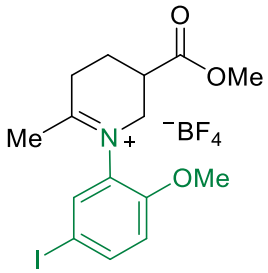

128

The synthesis of **128** was conducted on 5.0 mmol scale according to the general procedure with methyl 2-methylene-5-oxohexanoate as the electrophile and 5-iodo-2-methoxyaniline as the nucleophile. The cyclization was conducted for 43 h, and precipitation yielded **128** (1.23 g, 52% yield) a brown amorphous solid. ^{1}H NMR (600 MHz, CD_3CN) δ 7.92 – 7.86 (m, 1H), 7.70 (d, J = 2.2 Hz, 1H), 7.06 (dd, J = 8.9, 7.6 Hz, 1H), 4.07 – 3.99 (m, 2H), 3.88 (s, 3H), 3.72 (s, 3H), 3.21 – 3.10 (m, 3H), 2.27 – 2.18 (m, 1H), 2.18 (s, 3H), 2.12 – 2.00 (m, 1H). ^{13}C NMR (151 MHz, CD_3CN) δ 195.77, 172.06, 152.76, 142.21, 134.10, 131.51, 116.74, 82.34, 57.33, 57.19, 53.15, 37.77, 34.06, 25.04, 20.49. ^{19}F NMR (564 MHz, CD_3CN) δ -152.37. ESIHR (M-BF_4)$^+$ calc'd 388.0410, found 388.0412.

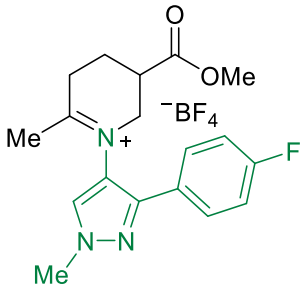

129

The synthesis of **129** was conducted on 5.0 mmol scale according to the general procedure with methyl 2-methylene-5-oxohexanoate as the electrophile and 3-(4-fluorophenyl)-1-methyl-1H-pyrazol-4-amine as the nucleophile. The cyclization was conducted for 43 h, and precipitation yielded **129** (1.67 g, 80% yield) as a light red amorphous solid. ^{1}H NMR (600 MHz, DMSO) δ 8.18 (s, 1H), 7.65 – 7.56 (m, 2H), 7.33 – 7.25 (m, 2H), 4.13 – 4.00 (m, 2H), 3.97 (s, 3H), 3.64 (s, 3H), 3.31 – 3.12 (m, 3H), 2.29 (d, *J* = 1.7 Hz, 3H), 2.17 (dq, *J* = 14.0, 5.3 Hz, 1H), 2.00 – 1.94 (m, 1H). ^{13}C NMR (151 MHz, DMSO) δ 195.91, 171.14, 162.37 (d, *J* = 246.4 Hz), 141.88, 129.64, 128.67 (d, *J* = 8.4 Hz), 126.65 (d, *J* = 3.2 Hz), 120.18, 116.27 (d, *J* = 21.7 Hz), 57.42, 52.31, 39.66, 36.55, 33.31, 25.24, 19.20. ^{19}F NMR (564 MHz, DMSO) δ -113.01, -148.86. ESIHR $(M\text{-}BF_4)^+$ calc'd 330.1618, found 330.1624.

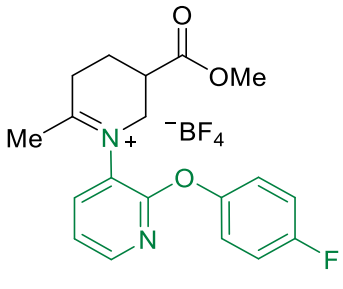

130

The synthesis of **130** was conducted on 5.0 mmol scale according to the general procedure with methyl 2-methylene-5-oxohexanoate as the electrophile and 2-(4-

fluorophenoxy)pyridin-3-amine as the nucleophile. The cyclization was conducted for 66 h at 140 °C, and precipitation yielded **130** (1.00 g, 47% yield) as a red amorphous solid. ^{1}H NMR (600 MHz, CD_3CN) δ 8.28 (td, *J* = 4.7, 1.8 Hz, 1H), 7.99 (ddd, *J* = 21.9, 7.8, 1.8 Hz, 1H), 7.36 – 7.30 (m, 1H), 7.29 – 7.16 (m, 4H), 4.37 – 4.28 (m, 1H), 4.26 – 4.15 (m, 1H), 3.60 (s, 3H), 3.28 – 3.18 (m, 3H), 2.36 (s, 3H), 2.30 – 2.22 (m, 1H), 2.17 – 2.08 (m, 1H). ^{13}C NMR (151 MHz, CD_3CN) δ 197.21, 172.06, 161.04 (d, *J* = 242.1 Hz), 156.29, 150.83, 149.37 (d, *J* = 2.6 Hz), 136.75, 125.72, 124.69 (d, *J* = 7.1 Hz), 120.93, 117.04 (d, *J* = 1.7 Hz), 57.54, 53.06, 37.74, 34.34, 25.54, 20.43. ^{19}F NMR (564 MHz, CD_3CN) δ -119.51, -152.30. ESIHR $(M\text{-}BF_4)^+$ calc'd 343.1458, found 343.1451.

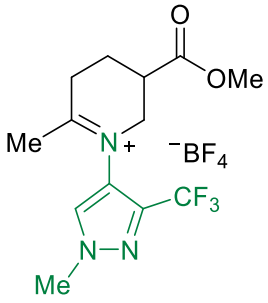

131

The synthesis of **131** was conducted on 5.0 mmol scale according to the general procedure with methyl 2-methylene-5-oxohexanoate as the electrophile and 1-methyl-3-(trifluoromethyl)-1H-pyrazol-4-amine as the nucleophile. The cyclization was conducted for 45 h, and precipitation yielded **131** (0.87 g, 45% yield) an orange amorphous solid. ^{1}H NMR (600 MHz, CD_3CN) δ 8.03 (s, 1H), 4.12 (dq, *J* = 6.2, 1.6 Hz, 2H), 3.98 (s, 3H), 3.71 (s, 3H), 3.32 – 3.08 (m, 4H), 2.33 (d, *J* = 1.5 Hz, 3H), 2.23 (dtd, *J* = 14.0, 6.1, 4.1 Hz, 1H), 2.11 – 2.01 (m, 1H). ^{13}C NMR (151 MHz, CD_3CN) δ 200.19, 171.88, 134.21 (q, *J* = 38.1 Hz), 131.05, 121.55, 121.07 (q, *J* = 268.7 Hz), 59.82, 59.77, 53.10, 41.20, 37.45, 34.26, 26.04, 19.82. ^{19}F NMR (564 MHz, CD_3CN) δ -62.76, -152.31. ESIHR $(M\text{-}BF_4)^+$ calc'd 304.1273, found 304.1276.

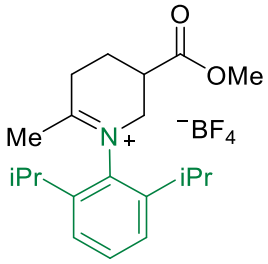

132

The synthesis of **132** was conducted on 5.0 mmol scale according to the general procedure with methyl 2-methylene-5-oxohexanoate as the electrophile and 2,6-diisopropylaniline as the nucleophile. The cyclization was conducted for 43 h, and precipitation yielded **132** (1.33 g, 66% yield) as a red amorphous solid. ^{1}H NMR (600 MHz, DMSO) δ 7.64 – 7.56 (m, 1H), 7.54 – 7.46 (m, 2H), 4.11 – 4.01 (m, 1H), 4.01 – 3.92 (m, 1H), 3.71 (s, 3H), 3.45 – 3.36 (m, 2H), 3.36 – 3.30 (m, 1H), 2.85 – 2.77 (m, 1H), 2.71 – 2.64 (m, 1H), 2.26 – 2.19 (m, 4H), 2.19 – 2.10 (m, 1H), 11.25 (d, *J* = 7.0 Hz, 6H), 1.17 (d, *J* = 6.6 Hz, 6H). ^{13}C NMR (151 MHz, DMSO) δ 194.79, 171.36, 142.01, 141.76, 135.93, 131.55, 126.17, 126.12, 56.84, 52.41, 36.22, 31.98, 27.51, 27.17, 27.15, 24.87, 24.75, 24.57, 24.10, 23.88, 18.86. ^{19}F NMR (564 MHz, DMSO) δ -148.95. ESIHR $(M\text{-}BF_4)^+$ calc'd 316.2277, found 316.2276. 5015553- 0222

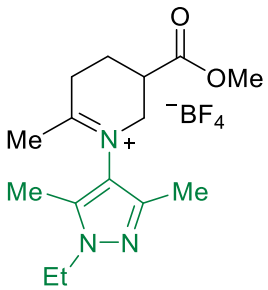

133

The synthesis of **133** was conducted on 5.0 mmol scale according to the general procedure with methyl 2-methylene-5-oxohexanoate as the electrophile and 1-ethyl-3,5-

dimethyl-1H-pyrazol-4-amine as the nucleophile. The cyclization was conducted for 44 h, and precipitation yielded **133** (1.24 g, 68% yield) as a purple-red amorphous solid. ^{1}H NMR (600 MHz, CD_3CN) δ 4.09 – 3.97 (m, 4H), 3.73 (s, 3H), 3.28 – 3.23 (m, 1H), 3.19 – 3.16 (m, 1H), 3.12 – 3.08 (m, 1H), 2.24 (s, 3H), 2.26 (m buried, 1H), 2.22 (s, 3H), 2.17 – 2.15 (m, 1H), 2.13 (s, 3H), 1.35 (td, J = 7.3, 1.4 Hz, 3H). ^{13}C NMR (151 MHz, CD_3CN) δ 197.19, 172.57, 140.83, 134.95, 121.13, 58.27, 53.16, 45.28, 37.54, 33.43, 25.18, 19.87, 15.17, 11.23, 9.07. ^{19}F NMR (564 MHz, CD_3CN) δ -152.38. ESIHR $(M\text{-}BF_4)^+$ calc'd 278.1869, found 278.1874.

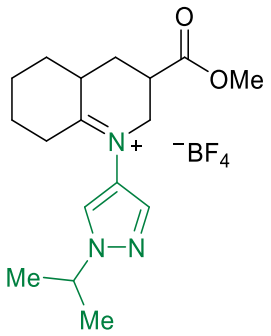

134

The synthesis of **134** was conducted on 5.0 mmol scale according to the general procedure with methyl methyl 2-((2-oxocyclohexyl)methyl)acrylate as the electrophile and 1-isopropyl-1H-pyrazol-4-amine as the nucleophile. The cyclization was conducted for 45 h, and precipitation yielded **134** (1.13 g, 58% yield) as an orange amorphous solid. ^{1}H NMR (600 MHz, CD_3CN) δ 7.90 (d, J = 2.0 Hz, 1H), 7.63 (d, J = 3.2 Hz, 1H), 4.59 – 4.50 (m, 1H), 4.15 – 4.06 (m, 2H), 3.69 (s, 3H), 3.27 – 3.16 (m, 1H), 3.01 (dq, J = 12.2, 6.2 Hz, 1H), 2.48 – 2.35 (m, 1H), 2.35 – 2.28 (m, 1H), 2.28 – 2.15 (m, 2H), 2.07 – 1.97 (m, 1H), 1.93 – 1.77 (m, 2H), 1.73 – 1.60 (m, 3H), 1.48 (d, J = 6.7 Hz, 6H). ^{13}C NMR (151 MHz, CH_3CN) δ 197.98, 171.98, 134.05,

125.06, 124.26, 60.06, 55.77, 52.96, 40.64, 37.29, 35.59, 34.30, 28.32, 26.90, 24.40, 22.75. ^{19}F NMR (564 MHz, CH_3CN) δ -152.22. ESIHR $(M\text{-}BF_4)^+$ calc'd 304.2025, found 304.2029.

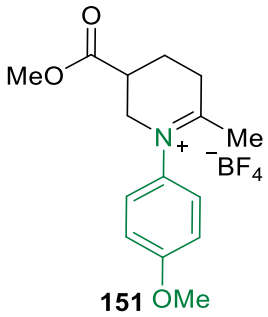

151

The synthesis of **151** was conducted on 5.0 mmol scale according to the general procedure with methyl methyl 2-methylene-5-oxohexanoate as the electrophile and 4-methoxyaniline as the nucleophile. The cyclization was conducted for 24 h, and precipitation yielded **151** (1.14 g, 58% yield) as a red oil. ^{1}H NMR (600 MHz, DMSO) δ 7.47 (d, J = 8.5 Hz, 2H), 7.23 – 7.14 (m, 2H), 4.18 – 4.01 (m, 2H), 3.83 (s, 3H), 3.70 (s, 3H), 3.36 – 3.29 (m, 2H), 3.15 – 3.03 (m, 2H), 2.20 – 2.15 (m, 4H), 2.02 – 1.96 (m, 1H). ^{13}C NMR (151 MHz, DMSO) δ 191.59, 171.45, 160.25, 134.53, 125.34, 115.46, 57.07, 55.67, 52.30, 36.48, 32.79, 24.76, 19.43. ^{19}F NMR (564 MHz, DMSO) δ -148.87. ESIHR $(M\text{-}BF_4)^+$ calc'd 262.1443, found 262.1443.

A3.5. Iminium Salt Derivatization:

General Procedure B: Iminium Salt Reduction

An 8 mL or 20 mL vial with a stir bar was charged with iminium salt (1.00 equiv) and DCM (0.10 M). Reducing agent ($NaBH_4$ 1.5 equiv or STAB 3.0 equiv) was added in one portion to the reaction mixture and stirred at room temperature. The reaction progress was followed by LCMS analysis to completion (usually 30 minutes to 3 hours). To the mixture was added 1 M aqueous sodium hydroxide or aqueous saturated bicarbonate solution (5 mL), and the mixture was stirred for 5 min. The organic layer was collected with a phase separator (Biotage Isolute), and the aqueous layer was extracted with DCM x 2. The solvents of the combined organic layer were evaporated, and the crude material was purified via silica gel chromatography.

General Procedure C: Iminium Salt Cyanation

An 8 mL or 20 mL vial with a stir bar was charged with iminium salt and DCM (0.25 M). TMSCN (2.00 equiv) was added to the mixture and stirred at rt. The reaction progress was followed by LCMS analysis to completion (usually 16 hours). The crude reaction mixture was concentrated and purified via silica gel chromatography.

General Procedure D: Iminium Salt Methylation

An 8 mL or 20 mL vial with a stir bar was charged with iminium salt. The vessel was degassed via three cycles of evacuation and nitrogen backfill. Toluene was added (0.10 M), and the reaction was cooled to 0 °C. A solution of $ZnMe_2$ (3.0 equiv) in Toluene (2.0 M) was added dropwise to

the reaction mixture with stirring. Upon completion of the addition, the reaction was warmed to room temperature and stirred overnight. The reaction progress was followed by LCMS analysis to completion (usually 16 hours). The reaction was quenched with an equal volume of H_2O and stirred for 5 minutes. The organic layer was collected with a phase separator (Biotage Isolute), and the aqueous layer was extracted with DCM x 3. The solvents of the combined organic layer were evaporated, and the crude material was purified via silica gel chromatography.

General Procedure E: Iminium Salt Trifluoromethylation

An 8 mL or 20 mL vial with a stir bar was charged with iminium salt (1.00 equiv) and IPAc (0.10 M). $TMSCF_3$ (2.00 equiv) and KHF_2 (2.00 equiv) were added, followed by TFA (2.00 equiv). The reaction mixture was stirred overnight at 50 °C. The reaction progress was followed by LCMS analysis to completion (usually 16 hours). The reaction was quenched with an equal volume of saturated aqueous solution of Na_2CO_3 and diluted with DCM (10mL). The organic layer was collected with a phase separator (Biotage Isolute), and the aqueous layer was extracted with DCM x 3. The solvents of the combined organic layer were evaporated, and the crude material was purified via silica gel chromatography.

General Procedure F: Iminium Salt Acylation

An 8 mL or 20 mL vial with a stir bar was charged with iminium salt (1.00 equiv) and Molecular sieves, 4A beads, 8-12 mesh (50 beads/mmol). The vial was capped with a cap containing a teflon septa. The mixture was placed under a nitrogen atmosphere, and DCM (0.20 M) was added. The

reaction mixture was stirred, and acyl chloride (1.20 equiv) was added followed by Hunig's base (2.00 equiv). The reaction progress was followed by LCMS analysis to completion (usually 1 hour). To the reaction mixture was added STAB (3.00 equiv), and the reaction progress was monitored by LCMS analysis to completion (usually 1-2 hour). Upon completion the mixture was diluted with DCM and quenched with aqueous saturated sodium bicarbonate solution. and the mixture was stirred for 5 min. The organic layer was collected with a phase separator (Biotage Isolute), and the aqueous layer was extracted with DCM x 2. The solvents of the combined organic layer were evaporated, and the crude material was purified via silica gel chromatography.

General Procedure G: Iminium Salt Allylation and Benzylation

An 8 mL or 20 mL vial with a stir bar was charged with iminium salt (1.00 equiv) and Molecular sieves, 4A beads, 8-12 mesh (50 beads/mmol). The vial was capped with a cap containing a teflon septa. The mixture was placed under a nitrogen atmosphere, and DCM (0.20 M) was added. The reaction mixture was stirred and alkyl halide was added (2.00 equiv for benzyl bromide or 3.00 equiv for allyl bromide), followed by Hunig's base (2.00 equiv). The reaction was warmed to room temperature, and the reaction progress was followed by LCMS analysis to completion (usually 18 hours). To the reaction mixture was added STAB (3.00 equiv), and the reaction progress was monitored by LCMS analysis to completion. To the mixture was added 1 M aqueous sodium hydroxide (5 mL), and the mixture was stirred for 5 min. The organic layer was collected with a phase separator (Biotage Isolute), and the aqueous layer was extracted with DCM x 2. The solvents of the combined organic layer were evaporated, and the crude material was purified via silica gel chromatography.

General Procedure H: Iminium Salt Alkylation with Methyl Vinyl Ketone

An 8 mL or 20 mL vial with a stir bar was charged with iminium salt (1.00 equiv) and Molecular sieves, 4A beads, 8-12 mesh (50 beads/mmol). The vial was capped with a cap containing a teflon septa. The mixture was placed under a nitrogen atmosphere and DCM (0.20 M) was added. The reaction mixture was stirred at room temperature and Michael acceptor (2.00 equiv methyl vinyl ketone) was added, followed by Hunig's base (2.00 equiv). The stirred at room temperature, and the reaction progress was followed by LCMS analysis to completion. To the reaction mixture was added STAB (3.00 equiv), and the reaction progress was monitored by LCMS analysis to completion. Upon completion the mixture was diluted with DCM and quenched with aqueous saturated sodium bicarbonate solution, and the mixture was stirred for 5 min. The organic layer was collected with a phase separator (Biotage Isolute), and the aqueous layer was extracted with DCM x 2. The solvents of the combined organic layer were evaporated, and the crude material was purified via silica gel chromatography.

General Procedure I: Iminium Salt Alkylation with Ethyl Acrylate

An 8 mL or 20 mL vial with a stir bar was charged with iminium salt (1.00 equiv) and Molecular sieves, 4A beads, 8-12 mesh (50 beads/mmol). The vial was capped with a cap containing a teflon septa. The mixture was placed under a nitrogen atmosphere and DCM (0.20 M) was added. The reaction mixture was stirred at room temperature and ethyl acrylate (3.00 equiv) was added, followed by Hunig's base (2.00 equiv). The reaction was heated to 50 °C, and the reaction progress

was followed by LCMS analysis to completion. To the reaction mixture was added STAB (3.00 equiv), and the reaction progress was monitored by LCMS analysis to completion. Upon completion the mixture was diluted with DCM and quenched with aqueous saturated sodium bicarbonate solution, and the mixture was stirred for 5 min. The organic layer was collected with a phase separator (Biotage Isolute), and the aqueous layer was extracted with DCM x 2. The solvents of the combined organic layer were evaporated, and the crude material was purified via silica gel chromatography.

General Procedure J: Telescoped Iminium Salt Synthesis and Cyanation

A microwave vial with a stirbar was charged with electrophile (1.00 equiv), amine (1.50 equiv), $LiBF_4$ (1.20 equiv), and TFE (4.0 M). The reaction vessel was sealed and heated to 90°C unless otherwise noted (usually 120°C for anilines that are less nucleophilic). The reaction progress was followed by LCMS analysis to completion (usually 20 hours). The mixture was cooled to room temperature, transferred to a 20 mL scintillation vial, and concentrated *in vacuo*. A stir bar was added, and the residue was diluted with DCM (0.10 M) followed by addition of TMSCN (2 equiv), and the reaction was capped. The crude mixture was stirred at room temperature, and the reaction progress was followed by LCMS analysis to completion (usually 18 hours). The crude reaction mixture was concentrated *in vacuo*, and the crude material was purified via silica gel chromatography.

General Procedure K: Telescoped Iminium Salt Synthesis and Trifluoromethylation

A microwave vial with a stirbar was charged with electrophile (1.00 equiv), amine (1.50 equiv), $LiBF_4$ (1.20 equiv), and TFE (4.0 M). The reaction vessel was sealed and heated to 90°C unless otherwise noted (usually 120°C for anilines that are less nucleophilic). The reaction progress was followed by LCMS analysis to completion (usually 20 hours). The mixture was cooled to room temperature, transferred to a 20 mL scintillation vial, and concentrated *in vacuo*. A stir bar, IPAc (0.10 M), $TMSCF_3$ (2.00 equiv), and KHF_2 (2.00 equiv) were added, followed by TFA (2.00 equiv). The reaction mixture was stirred overnight at 50 °C. The reaction progress was followed by LCMS analysis to completion (usually 16 hours). The reaction was cooled to room temperature and quenched with an equal volume of saturated aqueous solution of Na_2CO_3. The organic layer was collected with a phase separator (Biotage Isolute), and the aqueous layer was extracted with DCM x 3. The solvents of the combined organic layer were evaporated, and the crude material was purified via silica gel chromatography.

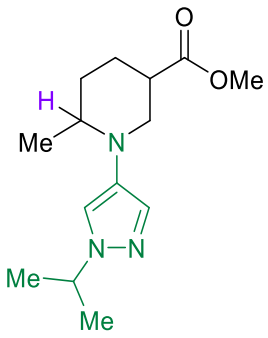

115

The synthesis of **115** was conducted according to general procedure B with iminium salt **114** (0.50 mmol) and $NaBH_4$ as reducing agent. The d.r. of the crude mixture was determined to be 1.4:1. Purification of the crude mixture by silica gel chromatography 0-15% EtOAc:EtOH (3:1) as eluent afforded **115** as a mixture of diastereomers (105 mg, 79% yield) as a pale yellow oil. Major Diastereomer: ^{1}H NMR (600 MHz, DMSO) δ 7.46 (d, *J* = 1.0 Hz, 1H), 7.17 (d, *J* = 0.9 Hz, 1H), 4.37 – 4.30 (m, 2H), 3.58 (s, 3H), 3.10 (dd, *J* = 11.7, 3.7 Hz, 1H), 2.90 – 2.85 (m, 1H), 2.78 – 2.74 (m, 1H), 2.61 (tq, *J* = 11.7, 3.9 Hz, 1H), 1.94 – 1.85 (m, 1H), 1.78 – 1.73 (m, 1H), 1.61 – 1.54 (m, 1H), 1.35 (d, *J* = 1.1 Hz, 6H), 1.33 – 1.28 (m, 1H), 0.89 (d, *J* = 6.3 Hz, 3H). ^{13}C NMR (151 MHz, DMSO) δ 173.50, 134.85, 131.82, 119.32, 55.00, 54.39, 52.91, 51.36, 40.75, 31.64, 25.00, 22.55, 22.54, 18.04. ESIHR (M+H) calc'd 266.1869, found 266.1875.

The same procedure with STAB as reductant provided a crude diastereomeric mixture of 1.4:1 (*trans*:*cis*). After column chromatography, **115** was provided as a mixture of diastereomers in 67% yield (89 mg). NMR spectra matched what is reported above.

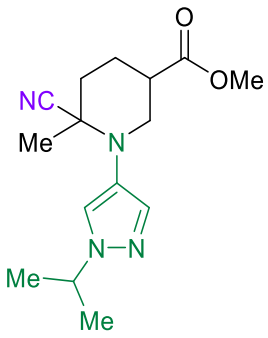

116

The synthesis of **116** was conducted according to general procedure C with iminium salt **114** (0.50 mmol). The crude reaction mixture was a mixture of diasteromers with a ratio of 2.9:1. Purification of the crude mixture by silica gel chromatography with 0-10% EtOAc:EtOH (3:1) in hexanes as eluent afforded **116** as a mixture of diastereomers (117 mg, 80% yield) as a pale yellow oil. Major Diastereomer: ^{1}H NMR (600 MHz, DMSO) δ 7.71 (d, *J* = 0.9 Hz, 1H), 7.35 (d, *J* = 1.0 Hz, 1H), 4.46 – 4.40 (m, 1H), 3.61 (s, 3H), 3.20 – 3.14 (m, 1H), 3.02 (t, *J* = 11.8 Hz, 1H), 2.68 – 2.63 (m, 1H), 2.09 – 1.97 (m, 2H), 1.72 – 1.55 (m, 2H), 1.38 (d, *J* = 6.7 Hz, 9H), 1.31 (s, 3H). ^{13}C NMR (151 MHz, DMSO) δ 172.61, 134.20, 129.99, 122.92, 119.73, 57.67, 53.35, 53.21, 51.62, 41.04, 36.19, 26.17, 24.42, 22.52, 22.51, 22.49, 22.46. ESIHR (M+H) calc'd 291.1821, found 291.1816.

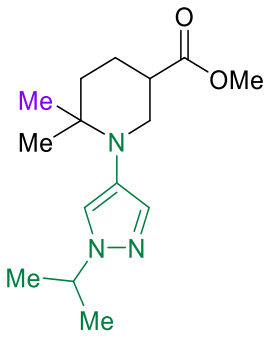

117

The synthesis of **117** was conducted according to general procedure D with iminium salt **114** (0.50 mmol). Purification of the crude mixture by silica gel chromatography with 0-10% EtOAc:EtOH (3:1) in hexanes as eluent afforded **117** (56 mg, 40% yield) as a pale yellow oil. Major Diastereomer: ^{1}H NMR (600 MHz, DMSO) δ 7.48 (s, 1H), 7.15 (d, *J* = 0.9 Hz, 1H), 4.36 (hept, *J* = 6.7 Hz, 1H), 3.59 (s, 3H), 3.09 – 3.05 (m, 1H), 2.93 (ddd, *J* = 11.8, 4.2, 1.4 Hz, 1H), 2.57 – 2.52 (m, 1H), 1.82 – 1.77 (m, 1H), 1.71 – 1.64 (m, 1H), 1.56 (dt, *J* = 13.1, 4.2 Hz, 1H), 1.46 (td, *J* = 12.5, 4.2 Hz, 1H), 1.36 (d, *J* = 6.7 Hz, 6H), 0.96 (s, 3H), 0.89 (s, 3H). ^{13}C NMR (151 MHz, DMSO) δ 173.60, 134.89, 131.63, 122.56, 52.92, 52.87, 51.36, 50.24, 41.93, 37.76, 28.70, 23.10, 22.57, 22.54, 18.37. ESIHR (M+H) calc'd 280.2025, found 280.2013.

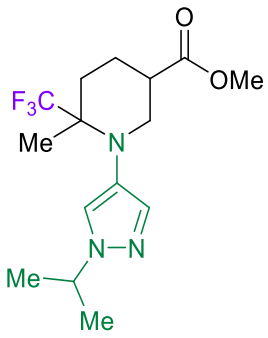

118

The synthesis of **118** was conducted according to general procedure E with iminium salt **114** (0.50 mmol). The crude reaction mixture was a mixture of diasteromers with a ratio of 1.8:1. Purification of the crude mixture by silica gel chromatography with 0-30% EtOAc in hexanes as eluent afforded **118** separated as a mixture of diasteomers (128 mg, 77% yield) as a pale yellow oil ^{1}H NMR (600 MHz, CD_3CN) δ 7.41 (s, 1H), 7.27 (s, 1H), 4.40 (hept, *J* = 6.7 Hz, 1H), 3.66 (s, 3H), 3.29 – 3.23 (m, 2H), 2.65 (ddt, *J* = 9.2, 7.5, 4.9 Hz, 1H), 2.03 – 1.80 (m, 4H), 1.42 (d, *J* = 6.7 Hz, 6H), 1.28 (s, 3H). ^{13}C NMR (151 MHz, CD_3CN) δ 174.53, 136.95, 132.28, 129.20 (q, *J* = 284.8 Hz), 124.95, 61.52 (q, *J* = 22.9 Hz), 54.60, 52.73, 52.21, 42.00, 31.11, 31.09, 23.01, 23.00, 22.53, 15.85. ^{19}F NMR (564 MHz, CD_3CN) δ -73.95. ESIHR (M+H) calc'd 334.1742, found 334.1737.

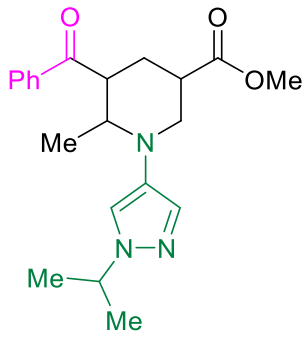

119

The synthesis of **119** was conducted according to general procedure F with iminium salt **114** (0.50 mmol) and benzoyl chloride as electrophile. Purification of the crude mixture by silica gel chromatography with 0-15% EtOAc:EtOH (3:1) in hexanesas eluent afforded **119** as a mixture of diastereomers (99 mg, 54% yield) as a pale yellow oil. Major Diastereomer: ^{1}H NMR (600 MHz, DMSO) δ 7.95 (d, *J* = 7.6 Hz, 2H), 7.70 – 7.59 (m, 1H), 7.57 – 7.53 (m, 2H), 7.33 (d, *J* = 1.0 Hz, 1H), 7.09 (s, 1H), 4.37 – 4.31 (m, 1H), 3.97 (dt, *J* = 12.3, 3.9 Hz, 1H), 3.86 – 3.83 (m, 1H), 3.69 (s, 3H), 3.32 – 3.26 (m, 1H), 3.06 – 3.03 (m, 1H), 2.93 – 2.87 (m, 1H), 2.05 – 1.98 (m, 1H), 1.99 – 1.90 (m, 1H), 1.35 – 1.33 (m, 6H), 0.74 (d, *J* = 6.7 Hz, 3H). ^{13}C NMR (151 MHz, DMSO) δ 200.75, 173.49, 136.05, 135.24, 133.19, 128.97, 128.04, 126.92, 114.17, 53.06, 52.95, 51.55, 45.34, 44.50, 37.89, 22.80, 22.49, 8.00. ESIHR (M+H) calc'd 370.2131, found 370.2113.

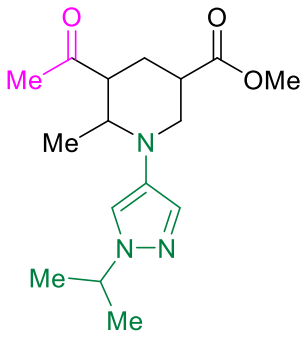

120

The synthesis of **120** was conducted according to general procedure F with iminium salt **114** (0.50 mmol) and acetyl chloride as electrophile. Purification of the crude mixture by silica gel chromatography with 0- 40% (3:1 EtOAc:EtOH) in hexanes as eluent afforded **120** as a mixture of diastereomers (83 mg, 54% yield) as a yellow oil. Major Diastereomer: ^{1}H NMR (600 MHz, DMSO) δ 7.38 (d, *J* = 0.9 Hz, 1H), 7.18 (d, *J* = 0.9 Hz, 1H), 4.33 (h, *J* = 6.7 Hz, 1H), 4.05 – 4.01 (m, 1H), 3.64 (s, 3H), 3.21 (ddd, *J* = 12.4, 4.5, 1.5 Hz, 1H), 2.94 (dt, *J* = 12.7, 4.0 Hz, 1H), 2.79 – 2.72 (m, 1H), 2.69 – 2.57 (m, 1H), 1.90 – 1.81 (m, 1H), 1.75 – 1.65 (m, 1H), 1.36 (d, *J* = 6.9 Hz, 9H), 0.75 (d, *J* = 6.7 Hz, 3H). ^{13}C NMR (151 MHz, DMSO) δ 208.35, 173.47, 135.32, 126.96, 113.99, 52.92, 51.54, 51.50, 50.42, 44.32, 39.38, 28.26, 22.56, 22.20, 7.75. ESIHR (M+H) calc'd 308.1974, found 308.1969.

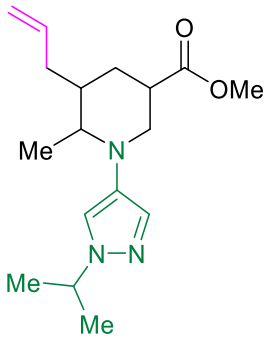

121

The synthesis of **121** was conducted according to general procedure G with iminium salt **114** (0.50 mmol) and allyl bromide as electrophile. Purification of the crude mixture by silica gel chromatography with 0-10% EtOAc:EtOH (3:1) in hexanes as eluent afforded **121** as a mixture of diastereomers (50 mg, 33% yield) as a pale yellow oil. Major Diastereomer: ^{1}H NMR (600 MHz, DMSO) δ 7.21 (d, *J* = 0.9 Hz, 1H), 7.02 (d, *J* = 1.0 Hz, 1H), 5.87 – 5.76 (m, 1H), 5.13 – 4.99 (m, 2H), 4.40 – 4.24 (m, *J* = 6.7 Hz, 1H), 3.59 (s, 3H), 3.39 – 3.31 (m, 2H), 2.89 (dd, *J* = 12.2, 3.9 Hz, 1H), 2.78 – 2.67 (m, 1H), 2.04 – 1.84 (m, 4H), 1.43 (ddd, *J* = 13.6, 11.8, 4.9 Hz, 1H), 1.34 (d, *J* = 1.7 Hz, 9H), 0.76 (d, *J* = 6.6 Hz, 3H). ^{13}C NMR (151 MHz, DMSO) δ 173.76, 136.80, 136.08, 127.28, 116.02, 114.08, 54.73, 52.78, 51.51, 44.80, 38.88, 36.94, 35.38, 24.86, 22.55, 5.34. ESIHR (M+H) calc'd 306.2182, found 306.2180.

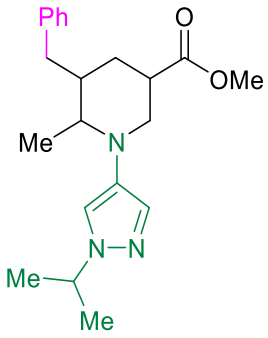

124

The synthesis of **124** was conducted according to general procedure G with iminium salt **114** (0.50 mmol) and benzyl bromide as electrophile. Purification of the crude mixture by silica gel chromatography with 0-5% (3:1 EtOAc:EtOH) in DCM as eluent afforded **124** as a mixture of diastereomers (62 mg, 35% yield) as a yellow oil. One diastereomer was cleanly separated while the rest of the material was isolated as a mixture of diastereomers.

Major diastereomer: ^{1}H NMR (600 MHz, DMSO) δ 7.33 – 7.28 (m, 2H), 7.24 – 7.17 (m, 4H), 6.99 (s, 1H), 4.32 (hept, *J* = 6.6 Hz, 1H), 3.54 (s, 3H), 3.41 – 3.27 (m, 2H), 2.93 (dd, *J* = 12.2, 3.9 Hz, 1H), 2.72 (p, *J* = 3.2 Hz, 1H), 2.59 – 2.55 (m, 1H), 2.40 (dd, *J* = 13.7, 9.2 Hz, 1H), 2.28 (td, *J* = 9.4, 4.4 Hz, 1H), 1.81 (dt, *J* = 13.8, 3.6 Hz, 1H), 1.46 (ddd, *J* = 13.5, 11.9, 4.9 Hz, 1H), 1.34 (d, *J* = 6.7, 2.1 Hz, 6H), 0.86 (d, *J* = 6.6 Hz, 3H). ^{13}C NMR (151 MHz, DMSO) δ 173.66, 140.07, 135.98, 128.70, 128.20, 127.38, 125.79, 114.22, 55.09, 52.77, 51.41, 45.15, 38.80, 38.37, 37.28, 24.49, 22.62, 22.54, 6.05. ESIHR (M+H) calc'd 356.2338, found 356.2330.

Minor mixture of diastereomers:

^{1}H NMR (600 MHz, DMSO) δ 7.30 (dd, *J* = 8.1, 7.1 Hz, 2H), 7.23 (d, *J* = 1.0 Hz, 1H), 7.22 – 7.18 (m, 3H), 6.99 (d, *J* = 1.0 Hz, 1H), 4.33 (p, *J* = 6.6 Hz, 1H), 3.61 (s, 3H), 3.31 – 3.27 (m, 1H), 3.22 – 3.17 (m, 1H), 2.98 – 2.85 (m, 2H), 2.83 – 2.72 (m, 2H), 1.91 – 1.87 (m, 1H), 1.78 (td, *J* = 13.1,

4.7 Hz, 1H), 1.61 (dt, *J* = 13.6, 3.5 Hz, 1H), 1.35 (s, 3H), 0.90 (d, *J* = 6.7 Hz, 3H). ^{13}C NMR (151 MHz, DMSO) δ 173.96, 140.92, 136.33, 128.96, 128.29, 126.80, 125.88, 113.86, 53.95, 52.82, 51.49, 45.04, 39.31, 37.78, 36.42, 24.81, 22.58, 11.21. ESIHR (M+H) calc'd 356.2338, found 356.2345

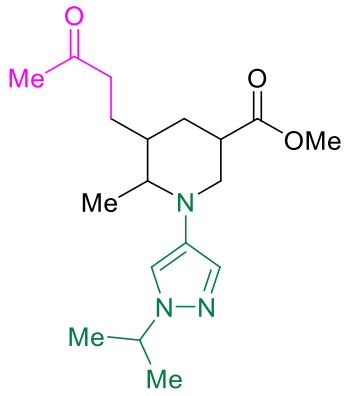

122

The synthesis of **122** was conducted according to general procedure I with iminium salt **114** (0.50 mmol) and methyl vinyl ketone as electrophile. Purification of the crude mixture by silica gel chromatography with 0- 20% (3:1 EtOAc:EtOH) in DCM as eluent afforded **122** as a mixture of diastereomers (71 mg, 42% yield) as a pale yellow oil. Major Diastereomer: ^{1}H NMR (600 MHz, DMSO) δ 7.23 (d, *J* = 0.9 Hz, 1H), 7.05 (d, *J* = 0.9 Hz, 1H), 4.32 (hept, *J* = 6.7 Hz, 1H), 3.59 (s, 3H), 3.41 – 3.34 (m, 2H), 2.87 (dd, *J* = 12.2, 3.9 Hz, 1H), 2.75 – 2.69 (m, 1H), 2.55 – 2.41 (m, 2H), 2.10 (d, *J* = 6.5 Hz, 3H), 1.91 – 1.88 (m, 1H), 1.83 – 1.78 (m, 1H), 1.45 – 1.39 (m, 1H), 1.37 – 1.35 (m, 10H), 0.75 (d, *J* = 6.6 Hz, 3H). ^{13}C NMR (151 MHz, DMSO) δ 208.33, 173.74, 136.13, 127.17, 113.90, 54.45, 52.79, 51.49, 44.60, 40.11, 38.89, 35.11, 29.79, 26.39, 25.04, 22.63, 22.55, 5.15. ESIHR (M+H) calc'd 336.2287, found 336.2282.

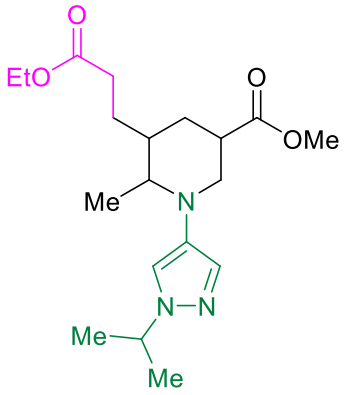

123

The synthesis of **123** was conducted according to general procedure I with iminium salt **114** (0.50 mmol) and ethyl acrylate as electrophile. Purification of the crude mixture by silica gel chromatography with 0-50% (3:1 EtOAc:EtOH) in hexanes as eluent afforded **123** as a mixture of diastereomers (62 mg, 34% yield) as a yellow oil. Major Diastereomer: ^{1}H NMR (600 MHz, DMSO) δ 7.24 (d, *J* = 0.9 Hz, 1H), 7.05 (d, *J* = 0.9 Hz, 1H), 4.32 (hept, *J* = 6.7 Hz, 1H), 4.06 (q, *J* = 7.1 Hz, 2H), 3.59 (s, 3H), 3.42 – 3.34 (m, 2H), 2.87 (dd, *J* = 12.2, 4.0 Hz, 1H), 2.72 – 2.71 (m, 1H), 2.34 (t, *J* = 7.8 Hz, 2H), 1.91 – 1.83 (m, 2H), 1.52 – 1.38 (m, 3H), 1.38 – 1.32 (m, 9H), 1.19 (s, 3H), 0.75 (d, *J* = 6.7 Hz, 3H). ^{13}C NMR (151 MHz, DMSO) δ 173.68, 172.85, 136.08, 127.16, 113.92, 59.72, 54.20, 52.79, 51.48, 44.64, 38.86, 35.13, 31.10, 27.61, 24.98, 22.55, 14.08, 5.20. ESIHR (M+H) calc'd 366.2393, found 366.2375.

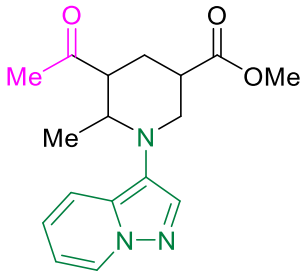

135

The synthesis of **135** was conducted according to general procedure F with iminium salt **125** (0.50 mmol) and acetyl chloride as electrophile. Purification of the crude mixture by silica gel chromatography with 0-30% (3:1 EtOAc:EtOH) in hexanes as eluent afforded **135** as

a mixture of diastereomers (82 mg, 52% yield) as a yellow oil. Major Diastereomer: ^{1}H NMR (600 MHz, DMSO) δ 8.51 (dq, *J* = 7.1, 0.9 Hz, 1H), 7.84 (s, 1H), 7.64 (dt, *J* = 8.9, 1.2 Hz, 1H), 7.10 – 7.05 (m, 1H), 6.83 – 6.74 (m, 1H), 3.64 (s, 3H), 3.50 – 3.41 (m, 1H), 3.18 – 3.11 (m, 3H), 2.76 – 2.71 (m, 1H), 2.15 (s, 3H), 1.99 – 1.90 (m, 1H), 1.80 – 1.73 (m, 1H). ^{13}C NMR (151 MHz, DMSO) δ 208.26, 173.35, 133.73, 131.52, 128.72, 125.01, 121.39, 117.03, 111.72, 51.31, 45.76, 28.18, 22.06, 7.95. ESIHR (M+H) calc'd 316.1661, found 316.1665.

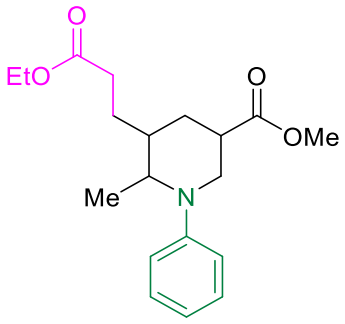

136

The synthesis of **136** was conducted according to general procedure I with iminium salt **126** (0.50 mmol) and ethyl acrylate as electrophile. Purification of the crude mixture by silica gel chromatography with 0-10% EtOAc:EtOH (3:1) in hexanes as eluent afforded **136** as a mixture of diastereomers (92 mg, 55% yield) as a pale yellow oil. Major Diastereomer: ^{1}H NMR (600 MHz, DMSO) δ 7.20 – 7.15 (m, 2H), 6.88 (d, *J* = 7.8 Hz, 2H), 6.72 – 6.68 (m, 1H), 4.08 – 4.05 (m, 2H), 3.91 – 3.84 (m, 1H), 3.83 – 3.78 (m, 1H), 3.04 (dd, *J* = 12.8, 3.8 Hz, 1H), 2.84 – 2.79 (m, 1H), 2.42 – 2.33 (m, 2H), 1.99 – 1.95 (m, 1H), 1.87 – 1.81 (m, 1H), 1.56 – 1.39 (m, 3H), 1.22 – 1.16 (m, 3H), 0.83 (d, *J* = 6.6 Hz, 3H). ^{13}C NMR (151 MHz, DMSO) δ 173.55, 172.85, 150.22, 128.91, 117.96, 115.78, 59.74, 52.36, 51.52, 42.53, 39.14, 35.45, 31.10, 27.89, 25.00, 14.10, 6.30. ESIHR (M+H) calc'd 334.2018, found 334.2017.

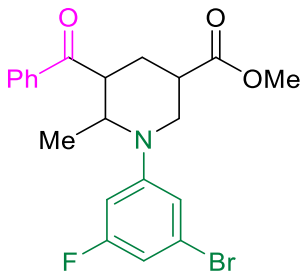

137

The synthesis of **137** was conducted according to general procedure F with iminium salt **127** (0.50 mmol) and benzoyl chloride as electrophile. Purification of the crude mixture by silica gel chromatography with 0-15% EtOAc in hexanes as eluent afforded **137** as a mixture of diastereomers (91 mg, 42% yield) as a colorless glass. Major Diastereomer: ^{1}H NMR (600 MHz, DMSO) δ 8.01 – 7.96 (m, 2H), 7.68 (ddt, *J* = 8.7, 7.3, 1.3 Hz, 1H), 7.61 – 7.53 (m, 2H), 6.91 (t, *J* = 2.0 Hz, 1H), 6.84 – 6.79 (m, 1H), 6.77 (dt, *J* = 12.9, 2.3 Hz, 1H), 4.39 – 4.24 (m, 1H), 4.00 – 3.88 (m, 1H), 3.73 (dd, *J* = 13.6, 4.3 Hz, 1H), 3.68 (s, 3H), 3.03 (dd, *J* = 13.3, 11.9 Hz, 1H), 2.79 – 2.74 (m, 1H), 2.12 – 2.00 (m, 1H), 2.00 – 1.90 (m, 1H), 0.82 (d, *J* = 6.7 Hz, 3H). ^{13}C NMR (151 MHz, DMSO) δ 200.26, 173.09, 163.34 (d, *J* = 244.7 Hz), 151.92 (d, *J* = 11.3 Hz), 135.95, 133.36, 129.04, 129.01, 128.14, 122.79 (d, *J* = 13.2 Hz), 114.08 (d, *J* = 2.5 Hz), 107.93 (d, *J* = 25.3 Hz), 101.66 (d, *J* = 25.6 Hz), 51.67, 51.48, 45.61, 42.29, 39.34, 23.12, 9.83. ^{19}F NMR (564 MHz, DMSO) δ -110.80 (dd, *J* = 12.5, 8.0 Hz). ESIHR (M+H) calc'd 434.0767, found 434.0771.

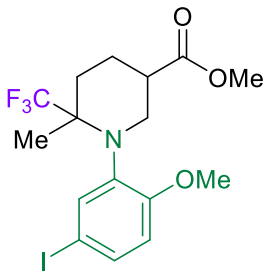

140

The synthesis of **140** was conducted according to general procedure E with iminium salt **128** (0.50 mmol). Purification of the crude mixture by silica gel chromatography with 25% DCM in hexanes as eluent afforded **140** as a mixture of diastereomers (139 mg, 61% yield) as a pale yellow oil. Major Diastereomer: ^{1}H NMR (600 MHz, DMSO) δ 7.54 – 7.45 (m, 1H), 7.44 – 7.38 (m, 1H), 6.86 – 6.83 (m, 1H), 3.73 (s, 3H), 2.99 (dd, *J* = 13.5, 4.6 Hz, 1H), 2.87 (d, *J* = 11.6 Hz, 1H), 2.79 (d, *J* = 11.8 Hz, 1H), 2.12 – 2.03 (m, 1H), 1.95 (s, 1H), 1.82 – 1.70 (m, 1H), 1.69 – 1.59 (m, 2H), 0.99 (s, 4H). ^{13}C NMR (151 MHz, DMSO) δ 173.25, 139.76, 138.34, 135.78, 128.73 (q, *J*= 294 Hz), 114.91, 83.77, 58.28 – 57.64 (m), 55.26, 51.36, 50.88, 40.37, 31.54, 23.06, 21.09. ^{19}F NMR (564 MHz, DMSO) δ -70.23. ESIHR (M+H) calc'd 458.0440, found 458.0440.

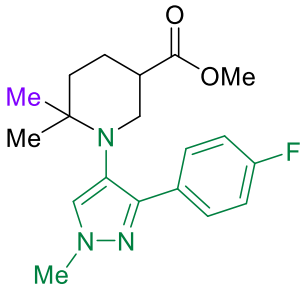

141

The synthesis of **141** was conducted according to general procedure D with iminium salt **129** (0.50 mmol) and benzoyl chloride as electrophile. Purification of the crude mixture by silica gel chromatography with 0-10% EtOAc:EtOH (3:1) in hexanesas eluent afforded **141** (100 mg, 58% yield) as a pale yellow oil. ^{1}H NMR (600 MHz, DMSO) δ 8.15 – 8.06 (m, 2H), 7.74 (s, 1H), 7.18 – 7.10 (m, 2H), 3.81 (s, 3H), 3.60 (s, 3H), 3.12 – 3.09 (m, 1H), 3.07 – 2.96 (m,

1H), 2.70 – 2.66 (m, 1H), 1.85 – 1.77 (m, 2H), 1.59 – 1.55 (m, 1H), 1.48 – 1.43 (m, 1H), 0.91 (s, 3H), 0.80 (s, 3H). ^{13}C NMR (151 MHz, DMSO) δ 173.68, 161.13 (d, *J* = 243.5 Hz), 144.41, 130.62 (d, *J* = 3.0 Hz), 129.05, 129.02, 128.33 (d, *J* = 7.7 Hz), 114.63 (d, *J* = 21.0 Hz), 41.54, 38.98, 37.75, 22.81. The two methyl carbons on the piperidine ring are believed to have broadened into the baseline. ^{19}F NMR (564 MHz, DMSO) δ -116.02. ESIHR (M+H) calc'd 346.1931, found 346.1935.

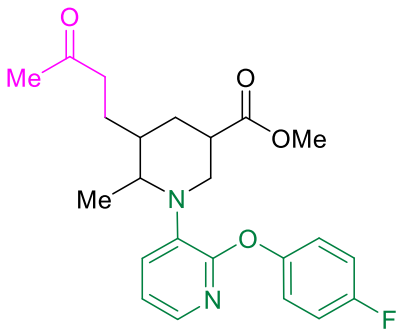

138

The synthesis of **138** was conducted according to general procedure I with iminium salt **130** (0.50 mmol) and methyl vinyl ketone as electrophile. Purification of the crude mixture by silica gel chromatography with 0-30% (3:1 EtOAc:EtOH) in hexanes as eluent afforded **138** (single diastereomer) (41 mg, 20% yield) as a yellow oil. ^{1}H NMR (600 MHz, DMSO) δ 7.70 (dd, *J* = 4.8, 1.6 Hz, 1H), 7.36 (dd, *J* = 7.8, 1.7 Hz, 1H), 7.24 – 7.13 (m, 2H), 7.08 (dd, *J* = 7.8, 4.7 Hz, 1H), 7.03 – 6.99 (m, 2H), 3.82 (dt, *J* = 11.0, 5.4 Hz, 1H), 3.47 (s, 3H), 3.41 (d, *J* = 11.4 Hz, 1H), 3.30 (dd, *J* = 12.3, 3.9 Hz, 1H), 2.78 – 2.76 (m, 1H), 2.41 (t, *J* = 7.7 Hz, 2H), 2.04 (s, 3H), 1.92 – 1.86 (m, 2H), 1.52 – 1.46 (m, 1H), 1.34 (q, *J* = 7.4 Hz, 2H), 0.81 (d, *J* = 6.8 Hz, 3H). ^{13}C NMR (151 MHz, DMSO) δ 208.17, 173.48, 158.36 (d, *J* = 239.2 Hz), 155.48, 150.76 (d, *J* = 2.4 Hz), 138.73, 136.73, 129.38, 121.76 (d, *J* = 8.5 Hz), 120.05, 115.91 (d,

J = 23.3 Hz), 53.63, 51.39, 44.42, 40.02, 39.01, 35.16, 29.72, 26.06, 25.19, 7.18. ^{19}F NMR (564 MHz, DMSO) δ -119.99 (tt, *J* = 9.2, 4.6 Hz). ESIHR (M+H) calc'd 415.2033, found 415.2032.

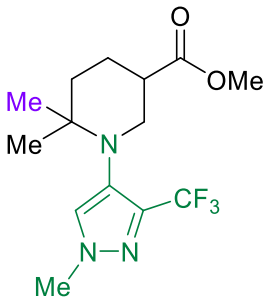

142

The synthesis of **142** was conducted according to general procedure D with iminium salt **131** (0.50 mmol). Purification of the crude mixture by silica gel chromatography with 0-30% (3:1 EtOAc:EtOH) in hexanes as eluent afforded **142** (116 mg, 73% yield) as a colorless oil. ^{1}H NMR (600 MHz, DMSO) δ 7.95 (s, 1H), 3.86 (s, 3H), 3.58 (s, 3H), 3.03 (dd, *J* = 12.1, 9.3 Hz, 1H), 2.91 (dd, *J* = 12.6, 4.3 Hz, 1H), 2.61 – 2.49 (m, 1H), 1.84 – 1.80 (m, 1H), 1.76 – 1.70 (m, 1H), 1.62 – 1.58 (m, 1H), 1.46 – 1.42 (m, 1H), 1.04 (s, 3H), 0.91 (s, 3H). ^{13}C NMR (151 MHz, DMSO) δ 173.87, 137.65 (q, *J* = 33.3 Hz), 130.79, 130.68, 122.01 (q, *J* = 269.5 Hz), 53.52, 52.09, 51.75, 41.89, 39.86, 38.28, 27.00, 23.33, 21.17, 21.03. ^{19}F NMR (564 MHz, DMSO) δ -59.18. ESIHR (M+H) calc'd 320.1586, found 320.1579.

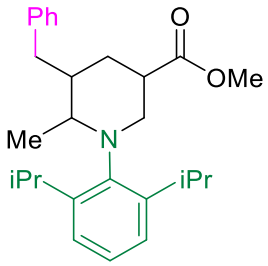

139

The synthesis of **139** was conducted according to general procedure G with iminium salt **132** (0.50 mmol) and benzyl bromide as electrophile. Purification of the crude mixture by silica gel chromatography with 0-20% DCM in hexanesas eluent afforded **139** as a mixture of diastereomers (83 mg, 41% yield) as a pale yellow oil. Major Diastereomer: ^{1}H NMR (600 MHz, DMSO) δ 7.32 – 7.28 (m, 2H), 7.24 – 7.20 (m, 2H), 7.20 – 7.18 (m, 1H), 7.13 (t, *J* = 7.6 Hz, 1H), 7.08 (dd, *J* = 7.7, 1.8 Hz, 1H), 7.06 – 7.03 (m, 1H), 3.77 (h, *J* = 6.1 Hz, 1H), 3.55 (s, 3H), 3.39 – 3.33 (m, 1H), 3.30 – 3.22 (m, 1H), 3.20 – 3.11 (m, 2H), 2.93 – 2.89 (m, 1H), 2.74 (d, *J* = 7.9 Hz, 2H), 2.14 – 2.10 (m, 1H), 1.83 – 1.71 (m, 1H), 1.67 – 1.63 (m, 1H), 1.20 – 1.08 (m, 12H), 0.85 (d, *J* = 6.9 Hz, 3H). ^{13}C NMR (151 MHz, DMSO) δ 173.79, 148.84, 143.55, 140.93, 128.86, 128.32, 126.34, 125.75, 124.05, 123.59, 56.93, 53.47, 51.44, 40.10, 37.76, 33.07, 29.07, 27.49, 27.12, 24.87, 23.42, 15.35. ESIHR (M+H) calc'd 408.2903, found 408.2901.

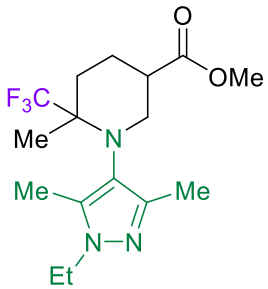

143

The synthesis of **143** was conducted according to general procedure E with iminium salt **133** (0.50 mmol). Purification of the crude mixture by silica gel chromatography with

0-40% (3:1 EtOAc:EtOH) in hexanes as eluent afforded **143** as a mixture of diastereomers (68 mg, 39% yield) as a pale yellow oil. Major Diastereomer: ^{1}H NMR (600 MHz, DMSO) δ 3.92 – 3.85 (m, 2H), 3.72 (dd, *J* = 12.4, 2.1 Hz, 1H), 3.61 (s, 3H), 3.19 – 3.12 (m, 1H), 2.69 (dt, *J* = 17.4, 4.3 Hz, 1H), 2.03 (t, *J* = 4.3 Hz, 4H), 1.94 – 1.88 (m, 1H), 1.86 – 1.79 (m, 1H), 1.78 – 1.73 (m, 1H), 1.23 (t, *J* = 7.3 Hz, 8H), 1.03 (s, 3H). ^{13}C NMR (151 MHz, DMSO) δ 173.66, 143.57, 135.04, 129.21 (q, *J* = 295.6 Hz), 125.16, 58.99 (dt, *J* = 40.8, 22.0 Hz), 51.48, 50.30, 43.45, 39.24, 29.75, 14.91, 12.20, 9.44. ^{19}F NMR (564 MHz, DMSO) δ -70.46. ESIHR (M+H) calc'd 348.1899, found 348.1901.

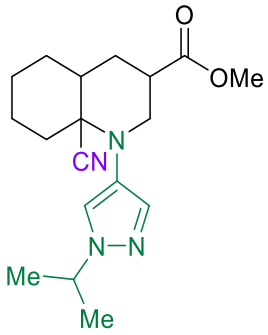

144

The synthesis of **144** was conducted according to general procedure E with iminium salt **134** (0.50 mmol). Purification of the crude mixture by silica gel chromatography with 0-40% EtOAc in hexanes as eluent afforded **144** as two mixtures of diastereomers (126 mg, 77% yield) which eluted as two peaks under the chromatography conditions.

Peak1 colorless oil (57 mg): ^{1}H NMR (600 MHz, DMSO) δ 7.63 (s, 1H), 7.29 (s, 1H), 4.42 (h, *J* = 6.1 Hz, 1H), 3.64 (s, 3H), 3.39 (dt, *J* = 12.6, 1.9 Hz, 1H), 3.34 (d, *J* = 3.7 Hz, 1H), 2.92 – 2.83 (m, 1H), 2.05 – 1.95 (m, 1H), 1.78 – 1.55 (m, 6H), 1.50 – 1.42 (m, 1H), 1.42 – 1.32 (m, 6H), 1.30

– 1.23 (m, 1H), 1.20 – 1.13 (m, 1H). ^{13}C NMR (151 MHz, DMSO) δ 173.19, 134.36, 129.16, 123.02, 118.06, 65.76, 53.13, 52.84, 51.74, 40.74, 38.63, 34.83, 29.63, 28.90, 24.43, 22.83, 22.52, 22.50. ESIHR (M+H) calc'd 331.2134, found 331.2139.

Peak 2 white solid (69 mg): ^{1}H NMR (600 MHz, DMSO) δ 7.70 (s, 1H), 7.34 (s, 1H), 4.43 (hept, *J* = 6.7 Hz, 1H), 3.62 (s, 3H), 3.20 – 3.17 (m, 1H), 3.13 (t, *J* = 11.8 Hz, 1H), 2.85 – 2.69 (m, 1H), 1.97 – 1.86 (m, 1H), 1.79 – 1.55 (m, 6H), 1.45 – 1.40 (m, 2H), 1.38 (d, *J* = 6.7 Hz, 6H), 1.33 – 1.16 (m, 2H). ^{13}C NMR (151 MHz, DMSO) δ 172.97, 135.04, 129.48, 123.66, 118.60, 65.62, 53.79, 53.67, 52.08, 43.28, 41.18, 35.28, 31.54, 30.03, 24.89, 23.26, 22.99, 22.94. ESIHR (M+H) calc'd 331.2134, found 331.2139.

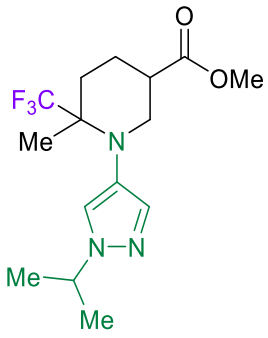

118

The synthesis of **118** was conducted according to general procedure K with methyl 2-methylene-5-oxohexanoate as the electrophile and 1-isopropyl-1H-pyrazol-4-amine as the nucleophile. The crude reaction mixture was a mixture of diasteromers with a ratio of 2.0:1 as determined by ^{1}H NMR. Purification of the crude mixture by silica gel chromatography with 0-10% EtOAc in hexanes as eluent afforded **118** as a mixture of diastereomers (101 mg, 61% yield) as a pale yellow oil. NMR Spectra is consistent for product reported above from isolated iminium.

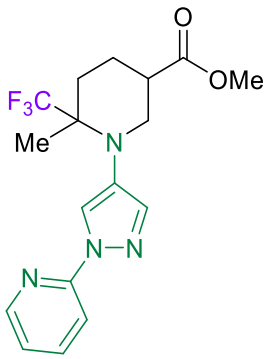

145

The synthesis of **145** was conducted according to general procedure K with methyl 2-methylene-5-oxohexanoate as the electrophile and 1-(pyridin-2-yl)-1H-pyrazol-4-amine as the nucleophile, except the cyclization was run at 120 °C. Purification of the crude mixture by silica gel chromatography with 0-5% EtOAc:EtOH (3:1) in hexanes as eluent afforded **145** as a mixture of diastereomers with a ratio of 2.3:1 as determined by ^{19}F NMR (48 mg, 26% yield) as a pale yellow oil. Major Diastereomer: ^{1}H NMR (600 MHz, DMSO) δ 8.44 – 8.43 (m, 1H), 8.40 (d, *J* = 0.9 Hz, 1H), 7.98 – 7.95 (m, 1H), 7.89 (s, 1H), 7.65 (s, 1H), 7.32 (dddd, *J* = 8.2, 4.5, 3.3, 1.1 Hz, 1H), 3.62 (s, 3H), 3.37 – 3.33 (m, 1H), 3.27 (dd, *J* = 12.3, 4.4 Hz, 1H), 2.74 – 2.69 (m, 1H), 1.98 – 1.75 (m, 4H), 1.28 (s, 3H). ^{13}C NMR (151 MHz, DMSO) δ 173.02, 150.77, 148.21, 139.39, 133.96, 127.95 (q, *J* = 288.5 Hz), 122.62, 121.73, 111.36, 60.08 (q, *J* = 22.9 Hz), 51.59, 51.57, 50.98, 40.12, 29.76, 21.09, 15.71. ^{19}F NMR (564 MHz, DMSO) δ -72.74. ESIHR (M+H) calc'd 369.1538, found 369.1538.

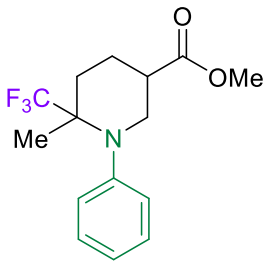

146

The synthesis of **146** was conducted according to general procedure K with methyl 2-methylene-5-oxohexanoate as the electrophile and aniline as the nucleophile, except the cyclization was run at 120 °C. The crude reaction mixture was a mixture of diasteromers with a ratio of 2.6:1 as determined by ^{1}H NMR. Purification of the crude mixture by silica gel chromatography with 0-10% EtOAc in hexanes as eluent afforded **146** as a mixture of diastereomers (106 mg, 70% yield) as a pale yellow oil. Major Diastereomer: ^{1}H NMR (600 MHz, DMSO) δ 7.29 (t, *J* = 7.8 Hz, 2H), 7.20 – 7.12 (m, 3H), 3.60 (d, *J* = 1.1 Hz, 3H), 3.36 (dd, *J* = 12.2, 7.3 Hz, 1H), 3.30 (dd, *J* = 12.3, 4.4 Hz, 1H), 2.713 – 2.69 (m, 1H), 1.99 – 1.74 (m, 4H), 1.25 (s, 3H). ^{13}C NMR (151 MHz, DMSO) δ 173.15, 149.19, 128.38, 128.27, 128.09 (q, *J* = 290.1 Hz), 125.73, 60.29 (q, *J* = 22.7 Hz), 51.48, 50.51, 40.34, 30.46, 21.26, 16.56. ^{19}F NMR (564 MHz, DMSO) δ -71.68. ESIHR (M+H) calc'd 302.1368, found 302.1358.

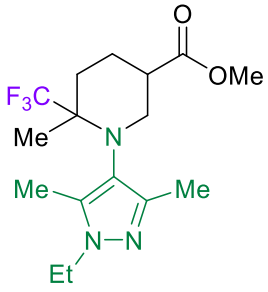

147

The synthesis of **147** was conducted according to general procedure K with methyl 2-methylene-5-oxohexanoate as the electrophile and 1-ethyl-3,5-dimethyl-1H-pyrazol-4-amine as the nucleophile. Purification of the crude mixture by silica gel chromatography with 0-

30% EtOAc in hexanes as eluent afforded **147** as a mixture of diastereomers (90 mg, 52% yield) as a pale yellow oil. Major Diastereomer: ^{1}H NMR (600 MHz, DMSO) δ 3.92 – 3.85 (m, 2H), 3.72 (dt, *J* = 11.3, 1.9 Hz, 1H), 3.61 (d, *J* = 2.0 Hz, 3H), 3.18 – 3.14 (m, 1H), 2.70 (p, *J* = 3.9 Hz, 1H), 2.09 (s, 3H), 2.04 (s, 1H), 1.95 (s, 3H), 1.95 – 1.88 (m, 1H), 1.86 – 1.80 (m, 1H), 1.79 – 1.71 (m, 1H), 1.23 (t, *J* = 7.2 Hz, 3H), 1.04 (d, *J* = 4.6 Hz, 3H). ^{13}C NMR (151 MHz, DMSO) δ 173.66, 144.26, 135.69, 129.19 (q, *J* = 291.6 Hz), 125.59, 59.43 – 58.71 (m), 51.47, 50.31, 43.45, 29.75, 21.27, 21.23, 14.91, 12.20, 9.44. ^{19}F NMR (564 MHz, DMSO) δ -70.47. ESIHR (M+H) calc'd 348.1899, found 348.1902.

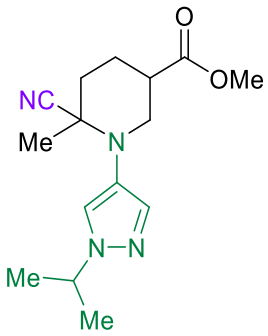

116

The synthesis of **116** was conducted according to general procedure J with methyl 2-methylene-5-oxohexanoate as the electrophile and 1-isopropyl-1H-pyrazol-4-amine as the nucleophile. The crude reaction mixture was a mixture of diasteromers with a ratio of 3.1:1 as determined by ^{1}H NMR. Purification of the crude mixture by silica gel chromatography with 0-10% EtOAc:EtOH (3:1) in hexanes as eluent afforded **116** as a mixture of diastereomers (75 mg, 52% yield) as a pale yellow oil. NMR Spectra is consistent for product reported above from isolated iminium.

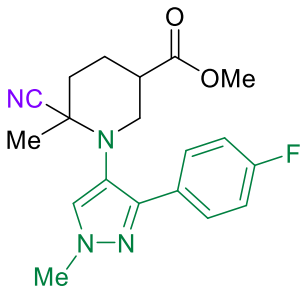

148

The synthesis of **148** was conducted according to general procedure J with methyl 2-methylene-5-oxohexanoate as the electrophile and 3-(4-fluorophenyl)-1-methyl-1H-pyrazol-4-amine as the nucleophile. The crude reaction mixture was a mixture of diasteromers with a ratio of 1.7:1 as determined by ^{1}H NMR Purification of the crude mixture by silica gel chromatography with 0-10% EtOAc:EtOH (3:1) in hexanes as eluent afforded **148** as a mixture of diastereomers (113 mg, 63% yield) as a pale yellow oil. Major Diastereomer: ^{1}H NMR (600 MHz, DMSO) δ 8.05 – 8.00 (m, 2H), 7.96 (s, 1H), 7.21 – 7.16 (m, 2H), 3.87 (d, *J* = 1.7 Hz, 3H), 3.61 (s, 3H), 3.28 – 3.16 (m, 1H), 2.98 (t, *J* = 11.9 Hz, 1H), 2.82 (tt, *J* = 11.6, 4.1 Hz, 1H), 2.14 – 2.03 (m, 2H), 1.74 – 1.61 (m, 2H), 1.14 (s, 3H). ^{13}C NMR (151 MHz, DMSO) δ 172.55, 161.40 (d, *J* = 244.3 Hz), 144.09, 129.55 (d, *J* = 3.1 Hz), 128.35 (d, *J* = 7.9 Hz), 127.48, 126.92, 120.07, 115.11 (d, *J* = 21.2 Hz), 115.11 (d, *J* = 21.2 Hz), 53.93, 51.62, 41.08, 39.20, 36.51, 24.58, 24.48. ^{19}F NMR (564 MHz, DMSO) δ -115.24 – -115.36 (m). ESIHR (M+H) calc'd 357.1727, found 357.1727.

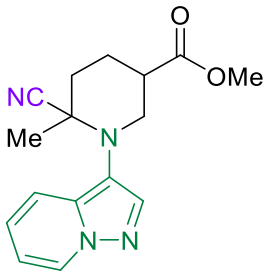

149

The synthesis of **149** was conducted according to general procedure J with methyl 2-methylene-5-oxohexanoate as the electrophile and pyrazolo[1,5-a]pyridin-3-amine as the

nucleophile. The crude reaction mixture was a mixture of diasteromers with a ratio of 1.7:1 as determined by ^{1}H NMR. Purification of the crude mixture by silica gel chromatography with 0-10% EtOAc:EtOH (3:1) in hexanes as eluent afforded **149** as a mixture of diastereomers (104 mg, 70% yield) as a pale yellow oil. Major Diastereomer: ^{1}H NMR (600 MHz, DMSO) δ 8.61– 8.59 (m, 1H), 8.09 (s, 1H), 7.62 (dt, *J* = 8.9, 1.2 Hz, 1H), 7.24 – 7.21 (m, 1H), 6.89 – 6.87 (m, 1H), 3.61 (s, 3H), 3.27 (t, *J* = 11.7 Hz, 1H), 3.20 (ddd, *J* = 12.1, 4.4, 1.6 Hz, 1H), 2.82 – 2.69 (m, 1H), 2.17 – 2.05 (m, 2H), 1.87 – 1.74 (m, 1H), 1.73 – 1.67 (m, 1H), 1.22 (s, 3H). ^{13}C NMR (151 MHz, DMSO) δ 172.59, 136.81, 136.26, 128.86, 123.73, 120.52, 120.51, 120.32, 116.53, 112.44, 58.25, 53.65, 51.71, 51.66, 41.38, 36.34, 25.53, 24.49. ESIHR (M+H) calc'd 299.1508, found 299.1515.

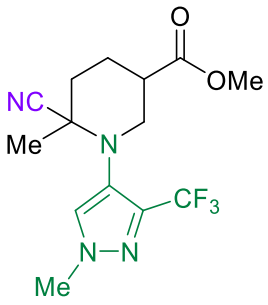

150

The synthesis of **150** was conducted according to general procedure J with methyl 2-methylene-5-oxohexanoate as the electrophile and pyrazolo[1,5-a]pyridin-3-amine as the nucleophile, except the cyclization was run at 120 °C. Purification of the crude mixture by silica gel chromatography with 0-40% EtOAc in hexanes as eluent afforded **150** as a mixture of diastereomers with a ratio of 2.2:1 as determined by ^{19}F NMR (106 mg, 64% yield) as a pale yellow oil. Major Diastereomer: ^{1}H NMR (600 MHz, DMSO) δ 8.12 (s, 1H), 3.91 (s, 3H), 3.61 (s, 3H), 3.19 – 3.12 (m, 1H), 2.93 (t, *J* = 11.8 Hz, 1H), 2.65 – 2.60 (m, 1H), 2.16 – 2.03 (m, 2H), 1.69 – 1.59 (m, 2H), 1.25 (s, 3H). ^{13}C NMR (151 MHz, DMSO) δ 172.34, 137.19 – 136.41 (m), 128.43,

128.41, 121.22 (q, J = 272.3 Hz) 120.11, 57.14, 54.58, 51.64, 41.04, 39.79, 36.47, 24.86, 24.31. ^{19}F NMR (564 MHz, DMSO) δ -60.13. ESIHR (M+H) calc'd 331.1382, found 331.1392.

A3.6. Sequential Difunctionalization of Iminium Salts:

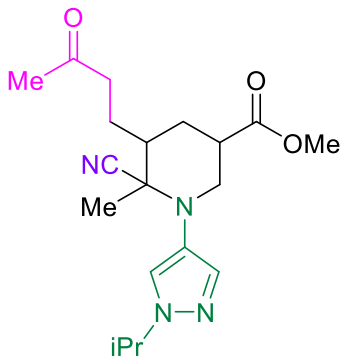

152

The synthesis of **152** was conducted on 0.5 mmol scale with iminium salt **114**. A 4 mL vial with a stir bar was charged with **114** (1.00 equiv) and Molecular sieves, 4A beads, 8-12 mesh (25 beads). The vial was fitted with a cap containing a teflon septa and DCM (2 mL) was added. The mixture was stirred for 5 minutes under a nitrogen atmosphere and methyl vinyl ketone was added (0.082 mL, 1.0 mmol, 2.00 equiv) followed by Hunig's base (0.096 mL, 0.55 mmol, 1.10 equiv). The reaction was stirred at room temperature, and the reaction progress was followed by LCMS analysis to completion (4 hours). Upon completion, TMSCN (0.134 mL, 1.0 mmol, 2.00 equiv) was added to the reaction mixture, and the reaction progress was monitored by LCMS analysis to completion (19 hours). To the reaction mixture was added a 1M solution of tetrabutyl ammonium fluoride (0.6mL, 0.6 mmol, 1.20 equiv). After 1 hour the reaction mixture was diluted with DCM (15 mL) and saturated aqueous sodium bicarbonate and the mixture was stirred for an additional 5 min. The organic layer was collected with a phase separator (Biotage Isolute), and the aqueous layer was extracted with DCM x 2. The solvents of the combined organic layer were evaporated, and the crude material was purified via silica gel chromatography. Purification of the crude mixture by silica gel chromatography with 0-50% (3:1 EtOAc:EtOH) in hexanes as eluent afforded **152** as

a mixture of diastereomers (110 mg, 61% yield) as a yellow oil. Major Diastereomer: ^{1}H NMR (600 MHz, DMSO) δ 7.72 (s, 1H), 7.35 (s, 1H), 4.46 – 4.39 (m, 1H), 3.63 (s, 3H), 3.38 – 3.32 (m, 1H), 3.22 (dd, *J* = 12.4, 3.6 Hz, 1H), 2.86 – 2.83 (m, 1H), 2.69 – 2.58 (m, 1H), 2.57 – 2. 52 (m, 1H), 2.27 – 2.19 (m, 1H), 2.12 (s, 3H), 1.95 – 1.84 (m, 1H), 1.67 – 1.56 (m, 1H), 1.43 – 1.15 (m, 14H) ^{13}C NMR (151 MHz, DMSO) δ 207.70, 172.90, 134.53, 130.17, 123.27, 118.84, 62.71, 53.22, 53.16, 51.61, 40.85, 40.00, 38.35, 29.71, 27.45, 24.97, 23.46, 22.50. ESIHR (M+H) calc'd 361.2240, found 361.2241.

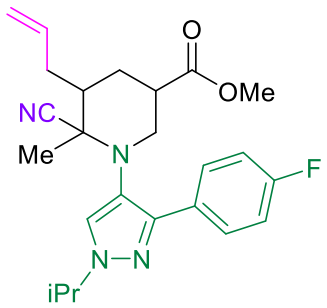

153

The synthesis of **153** was conducted on 0.5 mmol scale with iminium salt **129**. A 4 mL vial with a stir bar was charged with **129** (1.00 equiv), Molecular sieves, 4A beads, 8-12 mesh (25 beads). The vial was fitted with a cap containing a teflon septa, and DCE (2 mL) was added. The mixture was stirred for 5 minutes under a nitrogen atmosphere and Hunig's base was added (0.175 mL, 1.0 mmol, 2.00 equiv), followed by allyl bromide (0.130 mL, 1.5 equiv, 3.00 equiv). The reaction mixture was heated to 80 °C, and the reaction progress was followed by LCMS analysis to completion (26 hours). Upon completion, the mixture was allowed to cool to room temperature

and TMSCN (0.134 mL, 1.00 mmol, 2.00 equiv) was added to the reaction mixture, and the reaction progress was monitored by LCMS analysis to completion (19 hours). The reaction mixture was diluted with DCM (15 mL) and saturated aqueous sodium bicarbonate, and the mixture was stirred for 5 min. The organic layer was collected with a phase separator (Biotage Isolute), and the aqueous layer was extracted with DCM x 2. The solvents of the combined organic layer were evaporated, and the crude material was purified via silica gel chromatography. Purification of the crude mixture by silica gel chromatography with 0-35% EtOAc in hexanes as eluent afforded **153** as a mixture of diastereomers (117 mg, 59% yield) as a yellow oil. Major Diastereomer: ^{1}H NMR (600 MHz, DMSO) δ 8.06 – 8.01 (m, 2H), 7.97 (s, 1H), 7.23 – 7.13 (m, 2H), 5.85 – 5.68 (m, 2H), 5.11 – 5.03 (m, 2H), 3.87 (s, 3H), 3.60 (s, 3H), 3.29 – 3.19 (m, 1H), 3.05 – 2.95 (m, 1H), 2.91 (p, J = 2.6 Hz, 1H), 2.50 – 2.40 (m, 1H), 2.24 – 2.13 (m, 1H), 1.92 – 1.74 (m, 2H), 1.36 – 1.27 (m, 1H), 1.19 (s, 3H). ^{13}C NMR (151 MHz, DMSO) δ 172.45, 161.39 (d, J = 244.3 Hz), 144.29, 135.66, 129.51, 128.36, 127.43, 127.25, 118.93, 117.38, 114.96, 62.68, 53.84, 51.61, 43.63, 39.20, 35.72, 35.68, 29.81, 21.93. ^{19}F NMR (564 MHz, DMSO) δ -115.30. ESIHR (M+H) calc'd 397.2040, found 397.2033.

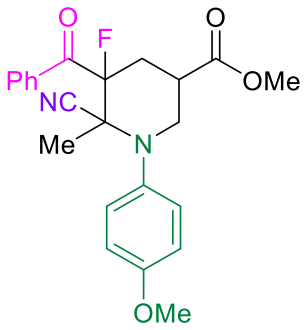

154

The synthesis of **154** was conducted on 0.5 mmol scale with iminium salt **151**. An 8 mL vial with a stir bar was charged with **151** (0.175 g, 1.00 equiv) and Molecular sieves, 4A beads, 8-12 mesh (25 beads). The vial was fitted with a cap containing a teflon septa and DCM (2mL) was added. The reaction mixture was placed under a nitrogen atmosphere and benzoyl chloride (0.070 mL, 0.6 mmol, 1.20 equiv) was added, followed by Hunig's base (0.175 mL, 1.0 mmol, 2.00 equiv). The reaction mixture was stirred at room temperature and the reaction progress was followed by LCMS analysis to completion (17 hours). Upon completion the reaction mixture was transferred to a 40 mL vial via pipette and concentrated to dryness with the aid of a rotary evaporator. The residue was dissolved in acetonitrile (2 mL). A separate 40 mL vial equipped with a stirbar was charged with NFSI (0.174 mg, 0.55 mmol, 1.10 equiv) and acetonitrile (4 mL). The solution was cooled to 0 °C in an ice water bath, and the cold mixture was stirred, followed by addition of TMSCN (0.101 mL, 0.75 mmol, 1.50 equiv) and pyridine (0.049 mL, 0.6 mmol, 1.20 equiv). The reaction mixture was stirred at 0 °C for 1 h. The reaction mixture was diluted with DCM (15 mL) and saturated aqueous sodium bicarbonate, and the mixture was stirred for 5 min. The organic layer was collected with a phase separator (Biotage Isolute), and the aqueous layer was extracted with DCM x 2. The solvents of the combined organic layer were evaporated, and the crude material was purified via silica gel chromatography. Purification of the crude mixture by silica gel

chromatography with 0-25% EtOAc in hexanes as eluent afforded **154** as a mixture of diastereomers (122 mg, 59% yield) as a yellow oil. Major Diastereomer: ^{1}H NMR (600 MHz, DMSO) δ 7.95 (dd, *J* = 28.1, 7.8 Hz, 2H), 7.73 – 7.60 (m, 1H), 7.56 – 7.52 (m, 2H), 7.22 (dd, *J* = 24.7, 8.3 Hz, 2H), 6.99 – 6.89 (m, 2H), 3.75 (s, 3H), 3.49 (s, 3H), 3.44 – 3.19 (m, 3H), 2.91 – 2.82 (m, 1H), 2.25 (q, *J* = 13.9 Hz, 1H), 1.22 (s, 3H). ^{13}C NMR (151 MHz, DMSO) δ 196.44 (d, *J* = 28.8 Hz), 171.20, 157.69, 138.56, 135.27 (d, *J* = 4.1 Hz), 133.38, 129.23, 128.51, 128.14, 116.83 (d, *J* = 3.0 Hz), 114.16, 96.14 (d, *J* = 196.7 Hz), 64.87 (d, *J* = 22.4 Hz), 55.19, 51.78, 51.47, 37.36 (d, *J* = 10.6 Hz), 33.47 (d, *J* = 22.1 Hz), 20.42. ^{19}F NMR (564 MHz, DMSO) δ -145.24. ESIHR (M+H) calc'd 411.1720, found 411.1730.

A3.7. References

(1) Larsen, M. A.; Hennessy, E. T.; Deem, M. C.; Lam, Y.; Saurí, J.; Sather, A. C. A Modular and Diastereoselective 5 + 1 Cyclization Approach to N-(Hetero)Aryl Piperidines. *J. Am. Chem. Soc.* **2020**, *142*, 726–732.

A3.8. NMR Spectra of Products

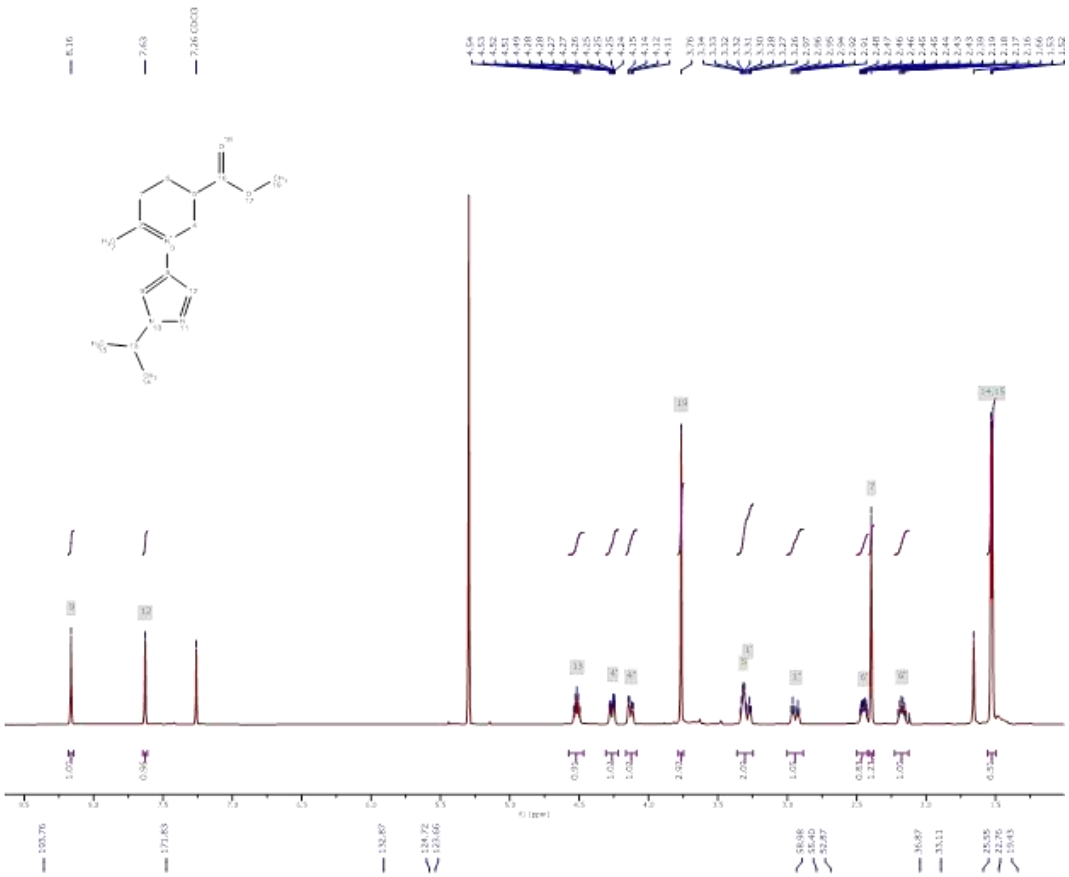

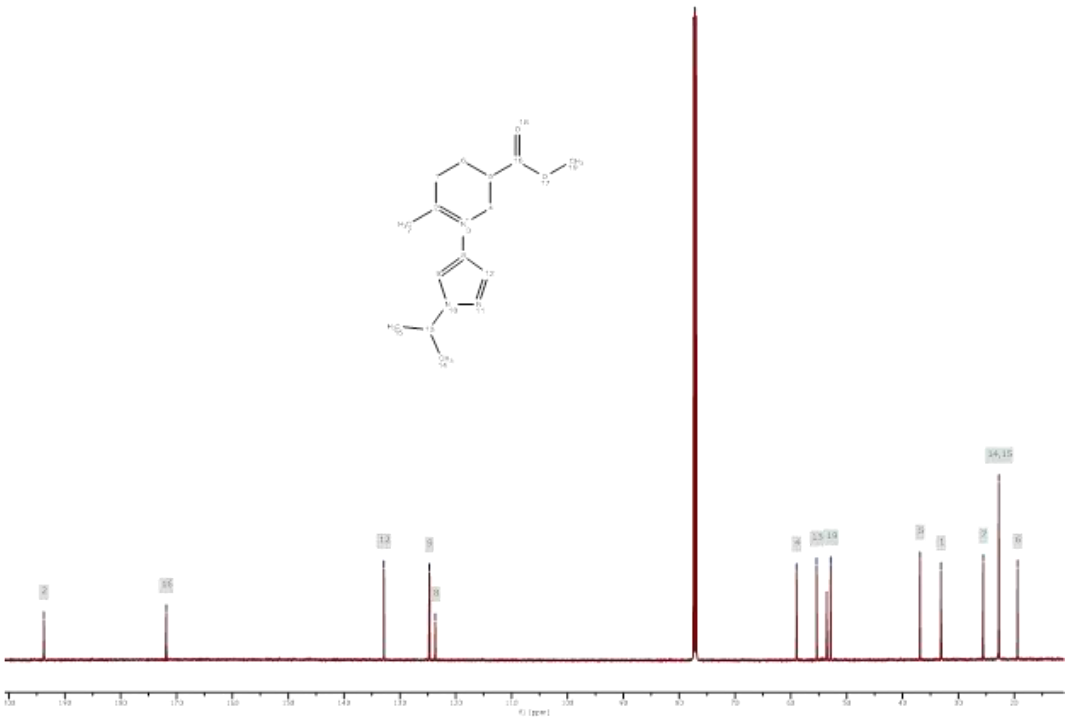

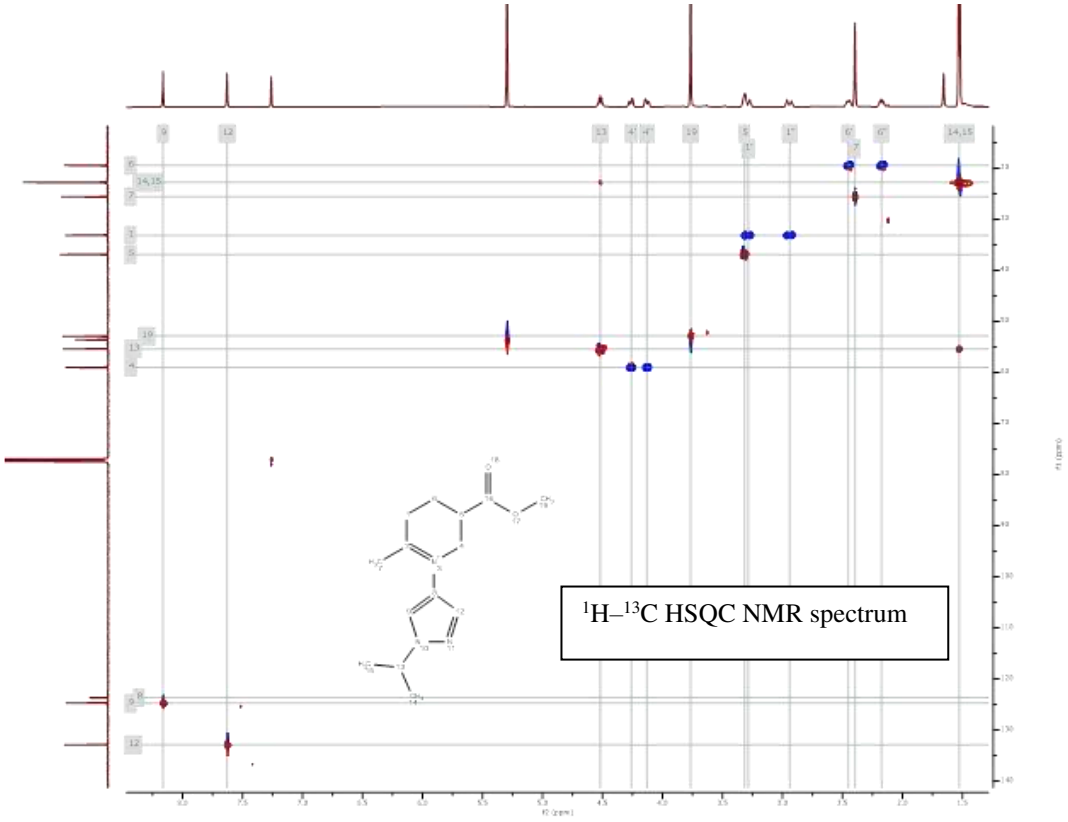

$^{1}H–^{13}C$ HSQC NMR spectrum

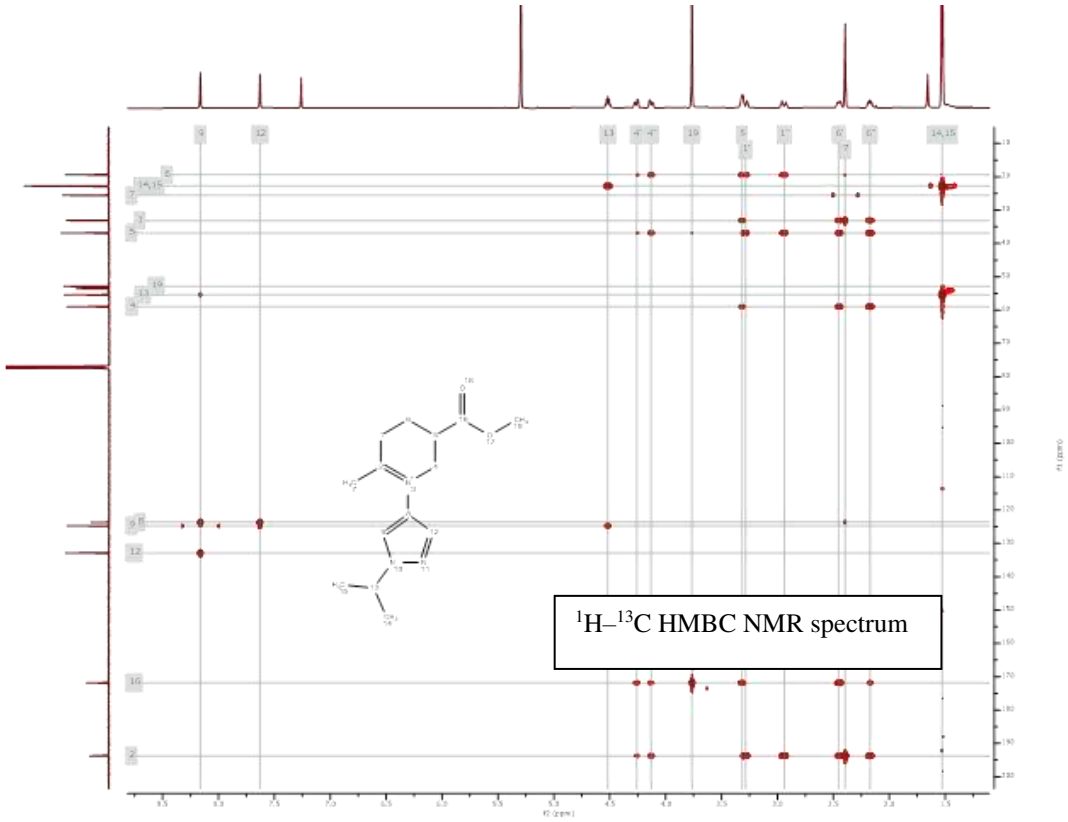

$^{1}H–^{13}C$ HMBC NMR spectrum

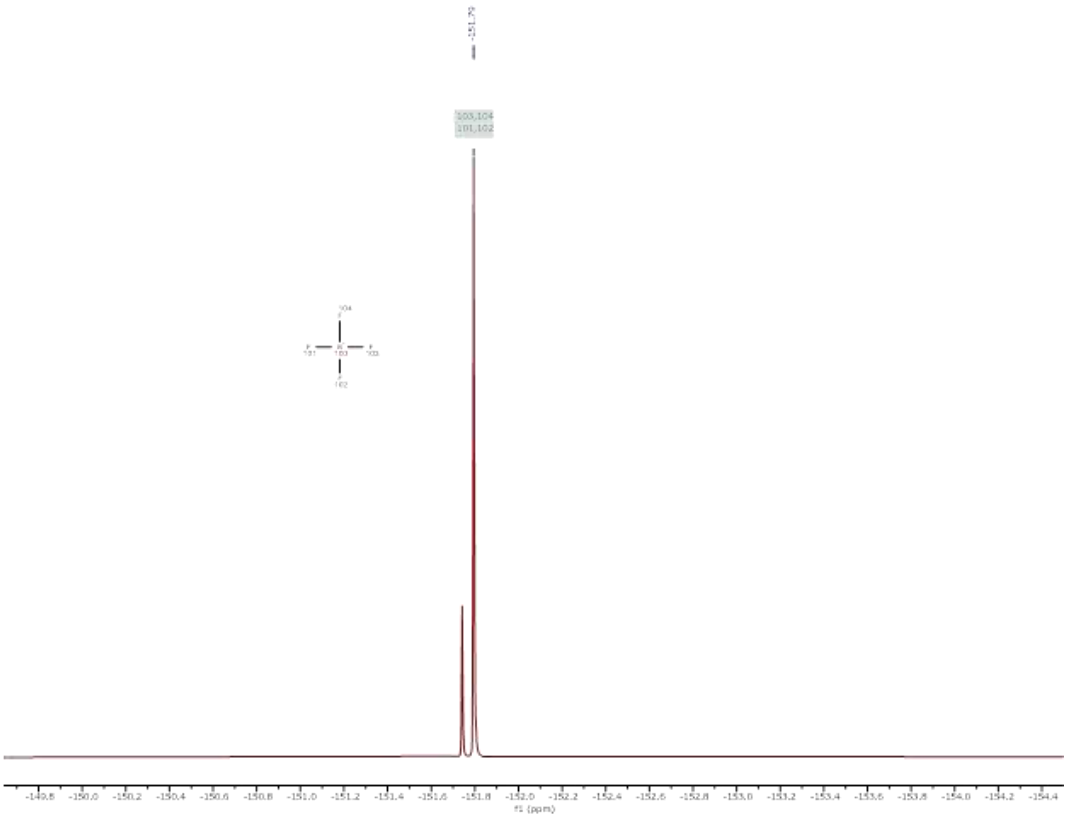

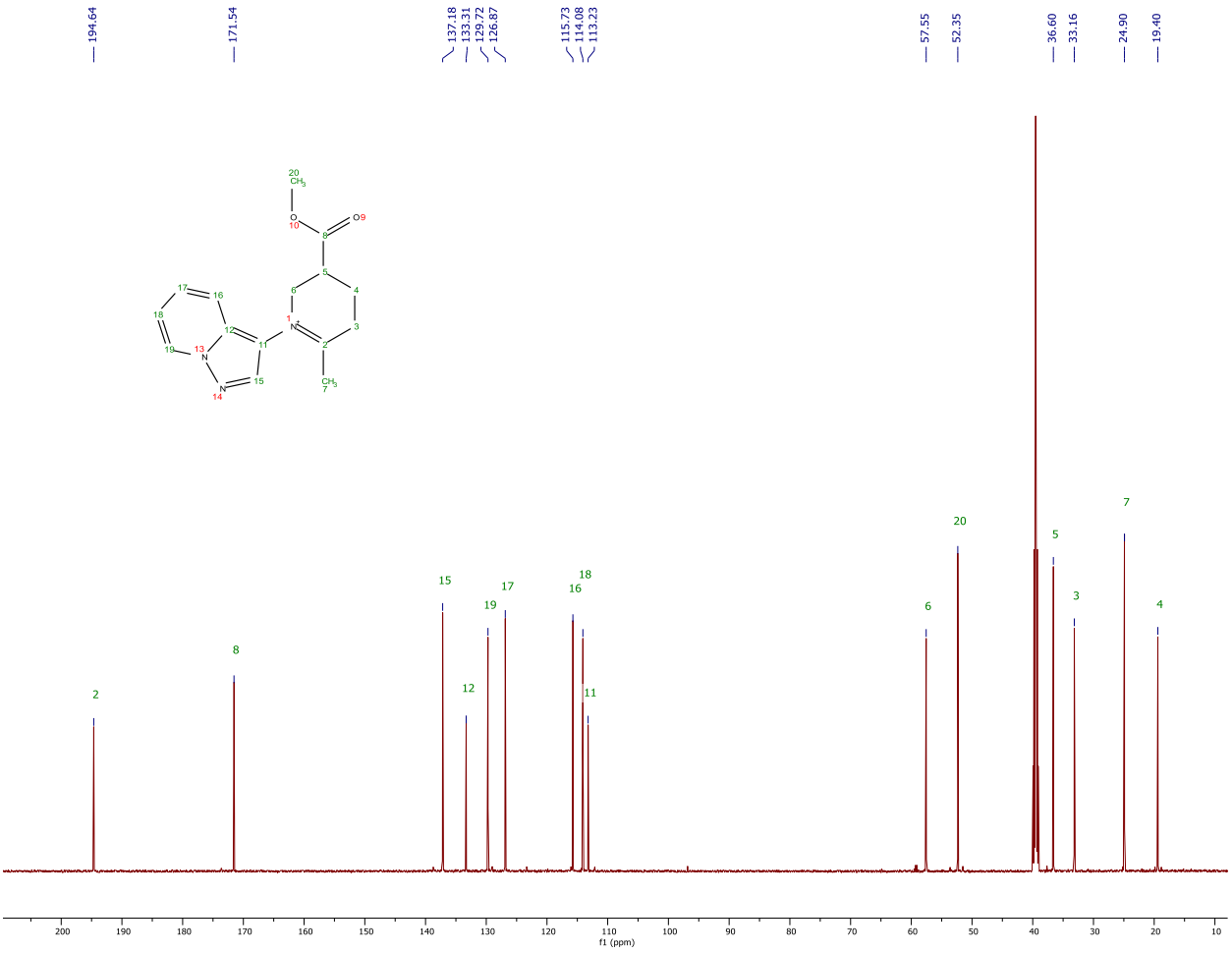
194.64
171.54
137.18
133.31
129.72
126.87
115.73
114.08
113.23
57.55
52.35
36.60
33.16
24.90
19.40
f1 (ppm)

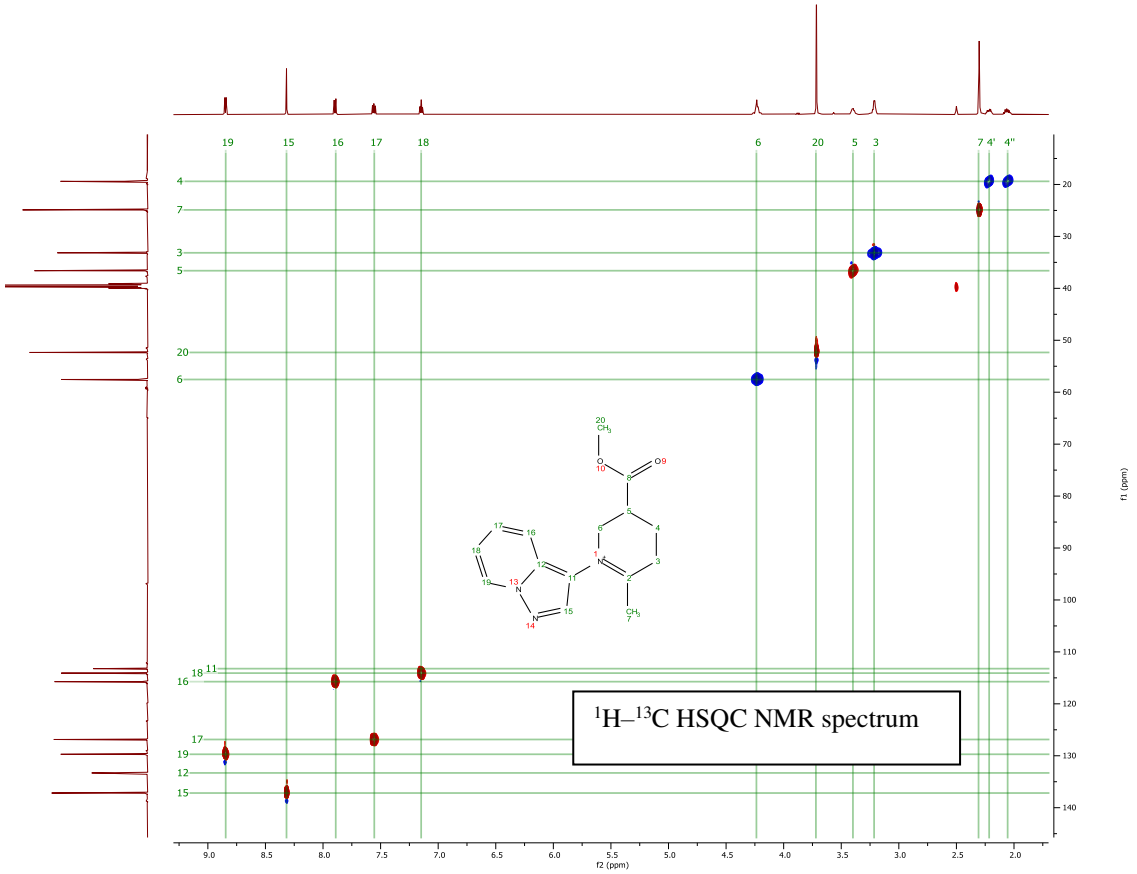

$^{1}H–^{13}C$ HSQC NMR spectrum

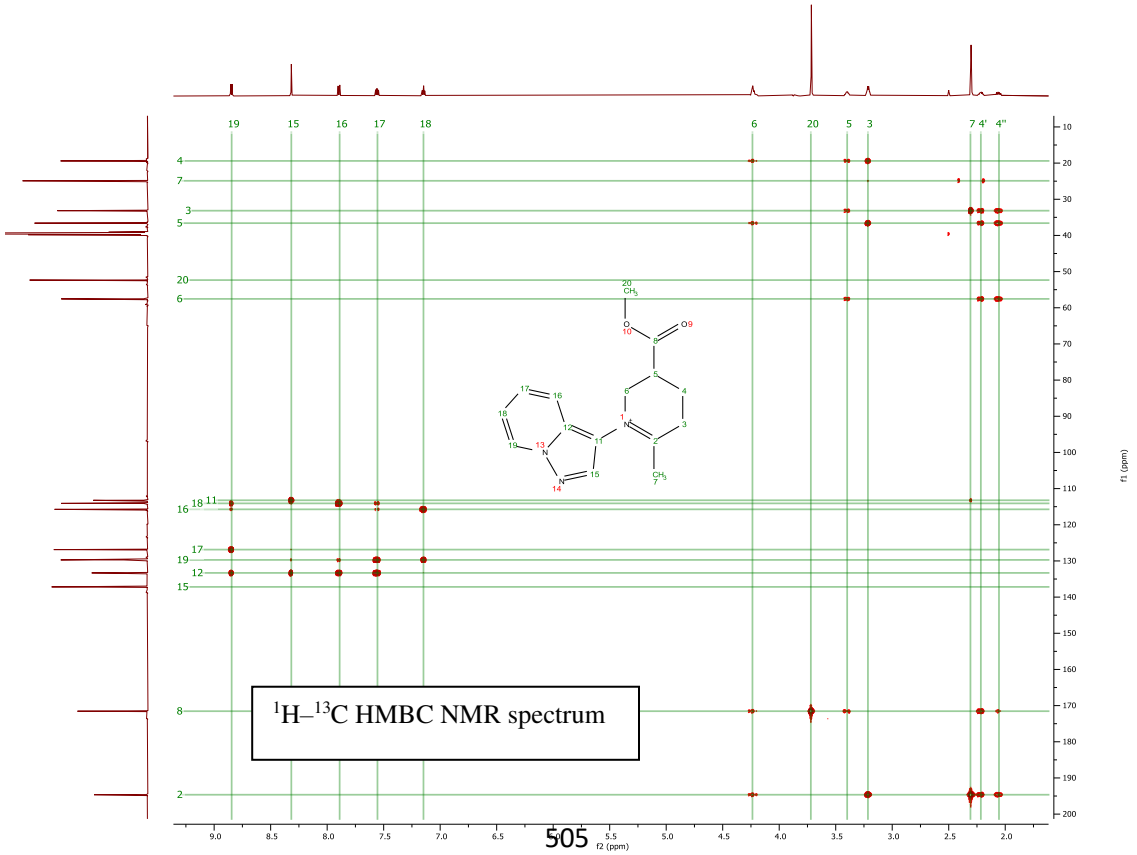

$^{1}H–^{13}C$ HMBC NMR spectrum

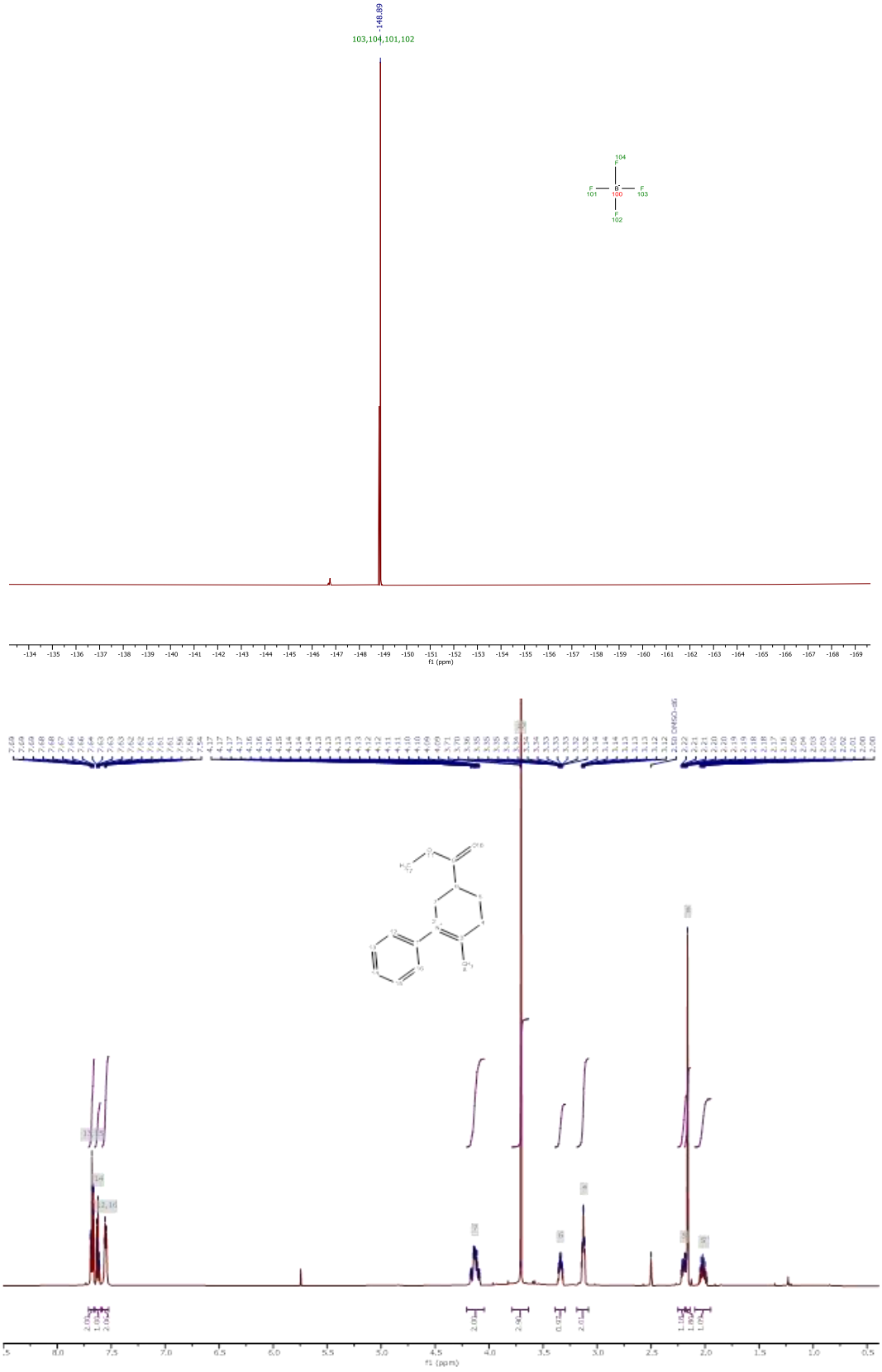
-148.89
103,104,101,102
104
F
F
101
B
100
F
103
F
102
f1 (ppm)
DMSO-d6
f1 (ppm)

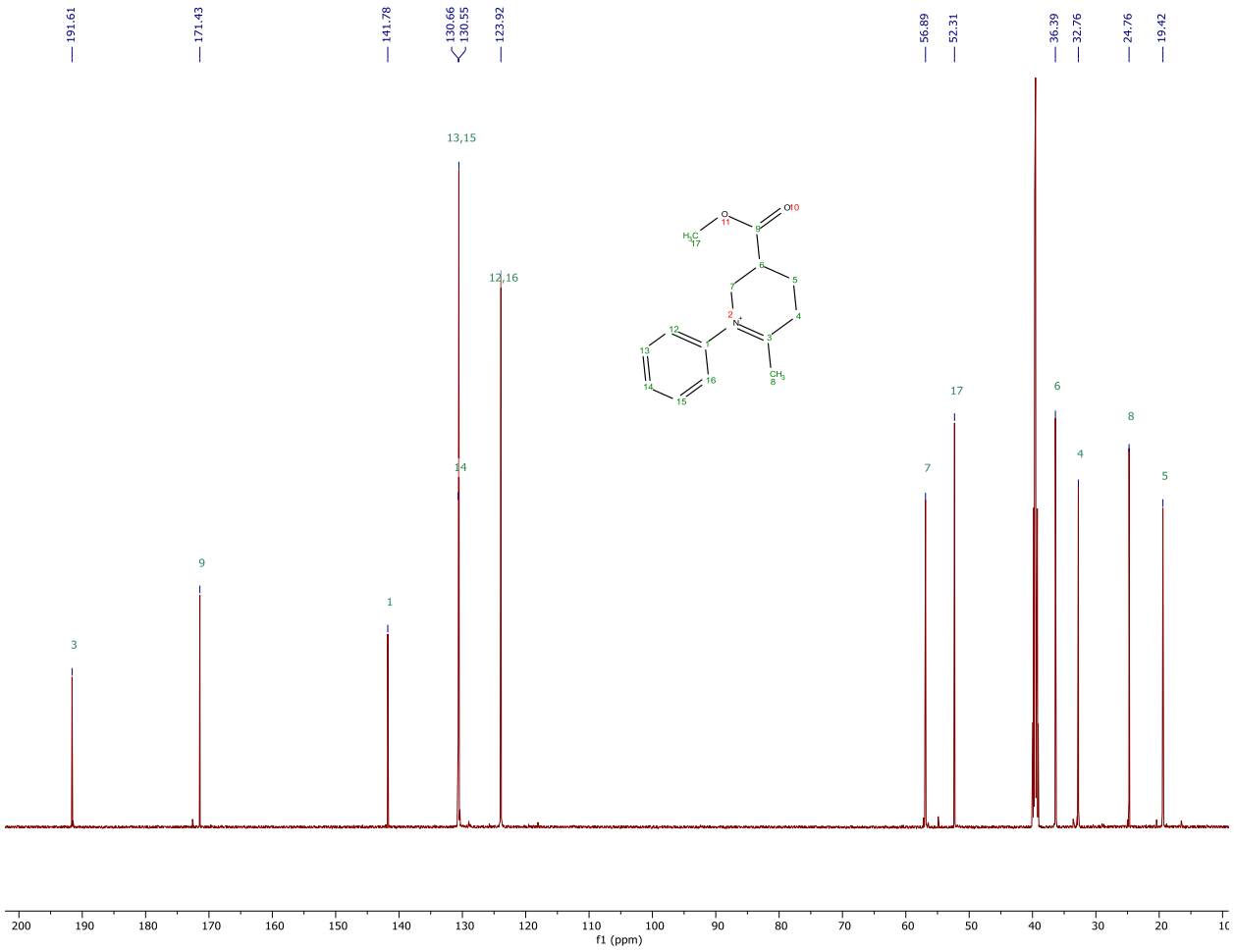
191.61
171.43
141.78
130.66
130.55
123.92
56.89
52.31
36.39
32.76
24.76
19.42
13,15
12,16
14
3
9
1
7
17
6
4
8
5
f1 (ppm)

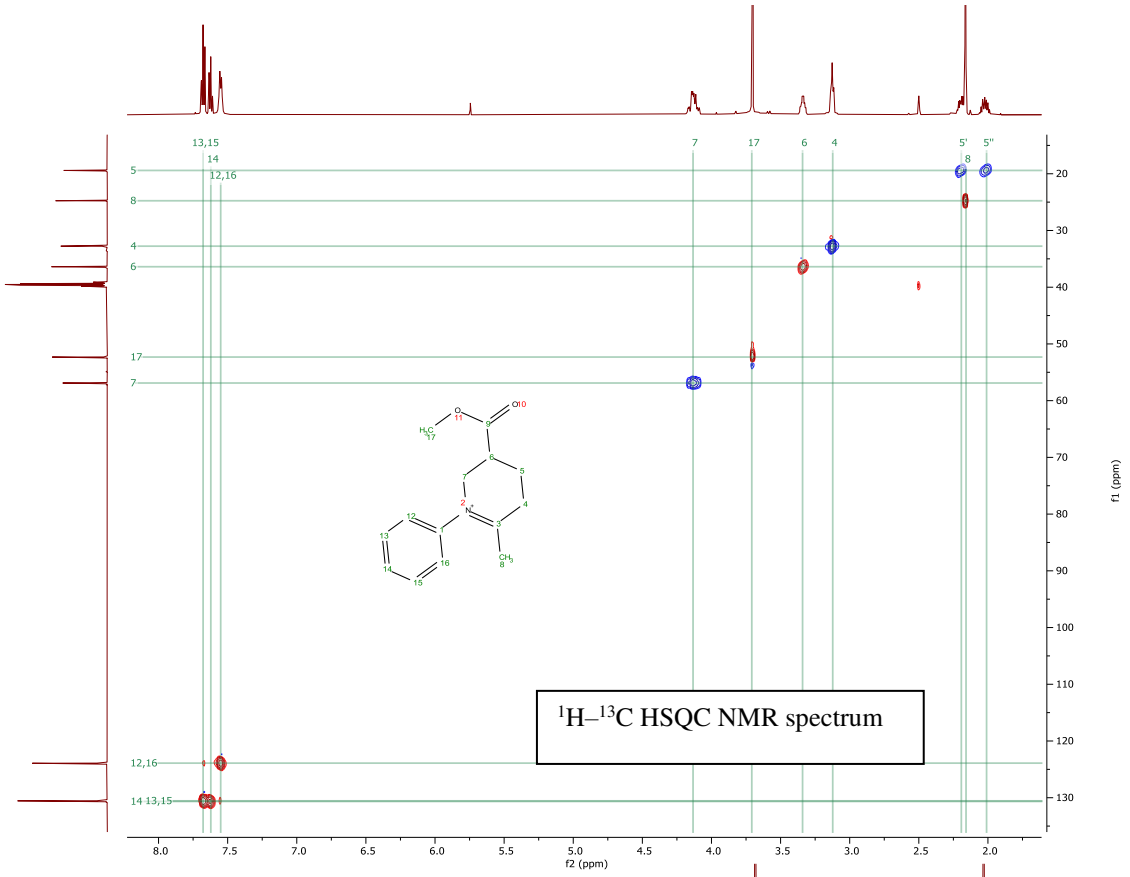

$^{1}H–^{13}C$ HSQC NMR spectrum

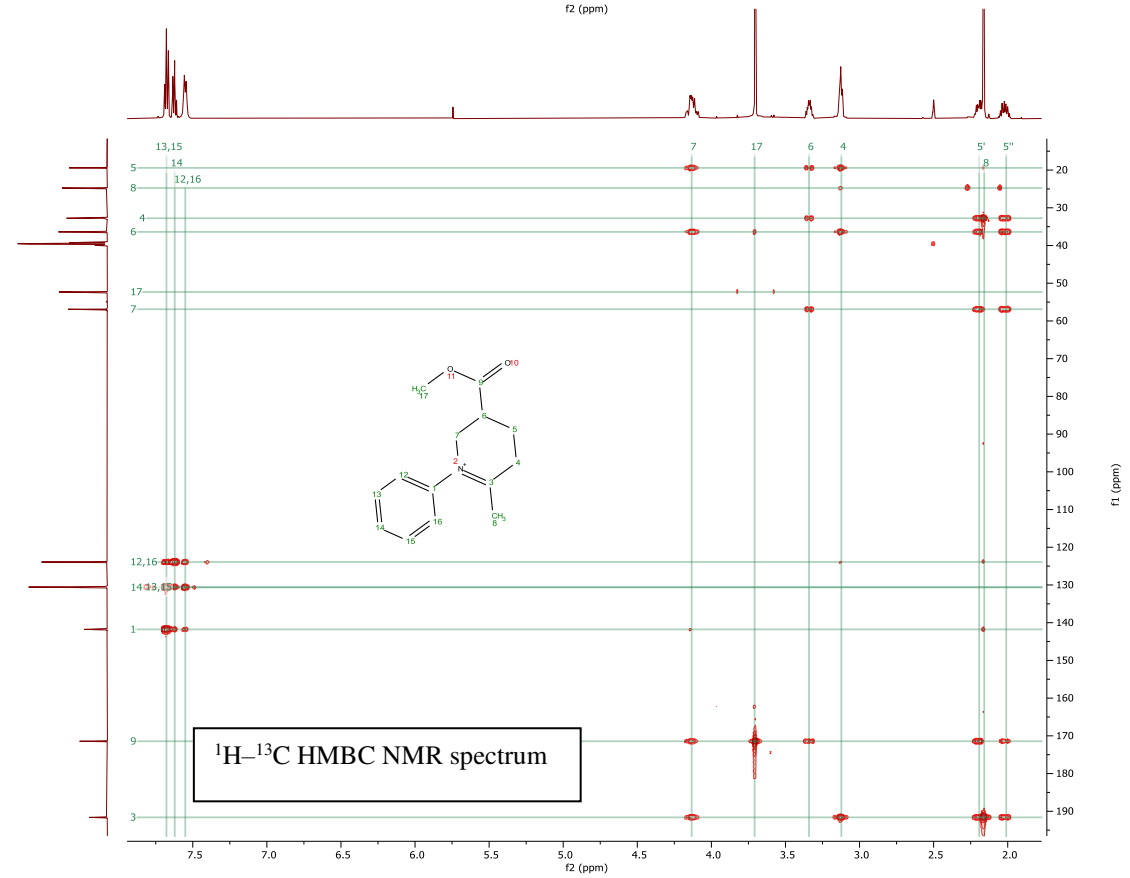

$^{1}H–^{13}C$ HMBC NMR spectrum

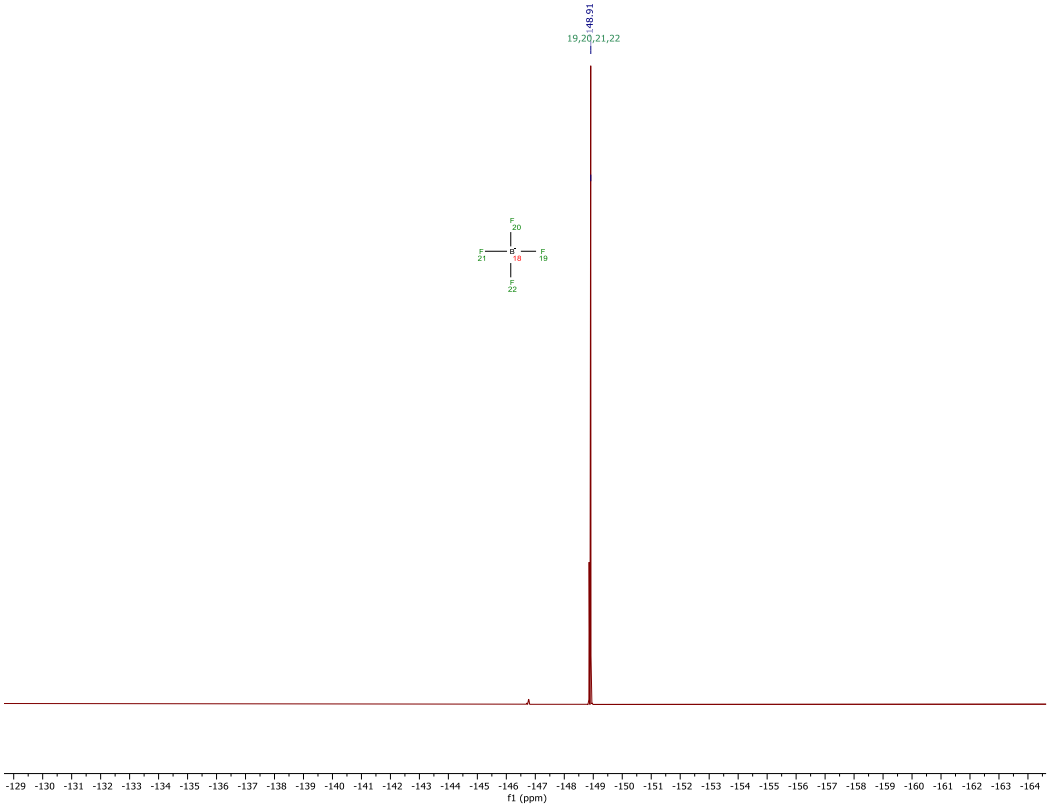
-148.91
19,20,21,22
F
20
F
21
B
18
F
19
F
22
-129 -130 -131 -132 -133 -134 -135 -136 -137 -138 -139 -140 -141 -142 -143 -144 -145 -146 -147 -148 -149 -150 -151 -152 -153 -154 -155 -156 -157 -158 -159 -160 -161 -162 -163 -164
f1 (ppm)

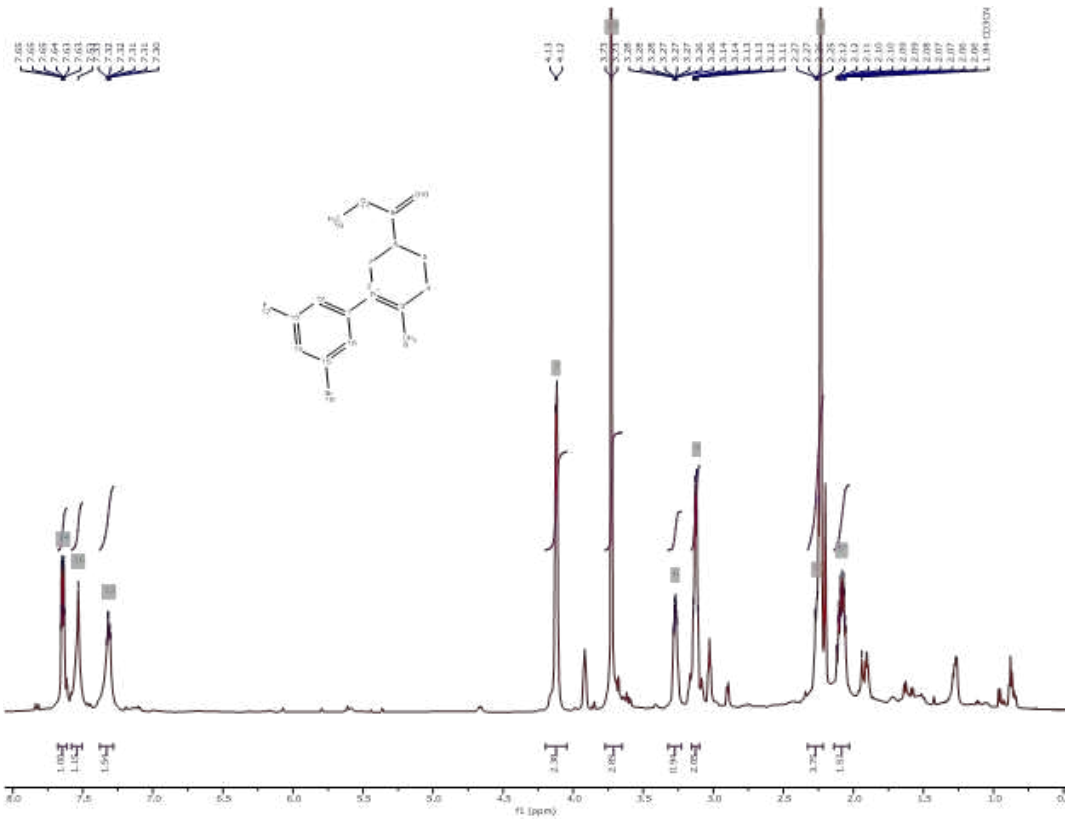
8.0 7.5 7.0 6.5 6.0 5.5 5.0 4.5 4.0 3.5 3.0 2.5 2.0 1.5 1.0 0
f1 (ppm)

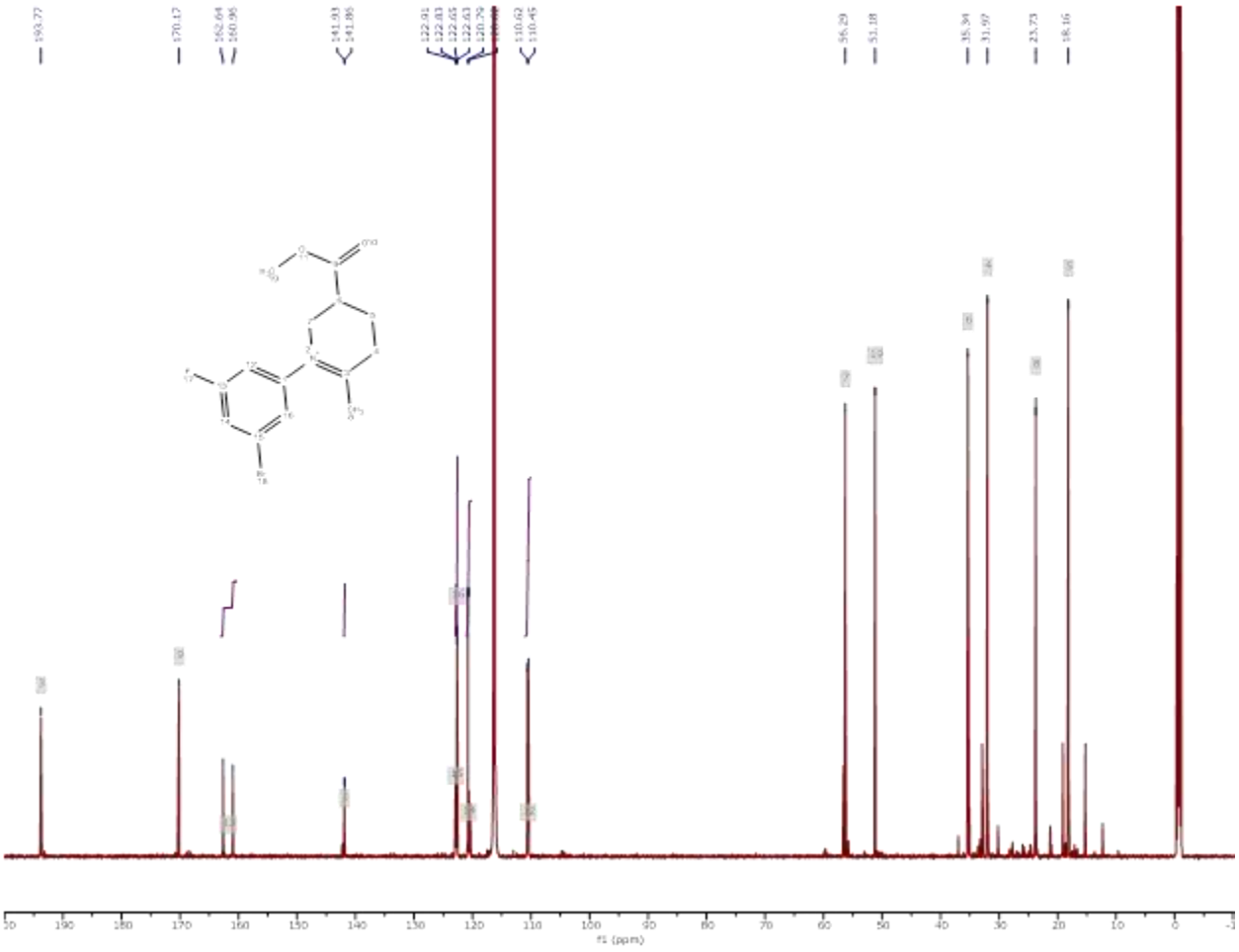
193.77
170.17
162.64
160.95
141.93
141.86
122.91
122.83
122.65
122.63
120.79
110.62
110.45
56.29
51.18
35.34
31.97
23.73
16.16
f1 (ppm)

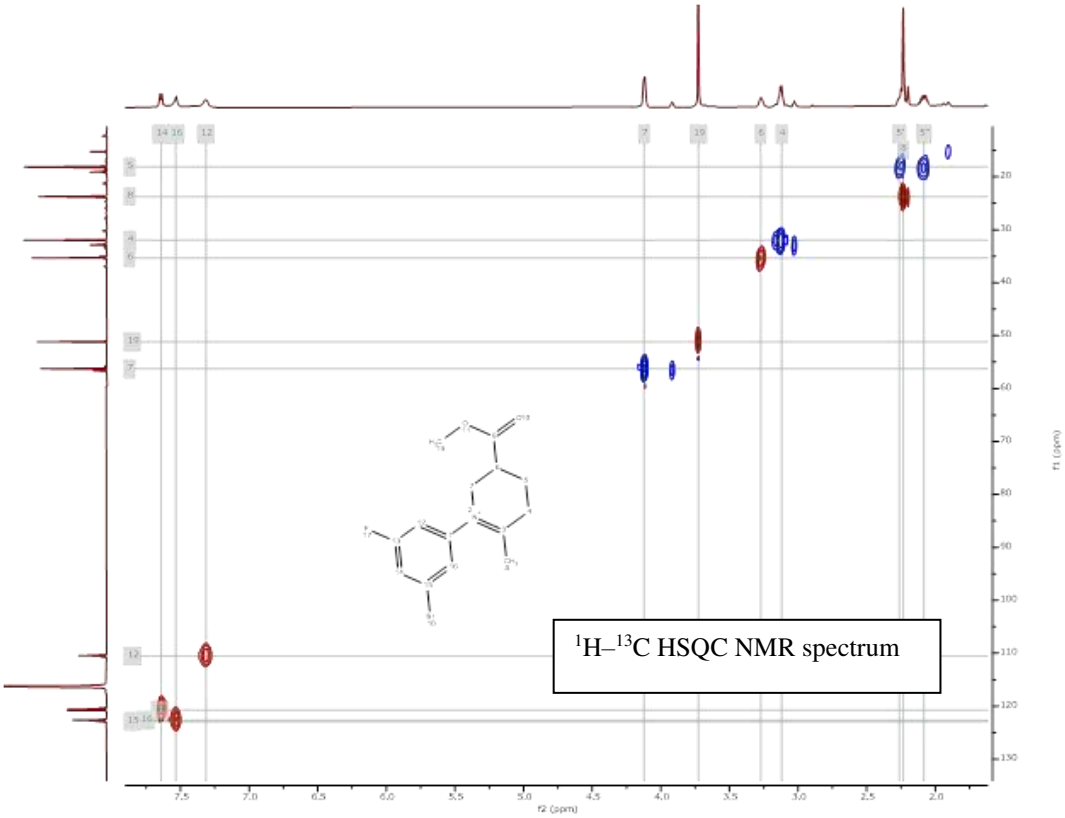
^{1}H–^{13}C HSQC NMR spectrum

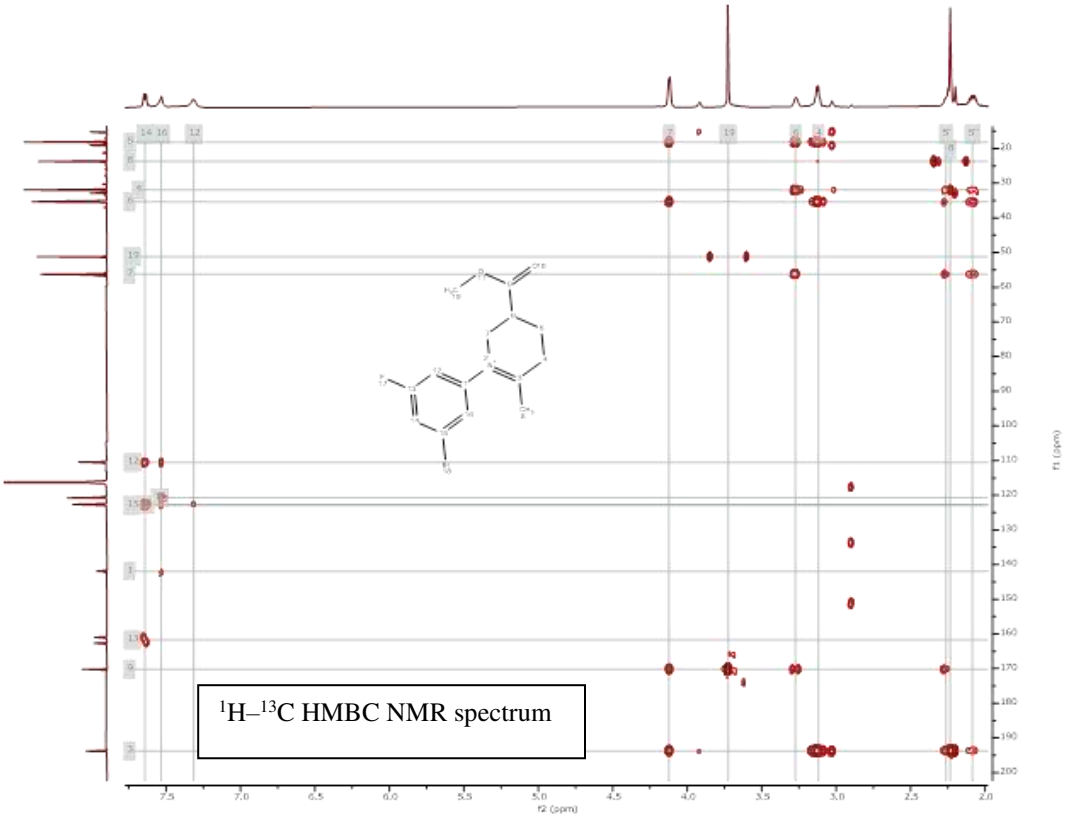
^{1}H–^{13}C HMBC NMR spectrum

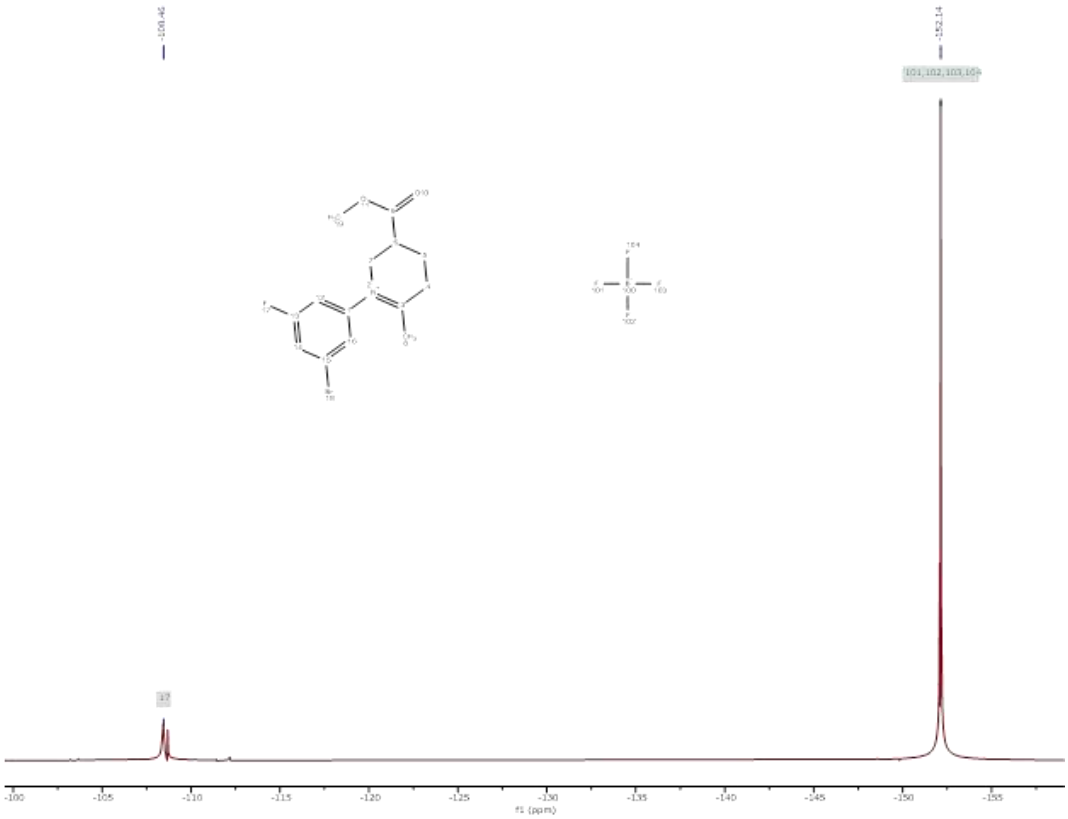

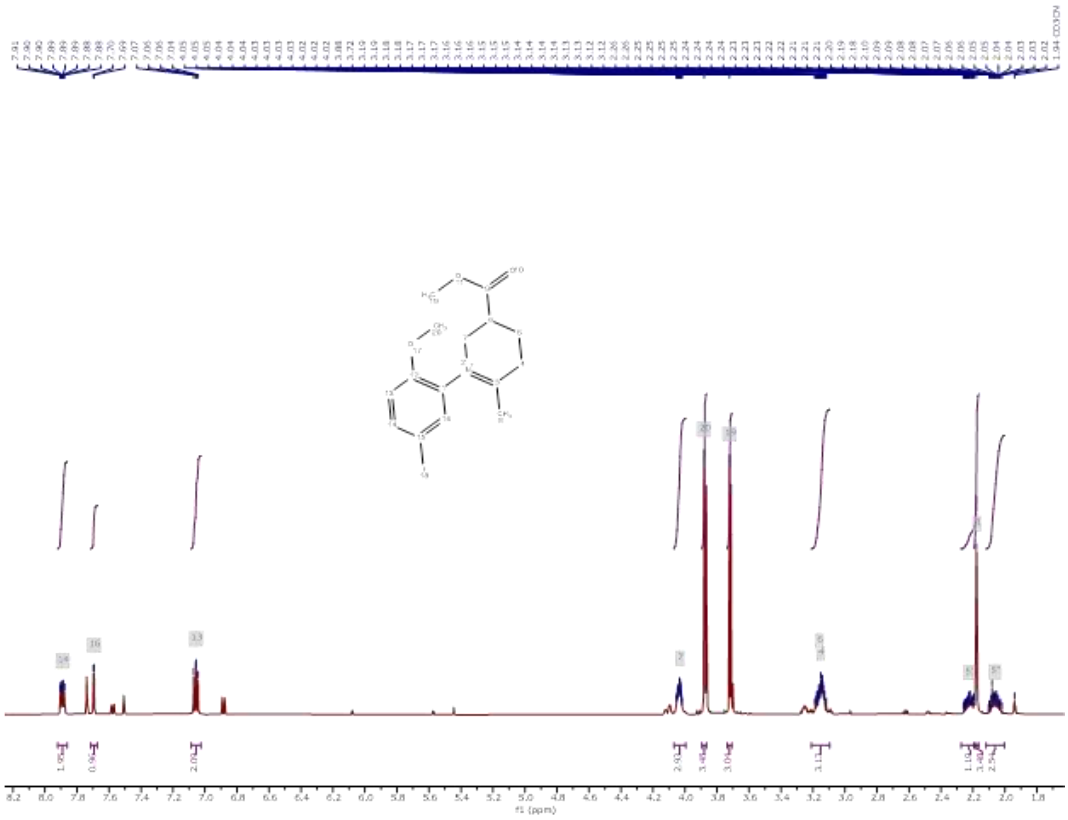

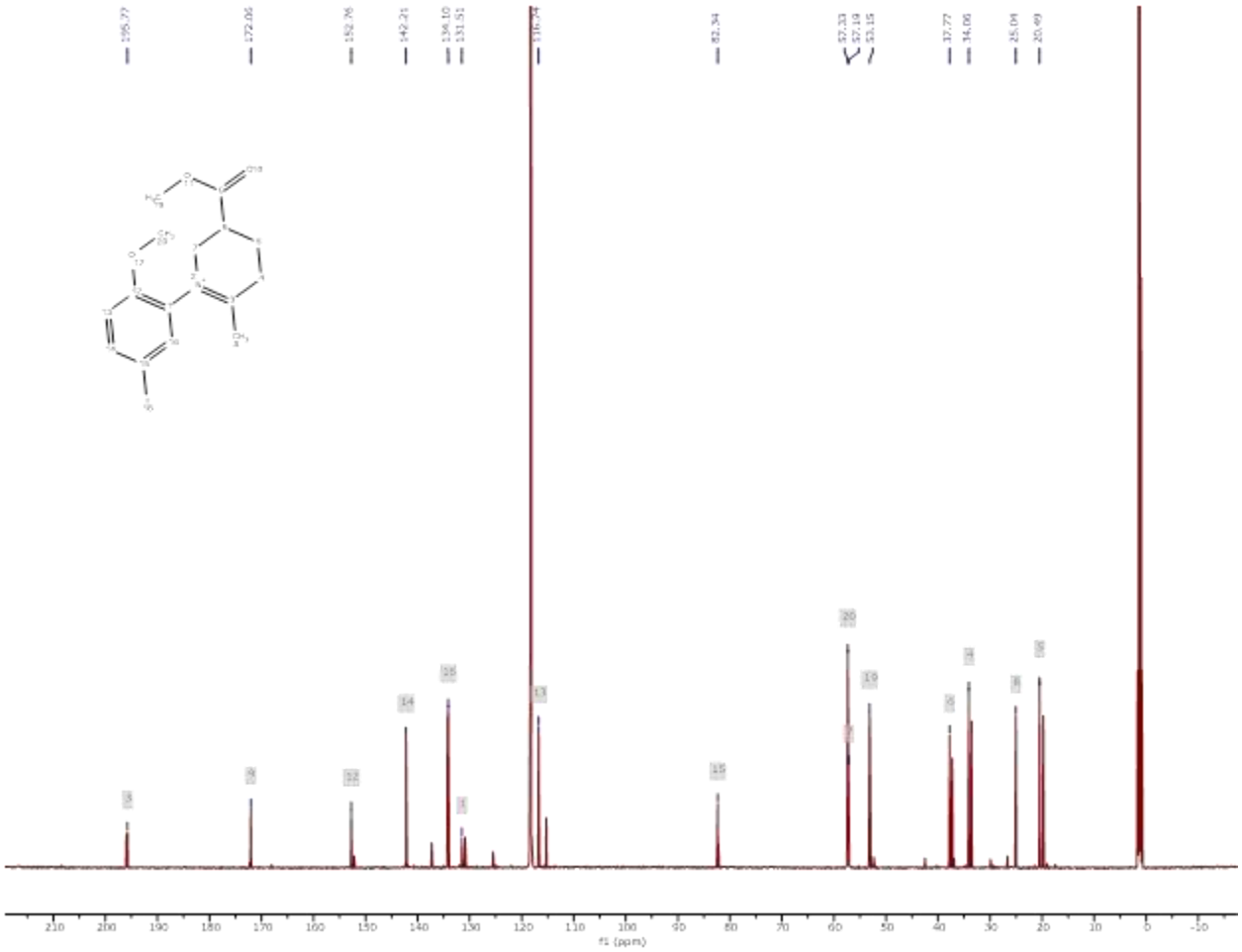
195.77
172.06
152.76
142.21
134.10
131.51
116.54
82.34
57.33
57.19
53.15
37.77
34.06
25.04
20.49
f1 (ppm)

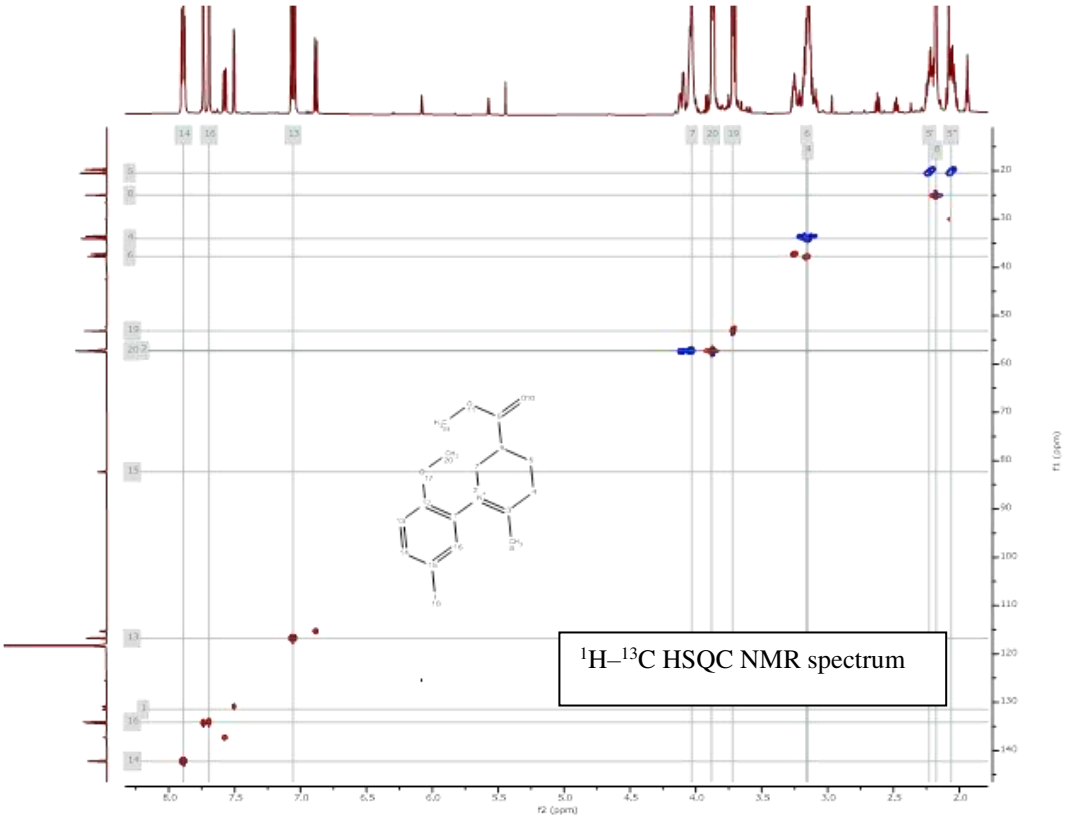

$^{1}H–^{13}C$ HSQC NMR spectrum

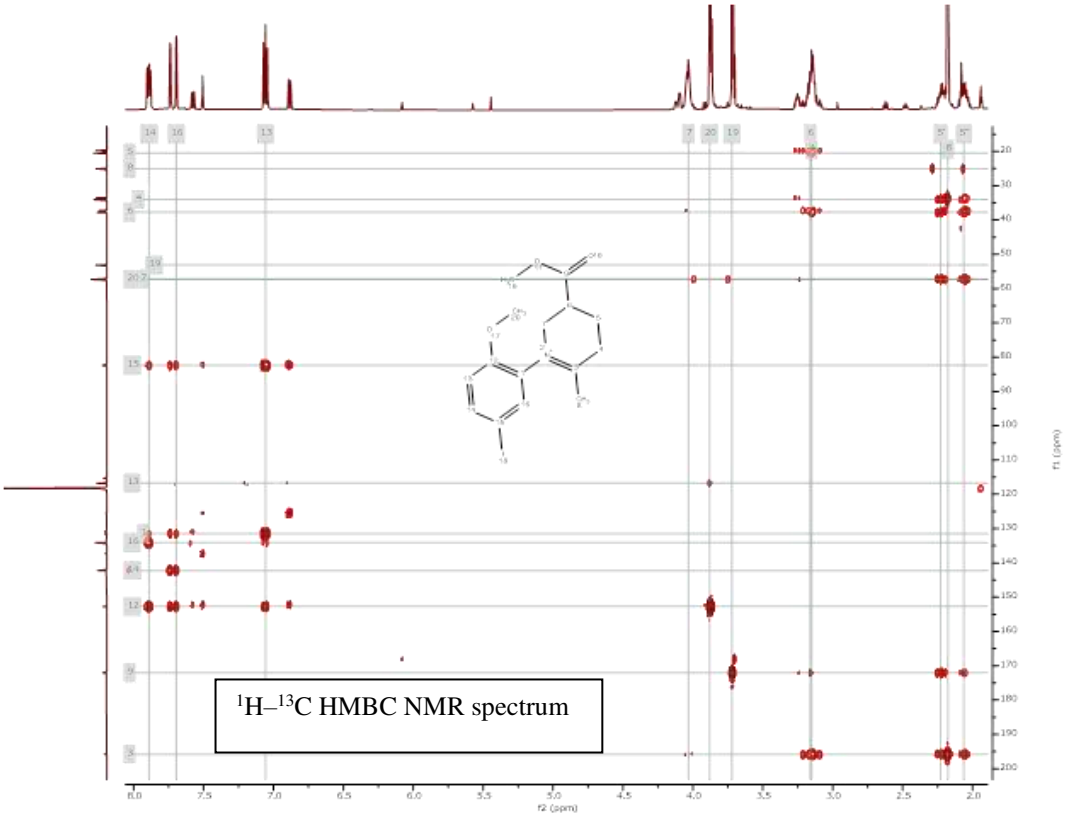

$^{1}H–^{13}C$ HMBC NMR spectrum

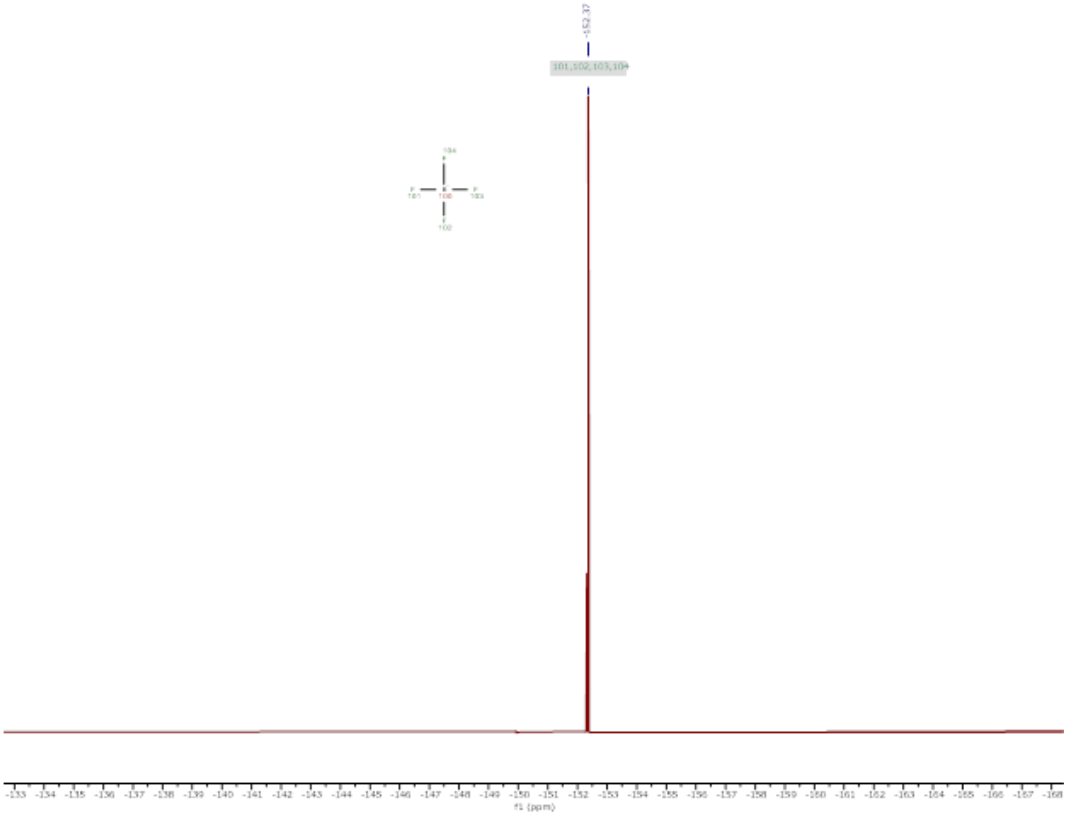

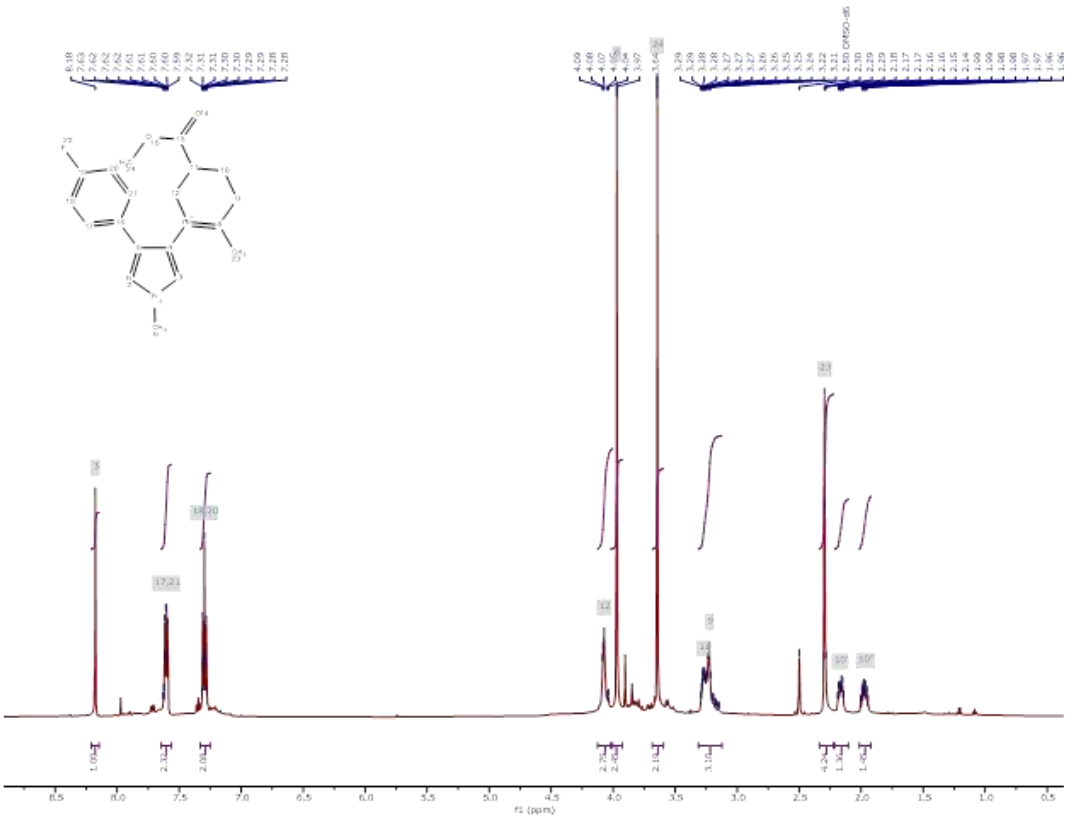

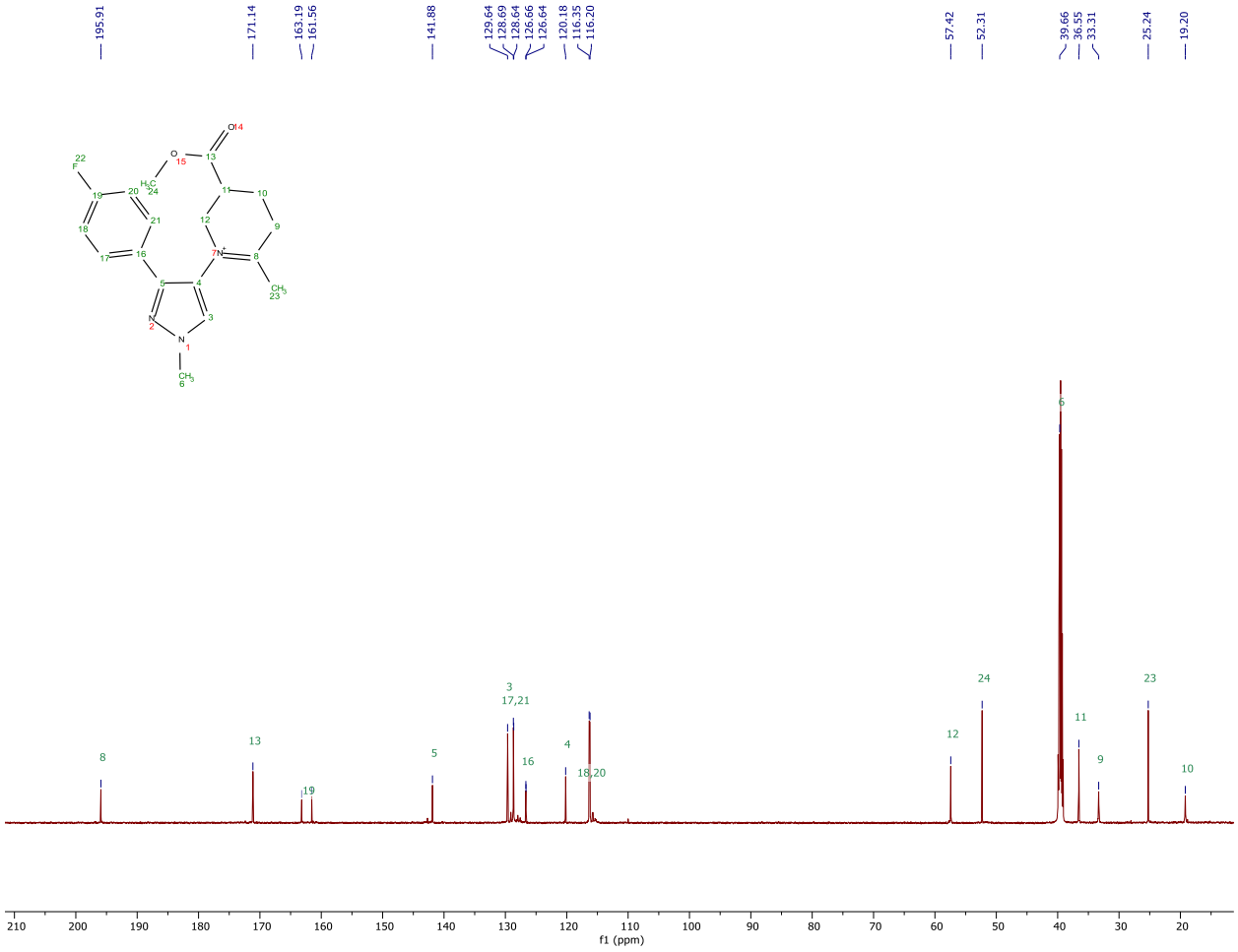
195.91
171.14
163.19
161.56
141.88
129.64
128.69
128.64
126.66
126.64
120.18
116.35
116.20
57.42
52.31
39.66
36.55
33.31
25.24
19.20
f1 (ppm)

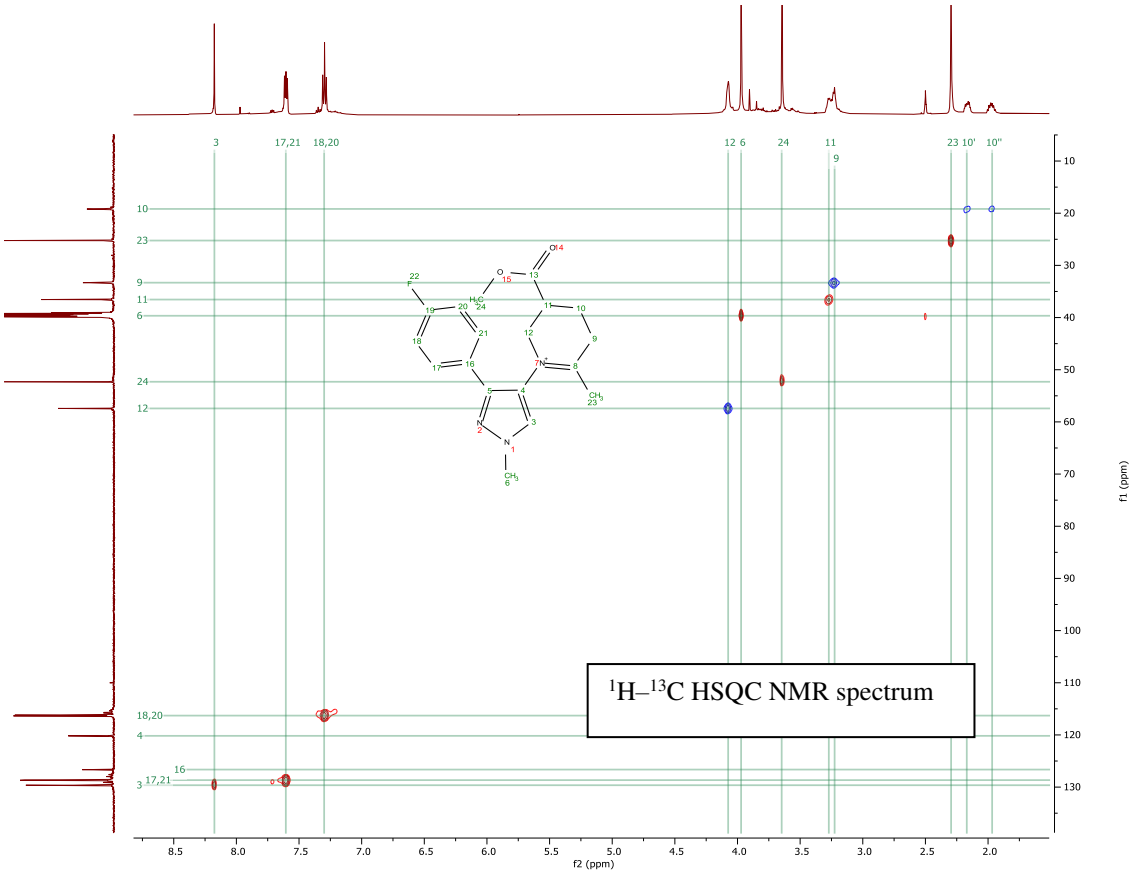

$^{1}H–^{13}C$ HSQC NMR spectrum

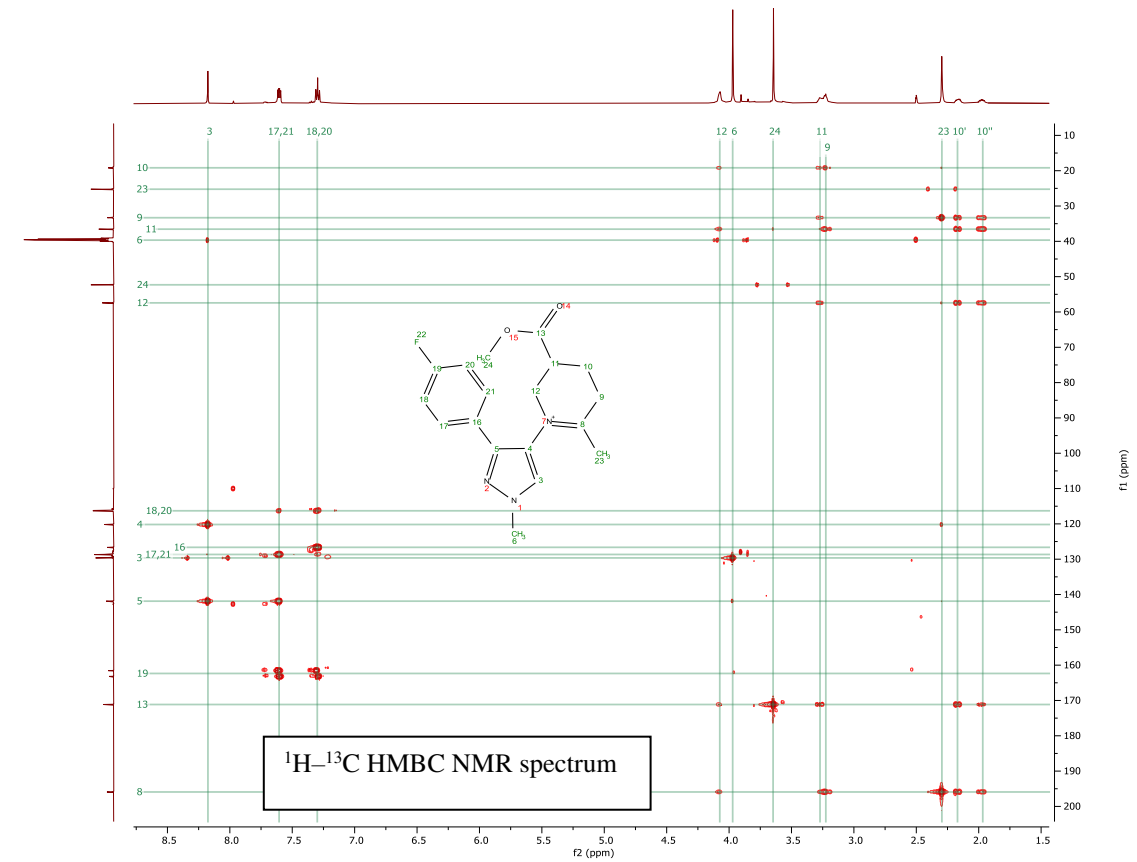

$^{1}H–^{13}C$ HMBC NMR spectrum

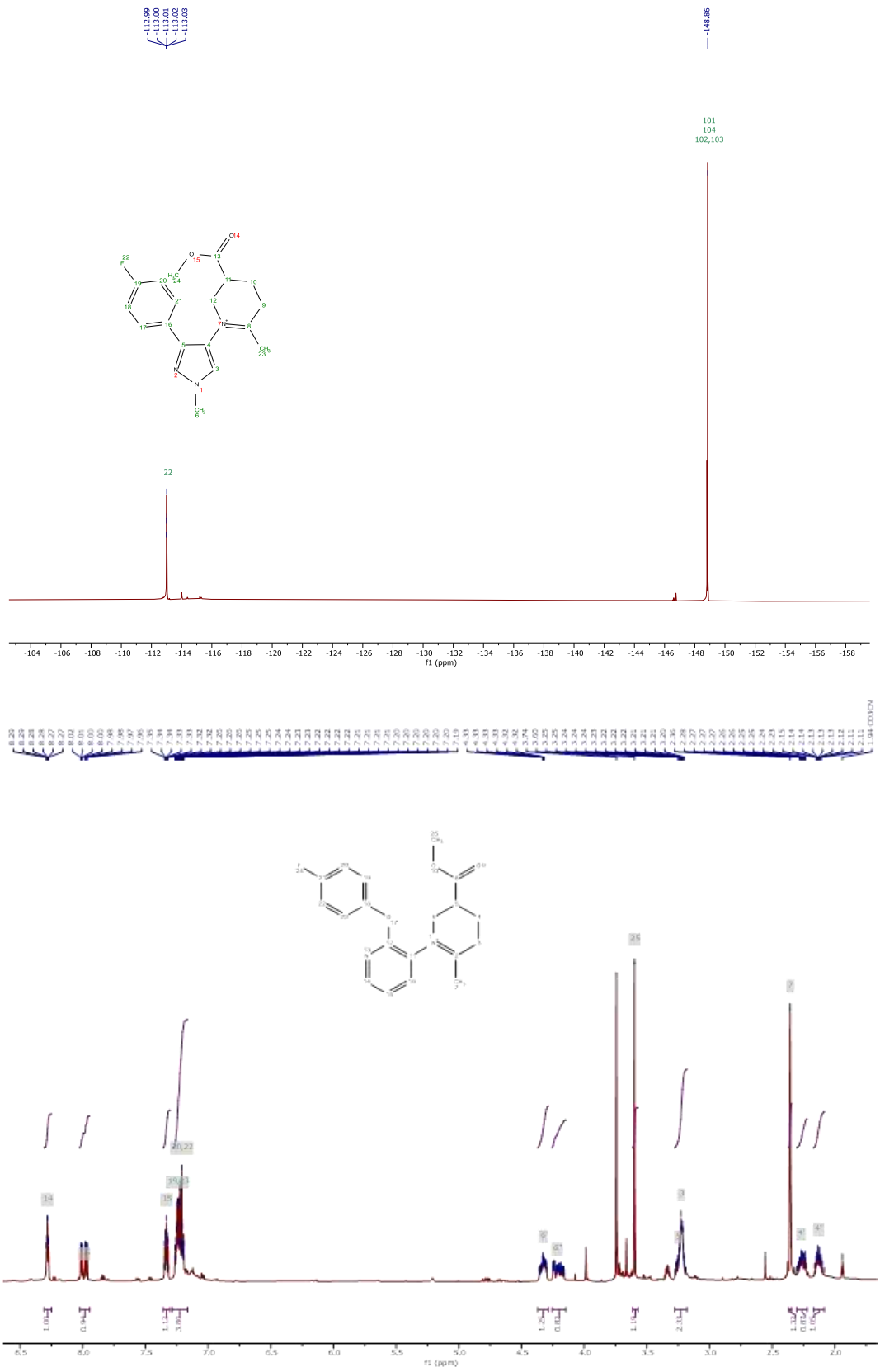
-112.99
-113.00
-113.01
-113.02
-113.03
-148.86
101
104
102,103
22
f1 (ppm)

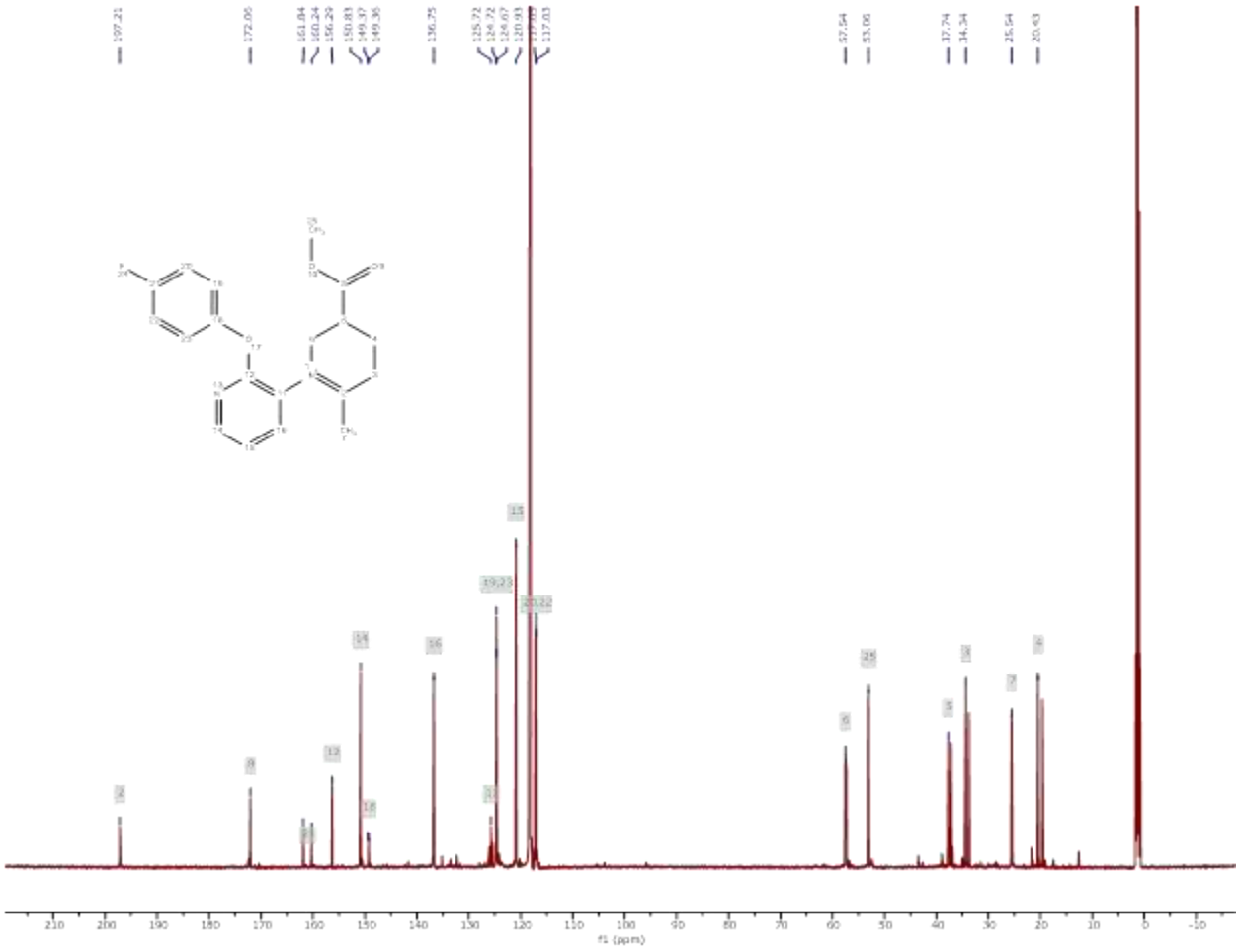
197.21
172.06
161.84
160.24
156.29
150.83
149.37
149.36
136.75
125.72
124.72
124.67
120.93
117.07
117.03
57.54
53.06
37.74
34.34
25.54
20.43
f1 (ppm)

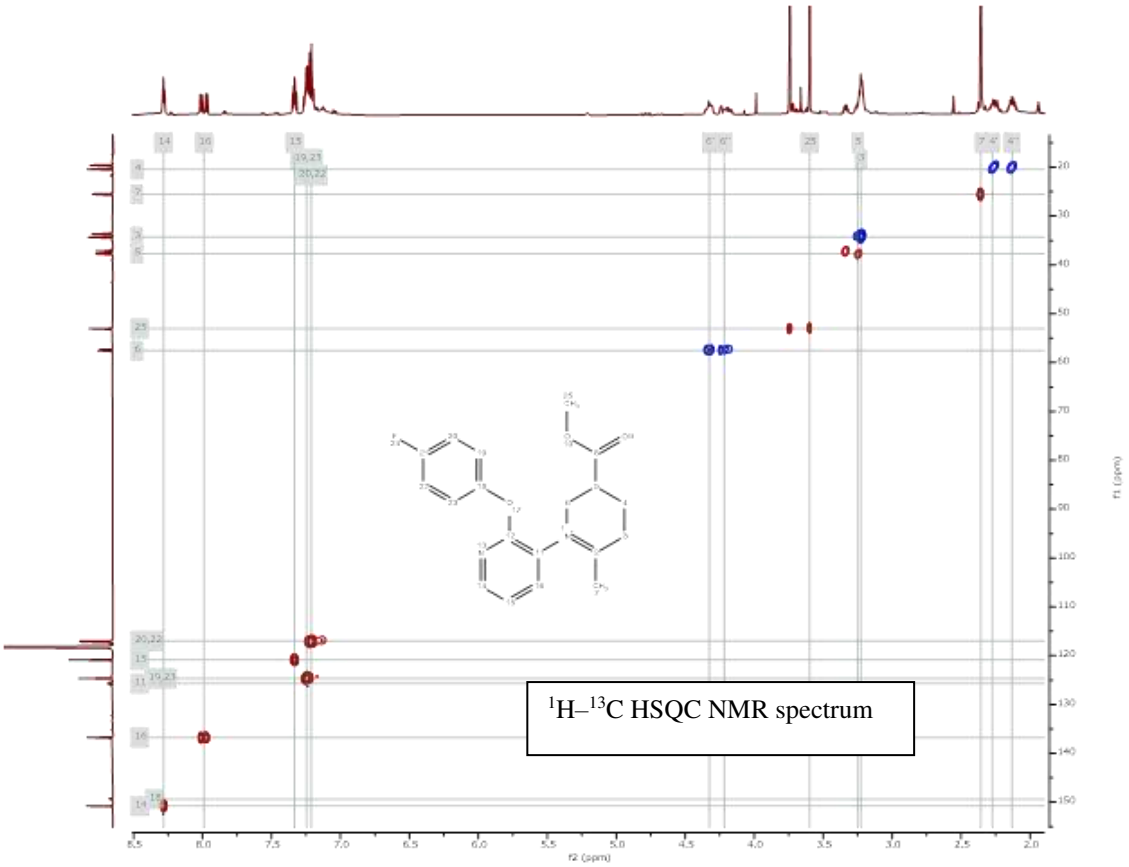

$^{1}H–^{13}C$ HSQC NMR spectrum

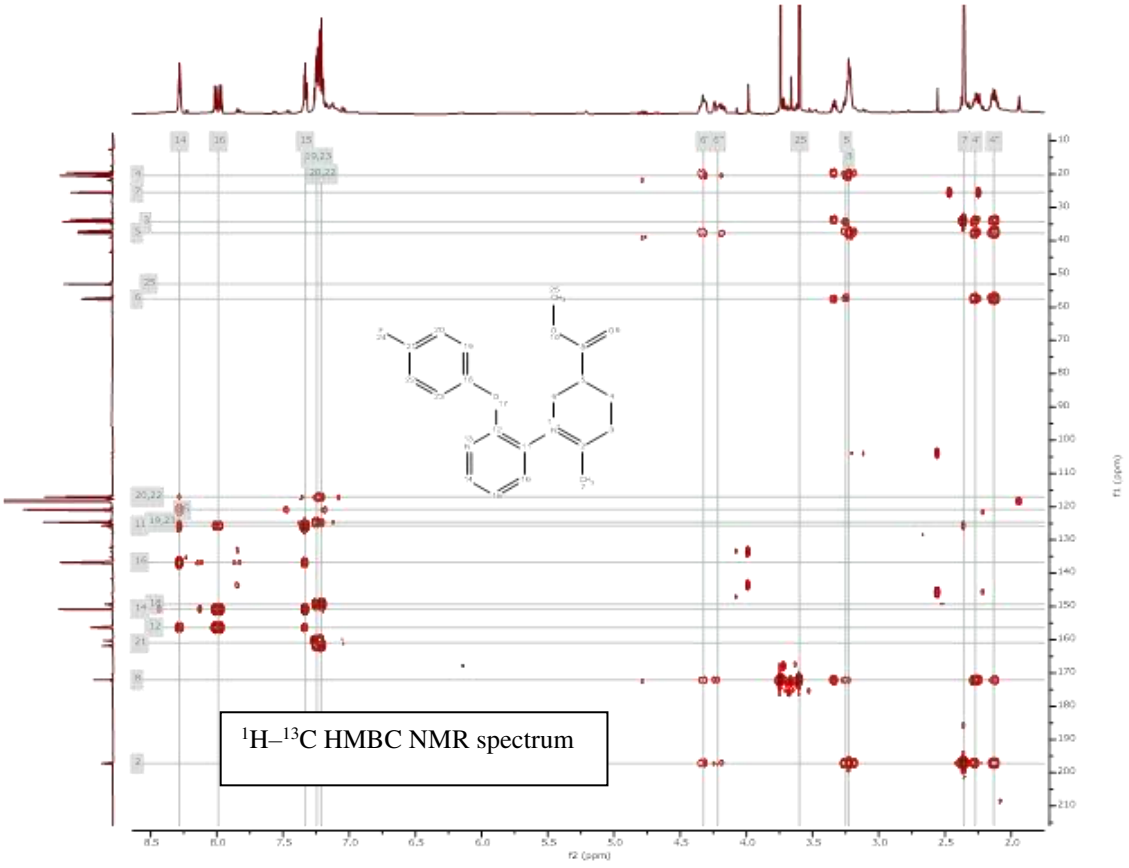

$^{1}H–^{13}C$ HMBC NMR spectrum

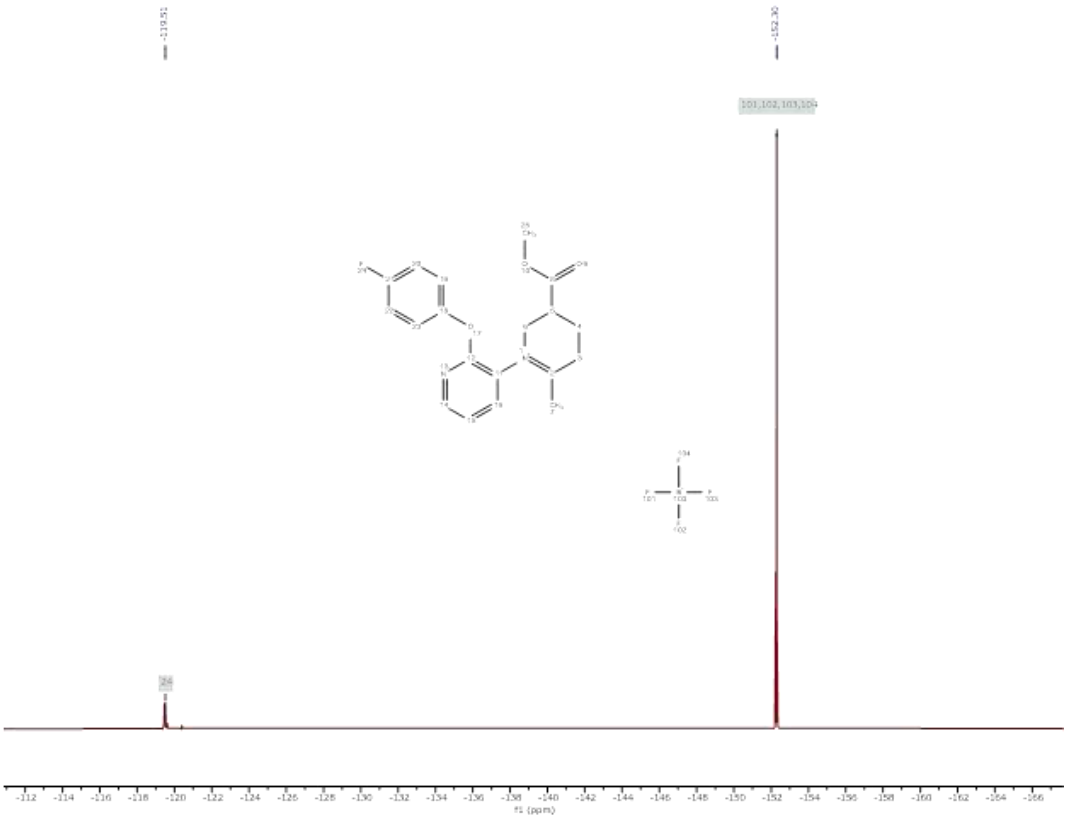

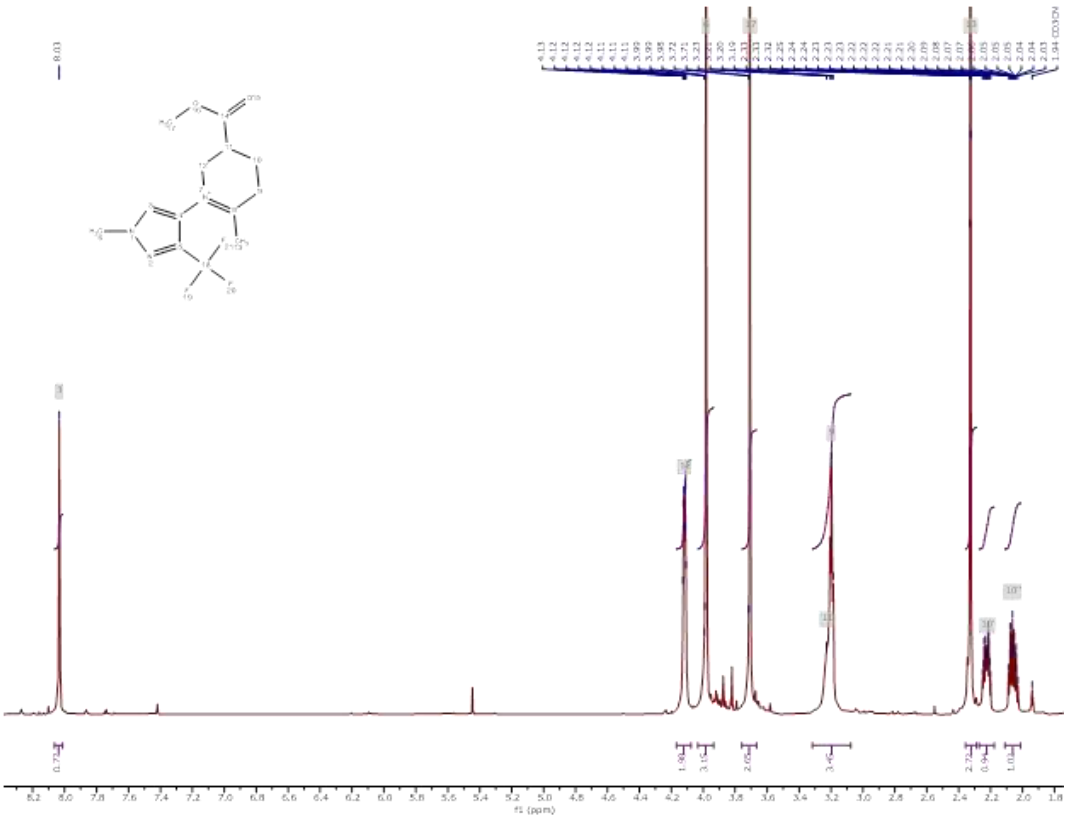

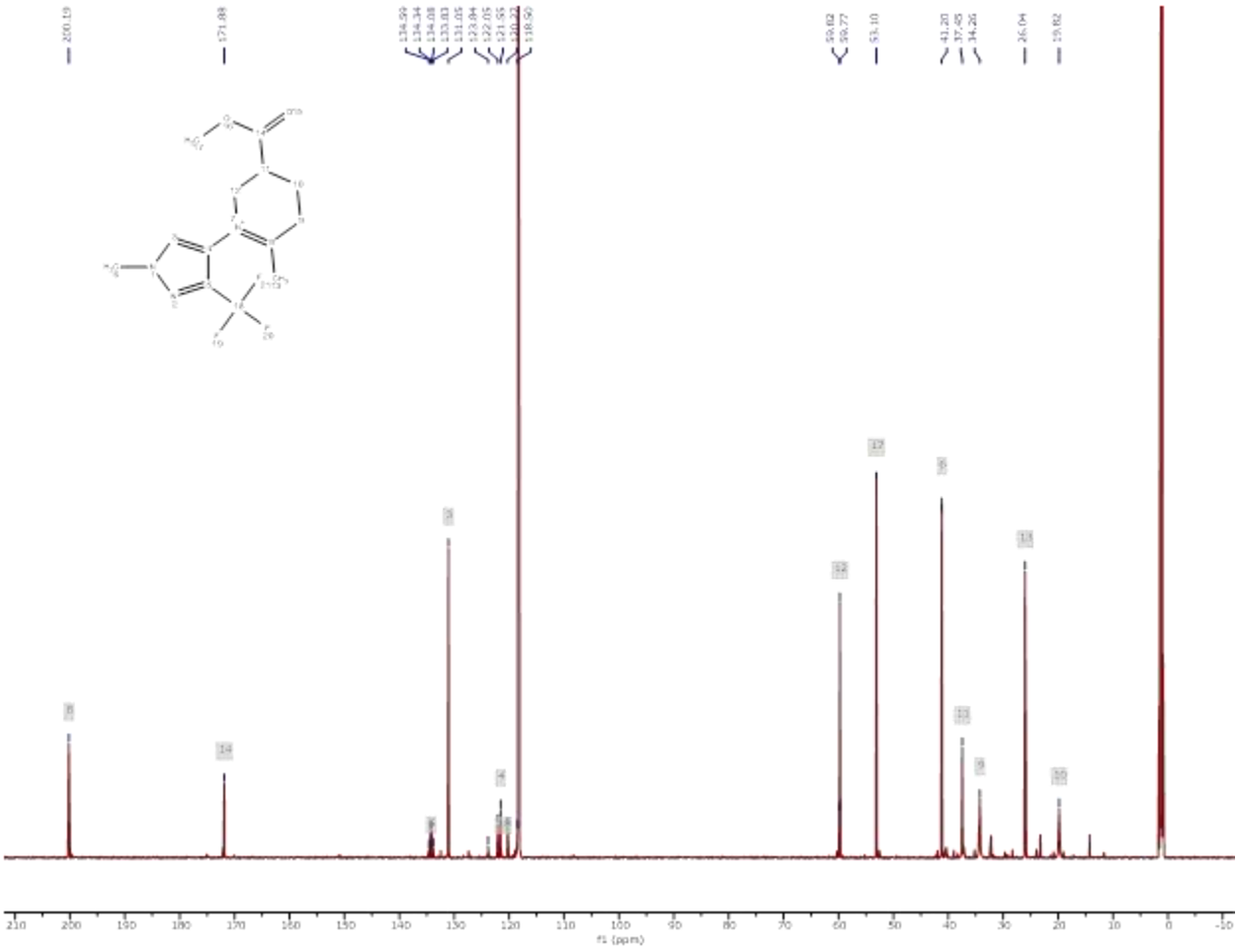
200.19
171.88
134.59
134.34
134.08
133.83
131.05
123.84
122.05
121.55
120.22
118.50
59.62
59.77
53.10
41.20
37.45
34.26
26.04
19.82
f1 (ppm)

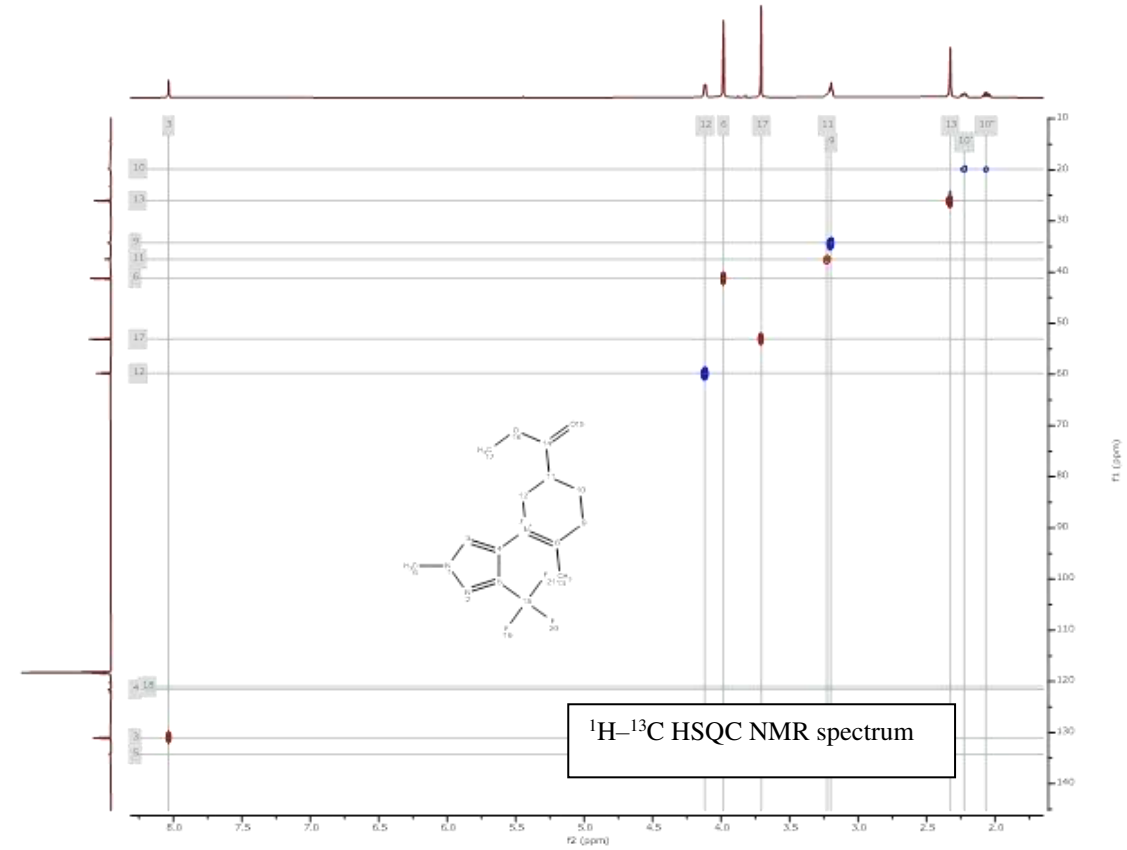
$^{1}H–^{13}C$ HSQC NMR spectrum

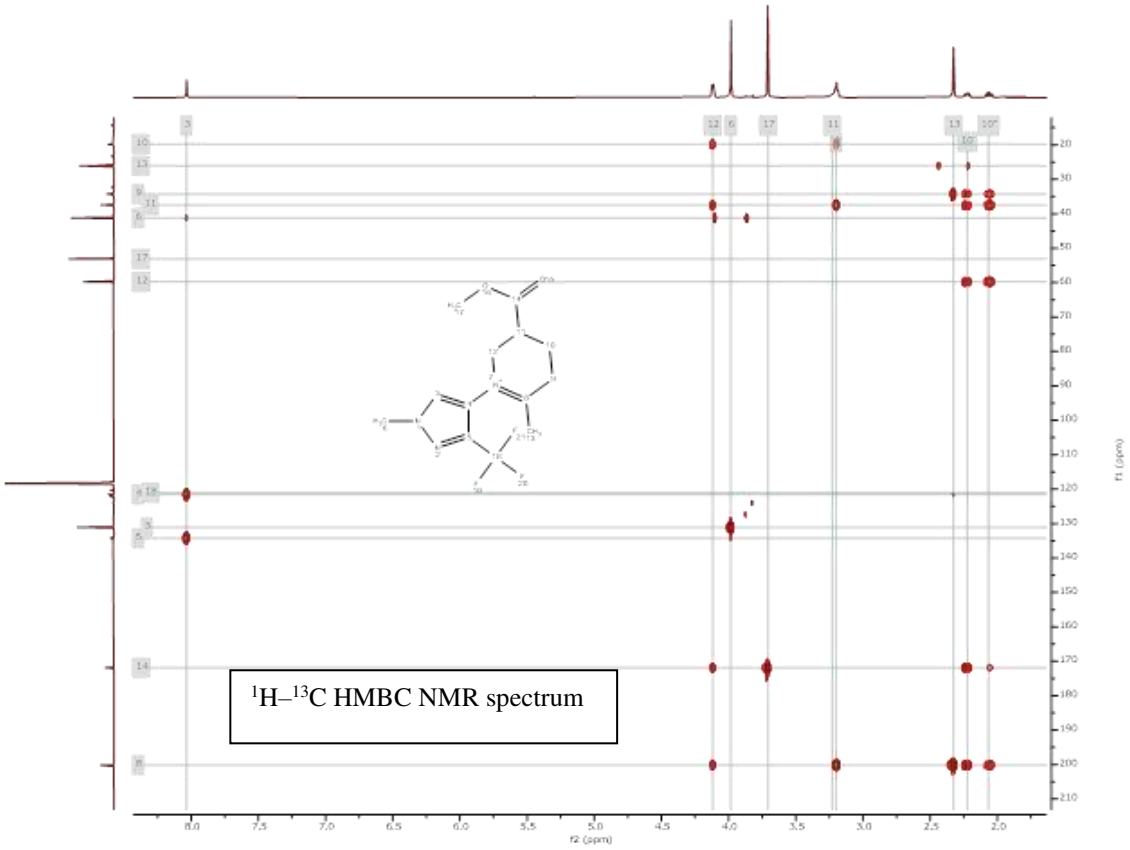
$^{1}H–^{13}C$ HMBC NMR spectrum

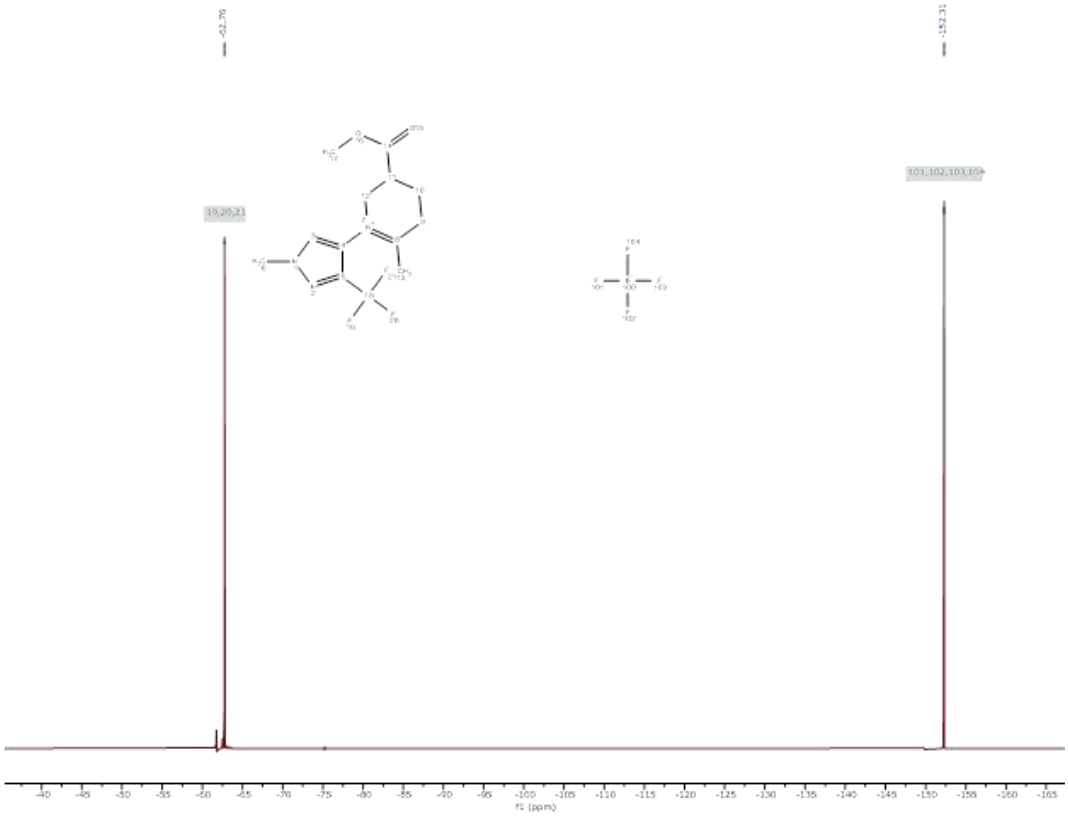

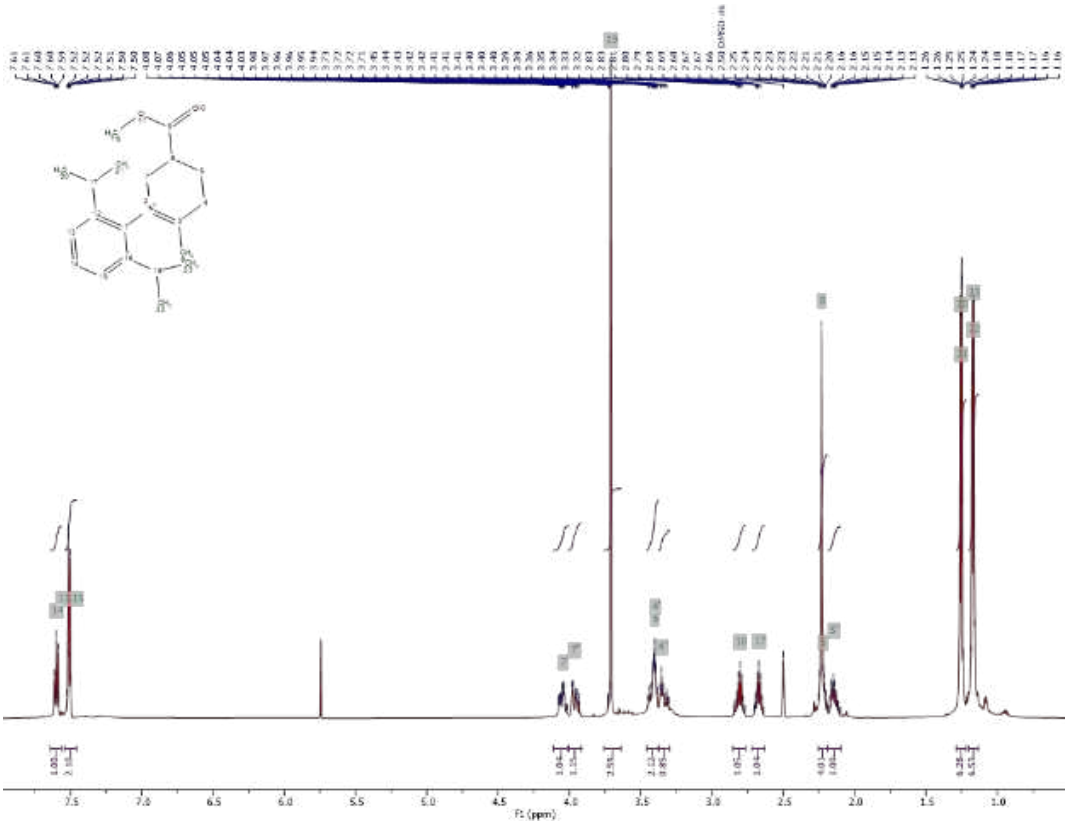

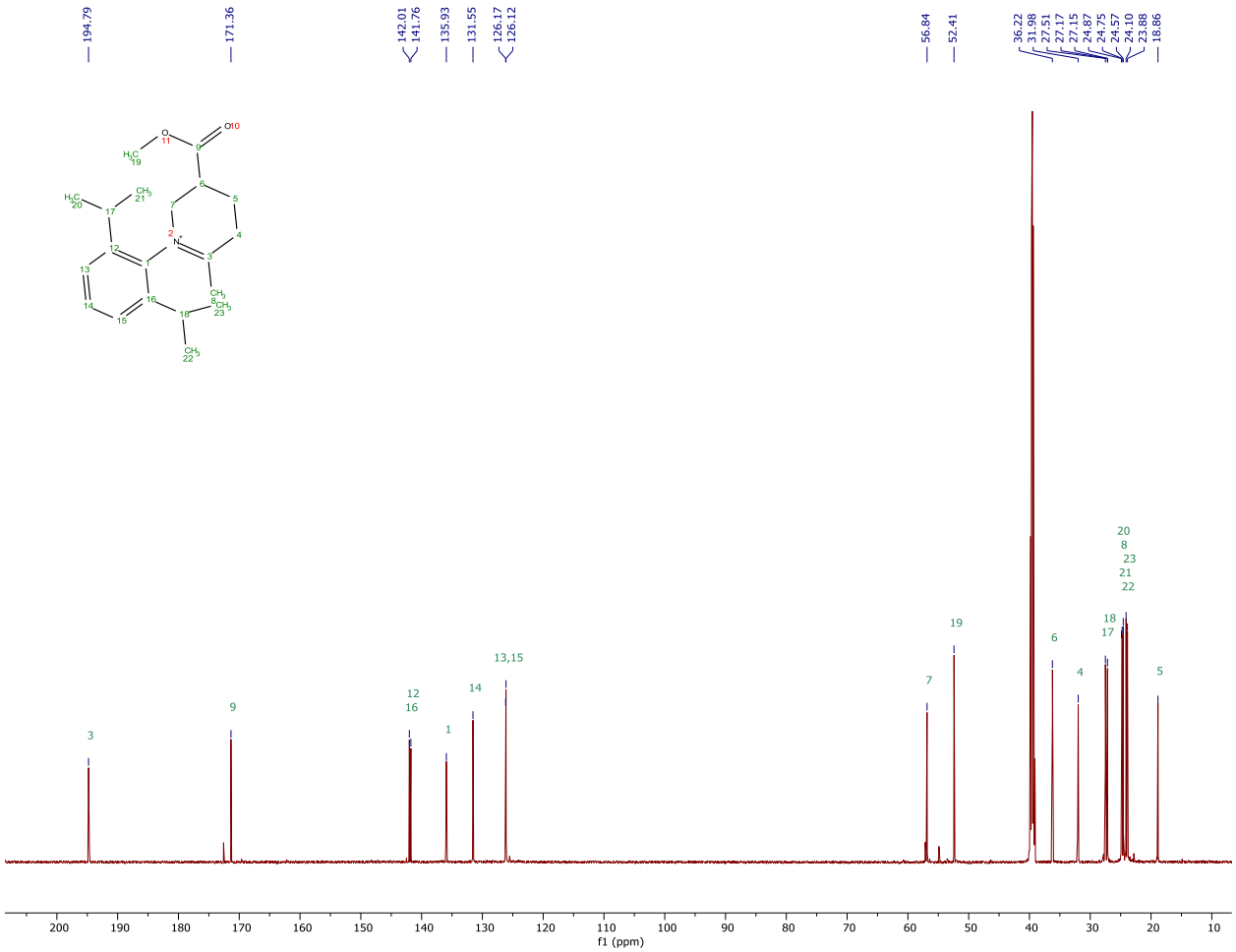
194.79
171.36
142.01
141.76
135.93
131.55
126.17
126.12
56.84
52.41
36.22
31.98
27.51
27.17
27.15
24.87
24.75
24.57
24.10
23.88
18.86
3
9
12
16
1
14
13,15
7
19
6
4
18
17
20
8
23
21
22
5
f1 (ppm)

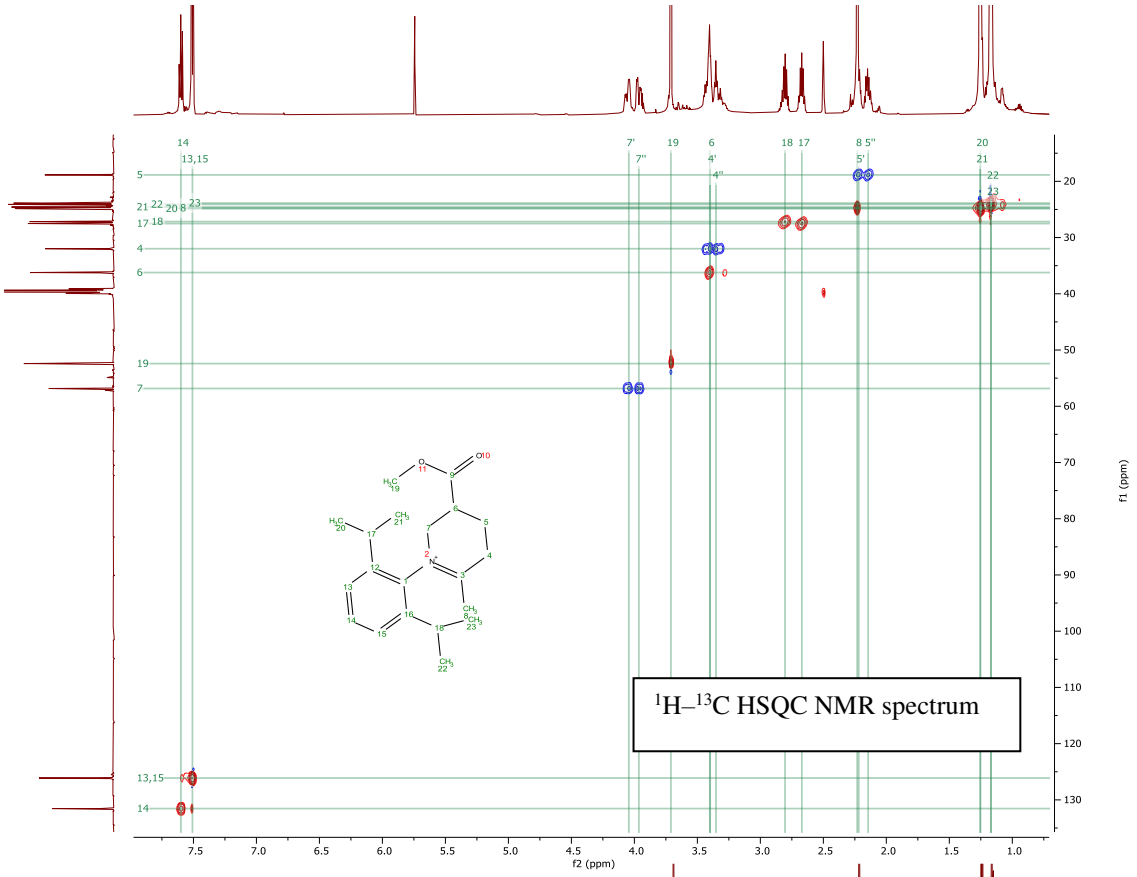
^{1}H–^{13}C HSQC NMR spectrum
f2 (ppm)
f1 (ppm)

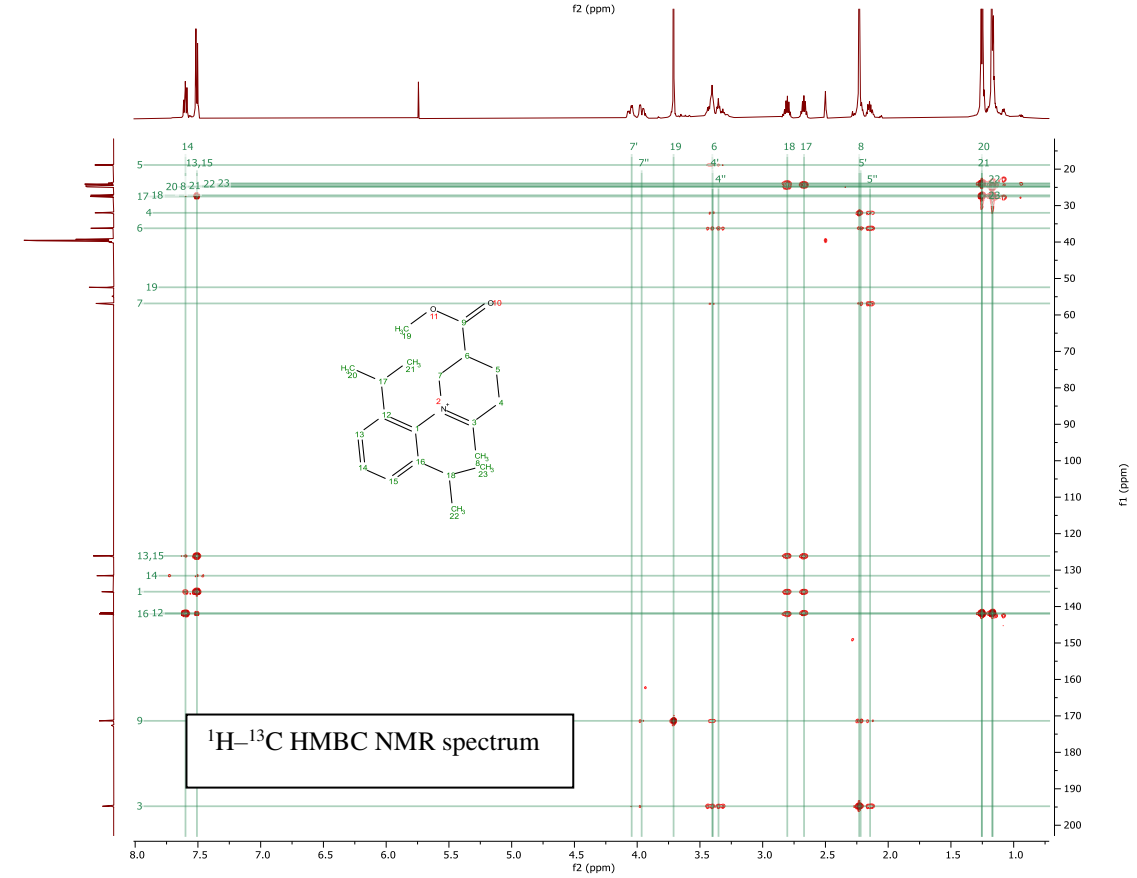
^{1}H–^{13}C HMBC NMR spectrum
f2 (ppm)
f1 (ppm)

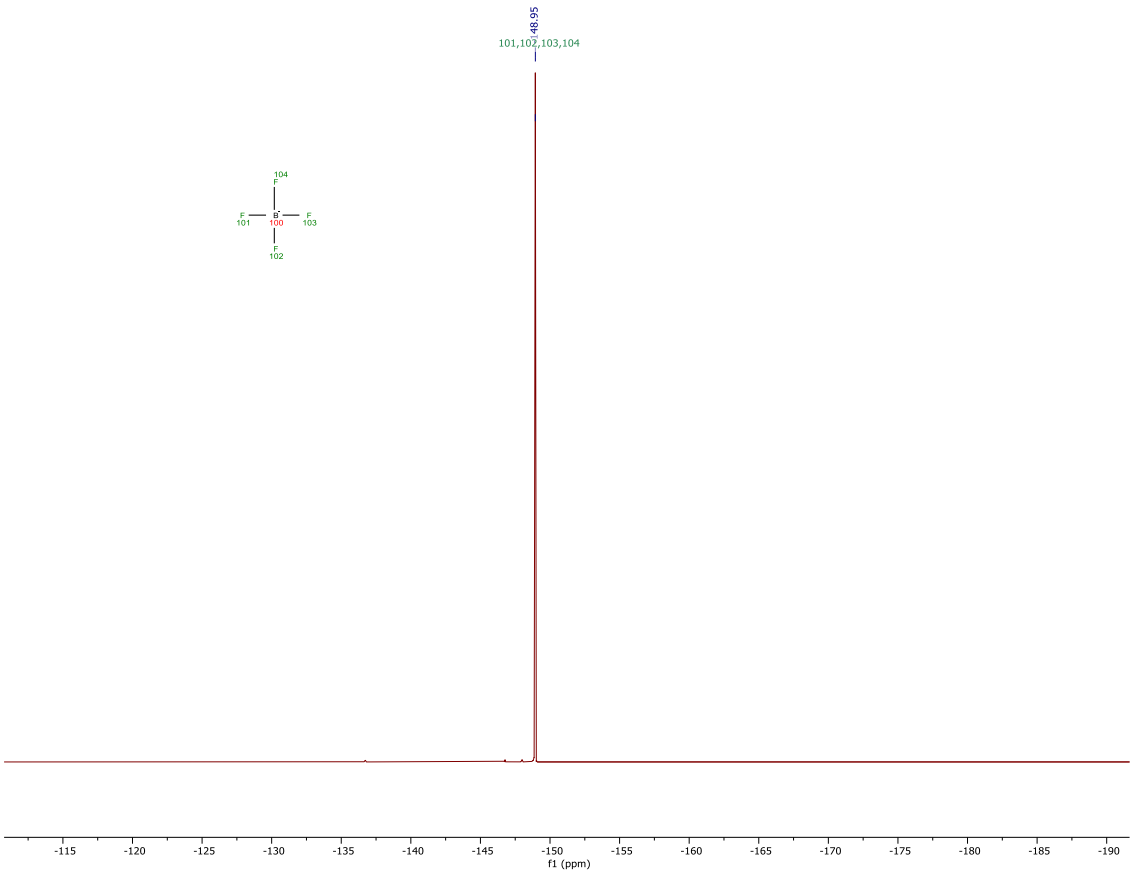
-148.95
101,102,103,104
104
F
F
101
B
100
F
103
F
102
-115
-120
-125
-130
-135
-140
-145
-150
-155
-160
-165
-170
-175
-180
-185
-190
f1 (ppm)

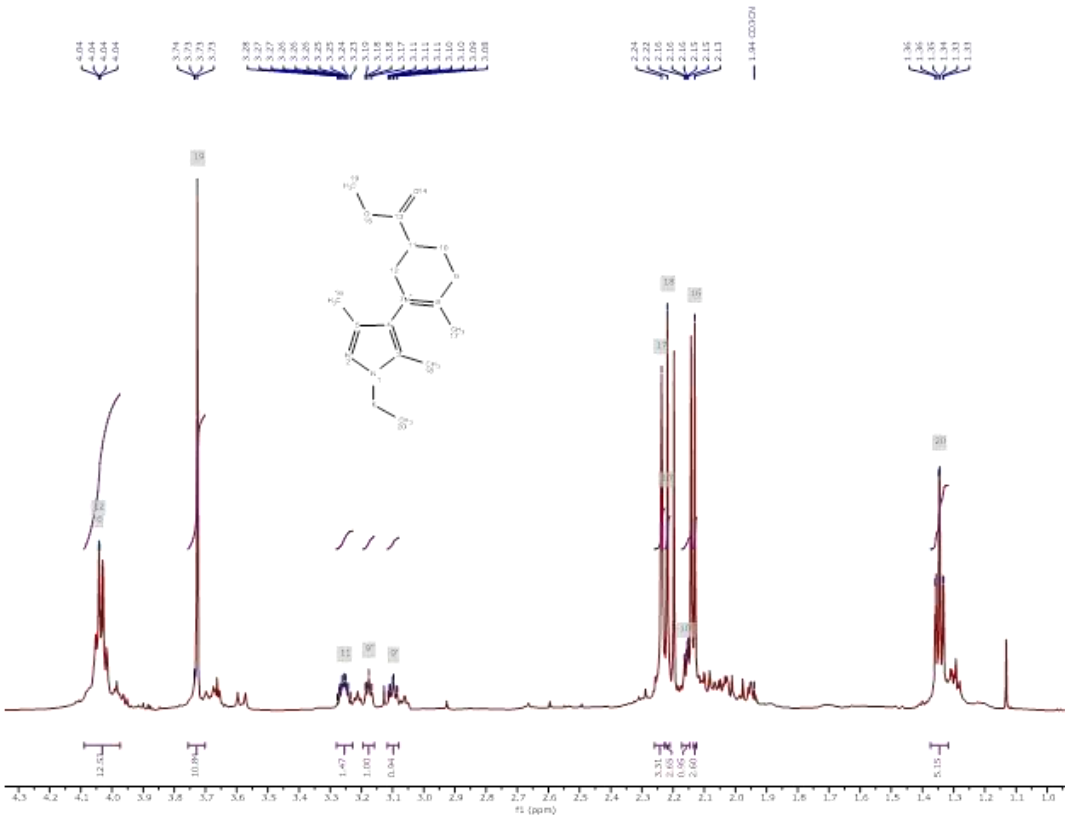
1.94 CD3OD
4.04
3.74
3.73
3.28
3.27
3.26
3.25
3.24
3.23
3.19
3.18
3.17
3.11
2.24
2.22
2.16
2.15
1.36
1.35
1.34
1.33
12.51
10.84
1.47
1.00
0.84
3.31
2.66
0.95
2.60
5.15
f1 (ppm)

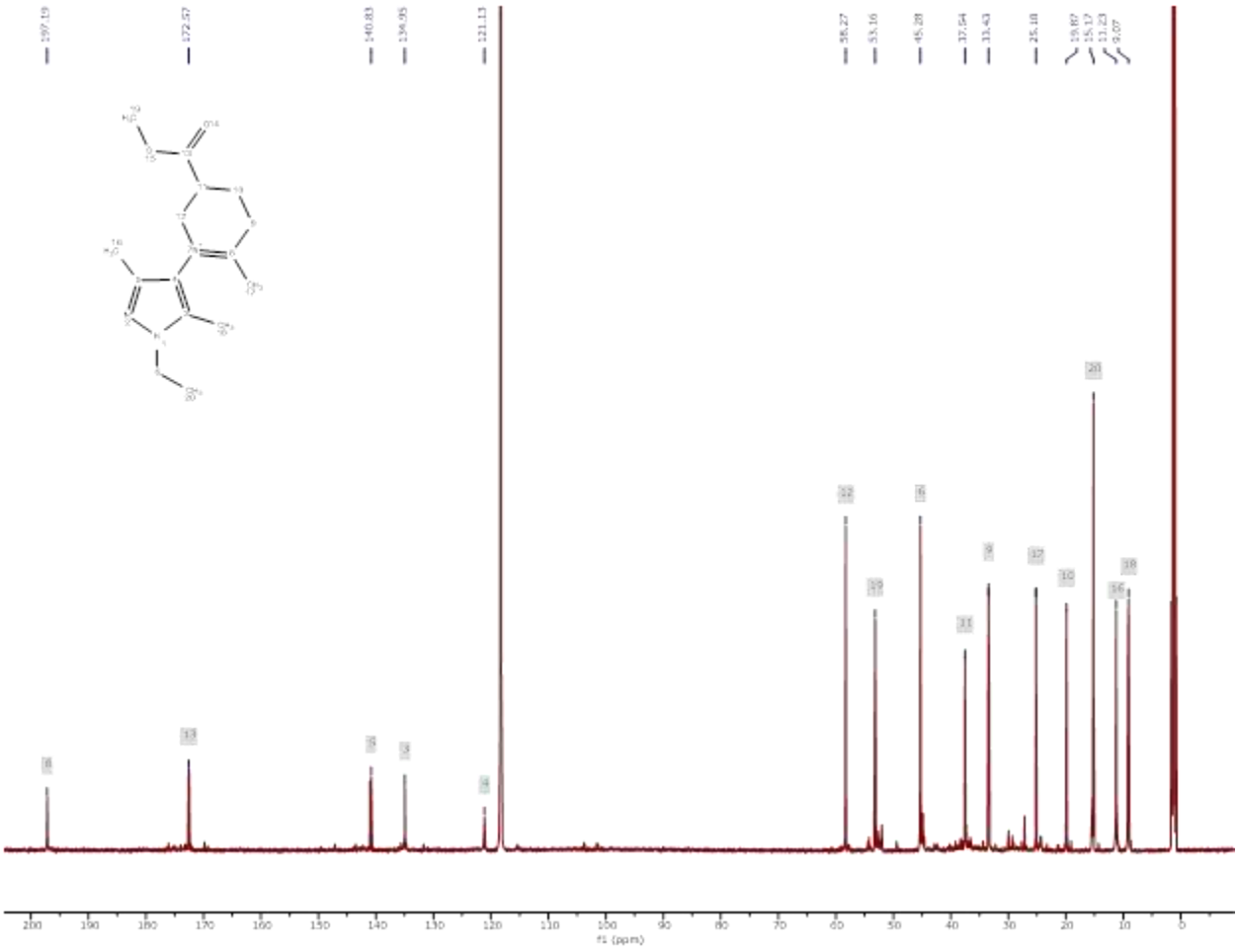
197.19
172.57
140.83
134.95
121.13
58.27
53.16
45.38
37.54
33.43
25.18
19.67
15.17
11.23
9.07
f1 (ppm)

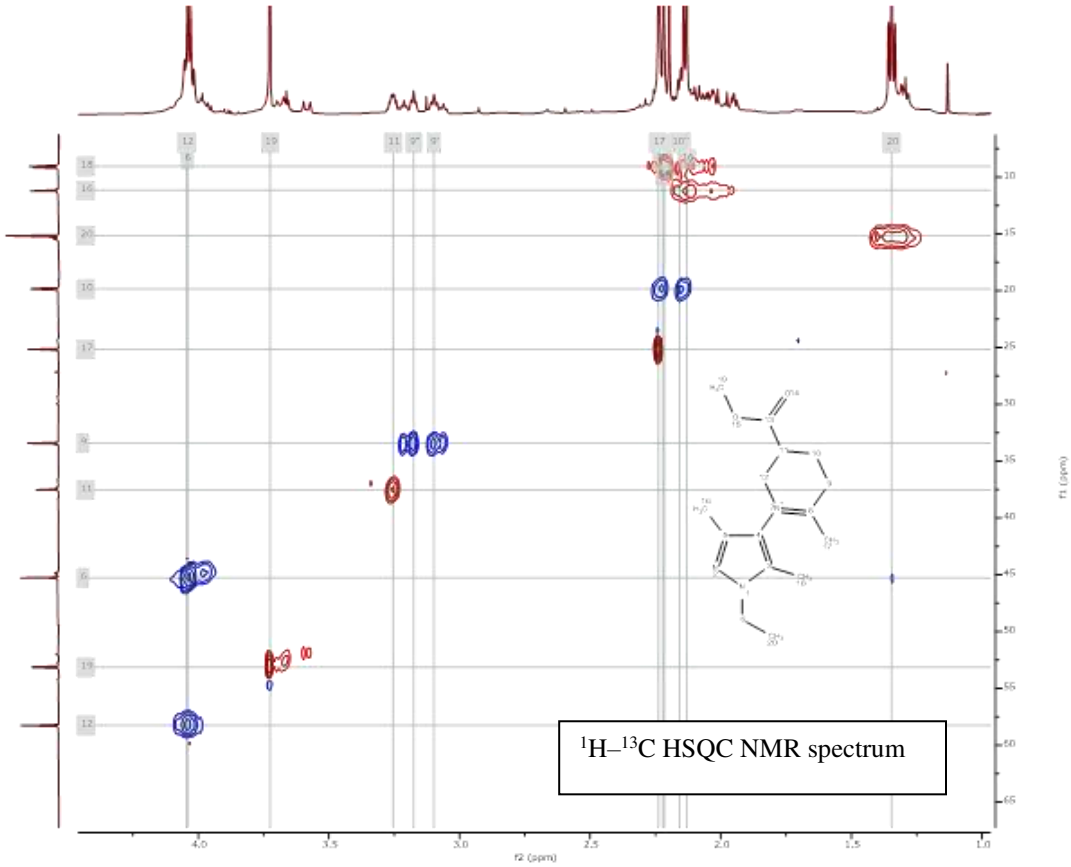

$^{1}H–^{13}C$ HSQC NMR spectrum

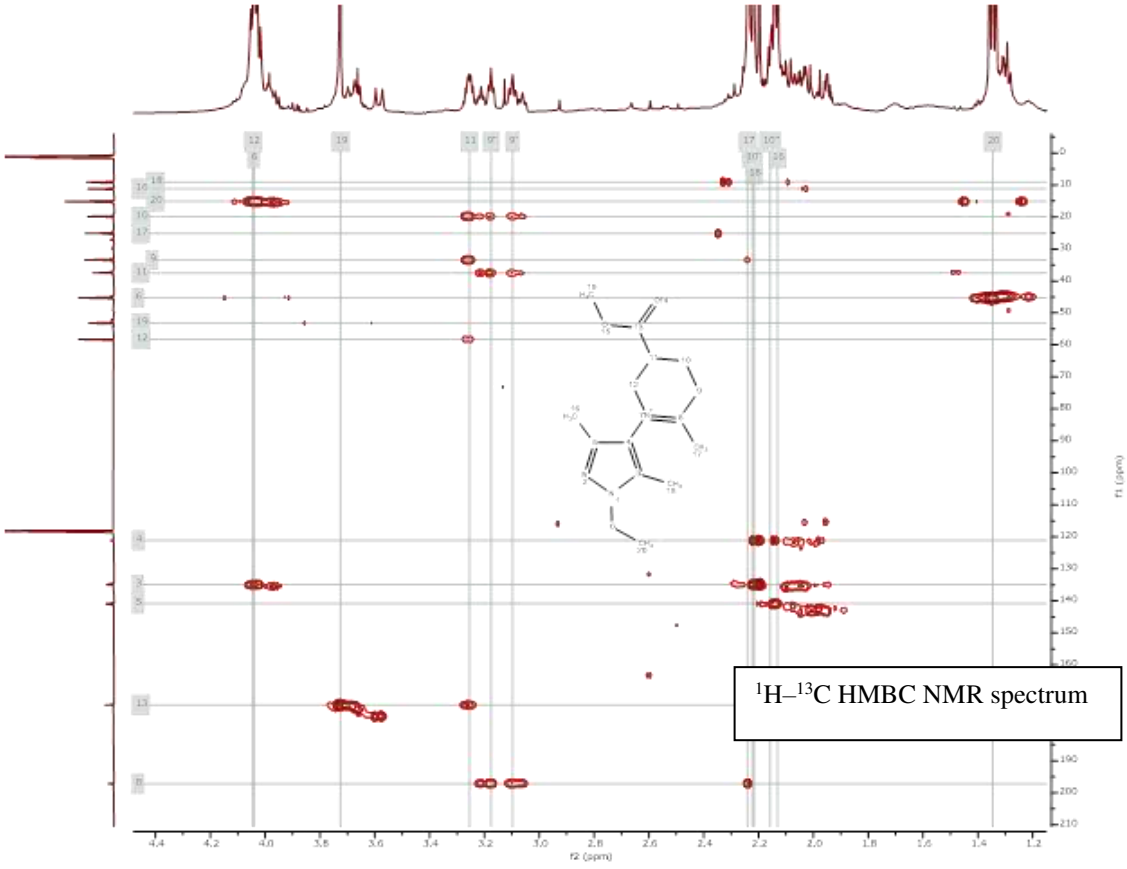

$^{1}H–^{13}C$ HMBC NMR spectrum

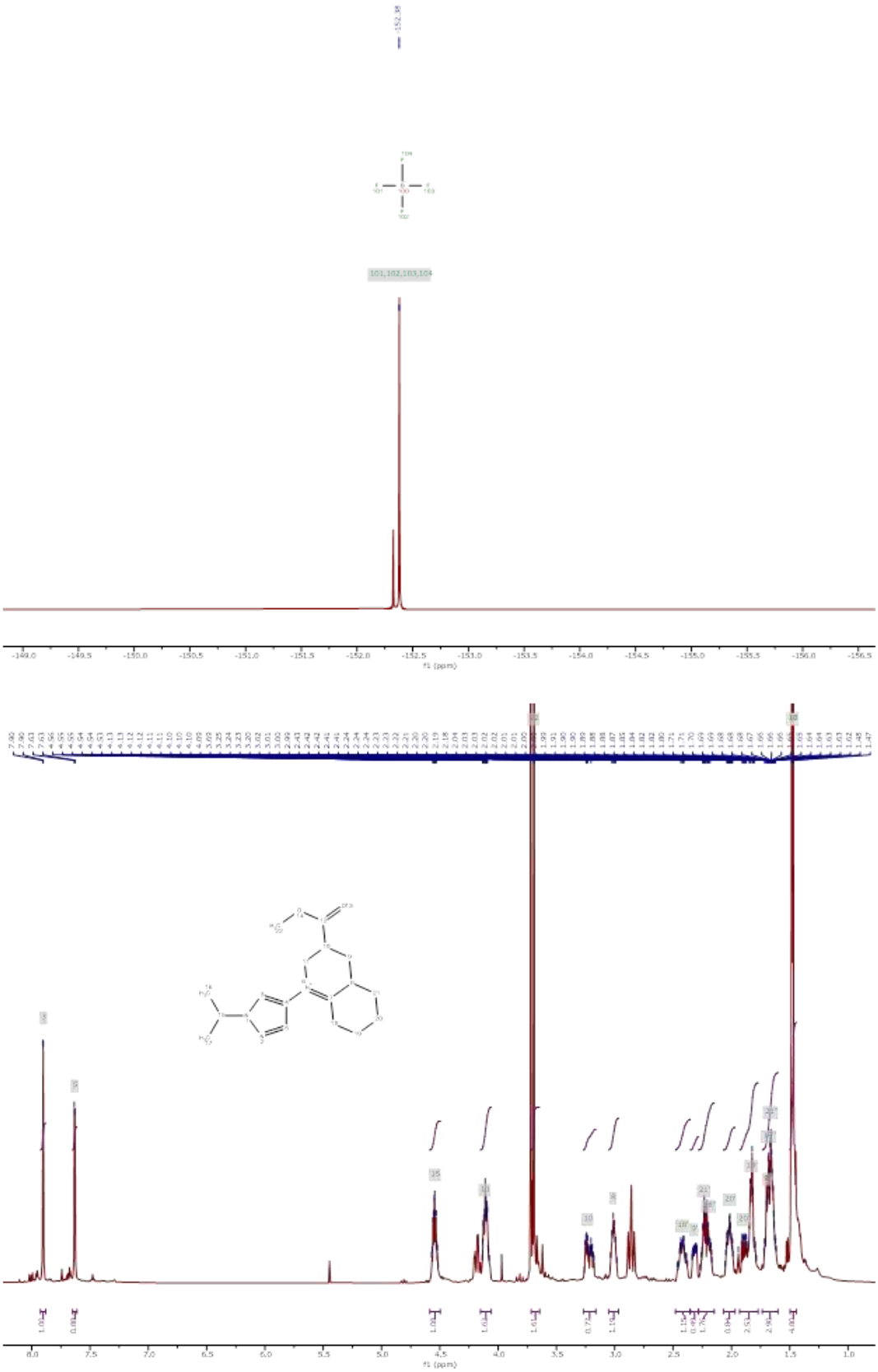

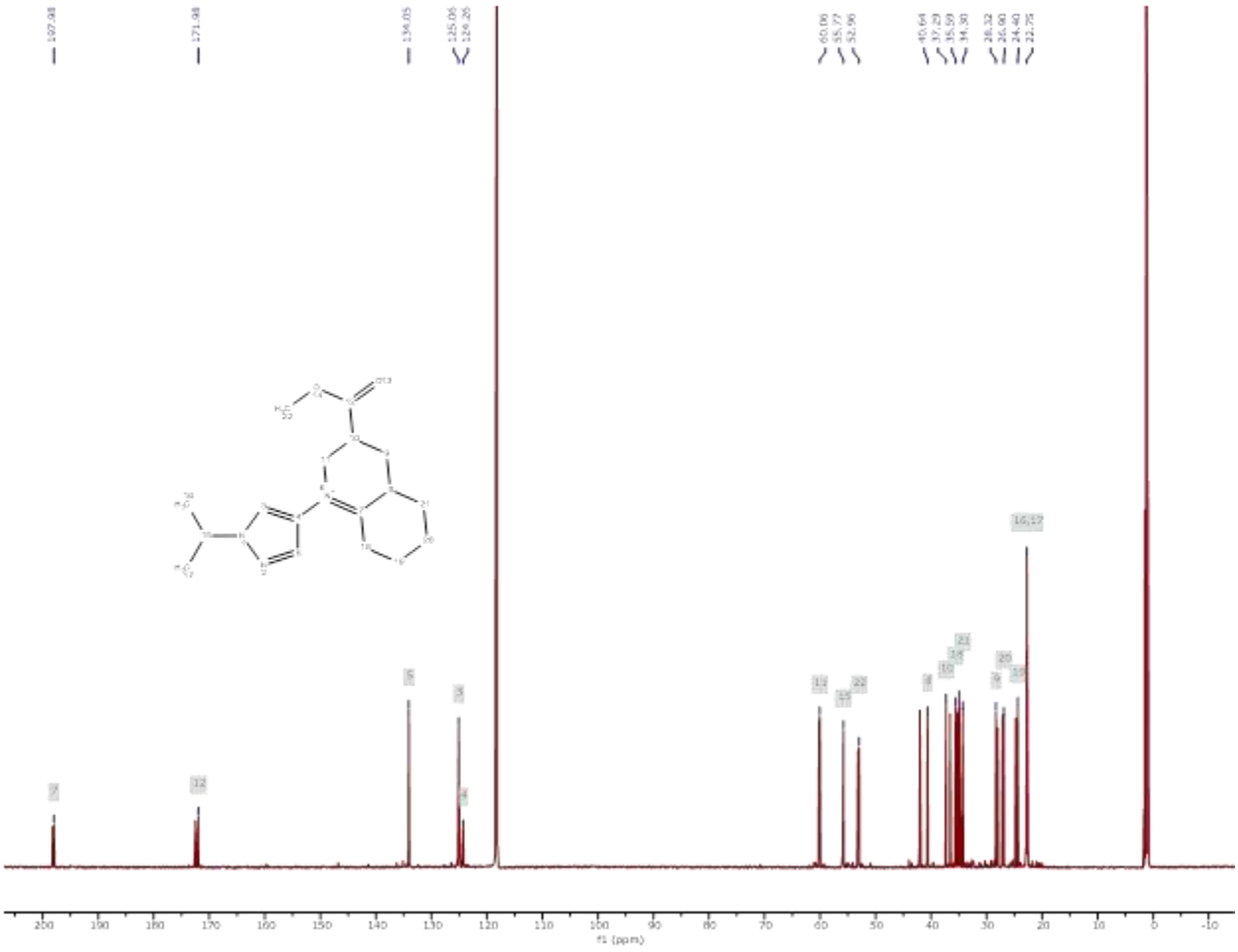
197.98
171.98
134.05
125.06
124.26
60.06
55.77
52.96
40.64
37.29
35.59
34.30
28.32
26.90
24.40
22.75
16,17
f1 (ppm)

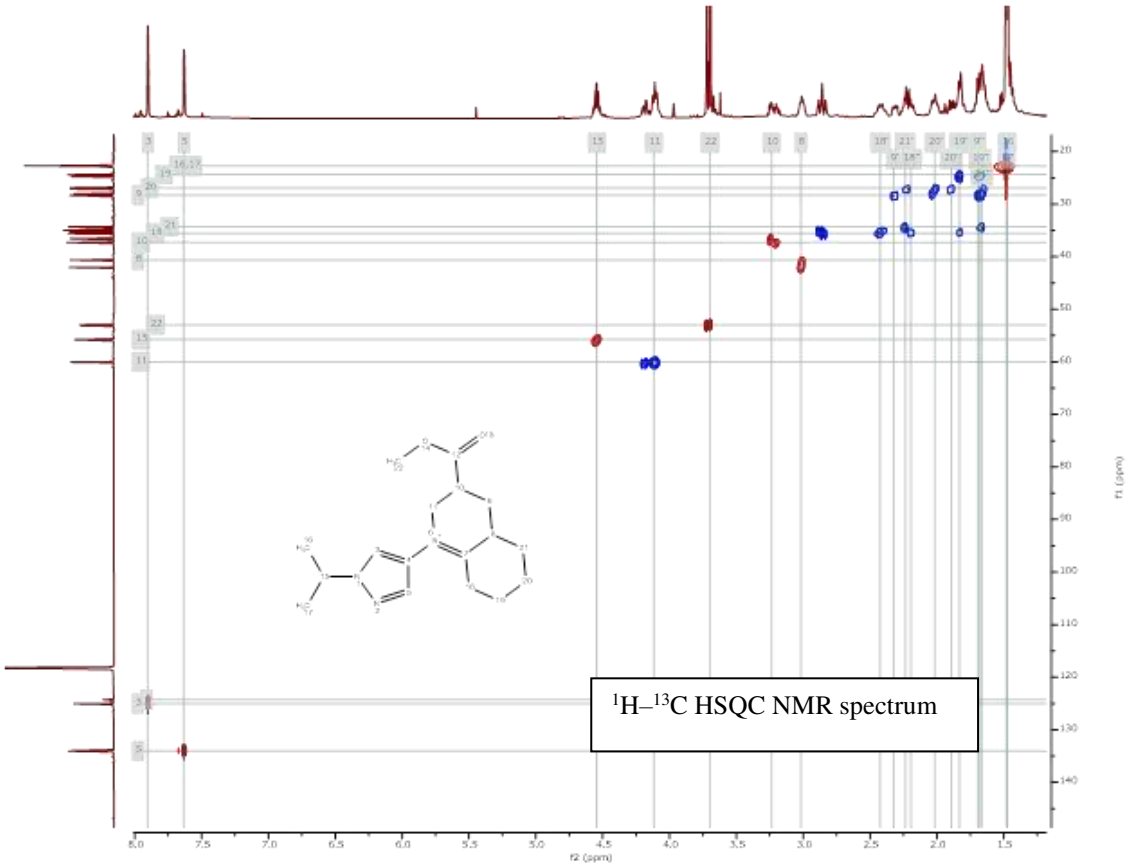
$^{1}H–^{13}C$ HSQC NMR spectrum

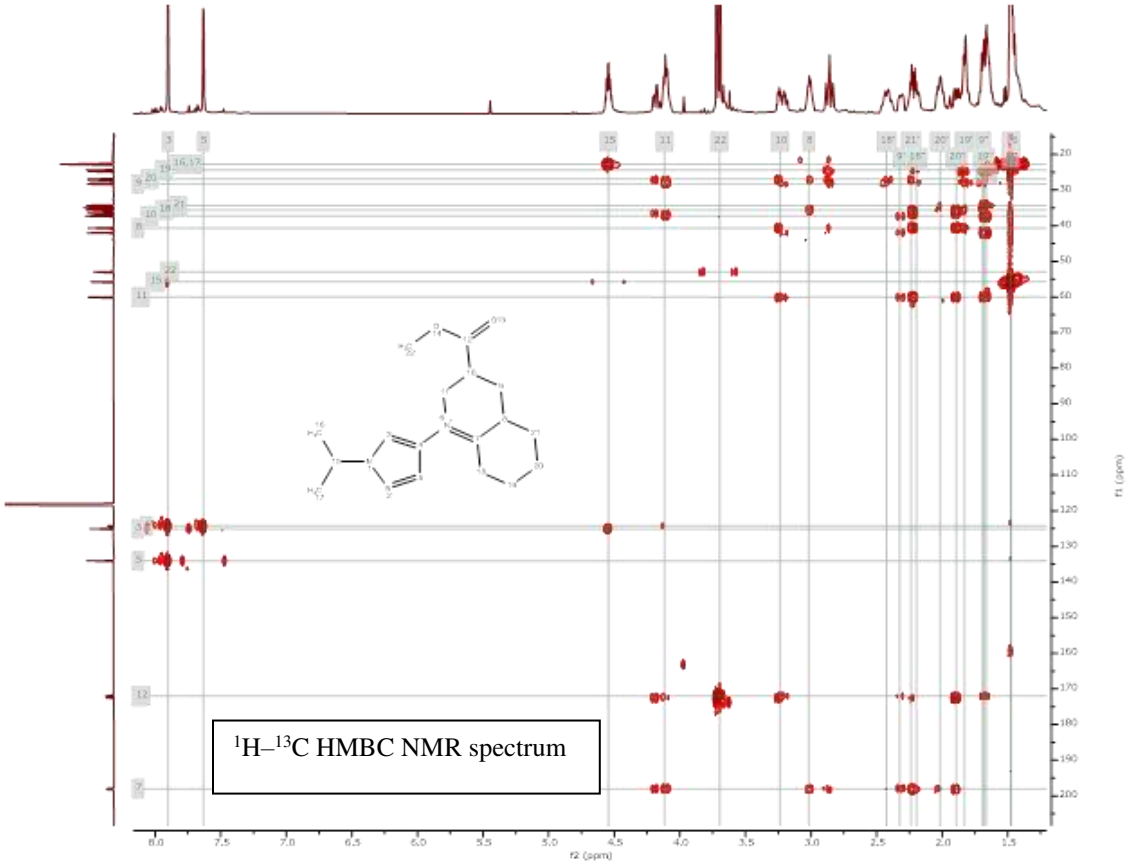
$^{1}H–^{13}C$ HMBC NMR spectrum

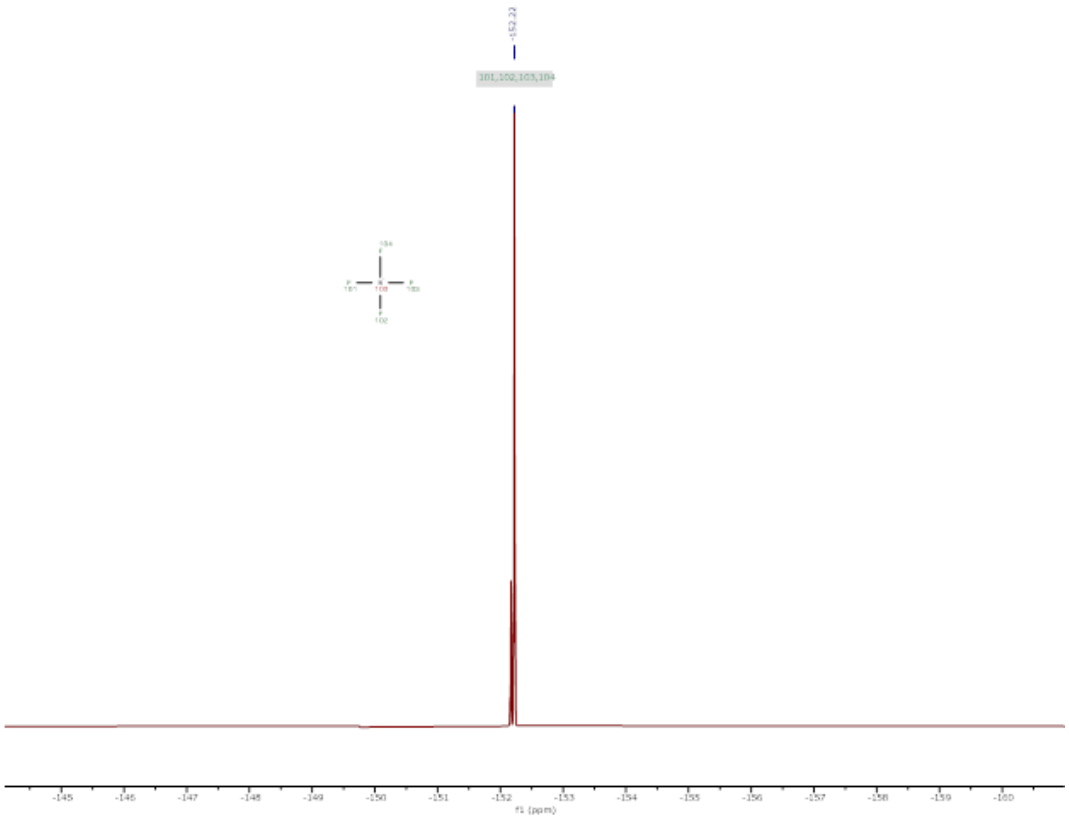

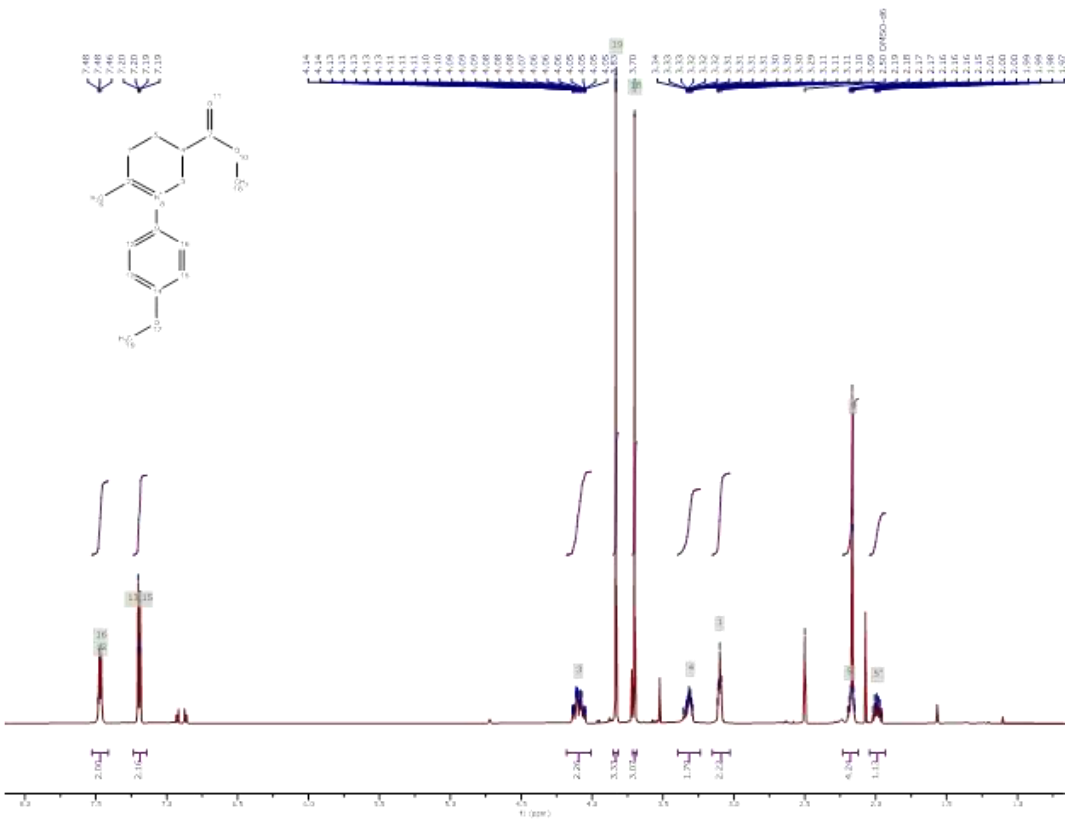

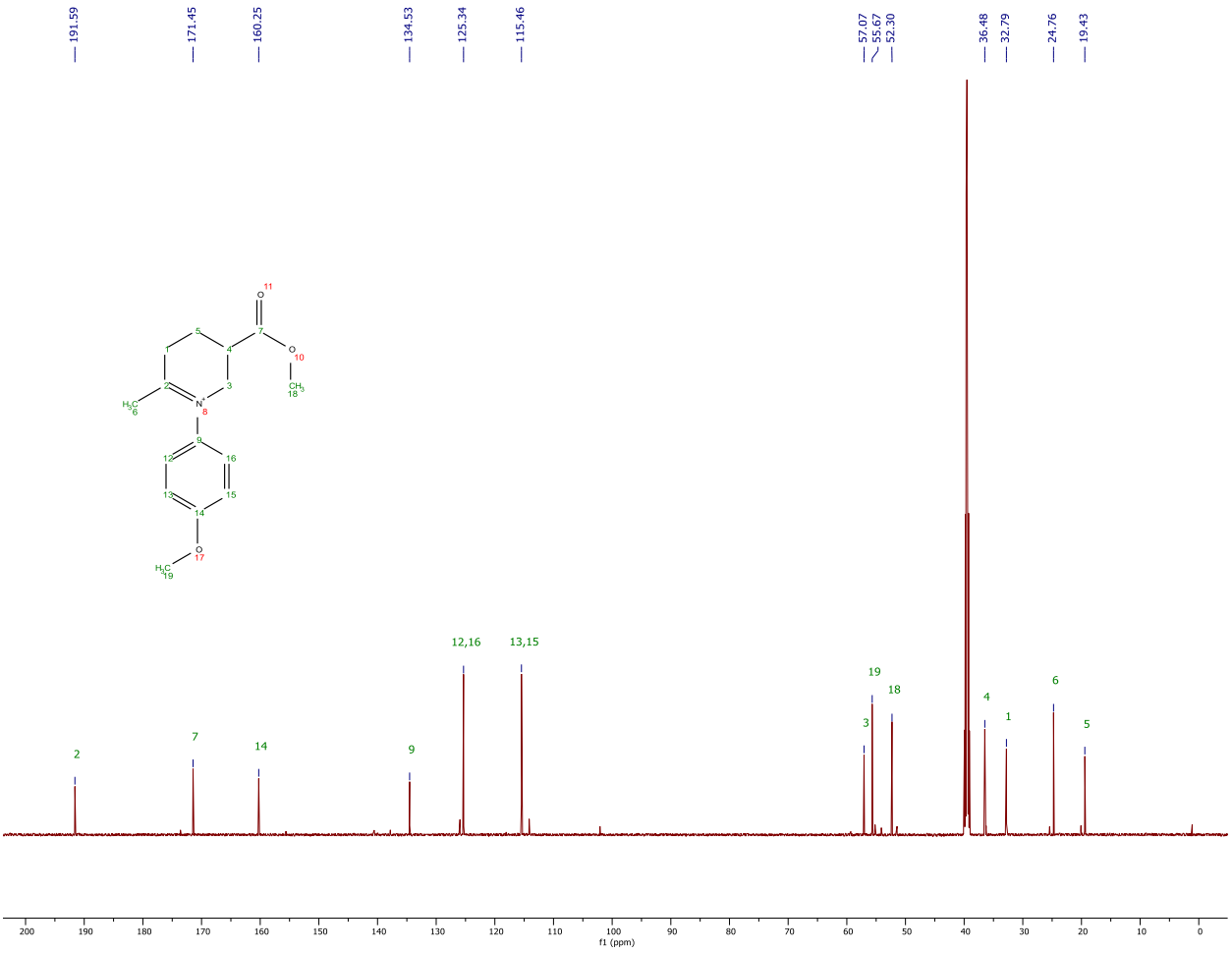
191.59
171.45
160.25
134.53
125.34
115.46
57.07
55.67
52.30
36.48
32.79
24.76
19.43
2
7
14
9
12,16
13,15
3
19
18
4
1
6
5
f1 (ppm)

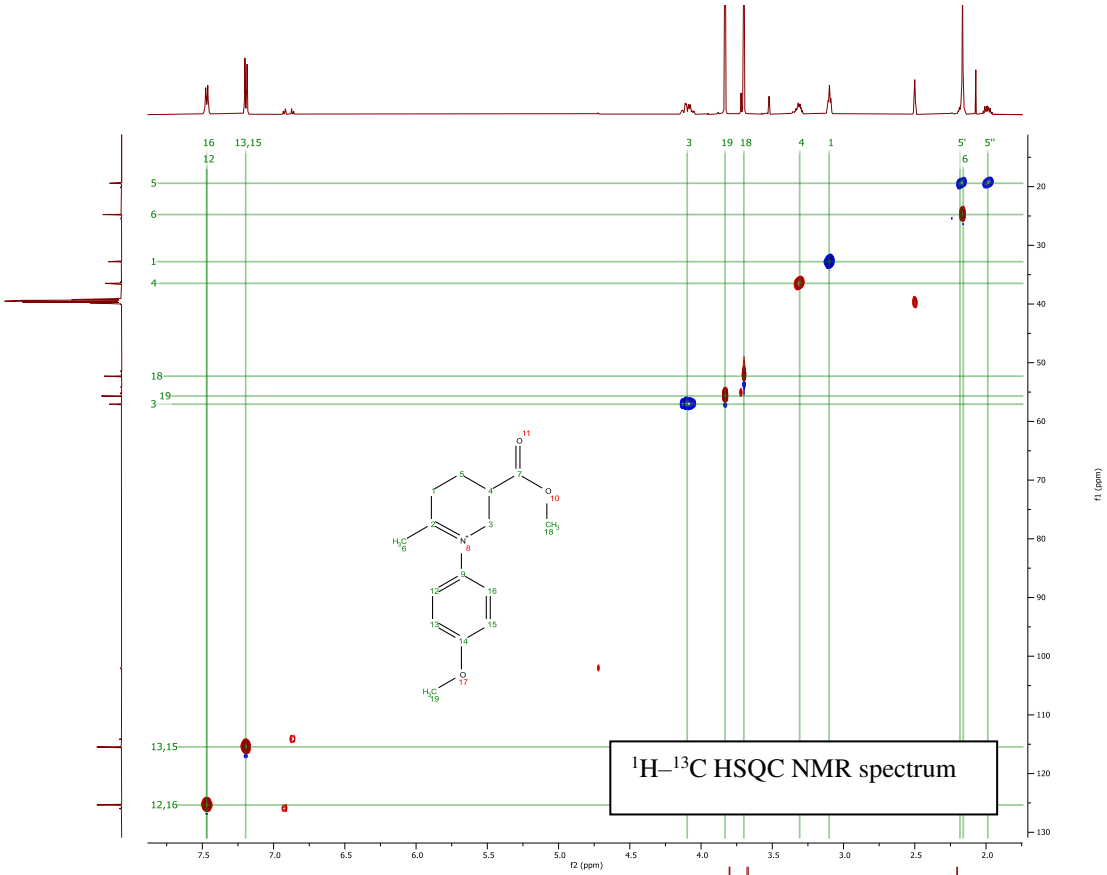

$^{1}H–^{13}C$ HSQC NMR spectrum

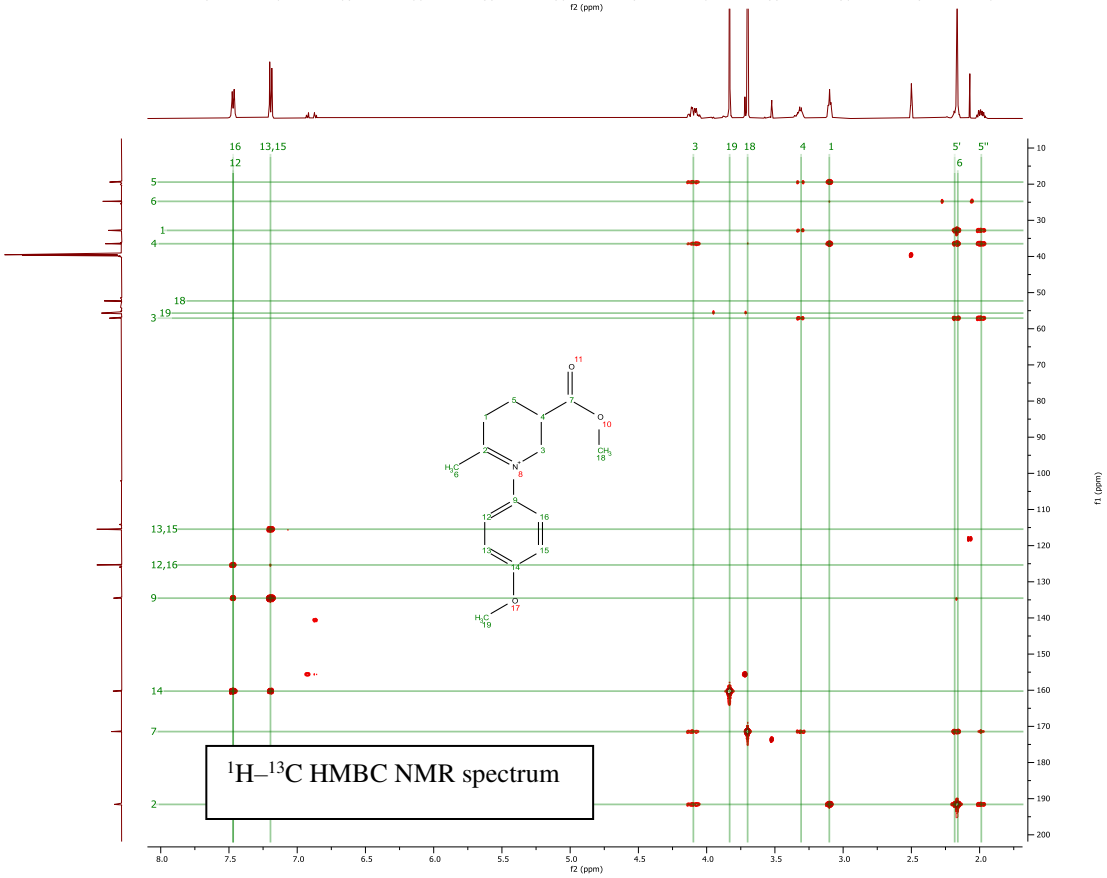

$^{1}H–^{13}C$ HMBC NMR spectrum

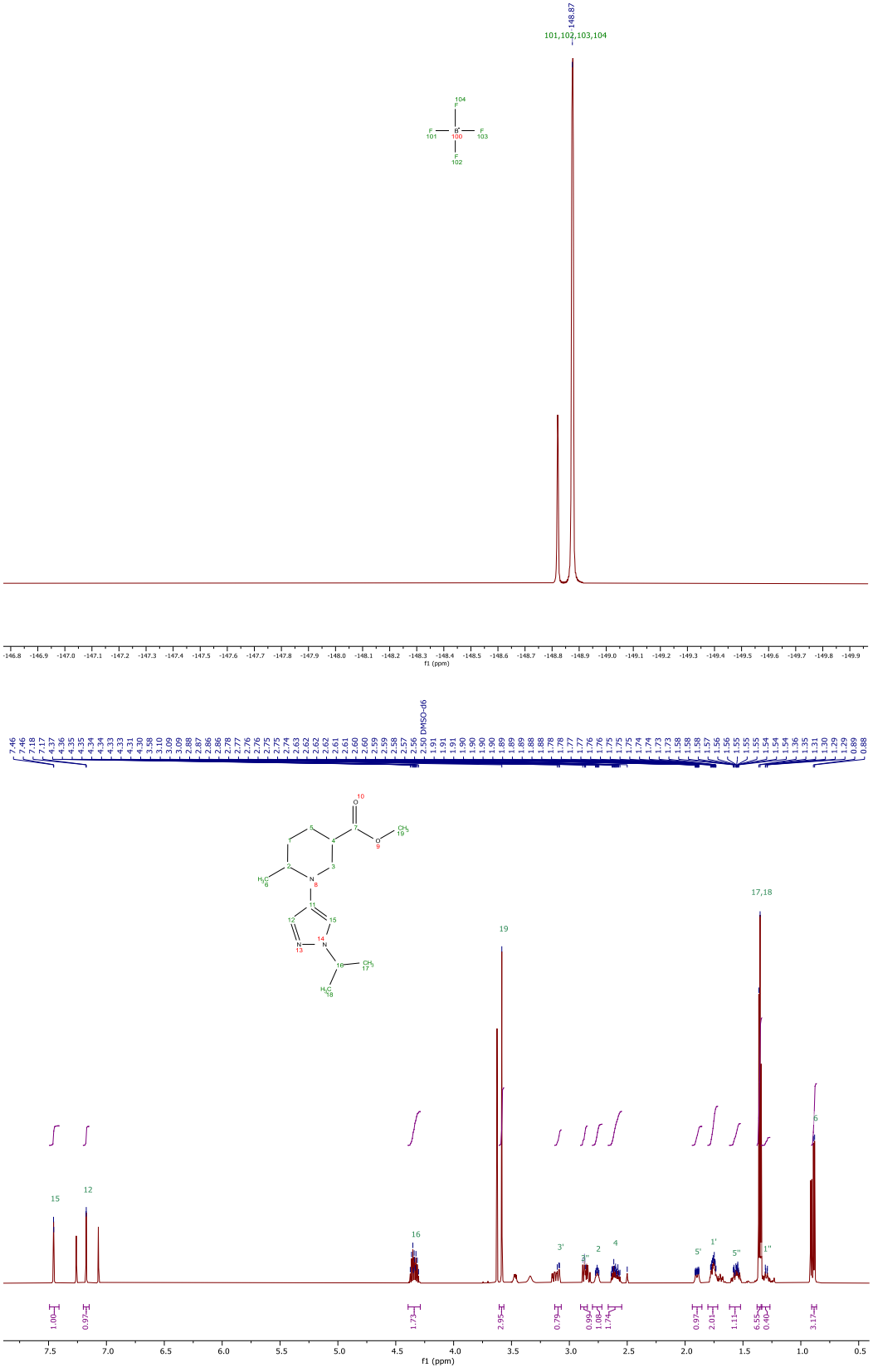
148.87
101,102,103,104
DMSO-d6
17,18
19
15
12
16
6
f1 (ppm)

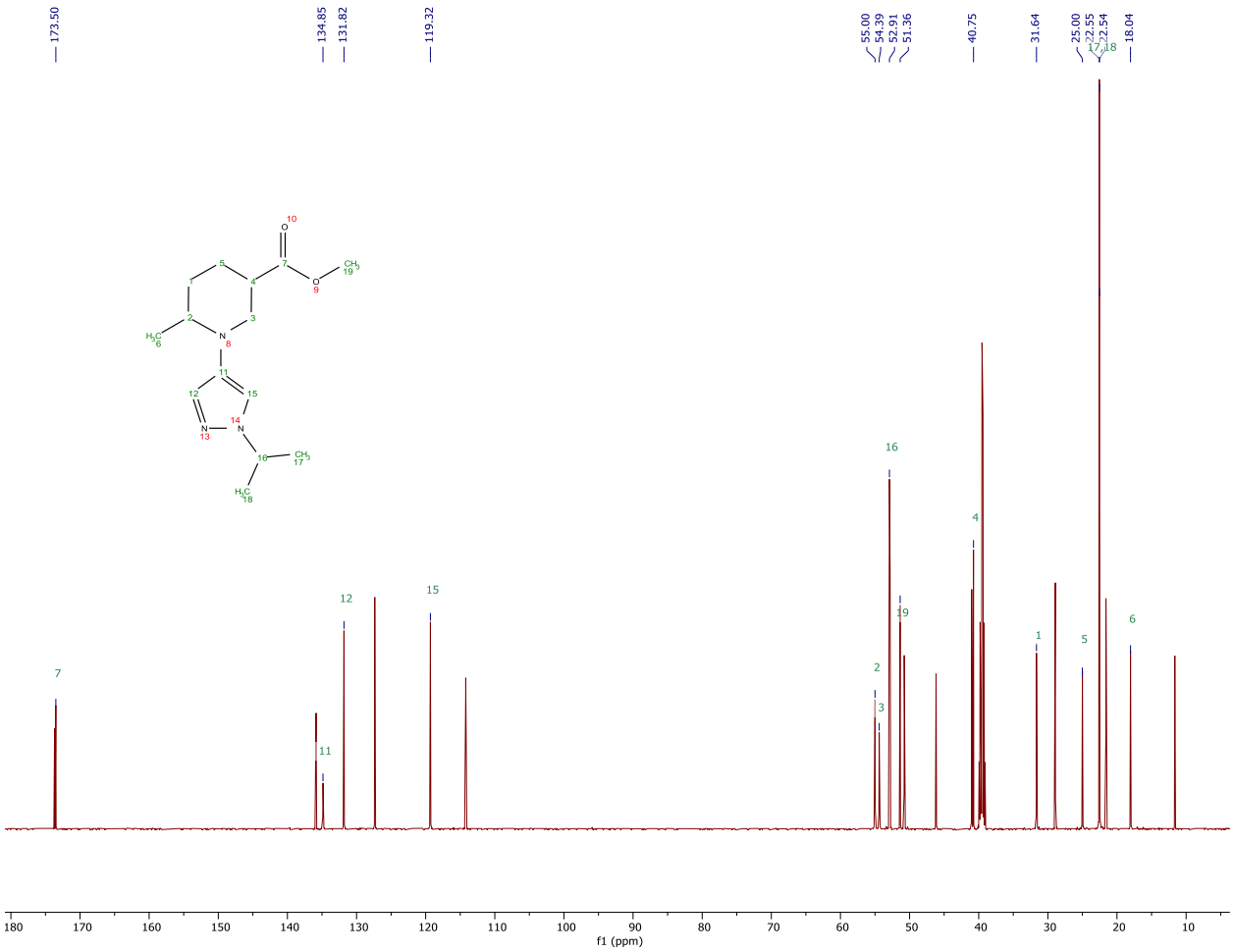
173.50
134.85
131.82
119.32
55.00
54.39
52.91
51.36
40.75
31.64
25.00
22.55
22.54
18.04
f1 (ppm)

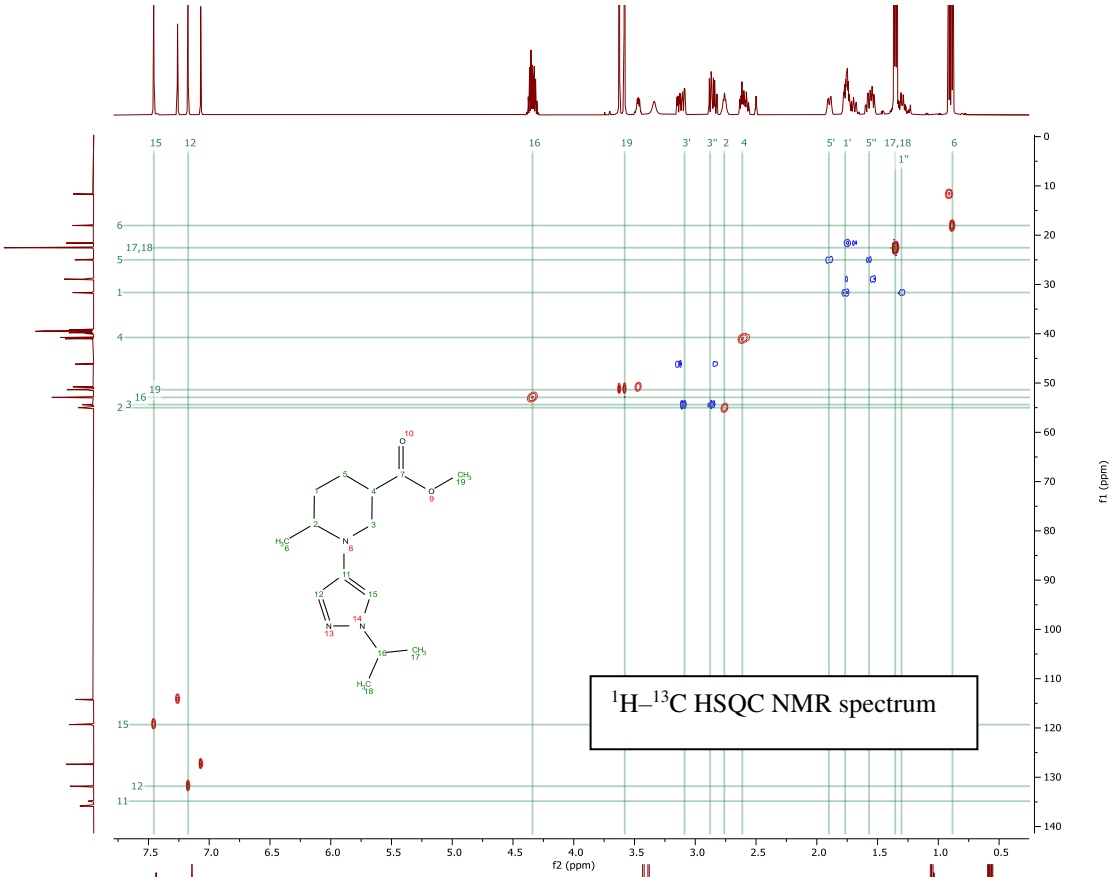
f2 (ppm)
f1 (ppm)
$^{1}H–^{13}C$ HSQC NMR spectrum

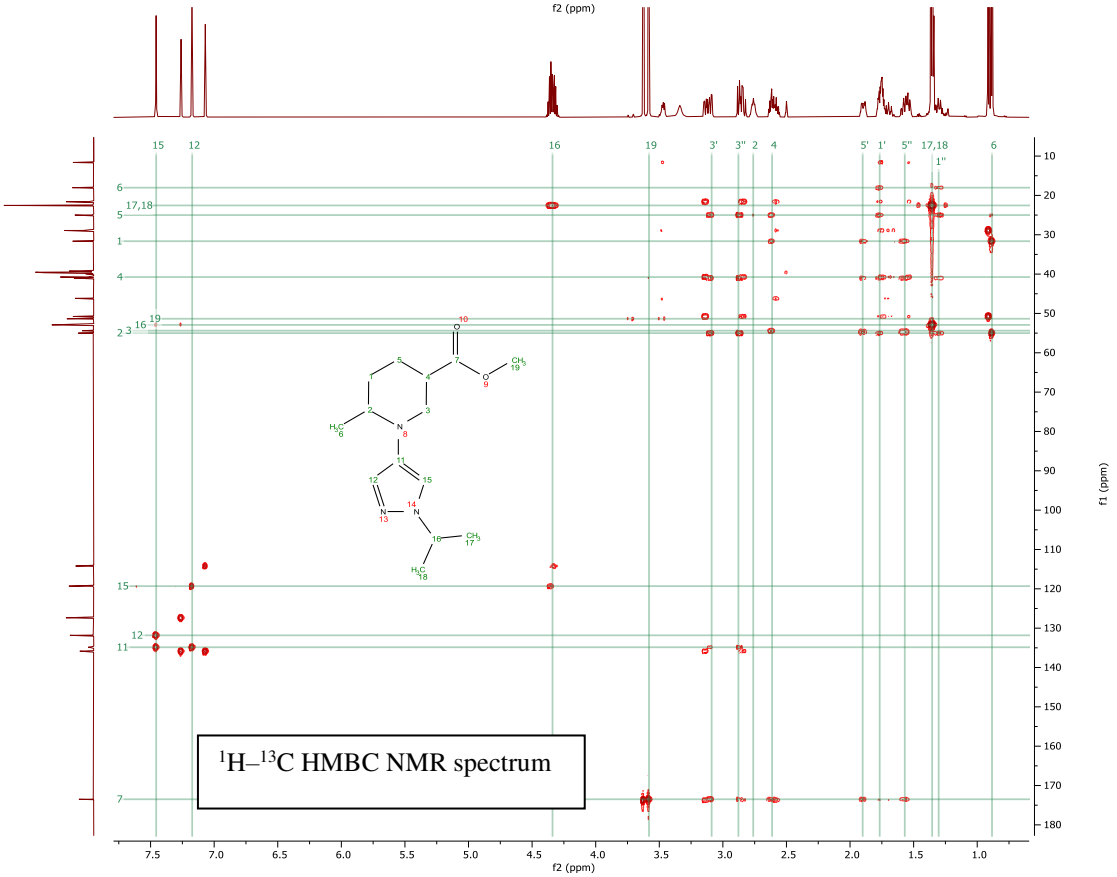
f2 (ppm)
f1 (ppm)
$^{1}H–^{13}C$ HMBC NMR spectrum

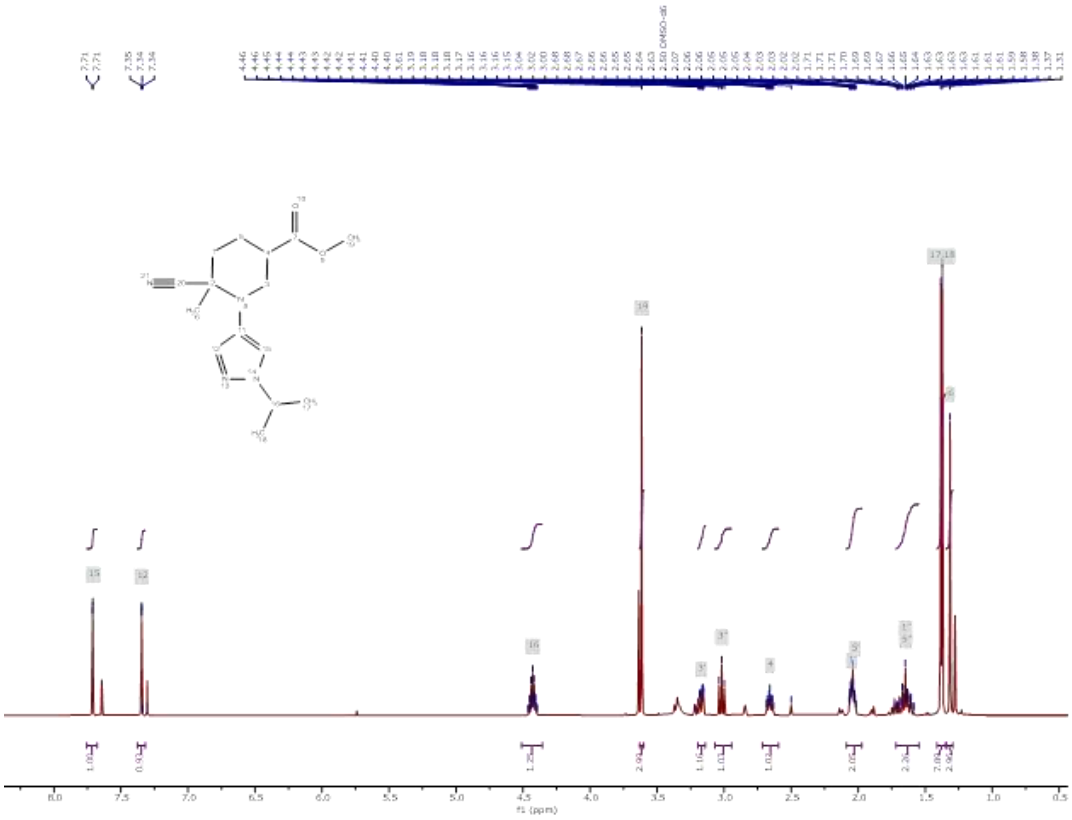

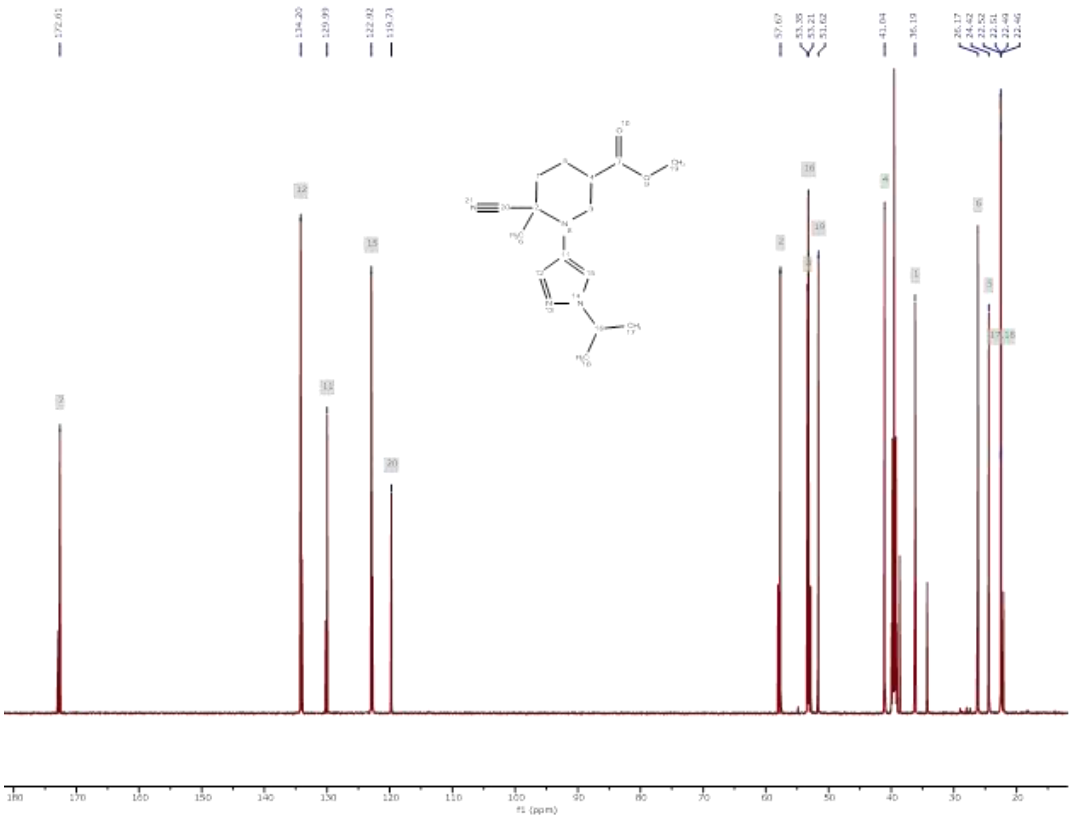

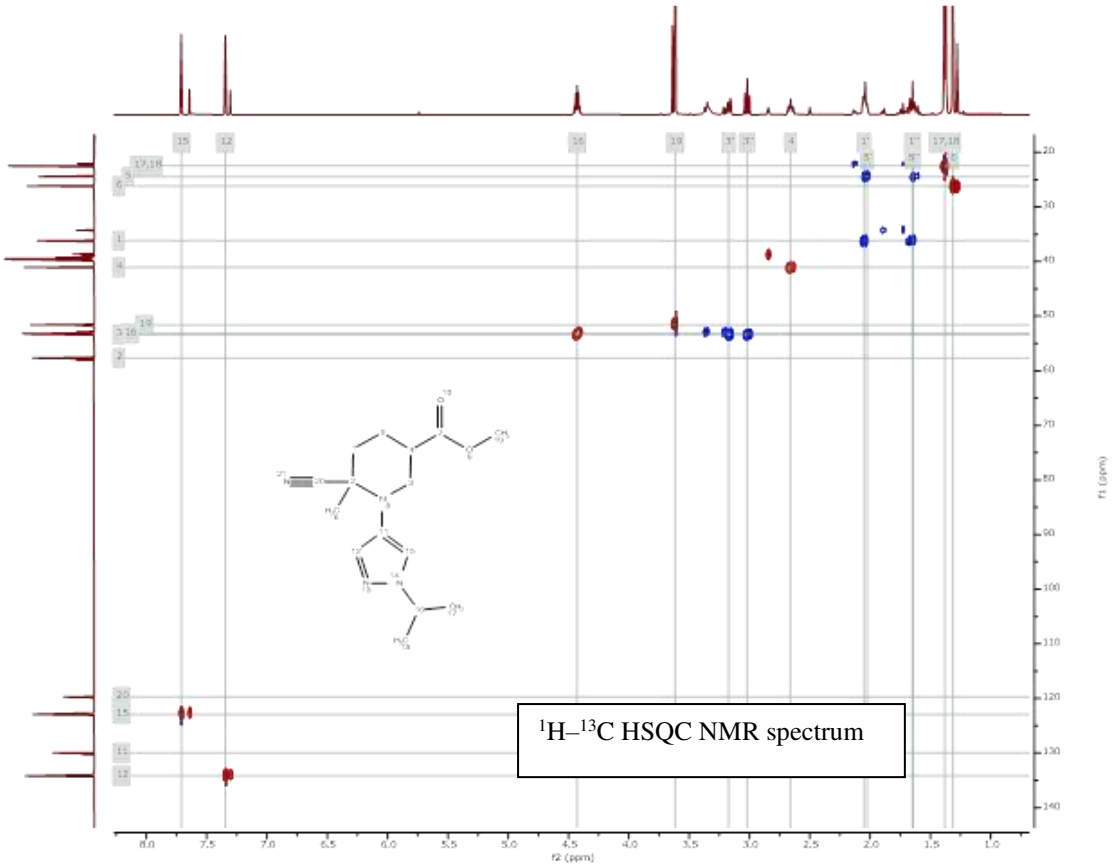

$^{1}H–^{13}C$ HSQC NMR spectrum

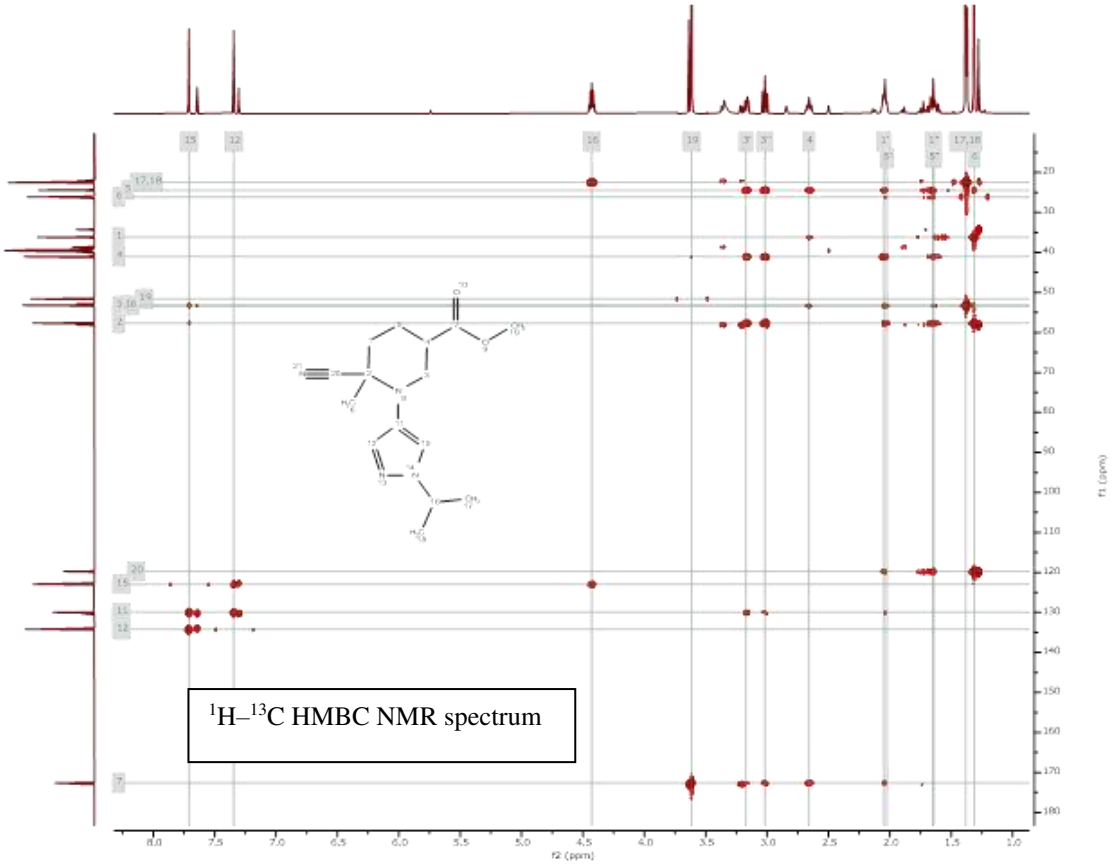

$^{1}H–^{13}C$ HMBC NMR spectrum

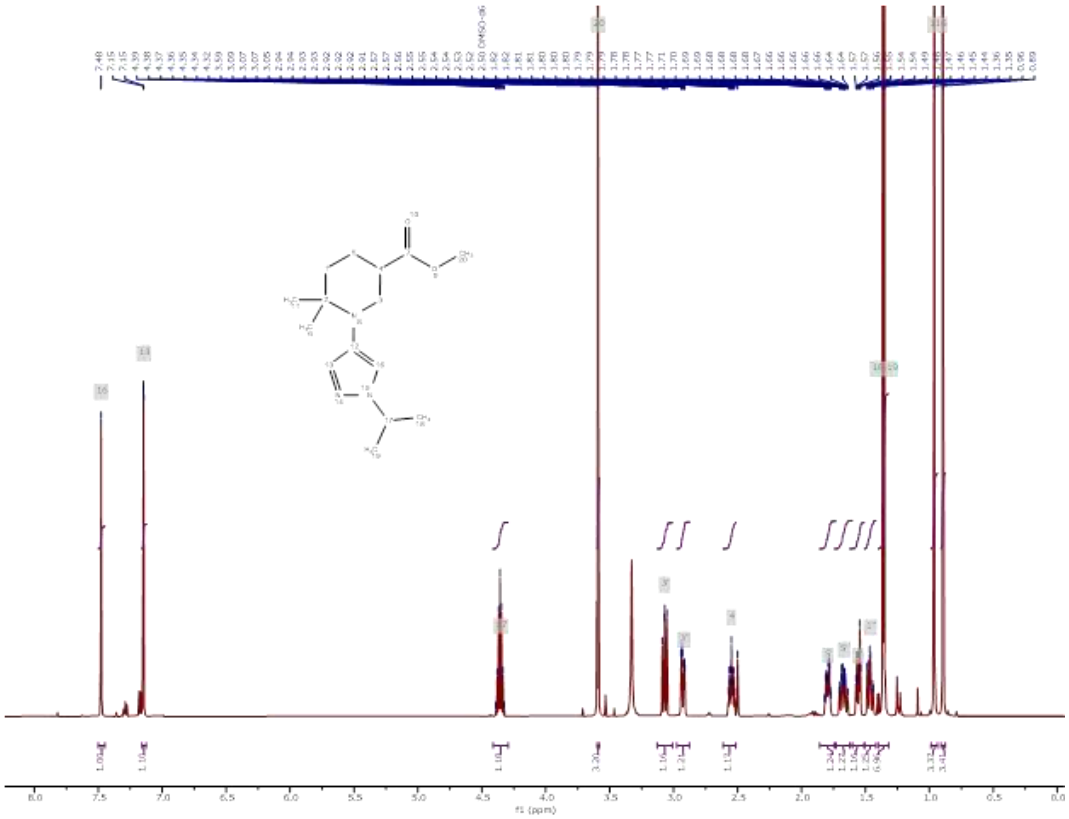

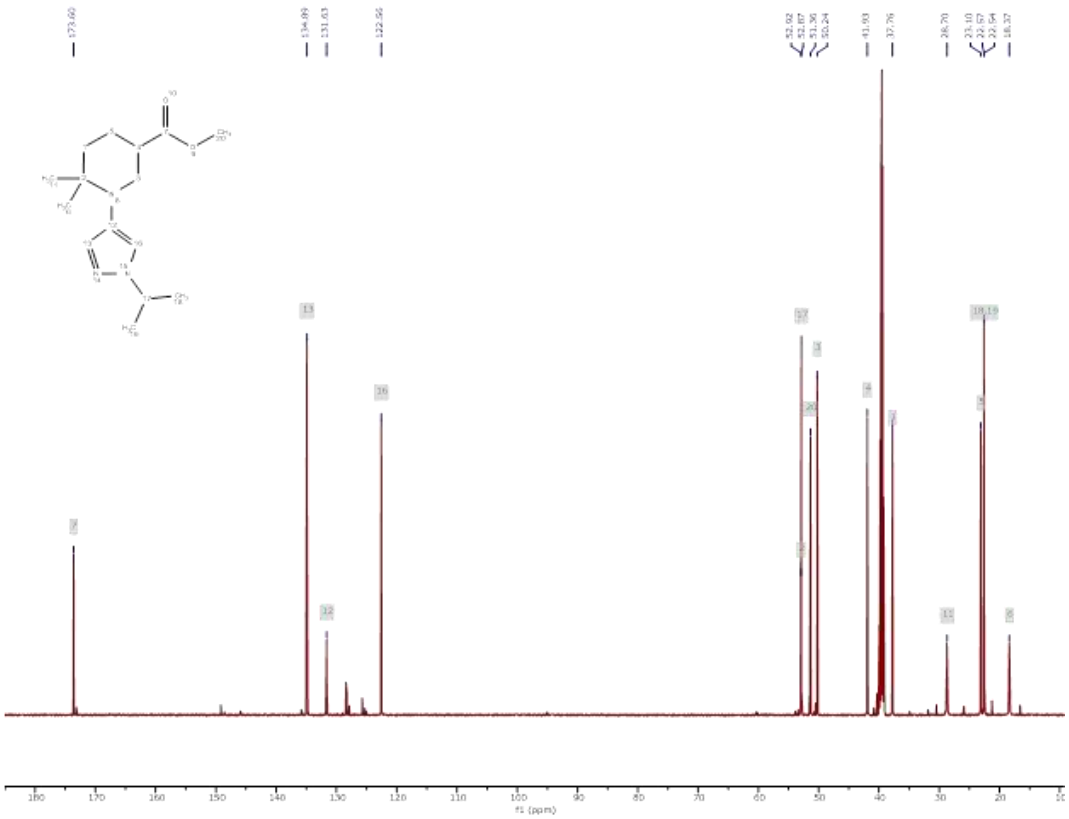

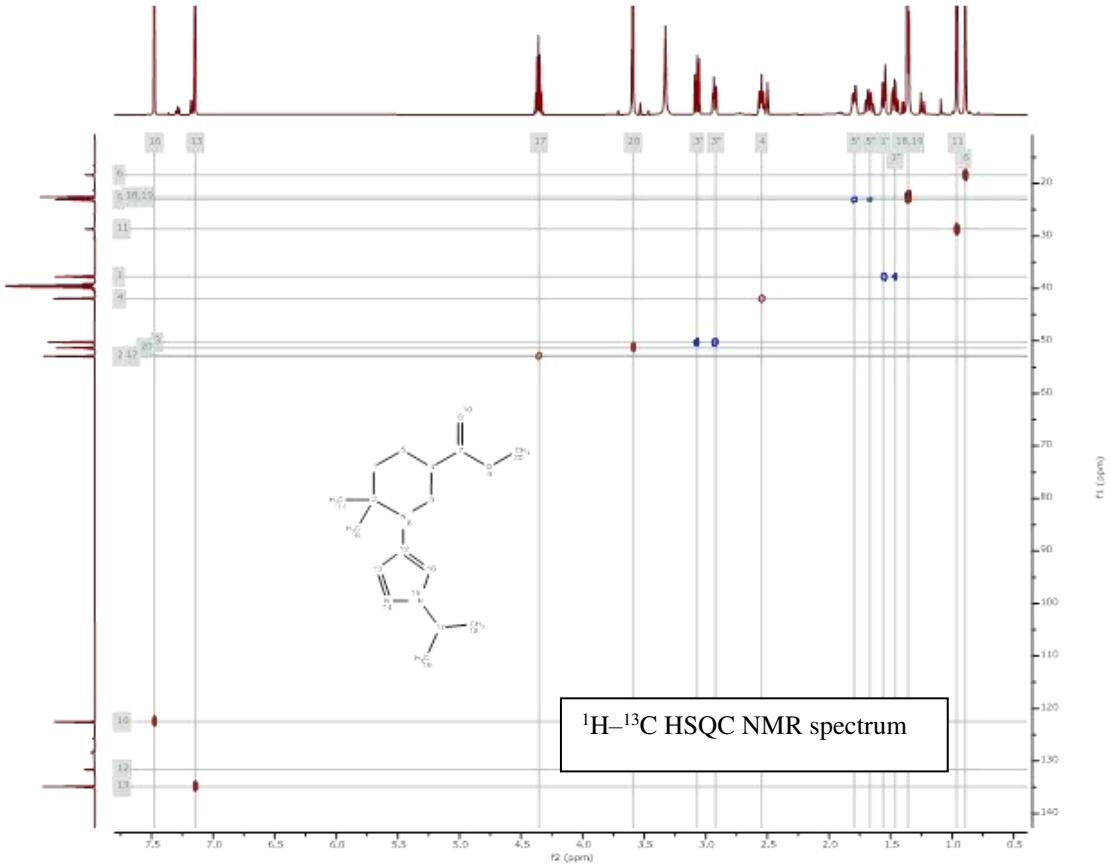
$^{1}H–^{13}C$ HSQC NMR spectrum

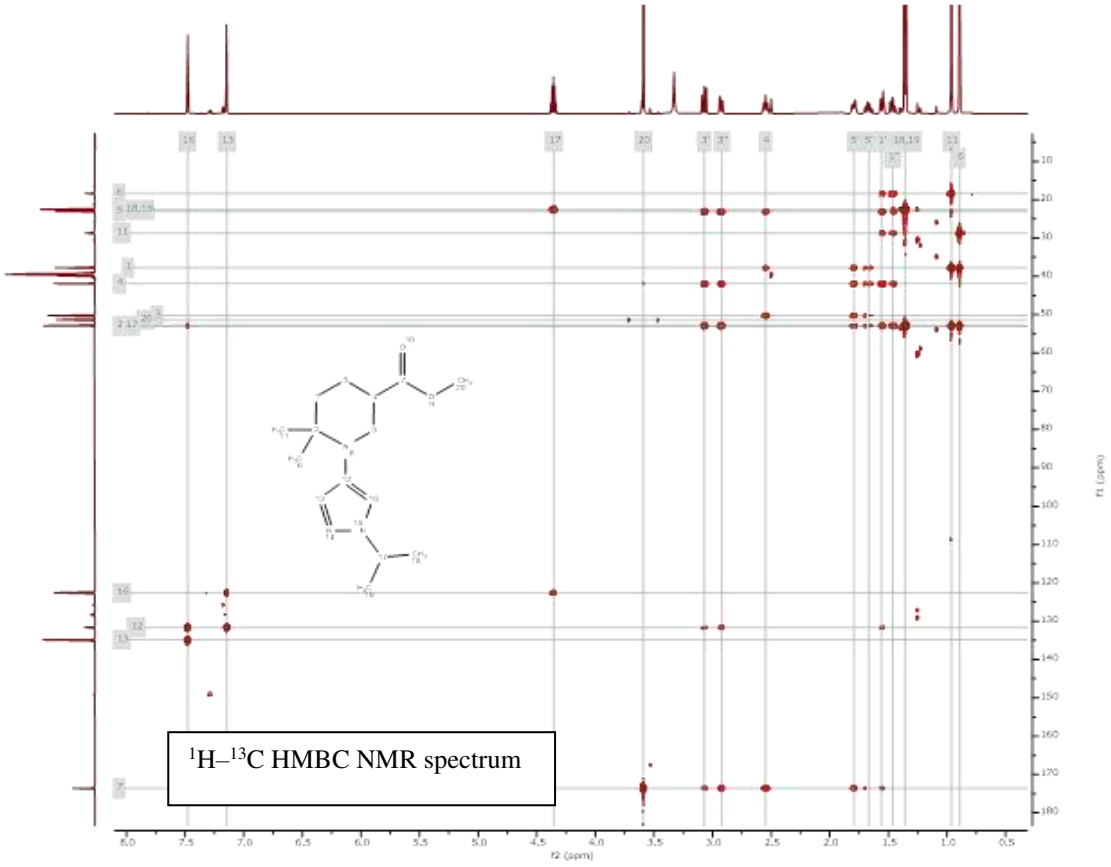
$^{1}H–^{13}C$ HMBC NMR spectrum

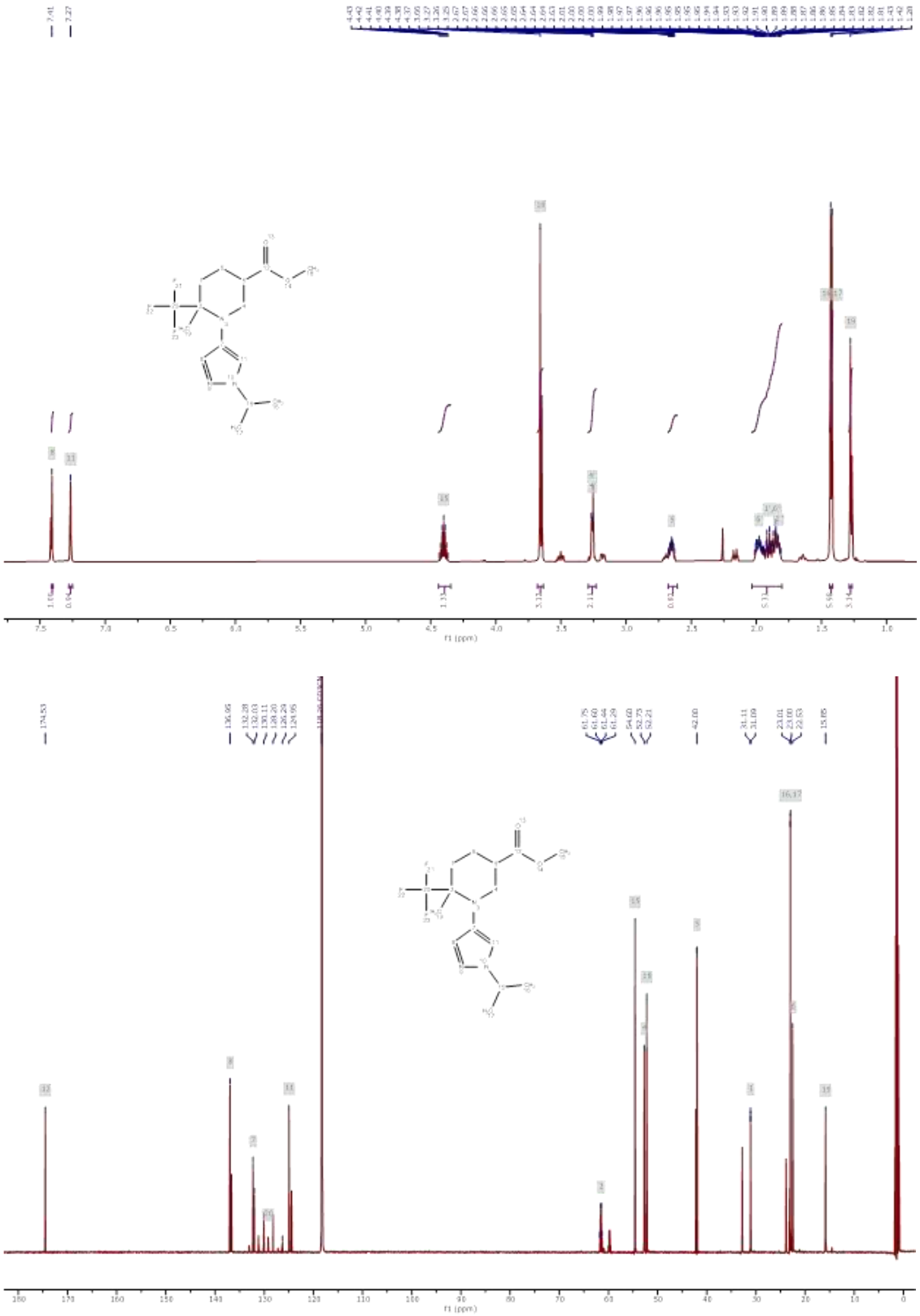

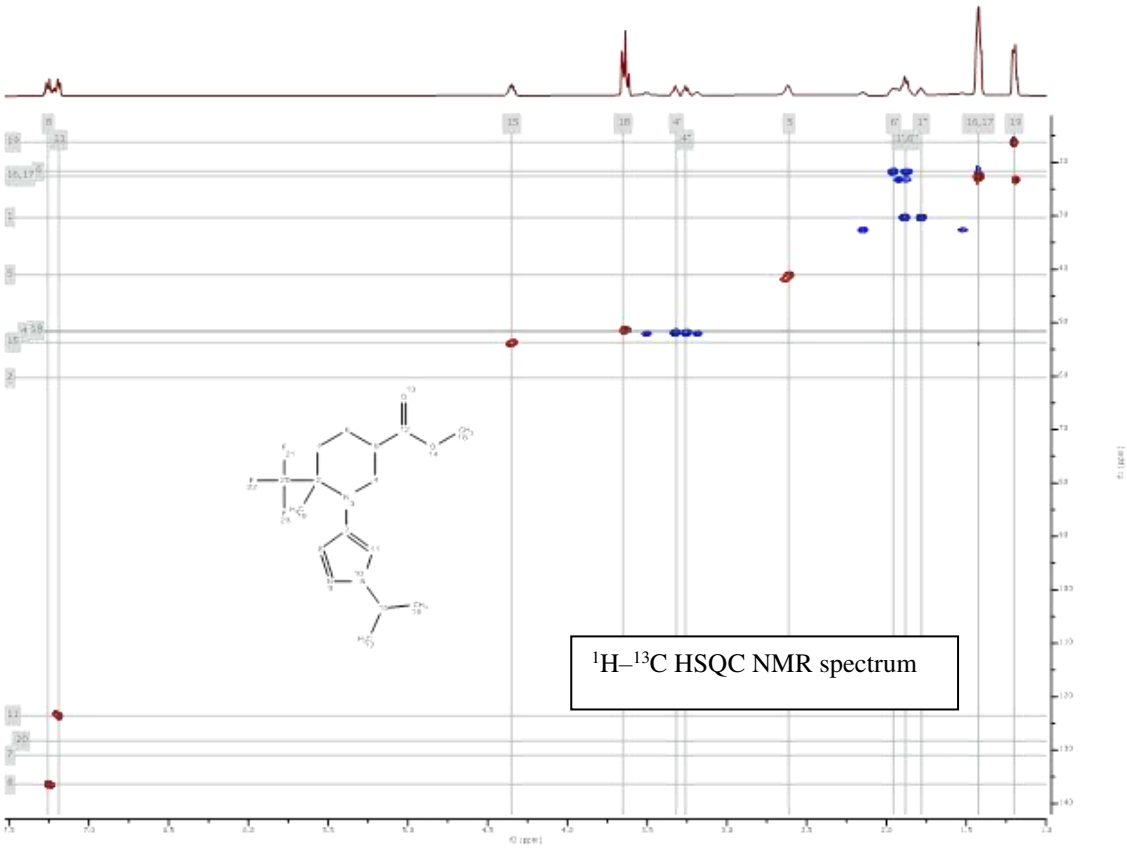

$^{1}H–^{13}C$ HSQC NMR spectrum

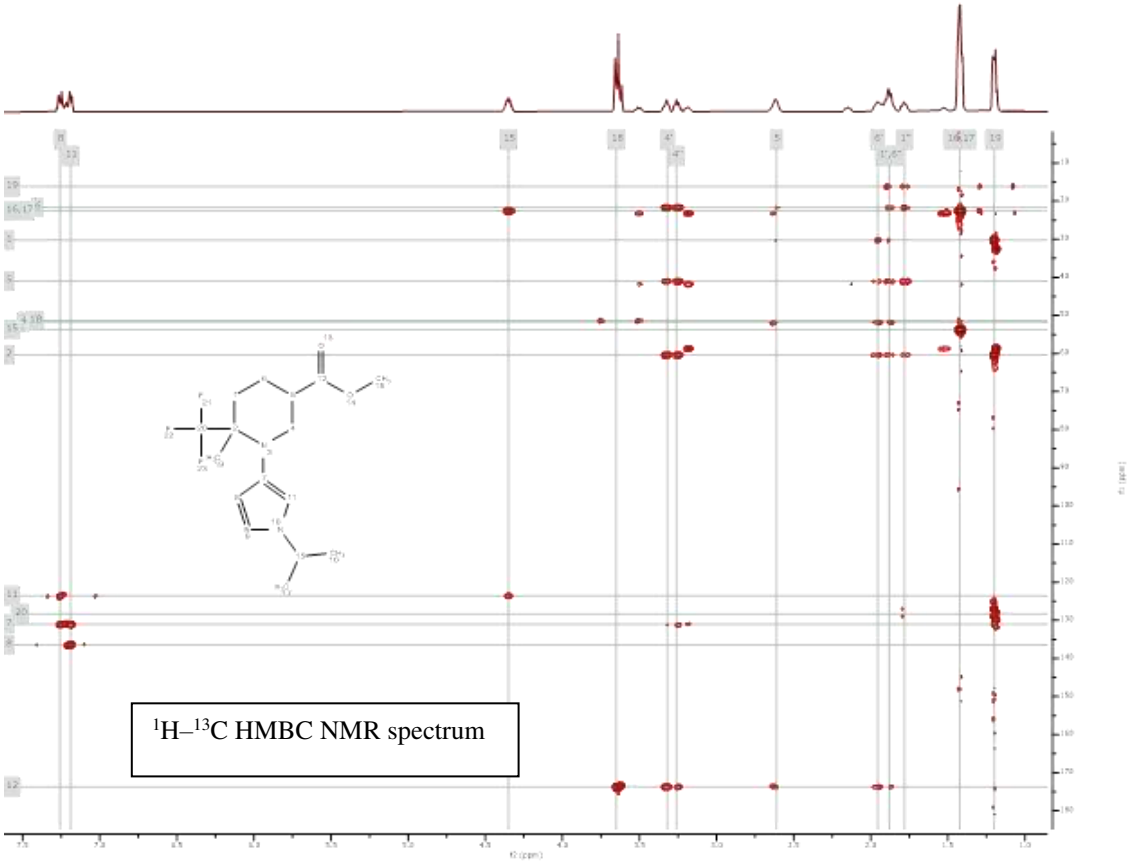

$^{1}H–^{13}C$ HMBC NMR spectrum

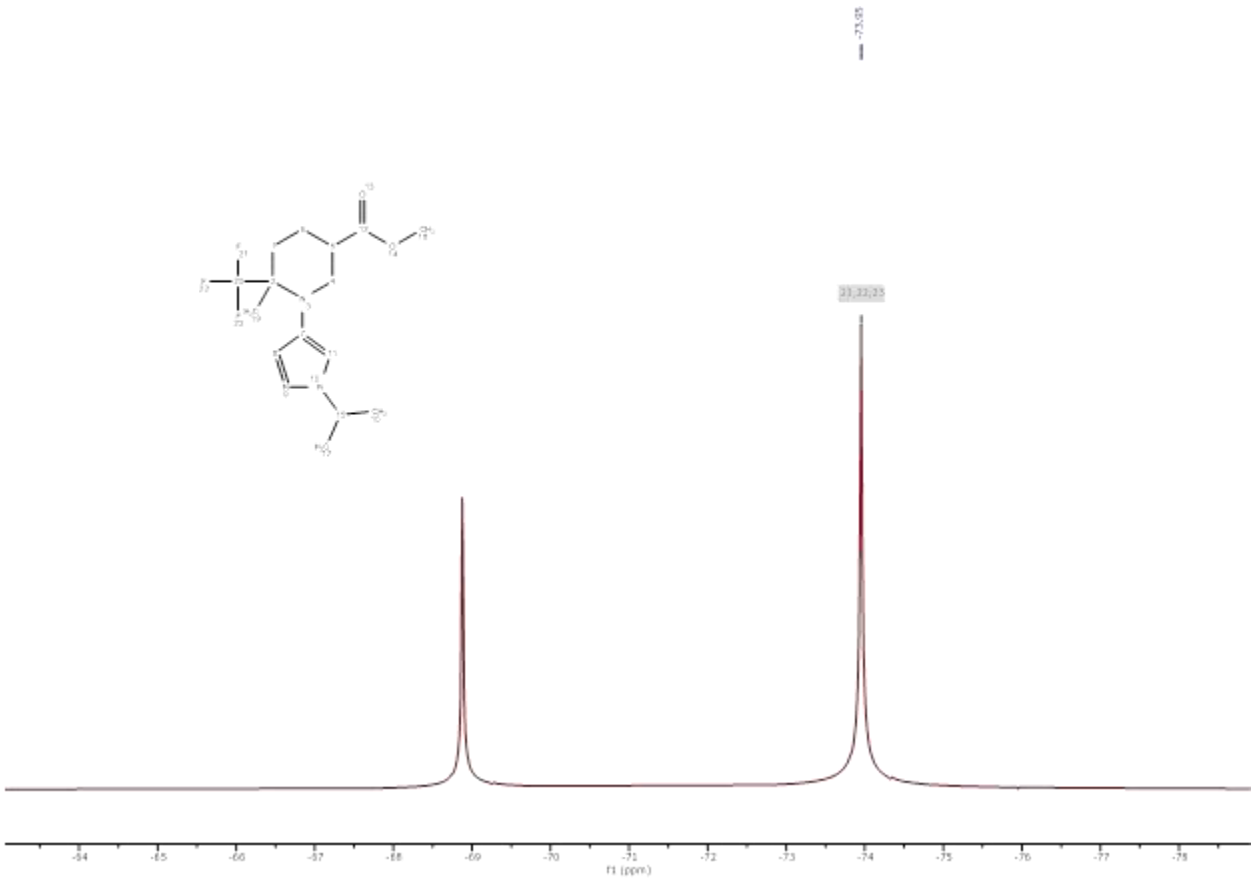
-73.65
33.33.33
-64
-65
-66
-67
-68
-69
-70
-71
-72
-73
-74
-75
-76
-77
-78
f1 (ppm)

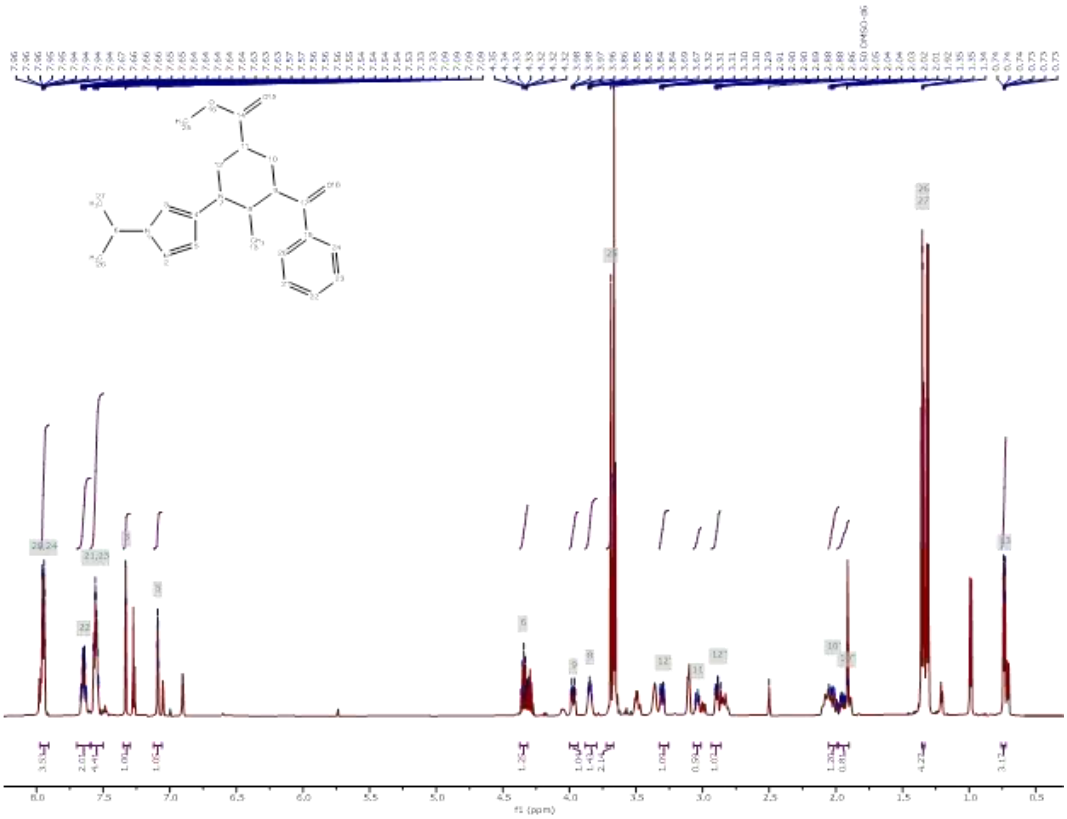

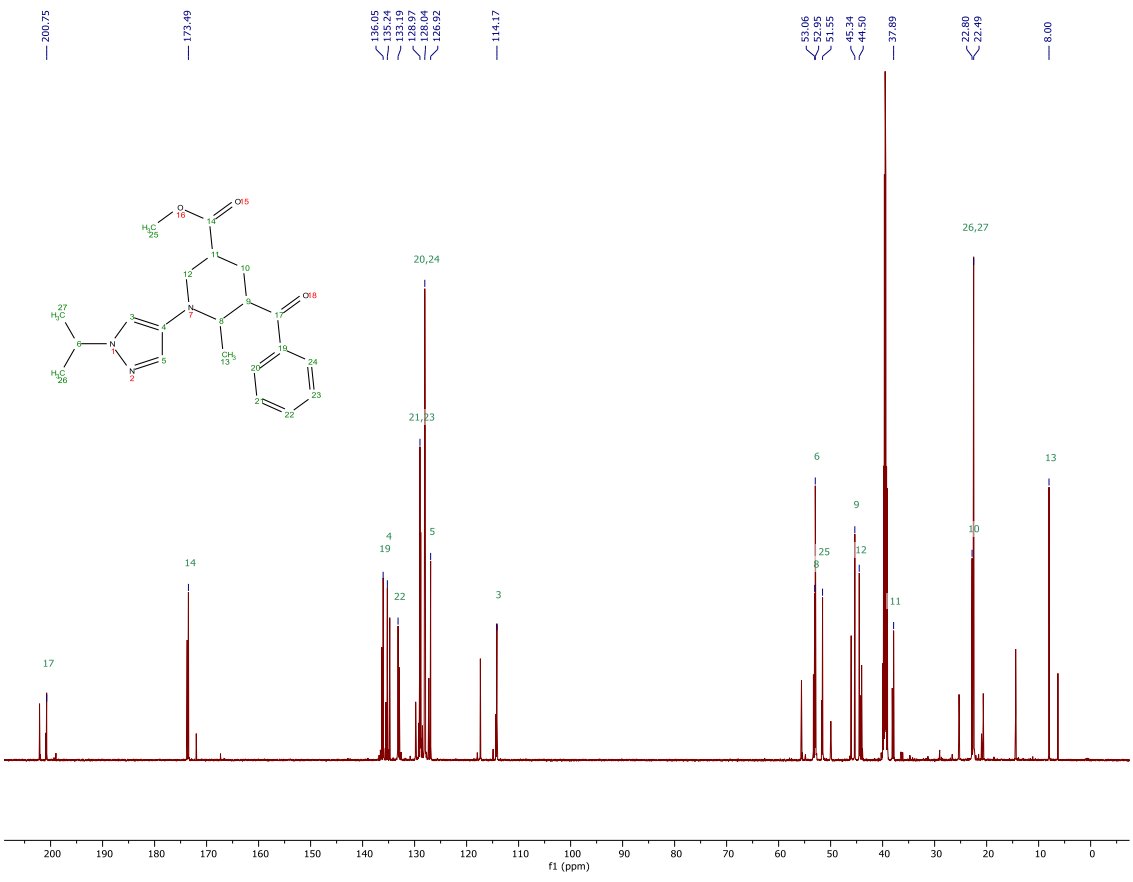

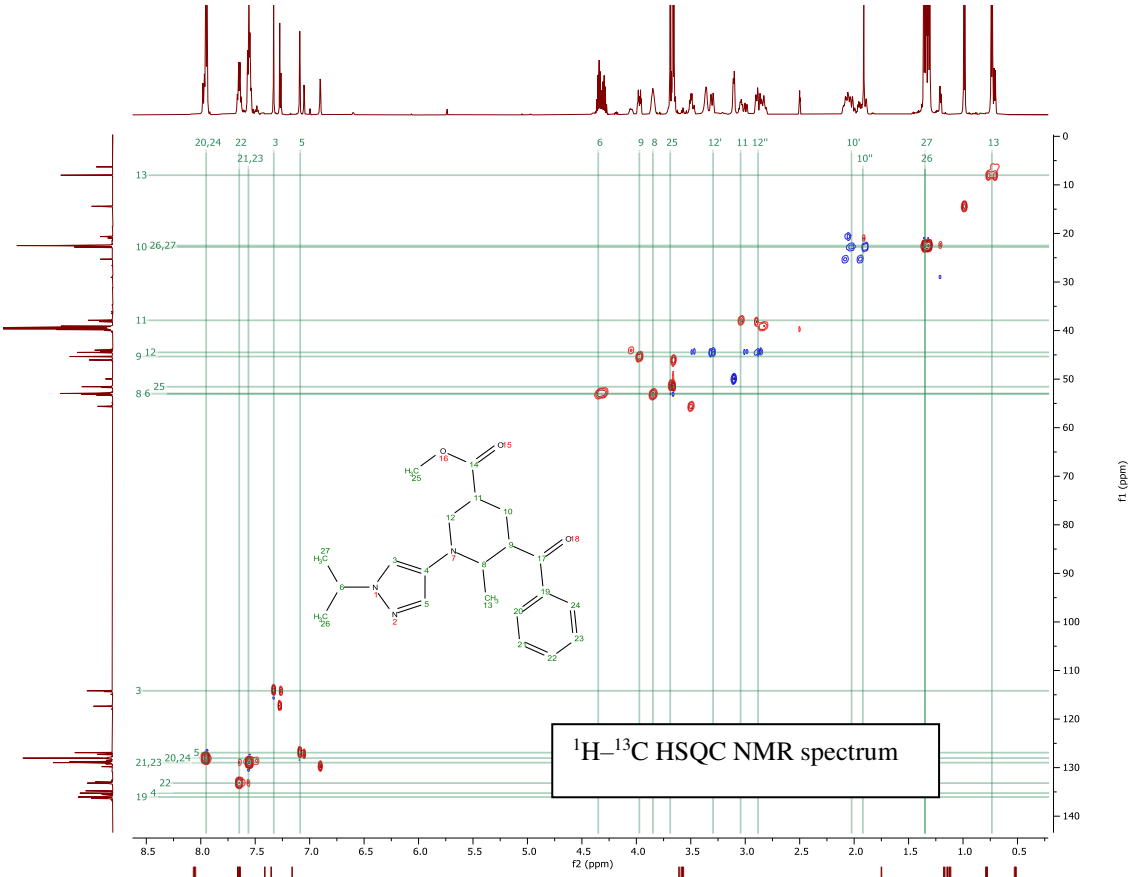
$^{1}H–^{13}C$ HSQC NMR spectrum
f2 (ppm)
f1 (ppm)

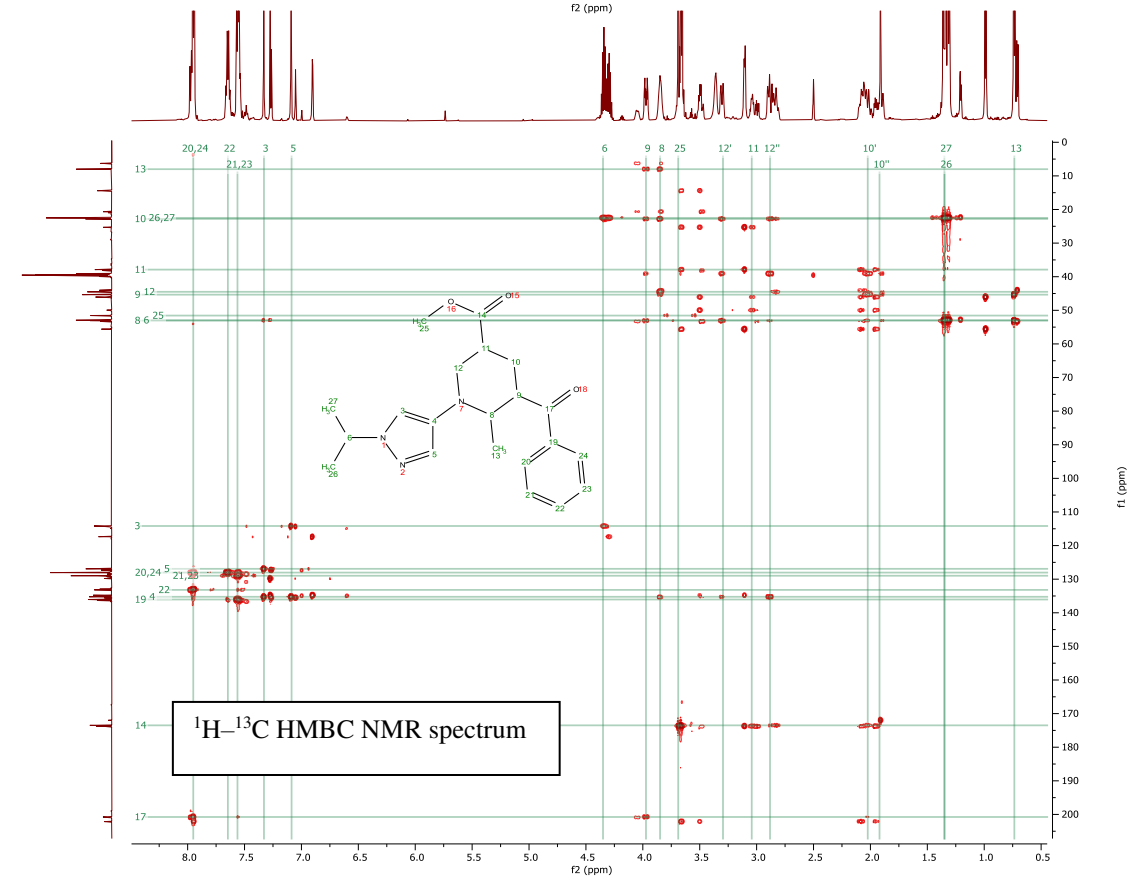
$^{1}H–^{13}C$ HMBC NMR spectrum
f2 (ppm)
f1 (ppm)

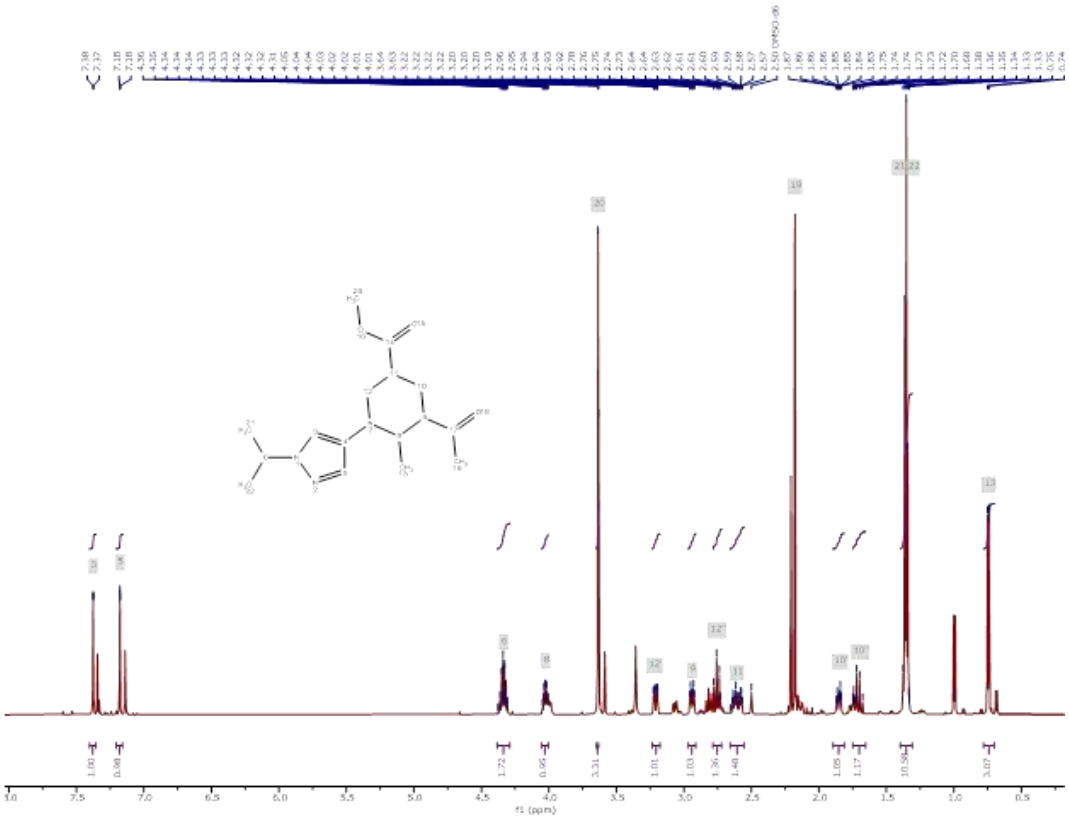

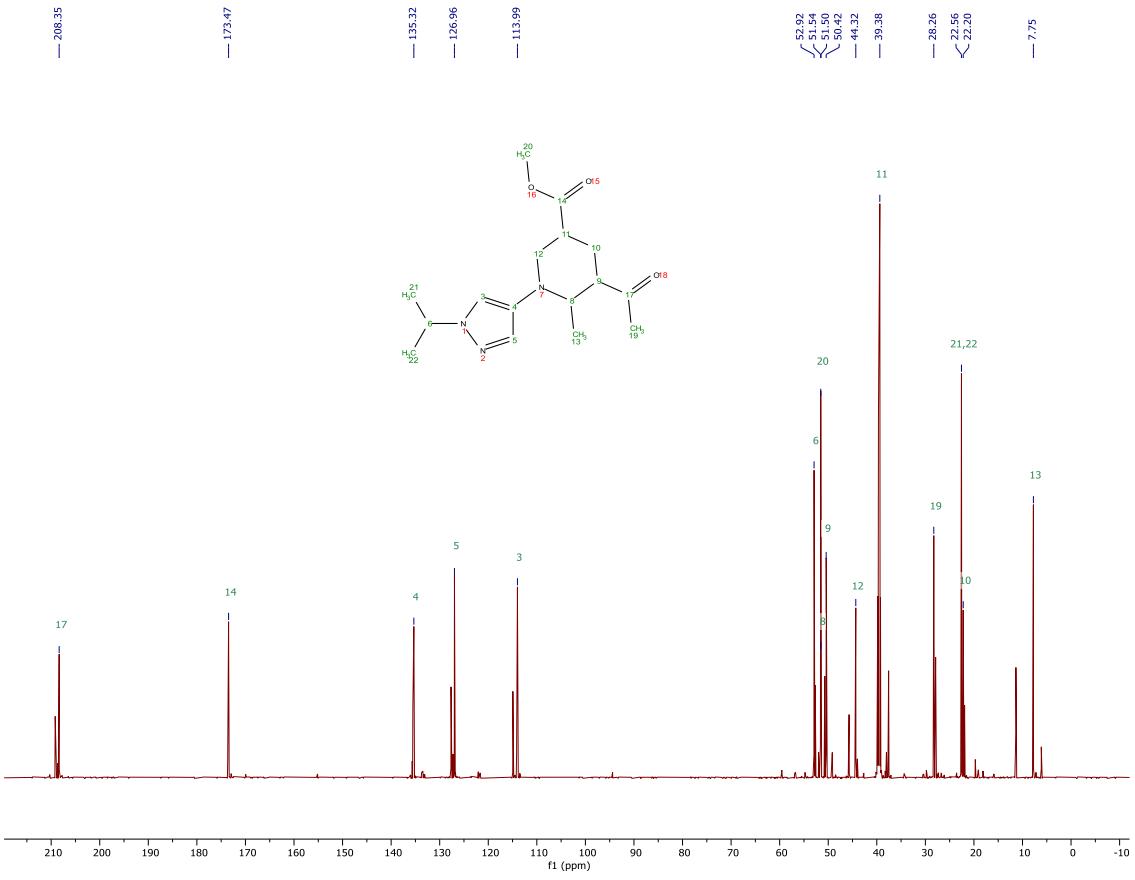

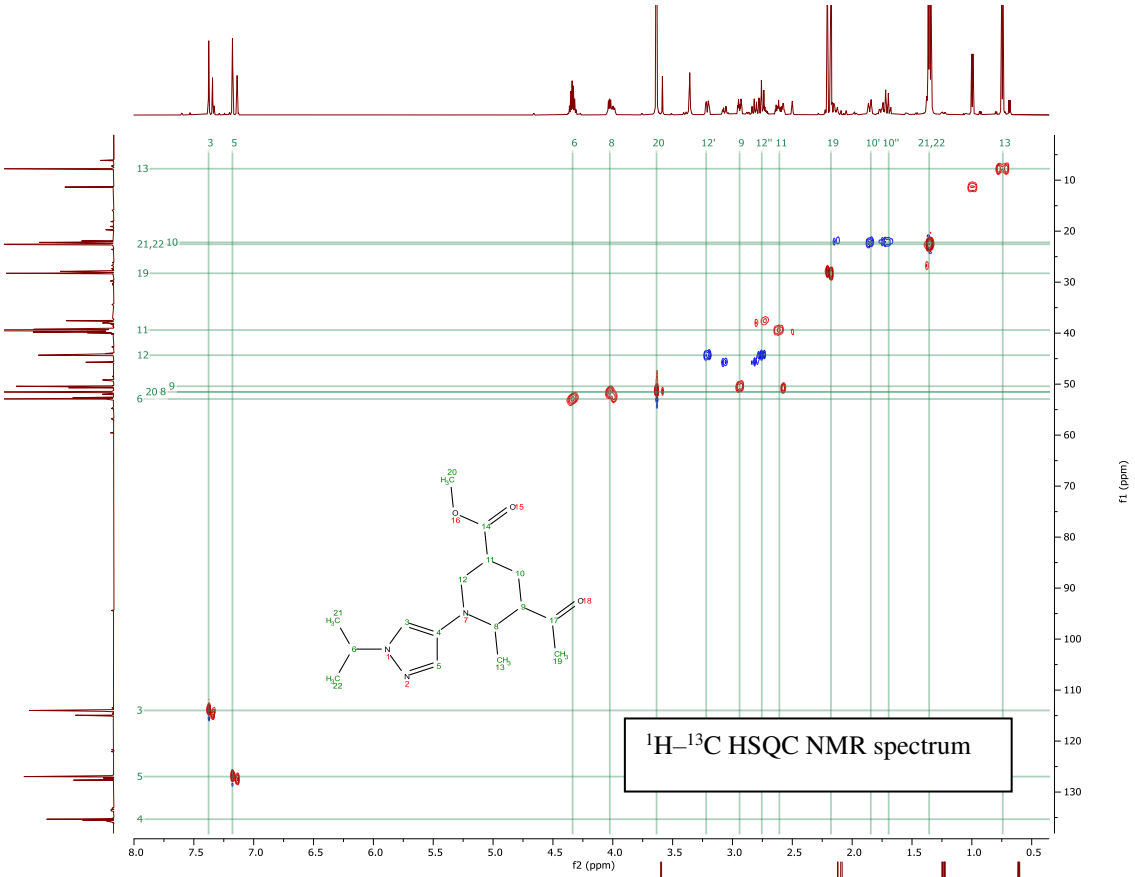

$^{1}H–^{13}C$ HSQC NMR spectrum

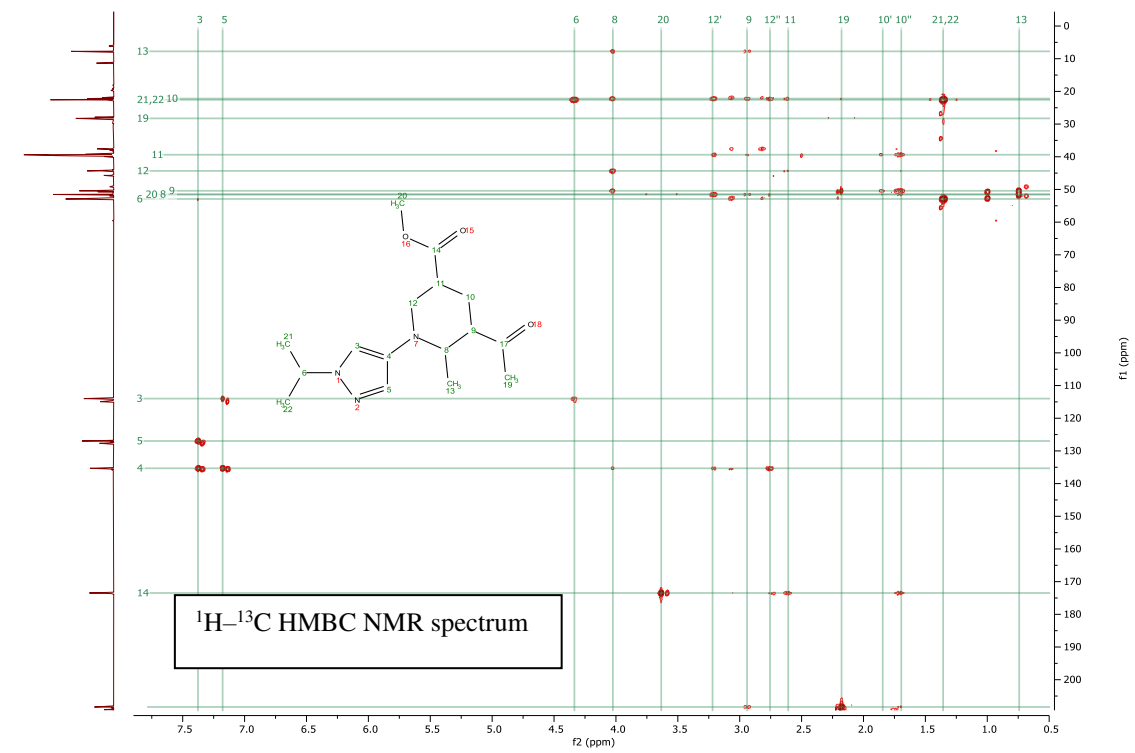

$^{1}H–^{13}C$ HMBC NMR spectrum

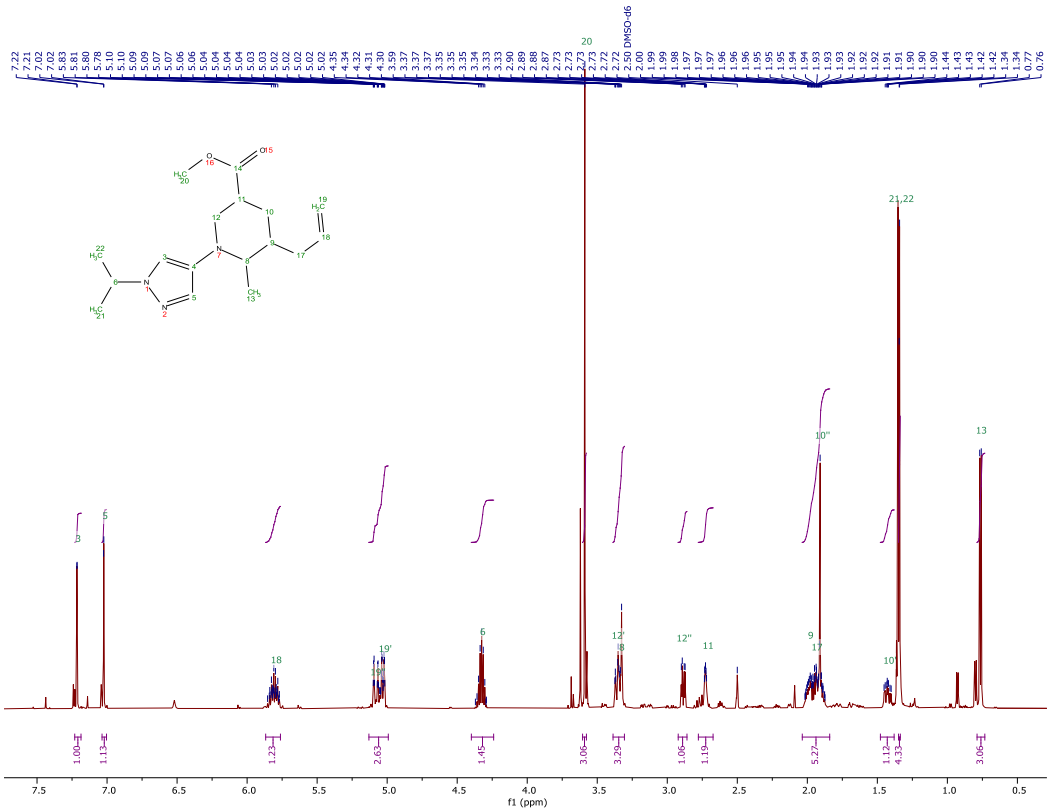
DMSO-d6
f1 (ppm)

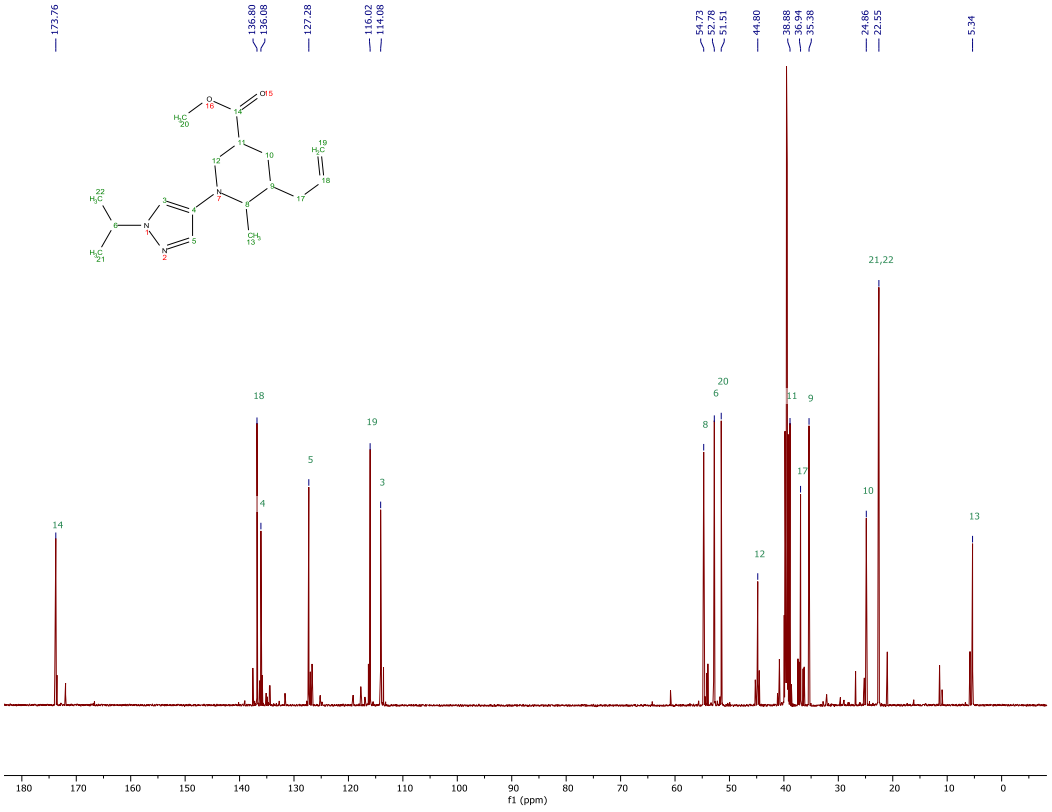
173.76
136.80
136.08
127.28
116.02
114.08
54.73
52.78
51.51
44.80
38.88
36.94
35.38
24.86
22.55
5.34
f1 (ppm)

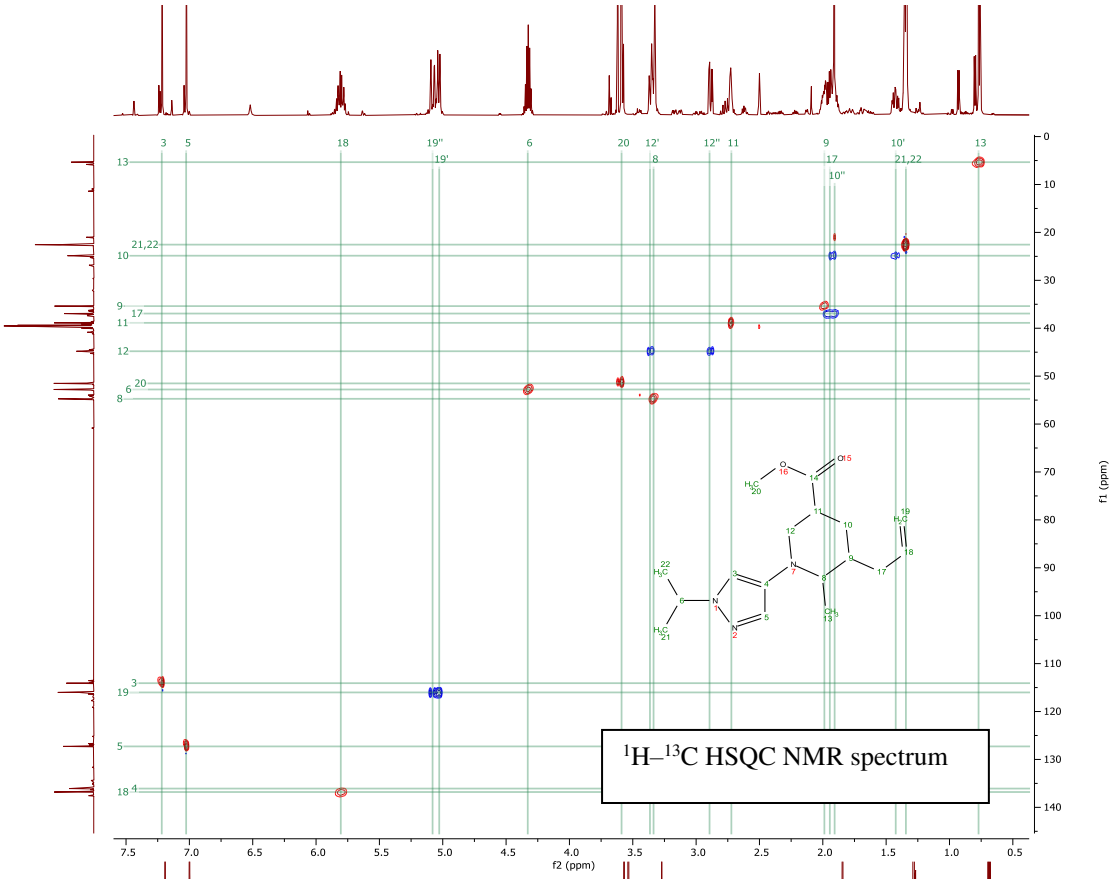

$^{1}H–^{13}C$ HSQC NMR spectrum

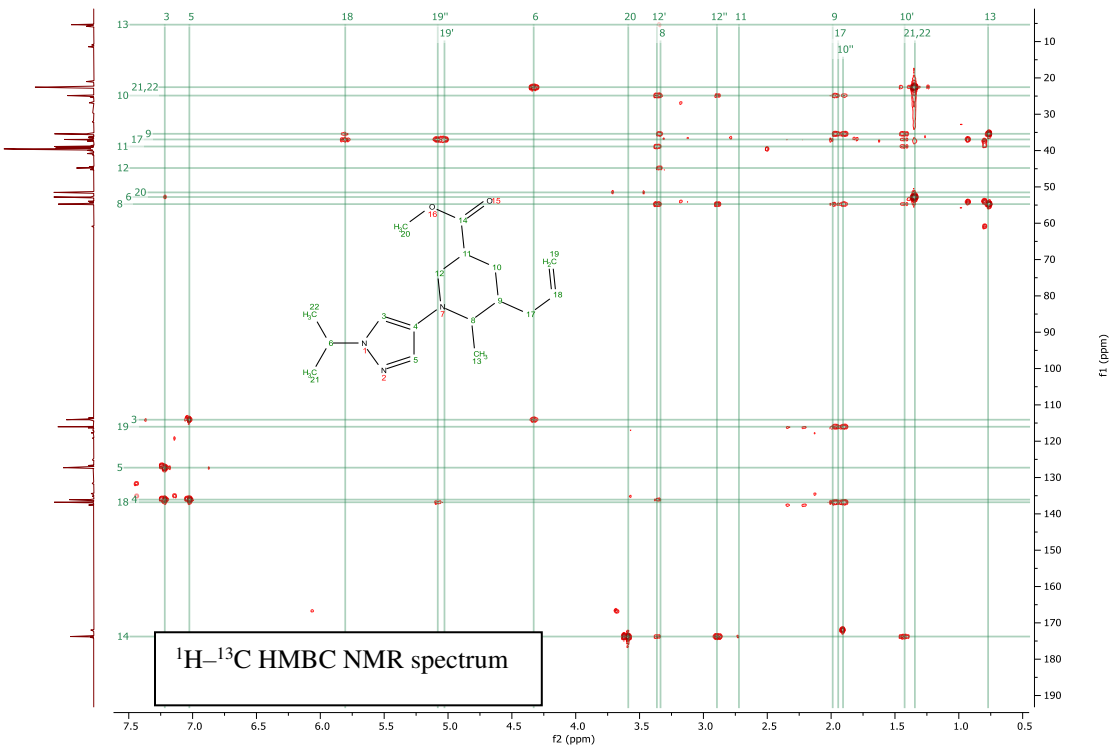

$^{1}H–^{13}C$ HMBC NMR spectrum

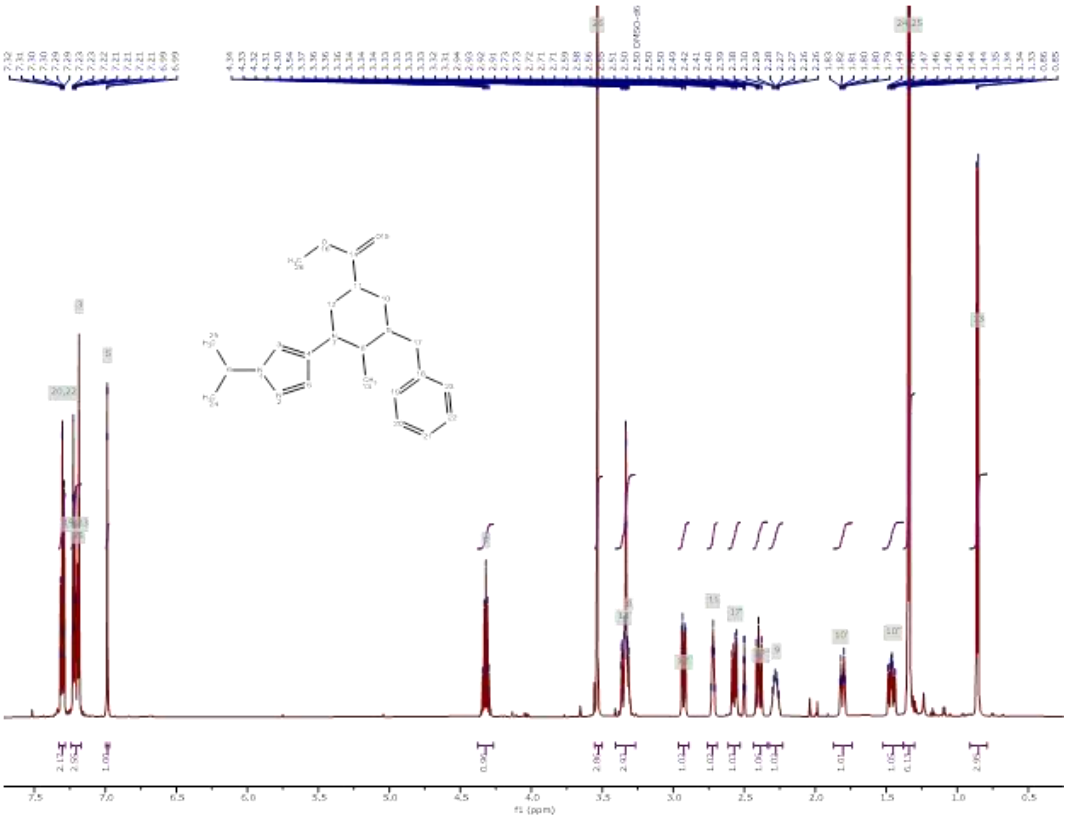

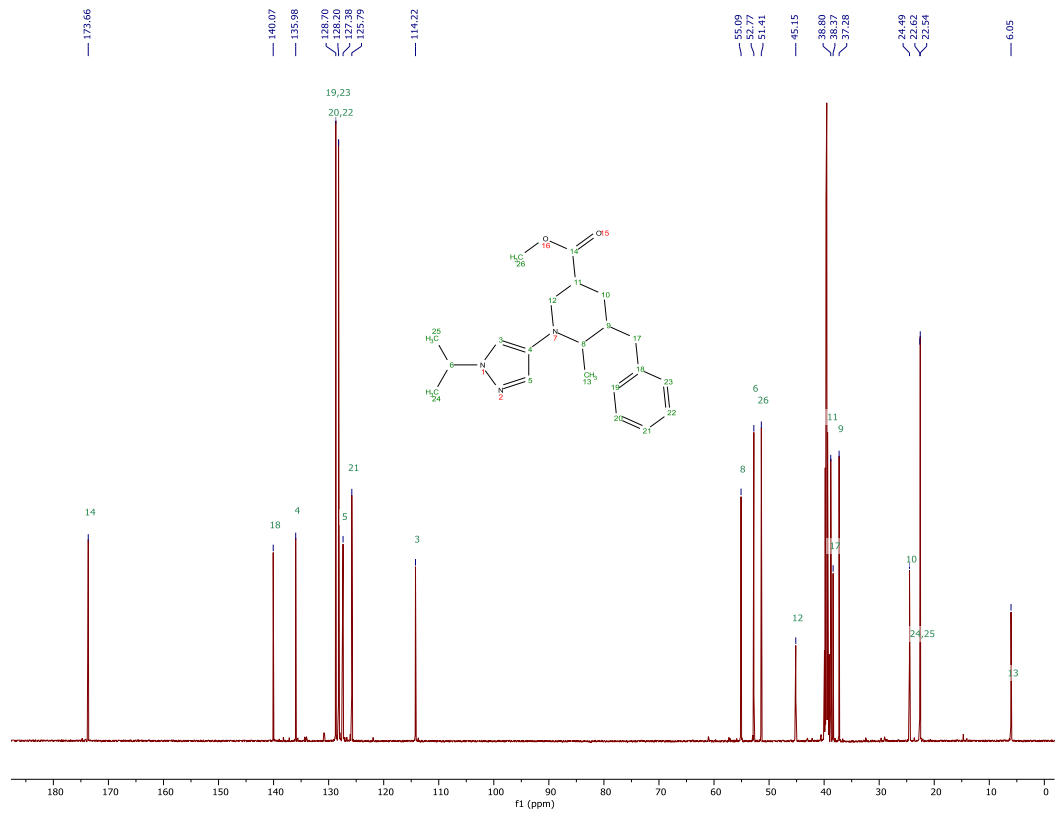

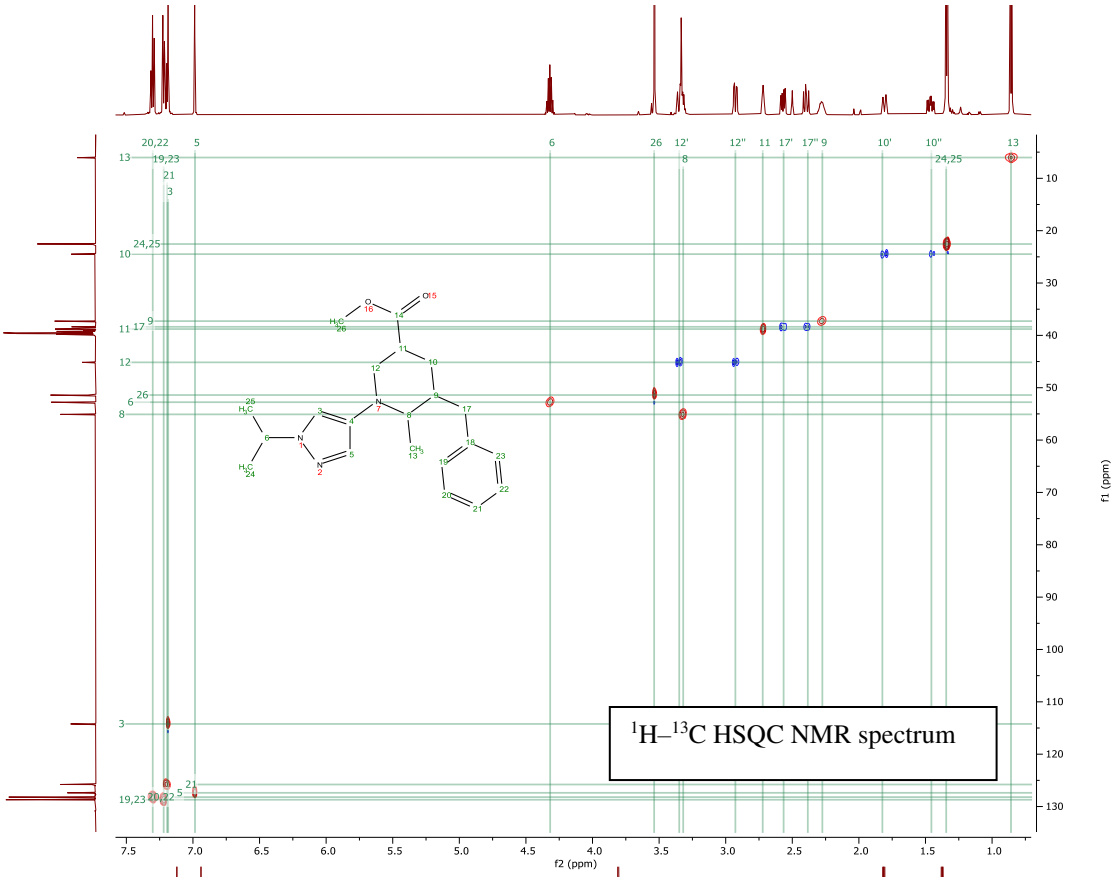

$^{1}H–^{13}C$ HSQC NMR spectrum

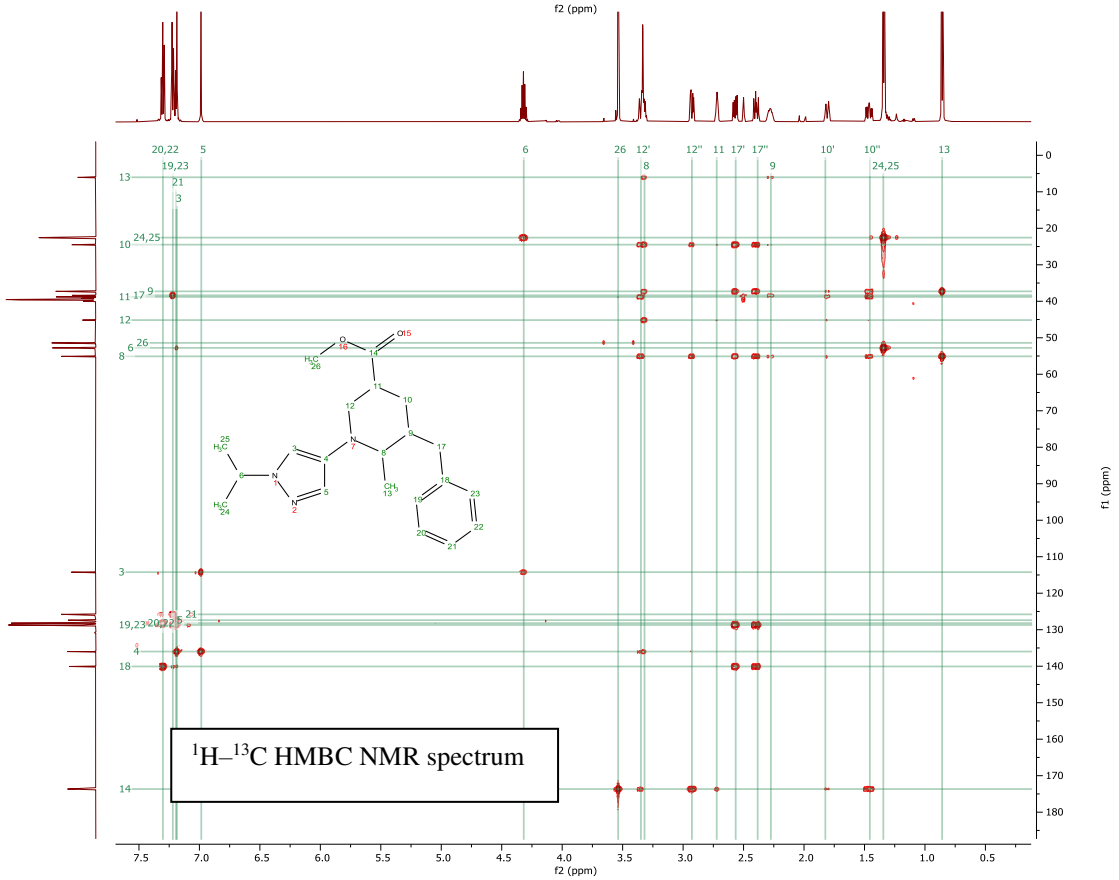

$^{1}H–^{13}C$ HMBC NMR spectrum

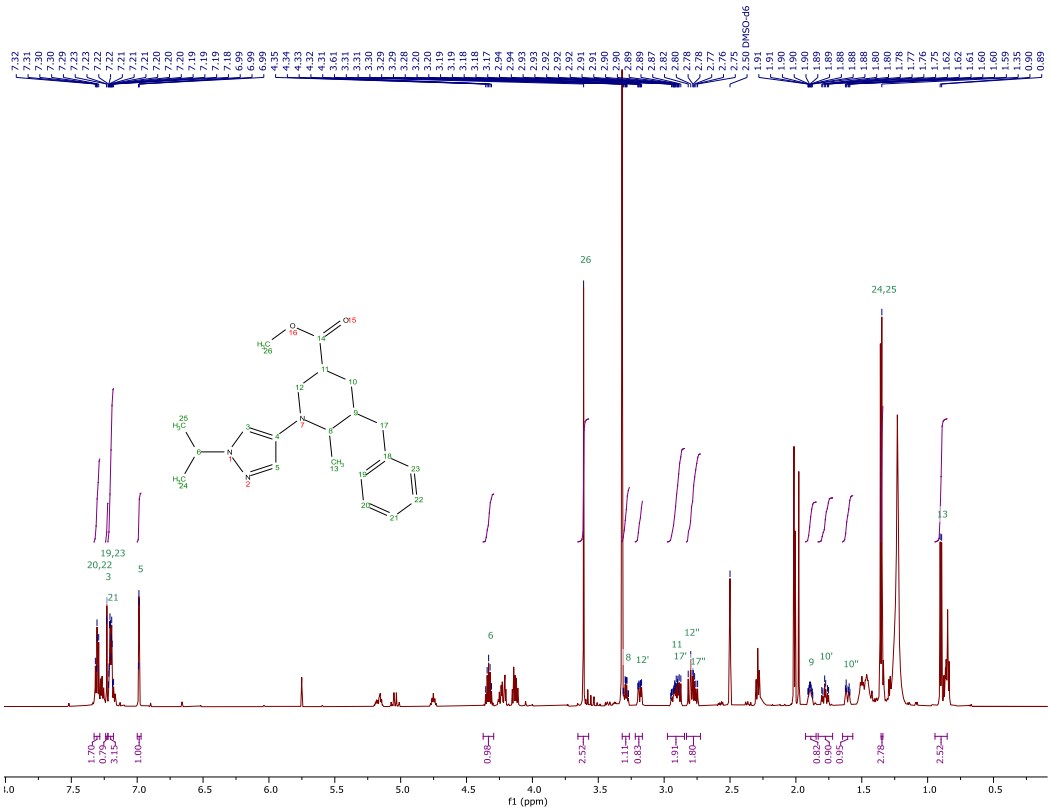
DMSO-d6
26
24,25
19,23
20,22
3
5
21
6
8
12'
11
17'
17''
12''
9
10'
10''
13
1.70
0.79
3.15
1.00
0.98
2.53
1.11
0.83
1.91
1.80
0.83
0.90
0.95
2.78
2.53
f1 (ppm)

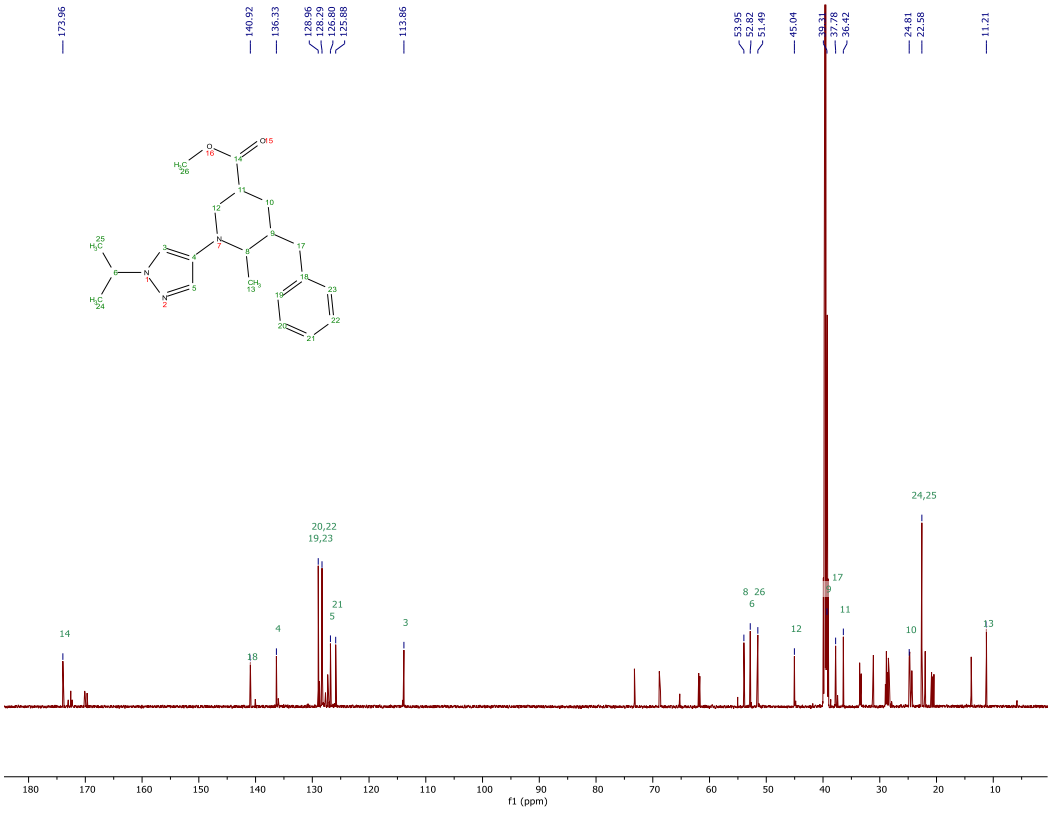
173.96
140.92
136.33
128.96
128.29
126.80
125.88
113.86
53.95
52.82
51.49
45.04
39.31
37.78
36.42
24.81
22.58
11.21
24,25
20,22
19,23
14
4
18
21
5
3
8
26
6
17
9
11
12
10
13
f1 (ppm)

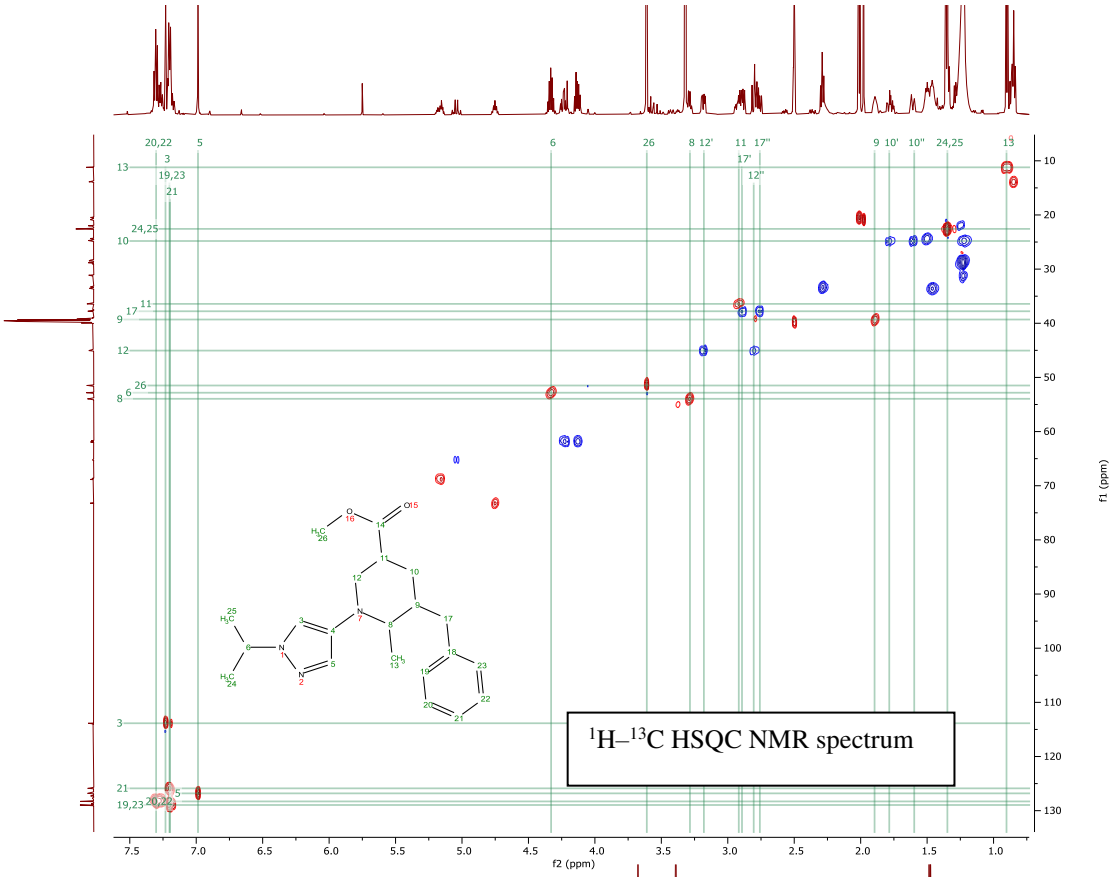

$^{1}H–^{13}C$ HSQC NMR spectrum

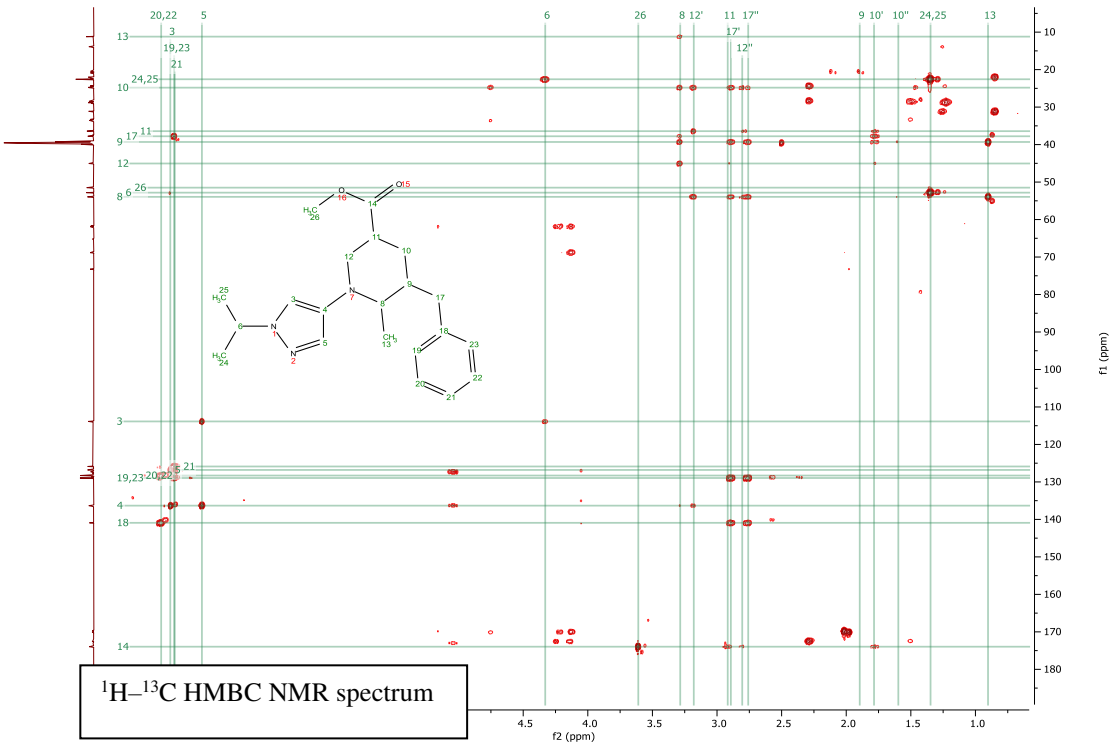

$^{1}H–^{13}C$ HMBC NMR spectrum

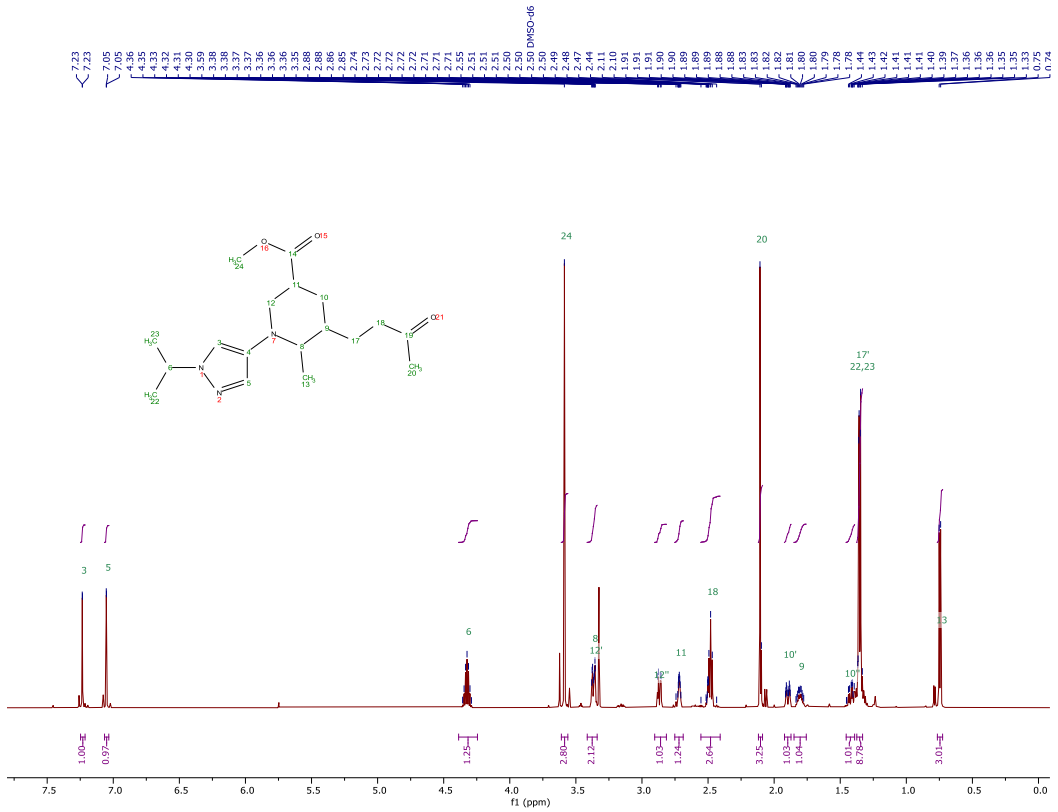
DMSO-d6
f1 (ppm)

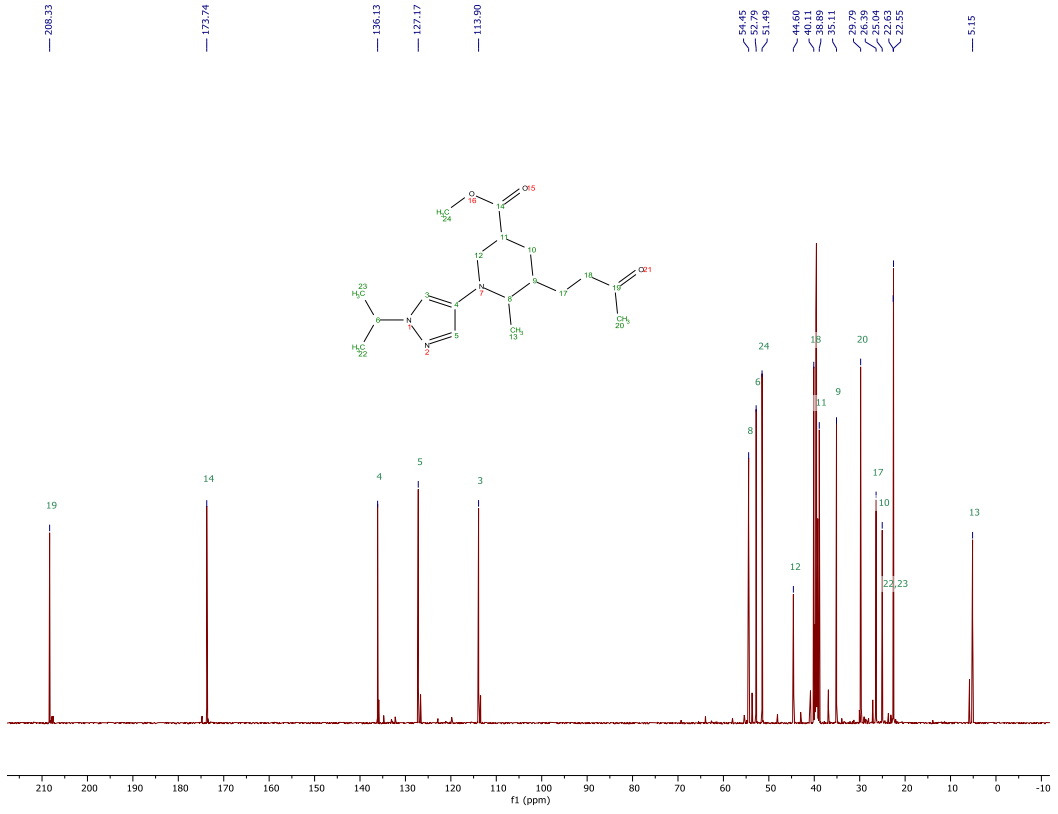
f1 (ppm)

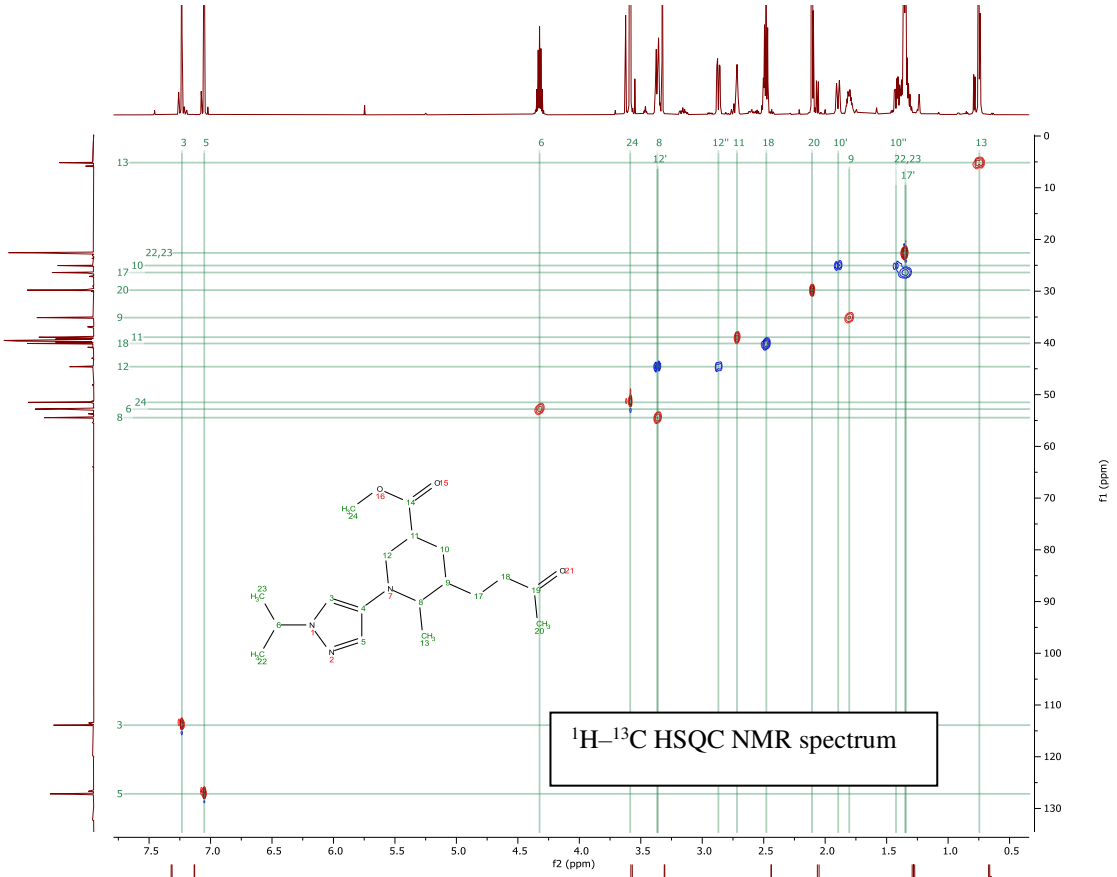

$^{1}H–^{13}C$ HSQC NMR spectrum

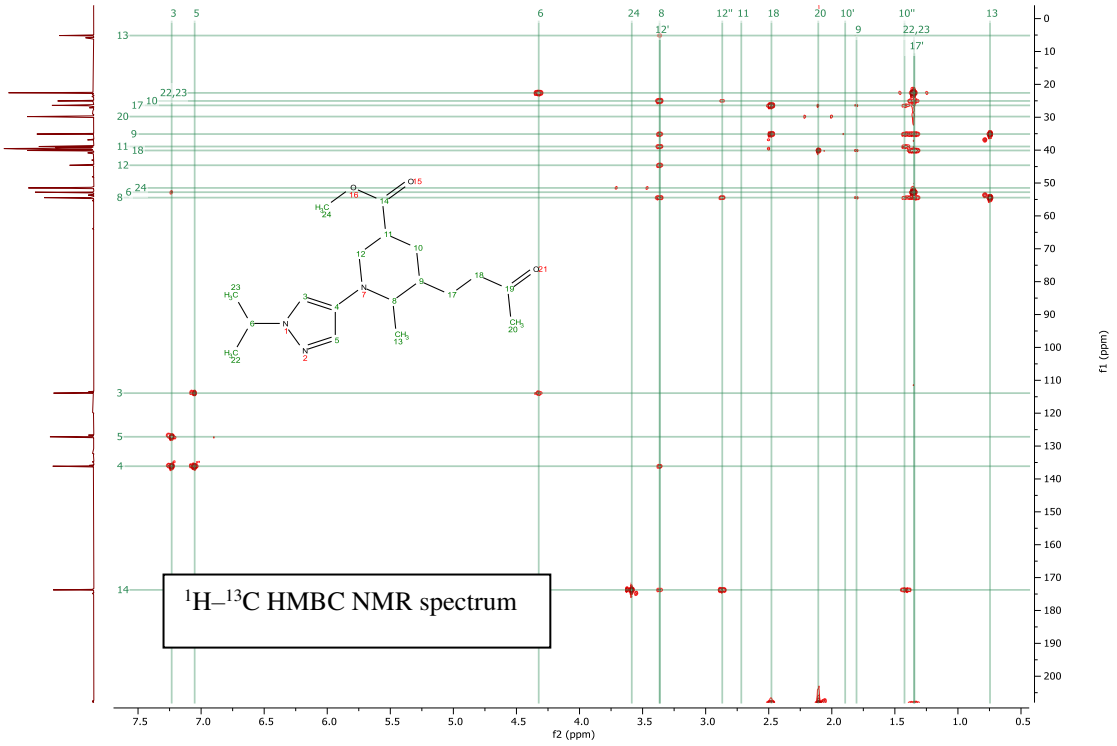

$^{1}H–^{13}C$ HMBC NMR spectrum

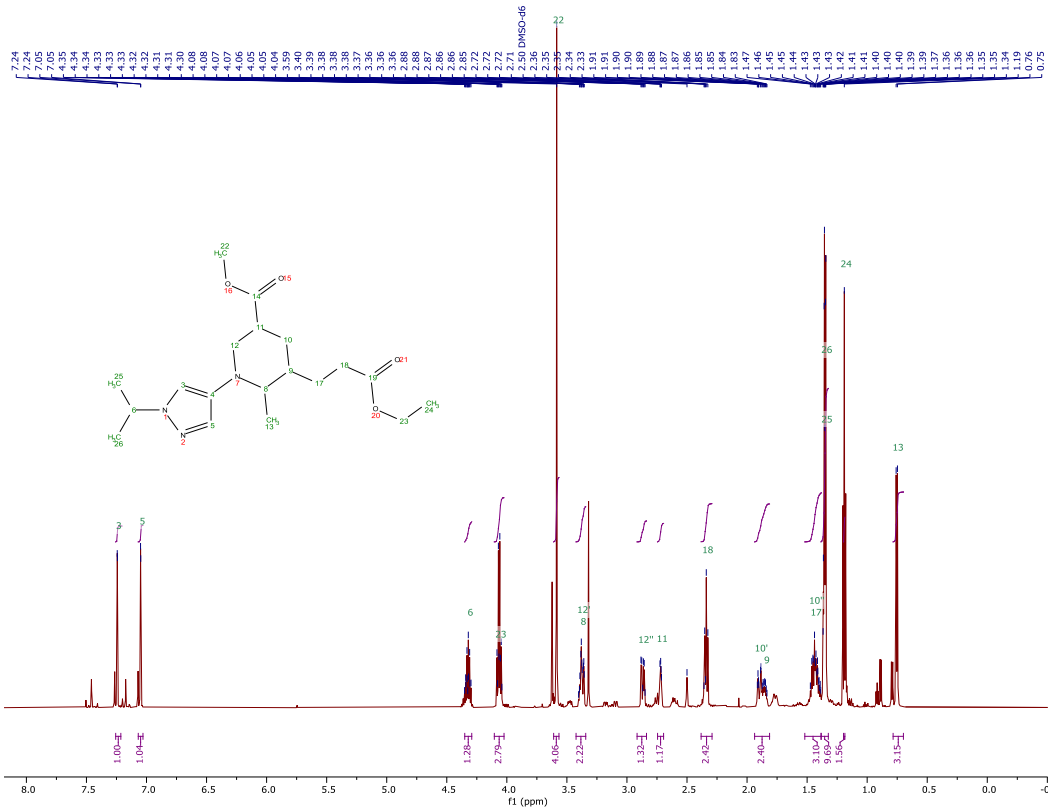
DMSO-d6
f1 (ppm)

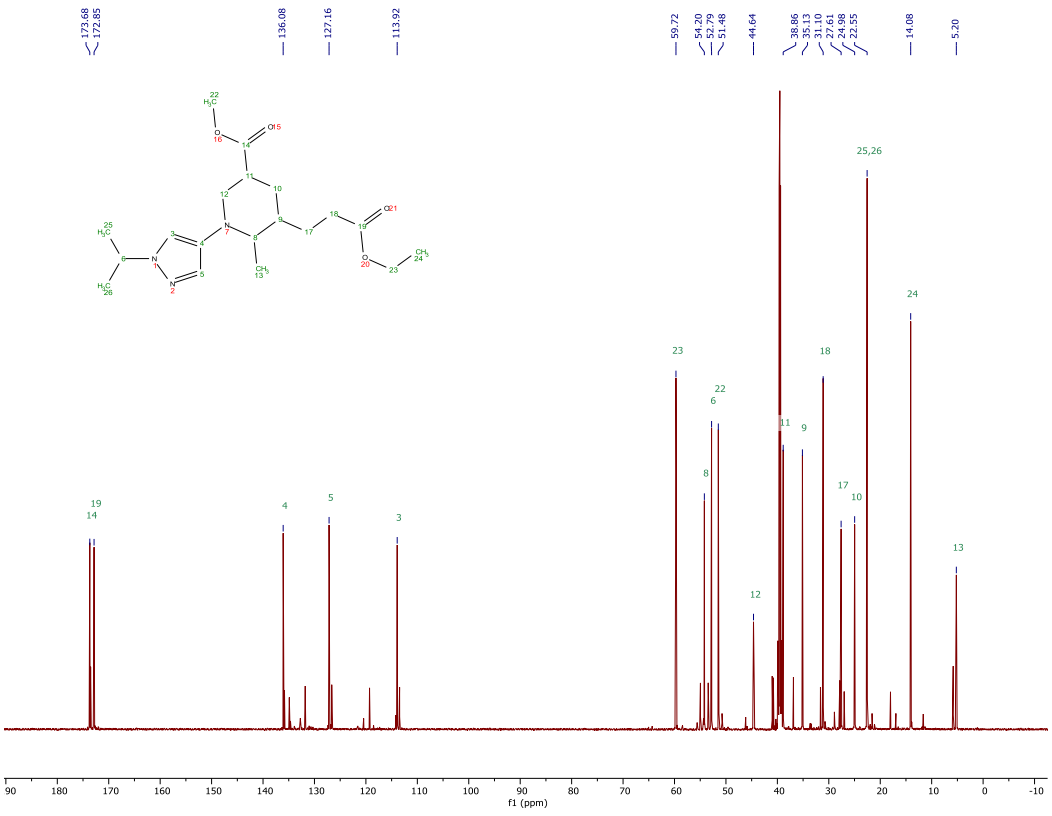
f1 (ppm)

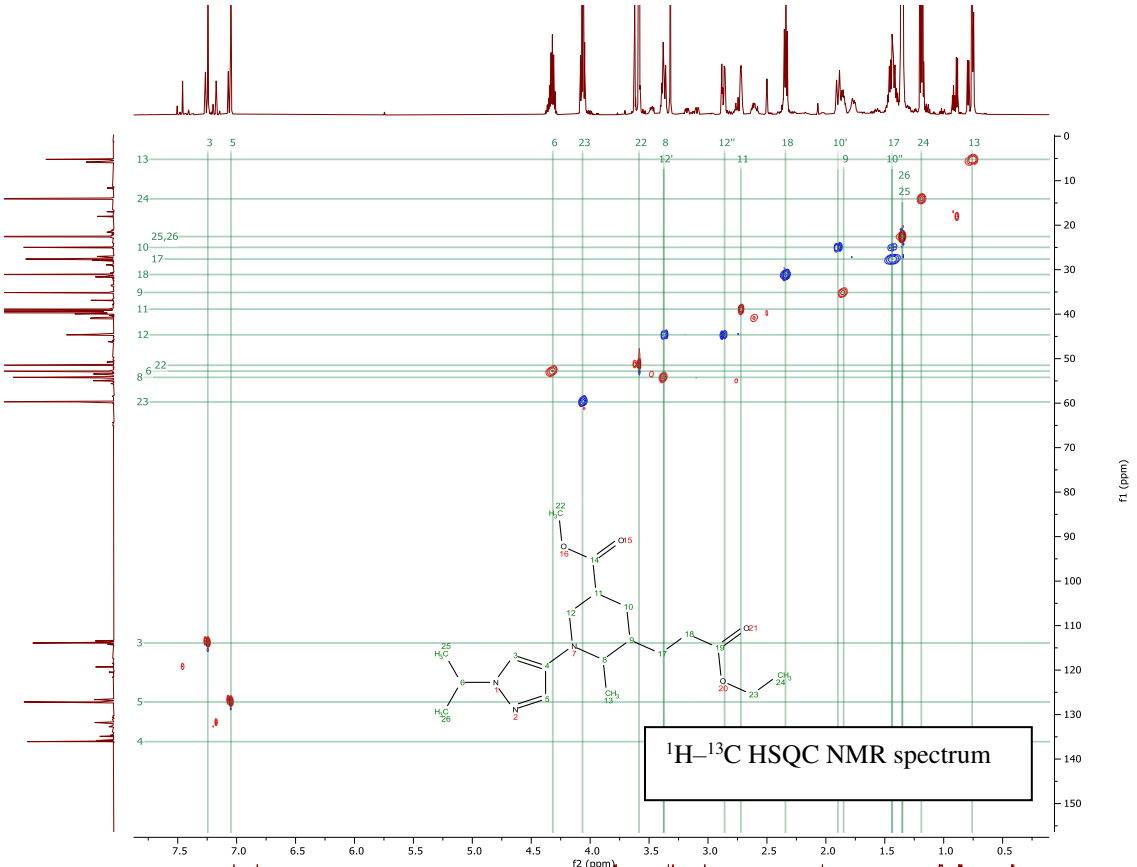
f2 (ppm)
f1 (ppm)
^{1}H–^{13}C HSQC NMR spectrum

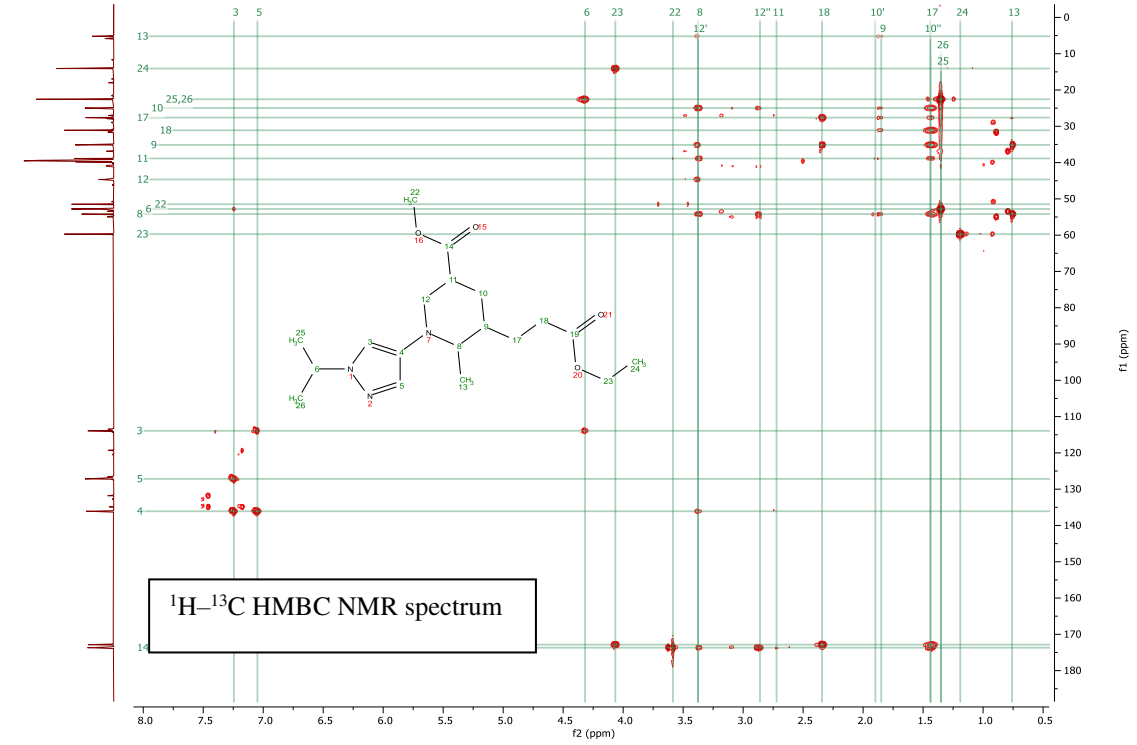
f2 (ppm)
f1 (ppm)
^{1}H–^{13}C HMBC NMR spectrum

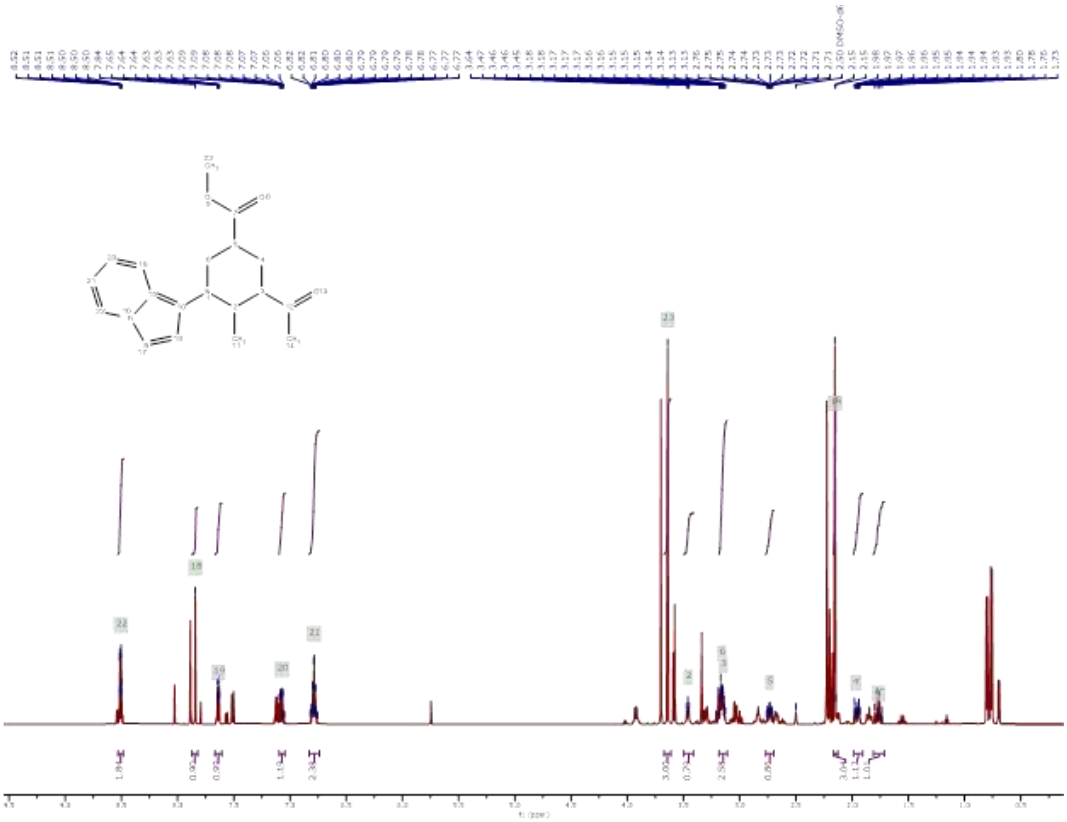

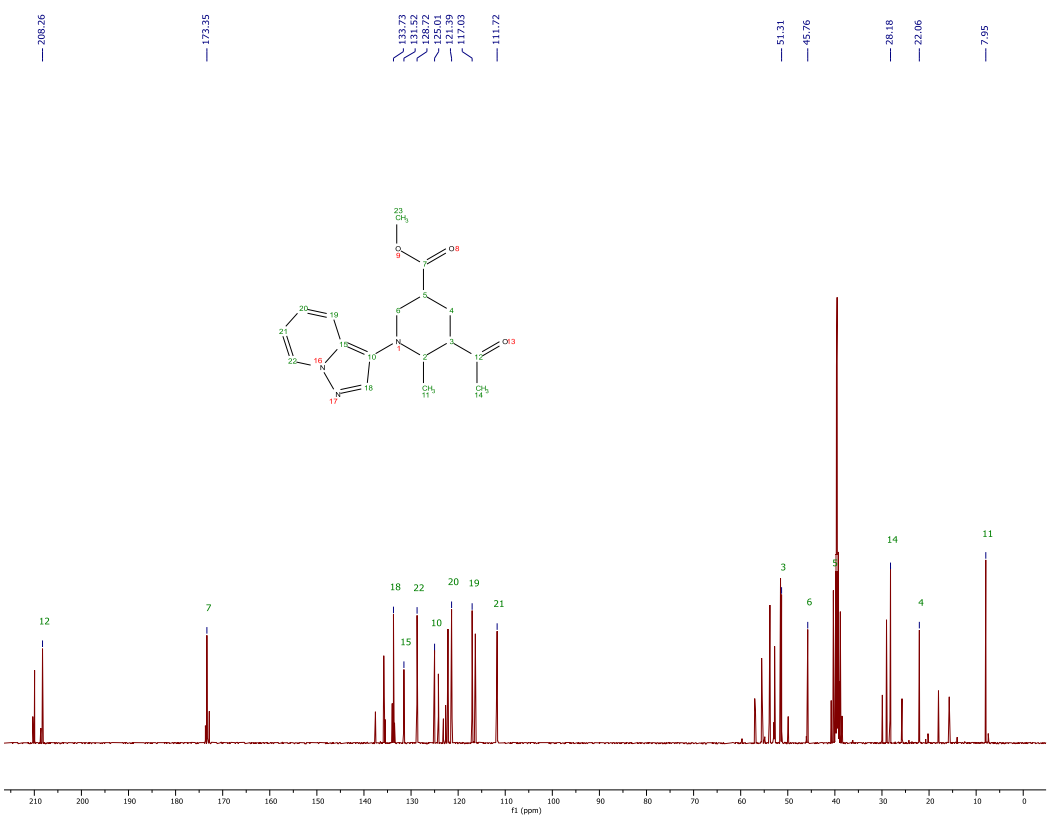

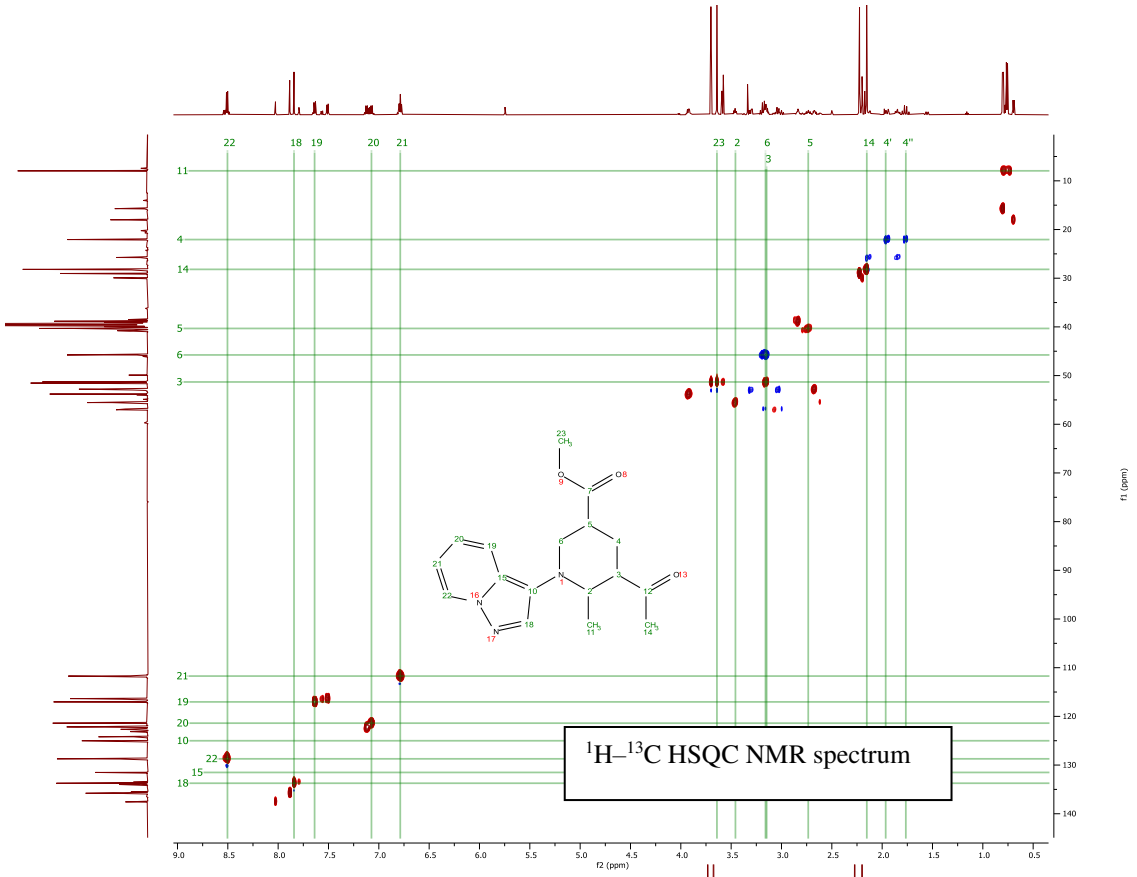
$^{1}H–^{13}C$ HSQC NMR spectrum

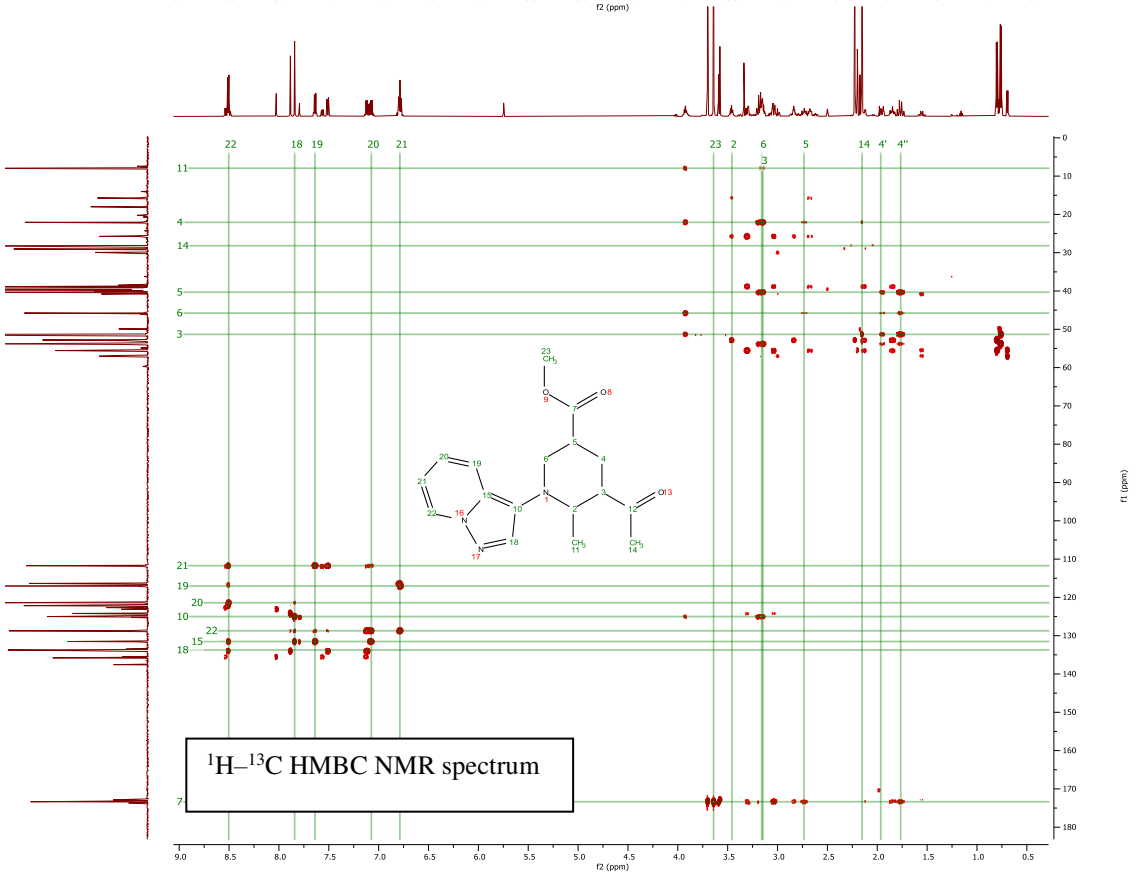
$^{1}H–^{13}C$ HMBC NMR spectrum

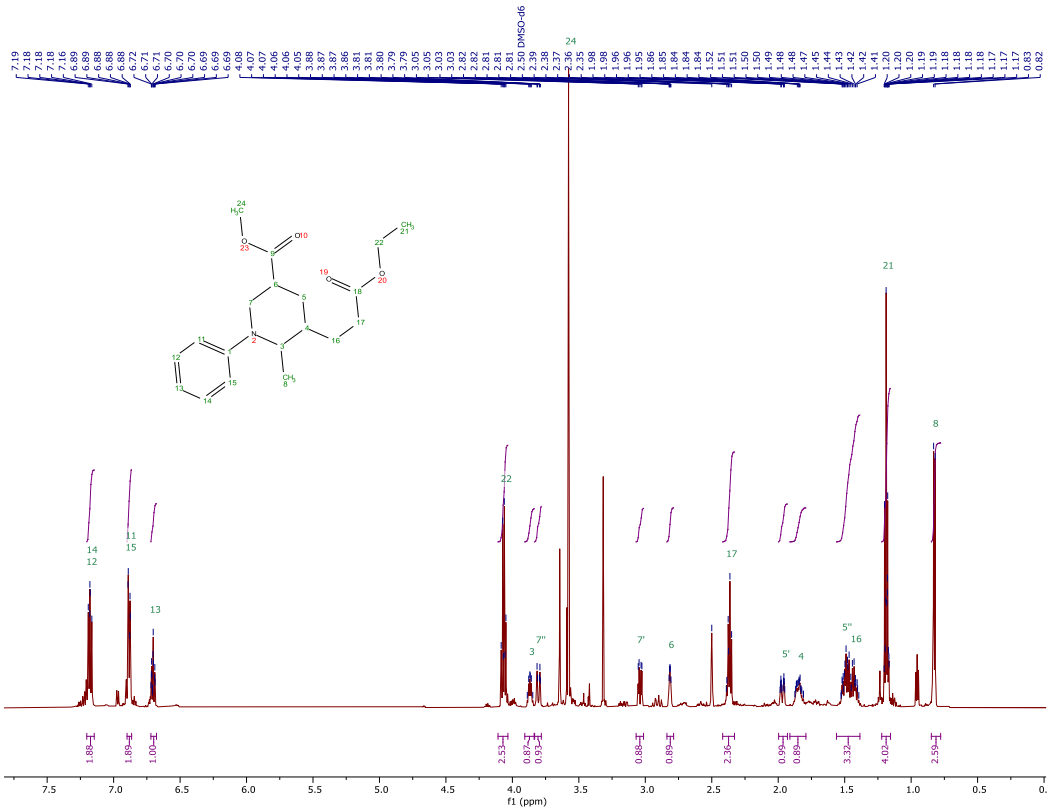
DMSO-d6
f1 (ppm)

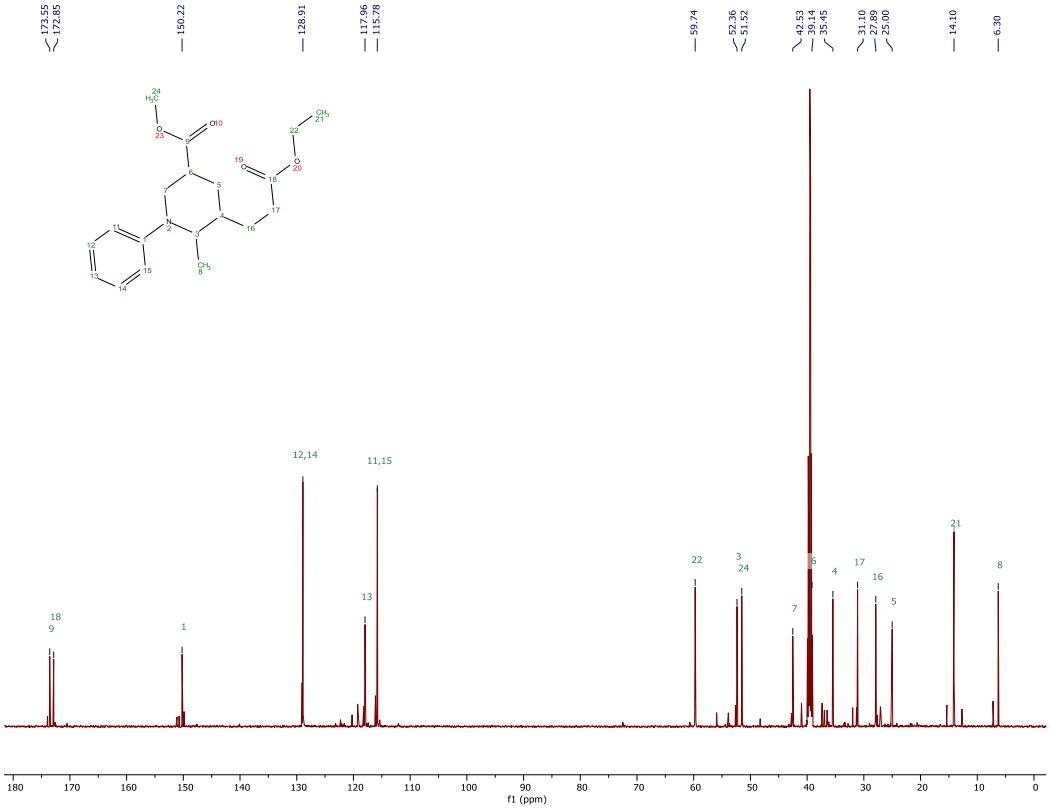
f1 (ppm)

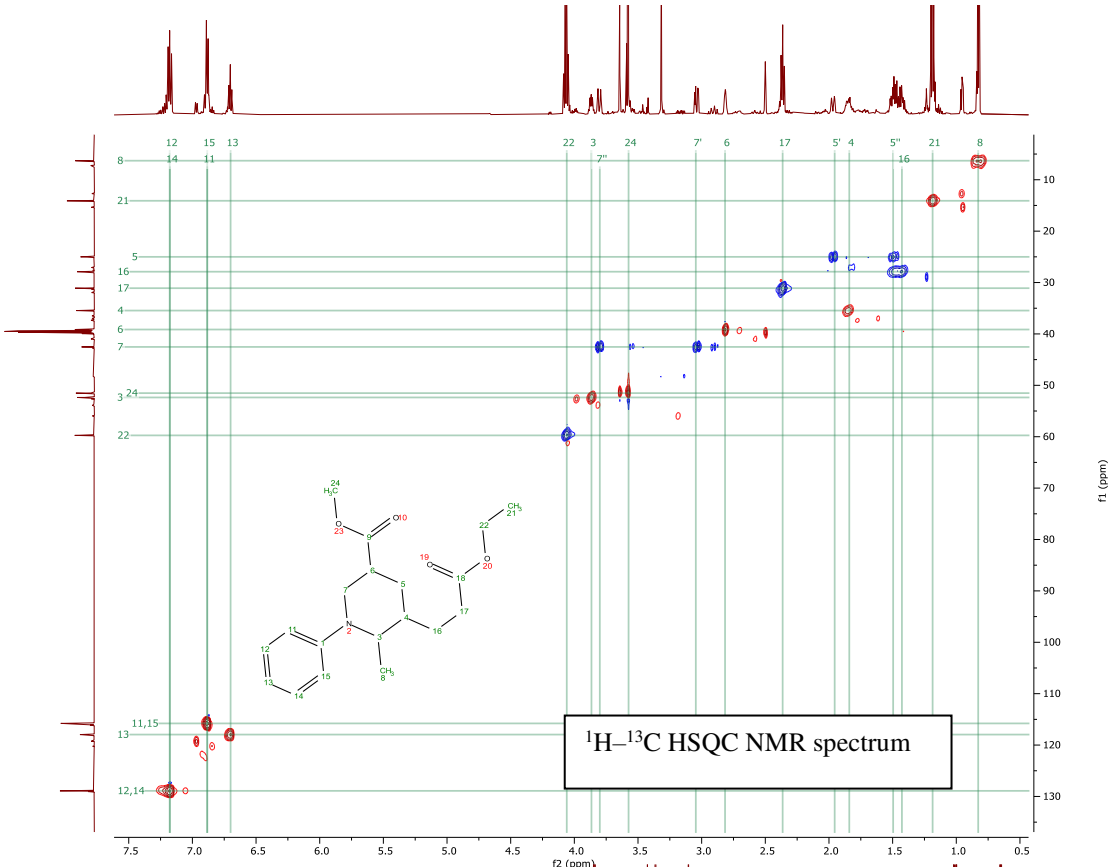
f2 (ppm)
f1 (ppm)
$^{1}H–^{13}C$ HSQC NMR spectrum

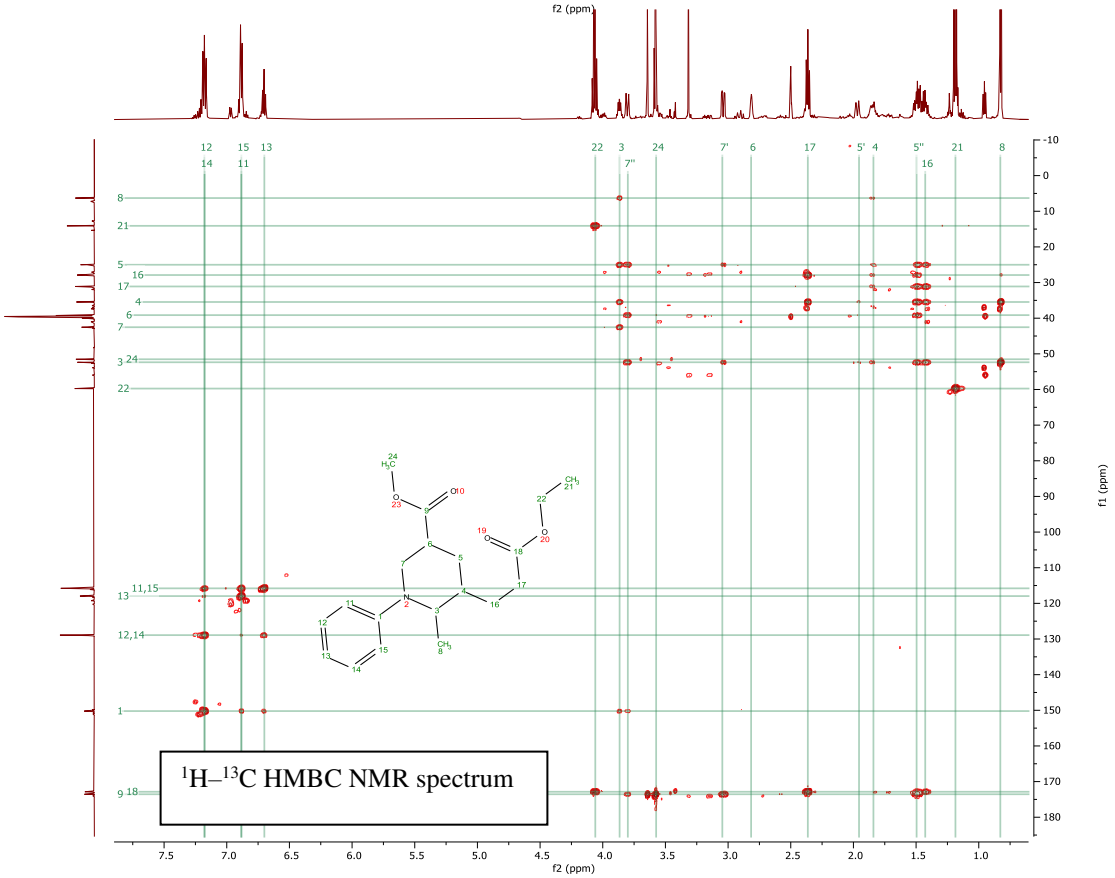
f2 (ppm)
f1 (ppm)
$^{1}H–^{13}C$ HMBC NMR spectrum

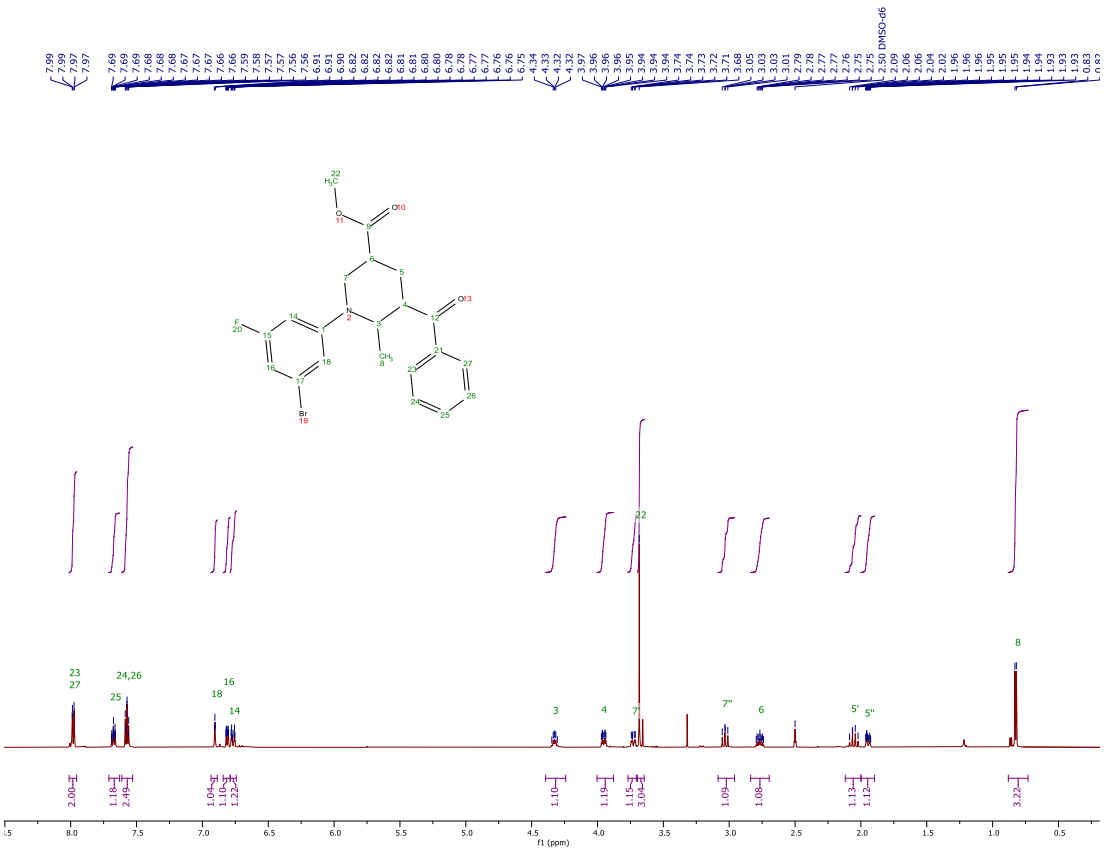

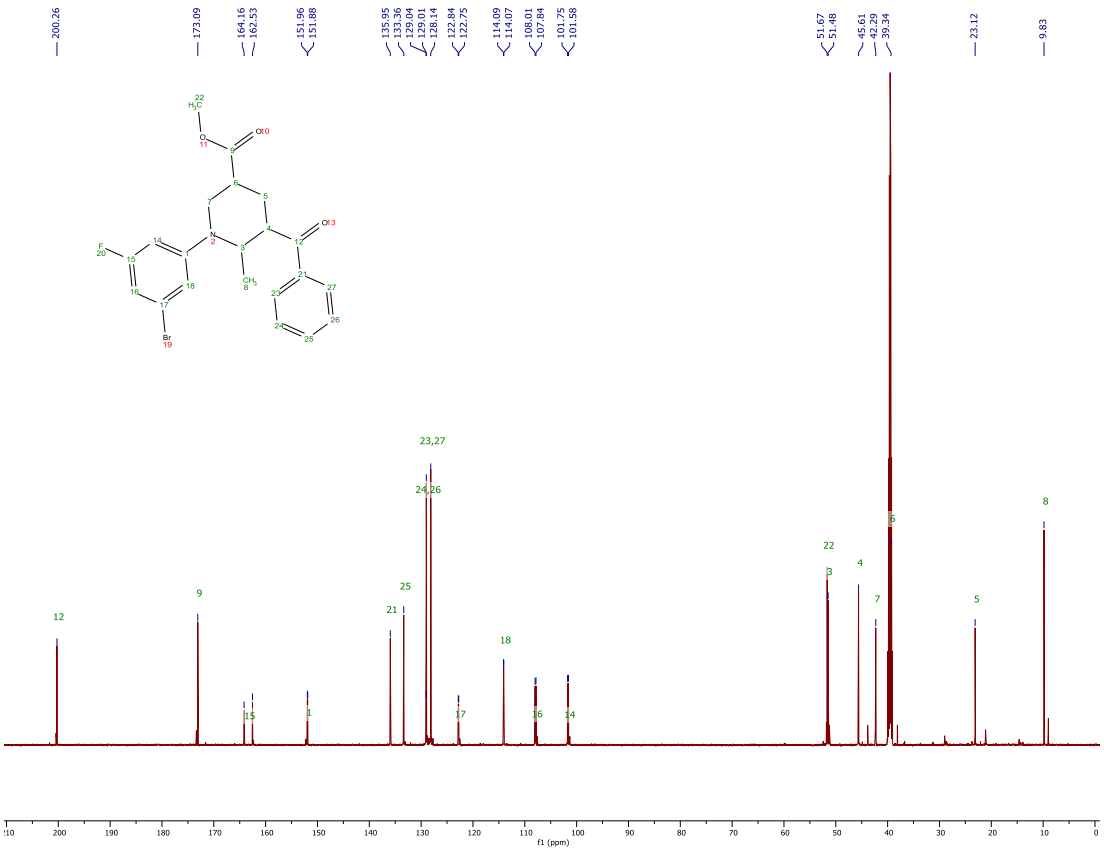

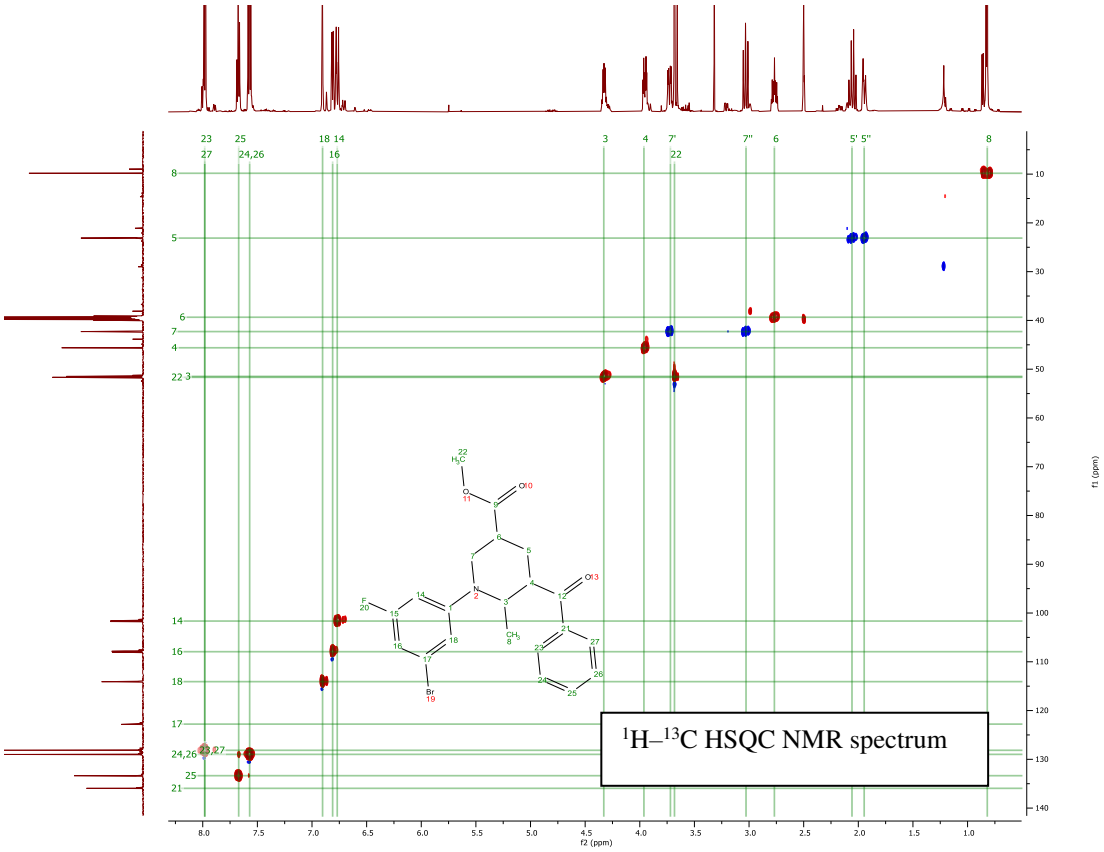
$^{1}H–^{13}C$ HSQC NMR spectrum
f2 (ppm)
f1 (ppm)

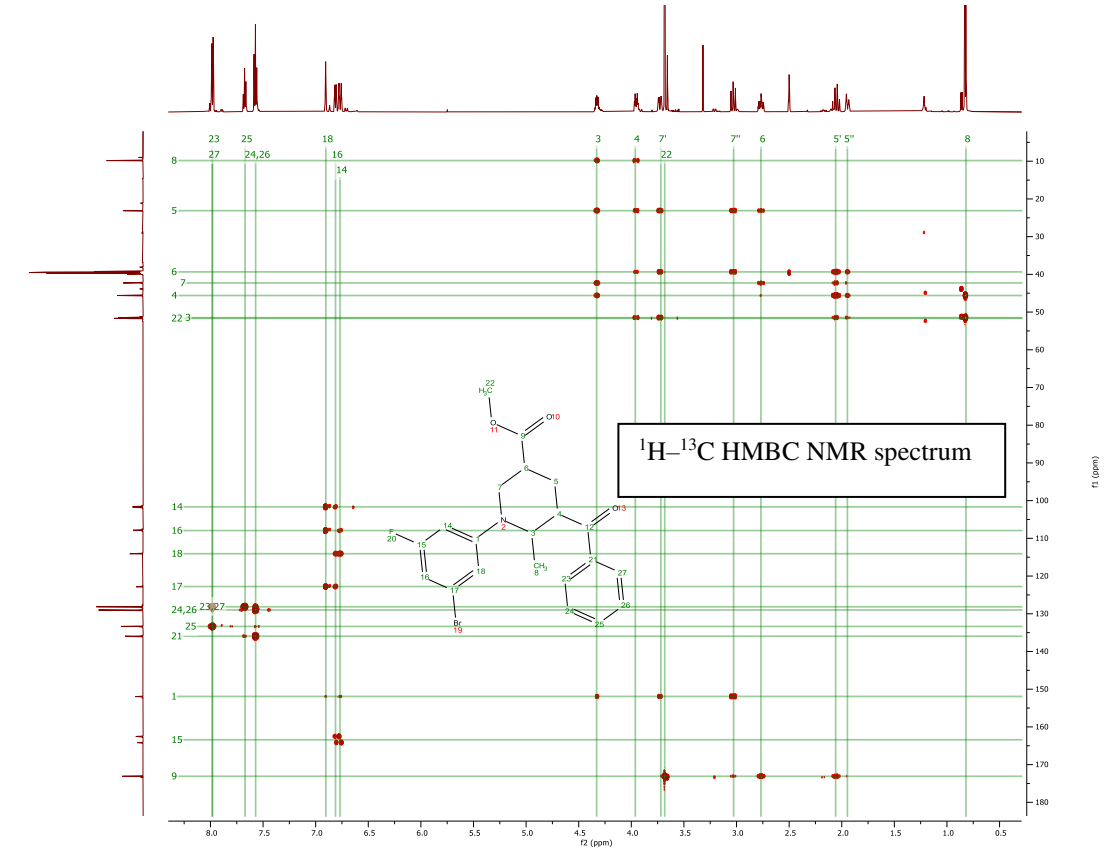
$^{1}H–^{13}C$ HMBC NMR spectrum
f2 (ppm)
f1 (ppm)

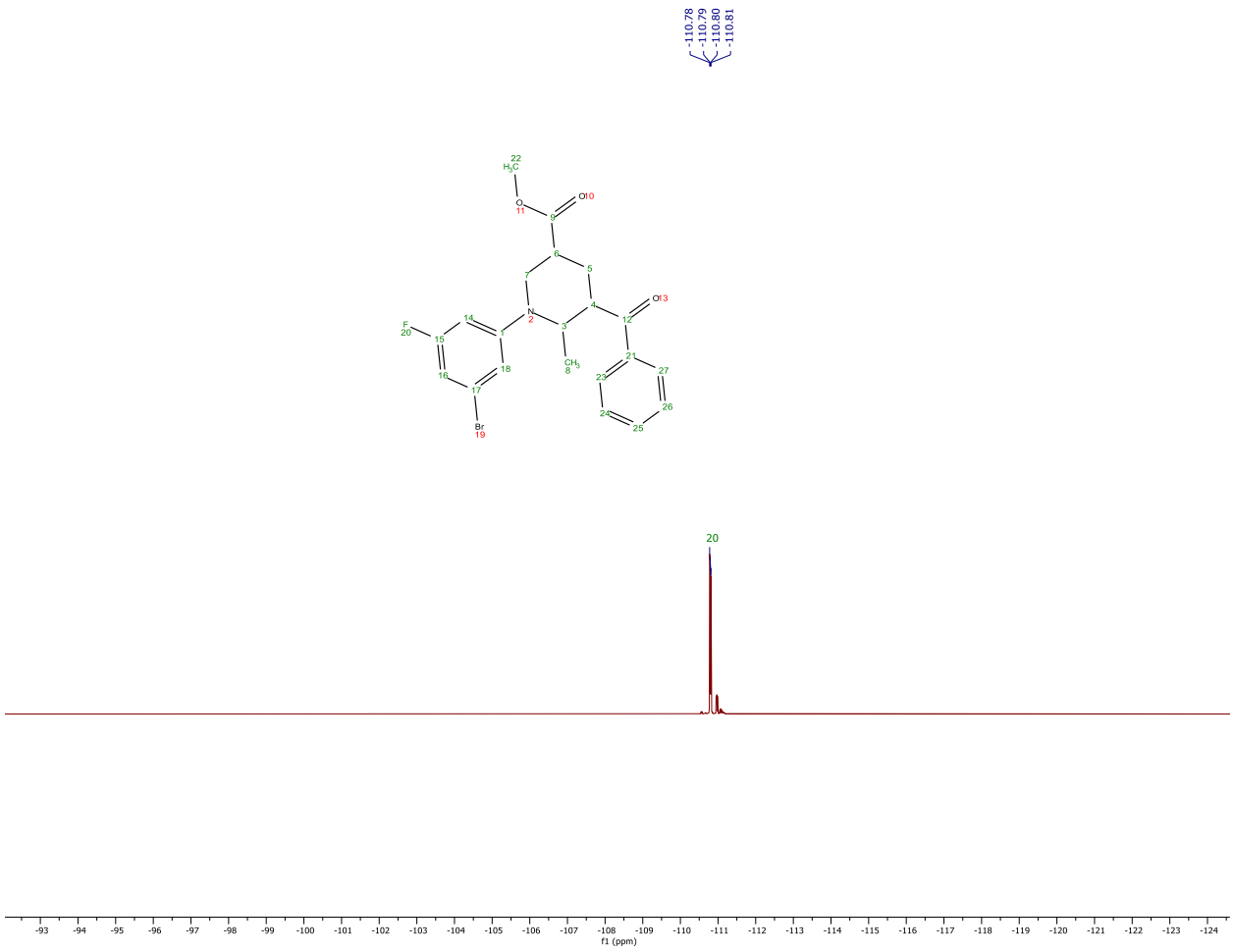
-110.78
-110.79
-110.80
-110.81
22
H3C
O
11
O10
9
8
7
6
5
4
O13
12
N
2
3
1
14
F
20
15
16
17
Br
19
18
CH3
8
21
23
27
24
26
25
20
-93
-94
-95
-96
-97
-98
-99
-100
-101
-102
-103
-104
-105
-106
-107
-108
-109
-110
-111
-112
-113
-114
-115
-116
-117
-118
-119
-120
-121
-122
-123
-124
f1 (ppm)

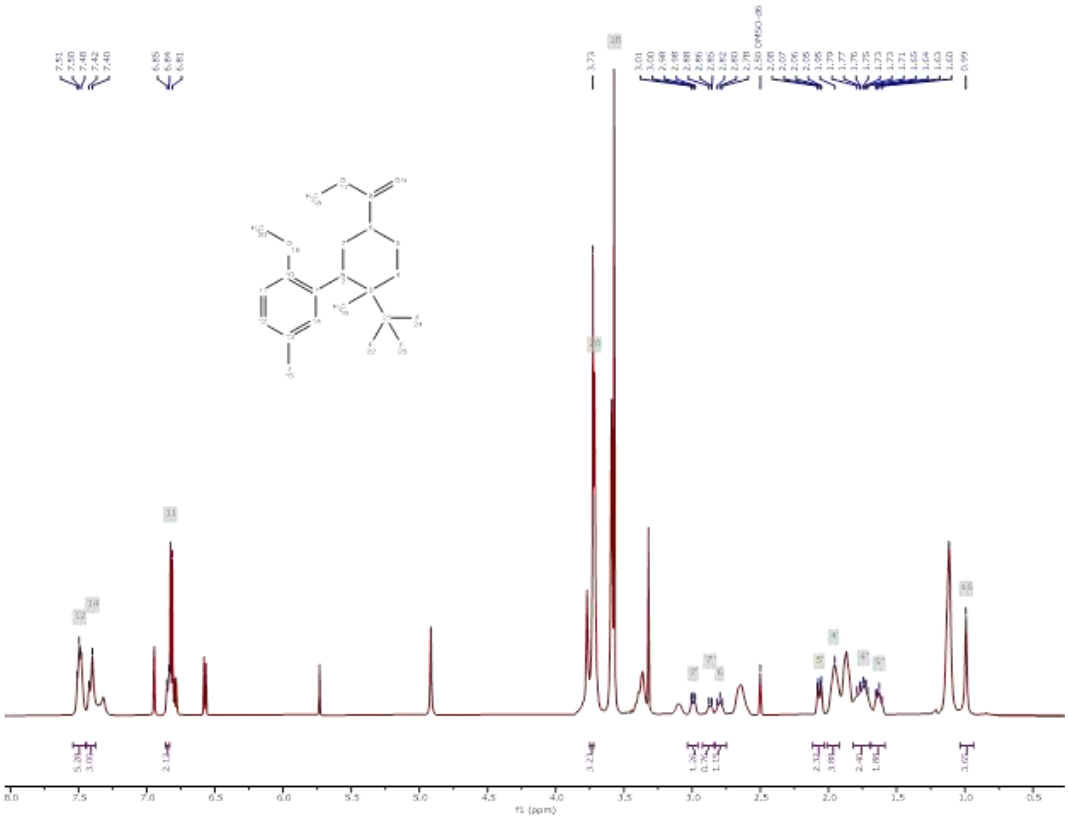

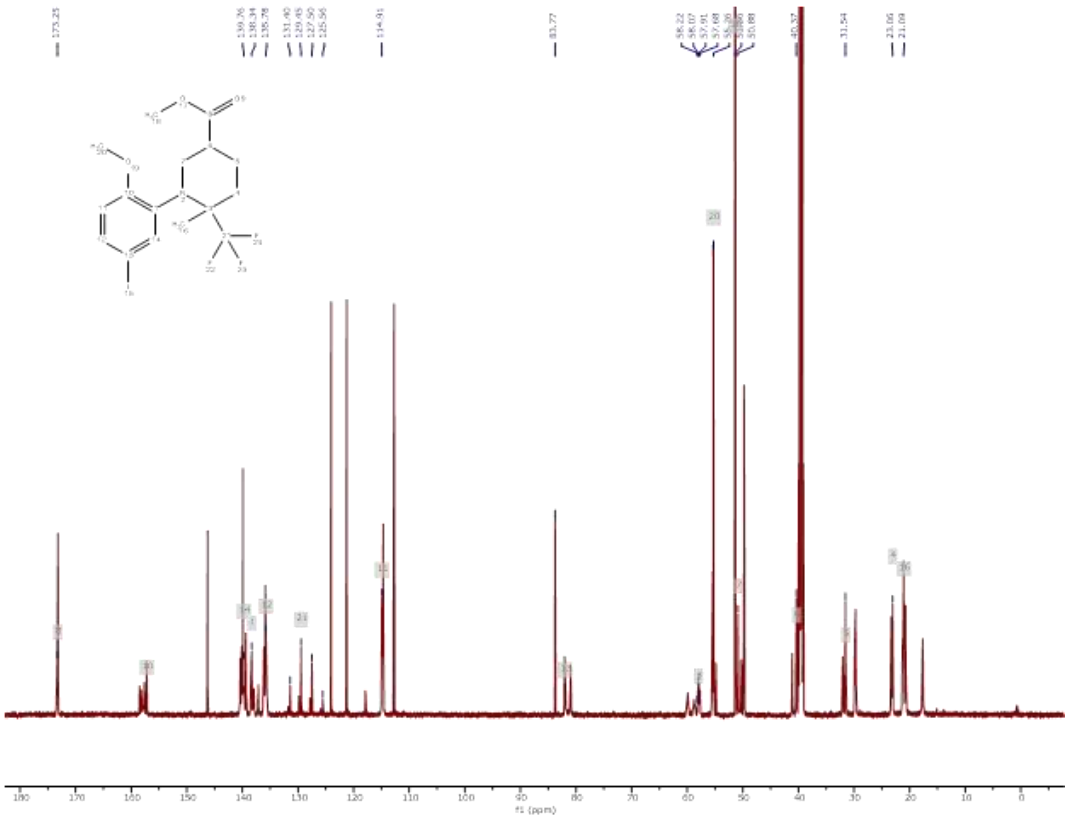

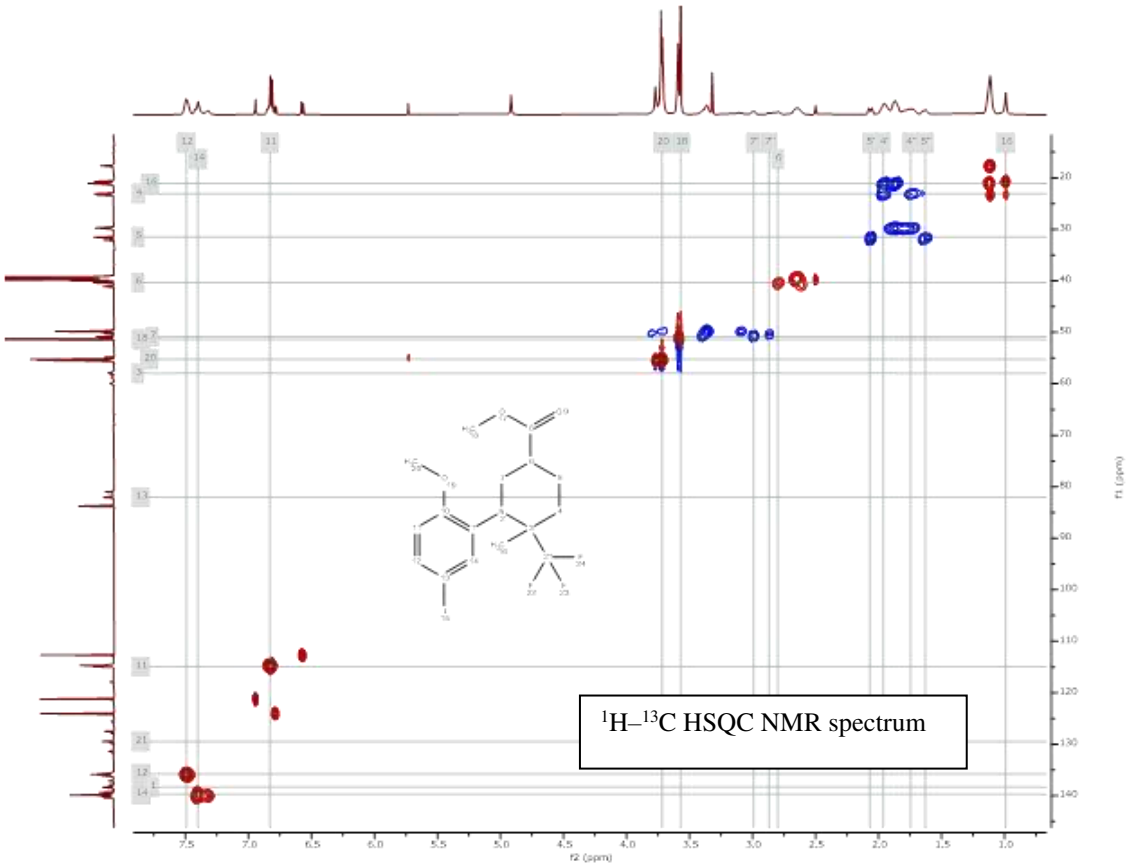
$^{1}H–^{13}C$ HSQC NMR spectrum

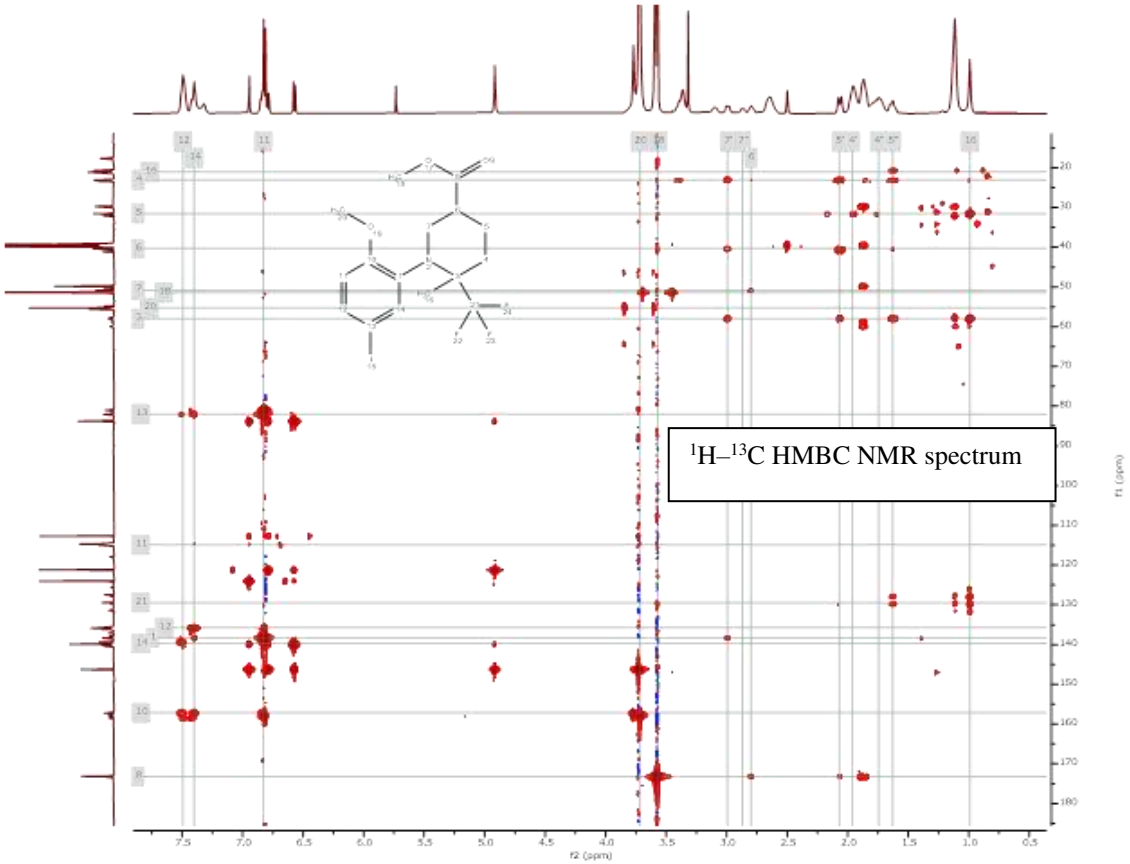
$^{1}H–^{13}C$ HMBC NMR spectrum

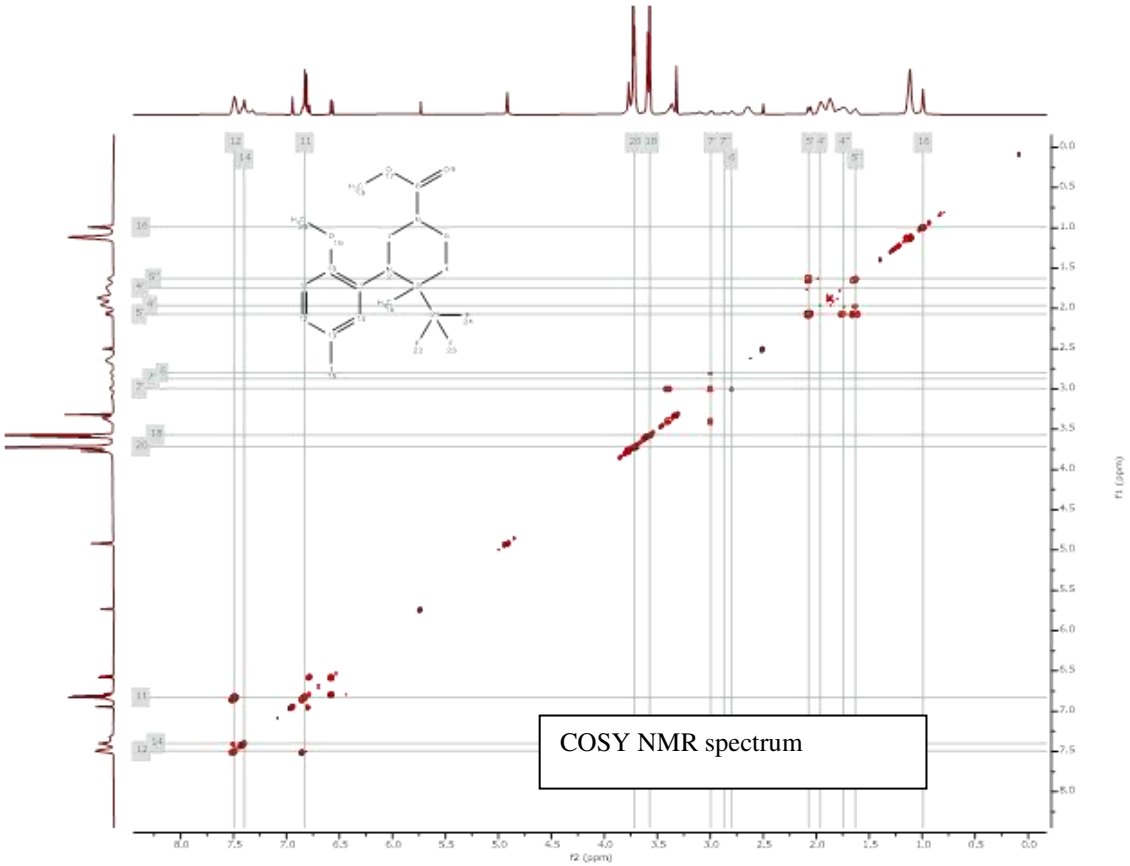
COSY NMR spectrum

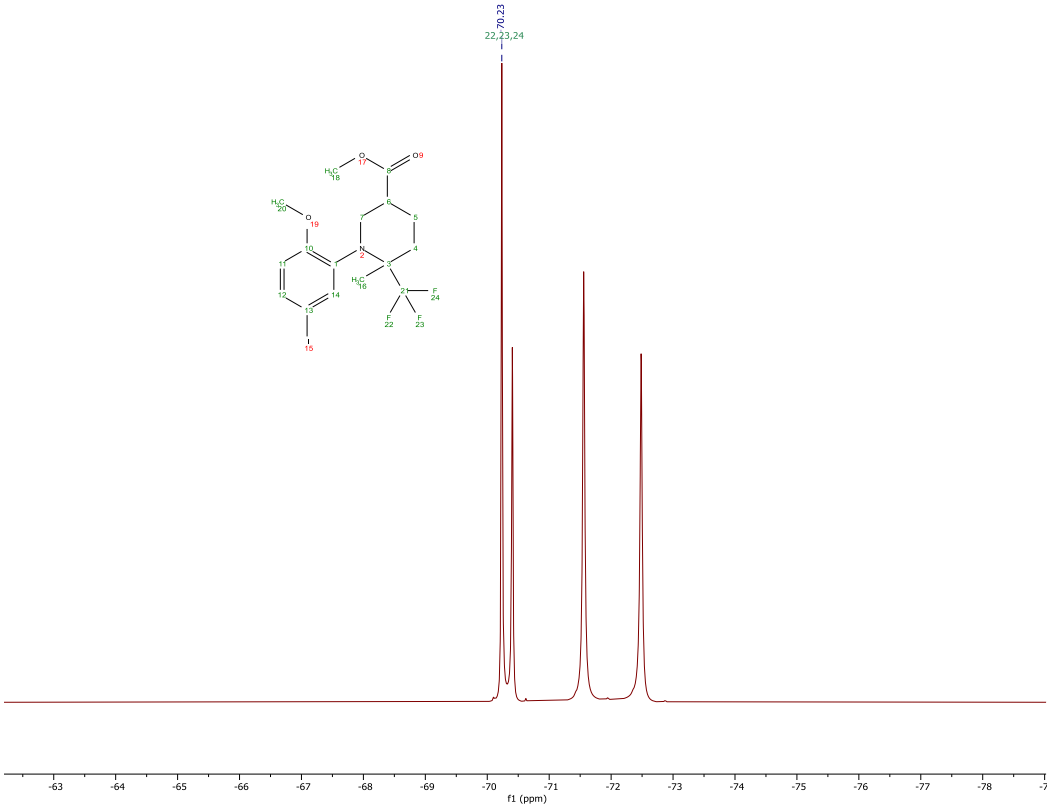
-70.23
22,23,24
f1 (ppm)

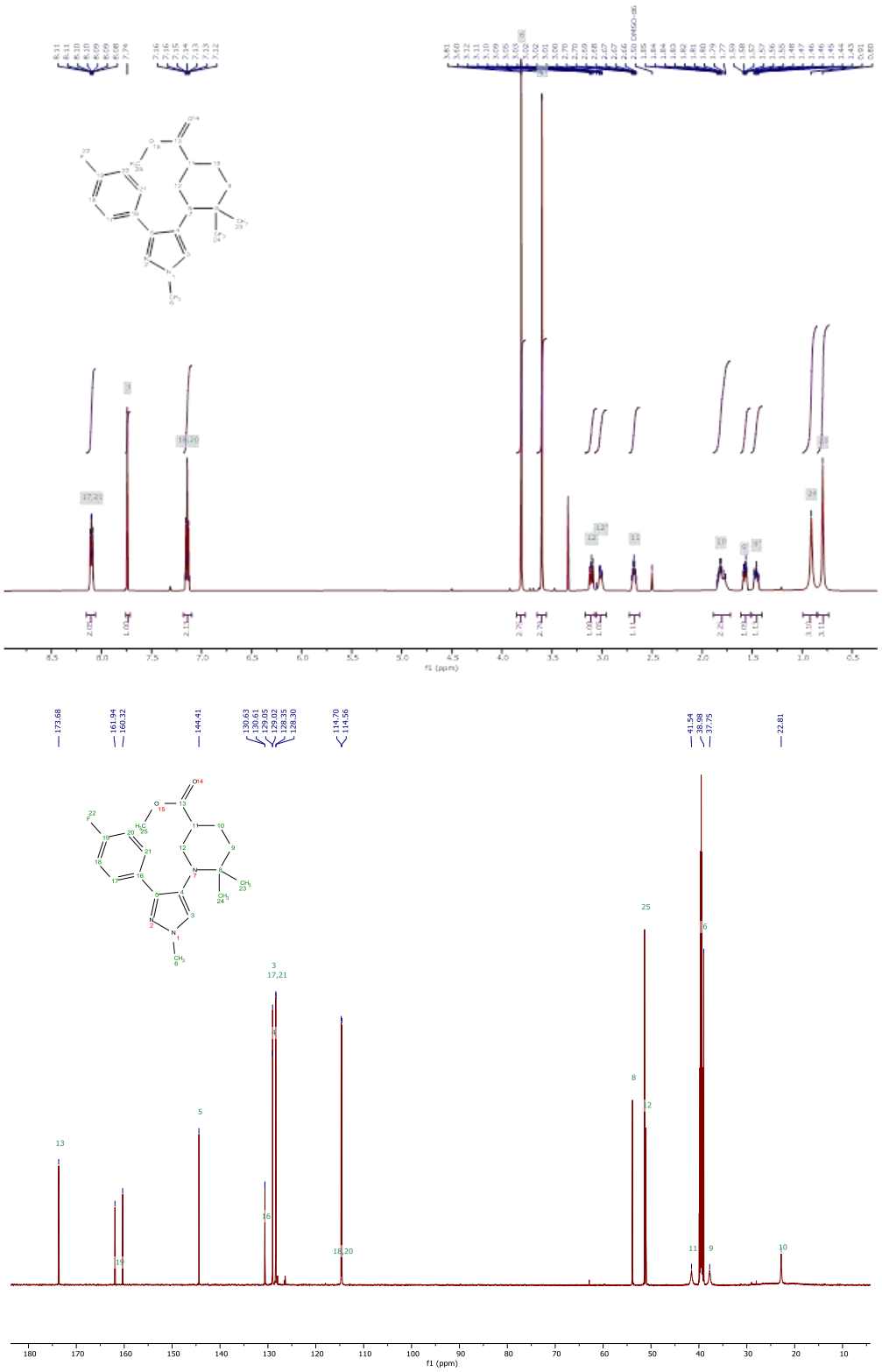

The two methyl carbons on the piperidine ring are believed to have broadened into the baseline.

Notice how carbons 9 and 11 are broad as well.

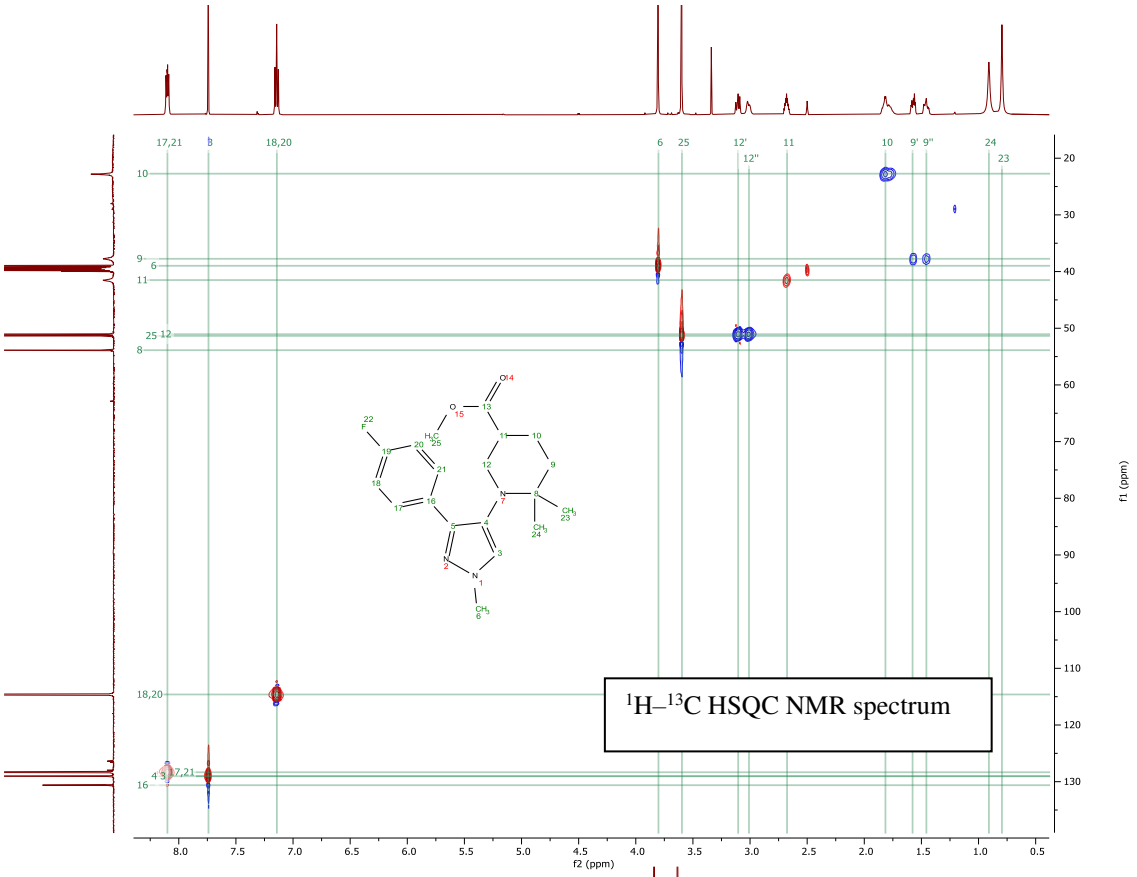
$^{1}H–^{13}C$ HSQC NMR spectrum
f2 (ppm)
f1 (ppm)

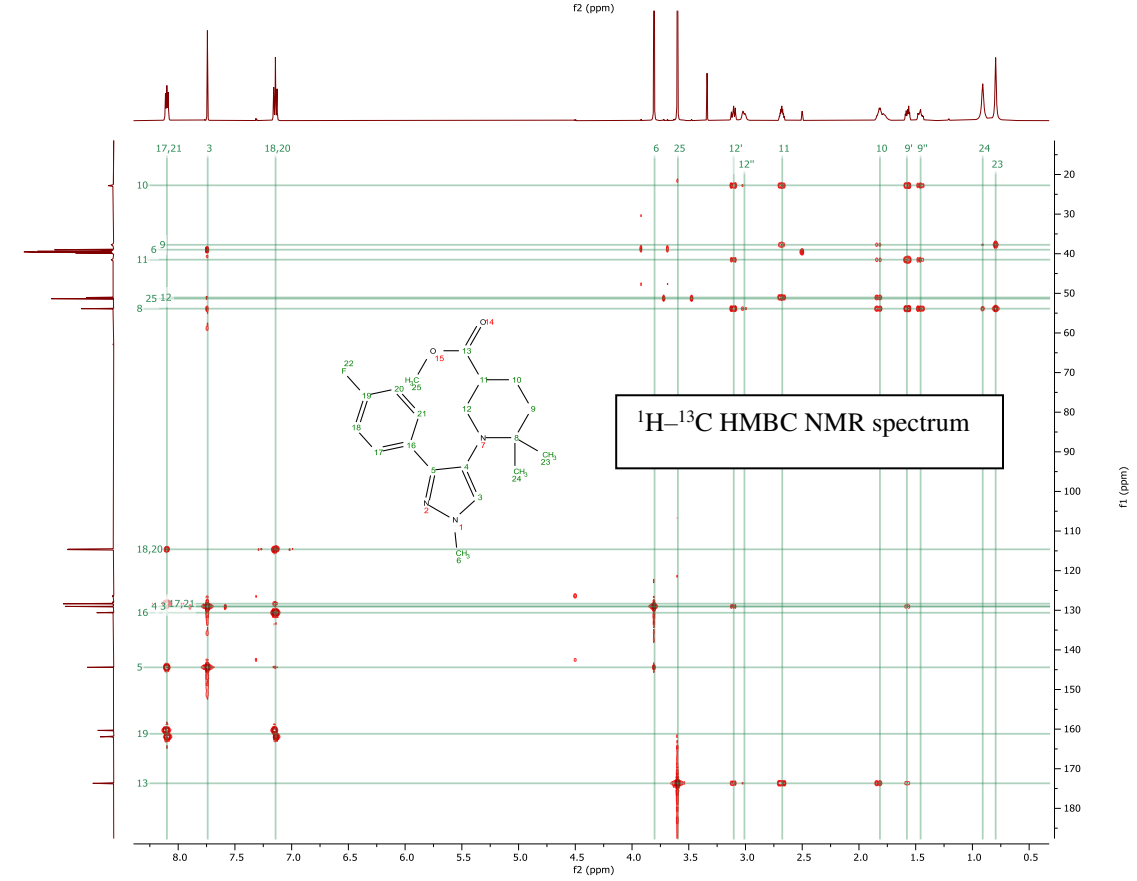
$^{1}H–^{13}C$ HMBC NMR spectrum
f2 (ppm)
f1 (ppm)

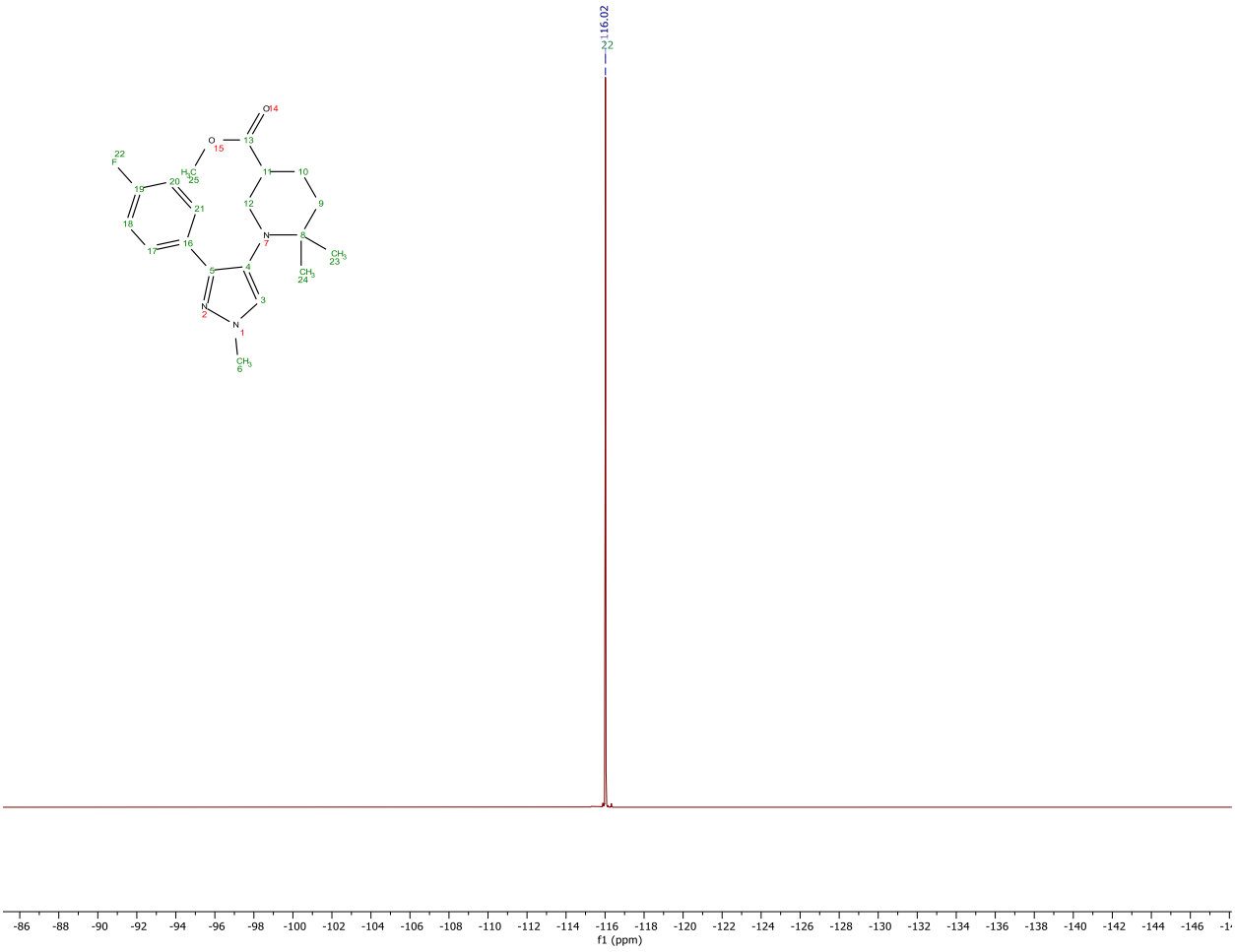
-116.02
-86 -88 -90 -92 -94 -96 -98 -100 -102 -104 -106 -108 -110 -112 -114 -116 -118 -120 -122 -124 -126 -128 -130 -132 -134 -136 -138 -140 -142 -144 -146
f1 (ppm)

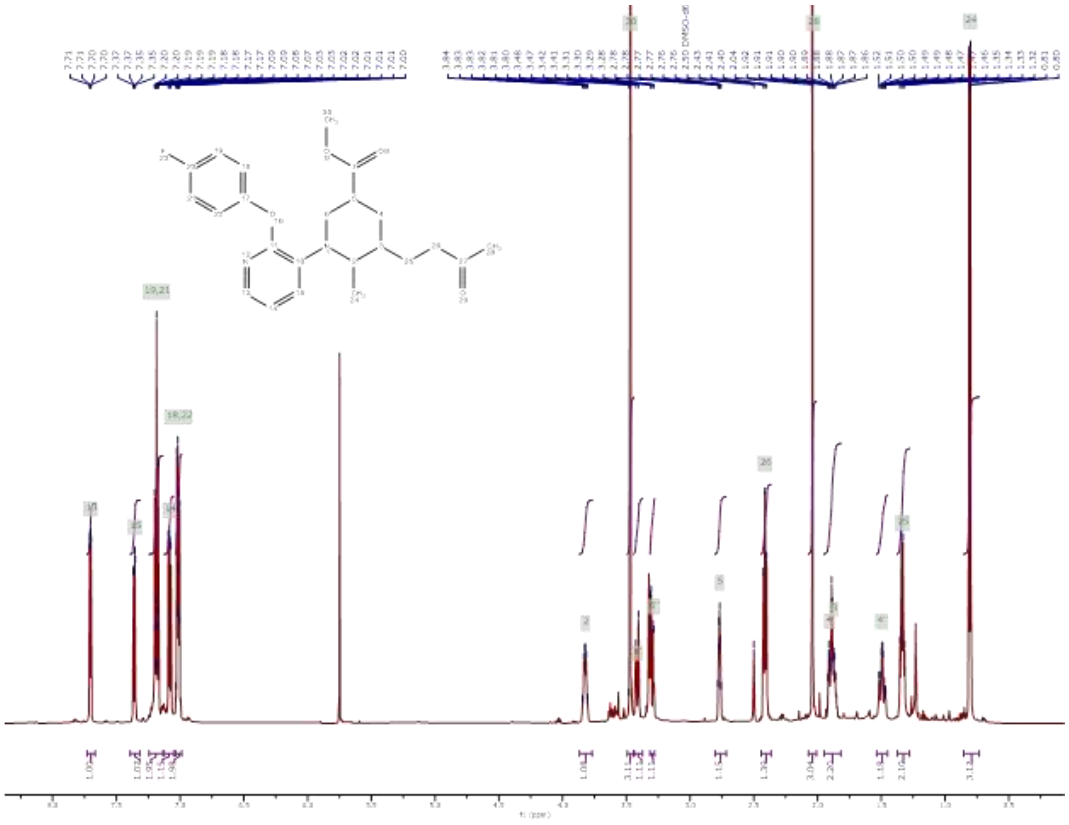

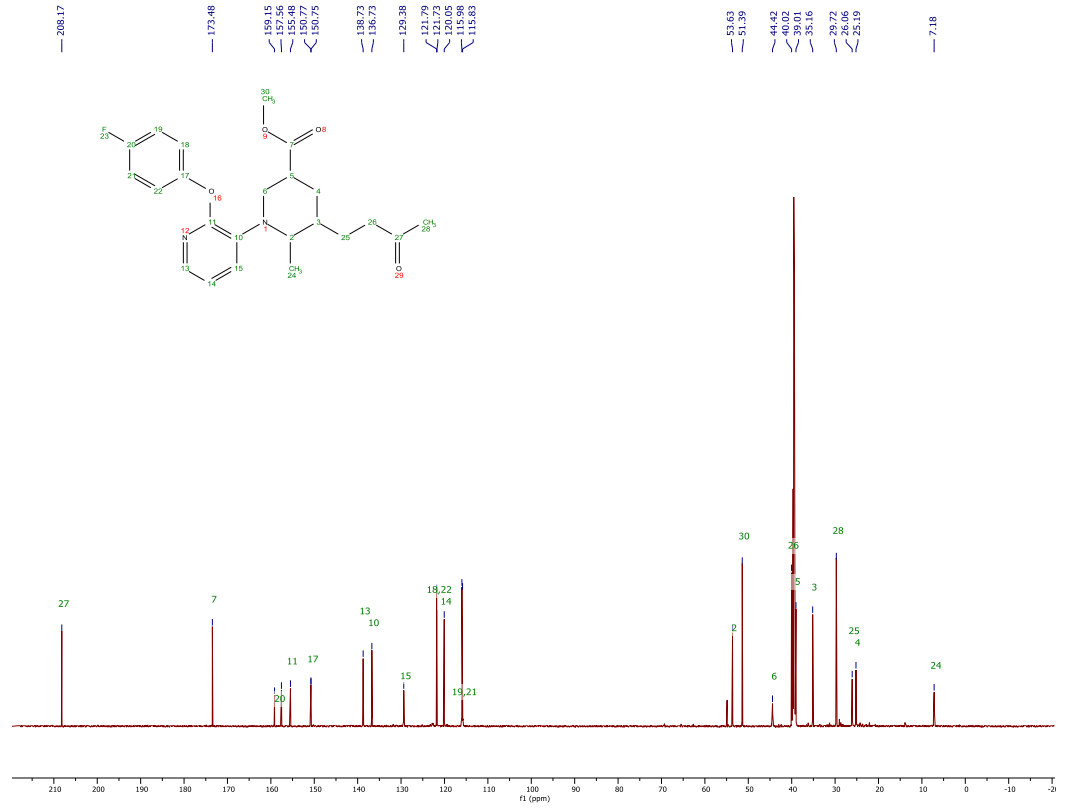

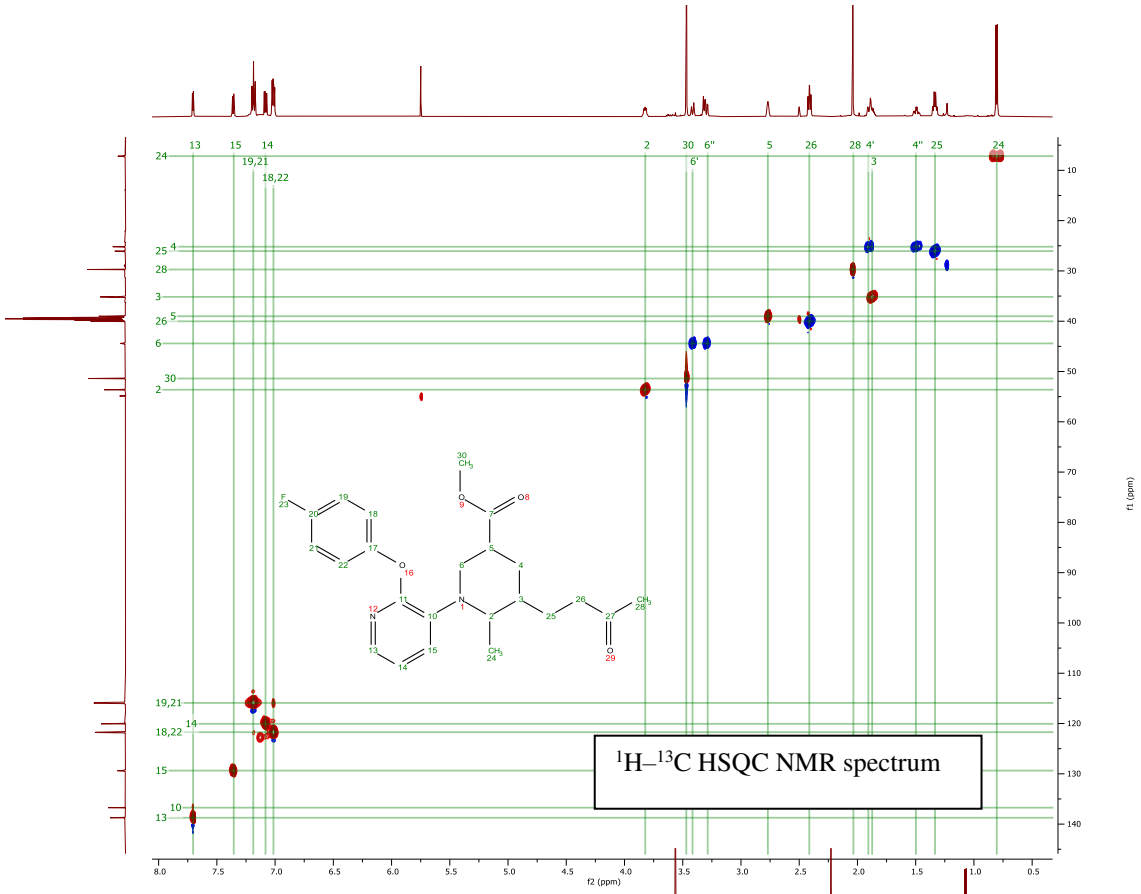
$^{1}H–^{13}C$ HSQC NMR spectrum

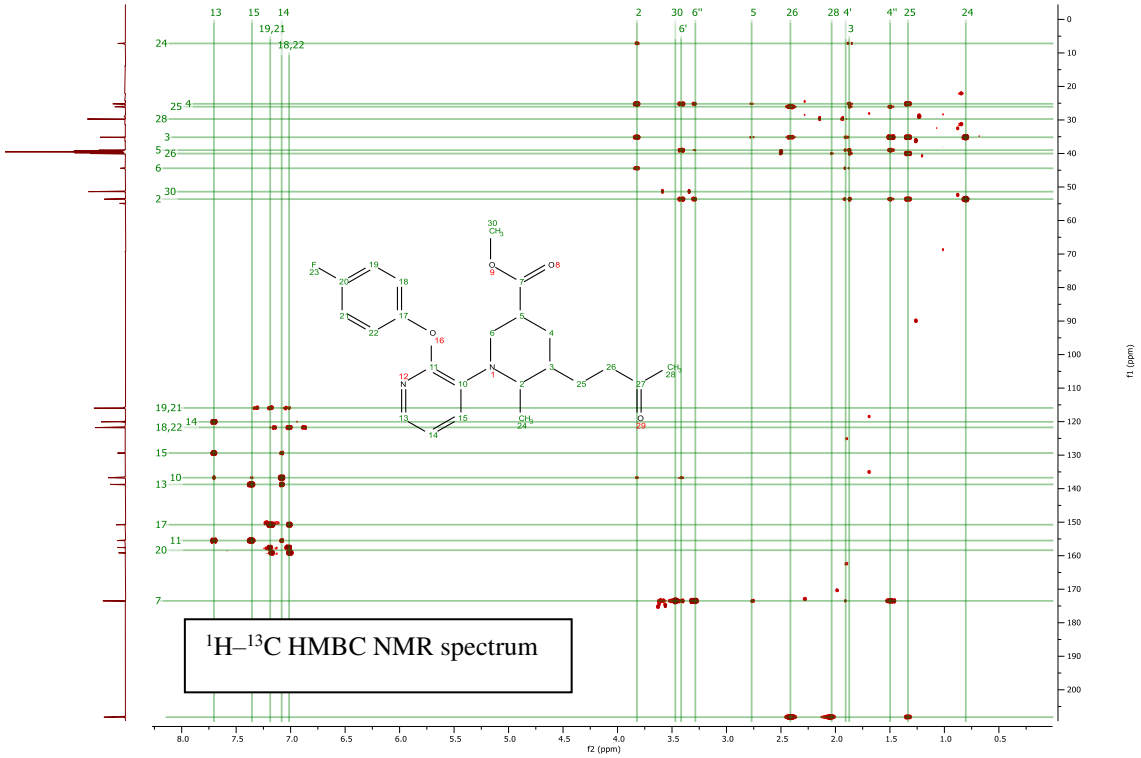
$^{1}H–^{13}C$ HMBC NMR spectrum

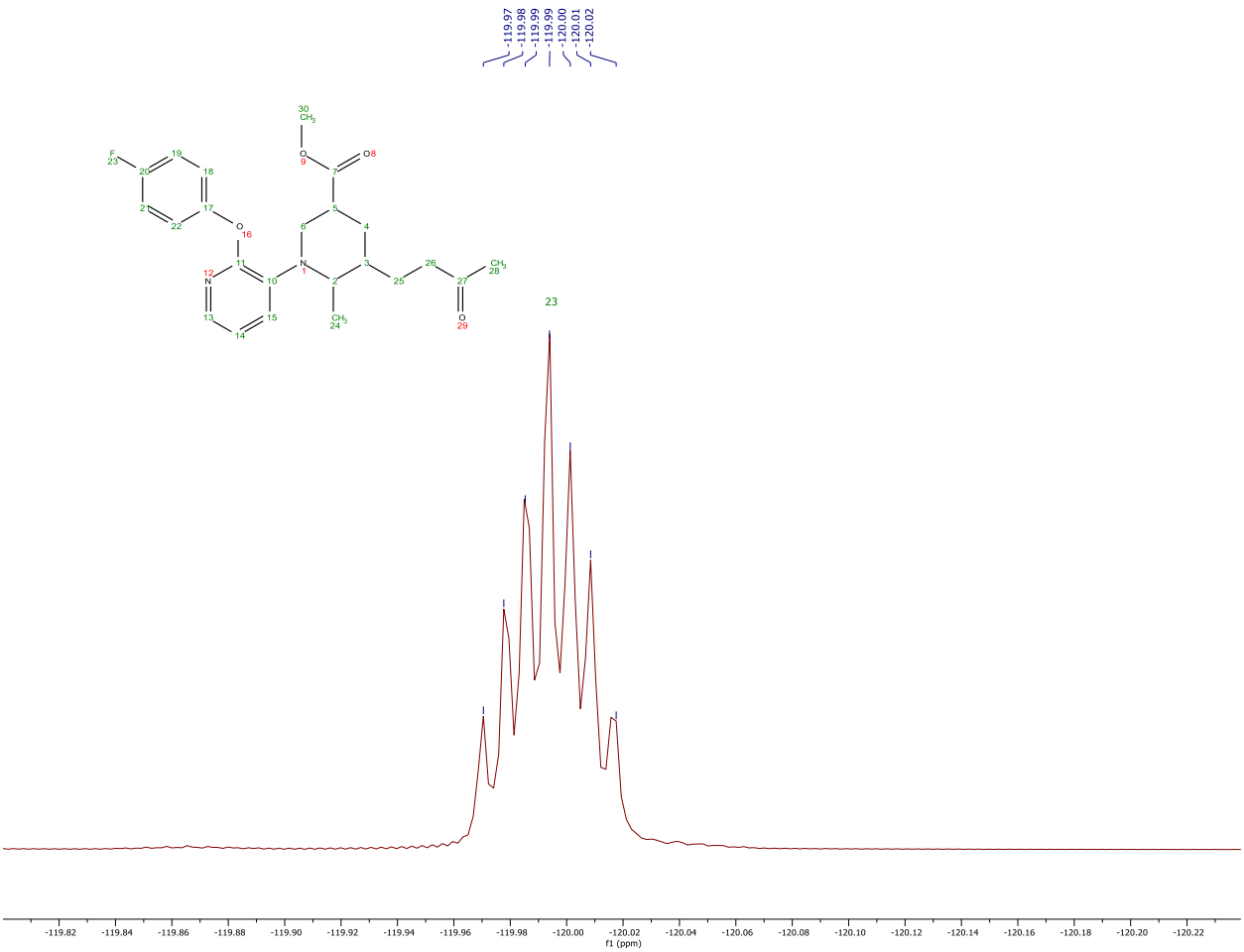
-119.97
-119.98
-119.99
-120.00
-120.01
-120.02
23
-119.82
-119.84
-119.86
-119.88
-119.90
-119.92
-119.94
-119.96
-119.98
-120.00
-120.02
-120.04
-120.06
-120.08
-120.10
-120.12
-120.14
-120.16
-120.18
-120.20
-120.22
f1 (ppm)

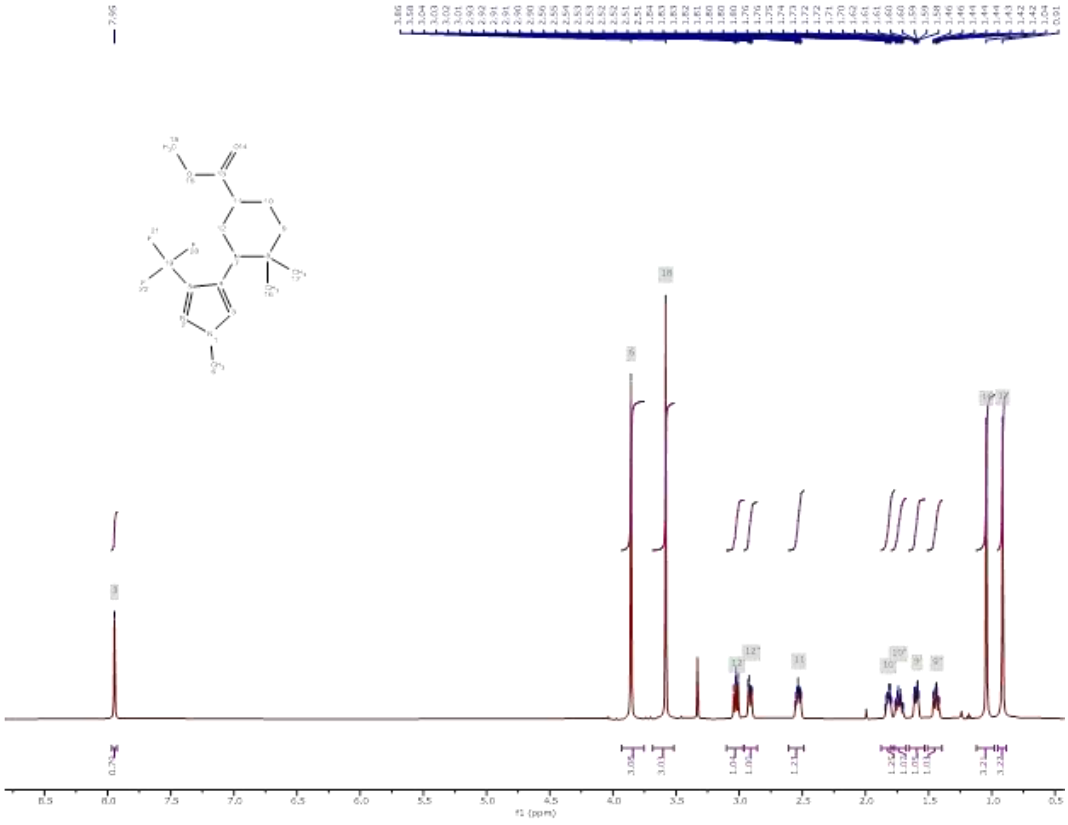

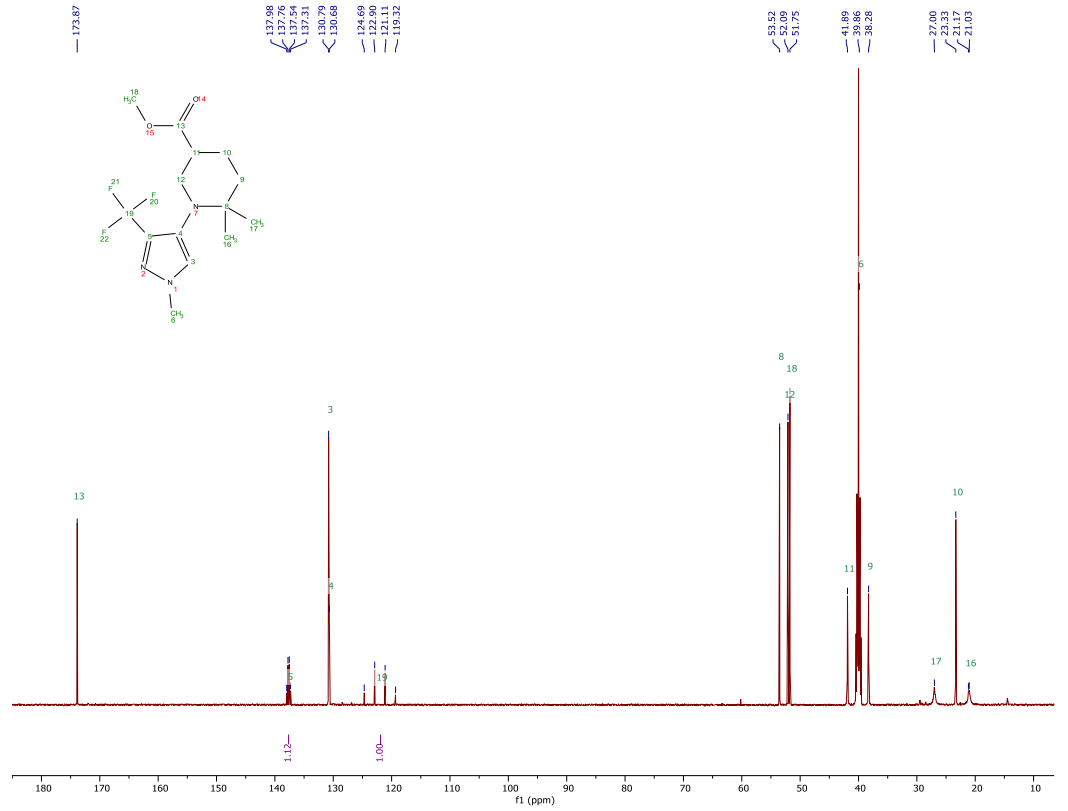

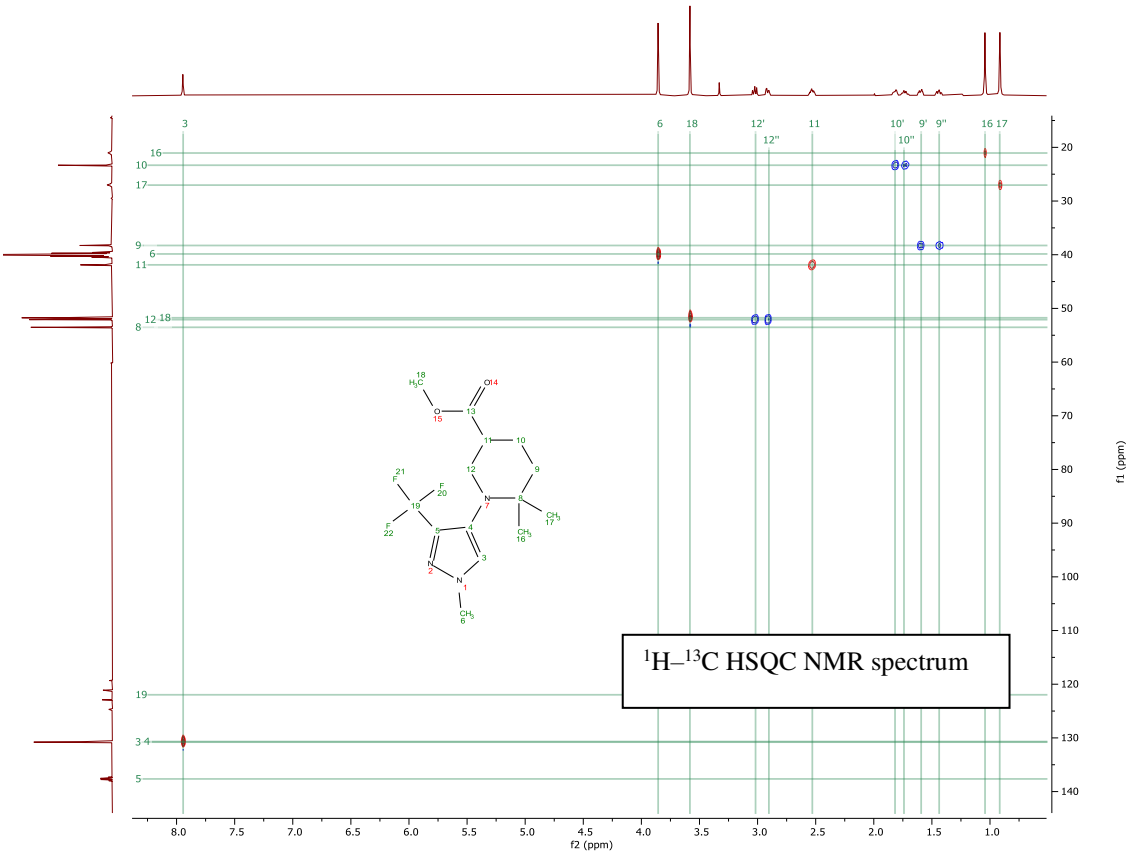

$^{1}H–^{13}C$ HSQC NMR spectrum

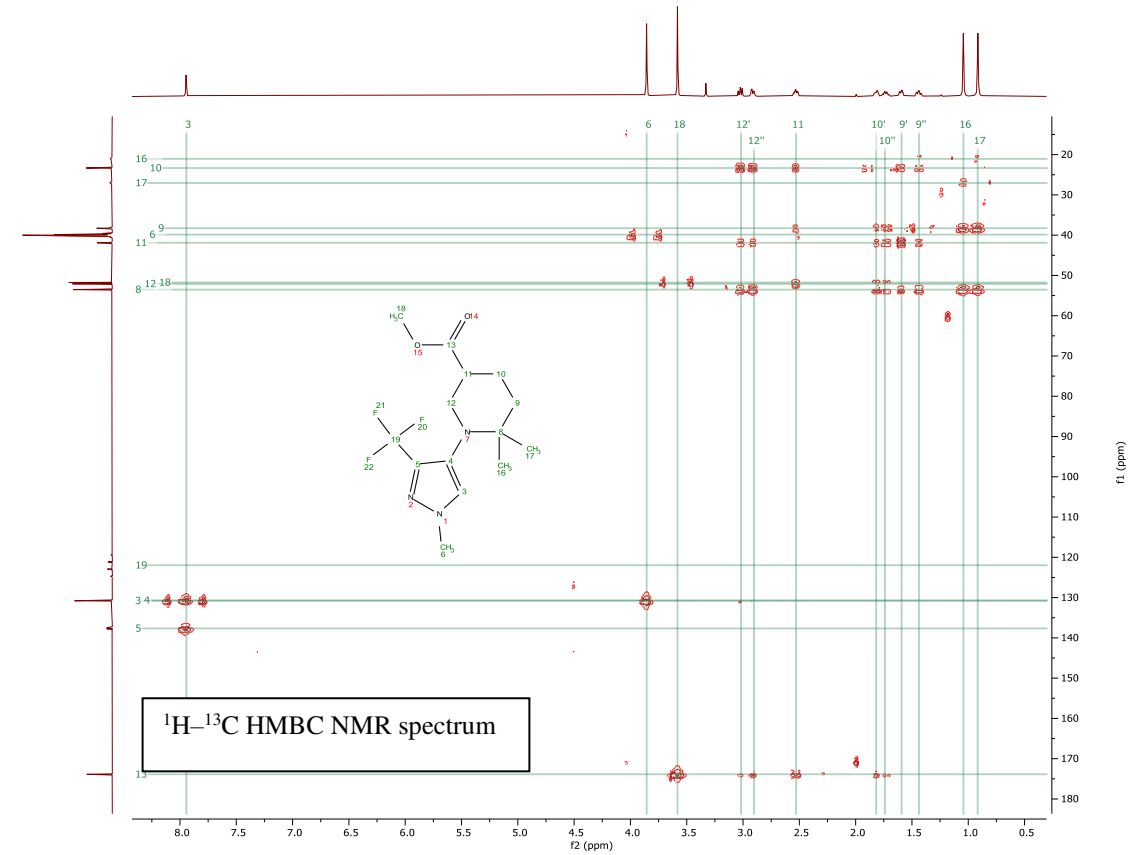

$^{1}H–^{13}C$ HMBC NMR spectrum

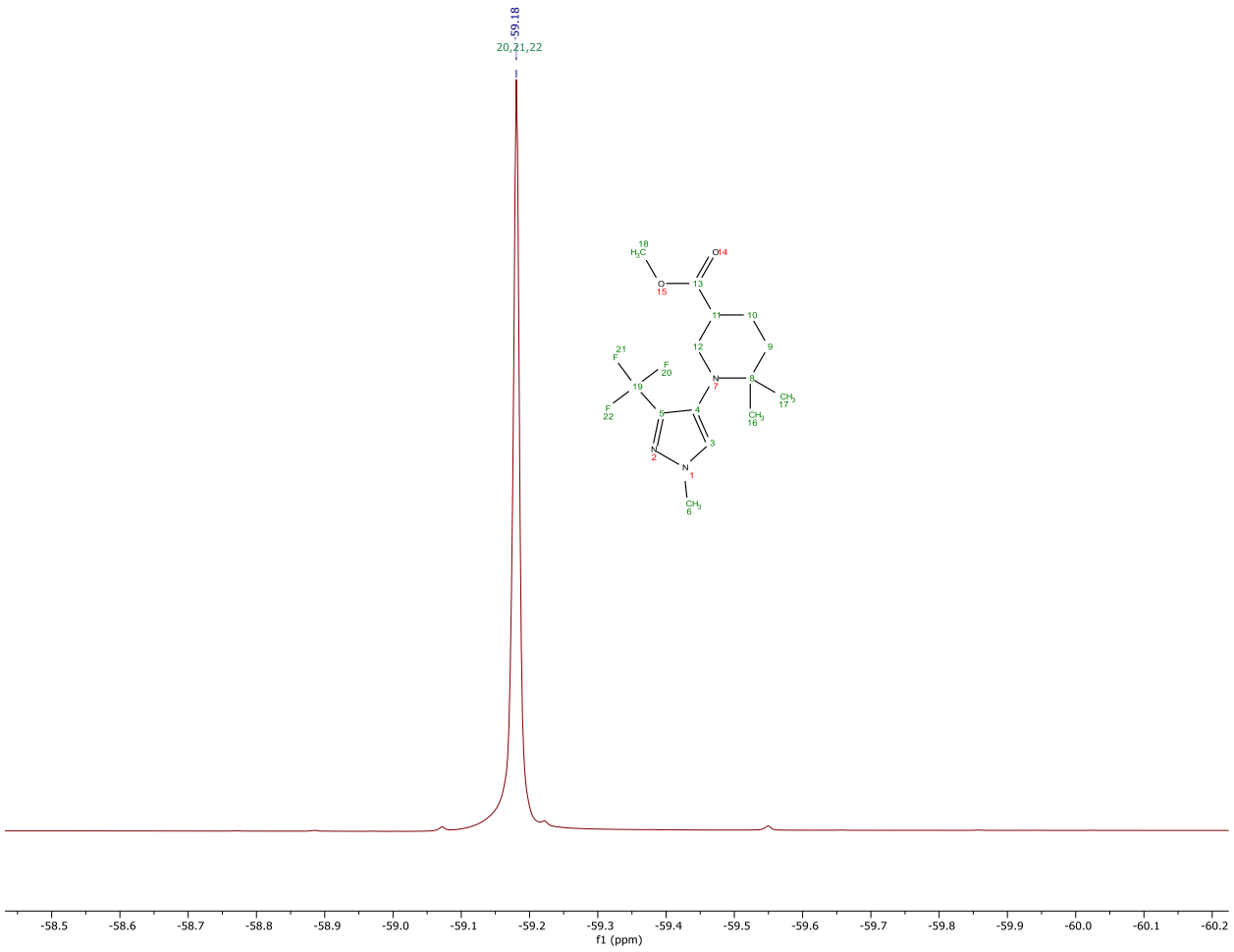
-59.18
20,21,22
-58.5
-58.6
-58.7
-58.8
-58.9
-59.0
-59.1
-59.2
-59.3
-59.4
-59.5
-59.6
-59.7
-59.8
-59.9
-60.0
-60.1
-60.2
f1 (ppm)

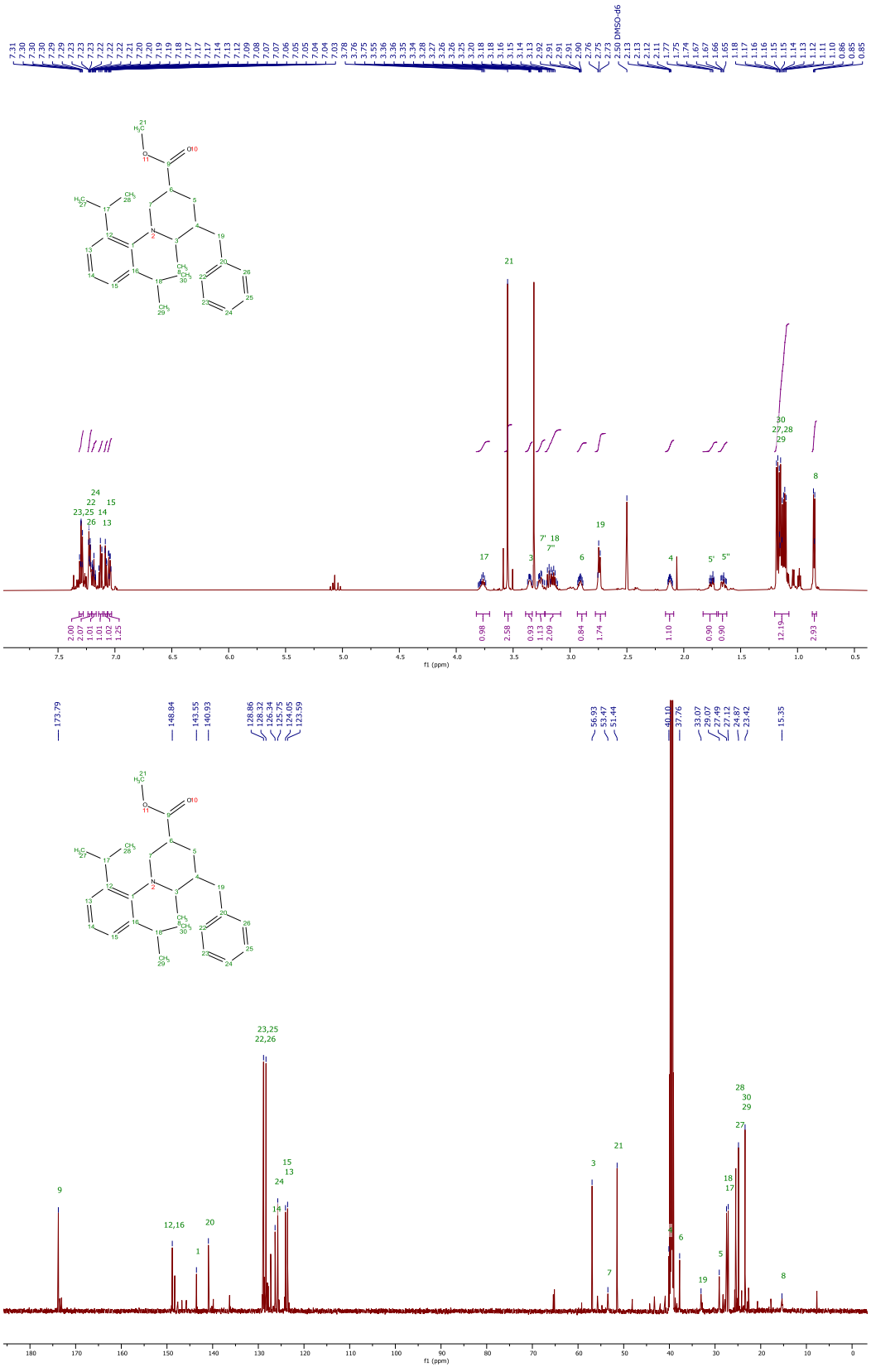
DMSO-d6
f1 (ppm)
f1 (ppm)

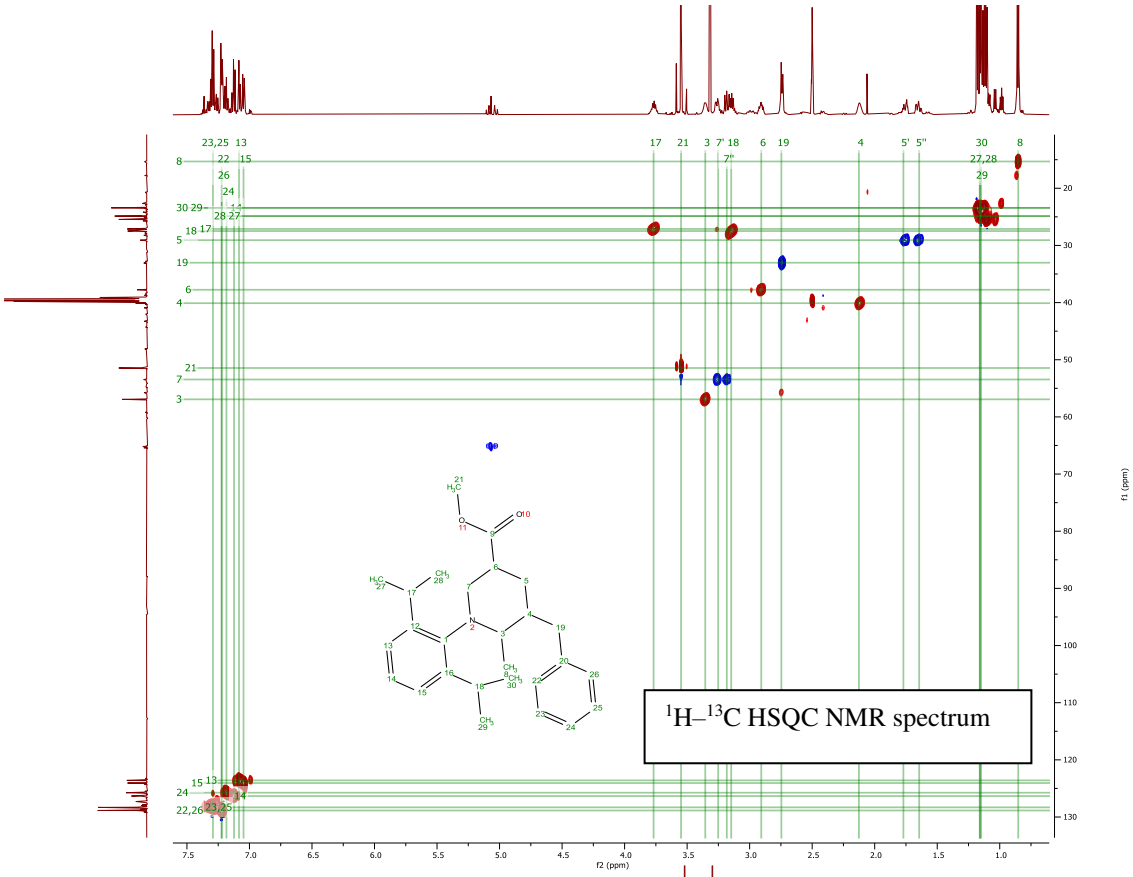
$^{1}H–^{13}C$ HSQC NMR spectrum
f2 (ppm)
f1 (ppm)

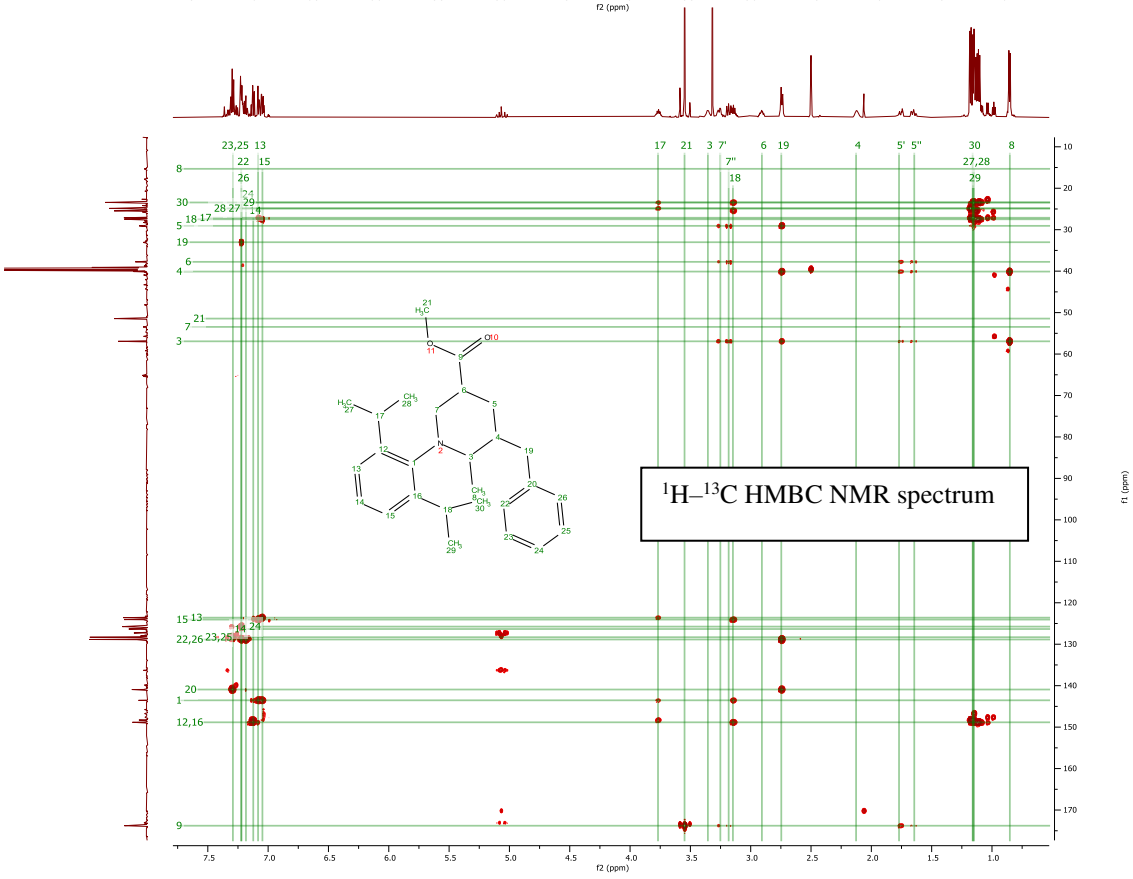
$^{1}H–^{13}C$ HMBC NMR spectrum
f2 (ppm)
f1 (ppm)

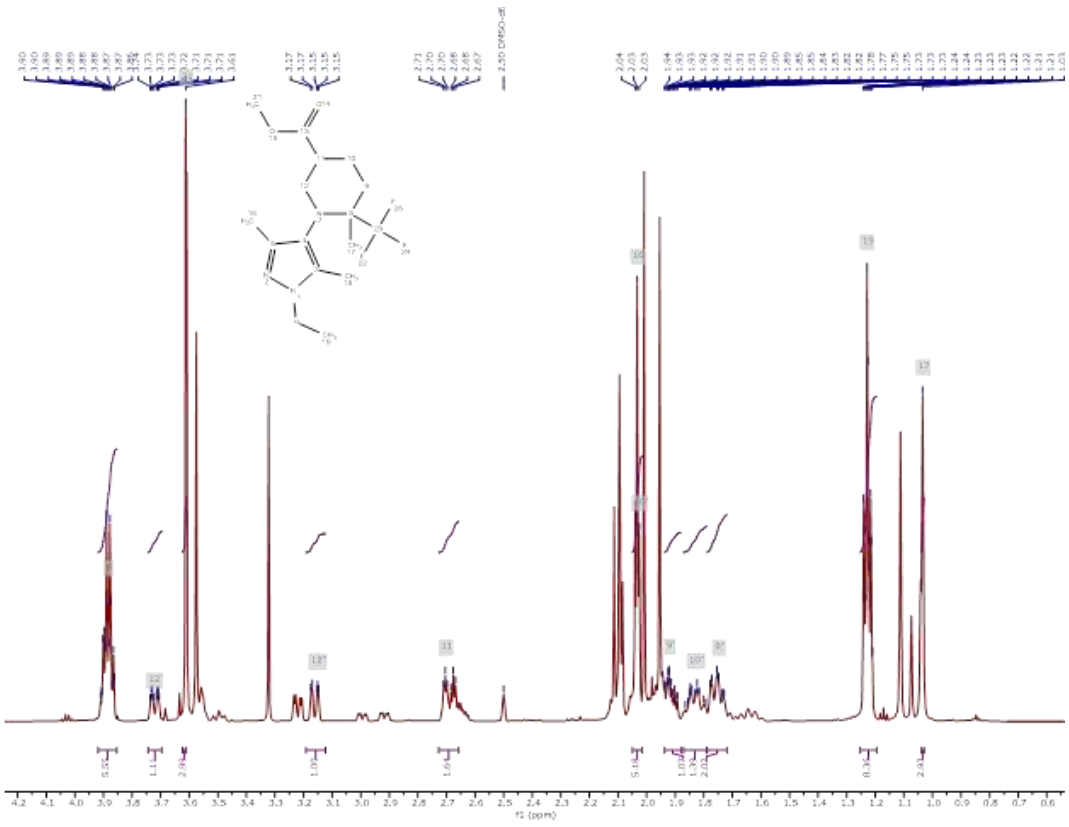

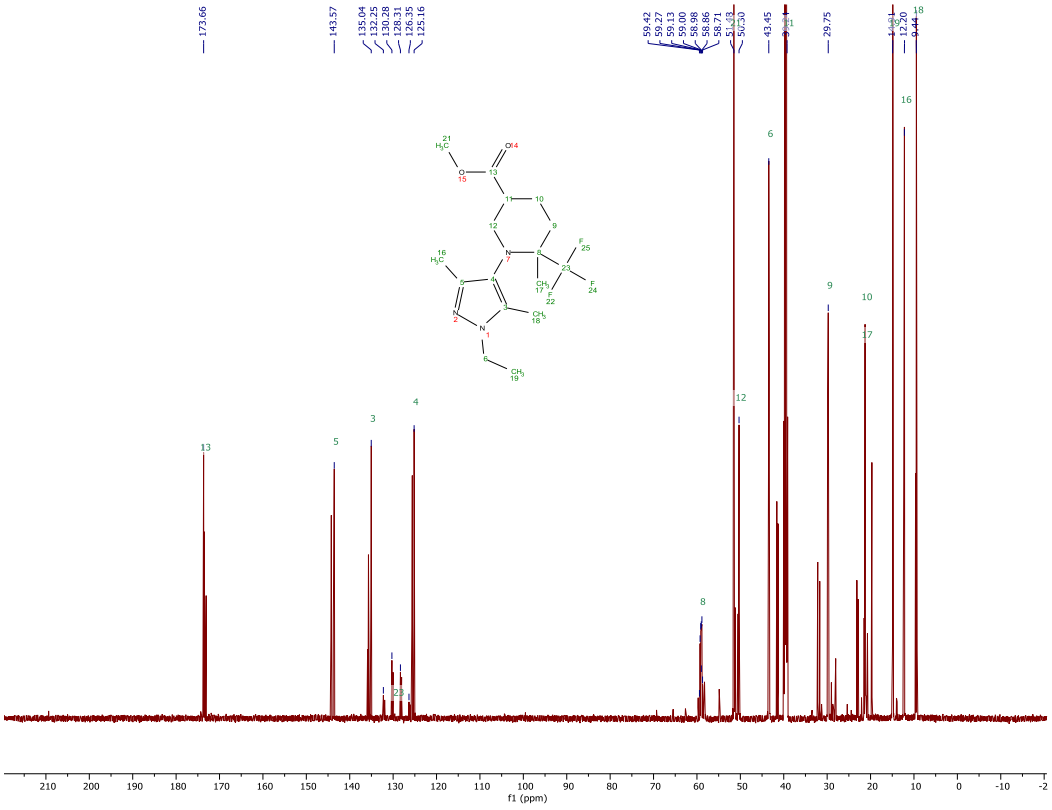

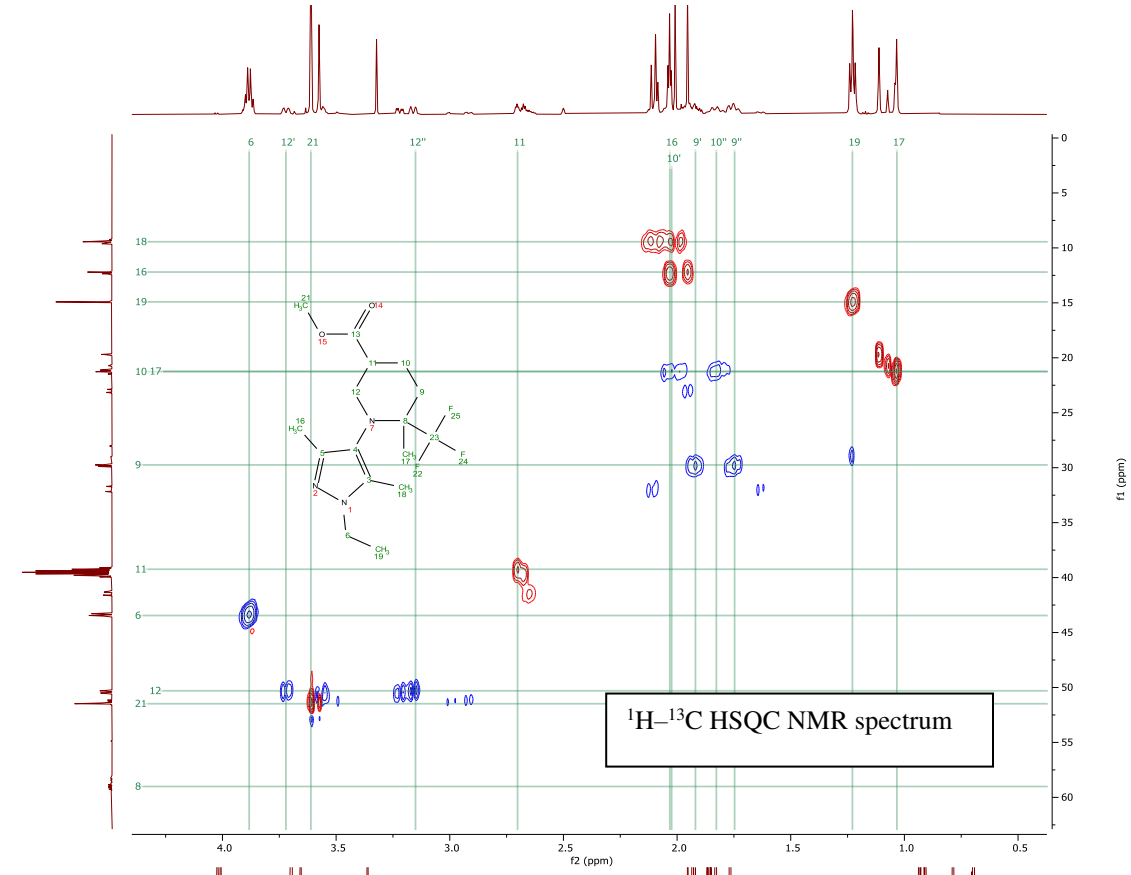

^{1}H–^{13}C HSQC NMR spectrum

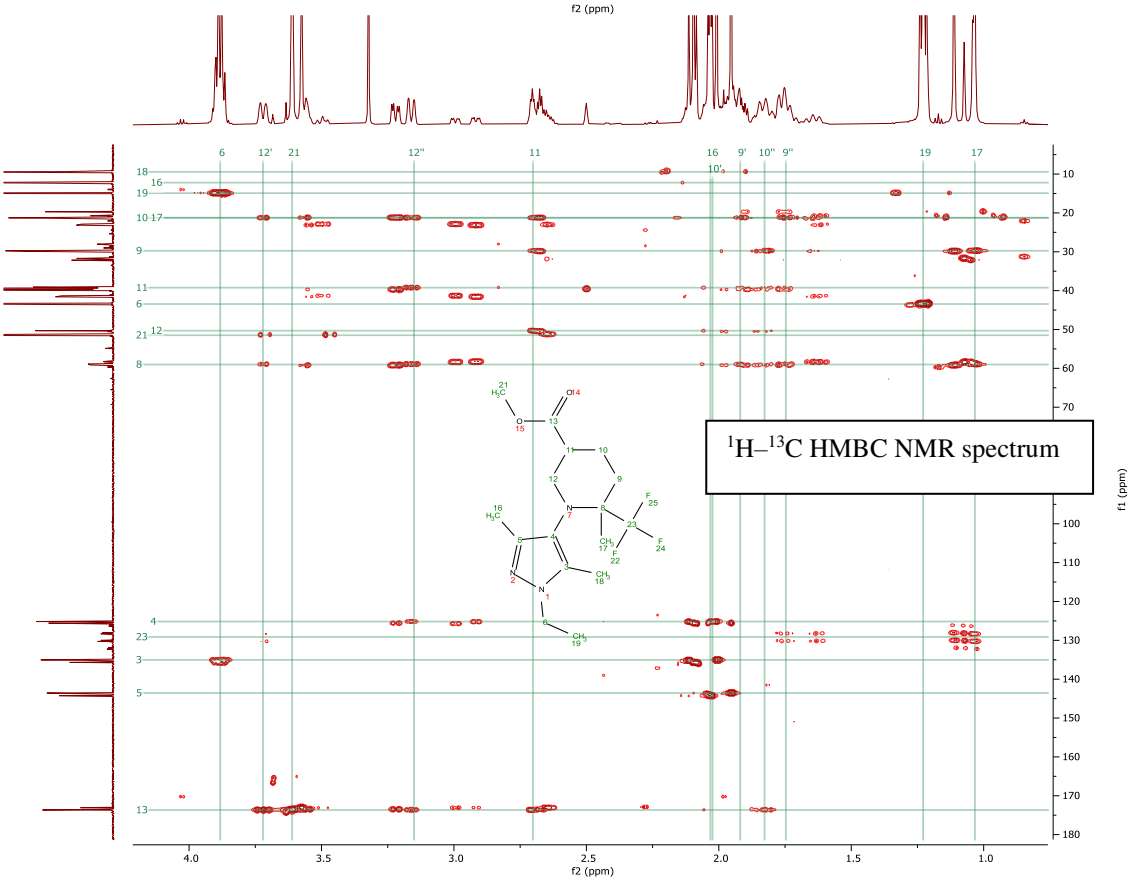

^{1}H–^{13}C HMBC NMR spectrum

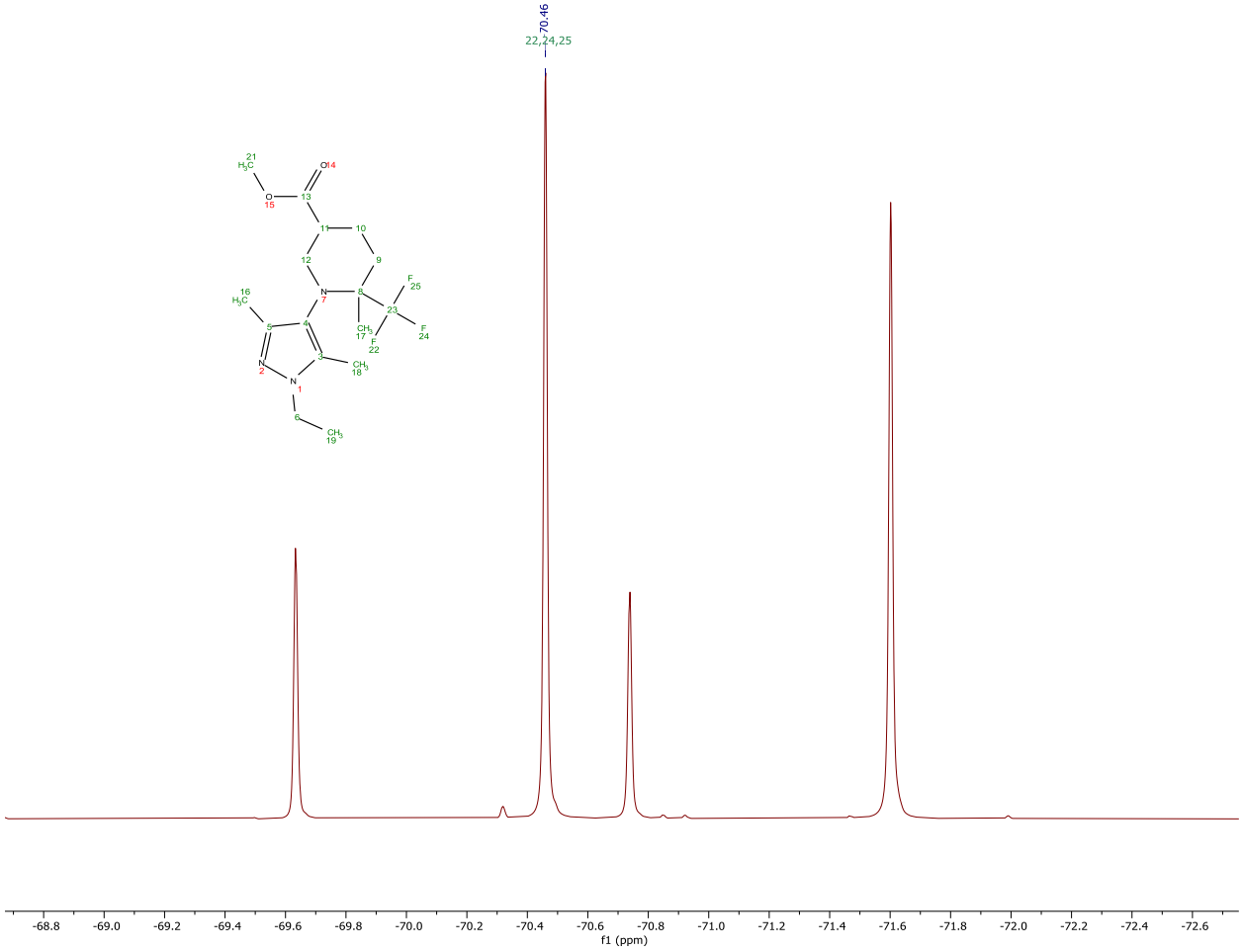
-70.46
-22,-24,-25
-68.8
-69.0
-69.2
-69.4
-69.6
-69.8
-70.0
-70.2
-70.4
-70.6
-70.8
-71.0
-71.2
-71.4
-71.6
-71.8
-72.0
-72.2
-72.4
-72.6
f1 (ppm)

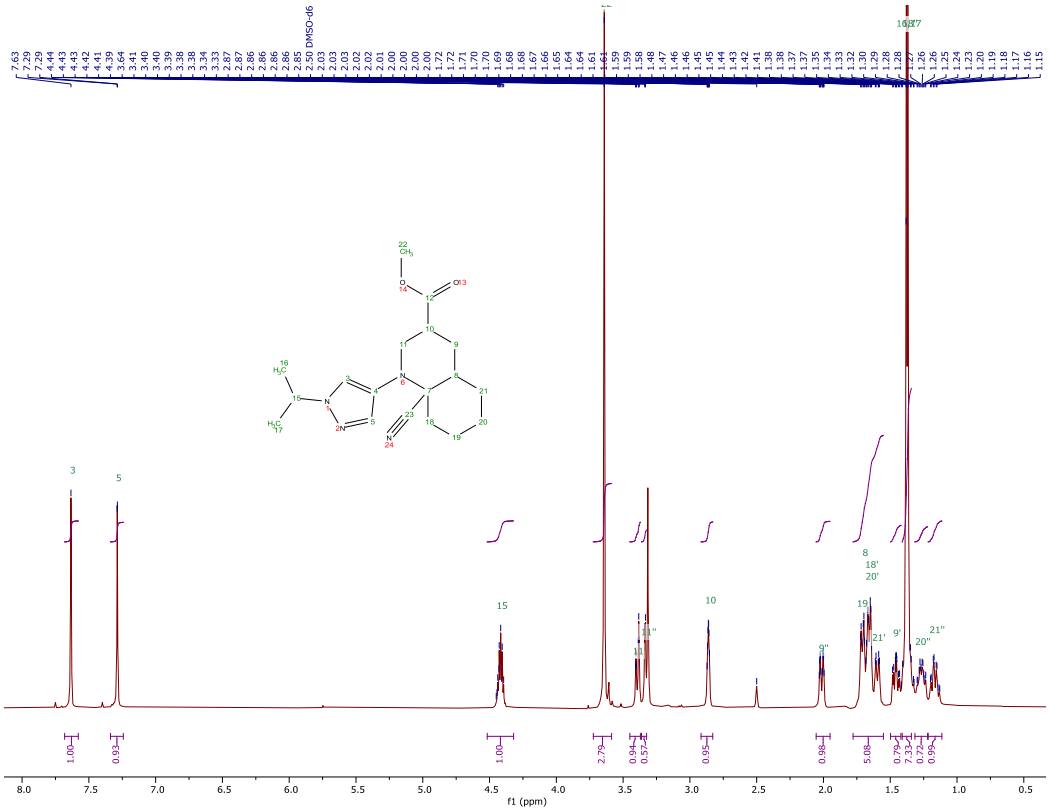
DMSO-d6
f1 (ppm)

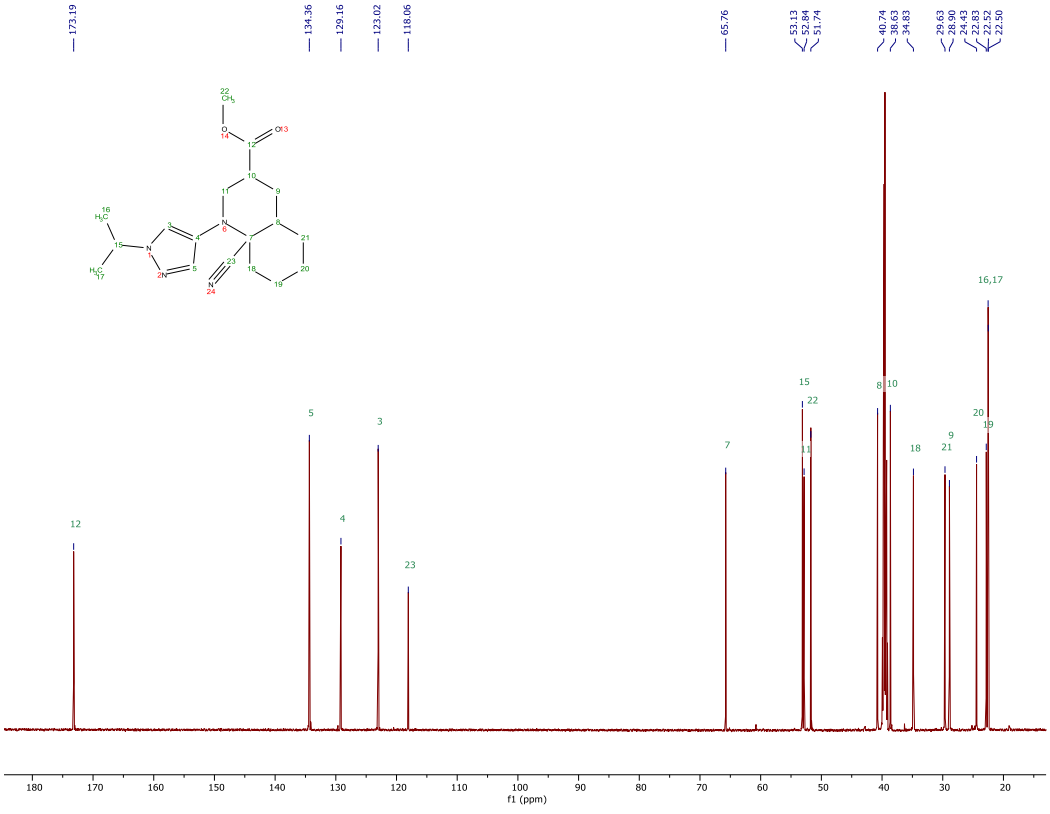
f1 (ppm)

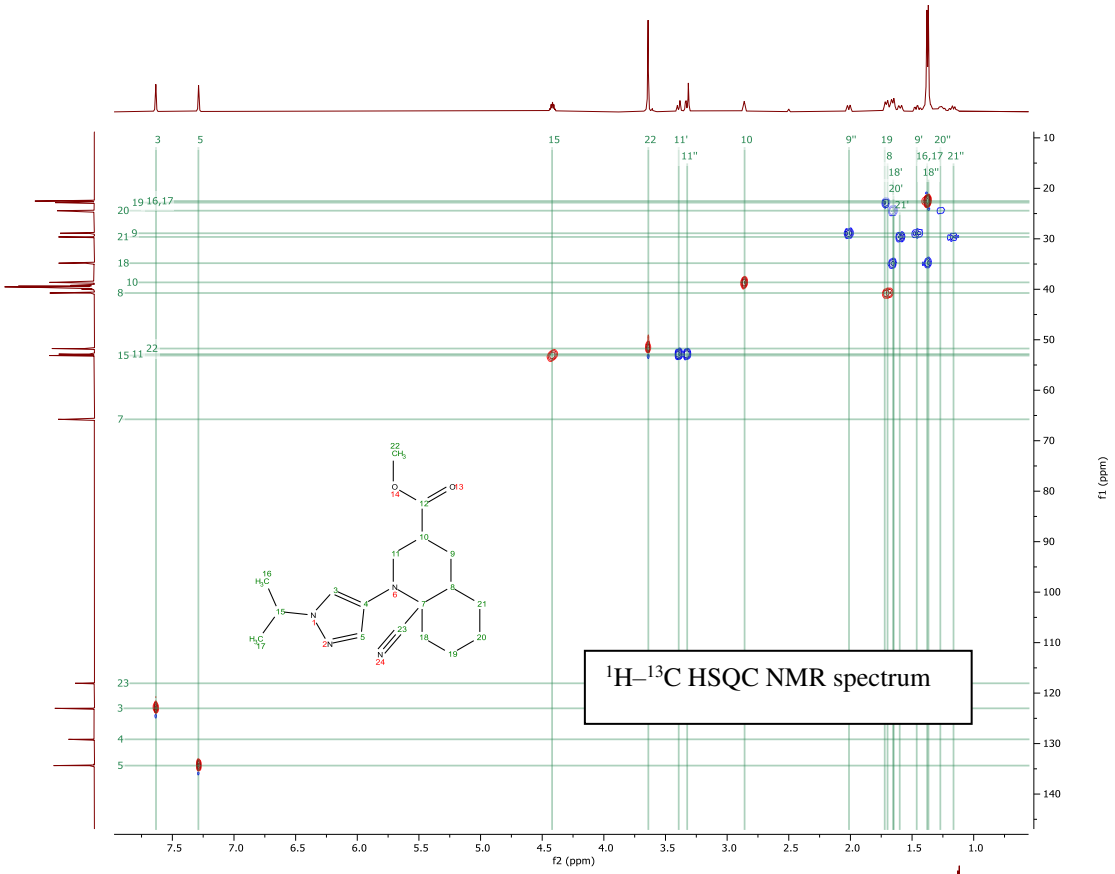

$^{1}H–^{13}C$ HSQC NMR spectrum

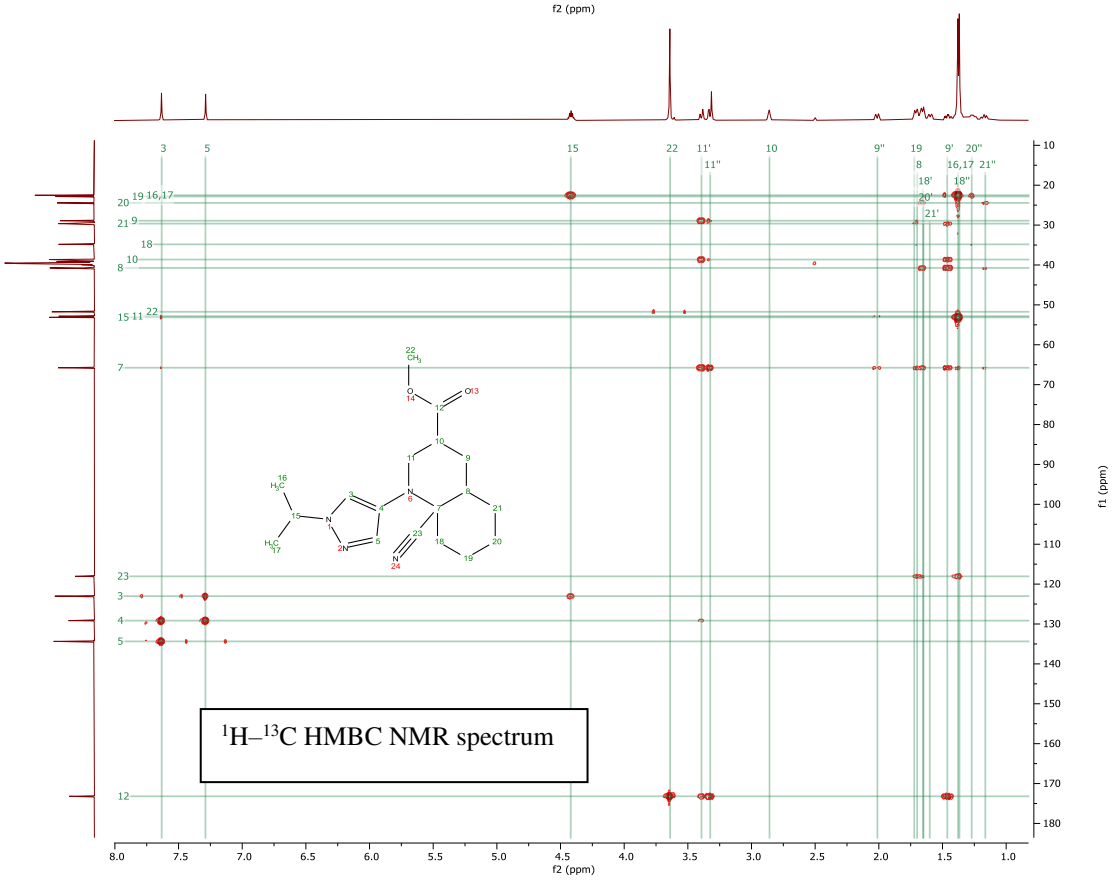

$^{1}H–^{13}C$ HMBC NMR spectrum

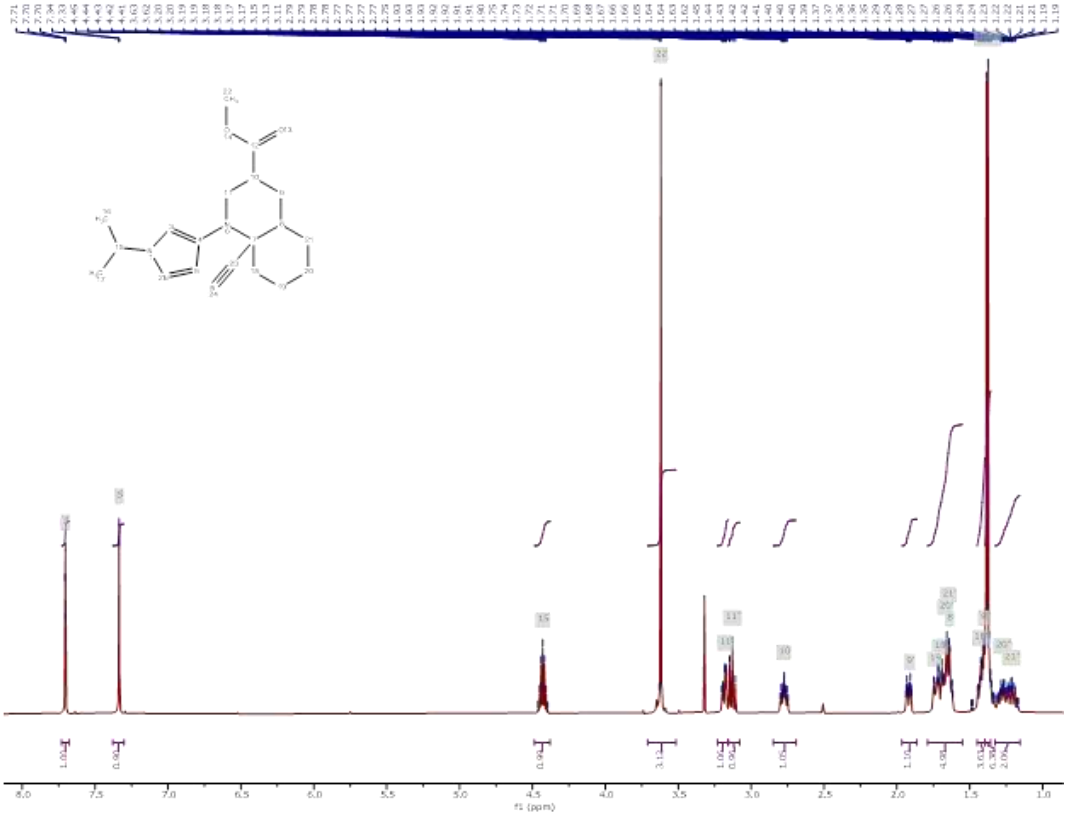

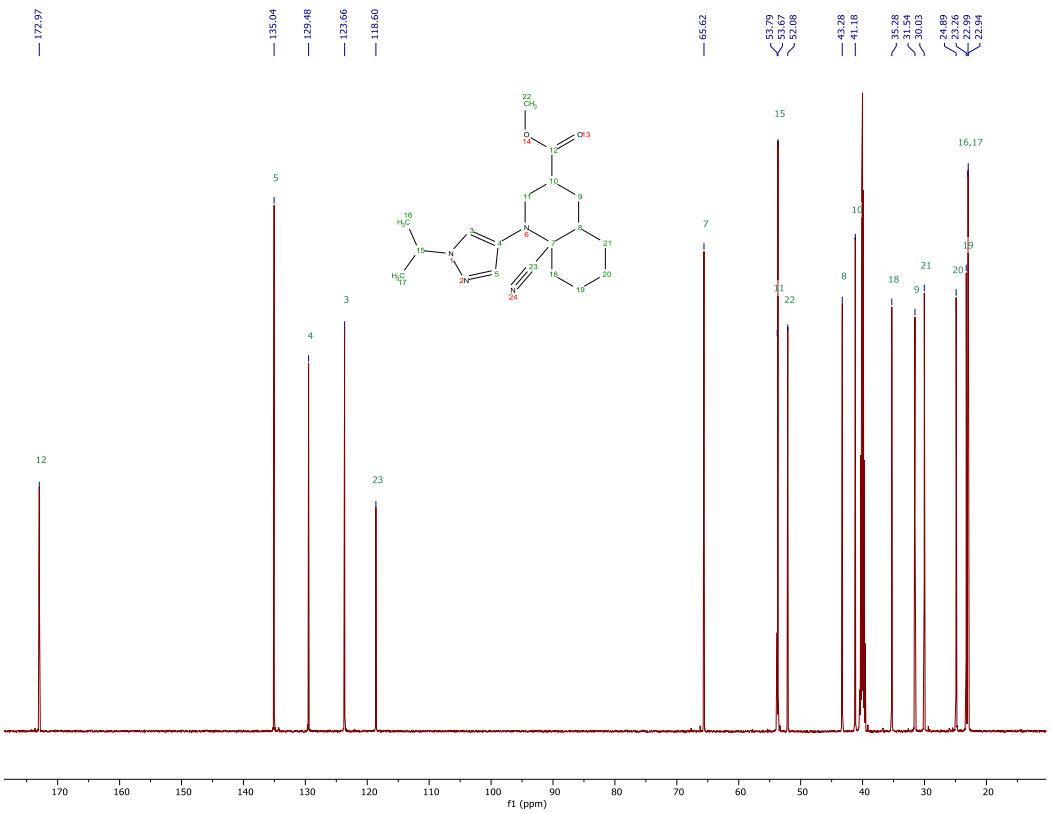

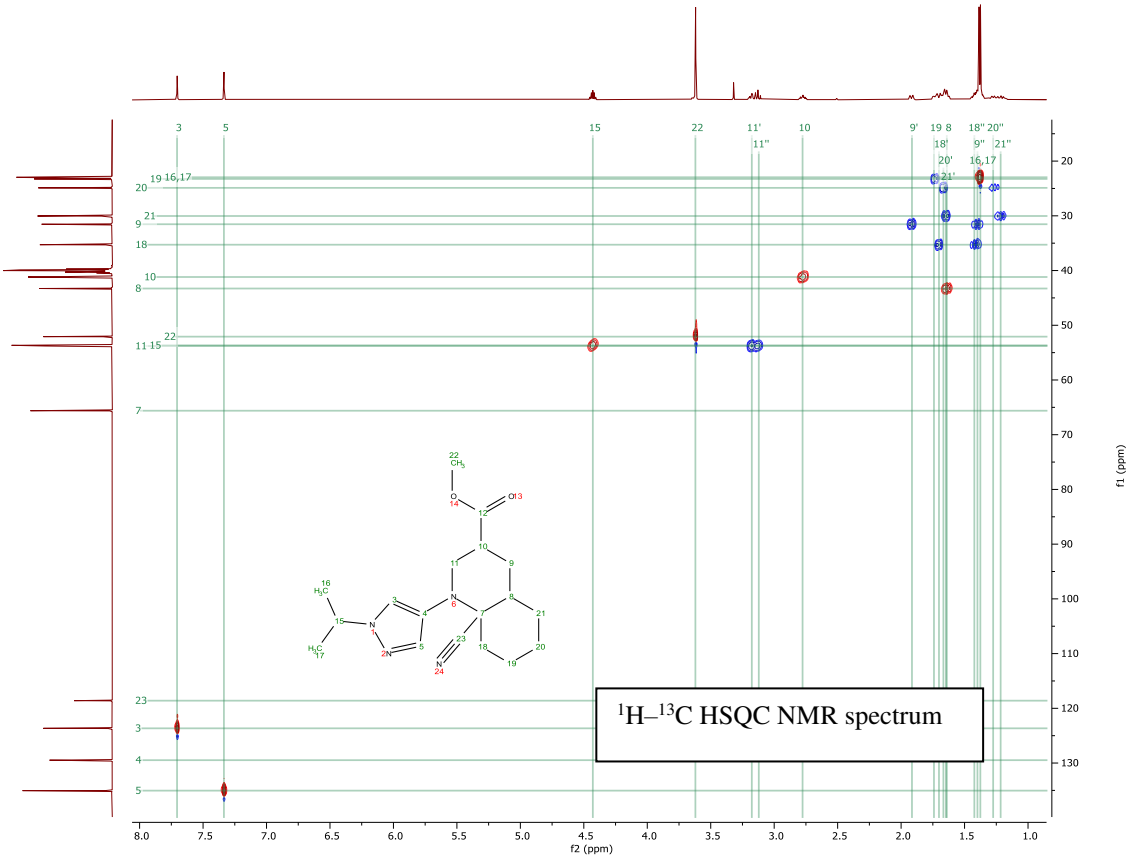

$^{1}H–^{13}C$ HSQC NMR spectrum

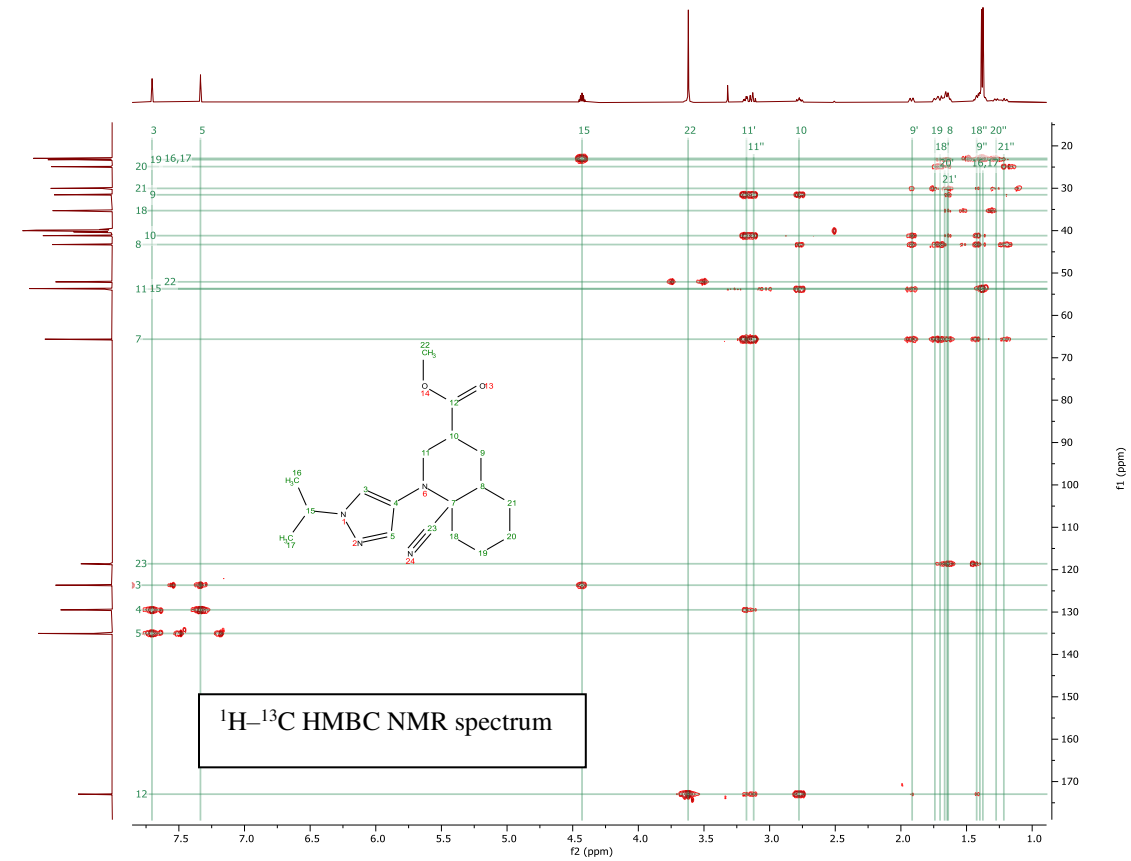

$^{1}H–^{13}C$ HMBC NMR spectrum

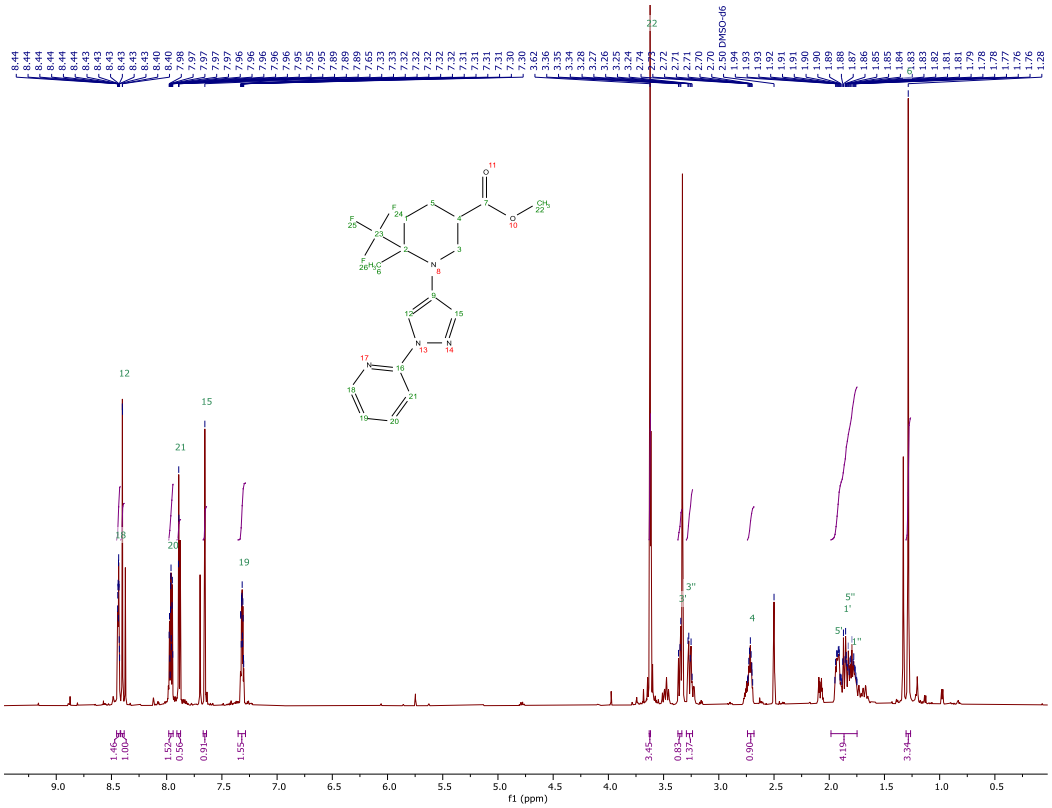
f1 (ppm)

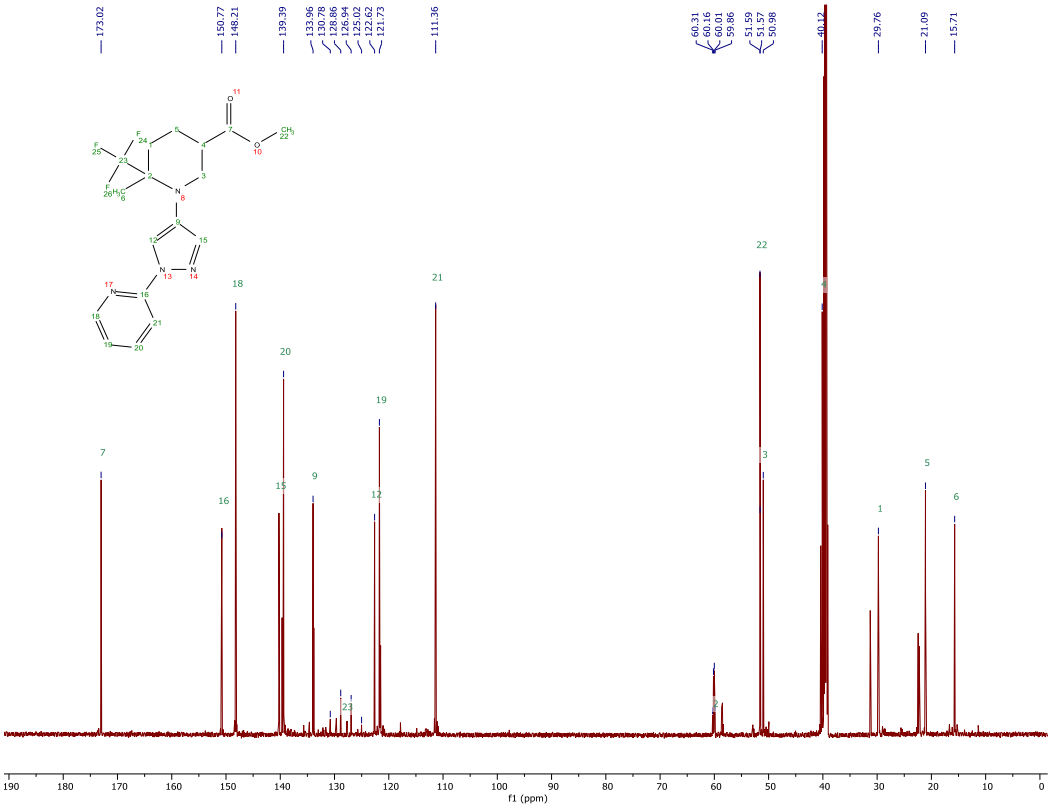
f1 (ppm)

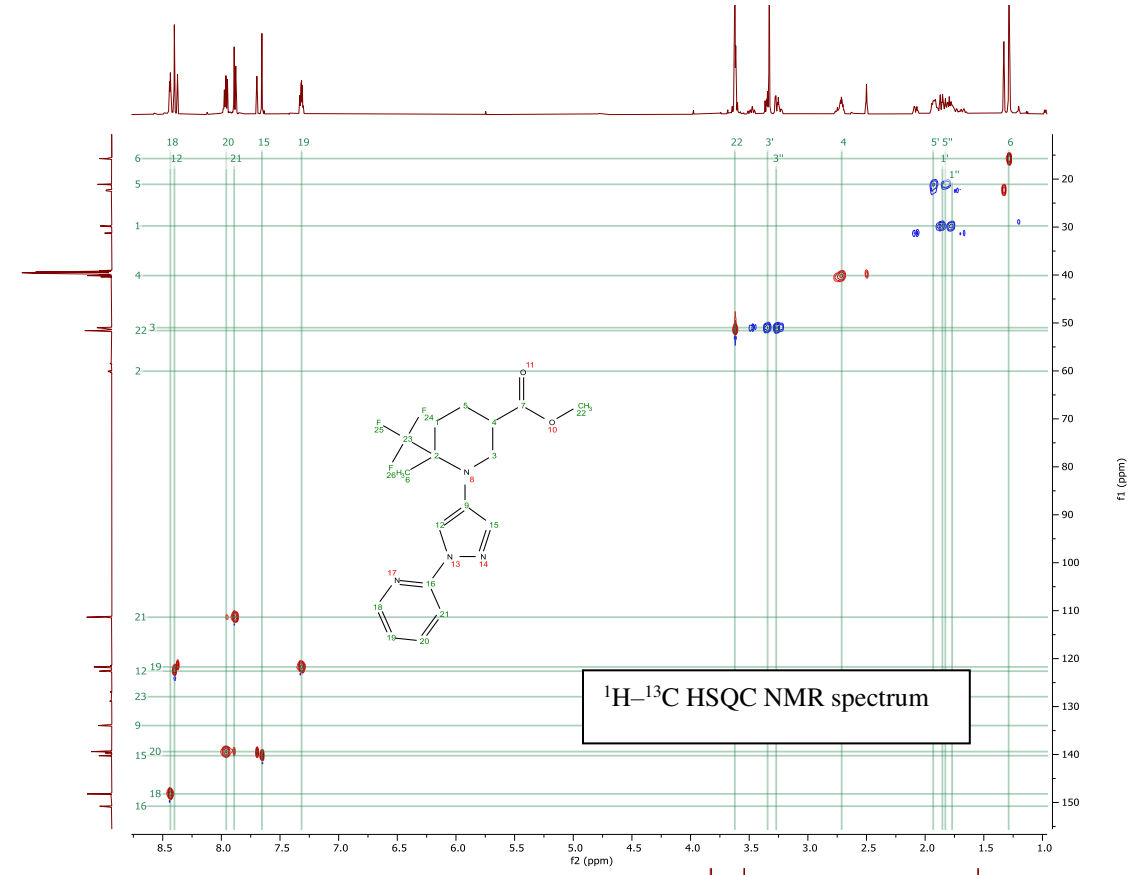

$^{1}H–^{13}C$ HSQC NMR spectrum

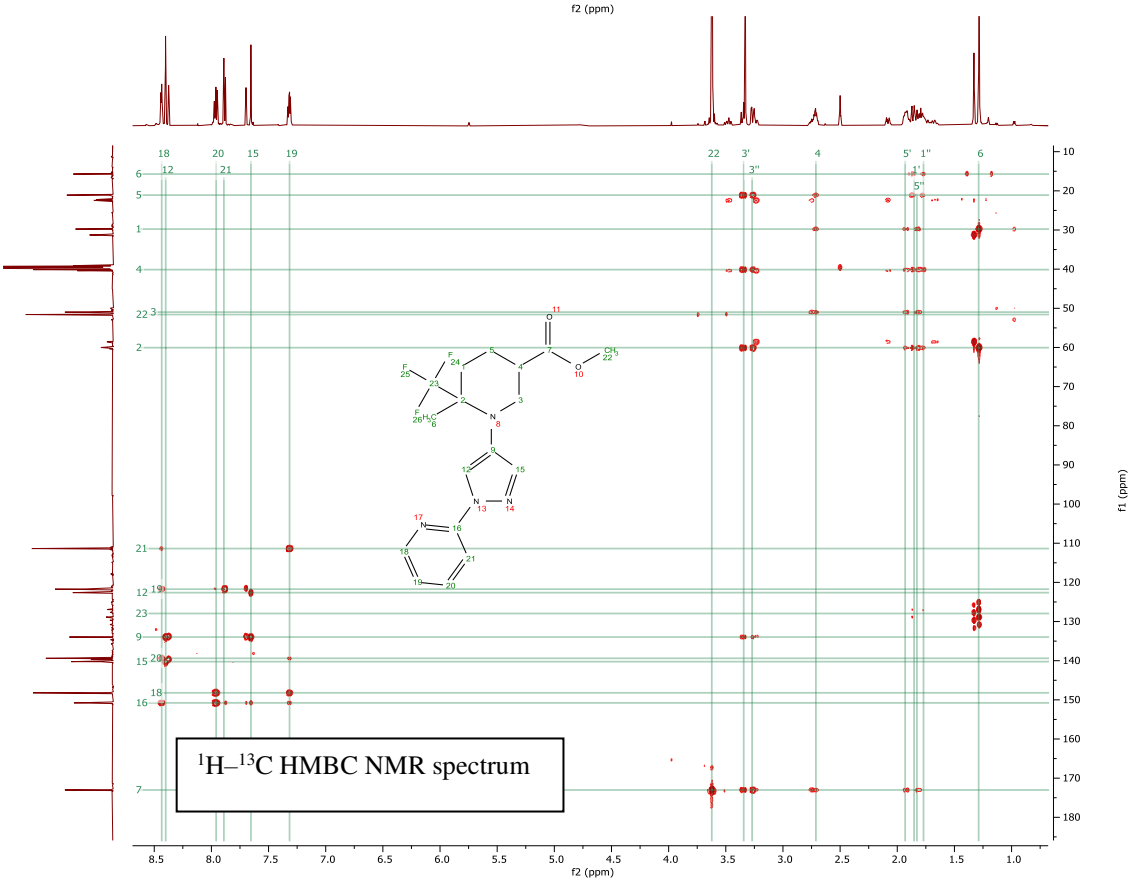

$^{1}H–^{13}C$ HMBC NMR spectrum

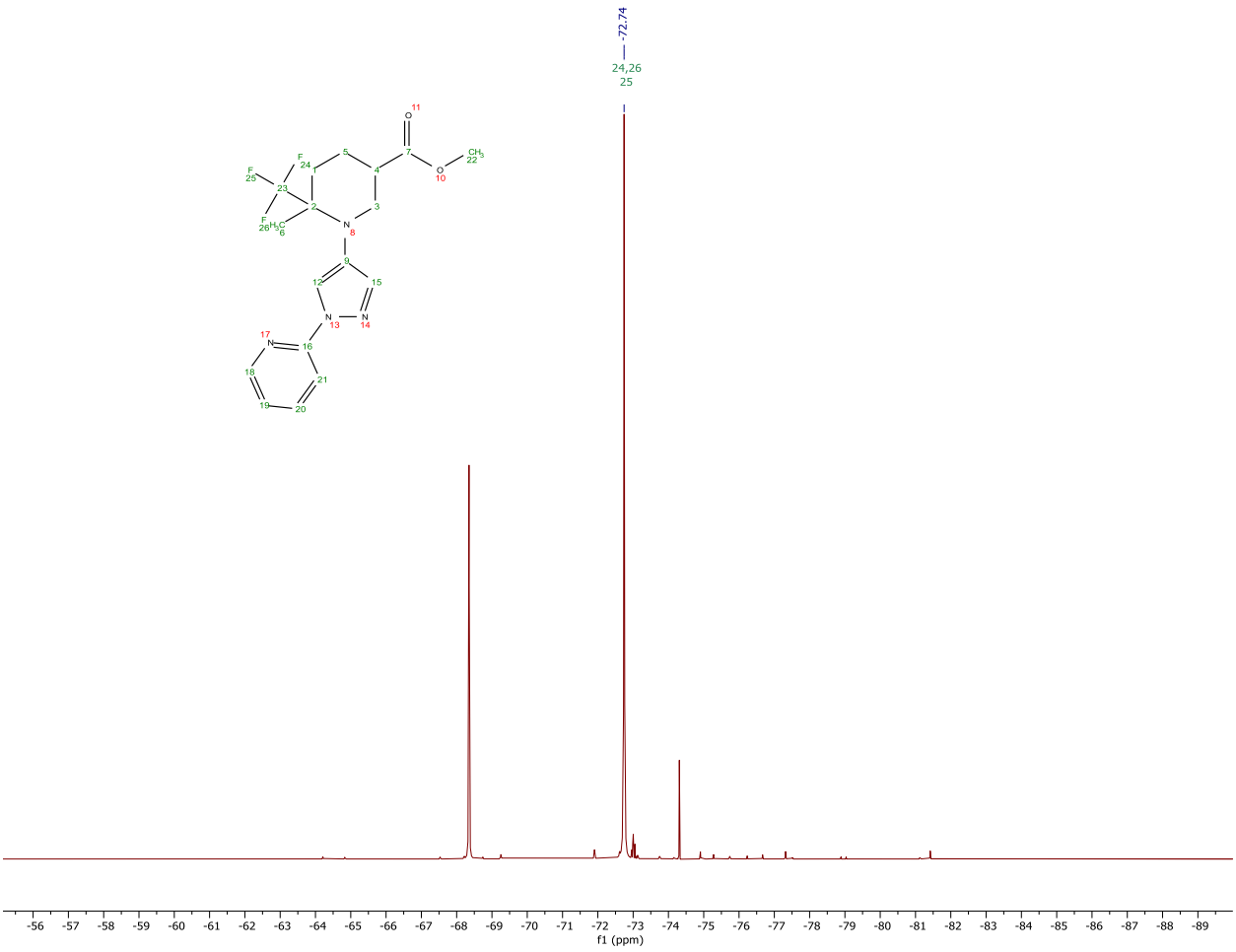
-72.74
24,26
25
-56 -57 -58 -59 -60 -61 -62 -63 -64 -65 -66 -67 -68 -69 -70 -71 -72 -73 -74 -75 -76 -77 -78 -79 -80 -81 -82 -83 -84 -85 -86 -87 -88 -89
f1 (ppm)

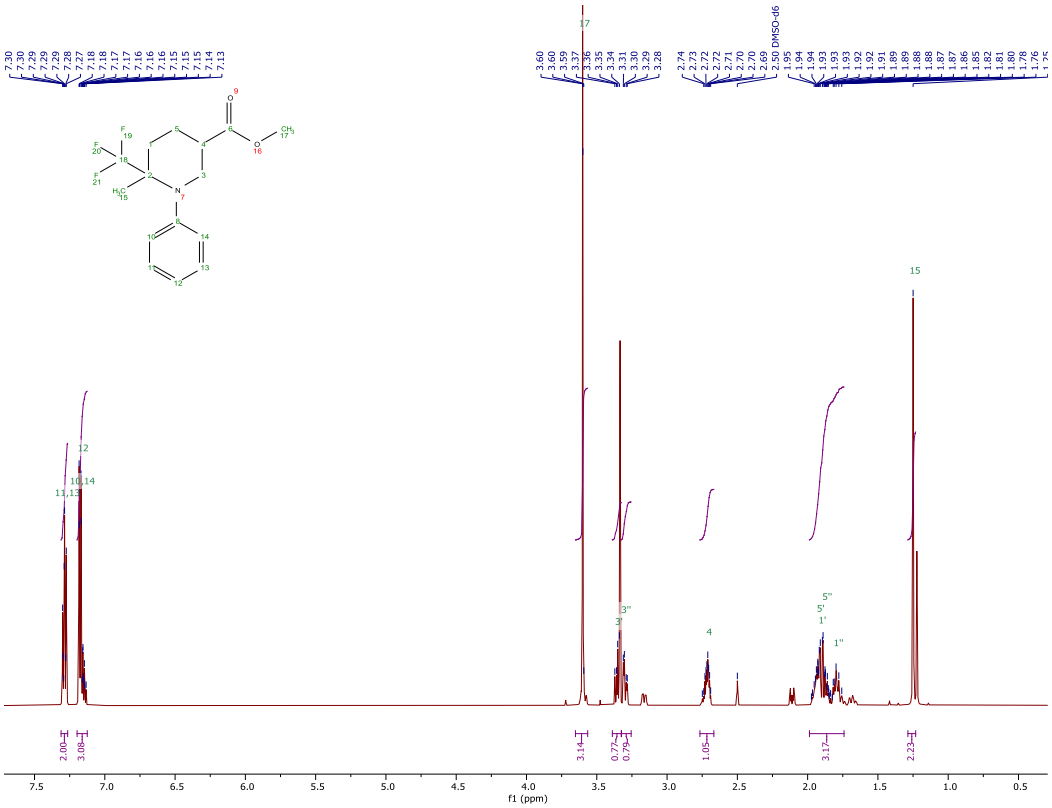
DMSO-d6
f1 (ppm)

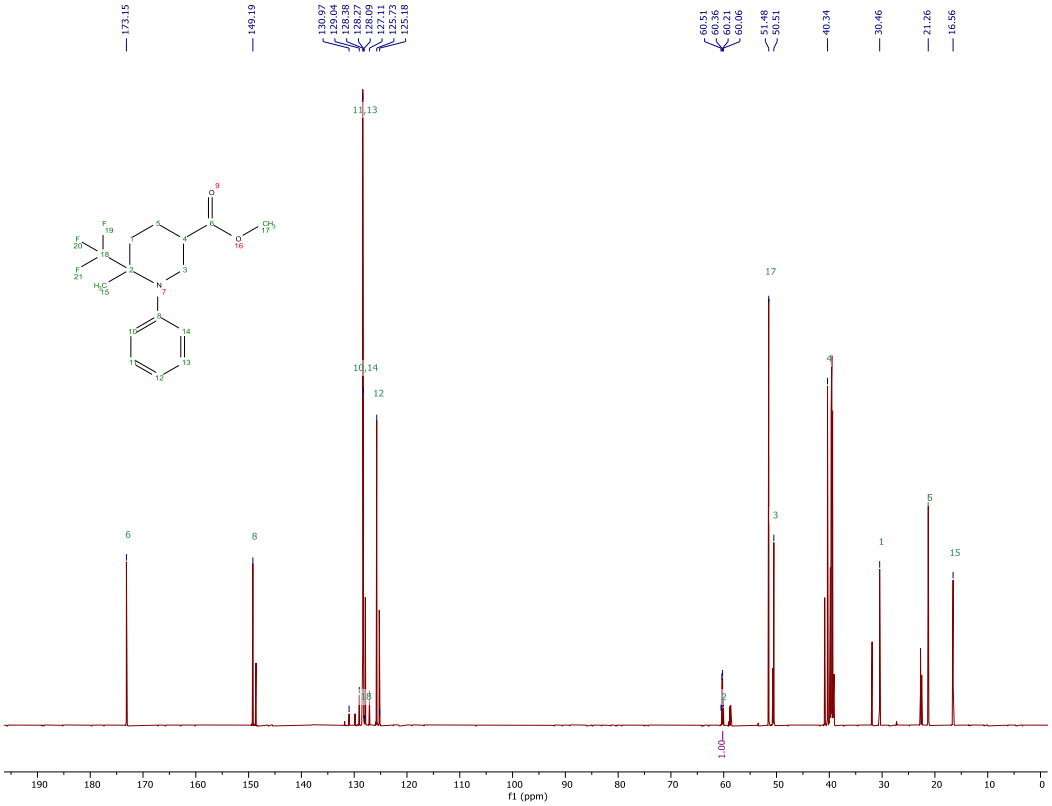
f1 (ppm)

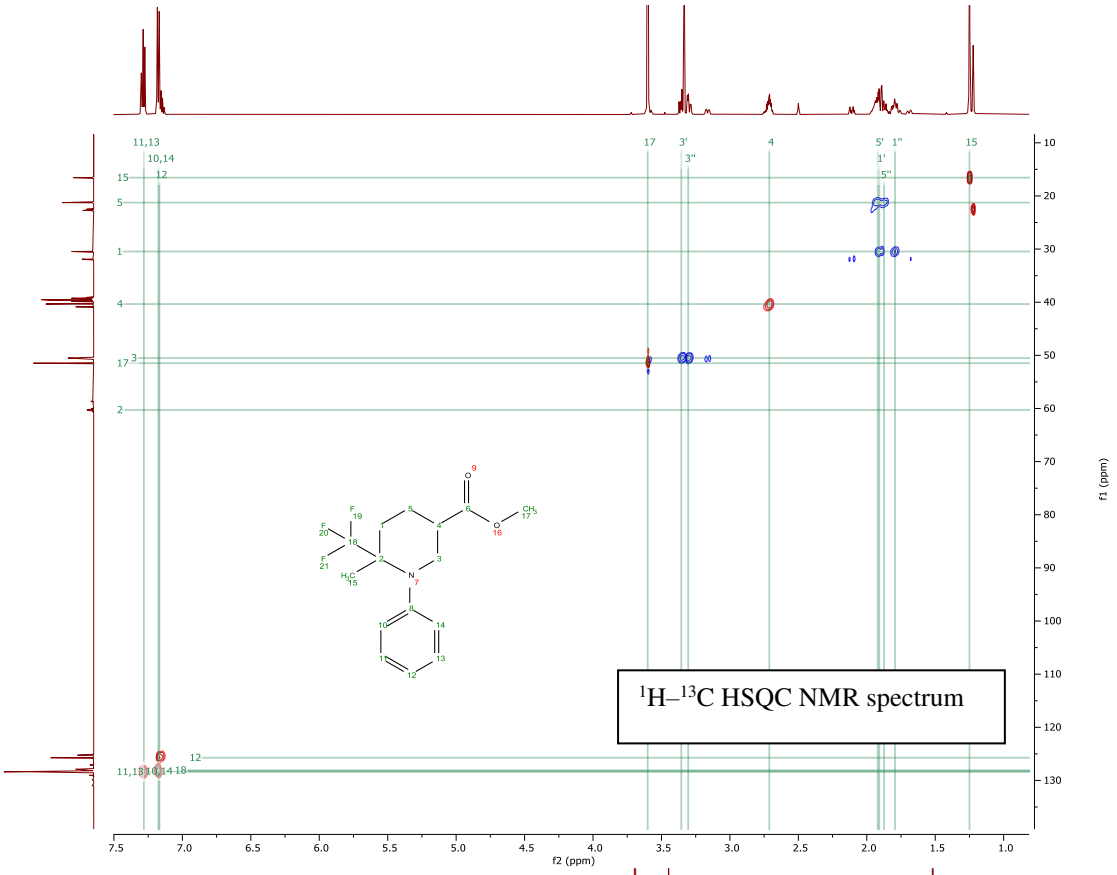

$^{1}H–^{13}C$ HSQC NMR spectrum

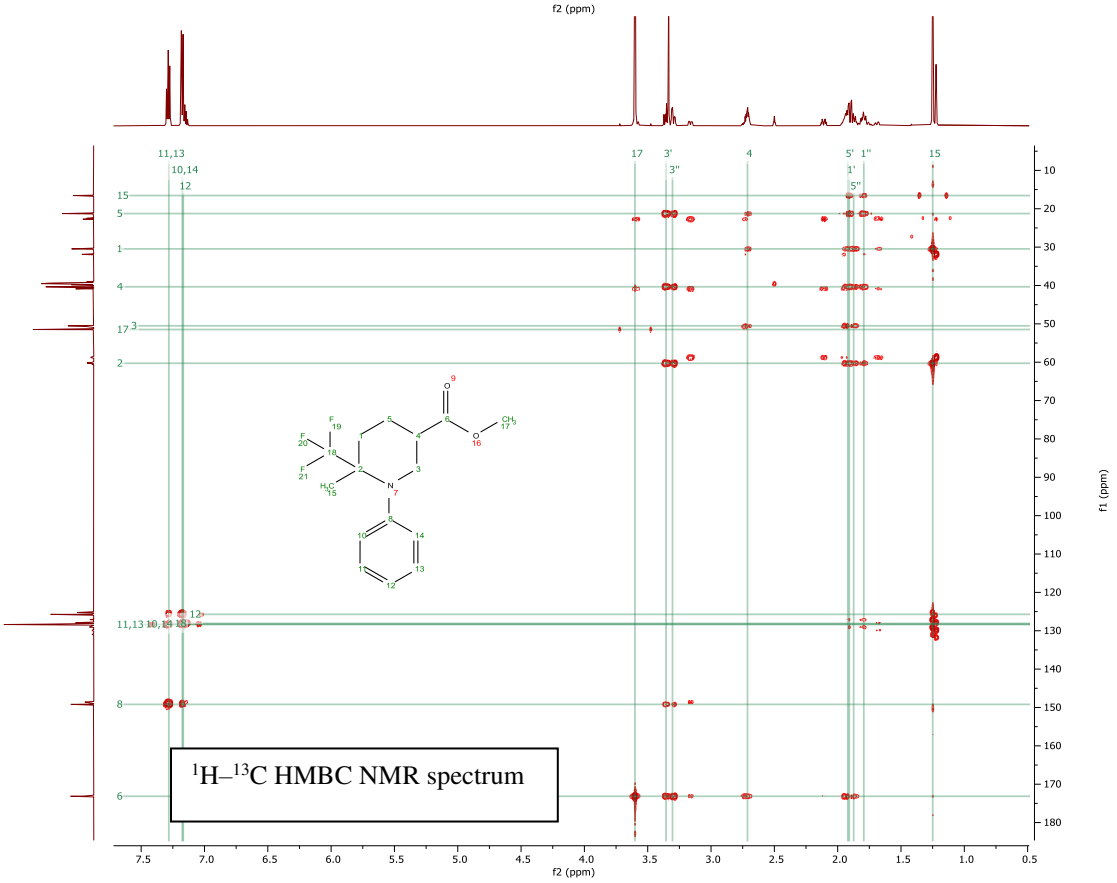

$^{1}H–^{13}C$ HMBC NMR spectrum

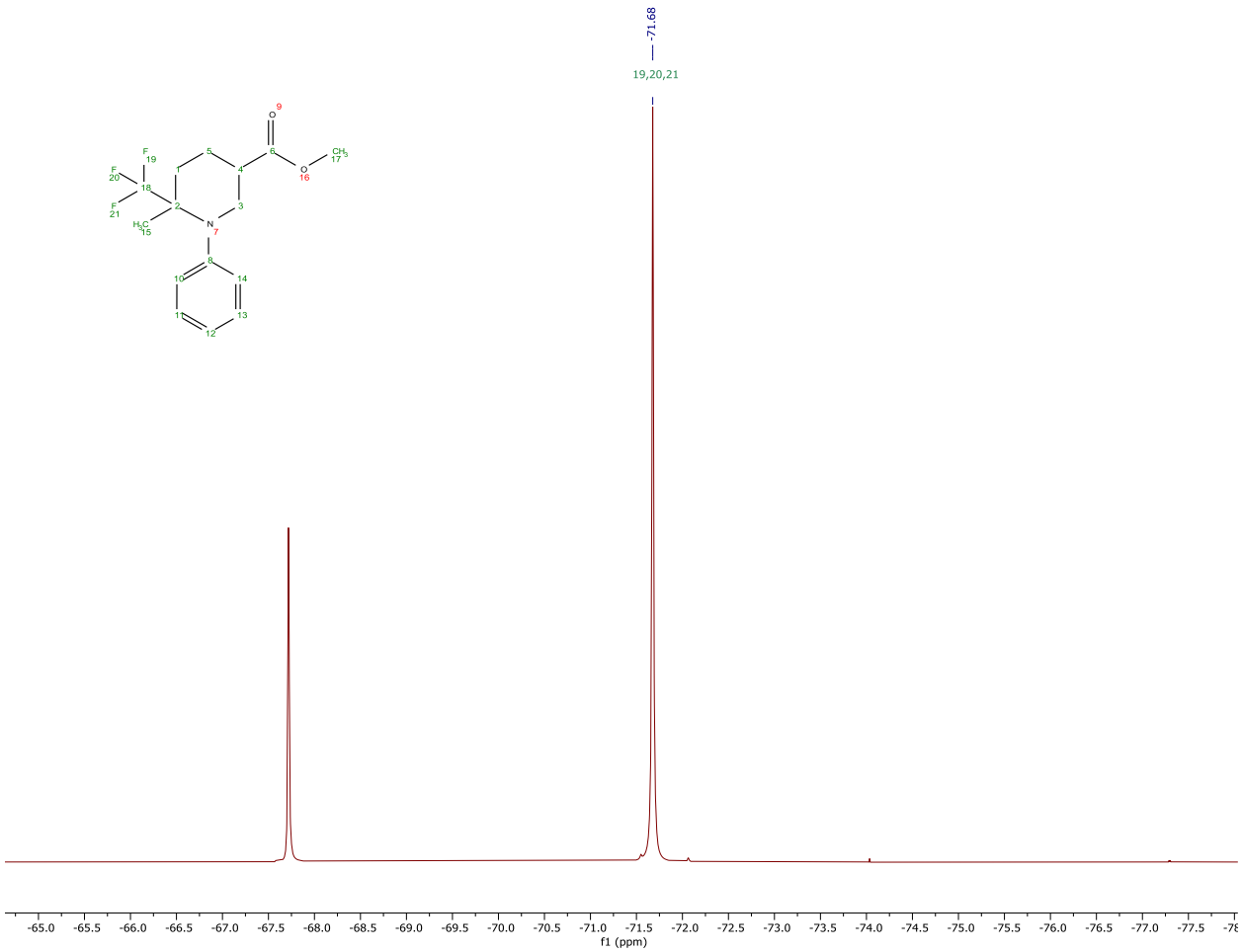
-71.68
19,20,21
-65.0
-65.5
-66.0
-66.5
-67.0
-67.5
-68.0
-68.5
-69.0
-69.5
-70.0
-70.5
-71.0
-71.5
-72.0
-72.5
-73.0
-73.5
-74.0
-74.5
-75.0
-75.5
-76.0
-76.5
-77.0
-77.5
f1 (ppm)

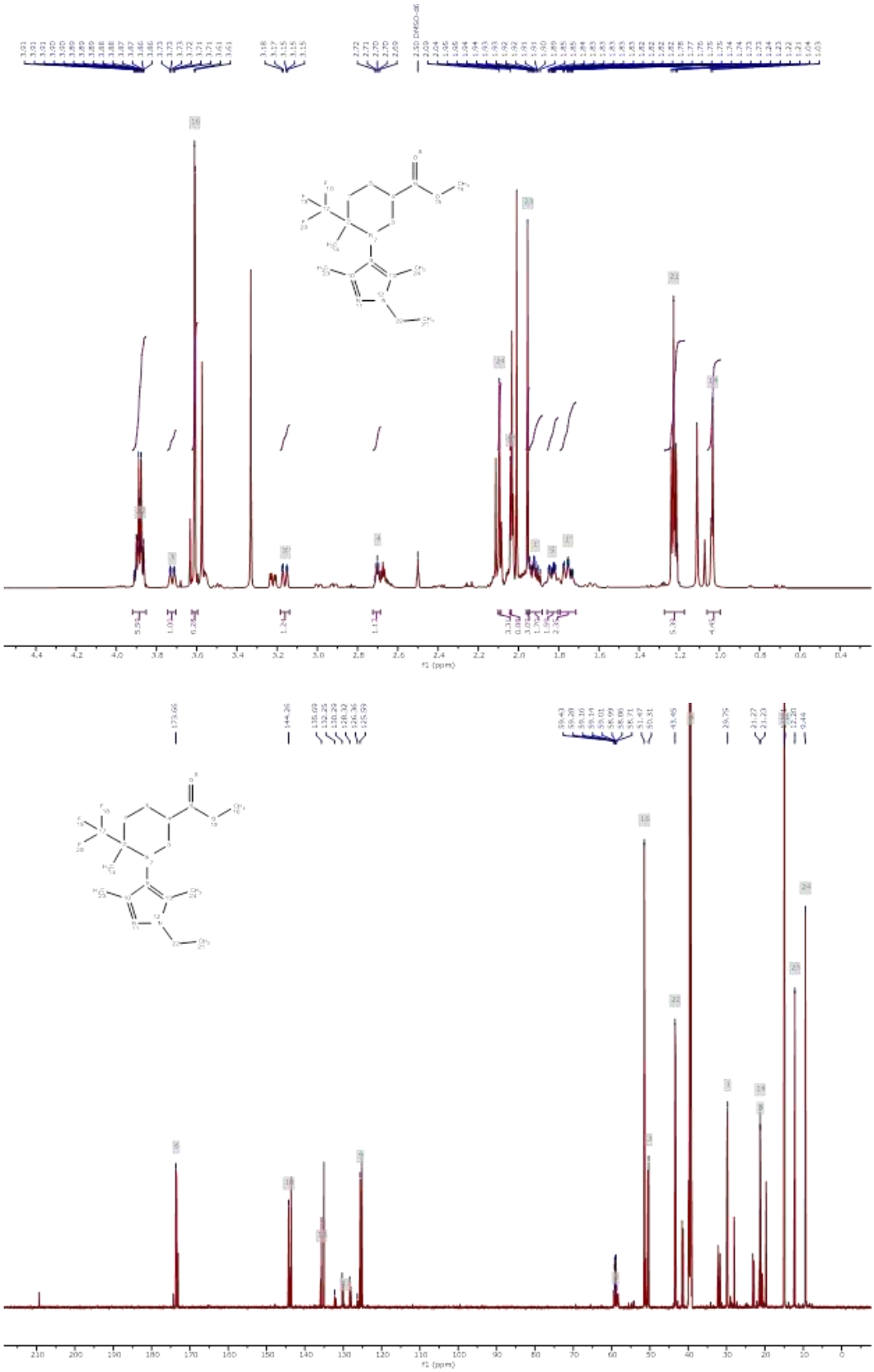

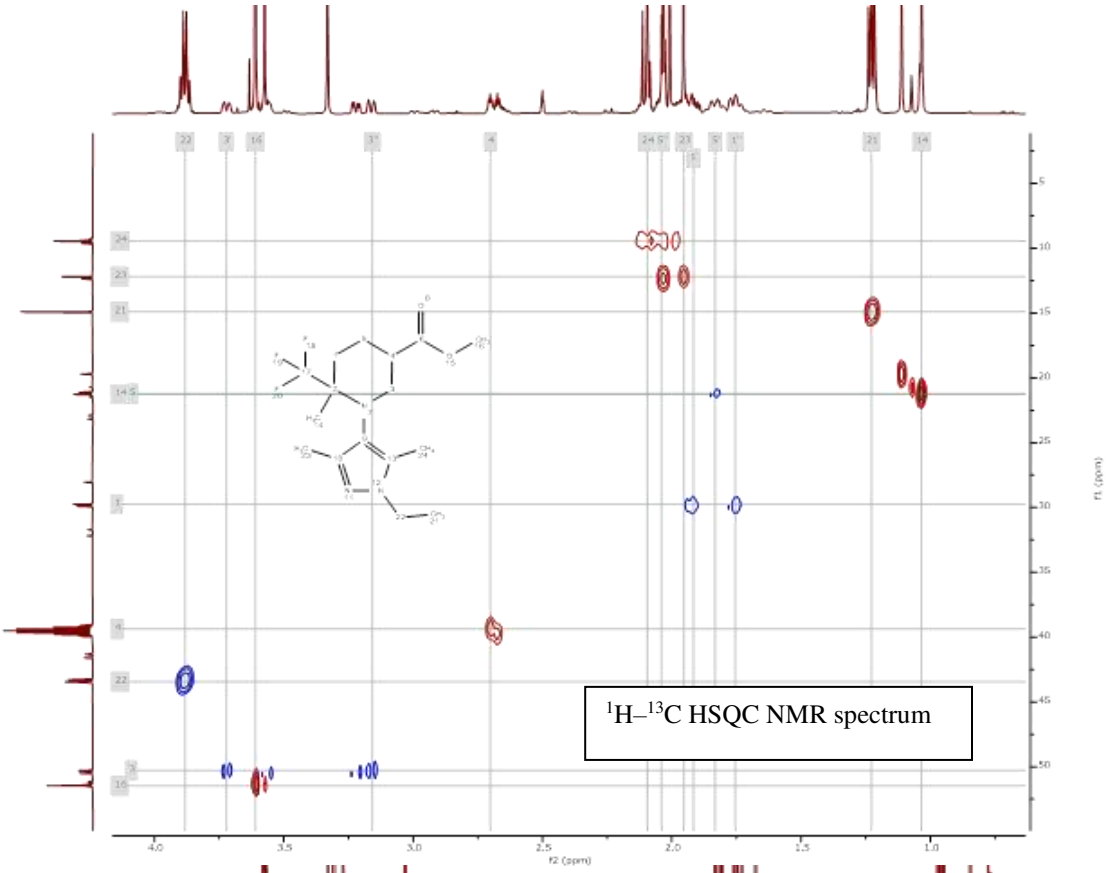
$^{1}H–^{13}C$ HSQC NMR spectrum

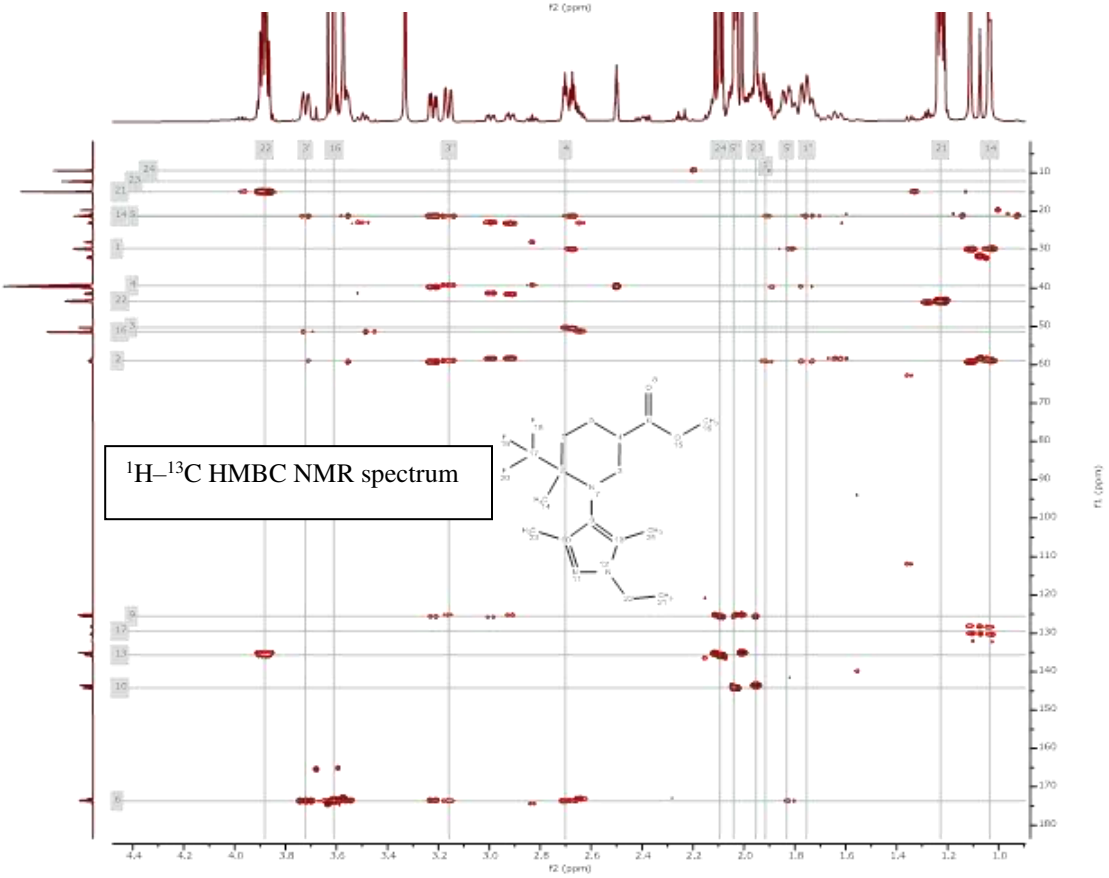
$^{1}H–^{13}C$ HMBC NMR spectrum

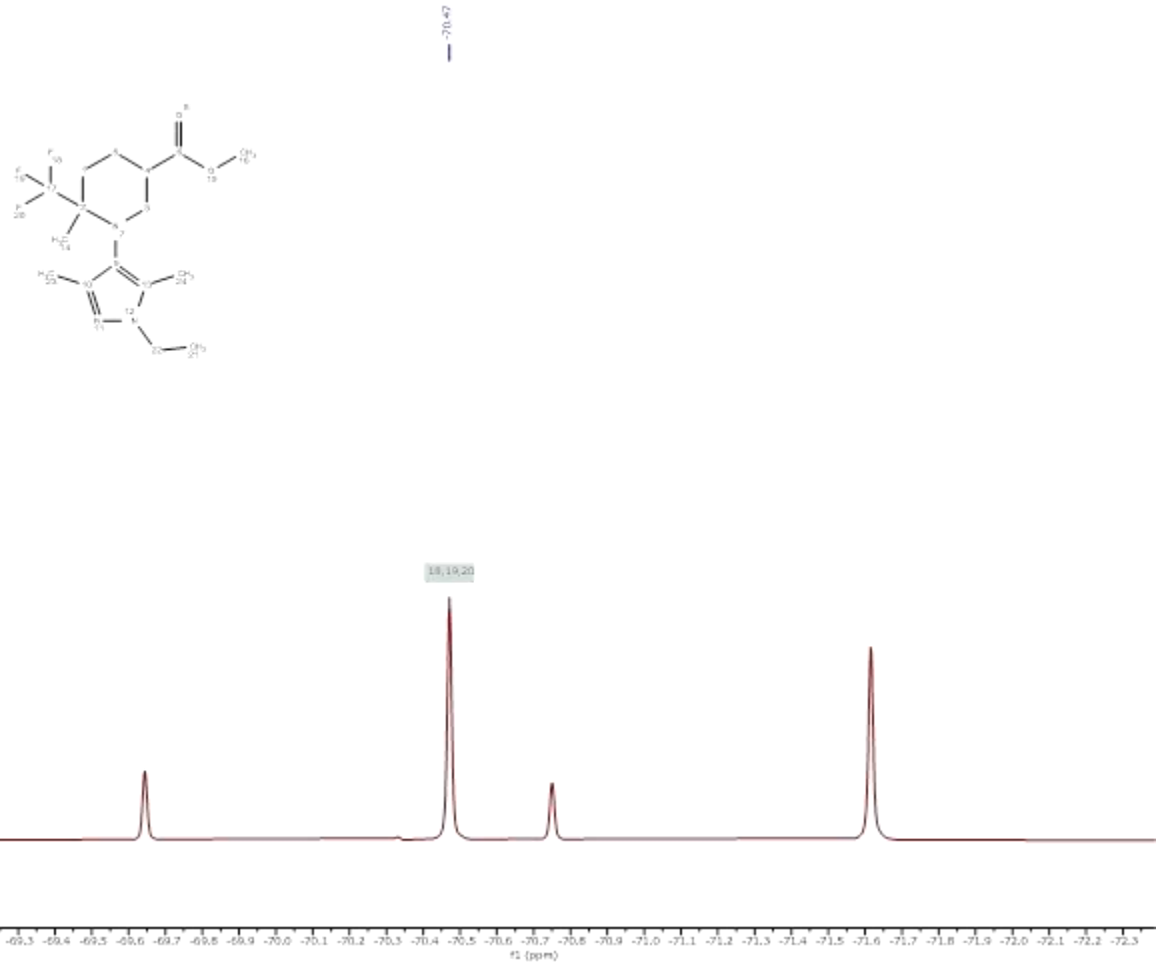
-70.47
18,19,20
-69.1 -69.2 -69.3 -69.4 -69.5 -69.6 -69.7 -69.8 -69.9 -70.0 -70.1 -70.2 -70.3 -70.4 -70.5 -70.6 -70.7 -70.8 -70.9 -71.0 -71.1 -71.2 -71.3 -71.4 -71.5 -71.6 -71.7 -71.8 -71.9 -72.0 -72.1 -72.2 -72.3
f1 (ppm)

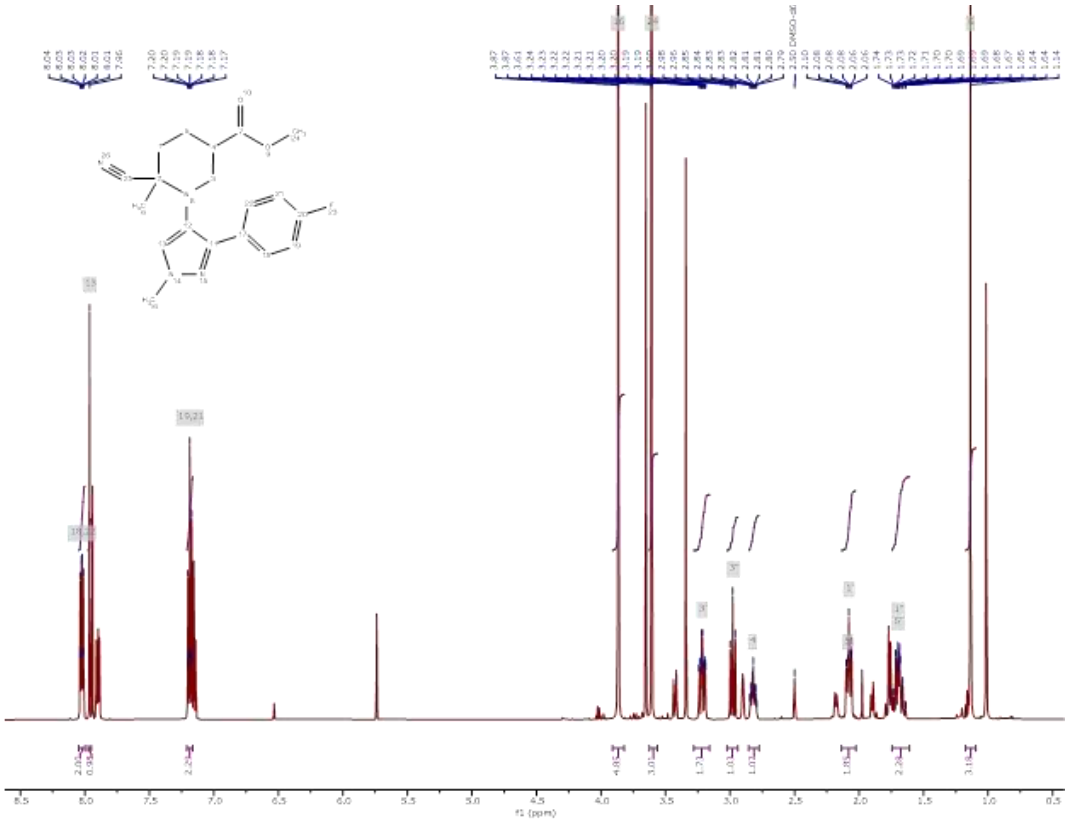

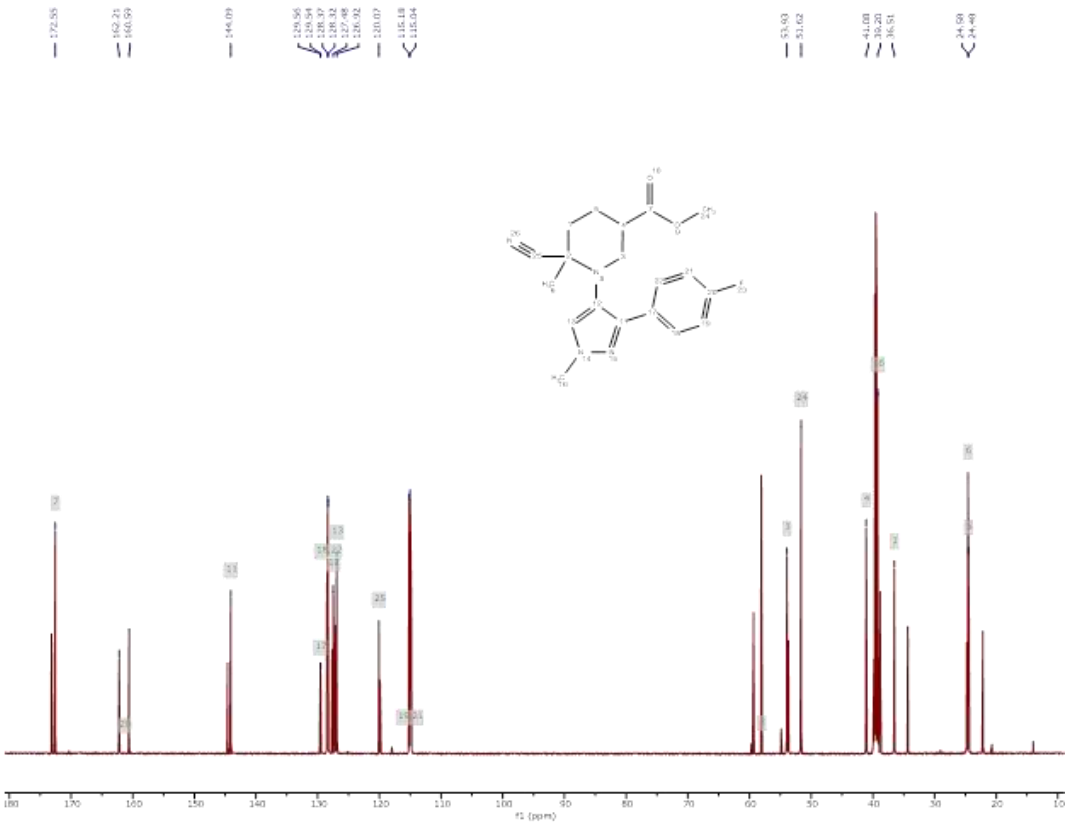

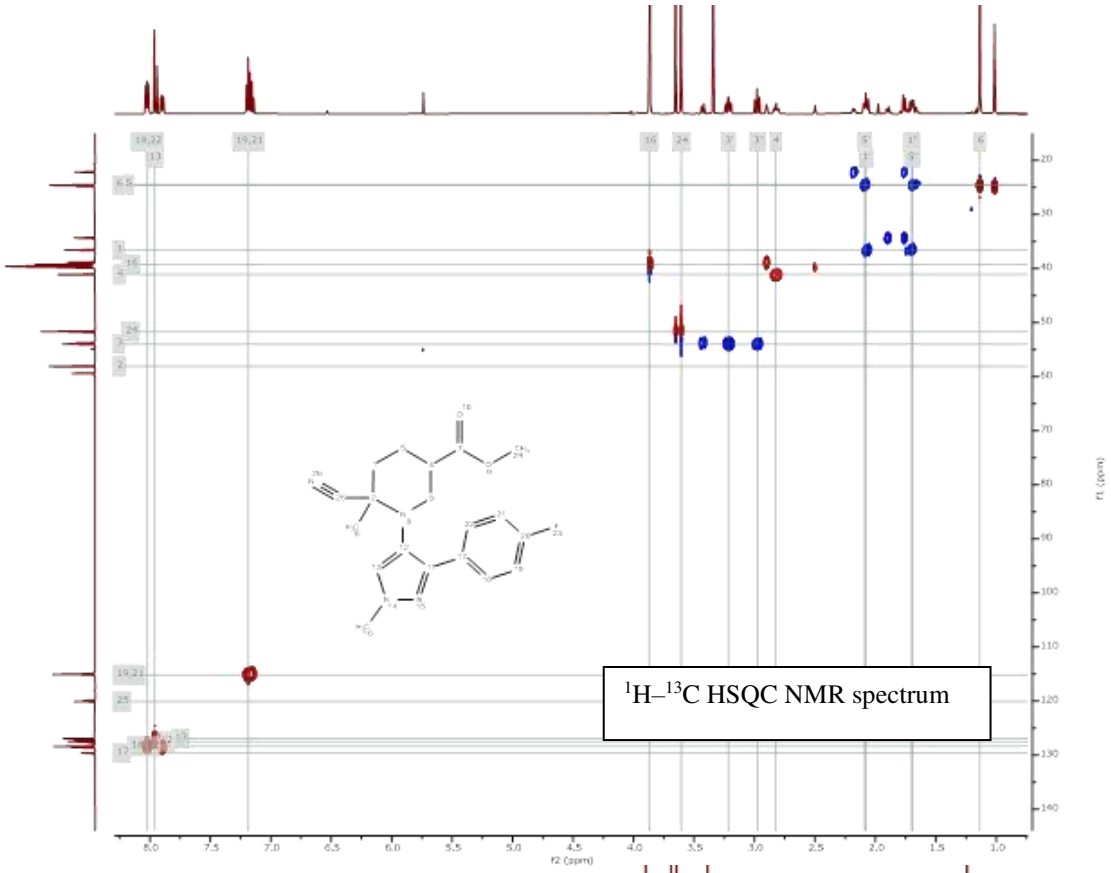
$^{1}H–^{13}C$ HSQC NMR spectrum

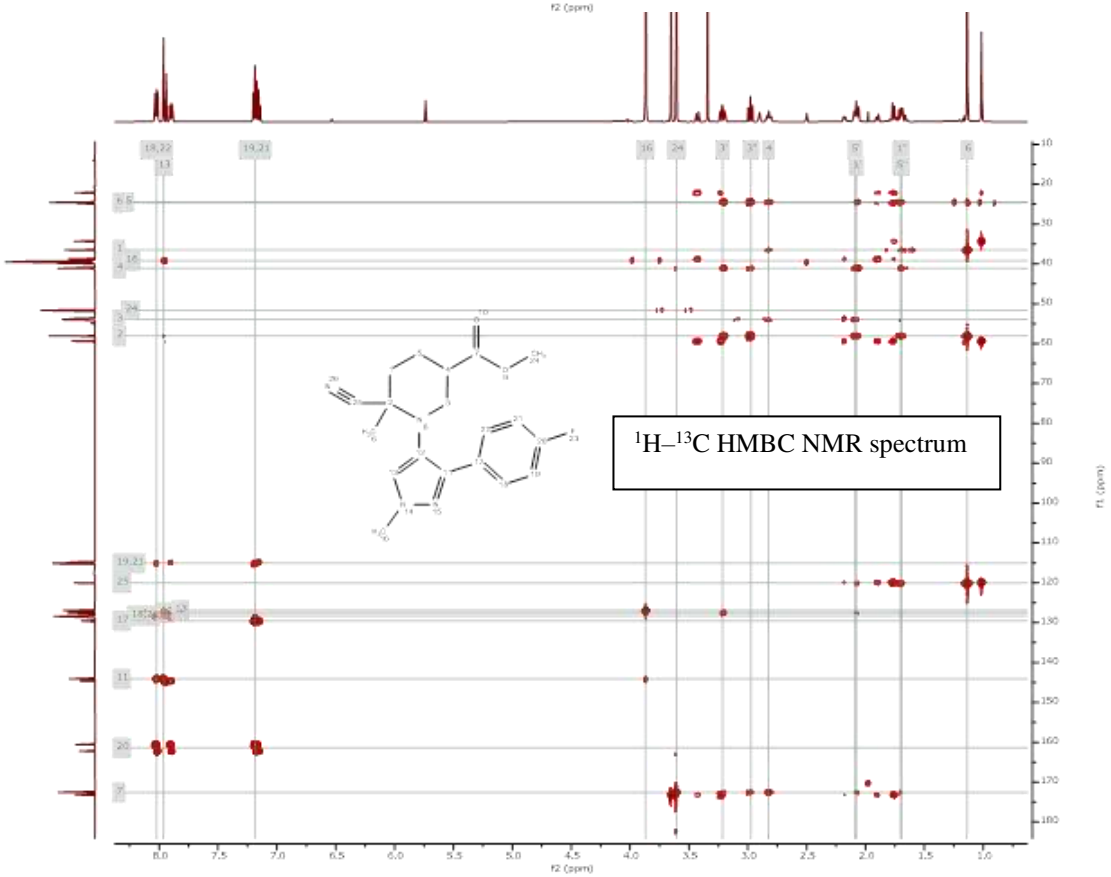
$^{1}H–^{13}C$ HMBC NMR spectrum

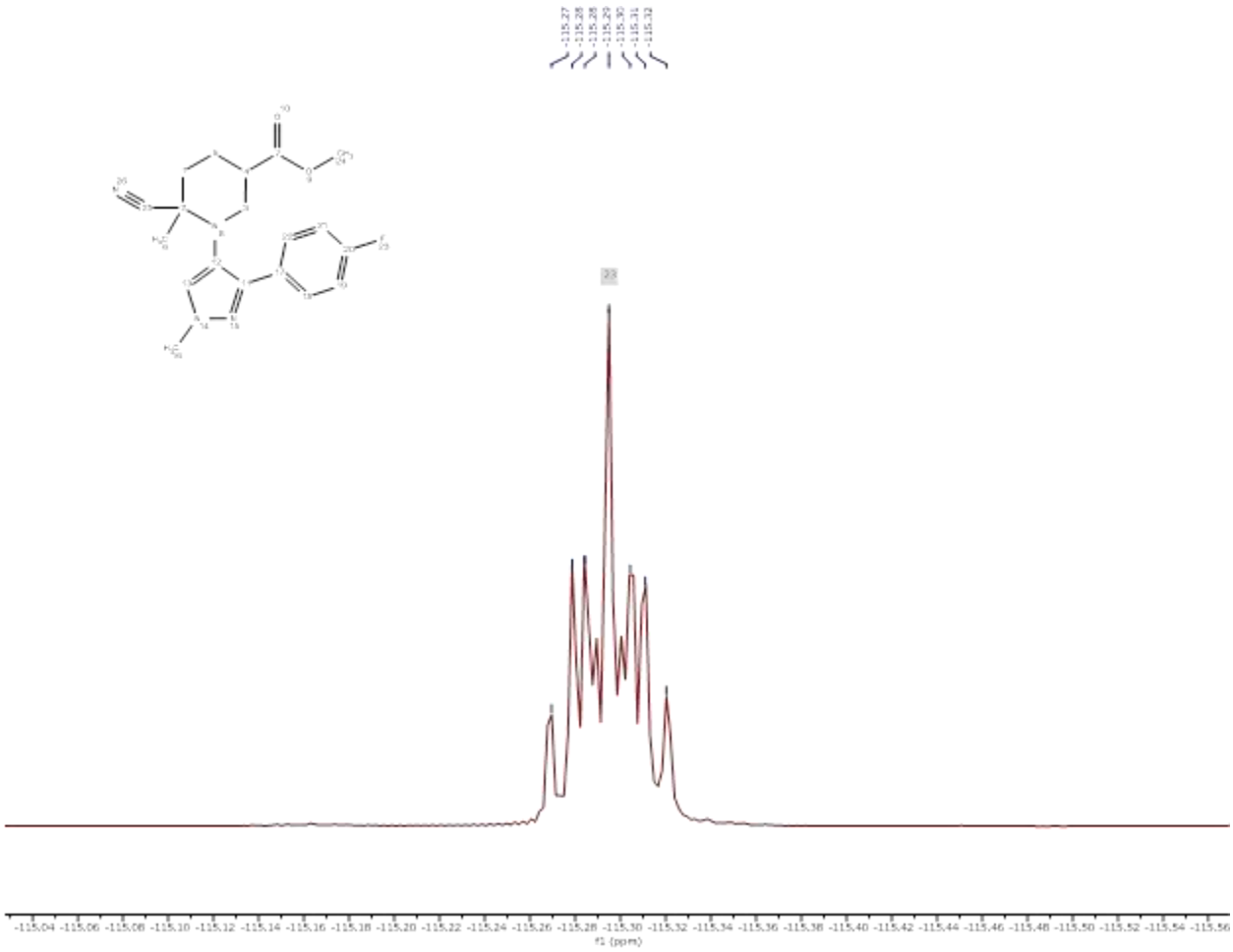
-115.27
-115.28
-115.28
-115.29
-115.30
-115.31
-115.32
23
-115.04 -115.06 -115.08 -115.10 -115.12 -115.14 -115.16 -115.18 -115.20 -115.22 -115.24 -115.26 -115.28 -115.30 -115.32 -115.34 -115.36 -115.38 -115.40 -115.42 -115.44 -115.46 -115.48 -115.50 -115.52 -115.54 -115.56
f1 (ppm)

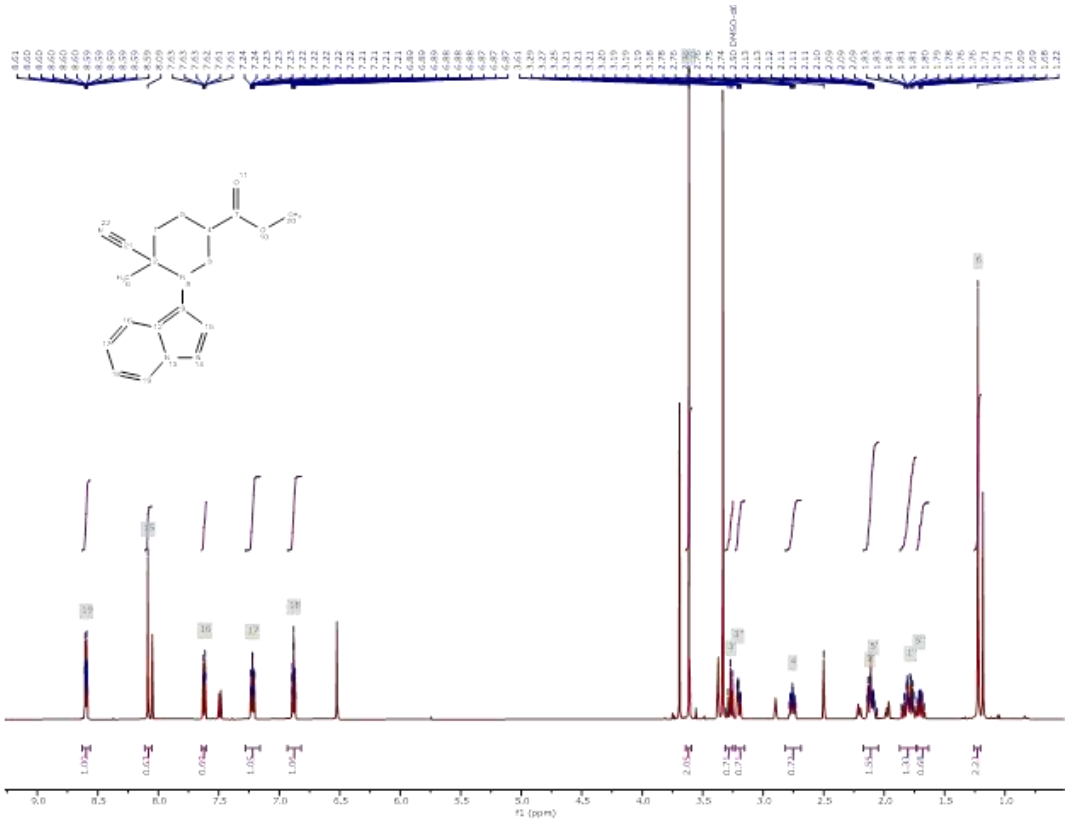

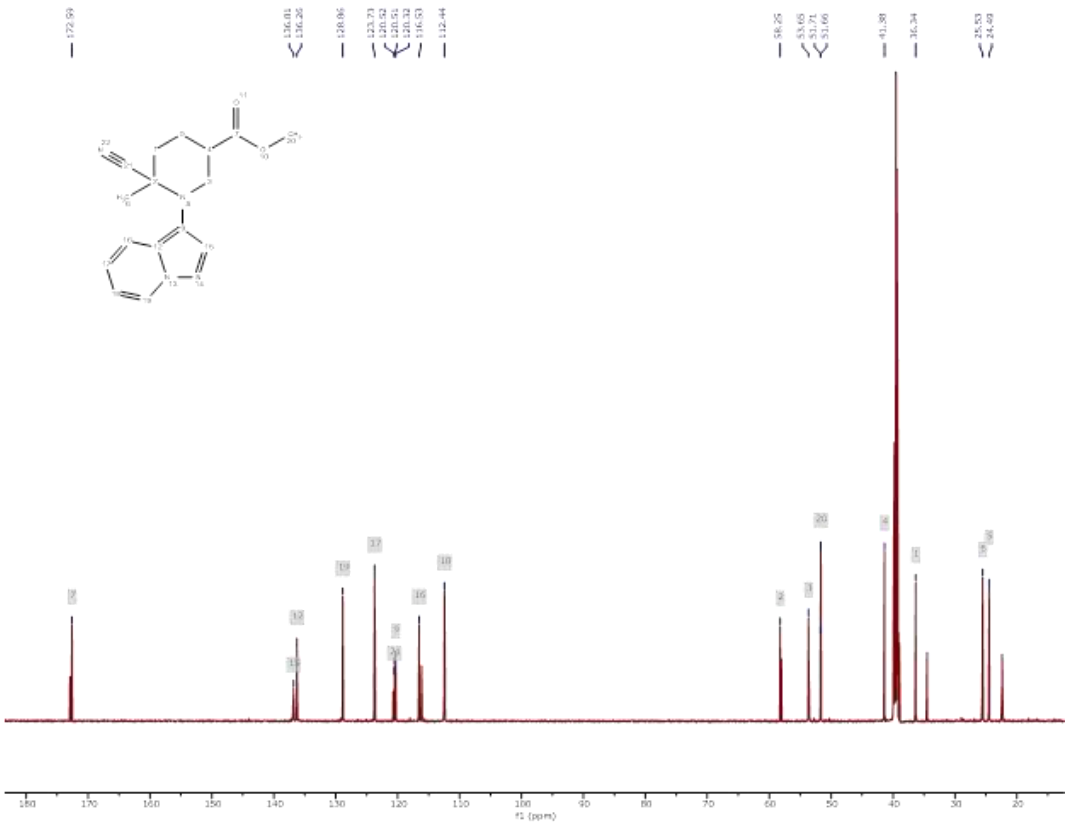

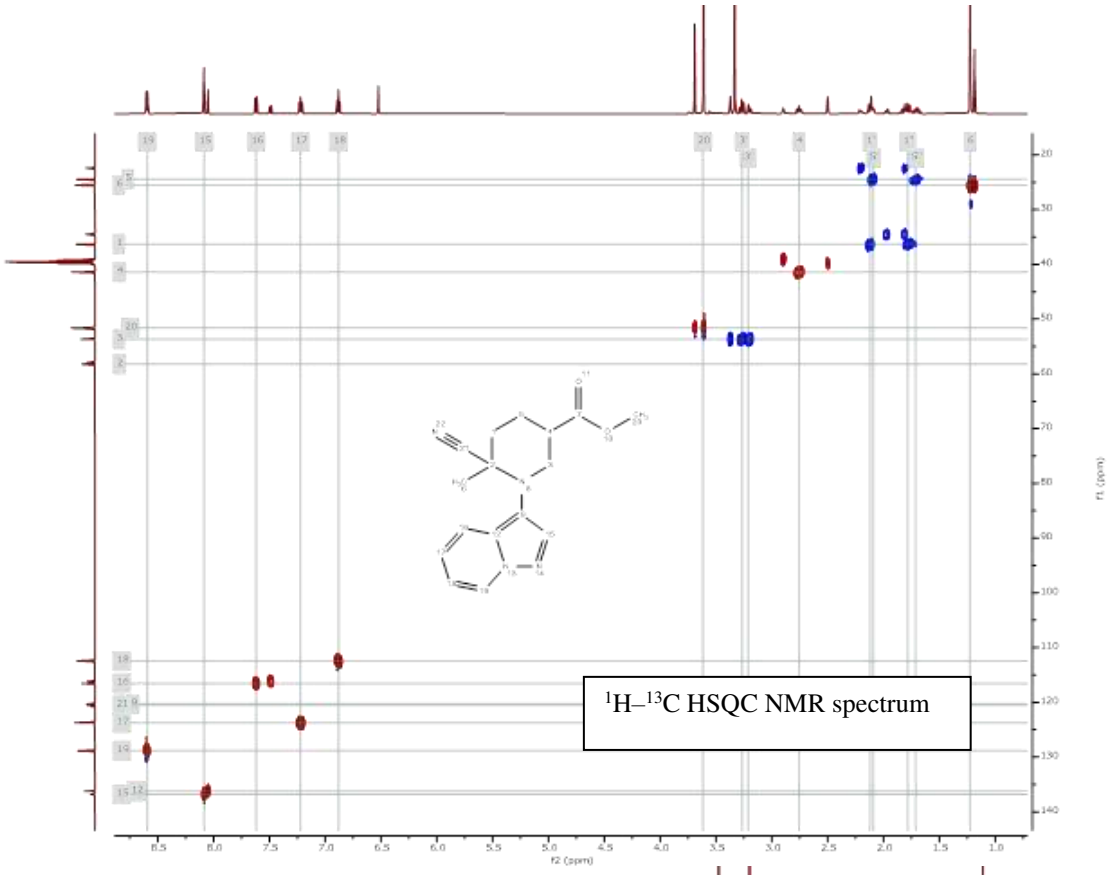
$^{1}H–^{13}C$ HSQC NMR spectrum

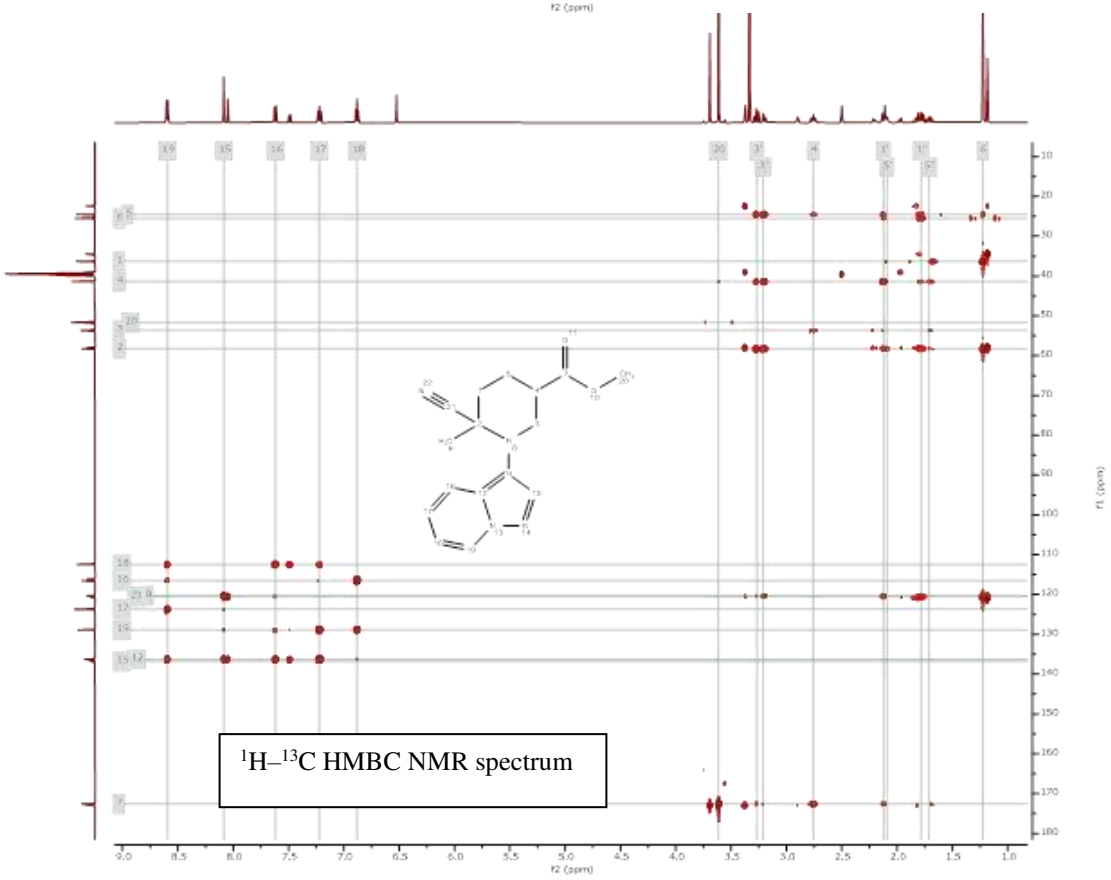
$^{1}H–^{13}C$ HMBC NMR spectrum

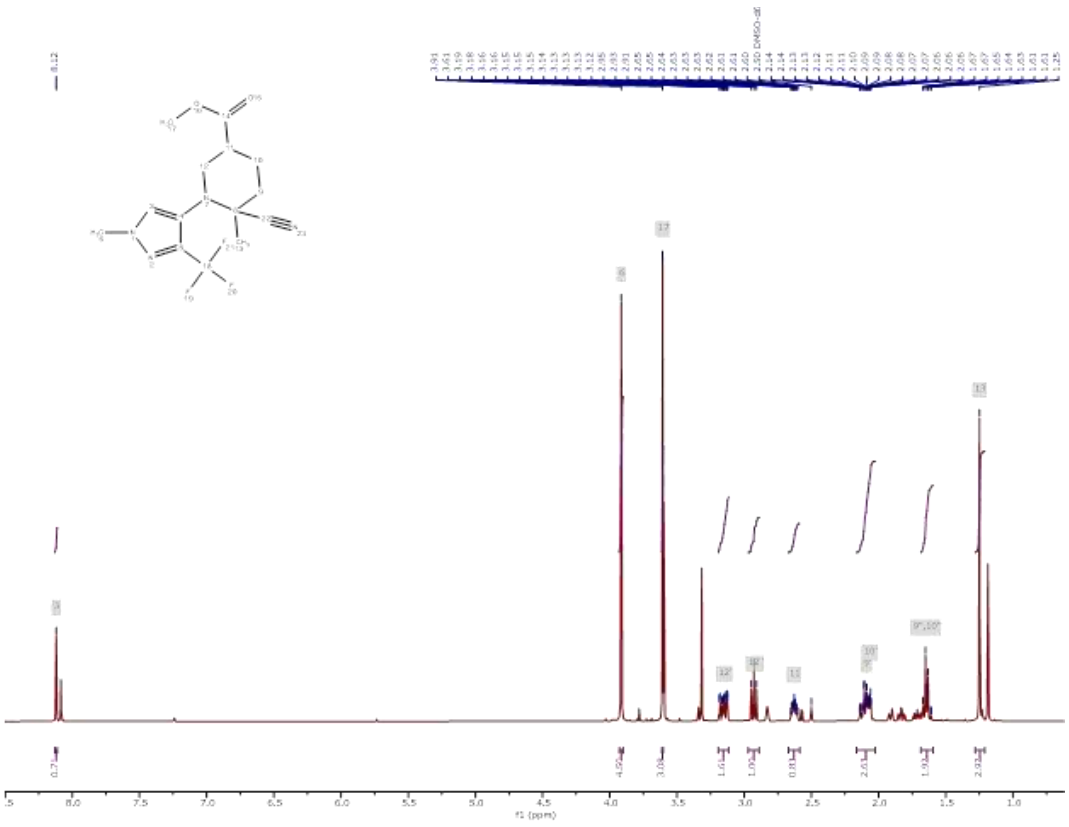

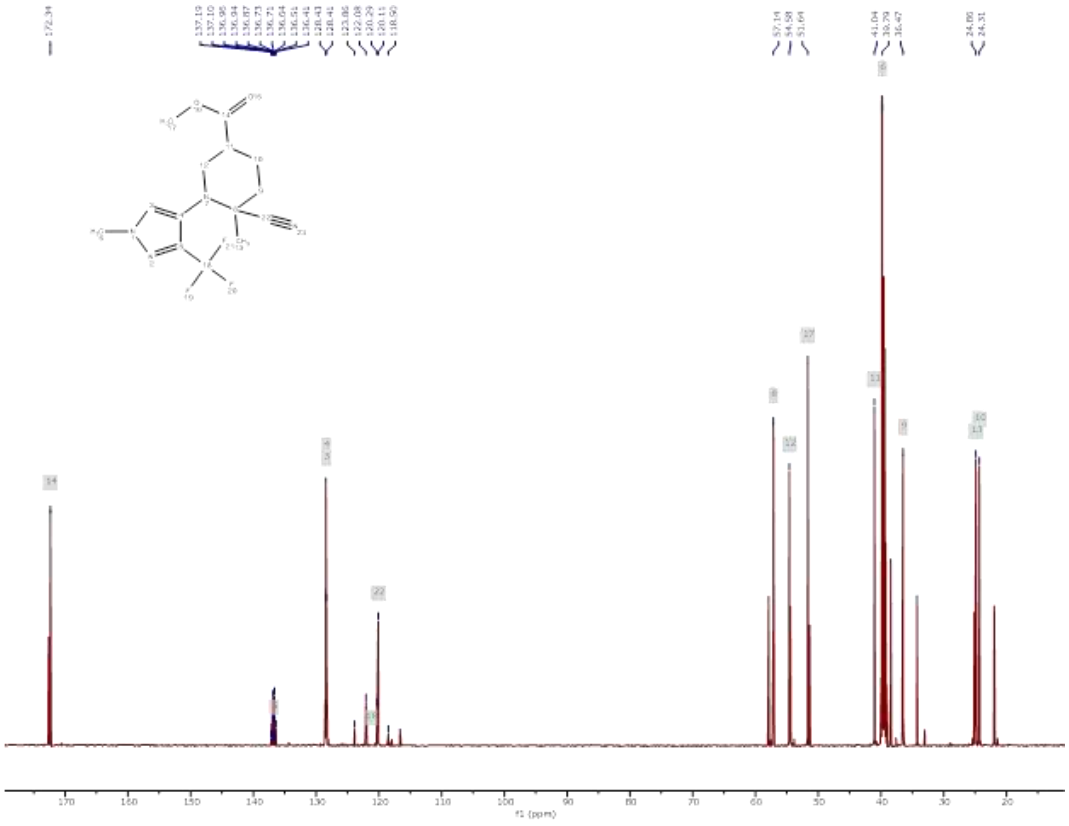

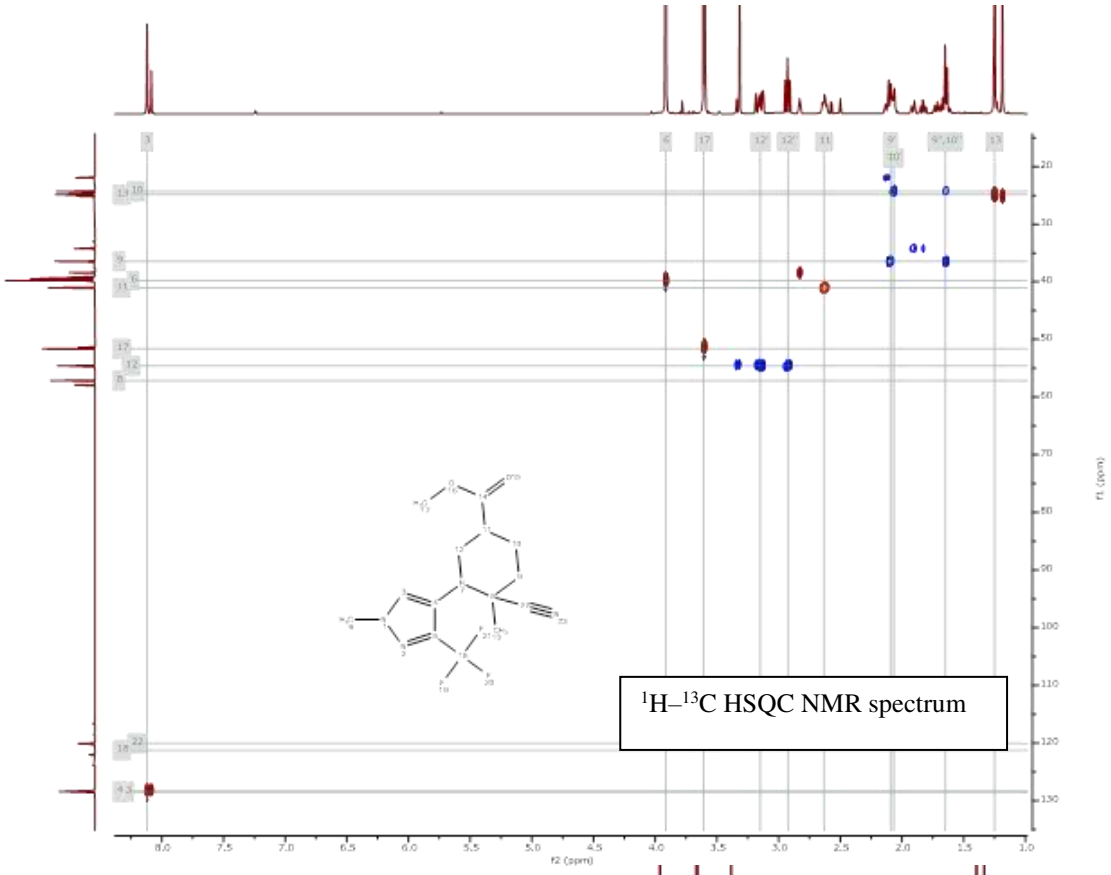

$^{1}H–^{13}C$ HSQC NMR spectrum

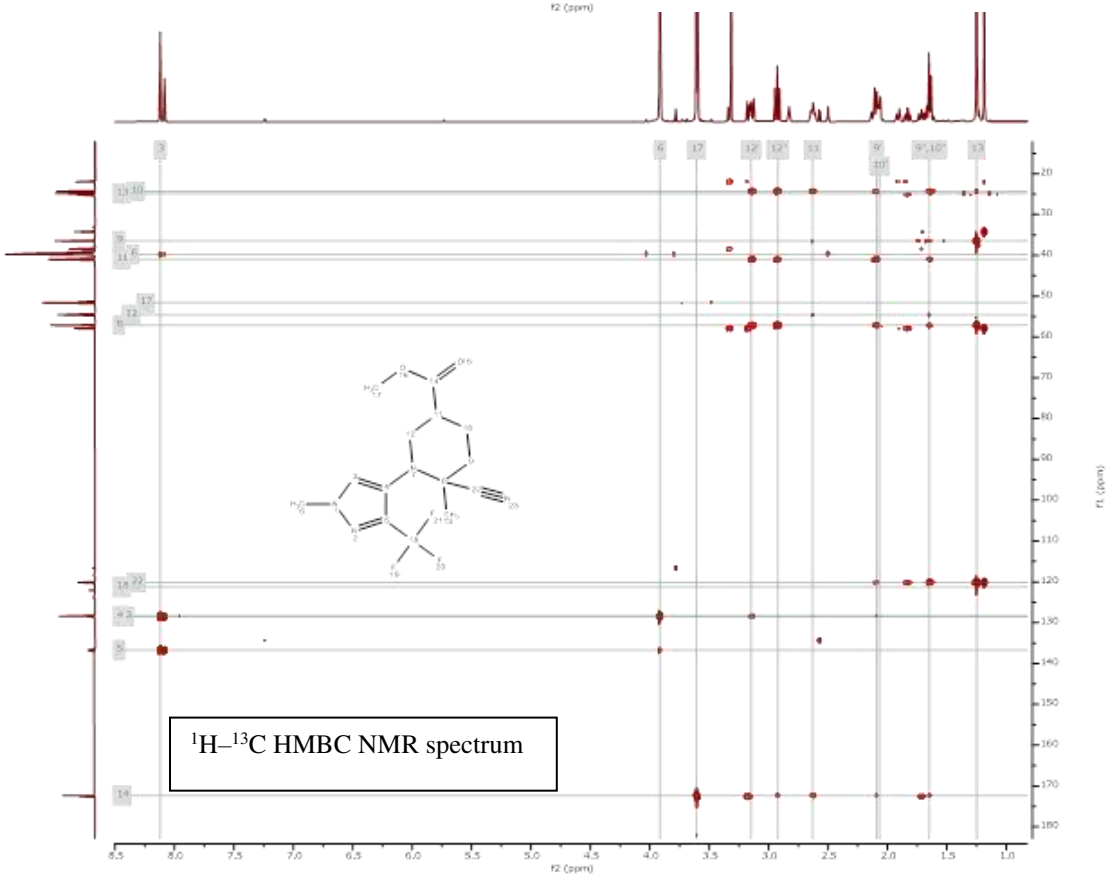

$^{1}H–^{13}C$ HMBC NMR spectrum

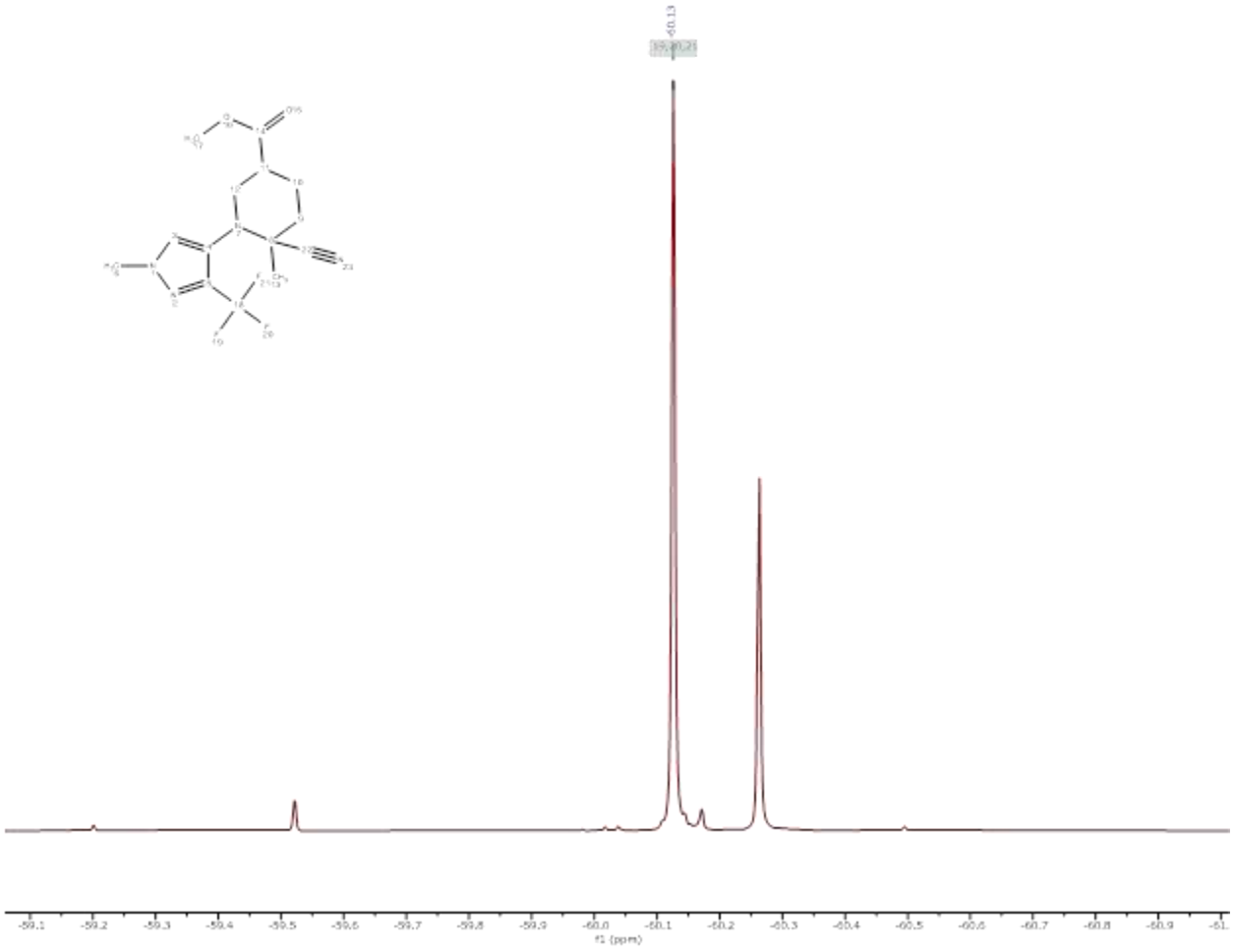
-60.13
-59.1
-59.2
-59.3
-59.4
-59.5
-59.6
-59.7
-59.8
-59.9
-60.0
-60.1
-60.2
-60.3
-60.4
-60.5
-60.6
-60.7
-60.8
-60.9
f1 (ppm)

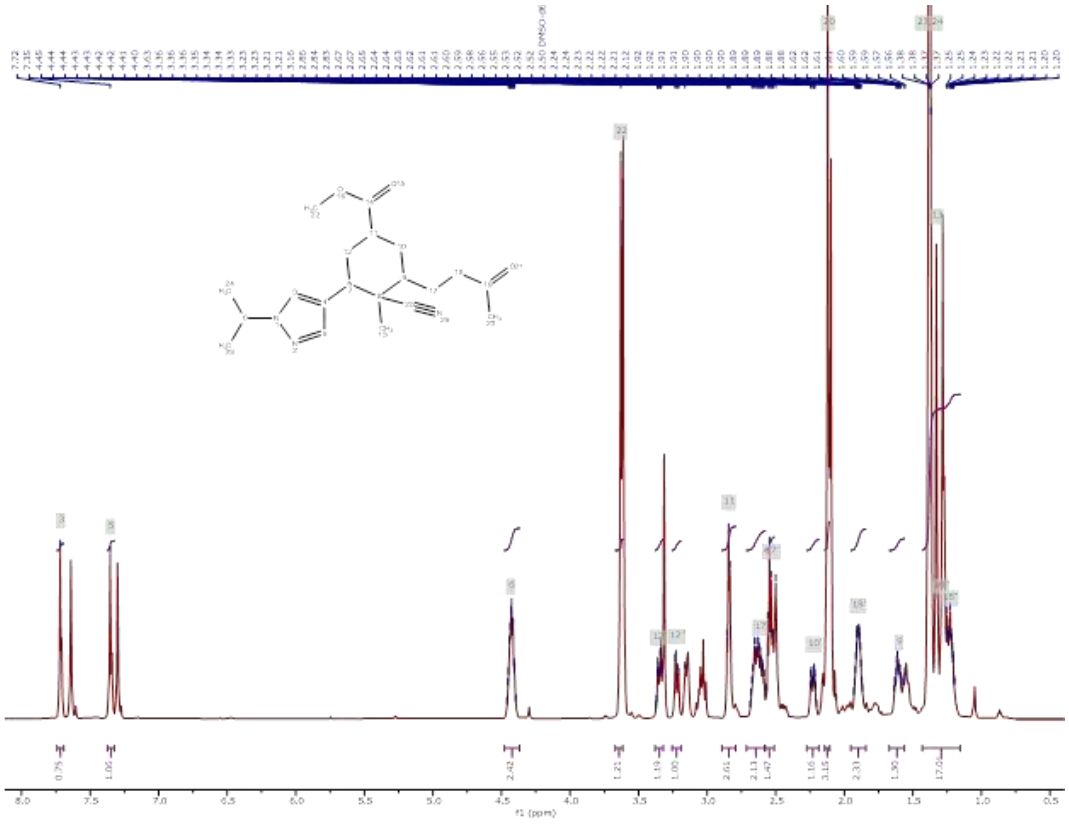

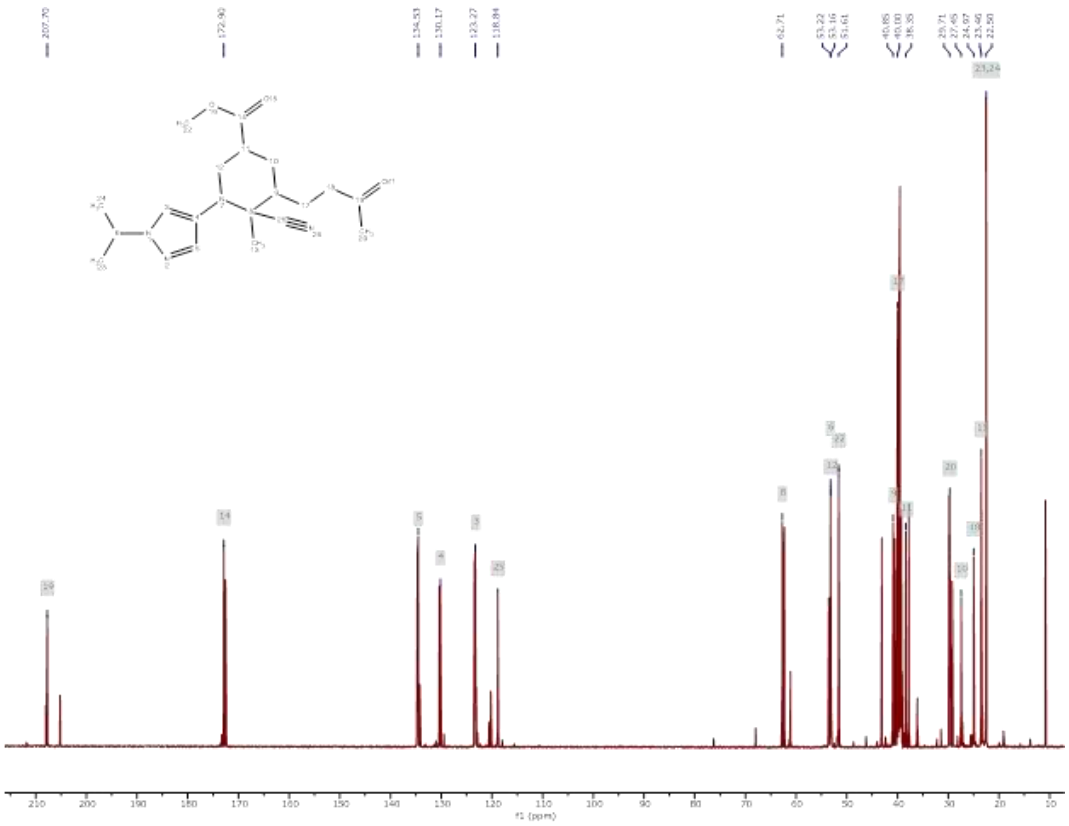

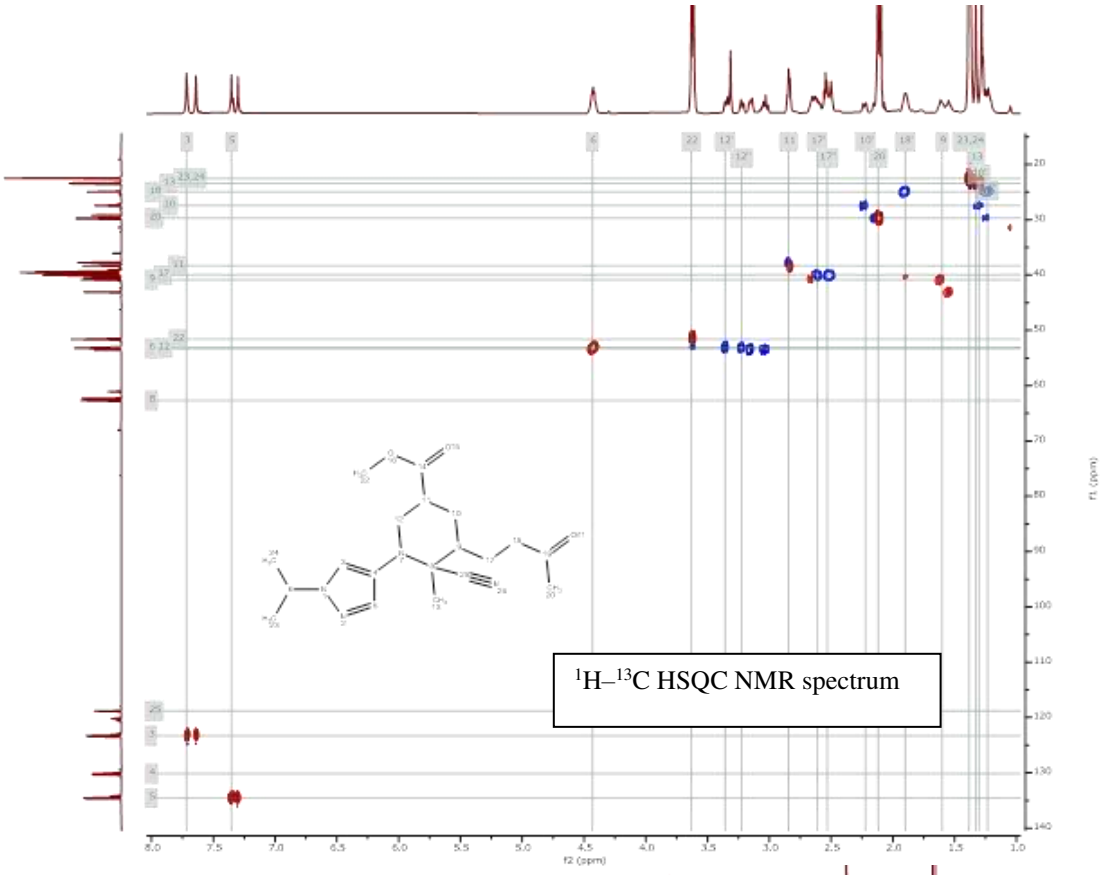

$^{1}H–^{13}C$ HSQC NMR spectrum

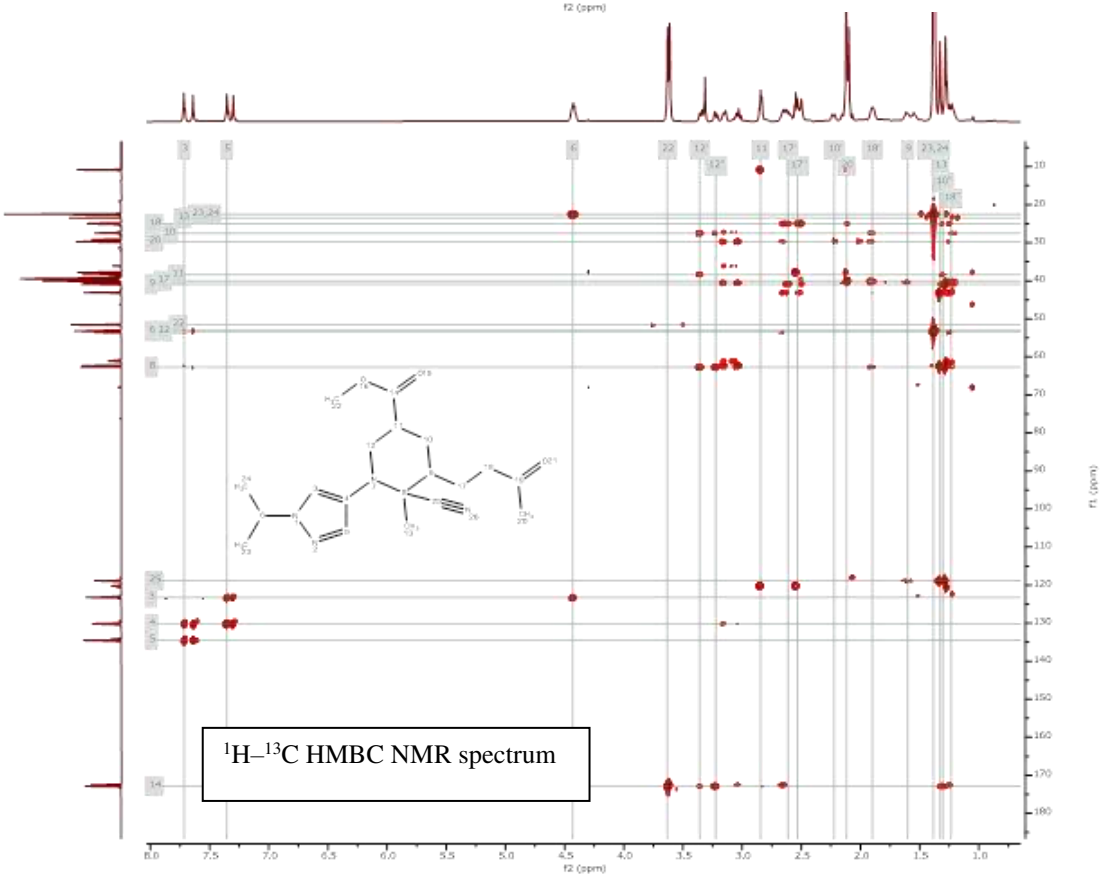

$^{1}H–^{13}C$ HMBC NMR spectrum

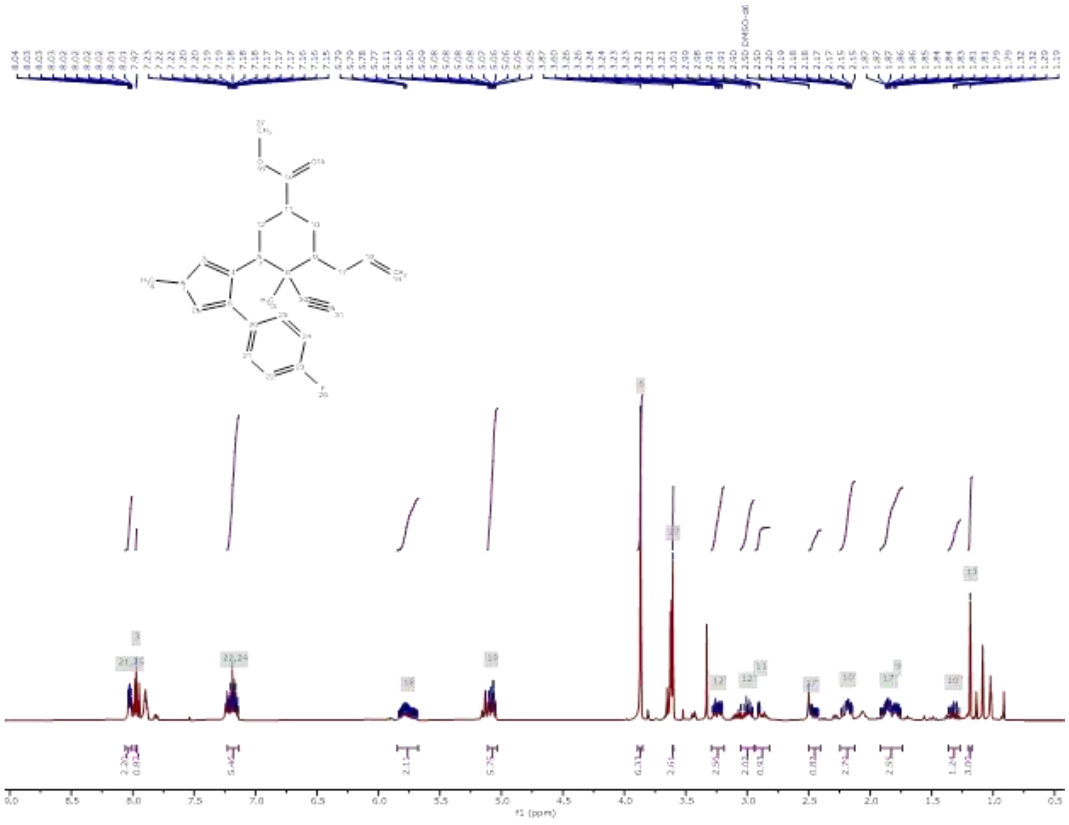

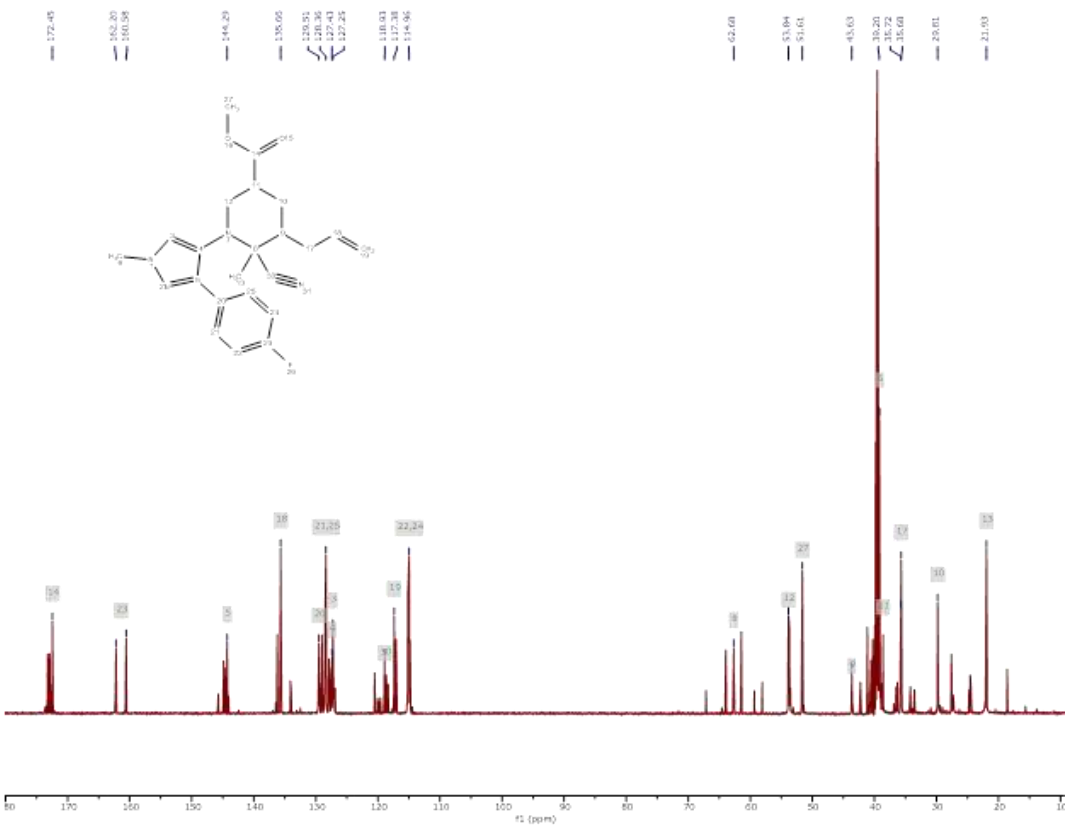

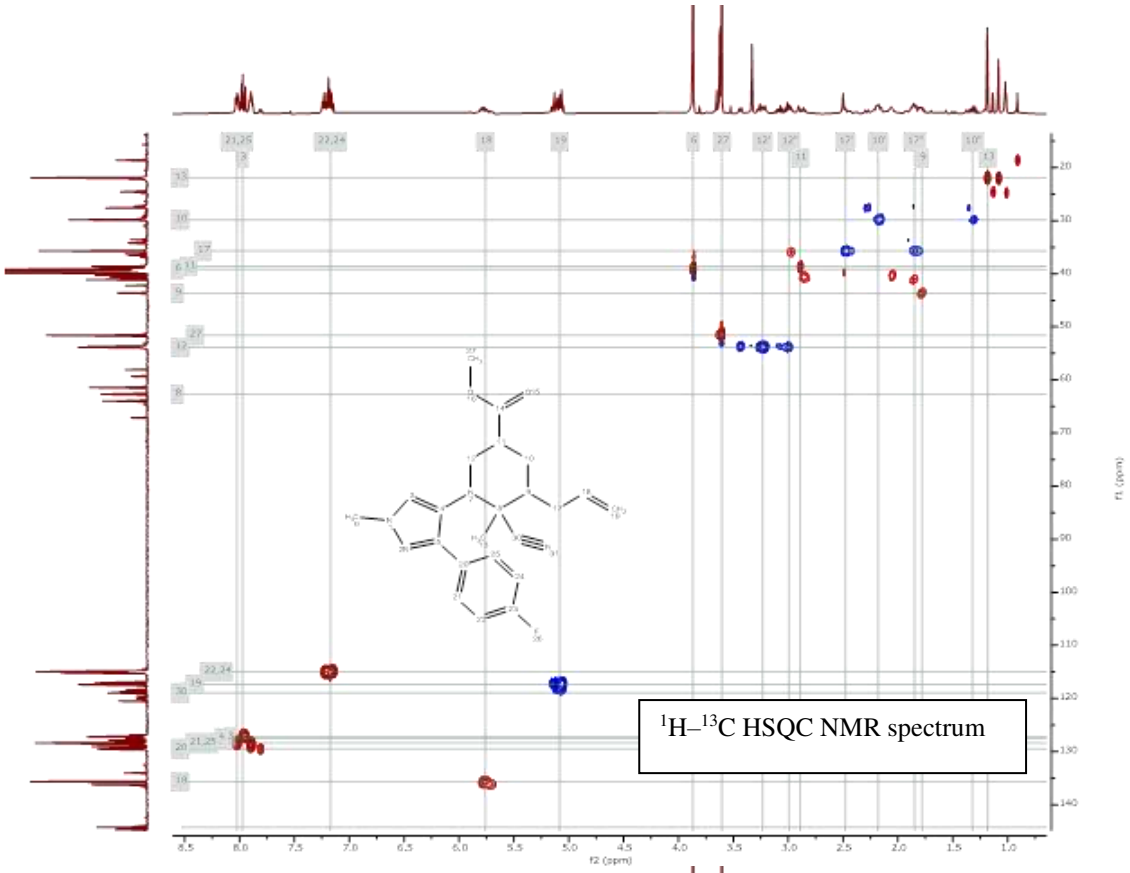
$^{1}H–^{13}C$ HSQC NMR spectrum

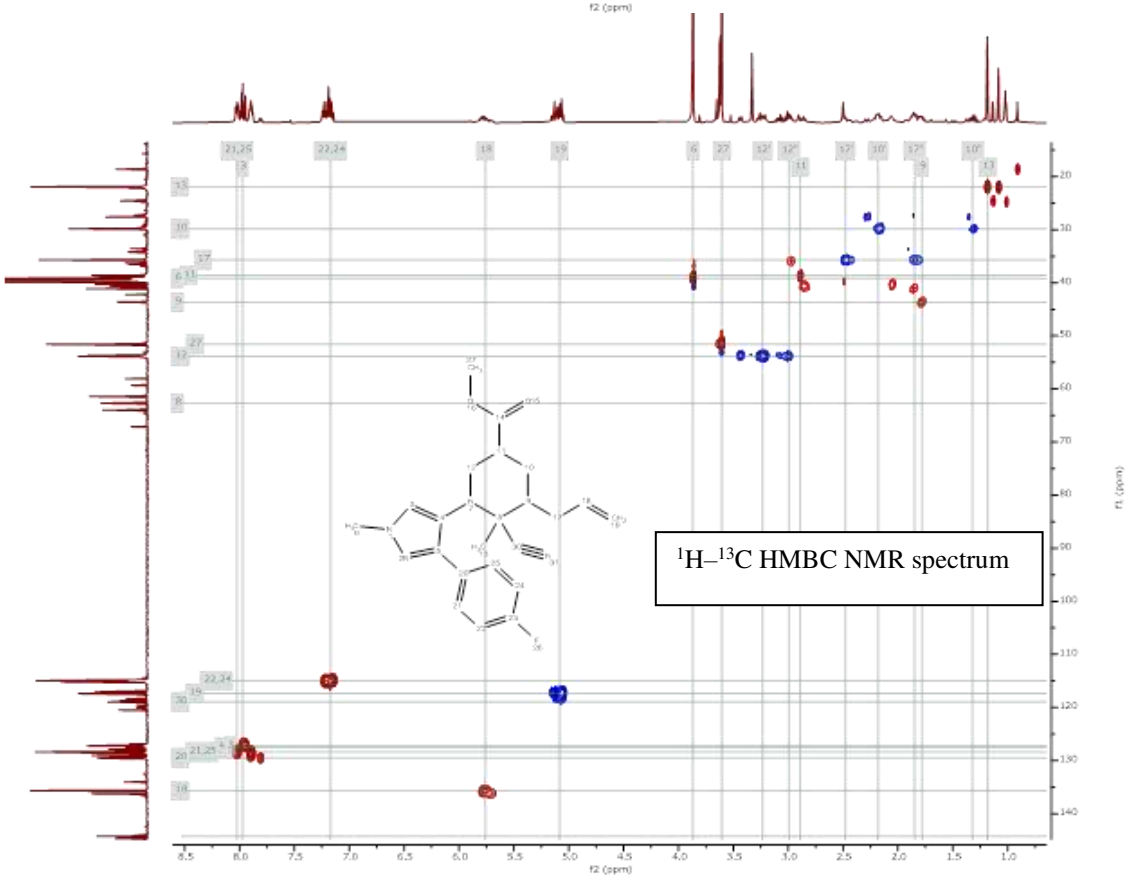
$^{1}H–^{13}C$ HMBC NMR spectrum

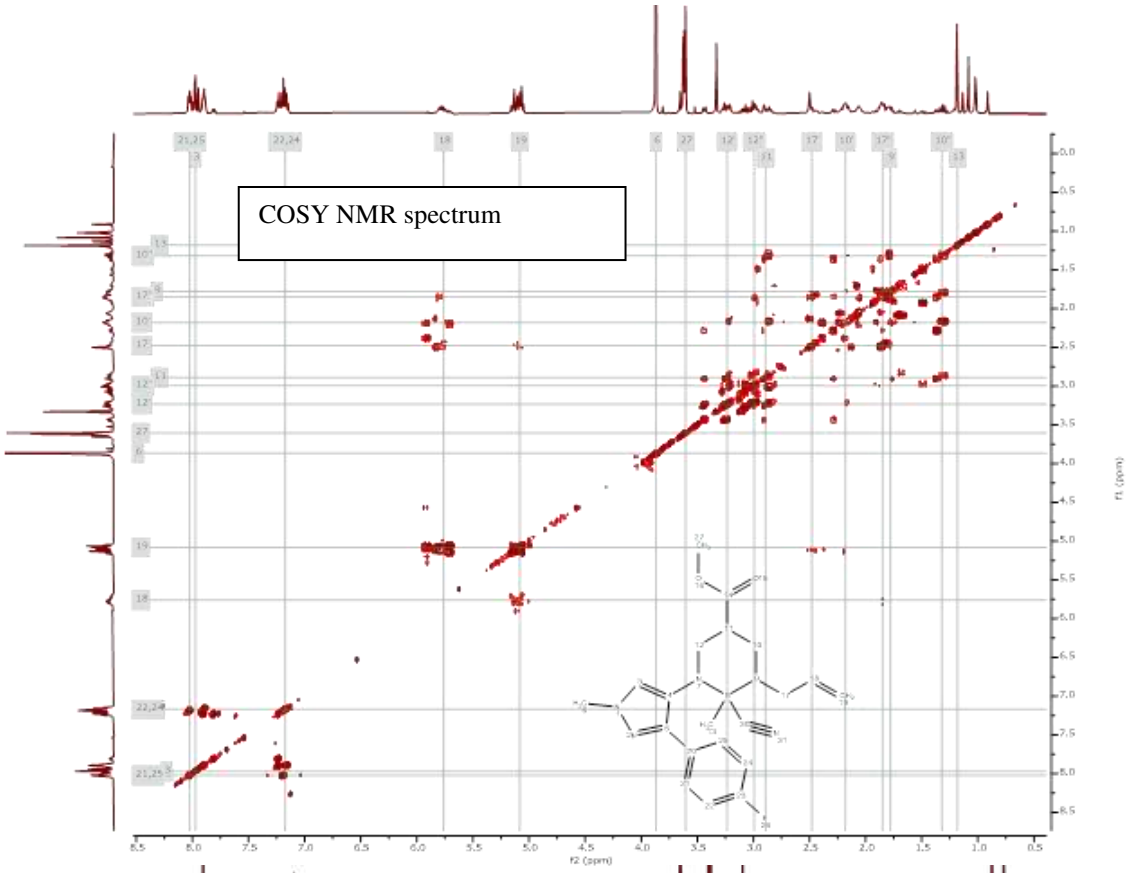
COSY NMR spectrum

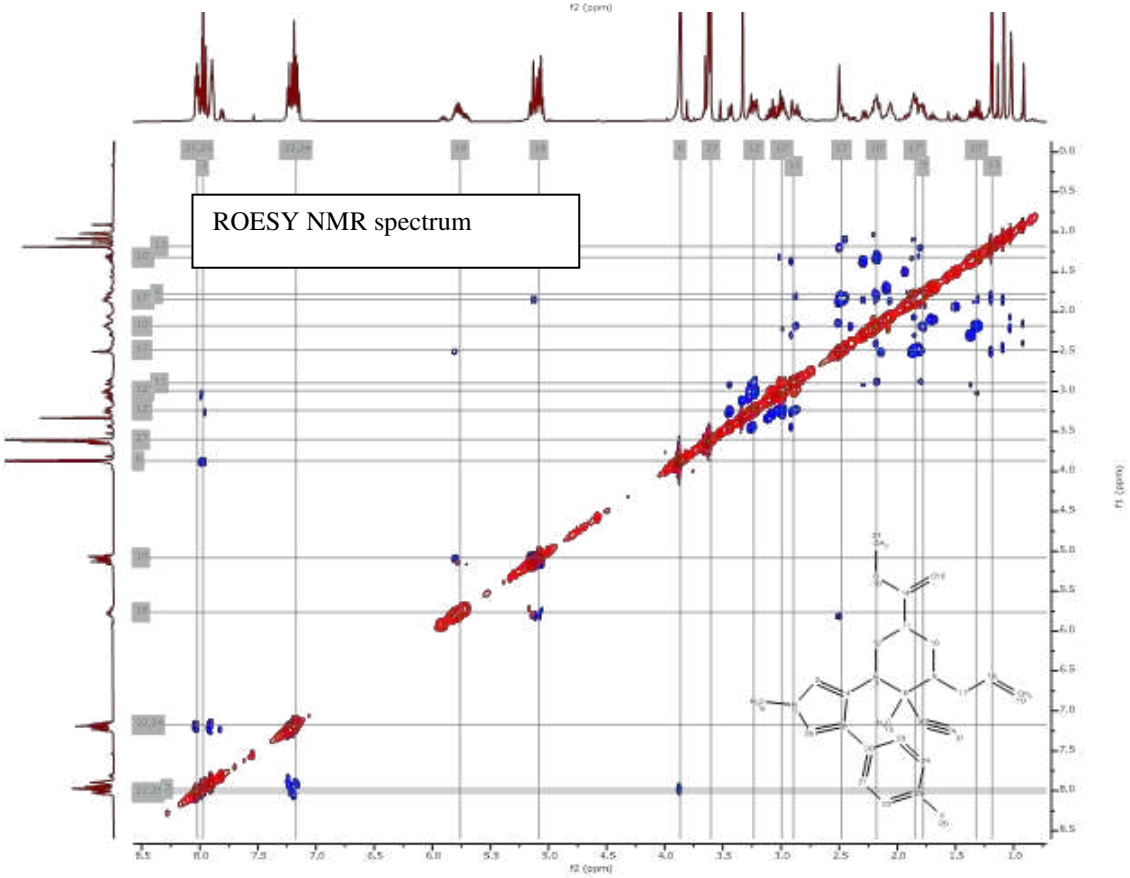
ROESY NMR spectrum

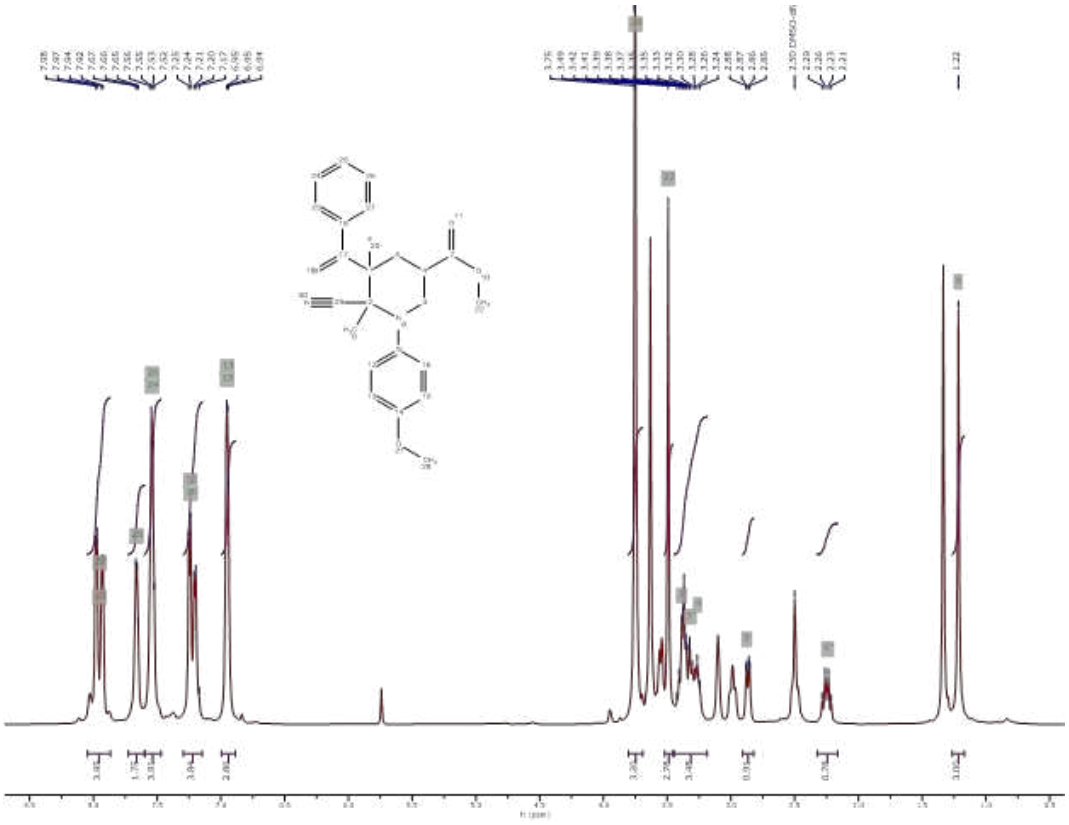

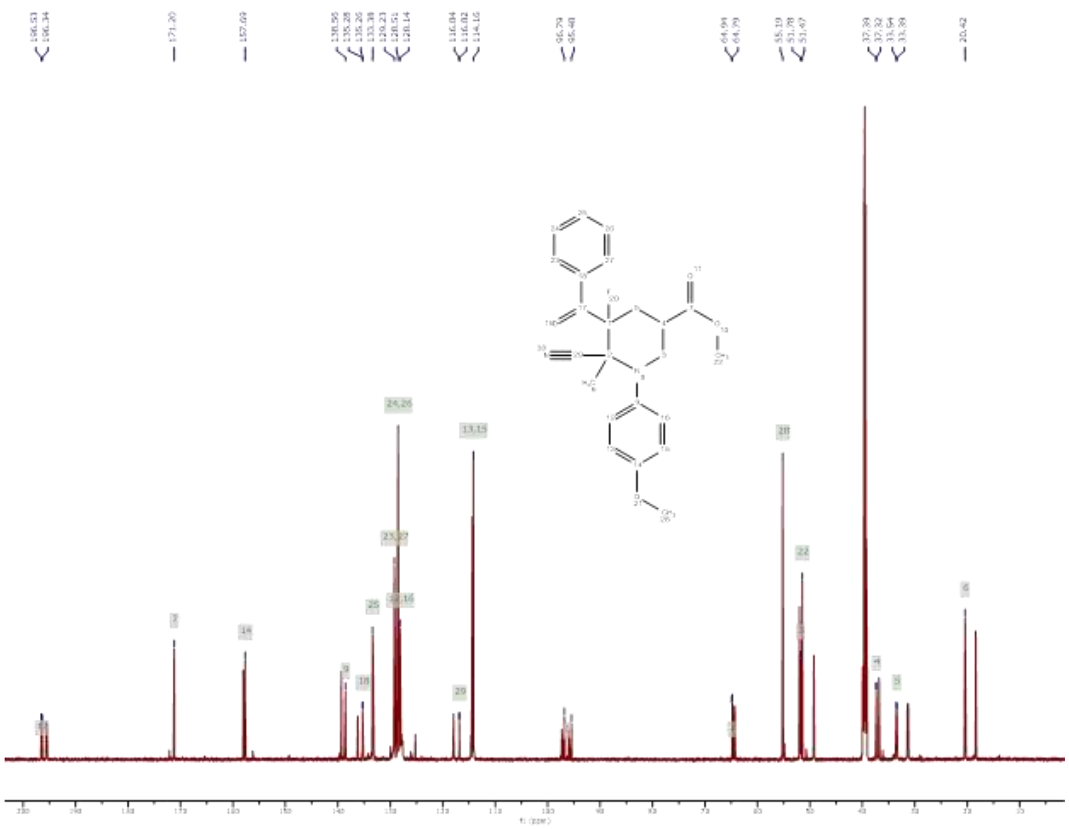

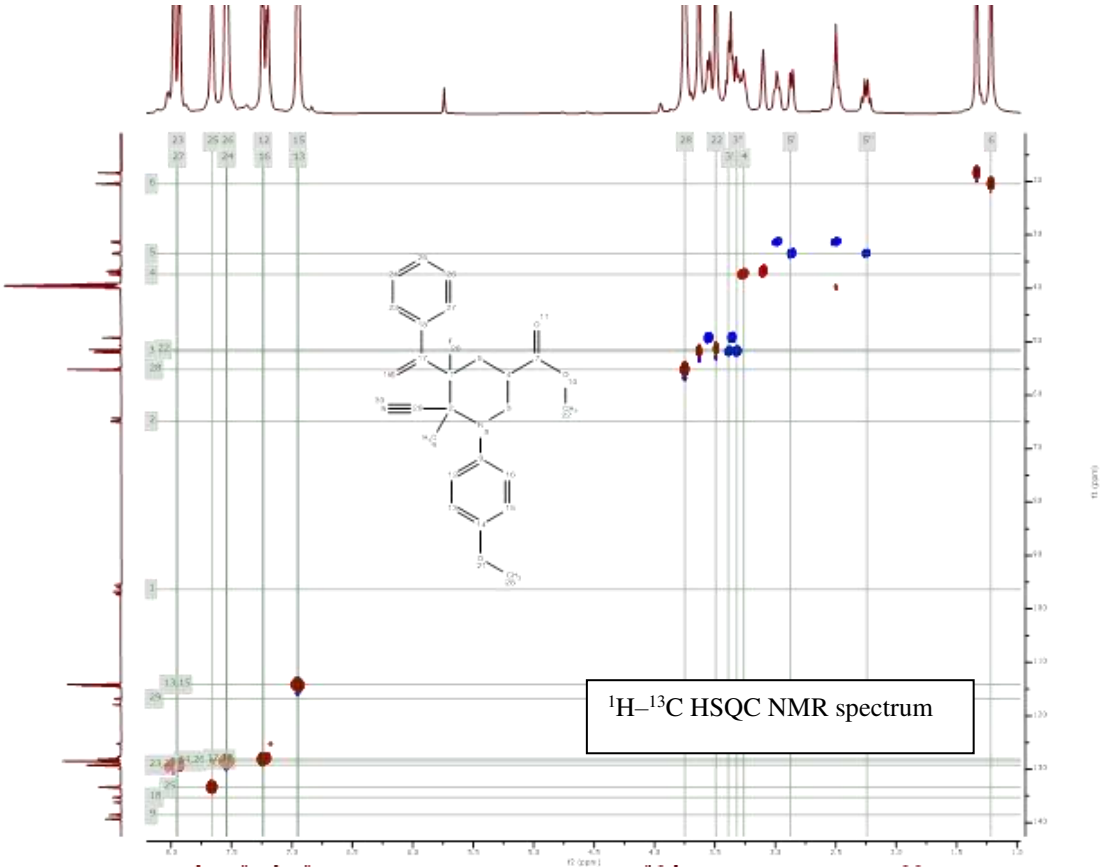

$^{1}H–^{13}C$ HSQC NMR spectrum

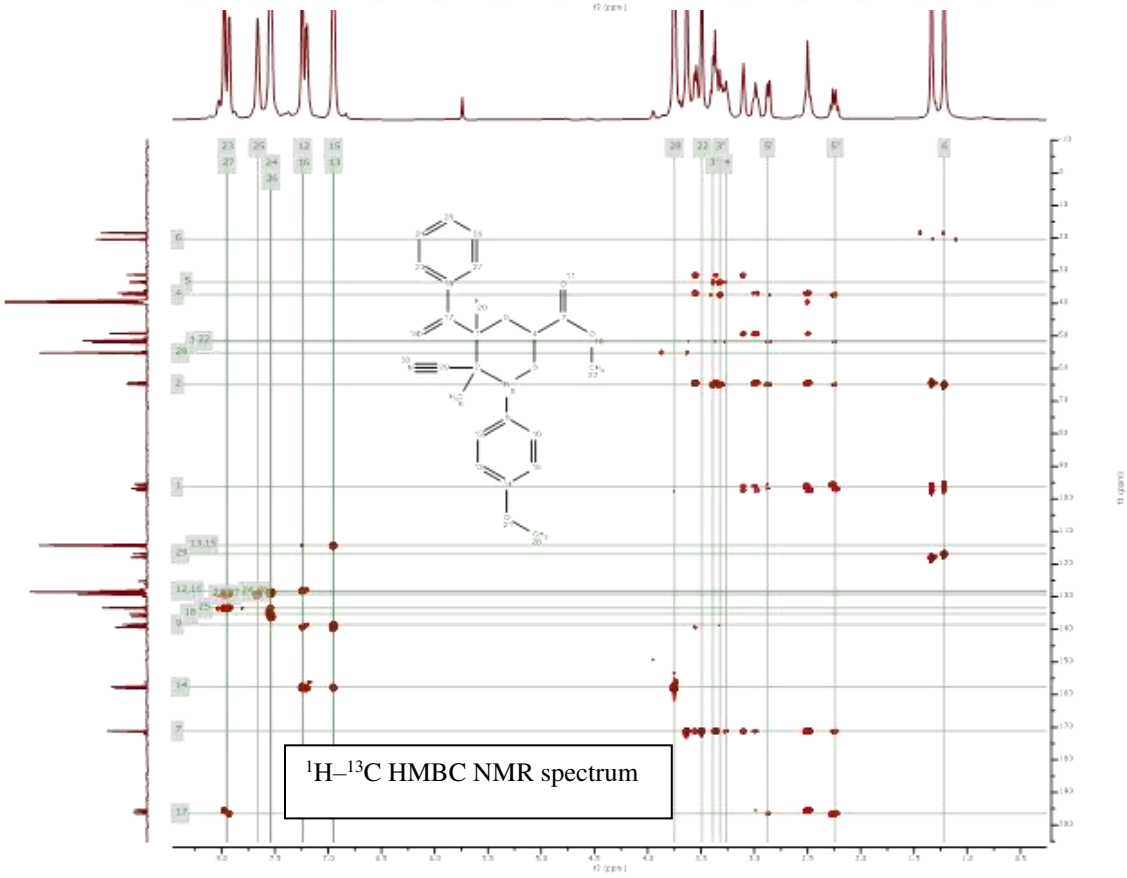

$^{1}H–^{13}C$ HMBC NMR spectrum

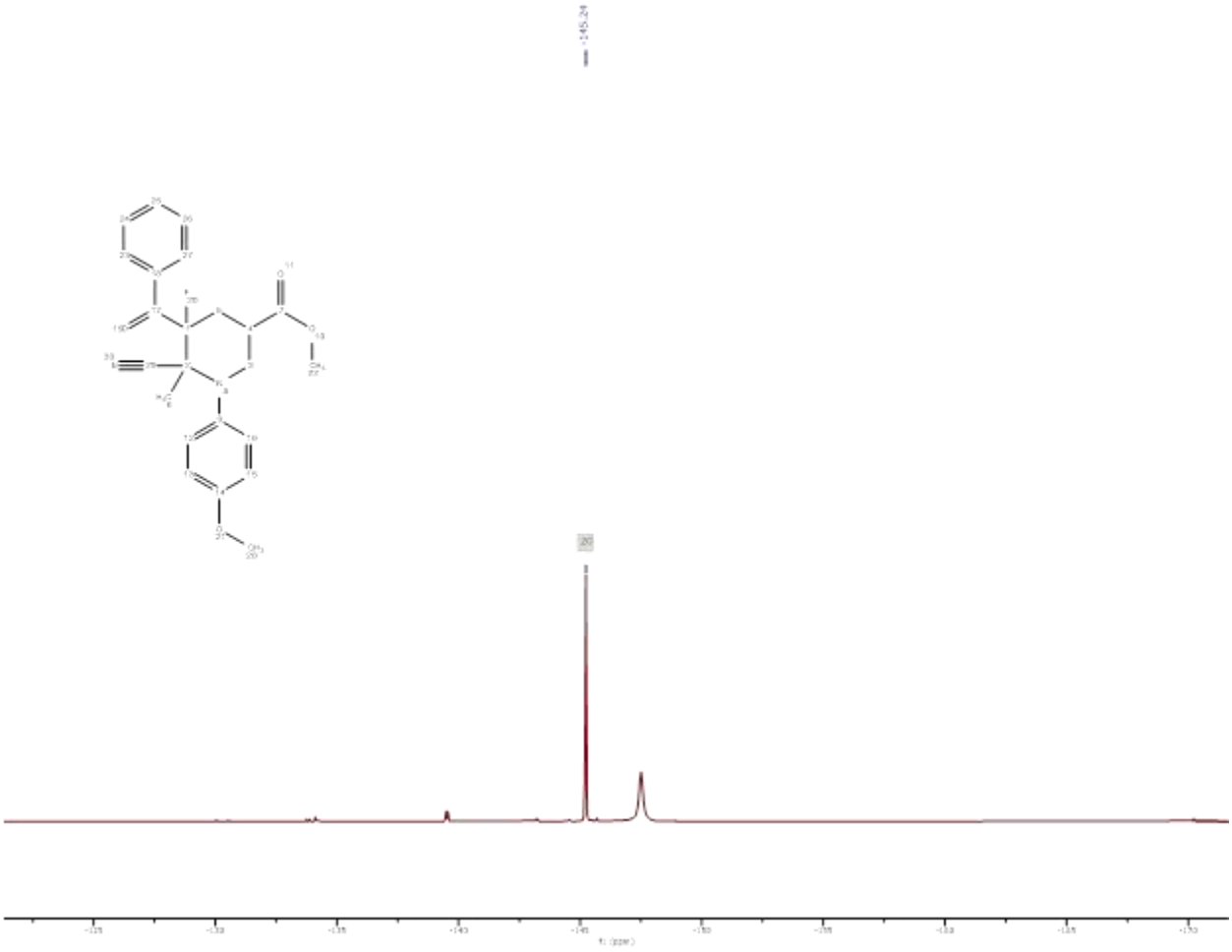

APPENDIX FOUR

COMPLEX PIPERIDINE SYNTHESIS ENABLED BY HYDROGENATION OF PYRIDINIUM SALTS: EXPERIMENTAL

A4.1. General Information

Proton nuclear magnetic resonance (^{1}H NMR) spectra were recorded at ambient temperature on either a Bruker Ultrashield–400 (400 MHz) spectrometer, a Varian 400 MR (400 MHz) spectrometer or an Agilent Inova 400 (400 MHz) spectrometer. Chemical shifts (δ) are reported in ppm and quoted to the nearest 0.01 ppm relative to the residual protons in $CDCl_3$ (7.26 ppm), C_6D_6 (7.16 ppm), $(CD_3)_2SO$ (2.50 ppm), CD_3OD (3.31 ppm) or CD_3CN (1.94 ppm) and coupling constants (*J*) are quoted in Hertz (Hz). Data are reported as follows: Chemical shift (number of protons, multiplicity, coupling constants). Coupling constants were quoted to the nearest 0.1 Hz and multiplicity reported according to the following convention: s = singlet, d = doublet, t = triplet, q = quartet, qn = quintet, sext = sextet, sp = septet, m = multiplet, br = broad. Where coincident coupling constants have been observed, the apparent (app) multiplicity of the proton resonance has been reported. Carbon nuclear magnetic resonance (^{13}C NMR) spectra were recorded at ambient temperature on either a Bruker Ultrashield–400 (100 MHz) spectrometer, a Varian 400 MR spectrometer (100 MHz) or an Agilent Inova 400 (100 MHz) spectrometer. Chemical shift (δ) was measured in ppm and quoted to the nearest 0.1 ppm relative to the residual solvent peaks in $CDCl_3$ (77.16 ppm), C_6D_6 (128.06 ppm), $(CD_3)_2SO$ (39.51 ppm), CD_3OD (49.00 ppm) or CD_3CN (1.32 ppm). DEPT135, NOE experiments and 2–dimensional experiments (COSY, HMBC, and HSQC) were used to support assignments where appropriate.

Low–resolution mass spectra (LRMS) were measured on an Agilent 6310 Quadrupole Mass Spectrometer. Infrared (IR) spectra were recorded on a Bruker Tensor 27 FT–IR spectrometer as either solids or neat films, either through direct application or deposited in $CHCl_3$, with absorptions reported in wavenumbers (cm^{-1}).

Analytical thin layer chromatography (TLC) was performed using pre–coated glass backed silica gel plates (Silicagel 60 F254). Flash column chromatography was undertaken on Silicycle silica gel (230–400 mesh) under a positive pressure of air. Visualization was achieved using ultraviolet light (254 nm) and chemical staining with ceric ammonium molybdate or basic potassium permanganate solutions as appropriate.

Tetrahydrofuran (THF), toluene, hexane, diethyl ether and dichloromethane were dried and distilled using standard methods.[1] Ethyl acetate (EtOAc), 1,2–Dichloroethane (DCE), 1,4–dioxane, chloroform, chlorobenzene and acetone were purchased anhydrous from Sigma Aldrich chemical company. All reagents were purchased at the highest commercial quality and used without further purification unless stated otherwise. Reactions were carried out under an atmosphere of nitrogen unless otherwise stated. All reactions were monitored by TLC, ^{1}H NMR spectra taken from reaction samples, and/or liquid chromatography mass spectrometry (LCMS) using an Agilent 6310 Quadrupole Mass Spectrometer.

A4.2. General Procedures

Zincke Imine Synthesis and Isolation

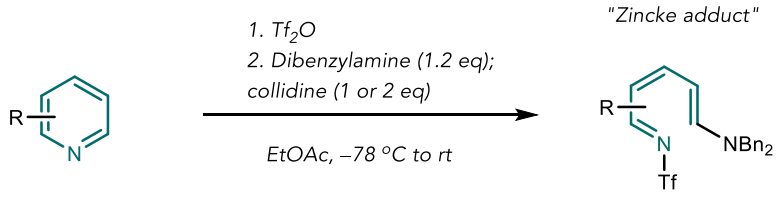

An oven dried 8 mL vial (≤ 0.5 mmol scale) or a round bottom flask (> 0.5 mmol scale) equipped with a stir bar was charged with the heterocycle (1.0 equiv) and placed under a nitrogen atmosphere. EtOAc (0.1 M) was added, the reaction vessel cooled to –78 ºC and Tf_2O (1.0 equiv) was added dropwise over 5 minutes. The reaction was stirred for 30 minutes before dibenzylamine (1.2 equiv) was added dropwise as a solution (1.0 M in EtOAc) followed by collidine (1.0 eq). The reaction was stirred for a further 30 minutes at –78 ºC. The cooling bath was removed and the reaction was allowed to warm to room temperature while stirring for approximately 30 minutes. The reaction was diluted with EtOAc then washed with H_2O (3x). The organic extract was dried ($MgSO_4$) and filtered. After filtration, the organic extract was added dropwise to excess hexanes (approx. 100 mL per 1.0 mmol) and the resulting oil was allowed to settle overnight in a –20 ºC fridge. After the oil has settled, the hexanes was decanted off and the residual oil was washed with hexanes and then dissolved in CH_2Cl_2 and concentrated *in vacuo* to provide the pure "Zincke imine" product.

Reaction Notes:

- Reaction is sensitive to excess of Tf_2O added (use of 1.2 eq results in substantial yield loss).
- Majority of substrates comparably with 1.0 equiv. and 2.0 equiv. collidine, 1.0 equiv. can be used regardless of substrate (Yields in scope table below denote how many equivalents

were used for that specific yield, but were within 5% when repeated with the other collidine amount).

- Stirring is critical to achieve consistent yields; recommended stirring 500-750 rpm
- For larger scales, it is recommended to allow the reaction to warm fully to room temperature, the 30 minutes was based on initial smaller scale reactions.
- Substrates with a 4-substituent (and unsubstituted pyridine) are susceptible to "bis-adduct" formation and care should be taken prior to crash out. Vaccing down prior to crash out results in significant (>20%) yield loss to bis-addition.
- If "bis-adduct" is observed, a short plug of silica (2-3 inches) and appropriate solvent eluent will remove it.
- Substrates with a 4-substituent (and unsubstituted pyridine) can be run with 1.0 eq Bn_2NH to minimize potential for bis-addition product formation.
- For substrates with a 2-R substituent, the organic extract can be concentrated *in vacuo* then redissolved in 2-10 mL CH_2Cl_2 prior to addition to the hexanes. This will provide higher yields.

N-Butyl Pyridinium Synthesis and Isolation

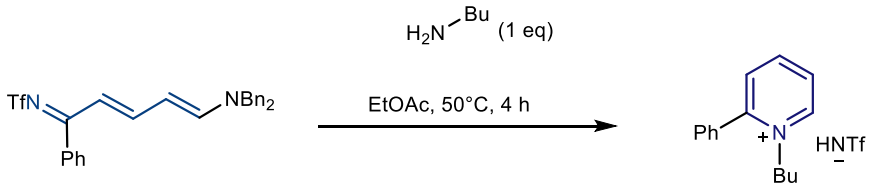

An oven dried 8 mL vial (≤ 0.5 mmol scale) or a round bottom flask (> 0.5 mmol scale) equipped with a stir bar was charged with the Zincke imine (1.0 equiv), EtOAc (0.1 M), and the *N*-butylamine (1.0 equiv). The reaction vessel was heated to 50 ºC and stirred for 4 hours. The reaction was cooled to room temperature and added dropwise directly to excess hexanes (approx. 100 mL per 1.0 mmol). The resulting suspension was allowed to settle overnight in a –20 ºC fridge and a thick oil results. The hexanes was decanted off and the residual oil was washed further with hexanes. The residue was dissolved in CH_2Cl_2, transferred to a round bottom flask and concentrated *in vacuo* to provide the pure pyridinium product. Yields range from 90%-98%.

Reaction Notes:

- Reaction ran with no precautions taken to exclude air or moisture proceeds with no change in yield
- Avoid any workup with water as the pyridinium product will partition into the aqueous layer.
- Reaction ran on 5.0 mmol scale following the general procedure yielded desired product in 98% yield. Product was kept in round bottom flask at room temperature on the bench for 5 weeks (from February 3rd, 2021 to March 11th, 2021) and no decomposition was observed via proton NMR.
- The crude reaction mixture can be concentrated *in vacuo* and reconstituted in CH_2Cl_2 prior to the crash out procedure if experiencing low yield upon precipitation.

- Depending on the substitution of the alpha position of the alkyl amine, (primary vs secondary or tertiary at the alpha position) different conditions are required for cyclization. Studies ongoing.

- Product decomposes upon prolonged reaction time. Reaction ran for 18.5 hours yielded pyridinium product in 72% yield.

- EtOH, CH_2Cl_2, and MeCN give comparable yields to EtOAc if required.

^{1}H NMR

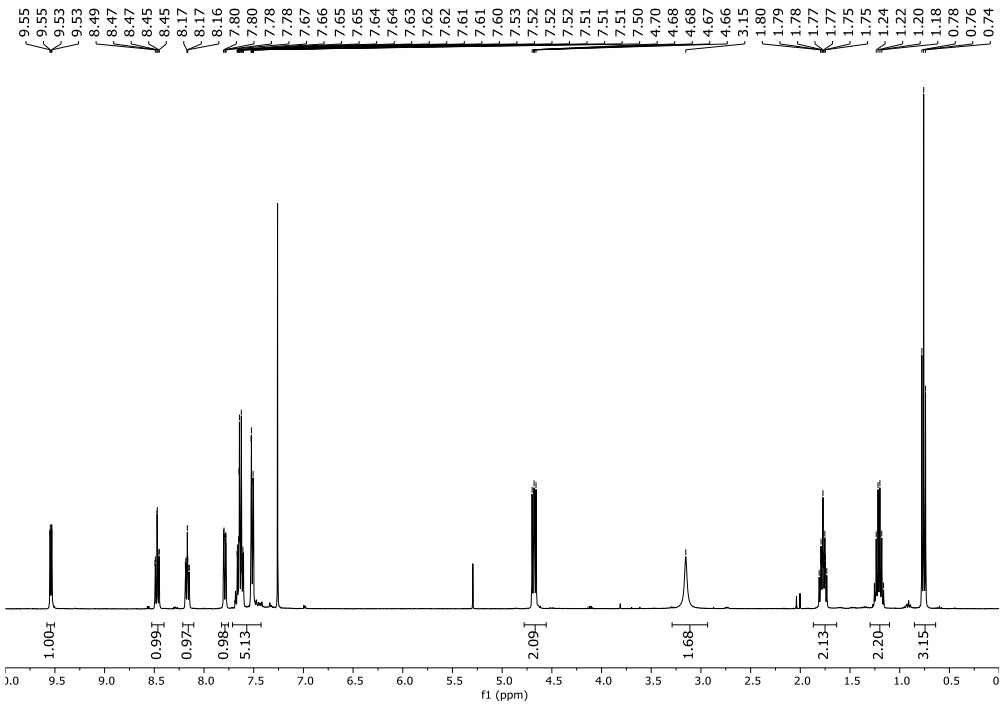

^{19}F NMR

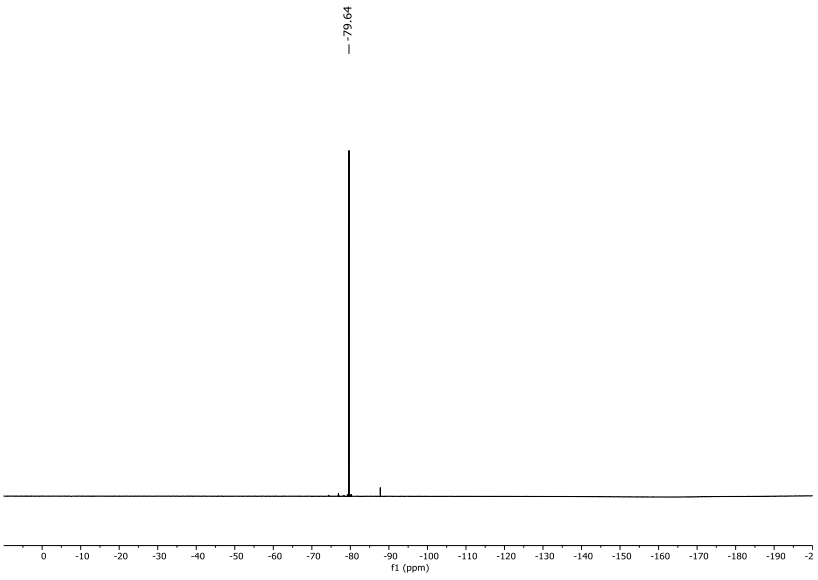

^{1}H NMR (400 MHz, $CDCl_3$) δ: 9.54 (dd, *J* = 6.3, 1.5 Hz, 1H), 8.47 (td, *J* = 7.8, 1.4 Hz, 1H), 8.17 (ddd, *J* = 7.8, 6.2, 1.6 Hz, 1H), 7.79 (dd, *J* = 7.9, 1.7 Hz, 1H), 7.70 – 7.59 (m, 3H), 7.55 – 7.48 (m, 2H), 4.76 – 4.59 (m, 2H), 3.15 (s, 2H), 1.85 – 1.69 (m, 2H), 1.21 (h, *J* = 7.4 Hz, 2H), 0.76 (t, *J* = 7.4 Hz, 3H).

^{19}F NMR (365 MHz, $CDCl_3$) δ: -79.64.

N-Phenyl Pyridinium Synthesis and Isolation

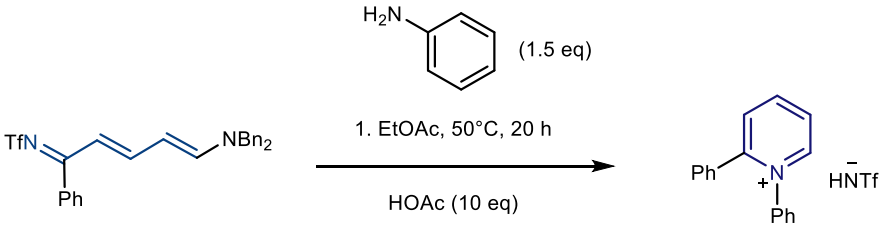

An oven dried 8 mL vial (≤ 0.5 mmol scale) or a round bottom flask (> 0.5 mmol scale) equipped with a stir bar was charged with the Zincke imine (1.0 equiv), EtOAc **(0.4 M)**, acetic acid (10 equiv) and aniline (1.5 equiv). The reaction vessel was heated to 50 ºC and stirred for 20 hours. The crude reaction was concentrated in vacuo and purified via flash column chromatography (basic alumina, gradient elution: 100% EtOAc to 5% MeOH:CH_2Cl_2) to afford the product as a viscous orange oil**.** Isolated yields 70-85%

- Reaction ran with no precautions taken to exclude air or moisture proceeds with no change in yield
- Reaction concentration (0.4M) is an important variable.
- Avoid any workup with water as the pyridinium product will partition into the aqueous layer. Investigation of a column chromatography-free purification method is ongoing.
- We suspect that this pyridinium is potentially susceptible to storage under ambient conditions and recommend long-term storage in a –20 ºC fridge.
- EtOH, CH_2Cl_2, and MeCN give comparable yields to EtOAc if required.
- It is possible that minor amounts of counterion exchange have occurred with acetate.

^{1}H NMR

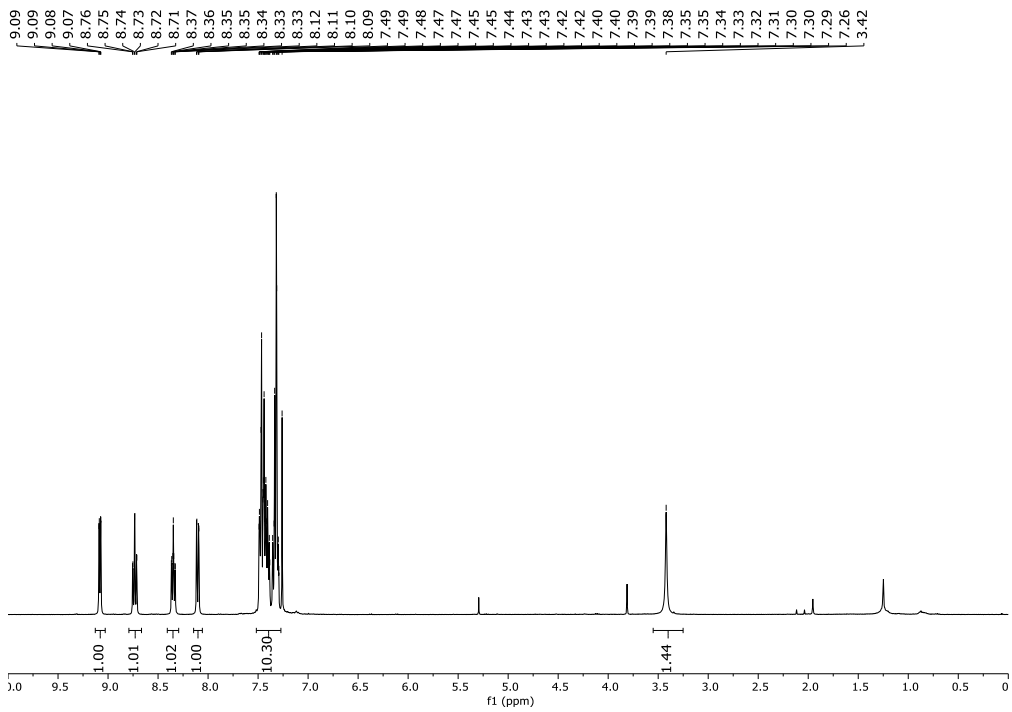

^{19}F NMR

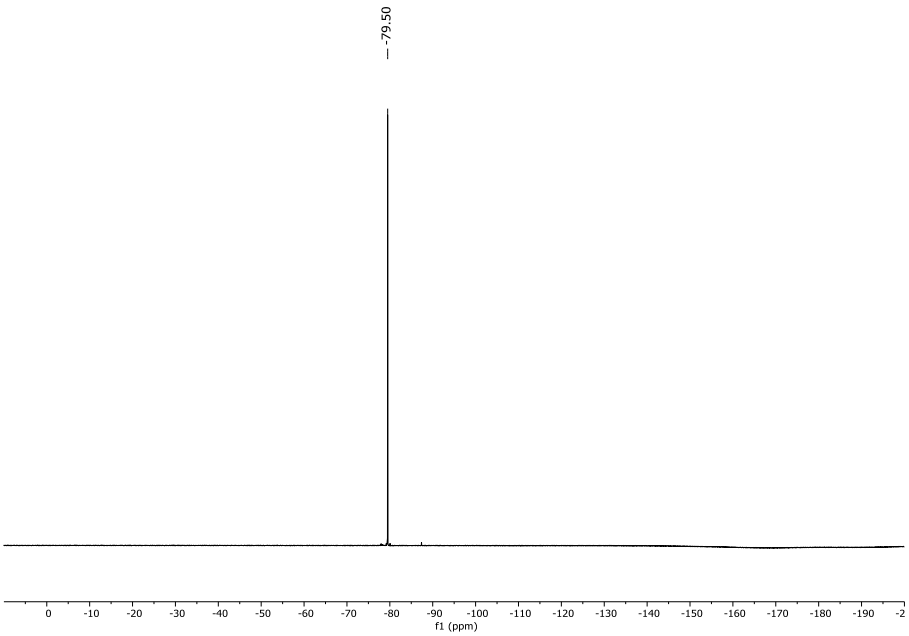

^{1}H NMR (400 MHz, $CDCl_3$) δ: 9.08 (dd, J = 6.2, 1.5 Hz, 1H), 8.73 (td, J = 7.9, 1.5 Hz, 1H), 8.35 (ddd, J = 7.8, 6.2, 1.5 Hz, 1H), 8.10 (dd, J = 8.0, 1.5 Hz, 1H), 7.56 – 7.37 (m, 6H), 7.37 – 7.28 (m, 4H).

^{19}F NMR (365 MHz, $CDCl_3$) δ: -79.50.